Forensic Engineering 2009

Pathology of the Built Environment

Proceedings of the Fifth Congress on Forensic Engineering

Edited by
Shen-en Chen, Alicia Díaz de León, Anthony M. Dolhon, Michael J. Drerup, and M. Kevin Parfitt

ASCE
AMERICAN SOCIETY OF CIVIL ENGINEERS

FORENSIC ENGINEERING 2009

Pathology of the Built Environment

PROCEEDINGS OF THE FIFTH CONGRESS ON FORENSIC ENGINEERING

November 11–14, 2009
Washington, D.C.

SPONSORED BY
Technical Council on Forensic Engineering
of the American Society of Civil Engineers

EDITED BY
Shen-en Chen
Alicia Díaz de León
Anthony M. Dolhon
Michael J. Drerup
M. Kevin Parfitt

ASCE AMERICAN SOCIETY OF CIVIL ENGINEERS
1801 ALEXANDER BELL DRIVE
RESTON, VIRGINIA 20191–4400

Cataloging-in-Publication Data on file with the Library of Congress.

American Society of Civil Engineers
1801 Alexander Bell Drive
Reston, Virginia, 20191-4400

www.pubs.asce.org

Any statements expressed in these materials are those of the individual authors and do not necessarily represent the views of ASCE, which takes no responsibility for any statement made herein. No reference made in this publication to any specific method, product, process, or service constitutes or implies an endorsement, recommendation, or warranty thereof by ASCE. The materials are for general information only and do not represent a standard of ASCE, nor are they intended as a reference in purchase specifications, contracts, regulations, statutes, or any other legal document. ASCE makes no representation or warranty of any kind, whether express or implied, concerning the accuracy, completeness, suitability, or utility of any information, apparatus, product, or process discussed in this publication, and assumes no liability therefore. This information should not be used without first securing competent advice with respect to its suitability for any general or specific application. Anyone utilizing this information assumes all liability arising from such use, including but not limited to infringement of any patent or patents.

ASCE and American Society of Civil Engineers—Registered in U.S. Patent and Trademark Office.

Photocopies and reprints.
You can obtain instant permission to photocopy ASCE publications by using ASCE's online permission service (http://pubs.asce.org/permissions/requests/). Requests for 100 copies or more should be submitted to the Reprints Department, Publications Division, ASCE, (address above); email: permissions@asce.org. A reprint order form can be found at http://pubs.asce.org/support/reprints/.

Copyright © 2010 by the American Society of Civil Engineers.
All Rights Reserved.
ISBN 978-0-7844-1082-0
Manufactured in the United States of America.

Preface

These proceedings are a collection of peer-reviewed technical papers presented at the Fifth Congress on Forensic Engineering, held in Washington, D.C. on November 11-14, 2009. The Congress was sponsored by the ASCE Technical Council on Forensic Engineering (TCFE), whose mission is to develop practices and procedures to reduce the number of failures, to disseminate information on failures, and to provide guidelines for conducting failure investigations and ethical conduct. TCFE uses the Forensic Congress to disseminate information on failures and the practices to mitigate failures, and to provide a forum to discuss ethical practice within forensic engineering. The publication of these papers is the result of the dedication and sacrifice of TCFE members who have volunteered many hours. TCFE collaborated closely with ASCE's Technical Council on Wind Engineering, and a number of excellent papers from this important discipline are also included herein. Each paper underwent a peer review process and received a minimum of two positive reviews. All of the papers in this proceeding are eligible for both discussions in the Journal of Performance of Constructed Facilities and ASCE awards.

In addition to paper presentations, the conference included two panel discussions, one forensic engineering education, and another on the potential impact of LEED certification on building performance. The education discussion was preceded by presentation of two papers regarding current university level forensic engineering programs in Ireland and Italy and also focused on a series of educator workshops presented by TCFE's Education Committee over the past several years.

On Wednesday, November 11, 2009, two Pre-Congress workshops were held. They were titled, "Forensic Practices" and "Facade Forensics." These workshops emphasized an interaction and exchange of information among the participants. The "Forensic Practices" workshop was based on the ASCE's *Guidelines for Forensic Engineering Practice*, 2003 and *Guidelines for Failure Investigation*, 1987. This workshop covered issues related to the practice of forensic engineering, including the investigation process, business aspects, and the legal system with an emphasis on the ethical issues. The "Facades Forensics" workshop introduced participants to key features of building facade failures including an historical overview and development of building facades, systems and materials, thermal performance, mechanisms of deterioration and failure, inspection and diagnosis, and repair and restoration.

On Thursday, November 12, 2009, the keynote presentation was given by Henry Petroski, Ph.D., P.E., Dist. M.ASCE, NAE. Dr. Petroski addressed a public event held in the Great Hall of the National Building Museum, which is the one of the great American buildings of the nineteenth century and one of Washington, D.C.'s most spectacular works of public architecture. Dr. Petroski is the Aleksandar S. Vesic

Professor of Civil Engineering and Professor of History at Duke University. Dr. Petroski is a renowned educator, author, researcher, and lecturer. He has achieved eminence for significantly advancing the practice of civil engineering and education. His published works, most notably *To Engineer is Human: The Role of Failure in Successful Design*, has increased the public's understanding of the role of the engineer. In 2008, Dr. Petroski was elected as a distinguished member of ASCE.

Shen-En, Chen
University of North Carolina at Charlotte
Proceedings Editor-in-Chief

Michael J. Drerup, P.E., M.ASCE
Exponent, Inc.
Congress Chair

Acknowledgements

The Steering Committee of the Fifth Congress on Forensic Engineering acknowledges the dedication of its members throughout the planning of the Congress, including Michael J. Drerup, P.E., M.ASCE (Congress Chair and ExCom); Shen-en Chen, Ph.D., P.E., M.ASCE (Proceedings Editor); Leighton Cochran, Ph.D., C.P.Eng., M.ASCE; Alicia E. Diaz de Leon, S.E., AIA, M.ASCE; Anthony M. Dolhon, P.E., M.ASCE; Mohamed Ettouney, Ph.D., P.E., M.ASCE; M. Kevin Parfitt, P.E., M.ASCE; David B. Peraza, P.E., M.ASCE; and Ziad M. Salameh, Ph.D., P.E., M. ASCE.

We also wish to thank the Executive Committeee (ExCom) of the Technical Council on Forensic Engineering, including David B. Peraza, P.E., M.ASCE (Chair); Leonard J. Morse-Fortier, Ph.D., P.E., M.ASCE (Past Chair); Norbert J. Delatte, Jr., Ph.D., P.E., M.ASCE (Past Chair); Anthony M. Dolhon, P.E., M.ASCE; Michael P. Lester, P.E., M.ASCE; and Michael J. Drerup, P.E., M.ASCE.

Throughout the planning process we collaborated closely with ASCE's Technical Council on Wind Engineering (TCWE), and appreciate the many excellent papers on various aspects of this important field included in this volume. TCWE's efforts, led by Leighton Cochrane, Ph.D, were integral to our planning and program development.

The Steering Committee also wishes to thank the authors, presenters, and session moderators, whose efforts form the heart of the Congress; and ASCE Staff, including Verna Jameson, TCFE Coordinator; Elaine Watson, Conference Manager; Donna Dickert, Publications Department; Mr. Patrick Driscoll of MIRA; and others whose names may have been inadvertently omitted.

Finally, we thank our families for their support throughout the planning and review process.

Reviewers

The Technical Council on Forensic Engineering wishes to thank the following individuals who served as reviewers for the Proceedings:

Kimball J. Beasley
Wiss, Janney, Elstner Associates, Inc.

Steven Camposano
High Velocity

Shen-en Chen
University of North Carolina at Charlotte

Xinzhong Chen
Texas Technology University

Leighton Cochran
Cermak Peterka Petersen, Inc.

Julie M. Cohen
Structural and Forensic Engineer

Michele Cyr
Exponent, Inc.

Kaoshan Dai
University of North Carolina at Charlotte

Norbert J. Delatte, Jr.
Cleveland State University

Alicia Diaz de Leon
Structural Engineer and Architect

Anthony M. Dolhon
Wiss, Janney, Elstner Associates, Inc.

Michael J. Drerup
Exponent, Inc.

Ibrahim Erdem
Exponent, Inc.

Mohammed Ettouney
Weidlinger Associates, Inc.

Jon Galsworthy
Rowan Williams Davies Irwin, Inc.

Rajaram Janardhanam
University of North Carolina at Charlotte

Kurtis Gurley
University of Florida

Gregory Kopp
University of Western Ontario

Michael P. Lester
Element Analytical, PLLC

Wanqiu Liu
University of North Carolina at Charlotte

Forrest Masters
University of Florida

Paul F. Mlakar
US Corp of Engineers

Felix Nieto
University of La Corunna

Terrance Paret
Wiss, Janney, Elstner Associates, Inc.

M. Kevin Parfitt
Pennsylvania State University

David B. Peraza
Exponent, Inc.

Wenya Qi
University of North Carolina at Charlotte

Kevin L. Rens
University of Colorado at Denver

Christine Reynolds
Wiss, Janney, Elstner Associates, Inc.

Ziad M. Salameh
ZSLLC

Gary Searer
Wiss, Janney, Elstner Associates, Inc.

Bin Su
Unitec New Zealand

David Thompson
KTA Structural Engineers

Rolando Vega
ABS Consulting, Inc.

J. Arn Womble
WindForce Associates

David Young
University of North Carolina at Charlotte

This page intentionally left blank

Contents

Building Envelope I: Performance

Practices to Reduce Common Failures **1**
Kenneth B. Simons

Case Studies of Roofing and Cladding Failures Involving Internal Pressurization **13**
Warren R. French

Water and Moisture Management with Sustainable Building Products **23**
Stephen M. Lattanzio and Roger G. Morse

Stone Veneer Wall Failure: A Small Earthquake Reveals a Large Problem **33**
T. N. Stubblefield and C. L. Searls

Thermal Inefficiencies in Building Enclosures—Causes of Moisture Related Performance Problems **43**
P. E. Totten and M. Pazera

Building Envelope II: Masonry Walls

Inspection, Rating, and Repair of a Residential Building Envelope Detail **55**
Kevin L. Rens and H. James Royston

Special Problems with Composite Multiwythe Masonry Walls **66**
David B. Peraza

Identification and Diagnosis of Building Façade Failures **74**
Kimball J. Beasley

Evaluation and Repair of a Distressed Masonry Veneer Façade: A Case Study of the Litton Reaves Repair Project **85**
J. E. Peterson and T. Shelton

To Seal or Not to Seal: A Practical Study of Masonry Surface Treatments **96**
Michael J. Drerup and Alicia E. Díaz de León

Bridges and Tunnels

The Bussey Railroad Bridge Collapse **105**
Steven M. Pennington

Assessing the Vulnerability of Large Critical Infrastructure Using Fully-Coupled Blast Effects Modeling **115**
Larry McMichael, Charles Noble, Jonathan Margraf, and Lee Glascoe

Development and Application of a Fast-Running Tool to Characterize Shock Damage within Tunnel Structures **125**
Lee G. Glascoe, Joseph P. Morris, Lewis A. Glenn, and Milovan Krnjajic

Collapse of the Wimer Covered Timber Bridge 133
Richard Dethlefs and Zeno Martin

Residential

Built-Up Column Stability in Wood Construction 143
Ryan Chancey, Stewart M. Verhulst, David W. Fowler, and Deepak Ahuja

Mold in Ductwork: A Forensic Analysis 153
Roger G. Morse and Stephen M. Lattanzio

The New FEMA 320 and FEMA 361—Highlights of the Wind and Flood Hazards Criteria for the Design and Construction of Residential and Community Safe Rooms (Shelters) 163
John Ingargiola and Scott Tezak

A Huff, and a Puff, and…It Blew the Chimney Down 175
Kerry S. Lee, Gary S. Dunlap, and Daniel M. Killian

Building Envelope III: Roofing and Drainage

Residential Roofing Evaluation 184
Luke M. Sharara, James W. Jordan, and Ross A. Kimble

Assessing Wind Damage to Asphalt Roof Shingles 194
Marco A. DeLeon and Pamela C. Pietrasik

The Roof Drainage Epidemic 204
Stewart M. Verhulst, Marco A. Deleon, and Bradley L. East

Soils I: Subsurface Conditions

Dimensional Study of Mine Subsidence Mapping Using Google Earth 214
Shen-En Chen, R. Janardhanam, and Mohiuddin Syed

Forensic Considerations in Sinkhole Investigations 224
E. D. Zisman

Case History: Sulfate-Induced Heave of Lime-Treated Soils beneath a Structure in Western Colorado 234
Aaron D. Bagley and Joseph A. Cesare

Forensic Engineering in the Assessment of Contaminated Land 244
L. A. Shah, C. L. James, and B. R. Thomas

Settlement Problems in Peat Due to Their High Compressibility and Possible Solution Using Cement Columns 255
Sina Kazemian, Afshin Asadi, Bujang B. K. Huat, Arun Prasad, and Irman B. A. Rahim

Soils II: Foundations

Bearing Capacity of Rectangular Foundations near the Slopes with Nonassociated Flow Rules 265
N. Ganjian, F. Askari, and O. Farzaneh

Assessment and Remediation of Geotechnical and Structural Deficiencies at a 5-Story Hotel Experiencing Large Differential Settlements **278**
Gregory L. Hebeler, Rafael I. Ospina, Darren K. Howard, and Ralf Leistikow

Optimization of Compaction Grouting in Collapsible Soils **288**
Jason M. Cumbers, Eileen M. Dornfest, Daniel D. Overton, and Joe Harris

Rethinking Waterproofing for Subsurface Structures **298**
Clinton Deckard and Peggy Hagerty Duffy

Floor Level Surveys and Their Use in Geotechnical Investigations: Case Studies **308**
K. Medji Sama, Debanik Chaudhuri, Michele F. Cyr, and Joanna L. Meldrum

Soils III: Vibrations and Blasting

Vibration Study of a Proposed Fitness Center Adjacent to a Server Room **318**
Prasad Samarajiva and Dilip Choudhuri

Shock and Blasting Effects on Power Transmission Structures **325**
Kaoshan Dai, Eric Connor, Antoneta Koleva, Wenya Qi, and David Young

Soil Contributions to Blasting Effects from Case Histories and Vibration Limits **335**
Mark R. Svinkin

Seismic Damage Control of Underground Structures Associated with Reduced Stiffness of Soil Foundation **348**
Mohammad Reza Okhovat and Koichi Maekawa

Collapse I: Shoring and Erection

Cantilever Roof Structural Failure Caused by Excessive Construction Loads, Flawed Design, and Poor Maintenance **358**
Hal K. Cain

Convention Center Steel Truss Collapse **368**
Benjamin Lavon and Andrew Goodrich

Structural Robustness Evaluation **378**
S. M. Marjanishvili, L. Leininger, M. Miraglia, and I. Alsharkawi

Partial Collapse of a Historical Masonry Building **387**
N. Augenti

Lessons Learned from Marcy Bridge Collapse **395**
D. J. Corr, D. M. McCann, and B. M. McDonald

Collapse II: Adjacent Construction, Overload, and Design Errors

From Concept to Collapse **404**
Stewart M. Verhulst, Deepak Ahuja, and Gregory G. Schober

Description and Analysis of Crib Wall Failures **414**
Gerald D. Lehmer and Chukwuma G. Ekwueme

Roof Collapse Case Study: Drainage Design Issues **424**
James W. Jordan and Luke Sharara

Failure of a Church Fresco: The Engineering of Art vs. the Art of Engineering 433
Michael P. Lester

Failures of Roofs under Snow Load: Causes and Reliability Analysis 444
M. Holicky and Miroslav Sykora

Collapse III: Wood Trusses

Analysis of an 1864 Long-Span Truss Roof 454
Donald Friedman

Load Duration Effect on Failure of an Overloaded Wood Truss Structure 465
Behnam Arya, Mohsen Kargahi, and Gary C. Hart

Structural Engineering Responsibilities and Structural Components: A Premanufactured Wood Truss Case Study 477
Stewart M. Verhulst and Deepak Ahuja

Investigation of Collapse of Wood-Framed Warehouse during Construction 487
R. Scott Silvester and Charles J. Russo

Ethics and the Expert Witness

Engineering Ethics and Structural Calculations 497
Joshua B. Kardon

Testifying Regarding the "Standard of Care" 504
Joshua B. Kardon

Education

The First University Master on Forensic Engineering 512
N. Augenti

Education: The Challenge and How Forensic Engineering Can Help 517
D. T. P. Phillips

Temporary Structures: Scaffolds, Cranes, and Towers

Wind Related Failures of Temporary Construction Installations 527
Dan Eschenasy

A Case Study of Failure Due to Inappropriate Usage of Forming Scaffold System 536
Y. Pashang Pisheh, H. R. Shafiei, and M. Hatambeigi

Defects, Damage, and Repairs Subject to High-Cycle Fatigue: Examples from Wind Farm Tower Design 546
Nestor A. Agbayani

Crane Safety—An Industry in Flux 556
David B. Peraza and Jeffrey A. Travis

Anatomy of a Tower Crane Collapse—An Opportunity to Learn 567
Charles J. Russo and Elizabeth A. Puchek

Investigative Methodology

Damage Assessment of Houses and Buildings from an Engineering Point of View **577**
Charles R. Norman

Investigation of Load Capacity and Serviceability of Assembled Concrete Blocks (Dox Plank) **587**
Anthony M. Dolhon, Dennis D. Rolander, Mark R. Chauvin, and David S. Finley

Uncertainty Information Processing in Repair and Rehabilitation **597**
Y. Ratna Divya, C. Natarajan, and A. Rajaraman

Failure and Repair in Cultural Heritage Conservation **607**
Miloš Drdácký and Zuzana Slížková

Non-Destructive Testing (NDT)

Forensic Evaluation Techniques for Masonry and Concrete Construction **617**
Gerald A. Dalrymple

Ground Penetrating Radar—Deciphering the Signals **627**
Amy S. Graver, Charles J. Russo, and Matthew R. Sherman

Integration of NDT Results into the Evaluation of Distressed Structures **637**
Keith Kesner and Michael D. Brown

The Application and Advantages of Surface Penetrating Radar in Subgrade Void Detection beneath Slabs-on-Grade **647**
Justin Norvell and John Grill

In Situ Evaluation of Structures Using Load Testing **657**
Nestore Galati and Tarek Alkhrdaji

Wind Engineering I: Wind Tunnels

A Method to Assess Peak Storm Wind Speeds Using Detailed Damage Surveys **668**
Gregory A. Kopp, Murray J. Morrison, Behareh Kordi, and Craig Miller

Wind Gust Phenomena on an Industrial Facility during Hurricane Gustav **678**
Rolando E. Vega and Ben F. Harrison

Wind-Induced Curtain Wall Damage and Moment Resisting Frame Performance: The Emergency Response, Stabilization, Analysis, Testing, and Retrofit of a 36-Story Urban High-Rise **688**
William D. Bast, Ken R. Maschke, Scott G. Nacheman, and Adam Abbes Yala

Wind Engineering II: Tornadoes

The Enhanced Fujita Scale: For Use Beyond Tornadoes? **699**
J. Arn Womble, Douglas A. Smith, Kishor C. Mehta, and James R. McDonald

Ground Damage Assessment from Tornado-Borne Projectiles **709**
Charles E. Pierce, Jonathan Jenkins, and Lesley Joseph

The Enhanced Fujita Scale: Development and Implementation 719
James R. McDonald, Kishor C. Mehta, Douglas A. Smith, and J. Arn Womble

Wind Engineering III: Hurricanes

Distinguishing between Storm Surge and Wind Damages to Buildings and Structures 729
Charles R. Norman

Cladding Performance of High-Rise Buildings in the Houston CBD during Hurricane Ike 739
Rolando E. Vega and Robert C. Konz

Structural Evaluation Procedures and Case Studies of Damage Related to Wind Storms, Tornadoes, and Hurricanes 749
Kerry S. Lee, Jessica M. Caffey, and Daniel M. Killian

An Investigation of Building Damage Caused by Thunderstorm Winds 759
Scott M. Adan, Rene Luft, and Nicholas G. Wetzel

Concrete and Masonry Structures

Repair and Rehabilitation of a 28 Year-Old Overhead Water Tank 769
C. Natarajan, S. E. Chen, and S. S. Fatima

Evaluation of Damage to Concrete Buildings for Insurance Claims: New Generation Approaches 779
Gary C. Hart and Anurag Jain

Structural Complexities and Durable Solutions for the Rehabilitation of a Reinforced Concrete High Rise Residential Building within a Marine Environment 789
Andrew Wilson, Tracy Marcotte, Mark Yerges, Robert Schaeffer, and Eric Godfrey

Forensic Assessment of Performance Deficiencies of a New Department Store 799
M. Holický

Restoration of Life Star Rooftop Heliport at Hartford Hospital 809
Howard Epstein and George Torello, Jr.

Indexes

Subject Index 817

Author Index 821

PRACTICES TO REDUCE COMMON FAILURES

Kenneth B. Simons[1], F. ASCE

Abstract

Common failures that occurred in the past continue to replicate themselves even though the analysis, design and construction phases have become more sophisticated and specialized. The mundane issues that designers and constructors may consider unimportant or uninteresting due to their low cost, visibility or low technical level can become huge factors in a constructed facility's performance and a tremendous drain on the nation's economy. This paper discusses ten common types of failures with examples and provides general recommendations to prevent or reduce these types of failures. The failures discussed herein vary from analysis and design consideration to construction practices and techniques.

Introduction

In 1998, the author presented a proposal to ASCE's Technical Council on Forensic Engineering to prepare a publication or series of publications that would digest down various common failures and provide general recommendations to reduce failures. Although the council has decided not to approach the reduction of failures in this manner, the author has presented the following practices developed based upon over thirty years of professional engineering experience in the design, construction, inspection, and forensic analysis of a variety of projects. These practices may not be appropriate for all situations and should be regarded as general in nature and used a resource or guide from which a reader can draw their own conclusions as to the appropriateness of these recommendations to their specific project.

The ten common failures presented are:

1. Foundation Movement
2. Leaking Basements
3. Asphalt Parking Lot Deterioration
4. Building Distortion from Wood Shrinkage
5. Deterioration of Light Wood Framed Roof Structures

[1] Principal Engineer, Damage Consultants, Inc., 9725 SE 36th Street Suite 102, PO Box 1336, Mercer Island, Washington 98040-1336

6. Wood Truss Collapse During Construction
7. Cracking and Leakage Portland Cement Stucco
8. Collapse of Rigid Frame Metal Buildings
9. Leakage of Flat Roofs
10. Detachment of Asphalt Shingles

Although these failures discussed may not be the most intriguing and exotic, they represent billions of dollars of expense to the economy of the United States. It is hoped that by discussing these mundane yet expensive failures in this forum will promote further discussion and create venues in which these failures can be reduced and eventually eliminated.

1. Foundation Movement

Soil conditions on a site can vary significantly; thus, making an assumption that one portion of a building site is equivalent to another can be erroneous. This incorrect assumption can take place at developed building sites as well as undeveloped property. These incorrect assumptions result in both settlement from consolidation and heaving from expansion (Simons 1991). In the case of a larger developed construction project where site development has taken place, the overlot grading process has disturbed the pre-existing surface and possibly subsurface features of a site. The importation of inexpensive (and possibly expansive) fill soils from a helpful donor may create conditions that are inconsistent with the original geotechnical information (see Figure 1). Also, re-distribution of excavated soils on a sloping site can create conditions that can cover underlying organic material such as downed trees and stumps and unsuitable soil materials (see Figure 2).

Figure 1
Expansive Soil Heaves Slab Upward

Figure 2
Fill Soils Cause Downhill Portion of Building to Settle

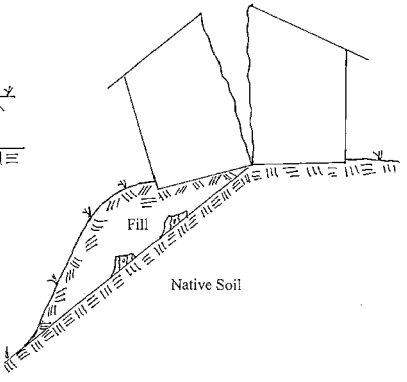

General recommendations to reduce differential movement from varying soil conditions include the following:

- Provide a minimum of two borings or open hole soil investigation on each building site regardless of size.
- Cursory underground penetrating radar surveys could be provided to determine the existence of buried objects and organic material.
- Structural fill should be limited to crushed rock/quarry spalls.
- In areas of expansive soils, the foundation configuration should be as simple as possible to maintain a more uniform pressure on the underlying soil.
- Steel reinforcement of concrete in excess of the code-required minimum in order to mitigate damage.

2. Leaking Basements

Sub-surface water infiltration (leaking basements) is a very common occurrence in many areas. Some are chronic conditions and others are only sporadic when there is heavy rainfall. Correction of these problems can often be quite expensive since providing deep excavation around the base of a foundation wall may affect adjacent structures, walkways, etc. around the building. In some cases it is more economically feasible to provide interior drainage, or simply accommodate the leakage if it is at a point source. One of the most common causes of water infiltration into a basement area is usually the placement of a perimeter sub-surface "footing" drain pipe directly on top of the footing. If water collects in the drain pipe at a depth equal to the interior concrete floor slab that is usually placed also on top of the footing, then the water seeps between the cold joint between the foundation wall and the footing and the interior slab (see Figure 3). A way of preventing this leakage is to initially place the footing drain below the top of the interior slab. That is, basically at the bottom of the footing. This installation requires a slightly larger excavation in order to place the footing at this location (see Figure 4). Other methods to prevent sub-surface water infiltration include the following:

Figure 3

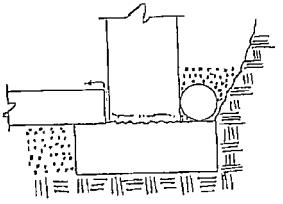

- If the surface area can not be drained by gravity, a pump can be installed. It is recommended that backup power requirements be considered depending on the use of the lower level area. It has been observed that complete sealing of the slab with a vapor barrier and bentonite (clay) panels can cause a hydrostatic uplift of concrete floor slabs

Figure 4

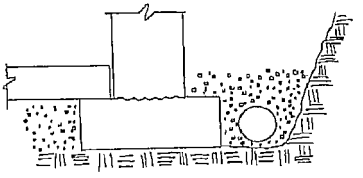

when emergency backup power is not provided for sump pumps.

- Often times it is found that basement footing drains could have been drained by gravity to an acceptable discharge point, if only the building had been raised slightly from its design position. This foundation elevation should be considered prior to final grading and placement of the footings.
- Roof drainage downspouts should not be directed into subsurface footing drains.
- Cleanouts should be provided for the footing drains at each change direction. Although this increases the costs of the initial construction, it may save the cost of installing a new footing drain at a later date. Rigid perforated plastic pipe is preferable to the corrugated flexible type of slotted pipe. There is less chance that there will be a low spot or a "sag" in the pipe where water will accumulate.
- At locations where it is determined more feasible to remove a portion or a "strip" of concrete adjacent to the foundation wall to install a drain inside the basement area, adequate lateral bracing should be provided for the base of the wall as the portions of the concrete slab are being removed.

3. Asphalt Parking Lot Deterioration

Asphalt pavement is a composite material of asphalt binder and mineral aggregate mixed together and then laid down in layers and compacted. Asphalt paving on roadways is well studied controlled and inspected by state and local agencies; however, at many parking lots of privately owned buildings, the same effort and oversight used during the design of the buildings is often overlooked when it comes to the construction of the asphalt paving. One of the most prevalent types of failures of asphalt parking lots is "alligator" cracking (interconnected cracks from a series of polygons that resemble alligator skin) (refer to Figures 5 and 6). These cracks are usually caused by a base or sub-grade failure. Poor surface drainage and traffic loads cause further wetting and loss of strength of the sub-grade causing further failure.

Figure 5
Alligator Cracking around a Storm Sewer Catch Basin

Figure 6
Close-up View of Alligator Cracking

General recommendations to consider enhancing the performance of asphalt parking lots include:

- Provide a minimum of 2% slope. This minimum applies to any cross slopes or valleys.
- Any soft or spongy area should be removed and replaced with a structural material that will not compress, such as crushed rock. This may not be a popular suggestion with the property owner since any spoil has to be removed and the crushed rock is an additional expense.
- All underground utility trenches, indulging excavations for manholes should be backfilled with crushed rock.
- The tops of the catch basins should be placed at or slightly lower than the theoretical height of the pavement.
- The sub-grade should be well-compacted including the utility trenches and other areas filled with crushed rock.
- A conservative selection of the base course and pavement thickness should be considered. Assuming good sub-grade conditions will allow for a thinner less expensive parking lot initially; however, allowing for poor sub-grade conditions will result in thicker asphalt and a deeper base course which will most likely enhance the pavement's long term performance.

4. Building Distortion from Wood Shrinkage

Settlement, if uniform throughout a structure, can usually be tolerated; however, when one part settles more than another, problems arise such as cracks and wracked doors. Even though these problems do not pose a threat to the strength or stability of the structure, they nevertheless can become very costly problems. These problems can be as minor as a hump in a single story, single-family home where the underlying floor joists are supported by a wood beam at one end and by a concrete foundation wall at the other. The shrinkage of the beam causes the foundation wall to become a hard point, not allowing the joists to "settle-in" with the rest of the floor framing (see Figure 7).

Figure 7
Hump at Floor Caused by Beam Shrinkage

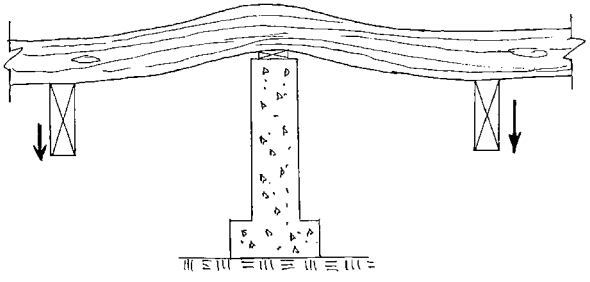

These problems can also manifest themselves as much more severe as in the case of a large five story, wood framed condominium building that required a large steel moment frame on one side of the building for lateral stability due to the large number of doors and windows. This differential shrinkage of the wood framing in relation to the steel moment frame was virtually non-existent at the lower levels; yet, by the time it had accumulated to the 5th floor, there was approximately 1-1/2" within an approximate 12' distance.

General recommendations in order to reduce the amount of differential settlement of wood framed buildings include the following:

- Accept that there will be shrinkage of the building during design and provide details that allow for uniform displacement.
- If varying structural materials are used, the designer should discuss the potential for differential shrinkage with the owner.
- If varying structural materials are used, the designer should consider increasing the horizontal distance that the differential displacement takes place, creating a less noticeable slope.
- Incorporate horizontal expansion joints within the exterior wall cladding to accommodate the differential shrinkage.

5. Deterioration of Light Wood Framed Roof Structures

Light wood framed roof structures are one of the most common building elements that suffer problems. These problems are related to the type and quality of materials selected in conjunction with the wall in which they are installed. The following recommendations should be considered in order to enhance the performance and to prevent failures of light wood framed roof structures:

- The designer should understand the performance differences between OSB roof panels in contrast to plywood roof panels.
- The designer should consider providing thicker roof sheathing than that required. Fore example: 15/32" sheathing with a 32/16 rating has an allowable live load of 70 psf while a 7/16" thick sheathing with a rating of 24/16 has a live load of 40 psf when the supports are placed at 24" center to center.[2]
- Provide solid blocking beneath all panel edges. Solid blocking prevents deflection between adjacent panels and provides greater lateral strength roof system. Care should be taken that solid blocking does not prevent adequate ventilation beneath the sheathing.
- Provide cross ventilation for the roof. Although the minimum code requirements (that is the area divided by 150) may be able to be met with ventilation from one source, better performance is usually obtained when cross ventilation is provided.

[2] APA – The Engineered Wood Association, E305 Table 25, May 2003.

- On very low sloping (flat) roofs, the designer should consider providing more slope than that which has been preliminary specified due to ponding at overlapping seams in the membrane and at cross slopes and corners where crickets are provided. Water that remains ponded on the roof for an extended period of time (typically greater than 24 to 48 hours) results in voiding the warranty from the roofing membrane manufacturer.
- The temporary lateral bracing of the trusses required by the truss manufacturer during erection of the trusses should be left in place to provide an additional degree of bracing and redundancy for the roof system. For simple gable roofs, these braces should include diagonal braces at the gable ends that are extended back towards interior load bearing walls. The designer should also consider providing additional horizontal lateral braces fastened to the bottom web members to help provide "joist action" in case of unintentional overloading of an individual truss.
- The designer should consider additional anchorage for uplift even if the analysis shows standard practice to be acceptable, especially at corners or discontinuities. A typical analysis may not anticipate special conditions that could occur during a high wind event.

6. Wood Truss Collapse During Construction

The major component in failure and collapses of plate connected wood trusses during construction involves the lack of adequate bracing and the improper handling of trusses at the job site. This industry has developed standards including the Truss Plate Institute (TPI). Building designers often rely on lumber companies to supply the manufactured trusses that are designed by an engineer working for the truss manufacturer. The temporary bracing standards including details normally included with the truss package. These instructions are usually included with the bill of lading and invoice and often get transferred to a supervisor or office. Thus, the crew erecting the trusses handle the trusses in a fashion which they have been successful with in the past. If the trusses are lifted into position and the sheathing begins immediately with no unusual winds or lateral force to the trusses, the roof is completed without all of the extra work to install (and subsequently remove) adequate temporary bracing; however, should a single truss rotate, a progressive (domino type) collapse can occur to all the trusses (see Figures 8 and 9).

Figure 8 – Progressive Collapse of Metal Plate Connected Wood Trusses

Figure 9- Rotation (Overturning) of Trusses due to Buckling of Light Gauge Metal Spacer Bars.

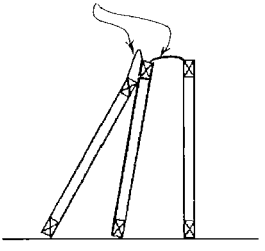

In order to prevent failures of these trusses during installation, the following recommendations should be considered:

- The building designer should include the temporary bracing diagrams in the set of building drawings. The diagrams could consist simply of Industry Standards that should be followed.
- The building designer should provide notes on the drawings that require a meeting of a representative of the Truss Manufacturer, general Contractor, truss erector and building designer prior to the erection of the trusses to discuss the erection process and answer any questions.
- As a minimum. Diagonal bracing should be provided on a continuous basis such that each truss is provided with a lateral load path down to the side walls.

7. Cracking and Leaking of Portland Cement Stucco

Stucco is a material used in a plastic state that can be troweled to form a hard covering for exterior walls. Coats of stucco are usually applied on a metal lath. The first coat is called the scratch coat because its surface is scratched to give it better bond to the second coat which is called the brown coat. The brown coat is finished accurately to a true surface ready to receive the finish coat. The finish coat of stucco has more recently been replaced with an acrylic finish. The total thickness of stucco usually varies from approximately 3/4" to 7/8". Several factors should be considered during the design and construction of the system including the following:

- Deflection design criteria for the substrate that a stucco assembly is attached to is required to be a minimum of an L/360. This is a live load requirement and it should be verified that the dead loads of the building are in place prior to the placing of the stucco wall cladding. The designer should consider shrinkage and compression of wood framing of the building especially in multi-story buildings. In addition, the structural designer should consider deflections or displacements between adjacent portions of the building. For example, shrinkage of the wood framing in deference to support of an adjacent portion of the building that is supported by steel or concrete.
- Careful selection of doors and windows should be considered. The popularity of "self-flashing" windows with nailing flanges requires special attention to "penetration warp" flashings. From a conservative basis, some designers consider leakage from window inevitable and thus provide complete sill pan flashings beneath the window assemblies to collect any water that may leak from a window.
- Proper placement and protection of the water resistive barrier (building paper, etc.) on the sheathing.
- Selection of a water resistant sheathing (such as siliconized gypsum sheathing board).
- Coordination of the metal flashings with the installation of the stucco. One of the most common flashing elements that causes water infiltration is the lack of an adequate diverter ("kick-out") flashing between roof and wall surfaces.

The cost of these flashings is insignificant; however, it is essential that it is verified that they are in place. Verify that the water resistive barrier is installed in weatherboard fashion.

- Verify the proper gauge of the metal reinforcement lath and the size of the fasteners.
- Verify that the placement of the upper trim accessories have been used such as casing beads, control joints, expansion joints and reveals.
- Make sure that the ambient temperature is 35° Fahrenheit (2° Celsius) or higher and moist cure the base coat for 8 hours after the set of the base coat if the temperature is above 77° Fahrenheit (25° Celsius) and allow a curing time of 7 days before providing the finish coat.

8. Collapse of Rigid Frame Metal Buildings

Rigid Steel frames can provide large economical structures including gymnasiums, churches, or auditoriums that require large unobstructed areas. Many of these buildings are of a proprietary nature, that is, designed and erected by a metal building manufacturer who has in house engineers design the building and, in many cases, an outside engineer designs the foundation. Failures can be avoided by considering the following:

- Verify the proper roof live (snow) loadings with the local building department. Verify the dead loads with the building manufacturer and owner including all equipment (current and future) that may be installed (hung) on the rigid frames.
- Provide hand sketches and calculations to determine if the rigid frame is stable and that the member sizes are consistent with the computer analysis.

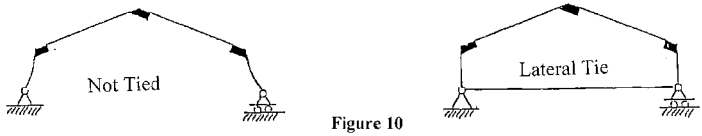

Figure 10
Typical Hand Sketches of Rigid Frame Conditions

- Provide a continuous horizontal lateral tie between the bases of the frame columns (legs) if possible. Often the designer(s) over-rely on the lateral restraint of the foundations by the backfill soils. Small horizontal displacements or rotations of the foundations can cause large stresses in the rigid frame.

Figure 11
Typical Hand Sketches of Rigid Frame Conditions

9. Leakage of Flat Roofs

Low sloping (flat) roofs cover more building area than any other type of roof. Expensive, sophisticated systems are sold annually to keep these buildings dry; however, the majority of leakage issues are not related to direct failure of a manufactured product, yet by a failure of understanding the limitations of the low sloping roofs. These leakages cause millions of dollars of property loss each year, not only to the building but also to the building contents. The following recommendations should be considered in order to enhance the performance and to prevent leakage through low sloping roofs.

- Provide as much slope as is economically and physically possible. An increase of 1/8" over 1'-0" slope results in a 12.5" increase in height of a building; yet will help prevent localized ponding on the roofing, specifically at the seams.
- Construct penetrations such as skylights, equipment curbs, and plumbing penetrations with greater height (freeboard) to prevent pounding water (and melting snow) from being driven by wind or gravity beneath the flashings.
- Increase the amount of roof slope down to drains. Often building shrinkage can raise drains slightly causing localized ponding at drains.
- Oversize the gutter and downspout sizing. The typical hydraulic calculations and tables used by designers do not consider obstructions.
- Provide redundant overflow drains and or scuppers at multiple locations to prevent ponding.

10. Detachment of Asphalt Shingles

Asphalt shingle roofing systems are consistently subject to failure. Approximately 80% of the current asphalt shingle market consists of replacing at least 12 billion dollars of existing shingles, resulting in 10 million tons of old shingles ending up in landfills each year. The failures are due to two factors: installation and materials. The type of fastener used can vary from corrosion resistant staples to stainless steel nails. Each shingle must seal to the layer below it to form a solid barrier against water and thus shingles should not be applied during cold weather. It is necessary for sunshine and heat to soften the underlying thermoplastic seal down strip is necessary during the early life of a new or replaced roof. Although typically allowed by shingle manufacturers, staples driven with pneumatic staple guns can puncture and tear the shingles.

General recommendations to enhance the performance of asphalt shingles include the following:

- Provide the installation of the shingles in conformance with the manufacturer's application instructions. These instructions are typically printed on the packaging that surrounds each bundle of shingles that arrives at

the job site. The packaging should be removed and discussed with each roofer on the project.

- Provide the fasteners in accordance with "high wind" recommendations as shown on the package – even if the project is not in a "high wind" area. This typically results in 6 fasteners instead of 4 for each shingle (see Figure 12).
- Use galvanized roofing nails with a minimum head diameter of 3/8" and a shank long enough to penetrate through the roof deck. There are rolls (belts) of pneumatically driven galvanized nails available which may be acceptable in most areas.
- Review the sealing of the thermoplastic adhesive (seal down) strips. Any shingle that is not sealed should be sealed by hand.
- Hand seal all shingles at the eaves to the starter shingles.

Figure 12
Typical 3-tab Asphalt Shingles

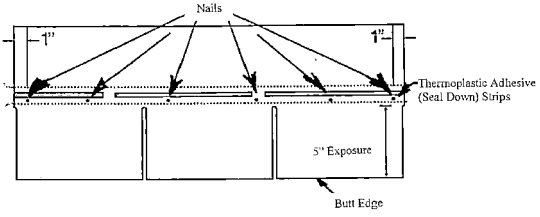

Closing Remarks

It is hoped that the brief discussions presented will help prevent or reduce the number of these types of failures. It is obvious that more in-depth analyses and recommendations could be developed for specific cases; yet, if the above succinct recommendations are at least considered, it is likely that failures in these categories will be reduced.

References

APA – The Engineered Wood Association E305, Table 25, Tacoma, Washington, May 2003.

International Code Council, *International Existing Building Code*, ICC, Country Club Hills, Illinois, 2003.

International Conference of Building Official, Uniform Building Code, ICBO, Whittier, California, 1991

International Council of Building Official, *Uniform Code for the Abatement of Dangerous Buildings*, ICBO, Whittier, California, 1997.

Nicastro, David H., Simons, Kenneth B., *Fenestration Frustration: Failure Mechanisms in Building Construction*, ASCE, New York, 1997.

Northwest Wall and Ceiling Bureau, Portland Cement Plaster and Stucco Resource Guide, Seattle, Washington

Sack, Ronald L. and Aune Petter. *The Norwegian Stave Church A Legacy in Wood, Classic Wood Structures*, ASCE, New York, 1989.

Simons, Kenneth B., Folding Bleacher Collapse: *An Accident Waiting to Happen, Forensic Engineering*, Proceedings of the Second Forensic Congress, ASCE, Reston, Virginia, 2000.

Simons, Kenneth B., *Imminent Collapse of Wood Structures Affected by Decay, Forensic Engineering*, Thames Telford Publishing, London U.K., November 2001, Pages 149-158.

Simons, Kenneth B., *Lateral Strength Evaluation of Existing Oriented Strandboard Wall Sheathing, Forensic Engineering*, Proceedings of the Fourth Forensic Congress, ASCE, Reston, Virginia, 2006.

Simons, Kenneth B., *Limitations of Residential Structures on Expansive Soils, Journal of Performance of Constructed Facilities*, Volume 5, No. 4, ASCE, New York, November, 1991.

Simons, Kenneth B., *Progressive Failure and Imminent Collapse of a Steel Storage Silo, Forensic Engineering*, Proceedings of the Third Forensic Congress, ASCE, Reston, Virginia, 2003.

Simons, Kenneth B., *Should I Notify the Building Department: The Dilemma of the Forensic Engineer, Forensic Engineering*, Proceedings of the First Forensic Congress, ASCE, Reston, Virginia, 1997.

Case Studies of Roofing and Cladding Failures Involving Internal Pressurization

Warren R. French, P.E., RRC, RWC, FRCI, CCS[1]

[1] President, French Engineering, Inc., Houston, Texas USA,
warren.french@frenchengineering.com

PRELIMINARY

Abstract
This paper will present the methods of evaluation utilized, as well as the results, of several forensic investigations involving the building envelopes of three different buildings. These case studies will present the conditions known regarding the original design and construction, as well as the storm circumstances that led to the observed failures. Where appropriate, discussions of the construction and workmanship realized for each project will be provided. It was determined during the investigations for each building that internal pressurization most likely played a part in the cladding or roofing failures, increasing the wind pressures incurred by these structures to levels exceeding the original design and the capacities of the various construction assemblies.

Introduction
Academic research papers, as well as building codes and practical experience, have shown that the cumulative wind pressures on structures and their cladding systems can be significantly affected by the contribution of internal pressures from within the structure. These internal pressures may arise due to stack effects, manipulation utilizing mechanical equipment (either planned, or inadvertently), as well as due to a catastrophic breach of the exterior building envelope during a storm event. Based on current calculation methods included in ASCE 7, such breaches of the cladding system (typically at openings, such as windows, doors, and storefronts, etc.), can result in an increase of the design wind pressure of 15 to 20 percent. This difference is derived by a determination whether the structure is "Enclosed" or "Partially Enclosed", utilizing an evaluation of the fenestration areas at each building elevation in conjunction with the formulas and criteria stipulated within ASCE 7. For structures located in hurricane prone regions, the current code prescribes that the building be considered as "Partially Enclosed" unless openings occurring within the lower 60 feet of the structure are composed of missile impact resistant glazing and components. This provision has not always been part of the code in the past, resulting in prior designs not generally allowing for the increases arising due to internal pressurization.

The buildings included within this paper are comprised of a tropical storm damaged curtain wall system on a multi-story office building located in Lafayette, Louisiana (**Case Study One**), hurricane damaged roof and wall cladding panels on a metal

building located in a New Orleans suburb (**Case Study Two**), and a hurricane damaged glass and aluminum curtain wall on a 30 year-old multi-story office building located in Houston, Texas (**Case Study Three**).

Case Study One

The first case study involves a multi-story office building located in Lafayette, Louisiana, which had incurred damage from Hurricane Lili in October of 2002. The existing building was originally constructed in 1969 as a three story bank building, and was composed of cast-in-place concrete framing system that had been designed for subsequent floors. These subsequent nine floors were added during a significant renovation that occurred during 1979, using a steel framed structure rising from the concrete "podium" and making the completed structure a total of twelve stories in height. See Figure 1.

At the time of our inspection approximately three weeks after the storm, the First and Second floors were occupied as offices and consisted of a cladding comprised of proprietary stainless steel and glass curtain wall. The Third floor is primarily utilized as a mechanical penthouse and was comprised of masonry walls. The First and Second floors are spatially connected via ascending and descending escalators that extend from the First floor to the Second floor through an opening within the Second floor framing that is approximately 4.73m by 7.3m (15'-6" by 24'-0") in size (34.6 m^2 - 372 S.F. total – or 2% of the floor area). See Figure 2.

The thirty-three year old curtain wall system at the First and Second floors consisted of prefabricated vertical and horizontal mullions composed of precision bent and punched stainless steel. Vertical mullions at the First floor spanned approximately 4.38m (14'-4½"), and ranged in spacing from 1.04m to 1.17m (3'-5" to 3'-10") on center, with 64mm (¼") thick tempered glass captured within dense neoprene gaskets. At the First floor, there was one horizontal mullion located approximately three feet from the sill. Vertical mullions at the Second floor spanned approximately 5.41m (17'-9"), and were consistently spaced at 0.61m (2'-0") on center, except at the corners, which exhibited a 12" wide glass lite on both sides of a butt-glazed corner sealed with clear silicone sealant. There were no horizontal mullions within the fenestration of the Second floor, resulting in long narrow glass lites, nominally sized at 0.61m by 5.31m (2'-0" by 17'-5").

During the 2002 hurricane season, this building had incurred significant weather events from both Hurricane Isidore and Hurricane Lili. Hurricane Lili resulted in significant damage to the building on October 3, 2002, causing partial loss of various portions of the curtain wall systems at the First and Second floors, water intrusion and damage to interior finishes, as well as abandonment of approximately 40% of the First floor and approximately 15% of the Second floor. Damage to the curtain wall consisted of significant portions of the of the glass and metal framing being removed or displaced at specific locations on all four elevations of the building at the Second floor, while a much more limited area of curtain wall was removed at the First floor (primarily the North and South elevations). See Figures 3 and 4.

Hurricane Lili originated from a tropical wave along the West coast of Africa on September 16, 2002. By September 21st, the cloud formations became sufficiently organized to be classified as a tropical depression, and followed a track across the Atlantic, moving Westerly between the Northern coast of South America and the Southern coast of Cuba. Hurricane Lili emerged from the strait located between the Yucatan Peninsula and Cuba as a Category Two hurricane, and strengthened to a Category Three in the middle of the Gulf of Mexico. Lili made land-fall on October 3rd, 2002 as a Category 4 hurricane with 125 MPH winds and remained at Category 4 wind speeds until well into Northern Louisiana. The track of the hurricane eye took it essentially right over, or perhaps slightly West of, the City of Lafayette, which would have subjected the city to the most significant winds during the storm. However, no monitoring stations were left undamaged in the immediate vicinity, so exact wind speeds at the building site are not known.

Based on reports from the building manager, as well as on-site observations, there was substantial evidence to indicate that the First floor curtain wall had blown inward, while the damaged portions of the Second floor curtain wall were blown outward. Our investigation determined that the First floor curtain wall had most likely either [a] experienced a failure of the head or sill connections to the structure allowing the framing to be displaced inward, or [b] was damaged by wind-blown debris resulting in significant framing damage and glass breakage. Failure of the First floor curtain wall by either of these methods would have produced a sudden and excessive internal "pressurization" of the Second floor space, due to the unrestricted communication between these floors occurring at the escalator opening. Internal pressurization of these spaces was "relieved" by the curtain wall framing failures and glass breakage occurring at the Second floor shortly after the First floor curtain wall breach. The Second floor curtain wall failures were generally located within the middle portion of the overall width at any given elevation, with an additional outward displacement occurring at the North elevation near the East end, which would have been subjected to significant separation vortexes and negative pressures during storm winds coming from the South. No pressurization of the Third floor spaces was experienced, since there are no significant openings between the Second and Third floors (other than the elevator shafts).

It should be noted that design wind pressures as derived by the codes in effect during the original construction, as well as during the 2002/2003 restoration work, could be significantly different. Based on our research, the wind loads differences could help explain the marginal connection details utilized for the original curtain wall installation. In addition, during the "infancy" period of the modern curtain wall design, unique proprietary systems were often half-engineered and half-designed using empirical methods. Furthermore, curtain wall design during that period often took advantage of the code-allowed "one-third increase" in the allowable stress when the loads were in combination with wind. Accordingly, it is not surprising that several of the curtain wall failures occurred because of, or in relation to, fasteners and

anchorage locations. A brief table of the cladding wind loads that could be expected using the two different calculation methods is provided below.

	1965 SBC	ASCE7-98
Field of Wall (Zone 4):	XXX	+26.0/-27.0 PSF
Corner of Wall (Zone 5):	XXX	+26.0/-39.0 PSF

Case Study Two

The second case study involves hurricane damaged metal roof and wall cladding panels on a metal-framed building located in a New Orleans suburb. The damage to this building was incurred during Hurricane Katrina on August 29th, 2005. The building was designed in 1987 and erected in 1989 to house production, bottling, and distribution facilities for a major soft drink manufacturer. During 2001 to 2002, the roof of this facility was renovated to provide increased resistance to wind uplift by installing retrofit "hurricane clips" with fasteners over the existing panels into the sub-purlins below.

The portions of the facility incurring the greatest damage were two interconnected buildings that constitute the main production and storage facilities of the plant. The first section was a high-bay storage portion of the facility, which exhibits a rectangular footprint of approximately 29.27 meters by 106.71 meters (96 feet by 350 feet), with an upper eave height at the North elevation of almost 30.2 meters (99 feet) above surrounding grade and a mean roof height of almost 29.88 meters (98 feet). This building utilized a unique structural framing system and was clad with 24 gage corrugated metal wall panels that utilized a concealed fastener at one rib placed against the girt and a proprietary, male/female, snap-lock, engagement that "connects" the other rib and conceals the previously placed rib fastener. The roof system was composed of a 24 gage, trapezoidal, standing seam metal roof panels with machine-crimped seams and concealed articulating clips in the seams that served to secure the panels to the purlins and sub-purlins.

The second section was a lower, 'U'-shaped building that surrounds the higher storage building and measures approximately 128 meters (420 feet) along the "legs" and 185 meters (607 feet) across the base. The lower building used for production and bottling surrounds the high bay building on the West, North, and east sides. It is a standard pre-engineered steel building with identical metal wall panel and metal roof panel assemblies as those installed on the high bay building. Interior spaces between the two large building sections communicate via two overhead roll-up doors placed within the separation wall of the two structures. See Figure 5.

The lower portion of the facility also features a rectangular building protrusion in the middle of its East elevation, measuring approximately 45.73 meters (150 feet) by 49.4 meters (162 feet), that includes at least twenty (20) large, overhead, roll-up doors at its North and South elevations. During Hurricane Katrina, at least five overhead doors were either totally or partially blown in along the North elevation of this

protruding building section. Based on reports from those familiar with the buildings, all of the exterior roll-up doors had been closed prior to the storm, however, all of the interior (communicating) roll-up doors had been left open allowing a free exchange of air between the two building sections.

Hurricane Katrina was an extraordinarily powerful and deadly hurricane that carved a wide swath of catastrophic damage and inflicted large loss of life. It was the costliest and one of the five deadliest hurricanes to ever strike the United States. Katrina was spawned by a complex series of meteorological events occurring over the Western Atlantic and the Bahamas after the degeneration of Tropical Depression Ten on August 14th, 2005. This series of events allowed the formation of Tropical Depression Twelve on August 23rd, which would later reach hurricane status and become Hurricane Katrina on August 25th. After making landfall as a Category 1 hurricane just North of Miami-Dade County, Katrina continued West-Southwesterly overnight and spent approximately six hours over land, where it briefly weakened. Emerging into the Gulf of Mexico and back over warm waters, Katrina began to strengthen, ultimately gaining to Category 5 status on August 28th, while doubling in size. Katrina turned Northward, but prior to making landfall at Buras, Louisiana, decreased in intensity to a strong Category 3 hurricane. The hurricane continued Northward and made its final landfall near the mouth of the Pearl River at the Louisiana/Mississippi border. It weakened rapidly after moving inland over Southern and central Mississippi, but of course, not without causing the wind and storm surge damage that we are all familiar with in New Orleans and surrounding areas.

Despite the extensive property loss, loss of life, and disruption of on-going society functions in New Orleans for an extended period of time, the strongest sustained surface wind speeds measured by dropwindsondes on the morning of August 29th was about 99 knots, which corresponds to only 113 MPH. In fact, with the closest approach of the eye of the hurricane approximately 20 nautical miles East of downtown New Orleans, most of the city, as well as metropolitan areas East and North of the city experienced sustained surface winds of Category 1 and Category 2 strength. Meteorological work done for the specific site where Case Study Two is located revealed that sustained winds in this area ranged between 78 MPH and 94 MPH, which was ostensibly lower than the original design wind speed. Obviously, periodic gusts may have exceeded those figures, and the occurrence of microbursts, tornadic activity, or rogue straight-line winds could possibly have resulted in increased wind pressures experienced by the structure and cladding.

With the exception of the roll-up doors that blew in at the North elevation, damage sustained by the low production building was minimal, essentially consisting of one corner panel that came “unsnapped” at the male/female snap-lock feature, as well as the loss of a few exhaust fan housings. However, damage to the high bay building included complete loss of the metal wall panels across the entire upper portion of the West elevation and around the Northwest and Southwest upper corners of the North and South elevations. Many panels were completely removed, while other panels remained attached to the building at their fastened rib, with the snap-locked rib

having been displaced or "disengaged". This left the panels still attached to the girts, but flagging in the wind and dysfunctional. There were additional smaller areas of panel removal or displacement at other building corners. In addition, a large portion of the metal roof panels had been removed by the storm along the North eave near the West end of the building. A sheet metal appurtenance utilized as an eave closure between the roof panels and wall panels was missing along a significant portion of the North eave (wider than the roof loss area). Whether the loss of this eave closure allowed additional internal pressurization or if it simply promoted lifting and peeling of the roof panels, the roof panels were removed and peeled back across the remaining roof in this area. It was noted that the maximum wind speeds of Katrina were experienced at this property from the North as the eye of the hurricane passed North and East of the city. One large HVAC unit at this roof level, weighing almost 1,136 kg (2,500 lbs), was also blown over and displaced from its through-roof curb.

Based on the analysis and evaluation of these construction assemblies and the associated storm wind pressures by several different parties, there have been various theories put forth related to the causes for the damage incurred at this building. One theory holds that a particularly difficult-to-construct special detail that was designed for the corner areas of the wall panels may not have been consistently achieved during the original construction. Another theory notes that the original design was based on old code wind "technology", which when applied as an "Enclosed" building and utilized with the "one-third increase" for wind, resulted in a marginal design of the wall panels, roof panels, and associated fastenings and anchorages. Apparently no serious consideration was given during the original design to the potential openings that could be created by the roll-up doors and the internal pressurization that would inevitably be experienced. More significantly perhaps is the fact that laboratory testing of several different configurations of the wall assemblies revealed that the metal panel manufacturer had published "design tables" related to the wall panel load capacities that were apparently based on ultimate loads rather than allowable loads. This would essentially result in the utilization of these panels on numerous building across the United States where the wind capacity of the panels effectively exhibited no factor of safety. Assuming these structures are not located in hurricane prone areas where the "code" prescribed wind load is likely to be experienced, there would be no problem. However, if these buildings are subjected to hurricane force winds, the capacity of the standard wall panels may not be sufficient in many areas.

In our opinion, the most significant factor in regard to the wind loads applied to these combined buildings is the fact that failure of the overhead roll-up doors, which were later discovered to have an allowable load of about 13 PSF (20 PSF ultimate load), allowed instantaneous internal pressurization that, in conjunction with the negative wind pressures at certain locations (particularly corner areas) resulted in combined pressures that exceeded the capacity of the marginally designed original construction assemblies. In addition, our analysis revealed a secondary factor that could have significant effect on the wind loads "felt" by this structure. Since the 1995 revision of ASCE 7, the wind load guide has provided coefficients and adjustments to the basic

pressure formula using topographic effects, which allows a rudimentary model of the wind "speed up" that can occur in relation to two-dimensional escarpments and ridges. See Figures 6 and 7. Our evaluation of this effect on wind pressures for those buildings thus affected indicates the increase can range between ten and twenty percent of the normal Enclosed or Partially-Enclosed condition. In our opinion, the low-rise building located to the North side of the high bay building and extending out approximately 97.56 meters (320 feet), with its mean roof height of about 12.2 meters (40 feet), acted like a two-dimensional escarpment, which increased the wind loads even further as the building experienced internal pressurization from the breach of the roll-up doors. In addition, the placement of the building on this property, in conjunction with the direction of the maximum sustained winds during the storm, most likely resulted in a condition where the wind struck the building from a slight quartering position at two critical corners where damage was experienced. As the winds struck these corners and continued blowing across the low-rise building, separation vortexes would have caused additional turbulence and disturbance of the otherwise laminar flow. See Figure 8.

Case Study Three

The third case study involves the glass and aluminum curtain wall on a 30 year-old eight-story commercial office building located in Houston, Texas, which had incurred damage from Hurricane Ike in September 13, 2008. The existing steel framed structure with curtain wall cladding was originally constructed in 1978. The South elevation represents the front of the building. Exterior wall components are comprised of glass and aluminum storefront glazing systems. The First and Second floors are comprised of a five and three-quarter inch deep aluminum mullions with an exterior "snap-cap" glazing keeper, while the curtain walls at the Third through Eight floors are comprised of seven and one-quarter inch deep aluminum mullions with an all neoprene gasket with separate "lock strip" center strip. The roof system consists of a modified bitumen roof membrane installed over lightweight insulating concrete (LWIC) with a mechanically fastened base sheet over steel bar joists and beams. See Figure 9.

Hurricane Ike moved through the Southeast part of Texas on September 13, 2008, making landfall in Galveston, Texas as a Category 2 storm, moving Northwest at 15 mph, passing directly over Houston, Texas, with winds up to 110 mph causing significant damage to many areas of Southeast Texas, including Harris County.

During our site survey, WE observed a number of conditions that could be problematic as a result of wind damage to the exterior cladding system on the building. Observations that may be contributing factors would entail negative and positive wind pressures that may have had increased winds due to the geographic layout of the property resulting in broken vision lites, sheared bolts within the curtain wall system, displaced metal spandrel panels, and displaced coping at the roof edge, causing the modified bitumen roof membrane to lose the integrity of its securement to

the LWIC deck and peel back, all a result of hurricane force winds caused by Hurricane Ike.

At the roof, WE observed approximately one-third of the modified bitumen roof membrane was displaced, presumably a result of the displaced metal coping (approximately 30 linear feet) at the Northwest end of the building. This damage was most likely a direct result of hurricane force winds caused by Hurricane Ike, which in turn, could have been contributing factors to the failure of the exterior cladding system.

In addition to the limited visual survey of the damage to the roof of the building, WE also performed an exterior survey of the curtain wall system. The information pertaining to the damage outlined below is included in tabulated below.

On the exterior cladding system of this building, we observed a total of 42 broken and boarded vision lites. Most of the damage to the curtain wall system suffered by Hurricane Ike, appeared to be on the exterior corners of the building, excluding periodic broken vision lites on various floors. This would indicate where the greater impact of hurricane force winds, as well as the greatest and negative and positive pressures that were present during the passing of Hurricane Ike.

On the West elevation, we also observed a total of twelve vision lites that had been removed by the contractor in charge of remediation in order to provide access for ventilation and trash chutes.

During the investigation, we also observed approximately 510 square feet (110 linear feet) of ⅛" thick, anodized, aluminum spandrel panels that had been displaced as a result of hurricane force winds created by Hurricane Ike. On the East elevation of the building, there appeared to be several locations between the Third and Fourth floors that sustained some visible damage to the ⅛" aluminum panels.

The following table illustrates the missing and broken lites and missing spandrel panels observed at this project:

	North Elev.	East Elev.	South Elev.	West Elev.	Total
Boarded Lites:	8	5	18	7	38
Broken Lites:	2	1	1	-	4
Spandrels Missing (L.F.): -		25	60	25	110 L.F.
Spandrels Missing (S.F.): -		116	278	116	510 S.F.

Upon conclusion of the exterior investigation, we observed several areas of the curtain wall system on various floors of the interior of the building (where gypsum board had been removed for remediation) that were damaged by Hurricane Ike.

On the Third Floor of the East elevation at the Northeast corner of the curtain wall system, we observed five sill anchor bolts that had been sheared at the sill plate. It

was noted that loss of the sill anchors allowed outward displacement of approximately 345 square feet of the curtain wall system, including vision lites and spandrel panels. The plastic shims that help support the vertical load of the curtain wall system were found to be loose and, in some locations, broken. This condition allowed the shims to be displaced within the curtain wall system causing the sill anchor bolts to bear additional vertical load of the curtain wall system.

On the Fourth Floor of the East elevation at the Northeast corner of the curtain wall system, we observed similar conditions as described for the Third Floor. There were two sill anchor bolts that had been sheared at the sill plate by hurricane force winds and two sill anchor bolts that were bent. Conditions described above regarding the plastic shims also occurred at various locations along the interior of the curtain wall system of the Fourth Floor. The shims were missing and broken and in some areas, had fallen down into the curtain wall system, seemingly as a result of the displacements of Hurricane Ike.

Based on our observations, it appeared that the outward displacement of the East elevation curtain wall at the Third and Fourth floors may have been a result of interior pressurization caused by the breach of the First and Second floor curtain wall at the West end of the building. Based on the wind design research, this type of curtain wall breach causes the building envelope to transition from "Enclosed" to "Partially Enclosed" and will typically cause an increase in design wind pressures applicable to the building exterior of fifteen percent (15%) to twenty five percent (25%). In our opinion this phenomenon could be responsible for the damage observed at the East end of the building.

Conclusions

It should be pointed out that past codes often did not include provisions for internal pressurization, and when included, were not as clear on when to apply the internal pressurization rules. Today's codes not only include this information with very specific formulas and criteria, but also include factors and coefficients for topographic effects, shape effects, etc.

Many designs in the past were developed based on Enclosed modeling. It has been our experience that some of these designs have led to failures when the margin of redundancy within the structural or cladding design was too small, or else when performance capacities of the cladding systems were overestimated or over stated by the manufacturer.

Certain provisions within the current codes provide better direction and guidance regarding when to apply the rules for internal pressurization, and in some cases, dictate their use when certain building configurations, building heights, construction materials, and geographic locations are involved.

It is incumbent on all designers to properly evaluate and apply the appropriate factors for interior coefficients when determining design wind pressures in order to more

fully realize the potential effect of internal pressurization on the roofing and cladding systems of constructed projects.

As may be ascertained from the case studies provided within this paper, damage to the cladding systems may occur in close proximity to where the breach in the exterior cladding occurs, or it may occur at an extreme distance from the breach. We have investigated buildings where the cladding failure due to internal pressurization has occurred many meters (several hundred feet) away from the location of the initiating breach that caused the internal pressurization. In many of these cases, the outward breach due to internal pressurization has occurred at an extreme location, a so-called "end of the line" location within the building enclosure. This phenomenon has not been extensively discussed in the literature that we have reviewed and may need to be formally studied in order to fully understand its impact.

Water and Moisture Management with Sustainable Building Products

Stephen M. Lattanzio, PE[1], Roger G. Morse, AIA[2]

[1] Morse Zehnter Associates, 165 Jordan Rd, Troy, NY 12180, PH (518) 283-7671, FAX (518) 283-9855, slattanzio@mzaconsulting.com, [2] Morse Zehnter Associates, 165 Jordan Rd, Troy, NY 12180, PH (518) 283-7671, FAX (518) 283-9855, rgmorse @mzaconsulting.com

Abstract

As the use of more sustainable building products is incorporated in the designs for both new construction and as well as building renovation, proper water/moisture management becomes a critical design consideration. Likewise, the understanding of moisture dynamics in and through the building envelope has become more important for the forensic engineer. Sustainable products generally do not have the same capacity to store moisture as traditional construction materials such as brick, block and concrete. Sustainable products also contain more organic matter, which make them more susceptible to mold growth. This paper will explore the various pathways of moisture intrusion; discuss strategies to investigate buildings to determine sources of moisture intrusion; and, provide calculation methodologies for predicting moisture intrusion. The paper will also describe the effects of leaking, condensation, and water vapor for their respective contributions to water damage and provide practical solutions to minimize the moisture damage to building materials.

Keywords: Sustainable Building Products, green design, moisture, moisture intrusion, building envelope, condensation, water vapor, infiltration.

There are three principle methods of moisture intrusion into buildings. These are liquid water intrusion, vapor diffusion and air infiltration. Liquid water enters a building through broken windows and cracks, deteriorated finishes and improperly designed weather barriers. An air pressure imbalance between interior and exterior spaces causes air infiltration. This air pressure imbalance is normally relatively low, but carries a large amount of water vapor along with the infiltrating air. Diffusion of water vapor through building envelope elements results from differences in vapor pressure arising caused by variance in the concentration of moisture in air inside and outside the facility. Moisture transfer through the building envelope is inevitable, but does not need to result in problems. It is only when moisture transfer is impeded in some way resulting in collection of moisture within an assembly, or when condensation occurs, that problems arise. Design and construction to control moisture transport through building envelopes is the key. In the past, this was easy, but present day, high performance construction has considerably upped the ante for moisture control.

In past eras, buildings were simple assemblies of inorganic materials with great mass and not much insulation. This resulted in a paucity of food for microbiological growth, great capacity for harmlessly storing moisture, and little thermodynamic

drive. Moisture control in these assemblies was so easy that nobody had to think about it and buildings were inherently moisture tolerant. All this changed through an evolutionary process over the past 100 years or so, as society increasingly demanded higher thermal performance and economy in material use and construction cost. Simply, society no longer tolerates wasteful building practices or thermal discomfort. Driven by societal demands, basic building construction has evolved from the technologically simple structures of the past into the sophisticated, high performance, technologically advanced buildings of today as shown in Figure 1. Recent trends toward sustainable design seek to maintain high quality indoor environments, but do so in a way that does not require more resources to build than can be recaptured by recycling at the end of the building's life cycle. This difficult, or even impossible, goal requires both the use of recycled and recyclable materials as well as diligent stewardship of new materials. Such materials are more fragile than those used in the past and must be used carefully to avoid damage, primarily from moisture. Sustainable design also seeks to minimize the energy required to operate the building, resulting in building envelopes that are, among other things, highly insulated.

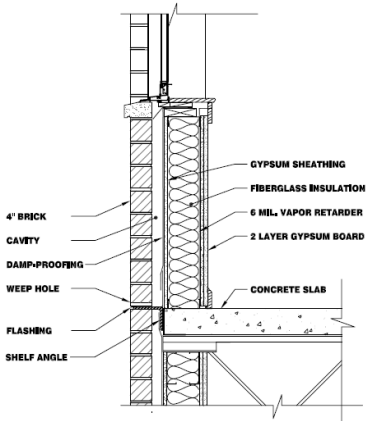

Figure 1 Typical Sustainable Construction

Demand for energy efficiency and thermal comfort increased levels of insulation in building envelopes. Insulating an envelope assembly increases the temperature gradient acting across it. For example, in the winter, the interior surface of an insulated assembly will be warmer and the exterior colder than in a less insulated assembly. This increased temperature difference results in a set of building conditions that that did not exist in the structures of old, but must be considered during design and construction of high performance sustainable buildings. Water vapor is driven into and through assemblies by the thermal gradient, creating what are called hygrothermal loads. Increased temperature differences result in thermal stresses on materials and increased problems from differential expansion. Air pressure from wind or other natural forces pushes air and moisture into, or pulls it out

of assemblies. These factors have turned the successful design of the building envelope into an exercise requiring not only knowledge of issues such as water penetration, structural loading and fire ratings, but also expertise in the application of sophisticated calculation methods to deal with the new set of issues involving control of moisture in envelope assemblies.

Liquid Water Intrusion

Water enters a wall through gaps or spaces in bonds of materials or leaks. It also enters through capillary action or the wetting and saturation of materials. Water generally flows down hill, but it also wicks upward through capillary action. Wind blown rain flows up, down and sideways.

In general, the two types of wall construction are 1) Drainage System or 2) Barrier System. The drainage system stops most water at the surface and has a drainage cavity that allows the drainage of water to the outside. A barrier system is a single massive wall of concrete or solid masonry with the surfaced sealed. Metal or glass walls are also examples of barrier systems.

There are some basic principles of construction concerning liquid water entry. Caulk will always fail, whether it is latex or silicone based. Relying solely on a caulk joint against liquid water intrusion is not enough, there needs to be a second line of defense. Additionally, periodic inspection and maintenance is necessary to verify that caulked joints are still functioning properly.

Flashing details are paramount to preventing water intrusion. It is important not to specify the type and design of flashing for the bulk of the building and leave the remaining details to the contractor. In this case, 90 % right is 100% wrong. Specify the corners, ends and transitions of the weatherproofing detail so that the building envelop will act as a system rather that independent parts with gaps between them. Finally, weep holes and drainage paths must be kept clear so they drain properly.

Air Infiltration

Compared to vapor intrusion, the potential amount of moisture introduced into an envelope assembly, or removed from it, by air infiltration is several orders of magnitude greater than that from vapor diffusion. Figure 2 illustrates the difference in moisture introduced through a one inch square from air infiltration and vapor diffusion.

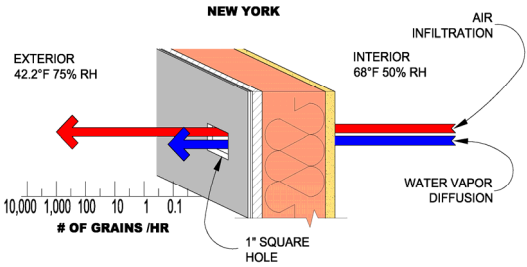

Figure 2 - Relative Moisture Intrusion

Air is driven into and through envelope assemblies by air pressure differentials. Air moves from an area of high pressure to a lower pressure. The major driving forces creating pressure differentials are 1) Wind Pressure, 2) Stack Effect and 3) Mechanical Ventilation.

The kinetic energy of moving air molecules in a wind translate into a high pressure zone when the wind piles up on the windward side of a building. This high pressure drives air molecules through the slightest imperfection, hole, crack or loose seal into and through the envelope assembly. Wind rushes past the sides of the building creating a negative pressure zone due to Bernoulli effect and then eddies on the lee side create another negative pressure. This all results in wind pressure higher on the windward side of the building than the pressure inside the building driving air into the building, and air pressure lower on the leeward side of the building than inside the building that is sucking air out of the building. Air infiltration enters the building and air exfiltration exits the building. Wind speed near the ground is slowed by friction with the ground and obstacles near the ground so that wind speeds and the resulting air pressure differentials become higher with increased elevation. This is illustrated in Figure 3. In high-rise buildings, this can result in a vertical airflow in the building. The methods of calculating the air pressure created by wind are in the ASHRAE Handbook (ASHRAE, 2009).

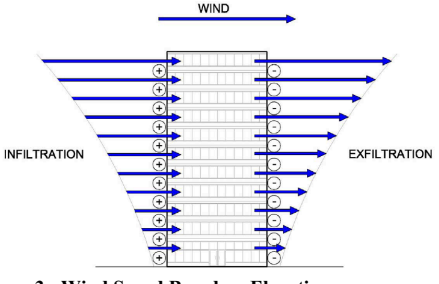

Figure 3 - Wind Speed Based on Elevation

Warm air rises as is evidenced by hot air balloons. Buoyancy of warm air causes air to rise through a heated building in a cold climate. This airflow resembles that of

smoke in a smoke stack and as such is referred to as “stack effect.” Airflow from the stack effect can be appreciable and can be calculated using methods and equations in the ASHRAE Handbook (ASHRAE, 2009). Stack effect depends upon temperatures and height of the building and is greater on cold days and in tall buildings. However, even a three-story building can exhibit airflow from stack effect. When the air rises in the building, it creates a negative pressure that sucks air into the building through the outside walls. Air collects in the top of the building creating a positive pressure that drives air through the walls and roof out of the building. The magnitude of the pressure differential, and hence air movement, will be greater as the distance from the pressure center of the building increases. This is illustrated in Figure 4.

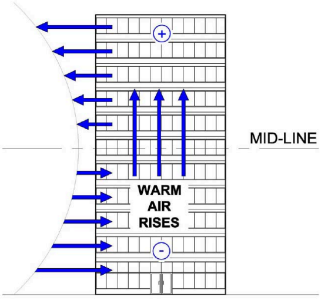

Figure 4 Stack Effect in Cold Climates

Figure 5 shows the reverse stack effect that occurs in air-conditioned buildings in warm climates. In this case, air enters through the upper floors, goes down the shafts and out the lower floors. The point of transition is the neutral plane. As with wind pressure calculations, ASHRAE has a methodology to calculate the stack effect pressures and flows (ASHRAE, 2009).

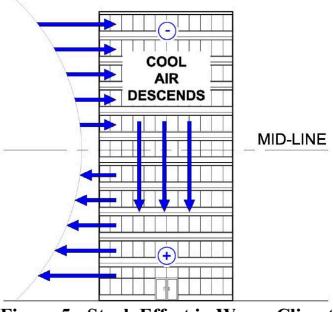

Figure 5 - Stack Effect in Warm Climates

Mechanical Ventilation

Exhaust fans pull air out of the building causing the air pressure inside of the building to become negative relative to the outside. In commercial buildings this is counteracted by ventilation air. Good practice in hot humid climates is to minimize infiltration by providing about 10% more ventilation than exhaust resulting in a slight positive pressure (USDOE, 2000). Typically, this will result in a

positive pressure on the order of 0.02 inches of water static pressure. Such a slight pressure is easily overcome by pressures from wind and stack effect. As such, the goal is to have the building, on average, operate at a slight positive pressure relative to outdoors. At any given time, if a wind is blowing, the windward side of the building exterior will be positive relative to inside, and the lee side will be negative. The air pressure differentials affecting a building are measured in fractions of an inch of water. Of this, the partial pressure of water vapor in the indoor atmosphere will only be hundredths of an inch of water. On the other hand, temperature and humidity driven vapor pressure differentials affecting buildings are measured in inches of mercury. For this reason, it is not practical to pressurize a building to a level that will overcome diffusion of water vapor through the building envelope into the building.

Air infiltration not only brings unwanted moisture into the building, which can change the dynamics of the conditioned air into the building, it can also increase the exhaust rate resulting in higher energy consumption. Allowing humid air across the building envelop, apart from the air make up and exhaust grills, means that moisture can effect unforgiving building materials. This may result in mold and bacteria proliferation. The only way to stop air infiltration is to provide air barriers that stop the passage of air and these must be tight and continuous. Figure 6 below shows some of the pathways that air enters a building

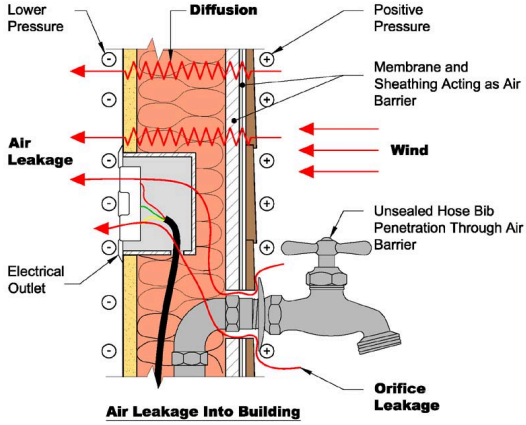

Figure 6 - Air Infiltration Pathways

Vapor Diffusion

The amount of moisture entering a building through vapor diffusion is dependent on the construction of the wall cavity and the relative humidity ratio between the inside and outside walls. Figure 7 illustrates the effect of humidity on the vapor diffusion rate.

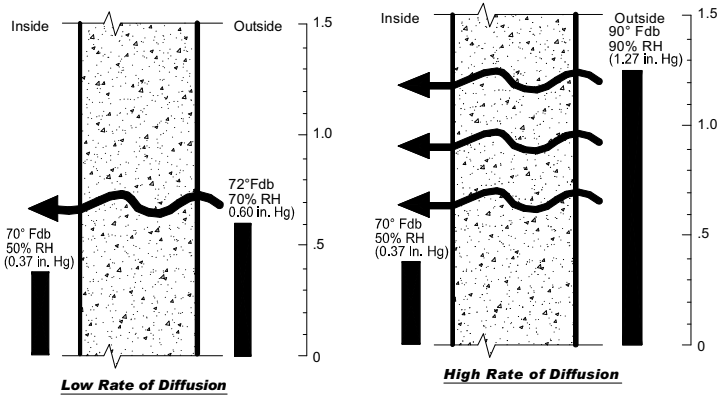

Figure 7 Comparison of Diffusion Rates

Humidity in the air is water as a gas. It is not an aerosol with small droplets of water suspended in the air. An aerosol of small water droplets is a fog and is visible. Water vapor is a gas and, along with oxygen and nitrogen, is part of the mixture of gases that make up the atmosphere. The difference between water vapor and the other gases in the atmosphere is that either it can exist as a gas or a liquid at the temperatures ordinarily found in the atmospheres or occupied buildings and in HVAC equipment. As water stays in a gaseous state due to kinetic energy, the warmer an atmosphere, the more water can remain as a gas. As the atmosphere cools water is less able to remain as a gas. Eventually it will reach saturation (100% relative humidity) and will then condense out on a surface, or small droplets will condense out of the air causing fog. Problems arise when the relative humidity inside a building envelope assembly is high enough to support corrosion or microbiological growth, or even worse, condensation occurs inside the envelope assembly.

Temperature in an insulated building assembly will decline with passage from the warm to the cold side. If the temperature falls below the dew point of the water vapor in the atmosphere, condensation will occur. This can cause liquid water to collect in the envelope component where it causes deterioration of the materials and can support microbiological growth and insect infestation.

Water vapor is a small enough molecule that it can pass through most materials. The ability of water vapor to pass through a material is referred to as the permeability of the material and is measured in terms of permeance, or perms. Perm ratings for materials range from zero for materials such as high performance glass or a metal sheet to 1000 for air spaces. If a material is relatively resistant to diffusion to water vapor it is referred to as a vapor retarder. To a greater or lesser degree all normal building materials will retard the passage of water vapor, but those with a perm rating between 1 and 10 are typically regarded as vapor retarders because they slow passage of water vapor sufficiently to require attention during design and construction of

assemblies. A material with a perm rating of 1 or less is commonly referred to as a vapor barrier because it dramatically slows the passage of water vapor sufficiently to virtually stop it. If a vapor barrier is included in an envelope, it is critical to the success of the assembly that it be properly located. Typically, a vapor retarder will be located on the warm side of the insulated portion of an assembly to prevent the passage of significant quantities of water vapor into the assembly (Morse, 2005). In this instance, there will be no vapor retarder between the insulated cavity and the cool side of the assembly. As the vapor drive is from the warm side toward the cool side, this allows any moisture that gets into the insulated cavity to pass out of the assembly into the atmosphere on the cool side. Typically, this arrangement results in a dry assembly. In locations with only a heating season the vapor retarder should be located in the inside, in areas with only a cooling load the vapor retarder should be located on the outside. The problem is that most areas have both a heating and cooling season, so with a vapor retarder in the assembly, it will inevitably be in the wrong place part of the time. The structures of old had sufficient moisture storage capacity, and gaps in construction, that periodically misplaced vapor retarders generally did not cause a problem as long as the vapor retarder was located on the side that was predominately warmer. The high levels of insulation, tighter construction and more moisture sensitive materials used in current high performance construction have changed this and moisture collection due to misplaced vapor retarders are increasingly causing problems.

Case Studies

Examples of moisture problems observed in the field illustrate the way that each of the moisture transport mechanism affects a building.

Case study 1: Liquid Water Intrusion

There were historic issues with water intrusion in a field operations center with a stucco exterior. The facility team adopted periodic maintenance treating walls using a waterproofing scheme of frequent painting and sealant (caulking) to face seal the walls and attempt to repel water from gaps, open mitering in corners of expansion joints and windows. Wet sealing of glazing stops on windows and plugging of weep holes on sill receptors provided limited relief.

The elevated moisture condition reported was from direct leaking into wall surfaces from rainwater sheeting down the face of the wall and windows with subsequent bridging to the interior base on the building envelope and mechanical issues noted. Wall leaks to the interior were strongly related to direct wetting and water penetration through cracks in the stucco face, from poorly detailed control joints as well as a missing or improperly installed drainage plane behind the stucco. Windows were a second major source of water entry from settling in the sill receptors and subsequent entry into walls.

The use of additional caulk to block off weep holes in window sills and to repair damaged control joints suggest that water may actually become entrapped and may increase the amount of bulk liquid against the surface of the wall rather than freely draining it. Such is the case of the windows on the east elevation of the Conference Room. Water apparently got into the sill through the gasket between the glazing and frame and through cracks in the jambs on both sides. This water ran to the low point, settling in the receptor and then made its way through joints in the frame, screw holes and the end dams. Water is supposed to run out the weep holes.

Additionally, the block and mortar faces are imperfectly sealed. This allowed water to leak through, especially at the network of control joints, which are not freely draining. The water entered the wall cavity, allowed the moisture penetration through the wall where it ultimately exited the cavity to the interior of the building wetting the inside finish materials. In addition, the use of a scrim face vapor retarder in between steel furring strips allowed for a relatively free passage of water and water vapor from the exterior to the interior of the building. Condensation was also occurring in the wall cavity of the conference room leading to corrosion of metal and adding to finish deterioration.

Case study 2: Vapor Intrusion

Floors in the great rooms of cottages have oak flooring installed over concrete ground supported slabs. This type of construction is common in new construction and normally presents no problems. However, within the first year of occupancy the floors in the cottages cupped, and in one instance, buckled. This happens when the backside of the wood flooring absorbs moisture, warping the oak boards. Water is mixed with concrete during construction, and water can be added by the weather. This moisture is enough to cause damage to wood flooring.

Investigation found that excessive moisture in the slab assembly was causing the cupping, and that moisture levels beneath the floor were high enough that it could lead to even further deterioration of the flooring. There are several factors that contributed to this problem:

- As designed, the floor included a layer of sand under the slab and on top of the vapor retarder. Design with a “sand layer” under a slab-on-ground above a vapor retarder is contrary to current good architectural practice.
- Exposure of the slabs to the weather allowed them to collect moisture. Moisture that collects in the sand/gravel layer under the slab is particularly difficult to dry out.

Case study 3: Air Infiltration

In a Midwestern dormitory, mold was found on drywall, windowsills and the window apron on the exterior wall in various locations in the summer of 2006. Observation of the pattern of mold growth shown in the videotaped inspections found that the pattern

of the growth was indicative of moisture resulting from condensation from infiltrating humid outside air. Evaluation of the building, weather data and operation found that this mold amplification resulted from a combination of factors. The exterior walls of the building permitted a relatively high level of infiltration, so that moisture-laden air could easily penetrate into the walls and reach the affected surfaces.

The building as a whole was operating at an air pressure that was negative relative to outdoors. In addition, exhaust fans in each dormitory unit exhausted more air than was replaced by the makeup air units in the hallway, resulting in a negative air pressure in the dormitory units. This increased the rate at which humid air infiltrated through the outside walls. Cooling the building to an unusually low temperature increased the risk of condensation on surfaces. The chilled air from the fan coil units in each dormitory unit blowing on the outside walls exacerbated this condition by chilling the walls below the room temperatures.

Discussion

Moisture intrusion into buildings is more important now than it ever was. Building envelop components not only do not have the water storage capacity that they once had, water has a more devastating effect on modern wall components and interior finishes. Designing modern buildings requires a complete engineered solution to prevent moisture intrusion. All of the detailed interfaces must be designed as a system rather than individual components. Hygrothermal modeling and air infiltration modeling programs can help predict the vapor diffusion and air infiltration (ASHRAE, 2009; WUFI).

References

ASHRAE. 2009. ASHRAE Handbook of Fundamentals. American Society of Heating, Refrigerating and Air Conditioning Engineers, Inc. Atlanta, GA.

USDOE Building America Builders Guide, 2000

Morse, R.G. and National Institute of Building Sciences. 2005. *Building Envelope Guide, Indoor Air Quality and Mold Prevention of the Building Envelope* in the National Institute of Building Sciences (NIBS) Whole Building Design Guide.

WUFI (Wärme und Feuchte Instationär) Version 4.1, and WUFI 2D, WUFI Plus, WUFI Mold. Fraunhofer Institute and Oak Ridge National Laboratory.

Stone Veneer Wall Failure: A Small Earthquake Reveals a Large Problem

T.N. Stubblefield[1] and C.L. Searls[2]

[1] Simpson Gumpertz & Heger, The Landmark @ One Market Street, Suite 600, San Francisco, CA, 94105; PH (415) 495-3700; FAX (415) 495-3550; email: tnstubblefield@sgh.com

[2] Simpson Gumpertz & Heger, The Landmark @ One Market Street, Suite 600, San Francisco, CA, 94105; PH (415) 495-3700; FAX (415) 495-3550; email: clsearls@sgh.com

Abstract

During a recent northern California earthquake of magnitude 4.4, a newly-built hilltop home experienced no structural damage, but some unexpected nonstructural damage. The golden sandstone veneer covering the top portion of an exterior wall dislodged and fell to the ground.

The owner hired a consulting engineer to investigate why the damage occurred and how to repair the wall. Given the extent of the stone veneer throughout the house – cladding both exterior and interior walls; in the bedrooms, living room, and kitchen – it became important for the engineer to also determine the extent of the problem throughout the house.

The cause of the failure was the contractor's omission of steel wires and dovetail anchors, and the poor bond between the stone and mortar. Repair recommendations consisted of providing supplemental out-of-plane anchorage for the stone veneer.

Introduction

During a recent small earthquake in northern California, a newly-built hilltop home experienced no structural damage, but the golden sandstone veneer covering the top portion of an exterior wall dislodged and fell to the ground.

The 3-inch thick stone veneer is anchored to fully-grouted concrete masonry unit shear walls using a system of steel dovetail anchors and steel wires running through the mortar joints. The integrity of the anchorage system depends on the bond between mortar and stone, and the distribution of anchors and wires throughout the system.

This paper describes the process by which the engineers conducted the forensic investigation. The paper discusses the cause of the failure, the test methods used to determine the extent of the problem throughout the house, the surprises revealed by the test results, and the repair recommendations the engineers developed for the owner.

This project, which began as an investigation of a small area of failed stone veneer under low earthquake loads, led to the discovery of widespread problems with the veneer construction throughout the house. The project required development of a unique laboratory test method to compare in-situ and new mortar performance. A simple diagnostic check of a stone sample led to a shift in focus, and resulted in surprising information about the stone itself.

The Earthquake and its Effects

According to the United States Geological Survey (USGS) website, an earthquake of Richter magnitude 4.4 occurred on August 2, 2006 in Petaluma, California. Based on records of nearby instruments, shaking at the site of the house was at most approximately 0.10g, or 10% of gravitational acceleration (32.2 ft/sec^2).

According to the owner, more than a dozen stones fell from the top corner of one exterior wall during this earthquake. The cap stones and some of the veneer stones at this wall and at an adjacent, parallel wall shifted laterally, but did not fall. The owner hired an engineering firm to investigate the cause of the damage, the adequacy of the anchorage system design, and how to repair the system, if required.

Stone Veneer Observations

The home features a golden-colored stone veneer throughout most of the exterior and interior walls. Stones of varying sizes are arranged in a split coursed rubble pattern, with discontinuous vertical joints and predominantly continuous horizontal joints (Photo 1). The stone is nominally 3 in. thick, and installed with its bedding plane parallel to the wall face, displaying the stone's naturally rough surface. Top, bottom, side, and back faces of the stone are smooth cut (sawn) surfaces. A nominal 2-inch wide cavity separates the veneer from the backup wall, a fully-grouted concrete masonry unit (CMU) shear wall. The veneer is anchored by steel dovetail clips installed in the mortar bed joints and connected to vertical steel channels bolted to the backup wall. Horizontal "pencil rods" (9 gauge steel wire) run through the bed joints and interconnect the steel anchors (Photo 2).

The engineers' initial site visit after the earthquake confirmed the owner's report: at the top corner of a 20-ft tall exterior wall, several stones had fallen out, exposing the CMU backup wall and vertical steel channels (Photo 1). Several remaining stone courses had shifted away from the wall, and mortar beds had shifted relative to the stones. No steel anchor clips remained attached to the vertical channels bolted to the CMU backup wall. The fallen debris on the ground below consisted of intact stones

and mortar beds that had separated from stones. No steel anchor clips or pencil rods were found in the debris, and no imprints of steel anchor clips or pencil rods appeared within the mortar beds. A close look at the failed wall area showed no evidence of any fallen steel anchor clips or pencil rods into the cavity between the veneer and CMU backup.

Initial Investigation Plan

The initial investigation plan included review of original construction documents, evaluation of the anchorage system design, a site visit with limited ground penetrating radar (GPR) testing to identify locations of anchorage components within the walls, determination of the as-built veneer conformance to the design and building code, in-situ bond strength testing, mortar analysis, and a report.

Information from Construction Documents

The original architectural drawings called for vertical steel channels at 16 in. on center, bolted to the CMU backup wall. Steel dovetail anchor clips are shown in the mortar beds and called out at 16 in. on center vertically. Horizontal pencil rods are placed at 16 in. on center in the mortar joints, interconnecting the steel anchor clips. The pencil rods are shown bent at discontinuities in horizontal joints due to differing stone heights.

The original structural drawings indicate that the design-level earthquake shaking for the site is 0.33g, or 33% of gravitational acceleration (32.2 ft/sec^2).

No stone veneer or mortar specifications were prepared for the project. The project architect indicated the stone is “Wyoming Valley Gold”, a sandstone quarried in Oklahoma. No daily reports, inspection reports, or other written records were available from the construction period.

Building Code Requirements

The applicable code for the project was the 2001 California Building Code (CBC) (CBSC, 2001), based on the 1997 Uniform Building Code (UBC) (ICBO, 1997). The code contains prescriptive requirements for anchored veneer (Chapter 14) and mortar mixes (Chapter 21).

Anchored veneer and its attachments are required to be designed to resist a horizontal force equal to at least twice the weight of the veneer. Wall ties shall be spaced so as to support not more than 2 sq ft of wall area but shall not be more than 24 in. on center horizontally. In Seismic Zones 3 and 4, wall ties shall have a lip or hook on the extended leg that will engage or enclose a horizontal joint reinforcement wire. The joint reinforcement shall be continuous with butt splices between ties permitted.

When the proportion of mortar ingredients is not specified for a project, the proportions must comply with Table 21-A. The table requires a cement-lime mortar

of type M, S, N, or O to have 1 part cementitious materials (cement plus lime) to 2-1/4 - 3 parts sand.

Laboratory Analysis of Mortar and Stone

A laboratory performed petrographic and chemical analyses on three samples of mortar: two from exterior walls, and one from an interior wall. The mortar is composed of Type I/II Portland cement, hydrated lime, and sand. Our findings are show in Table 1.

Table 1: Mortar Analysis Results

Mortar Sample	Cement	Lime	Sand	Cementitious Material to Sand Ratio
Interior	1	½	2 ½	1 : 1.67
Exterior	1	4 ½ -5	4-4 ½	1 : 0.66–0.82
Code (Table 21-A)	--	--	--	1 : 2 ¼ –3

The laboratory identified the stone as a ferruginous and argillaceous sandstone, regionally metamorphosed into a quartzite, with few pore spaces.

In-Plane Shear Testing for Mortar Bond Strength

A testing agency performed in situ in-plane shear testing of individual stones to check the mortar bond strength. This type of testing is common in brick construction, and is commonly used to establish the shear strengths of existing unreinforced masonry walls. The tests consisted of removing one stone to insert a jack, which pushes laterally on an adjacent stone. The mortar joint at the opposite side of the adjacent stone was cut to allow the stone to shift slightly within the plane of the wall.

Several codes were consulted to determine a minimum acceptable mortar shear bond strength. The 1997 Uniform Code for Building Conservation (UCBC) (ICBO, 1997) provided a reasonable lower-bound shear strength limit (intended for use on existing unreinforced masonry construction) of 30 psi (ultimate strength level). The gravity load stress of the masonry above the tested area must be subtracted from the tested shear strength value and compared to this limit.

Two locations at exterior walls and three locations at interior walls were tested. Mortar bond strengths ranged from 20-30 psi at exterior walls, and 60-80 psi at interior walls.

Initial Conclusions and Repair Recommendations

The engineers concluded that the anchorage system as designed meets the code, and the design is more stringent than the code. The anchorage system presumes adequate mortar bond strength to function properly.

The actual earthquake ground shaking at the site was approximately 1/3 of the design-level earthquake forces. The veneer, if all anchorage elements (anchor clips, channels, pencil rods, and mortar) were properly installed, should not have failed at this level of shaking.

The earthquake-damaged wall area of fallen stone lacked anchor clips and pencil rods and had poor mortar bond. There was no evidence that anchor clips were installed at the location of failure. Most of the stones on the ground had separated from their mortar beds, and the stone courses remaining near the areas of failure had shifted relative to their mortar beds.

The initial GPR testing revealed that some wall areas have channels spaced wider than 24 in. on center, and many anchor clips support more than 2 sq ft of wall. The installation did not comply with the code.

The mortar was not specified for the project and was therefore required to comply with the code. The samples tested do not comply with the code; the mix proportions differ significantly from the code requirements, and vary widely between the samples tested. The low proportion of aggregate can cause high shrinkage of the mortar, which affects the quality of the bond to the stone.

The initial repair recommendation consisted of removal of stones at full-height exterior walls starting from the top, and continuing removal until code-compliant anchor clips, pencil rod spacings, and well-bonded mortar are found. Stones could be numbered, saved, and reinstalled in the same locations.

If the stone veneer system would be reinstalled as originally designed, the engineers recommended laboratory mock-up testing of the mortar-to-stone bond prior to reinstallation. The engineers also recommended full-time inspection of stone reinstallation to ensure proper mortar mixing and placement of anchorage components. Alternatively, the stone could be reinstalled and anchored directly to the CMU backup by cutting kerfs in the tops of the stones, and providing bent anchor clips to connect the stone to the existing channels.

Due to the extent of stone veneer throughout the house's exterior and interior walls, and the areas missing anchors found during preliminary testing, the engineers recommended GPR testing of all walls prior to commencing repairs.

Laboratory Mortar Bond Testing

Because the in-plane shear test was used successfully on the building with a clear acceptance criteria, and because there was no standardized laboratory test equivalent to the field test, a new laboratory test was designed to mimic the field test for

evaluating alternate mortar mixes. This way, the performance of the mortar on the building could be directly compared to the performance of the mortar in the lab.

A skilled mason prepared three different code-compliant mortars designed by the engineers. Half the stone samples were used as-is with the smooth saw-cut surface, and half were sandblasted on the bed joint faces to produce a physical key for the mortar and increase the surface area to enhance mortar absorption and bond strength. The mason assembled test specimens consisting of a stack of 3 stone cubes (3 in. wide by 3 in. tall by 3 in. thick, matching the nominal thickness of the in-situ stone), with the middle stone offset. After moist curing for 28 days, the assembly was positioned on its side and placed in an MTS testing machine. The load cell pushed the top of the offset middle stone, causing the mortar joints to fail in shear as the stone slid past its neighbors. Confinement blocks were provided on either side of the specimen to maintain alignment and prevent other failure modes.

The shear bond strength was calculated as the failure load divided by the total mortar bed area, consistent with the UCBC (ICBO, 1997) method, which subtracts the gravity load contribution (of masonry in the wall above the test specimen) from the field test failure load.

The testing showed very low mortar bond shear strength in nearly all specimens (most less than 20 psi). Some specimens that did not receive sandblasting fell apart under their own weight during placement in the testing machine.

Questions About the Stone

The engineers now needed to understand why the mortar did not bond to the stone.

A colleague recently retired from a career as a masonry contractor stopped by to look at the stone samples after learning about the project and test results. He licked his thumb and pressed it to the stone surface. When the moisture did not disappear after several minutes, he suggested that the stone had a low suction, and could have difficulty absorbing water. If the masons pre-wet the stone during construction, the water could have filled the few available pore spaces, precluding a good mortar bond. (During construction, the stones were wet-cut immediately prior to placement, and were effectively pre-wetted during mortar application. The mason who prepared the lab test specimens also pre-wetted the stone surface prior to applying mortar, in accordance with standard masonry practice.)

Prior to this point, the engineers' focus had been on the mortar mix and anchorage system; now, the focus shifted to understanding the stone properties. The stone was tested for absorption and initial rate of absorption (IRA, also known as suction). The absorption was low (0.79%, per ASTM C 97 [ASTM International, 2002]; the normal range for sandstone is 1-20%), as was the initial rate of absorption (0.9 g/min/30in^2, per ASTM C 67 [ASTM International, 2005]).

The low absorption and initial rate of absorption values indicate that the ability of this stone to bond to any mortar is very low. Mortars generally bond best to masonry units having IRA values between 5-25 g/min/30in^2.

A myriad of factors affect the quality of bond between mortar and masonry; many of these factors are difficult to quantify, and it was not possible to fully investigate these factors during this investigation. These factors include: the mortar mix ingredients and proportions, physical properties of the masonry material, masonry surface preparation, curing methods and duration, and weather conditions during construction.

Research on similar applications of this stone yielded little information. The stone supplier's website showed the Wyoming Valley Gold stone used in rough rubble form in mass masonry walls or low retaining walls. No applications similar to the one at the project site were shown.

The stone assembly testing, physical properties, and research revealed peculiarities of the stone that brought into question its appropriateness for use in a wall veneer application with anchors in the mortar joints, rather than in the stone units.

Additional In-Plane Shear Testing of Mortar Bond Strength

Because the initial testing program consisted of only five locations, and given the poor mortar bond observed in the laboratory even with code-compliant mortar, the engineers decided to perform additional testing of the in situ mortar bond shear strength at interior and exterior walls.

A testing agency tested 13 interior and 22 exterior locations selected by the engineers. The results showed that the bond strength at 3 of 13 interior locations (23%), and most of the exterior locations, was less than 30 psi.

GPR Testing of All Stone Veneer

A testing agency used GPR to scan all interior and exterior stone veneer walls of the house to determine the existing anchorage layout. Several inspection openings were made to verify the test results. The test results showed that approximately 50% of the wall areas lacked code-compliant anchorage of the stone veneer. The problem areas were widely distributed throughout the walls: interior and exterior, high and low, and in irregular patterns.

This result was unexpected, disturbing, and required a change in approach to the repairs.

Revised Repair Recommendations

The engineers and owner were now faced two significant problems: the widespread lack of code-compliant anchorage, and the problematic in-situ and lab-tested mortar bond strengths. The initial repair approach would no longer work. The engineers

revised the repair strategy to anchor the stone veneer directly to the backup wall in problematic areas. This method would eliminate the reliance of the anchorage system on a good mortar bond. However, securing each stone with kerf anchors (as recommended in initial investigation report) would require disassembing the entire wall, cutting kerfs in the stone (which might not work due to the bedding plane orientation parallel to the wall face; the stone may cleave), and rebuilding the walls.

The engineers selected two alternate anchor types, specifically designed for in-situ repair of masonry veneer walls with cavities, to test on the house. The anchor manufacturer tested the selected anchors: a helical anchor and a dual expansion anchor (with one end embedded in the veneer, and the other end embedded in the backup wall). The proof load for each anchor was the code-based prescriptive design load multiplied by a factor of two.

The helical anchors developed very little load. The dual expansion anchors, however, developed the full proof load. The engineers prepared construction drawings and specifications for repairs to the stone veneer walls utilizing the dual expansion anchors. The repairs have not yet commenced.

Conclusions

An important lesson from this investigation is that a small earthquake revealed a large problem in the stone veneer walls' construction: widespread missing anchors and poor mortar bond, which could have been devastating in a larger earthquake. Although the failure was unfortunate, the damage was limited, and there were no injuries or other property damage. The damage caused by this relatively small earthquake was a warning signal to the engineer and the homeowners that a serious problem existed with the stone veneer system. This small earthquake provided an opportunity to address and correct the problem in advance of a larger seismic event. The owner now has the opportunity to correct the problem before the next, potentially larger, earthquake.

The project required development of a new laboratory test to compare the performance of in-situ mortar and repair mortar. The unexpected test results, combined with a simple diagnostic check of the stone suction, shifted the focus to the stone itself. Subsequent testing revealed surprising information: the unique stone chosen for the veneer may not have been appropriate for its application. The repair strategy changed dramatically as a result.

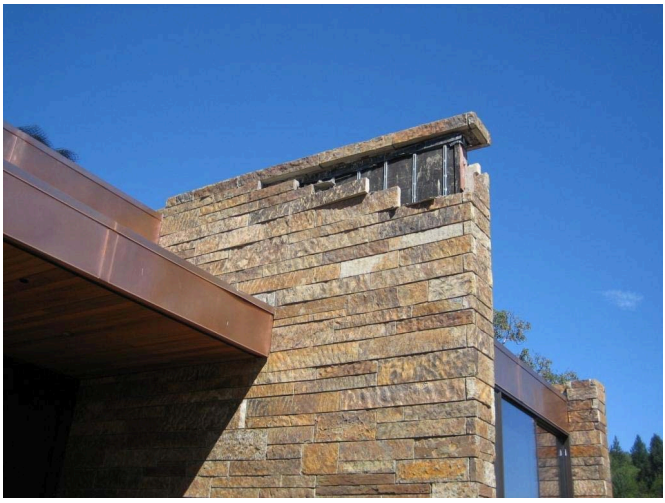

Photo 1: Typical stone veneer walls and the area of earthquake damage.

Photo 2: Typical stone veneer anchorage system, consisting of steel pencil rods, dovetail anchors, and vertical channels.

References

American Society for Testing and Materials (ASTM) International. (2002). *Standard Test Methods for Absorption and Bulk Specific Gravity of Dimension Stone (C 97),* West Conshohocken, PA.

American Society for Testing and Materials (ASTM) International. (2005). *Standard Test Methods for Sampling and Testing Brick and Structural Clay Tile (C 67),* West Conshohocken, PA.

California Building Standards Commission (CBSC). (2001). *California Building Code (California Code of Regulations Title 24, Part 2),* Sacramento, Calif.

International Conference of Building Officials (ICBO). (1997). *Uniform Building Code,* Whittier, Calif.

International Conference of Building Officials (ICBO). (1997). *Uniform Code for Building Conservation,* Whittier, Calif.

Thermal Inefficiencies in Building Enclosures – Causes of Moisture Related Performance Problems

P.E. Totten, PE[1] and M. Pazera, Ph. D. [2]

[1] Senior Project Manager, Simpson Gumpertz & Heger Inc., 2101 Gaither Road, Suite 250, Rockville, Maryland 20850; PH (301) 825-0518; Fax (301) 417.9825; e-mail: petotten@sgh.com
[2] Staff II – Building Technology, Simpson Gumpertz & Heger Inc., 2101 Gaither Road, Suite 250, Rockville, Maryland 20850; PH (301) 296-0167; Fax (301) 417.9825; e-mail: mpazera@sgh.com

ABSTRACT

In many buildings, thermal inefficiencies result in condensation problems. Some of these problems are readily visible, such as condensation on window surfaces, but some occur within our wall and roof systems. Condensation problems occur for several reasons, such as elevated humidity and stagnation of air.

We will discuss condensation related moisture problems, their cause and proposed remedial options. We will focus on presenting investigative approaches and tools used to evaluate these inefficiencies such as visual observation, tracer smoke testing, infrared thermography as well as thermal analysis.

We will discuss specialty building considerations using examples from past investigations. We will discuss considerations for structural retrofits for buildings such as blast resistance, seismic upgrades or structural retrofit for stabilization where the structural elements used form thermal bridges. We will discuss considerations for architectural features on buildings such as light shelves and sun shades and methods to reduce thermal bridging at these elements.

INTRODUCTION

Thermal inefficiencies can be caused by thermal bridges as well as unintended air flow and air leakage.

Thermal bridges are typically caused by the continuation of high-conductivity materials, such as steel and concrete framing, transferring through the thermal barrier for the building enclosure. Thermal bridges can result in significant heat loss and gain (depending on the season) and are elements that condensation can occur on or near.

Air leakage requires a pathway as well as a driving pressure. Pressure differences across the building enclosure include mechanically induced pressure, stack effect (natural buoyancy of air) and wind pressure. These pressures can make the building in question positive, neutral or negatively pressurized. Air leaks occur through voids; although the focus of this paper is not air barrier systems, these voids can be greatly reduced by the installation of a proper air barrier system. Several of the reference documents provided at the end of this paper provide additional information on air barrier systems and considerations.

Unintended air flow and air leakage is of importance with respect to condensation with most of the concern concentrated around the transportation of humid/moist air that is relatively warm to a significantly colder element that is at or below the dew point temperature of the air, such that condensation occurs. This hidden condensation is not easily detected if its accumulation is not significant and is typically found only after accumulation reaches a critical point of visible deterioration, or through observations made via destructive openings.

In order to understand the concerns of condensation, it is necessary to understand the mechanisms of heat transfer and the concept of dew point with respect to air flow. It is also important to understand the role of the interaction between our mechanical systems and our building enclosures, as this interaction can adversely affect the volume of condensation and locations of condensation.

HEAT TRANSFER MECHANISMS

Conduction, convection and radiation are three mechanisms that contribute to a total heat transfer through the building enclosure. Heat is conducted through solid components of the building enclosure including steel members, window frames, glazing, flashings and cladding materials. Heat transfer occurs through the path of least resistance and it is proportional to thermal conductivity of the material. The lower the thermal conductivity, the greater the resistance to heat transfer through the material. Metals and insulation materials are on the opposite ends of the thermal conductivity spectrum with the former being excellent conductors and the latter excellent insulators. At a microscopic level in conduction heat transfer is attributed to the energy exchange during molecular collision. It is during these collisions that the net exchange in energy occurs from more active molecules (at higher temperatures) to the less active molecules (at lower temperatures). Heat flow through the aluminum window frame components is an example of conductive heat transfer.

In convection, the energy exchange due to molecular collisions is also superseded by the bulk motion of the fluid. This means that in addition to energy exchange between individual molecules, there are also a large number of molecules moving collectively due to motion of the fluid. Convection heat transfer can be further subdivided into forced or free convection depending on the nature of the flow. Free convection occurs in instances when the bulk motion fluid is the result of buoyancy and forced convection is attributed to external forces such as wind. Convective heat transfer across the air gap in the insulating glass unit (IGU), on the exterior surface of building cladding (enclosure) due to increased wind velocities are just two examples of free and forced modes of convective heat transfer.

Thermal radiation is another mode of heat transfer, and it involves energy emitted in a form of electromagnetic radiation. Radiation requires a line of sight between the source and the receiver. Exchange of thermal radiation between the building enclosure surfaces, the surrounding environment and the sky plays an important consideration in condensation instances. Night time net exchange of thermal radiation can result in reduction of surface temperatures by as much as 7F to 10F on building enclosure components. When surface temperatures fall below the dew-point temperatures condensation will occur on these surfaces.

The discussion on the modes of energy transfer provides a basis for fundamental understanding of heat flow across the building enclosure. However, solving condensation problems requires evaluation of a variety of dynamic interactions, including air infiltration and exfiltration, building pressurization, and operating parameters of the HVAC systems. An important concept to understand in evaluating condensation problems is dew point temperature.

DEW POINT TEMPERATURE

Dew-point temperature is indicative of condensation and it is a temperature at which water vapor will condense into liquid. An air volume held at a constant barometric pressure will condense when its relative humidity reaches 100%. The relative humidity is a ratio that relates the actual amount of water vapor contained in the air to the maximum possible amount of air that can be contained at a specific temperature. In this context the dew-point is a temperature at which air cannot hold any more moisture; reducing the temperature below this point leads to condensation. Window glazing and window frame surfaces in cold and mix climates are usually more susceptible to condensation. We have performed numerous building investigations with winter time condensation occurring on the window frames and glazing components. Typically, resolving such problems involves a number of steps including an extensive field investigation, computer modeling and analysis, as well as development and evaluation of remedial (repair) options.

CONDENSATION STUDIES – INVESTIGATIVE AND ANALYSIS TOOLS

In order to complete an investigation of many condensation problems, a variety of investigative tools and analysis tools can be used. This includes, but is not limited to:

- visual observation, including observations at destructive opening;
- tracer smoke testing to examine unintended air flows and air leakage paths;
- infrared thermography to review thermal inefficiencies, including thermal bridges, and air leakage paths;
- two and three-dimensional thermal analysis.

Visual Observation

Before examining any condensation problem with thermography or tracer smoke, the human senses of sight and touch should first be used to evaluate the project. In completing a visual survey, documenting findings in notes and photographs, several key steps need to be undertaken prior to and during the study. These are:

- Review of drawings (architectural, mechanical and related as-built and shop drawings) and specifications to better understand the intended locations for the various building components and the location of related mechanical systems;

- Interviews/information from occupants/owners/property managers, and, if a fairly new structure, the design and construction team. In order to understand the condensation problem better, information shared by these individuals will be necessary in determining what has been observed, previously investigated by others, and potentially altered under past remediation/repair attempts. This includes understanding how the building was intended to operate and how it is actually performing;
- An field investigation to coincide with the times of year that the condensation problems occur;
- Field investigation, including visual survey.

Observations of both areas of reported condensation and those in similar conditions on the same property with no or limited reported condensation to compare what is different, such as positioning of heating sources, localized thermal bridges, such as structural framing, or changes in configurations of the various components, or potential localized air leakage.

Where condensation is reported above a drop ceiling or other moveable building component (i.e. an access panel, below a raised floor), then opening up elements to review potential causes is simplified. However, in most cases, condensation that is hidden within a system that appears at floor lines or at wall surfaces as staining, mold or other moisture-related damage can only be further reviewed by destructive openings to properly catalog all of the components of the enclosure and how they are installed. Assemblies should be removed by layers and documented at both the inboard and outboard surfaces to document any locations of moisture damage. In addition, tracer smoke should be used at each step to examine air leakage and air leakage paths as well as temperature and RH readings at any cavity locations immediately after gaining access to that space. This will provide the individual completing the investigation a more complete picture of all potential influences on the condensation problem. Visual survey techniques should be combined with tracer smoke testing and thermography as well as thermal analysis either before or after the field investigation to examine possible solutions to problems observed and/or documented.

Tracer Smoke Testing – Evaluate Air Flow Paths

All condensation problems are influenced to some extent by air, its temperature and humidity levels, how the air moves through the building enclosure and to the various elements of the enclosure and how the building enclosures reacts to this air. Tracer smoke is not only useful in examining air flow from air leakage through the enclosure or air flow within the enclosure from unintended air flow paths, such as a raised floor that is tied to the interior sheathing such that it communicates with the cavity between the exterior sheathing and interior sheathing and in turn communicates with a drop ceiling space creating a plenum that can transport air into the wall cavity and potentially to the wrong side of the insulation in the wall system, but also air flow at diffusers in forced air heating and cooling systems to examine the throw and flow rate from the diffuser.

Air leakage below window sills can provide significantly colder temperatures to the sill then intended by the design team (i.e. interaction of the HVAC and building enclosure systems) during winter months and can result in condensation problems that were not predicted by thermal analysis. In addition, drawing of this cold air elsewhere within the wall system by leaky mechanical return duct work can increase the range of influence of this cold air and result in condensation significantly higher up on the window than would normally be expected. By using tracer smoke at the window, leakage paths can be found, and by using smoke at destructive openings, many other air flow phenomena can be detected that may further explain the element being investigated and provide the investigator another set of components that may require a solution.

Review of air flow from diffusers is important to evaluate how this forced air might influence the window, and in most cases, the most likely source for condensation, the window sill. As window blind placement will typically isolate the window from the heat source when supplied in close proximity to the window system, tracer smoke can also be used to evaluate the risk of air stagnation behind the blind that can result in humidity build up.

In specialty buildings, such as ice rinks and natatoriums, this evaluation of air flow is needed to evaluate condensation problems. Many ice rinks now have extended operating seasons, sometimes year round. In humid climates during summer months, drawing in of warm moisture-laden exterior air can have a serious detrimental effect on the building enclosure as this air cools and eventually condenses within the building enclosure, should the building be placed under a negative pressure or overly influenced by wind. In natatoriums, if the mechanical system does not keep the entire pool under a slight negative pressure and some portion or all of the building is under a positive pressure, the reverse situation described for the ice rink occurs during winter months. As this warm, moisture-laden pool air is pushed to and across the enclosure, it will condense at elements below dew-point, worsening as the air cools. In both cases, it is air leakage that is the predominant driving force influencing the condensation, as driven by the interaction between the mechanical system and the building enclosure.

In addition to tracer smoke, touch and infrared thermography should be used to feel for significant temperature differences and for potential air leakage paths.

Infrared Thermography

In combination with visual observation, including any needed destructive openings, and tracer smoke to evaluate air flow that may be influencing the condensation problem, thermography is useful to examine thermal inefficiencies, such as thermal bridges, as well as air leakage paths. However, thermography by itself should not be relied on as the only tool to complete the condensation evaluation as the tool does have limits. Thermography is useful to examine thermal bridges and surface temperatures; if a large temperature difference is found and coincides with air leaks found with touch or smoke tracing, it is likely indicative of an air leak. The thermography will typically show the temperature influence of this air leak and may identify why a window or other element is condensing in a certain pattern. It is a

useful tool to find thermal bridges or insulation voids in some systems; however, in some configurations and with certain material thicknesses, there may not be enough of a temperature difference to see these paths.

Two and Three-dimensional Thermal Analysis

Two and three-dimensional computer based thermal analysis can be used to evaluate the as-built conditions as well as possible repair solutions. The examples in this paper use models developed by THERM (LBNL). THERM is a steady state numerical simulation software that performs two-dimensional heat flow calculations and computes temperature distribution within a building enclosure system based on defined system geometry, component materials, and boundary conditions. The software evaluates heat transfer by conduction and radiation, but does not evaluate convection and the possible influence of air leakage. The reviewer of the model will want to examine how heat transfer is predicted in the model versus field observations and thermography to validate the model, taking into consideration that the model tools used for this do not typically take into consideration air flow, and as air leakage may be unique to a particular case, programs like THERM will not tell you the influence of this leakage. We have good experience with correlation between the analysis software and field findings. Note that repair solutions determined by careful analysis may not supply the full solution, as air leaks still need to be stopped and mechanical systems may require reconfiguration, adjustment or new components/systems in order for the system to appropriately transfer heat to elements such as windows. The models accuracy is greatly improved with accurate dimensions of all components from a mix of field measurements, as-built drawings, shop drawings and original design drawings. If all components can be accurately measured for thickness and length, width, height in the field, then these measurements should be the measurements predominantly used for the model. Analysis should be completed for each unique condensation problem (windows and curtain wall with different frame extrusions require different models, each thermal bridge will require analysis).

Two common issues we are seeing in many building are thermal bridges formed by structural retrofit members, whether for blast, seismic or additional structural support. In these cases, the new elements require review by thermal analysis to see if heat transfer through new structural members will result in condensation and energy loss, and if so, how these problems can be solved. Figure 1 shows an example for a building that required new structural steel at the window surrounds to retrofit the system into an existing curtain wall. Additional insulation and a localized passive heat fin were supplied to reduce condensation risk and minimize heat loss and gain.

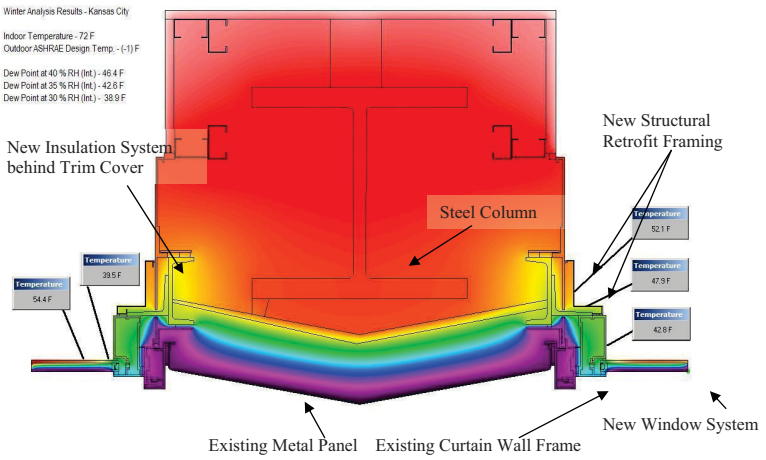

Figure 1. Thermal evaluation of structural retrofit of new energy efficient windows into an existing curtain wall.

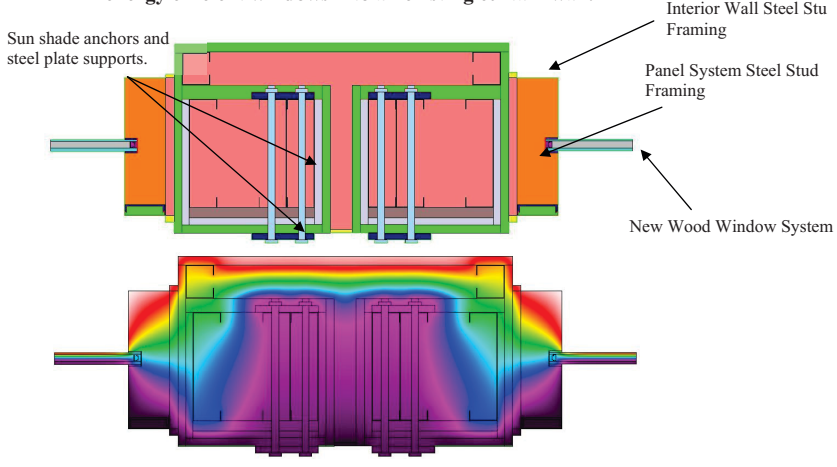

Figure 2. Sunshade evaluation. There is minimal effect due to thermal bridging due to the insulation strategies used.

A second issue is the attachment of sun shades and light shelves; in many buildings, these components and their attachment bypass the thermal break in the window or curtain wall system, or are tied into the building framing such that they transfer mostly or completely through the thermal barrier. Figure 2 (above) shows an

example of a sun shade, where the thermal bridge was minimized by placing insulation inboard of the structural attachment. In cases where this bridge is not dealt with, if the building is humidified, there is risk in winter for this bridge to result in condensation. In addition, heat loss and gain through the bridge will impact the overall energy efficiency of the structure.

CASE STUDIES

Case Study 1 – Ice Rink Roof

We conducted a field investigation to review issues with the building enclosure of an ice rink located in a mixed-humid climate. We were tasked with identifying the cause of condensation within the ice rink roof/ceiling assembly. Our findings are based on document review for the project including design drawings and specifications, and field investigation with inclusion of destructive openings. The roof assembly consisted of following elements listed from exterior to interior metal roof panel, fiberglass batt insulation installed between purlins, vapor barrier, fiberglass insulation installed between rafters and low-e vapor retarder ceiling membrane (Figure 3).

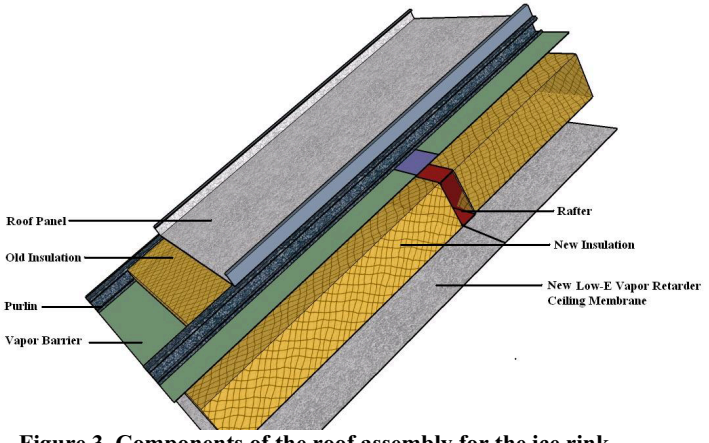

Figure 3. Components of the roof assembly for the ice rink.

Our findings indicated that water damage experienced in the roof assembly of the ice rink is mainly due to condensation of warm, moisture laden outdoor air that infiltrates into the roof assembly. The air enters the assembly at the soffit and condenses on the outboard surface of the interior insulation system. The airflow pattern that leads to this condensation is the result of the lack of a continuous air barrier system to prevent the infiltration of outdoor air into the roof assembly combined with a building that was susceptible to operating under a negative pressure. Pressurization measurements confirmed that the building was operated under negative pressure near the ceiling level allowing the warm, moist air to infiltrate. Smoke tracer tests were conducted to

verify the air flow paths from adjacent spaces and the roof elements i.e., soffits and roof ridge into the insulation system and confirmed the findings of negative pressure.

Case Study 2 – Hospital Window Condensation

We were contacted by a client to investigate condensing window problems in a 340, 000 sq. ft. hospital addition constructed on the east coast (Figure 4). We used a combination of visual observation, tracer smoke and thermal analysis to further assess this problem. The floor plan layout shows patient rooms along the perimeter at the north and south building elevation. The building enclosure consisted of precast concrete facade panels with punched and ribbon aluminum-framed windows and double glazed IGUs. The exterior wall consisted of following elements listed from exterior to interior, precast concrete panels, extruded polystyrene insulation with taped joints, a steel-stud-framed backup wall partly filled with fiberglass batt insulation, and interior gypsum wallboard.

Figure 4. Condensation on the window frame and glazing gasket at the sill.

The as-built condition showed numerous windows directly installed onto precast panels without shims, poorly taped joints between adjacent rigid insulation boards, lack of air barrier/air seal at the window surround (perimeter) and below the solid surface window sill. Condensation was limited to windows at the north building elevation that did not have fin tube radiant heating below the sill. We observed condensation on the; vertical leg of the aluminum-framed window extrusion and the glazing gaskets, 2-in. wide band of the glazing along the window frame at the sill and accumulation of bulk water on the solid surface sill. Window frames components and glazing at the jamb and at the head was not affected.

In the second phase of the project we applied 2-dimensional thermal modeling software (THERM 5.2) to assess the thermal performance of the as-built window sill condition and evaluate the extent and frequency of condensation occurrence. We proposed three remedial thermal improvement options and developed additional computer models to evaluate their predicted thermal performance. The two passive options included; installing spray foam (SPUF) insulation between the window frame at the sill and the existing rigid insulation to improve air tightness at the window sill (Option 1), and in addition to the SPUF providing a metal heat fin to improve heat flow from the interior to the window frame in the configuration shown on Figure 5 (Option 2). The active option involved installing heat trace system and provides direct heating to the window frame. In a final phase of the project, a mock-up for each of the remedial options discussed above was constructed in the field to further review its thermal performance and provide validation results for our numerical computer modeling.

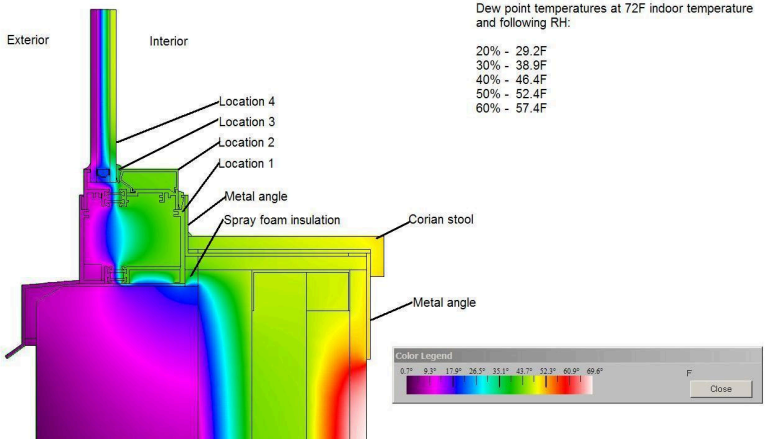

Figure 5. Temperature distribution for remedial thermal improvement Option 2 with inclusion of spray foam insulation, aluminum heat fin and thermal conductive gel.

The results of the modeling work confirmed the susceptibility of the as-built window sill detail to condensation at RH levels contemplated for the hospital's operation, and typical wintertime outdoor conditions. For the as-built condition, the model indicates that the window sill frame is at a higher risk for condensation than window jamb and head frames. At 30% interior RH and 72°F, the window sill frame is estimated to condense for 11 days a year. For the as-built sill condition, the predicted surface temperature is lowest at the window frame and gasket stops. The onset of predicted condensation is confirmed by field observations. The addition of insulation at the sill (Option 1) does not improve the condensation resistance of the frame and glazing assembly. The addition of aluminum heat fin, thermally

conductive gel, and spray foam insulation below the sill (Option 2) significantly reduces the condensation potential at the window frame sill from 11 to 0 days per year at RH levels at 30% or lower at 72°F. However, at higher indoor RH, the passive thermal improvement options increase the condensation resistance and reduce the number of condensation days, but do not fully eliminate the condenstaion.

Another option is to use heat trace cable. The heat trace can fully be configured to prevent condensation at outdoor design temperatures, however requires electrical circuits to incorporate monitoring devices to optimize performance and control operating expenses. The predicted annual operating cost of the heat traces system for individual windows with 30% and 40% interior RH and was estimated to be $1.50 and $4.80, respectively, at a $0.06 unit cost of electricity. This operating cost will be affected by changes in unit price of electricity, and climatic conditions (higher costs with severe winter conditions).

CONCLUSIONS

A combination of analysis and field assessment tools are needed to properly evaluate condensation problems, determine all sources influencing the condensation, and provide solutions that address the issues found. Simply relying on one tool for assessment without additional evaluation can result in an incomplete solution that can allow the condensation problems to continue to occur, albeit at potentially to a lesser extent than any remedial action. Investigators should evaluate which of the tools identified within this paper (and others not discussed that may fit the project needs, such as large scale air leakage testing) best fit the needs of their project in order to arrive at the most appropriate solutions within reasonable cost.

References

American Society of Heating, Refrigerating and Air Conditioning Engineers (ASHRAE) Standard 90.1 – “Energy Standard for Buildings Except Low-Rise Residential Buildings”, ASHRAE.

Blomsberg, T. and Claessen, Johan (2003), HEAT 3, Building Technology Group - MIT, Department of Building Physics – Chalmers Institute of Technology.

Incropera, F.P., and De Witt, D.P. (1990), “Fundamentals of Heat and Mass Transfer”, John Wiley & Sons, New York.

Pazera M., and V. Cammalleri (2008), “Avoiding Window Condensation in High-Humidity Buildings”. RCI Building Technology Symposium, Atlanta, GA.

Pazera M. (2008), “Condensing Window Problems”. The Construction Specifier.

Regents of the University of California, Lawrence Berkely National Laborotories (2003), THERM Finitie Element Simulator.

Totten, P.E., O'Brien, S.M, and Pazera, M. (2008), "The Effects of Thermal Bridging at Interface Conditions," Building Enclosure Science & Technology 1, Minneapolis, MN, (June 2008)

Totten, P.E., and O'Brien, S.M. (2007) "Air Barriers in High Interior RH Specialty Buildings: Considerations for Control of Moisture-Laden Air in Museums, Labs, and Natatoriums," Oakridge National Laboratories Buildings X, Clearwater, FL, (December 2007)

Inspection, Rating, and Repair of a Residential Building Envelope Detail

Kevin L. Rens[1] and H. James Royston[2]

Abstract: Building envelope failures resulting in water intrusion distress are well documented in the literature. Weather-resistive barriers underneath siding systems are often installed in haste by subcontractors or workers that do not understand lapping sequence to achieve the desired water-shedding installation. This paper documents a case study whereby a simple detail around a roof drain scupper caused significant damage to a residential house located in Denver Colorado. Non-destructive inspections and destructive tests were completed in order to determine the origin and cause of the damage. Economic ramifications as a result of the litigation are also discussed.

Introduction

Predock (2006) stated that "*The building envelope is more than a facade – it is the poetic mediation between an integral spatial realm and the outside world"*. Unnoticed and unwanted water intrusion though the building envelope facade and into the spatial wall cavity infrastructure is a growing problem accompanied with financial liability. With the exception of structural failures, it has been reported that about "*90% of all building problems are related to moisture in some way"* (Proskiw, 2008). In the Unitied States, the Insurance Information Institute estimates that $3 billion in building mold claims were paid in 2002 (Nadel, 2006). In Canada, losses in British Columbia alone are estimated in the hundreds of millions of dollars due to hundreds of filed law suits by building owners (Brindle, 2005).

Overview

This paper details a case study of a residential house of which various forms of water intrusion occurred over a 10 month period. In order to isolate the sources of all water infiltration, inspections were completed utilizing various destructive and nondestructive inspection technology. In the end, the total cost of inspections, repairs, and rehabilitation was estimated at around 33 percent of the value of the original 2004 construction costs.

1 Professor and Chair, Department of Civil Engineering, University of Colorado, Denver, Colorado 80217-3364
2 Principal, Western Engineering and Research Corporation, 2175 South Jasmine Street, Denver, Colorado 80222

Inspection History

According to local county property records residence was built in 2004. The residence was a single-family two-story wood frame home with a stucco exterior and concrete tile roofing. The residence experienced a late afternoon rainstorm on August 18, 2004 that reportedly produced approximately 4" of rainfall. As a result of this storm, damage occurred in the dining room as a result of water infiltration. In addition, water infiltration problems continued for months after the storm as the sump pit output pipe back flowed into the sump pit and the basement recreation room occasionally experienced leaks near the baseboard.

The four inspections were titled the Preliminary Report, Supplemental Report, Supplemental Report No. 2, and Supplemental Report No. 3. The basement bedroom flooded because of a blocked downspout extension that allowed water to flow into the window well serving the bedroom. The sump pit back flowed because of a negative sloping pipe and poorly connected pipe section seams. The sump pit issue was solved by video inspection and forcing smoke through the pipe to idenify the improper connection detail. The recreation room base board mold and deterioration problems were traced to a faulty sprinkler head assembly that was discharging water into the ground immediatley adjacent to the foundation. The remainder of this paper deals with the source of the water intrusion into the dining room and is derived from portions of the Preliminary report and the first two supplemental reports.

Figure 1 shows the west exterior wall of the dining room, and there was a 3-foot tall parapet wall around the flat roof above. The roof of the dining room consisted of modified bitumen rolled roofing with flashing on the inside face of the parapets. The drainage system for the flat roof consisted of 2 roof scuppers (identified by arrows in Figure 1) which penetrated the parapet. The numbers and drawn shapes in Figure 1 indicate the areas that were eventually water tested, as discussed later.

Figure 1. View of exterior dining room. Numbered areas are zones used in the water infiltration test. Arrows represent scupper locations (at top of downspouts)

The results of the preliminary inspection revealed that the sundeck roof above the dining room was low sloped and nearly flat in some areas – slope measurements ranged from about 0" to 1/2" in 4 feet. One possible source of dining room water infiltration was identified as the openings in the parapet walls for the drainage scuppers shown in Figure 2. Another possible source was the cracking in the stucco finish on the top of the parapet as shown in Figure 3. There was a deformed gutter located directly above the sunroof parapet wall shown in Figure 3 which during heavy rains likely overflowed and deposited significant roof drainage directly onto the cracked parapet wall cap.

The leak into the dining room presented as water on the floor and water staining on the dry wall adjacent to the French doors, and it was related to the sustained heavy rainfall, however, the exact path of the leakage was not determined in the preliminary report. During relatively normal Colorado rainfalls, minor leaks that result from stucco cracks or scupper deficiencies go unnoticed. However, during relatively intense rainfalls like that which occurred on August 18, normally minor leaks are exposed and magnified. It is likely that the leak that produced damage in the dining

room was present for some time, possibly since construction, and the heavy August 18th rainfall created more water infiltration which caused the leak to be noticed.

It was proposed that additional destructive and nondestructive testing be used to try to determine the exact origin and cause of the dining room leak. The additional work included water spray tests starting from the lowest elevation and ending at the top surface of the parapet wall. The zones included:

Zone 1: Lower area north of downspout

Zone 2: Middle area north of downspout

Zone 3: Top area north of downspout

Zone 4: Lower area between downspout and French doors

Zone 5: Upper area between downspout and French doors

Zone 6: Area above dining room French doors

Zone 7: Down spout below scupper

Zone 8: Scupper area draining from sun roof deck

Zone 9: Built up roof surface area

Zone 10: Outside surface of parapet wall

Zone 11: Inside surface of parapet wall

Zone 12: Top surface of parapet wall

Based on the visual examination of the construction, it was hypothesized that the leakage may have been coming from the joint between the stucco and the door trim (Zones 4 and 5), at the scupper exit from the parapet wall (Zone 10) as illustrated in Figure 2, at the scupper inlet, or through the open fractures in the top of the parapet walls (Zone 12) as illustrated in Figure 3.

Figure 2. Close up view of Scupper detail

Figure 3. Top of Parapet wall

There was repeated and known water leakage; water testing was completed using an unregulated light fan spray pattern to wet the surfaces. The authors had successfully used this method in the past to diagnose leakage problems. This method was used as it provides a less aggressive application of water than the American Architectural

Manufacturers Association (AAMA) standards (AAMA, 2003). Furthermore, it was not the purpose to complete a fenestration installation compliance test.

Portions of the drywall finish were removed around the door in the area of observed leakage. The insulation was removed to expose the wall cavities to allow observation for water infiltration during the spray tests. The water spray test was then completed, with water applied sequentially to the 12 identified zones. This diagnostic approach to the application of water began at the bottom of the wall and moved upward. The spray application was maintained on each area for a minimum of approximately 5 minutes before proceeding to the next zone. Throughout the testing the wall exposed wall cavity and surrounding finishes were observed for indication of water infiltration.

The results of the water infiltration test revealed that Zone 10 produced leakage into the interior wall cavity of the dining room. All other zones did not. It was then concluded that the scupper was a source of the dining room water intrusion. A contractor reported that they had sealed the scupper and that the leak subsequently subsided. The contractor had applied caulk around the perimeter of the scupper at the stucco interface as shown in Figure 4. However, 2 months later, mold and wetted dry wall again re-appeared in the dining room. Therefore, the stucco detail had to be more closely examined.

Figure 4. View looking down from top of Parapet wall to inside of scupper

Intrusive destructive testing of the exterior stucco, insulation, weather-resistive barrier (WRB) underlayment, and oriented strand board (OSB) sheathing was completed on May 5, 2005. Four areas were opened including:

1. The area around the scupper inlet on the east side of the parapet.
2. The top and west face of the parapet wall above the north scupper.
3. Around the north scupper in the west wall of the dining room.
4. The upper north corner of the exterior doorway.

The interior side of the parapet wall near the northwest scupper was destructively inspected as shown in Figure 5. Figure 6 shows that the WRB underlayment was lapped underneath the roofing wall flashing. This is referred to as a negative lap, and it allows water on the WRB to flow behind the flashing and into the exterior building envelope. The roofing was removed from the area in front of the scupper and moisture was observed on the sheet metal flashing for the scupper and the underlayment. The previous water testing did not reveal any leakage through the roofing system (Zone 9), so it was concluded that the moisture under the roofing probably originated from water infiltration through the stucco finish system. In addition, it was observed that the roofing membrane was not bonded to the underlayment at this location.

Figure 5. View of interior side of parapet wall above the northwest scupper with stucco removed

Figure 6. Close up of Figure 5. Note negative lapped wall flashing.

The stucco was removed from around the exterior of the north scupper as illustrated in Figures 7 through 9. Figures 7 and 8 illustrate that the WRB above the scupper was simply folded into the opening in the OSB wall sheathing, with no termination construction, such as a scupper flange behind the WRB above the scupper, to divert water out of the wall assembly. . Figure 9 shows the weather resistive barrier removed from the top and south side of the scupper. The OSB surface was wet below the scupper. Fungal growth was observed below the scupper.

Figure 7. View of exterior side of parapet wall above the northwest scupper

Figure 8. Close up view of Figure 7. Note underlayment detail folded inside

Figure 9. View of the OSB plywood below scupper area

Summary

This investigation revealed two improper weather-resistive barrier detailing issues on both sides of the scupper penetration as shown in Figures 5 and 6 (at the roofing flashing/wall weather-resistive barrier interface) and in Figures 7 through 9 (at the scupper/wall weather-resistive barrier interface). As background, remember that it was noted that in the Preliminary Inspection Report that the roof gutter system directly above the northwest scupper was deformed. Water shed from the upper clay tiled roof can overshoot the gutter and concentrate on the cracked sun deck parapet wall below it. This water concentration occurs directly above the northwest scupper. Water that penetrates the top of the parapet wall stucco material, either by diffusing through its cross section or by cracks, will shed to each side of the wall via the weather-resistive barrier. It was observed that the roofing flashing was negatively lapped and any trapped water that penetrates the parapet at the top and sheds east toward the sun deck will tend to drain behind the roof flashing, onto the sheathing and roof decking and through the exterior envelope and into the dining room. A similar situation occurs when water penetrates the top of the parapet wall and sheds towards the west away from the sun deck. Water on the surface of the weather-resistive barrier at the top of the scupper will tend to drain into the wall assembly. With the weather-resistive barrier wrapped inside the OSB wall sheathing as shown in Figures 7 and 8, the infiltrated water has a direct path into the wall and ceiling cavities. This is only amplified by the attempted sealant repair the contractor initiated

as shown in Figure 4. The result of this infiltrated water from these two improper weather-resistive barrier detailing issues accelerates the distress to interior finishes. At the top of the parapet wall, it was apparent that the weather-resistive barrier was not effective, as the underlying wood framing was wet and apparent biological growth was present.

References

AAMA (2003) 501.2-03, Quality Assurance and Diagnostic Water Leakage Field Check of Installed Storefronts, Curtain Walls, and Sloped Glazing Systems, American Architectural Manufacturers Association, 1827 Walden Office Square, Suite 550, Schaumburg, Il 60173, 7/2003.

Brindle, D. (2005) "Building Envelope Failures—Litigation and Insurance Industry Responses"Building Envelope Forum Online Newsletter, June. http://www.buildingenvelopeforum.com/index.html

Nadel, B. (2006) "21st Century Building Envelope Systems: Merging Innovation with Technology, Sustainability, and Function" McGraw-Hill Construction—Continuing Education Center. http://continuingeducation.construction.com/article

Predock, A. (2006) FAIA, 2006 American Institute of Architects Gold Medalist. http://continuingeducation.construction.com/article

Proskiw, G. (2008) "Building Envelope Solutions" Conference on Building Envelope Solutions. Edmonton, Alberta. http://www.buildingenvelopeforum.com/conferenceEDM08.html

Special Problems with Composite Multiwythe Masonry Walls

David B. Peraza, PE, Member ASCE [1]

[1] Exponent, 420 Lexington Avenue, Suite 1740, New York, NY, 10170;
PH 212-985-8100; email: dperaza@exponent.com,

Abstract

Composite multi-wythe walls for exterior walls, especially those that combine brick units and concrete masonry units (CMU), are vulnerable to certain special problems. There are a considerable number of existing structures that were built using this type of construction, and it is still occasionally used for new construction. These types of walls are prone to certain problems, and these problems are not generally well known among engineers and architects. The result is that existing buildings that show symptoms of these problems may be misdiagnosed, leading to inappropriate or expensive repairs, and that design professionals may not be fully aware of the pitfalls when they use this system for a new design.

This paper discusses the vulnerabilities of this type of construction, surveys the available literature on the topic, and illustrates the issues with a case study

Introduction

A composite multiwythe wall is one in which the wythes of masonry are bonded to each other, so that they act as one. Shear is transferred between wythes, allowing the full thickness of the wall to resist bending stresses induced by wind loads, as well as gravity loads and in-plane lateral loads. There are several mechanisms for bonding the wythes together, including the use of brick headers, the use of ladder-type joint reinforcement, and the use of discrete metal ties. This type of wall typically has a mortar-filled collar joint, usually less than 1 inch wide. This collar joint has several functions, it improves the moisture resistance of the wall, and it assists in transferring shear stresses between wythes.

In these types of walls, brick is usually used for the exterior wythe and CMU is typically used for the interior wythe. These walls may be load-bearing or non-load-bearing. If the walls are load-bearing, they typically do not include horizontal soft joints or relieving angles at floor levels. The author is aware of buildings that used this type of construction ranging from the 1960s to the 1990s.

The Problems

There are a number of difficulties that are created by using brick and concrete masonry units (CMU) together in a composite wall.

First, the two materials have conflicting volumetric characteristics. Brick tends to expand over time as it absorbs moisture from the atmosphere and CMU tends to shrink as it continues to cure and lose moisture, both through evaporation and chemical binding. If these materials are joined together, their natural and opposite volumetric changes will cause the wall to bow slightly, somewhat like a bimetallic strip, and will induce shear stresses along the collar joint.

One of the possible side effects of this behavior, especially if there are no horizontal soft joints at the floor levels, is that it may cause the parapets to lean inward, as shown in Figure 1.

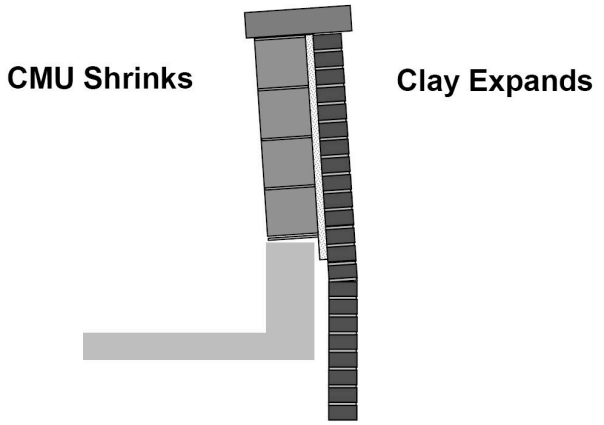

Figure 1: Leaning parapet caused by volumetric changes in brick and CMU, and by the lack of relieving angles.

Secondly, the joining of two wythes may cause the unintended transfer of stresses from one wythe to another. Often the inner wythe, which is CMU, is designed to be load-bearing. It may be directly supporting concrete plank floor, steel joists, or another type of floor construction. The load-bearing wythe may have horizontal joint reinforcement, and may include vertical reinforcement grouted into the cells. The outer wythe, which is brick, is usually not intended to be load-bearing, and may not have any reinforcement at all. At best, it may have some horizontal joint reinforcement. But since the two wythe are joined compositely, stresses due to gravity loads will be transferred from the CMU wythe across the collar joint to the brick wythe. This may result in distress to the brick wythe. A similar situation can occur with lateral loads. If the outside walls are shearwalls that are part of the lateral load resting system, in-plane lateral loads delivered from the floors to the CMU will also bleed over to the brick wythe, possibly causing distress.

A further complication regarding shear transfer arises when flashing is installed in the wall. Flashing was not used in traditional barrier walls, which rely on their mass to resist moisture penetration. But flashing is an integral part of modern-day cavity wall construction. Composite brick-CMU walls are neither barrier walls nor cavity walls, so designers do not always know whether to include flashing. Flashing is desirable from the point of view of reducing water penetration, especially since these walls, unlike traditional barrier walls, contain hollow units and are relatively thin. But the flashing has the potentially adverse effect that it serves as a bond breaker between the two wythes, preventing shear transfer in the areas where the flashing is located. This can have the effect of concentrating the shear transfer in the areas immediately above and below the flashing, possibly causing distress in the brick wythe where the flashing terminates.

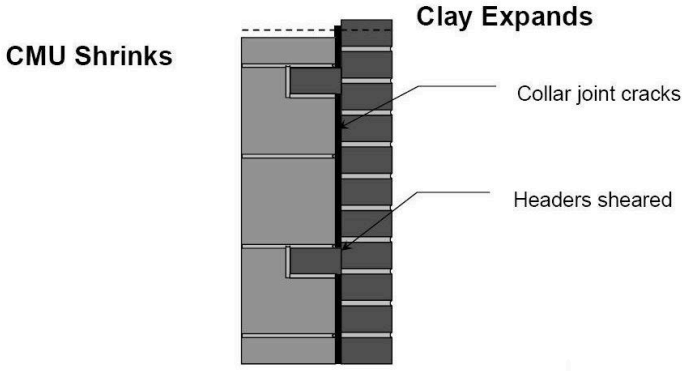

Figure 2: Brick headers can be fractured by differential volumetric changes, potentially destabilizing the brick wythe

Another potential problem is that the mechanisms for transferring shear between wythes may not be adequate for the purpose. There are two mechanisms for transferring shear: shear-friction across the collar joint, and shear across the ties or other components that bond the wythes together. If, for example, brick headers are used, the shear stresses could snap the headers, as illustrated in Figure 2. This would leave the exterior wythe freestanding, which could ultimately result in the collapse of the exterior wythe. Metal ties have more ductility, and are therefore better able to accommodate differential movement without failure. The adequacy of the shear transfer mechanisms is something that is rarely considered by design professionals.

Available Literature

As was mentioned previously, brick expands over time and CMU shrinks. Brick, which is a fired-clay product, expands as it absorbs atmospheric moisture. The amount of expansion varies due to the type of clay, the firing and handling practices, age, and the ultimate service environment of the brick. For design purposes, ACI 530 provides a coefficient of expansion, k_e, of 0.0003 inches/inch. Technical Note #18 of the BIA provides a value of 0.0005 inches per inch. The same source estimates that about 60% of brick's moisture expansion takes place within the first two years. Estimates for the amount of shrinkage that concrete masonry units (CMU) experience are also given by various sources. ASTM 426 estimates that the linear drying shrinkage ranges between 0.0002 to .00045 inches per inch. For non-moisture-controlled units, the linear drying shrinkage is multiplied by a factor of 0.5 to obtain the shrinkage coefficient.

In spite of the industry knowledge and guidance available regarding the expansion and shrinkage characteristic of these two individual materials, there are a few warnings in the literature regarding the use of these materials together. For example, an NCMA bulletin states, "Differential movement deserves particular attention on high-rises where concrete masonry is clad with clay brick. Concrete materials tend to shrink, while clay tends to expand." It goes on to describe a high rise project where vertically slotted anchors were used between the brick and the block. It appears from this description that the problem is limited to high-rises. Beall (1987) also recognizes the potential problem, but does not limit it to high-rises, "Clay masonry expands with moisture. …When combined with other types of movement and with the conflicting shrinkage of other materials, this expansion can be significant, and must be anticipated." However, Beall does not provide any specific recommendations on how to anticipate, avoid, or deal with this phenomenon. Newman (2001) also points out the problem, "The main problem of walls made of brick veneer and concrete block is that these two materials, even though both are called masonry, are radically different in nature. Brick is made of clay; it is fired in the oven and contains practically no moisture immediately after fabrication. As brick ages, it gains moisture and steadily expands in the process. A concrete masonry unit begins its life as a wet mix and is later cured saturated with water. As a CMU wall ages, it gradually loses moisture and shrinks." Again, this reference provides no specific recommendations or prohibitions. Searls and Bronski (2000) are keenly aware of this exact issue, of combining clay products with cementitious products, and they describe the possible consequences, "If the outer wythe masonry expands but is restrained by the structure, it will eventually crack, spall, or buckle under the accumulated stresses."

Despite these warnings, most codes and standards allow, and even encourage, the use of composite brick and block walls. A 1976 NCMA publication shows a composite wall composed of brick veneer and load-bearing concrete block wythe, connected to each other with a collar joint and metal ties.

Lest we think that this is a detail from "days gone by", a rapid review of prominent contemporary design guides reveals that this type of construction is still promoted.

For example, nearly a quarter century later, Architectural Graphic Standards (2000) has an almost identical detail and it states “The most common multiwythe wall is the composite wall, which consists of a clay brick wythe and a concrete masonry wythe with a ¾ in. collar joint, and brick headers or anchors.” A 2005 NCMA publication states, “One way to construct a brick and block wall is to separate the two wythes with an airspace, creating a cavity wall. Another is to use a composite wall design. The composite wall consists of an exterior wythe of brick directly mortared or grouted and tied to an inner wythe of CMU. The collar joint between the two wythes should be 100% solid as it is the only defense against water penetration.”

Furthermore, codes do not prevent or restrict use of this construction. ACI 530 (2005) states in the commentary that, “Composite masonry walls generally consist of brick-to-brick, block-to-block, or brick-to-block wythes. The collar joint can be filled with mortar or grout, or the wythes can be connected with metal ties.” The only mention of differential movement, due to any cause, is, “The influence of differential movement is especially critical when headers are used.” Apparently the concern here, which is well-founded, is that the inter-wythe differential movement will snap the brick headers, allowing the outer wythe to separate from the backup wythe. Such an event could indeed be disastrous, since it could result in a partial wall collapse.

Case Study

The author was retained as an expert, by attorneys representing the structural engineer-of-record, on a case that involved distress of a brick masonry façade. The building was a seven story hospital, located in New York City, which was roughly rectangular in plan and measured approximately 50 feet by 300 feet in plan. The structure consisted of hollow-core precast concrete floor planks, spanning in the transverse direction supported on load-bearing CMU walls. The lateral load system consisted of shear walls. The façade consisted of load-bearing concrete masonry units (CMU), and 4 inch-thick glazed jumbo brick. The building was constructed circa 1992.

Originally, the façade was designed as a cavity wall. The CMU wythe was designed as load-bearing, and the brick wythe was not. Prior to awarding the contract, the construction manager recommended, as a cost-saving measure, to eliminate the cavity, substitute a 7/8” wide filled collar joint between the brick masonry and the load-bearing CMU, and eliminate the relieving angles. This change effectively made the brick composite with the CMU. The change was accepted by the owner and the design team, and the drawings were revised accordingly.

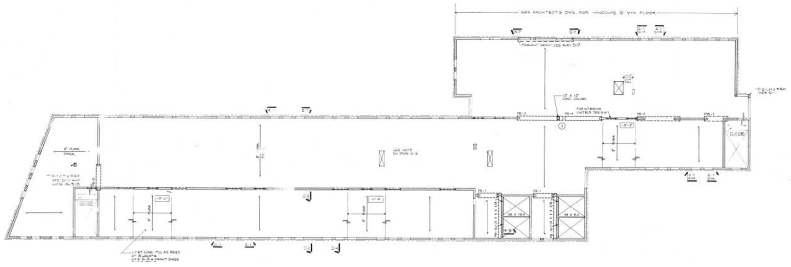

Figure 3: Plan view of hospital building

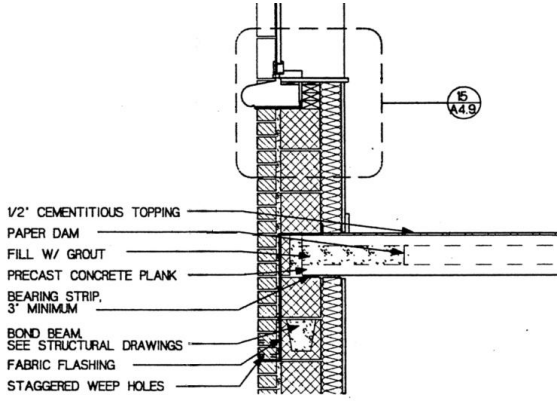

Figure 4: Typical wall section for hospital building

After about 12 years, the brick façade began exhibiting distress at certain locations. The distress typically consisted of prick spalling, and it was located along a horizontal band aligned with the window head. Most of the distress was located at the 2nd floor, but there was scattered distress at other floors. The majority of the distress was located on the south façade.

One of the theories for the distress, which was initially generally accepted by the design and construction team, was that it was caused by the use of a heavy gauge copper flashing. The mason reportedly experienced difficulties field bending the flashing crisply, which then provided soft support for the CMU that was placed on the flashing. The mason requested substituting lighter gauge copper flashing for the upper floors, which was accepted by the design team. It was theorized that the springiness of the flashing allowed the CMU to "settle" as weight was added during construction, causing the cracking. This theory was not adopted by any of the experts in the case.

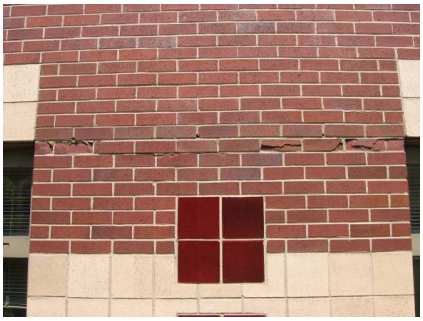

Figure 5 (left): Brick distress was typically located along bands aligned with the window head.

Figure 6 (right): Probes found that the as-built condition substantially matched the drawings, except that the collar joint was not filled

The owner retained an engineer to investigate the problem and to make recommendations. Probes were made through the brick to investigate the underlying conditions. Adjustable metal ties were found, in accordance with the drawings, and flashing was located as per the drawings. The only deviation from the drawings found was that the collar joint was not filled with mortar. It appeared that the collar joint was filled at perhaps 25% of the wall area.

After inspecting probes and performing structural analyses related to the lateral load resting system of the building, the owner's engineer came to the conclusion that the cracking was due to the lack of relieving angles, which allowed the weight of the brick to accumulate. The owner's engineer stated that if the condition was not corrected, cracking would continue and the wall could potentially become unstable. The remedy, therefore, was to install relieving angles at every floor. And according to the owner's engineer, installation of relieving angles could only safely be accomplished by removing the entire brick façade. The owner's engineer also partially attributed the cracking to an increase in thickness of the CMU bearing wall, which "potentially created an eccentricity." The cost to carry out the recommendations made by the owner's engineer was on the order of $4.5 million.

Conclusions

The use of brick masonry together with CMU in a composite wall has many pitfalls, which can result in distress to the façade. There is very little information available to the profession about the potential problems and how to avoid them and how to diagnose them. Some authoritative resources, such as Architectural Graphic Standards, even appear to encourage the use of this type of construction. Masonry codes do not prohibit or restrict the use of this type construction. This type of construction, along with its special problems, issue needs to be studied by industry organizations, and suitable warnings should be developed and promulgated.

References

ACI 530, 2005 “Building Code Requirements for Masonry Structures,” American Concrete Institute

Brick Industry Association, (BIA) Technical Notes 18, *Volume Changes and Effects of Movement, Part 1* (revised in January 1991).

NCMA TEK 3-12 (1998), “Construction of High-Rise Concrete Masonry Buildings”:

“Masonry Design and Detailing" by Christine Beall, 1987, McGraw Hill

“Structural Renovations of Buildings” by Alexander Newman (2001), McGraw Hill (Pg 795)

Searls and Bronski, “Early Twentieth Century transitional facades in the United States: Common Maladies,” Proceedings of ARCHI2000, UNESCO-ICOMOS & Bethlehem 2000 Project

“Architectural and Engineering Concrete Masonry Details for Building Construction” by A. Elmiger, 1976, NCMA, Page 27.

Architectural Graphic Standards (2000), by Ramsey and Sleeper, Tenth edition. Pg. 226-7

NCMA TEK 3-13 (2001, and 2005), “Construction of Low-Rise Concrete Masonry Buildings”:

ACI 530, 2005 “Building Code Requirements for Masonry Structures.” Commentary Section 2.1.5. American Concrete Institute

IDENTIFICATION AND DIAGNOSIS OF BUILDING FAÇADE FAILURES

Kimball J. Beasley, M.ASCE, MBA, BSEngr

Wiss, Janney, Elstner Associates, Inc., Building 5, 14 Washington Rd., Princeton Jct., New Jersey, 08550 USA. Phone: (609) 799 7799, email: kbeasley@wje.com

ABSTRACT

Early building walls were usually constructed of stone or masonry and were intended to support the structure and to shelter the building occupants. Over the past 100 years building walls have become lighter and thinner. While they still serve to keep the weather out, these newer walls no longer support the structure. They often contain complicated interdependent components which can increase the likelihood of failure. Facade failures are not just limited to collapse, cracks, or excessive water or air infiltration. Building facades that do not comply with project specifications, governing building codes, or industry standards have also failed. Even facades that do not meet aesthetic standards or the desired appearance may also be considered to have failed to the owner or architect. Considering the complexity of contemporary wall systems, understanding why they fail to perform as expected is seldom an easy task. Failures can originate from a wide variety of influences; such as accumulated differential thermal or moisture expansion, inadequate wall cavity drainage, or material incompatibility. Complicated internal leak control systems or intricate connection or support mechanisms further increase the probability of facade failures. Special diagnostic techniques and tools are needed to properly identify facade failures to enable effective remediation (Beasley 2001).

FACADE TYPES

Building walls may be divided into two broad categories: load bearing and non-load bearing. The facade may either share the structure's gravity load (load bearing walls) or may simply hang from the structure serving as the building's skin. In any case, the facade must be designed and connected to the structure in a manner to support its own weight and resist any imposed forces with an adequate factor of safety. Over the past several decades, many building facades have evolved from mortar-bedded unit masonry to thin dimension stone or composite panel building veneers. Each type of facade has distinct benefits and potential problems. Traditional solid barrier walls or cavity walls may be constructed of brick, terra cotta, precast concrete, cast stone, or concrete masonry. Contemporary facades may be skin barriers or rain screen systems constructed of cementitious tiles, thin stone, metal plates, composite panels (e.g., metal sandwich panels, tile-faced panels, or thin stone on cementitious backer board), or metal and glass curtain wall.

FACADE FAILURES

Failure is often a misunderstood term in the context of building systems. A wall collapse is an obvious failure. However, a facade that appears to be intact but would not sustain normal wind loads because of missing or corroded anchors behind the wall surface is also a failure. Such latent failures can be more insidious because they are difficult to detect and may collapse without warning. Loss of function of building facades (e.g., leaking or cracking) is far more common than failures that result in a catastrophic collapse that claims life and property (see Figure 1). The collective economic consequences of such serviceability failures may be far greater than of collapses.

Facades are subjected to a wide variety of conditions that may lead to failure. Deterioration of facade or connection materials undermines their ability to resist normal loads. External forces of a magnitude or orientation not anticipated in design can damage facade and attachment elements. Defects introduced during construction may affect the facade's ability to perform as designed (Carper 1988).

Since facades are generally considered non-structural, the responsibility for design of the facade support system may be shared between the design architect and structural engineer. Often, the project designer and the project engineer avoid dealing with the facade by relying on the contractor's shop drawings to detail the connections and supporting elements. This fragmenting of responsibility and the resulting potential lack of coordination are also frequent indirect contributors to failures.

Figure 1. Total collapse of a load bearing wall

Forces

While most contemporary building facades do not intentionally carry loads imposed by the building's structure, they must resist a variety of externally and internally imposed forces. External forces may include lateral loads from wind or earthquakes and vertical loads from the facade's own weight (gravity load). The facade also may be subjected to localized internal forces imposed by expanding elements embedded in the wall (e.g., corroding shelf angles or reinforcing steel) or by differential planar movements between the facade element and the wall's substrate or the building's structural frame.

External loads are usually well understood and the response of the facade to these forces may be predictable. Wind, gravity, and even earthquake loads can be quantified and analyzed. The facade's strength properties and connection system can be designed to accommodate such forces with an appropriate factor of safety. However, internal forces are more complex and may vary substantially from structure to structure and within the same structure depending on the facade materials, configurations employed and exposure to various environments. Such forces are often overlooked or misunderstood, leading to failures that are difficult to analyze.

Water

Aside from erosion of mortar joints or soft stone, water may damage facade and wall elements in a variety of ways. Water that enters and is retained in the wall leads to corrosion of embedded metal, which both reduces the strength of the steel support/anchor and produces corrosion scale that expands which spalls or cracks the surrounding masonry. Figure 2 illustrates spalling of the concrete surface from embedded reinforcing steel corrosion scale expansion. When saturated with water and subjected to cyclic freezing and thawing temperatures, stone, concrete, mortar, or fired clay masonry materials can deteriorate. Identifying water related failures requires an understanding of wall water management principles, or potential water entry points and migration paths within the wall. Water management means that water that penetrates the exposed facade surface or water vapor that condenses within the wall is collected and diverted out of the wall by an internal wall drainage system. Early traditional masonry walls minimized water leakage because the solid masonry mass would absorb water and gradually expel it as a vapor. With contemporary wall systems water that penetrates the facade must be conveyed via internal cavities to wall flashings that are watertight, continuous, and properly enveloped. Weepholes must be configured to easily drain water collected by the flashing. Blocked or bridged wall cavities, breached flashings, and blocked or poorly positioned weepholes may individually or collectively result in water leakage to the interior. Failure of the wall flashing/weep system in exterior walls built directly above occupied spaces, referred to as "rising walls", has a high probability of water leakage because water that bypasses the flashings readily enters the building.

Figure 2. Concrete spall from corroded reinforcing steel

INVESTIGATION METHODS

The type of facade investigation required depends on the nature, severity, and consequences of the failure (Beasley 1989). Facade failure investigations normally contain four common steps:

1. Acquisition of data
2. Analysis of data
3. Development and evaluation of failure hypotheses
4. Formulation and communication of opinions

Document Review

Review of available relevant drawings, specifications, prior reports, photographs, media coverage, etc. can usually provide background information on the design of the facade system and possibly the circumstances of the failure. However, since as-built construction often deviates significantly from the design documents, confirmation by investigation is necessary.

Inspection and Condition Surveys

Inspection methods can range from cursory binocular surveys to detailed examination, probe openings, and testing or monitoring. Inspection may help to identify and document the severity or nature of facade distress in order to assess possible causes of failure. Facade cracking, bulging, delamination, or leaking usually occur with patterns or features that can offer clues to their causes. Periodic inspection can also serve to determine the rate of deterioration and can help determine the service life of facade components. A visual condition survey of

building facades usually involves documenting observations by annotating conditions onto building elevation drawings or by high-resolution photographs. The condition survey objectives include identifying the location and nature of distress, identifying patterns of deterioration, establishing potential scope and locations for repair work, and establishing a baseline for subsequent detailed inspections. The visual condition survey also helps to establish locations for close-up observation.

Binoculars or telephoto equipment are often used to facilitate observation of small cracks, bulges, and spalls. The condition survey drawings offer a valuable method of documenting the nature and location of facade distress and for visualizing the overall patterns of distress and force paths.

Conditions identified during the survey will usually help to determine the need for and type of additional studies and laboratory tests. The distress patterns provide clues to the underlying cause(s). Conditions often identified during a condition survey include cracks, spalls, displacements, corrosion, delamination, efflorescence, honeycombs, scaling, and staining (Erdly 2004).

Detailed Inspection

Close-up visual examination of collapsed and damaged facades and of adjacent areas that are representative of the undisturbed wall is essential to gain knowledge of as-built construction and the conditions likely to have existed prior to the collapse. Safe access for such close-up examination may be from roof setbacks, balconies, swing or pipe scaffolding, or rappelling. Examination of subsurface wall elements, facade connections, and adjacent construction requires probe openings (removal of surface materials) or inspections via an optical borescope (see Tools and Equipment). Special access and contractor assistance are usually required for close-up inspections and for making and patching probe openings. Detailed inspections will almost always include various measurements such as dimensions of typical wall panels, masonry units, joint widths, displacements, crack widths, etc. Measurements also help to confirm whether the original construction documents accurately represent existing conditions.

Tools and Equipment

A wide variety of simple, traditional, or advanced new equipment is available to the facade investigator.

Common Tools

The tools and equipment required to investigate facade failures vary with the type of failure being investigated. However, certain simple tools are common to many investigations. These include: camera, flashlight, tape measure, binoculars, hammer, etc. Tools that are more sophisticated, more accurate, or dedicated to a specific purpose may also be helpful.

Photographic Equipment

A high quality digital camera and in some cases a video camera are fundamental tools. Sometimes a professional photographer may be needed for high resolution or aerial views. Specialized photographic methods may be used to measure and document a multitude of conditions. Infrared photography can be used in some cases to

determine if delaminations, cracks, spalls, or voids exist inside solid walls. Minute variations in the facade's surface temperature may correlate with discontinuity in thermal conductivity within the wall. Photogrammetry, which involves stereoscopic images, helps to detect irregular or displaced wall surfaces.

Borescope

The borescope employs fiberoptics or a micro-miniature video camera to view behind the facade. The borescope's small-diameter (6 or 8 mm) metal tube or camera head is inserted through a small hole or joint. The device includes a power supply and light source. Figure 3 shows a flexible fiber optic borescope in use.

Figure 3. Optical borescope is used to examine wall connection

Measuring Devices

Simple measuring devices include a tape measure, plumb bob, or optical crack comparator. More sophisticated devices such as a theodolite, laser level, and electronic distance measuring instrument may be used to measure precise relative positions of visible building facade areas relative to a reference point. Current technology allows precise measurement using a variety of high-tech methods. High precision global positioning systems (GPS) and various inclinometors, accelerometers, and other electronic sensing devices can accurately monitor building movements.

Metal Detector/Pachometer

The location and size of embedded steel reinforcement and steel support or anchor elements beneath the surface may need to be known to fully evaluate the wall or

facade. The pachometer measures changes in electric inductance to indicate the presence and depth of underlying metal.

Pulse Velocity Methods

The velocity and waveform of a sonic pulse traveling through concrete, stone, or solid masonry corresponds to the material's relative strengths. Sonic pulse characteristics can also help to detect internal discontinuities. The test may be conducted in accordance with ASTM C597-02, *Standard Method for Pulse Velocity Through Concrete*. A transmitting transducer introduces an ultrasonic or sonic energy pulse into the concrete or masonry and a receiving transducer detects the signal. Timing circuits in the device measure and display the elapsed time of transit. The pulse velocity is determined by dividing the distance between the transducers by the transit time. The velocity of sonic pulses traveling in concrete or solid masonry generally corresponds to the material's elastic modulus and strength.

Strain Relief

Strain relief testing involves adhering carbon-filament strain gages to the wall surface (see Figure 4). The instrumented area is then isolated from the surrounding wall by saw cutting. The strain value is measured before and after saw cutting. The in-situ residual stress is computed by multiplying the modulus of elasticity of the wall material by the measured strain change. This technique is particularly useful to determine potential for compression or buckling failure or cracking of masonry facades.

Figure 4. Carbon filament strain gage is adhered to the façade surface to measure in situ facade stress levels

Instrumentation and Monitoring

The behavior of facade or wall elements under controlled load application often helps to establish their strength, deflection characteristics, or mode of failure. A wide variety of devices are available to measure facade strain and deflections. Computerized data acquisition systems can collect, store, and display data rapidly during the test.

Water Penetration Testing

Water leakage into the building interior is one of the most common and insidious types of facade failures. Several standards provide controlled water penetration testing methods for diagnostic tools or for proof testing to assess the facade's compliance with project specifications, standards, or codes. A standard that is commonly used for diagnostic water leak testing is AAMA 501.2-03, *Quality Assurance and Diagnostic Water Leakage Field Check of Installed Storefronts, Curtain Walls, and Sloped Glazing Systems*. A standard which is commonly used for water penetration resistance proof testing is ASTM E1105-00, *Standard Test Method for Field Determination of Water Penetration of Installed Exterior Windows, Skylights, Doors, and Curtain Walls, by Uniform or Cyclic Static Air Pressure Difference*.

Models

Testing of mockups and models may help to understand the behavior of complex building facade systems. Service loads can be duplicated while monitoring displacements and strains in a controlled environment. Loads can be increased to test the mode of failure. Tests may focus on connections or facade components of concern. Duplicating an actual failure with a mockup of the as-built elements offers verification of a failure hypothesis.

Laboratory Testing

Numerous laboratory tests are available to determine the properties of facade materials, the nature of deterioration, and the effectiveness of remedial measures.

Petrographic Microscopy

Petrography involves a standardized microscopic examination of stone, concrete, brick, or mortar based on the methods outlined in ASTM C856, *Standard Practice for Petrographic Examination of Hardened Concrete*. The objectives of a petrographic examination are to identify the presence of microscopic defects and visible indicators of deterioration; evidence of unsound or reactive aggregate, unhydrated cement, and carbonation of the concrete and mortar. Petrographic examination is also used to estimate the cement content, water-cement ratio, percent of entrained air, characteristics of the air void system, and the degree of consolidation of concrete or mortar. In general, petrography indicates the overall quality and soundness of the stone, brick, concrete, or mortar.

Chloride Content

The chloride ion content and profile (variation in chloride concentration with distance from the surface) in concrete or mortar provides quantitative evidence of the potential for corrosion of embedded steel elements. The chloride content is determined

by an acid-digestion, potentiometric titration procedure described in ASTM C1218, *Standard Test Method for Water-Soluble Chloride in Mortar and Concrete* and in ASTM C1152, *Standard Test Method for Acid-Soluble Chloride in Mortar and Concrete*.

Freeze-Thaw Testing

Sensitivity of masonry and concrete materials to cyclic freezing and thawing is measured by alternately exposing uniformly sized, critically saturated samples to temperatures above and below freezing. Deterioration is measured by weighing the samples periodically during the test to assess weight loss from fragmentation. A dynamic modulus test measures variations in the sample's resonant frequency as an early detection of internal sample degradation. Procedures for freeze-thaw testing of prepared concrete prisms are provided in ASTM C666, *Standard Test Method for Resistance of Concrete to Rapid Freezing and Thawing*. ASTM C67, *Standard Test Methods of Sampling and Testing Brick and Structural Clay Tile* provide guidelines for freeze-thaw testing of brick specimens. Saturation coefficient can also be used as a measure of the potential freeze-thaw durability of brick. The method of measuring saturation coefficient is described in ASTM C67 and the criteria are described in ASTM C216, *Standard Specification for Facing Brick (Solid Masonry Units Made from Clay or Shale)*. Saturation coefficient is the ratio of brick absorption in cold water and in boiling water. This value essentially quantifies the free pore space that is available to accommodate ice formation in the water-saturated brick body.

ORGANIZATION AND COMMUNICATION OF FINDINGS

Depending on the goal of the investigation, the report may take a variety of forms. The information provided usually follows a logical sequence from facts to opinions to recommendations. The report may start with an introduction and background. Observations and factual information gained during the investigation may be provided next. Analysis and discussion involves assessment and interpretation of verifiable facts. Finally, opinion and conclusions express the investigator's determination of the cause of the failure or condition. Reports may also include recommendations for remediation.

If a preliminary determination and early report are needed before an investigation is complete, all assumptions and limitations due to incomplete data which formed the basis of the report should be described. However, discrepancies must be explained if later investigations and evaluation of additional data leads to opinions that differ substantially from the preliminary report.

Depending on the client's needs, communication of investigation findings may also include presentations or development of physical models and court exhibits.

CONCLUSIONS

The scope and method of the facade investigation, diagnosis, and remediation will vary depending on the nature of the facade failure or non performance. The key objective is to collect sufficient reliable data in order to accurately determine the underlying cause(s) of the failure. The investigation tools and methods used should be selected to provide the most useful and accurate information in order to understand the forces and conditions leading to the failure. Facade failures can occur from a variety of circumstances; however, they occur more often with facade designs that employ overly complex features with materials, connections, and details that do not include redundant facade support mechanisms or effective wall drainage systems.

REFERENCES

AAMA 501.2-03, *Quality Assurance of Diagnostic Water Leakage Field Check of Installed Storefronts, Curtain Walls, and Sloped Glazing Systems,* American Architectural Manufacturers Association, Schaumburg, IL.

ASTM C67-07a, *Standard Test Methods for Sampling and Testing Brick and Structural Clay Tile*, American Society for Testing and Materials, West Conshohocken, PA.

ASTM C216-07a, *Standard Specification for Facing Brick (Solid Masonry Units Made from Clay or Shale)*, American Society for Testing and Materials, West Conshohocken, PA.

ASTM C666/C666M-03, *Standard Test Method for Resistance of Concrete to Rapid Freezing and Thawing*, American Society for Testing and Materials, West Conshohocken, PA.

ASTM C856-04, *Standard Practice for Petrographic Examination of Hardened Concrete*,
American Society for Testing and Materials, West Conshohocken, PA.

ASTM E1105-00, *Standard Test Methods for Field Determination of Water Penetration of Installed Exterior Windows, Skylights, Doors, and Curtain Walls by Uniform or Cyclic Static Air Pressure Difference.* American Society for Testing and Materials, West Conshohocken, PA.

ASTM C1152-04, *Standard Test Method for Acid-Soluble Chloride in Mortar and Concrete*, American Society for Testing and Materials, West Conshohocken, PA.

ASTM C1218/C1218M-08, *Standard Test Method for Water-Soluble Chloride in Mortar and Concrete*, American Society for Testing and Materials, West Conshohocken, PA.

Beasley, K.J., Greenspan, H.J., Okon, J., Ward, J. (1989), *Guidelines for Failure Investigation*, American Society of Civil Engineers, New York.

Beasley, K.J. (May 2001), Vol. 15, No. 2, *Contemporary and Traditional Wall System failures,* Journal of Performance of Constructed Facilities, American Society of Civil Engineers, Technical Council on Forensic Engineering.

Carper, K.L. (1988). *Forensic Engineering*, Elsevier Science Publishing Co., Inc., New York.

Erdly, J.L., Schwartz, T.A., (2004), *Building Façade Maintenance, Repair and Inspection*, ASTM STP 1444, ASTM International, Conshohocken, PA.

Evaluation and Repair of a Distressed Masonry Veneer Façade: A Case Study of the Litton Reaves Repair Project

J. E. Peterson[1] and T. Shelton[2]

[1]Whitlock Dalrymple Poston & Associates, P.C., 10621 Gateway Boulevard, Suite 200, Manassas, Virginia 20110; PH (703) 257-9280; FAX (703) 257-7589; email: epeterson@wdpa.com

[2]Viginia Polytechnic Institute and State University, 90 Sterrett Facilities Complex, Blacksburg, Virginia 24061; PH (540) 231-4076; email: sheltont@vt.edu

ABSTRACT

The Litton Reaves facility is a multi-use laboratory and classroom building for the Animal Science Department of Virginia Tech. Constructed in the early 1980s, the facility had been in service for almost 20 years before symptoms of distress began to appear in the exterior cladding of the building. The severity of the distress was punctuated by the partial failure of a section of oolitic limestone panel that fractured and had to be removed from the facility. This case study offers an overview of the evaluation performed on the exterior cladding system of the building and discusses the mechanisms that led to the problems in the brick and limestone veneer. The paper discusses the repair program and highlights several structural repair and sequencing challenges that were encountered due to the redistribution of forces within the veneer. Correction of nagging water penetration and air infiltration problems were sequenced and performed in conjunction with the structural repairs in order to improve the building's interior conditions while meeting the University's "design-to" budget.

INTRODUCTION

The Litton Reaves facility is a three story building on the campus of Virginia Tech consisting of a combination of classrooms, office spaces and laboratory facilities (Figure 1). In August of 1999, a portion of one of the limestone panels fractured, became loose and consequently had to be removed from the building for safety purposes. A preliminary review of the exterior cladding by University personnel identified other areas of similar distress throughout the façade including displaced and cracked exterior brick masonry, cracked and spalled limestone panels, displaced interior slabs, cracked concrete masonry interior walls and other cladding related problems throughout the facility. The University undertook an initial repair program to stabilize some of the limestone by installing threaded steel rods set in high-strength epoxy at displaced or cracked panels. Ultimately, a more in-depth investigation was undertaken to determine the underlying causes of the distress. Repairs were then

designed to restore the integrity and support of the building's exterior façade while maintaining occupancy of the facility.

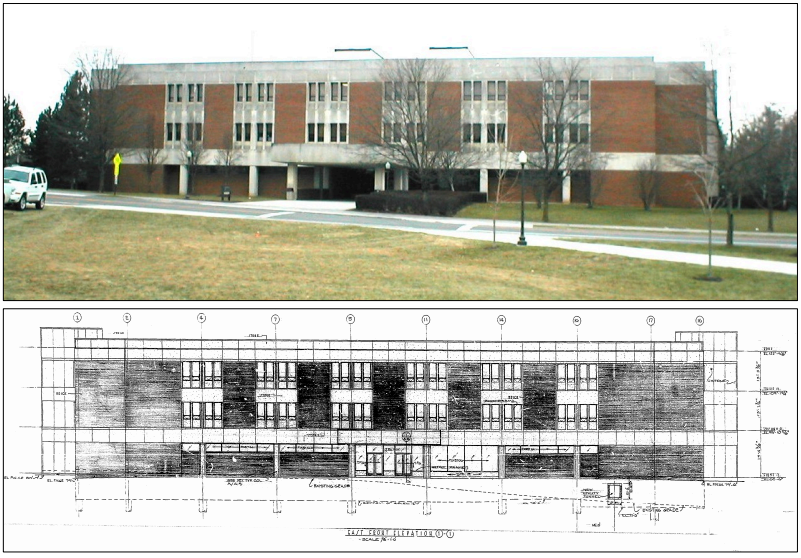

Figure 1. Litton Reaves front elevation.

BUILDING EVALUATION

The Litton Reaves building was constructed with a reinforced concrete frame founded on concrete caisson foundation systems. The exterior skin of the building consisted of brick veneer with bands of limestone panels and limestone window surrounds. The exterior veneer was supported by concrete grade beams spanning between the caissons at the first floor level and by structural steel angles connected to embedded plates at each floor line. Limestone window surrounds were supported on the exterior perimeter beams and clipped to the concrete with bolted steel angles. Figure 2 shows a typical elevation and wall section for the building at the window stack.

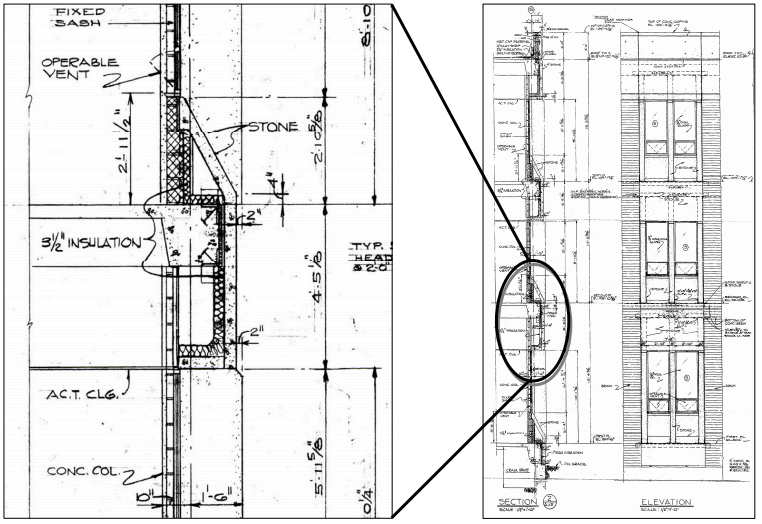

Figure 2. Typical building section and window detail.

The evaluation of the building generally consisted of a visual survey of the facade distress, probe openings at critical points of lateral and vertical restraint, water testing of exterior brick veneer and window systems, non-destructive testing of structural framing systems and material testing of façade components. The brick was found to be of generally good quality with little to no evidence of durability problems that would require a complete recladding. Localized areas of distress such as through-brick cracks and spalls were observed sporadically at the shelf angle locations and building corners. The condition of the brick at the upper floors was appreciably worse with visible cracking and out-of-plane displacement. The masonry mortar exhibited some minor shrinkage cracking, but otherwise appeared to be in reasonably good condition in most areas of the building. Occasional voids in the head joints were observed in probe openings which, combined with the shrinkage cracking, contributed to moderate rates of water penetration.

During the inspection of the limestone panels, the anchors for lateral restraint were found to be incorrectly installed into oversized holes in the panels that were not filled with mortar as recommended by the Indiana Limestone Institute. This permitted excessive free play of the panel connections prior to engaging the lateral restraint and allowed many of the panels to displace out-of-plane. The brick masonry veneer ties were located non-destructively using a pachometer (ferrous metal detector). The spacing between ties was somewhat inconsistent and there were large areas where no ties were detected, such as at the corners of the building. Random probe openings indicated that the galvanized ties displayed very little corrosion, even after 25 years of service; however, because the tie spacing was often excessive, parts of the masonry veneer were not adequate to resist the design lateral loads. Both the

limestone panels and the brick veneer would require supplemental lateral restraint to stabilize the veneer.

The original design did not include horizontal expansion joints below the shelf angles to accommodate expansion of the veneer as is required in current industry recommendations. Distress resulting from restrained differential movement was obvious and widespread. Frame shortening combined with clay brick moisture expansion had taken a severe toll on the structural integrity the cladding. Based on coefficients of volume change for these conditions, maximum relative displacements for the veneer were likely as much as 1" with almost 1/2" at the mid height shelf angles. Figure 3 schematically depicts this phenomenon and the resultant distress.

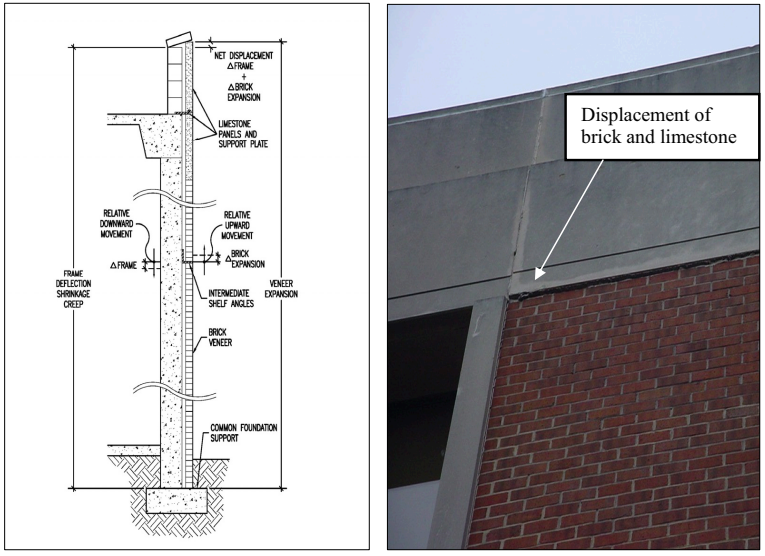

Figure 3. Schematic illustration of relative movement for brick veneer over a concrete frame and resultant displacements of brick and limestone.

The horizontal legs of the masonry shelf angles were typically set in contact with the brick below, developing internal stress as the veneer expanded into the bottom of the angle. This was most evident where hard plastic shims were found between the shelf angle and the brick below, likely to level the shelf angle. Because the shims were never removed, the compressive stresses formed between the angle and the brick crushed and split the plastic shims, leaving an indentation from the brick cores. The masonry veneer below the two plastic shims was also cracked due to the stresses generated. The original design specified bolted connections between the shelf angle and the embedded angle. However, due to irregularities in the concrete slab edges, the original bolted connection was often abandoned and the angle was welded either along the heel of the angle or along the toe of the vertical leg. Where the veneer came in contact with the shelf angles, the forces created by the restrained movement

cracked and spalled the masonry and limestone, or in some cases, distorted bolts and fractured the welds of the supporting elements. With the connection to the building severed, the masonry above the shelf angle became predominantly supported by the masonry below, thus increasing the internal stresses on the veneer of the lower levels (Figure 4).

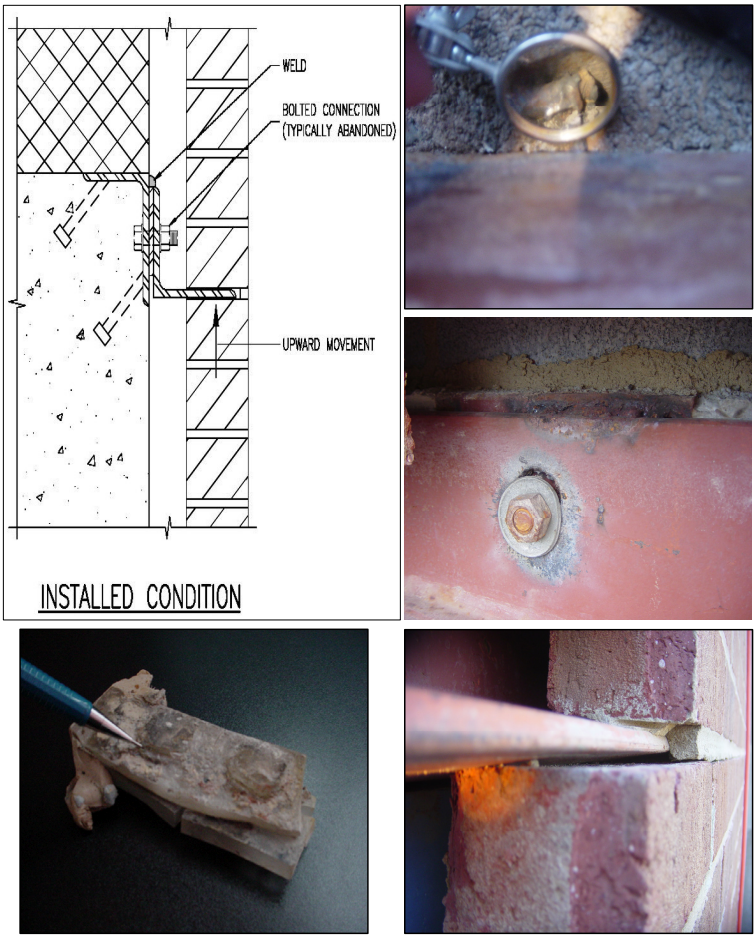

Figure 4. Restrained movement in brick veneer and resulting damage. Clockwise from top right 1) broken weld connection behind angle; 2) overstressed bolts with deformed washers; 3) rotation of shelf angle and cracking of mortar joints; 4) crushing of embedded shims with indentations from brick cores.

Limestone panels installed at the roof elevation were constructed to bear on a galvanized plate with a toe bar welded to the leading edge at the top of the spandrel beam. The inside face of the panel was notched at the bottom to receive the lipped plate connection, but no mortar was installed between the stone and the steel. On many of the panels, the front edge was observed bearing directly on top of the panel below and the panel was completely disengaged from the bearing connection. This condition resulted in fractured welds at the support points and spalling on the interior face of the panel from the masonry expansion (Figure 5).

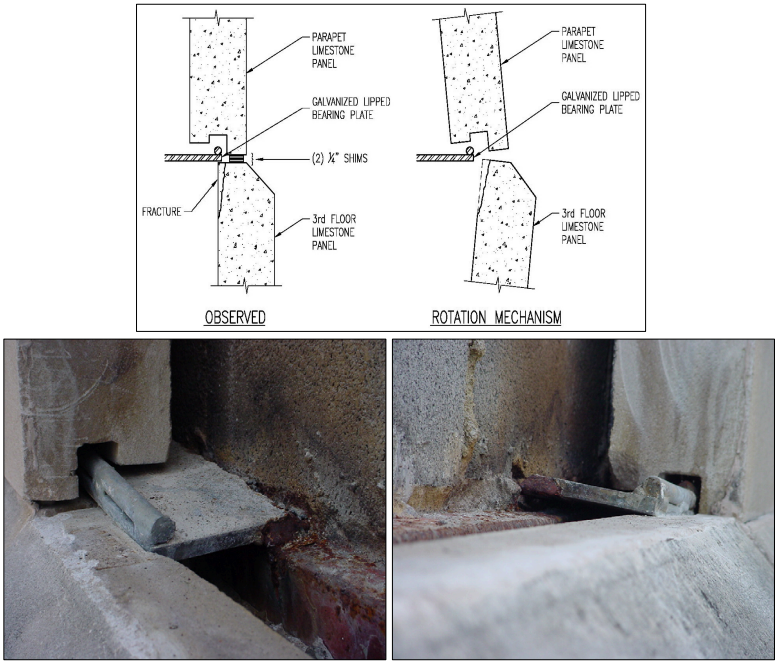

Figure 5. Condition of limestone panels at supports and broken weld on support plate.

In addition to the structural deficiencies noted in the façade, several serviceability problems were observed in the exterior wall system. Significant air infiltration through the building envelope was apparent while walking through the hallways on windy days that originated from the window systems and ceiling plenums. Severe air exfiltration was observed from the masonry cavities on the exterior due to positive building pressurization and an incomplete air/moisture barrier for the building. A study of the drawings and the interior plenum spaces above the drop ceilings indicated that there were large areas where air could migrate into the cavity of the veneer from behind the limestone panels and around the windows and doors.

Flashings were often terminated at the limestone window surrounds and other interruptions without end dams and were held back from the exterior face of the brick. The sections of the through wall flashing spanning the wall cavity were filled with mortar and often sagged in the cavity, which inhibited the drainage of water. Coping stone flashings were not terminated correctly on the leading edge, nor were they tied into the roof membrane on the back side of the parapet (Figure 6). Because of these deficiencies, testing was performed on the masonry in accordance with ASTM C1601, "Standard Test Method for Field Determination of Water Penetration of Masonry Wall Surfaces" to determine how much water would be expected to penetrate the veneer during a severe rain event. The testing revealed that the veneer was relatively permeable and would experience significant volumes of water in the cavity during periods of heavy wind driven rain. Thus, the condition of the flashing system was critical to the overall performance of the wall system and would have to be repaired.

Figure 6. Poorly installed flashing including shelf angles with missing end dams and cavity.

Sealants installed around windows, between brick and limestone, at limestone panel joints, at window perimeters and at capstone joints had all failed. The sealant texture was hard and brittle, and sealant was often cracked or extruded from the joints at material transitions due to expansion of the veneer. The sealants on the building appeared to be original, indicating that they have been in service for approximately 25 years, far beyond the anticipated service life of most sealant materials. Because there were no secondary barriers to water penetration, failures of these sealants allowed water to enter directly into the building through limestone panels above the window heads. Water damaged fiberglass insulation and water staining on the ceiling tiles were observed at several locations above and around the windows (Figure 7).

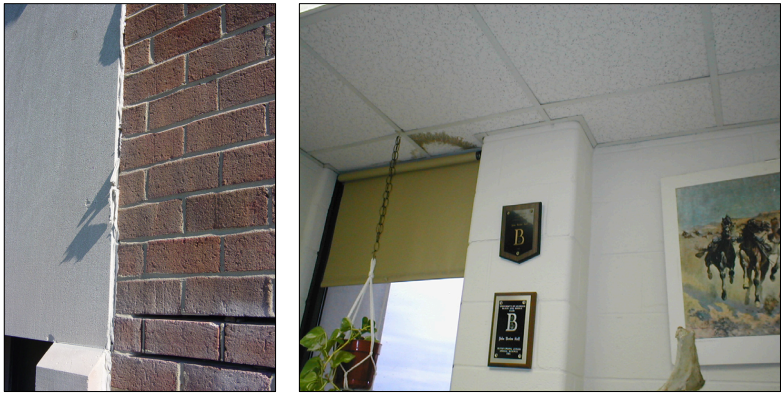

Figure 7. Failed panel sealant joints and resultant leakage over windows.

Water tests performed on the operable windows in accordance with ASTM E 1105, "Standard Test Method for Field Determination of Water Penetration of Installed Exterior Windows, Skylights, Doors, and Curtain Walls, by Uniform or Cyclic Static Air Pressure Difference" resulted in severe water penetration into the building. The leakage was the result of failed internal sealants, worn glazing and sash gaskets and ineffective weep components. Since refurbishing the windows would only solve a portion of the leakage issues during severe weather events, it was recommended that the windows be replaced.

REPAIR PROGRAM

Based on the findings of the forensic investigation, the University initiated a repair program for the building. Since funding for the program was limited, and the building was to remain occupied during the restoration, a re-cladding scenario was ruled out and a selective repair program was initiated. The repairs were prioritized based on the funds available to correct the structural deficiencies first, with the remaining funds used to improve the serviceability problems such as water management and energy losses. The program objectives were as follows:

- Re-establish reliable support of the veneer at each floor level;
- Relieve the stresses currently stored in the building façade;
- Provide for additional future movements from any residual long-term expansion and cyclic thermal movements;
- Improve the water management capability of masonry flashings and weep systems;
- Reduce the water penetration through the masonry veneer and limestone panels; and
- Replace the existing window systems throughout the building.

Coincidentally, a new stone masonry building was slated to be constructed directly adjacent to the Litton Reaves facility that would share the loading dock space and have a common wall in the southeast corner of the building. Both construction projects shared work areas and lay-down space, which required careful sequencing of

the work to prevent delays to both projects. The most significant challenge was to maintain operations in the facility during construction. Primary and emergency egress points had to be maintained at all times throughout construction. Lighted sidewalk sheds were designed to provide protection from potential overhead hazards from the distressed cladding and were erected two years prior to construction. The same systems were also designed and utilized to isolate and protect the pedestrians from the construction operations and support the scaffold systems during construction.

As the work was to be done with the veneer in place, the repairs were sequenced to incrementally reduce the load in the facade while establishing new connections to the building frame. This was performed by working in a "top down" approach on the building. Existing shelf angles were removed in sections while shoring each floor of masonry (Figure 8).

Figure 8. Shoring of existing masonry after replacement of shelf angle sections.

Because of lead based paint on the structural steel, and asbestos mastics found on the existing flashing materials, shelf angles were replaced with new galvanized steel angles bolted into the existing concrete frame. Angles were mounted to create room for future expansion and contraction of the floors below and new flashing elements were installed with hemmed drip edges and end dams at each floor to improve the water management system. After isolating and re-supporting the masonry at the top shelf angle, the process was repeated sequentially on the floors below.

The limestone panel systems around the entire perimeter of the building at the third floor and parapet levels were temporarily removed from the building to obtain access to the damaged supports. Removal of the panel systems was complicated by the fact that the building envelope was breached at each window by the removal of the limestone panels that served as the primary weather resistive barrier in these locations (Figure 9). Building occupants were temporarily relocated while the panels were removed and the repairs were performed in the area. The removal of the panels to repair the supports also facilitated access to the most severe air infiltration points and allowed for supplemental sheathing and framing to be added behind the limestone in order to seal the gap between the window head and the slab above. Once the closure panel was installed, the building occupant was free to re-occupy the office. The

entire process took approximately 3 days per window to complete from beginning to end and the impact to the office occupant was minimized where possible.

Figure 9. Removal of limestone panel exposing breach in exterior envelope and installation of envelope closure panels.

To reduce the amount of water penetration through the veneer, the mortar joints of the entire masonry exterior were tuck-pointed. This also permitted the repair of the existing masonry cracks and allowed the mortar from the repairs to the shelf angles to be replaced with the tuck-pointing, resulting in a more uniform appearance of the building façade. Because of the unusual color of the original brick, a suitable replacement could not be obtained to install where the brick could not be salvaged. Even with an approximate 80% salvage rate, new brick would be required to be blended with the old in most areas of the building. A decorative plaza perimeter wall constructed with an identical brick to the main building was demolished and the brick was salvaged to be used on the building in order to make replaced brick less noticeable.

After the project was underway, the University elected to replace all the windows in the facility as a supplemental project that ran concurrently with the repairs to the cladding. A thermally broken heavy commercial window system with low E glass was installed to further improve the energy efficiency of the building. This work was sequenced into the phasing of both the repair project and the newly constructed facility adjacent to Litton Reaves.

After the repair project and the window installation were complete, the University elected to stain the brick masonry to allow it to blend aesthetically with the stone masonry buildings in the vicinity, including the new building with which it shared a loading dock. The completed exterior facade is shown in Figure 10.

Figure 10. Elevations of Litton Reaves after installation of masonry stain.

CONCLUSION

The project was completed in 2008. The University spent approximately 2.9 million dollars on the renovation which was performed on-schedule, under budget, and with minimal disruption to the building occupants. Since the renovation, the water leakage observed through exterior walls and window systems was eliminated and the severe air infiltration experienced during the winter months was significantly reduced. On the exterior, the improvements made to the lateral and vertical support conditions, coupled with the new horizontal and vertical movement joints installed, allow the veneer to expand and contract without developing the internal stresses that led to the previous cladding failures. Recent exterior surveys of the building indicate that the lateral and vertical displacements have been arrested and there is no evidence of distressed veneer or masonry cracking. Overall, the Litton Reaves Repair project demonstrates how significant serviceability and energy efficiency improvements can be implemented into a structural and architectural repair program without imparting substantial additional costs to the project.

REFERENCES:

Indiana Limestone Institute of America, Inc., Bedford, Indiana
Brick Industry Association Technical Notes 18 and 18A (2006). “Volume Changes – Analysis and Effects of Movement.” Brick Institute of America, Reston, Virginia
ASTM International, West Conshohocken, Pennsylvania

To Seal or not to Seal
A Practical Study of Masonry Surface Treatments

Michael J. Drerup, P.E., SECB, LEED AP, M. ASCE[1]
Alicia E. Díaz de León, S.E., AIA, LEED AP, M. ASCE[2]

[1]Senior Managing Engineer, Exponent Failure Analysis Associates, Inc., 17000 Science Drive, Suite 200 Bowie, MD 20715; PH (301) 291-2500; FAX (301) 291-2599; e-mail: mdrerup@exponent.com
[2]Structural Engineer and Architect; e-mail: alicia.e.diazdeleon@gmail.com

ABSTRACT

An 80-year-old school building in Brooklyn, New York, with pervasive water leakage and deteriorating brick exterior walls was a potential candidate for a treatment to stabilize and seal the surface. The building continued to experience extensive water leakage despite the recent installation of a new roof and flashing repairs. An investigation was conducted to evaluate the cause of the leakage and to evaluate the potential effectiveness of four prospective surface treatments to seal or consolidate the brick. Each of the four products tested was a commercially available proprietary product specifically marketed for use on brick masonry.

This paper presents the findings of our field and laboratory studies, which identified critical defects in the extensive recent repair work, and indicated that surface treatment of the brick masonry was inadvisable.

INTRODUCTION

Masonry surface treatments have been around almost as long as masonry itself. More than 2,500 years ago the ancient Babylonians mastered the art and science of glazed masonry, and their craft can still be seen in the reconstructed Ishtar Gate now in Berlin's Pergamon Museum (Figure 1). Many of the ancient bricks are still in remarkably good condition, their glazing and color still intact. Glazed brick continues to be popular to this day.

On the other hand, masonry surface treatments are often less successful. The authors recently observed a late 19th century firehouse in Utica, New York with newly painted brick exterior walls. The front wall, which had been painted many decades ago, continues to perform well, but a previously uncoated side wall exhibited widespread deep spalling within a year of painting (Figure 2). In some cases entire bricks had disintegrated as a result of improper coating.

To understand why some surface treatments are successful while others are quite harmful, it is important to understand the characteristics of the brick, the surface treatment used, the performance and maintenance history of the brick, and the service environment. Of particular importance are the porosity and pore structure of the

brick, whether the surface treatment is fired into the brick (i.e. a glaze) or applied later, and the extent to which the brick is exposed to moisture and cyclic freezing.

Figure 1. The Ishtar Gate at the Pergamon Museum in Berlin.

Figure 2. Brick deterioration on a previously uncoated masonry wall at a late 19th Century firehouse in Utica, NY.

This paper presents the findings of field and laboratory studies of an 80-year-old brick masonry school building that exhibited visually severe surface deterioration and continued water intrusion despite numerous apparently reasonable attempts to repair the exterior masonry walls. After these unsuccessful attempts, a surface treatment was being considered and one goal of the studies was to determine if a masonry surface treatment could be a successful repair for this building.

BACKGROUND

New York City is home to the largest public school system in the United States, with more than 1,200 buildings serving over one million students. These buildings form a rich practical workshop representing construction technology from four centuries, dating as far back as 1786 and continuing into the 21st century. Over a five-year period the authors investigated building performance problems at dozens of schools throughout the city. Many of these investigations focused on long-term deterioration and water intrusion through exterior multi-wythe masonry walls.

Figure 3. Overview of the school.

The building discussed in this paper is a primary school constructed circa 1924 located in the Bensonhurst section of Brooklyn. The school is about two miles north of the Atlantic Ocean and one mile east of Lower New York Bay. The building has a steel frame encased with multi-wythe brick masonry and is representative of dozens of New York City school buildings currently in use (Figure 3). The building had exhibited water leakage and deterioration of the exterior brick masonry.

INVESTIGATION

Field Investigation

The field investigation consisted of a visual condition survey, interviews with school staff about the maintenance and service history of the building, assessment of existing interior leaks, controlled water spray testing, and inspection openings. Numerous areas of limited masonry replacement were observed; these included narrow, generally vertical bands of newer brickwork consistent with crack repair, and horizontal sections of replacement brickwork at some window heads, indicative of flashing installation and replacement or repair of steel lintels. Custodial staff reported that the school had been painted for about 20 years, and that the paint had been

stripped within the past 2 years. Close observations revealed a few fragments of paint still adhered to the brick. The brickwork had an uneven surface texture and appearance because portions of the hard-fired surface had spalled away and exposed the lighter-colored bisque.

Six representative areas of the exterior masonry walls were spray tested to evaluate potential water infiltration points and potential paths of water migration within the wall system. The selected test locations were areas of known water leakage, both with and without visible masonry repairs. Testing was conducted using a calibrated grid of spray nozzles, and was based on ASTM E1105 *Standard Test Method for Field Determination of Water Penetration of Installed Exterior Windows, Curtain Walls and Doors by Uniform or Cyclic Static Air Pressure Difference* (ASTM E1105). Tests were performed without an applied air pressure differential. The testing replicated reported leakage at window heads and through the roof parapet walls.

Inspection openings were made in the masonry wall at or near locations where leakage was observed during spray tests. An opening at a window head with no evidence of prior repairs, revealed an absence of flashing at the window lintel (Figure 4). An opening at a rebuilt window head revealed flexible PVC flashing that lapped onto the vertical leg of the steel window lintel but did not turn onto the horizontal leg and did not have end dams (Figure 5).

Figure 4. Opening at unrepaired window head

Figure 5. Opening at rebuilt window head

Figure 6. Opening at inside of parapet wall

Figure 7. Opening at inside of parapet wall

Two additional openings were made at the inside of the masonry parapet wall, just above the roof flashing (Figures 6 and 7). These openings revealed that new sheet metal flashing had been installed one course of brick above the original internal copper flashing, which remained in place. The new flashing was surface mounted, while the original copper flashing was installed through the full thickness of the outer wythe of masonry. Water traveling through the masonry could bypass the newer flashing and be directed under the roof when it reached the older, lower flashing because of this configuration.

The field investigation demonstrated that defects in the design and execution of repair work, especially at roof and window head flashings, were causing continued water intrusion.

Laboratory Studies

A program of laboratory observation and testing was performed to evaluate the durability of the existing brick and the potential effectiveness of a water repellant or consolidating surface treatment. The purpose of the studies is to help understand the characteristics of the brick and its interaction with the proposed surface treatments. These studies included visual and microscopic observation, and physical testing for initial rate of absorption (IRA), saturation coefficient (SC), and freeze thaw resistance (FT). Approximately 100 bricks were extracted from the north and south exterior walls of the rooftop mechanical room walls for testing, with roughly equal numbers removed from each wall to represent different weather exposures. The brick specimens were divided into five groups for physical testing – one control group and four groups that were treated with different surface treatments, as indicated in Table 1. Laboratory studies were based on applicable ASTM Standards current at the time of the investigation. The details and results of these studies are discussed in the following sections.

Product Type	Location	IRA[1]	SC[2]	FT[3]
Control-Untreated	A	1.3720	0.7476	Pass
	B	6.1097	0.7044	Pass
40% Silane Sealer	A	0.2117	0.0626	Fail
	B	0.1493	0.0560	Fail
90% Water Repellant/10% Consolidant Hybrid	A	0.3623	0.0386	Fail
	B	0.1503	0.0376	Fail
10% Water Repellent/90% Consolidant Hybrid - 1	A	0.2193	0.1286	Fail
	B	0.2293	0.1106	Fail
10% Water Repellent/90% Consolidant Hybrid - 2	A	0.1507	0.0792	Fail
	B	0.2293	0.0468	Fail

[1] Per ASTM C-67, grams per 30 sq. in. of contact surface per minute
[2] Per ASTM C-67, ratio of cold water absorption to boiling water absorption
[3] Per ASTM C-666, Method B and ASTM C-216 failure criteria

Table 1 - Summary of Brick Testing Results

Brick Testing

Bricks extracted from the two sample locations were tested in accordance with ASTM C67 *Standard Test Methods for Sampling and Testing Brick and Structural Clay Tile* for absorption and saturation and ASTM C666 *Standard Test Method for resistance of Concrete to Rapid Freezing and Thawing* for freeze-thaw resistance. Test results were evaluated based on ASTM C216 *Standard Specification for Facing Brick (Solid Masonry Units Made from Clay or Shale)*.

Visual and microscopic laboratory observations of brick samples indicated that they had a low-to-moderate IRA and appeared to be reasonably well fired. The bricks exhibited minor, randomly distributed cracking, a characteristic typical of un-cored brick units. They appeared to have good bond characteristics, but exhibited significant local variation in properties, including porous nodules and voids. These nodules and voids can collect and hold water, increasing the potential for local FT induced fractures.

Absorption testing of the brick samples based on ASTM C67 *Standard Test Methods for Sampling and Testing Brick and Structural Clay Tile* yielded saturation coefficients between 0.600 and 0.839. ASTM C216, *Standard Specification for Facing Brick,* requires an average SC of 0.78 for new Severe Weathering (SW) grade brick, with no single value exceeding 0.80. The testing indicates that the bricks are fairly durable since they nearly meet this standard even after 80 years of service. FT testing confirmed these findings; no failures were induced by FT testing of the control group or untreated bricks (see Table 1).

Sample groups of bricks from each weather exposure group were prepared with each of four prospective surface treatments that represented various combinations of water repellents and consolidation products. These products were being considered to limit interior water leakage and control continued surface deterioration of exterior bricks. Each surface treatment product evaluated was specifically marketed for use on brick masonry. A control group of untreated bricks was also included in the test regimen for each exposure for comparison purposes and to evaluate the properties of the bricks further.

The Products

The products tested were water repellents, consolidants, or combinations of the two. Water repellents are penetrating substances specified for use on masonry surfaces to limit ingress of water and waterborne contaminants by chemically bonding water repellent molecules onto the surface. Consolidants are typically ethyl silicate/silane (or similar) treatments that penetrate into deteriorated masonry surfaces by “replacing” the natural binding materials while protecting the treated surfaces from further deterioration. The first product was a widely used water repellant silane sealer. The second product was a hybrid of 10% water repellent and 90% consolidant. The remaining two products were each 90% consolidant and 10% water repellent.

Initial Rate of Absorption

The IRA is the weight of water absorbed (expressed in grams per 30 sq. in. of contact surface) when a brick is partially immersed for one minute in accordance with ASTM C67. It indicates how "thirsty" the bricks are when initially exposed to water. IRA can also be evaluated qualitatively by placing a drop of water on the surface of the brick. A brick with a high IRA will absorb the water quickly, and may appear dry after a few seconds. A water drop placed on a brick with a low IRA will absorb the water much more slowly, and it may form a bead on the surface. The tests indicate that the untreated bricks have a low-to-moderate IRA, which is considered desirable. Values obtained for individual samples vary significantly within this range. All surface treatments substantially reduced IRA values. These reduced values, however, do not necessarily represent increased durability.

Saturation Coefficient

The SC is the ratio of the weight of water absorbed by a masonry unit during immersion in cold water to weight absorbed during immersion in boiling water. This test provides an indication of the probable resistance of brick to cyclic freezing and thawing because water expands both during freezing and boiling. All surface treatments substantially reduced SC values. These reduced values, however, do not necessarily represent increased durability. As revealed by the freeze-thaw testing described below, every surface treatment tested actually reduced the durability of the brick; even though surface treatments may keep water out of the brick, they may also trap water inside the brick.

Freeze-Thaw Resistance

All samples were tested using ASTM C666 Method B, which specifies freezing in air and thawing in water. The failure threshold for the brick samples tested, however, was defined using ASTM C-216 criteria as having individual units that separate or disintegrate resulting in a weight loss greater than 0.5% of its original dry weight or develop a crack that exceeds the unit's least length dimension for Grade SW bricks. Samples were subjected to 54 freeze-thaw cycles at a rate of 6 cycles per day. After freeze-thaw testing, the control (untreated) group exhibited no failures. Every treated group exhibited a high rate of failure. Failure modes included fracturing and surface disintegration. There was no significant difference in the failure rate between sample groups from each of the two exposures. Table 1 summarizes the average results of the laboratory studies.

Test results indicated that all of the tested surface treatments would adversely affect the durability of the brick, and that the untreated bricks are in better condition than they appear. All of the surface treatments likely trapped moisture beneath the face of the brick rather than allowing the moisture to evaporate. In cold weather, trapped moisture freezes and expands, creating fracture stresses within the brick (Figure 8), as likely occurred in the Utica firehouse case discussed in the Introduction.

Figure 8. Fractured surface-treated brick unit after freeze-thaw testing.

DISCUSSION

When confronted with a leaking building with porous brick walls, applying a sealer or consolidant can seem like an attractive option. Unfortunately, surface treatments typically provide little long-term benefit, and leave fundamental underlying conditions unaddressed. Furthermore, any treatment that keeps water out may also keep water in. Brick masonry is inherently porous and naturally absorbs and releases water in response to rain and variation in humidity. When the masonry is sealed, water inside the wall may become trapped and exacerbate deterioration, especially in a freeze-thaw environment.

Flashing systems are highly vulnerable to workmanship deficiencies, and these deficiencies are easy to hide, because they are quickly concealed during the construction process. Consequently, flashings always need to be evaluated as a culprit in any leakage investigation. Other sources, including roof and parapet leaks, and even plumbing leaks should be considered. If a thorough water leakage study indicates that water absorption through the masonry is the primary culprit, all other significant sources of water leakage have been repaired, and provisions have been included to allow water to drain from within and behind the masonry (i.e. through-wall flashings and clear weep openings), it may be time to consider sealers, although cautiously. Materials studies such as the one presented here should be done to evaluate the compatibility of the proposed sealer with the brick or other masonry material.

CONCLUSION

In lieu of surface treatments, correctly detailed and executed flashing installation, selective reconstruction, tuckpointing, and selective overcladding can abate water intrusion through masonry walls. These approaches should always be explored first. Flashings should have end dams and drip edges. Selective reconstruction will be necessary only on units severely distressed due to cracking, separation, and out-of-plane displacement. Tuckpointing must have the proper pointing depth, mortar mix and application technique to prevent water penetration through joints. Selective overcladding, using either stucco or metal panels, particularly at roof bulkheads and parapets, can help address flashing deficiencies, protect the brick and create a new waterproofing layer. Copings should be sealed properly or protected with a metal cap where necessary.

Masonry sealers should be considered only after the other available options are explored and as determined through investigation and testing. The field investigation of the Brooklyn school building showed that improper flashing and poorly performed masonry repairs contributed significantly to the water intrusion problems. In addition, the laboratory study of bricks taken from this building and treated with commonly used surface treatments indicated that these treatments would adversely affect the brick.

ACKNOWLEDGMENTS

The authors extend their appreciation to their colleagues at Wiss, Janney, Elstner Associates, Inc. who participated in this study, especially Lisa Backus and Ross Martinek. Their expertise and collaboration were indispensable.

REFERENCES

Trachtenberg, M. & Hyman, I. (1986). Architecture: From Pre-History to Postmodernism. Prentice Hall, Englewood Cliffs, New Jersey.

"Standard Test Method for Field Determination of Water Penetration of Installed Exterior Windows, Skylights, Doors, and Curtain Walls, by Uniform or Cyclic Static Air Pressure Difference." ASTM E1105. ASTM International, West Conshohocken, PA

"Standard Test Methods for Sampling and Testing Brick and Structural Clay Tile." ASTM C67. ASTM International, West Conshohocken, PA

"Standard Test Method for Resistance of Concrete to Rapid Freezing and Thawing." ASTM C666. ASTM International, West Conshohocken, PA

"Standard Specification for Facing Brick." ASTM C216. ASTM International, West Conshohocken, PA.

The Bussey Railroad Bridge Collapse

By

Steven M. Pennington, PE, PLS, MASCE
Associate
Facility Engineering Associates
Fairfax, Virginia
pennington@feapc.com

Abstract

On March 14, 1887 a Boston bound train, near full capacity and after departing Roslindale Station, crossed an iron frame bridge. The locomotive along with the first three cars safely crossed but the remaining six cars fell to the street below as the bridge collapsed. Failure of two iron hangers was the cause, however contract mismanagement on the part of the railroad company was an underlying factor. This paper presents an overview of the Bussey Bridge collapse, its historical background, the engineering and construction.

Introduction

Bridges are among the most public of all engineering structures. They are visual and, in many respects, the most dramatic of all engineering structures. They provide both function and art and when one collapses it brings immediate public reaction. Bridge failures happen swiftly, they present a somewhat horrifying visual image and more often than not, the loss of life. When considering the complex nature of bridge dynamics, failure invariably results from a small detail. Attention to detail, whether in design or construction is a frequent scenario throughout the historical record.

Robert Stephenson, the famed 19th century British engineer offered these words;

> nothing was so instructive to the younger members of the profession, as records of accidents in large works, and of the means employed in repairing the damage. A faithful account of those accidents, and of the means by which the consequences were met, was really more valuable than a description of the most successful works… (Hammond, 1956)

Today, the demand for bridges higher, longer and more economical pushes the limits of engineering design and construction. However, the historical background remains a knowledge base and Stephenson's words provide a useful segue to the importance of examining historical failures.

The Bussey Bridge Historical Background

The Boston and Providence Railroad was founded in 1831 to link the two cities. The first section of track was completed in 1834 connecting Boston with Canton and a branch line to Dedham, Massachusetts. The remaining track was completed to Providence in 1835, where by 1837 a ferry would take the cars across the Providence River for connections to New York City. [1]

The branch rail line to Dedham traversed the Massachusetts country side stopping at Spring Street, West Roxbury, Highland, Central, Roslindale, Forest Hills and other points northward on its route into Boston. Between Roslindale and Forest Hills the route crossed South Street on a bridge referred to as the Bussey Bridge. (See Fig. 1a and 1b)

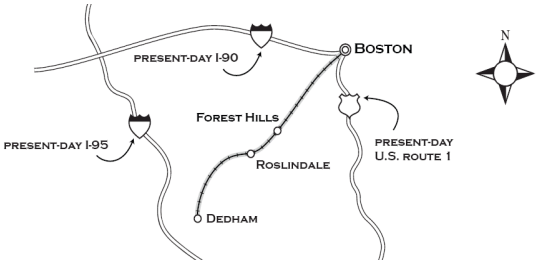

Figure 1a

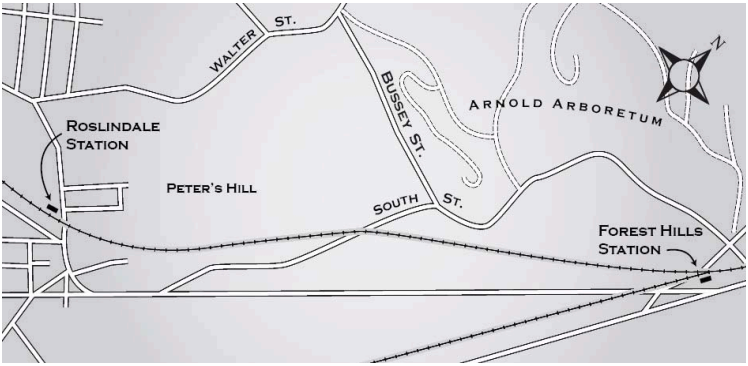

Figure 1b.

The bridge alignment is skewed at an oblique angle, near sixty-five degrees from the perpendicular and, in its original form, was a Howe type wooden deck truss with the record not giving an original construction date. (See Fig. 2) At some point in the past individual wooden truss members were covered with tin sheeting as protection from both water and fire.

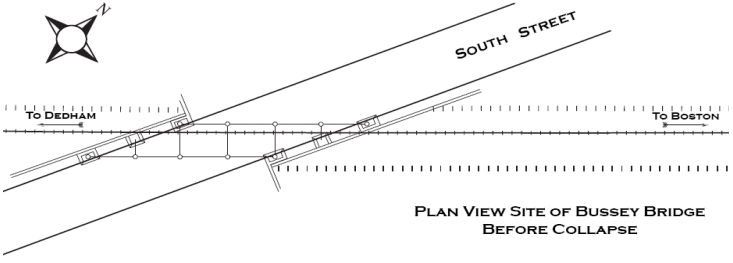

Figure 2

In 1870 the wooden truss on the west side was replaced with an iron truss creating a mix of materials, one truss of iron and one of wood. In 1876, the remaining wooden truss was removed, the existing iron truss moved to replace it and a new iron truss erected to take

the place of the other. The original iron truss which replaced the first wooden truss was manufactured by the National Bridge Company with a design by C.H. Parker. It was a rectangular truss with iron components. The new iron truss was manufactured by Metropolitan Bridge Company with a design by Edmund H. Hewins. In this bridge configuration the Parker truss was on the east side of the bridge with the Hewins truss on the west. (See Fig. 3)

Figure 3 – Looking south, Hewins truss in the fore-ground.

The bridge crossed South Street with a single track but was planned for a second. The design distance between trusses was twenty feet (6.1 m) with the perpendicular span between abutments on the order of seventy-five feet (22.9 m). The horizontal track alignment comprised a short tangent section for the crossing with a two degree curve on the southern side and a 3 degree curve on the northerly side. As the road bed approached the crossing from the south the vertical alignment had a downgrade of just under 1%. [2]

The Incident

It was early Monday morning with a generally heavier passenger volume than other days. Leaving Dedham the engine and tender pulled nine passenger cars. Later in the run, as

the train stood in the Roslindale station, the passenger count stood at slightly under 300 and due to the day and time there were relatively no children on board. The train was half way to Boston when out from Roslindale the train approached the Bussey Bridge over South Street.

There were few witnesses due to the early hour. The engine and tender successfully crossed the span along with cars one, two and three. As the fourth car crossed, the bridge collapsed pulling the undercarriage of the fourth into the void below leaving only the roof of the fourth on the tracks above. The shearing of the fourth caused the first three to derail and further causing the engine to separate from the tender. With their forward momentum the trailing five cars all plummeted onto South Street with car five landing on, the now roofless, car four. (See Fig. 4)

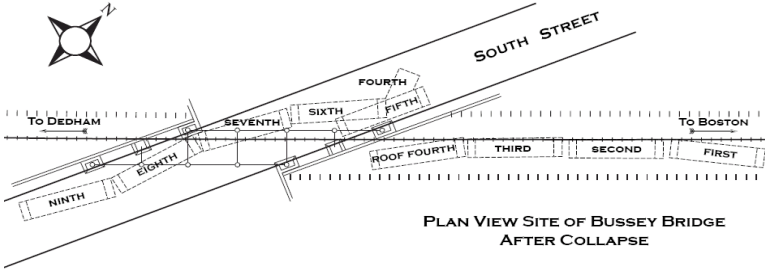

Figure 4

The construction of typical passenger cars contributed to the injury and fatality count. Those cars, which fell onto South Street, were found to be ripped apart, upside down,

twisted and one on top of the other. Of the near 300 passenger count just under half were either killed or injured with 23 deaths and over 100 injured, many of them seriously.[3]

The Investigation

The Massachusetts Board of Railroad Commissioners convened the following day to investigate. The resulting report alluded to improper oversight during bridge component fabrication, field construction and maintenance with allegations of impropriety leveled at the railroad, the bridge company and the designer.

In 1876, when the Parker truss was moved from the west side of the bridge to the east, a new iron truss was contracted by the railway company for which two bids were received. One bid from the National Bridge Company, with a Parker design, and a second bid from the Metropolitan Bridge Company, represented by Edmund Hewins. The Metropolitan, with Hewins as its agent, won the award.

In actuality the Metropolitan Bridge Company did not exist. It was the intention of Edmund Hewins to form his own bridge company of that name, but at the time of the contract award the company did not exist. Hewins prepared design plans and arranged for truss fabrication at the Trenton Iron and Steel Company with some of the components manufactured elsewhere, specifically tension members. The truss components were field erected at the site by the railway company under the supervision of Hewins who had total control of every aspect of fabrication. The railway company did not undertake, either on

its own behalf or by a third party, any oversight of the Hewins design or the quality of manufactured materials.

Further complications resulted from the skew of the bridge alignment. As a train approached the span there would be a brief moment when only one truss carried the full load. The single track was situated on the Hewins truss side. The Hewins design also had a peculiar joint detail. At certain locations in the top chord there were cast iron joint blocks from which the tension hangers were pinned. (See Figs. 3 and 5) These joint blocks were at compression points of the top chord with primary diagonals. The diagonals were comprised of built up standard sections and from the joint blocks short tension hangers were used to suspend the floor beams. [4]

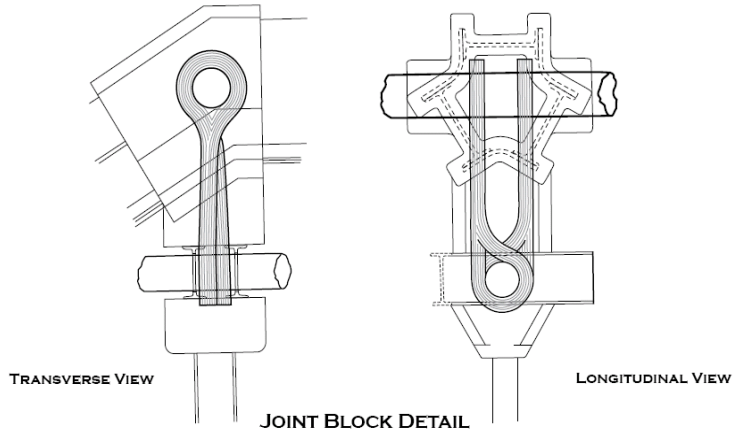

Figure 5 see also Figure 3

The Cause

Collapse of the bridge occurred with failure of the Hewins truss. Fracture occurred in two of the short tension hangers in the top chord joint blocks. These tension hangers were in the form of iron rods with a curved eye at each end for a pin connection with the truss members. The "joint blocks" were integral to the connections between compression members of the top chord and contained a pocket where the top eye of the tension hanger was inserted and held with a pin.

The disadvantage of such a design was it prevented visual inspection of the pinned connection. The rods were also loop welded and not drop forged with the hooked eye non-symmetric with the shaft of the rod, thus creating an eccentric loading condition. (See Fig. 6)

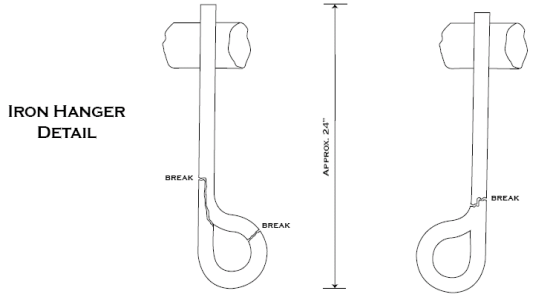

Figure 6

Failure occurred at the north end of the Hewins truss with fracture of the tension hanger eyes inside the joint blocks. Evidence revealed the collapse may have been instantaneous but distress to the rods had been ongoing for some time due primarily to strains resulting from the combination of materials, hanger rod size and eccentric design. [5]

The Board Recommendations

The Board of Railroad Commissioners' admonished the railway company for not investigating the bridge building contractor revealing that all the parties involved were shown to not have adequate bridge building experience and engineering experience in both design or specification. There was no oversight of construction by the company, no materials testing and no bridge inspection program.

General recommendations were made for proper engineered bridge design and construction to be followed by inspection. These were made in light of the trend, at the time, for increased railway loadings. The Board further recommended legislation requiring all railway companies to inspect their bridges once every two years by a competent and experienced civil engineer.[6]

Conclusion

To paraphrase Robert Stephenson's words; the accidents of our predecessor engineering professionals provide lessons. In the case of the Bussey Bridge the times were different, the materials were different and construction methods differed but the lessons are there none the less. It becomes apparent with a study of the Bussey Bridge collapse there were two common themes lacking; diligence and professionalism. Two attributes, which go without saying, are necessary for today's engineering professional.

Holt Hammond in his book *Engineering Structural Failures*, although dated, puts a perspective on the relevance of studying and understanding historic failures;

> "Some of the most spectacular structural failures in engineering history have been those suffered by bridges and although the loss of life on some of these occasions was deplorable, lessons of the most far reaching and permanent value have been gained." (Hammond, 1956)

Phrased with other words, great works are not in of themselves the teaching tool but rather it is the journey getting there.

Endnotes

1. Wikipedia, "Boston and Providence Railroad," 2009.
2. Sweeney, Edward J. "The Bussey Bridge Disaster," 1975.
3. Railroad Commissioner's Report, 1887.
4. Ibid.
5. Ibid.
6. Ibid.

Illustration Credits

Figure 1a. Joan Pennington
Figures 1b, 2, 4, 5 and 6. Joan Pennington, adapted from Investigative Report, in the public domain
Figure 3. Investigative Report, in the public domain

Reference Material

Hammond, Holt, 1956, *Engineering Structural Failures*, London: Odhams Press Limited.

Massachusetts Board of Railroad Commissioners, 1887, *Bussey Bridge Investigation*, Boston.

"A Miserable Death Trap; The Bussey Bridge Faulty in Construction," *The New York Times*, March 27, 1887.

Sweeney, Edward J. "The Bussey Bridge Disaster," *Yankee Magazine*, March 1975, p.66.

"The Bussey Bridge Disaster," *The New York Times*, May 1, 1887

Wikipedia."Boston and Providence Railroad," (2009), http://en.wikipedia.org/wiki/Boston_and_Proficence_Railroad.

Assessing the Vulnerability of Large Critical Infrastructure Using Fully-Coupled Blast Effects Modeling

Larry McMichael[1], Ph.D., Charles Noble, Ph.D., Jonathan Margraf,
and Lee Glascoe, Ph.D., P.E., Assoc. M. ASCE
Lawrence Livermore National Laboratory
Livermore, California, USA
[1] PH: 925-423-4911, e-mail: ldmcmichael@llnl.gov

Abstract
Structural failures, such as the MacArthur Maze I-880 overpass in Oakland, California and the I-35 bridge in Minneapolis, Minnesota, are recent examples of our national infrastructure's fragility and serve as an important reminder of such infrastructure in our everyday lives. These two failures, as well as the World Trade Center's collapse and the levee failures in New Orleans, highlight the national importance of protecting our infrastructure as much as possible against acts of terrorism and natural hazards. This paper describes a process for evaluating the vulnerability of critical infrastructure to large blast loads using a fully-coupled finite element approach. A description of the finite element software and modeling technique is discussed along with the experimental validation of the numerical tools. We discuss how such an approach can be used for specific problems such as modeling the progressive collapse of a building.

Introduction

The ramifications of structural failures extend far beyond the lost physical use of the structure. The World Trade Center collapse, New Orleans levee failure, and Minneapolis I-35 bridge failure are just three recent examples of the psychological and financial impacts that the loss of critical infrastructure can have on regional and national economies. The MacArthur Maze I-880 overpass collapse from a gasoline tanker collision and resulting fuel fire highlights our infrastructure vulnerability to accident scenarios that can result from its normal everyday use. The terrorist use of explosives against buildings and transit systems is illustrated by the bombings at the Marine barracks in Beirut (1983), Murrah Federal Building (2000), and U.S. embassies in Kenya (1998), Tanzania (1998), and Yemen (2008) and train bombings in Madrid (2004), Mumbai (2006), and Russia (2007). Understanding critical infrastructure vulnerabilities to accidents, natural hazards and directed terrorist attack is recognized as a topic of national concern.

Considerable efforts have been made to understand the evolution of progressive damage in large infrastructure (e.g. NIST, 2005), the uncertainty in failure analysis (Fong, 2006), and the probabilities associated with system reliability during progressive failure (Guers, 1988). The federal government has adopted design guidelines (GSA, 2005 and DoD, 2005) that use a threat independent methodology to reduce the progressive collapse potential for new and retrofitted federal facilities. These efforts reflect the need to understand how blast energy is imparted to a structure, the initiation of local (component) failure, damage evolution as loads are redistributed, and the overall structural stability of a damaged structure.

Vulnerability Assessment Process

Modeling the nonlinear, dynamic response of large-scale infrastructure from explosive detonation to final structural stability is a computationally demanding endeavor. As a national science and technology laboratory operated for the Department of Energy (DOE), Lawrence Livermore National Laboratory (LLNL) has the computational resources and finite element software capabilities that enable high-fidelity simulation of critical infrastructure to a range of dynamic insults. LLNL's approach for assessing the terrorist threat to structures leverages a history of high-fidelity infrastructure analysis that extends back to the 1970s with assistance to the Nuclear Regulatory Commission (e.g. Bohn et al 1984) and DOE complex (e.g. Coats et al 1981) on earthquake safety. LLNL has also been actively involved in assessing the seismic safety of buildings, bridges and dams (e.g. McCallen and Romstad 1994; McCallen and Astaneh-Asl 2000; and Noble and Nuss 2004). The approach used by LLNL engages a multi-disciplinary team of engineers (civil, mechanical, geotechnical), physicists, computer scientists, geoscientists, and statisticians. Extensive experimental facilities for high explosive research, development, and testing at LLNL's High Explosives Applications Facility complement the available computational resources. This unique combination of personnel, computational resources, and experimental facilities enables LLNL to perform a complete characterization of threats, vulnerabilities, and countermeasures for critical infrastructure.

Blast effects modeling is an integral component of the vulnerability assessment process which uses a systematic approach to determine infrastructure vulnerability and assist stakeholder decisions. A system level analysis evaluates the system as a whole and establishes the overall consequences from a particular, local, component failure. Component level analysis determines the threat required to initiate a specific failure. Risk, adversary and consequence analysis allows for countermeasure prioritization. This approach allows threat considerations to be tailored to the type of infrastructure and any unique site/system characteristics.

The process begins by identifying what kinds of threats are of concern (explosives, shaped charges, fire events), what structures are likely to be the most vulnerable (age, construction technique and materials, accessibility), and which vulnerabilities have the highest consequence (casualties, economics). Threat size and type are influenced

by facility access and physical constraints. For example, a transit system may be more susceptible to a man portable explosive, while a building might be easily subjected to a vehicle borne explosive. A detailed vulnerability assessment is then performed to determine how vulnerable a specific structure is to high consequence threats. A finite element model of the structure is developed and high-fidelity, physics based, structural analysis is performed to simulate exposure to a variety of dynamic insults, e.g. vehicle impact, explosive detonation, explosively formed projectile. Stochastic inferences can be made from analysis results to evaluate confidence levels and estimate uncertainty (Glascoe et al 2009; Koutsourelakis et al 2006). The process continues by identifying practical countermeasures and the Concept of Operations (CONOPS) required to effectively protect the structure. Countermeasures for structurally robust structures may focus on security and response enhancements, while countermeasures for weaker structures will also include bounding vulnerabilities and developing actionable mitigation strategies. A detailed countermeasure evaluation is performed using systems analysis, high-fidelity modeling, and stochastic inference to determine the effectiveness of a particular countermeasure. The countermeasure is evaluated not only with respect to its effectiveness to mitigate a threat, but also how well it works with CONOPS and maintains system functionality.

Finite Element Analysis Software

Vulnerability assessments are performed using two finite element analysis codes developed by LLNL: ParaDyn (DeGroot et al 2008) for system level response to structural failures and ALE3D (Nichols 2008) for fully coupled blast analysis. ParaDyn, the parallel version of DYNA3D (Lin 2007), is an explicit, transient dynamic analysis code for solid and structural mechanics which uses a Lagrangian formulation. Component failures can be accommodated through element erosion and the conversion of failed elements into SPH particles which preserve the system's mass and momentum balances. The SPH particles can interact with other particles and intact elements which provides a means to transfer the kinetic energy of failed components into other parts of the structure.

ALE3D is an arbitrary-Lagrangian-Eulerian hydrodynamic analysis code that simulates the fluid and elastic-plastic material response. The code incorporates continuum mechanics, thermal diffusion, chemistry, incompressible flow, multiphase flow, and magneto-hydrodynamics. The detonation energy released by the explosive is represented using a Jones-Wilkins-Lee (JWL) equation of state (Dobratz 1981). The resulting shock wave is propagated through the surrounding medium (e.g. air or water) using advection and mesh relaxation techniques to allow material flow through the mesh without tangling elements. The code tracks the wave propagation and interactions (reflections), so the blast pressures applied to the structure vary temporally (arrival time) and spatially (stand-off distance) as the blast wave travels over and around the structure. The materials representing the structure can be held Lagrangian to best preserve material history parameters or allowed to advect if extensively damaged.

Several material models are available in both codes to represent the component materials' deviatoric strength and pressure-volume relationship (i.e. equation of state). Structural components can be modeled using a combination of beam, shell, and solid elements. Steel members are often modeled using beam elements with user defined integration rules to represent the joist, girder, and column cross-sections and account for partial yielding through a cross-section. The constitutive response is represented by an isotropic plasticity model; there are options for bilinear, power law, and piecewise linear hardening relationships and strain rate dependent yield strength. Concrete members are typically modeled with solid elements and often use the Karagozian & Case (K&C) concrete model (Malvar et al 1997; Malvar et al 2000). The K&C model determines concrete strength with respect to confining pressure, damage, and strain rate. The K&C model also allows a homogenized representation of reinforcement using volume fractions.

Considerable efforts have been made to validate the blast responses predicted by these simulation tools (e.g., Noble et al 2005). The experimental studies used for the validation efforts include, among others, the U. S. Army Engineer Research and Development Center Precision Test Wall Study and the Defense Threat Reduction Agency Divine Buffalo test series. Validation efforts include simulations of air blasts (Figure 1a), underwater explosions, and comparisons of discrete and homogenized rebar models (Figure 1b).

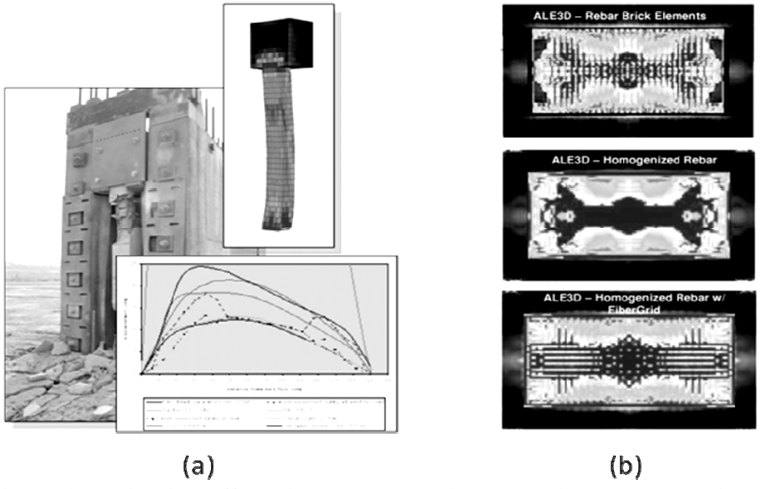

Figure 1. Validation efforts include comparing numerical results against experimental data (a) and verifying modeling assumptions like the use of homogenized rebar (b).

Evaluating Structural Stability

The consequences that a particular threat has on a structure can range from cosmetic damage to initiating progressive collapse. If a structural breach (localized failure)

does occur, the effects may extend to a single structural component, a section of the structure (localized collapse), or a large portion of the structure (progressive collapse). Evaluating a threat's consequences requires determining the energy released by the threat and imparted to the structure, the resulting structural damage and potential structural component failures, and the damaged structure's ability to redistribute the loads that had been carried by failed members. Typically, the threat is generalized as a sphere of trinitrotoluene (TNT). This allows other explosives and shapes to be converted to an equivalent weight of TNT and be related to the results obtained. Alternatively, other explosives and shapes can be explicitly represented to account for differences in the energy release rate and focusing effects. Two approaches are used at LLNL to evaluate a damaged system's structural stability.

The first approach initially uses a threat independent technique that presupposes a localized component failure and evaluates the system impact of that failure. For the high consequence failures, i.e. where a local component failure propagates into localized or progressive collapse, the threat required to cause the initial failure is determined with respect to charge weight and stand-off distance. An example application of this approach is looking at the potential for progressive collapse of a building. The building is represented using beam, shell, and solid elements as appropriate (refer to Figure 2a) and ParaDyn is used to determine the system response. The first analysis step is to statically initialize the building with gravity loads and create a restart file (which allows the static initialization to be performed only once and provides a starting point for all the subsequent failure analyses). The failure of one or more structural members is represented by specifying the elements to be removed and restarting the analysis. The element deletion causes an imbalance between the external applied loads and internal stresses which forces the structure to attempt to redistribute loads. If the redistributed loads cause additional component failures (e.g. excessive plastic strain, damage or buckling), then the code tracks the failure propagation until an alternative load path with adequate strength is reached or

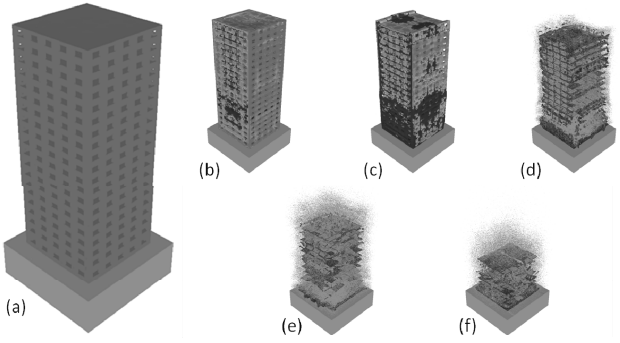

Figure 2. When a basement column failure is simulated, the building (a) experiences large deformations and extensive concrete damage which leads to structural collapse (b-f).

the structure collapses (refer to Figure 2 b to f). Metrics for evaluating the structure's damaged state include equivalent plastic strains (EPS) in the steel, damage parameter in the concrete and nodal displacement time histories. Displacement time histories with continually increasing magnitudes indicate failure propagation, while displacement time histories that oscillate about a stable value indicate that the structure has stabilized and is just ringing from the dynamic loading.

The second analysis step is to determine the threat required to cause the initial failure by performing a fully coupled blast analysis using ALE3D. The finite element model might contain only the component of interest to evaluate a single point failure mode, or a subsection of the structure to evaluate a multi-point failure mode or floor heave (refer to Figure 3). The model can represent the structural members using a combination of beam, shell, and solid elements. The metrics used for evaluating damaged components is similar to those used for the system analysis, including EPS for steel, concrete damage, and displacement time histories.

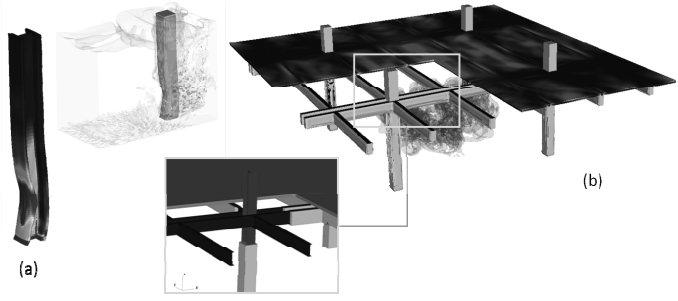

Figure 3. A component model (a) provides a good estimate for a single point failure mode, while multi-point (multi-component) failure modes or floor heave require a section of the structure to be modeled (b).

The second approach performs a fully coupled blast analysis on a full system model. The domain space can be limited by symmetry planes and boundary conditions where appropriate to reduce model complexity. The resulting finite element model is typically much larger than a corresponding model in ParaDyn due to the necessity to include the medium propagating the blast wave. This approach is used when specific threat scenarios are being considered or component failures are intimately connected to the overall structure geometry. An example application of this approach is the tunnel vulnerability assessment shown in Figure 4. The tunnel is constructed from reinforced concrete waffle sections (Figure 4b) and subjected to the detonation of a high explosive charge near the tunnel wall (Figure 4a). The concrete shelf acts as a reflecting surface and increases the damage caused by the high explosive. Figure 4c shows a simulation result where the explosion directly breached the tunnel wall near the charge location and the reflected blast waves caused secondary breaches near the tunnel top and on the opposite tunnel wall.

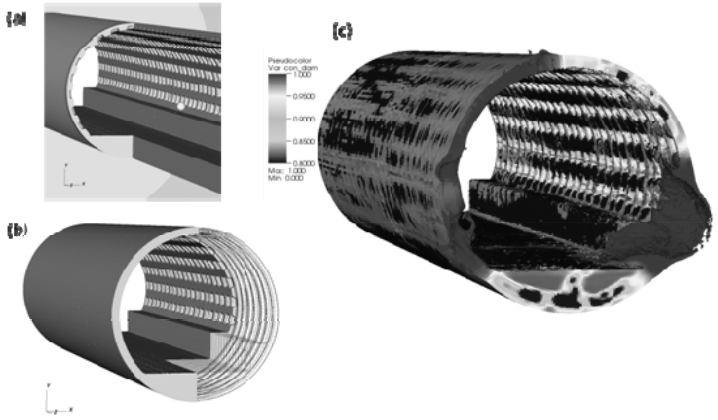

Figure 4. A spherical TNT charge is placed near the wall (a) of a reinforced concrete tunnel composed of waffle sections (b). The explosion breaches the tunnel in three locations (c).

In addition to characterizing the structural damage from an explosive detonation, ALE3D can be used to predict personnel injuries from the blast. The simplest indicator is to track the peak overpressure over the problem domain and construct casualty contours based on those peak pressures (refer to Figure 5). This approach neglects the relationship between pressure and exposure duration with respect to injury and lethality (Bowen, 1968), but provides the stakeholders with a conservative injury estimate that can be used for emergency planning and mitigation assessment.

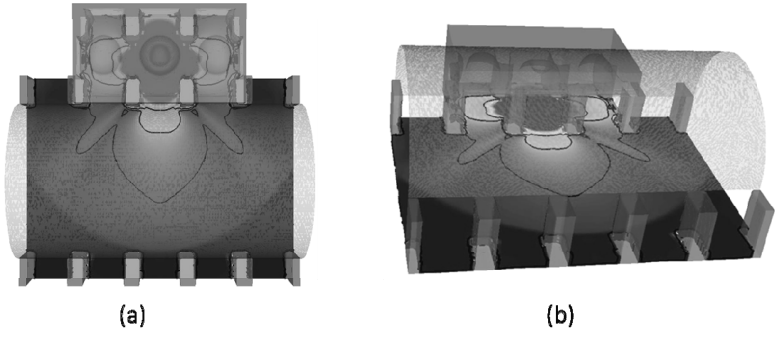

Figure 5. Personnel injury estimates are shown for a particular threat scenario from a top view (a) and oblique view (b) of the structure.

Basing Stochastic Inferences on High-Fidelity Simulations

A single analysis provides a deterministic approximation for the structural response for a given threat and set of material parameters. If a series of analyses are performed,

with carefully chosen variations in input parameters, then stochastic inferences can be made regarding result uncertainty and sensitivity to constitutive parameters, threat size, etc. An example application of this technique is shown in Figure 6. A series of high-fidelity hydrodynamic analyses were performed using ALE3D's fully coupled physics models to determine the predicted breach diameter in the tunnel for a subset of material parameter variations. A multivariate regression technique can then be used to establish confidence levels and predict the breach diameter for a range of charge stand-off distances (Glascoe et al 2009; Koutsourelakis et al 2006).

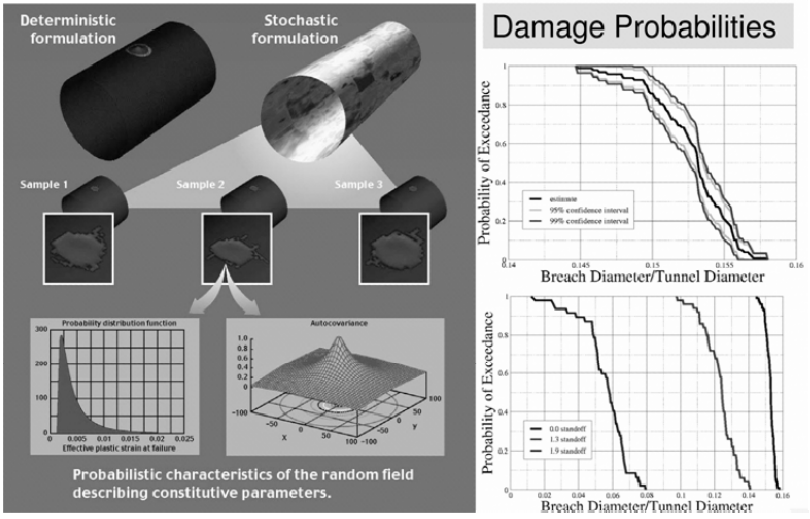

Figure 6. Stochastic inferences predict the breach diameter for several stand-off distances based upon the results of several high-fidelity, hydrodynamic analysis realizations.

Conclusions

Critical infrastructure protection requires a systematic approach that identifies credible threats, evaluates the overall consequences from vulnerabilities being exploited, determines the threat required to initiate a failure and deploys actionable countermeasures to protect the system. By combining high-fidelity, multi-physics modeling and materials testing capabilities with expertise in understanding emerging terrorist threats, LLNL provides end-to-end analysis of critical infrastructure with resultant assessments of likely vulnerabilities and potential consequences as well as recommendations for the development and deployment of mitigation strategies. Such analyses are used by government agencies and infrastructure owners to guide security efforts nationwide.

Acknowledgements

This work was performed under the auspices of the U. S. Department of Energy by Lawrence Livermore National Laboratory under Contract DE-AC52-07NA27344.

The authors want to acknowledge the Department of Homeland Security's Science and Technology Directorate for supporting this effort and would like to thank Dr. John Fortune of DHS/S&T and Mr. Christopher McKay of the Transportation Security Administration for their assistance and support.

References

Bohn, M. P., Shieh, L. C., Wells, J. E., Cover, L. C., Bernreuter, D. L., Chen, J. C., Johnson, J. J., Bumpus, S. E., Mensing, R. W., O'Connell, W. J., and Lappa, D. A. (1984). "Application of the SSMRP Methodology to the Seismic Risk at the Zion Nuclear Power Plant." NUREG/CR-3426 and UCRL-53483, Lawrence Livermore National Laboratory.

Bowen, I. G., Fletcher, E. R., and Richmond, D. R.(1968). "Estimate of Man's Tolerance to the Direct Effects of Air Blast." DASA-2113, Defense Atomic Support Agency, Washington, D. C.

Coats, D. C., Murray, R. C., and Bernreuter D. L. (1981). "Methods for Developing Seismic and Extreme Wind Hazard Models for Evaluating Critical Structures and Equipment at U. S. Department of Energy Facilities and Commercial Plutonium Facilities in the United States." *6th International Conference on Structural Mechanics in Reactor Technology*, Paris, France, August 17-21, 1981.

Department of Defense (DoD). (2005). "Design of Buildings to Resist Progressive Collapse." Unified Facilities Criteria, UFC-4-023-03.

DeGroot, A. J., Sherwood, R. J., and Hoover, C. G. (2008). "ParaDyn, a Parallel Nonlinear Explicit, Three-Dimensional Finite Element Code for Solid and Structural Mechanics," Version 8.1 User Manual, LLNL-SM-407000, Lawrence Livermore National Laboratory.

Dobratz, B. M. (1981). "LLNL Explosives Handbook, Properties of Chemical Explosives and Explosive Simulants," UCRL-52997, Lawrence Livermore National Laboratory.

Fong, J.T., Filliben, J.J., deWit, R., Fields, R.J., Bernstein, B., and Marcal, P. (2006). "Uncertainty in Finite Element Modeling and Failure Analysis: A Metrology-Based Approach." *J. Pressure Vessel Tech*., 128, pp. 140-147.

General Services Administration (GSA). (2003). "Progressive Collapse Analysis and Design Guidelines for New Federal Office Buildings and Major Modernization Projects.", U.S. Government Printing Office, Washington, D.C.

Glascoe, L., Morris, J.P., Glenn, L.A., and Krnjajic, M. (2009). "Development and application of a fast-running tool to characterize shock damage within tunnel structures." *ASCE Fifth Congress on Forensic Engineering,* Washington, D.C., November 10-15, LLNL-CONF-411709.

Guers, F., Dolinski, K., and Rackwitz, R. (1988). "Probability of Failure of Brittle Redundant Structural Systems in Time." *Structural Safety*, 5, pp. 169-185.

Koutsourelakis, S., Noble, C., and Glascoe, L. (2006). "The effect of material uncertainty on evaluating infrastructure vulnerability." *ASCE Bridge and Tunnel Security Workshop,* UCRL-PRES-222951.

Lin, J. I, (2007), "DYNA3D: A Nonlinear Explicit, Three-Dimensional Finite Element Code for Solid and Structural Mechanics." Release 7.1 User Manual, UCRL-MA-107254, Lawrence Livermore National Laboratory.

Malvar, L. J., Crawford, J. E., Wesevich, J. W., and Simons, D. (1997). "A Plasticity Concrete Material Model for DYNA3D." *Int. J. Impact Eng*., 19(9-10), pp 847-873.

Malvar, L. J., Crawford, J. E., and Morrill, K. B. (2000). "K&C Concrete Material Model Release III – Automated Generation of Material Model Input." TR-99-24.3, Karagozian & Case, Structural Engineers, Glendale, CA.

McCallen, D. B., Astaneh-Asl, A., and Larsen, S. (2000). "Seismic Studies of the San Francisco-Oakland Bay Bridge." *12th World Conference on Earthquake Engineering*, Auckland New Zealand, January 30 – February 4, 2000.

McCallen, D. B., and Romstad, K. M. (1994). "Nonlinear Model for Building-Soil Systems." *J. Eng. Mech.*, 120(5), pp. 1129-1152.

National Institute of Standards and Technology (NIST). (2005). "Final Report on the Collapse of the World Trade Center Towers." NIST NCSTAR 1, U.S. Government Printing Office, Washington, D.C.

Nichols III, A. L., ed. (2008). "Users Manual for ALE3D, An Arbitrary Lagrange/Eulerian 2D and 3D Code System." Volumes 1 and 2, UCRL-MA-152204 Rev. 7, Lawrence Livermore National Laboratory.

Noble, C., Kokko, E., Darnell, I., Dunn, T, Hagler, L., and Leininger, L. (2005). "Concrete Model Descriptions and Summary of Benchmark Studies for Blast Effects Simulations." UCRL-TR-215024, Lawrence Livermore National Laboratory.

Noble, C. R., and Nuss, L. K. (2004). "Nonlinear Seismic Analysis of Morrow Point Dam." *13th World Conference on Earthquake Engineering*, Vancouver, Canada, August 1 – 6, 2004.

DEVELOPMENT AND APPLICATION OF A FAST-RUNNING TOOL TO CHARACTERIZE SHOCK DAMAGE WITHIN TUNNEL STRUCTURES

Lee G. Glascoe[1], Ph.D., P.E., Assoc. M. ASCE, Joseph P. Morris, Ph.D., Afill. M. ASCE, Lewis A. Glenn Ph.D., Milovan Krnjajic, Ph.D.
Lawrence Livermore National Laboratory, Livermore (LLNL), CA 94550
1. glascoe@llnl.gov, 925-423-2922

Abstract

Successful but time-intensive use of high-fidelity computational capabilities for shock loading events and resultant effects on and within enclosed structures, e.g., tunnels, has led to an interest in developing more expedient methods of analysis. While several tools are currently available for the general study of the failure of structures under dynamic shock loads at a distance, presented are a pair of statistics- and physics-based tools that can be used to differentiate different types of damage (e.g., breach versus yield) as well as quantify the amount of damage within tunnels for loads close-in and with standoff. Use of such faster running tools allows for scoping and planning of more detailed model and test analysis and provides a way to address parametric sensitivity over a large multivariate space.

Introduction

High fidelity computational hydrodynamic and structural analysis tools, e.g., the ALE3D, DYNA3D and CTH codes (Sharp, 2004; Lin, 2005; McGlaun et al., 1990), are useful for predicting the response of structures to shock loads (see Figure 1) and can ultimately be used to assist vulnerability corrective measures and reduce overall risk (e.g., Noble et al., 2008; Glascoe et al., 2009; McMichael et al., 2009). Unfortunately, such tools require significant computational resources which can undermine timely assessment involving a large range of threats and threat locations. In addition, high fidelity tools are typically deterministic in nature and, therefore, must assume a specified set of material properties for the structure itself. Large uncertainties associated with, for example, material strength need to be at least bounded for a proper risk assessment. Consequently, there is a need for capabilities that can rapidly evaluate effects associated with various threat sizes, threat locations, and system states while quickly highlighting uncertainties associated with structural and system response.

This paper presents two components of a proposed fast-running tool for confined spaces such as tunnels. The first component is a physics-based approach for predicting shock propagation in tunnels that runs in minutes on a standard single processor platform. This capability can be used to rapidly determine the spectrum of loading environments associated with the range of credible threats, threat locations and tunnel networks. The second component is a statistical treatment for predicting and bounding close-in structural response at varying standoff using previously executed high fidelity loading realizations.

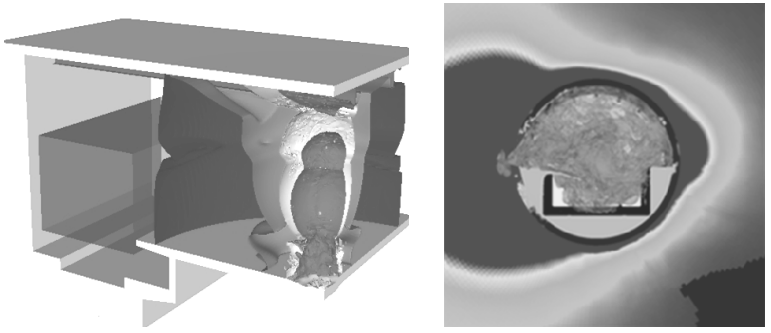

Figure 1: Two examples of high fidelity ALE3D simulation of a blast within enclosed tunnel structures. The plot on the left illustrates different pressure contours after a shock within an enclosed station, the plot on the right highlights a fully-coupled three-dimensional fluid/structure/soil blast simulation.

A Fast-running Tool for Blasts in Tunnels: the STUN code

Direct simulation of blast propagation in tunnels is a formidable task due to a combination of factors. Firstly, flow in long tunnels is dominated by boundary layer effects, such as wall drag, that require high resolution zoning. Tunnels, by nature, have high length over diameter ratios, resulting in highly protracted computational domains relative to tunnel diameter. Such long domains, coupled with high resolution requirements needed to capture boundary effects, makes direct three-dimensional simulation of long tunnels prohibitively expensive. Even two-dimensional simulations of extensive tunnel lengths become computationally expensive when considering multiparameteric study. The sphere and tunnel code (STUN) employs a simpler algorithm that captures the essential physics of blasts in tunnels (Glenn, 2001), but runs in minutes on standard personal computing hardware. STUN is based on an algorithm originally developed for the study of hypervelocity launchers and gas guns (e.g., Glenn, 1990 and 1997) and is, in part, based on the one-dimensional wall drag model:

$$\frac{du}{dt} + \frac{1}{\rho}\frac{\partial p}{\partial x} + \frac{f}{4r}u|u| = 0$$

where u is the particle velocity in the x direction, ρ is the air density, p is pressure in the tunnel, A is the cross-sectional area of a tunnel of radius r, and the friction coefficient, $F = f/4r$. The friction factor, f, the Prandtl-Karman "Law of the Wall", is a function of the Reynolds number:

$$f^{-1/2} = 2\log_{10}\left(\mathrm{Re}f^{1/2}\right) - 0.8$$

The STUN code works by coupling several one-dimensional representations of the tunnel and blast into a higher dimensional representation. Specifically, STUN includes a spherical flow region for the detonation that is coupled to an axial one-dimensional model of tunnel segments. By varying the cross section of the tunnel along its length, it is possible to account for the effect of platforms (larger cross section) and trains (restricted cross section) upon the blast wave propagation and attenuation. The code can predict the effect of an arbitrary number of bends in a tunnel and supports coupling to additional 1-D segments to simulate the effect of tunnel intersections upon the shock wave. STUN incorporates treatments for blast doors displaceable and potentially fragmented by dynamic loading.

STUN has been validated against several sets of data involving a range of threat sizes and tunnel configurations. Consider results from a specific experiment involving blast loading on a single straight tunnel section containing two doors (see Figure 2). This particular test configuration has a relatively low length to diameter ratio allowing response prediction with high fidelity codes in two-dimensions. For this example high fidelity CTH simulations were exercised for comparison. Figure 3 illustrates consistency between experiment and the two numerical solutions and demonstrates that STUN results can track experimental results better than the higher fidelity CTH results at the first gauge.

The addition of an intersection, or bend in the tunnel makes this example inherently three-dimensional and far more expensive for a high-fidelity code to execute. In sharp contrast, the cost of the corresponding STUN calculation is minimal. Such a fast-running tool is ideally suited for providing pressure histories at a distance along a complex tunnel/station configuration to examine, for example, down-tunnel blast effects on personnel or impulse loading of structural components.

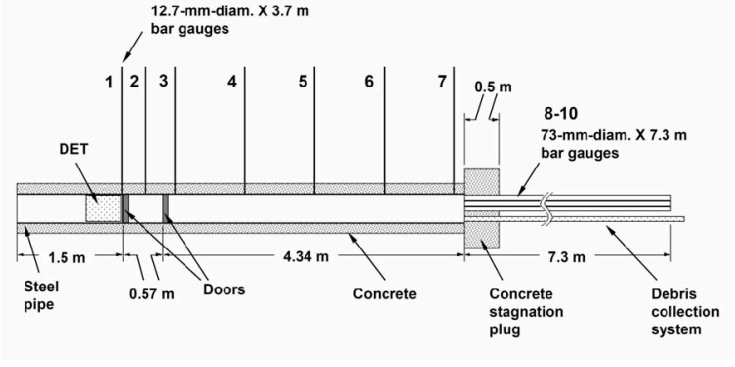

Figure 2: Experimental configuration with Dilute Explosive Tile placed against blast door outside a single, straight tunnel.

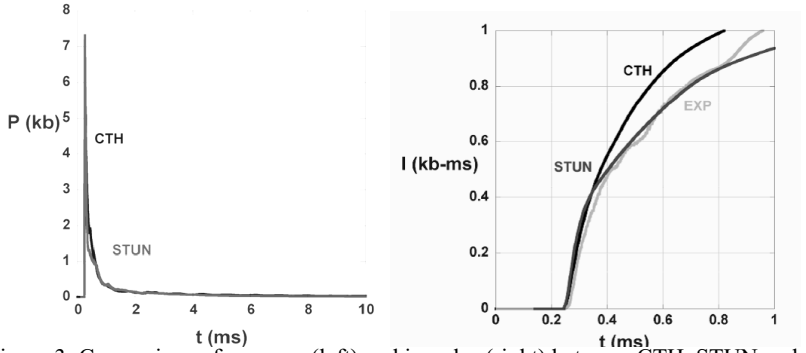

Figure 3: Comparison of pressure (left) and impulse (right) between CTH, STUN and experimental result at the location of gauge #1.

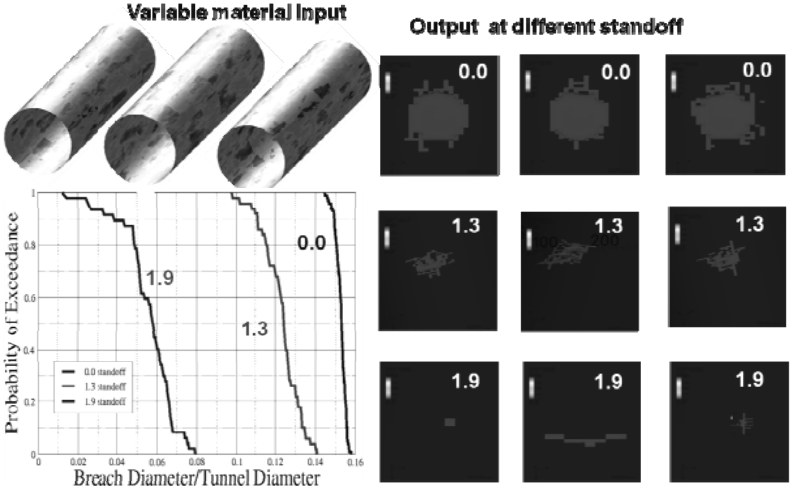

Figure 4. Three stochastic realizations (top left three tunnels with spatially varying material strength) of breach failure for three stand-off distances (right close-ups of breach hole at standoff 0.0, 1.3 and 1.9); based upon the results over hundreds of high fidelity 3-D finite element realizations.

Fast-running Failure Assessment with Uncertainty Quantification

Analysis of close-in structural response within confined tunnel environments to idealized explosive blast scenarios is an inherently difficult three-dimensional problem (Figure 1). Accounting for uncertainty requires more than a single deterministic simulation and can greatly benefit from faster running techniques. The tradeoff, of course, is that simplifications associated with faster-running techniques can introduce additional uncertainty. Under carefully considered conditions, trends gleaned from high fidelity 3D analysis and experiments can be used to generalize response curves. Such easily referenced curves may include the effect of uncertainties when cast in a probabilistic framework (Koutsourelakis et al., 2006). Uncertainty associated with, for example, material properties throughout a given structure can be incorporated into assessments to highlight probabilities of failure under specific threat conditions (Figure 4).

Generalized but structurally detailed 3D scenarios can be considered to address tunnel types based on construction (e.g., 3/8" steel shell structures versus 3' thick reinforced concrete structures) at different threat size and standoff configurations. Each scenario can account for uncertain parameters associated with considerations affecting the defined tunnel type, such as material strength or local geologic conditions. Advanced regression techniques can utilize and then inform on computationally demanding 3D finite element simulations of these tunnel scenarios by sampling model output over a multivariate space (e.g., Mardia et al., 1979). For example, a statistical approach comprising a logistic and a regular regression could evaluate damage to a specific tunnel structure in terms of engineering plastic strain (EPS) and the area exceeding a predefined threshold of EPS as a function of threat size and standoff. Specifically, the dependence of a subset of the finite element output, such as strain damage and damaged area, on a part of its input, such as threat weight and distance, is fit to a two-step regression:

- Step 1: logistic regression on the whole data set for two categories: "no breach" and "breach".
- Step 2: Regular regression for the part of the set with non-zero values of maximum EPS.

The variables in the regression models include finite element input along with the corresponding output of maximum EPS and the size of the yield area for different EPS thresholds. To analyze how different failure modes depend on the range of inputs, a failure criterion needs definition, such as 'a breach occurs when plastic yielding exceeds a specified threshold, and the size of the related area exceeds a specified value'. In statistical terms, this definition is a binary response, Z, which is "1" when breach occurs, and "0" otherwise. Breach is analyzed as a function of covariates (threat size and standoff) using a logistic regression model. Specifically, logistic regression relates the probability of breach to the covariates, X_i, as follows:

$$\log\left(\frac{p_i}{1-p_i}\right) = X_i^T \beta + \epsilon, \quad i = 1, \ldots, n$$

where $p_i = \Pr(Z_i = 1|X_i)$ and n is the number of data points.

In addition to the binary breach mode, another finite element output is the damage area, *Y,* that is a positive number wherever there is a breach, otherwise $Y = 0$. For a subset m of n data points for which the failure $Z_i = 1$, area $Y_i \geq y_{threshold}$, and maxEPS $\geq max\text{EPS}_{threshold}$, a second stage to the statistical model can be added,

$$\log(Y_i) = X_i^T \gamma + \delta, \quad i = 1, \ldots, m$$

Fitting the compound regression model provides estimates of coefficients, β and γ, along with the corresponding error bounds. Fitted values are in turn used in a simulation to calculate predictive distributions of the probability of breach and distributions of breach size at a desired set of values for threat weight and distance.

As an example, consider a study with 94 three-dimensional finite element realizations for two tunnel structures similar to that pictured on the right in Figure 1: a strengthened tunnel breaching at a high strain, and a weakened tunnel breaching at a low strain. The logistic response curve is generated using the approach described on breached (solid points) and non-breached (open points) realizations; this is plotted as a function of threat size versus standoff in Figure 5. Figure 6 illustrates the second stage fit of the standard regression on extent of damage as a function of threat size (shown for three standoff values). Figure 7 highlights the role of uncertainty captured by the regression fit with 99% confidence intervals banding the damage area versus threat size (shown at 10 inches standoff).

This statistical model is only a first and demonstrative step in quickly characterizing response and uncertainty associated with detailed high-fidelity simulation. It can be thought of as a statistical approximation of the finite element model for a given set of inputs and outputs. Such a statistical model can provide both qualitative and quantitative insight into the input/output dependencies of interest and associated uncertainties. Improved statistical approximation and improved efficiency of assembly of finite element input may be attained using informed sampling techniques such as Latin Hypercube or Sequential Importance Sampling (e.g., pp. 227-246 of Doucet et al., 2001) to reduce the number of realizations necessary to generate the response curves.

Conclusions

Fast-running tools can be used to predict blast effects within confined structures in a timely manner allowing for uncertainty assessment. Two different approaches to building a fast-running capability have been discussed: a one-dimensional physics-based pressure propagation tool and a statistical treatment of high fidelity effects analysis. The former provides rapid theory-based analysis of blast effects within a confined structure at a distance; the latter is useful for estimates of close-in structural integrity at a specific location accommodating some degree of uncertainty and is entirely based on previously examined high fidelity deterministic analysis. The combination of these capabilities into a single integrated model can provide engineers and decision-makers with a tool allowing timely analysis when considering shock loading events within confined environments, such as tunnel structures.

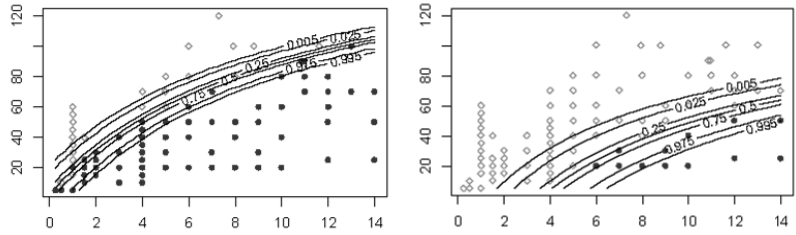

Figure 5. Response curves of **threat size vs standoff** for a strengthened structure (left) and a weakened structure (right) where solid points indicate breached realizations and open circles indicate nonbreached realizations.

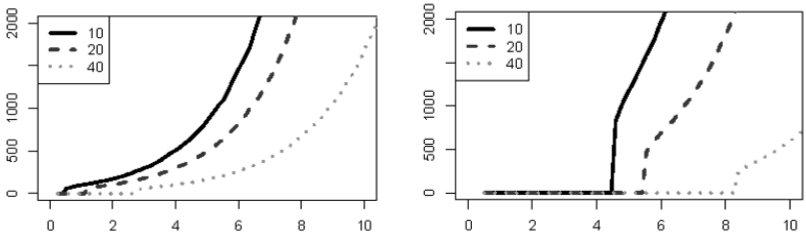

Figure 6. Reponse curves of **breached area as a function of threat size** for a strengthened structure (left) and a weakened structure (right) for three standoff distances (10 inches, 20 inches, and 40 inches).

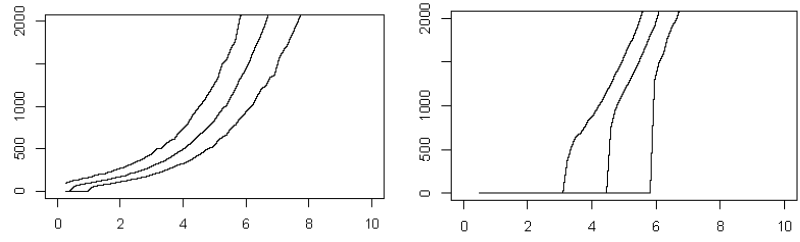

Figure 7. Pointwise 99% confidence intervals for **breached area versus threat size** for a strengthened tunnel (left) and a weakened tunnel (right) at 10 inches standoff. The three curves indicate the mean and the 99% pointwise confidence interval for each response fit.

Acknowledgements

This work was performed under the auspices of the U. S. Department of Energy by Lawrence Livermore National Laboratory under Contract DE-AC52-07NA27344. We want to acknowledge the Department of Homeland Security's Science and Technology Directorate for supporting this effort and would like to thank Dr. John Fortune of DHS/S&T and Mr. Christopher McKay of the Transportation Security Administration for their assistance and support.

References

Doucet, A., de Freitas, N., and Gordon, N. (2001). *Sequential Monte Carlo Methods in Practice.* Springer-Verlag, New York.

Glascoe, L., Noble, C., Reynolds, J.G., Kuhl, A., and Morris, J. (2009). "Securing Transportation Systems from High Explosive Threats." *Proceedings of the 2009 IEEE International Conference on Technologies for Homeland Security*, May 11-12, Waltham, MA, LLNL-PROC-411500.

Glenn, L. A. (2001). "Simulating MARVEL with the STUN Code." LLNL UCRL-ID-143993 (June 6, 2001).

Glenn, L. A. (1997). "On how to make the fastest gun in the West." *Proc. of the International Workshop on New Models and Numerical Codes for Shock Wave Processes in Condensed Media*, St. Catherine's College, Oxford, U. K. (September 15-19 1997).

Glenn, L. A. (1990). "Design limitations on ultra–high velocity projectile launchers." *Int. J. Impact Engrg,* 10, 185.

Koutsourelakis, S., Noble, C., and Glascoe, L. (2006). "The effect of material uncertainty on evaluating infrastructure vulnerability." ASCE Bridge and Tunnel Security Workshop, UCRL-PRES-222951 (July 2006).

Lin, J. (2005). " DYNA3D: A Nonlinear, Explicit, Three-Dimensional Finite Element Code for Solid and Structural Mechanics User's Manual." UCRL-MA-107254.

Mardia, K.V., Kent, J.T., and J.M. Bibby. (1979). *Multivariate Analysis.* Academic Press, New York.

McGlaun, J.M., M.G. Thompson, and M.G. Elrick. (1990). "CTH: a three-dimensional shockwave physics code." *Int. J. Impact Engng,* Vol. 10: 351-360.

McMichael, L.M., Noble, C., Margraf, J., and Glascoe, L. (2009). "Fully-Coupled Blast Effects Modeling of Large Critical Infrastructure." *ASCE Fifth Congress on Forensic Engineering,* November 10-15, LLNL-CONF-411649.

Noble, C.R., Wemhoff, A.P., and McMichael, L.D. (2008). "Thermal-structural analysis of the MacArthur Maze Freeway collapse." *ASME 2008 Summer Heat Transfer Conference*, Jacksonville, FL, August 10-14.

Sharp, R. (2004). "Users Manual for ALE3D: An Arbitrary Lagrange/Eulerian 3D Code System, Volume 1." UCRL-MA-152204 Rev. 2 (June 1, 2004).

Collapse of the Wimer Covered Timber Bridge

Authors:

Richard Dethlefs, Wiss, Janney, Elstner, Associates, Inc., Seattle, WA, rdethlefs@wje.com
Zeno Martin, Wiss, Janney, Elstner, Associates, Inc., Seattle, WA, zmartin@wje.com

ABSTRACT

On, July 6, 2003, the Wimer Covered Bridge, an historic covered wooden bridge located in southern Oregon, collapsed shortly after a pickup truck crossed over it. A local resident and his two grandsons were on the bridge at the time and sustained serious injuries. The bridge was originally built in 1892 and substantially rebuilt in 1927. The bridge underwent major rehabilitations in 1962 and 1985. The 2001 bridge rating concluded that it was safe to keep the bridge open to restricted traffic loads.

The bridge collapsed due to extensive decay in the bottom chord at a panel point on the upstream truss. Engineers involved had numerous opportunities to identify the critical nature and deteriorated condition. Mistakes were made in both the analysis and in the inspections of the bridge. This paper addresses standard of care and the importance of assessing wood decay when analyzing a timber bridge structure.

RESIDENTS BID FAREWELL TO A LOCAL LANDMARK

On Sunday afternoon, July 6, 2003, residents were astonished to find that their beloved historic wood covered bridge had suddenly collapsed into Evans Creek. Witnesses rushed to free a local man and his two young grandsons from the debris. The three sustained serious but not life-threatening injuries.

The original Wimer Covered Bridge was built in 1892 by J. W. Osbourne. It was listed on the National Register of Historic Places. The Oregon Department of Transportation (ODOT) provides the following description of the bridge [3], presumably written not long before its collapse:

> The Wimer Bridge was saved from destruction when local residents battled to initiate a rebuilding of the weakened structure in 1962.

Community members insist that the original bridge was built in 1892, and a sign posted on the bridge claims title to that date. The Hartman brothers, bridge builders of Jacksonville, replaced the Wimer Bridge in 1927.

Features of the Wimer covered span include a shingle roof, the usual daylighting narrow windows above the trusses, wooden flooring, and a Queenpost truss design. The bridge appears not unlike a barn from downstream and only the flying buttresses indicate it to be a covered bridge and not a barn over water.

Although refurbished in 1962, the bridge had a load limit of 8 tons placed on it by the mid 1970s and deterioration soon closed it to vehicular traffic. In 1985, the wooden bridge was rehabilitated and the 8-ton load limit restored.

However, the span of 85 feet is too long for the Queenpost truss, and the buttresses do not adequately support the top chord. Now, the east truss has severe bowing and sweep, and the bridge exhibits large movements when cars pass, so the bridge currently has a 3-ton load limit and is slated for rehabilitation using National Historic Covered Bridge funds.

BRIDGE DESCRIPTION

The Wimer Covered Bridge was a 6 span, 171 foot long timber structure composed of an 86 foot main span supported by two timber Queenpost trusses, and three north and south timber stringer approach spans. The substructure was timber bents supported on concrete pedestals and footings.

The Queenpost truss was composed of five 17 foot 2 inch panels. The top and bottom chords were continuous bolt-laminated untreated timber members with staggered joints in the plies. The diagonals and lower portion of the top chord in the center panel were solid sawn untreated members. The vertical tension members were double steel rods. The rods were anchored at the top of the top chord and passed through the bottom chord supporting the floor beams at each of the bottom chord panel points. The floor beams were originally 12 by 19-1/2 inch heavy timbers that extended approximately 4 feet 6 inches beyond the house. Attached to the ends of the cantilevered floor beams were diagonal buttresses that braced the top chords of the trusses. The deck was composed of timber stringers and decking and had an asphalt overlay.

The truss bottom chords were composed of five vertically laminated Douglas-fir timber members, each approximately 2-3/4 inches wide by 11-1/2 inches deep. The bottom chord had an overall measured width of 13-7/16 inches and depth of 11-1/2 inches. The members were periodically cross-bolted with 3/4-inch diameter bolts. Butt joints in the plies were staggered and there were hardwood shear keys notched between intermittent plies.

OBSERVATIONS AFTER COLLAPSE

An investigation attended by a number of engineers immediately following the collapse concluded that the failure initiated at the first panel point in the bottom chord on the upstream (east) truss (Figure 1). The bottom chord failed in tension while primarily under dead load. Inspections found extensive fungal decay in the bottom chord at the point of failure.

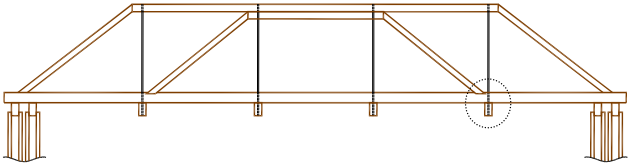

Figure 1. Queenpost truss schematic with bottom chord failure location shown circled.

In a report by one of the investigating engineers, the decay was described as "the chord at L1 showed moisture related deterioration of up to 2 inches deep over the area in contact with the original and added floor beam members. In addition, it was estimated that each of the 2-1/2 inch diameter hanger rod holes through the chord had a 1/2 inch wide band around the hole that was deteriorated. The 4th ply from the interior face of the chord was determined to be deteriorated through most of its section from top to bottom." Reasons why the decayed condition of the bottom chord member were not accurately appraised prior to the collapse are discussed in this paper.

In addition to the decayed condition of the chord at the point of failure, there were also a number of notches and borings, which not only substantially reduced the effective cross sectional area but were also primary reasons why this location was susceptible to decay (Figures 2 and 3). Figure 3 illustrates the notches and borings present at this location, which included the following:

- A 2-3/8 inch deep dap at the top of the chord (Area = 31.9 in^2)
- Two, 2-1/2 inch diameter full depth holes for hanger rods (Area = 45.6 in^2)
- A 1-1/4 inch wide full depth notch for a shear key (Area = 11.4 in^2)
- A 3/4 inch diameter bolt hole across the full width (Area = 5.4 in^2)

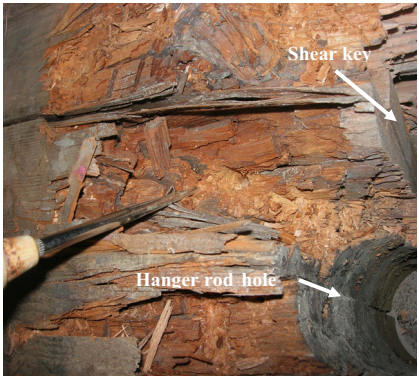

Figure 2. Extensive decay at bottom half of failed section. Shear key and hanger rod hole sections are also visible.

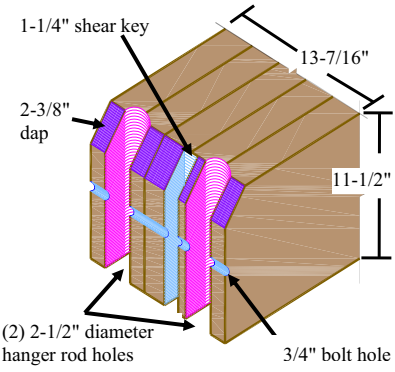

Figure 3. Bottom chord cross section at failure location.

The gross cross sectional area of the bottom chord was 154.5 in^2. However, after reducing the cross section to account for all of the notches and borings at the critical cross section, the remaining effective area was only 60.2 in^2. Subtracting the area of wood that was considered completely decayed results in only 17.1 in^2 of effective wood (11% of the gross section) in the bottom chord at the first panel point.

COMPLACENCY AND POOR JUDGMENT DOOM BRIDGE

Following an informal inspection of the bridge by a Jackson County (County) employee in 2000, where it was observed that the top chords of the trusses were substantially out of alignment, the County contacted the same engineering firm (Consultant) that had designed the rehabilitation of the bridge in 1985. The Consultant was asked to assess the current condition of the bridge and to perform a load rating of the structure. In their October 2001 report, the Consultant found that the current 3-ton posting on the bridge was appropriate and that "this bridge is in desperate need of rehabilitation." The Consultant performed only a walk-through visual inspection of the bridge prior to preparation of the load rating.

A routine bi-annual inspection of the bridge in August 2001, which was performed by a bridge inspection company not affiliated with the Consultant, assigned the bridge superstructure a fair (5) rating. The inspection report noted that the top chords of both trusses were substantially out of alignment with the bottom chords. The report recommended geometric surveys to monitor the deflection in the truss members. The inspection did not include up-close inspections of the underside of the bridge deck nor did it include any borings in the bottom chord members.

In October 2001, the County received funding from the National Covered Bridge Preservation Program to rehabilitate the bridge. Following a formal proposal review

process, the County retained the Consultant in January 2002 to perform an evaluation of the bridge and provide design services for a major rehabilitation.

Throughout 2002 and early 2003, the Consultant performed analyses of the bridge and its members and developed repair drawings for the bridge rehabilitation. However, not once during this period did the Consultant perform an in-depth inspection of the bridge that included gaining access to the underside of the superstructure to inspect the condition of the bottom chord members. Even so, the Consultant was only weeks away from delivering the final repair drawings when the bridge collapsed in July 2003. A review of the rehabilitation drawings revealed that no repairs were planned to address the condition of the bottom chord member.

Following the collapse in 2003 a review of available records found that the bridge was load rated on three occasions between 1984 and 2001. The Consultant performed load ratings of the structure in 1984 and again in 2001. In 1994 a different engineering company performed a load rating of the structure. A summary of the three load ratings performed in 1984, 1994, and 2001 are provided below.

January 1984 – Inspection and load rating by Consultant.
In the 1984 load rating, the cross sectional area of the bottom chord assumed present (109.25 in^2) only accounted for a reduction due to two 2 inch diameter hanger rod holes. The area was not reduced for the dap at the top of the chord, the horizontal bolt hole, or the shear key. The diameter of the hanger rod hole used in the analysis was less than the actual 2-1/2 inch diameter.

Had the Consultant included a reduction in cross-sectional area of the bottom chord to account for the 2-3/8 inch dap *and* used the actual diameter of the two hanger rod holes of 2-1/2 inches, the Consultant would have calculated an effective area of only 77 in^2 instead of 109.25 in^2. Both the dap and the hanger rod holes were visibly apparent and could have been detected by a careful visual inspection. Using the assigned F't of 900 psi and an effective area of 77 in^2 results in an allowable tensile capacity of the bottom chord of only 69.3 kips, which is barely more than the calculated dead load forces in the bottom chord. Had this analysis been performed, the bridge would have been closed to traffic.

June 1994 – Load rating by second engineering firm.
In the analysis of the bottom chord capacity, the assigned bottom chord dimensions were 13-1/8 by 11-1/2 inches for a gross cross sectional area of 150.9 in^2. The cross sectional area assumed present (76.6 in^2) accounted for a reduction due to two 3 inch diameter hanger rod holes plus one 3/4 inch diameter horizontal bolt hole. The diameter of the hanger rod holes used in the analysis was more than the actual 2-1/2 inch diameter, which offset the fact that they did not reduce the cross section to account for the 2-3/8 inch dap at the top of the chord.

In the analysis, the engineer assigned a nominal allowable tensile stress for Douglas-fir Dense No. 1 of 1200 psi. In determining this allowable value, the engineer

referenced an unspecified AASHTO document. No adjustment factors for load duration were applied.

Design values associated with "dense" grades have typically pertained to *Timbers* which are nominally 5 inches by 5 inches and larger. The actual wood laminations making up the truss bottom chords were only 2-3/4 inches in width and thus would be more appropriately considered dimension lumber. The 1991 National Design Specification for Wood Construction (NDS) [1] provides a nominal design value of 675 psi for Douglas-fir No. 1 visually graded dimension lumber in tension parallel to grain. The use of 1200 psi in the 1994 load rating analysis was not appropriate even if the wood material were in new condition. The engineer did not perform a detailed inspection of the bottom chord members and did not make any reductions in allowable tensile stress to account for the aged and deteriorated condition of the wood.

With the net effective cross sectional area of only 76.6 in^2, any reasonable assignation of allowable tensile stress to the wood would have resulted in the bridge being closed to traffic.

October 2001 –Load rating by Consultant.
In the analysis of the bottom chord capacity, the cross sectional area assumed (128.3 in^2) only accounted for a reduction due to a 2 inch dap at the top of the chord. The cross sectional area was not reduced for the hanger rod holes even though an analysis by the same firm in 1984 included a reduction for the hanger rod holes.

The nominal allowable tensile stress assumed in the analysis was 600 psi for a "fair" condition of the wood. The value was then adjusted upward with a 1.15 load duration factor so that the allowable tensile stress assigned was 690 psi. Use of a load duration factor when performing traffic live load ratings for timber bridges that have been in service for a number of years is inappropriate.

Apparently, the engineer did not review the past load ratings of the bridge, or else they would have realized that the assigned cross sectional area was too high and the calculation should include a reduction for the two hanger rod holes. With the assigned allowable tensile stress of 690 psi, a realistic calculation of effective area would have resulted in the bridge being closed to traffic.

None of the analyses by the two engineering consultants included a reduction in effective area for the 1-1/4 inch hardwood shear key between the timber plies. None of the load ratings since 1984 included a detailed survey of the bridge including up-close inspection of the bottom chord members. As a result, none of the assessments identified the presence of the extensive wood decay in the bottom chord and none of the load ratings accounted for the effects of the wood decay in the analyses. A summary of the three load rating analyses is included in Table 1.

Table 1. Summary of Bridge Load Ratings

By	Date	F't (psi)	Area (in^2)	Bottom Chord Capacity (kips)	Dead Load Effect (kips)	Load Rating
Consultant	1984	900	109.25	98.3	67.9	3 tons
Other firm	1994	1200	76.6	91.9	71.8	6 tons
Consultant	2001	690	128.3	88.5	71.9	5 tons

DISCUSSION

Reviewing the load ratings for the bridge since 1984 raises a number of questions about what the standard-of-care should be for performing load ratings of timber bridges. Questions raised include:

- Should it be expected that an engineering consulting firm will review project files including prior analyses to ensure logical consistency?
- What level of inspection is required to determine effective areas of wood members?
- How in-depth should inspections be to determine the presence and extent of wood decay?
- Should the presence of wood decay be considered to reduce the effective cross section of the wood; or should the presence of the decay be accounted for with a reduction in the assigned allowable stress values?
- What level of conservatism should an engineer apply to their analysis when they do not possess detailed information regarding member geometry and properties?

Effective Net Area

A number of mistakes were made by both engineering consultants regarding the net effective cross sectional area of the bottom chords; however, the biggest mistake was made in the most recent 2001 load rating, which is difficult to understand since the Consultant should have had the benefit of all of the prior analyses. The mistakes display a lack of careful or accurate accounting of actual conditions. In fact, the effective cross sectional area assigned by the Consultant in 2001 was 17% larger than was assigned in 1984 for the same member. None of the analyses included the reduction in area for the 1-1/4 inch hardwood shear key, and none of the analyses included reductions for both the 2-3/8 inch dap *and* the two 2-1/2 inch diameter hanger rod holes, both of which were easily visible.

Even a remotely close determination of the effective area of the bottom chord, one accounting for reductions due only to the dap and the hanger rod holes, would have yielded an effective area of approximately 77 in^2. Dividing the dead load force in the bottom chord (71.9 kips) by this effective area results in a tensile stress of 934 psi, which exceeds the allowable stress assigned by the Consultant in 2001 (690 psi) by 35%. Had this analysis been performed, the bridge would have been appropriately closed to vehicular traffic.

Allowable Stress

As shown in Table 1, the allowable tensile stress assumed for the bottom chord in determining the load ratings had wide variations. In their analyses, the engineering consultants often referenced the highest possible published design values for Douglas-fir wood, typically referencing No. 1 to Dense No. 1. In 1984, the Consultant made an effort to adjust the selected tabulated allowable stress by arbitrarily picking an allowable tensile stress of 900 psi. This value represented a 10 to 25% reduction from the 1000 to 1200 psi values cited by the Consultant in their analysis.

In the 2001 load rating calculations by the Consultant, the nominal tensile stress for Douglas-fir No. 1 was cited as 675 psi from the "current NDS." However, a value of 600 psi was used as the nominal value to account for a "fair" condition. A 1.15 load duration factor was applied so that the allowable tensile stress used was 690 psi. The 1997, 2001, and 2005 NDS all provide a nominal reference design value of 675 psi for Douglas-fir No. 1 visually graded dimension lumber in tension parallel to grain.

In general, the allowable tensile stresses used in the load ratings did not account for the possibility of decayed conditions. The allowable tensile stresses used in the 1984 and 2001 load ratings were reduced by various amounts to account for "fair" conditions. No comments were provided as to why the specific reduction magnitudes were selected and it is assumed to be based on engineering judgment. Since the initial assumption by the engineers was that the wood was of the highest possible quality, the nominally applied reductions only served to reduce the allowable stresses to levels consistent with good quality, new Douglas-fir.

Understanding Wood Decay

The purpose of covering a wood bridge is to presesrve the supporting timbers by physically providing shelter from the elements [2]. While covers do provide some degree of protection, they cannot protect a deck from moisture transported by vehicles and typically do not provide complete protection to all of the structural members. The wood members making up the main trusses of the Wimer Covered Bridge were not preservative treated and therefore had the potential to decay in the outdoor environment.

The 1984 and 2001 load ratings contained some accounting of the "fair" wood condition but rationale for appropriate allowable design values was not provided. Furthermore, the wood considered fair in 1984 was still considered fair in 2001. Assumptions of allowable stress values by both consultants did not indicate an understanding of wood decay effects on the strength of wood fibers.

Wood is subject to deterioration by a variety of agents as soon as it is formed in the tree. Wood decay is the primary cause of wood bridge deterioration, and therefore it is essential for timber bridge inspectors, and engineers involved in rehabilitation or load rating, to understanding the factors associated with wood decay in a given environment for accurate assessment.

Connections and notches are locations where decay potential can be the most severe because these can be areas of moisture intrusion, entrapment, and where air circulation and drying are inhibited. The Wimer Covered Bridge had extreme decay in the section where the notches, bolt holes, and hanger rod holes were present.

Timber Bridges – Design, Construction, Inspection, and Maintenance [4] provides a good basis for a reasonable standard of care, and emphasizes some relevant points as follows:

- *For timber bridges, it is critical that all decay and its location be accurately and completely described. This must include both the location of the deterioration in specific components and the longitudinal and transverse dimensions of the decayed wood.*
- *Decay effects on strength can be many times greater than visual observation indicates, with possible strength losses of 50 to 70 percent for a corresponding weight loss of only 3 percent.*
- *...it is recommended that no strength value be assigned to wood showing evidence of decay in any stage of development.*

Detailed Inspections Required to Locate Decay and Identify Member Sections

It was known in 1984 that the floor beams were extensively decayed. The repairs designed by the Consultant in 1985 included adding preservative treated timbers to either side of the floor beams to carry the deck loads - essentially ignoring any remaining capacity in the existing beams. The floor beams are supported at each end by the hanger rods and are in contact with the bottom chords of the trusses. The inspection records for the bridge indicate that decay and deterioration of the deck members was an ongoing concern.

With all of the known decay in the vicinity of the bottom chords and the extent of decay in members in contact with the bottom chords, it would be reasonable to expect that some level of decay would be occurring in the bottom chords. Especially when considering it had been sixteen years since the last substantial maintenance and repairs had been performed.

In the Consultant's Statement of Qualifications/Statement of Proposal submitted to the County in pursuit of the rehabilitation design work in 2002, the Consultant clearly indicates that detailed inspections would be a necessary component of any bridge rehabilitation design. The Consultant even goes so far as to state that "*All timber members will be inspected for decay and the design section verified for possible reuse vs. replacement*."

In fact, the bottom chord members were not inspected for decay and the design sections were not accurately verified.

RECOMMENDATIONS

Structural engineers involved in the evaluation of existing timber bridges must understand how to identify the extent of wood decay and account for it in their appraisal. Uncertainties in determining the extent of decay should lead to a more conservative appraisal with the understanding that reductions in wood strength due to decay are known to be substantial.

Up-close visual inspections and field measurements should be used to develop actual cross sections that accurately account for cross sectional removal resulting from notches and/or holes.

When assigning allowable stresses to existing lumber, an engineer should not immediately default to published allowables. Wood that has been exposed to the environment may be affected by any number of wood-deteriorating organisms and fungal decay. In addition, for older structures, heavy sustained dead loads and the possibility for periodic overstressing and wear-and-tear are all factors that should go into the engineer's decision of what allowable stress is appropriate to assign to the members. When an engineer does not have the benefit of a recent up-close detailed inspection of the bridge to guide the selection of an appropriate allowable stress value, good engineering judgment should lead to the selection of a value that errs on the side of conservatism.

Recommended resource documents include:

- *Covered Bridge Manual* [2]
- *Timber Bridges – Design, Construction, Inspection, and Maintenance* [4]

REFERENCES

American Forest and Paper Association, Washington, D.C. (editions published in 1991, 1997, 2001, and 2005), National Design Specification (NDS) for Wood Construction [1]

Federal Highway Administration, Publication Number: FHWA-HRT-04-098, <http://www.tfhrc.gov/structur/pubs/04098/index.htm> *Covered Bridge Manual* (accessed March 2009) [2]

Oregon Department of Transportation Website: <http://www.oregon.gov/ODOT/HWY/BRIDGE/docs/covbrdg/Descriptions/wimer.pdf> (accessed March 2009) [3]

United States Department of Agriculture Forest Service, Publication Number: EM7700-8 (August 1992) *Timber Bridges – Design, Construction, Inspection, and Maintenance* [4]

Built-up Column Stability in Wood Construction

Ryan Chancey, Ph.D., M.ASCE[1]; Stewart M. Verhulst, M.S., P.E., M.ASCE[2]; David W. Fowler, Ph.D., P.E., F.ASCE[3]; Deepak Ahuja, M.S., P.E., M.ASCE[4]

[1] Senior Associate, Nelson Architectural Engineers, Inc., 2740 Dallas Parkway, Suite 220, Plano, Texas 75093; phone: 469-429-9000; email: rchancey@architecturalengineers.com

[2] Branch Director, Nelson Architectural Engineers, Inc., 9701 Brodie Lane, Suite 201, Austin, Texas 78748; phone: 512-610-2800; email: sverhulst@architecturalengineers.com

[3] University Distinguished Teaching Professor Joe J. King Chair in Engineering No. 2 Director, International Center for Aggregates Research, The University of Texas at Austin, 1 University Station, C1755, Austin, TX 78712-0277; email: dwf@mail.utexas.edu

[4] Vice President, Nelson Architectural Engineers, Inc., 2740 Dallas Parkway, Suite 220, Plano, Texas 75093; phone: 469-429-9000; email: dahuja@architecturalengineers.com

ABSTRACT

Wood construction is common for low-rise buildings, including residential and light commercial structures. For these types of structures, vertical structural members may consist of multiple wood studs, called built-up columns. As wood-framing becomes increasingly common for multi-story structures, concerns of both structural strength and stability of the wood members should be of paramount importance to the engineer. Specifically, the engineer must have knowledge of the type and extent of bracing present to properly determine the capacity of each member.

Most commonly, wood studs in low-rise buildings are braced in the weak direction by fastening wall sheathing to the face of the stud of the narrower dimension. The use of gypsum board wall finishes to brace wood stud walls (and for lateral shearwall diaphragms) has become common in the design of wood structures. However, engineers must remain aware of the limitations of gypsum board when designing heavily loaded, non-repetitive members such as columns. These limitations are particularly important for the design and detailing of built-up columns.

Design and construction defects related to wood columns in a wood-framed townhome project are presented herein. The subject three-story structures utilized built-up wood columns that depended on gypsum board for stability bracing. The columns did not satisfy the National Design Specification requirements for built-up columns. The proper design of the columns and the implications of using gypsum board for bracing will be discussed.

BACKGROUND

The case study presented herein is based on a wood-framed condominium complex located in Dallas, Texas. The complex included 17 three-story (plus attic) condominium units in three buildings of similar construction. The complex featured only four distinct floor plans; thus, the unit layouts were repeated in the three buildings. The buildings were constructed in 2000 and 2001. The 1997 Uniform Building Code (UBC) was adopted with amendments by the City of Dallas in 1999 and was the Building Code enforced at the time of the building design and construction. The 1997 UBC references the 1991 National Design Specification (NDS) for Wood Construction (AFPA 1993) for the design of wood structures.

The first floor of each building was supported by a slab-on-grade foundation with piers. The framing at the second and third floors consisted of metal plate connected wood trusses and engineered glu-laminated (glulam) and parallel strand lumber (PSL) beams. The vertical support consisted primarily of wood stud walls, with "stud packs" (groups of studs). The interior finishes were typical for residential construction and included wood floors, carpet, and gypsum board walls and ceilings. In addition to the floor loads, the framing supported some brick veneer (i.e., the veneer was not continuously supported to the foundation at some areas).

Forensic engineers investigated complaints of several of the unit owners. Such complaints included, but were not limited to, uneven floors, sloping countertops, cracks in finishes, separations in wood flooring, cracks in brick veneer, and sticking and swinging doors. Specifically, the structural design was evaluated to determine if structural deficiencies were contributing to the damage and floor levelness issues. Although the investigation encompassed several issues and causes of distress, this discussion is limited to the issues related to the design and bracing of the vertical load-resisting members, specifically built-up columns. A study of issues related to the design of the floor framing was previously presented by Verhulst and Ahuja (2008).

A relative floor elevation survey was performed for each unit type to determine the extent and pattern of floor unlevelness for each framing layout. Based on these elevation surveys and the visible distress, a pattern of deflection at some of the interior walls and/or framing support locations was apparent. The surveys ruled out foundation movement as a cause of unlevelness at the second and third floors.

DESIGN AND CONSTRUCTION

The subject condominium units required columns at the first, second, and third stories. The columns at the subject structures consisted of multiple studs (commonly called "stud packs"), typically ranging from two to five studs (although some columns with more studs were observed). The columns were not consistent throughout the project, even at repetitive units with the same framing design. It should be noted that the terms "stud pack" and "built-up columns" are not interchangeable; "stud packs" are groups of individual studs and the term "built-up column" refers to multiple studs

fastened together in a specific manner so that they act together as a column. This is discussed further in the following sections.

Design

The only column specification for the subject structures was included in the framing details. "Shearwall Detail" 20 on Sheet S5.1 of the Structural Drawings is presented in Figure 1, below, and indicates that beams and truss girder supports were to consist of three 2x4 studs in a cluster or "stud pack," unless noted otherwise. The "stud packs" ranged from 8' to 10' (2.44m to 3.05m) in length. This was the only specific guidance regarding the column requirements for the project.

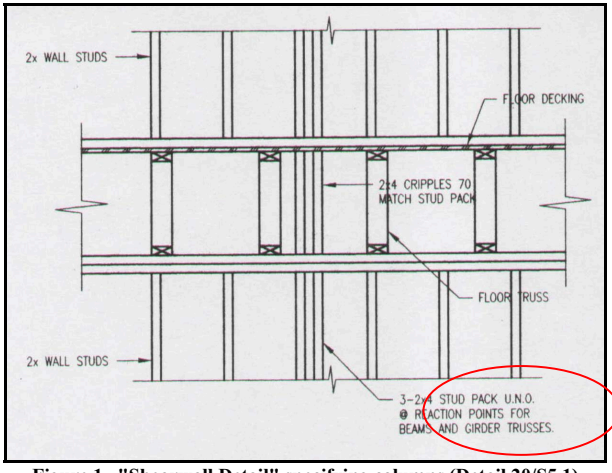

Figure 1. "Shearwall Detail" specifying columns (Detail 20/S5.1)

Based on an engineering review of the structures and the loading conditions, the columns were intended to behave as if continually braced, thus requiring the design of column bracing. However, the Structural Drawings did not include any design guidance regarding the bracing requirements of the studs/columns and no schedule for nailing the sheathing to the columns was included.

In addition, for the columns at the subject structures to be considered as built-up columns, the multiple studs must have been attached per the 1991 NDS (AFPA 1993). Studs which are not attached as indicated in the NDS act as individual studs, and do not gain additional design capacity from grouping. Compounding the structural deficiencies, even continually braced or "built-up" columns consisting of three 2x4 studs would not have been sufficient for the design loading conditions at many locations.

No attachment schedule for the studs/columns was included on the drawings. A "Nailing Schedule" indicated that "Double Studs" required 16d nails spaced at 16" (40.64cm) on-center and "Built-Up Corner Studs" required 16d nails spaced at 24" (60.96cm) on-center. These guidelines did not apply to the columns located in the walls nor did they conform to the NDS specifications for built-up columns.

It is the authors' opinion that the column design provided by the Structural Engineer was insufficient to support the design loads.

Construction

Excessive compressive load on a slender column will cause it to deflect or "bow" perpendicular to the weak axis (Breyer 1993). This deflection causes gaps between the studs of a stud grouping. Such gaps were observed between the studs at heavily-loaded "stud packs" at the subject structures. Column bowing of up to 7/8" (2.22cm) was observed at the subject structures, as measured by the distance between studs at mid-height in comparison with the distance between the studs at the top and bottom, as presented in Figures 2 - 4, below, and on the next page.

Figure 2. Bottom of two adjacent stud groups. The left group exhibits perceptible bowing. Measurement between columns was 1 1/16" at the bottom.

Figure 3. Measurement at mid-height of columns is 3/16".
The studs have displaced laterally and are also separated individually.

Figure 4. Top of columns. Distance between columns same as at base.

In addition, bowing studs were observed during the construction of the structures by a firm monitoring the overall construction. The Structural Engineer was notified.

Evidence of downward column deflection was observed due to bowing of the column under load. At one attic space, a heavily-loaded beam had separated more than 1" (2.54cm) from the framing at the attic, as shown in Figure 5, below. Despite the observed column failures, it should be noted that the structure had likely not been subjected to the full design load at the time that these conditions were observed.

Figure 5. Separation of framing at attic level above a heavily-loaded column.

Considering the significant amounts of overstress on the columns at the site, several factors prevented a collapse or catastrophic column failure. The actual loads at the time of the authors' observations did not approach the design loads, and load sharing with other structural elements such as adjacent wall studs provided many degrees of structural redundancy. Additionally, some bracing was provided by non-structural elements. Finally, the inherent factor of safety in the design capacities of the columns prevented catastrophic failure. Factors of safety may provide additional capacity but cannot be counted on by a designer for long-term load-carrying capacity. Building codes do not allow the designer to reduce these factors to increase the load-carrying capacity (UBC 1997; Breyer 1993; and Salmon 1996). Furthermore, the capacity provided by non-structural elements cannot be considered when determining the design capacity of the columns.

The unsafe conditions created by the insufficient column design necessitated significant column repairs at the subject structures. Inadequate columns were repaired or replaced with "built-up" stud columns (conforming to NDS specifications) or with glulam members. These repairs were necessarily invasive, and required relocation of the unit owners. Significant shoring was required to perform the column repairs. Additionally, some of the columns proved difficult to access and required the removal of architectural features. **The cost of the repair work far exceeded the cost of providing proper column support during construction.**

REQUIREMENTS FOR STUDS AS BUILT UP COLUMNS

Groups of studs, commonly called “stud packs”, are frequently used to support large concentrated loads, such as reactions from beams. In such applications, the studs are generally nailed together in a random manner, if at all. To be effective as a column, however, the individual laminations must be connected in the proper manner to function as a built-up column.

The NDS (AFPA 1993) provides requirements for built-up columns. Built-up columns may be either bolted or nailed and contain two to five laminations. The NDS requires that:

- Each lamination must be at least 1-1/2" (3.81cm) thick;
- All laminations must have the same depth (face width);
- The faces of adjacent laminations are to be in contact;
- All laminations must be full column length; and
- Specified connection requirements must be met.

The nailing and bolting requirements of the NDS are very specific. When nails are used, the following provisions must be met:

- Adjacent nails are driven from opposite sides of the column;
- All nails must penetrate at least 75% of the thickness of the last lamination [A 30d nail, for example, has a length of 4-1/2" (11.43cm), and the column thickness would be limited to three 1-1/2" (3.81cm) laminations]; and
- Nail spacing and end and edge distances are specified [For example, for 30d nails the minimum end distance is 3-1/2" (8.89cm), the minimum edge distance is 1-1/2" (3.81cm), and the maximum spacing in the parallel to grain direction is 9" (22.86cm)].

When bolted columns are used, the NDS requires that:

- Two or more longitudinal rows of bolts are required when more than three laminations are used;
- Metal washers or plates are required beneath the bolt head and the nut; and
- Typical bolt locations for 1/2" (1.27cm) diameter bolts are 3-1/2" (8.89cm) end distance, 2" (5.08cm) edge distance, and 8" (20.32cm) longitudinal spacing.

The built-up column is designed as a solid wood column, except that in the direction perpendicular to the face grain, the allowable axial load based on stability equals the load permitted for a solid column multiplied by K_f, where $K_f = 0.6$ for a built-up column nailed in accordance with NDS Section 15.3, and $K_f = 0.75$ when bolted in accordance with NDS Section 15.3. In effect, the allowable load (considering the designated axis) is reduced by 40% when the column is nailed and 25% when the column is bolted compared to a solid wood column having the same size. The reduction in load is due to the fact that the contact faces of the laminations are not fully restrained from slipping, and as a result the column does not fully behave as a solid column.

If the provisions of the NDS 15.3 are not met for built-up columns, the members cannot be considered to act as an integral unit; each stud must be considered as an individual column. Since the maximum L/D = 50 for a wood column, a non-braced stud with an unsupported length of 50 x 1.5 = 75" (190.5cm) or greater (as encountered at the previously-mentioned structures) would have an allowable load, P = 0. Typically, gypsum board is used to brace individual studs, but if gypsum board is nailed to one of the members in the stud pack, the other members would not be considered as braced in the direction of the least dimension. Only the nailed member could be considered as braced, but **only if the bracing were adequate**.

In the opinion of the authors, nailed gypsum board or paneling should **never** be assumed to provide bracing for a stud pack to function as a composite column for the following reasons:

- Neither gypsum board nor paneling is a permanent brace. During future remodeling either could be removed, and the column would then have no allowable axial load capacity. That is not a risk that either the design engineer or the owner should accept.
- If gypsum board were to become water saturated, perhaps due to a roof or plumbing leak, the gypsum board would have little or no bracing capacity.
- It is very difficult to verify during construction that the nailing into the individual laminations was in accordance with the design, e.g. some nails might be driven into the interface or nearer to the edge of the lumber than permitted by the NDS. For example, Figure 6, on the next page, shows nails

at the edge of one of the studs at the subject condominium project when only a single line of nails was used.

Verification of correct nailing would require much greater levels of inspection than is practical. With the studs covered by gypsum board, it would be very difficult for the drywall contractor to ensure that the gypsum board was nailed adequately and for the engineer to inspect the nailing.

Figure 6. Nails attached near the edge of a stud in a "stud pack".

Individual studs can be braced using nailed gypsum board or paneling; however, individual studs carry a relatively small axial load, and if one or two studs were rendered unbraced, adjacent studs would provide support. When stud packs are required to carry large loads, e.g. 5 kips to 10 kips (2268kg to 4536kg) or more, no such adequate nearby support is generally available.

RECOMMENDATIONS

The issues discussed herein deal with column design capacities, which is an issue of public safety. The limitations of multiple wood studs used as columns and of gypsum board as a bracing material were discussed. The authors recommend that building codes and the applicable standards be revised to reflect these limitations. Structural

Engineers should be aware of the above-noted limitations when performing wood design.

The authors recommend that applicable codes be changed to reflect the following:

1. Two or more studs that are required to carry a greater load than permissible using a single stud should be designed as a built-up column.
2. Gypsum board or other wall paneling is not to be considered as bracing for more than one stud in a group. Also, these materials should not be considered as bracing for columns (solid or built-up) with a design load greater than the capacity of one stud.
3. Built-up columns should be called out on Structural Drawings and be detailed in accordance with NDS requirements.

REFERENCES

American Forest & Paper Association (AFPA). (1991) *ANSI/NfoPA NDS-1991: National Design Specification for Wood Construction*, Revised 1991 Edition.

Breyer, Donald E. (1993) *Design of Wood Structures*, *Third Edition*. St. Louis: McGraw-Hill, St. Louis.

International Conference of Building Officials (ICBO). (1997) *Uniform Building Code*, *1997 Edition*.

Salmon, C.G. and Johnson, J.E. (1996) *Steel Structures: Design and Behavior, Emphasizing Load and Resistance Factor Design*, Fourth Edition. New York: HarperCollins College Publishers.

Verhulst, S. and Ahuja, D. (2008). *Structural Engineering and Structural Components: A Wood Truss Case Study.* The Institution of Civil Engineers (ICE), The Fourth International Forensic Engineering Conference, December 3-4, 2008.

Mold in Ductwork: A Forensic Analysis

Roger G. Morse, AIA[1] , Stephen M. Lattanzio, PE[2]

[1] Morse Zehnter Associates, 165 Jordan Rd, Troy, NY 12180, PH (518) 283-7671, FAX (518) 283-9855, rgmorse @mzaconsulting.com, [2] Morse Zehnter Associates, 165 Jordan Rd, Troy, NY 12180, PH (518) 283-7671, FAX (518) 283-9855, slattanzio@mzaconsulting.com,

Abstract

Mold growth in ductwork is an abnormal, but not an unusual condition. One of the prerequisites for mold growth to occur is that the interior surface of the duct must become wet. Moisture in ductwork can occur for a number of reasons, including, but not limited to: water can be stripped off cooling coils and carried down the ductwork; operation of the equipment can result in condensation inside the ductwork; or, a fog could be created inside the duct. This paper will describe the causes of moisture inside ductwork, the factors allowing mold growth to occur, and strategies to correct or avoid these problems. After the moisture problems are resolved, mold will cease to grow; but microbiological debris will be left in the ducts. The pros and cons of duct cleaning to deal with this debris, as well as alternative duct cleaning methods, will also be discussed.

Keywords: mold, ductwork, condensation, duct cleaning, temperature, relative humidity

Introduction

Mold growth in ductwork is an abnormal condition, but not unusual. One of the prerequisites for mold growth to occur is that the interior surface of the duct must become wet. Moisture in ductwork can occur for multitudes of reasons, including, but not limited to: water stripped off cooling coils and carried down the ductwork, operation of the equipment resulting in condensation inside the ductwork; or, a fog could be created inside the duct. The solutions to these issues are straightforward. After the moisture problems are resolved, mold will cease to grow, but microbiological debris will be left in the ducts. There are established standards for cleaning ductwork.

Mold – Requirements for growth

Three conditions must be present for mold to germinate and grow. These are moisture content, temperature and nutrients. Ductwork typically has two of these, temperature and nutrient sources. Among the nutrient sources typically found in ductwork are the following.

- Resin binding glass fibers together
- Paper dust

- Skin cells
- Fiber (cotton, wool)
- Construction dust
- Oil
- Hydrocarbon deposition
- Rubber dust

Mycologists have determined if the Equilibrium Relative Humidity is at least 80% then mold can germinate and grow. There are multiple potential sources of moisture in ductwork from the condensate drip pan to the humidity of the supply air.

A primer on AC Equipment operation

Figure 1 – Air Handling Unit shows a typical single fan AC unit. The fan draws the air though a chilled water coil or a DX coil. The fan shown below is a draw through unit. If the fan were on the other side of the coil, it would be a blow through unit.

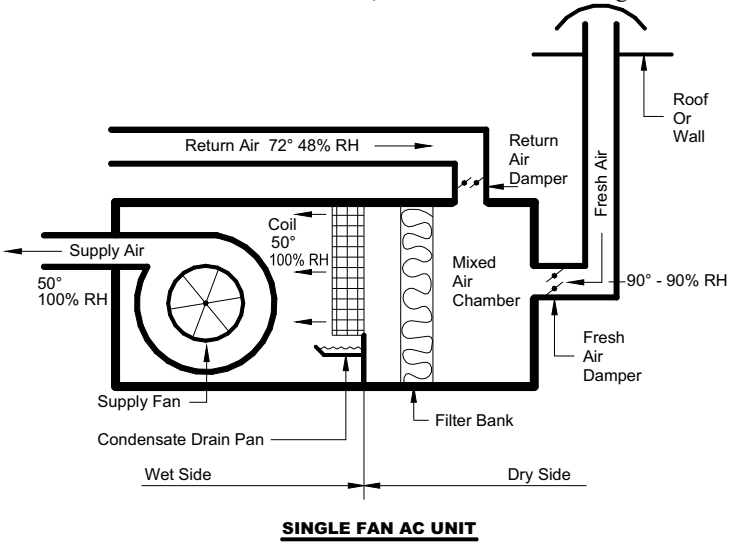

Figure 1 Air Handling Unit

This particular unit shows the fresh air at 90°F and 90% RH. The coil cools this air down to 50°F and 100% RH. This air is still saturated, but it holds less water than it would at 90°F. As this air mixes with the room air and warms back up to 70°F, the humidity is reduced to 48%. Figure 2 - Psychometric Chart shows that the humidity ratio (grains of water vapor per pound of dry air) drops from about 195 grains at 90°F and 90% RH to 53 grains at 50°F and 100% RH. The remaining grains of water end up in the drainage pan. Since no more grains of water are added when the air is heated back up to 70°F, the relative humidity reduces to 48%.

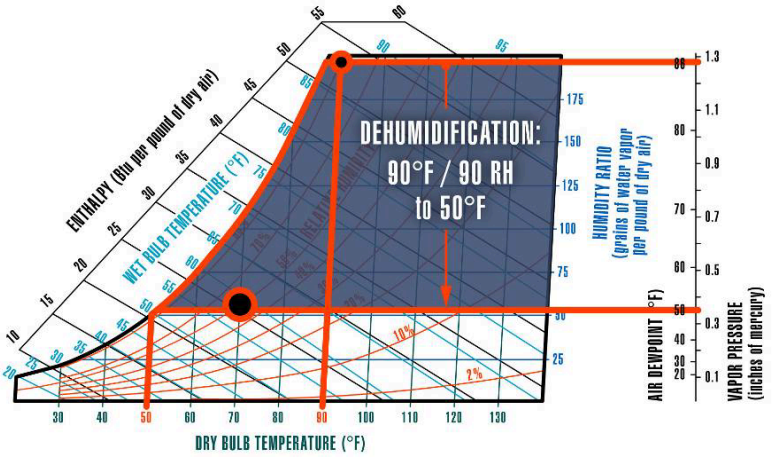

Figure 2 - Psychometric Chart

In summary

- Air conditioning systems dehumidify by chilling air below the dew point
- Water condenses out on the fins of the cooling coil
- The leaving air has a reduced dew point and specific humidity
- The leaving air will be saturated and have a relative humidity of about 100%

It was stated earlier that if the Relative Humidity was over 80%, then mold can germinate and grow. The air leaving the coil is at 100% RH. These leads to the question, why is mold not present in all ductwork? This is due to the dew point. Dew point is the temperature at which the air can no longer hold the moisture that is in it.

The important items to know about dew point are as follow. If the temperature of the surface falls below the dew point of the water vapor, condensation will occur on the surface. If the temperature of the surface is above the dew point, then the surface will stay dry. If the air temperature is below the dew point, then fog will occur. The ductwork is not in a static condition - the air is constantly flowing in the ductwork. Below are results of field measurements taken on a ductwork. Since the room temperature is higher than the air inside the ductwork, there will be a temperature gradient across the ductwork. Figure 3 – Ductwork Temperatures and Relative Humidity shows that the interior surface of the ductwork is above the dew point so the ductwork stays dry. Ducts should stay dry as long as the air conditioning system is operating.

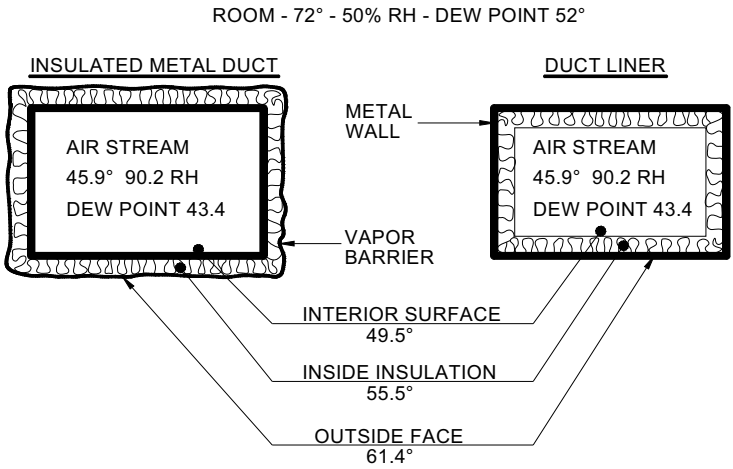

Figure 3 - Ductwork Temperatures and Relative Humidity

Causes of Mold Growth in HVAC Equipment

There are several causes of mold growth in HVAC equipment. The first is the introduction of humid outside air to chilled surfaces inside ductwork. Oversized AC coils exacerbate this. When the coil shuts down, the humid air will pass through the coil and condense out in an area of the ductwork that does not have a drain pan. A second condition is coil carry over. If the face velocity of the coil is too high, then the condensed water droplets will not drop to the drainage pan, but be carried with the air steam and deposited onto surfaces downstream. If the condensate drain pans are improperly sized or the drainage system is not designed properly, the pan can cause localized flooding of the ductwork. The last two less common issues causing mold are stratification causing fog in ductwork and the problems associated with gradually increasing coil temperatures.

In order to correct problems associated with the introduction of humid air the following are practices to consider:

- Precondition outside air
- Properly size or undersize cooling equipment
- Maintain constant coil temperature
- Allow drying out period without ventilation air, or cooling

Water stripped off the coil by the air stream is usually caused by the face velocity of the air stream being too high (over 500 fpm), tall coils which require more time for the water droplets to drain to the condensate pan, localized high velocity or non uniform air flow through coil, blow-through units without baffles, or blocked and

dirty coils. There are several options for correcting coil carryover. These include reducing fan speed to slow air flow through coil, install louvers (Mist Stop) to stop drops, extend drain pan to catch drops, and possibly control with a drying cycle by circulating room air with no cooling.

Specifying and installing a condensate drain pan properly is of the most cost effective measure to minimize mold in ductwork. There are several simple requirements for the pan. A properly designed pan will have the following features.

- 0.25" per foot minimum slope.
- Bottom drain or side drain in a sump.
- Recess drain so that it is flush with surface of pan.
- Large enough to catch stripped off water.
- Smooth cleanable surfaces.
- Free draining.
- Double wall insulated

If existing pan meets all requirements, make sure the drains are clean and initiate an Operations and Maintenance program.

Case Studies

Case Study 1 - Stratification causing fog in ductwork

As designed, the air handling unit (AHU) operated in a manner that resulted in wetting of the duct liner in the supply air ductwork. During normal operation, the surface of the duct liner is chilled to the temperature of the supplied air stream (approximately 50° F.). The chilled water coil in the air-handling unit modulates on and off to maintain comfort conditions. Unfortunately, AHU was designed in a manner that left the fresh air damper open when the chilled water coil was modulated off. At these times, unconditioned hot, humid outside air was admitted to the ductwork where the humidity condensed out on the chilled surfaces of the duct liner. This caused a wet condition. The conditions were exacerbated by the fact that the air conditioning was evidently operated during the later phases of construction of the building. Dust from drywall taping compound was found in locations of mold amplification. At the time that a musty odor was reported, the duct liner was observed to be saturated with water.

The operation of AHU was subsequently changed to correct the wetting condition. The chilled water coil was set so that it never modulated off. In this way, the coil dehumidified all outside air admitted to the ductwork. This resulted in overcooling of the space, but corrected the situation that allowed hot, humid outside air to impact on chilled surfaces inside the air-handling unit and ductwork. Figure 4 Stratification of Air Streams illustrates this lack of mixing.

.

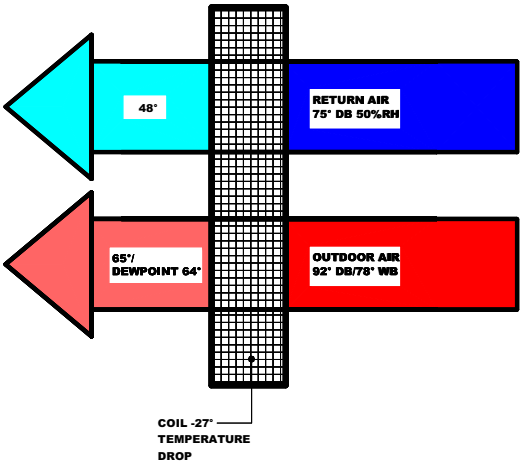

Figure 4 Stratification of Air Streams

The mold amplification was so well established in some locations however that it was able to hydrate itself and survive by drawing moisture directly from humidity in the air in the ductwork.

Testing has demonstrated that in most locations the mold is growing on construction dust, is found only on the surface and has not penetrated into the liner. In one location, the situation is more adverse. In the trunk duct connected directly to the AHU, the surface and interior of the liner have been contaminated with mold growth. In addition, this location is periodically dampened by aerosolized water stripped from the chilled water coil in the air-handling unit.

Case Study 2 - Gradually increasing coil temperatures

The supply air system on each floor consisted of an air handling unit, located in a central mechanical room, and lined sheet metal ductwork carrying air to the occupied floor. The supply air plenum on the air handling units are of double-wall construction with insulation sandwiched between two layers of sheet metal. Figure 5 shows the interior of the ductwork. The supply ductwork extending from this plenum is lined

with sound absorbent fiberglass insulation with a surface designed to prevent air erosion.

Figure 5 – Interior Ductwork

Air handling units are located in a mechanical room on each floor. Fresh air and return air are ducted to the mechanical room, which serves as a mixed air plenum. An air handling unit consisting of a painted steel case with a filter bank, followed by a chilled water coil and then a fan, is located in each mechanical room. Air is drawn from the mechanical room (mixed air plenum) through the filters and coil by the fan and is then blown into a supply air plenum that extends above the air handling unit. This plenum is of double-wall construction with insulation sandwiched between two layers of sheet metal. The inner layer of sheet metal is perforated to provide sound attenuation of machine noises. Supply air ductwork connects into the plenum above the air handling unit and carries conditioned air to the occupied floor. The supply air ductwork is fabricated of galvanized sheet metal and is lined with fiberglass duct liner equipped with a coating on the inner surface that is designed to prevent air erosion of the underlying fiberglass. Water damage and staining occurred on the surface of the duct liner, particularly where the HVAC units operated 24 hours per day.

As in most commercial buildings, the HVAC system serving this building dehumidifies air by chilling it below its dew point. Much like condensation on a pitcher of ice water, when air is chilled, the water vapor in the air condenses out of the air and collects on the cooling coil, where it drips into a condensate pan and carried away by a drain. As the air cooled to its dew point, the relative humidity of the air leaving the cooling coil is near 100% and the air is referred to as “saturated.” Normally, the inside face of the ductwork remains dry as it is warmed slightly by heat from the air surrounding the duct that is conducted through the wall of the duct and

insulation. If the coil temperature increases, the air temperature and the dew point of the air leaving the coil increased. If this dew point is above the temperature of the surface of the duct liner, water condenses out of the supply air stream, wetting the surface of the liner. In a variable air volume (VAV) system, this situation should not occur; the leaving air temperature in a VAV system should remain relatively constant, and the temperature in the occupied spaces would be controlled by varying the amount of air admitted to the space. However, in the units monitored during this study, the occupied space was sub-cooled prior to occupancy and the temperature was allowed to drift up during the course of the day. Mixed air temperatures measured were typically 68°F just before occupancy, rising to about 75°F by the end of the work day. The temperature of air leaving the chilled water coil increased gradually throughout the day from about 48°F to about 54°F. This is depicted in Figure 6 – Air Leaving Coil Conditions

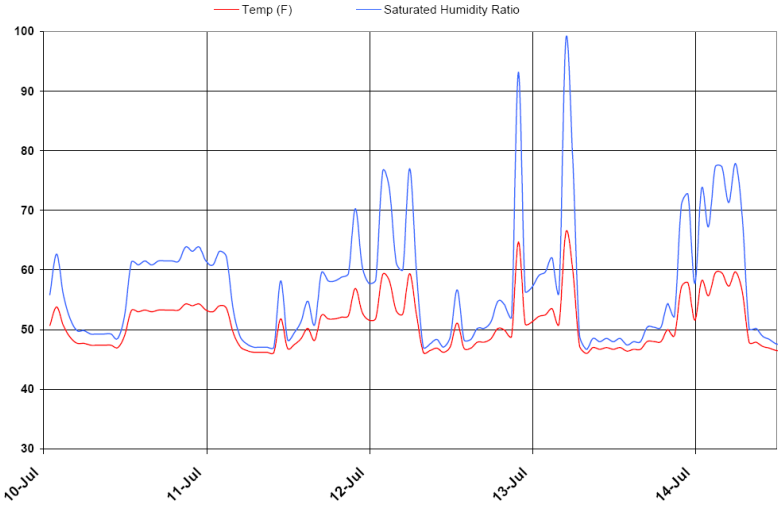

Figure 6 - Air Leaving Coil Conditions

This resulted in gradually warmer air impacting upon the chilled surfaces inside the supply air ductwork, causing condensation on the surface of the duct liner. Since the relative humidity of the air being carried by the duct work is near saturation, the water condensed on the surface does not dry out and the surface remained wet.

Moisture damage to the supply air ductwork is caused by current operation of the chilled water coil in air handling units on each floor of the building. These coils were gradually warmed during the work days, resulting in relatively warmer saturated air impacting on chilled surfaces in the supply air path, causing condensation. As this condition persisted for the entire working day, the duct liner remained wet and

became water-damaged. This condition is particularly acute on floors where the air conditioning units ran all day and night. On these floors, the duct liner never had the opportunity to dry out, resulting in moisture damage to the duct liner.

Cleaning Ductwork

According to the Environmental Protection Agency, regarding residential ductwork:

- It is unknown if duct cleaning reduces health problems
- It is unknown if dirty ducts result in higher particulate levels in occupied spaces
- There is no evidence that dust and other particulate in ducts is a health problem
- It is recommended to clean ducts if there is visible mold

Commercial buildings have different requirements for cleaning. Commercial buildings typically shut down the HVAC systems at night. This allows the dirt to settle. During the morning start of the HVAC equipment, the settled dust becomes airborne again and will eventually come out of the diffusers. If there is dirt or debris dumping out of the diffusers, then cleaning ducts becomes worthwhile to satisfy the building occupants. There are two organizations that provide standards for duct cleaning based on the type of duct you have.

- Hard duct surfaces in the supply air plenum should be cleaned using procedures published by NADCA (NADCA, 2004).
- NAIMA (NAIMA Pub. No. AH122) sets forth the procedures for cleaning lined duct surfaces.

In addition to cleaning these surfaces according to the above-published standards, the following additional cleaning strategies are recommended:

- Install access hatches no farther than 12’ apart to provide access for cleaning, inspection and encapsulation.
- Perform direct contact vacuuming to clean the ductwork.
- Cleaning of fiberglass duct liner should be accomplished by direct contact vacuuming followed by cleaning with an air whip.
- Subsequent to cleaning and passing a visual inspection, with cleanliness verified as necessary by direct contact vacuuming, acceptance samples should be collected on mixed cellulose filters using the micro-vacuum collection technique in ASTM D5755. The filters should be analyzed using NIOSH 7400 procedure, with all particles being counted, except fiberglass. Surfaces are acceptable if all samples have particle counts as low as or lower than that in the criterion area with the diversity of particles the same between the test and criterion area. Ventilation air ductwork can be used as a criterion area for this purpose.
- After clearance, the surface of the duct liner is treated with a penetrating type encapsulant that contains a biostat additive (Fiberlock IAQ 8000™).

- After the penetrating encapsulant has dried, the surface of the liner should be coated with a heavy coating of encapsulant to bind the surface together and prevent release of fiberglass from the liner. This coating should be white to permit future inspection and contain a biostat (Fiberlock IAQ 7000™).
- The cleaned ductwork should be inspected on a periodic basis to make sure that the wet condition has not reoccurred and that there is no new water damage or staining.

Conclusions

Air handling units and cooling and heating equipment are necessary equipment in most every building. These systems must be designed properly to provide comfort for the occupants. Designing these systems to maintain dry systems and provide maintenance access is part of a proper design. Designing the ductwork so that it stays dry during operation will eliminate most causes of mold in ductwork.

References:

NADCA (2004) General Specifications For The Cleaning of Commercial Heating, Ventilating and Air Conditioning Systems, Copyright by National Air Duct Cleaners Association, Washington, D.C.

Cleaning Fibrous Glass Insulated Duct Systems - Recommended Practices, NAIMA Pub. No. AH122, North American Insulation Manufacturers Association, 44 Canal Center Plaza, Suite 310, Alexandria, VA 22314

Fiberlock IAQ 8000™ Duct Liner Insulation Sealer/Adhesive/Basecoat, www.fiberlock.com

Fiberlock IAQ 7000™ Duct Liner Adhesive Coating/Encapsulant, www.fiberlock.com

The New FEMA 320 and FEMA 361—Highlights of the Wind and Flood Hazards Criteria for the Design and Construction of Residential and Community Safe Rooms (Shelters)

John Ingargiola, CFM – FEMA, Mitigation Directorate, Building Science Branch, 500 C Street, SW, Washington, DC 20007 John.Ingargiola@dhs.gov

Scott Tezak, PE, BSCP – URS Corporation, Infrastructure Protection & Risk Assessment Team, 260 Franklin Street, Suite 300, Boston, MA Scott_Tezak@URSCorp.com

Abstract

In August 2008, the Federal Emergency Management Agency (FEMA) released the Third Edition of FEMA 320, *Taking Shelter From the Storm: Building a Safe Room For Your Home or Small Business,* and the Second Edition of FEMA 361, *Design and Construction Guidance for Community Safe Rooms*. First released in 1998, FEMA 320 is the benchmark publication that provides prescriptive designs to be used in the design and construction of **residential** safe rooms (shelters) to protect occupants from hurricanes and tornadoes. Originally released in July 2000, FEMA 361 provides technical guidance for design and construction of **community** safe rooms to protect larger groups of occupants from hurricanes and tornadoes.

These FEMA documents were the basis for the development of the new ICC/NSSA *Standard on the Design and Construction of Storm Shelters* (ICC-500) released in August 2008. This paper presents the criteria and levels of protection from the FEMA documents and compares them to new ICC-500.

Introduction

Federal Emergency Management Agency (FEMA) publications presenting design and construction guidance for both residential and community safe rooms have been available since 1998. Since that time, thousands of safe rooms have been built using FEMA's criteria, many in part with funding from the FEMA. A growing number of these safe rooms have already saved lives in actual events. Since the initiation of its safe room program, FEMA has provided federal funds through its Hazard Mitigation Assistance Program totaling over $200,000,000 for the design and construction of more than 500 community safe rooms. Through residential safe room initiatives over the same time, FEMA has provided support for the design and construction of nearly 20,000 residential safe rooms with federal funds totaling more than $50,000,000. These safe rooms were constructed in tornado and hurricane-prone regions.

The new Third Edition of FEMA 320, *Taking Shelter From the Storm: Building A Safe Room For Your Home or Small Business*, 2008, presents updated hazard evaluation, prescriptive safe room designs, and consumer guidance. The new Second

Edition of FEMA 361, *Design and Construction Guidance for Community Safe Rooms,* 2008, presents updated and refined design criteria for safe rooms when compared to the First Edition's 2000 criteria. The criteria presented in the publications address how to design and construct a safe room that provides near-absolute protection for groups of individuals sent to a building or structure expecting it to be capable of providing them life-safety protection from wind, windborne debris, and flooding. The changes to the publications are the result of post-disaster investigations into the performance of safe rooms and shelters and also consider the new consensus standard from the International Code Council® (ICC®) and the National Storm Shelter Association (NSSA), the ICC/NSSA *Standard for the Design and Construction of Storm Shelters* (ICC-500, 2008).

FEMA continues to support the development of consensus codes and standards that provide minimum acceptable requirements for the design and construction of hazard-resistant buildings; and FEMA supported and participated in the development of the ICC-500. Although these two documents present essentially the same criteria, some design criteria remain different. The technical differences are evident in some wind design criteria, the design missile criteria for hurricane safe rooms, peer review requirements, and flood hazards siting requirements.

Levels of Protection: Defining the "Safe Room"

"Safe room" and "shelter" are two terms that have been used interchangeably in past publications, guidance documents, and other shelter-related materials. However, with the release of the ICC-500 standard, there is a need to identify or describe shelters that meet the FEMA criteria for life-safety protection and those that meet the ICC-500 standard. To help clarify the difference between shelters designed to the ICC-500 standard, and all other shelters (such as evacuation, recovery, long-term, etc.) and structures being designed to comply with the FEMA 320 and FEMA 361 guidance, FEMA refers to all shelters constructed to meet their criteria as **safe rooms**. A safe room provides occupants "near-absolute protection" from extreme-wind events. All safe room criteria in set forth in the FEMA publications meet or exceed the shelter requirements of the ICC-500. The different approaches to protection are seen in the FEMA and ICC definitions below:

FEMA 361, Section 1.2."*Near-absolute protection means that, based on our current knowledge of tornadoes and hurricanes, the occupants of a safe room built according to this guidance will have a very high probability of being protected from injury or death. Our knowledge of tornadoes and hurricanes is based on substantial meteorological records as well as extensive investigations of damage from extreme winds."*

By comparison, the purpose of the ICC-500 standard was set forth as:
ICC-500, Section 101.1 Purpose. *The purpose of this standard is to establish minimum requirements to safeguard the public health, safety, and general welfare relative to the design, construction, and installation of storm shelters constructed for protection from high winds associated with tornadoes and hurricanes. This standard*

is intended for adoption by government agencies and organizations for use in conjunction with model codes to achieve uniformity in the technical design and construction of storm shelters.

It is up to a community or jurisdiction to determine if the level of protection they desire is that of a safe room, an ICC-500 shelter, or another shelter that may provide some level of protection between that of an engineered building and the FEMA or ICC-500 levels of protection. The 2009 IBC and IRC have adopted the ICC-500 Storm Shelter Standard as the code minimum requirements for the design and construction of tornado and hurricane shelters. Table 1 summarizes and compares different levels of protection afforded by the different criteria that is being enforced in various jurisdictions around the country. This table is a condensed version of FEMA 361, Table 2-1; a complete summary of the table is in FEMA 361, Section 2.2.

General Design Approach

The FEMA safe room design and construction criteria are presented in Chapter 3 of FEMA 361without detailed discussion or guidance. The remaining chapters of the publication provide both discussion and guidance on the design and construction criteria presented in Chapter 3. These criteria are based on codes and standards available for adoption by any jurisdiction. Should a designer, builder, or manager have any questions regarding design criteria presented in FEMA 361, the following approach should be taken (if not, the safe room cannot be considered to be a FEMA safe room.):

1. When differences between FEMA 361 criteria and another code or standard (such as the ICC-500) are identified, the criteria in FEMA 361 should govern.
2. When design and construction criteria are not presented in FEMA 361, but provided in the ICC-500, the criteria of the ICC-500 should be used.
3. When criteria or requirements are not addressed by FEMA 361 or the ICC-500, the 2006 IBC and 2006 IRC (with references to ASCE 7-05 and ASCE 24-05) should be used.
4. Where the purpose of a safe room is to provide life-safety protection from both tornadoes and hurricanes, the entire safe room should be designed and constructed using the most restrictive of the two sets of criteria.

Table 1 –Safe Room and Shelter Criteria from Existing Codes and Standards

Shelter Design Standard, Code, or Document	Data[1]	Example Location #1: Miami, FL (Both tornado and hurricane hazards)	Example Location #2: Galveston, TX (Both tornado and hurricane hazards)	Example Location #3: Greenburg, KS (Tornado hazard only)
FEMA 320/361 (August 2008)	Design wind speed	200 mph (tornado) 225 mph (hurricane)	200 mph (tornado) 160 mph (hurricane)	250 mph (tornado)
	Pressure on windward wall[2]	107 psf (tornado) 136 psf (hurricane)	107 psf (tornado) 69 psf (hurricane)	167 psf (tornado)
	Pressure on roof section[2]	257 psf (tornado,) 325 psf (hurricane)	257 psf (tornado) 202 psf (hurricane)	401 psf (tornado)
	Test missile momentum at impact[2]	62 lb_f-s (tornado) 46 lb_f-s (hurricane)	62 lb_f-s (tornado) 33 lb_f-s (hurricane)	68 lb_f-s (tornado)

Shelter Design Standard, Code, or Document	Data[1]	Example Location #1: Miami, FL (Both tornado and hurricane hazards)	Example Location #2: Galveston, TX (Both tornado and hurricane hazards)	Example Location #3: Greenburg, KS (Tornado hazard only)
ICC-500 (August 2008) [3]	Design wind speed	200 mph (tornado) 225 mph (hurricane)	200 mph (tornado) 160 mph (hurricane)	250 mph (tornado)
	Pressure on windward wall[2]	107 psf (tornado) 136 psf (hurricane)	107 psf (tornado) 69 psf (hurricane)	167 psf (tornado)
	Pressure on roof section[2]	257 psf (tornado,) 325 psf (hurricane)	257 psf (tornado) 202 psf (hurricane)	401 psf (tornado)
	Test missile momentum at impact[2]	62 lb_f-s (tornado) 36 lb_f-s (hurricane)	62 lb_f-s (tornado) 26 lb_f-s (hurricane)	68 lb_f-s (tornado)
FBC EHPA (as required per FBC Section 423.25)	Design wind speed	146 mph	N/A	N/A
	Pressure on windward wall[2]	39 psf	N/A	N/A
	Pressure on roof section[2]	117 psf (suction)	N/A	N/A
	Test missile momentum at impact[2]	14 lb_f-s	N/A	N/A
ASCE 7-05/IBC 2006 (referencing ASTM E 1996)	Design wind speed	150 mph	105 mph	90 mph
	Pressure on windward wall[2]	41 psf	18 psf	15 psf
	Pressure on roof section[2]	124 psf	52 psf	44 psf
	Test missile momentum at impact[2]	14 lb_f-s	Not required	Not required
ARC 4496	Design wind speed	Not Specified	Not Specified	Not Specified
	Pressure on windward wall[2]	Not Specified	Not Specified	Not Specified
	Pressure on roof section[2]	Not Specified	Not Specified	Not Specified
	Test missile momentum at impact[2]	Not Specified	Not Specified	Not Specified

TABLE NOTES:

1. Wind pressures were calculated based on a 40-foot x 40-foot square building, with a 10-foot eave height and a 10-degree roof pitch.
2. psf – Pounds per square foot; lbf -s – Pounds (force) seconds. Suction or outward acting forces.
3. ICC-500 Hurricane design criteria used the most restrictive case that may be appropriate, which results in the use of GCpi=+/-0.55 and Exposure Category C at the site.

The primary difference in a building's structural system designed for use as a safe room, rather than for conventional use, is the magnitude of the wind forces that it is designed to withstand. Conventional (normal) buildings are designed to withstand forces associated with a certain wind speed (termed "design [basic] wind speed") presented in design standards such as the American Society of Civil Engineers (ASCE) 7-05, *Minimum Design Loads for Buildings and Other Structures*. The highest design wind speed used in conventional construction, near the Atlantic and Gulf coasts, is in the range of 140 to 150 mph (3-second gust). By contrast, the design wind speed recommended by FEMA for safe rooms in these same areas is in the range of 200 to 225 mph (3-second gust) and is intended to build safe rooms that can provide "near-absolute protection" for occupants.

For envelope or cladding systems, the governing design criterion is windborne debris, commonly referred to as missiles. Windows, and glazing in exterior doors, of conventional buildings are not required to resist windborne debris except when the

buildings are located within windborne debris regions; when openings must have impact-resistant glazing systems or protection systems. These systems can be laminated glass, polycarbonate glazing, or shutters. The ASCE 7-05 missile criteria were developed to minimize property damage and improve building performance; they were not developed to protect occupants and notably do not require walls and roof surfaces to be debris impact-resistant. To provide occupant protection for a life-safety level of protection, the criteria used in designing safe rooms include greater resistance to penetration from windborne debris. Sections 3.3.2, 3.4.2, and 3.5.2 present the debris impact-resistance performance criteria for the tornado, hurricane, and residential safe rooms, respectively. FEMA 361 defers to Chapter 8 of the ICC-500 for protocols for testing and acceptance of safe room components providing life-safety protection subject to wind pressures and debris impact.

The remaining design criteria for the safe rooms is also identified in Chapter 3 of FEMA 361. The criteria may be found as follows:

- Section 3.6 – Flood design criteria
- Section 3.7 – Product testing
- Section 3.8 – Permitting, code compliance, professional design oversight and peer review
- Section 3.9 – Construction documents, signage, and labeling
- Section 3.10 – Quality assurance and special inspections

Many other factors need to be considered when designing, constructing, permitting, and managing a safe room. In addition to the safe room design criteria for wind, and flood hazards, FEMA 361 provides design guidance for a variety of human factors, emergency management, and construction and permitting issues.

Finally, the use of "ultimate" wind speeds in the safe room design wind speed maps requires the adjustment of wind load factors in the load combinations presented in Chapter 2 of ASCE7-05. To correctly account for the return periods provided in the safe room design wind speed maps (Figures 1 and 2 of this paper), modifications to the load combinations are necessary. These modifications are addressed by Section 3.2 of FEMA 361.

FEMA 320 Criteria and Prescriptive Designs for Small Safe Rooms

FEMA provides prescriptive designs to meet the need for safe room solutions for residential and small, community safe rooms with occupancies of 16 persons or less. The FEMA prescriptive solutions are a vetted set of designs for different materials. With the release of the 3rd Edition of FEMA 320, FEMA has expanded the prescriptive designs which provide a universal solution to safe room protection via one set of design criteria to include both residential and small, community safe room designs. FEMA 361 and FEMA 320 define the small safe rooms as follows:

***"A residential safe room** is intended to provide protection for a small number of people (16 or less)……..An in-residence safe room is a small, specially designed ("hardened") room, such as a bathroom or closet, which is intended to provide a*

place of refuge for the people who live in the home. An external residential safe room is similar in function and design, but it is a separate structure installed outside the home, either above or below ground. The residential safe room criteria presented by FEMA are for the combined tornado and hurricane hazards and are capable of proving life-safety protection as defined in Section 3.5 of this publication."

FEMA has studied the costs of safe room design and construction and has found these solutions to be a viable alternative to site-specific design solutions. As such, safe rooms designed to these criteria for a universal set of criteria meet the combined-hazard criteria identified in both the FEMA and the ICC documents. Table 2 presents a summary of key design criteria for the safe room designs presented in FEMA 320 (and in Section 3.5 of FEMA 361) along with the criteria for community safe rooms.

FEMA 361 Design Criteria for Community Safe Rooms

When the design of safe rooms is intended for non-residential use or the safe room population exceeds 16 persons, FEMA provides performance-based, design criteria for the community safe room. For a complete listing of all safe room design criteria, the reader is directed to FEMA 361, Sections 3.3 and 3.4 for tornado and hurricane safe room design criteria, respectively; using the highest of either criteria when a combined hazard safe room is determined to be appropriate. Specifically, FEMA 361 defines a community safe room as follows:

*"A **community safe room** is intended to provide protection for a large number of people, anywhere from approximately 16 to as many as several hundred individuals. These safe rooms include not only public but also private safe rooms for business and other types of organizations. Tornado and hurricane community safe rooms are buildings or portions thereof that have been designed and constructed to the criteria set forth in Sections 3.3 and 3.4, respectively."*

Community Safe Room Design Criteria

Table 2 presents a summary of key design criteria for the safe room designs presented in FEMA 361 and as outlined in Sections 3.3 and 3.4 of FEMA 361.

Table 2 – Key Wind and Debris Impact Design Criteria for Residential and Community Safe Rooms from FEMA 361

Safe Room Design Criteria	Tornado Hazard Design Values – *Community* Safe Room	Hurricane Hazard Design Values – *Community* Safe Room	Combined Hazard Design Values – *Residential* Safe Room
Safe Room Design Wind Speed	130 - 250 mph (3-second gust @ 33 ft), varies based on geographic location	160 - 255 mph (3-second gust @ 33 ft), varies based on geographic location	250 mph (3-second gust @ 33 ft)
Importance Factor	I = 1.0	I = 1.0	I = 1.0
Exposure Category	C	C	C
Directionality Factor	K_d = 1.0	K_d = 1.0	K_d = 1.0
Topographic Effects	K_{zt} need not exceed 1.0	K_{zt} need not exceed 1.0	K_{zt} need not exceed 1.0
Enclosure classification	Partially Enclosed recommended, Enclosed may be used if conditions	Partially Enclosed recommended, Enclosed may be used if conditions	Partially enclosed.

Safe Room Design Criteria	Tornado Hazard Design Values – *Community* Safe Room	Hurricane Hazard Design Values – *Community* Safe Room	Combined Hazard Design Values – *Residential* Safe Room
	are met	are met	
Atmospheric Pressure Change contribution	Estimated using CG_{pi} = +/- 0.55 (recommended), direct calculation of APC (allowed)	Need not be considered	Estimated using CG_{pi} = +/- 0.55 (partially enclosed)
Max safe room height	Not limited	Not limited	8 feet of vertical wall
Duration of Protection	2 hours	24 hours	24 hours
Maximum Occupancy / Population	Not specifically limited, consult FEMA Policy	Not specifically limited, consult FEMA Policy	16 persons (square footage requirements must be met)
Occupancy Classification	Use the occupancy classification as defined by IBC for primary use. If single use, use A-3 Occupancy as defined in IBC.	Use the occupancy classification as defined by IBC for primary use. If single use, use A-3 Occupancy as defined in IBC.	▪ 3-5 sf/per person (depending on 1- and 2-Family Dwellings, Other residential, or small/ community)
Maximum Population Densities - Note: Net square footage design criteria may apply	▪ 5 sf/per person (standing or seated) ▪ 10 sf/per person (wheel-chair bound) ▪ 30 sf/per person (bedridden)	▪ 20 sf/per person (standing or seated) ▪ 20 sf/per person (wheel-chair bound) ▪ 40 sf/per person (bedridden)	▪ 7 sf/per person (1- and 2-Family Dwellings) ▪ 10 sf/per person (Other residential and small, community up to 16 person occupancy)
Design Missile for Debris Impact	15-lb 2x4 wood member	9-lb 2x4 wood member	15-lb 2x4 wood member
Design Missile Impact Speed (as a function of the Safe Room Design Wind Speed)	Varies from 80-100 mph on vertical surfaces and 53-67 mph on horizontal surfaces	Varies from 80-128 mph on vertical surfaces (0.5 x safe room design wind speed) and 16-26 mph on horizontal surfaces	100 mph on vertical surfaces 67 mph on horizontal surfaces
Surfaces that must meet debris impact criteria	All areas protecting occupants (exceptions apply for soil covered safe rooms and for doors and windows shielded by alcoves)	All areas protecting occupants (exceptions apply for soil covered safe rooms and for doors and windows shielded by alcoves)	All areas protecting occupants (exceptions apply for soil covered safe rooms and for doors and windows shielded by alcoves)
Peer Review of Safe Room Design Elements	Always recommended, but must be performed when occupancy is 50 persons or more	Always recommended, but must be performed when occupancy is 50 persons or more	Always recommended, but not required

Safe Room Design Wind Speed Maps

Figures 1 and 2 are the safe room design wind speed maps from FEMA 361 for the design of tornado and hurricane safe rooms, respectively. These maps are important as they are the basis not only for the wind design of the safe rooms, but also because the debris impact speeds of this criteria (and the ICC-500) are presented as a function of the safe room design wind speed at the site.

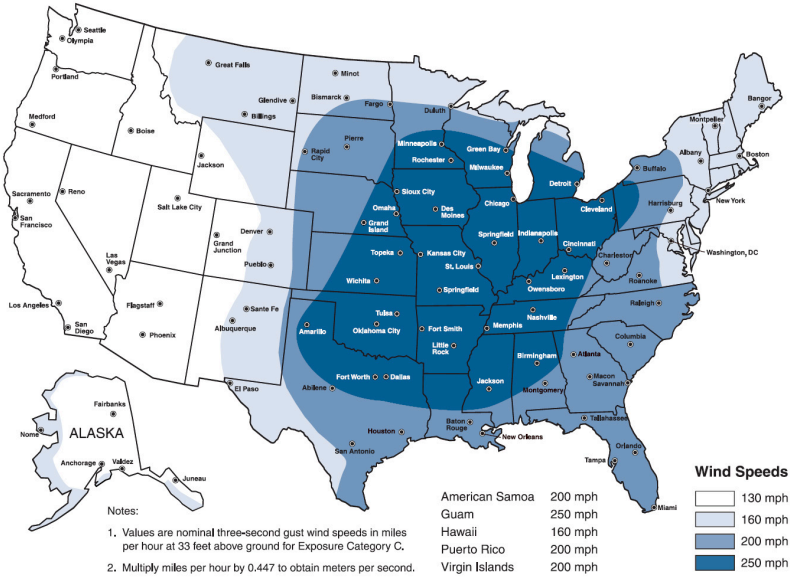

Figure 1 – Tornado Safe Room Design Wind Speed Map (consistent with ICC-500 Tornado Hazard Map)

Most wind speed maps in use today reflect a specific MRI that was adopted as a risk indicator for that design standard. ASCE 7-05 wind maps, for example, use a 50-year MRI to determine the basic wind speeds for non-hurricane-prone areas. Some occupancies categorized by ASCE 7-05 as Category III and IV buildings are required to be designed for 100-year wind events, which necessarily involves higher wind speeds. This adjustment in the MRI is accomplished through the use of an importance factor (I) in the wind load calculations. The FEMA 361 map for tornado hazards, which is identical to the ICC-500 tornado map, uses 10,000 to 100,000 MRI wind events to determine the wind speed zones for tornado safe rooms. The low probability of occurrence or the mean recurrence interval of 10,000 to 100,000 years is used in order to make sure that safe rooms are protected even against the rarest of wind storms with extreme-wind speeds of 250 mph (3-second gust).

For the hurricane hazard, NOAA and other meteorological groups have more readily available tracking maps to illustrate the occurrence of hurricanes. Furthermore, the ASCE 7-05 basic wind speed map was developed from a combination of historical and probabilistic storm events (which include hurricanes, but not tornadoes). As a result, for the hurricane-prone regions the mapped speeds reflect the hurricane influence and hazard and should be considered to be 100-year MRI basic wind speeds

(For a more complete discussion on the MRI used for hurricane and non-hurricane wind speeds on the ASCE 7-05 Basic Wind Speed Map, see the commentary for Chapter 6 of ASCE 7-05.). The FEMA 361 map uses the ICC-500 Shelter Design Wind Speeds for Hurricanes Map (ICC-500, Figure 304.2.2), which has been developed using the same modeling approach and inputs as the ASCE 7-05 basic wind speed map. However, it has been developed for an ultimate wind event of 10,000 MRI (based on both historical and probabilistic storm data). As a result, appropriate maximum hazard wind speeds associated with the hurricane event alone (tornadoes are not included in this model) are 225 mph for the mainland U.S. and 255 mph for certain U.S. island territories (3-second gust).

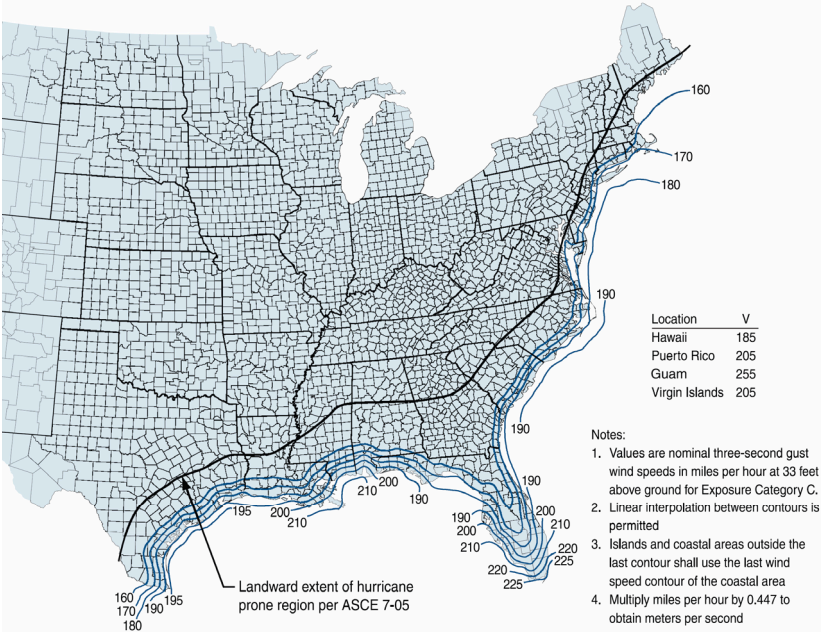

Figure 2 – Hurricane Safe Room Design Wind Speed Map (consistent with ICC-500 Tornado Hazard Map)

Source: *ICC/NSSA Standard for the Design and Construction of Storm Shelters* (ICC-500). Copyright 2008, Washington, DC: International Code Council. Reproduced with permission. All rights reserved. www.iccsafe.org < http://www.iccsafe.org >

Flood Hazard Design Criteria

It is also important to address the flood hazards that may exist at a safe room site. Safe rooms subject to flooding should be designed in accordance with the provisions of Section 3.6 of FEMA 361, ASCE 7-05, Section 5, and ASCE 24-05. If the flood hazard does not exist at the site, a statement identifying that there is not a flood hazard should be included on the project plans.

Community Safe Room Flood Design Criteria

Flood loads acting on a structure containing a safe room will be strongly influenced by the location of the structure relative to the flood source. Therefore, the safe rooms should be located ***outside*** of the following high-risk, special flood hazard areas (SFHAs):

a. The Coastal High Hazard Area (VE zones) or other areas known to be subject to high-velocity wave action; or
b. Areas seaward of the Limit of Moderate Wave Action (LiMWA) where mapped, also referred to as the Coastal A Zone in ASCE 24-05; or
c. Floodways.

Structures containing community safe rooms should be located in areas at low risk to flooding and mapped as unshaded Zone X (outside the 500-year [0.2 percent annual change] floodplain) wherever possible. Siting of safe rooms in SFHAs is not a desirable option, and should be avoided except in special circumstances. When the safe room is sited in a floodplain, the lowest floor used for safe room space and/or safe room support areas ***should be elevated to the higher of the following elevations***, which should be used as the design flood elevation (DFE) for flood load calculations:

1. Two feet above the base flood elevation (BFE), i.e., 2 feet above the flood elevation having a 1 percent annual chance of being equaled or exceeded in any given year (100-year event); or
2. The stillwater flood elevation associated with the 0.2 percent annual chance of being equaled or exceed in any given year (500-year event); or
3. The lowest floor elevation required by the community's floodplain ordinance, if such ordinance exists; or
4. Two feet above the highest recorded flood elevation in an area, if the area is designated as Zone D on a FIRM, or if the area has not been evaluated as part of a NFIP flood study (or equivalent flood study); or
5. If the community safe room is in an area subject to coastal storm surge inundation:
    a. The maximum stillwater inundation elevation associated with a Category 5 hurricane
    b. The wave crest elevation having a 0.2 percent annual chance of being equaled or exceeded in any given year.

Residential Safe Room Flood Design Criteria

Flood hazards should also be considered when designing and constructing a combined-hazard tornado, hurricane residential safe room. The residential safe room should be located ***outside*** of the high-risk flood hazard areas listed below, in addition to the areas listed for the community safe rooms (items a.-c. above):

d. Areas subject to coastal storm surge inundation associated with a Category 5 hurricane (where applicable, these areas should be mapped areas studied by the U.S. Army Corps of Engineers [USACE], NOAA, or other qualified source).

A residential safe room should not be located within the SFHA if at all possible. If the safe room needs to be located within the SFHA, the lowest floor of the safe room

should be elevated to the highest of flood hazard elevations identified in this section. It is important to note, if the residential safe room plans from FEMA 320 are used, the designs are restricted by a maximum allowable height above grade as specified on the drawing sheets; for a maximum elevation above existing grade of 3 to 5 feet. The ***elevations that should be considered when designing a safe room are the highest of***:

1. The minimum elevation of the lowest floor required by the floodplain ordinance of the community (if such ordinance exists); or
2. Two feet above the BFE, (i.e., 2 feet above the flood elevation having a 1 percent annual chance of being equaled or exceeded in any given year [100-year event]); or
3. The stillwater flood elevation associated with the 0.2 percent annual chance of being equaled or exceed in any given year (500-year event).

Residential Tornado Safe Room Exception: Where a residential tornado safe room is located outside of the hurricane-prone region as identified on Figure 2 of this paper (FEMA 361, Figure 3-2), and the community participates in the NFIP, the safe room need only be elevated to the minimum lowest floor elevation identified by the floodplain ordinance of the community.

Conclusions

The August 2008 release of the FEMA safe room guidance documents and the ICC storm shelter standard were significant milestones in the standardization of criteria for structures to be used to provide life-safety protection from tornadoes and hurricanes. With the publishing of the ICC-500 Storm Shelter Standard, and the incorporation of the Standard into the 2009 IBC and IRC, the majority of the FEMA safe room criteria in use since the 1990s have new been codified. It is now the challenge of designers, emergency managers, owners/operators, and industry groups and participants to strive towards producing quality safe rooms that meet the new criteria.

This paper highlights the primary design and construction criteria for safe rooms. However, due to the limitations of the length of this paper some criteria may not have been presented. Any safe room design should be completed referencing the complete FEMA 320 and FEMA 361 documents and not this paper alone.

References

1. American Red Cross, 1992, *Guidelines for Hurricane Evacuation Shelter Selection*, ARC 4496
2. State of Florida, Department of Community Affairs, Division of Emergency Management, 1997, *Model Hurricane Evacuation Shelter Selection Guidelines*
3. American Society of Civil Engineers, 2005, *Minimum Design Loads for Buildings and Other Structures*, ASCE Standard ASCE 7-05
4. Federal Emergency Management Agency, 2008, *Taking Shelter From the Storm: Building a Safe Room for Your Home or Small Business*, FEMA 320

5. Federal Emergency Management Agency, 1999, *National Performance Criteria for Tornado Shelters*, May 1999
6. Federal Emergency Management Agency, 1999, Midwest Tornadoes of May 3, 1999, FEMA 342
7. Federal Emergency Management Agency, 2008, *Design and Construction Guidance for Community Safe Rooms*, FEMA 361
8. Insights from IBHS, http://www.ibhs.org
9. International Code Council, 2008, *Standard for the Design and Construction of Storm Shelters*, ICC-500
10. National Storm Shelter Association, 2001, *Standard for the Design, Construction, and Performance of Storm Shelters*, http://www.nssa.cc/association_standard.htm

A HUFF, AND A PUFF, AND… IT BLEW THE CHIMNEY DOWN

Kerry S. Lee, P.E., MBA, M.ASCE[1]
Gary S. Dunlap, AIA[2]
Daniel M. Killian, P.E., B.S.[3]

[1] Director of Engineering, Nelson Architectural Engineers, Inc., 2740 Dallas Parkway, Suite 220, Plano, Texas 75093; email: klee@architecturalengineers.com; phone: 469-429-9000
[2] Assistant Director of Architecture, Nelson Architectural Engineers, Inc., 2740 Dallas Parkway, Suite 220, Plano, Texas 75093; email: gdunlap@architecturalengineers.com; phone: 469-429-9000
[3] Project Director, Nelson Architectural Engineers, Inc., 2740 Dallas Parkway, Suite 220, Plano, Texas 75093; email: dkillian@architecturalengineers.com; phone: 469-429-9000

Abstract

This paper will present case studies and assessment of collapses of tall, free standing residential masonry chimneys resulting from windstorms in North Texas. The case studies will outline the assessment of the causes of the collapses and a discussion of design and/or construction defects.

A review of limited and highly lacking documentation on design, construction and code requirements governing the architectural and structural "design" and construction of residential chimneys will be conducted. The paper will provide a discussion of the lack of design standards and poor construction practices used for residential load-bearing masonry chimneys.

This paper will illustrate how the lack of design, construction, and code requirements results in chimneys lacking sufficient capacity to resist below design wind loads leading to unsafe conditions. It is only a matter of time before the collapse of one of these elevated masonry chimney "missiles" results in severe injury or death of an inhabitant.

Introduction

The majority of residential structures being built throughout the country today rely on construction requirements outlined within the International Residential Code (IRC). The IRC provides a prescriptive outline of minimum requirements that must be met during the construction of one and two-family dwellings, not exceeding three stories in height. In today's typical residential construction, a minimal amount of actual engineering of the structure and structural components is performed. In fact, according to the IRC, only those structural components exceeding or not conforming to the empirical design specifications as set forth in the IRC require design by a professional engineer.

Masonry chimneys are prevalent in residential construction in North Texas with tall, slender chimneys rising above rooftops almost anywhere you turn. The minimum required height that a chimney must extend above a roof has been consistent across different building codes as far back as the 1980's. Codes have and still require a chimney to extend a minimum of 2 feet above any adjacent construction located within 10 feet of the chimney. Steep roof pitches are common in North Texas which leads to taller chimneys. However, the overall required height of the masonry chimney is ultimately regulated by the sizing and subsequent ability for air to properly flow through the flue. The three basic elements of residential chimney design are: the area of the fireplace opening, the area of the flue, and the height of the chimney. The size of the fireplace opening is directly proportional to the height and area of the flue. In essence, the larger the fireplace opening gets the taller the chimney becomes.

As the chimneys extend past the roof line, no lateral resistance is provided and they act as cantilevered masonry elements. In fact, residential construction is typically not designed by a structural engineer and the code does not require lateral support for the chimney in low seismic zones; therefore, any lateral resistance provided by the framing of the house is undetermined and not designed and therefore, should not be relied upon.

Lateral Resistance

In North Texas, design of structures for lateral forces is typically governed by the forces imparted by wind due to the low seismic activity in the region. The design wind speed in the area is 90 mph (3-second gust). As the chimneys increase in height above the roof line, the moment induced on the masonry assembly from the cantilevered section increases as well. The moment at the base of a chimney extending ten feet above the second story roof can be as much as 11 times greater than at a chimney extending only three feet above the same roof line. As these lateral forces increase, the amount of available resisting force must increase as well. Resistance to overturning from lateral force is typically provided by the installation of vertical reinforcement within the masonry assembly since unreinforced masonry construction is extremely weak in tension.

Previous building codes, such as the Uniform Building Code (UBC) and Building Officials and Code Administrators International, Inc. (BOCA), required a minimum amount of vertical reinforcement for masonry chimneys located in seismic zones 2, 3, and 4; however, no minimum amount of reinforcement was specified due to forces from wind. No specific minimum reinforcing requirements were provided within versions of the Standard Building Code (SBC).

As stated above, design for lateral forces is typically governed by wind in North Texas. Due to the lack of clear empirical direction for required amounts of vertical reinforcement in masonry chimneys, coupled with the fact that the chimneys are typically erected using unskilled labor, masonry chimneys erected in North Texas are

built with little to no vertical reinforcement and rely on the weight of the masonry to provide the resistance to wind loads. This lack of reinforcing severely reduces the chimneys' ability to resist lateral forces.

In addition to the lack of design, defects in chimney construction have been identified which contribute to a decrease in the chimneys' ability to resist external loading, including: improper installation of metal flashing at the roof intersection, lack of roof crickets at the upslope side of the chimney, improper/incomplete installation of mortar at bed and head joints, lack of masonry unit interlock between the core and veneer of the chimney, and the lack of horizontal joint reinforcement.

Load Bearing Masonry

When built according to the empirical methods set forth in current and previous editions of the building code, a masonry chimney may not support any additional structural load unless it has been specifically designed and constructed to do so. Therefore, unless the chimney has been designed by a structural engineer, the walls of the chimney are not permitted to be used as a bearing wall for floor or roof framing.

Vertical loads from the self weight and any additional building dead and live loading must be transferred into the foundation below. Many of the researched building codes provide a minimum footing thickness of 12 inches for conventionally reinforced concrete foundation construction. The concentration of vertical and overturning loads imparted on the foundation by these full height masonry chimneys must be accounted for by residential foundation designers. This is particularly important in the North Texas region where the high shrink/swell potential of soils creates the need for specialized foundation systems such as pier and beam and post-tensioned concrete slabs-on-grade. As illustrated in Case Study B, foundation designers do not always account for the lateral loads from the chimney in their foundation designs.

Case Studies

Two individual case studies are presented below which exhibit failure of the chimneys from wind due to the lack of structural design combined with poor quality of construction and construction defects.

Case Study A: In the early morning hours of April 10, 2008, a line of severe thunderstorms moved through North Texas producing large hail, tornadoes, and damaging straight-line winds. The straight-line winds were recorded at up to 87 miles per hour in the vicinity of the subject site.

The subject chimney was constructed of brick masonry. Based on pre-storm photographs, the overall height of the masonry chimney was estimated to be over 35 feet above grade with an extension of approximately 12 to 15 feet above the eave. The chimney was measured to be 6 feet wide by 1 foot 8 inches in depth at the base; however, the top portion of the chimney was corbelled for aesthetic appeal and was

wider than the supporting base. This effectively created a large elevated mass at the top of the chimney and resulted in a top-heavy condition.

Figure 1. Pre-storm Chimney at Case Study A (Google Maps Street View)

The addition of the solid masonry core at the top of the chimney contributed to the overturning moment and subsequent collapse of the chimney. The top portion of the chimney is visible in Figures 2 and in the left side of Figure 3 below. The bottom section of the masonry chimney was erected such that hollow cavities existed on each side of the flue. These hollow cavities terminated approximately 4 feet from the top where the solid masonry core began as shown in Figure 2.

Figure 2. Solid Masonry Core Formerly at Top of Chimney

Due to the lateral forces imparted on the chimney by high winds, (but still less than the required 90 mph design wind speeds), the cantilevered portion of the masonry chimney failed, falling into and causing significant damage to the structure below.

Figure 3 below shows the collapsed masonry chimney as well as the detached top portion of masonry that punctured through the roof deck and framing. The second floor ceiling and wall framing stopped the detached section of masonry from crashing into the bedroom below where two young girls were sleeping at the time of the chimney collapse.

Figure 3. Collapsed Section of Chimney Above Children's Bedroom

Investigation of the remaining chimney shaft revealed the following deficiencies which most likely contributed to the failure:

- Continuous vertical reinforcement had not been installed within the masonry.
- A roof cricket had not been installed at the upslope side of the chimney.
- Metal flashing had been installed in place of the cricket and penetrated through the full width of the mortar bed (Figure 4). The full penetration of flashing effectively broke the masonry bond, creating a weak joint in the chimney construction.

Figure 4. Full Penetration of Metal Flashing

The lack of continuous vertical reinforcement effectively limited the tensile forces that the chimney could resist. In this case, the addition of a top-heavy masonry "missile" aided in the chimney collapse. Wind forces laterally displaced the chimney, creating an eccentric loading condition from the solid masonry top section and a subsequent moment that exceeded the tensile strength of the as-built masonry construction. The chimney collapsed at the base of the cantilevered section and into the structure. Fortunately, the roof framing absorbed enough of the chimney's kinetic energy for the second floor ceiling and wall framing to stop the masonry "missile's" further decent into the structure; otherwise, the two young girls sleeping in the bedroom below may have been severely injured or even killed.

Case Study B: The masonry chimney outlined in this case study failed due to winds with significantly less intensity than the design wind speed for the region or those recorded in Case Study A. The recorded wind speed at the time of collapse was only 39 mph (3-second gust). Wind speeds of this magnitude and higher are frequent in the North Texas area.

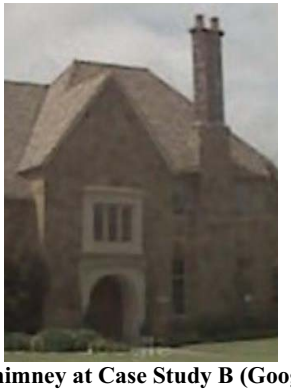

Figure 5. Pre-storm Chimney at Case Study B (Google Maps Street View)

The design and construction for the structure was based on the 1997 UBC with a seismic zone classification of 0 and a 70 mph design wind speed. The chimney was constructed of generally un-mortared, rubble-type construction and was clad with a fieldstone and brick veneer. The height of the chimney was approximately 40 feet above grade; almost half of which stood laterally unsupported above the roof line. This can be seen in Figure 5 above. The shape of the chimney was unusual and transitioned above the roof line from a single rectangle to a pair of parallel rotated squares. The shape transition required the flue to not only offset, but to rotate 45 degrees as well. Information provided indicates that the driving force for the unusual shape and height of the chimney was purely architectural in nature.

Failure of the chimney occurred at the roof line, allowing for the full cantilevered portion to overturn and fall into the structure below as seen in Figure 6. The collapsed chimney fell through the second floor bedroom and into the first floor

dining room. Review of the construction documents indicated specific portions of the structure were required to be designed by a structural engineer; however, the design of the chimney was not included in the structural requirements. Additionally, the post-tensioned foundation did not account for the additional weight imparted by the solid core masonry chimney at that location and did not account for the lateral wind loads acting to overturn the chimney.

Figure 6. View of Collapsed Chimney

Further investigation of the post-collapse debris revealed that no vertical or horizontal reinforcement had been installed. Additionally, the brick masonry core had been poorly constructed and did not have proper continuous mortar bedding for the bricks. Much of the brick within the masonry core appeared to have been laid loosely with no structure or organization as seen in Figure 7 below. No interlock was observed between the brick core and veneer, allowing for subsequent delamination from the core during collapse. Debris, including aluminum cans, was observed within the rubble of the collapsed chimney.

Figure 7. Lack of Mortar and Interlock at Masonry Core

In addition to the lack of continuous vertical reinforcement, the narrowing of the chimney section and transition from a rectangular section to two separate rotated square-shaped flues aided in the chimney's inability to resist lateral forces. As stated

previously, the chimney failed from wind forces far less than those outlined in the building code. Similar to Case Study A, the chimney collapsed above a second floor bedroom; however, in this scenario, the ceiling framing was not able to retard the masonry's decent into the structure. In addition, potential injury and/or death were averted simply because the occupant of the bedroom below the chimney was away at school and another occupant had recently left the room at the time of the collapse after investigating a strange bumping sound (likely the chimney swaying prior to collapse).

Conclusion

The two case studies presented above showcase some of the poor construction associated with non-engineered freestanding masonry chimneys in North Texas. In addition, the lack of clear empirical direction for the construction of brick masonry chimneys contributes to the erection of structures with deficient load resisting capability. In both case studies, the collapsed chimneys fell on bedrooms. Thankfully, no one was injured associated with either of these collapses; however, it is only a matter of time before someone is injured or killed when a tall freestanding masonry chimney collapses due to inadequate design and/or construction.

The authors of this paper strongly recommend that the requirements for the structural design of free-standing chimneys in no or low seismic regions be strengthened immediately in order to reduce the potential for injury and/or loss of life. This includes strengthening the requirements for the design of the foundation systems supporting these chimneys as well as the requirements for continuous vertical reinforcing. The authors further recommend that the requirements for the inspection of the quality of construction by the design professionals also be strengthened and that homeowners with free-standing masonry chimneys have their chimneys evaluated for possible deficiencies and concerns for safety.

References

Building Officials and Code Administrators, International, Inc (BOCA). 1993. *The BOCA National Building Code/ 1993,* Twelfth Edition.

Building Officials and Code Administrators, International, Inc (BOCA). 1996. *The BOCA National Building Code/ 1996,* Thirteenth Edition.

Council of American Building Officials (CABO) 1995. *1995 CABO One and Two Family Dwelling Code,* Sixth Printing.

Google Maps Street View, maps.google.com, viewed 2009.

International Code Council, Inc (ICC). 2000. *2000 International Building Code,* First Printing.

International Code Council, Inc (ICC). 2002. *2003 International Building Code,* First Printing.

International Code Council, Inc (ICC). 2006. *2006 International Building Code, Code and Commentary Volume II,* First Printing.

International Code Council, Inc (ICC). 2000. *2000 International Residential Code for One- and Two-Family Dwellings,* Fourth Printing.

International Code Council, Inc (ICC). 2003. *2003 International Residential Code for One- and Two-Family Dwellings,* First Printing.

International Code Council, Inc (ICC). 2006. *2006 International Residential Code for One- and Two-Family Dwellings,* First Printing.

International Conference of Building Officials (ICBO) 1988. *1988 Uniform Building Code.* Fifth Printing.

International Conference of Building Officials (ICBO) 1991. *1991 Uniform Building Code.* Sixth Printing.

International Conference of Building Officials (ICBO) 1994. *1994 Uniform Building Code, Volume 1 – Administrative, Fire- And Life- Safety, And Field Inspection Provisions.* First Printing.

International Conference of Building Officials (ICBO) 1997. *1997 Uniform Building Code, Volume 1.* First Printing.

International Conference of Building Officials (ICBO) 1997. *1997 Uniform Building Code, Volume 2.* First Printing.

Southern Building Code Congress International, Inc (SBCCI). 1985. *1985 Standard Building Code.* Third printing.

Southern Building Code Congress International, Inc (SBCCI). 1994. *1994 Standard Building Code.* Fourteenth printing.

Southern Building Code Congress International, Inc (SBCCI). 1997. *1997 Standard Building Code.* Sixteenth printing.

RESIDENTIAL ROOFING EVALUATION

Luke M. Sharara, PE, M.ASCE[1]
James W. Jordan, SE, PE, M.ASCE[1]
Ross A. Kimble, PE, M.ASCE[1]

Abstract: As civil / structural engineers in the field of forensic engineering, we are often asked to evaluate roof coverings for storm damage. Of the myriad of roof coverings available for the numerous types of buildings, roofing types used for residential applications comprise a substantial portion of this wide spectrum.

The purpose of this paper is to characterize and describe storm damage that affects roof coverings typically used in residential construction. It will address damage induced by hailstorms and windstorms to asphalt composition shingles, wood shingles and shakes, and slate and clay tile roof coverings. The paper will also discuss the typical steps involved in this type of forensic investigation, including obtaining and analyzing weather data, safely performing a physical inspection, and providing repair or replacement recommendations. It will also touch on the common material defects, installation problems, and reparability concerns encountered when evaluating these roof coverings.

[1]Rimkus Consulting Group, Inc., 8910 Purdue Road – Suite 170, Indianapolis, IN 46268; PH (317) 510-6484; FAX (317) 510-6488; email: lmsharara@rimkus.com, jwjordan@rimkus.com, rakimble@rimkus.com .

Introduction

In the field of forensic engineering, civil/structural engineers are often asked to evaluate the condition of roof coverings with respect to reported storm damage. The professional, unbiased and substantiated technical opinions of civil/structural engineers are often sought in such matters as they relate to insurance and legal issues. Many civil/structural engineers qualify as experts in this field based on their education, experience and training.

The purpose of this paper is to provide a basic understanding and general review of roofing assessment for the civil/structural engineer. Given the broad nature of this topic, the authors chose to focus the discussion on the evaluation of wind and hail damage to common residential roofing materials.

Forensic Investigation

The following outlines the basic steps involved when inspecting and evaluating a residential roof covering for storm damage:

- Prepare for the inspection by becoming familiar with the storm event and the area where the residence is located. This may involve obtaining weather information, maps, and aerial photographs. The inspector must take adequate precautions to access the roof safely for a detailed inspection.

- Interview the property owner/resident for their knowledge of the storm event, age of the roof covering, history of repairs, etc.

- Inspect areas surrounding the subject roof for evidence of collateral damage or tell-tale markings. Examples may include fallen trees/limbs and other wind-blown debris; smooth, round, and randomly located indentations in metal materials (mailboxes, utility enclosures, etc.); and hail spatter marks (randomly located hail impact markings on oxidized surfaces) on various objects such as electrical transformer enclosures and wood privacy fences.

- Inspect the roof covering. This should include observing all roof slopes to determine the general condition of the roof covering and to identify the general locations of any specific damage. A more detailed inspection of "test squares" (100 square foot inspection areas) should then be performed to quantify specific damage when applicable.

- Formulate opinions based on the physical inspection and information gathered from various resources. Some research may need to be performed to determine if a particular roof covering has any known history of defects.

- Report findings to the client. This may be verbal or written, depending on the client's request. The report should define the condition of the roof covering and the amount of storm damage (if present). The client may also ask for general repair recommendations.

Asphalt Composition Shingles

Hail Damage Assessment

Hailstorms produce a significant amount of damage to buildings every year. While the science behind the formation of hailstorms, the characteristics of hailstones, and the physics behind the falling hailstone are beyond the scope of this paper, it is important to note that hailstorms produce hail that is not of uniform size, shape, or density. In addition, hailstorms may vary in intensity over a short distance. This randomness, combined with numerous variations in individual roof coverings, necessitates detailed and independent evaluation of each subject roof covering as described in subsequent sections of this report.

Roof covering manufacturers test their materials to determine their resistance to hail impacts in accordance with published standards. One of the most common standards, UL 2218 "Impact Resistance of Prepared Roof Coverings", is produced by Underwriter's Laboratory and groups roof coverings into classes (Class I to Class IV) with Class I being the least hail resistant and Class IV being the most hail resistant. Other technical organizations involved with roofing materials include: American Society of Testing and Materials (ASTM), Factory Mutual Research Corporation (FMRC), and the National Institute of Science and Technology (NIST). These standards provide important guidance when evaluating roof coverings and determining susceptibility to hail impacts.

As would be expected, hail impacts to asphalt composition shingles can damage shingles to varying degrees of severity. When assessing hail impact damage to asphalt shingle roofs, it is necessary to determine or define the term "damage". A generally accepted definition of such damage is "the loss of water-shedding capability or a reduction in the expected long term life of the roofing material." This is a functional definition which has industry acceptance. This definition has two components, either of which may qualify a specific location as damaged.

The first component is the loss of water-shedding capability. Large hail may immediately puncture or tear shingles, resulting in a potential leak (reduction in water shedding ability). The second portion of the definition is the reduction in the expected long-term life of the roof covering. Asphalt shingles have a granular coating which serves both functional and aesthetic purposes. Functionally, the coating provides a wearing surface for the roof. The granular coating also protects the underlying asphalt impregnated base mat from the sunlight's ultraviolet rays as well as from mechanical abrasions such as that from foot traffic and other forms of incidental contact. When this granular coating wears off or is removed, the underlying asphalt base mat becomes exposed and is more susceptible to mechanical damage and will experience accelerated degradation due to ultraviolet rays. This accelerated degradation may result in a reduced service life in the area of granule loss and therefore might meet the criteria of "damage", depending on the severity.

Hail impacts may produce randomly located areas of damage that are round and localized. Damage severity increases with greater hailstone sizes. The more severe damage typically consists of bruising (localized softness due to material fracture) or physical tearing of the shingle base mat.

Because one of the characteristics of hail damage is granule loss, some controversy arises due to granule loss that is caused by other conditions. The most common of these conditions are referred to as weathering, blistering, scuffing, marring, flaking and mechanical damage. Weathering or aging of the shingles typically manifests itself as broad, irregularly shaped granule loss that exposes the underlying asphalt impregnated base mat. Weathering will affect large areas of the shingle and the roof, and will typically be more pronounced on slopes exposed to direct sunlight and on roof coverings with inadequate ventilation. Blistering is a condition that occurs when gas pockets from within the base mat rise to its surface and release the air within

them displacing a few granules. The size of these individual blisters is typically smaller than what is caused by hail impacts. Blistering also occurs more often on areas of the roofs with inadequate ventilation. Scuffing is caused by abrasive forces against the shingle surface, most notably due to foot traffic. As a result, scuffing is often found in areas where people have a tendency to walk, such as valleys or slopes that lead from upper to lower roofs. Marring occurs when forces push or shift (without removal) portions of the granule coating and the top surface of the base mat. This typically occurs when the roof covering is hot, and often occurs due to foot traffic as well. Flaking is characterized by the loss of small groups of granules that are not adequately adhered to the base mat. Often walking upon or application of light finger pressure to areas which are flaking will cause the loss of additional groups of granules. Because of the brittle condition of the granule coating, shingles exhibiting flaking are prone to additional loss of granules from hail impact. The round and localized nature of hail impact damage helps to distinguish it from flaking damage, which often is irregular in shape and size. Mechanical damage covers a broad range of incidents which may physically damage shingles or remove the granular roof coating, including golf ball strikes, tree limb contact, and in some cases intentional damage. Becoming familiar with these conditions will help the inspector properly identify damage caused by hail impacts.

Figure 1: Actual hailstones (2.5-inch diameter) from April 14, 2006 hailstorm in Indianapolis, Indiana.

Wind Damage Assessment

Just as for hail damage assessment, in order to evaluate wind damage to asphalt composition shingle roof coverings, a working definition must be established. Accepted industry definitions and experience support the definition that wind damage is typically manifested in one of three ways. These include torn or missing shingle tabs, creased shingles, and what is referred to as “hidden damage”. Hidden damage is a phrase used to describe torn conditions which are not readily visible when walking on the roof.

Strong wind may completely tear or separate shingles or shingle tabs from the roof. The phrase “shingle tab” refers to the exposed portion of the shingle. Common strip

Figure 2: Examples of hail damage from Indianapolis hailstorm.

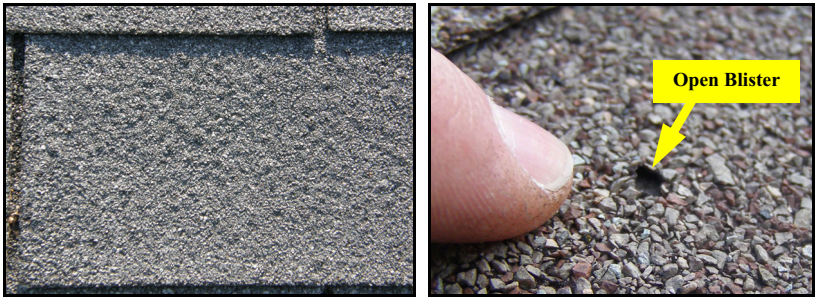

Figure 3: Examples of blistering (often mistaken as hail impact damage).

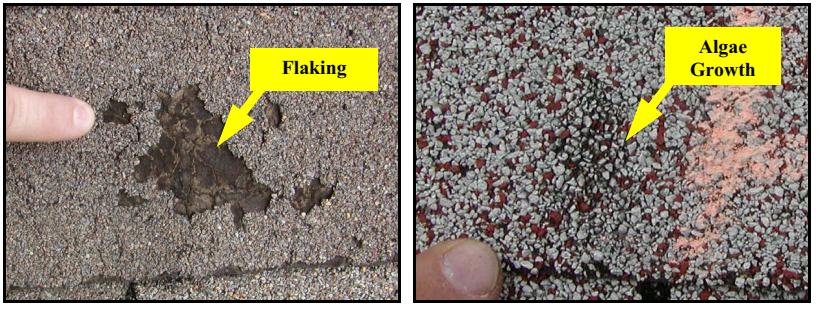

Figure 4: Other anomalies commonly mistaken as hail impact damage.

shingles may have three or four tabs. Some shingles have extra layers or laminations (often referred to as "architectural", "laminated", or "dimensional" shingles). Wind damage is most common on the windward side of the building. Eaves, rakes, and ridges are often vulnerable due to increased wind pressures in these areas. A creased condition occurs when strong wind bends a shingle tab upward. If shingle tabs crease, it is an indication that wind was sufficient to bend back the affected

shingle tab to the point where a line of exposed asphalt bitumen will form in the shingle at the area where it was bent back, typically close to the edge of the overlying shingle. Once the shingle creases, it becomes prone to tearing along the crease, especially if the wind causes repetitive lifting (flapping condition). A discussion of the sealing condition of the shingle, which may (or may not) lead to the creasing of the shingle is explained in a subsequent section of this report.

Wind may also damage shingles by separating or tearing them from their fasteners without removing them from the roof. This typically occurs to groups of shingles. This form of damage is often hidden since the affected shingles may lie back to their original positions thus covering the underlying damage. Because this type of damage is typically hidden, representative testing (gentle lifting using hand pressure) of the shingle is commonly required for identification. If a shingle tab is loose, the fasteners and surrounding shingle surfaces may be examined for torn conditions. A torn condition may impair the shingles' ability to remain on the roof.

An unsealed condition in and of itself is generally not considered to be wind damage, because the shingle may be unsealed for a variety of reasons. Unsealed shingles do, however, make the roof covering more prone to wind damage, since the unsealed condition may allow wind to more easily lift the affected shingle tab upward and bend it backward, resulting in a creased or torn condition. It can also allow the affected shingle to more easily tear or to pull from its fasteners (possible hidden damage). The challenge for the inspector becomes the determination of whether or not the wind event caused or contributed to the unsealed condition of the shingles. An examination of the degree of transference between the sealing strip and the underside of the shingle may provide an indication of the adequacy of the seal prior to the storm event. That is, if there is no transference of the sealant between overlying shingles, the shingles were likely not properly sealed prior to the wind event. The roof covering should be evaluated in its entirety, putting into consideration prevailing wind direction and other forms of damage which may accompany the unsealed shingles. The inspector should note any patterns in the unsealed conditions of the shingles. Unsealed groups of shingles at roof locations where wind pressures would tend to be greater may be consistent with wind damage, whereas localized unsealed shingle tabs that follow the installation pattern of the roof covering may not be consistent with the effects of wind.

When evaluating asphalt composition shingles for wind damage, special attention should be given to the fastening condition of the roof covering. Improper fastening will directly impact the susceptibility of the roof to wind damage. Proper fastening is of paramount importance to the performance of an asphalt shingle roof covering. One of the most common improper installation techniques concerns the location of the fasteners. Installation of nails or staples on or above the sealing strip is referred to as "high-nailing". A nail or staple installed at a location significantly higher than what is required may miss the upper edge of the shingle underneath. This means that a reduced number of fasteners will hold the shingle, which has a direct bearing on its ability to resist wind pressures. A fastener that is installed over the sealing strip may hinder the shingle's ability to seal properly, which could make it prone to lift up,

crease, and eventually tear due to wind events. Another condition is missing fasteners, which has a strong impact on the shingle tab's ability to withstand wind pressures. A condition where edge fasteners are missing is typically caused by a "racked" installation method. Racking is an installation technique where shingles are installed in a staggered column formation rather than in a stair-step pattern, as recommended by most manufacturers. One of the concerns of racked installations is the likelihood of omitting the last fastener on the shingle, because a blind-nailing condition will occur at every other course. Another installation concern arises due to overdriven fasteners. Nail heads or staples are required to be flush with the surface of the shingle without penetrating its surface. Overdriven nails or staples may promote a tear around the fastener.

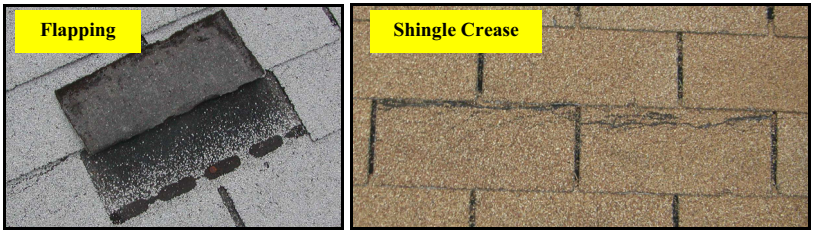

Figure 5: Examples of wind damage to asphalt shingles.

Repair Recommendations

Throughout the evaluation of the shingles for hail or wind damage, consideration should be given to the potential repair recommendations. Newer roofs are typically more resilient and more easily repaired, while older or weathered roofs tend to be more difficult to repair due to their brittleness and reduced pliability. The season or weather also affects ease of repair as asphalt shingles become more brittle in cold weather and soft in hot weather. When asked to provide repair recommendations, the engineer should consider the degree of damage, season, and overall condition of the roof covering. A break-even analysis will provide an approximation of the amount of damage required to warrant a replacement recommendation based upon economic concerns.

Wood Shingles and Shakes

Hail Damage Assessment

Functional hail damage affecting wood shingles and shakes causes the individual shingles/shakes to split. This split exposes previously protected wood and is typically noticeable by variations in color at the fracture location. A mark or indentation where the hailstone impacted the shingle or shake should be evident if caused by a hailstone strike. The engineer should note that wood shakes often split due to long-term deterioration and foot traffic. Lightly pressing on the exposed corners of the affected shingle/shake may expose the split edge during an inspection.

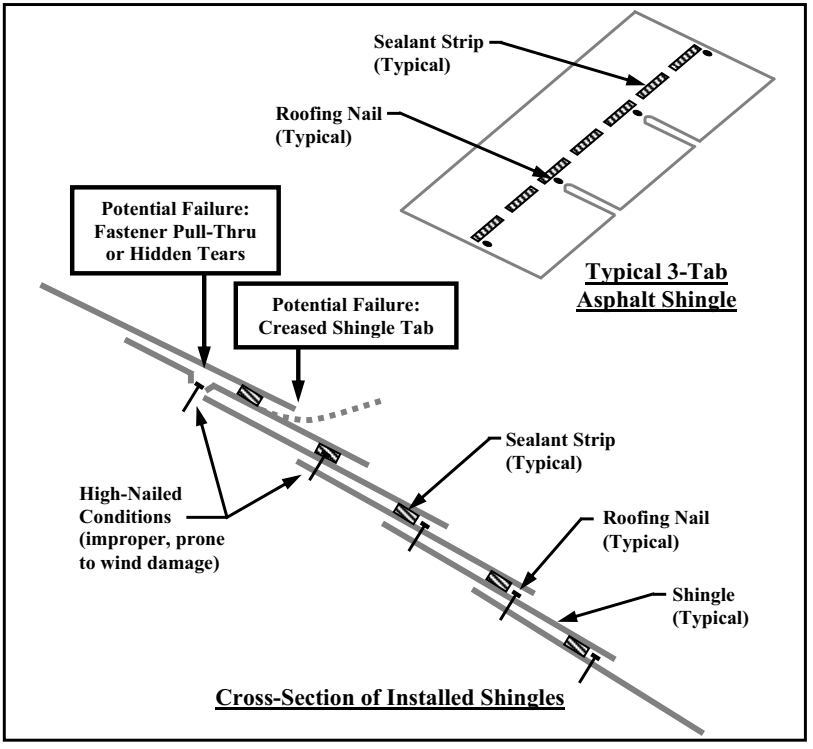

Figure 6: Diagram of installed asphalt shingles (potential wind damage cited).

Similar to other types of roof coverings, randomness of damage plays a crucial role in the evaluation of the roof covering for hail damage. Spatter marks may also be evident on the wood roof. Spatter marks are discolored areas that occur due to hail impacts. These markings fade over time and are not considered to be functional hail damage, because they do not reduce the service life of the roof covering. However, spatter marks (on roofs and other surfaces) provide a clear indication of the prevalent direction of the hail event.

Wind Damage Assessment

Wind damage to wood shingles or shakes typically consists of missing, displaced, shifted, or fractured wood shakes. Correlating affected roof areas to the reported wind direction is useful in determining whether or not the damage was attributable to the storm event. Wind damage should be discerned from loose or damaged conditions attributable to long-term deterioration or decay.

Figure 7: Examples of hail impact damage to wood shakes.

Slate and Clay Tile

Hail Damage Assessment

Clay and slate tile are among the hardest materials used for roof coverings and therefore are very weather resistant. As such, this roofing material typically requires relatively large hail to elicit damage. Hail damage to clay and slate tiles consists of fractures to the tile. Similar to other roof coverings, the randomness and recent nature of the fractures are key characteristics that distinguish a fracture caused by hail impacts versus other means. Damaging hail impacts to slate tile often results in round fractures when in the central or upper portion of tile. It is not uncommon to find repetitive fractures or breaks that exist at associated areas of the tiles such that a pattern is established, which is an indicator that they may not be attributable to hail impacts. The recentness of the fracture can be evaluated from the color of the exposed edge, accumulated dirt, and algae growth. These observations may provide physical evidence of long-term or pre-existing conditions.

Wind Damage Assessment

Because of their relative weight, slate and tile roof systems are relatively resistant to most wind events. Should sufficiently strong winds occur, tiles may be lifted from the roof, become airborne, and impact adjacent areas of the roof, resulting in chipped, cracked and fractured tiles.

Figure 8: Examples of hail impact damage to slate roofing tiles.

Conclusion

Forensic civil/structural engineers are often asked to evaluate roof coverings for storm damage. Considering civil/structural engineers' knowledge of the effects of weather on buildings, their understanding of the behavior of roofing materials subjected to impact forces, and upon gaining experience examining storm damage, civil/structural engineers are well suited for evaluating storm damage to roof coverings. In this paper, we reviewed some of the basic steps to the forensic engineering investigation of residential roof coverings. We reviewed several common types of residential roof coverings, and discussed key aspects of assessing these roofing materials for wind and hail damage. We also discussed issues related to determining the reparability of some roof coverings. This information should prove valuable to forensic engineers performing residential roofing evaluations.

References

Cullen, William C. "Hail Damage to Roofing: Assessment and Classification", Proceedings of the Fourth International Symposium on Roofing Technology, National Roofing Contractors Association (NRCA), Washington D.C.

Cedar Shake & Shingle Bureau (2005). "Certi-label Cedar Roofing: A Claim Adjuster's Guide to Handling Hail-Related Claims".

Roofing Industry Committee on Weather Issues, Inc. (RICOWI, 2005). "Hailstorm Investigation – Oklahoma City, OK – April 21, 2004".

Vickie Crenshaw and Jim D. Koontz, P.E. (2000). "Simulated Hail Damage and Impact Resistance Test Procedures for Roof Coverings and Membranes", Article based on presentation at Roofing Industry Committee on Weather Issues Meeting in Dallas, Texas.

Levine, Jeffery S. (1992). "Preservation Brief 29: The Repair, Replacement & Maintenance of Historic Slate Roofs", Technical Preservation Services, National Park Service, U.S. Department of the Interior.

Underwriter Laboratories Inc. (UL, 1998). "UL 997 – Wind Resistance of Prepared Roof Covering Materials".

Patterson, Stephen and Mehta, Madan (2001). "Roofing Design and Practice". Upper Saddle River, New Jersey. Prentice-Hall, Inc.

Jenkins, Joseph. 2003. "The Slate Roof Bible – 2nd Edition".

Assessing Wind Damage To Asphalt Roof Shingles

Marco A. DeLeon, M.E., P.E., M.ASCE[1]
Pamela C. Pietrasik, M.S., P.E., A.M.ASCE[2]

[1] Assistant Director of Engineering, Nelson Architectural Engineers, Inc., 2740 Dallas Parkway, Suite 220, Plano, Texas 75093; email: mdeleon@architecturalengineers.com; phone: 877-850-8765

[2] Project Director, Nelson Architectural Engineers, Inc., 2740 Dallas Parkway, Suite 220, Plano, Texas 75093; email: ppietrasik@architecturalengineers.com; phone: 877-850-8765

ABSTRACT

Distress to asphalt roof shingles due to high wind events, beyond obvious physical dislocation, might not be evident and is often overlooked, improperly evaluated and/or is a source of debate among insurance adjusters, roofing contractors, building inspectors, and design professionals.

This paper presents an overview of asphalt roof shingles including material composition, style, grade, and installation, and their impact on wind resistance. A practical non-destructive method for identifying, quantifying, and categorizing wind distress is presented. Distress not related to wind is briefly considered including installation deficiencies and manufacturing defects. Recommendations for repairing or replacing a damaged roof are also discussed, considering material properties and type and extent of distress.

Finally, this paper highlights the role of the builder and/or design professional regarding the proper specification and application of shingles based on the geographical region and climate in which they are installed. Regulation which correlates with existing guidelines needs to be specified and enforced.

BACKGROUND

The apparent recent increase of tornado and hurricane activity impacting U.S. territories, including densely populated areas, has augmented the need for accurate and thorough assessment of wind damage to residential structures. The roof covering is one of the primary building envelope components in residential construction to suffer damages related to high winds.

In the authors' experience, evaluation methods for wind damage to asphalt shingle roofs vary widely among insurance adjusters, roofing contractors, building inspectors, and design professionals. Often, evaluator opinions of wind damage to asphalt roof shingles on a given roof can range from minor or no damage to significant damage that requires a complete roof replacement. Therefore, standard methods for identifying and quantifying wind distress beyond a qualitative analysis are needed.

Asphalt shingle is the preferred roof covering in residential structures in most parts of the country including areas subjected to high winds. Based on the authors' experience, roofing and re-roofing projects in some of these regions incorporate inappropriate shingle grades and/or improper shingle installation methods. In the authors' opinion construction and design industries must self regulate to ensure that building code mandates are enforced in roof structures with asphalt shingles.

ASPHALT ROOF SHINGLES – GENERAL DISCUSSION

The shingle material properties, grade, style, installation method and quality, and wind rating influence its wind resistance and plays an important role in the assessment of wind related damage.

Materials. Asphalt shingles consist of a reinforcing mat (fiberglass or organic based) with top and bottom asphalt coatings, and a top surface layer of coarse mineral granules. The mineral granules protect the asphalt from ultraviolet rays and weathering, increase the external fire resistance, add weight, and provide a variety of aesthetic appearances to the shingles (NRCA 2006).

Asphalt shingles contain heat sensitive, self-sealing adhesive strips that secure the leading edge of the shingle to the shingle underneath, resulting in increased wind resistance (NRCA 2006). If installation occurs during the winter, self-sealing may not occur until the following spring. For winter installation, a process referred to as "hand sealing" or "hand tabbing" may be performed as discussed later in this paper.

Grade. Shingle weights and dimensions vary by manufacturer. Generally, higher grade shingles have greater asphalt content and are heavier, last longer, and have an improved aesthetic appearance. Higher grade shingles also have higher wind ratings.

Style. The two most common styles of asphalt shingles are strip shingles and laminated shingles. Strip shingles, commonly referred to as "3-tab" shingles, consist of one laminate layer with interior keys that divide the lower half section of the shingle into three tabs. Standard size shingles are generally 12" x 36" in length with a typical 5" exposure. Laminated shingles, commonly referred to as "dimensional" or "architectural" shingles, have additional laminate layers and do not contain interior keys. **Figures 1a** and **1b** provide a representative depiction of each shingle style.

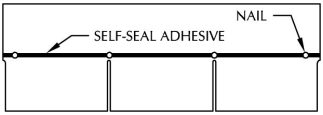

Figure 1a. 3-Tab Shingle

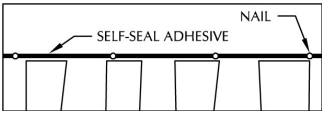

Figure 1b. Laminated Shingle

Installation. The National Roofing Contractors Association *Roofing and Waterproofing Manual* (NRCA) is considered the industry standard for the specification and installation of asphalt shingles. NRCA recommends a minimum roof slope of 2:12 (2" rise on a 12" horizontal projection) for shingle application. Most shingle roofs typically have slopes between 4:12 and 8:12. Applications on roofs with slopes between 2:12 and 4:12, and greater than 20:12 (i.e. mansard application), require special installation requirements including the use of special underlayment, flashing, and/or additional fasteners.

NRCA recommends using nails for the application of asphalt shingles to wood based decking. Shingles can also be fastened with staples. Although staples are not prohibited by manufacturers or building codes, based on the authors' experience, the use of staples is often prone to installation deficiencies. Asphalt shingles should have the minimum number of fasteners required by the manufacturer and applicable building codes. Some manufacturers increase the wind rating of shingles with increased number of fasteners. The current International Residential Code (ICC 2006) requires that asphalt shingles be secured with at least four fasteners per strip shingle; however, additional fasteners and/or special methods of fastening are required under certain circumstances.

Manufacturer's Wind Rating. It is important to install only shingles that have a wind capacity equal to or higher than the design wind speeds for the roof structure. Standard grade 3-tab shingles have a typical manufacturer wind rating of 60 mph. Higher-grade 3-tab shingles have manufacturer wind ratings up to 80 mph. Standard grade laminated shingles have manufacturer wind ratings between 70 and 80 mph. High grade laminated shingles have manufacturer wind ratings of up to 110 mph. As described in the next section, the manufacturer's wind ratings do not correlate to basic design wind speeds as described in the International Residential Code (IRC), but are rather based on a standardized American Society for Testing and Materials (ASTM) test procedure.

STANDARIZED ASPHALT SHINGLE WIND TESTING

Available standardized tests for shingle wind resistance focus on design and/or rating requirements, not on field performance or condition assessment. The International Building Code (IBC) requires that asphalt shingles be tested in accordance with ASTM D3161 *Standard Test Method for Wind-Resistance of Asphalt Shingles (Fan-Induced Method)* (ASTM 2003). This test classifies shingles into three classes. Class A shingles pass the test at a velocity of 60 mph, Class D shingles pass the test at a

velocity of 90 mph, and Class F shingles pass the test at a velocity of 110 mph.

According to the ASTM D3161 test procedure, the test results do not correlate directly to wind speeds experienced in service and intrinsically do not correlate to the 3-second basic design wind speeds (the testing lasts for 2 hours or until such lesser time as a failure occurs).

SHINGLE WIND RATING - BUILDING CODE REQUIREMENTS

Presently, the IBC and IRC provide wind resistance code requirements for roofing assemblies and roof coverings. In the authors' experience, some of the code requirements for asphalt shingles are not well defined and can lead to the specification of underperforming shingles in certain areas of the country.

For roofing assemblies the codes reference *ASCE 7 Minimum Design Loads for Buildings and Other Structures* (ASCE 2005). In practice, the degree of wind shingle distress correlates closely with higher wind pressures as calculated by ASCE 7, namely higher distress at the ridges and corners of roofs.

In regards to wind resistance of asphalt shingles, the IRC states that shingles meeting ASTM D3161 are acceptable for use in wind zones less than 110 mph (3-second). However, no shingle classification as per ASTM D3161 (i.e. Class A, Class D, Class F) is specified. The code does require Class F shingles for areas where the basic wind speed is 110 mph or higher and where special fastening is required.

In the author's experience, Class A shingles, including most 3-tab shingles, under-perform in wind zones with basic wind speeds over 90 mph (3-second). Yet, 3-tab shingles are readily seen in residential construction in most of the east coast where basic wind speeds are in excess of 110 mph (3-second) and where yearly tropical storms and hurricanes result in the dislocation of such shingles. In the authors' opinion, there is either a lack of compliance or lack of proper regulations and enforcement from local authorities to require a shingle with an appropriate wind rating.

Based on the authors' experience of underperforming Class A shingles in wind zones above 90 mph (3-second) and due to the lack of shingle class specification in the IRC for wind zones below 110 mph (3-second), the authors propose the following guideline which is in agreement with regulations by the Florida Building Code Residential (FBCR):

> *ASTM D3161 Class D shingles (90 mph) should be used on wind zone regions of 100 mph (3-second) or less. ASTM D3161 Class F shingles (110 mph) should be used on wind zone regions of 110 mph (3-second) or more.*

TYPICAL WIND DAMAGE TO ROOF SHINGLES

Typical damage to shingles related to high winds includes partially or fully un-adhered shingle tabs, bent/failed shingle tabs, and missing shingles. During high wind events, such as during a tornado or hurricane, damage can also occur due to wind-blown debris such as punctured and scuffed shingles.

Partially or fully un-adhered shingles. A partially or fully un-adhered shingle or shingle tab can usually be easily lifted by hand (**Figure 2a**). An un-adhered shingle or shingle tab may or may not show signs of surface distress depending on whether it has been subjected to repeated high wind speed cycles. An un-adhered shingle or shingle tab is usually related to wind uplift but can also be affected by manufacturing and/or installation defects, natural weathering, and/or improper storage prior to installation. Depending on the degree and extent of un-adherence, partially or fully un-adhered shingles or shingle tabs can be either repaired or replaced.

Bent/Failed shingles. Bent/failed shingle or shingle tabs show flexural distress in a pattern usually parallel to the edge of the exposed shingle or shingle tab (**Figure 2b**). In many cases, the shingle or shingle tab is partially or completely detached from the underlying shingle. The uplift pressures and/or lateral wind loads lift the shingle tab during a windstorm and bend the shingle tab back and forth as wind speeds increase and decrease, thus weakening the tab at the location of the bend. A crease in the shingle is evidence of flexural distress and shingle replacement is required.

Missing shingles. Fully dislocated shingles with exposed underlayment and/or roof decking (**Figure 2c**) are typically associated with high wind distress, but are also associated with improper installation such as improper number and/or application of fasteners. Typically, areas of higher wind pressure concentrations such as at ridges and corners are the first to show this type of distress. Missing shingles must be replaced.

Punctured, scuffed shingles. Wind-borne debris can impact a shingle. Depending on the severity of the impact, a scuff mark or puncture may result. A scuff mark may remove only granules from the shingle surface, reducing UV protection. This type of distress typically is localized and requires individual shingle replacement.

Figure 2a. Fully Un-adhered Shingle

Figure 2b. Bent/Failed Shingle Tab

Figure 2c. Missing Shingles

REPAIR PROCEDURE FOR UN-ADHERED ASPHALT SHINGLES

When wind lifts a shingle and breaks the seal, it is not likely that the shingle will re-seal itself (GAF). Whether a shingle will re-seal or not depends on many factors, such as the age of the shingle, time and amount of high temperature exposure, previous high wind exposure, and contamination of the sealant by dirt and debris. In addition, re-sealing of the shingles will more than likely result in a weaker bond that the bond provided by the original seal. Depending on the extent of un-adhered shingles and other considerations, hand sealing of shingles can be performed.

Hand sealing of shingles may be performed as a repair on partially and fully un-adhered shingles. Hand sealing should not be considered as effective as the original seal and the shingle does not regain its full original wind resistance. Hand sealing is performed by placing daubs of adhesive under the shingle to be sealed using a caulking gun or small trowel. Most shingle manufacturers allow hand sealing under certain circumstances.

PRACTICAL WIND DAMAGE ASSESSMENT PROCEDURE

As part of the wind assessment of roof shingles, the evaluator must evaluate the wind speeds that the structure experienced. Site-specific weather information including wind speeds and wind directions can be obtained from several sources including the National Oceanic and Atmospheric Administration (NOAA). Knowledge of the magnitude and duration of wind speeds can provide the evaluator an idea of expected distress based on the wind rating of the shingles. Sustained wind speeds (1-minute) in excess of shingle manufacturer ratings typically result in some form of shingle distress. Lower speeds can also result in shingle distress due to aged and/or deficient and/or improperly installed asphalt shingles.

In assessing shingle damage, the roof must be walked thoroughly and a roof plan should be drawn. When evaluating a roof for wind damage, distress which is not related to wind should be noted and manufacturing and installation deficiencies must also be considered.

Sampled Areas. To obtain a representative sampling of the roof distress, 10' x 10' sample roof areas are used. A 10' x 10' area equates to what is normally referred to as "one square" (100 SF) of roofing. It is recommended that one sample area be taken on each roof plane for every 1000 SF of roofing area at representative roof areas. For a typical shingle roof, one square of roofing consists of approximately 80 shingles and 240 shingle tabs (3-tab shingles).

Analysis. Shingles within the sample areas should be evaluated for the four types of distress mentioned previously: un-adhered shingles (partial and full), bent shingles,

missing shingles, and punctured/scuffed shingles. The testing consists of both visual observations and hand lifting of the bottom edge of each shingle throughout the sample areas. The distressed shingles are then marked and quantified.

The types of distress are separated by Groups (I and II) for categorizing purposes. Bent, missing, and punctured/scuffed shingles are grouped together in Group I. Shingles within Group I require replacement. Partially un-adhered shingles or shingle tabs and fully un-adhered shingles or shingle tabs are grouped separately in Groups IIA and IIB respectively. Shingles or shingle tabs within Group II may require repair or replacement. A summary of Groups distress is shown on **Table 1**.

Table 1. Shingle Group Distress Categories

Group I	Group II	
	A	B
Bent, Missing, Punctured	Partially un-adhered	Fully un-adhered

Note the quantification for Group I type of shingle distress is based on the entire surface of one shingle. If the shingle is a 3-tab shingle, the distress is only counted once for each shingle even if two or three tabs show the same type of distress. This accounts for the fact that if any one of the three tabs is damaged, the entire shingle must be replaced. **Equation 1** below can be used to determine the percentage of damaged shingles on a square of shingles with Group I distress, where N_s represents the number of damaged shingles observed in the 10' x 10' sample area.

$$(N_s / 80) * 100 \qquad \textbf{(Eq. 1)}$$

Quantification for Group II distress varies depending on the type of shingle. For laminated shingles a partial un-adhered shingle is considered to be one where one third or less of the shingle is un-adhered. A shingle that has more than 1/3 of its surface un-adhered is considered a fully un-adhered shingle. For 3-tab shingles, individual tabs are quantified. For these, a partial un-adhered shingle tab is one where tab corners are able to be lifted. A fully un-adhered shingle tab is one where the complete shingle tab can be lifted by hand.

Equations 1 or **2** can be used to determine the percentage of damaged shingles with Group II distress. Equation 1 should be used for laminated shingles and Equation 2 should be used for 3-tab shingles. In Equation 2, N_t represents the number of damaged shingle tabs observed in the 10' x 10' sample area.

$$(N_t / 240) * 100 \qquad \textbf{(Eq. 2)}$$

Table 2 below shows a sample form used to document laminate shingle distress within three sample areas.

Table 2. Example Shingle Distress Documentation for Laminated Shingles

Area	Group I Distress		Group II Distress			
			A - Partially Un-adhered		B - Fully Un-adhered	
	N_s (Qty.)	%	N_s (Qty.)	%	N_s (Qty.)	%
A	7	9	10	13	7	9
B	3	4	5	6	5	6
C	8	10	18	23	9	11

Damage Assessment and Recommendations. Based on the type and percent of distress at the roof sample areas, one can estimate the percentage of overall roof damage. Depending on the type and percentage of overall distress, the roof shingle distress can be categorized as minimal, moderate, or severe. Based on the authors' experience, percentage threshold recommendations are provided below and are summarized on **Figure 3**. Note that the overall condition of the subject roof (and often each individual plane) should be considered including the type, degree and extent of distress, overall condition of the shingles, quality of installation, and the age of the roof. In some cases individual planes may require separate analysis depending on factors such as different age slopes (additions or previous repairs) or differing degrees of damage due to the direction of a traveling storm. The final decision when considering repair versus replacement may be based on other factors than engineering judgment such as availability of like kind and quality shingles and local code requirements.

Minimal Damage. A roof with minimal wind damage will have very low, if any, Group I type of distress (typically less than 2%) and low Group II type of distress (typically up to 7%). For this level of distress, we recommend replacement of individually bent, punctured, or missing shingles and hand sealing of partially un-adhered shingles in accordance with shingle manufacturer recommendations.

Moderate Damage. A moderately damaged roof will have moderate Group I distress, typically below 15% and low to moderate Group IIB distress ranging from 8% to 15%. In addition, the total percentage of Group II distress (IIA + IIB) should not exceed 25%. Recommendations for moderate damage are more difficult to specify. For example, consideration must be given to the age of the shingles. Newer shingles that are lying mostly flat can be hand sealed. However, if the shingles are older, then full replacement should be considered.

Severe Damage. A severely damaged roof will have moderate to high each Group I and IIB distress (above 15%). However if the total of Group II distress (IIA + IIB) is more than 25%, it should be categorized as severe. This accounts for the fact that it is unlikely to be economical to repair (hand seal) shingles in excess of 25% of the roof area. A roof with severe shingle damage requires replacement of the entire roof.

Figure 3 below provides a summary for determining the type of roof distress. Engineering judgment should be used, especially when numbers fall near the boundary values of each category.

MINIMAL	MODERATE	SEVERE
Group I < 2% Group II (A+B) ≤ 7%	Group I < 15% 8% ≤ Group IIB ≤ 15% and Group II (A+B) ≤ 25%	Group I > 15% Group IIB > 15% and Group II (A+B) > 25%

Figure 3. Summary of Categorized Roof Distress

CONCLUSION

The wind resistance of asphalt shingles depends on many variables including the shingle material properties, grade, style, quality of installation, age of shingles, and the direction of weather exposure.

The building code wind requirements for residential asphalt shingles are not well defined and can lead to the specification of underperforming shingles in certain areas of the country. The authors recommend that ASTM D3161 Class D shingles should be used on wind zone regions of 100 mph (3-second) or less and ASTM D3161 Class F shingles should be used on wind zone regions of 110 mph (3-second) or more.

A practical non-destructive procedure for identifying and quantifying shingle wind distress includes on-site visual and physical evaluations of sample roof areas representative of overall roof distress. Roof distress including bent, missing, punctured, scuffed, and partially and fully un-adhered shingles is categorized as minimal, moderate, and severe. Depending on the type and extent of the roof distress, different repair procedures are recommended. The final decision when considering repairing versus replacement may be based on other factors than engineering judgment such as availability of like kind and quality shingles and local code requirements.

REFERENCES

American Society of Civil Engineers (ASCE). 2005. *ASCE 7-05 Minimum Design Loads for Buildings and Other Structures,* U.S.A.: ASCE.

American Society for Testing and Materials (ASTM). 2003. *D3161-03b: Standard Test Method for Wind-Resistance of Asphalt Shingles (Fan-Induced Method)*, West Conshohocken, PA: ASTM International.

GAF Materials Corporation. “Steep Slope Technical Points & Observations Documents,” http://www.gaf.com/General/GafIntro_MAIN.asp.

International Code Council (ICC). 2006. *International Building Code*, U.S.A.: International Code Council, Inc.

International Code Council (ICC). 2006. *International Residential Code*, U.S.A.: International Code Council, Inc.

International Code Council (ICC). 2007. *Florida Building Code Residential*, U.S.A.: International Code Council, Inc.

National Roofing Contractors Association (NRCA). 2006. *The NRCA Roofing and Waterproofing Manual*, 5th Edition. Rosemont, Illinois: National Roofing Contractors Association.

The Roof Drainage Epidemic

Stewart M. Verhulst, M.S., P.E., M.ASCE[1]
Marco A. Deleon, M.E., P.E., M.ASCE[2]
Bradley L. East, M.S., M.ASCE[3]

[1]Nelson Architectural Engineers, Inc., 9701 Brodie Lane, Suite 201, Austin, Texas 78748; PH (512) 610-2800; email: sverhulst@architecturalengineers.com
[2]Nelson Architectural Engineers, Inc., 2470 Dallas Parkway, Suite 220, Plano, Texas 75093; PH (469) 429-9000; email: mdeleon@architecturalengineers.com
[3]Nelson Architectural Engineers, Inc., 9701 Brodie Lane, Suite 201, Austin, Texas 78748; PH (512) 610-2800; email: beast@architecturalengineers.com

ABSTRACT

Poor roof drainage can cause accelerated deterioration of a roofing system and in extreme cases, roof collapse. It is the authors' experience that roof collapses related to poor roof drainage are almost exclusively limited to low-slope roofs with parapet walls that prevent drainage over the roof edge.

For roofs with parapet walls, the proper function of the primary and secondary drain systems is essential for roof performance and safety. However, many buildings with parapet walls do not have adequate drain systems. The authors consider this to be an "epidemic", akin to the much-publicized deficiencies in public infrastructure.

With this study, we propose to discuss common roof drainage issues and to offer a set of conditions for the oversight and approval of roofing projects. For both new construction and existing buildings undergoing roof repairs, compliance with these roof drainage conditions should be mandatory and specifically enforced by the local building officials.

INTRODUCTION

Many commercial and/or high occupancy buildings, especially those with large roof areas, are constructed with low-slope roof systems. Examples of such buildings include those utilized for commercial/retail purposes, as well as hospitals and schools.

Problems associated with low-slope roof systems, or "roof failures", occur for various reasons. The authors' definition of the term "roof failure" is discussed below in the discussion section of this paper. It is the authors' experience that a large number of roof failures are caused by improperly designed primary and secondary roof drain systems, and by a lack of and/or improper maintenance. Additionally, it is our

experience that extreme cases of roof failures, including roof collapses, are almost exclusively limited to low-slope roofs with parapet walls that prevent drainage over the roof edge. It is the purpose of this paper to present our findings for several roof failure cases that we have personally investigated.

It is our opinion that if proper oversight is performed during new roof construction and/or during the re-roofing of existing buildings, most extreme or catastrophic roofing failures can be prevented. Therefore, it is the intent of the authors to propose a set of standards for the oversight of new and existing roof construction. Our proposal will be limited to high occupancy buildings with low-slope roof systems. Additionally, we will propose a more strict set of standards for "important buildings" based on the International Building Code (IBC) occupancy categories and building use.

Low-slope roof systems. It is not the intent of this paper to detail low-slope roof systems; however, the authors feel it necessary to briefly describe the major components associated with these types of roofs. Generally, low-slope roof assemblies consist of a roof covering or membrane, insulation boards, and a roof substrate or decking. Insulation generally consists of rigid boards stacked one over another to achieve a desired thermal "R" rating. The insulation is sometimes tapered to accommodate drainage requirements. The substrate consists of the building superstructure framing and a deck over which the roofing assembly is installed. In some cases, the superstructure framing is sloped in lieu of tapered insulation.

The National Roofing Contractors Association (NRCA) categorizes low-slope roof coverings or membranes into six general categories: built-up, polymer-modified bitumen, thermoplastic, thermoset, metal panels, and sprayed polyurethane foam-based. The primary waterproofing mechanism of low-slope roofing systems is impermeability of the roofing membrane. In contrast, high-slope roofing systems rely on gravity shedding of water over semi-impervious roof coverings. The roof designer should select a roof membrane(s) for a particular project based on a set of criteria, as well as site and building-specific issues (NRCA, 2006).

Drainage. It is the authors' experience that drainage is the roof component that is most neglected and whose purpose or function is often misunderstood by roofers, owners, and even design professionals. Drainage generally consists of either an array of interior drains or perimeter drainage in the form of free-fall edges or thru-wall scuppers at parapet walls.

As noted earlier, the culprit for many roof collapse cases on roofs with parapet walls is poor roof drainage. Poor roof drainage can be caused by a number of different factors, including improper or deficient design. Typical design drainage requirements include a minimum number of drains based on service areas and the inclusion of secondary drains. Secondary drains are drains that will become active during an emergency situation where the main (primary) drains are not functioning properly

and/or the design rainfall rate is exceeded. For low-slope roofs with parapet walls, secondary drains typically consist of overflow drains or scuppers.

The design of primary roof drainage is typically based on the 100-year hourly rainfall rate (theoretical) for a given location as specified in the International Plumbing Code (IPC) or from an approved local weather source. The IPC provides tables based on the design rainfall rate and horizontally projected roof area (or tributary area for a given drain), which allows the user to easily size primary drainage. Secondary drainage is sized using the same method; and flow through the primary system is not considered when sizing the secondary roof drain system (ICC, 2006).

Ponded water and roof collapse mechanism. Ponding takes place when rainwater does not drain properly and collects at confined spaces and in deflections or irregularities on the surface of a roof. Acceleration of ponding occurs when the weight of the collected water causes significant deflections in the roof framing, causing progressively more water to drain to the area and creating instability in the roof framing. Considering structural design of roof framing, the strength and stiffness of the roof framing and the drainage conditions must be adequate to prevent the acceleration of ponding at the roof. However, in extreme cases, ponding instability can occur; especially in the presence of poor roof drainage and in older structures which were not designed to comply with more recent building codes. While roof failure and collapse can occur without ponding instability, it is important to consider this mechanism when a given roof structure is analyzed.

DISCUSSION

The primary purpose of roof systems is to shed water off the roof assembly and prevent it from infiltrating the interior of the structure. Therefore, it is the authors' opinion that roof systems have failed if moisture infiltrates the interior of a structure as a result of the roof system and/or the roof does not adequately shed rain runoff, which results in ponded water on the roof surface. Ponded water that persists for an extended amount of time provides conditions conducive to roof deterioration, reducing the lifespan of the roof. NRCA states, "The criterion for judging proper slope for drainage is that there be no ponding water on the roof 48 hours after a rain during conditions conducive to drying (NRCA, 2006)". Structural failure of the roof framing, such as a roof collapse, is also considered to be a roof failure. As noted above, in extreme cases, poor drainage can result in roof collapse.

The authors have evaluated many low-slope roof failures related to poor drainage. Common roof drainage issues include poor design/construction of primary and secondary drain systems, lack of maintenance, improper roof repairs, and drain system modifications. The following case studies are presented to highlight some of the aforementioned drainage issues.

Poor design/construction. The subject structure in our first case study was a large public high school located in south Texas, near the Gulf of Mexico. The roof at the

subject structure was a multi-level low-sloped roof with multiple roof areas that were bounded by parapet walls. **Figure 1** is an overall view of several roof areas at the subject structure. Roofing types included modified bitumen roofing (both smooth and granule surfaced) and built-up roofing with gravel ballast. The roof drain systems throughout consisted of primary roof drains and associated secondary scuppers along the roof edges.

Figure 1. General view of a portion of the school roof.

It was observed during our investigation that several of the scuppers were located approximately 4" to 7" above the adjacent roof drains. **Figures 2 and 3** are examples of two of the scuppers that were measured during our site visit. Previous building codes (dating back at least to the 1997 Uniform Building Code [UBC]) required that the secondary drain system be located 2" above the primary drains (ICBO, 1997). The requirements of the more recent IBC are based on the design of the roof structure and differ from the UBC prescriptive requirements. Regardless, it has been our experience that the 4" to 7" distance between the scuppers and primary drainage at the high school roof was too high. In our opinion, this condition was potentially unsafe if the roof structures were not designed for the hydrostatic loading from water accumulation to these heights. Additionally, the significant amount of water allowed to pond on the roof due to the location of the scuppers provided a condition conducive to significant water intrusion and accelerated roof deterioration.

Figure 2. Scupper is located approximately 5" above the roof surface.

Figure 3. Additional scupper located 7" above the roof surface.

Lack of maintenance. For our second case study, the authors investigated a commercial building with a low-slope roof that had been overlaid with a foam roof system. Roof drainage consisted of two (2) small roof drains that also served two (2) evaporator coil condensate lines, and six (6) thru-wall scuppers along the south side of the roof edge (roof was sloped towards this edge). There were no strainers over the roof drains.

There was a significant amount of debris along the south end of the roof around the scuppers. **Figures 4 and 5** below depict the debris build-up at the subject roof. The debris was obstructing the roof drainage. Vegetation was observed growing from the debris, indicating a long-term condition. Additionally, staining was observed at the roof consistent with previous standing water, and unevenness at the foam roof surface, which created several localized low spots for standing water. These conditions resulted in poor roof drainage, which contributed to roof failure and water intrusion at the building interior. Proper maintenance at the roof level would have prevented the significant debris build-up and provided conditions favorable for proper drainage.

Figure 4. Debris build-up at roof.

Figure 5. Debris build-up around scupper.

Improperly applied repair. Improper roof repairs can radically affect roof drainage. The subject structure in our third case study was a medical office building in Houston, Texas. The roof at the structure consisted of a ballasted built-up roof system. It was reported that the roof at the west side of the building was damaged during Hurricane Ike. The roof in this area had been replaced with a modified bitumen membrane prior to our site visit.

It was observed during our investigation that the roof surface around several of the drains had been patched; however, the strainers at most of these drains were missing. It was also observed that the overflow scuppers along the north parapet wall had been flashed over by a modified bitumen membrane repair, thus eliminating the overflow drain system. This created a potentially unsafe condition at the roof: if the primary drain system was to become impeded (more likely due to the lack of strainers), there would be no secondary means by which the roof could drain, which would create

conditions conducive to a roof collapse. **Figure 6** shows an area at the roof where the overflow scupper had been patched over and **Figure 7** shows the same scupper as viewed from the exterior of the structure.

Figure 6. Patched over overflow scupper.

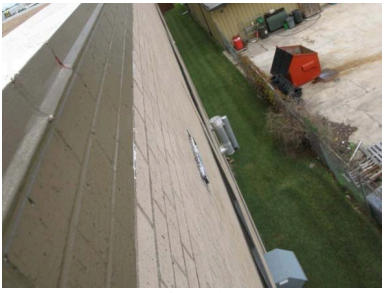

Figure 7. Non-functional scupper viewed from exterior.

Inadequate drain covers. The subject building in our fourth case study was a multi-story office building with recessed roofs at the three top-most floor levels, as shown in **Figure 8**. The recessed roofs consisted of rectangular gravel ballasted built-up roofs with perimeter parapet walls at three edges. The fourth edge consisted of a building exterior wall with windows over a low curb wall. An overall view of one of the recessed roofs can be seen in **Figure 9**. Drainage for each roof consisted of two pairs of primary and secondary drains. Drainage for roofs cascaded down from upper to immediately lower roofs. Therefore the bottom-most recessed roof received the drainage from all upper roof areas.

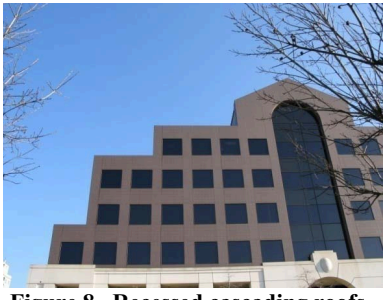

Figure 8. Recessed cascading roofs.

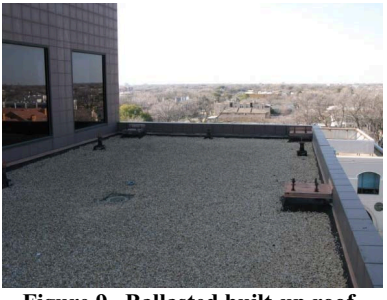

Figure 9. Ballasted built-up roof.

Water intrusion occurred at two of the roofs during a high precipitation storm. Improper/deficient drain strainers were reportedly clogged with debris. As a result, water ponded over the roofs to a height that exceeded the curb height adjacent to the exterior wall of the building. Water infiltrated over the curb and below the windows causing extensive water damage to the offices below the roofs. It should be noted that the secondary drains were sized appropriately even considering the cascading conditions of the roofs.

It was determined that improper drain strainers caused the drain systems to fail. **Figure 10** shows both primary and secondary drains that were reportedly cleaned after the storm event. Note that the primary drain strainer was installed flush with the drain and a square low-profile ballast retainer was located outside the drain. The ballast easily overcame the ballast retainer and clogged the primary drain strainer. There was no strainer at the secondary drain and more than likely it was also covered by debris during the storm. Neither the primary nor the secondary roof drains conformed to building code standards, including requirements that strainers or drain covers extend a minimum of 4" above the surface of the roof (ICC, 2006). This case exemplifies at least two typical roof deficiencies: improper drain strainers and/or deferred maintenance resulting in clogged drains.

Figure 10. Primary and Secondary Drains.

Modified drainage. The subject building in our fifth case study was a nearly 100 year old retail strip-mall building. It had original wood truss roof construction with multiple layers of roofing membranes. The roof profile was unusual and consisted of low-sloped roof sections with gable-style cross-sections in an apparent attempt to direct water to the sides of the roof. Thru-wall scuppers were located on a high parapet wall at the downward slope of the roof. An overall view of the building can be seen in **Figure 11**. The roof partially collapsed during a storm event, as shown in **Figure 12**. Fortunately, there were no injuries.

Figure 11. Strip mall.

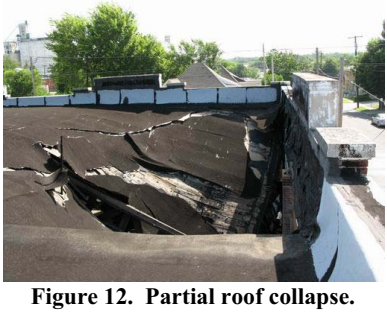

Figure 12. Partial roof collapse.

The cause of the collapse was determined as improper drainage. The roof drain system was modified upon the numerous re-roofing applications performed on the structure over the years. As **Figures 13 and 14** show, at some time the drain system changed from interior roof drains to exterior scuppers. The new scuppers became undersized due to the numerous re-roofing layers that reduced the available scupper cross-sectional drainage area and also by a reduction in size of the downspouts located on the exterior walls. Clearly, the original drain system was changed substantially and resulted in the partial collapse of the roof.

Figure 13. Modified drainage – scupper above sealed-over drain.

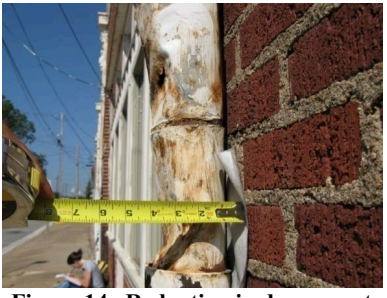

Figure 14. Reduction in downspout cross-section.

PROPOSED CHANGES

It is the intent of this paper to propose a set of standards for the oversight of new and existing non-residential low-slope roof construction with parapet walls. We exclude residential construction due to the lesser occupancy and the relatively low percentage of low-slope roofs with parapets, which may make additional oversight impractical. In addition, for "Important Buildings", which have higher occupancy and/or critical functions, we recommend a higher standard of review.

Important Buildings. Although the classification of "Important Buildings" is subjective, we propose that these "Important Buildings" include the buildings in IBC Occupancy Category IV and the following buildings from Occupancy Category III: schools, jails/detention facilities, and buildings with an occupancy load exceeding 5,000 (ICC, 2006).

We propose that for these "Important Buildings" with low-slope roofs and parapets restricting free drainage over the roof edge, the roof drain systems must be in compliance with the current building code at all times. This includes immediately following completion of new construction and/or re-roofing. For new construction, we propose that a drainage analysis be submitted to the city (or building official) of jurisdiction. This analysis will require signature and seal by a licensed Professional Engineer. Furthermore, we propose that the construction of the roof drain system must be certified by a licensed Professional Engineer or Architect.

To enforce these standards we propose that the issuance of a building permit be contingent on the submittal of the drainage analysis. Likewise, we propose that the issuance of the Certificate of Occupancy be contingent on the certified review of the constructed roof drain system by a licensed Professional Engineer or Architect.

For re-roofing of "Important Buildings" with low-slope roofs and parapets restricting free drainage over the roof edge, we propose that inspection of an existing roof shall be performed if greater than 25% of the roof area is repaired or replaced, or if the existing drainage system is changed in any way. This inspection should be performed by a licensed Professional Engineer or Architect. Also, we propose that any changes to the roof drain systems require a complete drainage analysis by a licensed Professional Engineer. Changes to an existing roof drain system would include removing, resizing or relocating drains, or altering drainage flow. Enforcement methods similar to those proposed above for new structures should be applied to existing structures, including the possible revocation of the Certificate of Occupancy if the roof drainage is not properly analyzed and certified. Finally, we propose that the owners of these "Important Buildings" be required to have periodic roof evaluation/maintenance by their personnel to ensure that the roof drain systems are performing and that the drains and scuppers are free from obstruction.

All other buildings. For all remaining non-residential buildings with low-slope roofs and parapets restricting free drainage over the roof edge, it is the objective of the authors' recommendations to increase the level of inspection following new construction and re-roofing projects.

For new construction, the roof drain systems should already be properly sized and designed; however, this is not always the case nor is it closely evaluated. We propose that all new construction for low-slope roofs with parapets restricting free drainage over the roof edge require a roof drainage analysis signed and sealed by a licensed Professional Engineer. After construction, we propose that the building official inspect the roof drain systems for compliance with the design, with special attention to the presence and location of the secondary drain system. We propose that the Certificate of Occupancy be contingent on this review.

For re-roofing projects on existing buildings, we propose that the city (or building official) require that the contractor submit information about the roof drainage with the permit application. The required information from the roofing contractor should include the type of roofing to be installed, the type of roof structure supporting the roof, the nominal roof slope that will be achieved, the number and size of the primary and secondary drains, and the proposed location of the primary and secondary drains (including the height of the secondary drains above the level of the primary drains). After construction, we propose that the building official perform an inspection of the roof drain system. It is likely not economically feasible to require inspection by a licensed Professional Engineer or Architect for all roofs (other than "Important Buildings", as noted above), so we propose that the building official use the building code as a guide for the drainage requirements.

It is also our opinion that a secondary roof drain system be required for all re-roofed low-slope roofs with parapets restricting free drainage over the roof edge. This includes existing buildings that do not have a secondary drain system. We propose that this requirement should take effect upon repair of more than 25% of the roof system or if the existing roof drain system is changed in any way.

SUMMARY AND CONCLUSION

Based on our experience, it is our opinion that a lack of roof drainage oversight for buildings with low-slope roofs and parapets restricting free drainage over the roof poses a safety concern to the general public. Therefore, the authors feel it is necessary to increase the level of inspection of roof drain systems for such buildings, both for new construction and for re-roofing projects. For "Important Buildings" that have essential functions or high occupancies, we recommend an even higher level of analysis and inspection to ensure proper roof drainage. We further propose that these increased standards be enforced by the city or building official of jurisdiction.

Based on our experience, it is the authors' belief that these higher standards can improve roof performance and significantly decrease the number of roof collapses. This is of great benefit to public safety and in most cases will not require a significant additional expenditure of money or effort.

REFERENCES

International Conference of Building Officials (ICBO). (1997). *Uniform Building Code*, Whittier, California.
International Code Council (ICC). (2006). *International Building Code: Code and Commentary, Volumes 1 and 2*.
International Code Council (ICC). (2006). *International Plumbing Code*.
National Roofing Contractors Association (NRCA). (2006). *The NRCA Roofing and Waterproofing Manual*, Rosemont, Illinois.

Dimensional Study of Mine Subsidence Mapping Using Google Earth™

Shen-En Chen, R. Janardhanam and Mohiuddin Syed

Dept. Civil and Env. Eng., University of North Carolina at Charlotte, 9201 University City Blvd., Charlotte, NC 28223-0001, USA

ABSTRACT: Problems arising from subsidence pose danger for future land development above abandoned coal mines and are challenging to forensic engineers to substantiate these damages and differentiate the effects due to mine subsidence from other possible non-mine related damages. Forensic investigators commonly asked to provide evidence that the structures-of-interest are in fact above or close to the coal mines by associating the structures to possible mine activity sites, such as within the angles of draw to the underground mine. This paper discusses the problems and errors associated with abandoned mine mapping using Google Earth™ and historical mine maps. Analyses of dimensions are performed to validate the results of error analysis.

KEYWORDS: geophysical testing, wave phenomena, stress wave techniques, sinkhole and abandoned mine detections.

INTRODUCTION

Coal occurs beneath an overburden composed of weak bedrock deposits having depths reaching hundreds of feet. Extensive exploitation of underground minerals using excavation techniques is leading to more coal mining by underground excavation (Dunrud & Osterwald 1980). After being depleted, these mines are usually left abandoned. Abandoned mines, which are left untreated, can create problems such as sinkholes and surface depressions, any of which may increase with time and cause damages to properties and structures on the surface. Damages to structures due to mine subsidence have been observed for many areas throughout the United States including Alabama, Colorado, Illinois, Missouri, Ohio, Kentucky, Tennessee, Virginia, Utah, and Wyoming. (Gennaro et al. 1986) identified the resulting differential movements in the ground surface caused damages to nearby structures and utilities. These problems resulted in legal claims and the need for forensic investigations.

Forensic investigators rely on strong evidence in order to substantiate their assumptions. One common assumption is that the main cause of damage to structures overlaying abandoned mines is from mine subsidence. To prove this assumption, mapping of abandoned mines using historical data superimposed to the geographical positions of the damaged structures is performed. However, the potential errors resulting from mapping is difficult to substantiate.

In this study, errors in mapping abandoned coalmines using Google Earth™ and historical mine maps are studied by performing an error analysis and analyses of dimensions. Mary Lee # 1 mine in Alabama is used as case study. Mapping of the mine onto property locations is done by applying Google Earth™ results on to property data provided by historical mine maps. Mapping is completed by taking in to

consideration the geological features such as rivers, highways, and latitude and longitude locations.

QUALITATIVE ERROR ANALYSIS

The error analysis considers the mapping of geographical features that are recognizable using Google Earth™. Many parameters have been considered for the error analysis including errors associated with the area of the mine, perimeter of the mine, geographical feature recognition and as well as the influence area of these mines. Influence area is defined as the potential zone that may experience mine subsidence and is usually established by assuming the angle of influence or the angle of draw. Analysis of dimension has been conducted to verify the analytical results. Error analysis of parameters such as eye altitude, area, perimeter, geographical features and influence area of the superimposed mine map as compared to the original mine map, has been performed.

Percentage Variance in Eye Altitude, Area and Perimeter

To map geographical features of a mine map on top of the Google Earth™, the altitude is adjusted in such a way that the features from different sources can be superimposed. This mapping technique is approximate, as it is based on eyeball judgment. Hence, eye altitude plays an important role in the mapping technique and the error involved in mapping must be calculated in order to improve on the technique and reduce the overall percentage error. This error, which is resulted from the percentage variance, should be added to the overall errors involved in area and perimeter estimations.

In order to calculate the eye altitude error, five independent trial mappings have been made by superimposing the abandoned mine map over the region in Google Earth™. The mine map under consideration belongs to the Mary Lee # 1 mine in Alabama (Figure 1). After superimposing the mine map over Google Earth™, the corresponding values for eye altitude are recorded and the area and the perimeter have been calculated.

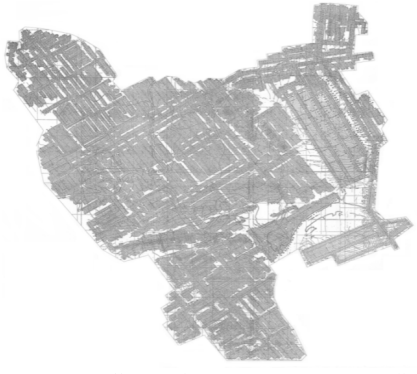

Figure 1. Abandoned Coal Mine Map – Mary Lee # 1, Alabama.

The area and the perimeter have been calculated using AutoCAD™ 2007 and Google Earth™, respectively. The percentage variances (coefficients of variation) are then calculated from the five trials as:

$$v_i = \frac{\sigma}{\mu} \text{ x } 100\,\% \tag{1}$$

where, σ = standard deviation and μ = average values. The super imposed mine map over Google Earth™ is shown in Figures 2.

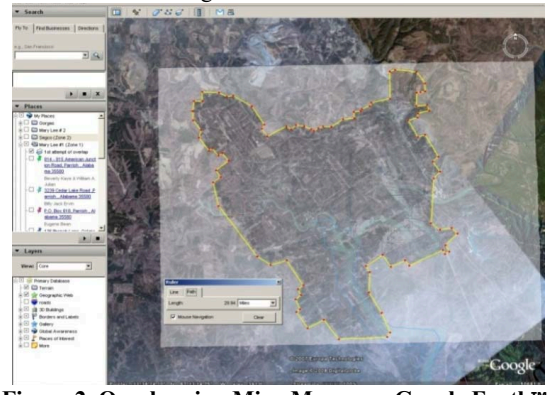

Figure 2. Overlapping Mine Map over Google Earth™.

The statistical values for the eye altitude, area from the AutoCAD™ and perimeter from Google Earth™ from the five trials are listed in Table 1. As shown, eye altitude has the same order of magnitude as perimeter, but results in higher order of error in area calculation. This may be due to coupling errors in both x and y directions.

Table 1. Statistical Average, Standard Deviation and Coefficient of Variances

Description	1st trial	2nd trial	3rd trial	4th trial	5th Trial	Average μ	Standard Deviation σ	COV %
Eye Altitude (ft.)	53380	47486	51206	47165	47249	49297	2843.50	5.77
Area $(mi.)^2$	24.77	24.70	20.00	20.44	27.10	23.40	3.07	13.10
Perimeter (mi.)	29.94	25.68	28.08	25.45	25.51	26.93	2.01	7.46

Area and Perimeter of the Mine

Area and the perimeter of the superimposed mine and the original mine maps have been calculated by using AutoCAD™ (2007). Figure 3 below shows the mine maps in 2007 AutoCAD™. The values are tabulated in Table 2 and the percentage errors are calculated as:

$$\% \text{ Error in Area} = \frac{\text{Original Mine Map Area} - \text{Superimposed Mine Map Area}}{\text{Original Mine Map Area}} \times 100 \qquad (2)$$

$$\% \text{ Error in Perimeter} = \frac{\text{Original Mine Map Perimeter} - \text{Superimposed Mine Map Perimeter}}{\text{Original Mine Map Perimeter}} \times 100 \qquad (3)$$

The errors in area and perimeter calculations have an impact on the projected mine influence area. The errors come from the lack of precision in estimating the outlines of the mapped area. As shown, the superimposed mine map has a reduced influence area relative to the original map.

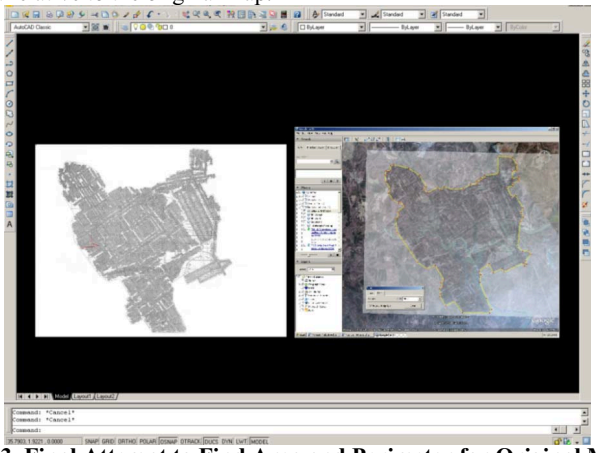

Figure 3. Final Attempt to Find Area and Perimeter for Original Mine & Superimposed Mine Map Using AutoCAD™.

Table 2. Area, Perimeter and Respective Percentage of Errors

Description	Area (mi.)^2	Perimeter (mi.)	% Error in Area	%Error in Perimeter
Superimposed Mine Map in Google Earth™	32.35	33.73	28.15 %	14.92 %
Original Mine Map	45.02	39.64		

Geographical Feature Recognition

In order to fit the abandoned mine map over Google Earth™, geographical features identified on the abandoned mine map must match the Google Earth™ features including rivers and roads. For the Mary Lee # 1 mine, a segment of a river has been used as the target feature for overlapping. The distances are measured from the geographical feature (river) to a fixed location (property) on the Google Earth™ and on the mine map. Distances in both X and Y directions are being measured on Google Earth™. Table 3 below tabulates all the distances in the x and y directions. These two distances have been compared and Root Mean Square (RMS) of the distance has been calculated by using the following formula:

$$\text{RMS} = \sqrt{(\text{L}_\text{x} - \text{L}'_\text{x})^2 + \left(\text{L}_\text{y} - \text{L}'_\text{y}\right)^2} \quad (4)$$

where, L_x = Distance from fixed location to the geographical feature in X – direction on Google Earth™; L_y = Distance from fixed location to the geographical feature in Y – direction on Google Earth™; L_x = Distance from fixed location to the geographical feature in X – direction on mine map; and L_y = Distance from fixed location to the geographical feature in Y – direction on mine map. Error is defined as:

$$\%\ \text{Error in X Direction} = \frac{\text{X Length before Mapping} - \text{Length on Superimposed Mine Map}}{\text{Length before Mapping}} \text{ x } 100 \quad (5)$$

$$\%\ \text{Error in Y Direction} = \frac{\text{Y Length before Mapping} - \text{Length on Superimposed Mine Map}}{\text{Length before Mapping}} \text{ x } 100 \quad (5)$$

The superimposed mine map and the original mine map have a RMS distance of 74.67 feet. The error in x-direction is higher compared to the y-direction. These errors provide a sense of scale of the superimposed mine map. One can interpret from the above values that the superimposed mine map has a high error in x-direction than in y-direction, as shown in Figure 4 and 5. However, this percentage error may be due to the shape of the selected geographical feature.

Table 3. Percentage Errors in Length in X and Y Directions

Description	Length in X direct. (ft.)	Length in Y direct. (ft.)	% Error in Length in X direct.	% Error in Length in Y direct.
Google Earth™	158.42	950.43	33.33 %	5.26 %
Mine Map	105.64	1003.22		

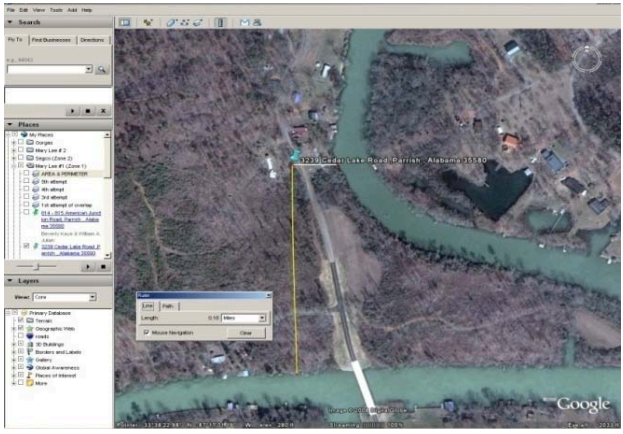

Figure 4. Distance in X and Y Directions from the Property in Google Earth™.

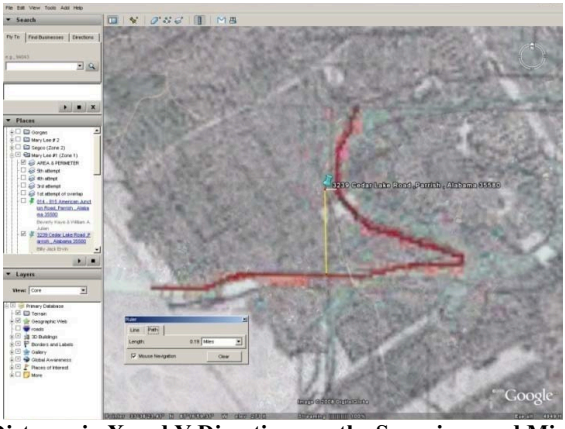

Figure 5. Distance in X and Y Directions on the Superimposed Mine from the Property in Google Earth™.

Table 4. Description of Actual Area

Map	Length (ft.)	Width (ft.)	Actual Area on ground surface (ft^2.)
Superimposed Mine Map	41991.84	39119.52	1.643×10^9
Original Map	49362.72	46696.32	2.305×10^9

To calculate the influence area, an approximate method has been used: The approach is similar to the 2:1 method used for calculating stress influence at depths. Based on the method, a slope of 1 horizontal to 2 vertical from the edge of the area is taken to compute the influence area, as shown in Figure 6 and Table 5 (Coduto 1999). This approximation would result in an angle of draw of 45˚. The Influence area for an angle of draw of 35˚ are investigated in Table 6. Compare the results for 35˚ and 45˚ angles of draw, it is shown that the the angle of draw has significant influence on the ground level subsidence. Table 7 tabulates the differences between the projected influence areas by considering the two angles of draw. To give an idea about the influence of subsidence at the ground surface due to these mines, Table 8 compares the projected area to the influence area due to 0^o and 35˚ angles of draw. It is therefore concluded that the subsidence influence zone is minimal for a mine depth of 500 ft (< 4%).

Table 5. Projected Influence Area by Considering an Angle of 45˚

Map	Depth (ft.)	Projected Length (ft.)	Projected Width (ft.)	Projected Influence Area (ft^2.)
Superimposed Mine Map	300	42591.84	39719.52	1.692×10^9
	400	42791.84	39919.52	1.708×10^9
	500	42991.84	40119.52	1.725×10^9

Table 6. Projected Influence Area by Considering an Angle of 35˚ for Superimposed Mine Map

Map	Depth (ft.)	Projected Length (ft.)	Projected Width (ft.)	Projected Influence Area (ft^2.)
Superimposed Mine Map	300	42411.96	39539.64	1.676×10^9
	400	42552.00	39679.66	1.688×10^9
	500	42692.04	39819.71	1.699×10^9

Table 7. Comparison of Projected Influence Area for Angles of 35˚and 45˚

Depth (ft.)	Projected Areas x 10^9 (Sq. ft.)		% Difference
	Superimposed Mine Map		Superimposed
	45˚	35˚	
300	1.69	1.68	0.95
400	1.71	1.69	1.12
500	1.73	1.70	1.51

Table 8. Comparison of Projected Influence Area for Angles of 0˚and 35˚

Depth (ft.)	Projected Areas x 10^9 (Sq. ft.)		% Difference
	Superimposed Mine Map		Superimposed
	0˚	35˚	
300 ft.	1.64	1.68	1.97
400 ft.		1.69	2.67
500 ft.		1.70	3.30

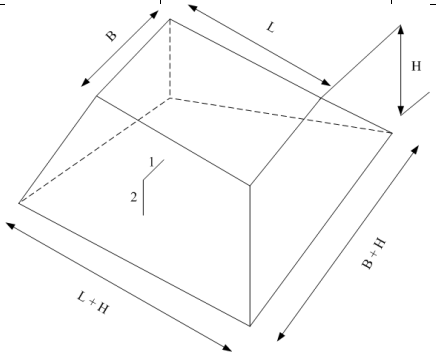

Figure 6. Approximate Method for Calculating Influence at Depths.

Analyses of Dimensions for Area & Perimeter

Analysis of dimensions is a tool used to determine the effects of physical dimensions to certain derived quantities. In order to use this analysis, one has to know the variables of the physical quantities (Bridgman, 1922). In this case, the physical quantities are areas and perimeters that have a basic physical dimension of length (L). The dimensions for the area and the perimeter are L^2 and L, respectively. The map is considered rectangular and hence has physical dimensions of length, L and width, W. In this section, the length and the width for both the original and superimposed mine maps are taken into consideration and are tabulated below in Table 9. The area and the perimeter are tabulated and the percent difference is calculated below in Table 10.

Table 9. Analysis of Dimensions of Length and Width for Original and Superimposed Mine Maps

Description	Dimension	Original Mine Map	Superimposed Mine Map	% Difference
Length, L (ft.)	L	49362.72	41991.84	14.93
Width, W (ft.)	L	46696.32	39119.52	16.23

Table 10. Analysis of Dimensions of Area and Perimeter for Original and Superimposed Mine Maps

Description	Dimension	Original Mine Map	Superimposed Mine Map	% Difference
Area (Sq. ft.)	L^2	2.31×10^9	1.64×10^9	28.72
Perimeter (ft.)	L	1.92×10^5	1.62×10^5	15.52

To determine the percent difference of the area (Area: L^2), the following formula is used:

$$\% \text{ Difference} = \frac{(L+\Delta L)^2 - L^2}{L^2} \times 100\% = \frac{\left(\Delta L^2 + 2L\right)}{L^3} \times 100\% \quad (7)$$

where change in length: ΔL and original length: L. The percent difference of the area which has been calculated to be 28.43 % and the area is 32.3 %.

To check the percent difference of the perimeter, the following formula is used.

$$\% \text{ Difference} = \frac{(L+\Delta L) - L}{L} \times 100\ \% = \frac{\Delta L}{L} \times 100 \quad (8)$$

The percent difference of the perimeter came out to be as 15.10 % and the perimeter from the above check is 15 %. The check shows that the percent difference of the length and the perimeter are almost equal, as they have the same dimension 'L'. The area having the dimensions as 'L^2' and should have a value close to twice that of the perimeter. By using the analysis of dimensions, it can be concluded that the area and perimeter and their respective percent difference are close and in the same orders of magnitude.

Discussion

The overall error analysis gives a clear idea about the errors due to approximation involved in the estimation of area, perimeter, and geographical feature recognition and influence area. The coefficient of variation is very useful in determining the overall percentage errors involved with area and perimeter estimations. The overall percentage of error in area is 28.43 % and that of the perimeter is 15.10 %. The percentages of errors while mapping the geographical features of the mine over the Google Earth™ are calculated to be 33.33% in the x-direction and 5.26% in the y-direction. This error reveals that the mapping of mines over Google Earth™ resulted in a much higher percentage of error in the x-direction than in the y-direction.

The projected influence areas were calculated with the approximate method by taking the angle of draws of 35˚ and 45˚ respectively, and revealed that the projected influence area was less for an angle of draw of 35˚ than for 45˚.

Analyses of dimensions were done to verify the results of error analysis and were done by taking into consideration the physical quantities of area and perimeter. This step revealed reasonable accuracy for error analyses for both area and perimeter.

CONCLUSION

This study presents the outcomes of a study into the use of Google Earth™ in forensic investigations to substantiate structural failures due to mine subsidence. The specific conclusions related to Google Earth™ mapping are as follows:

- Overall error analysis using Google Earth™ for geo-referencing the Mary Lee # 1 mines revealed directional implications: % errors are 33.33% and 5.26% in X and Y directions, respectively.
- The errors may be introduced by the eye altitude, which has a coefficient of variation of 5.77%.
- The percentage errors resulting from mapping the superimposed area and perimeter have been calculated. The projected influence area of the abandoned underground coal mines gives a clear indication about the influence of subsidence of these mines on the ground surface.
- The specific percentage error in projected area is 28.43% and that of the perimeter is 15.10%.
- The percentage of area calculated from analyses of dimensions is 32.30% and for perimeter is 15.00%. The differences in percentage of error between the two analyses are 3.90% and 0.10%, for area and perimeter, respectively.

The abilities to demonstrate geo-referenced bird view images of locales make Google Earth™ a useful tool that has the potential of demonstrating effects of mine subsidence to residential structures. However, as the results of this study indicate, mine subsidence professionals should caution of the potential sources of errors that may be introduced in the analytical process.

REFERENCES

Anderson N and Ismail A. (2003). "A generalized protocol for selecting appropriate geophysical techniques." *Geophysical Technologies for Detecting Underground Coal Mine Voids Forum*, July 28-30, 2003, Lexington, Ky.

Benson RC. (2000). "An overview of geophysical and non-destructive methods for characterization of roads and bridges", *Use of Geophysical Methods in Construction, ASCE, Geotechnical Special Publication* No. 108, p.1-14.

Chen SE, Syed M and Janardhanam R. (2007). "Surface geophysical testing techniques for forensic geotechnical studies." *Journal of Performance of Constructed Facilities.* ASCE Publications (Submitted).

Delatte N, Chen SE, Maini N, Parker N, Agrawal A, Mylonakis G, Subramaniam K, Kawaguchi A, Bosela P, McNeil S and Miller R. (2003). "Application of

nondestructive evaluation to subway tunnel systems." *Transportation Research Record 1845*, Transportation Research Board, 127-135.

Dunrud CR. (1976). "Some engineering geological factors controlling coal mine subsidence in Utah and Colorado." *Geological Survey Professional Paper 969*. United States Dept. of Interior and Geological Survey.

Dunrud CR and Osterwald WF. (1980). "Effects of Coal Mine Subsidence in the Sheridan, Wyoming Area." *Geological Survey Professional Paper 1164*. United States Dept. of Interior and Geological Survey.

Gennaro GM, James WM, Larry RP, and Richard ET. (1986). "Ground subsidence and structural damage over an abandoned room and pillar coal mine at Hegeler, IL." *Information Circular 9072.* United States Dept. of Interior and Bureau of Mines.

Griffin LM and Hiltunen DR. (2000). "Precision of seismic wave propagation methods in construction applications." *Use of Geophysical Methods in Construction, ASCE Geotechnical Special Publication No. 108*, 109-125.

Gucunski N, Antoljak S and Maher A. (2000). "Seismic methods in post construction condition monitoring of bridge decks." *Use of Geophysical Methods in Construction, ASCE Geotechnical Special Publication No. 108*, 35-51.

Hanson DR, Haramy KY and Neil DM. (2000). "Seismic tomography applied to site characterization." *Use of Geophysical Methods in Construction, ASCE Geotechnical Special Publication No. 108*, 65-79.

Huang H and Fraser DC. (2001). "Mapping of the resistivity, susceptibility, and permittivity of the earth using a helicopter-borne electromagnetic system." *Geophysics*, 66(1), 148-157.

Monaghan WD, Trevits MA, Mucho TP and Wood J. (2003). "Recent national institute for occupational safety and health research using ground penetrating radar for detection of mine voids." *Geophysical Technologies for Detecting Underground Coal Mine Voids Forum*, July 28-30, 2003, Lexington, Ky.

Nasseri-Moghaddam A, Cascante G, Phillips C and Hutchinson DJ. (2007). "Effects of underground cavities on Rayleigh waves – field and numerical experiments." *Soil Dynamics and Earthquake Engineering*, 27(4), 300-313.

O'Conner K, Dowding CH and Su MB. (1986). "Quantification of rock caving within sinkholes by time domain reflectometry." *Karst Hydrogeology: Engineering and Environmental Applications, Proceedings of 2nd Multidisciplinary Conference on Sinkholes and the Environmental Impacts of Karst*, Beck, B.F. edit, AA Belkema, Accord, Ma., 157-60.

Forensic Considerations in Sinkhole Investigations

E. D. Zisman, P.E., P.G.[1]

[1] E. D. Zisman, P.E., P.G., M ASCE, ATC Associates, 5602 Thompson Center, Tampa, FL 3334

Abstract

Determination of the causes of structural damage that can result from sinkhole activity is a difficult process requiring consideration of many arcane factors. Most investigations are directed to analysis of subsurface conditions as they relate to signature conditions known to occur when sinkhole activity is present. Missing in many sinkhole investigations is a thorough analysis of structural damage as it relates to causal subsurface conditions. Several case studies are presented where careful analysis of site conditions and structural damage has provided valuable clues to subsurface conditions responsible for structural distress. Also presented is an outline of the typical phases of a sinkhole investigation that will help the investigator adequately consider failure analysis in understanding how subsurface conditions interact with the structure.

1. Introduction

This manuscript is intended to make the investigator more aware of the forensic tools available to help in the identification of the causes of building distress. Emphasis is placed on subsurface conditions, not only related to sinkholes, but to other subsurface conditions that can cause distress in structures. It is vital to an investigation that the origin and nature of these causes be understood and considered in the analysis of structural damage so an accurate determination of causal factors can be made.

Most of us are familiar with pictures of the catastrophic collapse of the ground surface depicting the progressive destruction of one or more homes illustrating the destructive nature of ground movements associated with sinkholes. However, in Florida, the majority of sinkhole damage occurs from minor ground movement sufficient only to result in varying degrees of distress in the structure. The types of sinkhole damage can be classified as 1) cosmetic, involving only the appearance of the building; 2) functional, involving the use of the building; or 3) structural, involving the structural integrity of the building. Distress in the building can be the result of structural deficiencies in the building, deficiencies in the subsurface or a combination of both. It is the investigators responsibility to determine the severity and origin of distress by employing forensic methods to establish the cause of damage as it relates to sinkhole activity or other causes.

Obviously, adverse subsurface conditions can be caused by other factors besides active sinkhole conditions. These factors are discussed in subsequent sections of this

manuscript and for a detailed discussion see Zisman, 2001. All of these conditions must be addressed by the geotechnical engineer or geologist.

2. Sinkhole Investigation

2.1 General

It is essential in any sinkhole investigation that the investigators obtain a complete picture of all factors that can affect the structure. This requires that the investigation be structured to consider all possible failure scenarios that can result from above ground and below ground causes.

2.2 Steps in an Investigation

Every sinkhole investigation should be structured to meticulously consider all possible clues that become apparent in each part of the investigation. Similar to solving a puzzle, one must be vigilant to consider all information that can be gleaned from the site investigation. Figure 1 provides an outline for a typical subsurface investigation that should be helpful in the evaluation of site conditions. Each site has its unique constraints and requirements that will require some modification of the outline to meet site conditions. Although, detailed discussion of this outline is beyond the scope of this document its inclusion herein should provide guidance to investigators a more complete discussion can be found in Zisman, 2001.

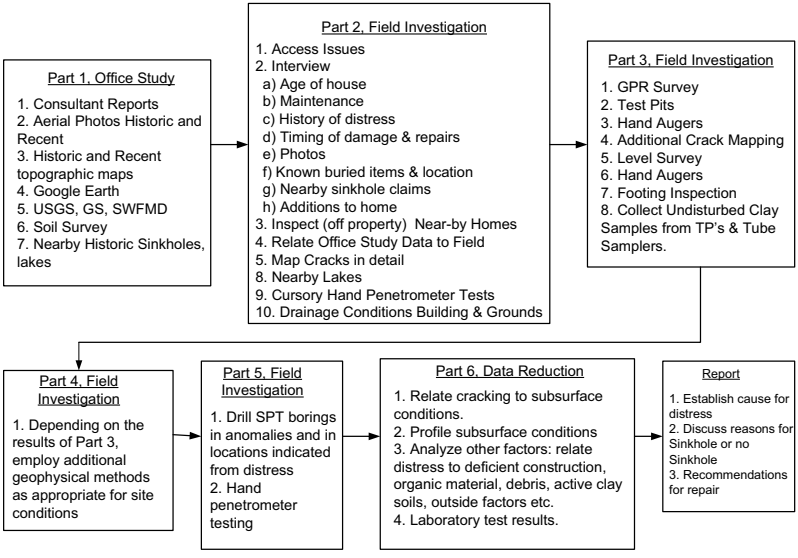

Figure 1, Outline of the Typical Parts in a Sinkhole Investigation

3. Causes of Structural Distress

3.1 General

The initial phase of the investigation should include an investigation of all manifestations of building distress. If building distress in any form (cosmetic, functional or structural) is present, it is the responsibility of the investigator to determine the cause of cracking. The first consideration is to determine if cracking is caused by above ground conditions such as shrinkage of masonry, inadequate design of structural members, deterioration of building components etc or is the result of below ground causes such as inadequate foundations, buried organic material, expansive clay, loose or soft soils etc. The starting point in answering these questions is to carefully examine building distress to understand what condition or combination of conditions can cause the observed damage.

In many sinkhole investigations, the investigator only notes where the cracking is but does not analysis the cracking to determine how the cracking is related to potential ground or structural conditions. Consider the simple case where a building is effected by an unstable slope. In this instance, one would expect to find tension cracking in the wall perpendicular to slope movement. That is, greater displacement should be found at the top of the wall than at the bottom of the wall. In this example observation of building damage provides a clue to the cause of building distress. This type of analysis can be applied to other types of cracking as discussed later. In addition to considering where cracking occurs in the building, it is also necessary to analyze the displacement and offset along the cracks to relate cracking to the overall building geometry and building movement. Such an examination can lead to an understanding of the cause of cracking.

3.2 Mapping Cracks

To aid in the understanding of distress as it relates to the building and subsurface conditions, a valuable technique in forensic engineering is to develop maps drawn to scale for each side of the building. The maps should show the size, shape, pattern displacement and location of the cracks on both interior and exterior walls. Any deflection found in the floor behind the wall should also be indicated. These maps should be supplemented with photographs of the walls. The photos should be taken in favorable light conditions and at angles that will enhance the distress seen in the walls. Photographs should show close ups of the cracking as well as overall views of the entire section of the wall to depict cracking in relation to the entire side of the building.

The maps and photos should be used for further office study in the analysis of structural movements. In many cases initial assessments are made in the office following Part I of the Field Investigation and are later enhanced in Part 2 of the Field Investigation. Information obtained in Parts 1 and 2 should be used to develop

Part 3 and 4 of the field investigations. All of this data is brought together in Phase 6, Data Reduction.

3.3 Significance of Various Types of Cracks

3.3.1 Basic Cracking

A brief discussion of the type of cracking that can be found in the field follows; however, it should be recognized that when multiple causes of distress are present interpretation of cracking and other forms of distress will require careful analysis of the many possible conditions that can cause the observed distress.

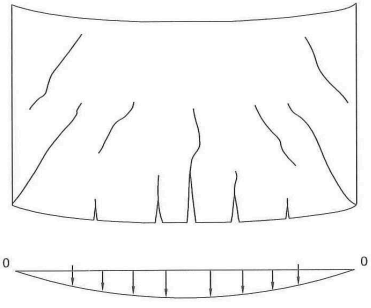

Figure 2, Concave Settlement

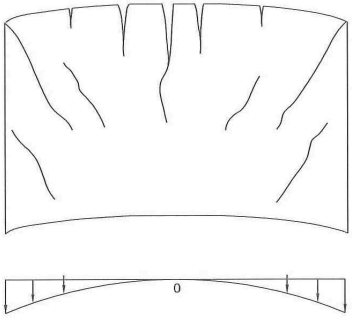

Figure 3, Convex Settlement

Figure 2 shows the idealized cracking that can occur in a homogeneous material when differential settlement results in a dish-shaped (concave) settlement as shown in the figure. Notice that the greatest displacement in the cracks occurs where the largest tensile forces are present in the bottom of the section as shown in the idealized settlement profile shown at the bottom of the figure.

Similarly, in Figure 3, the condition where differential settlement results in convex settlement of the foundation, a condition results where the greatest crack displacement occurs in the top of the wall where tensile forces are greatest. The relative settlement profile is shown at the bottom of the figure.

These figures illustrate how observation of cracking should include the orientation and measurement of crack displacement so this information can be used to analyze overall wall movement. In Figure 2 one would be inclined to investigate near the center of the wall where the maximum movement has occurred. Conversely, in Figure 3 one should investigate near the ends of the wall were most movement has occurred.

3.3.2 Other Considerations in the Formation of Cracks

There are essentially two types of cracks in concrete: shrinkage and settlement cracks. These cracks can generally be distinguished by the usual discontinuous and of relatively uniform displacement found in shrinkage cracks while settlement cracks tend to be continuous, and may have varying displacement.

Concrete masonry units (CMU) shrink as they cure and uncured CMU may be used in construction. Shrinkage cracks in CMU are generally uniform in thickness and appear in the weakest section of the wall (middle of a span without an interior opposing wall).

A horizontal crack in a masonry wall may result from creep of the lower portion of the wall where it joins a slab or footing. In this instance, if reinforcement is inadequate or no reinforcement is used to secure the masonry wall to the concrete footing a crack may form where the two materials meet.

Another consideration is stair-step cracking in adjacent corners of a CMU wall. This condition may indicate settlement of that corner of the building. The cracking that occurs generally forms a line that will intersect the wall and the floor (see Figure 4, Convex Settlement). Also, when viewing cracking distress, it should be remembered that masonry generally shrinks with the passage of time while brick will generally grow as moisture is absorbed. Uncured masonry units will exhibit significant cracking as the CMU ages.

Other causes of settlement that can result in distress are: 1) absence of a footing, 2) decomposition of organic material below a footing or slab, 3) inadequate design of the footing or structure, 4) inadequate compaction below the slab or footing, 5) expansive soils, 6) settlement resulting from sinkhole activity, 7) erosion of supporting soil, or 8) variation in stiffness of subsurface materials.

4. Case Studies

4.1 Case Study No. 1

In any forensic investigation, the study should begin with a complete analysis of all available information as shown in Part 1, Office Study of Figure 1. In this example, two aerial photographs were available in the initial stages of the investigation one taken in 1941 before the area was developed the other taken in 1998 after completion of most area development.

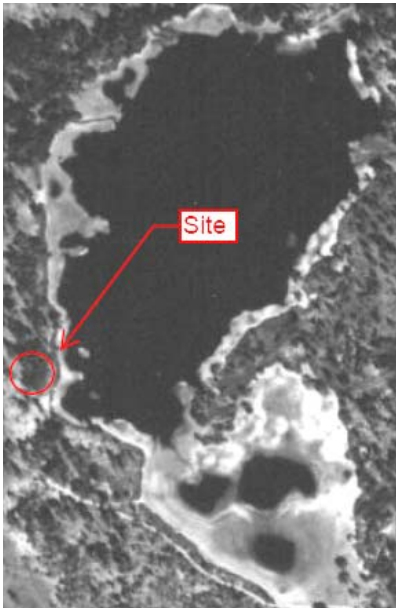

Figure 4, 1941 Aerial Photograph

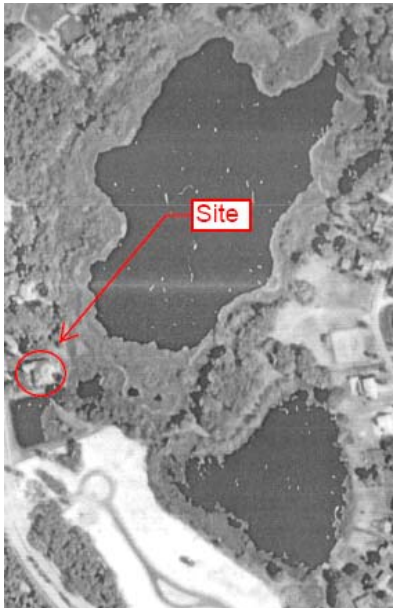

Figure 5, 1998 Aerial Photograph

Both figures show sinkhole lakes, formed by the coalescence of smaller sinkholes (for example see the lower part of Figure 4). The figures show the locations of a home built in 1997 and the position of the home, as it would have appeared in the 1941 aerial photo. Both photos are shown at the same scale.

A couple of features are apparent in the photos that will help in identification of site conditions. First it is seen that in 1941 the lake was much larger than that seen in the 1998 photo and that the home is located on the shore or possibly in the position of the 1941 lake. It is apparent that the original lake had been filled to create land for construction of the home. This conclusion is also apparent from careful observation of 1998 photo where it can be seen that a substantial zone of new vegetation (no large trees) exists around the shore of the lake shown in the 1998 photo.

The conclusion that the house was built on the shore of the sinkhole lake should result in the preliminary conclusion that karst conditions are likely to exist under this home. Subsurface conditions found in the borings are shown in Figure 6 which depicts the distribution of subsurface conditions found on all sides of the building (see boring location plan shown in Figure 7).

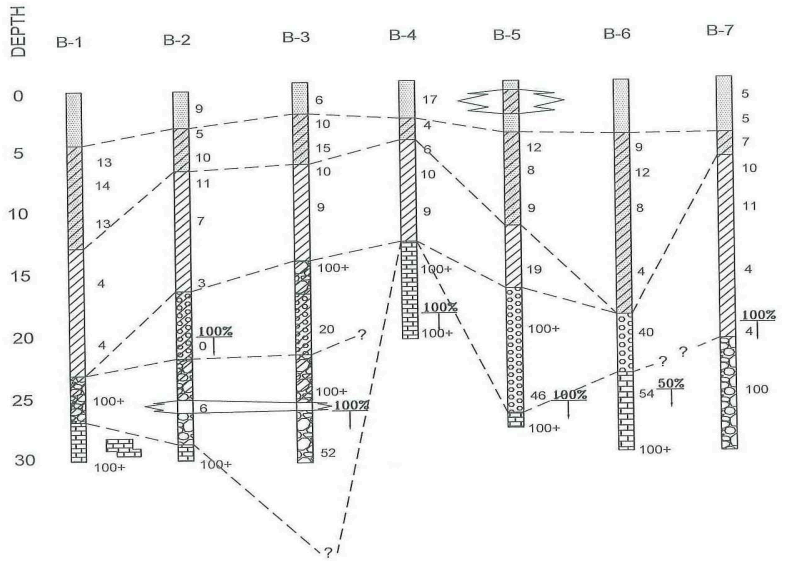

Figure 6, Boring Profile along the Outer Boundary of the Home

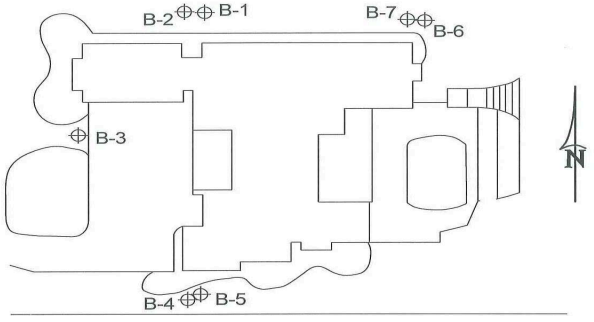

Figure 7, Boring Location Plan

In this case study, it is apparent that even before beginning geophysical or drilling programs substantial information is available in the first phase of the investigation (see Part 1, Office Study shown in Figure 1). This information together with analysis of distress in the building can be used to limit and direct the subsurface investigation to specific areas of interest for remediation of the building. One note of caution, from the subsurface conditions found in this investigation, it was apparent that the building needed to be underpinned therefore, the investigation should determine the competency of the underlying rock to support pile loads. This requires

extending the borings 10 to 20 feet into the underlying rock to assure competency of the supporting material.

4.2 Case Study No. 2

The next example shows how information obtained in Parts 1 and 2 of the investigation can be used to characterize the site and allow the investigation to focus on meaningful aspects of site conditions. In this example, it was initially required to perform a sinkhole investigation; however, study of information obtained in Parts 1 and 2 (aerial photo study and site reconnaissance) indicated that a stability problem likely existed at the site and the site may not have been impacted by active karst conditions.

Figure 8 shows the floor slab of a two-year-old commercial building that had undergone significant settlement in the order of 2 to 4 inches (5.1 to 10.2 cm) on one side of the building. The settlement was found after removing the floor covering in preparation for a new tenet. Following closer inspection of the building, it was found that settlement also occurred in the columns and roof trusses in the area of slab movement.

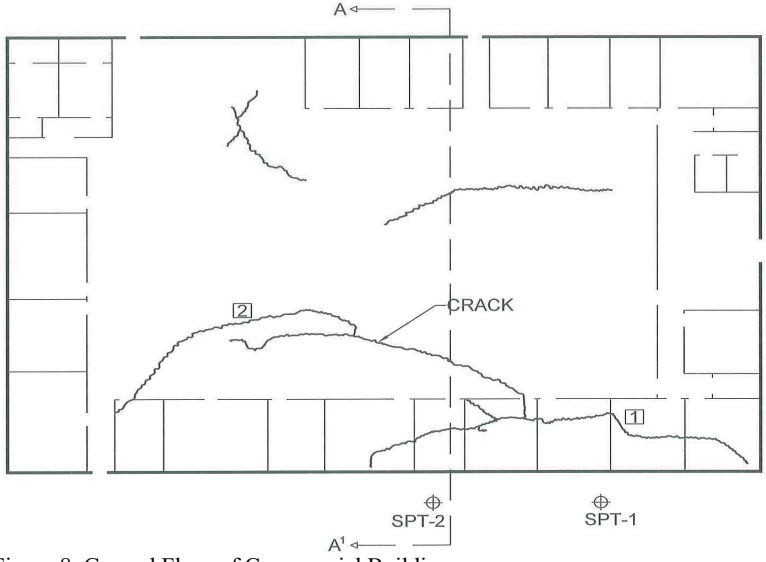

Figure 8, Ground Floor of Commercial Building

Although the owner was concerned with the possibility of a sinkhole, review of historic aerial photos disclosed no sinkhole activity in the area. However, it was observed in the aerial photos that the original flat lying landscape of the site and surrounding area was disturbed by the excavation of several borrow pits one that

extended near the boundary of the site. Subsequently, in an effort to facilitate drainage in the area and to use the nearby borrow pit as a catch basin, a drainage channel was constructed along the side the building. The ditch was later deepened, after construction of the building, creating a steep slope on one side of the building as shown in Figure 9. Subsequent analysis of the stability of this slope (see lines 1 and 2) disclosed a marginal factor of safety that confirming the circular nature of cracking in the floor slab was the result of slope movement caused by the inadvertent deepening of the drainage ditch.

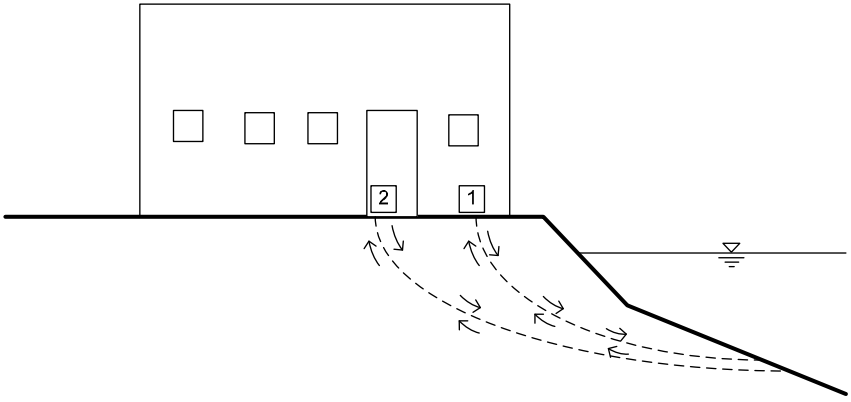

Figure 9, Generalized View of Slope Stability (see Section A-A' in Figure 8)

The subsurface conditions found in the sinkhole investigation are shown in the boring profile in Figure 10. Although a few signature features associated with sinkhole activity were found in the borings, it was concluded that sinkhole activity was not a factor in building distress. This conclusion was based on aerial photographic information, the absence of known sinkhole activity in the area, the absence of a significant number of signature sinkhole features in the borings and the fact that distress occurred in only the area of instability.

Because of space limitations, additional aspects of sinkhole investigations cannot be discussed. The reader is encouraged to review some of the other articles written by the author on this subject such as Zisman, 2001 and 2005.

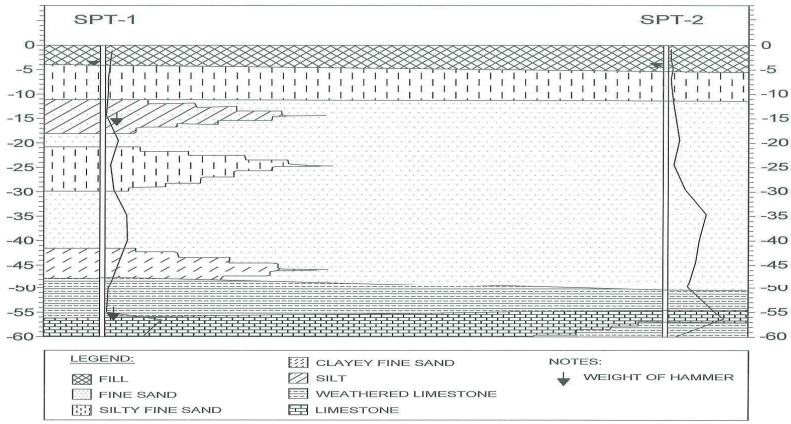

Figure 10, Boring Profile

5. Conclusions

The vast majority of sinkhole claims made to insurance companies are for damage caused by discrete zones of loose soil associated with sinkhole activity. That is, there is in most cases (in west central Florida) no large chasm in which a home has fallen into only a progressive loosening of the soil resulting in a minor depression in some discrete area under the home or progressive loosening of the soil that has resulted in a loss of bearing capacity under the building Zisman, 2005. This means that geotechnical engineers and geologists do not have a readily apparent "smoking gun" but must interpret the cryptic nature of the subsurface to determine the cause(s) responsible for building distress. In many instances, there are "clues" present in the manner in which distress has occurred in a building. It is the investigators responsibility to record and analysis all signs of distress to analysis the differing set of conditions that can cause distress. The procedure is, in many ways, similar to the methods used by a physician in eliminating potential causes of an illness.

References:

Zisman, E. D. (2001) "A Standard Method for Sinkhole Detection in the Tampa, Florida, Area", Environmental & Engineering Geoscience, Vol. VII, No. 1, February 2001, pp 31-50

Zisman, E. D. (2005) "Sinkhole Case Studies—Is it or Isn't it a Sinkhole, Geotechnical Special Technical Publication No. 144, Sinkholes and the Engineering and Environmental Impacts of Karst, Edited by Barry F. Beck

Case History: Sulfate-Induced Heave of Lime-Treated Soils Beneath a Structure in Western Colorado

Aaron D. Bagley, P.E.[1] and Joseph A. Cesare, P.E.[2]

[1]Senior Engineer, Joseph A. Cesare and Associates, Inc./Construction Technical Services, 7108 South Alton Way, Building B, Centennial, Colorado 80112; PH -(303)-220-0300; FAX (303)-220-0442; email: abagley@jacesare.com
[2]President/Senior Principal, Joseph A. Cesare and Associates, Inc./Construction Technical Services, 7108 South Alton Way, Building B, Centennial, Colorado 80112; PH -(303)-220-0300; FAX (303)-220-0442; email: joecesare@jacesare.com

ABSTRACT

A commercial structure in western Colorado constructed circa 2001/2002 began to exhibit drywall distress within a few months of completion. The foundation consisted of a monolithic, cast-in-place footing and structurally connected slab-on-grade bearing on 0.3 to 0.8 meters of lime-treated, clay soils. The clay soils were documented to have low expansion potential and high sulfate contents. A survey of the building in 2004 showed an elevation difference of 27.9 centimeters over 15.2 meters. A Scanning Electron Microscope showed the presence of ettringite beneath the foundation. Sulfate induced heave is caused by the volume change associated with the formation of ettringite. Water entered the lime-treated soils beneath the foundation and was the catalyst for soluble sulfates to react with calcium in the lime to form ettringite. This reaction resulted in the structure's distress.

INTRODUCTION

A commercial structure was constructed between 2001 and 2002 with a monolithic cast-in-place footing and structurally connected slab-on-grade foundation bearing on a lime-treated structural fill blanket. Shortly after the structure was occupied indicators of vertical foundation movement were observed. An elevation survey of the building in 2004 indicated over 27.9 centimeters of differential elevation across the structure. A second elevation survey in 2006 indicated that approximately 1.3 to 2.5 centimeters of additional movement had occurred between the two surveys.

High soluble sulfate contents within the native soils indicated a likely cause of the movement was sulfate induced heave within the lime-treated structural fill blanket. The purposes of the paper are to describe the site conditions, history, building distress evaluation of heave mechanisms, and repair options.

GENERAL SITE CONDITIONS

The site is located in western Colorado. The building is a single-story, wood-framed structure with pressboard veneer siding. The building consists of a central common area with north and south portions. Each portion consists of three wings.

The structure is founded on a monolithic concrete cast-in-place footing foundation with a slab-on-grade floor system bearing on lime-treated, on-site clay soils. The slab-on-grade floor is structurally connected to the foundation walls and footings by steel reinforcing.

The existing topography is relatively flat with areas of localized low spots where water ponding occurs. Storm water detention ponds are located to the southwest and northwest of the building. An asphalt parking lot is located along the west side of the building. A concrete sidewalk surrounds the building. Landscaping consists of rock and shrubs adjacent to the building and lawn areas. A general site plan is shown on Figure 1.

SITE SUBSURFACE CONDITIONS

Twelve test borings were performed for a pre-development geotechnical investigation. The borings encountered 2.4 to 9.1 meters of silty, sandy clay overlying Mancos Shale bedrock. The clay soils were soft and moist to wet. Five swell-consolidation tests were performed on the native clay soils. Four of the five samples consolidated less than 1/2 of a percent when wetted under a 4.78 kPa surcharge. The remaining sample swelled approximately 1/4 percent when wetted under a 4.78 kPa surcharge with a swell pressure of 16.75 kPa. Groundwater was encountered between 1.5 and 3 meters in several of the borings. Soluble sulfate contents greater than 200 parts per million (ppm) (0.02 percent) were reported.

We performed an investigation in 2005. Our investigation consisted of six exterior borings, eight interior borings, and four exterior test pits. Figure 1 shows the locations of the test holes and test pits.

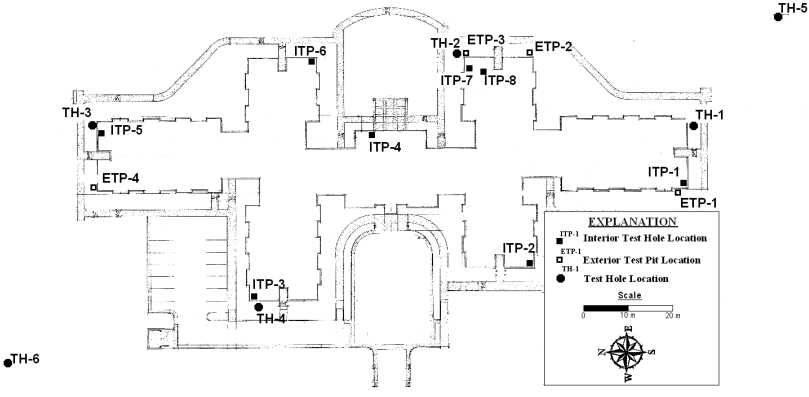

Figure 1. General Site Plan and Test Hole and Test Pit Locations

Subsurface conditions encountered in exterior test borings consisted of approximately 1.8 to 9.1 meters of sandy clay to clay overlying sandy claystone. The clay soils

encountered were very soft to medium stiff, moist, and brown to dark brown in color. The clay soils were very soft to medium stiff, very moist to wet, and light brown in color. The claystone encountered was firm to very hard, slightly moist, and light brown to gray in color.

Groundwater was encountered in the exterior borings at the time of drilling between depths of approximately 2.4 to 3.3 meters in all of the test holes with the exception of TH-6, where water was not encountered. The subsurface conditions encountered in our 2005 investigation are generally consistent with those encountered in the pre-development investigation.

BACKGROUND

Foundation Recommendations

Initially the project geotechnical engineer provided foundation options and criteria for driven piles, drilled piers, and footings. Floor system options were a slab-on-grade floor on structural fill or a structural floor above a crawlspace. A subsequent option for founding the structure on a 0.6-meter thick blanket of structural fill was also provided at the request of the project architect. The structural fill blanket could consist of either imported non-expansive granular fill or on-site, lime-treated soils. Lime-treatment of the on-site soils was selected for construction of the structural fill blanket.

Lime-Treated Fill Construction

The lime-treatment was applied to the building area as follows:

- Approximately 38.1 to 45.7 centimeters of native soil was removed from the building pad area and stockpiled on-site.
- The first lift or bottom 38.1 to 50.8 centimeters of the building pad subgrade was scarified and lime-treated. The lime was applied as dry quicklime on the subgrade surface and then rototilled into the soil. The amount of lime used was between 5 and 10 percent by dry weight of the combined lime/soil mixture.
- Water was added to the subgrade at the same time the lime was blended into the soils. The lime-treated soil was allowed to cure for one to two days and then was remixed prior to being compacted. No data existed on the moisture contents the lime-treated soil was kept at during the curing period.
- The first lift was compacted and tested for compaction.
- The second lift of 38.1 to 50.8 centimeters in thickness was placed with lime-treated soil. This soil was lime-treated and mixed near its stockpile location, allowed to cure for one to two days, then imported to the building pad site.
- The second lift of lime-treated soil was remixed after being placed on the building pad. The second lift was compacted and tested for compaction.

Foundation Construction

Our investigation indicated that the foundation walls and footings were constructed by excavating trenches through or into the lime-treated soil. A foam insulation board was placed adjacent to the exterior trench wall prior to concrete placement for

insulation and to act as a form for the concrete. The concrete slab-on-grade floor was connected to the foundation wall and footings with reinforcing bars. The concrete floor and footing were poured monolithically.

The as-constructed conditions beneath the slab-on-grade floor generally consisted of approximately 2.5 to 5.1 centimeters of sand on top of 7.6 to 22.9 centimeters of 1.9 centimeter angular gravel overlying 0.3 to 0.82 meters of lime-treated fill soils. Native clay soils were encountered beneath the lime-treated layer in all of the interior test holes with the exception of ITP-7 and ITP-8 where a light brown clay fill was encountered. A detail of the as-constructed foundation conditions is shown on Figure 2.

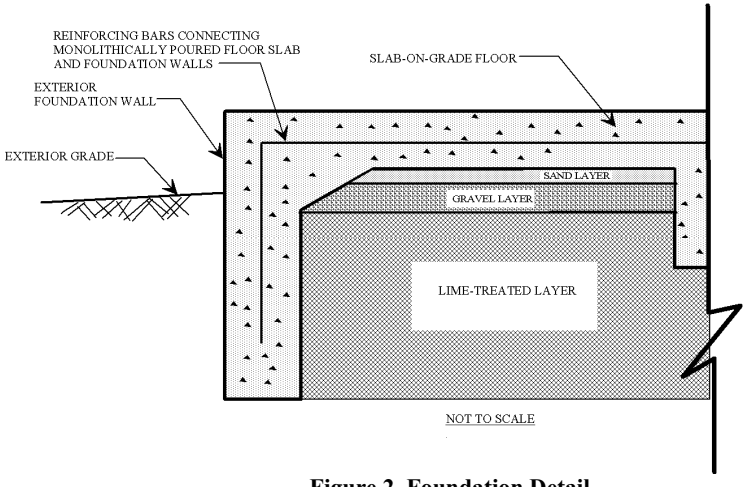

Figure 2. Foundation Detail

The bottoms of the exterior footings were encountered at depths of 0.76, 0.64, 0.64, and 0.61 meters below the ground surface in ETP-1 through ETP-4, respectively. Soft and very moist soils were encountered below the footing in ETP-1 and ETP-2. These soils did not appear to be lime-treated. Lime-treated soils were encountered beneath the footing in ETP-4. A 5.1 to 7.6 centimeter void was observed beneath the footing in ETP-1.

BUILDING DISTRESS

Within a few months of occupying the building, occupants observed drywall cracks in the south wing of the building. The drywall distress increased with time and migrated towards the north. By 2004, a unit located at the northeast corner of the southeast wing was vacated due to the severity of the distress. Drywall cracking was also reported in the southern end of the north wing. The following conditions were observed during our December 2004 site visit:

- Distress consisted of drywall cracks, racked doors and windows, cracks in the slab-on-grade floor, separation of molding of countertops and cabinets, and gaps between the floor and the base of partition walls.
- The areas with the most severe distress were located in the eastern end of the southeast wing and the south end of the south wing.
- Monitoring indicated that the cracks were increasing in length at some but not all of the locations.
- A white mineral precipitate was observed on the soil surface at locations along the southern and the southeastern portions of the structure where occupants indicated standing water occurs after storm events.

BUILDING MOVEMENT

An initial relative elevation survey of the structure was performed in December of 2004. This survey indicated 30 centimeters of floor slab elevation differential across the entire building. Approximately 27.9 centimeters of relative elevation difference over a distance of 15.2 meters along the east wall of the southeast wing. A second relative elevation survey was performed in April of 2006. The April 2006 survey indicated 32.2 centimeters of floor slab elevation differential. The high point in both surveys was located in the northeast corner of the southeast wing. The survey data indicated 3.3 centimeters of additional movement to portions of the southeast wing, approximately 2.5 centimeters of additional movement to portions of the south wing, and approximately 1.3 centimeters of additional movement to the southern portion of the north wing. Contour maps of the relative elevation survey data were prepared using the computer program SURFER (Golden Software 2007). A contour map of the 2006 floor slab survey data is shown in Figures 3.

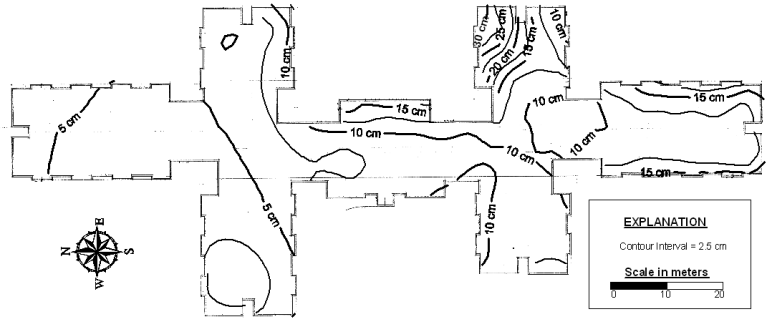

Figure 3. Contour Map of 2006 Floor Slab Relative Elevation Survey Data

EVALUATION OF HEAVE

The survey data, observed building distress, and test pit observations indicate upward movement (heave) of the outside edge of the floor slab and exterior footings. The addition of water to the on-site expansive clay soils and sulfate-induced heave within the lime-treated fill blanket were identified as potential mechanisms for the

foundation movement. Laboratory tests were performed on various samples collected during our field investigation in order to evaluate these two mechanisms. The tests performed were swell-consolidation, gradation, Atterberg limits, natural moisture content, in-situ dry density, pH, and soluble sulfate tests. A summary of our laboratory test results is shown on Table 1. Ten samples collected from the interior test holes and exterior test pits were sent to the Colorado School of Mines (CSM) Mineralogy Laboratory for a Scanning Electron Microscope (SEM) and X-ray diffraction analysis to determine the minerals present within the soil samples.

Evaluation of On-Site Expansive Clays

For expansive clay soils to be a viable heaving mechanism at this site, the percent swell and swell pressures of the soils beneath the footings and above the historic groundwater table need to be high enough to account for approximately 27.9 centimeters of differential movement experienced at the southeast wing. The groundwater table represents the maximum depth of potential heave of the clay soils. The depth of the groundwater beneath the southeast wing is approximately 2.7 meters. The base of the lime-treated blanket is at an average depth of 0.91 meters. The soil heave would have to be realized within a soil column of 1.8 meters. In order to experience 27.9 centimeters of heave over a depth of 1.8 meters, the percent swell of the clay soils would have to average approximately 15 percent. Data from the pre-development and post-development investigations indicated either consolidation or less than 1 percent swell within the native clay soils.

The low swell potential, high moisture contents, and soft to very soft consistency of the native soils indicate that addition of water to the on-site clay soils was not a probable source of the movement.

Evaluation of Sulfate-Induced Heave

Sulfate induced heave problems occur when sulfate rich soils are stabilized with calcium based chemicals such as lime and ordinary Portland cement. The sulfate induced heave occurs when the calcium stabilizers in the lime-treated soil react with free alumina and soluble sulfates in the soils in the presence of water to form calcium-aluminate-sulfate-hydrate minerals (Mitchell 1986; Hunter 1988; Petry et al. 1991; Little 2000).

Sulfate induced problems in soils stabilized with calcium-based chemicals have been documented since the late 1950's (Little, 2000). Sulfate induced heave, as a geotechnical concern, became known through papers authored by Mitchell (1986) and Hunter (1988) describing pavement distress in Las Vegas, Nevada.

The most discussed mineral in the literature that causes distress is ettringite-thaumasite solid solution series (Hunter 1988; Mitchell and Dermatas 1990, Petry et al. 1991, Little 2000). Ettringite-thaumasite holds large quantities of water within its structure and during its formation can develop large volume increases and high swell pressures. Volume increases for extreme cases can be as much as 250 percent of the initial volume (Little 2000).

Table 1. Summary of JAC/CTS Laboratory Test Results

Sample Location		Natural	Natural	Gradation			Atterberg Limits		Water	Swell Potential When Wetted	
Test Hole	Depth (m)	Moisture Content (%)	Dry Density (kg/m^3)	Gravel (%)	Sand (%)	Silt/Clay (%)	Liquid Limit (%)	Plasticity Index (%)	Soluble Sulfates (%)	Under 1000 psf Load (%)	PH
ITP-1	0.52	32.2	1287.8	-	-	-	-	-	0.02	-0.1	-
ITP-1	0.61-0.91	27.9	1375.9	-	-	-	-	-	0.11	-	9.9
ITP-2	0.52	25.3	1283.0	-	-	-	-	-	-	-2.3	8.9
ITP-3	0.49	50.5	1278.2	-	-	-	-	-	-	0	-
ITP-3	0.61-0.91	-	-	-	-	-	-	-	0.04	-	-
ITP-4	1.14	23	1584.2	-	1.3	98.7	38	15	0.01	-0.9	9.3
ITP-4	0.61-0.91	-	-	-	-	-	-	-	negligible	-	-
ITP-5	0.43	26.3	1451.2	-	-	-	-	-	-	-0.4	-
ITP-5	0.88	32.7	1540.9	-	23.1	76.9	39	13	0.08	-0.4	10.3
ITP-5	0.61-0.91	-	-	-	-	-	-	-	0.01	-	11.7
ITP-6	0.37	59.1	1204.6	-	-	-	-	-	-	-0.2	-
ITP-6	0.61-0.91	-	-	-	-	-	-	-	negligible	-	-
ITP-7	0.37	26.7	1500.9	-	-	-	-	-	-	-0.7	-
ITP-7	0.61-0.91	-	-	-	-	-	-	-	0.03	-	-
ITP-7	1.01	57.2	-	-	14.1	85.9	56	19	negligible	-	9.3
ITP-8	0.37	-	-	-	-	-	-	-	0.01	-	10.4
ITP-8	0.61-0.91	-	-	-	-	-	-	-	-	-	9.6
ETP-1	0.61-0.91	34	-	5.2	12.2	82.6	41	13	-	-	-
ETP-1	0.91	37.3	-	0.6	24.7	74.7	40	19	negligible	-	9.1
ETP-2	0.61	35.6	-	2.5	8.4	89.1	44	16	-	-	8.9
ETP-3	0.61	-	-	-	-	-	-	-	-	-	10.5
ETP-4	0.61	-	-	-	-	-	-	-	0.01	-	10.5
TH-1	0.00	28.8	1467.2	-	-	-	-	-	-	-	-
TH-1	0.76	22.8	1633.8	-	-	-	-	-	-	-	-
TH-1	1.52	22	1483.3	-	-	-	-	-	0.09	-	-
TH-1	3.05	16.3	1882.1	-	-	-	-	-	-	-	-
TH-2	0.00	38.8	1307.1	-	-	-	-	-	-	-	-
TH-2	0.76	33.4	1454.4	-	-	-	-	-	-	-	-
TH-2	1.52	27.1	1542.5	-	-	-	-	-	0.11	-	-
TH-2	3.05	10.6	1997.4	-	-	-	-	-	-	-	-
TH-2	4.57	11.2	2013.5	-	-	-	-	-	-	0.3	-
TH-3	0.00	47.3	1191.7	-	-	-	-	-	-	-	-
TH-3	0.76	21.3	1638.6	-	-	-	-	-	-	-	-
TH-3	1.52	24.1	1629.0	-	-	-	-	-	0.17	-	-
TH-3	3.05	16.7	1859.7	-	-	-	-	-	-	-	-
TH-4	9.14	14.3	1867.7	-	-	-	-	-	-	0.8	-
TH-5	1.52	-	-	-	-	-	-	-	0.08	-	-
TH-6	0.30	-	-	-	-	-	-	-	0.14	-	-

Little (2000) presents guidelines for stabilization of soils containing sulfates. Little (2000) indicates that soluble sulfate contents in the soil below 0.3 percent should not be of significant concern. Soluble sulfate contents between 0.3 percent and 0.5 percent represent a moderate risk of a harmful reaction. Soluble sulfate contents between 0.5 percent and 0.8 percent represent a moderate to high risk and contents above 0.8 percent represent a high and unacceptable risk for routine work. Little indicates that if lime-treatment is used for soils above 0.8 percent special application techniques should be considered such as applying the lime as a slurry mixture, extending the mellowing period to at least three days and possibly as long as seven days, and providing a double application technique. Petry et al. (1991) indicated that sulfate-induced heave may occur at sulfate contents on the order of 0.3 percent. A post-construction investigation by the original geotechnical engineers indicated soluble sulfate contents of 0.37, 0.48, 1.18, 1.20, 1.30, 1.54, and 1.65 percent.

The SEM and X-ray diffraction analysis performed by CSM for our study confirmed the presence of the ettringite-thaumasite solid solution series in the samples collected from beneath the exterior footings and the floor slab. A representative SEM photo of ettringite-thaumasite found in the field samples is shown in Figure 4.

Water has to be available for the reaction that causes sulfate heave to occur. Our study indicated that surface water infiltration from poor surface drainage adjacent to the structure, lack of roof downspouts, and irrigation were the probable sources of water.

We performed calculations to determine the amount of ettringite that can form from the reaction of sulfate ions with the calcium in the lime. We assumed that the poor drainage condition and relatively shallow groundwater conditions provide a constant source of sulfate-ion rich water. Our calculations indicate that enough ettringite could form to result in a volume increase of approximately 40 percent. The lime-treated fill layer ranged between 0.3 and 0.82 meters. Forty percent of this layer corresponds to 12.2 to 33 centimeters of potential heave and correlates with the measured heave.

The lime application technique used at this site did not account for the high sulfate soils. The application of the lime should have, as a minimum, been applied as a slurry mixture, cured a minimum of three days prior to compaction, and utilized a double application technique. Even with these precautions, however, intolerable amounts of sulfate-induced heave may have occurred due to the very high sulfate contents of the soil.

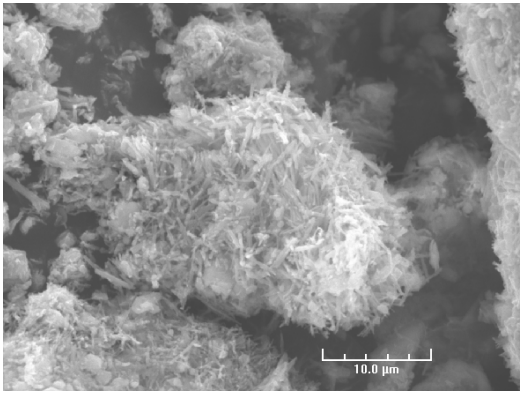

Figure 4. SEM Photo of Cluster of Ettringite-Thaumasite Crystals at 2000X Magnification

REPAIR OPTIONS

The results of our investigation did not show a significant difference in subsurface conditions beneath the portions of the structure that have experienced distress versus the portion that to date has not experienced distress. We did not see evidence that indicated the observed movement in the southern and southeastern portions of the structure could not occur at other locations throughout the building.

If the lime-treated soil remains beneath any portion of the structure, repairs should include precautions to limit migration of surface and subsurface water to the lime-treated soils. A groundwater cutoff trench around the perimeter of the building in combination with re-grading and placement of an impervious membrane adjacent to the structure is a reasonable means to reduce the amount of water migrating to the lime-treated soils but cannot eliminate all possibility. Sumps located within the interior of the cutoff trench can be spaced around the building in order to remove water that may become trapped inside the cutoff trench from utility leaks and rising groundwater. The amount of observed distress to the south and southeast wings of the structure warrant re-construction of the foundations at these locations.

CONCLUSIONS

1. Distress to the structure was the result of sulfate induced soil heave, which can occur when high sulfate content soils are lime-treated and have access to water.
2. The poor site drainage, lack of roof downspouts, and landscape irrigation adjacent to the structure provided the water necessary for the chemical reaction to occur.
3. The application of the lime should have, as a minimum, been applied as a slurry mixture, cured a minimum of three days prior to compaction, and utilized a double application technique. Even with these precautions, intolerable amounts of sulfate-induced heave may have occurred due to the very high sulfate contents.
4. The south and southeast portions of the foundation required replacement.
5. Repairs to the remaining areas included precautions to limit migration of surface water and subsurface water to the lime-treated soils.

REFERENCES

Golden Software, Inc. (2007). SURFER Mapping Software Program, Version 8.08. Golden, Colorado

Hunter, D. (1988). "Lime-induced heave in sulfate-bearing clay soils." Journal of Geotechnical Engineering, ASCE 114(2), 150-167.

Little, D.N. (2000). "Technical Memorandum, Guidelines for Stabilization of Soils Containing Sulfates Austin White Lime, Chemical Lime, Texas Lime" Soil Stabilization Seminar, Sulfate Soils, Dallas Texas. Sponsored by Lime Association of Texas.

Mitchell J.K. (1986). "Practical problems from surprising soil behavior." Journal of Geotechnical Engineering. Div., ASCE, 112 (3), 259-289.

Mitchell, J.K. and Dermatas, D. (1990). "Clay soil heave caused by lime-sulfate reactions." ASTM Special Technical Publication 1135, 41-64.

Petry, M.T. and Little, D.N. (1991). "Update on Sulfate Induced Heave in Lime and Portland Cement Treated Clays; Determination of Potentially Problematic Sulfate Levels", 1992 Annual Meeting of the Transportation Research Board.

Puppala, A.J., Griffin J., Hoyos, L.R., and Chomtid, S. (2004). "Studies on Sulfate-Resistant Cement Stabilization Methods to Address Sulfate-Induced Soil Heave." Journal of Geotechnical and Geoenvironmental Engineering, ASCE, 130 (4), 391-402.

Puppala, A.J., Intharasombat, N., and Vempati, R.K., (2005). "Experimental Studies on Ettringite-Induced Heaving Soils." Journal of Geotechnical and Geoenvironmental Engineering, ASCE, 131 (3), 325-337.

Forensic Engineering in the Assessment of Contaminated Land

L. A. Shah,[1] C. L. James[2] and B. R. Thomas[3]

[1]L. A. Shah BEng MSc CEng MICE; e-mail: la.shah@grontmij.co.uk
[2]C. L. James BSc CEnv MCIWEM; e-mail: christopher.james@grontmij.co.uk
[3]B. R. Thomas MSc PhD CEng EurGeol; e-mail: bryn.thomas@grontmij.co.uk
[1, 2, 3]Grontmij Limited, 41 Corn Street, Bristol BS1 1HS UK;
PH +44(0)1179 278850; FAX +44(0)1179 278888

Abstract

Land affected by a legacy of industrial and commercial activities including domestic and accidental contaminative spillages is termed contaminated land. Recent research estimates there are approximately 325,000 contaminated sites in the UK (1) with an annual spend of approximately £1.2 billion on regeneration and remediation. (4)

Following the 'polluter pays' principle, those involved in pollution are liable to take appropriate action and return the land to its original form. Where the polluter cannot be identified, remedial and regeneration costs are borne by the public exchequer. Alternatively, forensic engineering can be applied to identify persons liable of polluting air, land, groundwater and surface waters and also to assist in recovering remedial costs through litigation.

This paper describes effective and practical methodologies for the forensic assessment of contaminated sites with regard to determination of polluter responsibility and allocation of associated liabilities under UK and European legislation.

Introduction

Contaminated land is defined as "any land which appears to the local authority in whose area it is situated to be in such condition by reason of substances in, on or under the land, that; significant harm is being caused or there is a significant possibility of significant harm being caused; or, significant pollution of controlled waters is being caused or there is a significant possibility of such pollution being caused" in the context of the Environmental Protection Act 1990, the Water Act 2003 and associated guidance.

Land and groundwater contamination can be identified years after contaminative activity ceases on site with ownership passing onto several entities. Local Councils are often burdened with remediation costs when their options are either to spend developmental funds on remediation or ignore potential health hazards to the local population and environment, until funds are available.

Environmental forensics has been defined as *'the study, analysis and evaluation of environmental issues in a legal dispute.*' (2) Forensic engineering is defined as *'the investigation of materials, products, structures or components that fail or do not operate as intended, causing personal injury or damage to property.'* (3) Forensic

geology is concerned with the applications of geology to solving crimes whilst forensic geophysics has been defined by researchers as '*the application of geophysical methods related to legal investigations*.' [5]

Forensic investigation in the assessment and remediation of contaminated land involves horizontally expanding the engineering and earth science inputs and determining who pays and how much. In the legal context the forensic engineer/scientist seeks to establish the 'truth' (actual state of matter or reality) for every technical issue in contaminated land litigation.

UK and European Legislation

UK and European Environmental law comprises a combination of statutes and common laws. Litigation processes involving current or historical incidents of environmental pollution in the UK encompass the prevalent legal framework illustrated in figure 1.

On completion of forensic analysis and liability allocation process, enough tangible evidence can be gathered to initiate a litigation process. This may involve past and present site occupiers and owners, the state, members of the public, solicitors, expert witnesses (e.g. engineers and scientists), arbitrators and mediators.

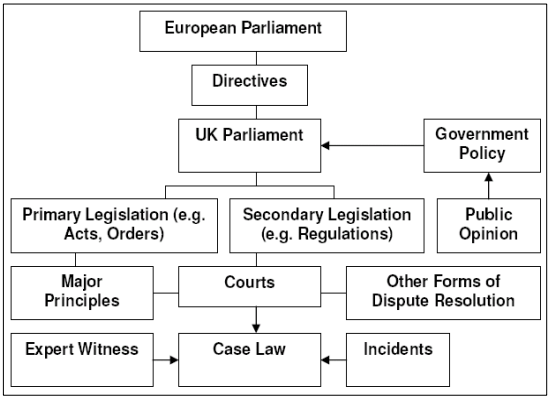

Figure 1 The UK legal framework in environmental prosecution

Key environmental legislation governing contaminated sites in the UK includes:

1. Water Resources Act (1991)
2. Environmental Protection Act (EPA-1990) as amended by the Environment Act (1995)
3. Pollution, Prevention and Control (England and Wales) Regulations 2000
4. The Environmental Liability Directive (EU – 2004)
5. The Environmental Damage (Prevention and Remediation) Regulations 2009

Environmental Liability and the 'Polluter Pays' Principle

Most of the UK's industrial pollution occurred historically with little or no public accountability, with costs being borne not by the polluter but by society as a whole. The 'polluter pays' principle was first introduced in the European Economic

Community (EEC) by the Treaty of Rome (1957) that was further modified in the Single European Act (1986) and the Maastricht Treaty (1991). Article 130R of the treaty states that '*where pollution is caused the polluter should pay for the clean up of the environment; where pollution is allowed the polluter should pay for the privile*ge'. [15] This includes environmental costs, plus costs to people or property and costs to avoiding pollution.

The European Union (EU) Environmental Liability Directive was introduced in 2004 and was intended to give effect to the "polluter pays" principle by imposing liability for prevention and remediation of environmental damage. The EU member states are under a duty to ensure that necessary preventive or restorative measures are taken in prevention, mitigation and remediation of polluting events, by the relevant operator, the competent authorities or a third party. [17]

There are four possible options under the 'polluter pays principle':

- Polluter could be made liable
- Current owner/occupier could be made liable
- The state could pay (via some form of public clean-up mechanism)
- Loss could lie where it falls (environment and local community 'pay')

Two forms of liability are considered in the environmental prosecution scenario:

a) Civil Liability

The legal principles in the UK underlying civil liability for environmental damage have developed through application and refinement of common law. Common law actions for environmental damage particularly involve allegations of nuisance and/or negligence. Such actions give rise to the possibility of a civil remedy (damages or an injunction) rather than a criminal sanction (imprisonment or a fine payable to the state).

b) Strict Liability

Applies when a liability can be established irrespective of fault. It is then only necessary to prove that a particular event caused damage. This means the claimants need to establish a substantial link between the activities of the alleged polluter and the damage caused without having to demonstrate actual fault.

Duty of Care

A concept that occurs frequently in environmental cases, especially those including the tort of Negligence. Duty of care aims to prohibit injuries to others by acts or omissions. EPA – 1990 specifically defines the duty of care in general environment and waste management scenarios.

Torts and Toxic Torts

A tort is a wrong against an individual. The primary function of the law of torts is to provide a method of redress for individuals who have suffered loss. The object of the law of torts is to compensate rather than to punish. The most commonly applied torts in environmental litigation are Nuisance (Public and Private), Negligence and Trespass.

A toxic tort relates to a special type of personal injury lawsuit in which the plaintiff claims that exposure to a chemical caused the plaintiff's toxic injury or disease. Environmental forensics is applied to assess and quantify the exposure and dose of historical chemical concentrations in air, water, soil or edibles.

Environmental Protection Act (EPA-1990) Part IIA

The law is becoming more concentrated in a smaller number of Acts. The main controls over historically contaminated land are via the statutory framework in Part IIA, which sets out the structure of systems to deal with contaminated land. Supplementary secondary legislation in the Contaminated Land (England) regulations 2000 (SI 2000/227) defines 'special sites' and provides detailed arrangements for remediation notices. Most important are tertiary rules in the statutory guidance documents and in Circular 2/2000, *Contaminated Land: Implementation of Part IIA of the Environmental Protection Act 1990*.

The Environment Act 1995 combines various tools to protect public interest by a combination of mechanisms that borrow from public, private and criminal law to provide a set of different tools to achieve protection of the environment. For contaminated land someone has to 'pay' for the contamination, either by cleaning it up or living with the consequences. Legal tools are accepted as legitimate devices for helping to solve environmental problems alongside science, technology, engineering, social and economic factors.

Environmental Damage Regulations (2009)

The Environmental Liability Directive (2004) has been adopted in the UK legislation as the Environmental Damage (Prevention and Remediation) Regulations in 2009. The Regulations require action in response to the most significant cases, covering specific types of damage from contamination to:

- species and habitats
- water, or
- human health

It also imposes a 'strict liability' for the operators when there is an imminent threat or actual environmental damage has occurred.

The onus remains on the responsible party to take preventive action and report to the relevant enforcing authority which is responsible for overseeing the effective operation of the Regulations. [27]

Process and Methodology

A three tiered approach in the form of interconnected preceding levels is followed as part of the liability analysis ahead of any litigation process. This enables comprehensive collection and collation of relevant data and avoids the possible collapse of the lawsuit in the absence of tangible evidence. The main steps in forensic analysis is illustrated in Figure 2 and detailed below.

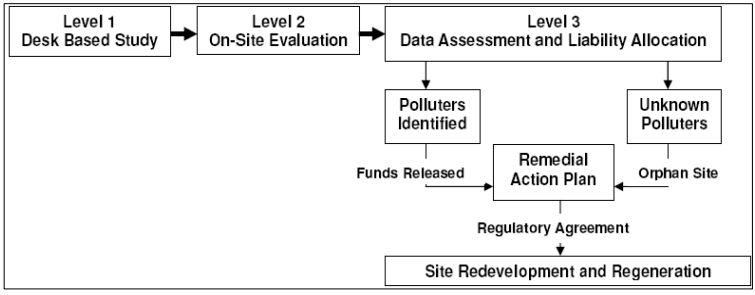

Figure 2 Process Flow Diagram – Forensic Analysis of Contaminated Land

Level 1: Desk-Based Study

A Phase 1 geo-environmental desk study comprises the collation and assessment of available information sources such as geological and hydrogeological mapping, historical land uses from Ordnance Survey maps, aerial photographs and site walkover surveys. Approximately 40% of the relevant environmental forensic data can be collated during Level 1. This level 1 process enables creation of an initial Conceptual Site Model (CSM – see figure 3) of the site's geo-environmental setting and is mainly a qualitative approach (i.e. no site specific data may exist at this stage).

Level 2: On-site Evaluation

The second and most useful level of environmental forensic analysis is on-site geo-environmental appraisal and evaluation via a targeted intrusive site investigation. A site investigation typically comprises the advancement of trial pits and boreholes/probe-holes to obtain detailed site-specific information on the ground and/or groundwater conditions with geo-environmental logging and sampling undertaken to recognised standards (e.g. BS5930 [18], Eurocode 7 [19]).

Substantial quantitative information is obtained and re-evaluation of the initial CSM. The assessment of risks with respect to potentially contaminated land follows the source-pathway-receptor methodology. For instance, if a potential contamination source is confirmed and able to reach a receptor (such as humans or controlled waters) via a relevant pathway, then a pollutant linkage may be said to be present. A targeted site investigation approach ensures that identified potential sources of contamination and likely pathways by which the contamination is able to reach receptors are appropriately quantified. For example an electricity substation site with a history of oil spillages may have solid, liquid and vapour form contamination in

different strata beneath the site. Forensic analysis also requires the time-lag factor to be considered if a significant gap exists between the conclusion of the polluting activity and timing of any site investigation.

Sampling Plans

The main contaminated land sampling approaches include representative, probabilistic, random, systematic and targeted sampling. The retrieved samples are examined for evidence of visual and olfactory contamination prior to off-site chemical analysis. Selected soil samples are scheduled for a range of chemical determinants relevant to the contaminative activity e.g. at a former oil refinery site, hydrocarbons will be the major chemicals of concern.

Chemical Fingerprinting

In a forensic engineering perspective, site environmental analytical data needs to be evaluated in greater detail to determine its value as substantial evidence. Chemical fingerprinting can be employed to identify the 'who', 'what', 'when' and 'why' questions that may exist with respect to chemical pollution. [(2)] The presence or absence of specific chemical compounds can also be used for chemical finger printing purposes. One of the common chemical finger printing analysis techniques is chromatography which includes techniques such as high-pressure liquid chromatography, thin-layer chromatography, mass and visible spectroscopy.

Level 3: Data Analysis and Liability Allocation

Using laboratory data obtained from levels 1 and 2, correlations can be established between the time and contaminative activity on site.

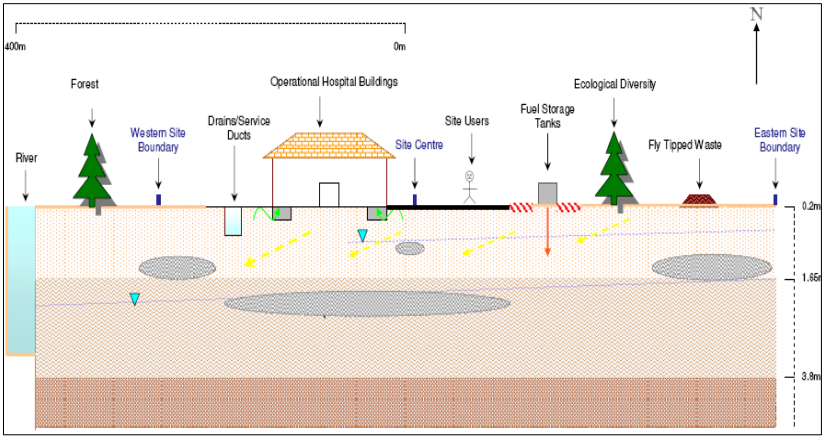

Figure 3 A typical conceptual site model (CSM)

A key element during Level 3 is re-examination of the initial CSM. A clearly illustrated site specific conceptual model can portray linkages between contamination

sources, pathways and receptors (Figure 3). This approach allows clear understanding of the pollutant source and contaminative activity on the site. The nature and extent of liability is then determined using a quantified risk matrix.

Remedial Action Plan

Environmental liabilities (either statutory or development based) identified at a site will require some form of active remediation to mitigate these liabilities. Remediation techniques can be generally split into *in-situ* (where contamination is treated in-ground) and *ex-situ* (where contamination is excavated before treatment is applied). [8] The key parameters which determine which method is employed are the nature and extent of the identified contamination, agreed clean-up targets (linked to the proposed end-use) and remediation timescales. A number of different techniques can be utilised at different stages of the remediation process e.g. the remediation strategy at a former fuel filling station with sub-surface contamination may comprise primary treatment methods (such as physical removal of grossly contaminated material and associated structures) followed by secondary treatment techniques such as soil sparging/vacuum extraction (to treat residual contamination in deeper soils) and/or groundwater treatment.

Case Study – Brofiscin Quarry, South Wales

Background

Brofiscin Quarry is a former limestone quarry in the village of Groesfaen, near Llantrisant in Rhondda Cynon Taff County Borough Council (RCTCBC), South Wales which was used as a disposal site for industrial and chemical waste between 1965 and 1970. The issues identified at Brofiscin provide a very good example of a Part IIA site which has attracted significant local and media interest, and where a number of site investigations have been undertaken since 1978 to determine the 'appropriate person' liable for the pollution. [20], [22]

Photo 1 Aerial view of the Brofiscin Quarry Site

The site occupies approximately 1.5 hectares with deposited waste confined to the western end of the quarry. The deposited waste is understood to include particularly hazardous compounds such as chlorinated hydrocarbons (including trichloroethylene and dichloromethane) phenols, PCBs, organo-phosphorous compounds and various heavy metals.

It is understood that the major producer of the waste chemicals deposited within Brofiscin Quarry was The Monsanto Group (currently operates as Solutia UK) which in 1971 shifted the majority of its PCB production from Anniston, Alabama (USA) to its Newport (UK) site. According to government statistics the company made

61,500 tonnes of PCBs at Newport. However the site was not used exclusively by the Monsanto Group and accepted wastes from other businesses in the area.

Investigations

Initial studies in the 1970s and 80s and further investigations since 2001 have been undertaken to identify potential pollution at the site. The main focus has been to identify if waste deposited at the quarry poses significant risks to surface water, groundwater, air or human health. Although initial studies concluded that there is no identifiable harm or immediate danger to human health, some unquantifiable pollution of deep groundwater and surface water exists at the site. In March 2005 the site was determined by RCTCBC as contaminated land, under Part IIA of the EPA 1990, by way of pollution of controlled waters and subsequently designated a Special Site. The site was designated specifically because of the nature of the geology and contamination present and was based on sixty-seven significant pollutant linkages for controlled waters. This meant that the Environment Agency Wales (EAW) became the lead regulator for the site, responsible for securing remediation.

Following this determination, an investigation was undertaken in 2006 which included the installation of multi-level groundwater sampling wells in six deep boreholes advanced through the Limestone bedrock that surrounds the quarry. One of the objectives of this investigation was to understand the interaction between the waste mass and the surrounding geology, and it concluded that Brofiscin Quarry is causing ongoing contamination of controlled waters within the Limestone Major Aquifer (via leaching of the waste mass). This contamination was identified at depths greater than 50m below ground level. The investigation also concluded that waste contained in the quarry does impact the surface water ditch within the adjoining fields, but only when there is sufficient rainfall or a high water table at the site (rainwater effectively 'flushes' through the waste mass causing polluted surface waters to discharge the site). However no impact has been identified to the water quality of the nearest rivers and tributaries to the site, as a direct result of the deposited waste.

Remedial Options Appraisal

Following issue of the 2006 investigative report, EAW commissioned an environmental consultant to update the Remedial Options Appraisal (ROA) to identify the Best Practical Technique (BPT) to remediate the site, to meet Part IIA standards of remediation, taking into account reasonableness, practicability, durability and effectiveness. The ROA identified three possible remedial packages:

1. Excavation, pre-treatment of contaminated material and either disposal to landfill or incineration
2. Treatment of surface water that currently discharges from the site with Monitored Natural Attenuation of both groundwater and surface water
3. Monitored Natural Attenuation of groundwater and surface water

It is understood that the preferred remedial package is surface water treatment and Monitored Natural Attenuation (MNA), possibly utilizing reed beds as a natural

solution to capture other contaminants. It is estimated that it will take three years to implement with the cost of the work in the region of £2 million.

Liability Allocation

Since 2005/06 the Welsh Assembly Government has provided £383,000 to the EAW to undertake investigations (£274,000 in 2005/06 and £109,000 in 2006/07) at the site. [21] In line with the 'Polluter Pays' principle, EAW has sought to identify the "appropriate persons" for remedial work (i.e. who is responsible for remedial costs) and it is understood that EAW have agreed with Solutia Inc and Monsanto Company that Brofiscin Quarry will be added to a list of sites that Monsanto will assume environmental liability for. On 29th November 2007 the U.S Bankruptcy Courts confirmed Solutia's reorganization plan and a related global settlement between Solutia and Monsanto, although details of this settlement have not been disclosed.

The Welsh Assembly Government has made a potential contingency liability of £20 million for remediation works at the site. Specific requirements will be dependant on the outcome of the investigative studies. [21], [22]

Current Position

It is understood that EAW have commenced work relating to the preferred remedial option by gauging flow measurements of surface water discharges from the site and measuring water quality on site. EAW are also due very shortly to review an outline report which contains qualitative and quantitative information on surface water discharges to both determine the appropriate remedial technology for treatment of these waters, and review the effectiveness of MNA in reducing groundwater contaminant concentrations at the site. It is also understood that RCTCBC secured Welsh Assembly Government funding to investigate the presence or absence of vapours from the quarry site to evaluate any potential risk to human health. The latest monitoring include continuous monitoring of sub-surface and ambient gases from newly installed boreholes within and around the quarry perimeter (including within gardens of residential properties). It is understood that sampling commenced end of 2008, with monitoring to be undertaken over a 12 month period.

Photo 2 Westerly view of the Brofiscin Quarry Site

In terms of apportioning the remediation costs for the site, it is understood that EAW are currently in consultation with the 'appropriate persons' (including Monsanto) and are pursuing voluntary agreement between all parties (as opposed to litigation), although the timescale for reaching an agreement is not known.

Uncertainties and Limitations

A number of uncertainties can apply in the forensic assessment of contaminated land, including:

- Determination of a real-time status of the polluter could be erroneous when the land ownership/lease has transferred to a number of persons/organizations.
- Chemical decay factors vary for different substances. A newly formed chemical compound due to the oxidation/reduction processes could have a significant impact on the liability analysis picture.
- Costs i.e. funds not available for site assessment or remediation.
- Risks of achieving non-tangible evidence.
- Allocation and apportionment of retrospective liability often faces great practical difficulties when attempting to allocate or apportion (retrospective) liability for historic contamination, factual background complex.

References

1. Environment Agency (http://www.environment-agency.gov.uk/research/library/data/34403) accessed 02/03/2009.
2. Sullivan, P. J., Agardy, F. J and Traub, R. K (2001). *Practical Environmental Forensics, Process and Case Histories*, John Wiley and Sons.
3. Wikipedia (http://www.en.wikipedia.org/wiki/Forensic_engineering) accessed 02/03/2009.
4. University of Aberdeen, Scotland (http://www.abdn.ac.uk/mediareleases/release.php?id=1251) accessed 02/03/2009.
5. Fenning, P. J and Donnelly, L. J. (2004). *Geophysical Techniques for Forensic Investigation*, Geological Society, London, Special Publications; v. 232; p. 11-20.
6. Pye K and Croft, D. J. (2004). *Forensic Geoscience: Introduction and Overview*, Geological Society, London, Special Publications; 2004; v. 232; p. 1-5.
7. Ashley; P. R. (1998). *Foreseeability of Environmental hazards; the implications of the Cambridge Water Company case*, Geol. Soc. London, Special Publication. v. 128; p. 23-26.
8. James, C. L., Shah, L. A and Thomas, B. R.; (2007). *Case Study of a Sustainable Approach to Management and Re-use of Soils Arising from a Brownfield Site in the UK,* Institute of Materials, Minerals and Mining, London, Conference Proceedings, p. 21-28.
9. Robins, N. S., Dumpleton, S and Walker, J., (2002). *Coalfield Closure and Environmental Consequence – the Case in South Nottinghamshire*, Geological Society, London, Special Publications; v. 198; p. 99-105.
10. The Landfill Directive (1999/31/EC); (http://www.eurlex.europa.eu/LexUriServ) accessed 02/03/2009.
11. The Hazardous Waste (England and Wales) Regulations, 2005.
12. The Special Waste Regulations (England, Wales and Scotland) 1996.

13. Environment Agency, Technical Guidance on Hazardous Waste: Interpretation of the definition and classification of hazardous waste, 2nd Edition v2.1, October 2006.
14. Environment Agency, Briefing Note; 'Update on the use of higher landfill waste acceptance criteria limit values for hazardous waste'. Version 1, March 2007.
15. The EEC treaty of Rome (1957) (http://www.eur-lex.europa.eu/en/treaties) accessed 02/03/09.
16. The European Union; Environmental Liability Directive (2004/35/CE).
17. DEFRA; Consultation on Transposition of the Environmental Liability Directive, June 2007 (http://www.defra.gov.uk/environment/liability/pdf/implementation-summary) accessed 02/03/2009.
18. British Standards Institute BS 5930: 1999; The Code of Practice for Site Investigations.
19. British Standards Institute BS EN 1997 Eurocode 7: Geotechnical design.
20. Environment Agency Wales; Brofiscin Quarry (http://www.environment-agency.gov.uk/regions/wales) accessed 10/03/2009.
21. Jones, Carwyn (Minister for Environment, Planning & Countryside), Welsh Assembly Government, Cabinet Statements 2007; '*Recovering the clean-up costs at Brofiscin Quarry from contaminated waste produced by the Monsanto Group*.'
22. Guardian News; '*The wasteland: how years of secret of chemical dumping left a toxic legacy*.' February 12, 2007.
23. Bell, S and McGillivray, D. (2002). Environmental Law: *The Law and Policy relating to Protection of the Environment'* 5th Edition, Blackstone Press Limited, London.
24. Murphy, B. L and Morrison, R. D.; (2007). *Introduction to Environmental Forensics (Second Edition)*; Elsevier Academic Press.
25. Environment Agency & DEFRA, CLR 11; Model Procedures for the Management of Land Contamination, September 2004.
26. DETR Circular 02/2006, Contaminated Land Environmental Protection Act 1990: Part IIA, September 2006.
27. DEFRA, Guidance for England Draft Guidance for Wales: The Environmental Damage (Prevention and Remediation) Regulations, February 2009.
28. Shah, L. A., James, C. L. and Thomas, B. R.; (2008). *Forensic Engineering in Assessment and Remediation of Contaminated Land*, ICE 4th International Conference on Forensic Engineering, London, December 2008.

Settlement Problems in Peat Due to Their High Compressibility and Possible Solution Using Cement Columns

Sina Kazemian, Afshin Asadi, Bujang B. K. Huat, Arun Prasad and Irman B. A. Rahim

Civil Engineering Department, University Putra Malaysia, Serdang, Selangor, Malaysia, PH (601) 7393-9404; FAX (603) 5636-8528; email: sina.kazemian@gmail.com

ABSTRACT

Tropical peat soils are considered as extremely soft, wet, unconsolidated deposits. These kinds of soils are geotechnically problematic due to their high compressibility or high settlement and low shear strength. Cement columns may be used to improve the settlement problem of these soils. This paper describes the results of the effects of cement columns on the compressibility of fibrous tropical peat soils. Coefficient of consolidation, compression index, coefficient of secondary compression, and coefficient of volume compressibility were obtained by a Rowe cell test for both, untreated peat soil and peat soil treated with cement column. The results indicate that installing cement columns and increasing cement ratio could reduce the compressibility of peat soils and decrease its settlement dramatically.

INTRODUCTION

All soils with organic content of greater than 20% are known as organic soil. Peat soil is an organic soil with organic content of more than 75% (Huat, 2004). Peat soils have been classified to 10 degrees of humification (H_1-H_{10}) by Von post (1922) based on degree of humification, botanical composition, water content and content of fine and coarse fibers. In modern classification, they have been narrowed to 3 classes: (i) *Fibric* or fibrous (least decomposed), (ii) *Hemic* or semi-fibrous, and (iii) *Sapric* or amorphous (most decomposed) (Magnan, 1980).

Peat soils are found throughout the world and constitute 5 to 8% of the land surface of the earth. The most extensive areas are located in the northern hemisphere (Mesri and Ajlouni, 2007). In recent years, they are increasingly being utilized for the construction purpose since the coverage of the soil is quite extensive.

Fibrous peat has high organic and fiber content with low degree of humification. The behavior of fibrous peat is different from mineral soil because of different phase properties and microstructure (Edil, 2003). Landva and Pheeney (1980) described

fibrous peat particles as consisting of fragments of long stems, thin leaves, rootlets, cell walls and fibers, often very large.

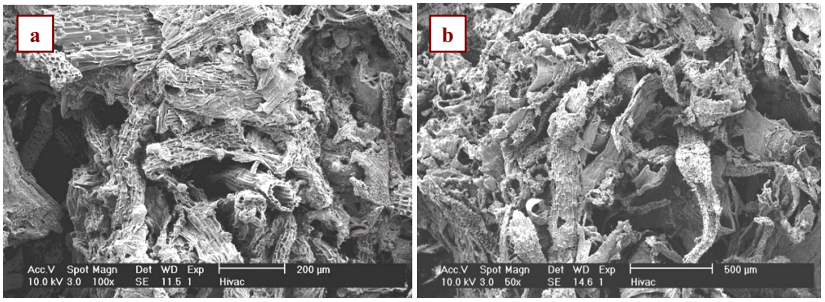

Figure 1. Scanning electron microphotograph of peat (a) vertical section and (b) horizontal section (after Mesri and Ajlouni, 2007)

Since fibrous peat has hollow perforated cellular structures (Fig. 1) and a network of fibrous elements in vertical and horizontal sections, it is most likely to have very low shear strength, high compressibility and the long-term consolidation of peat results in a large deformation. Peat lands have presented difficult subsurface conditions for the construction of roads, dikes, housing developments, storage facilities, industrial parks, and so on, including high initial costs and/or continued maintenance operation for years (Colley, 1950; Hanrahan and Rogers, 1981). Peat soils are geotechnically problematic soils as the compression and settlement processes may take a considerably longer time and it increases when the ground water level decreases. Besides settlement, stability problems during construction such as localized bearing failures and slip failures need to be considered (Duraisamy et al, 2009). Figure 2 shows a badly damaged house constructed on peat soil due to differential settlements.

Figure 2. A badly damaged house due to differential settlement in peat soil in Sibu, Malaysia (after Huat, 2004).

Compressibility parameters of peat. High organic maters are indicator of high compressibility and swell characteristics of the soils (Mesri and Ajlouni, 2007; Kazemian et al., 2009). Tropical peat soils undergo large settlements in comparison to

clays when subjected to loading. The compression behavior of fibrous peat varies from the compression behavior of other types of soils in two ways: first, the compression of peat is much larger than of other soils and second, the creep settlement plays a more significant role in determining the total settlement of peat. The primary consolidation of the fibrous peat is very rapid, a large secondary compression and even tertiary compression is also observed. Secondary compression is generally found as the significant part of the total compression because the time rate is much slower than the primary consolidation (Yulindasari, 2006).

Larson (2003) emphasized that the deep mixing method is today accepted world-wide as a ground improvement technology in order to improve the permeability, strength and compressibility properties of the soil. Binders, such as lime or cement are mixed with the soil by rotating mixing tools. The stabilized soil, often produced column shapes, has higher strength, lower compressibility, and lower permeability than the original soil. Experience has been positive and the method has great development potential. The method is undergoing rapid development, particularly with regard to its applicability, cost effectiveness and export potential. Cement is one of the most commonly used binders for deep mixing method. The reactions that provide effective soil stabilization are (i) the reaction of cement with the water in the soil, (ii) pozzolanic reactions between $Ca(OH)_2$ from burnt lime or cement and pozzolanic minerals in the soil, and (iii) ion exchange between calcium ions from lime or cement and ions in the clay (Janz and Johansson, 2002).

This study is focused on the compressibility characteristics of fibrous peat from consolidation tests. The main compre-ssibility parameters examined to assess the effect of the cement column on consolidation and settlements of fibrous peat are: coefficient of consolidation (c_v), compression index (c_c), coefficient of secondary compression (c_α) and coefficient of volume compressibility (m_v).

EXPERIMENTAL DESIGN AND LABORATORY WORK

As mentioned earlier that settlement is affected by the compressibility parameters in peat soils, this paper is mainly concerned with fibrous peat and presents an interpretation of the compressibility parameters of fibrous peat soil before and after installation of cement column with different cement-soil ratio by using the results from Rowe cell consolidation test on undisturbed samples for investigating the effects of cement column on settlement of the soil.

Sample preparation. Undisturbed samples of peat soil were collected from Jawa Klang, Selangor, Malaysia using a sampling tube, sealed to prevent the loss or gain of moisture and transported to UPM laboratory for testing taking all care not to disturb the samples. Samples of size 150 mm diameter and 230 mm high were taken out from the sampling tube using auger, top and bottom faces trimmed and the specimens prepared were transferred to Row cell for testing, following BS 1377-1. As fibrous soil such as peat is easily disturbed, the trimming process was done carefully and quickly to minimize any change in water content of the soil sample. All the tests reported here were performed in the laboratory at a constant temperature at 20±2°C.

The height and diameter of each specimen was 50 and 150 mm respectively, as shown in Figure 3(a).

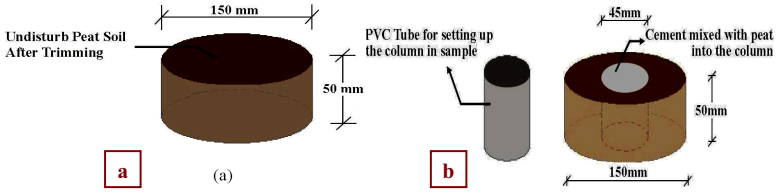

Figure 3. (a) A cylindrical specimen from the original soil sample after trimming (b) Method used to set up cement column in the specimen.

In order to investigate the compressibility parameters of peat reinforced with cement column, a smooth PVC tube of outer diameter 45 mm was used to remove a core of peat soil from the center of the specimen. This annular opening was subsequently filled by a cement-peat column. The dose of cement was at the rate of 250 kg/m^3. The cement column was prepared by adding cement equal to 10, 20, 30 and 50% of the weight of the cement dose to the peat extracted from the sample. The proportions of cement (as calculated above) and added to extracted peat with different ratio are presented in Table 1. The diameter of cement column was 45 mm and the area ratio of column to sample was 0.09 (Figure 3(b)).

Table 1. Mix Proportions of Cement-Peat Column.

Samples	Mix Proportion
Control sample	Untreated peat soil
Sample I	Peat soil 90% & cement 10%
Sample II	Peat soil 80% & cement 20%
Sample III	Peat soil 70% & cement 30%
Sample IV	Peat soil 50% & cement 50%

The samples were cured for 28 days in a soaking basin with natural peat water (Figure 4) collected from peat site, before performing the compressibility test.

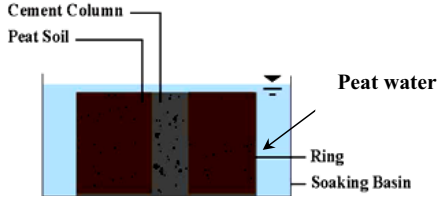

Figure 4. Curing peat cement column specimen (Kazemian et al. 2008)

Testing programs. The physical properties of the natural peat soil determined were organic content, water content, liquid limit and specific gravity in accordance with BS

1377-3(4) (1990), BS 1377-2(3) (1990), BS 1377-2(4) (1990) and BS 1377-2(8) (1990) respectively. The fiber content of the peat samples was determined based on test procedures following ASTM D 1997-91 and used to find the degree of humification as per Von Post scale. The samples were then tested in a Rowe cell to overcome most of the disadvantages of the conventional oedometer apparatus when performing consolidation tests on soils with low permeability, including non- uniform deposits. The two most important features of a Row cell is the ability to control drainage and to measure pore water pressure during the course of consolidation tests (Duraisamy et al., 2009).

The test set up comprised of a Rowe cell apparatus, gradually diverging system (GDS), pressure and volume controllers and GDS laboratory software. The consolidation pressure (σ) of 50, 100, 200 and 300 kPa was applied to the sample surface either via a flexible diaphragm, using a hydraulic loading system, to give a uniformly distributed pressure (free strain) or via a rigid plate to give uniform settlement (equal strain). The bottom drain is provided with a tapping to a pressure transducer. The consolidation test was performed on peat, a soil with low permeability, based on BS 1377-6 (1990) and the compressibility parameters of the specimen were calculated without having to remove it from its sampling tube. The specimens therefore didn't suffer disturbance due to preparation and the moisture content of the soils at the respective test horizons could be reported. The compressibility parameters of peat soil and soil with cement column were evaluated to assess the effect of the cement column with different cement ratio. The parameters evaluated are: (i) c_v, (ii) c_c, (iii) c_α, and (iv) m_v.

RESULTS AND DISCUSSION

PHYSICAL CHARACTERISTICS OF UNTREATED (NATURAL) PEAT

Some preliminary tests, such as moisture content, specific gravity, degree of humification, organic content, fiber content, pH, and bulk density were performed on fibrous peat soil and the results are presented in Table 2.

Table 2. Physical Characteristics of Untreated Peat Soil.

Parameters	Results
Moisture content (%)	524
Liquid limit (%)	169.6
Specific gravity	1.24
Degree of humification (%)	H_4
Organic content (%)	89.35
Fiber content (%)	94
Bulk density (kN/m^3)	10.01
pH	4.8

The results present the characteristics and indications of the concentration at which all of the organic compound are usually found in soils. It was observed that the results

agree well with the findings of Ajlouni (2000), Huat (2004), Alwi (2007), Kazemian et al. (2009), and Kalantari and Huat (2009).

Compression index (c_c). The c_c is defined by the slope of the final part of the void ratio versus logarithmic of consolidation pressure (log σ) curve. Based on Figure 5, the c_c values calculated from Rowe cell consolidation test results for the natural fibric peat, sample I, II, III and IV were 1.79, 1.70, 1.46, 1.32, and 1.08 respectively, for σ of 50 kPa. It implies that by increasing the cement ratio the c_c is decreasing gradually.

The results do not follow closely the results reported by other researchers and the reason may be that the reinforced peat specimens were cured in peat water and not natural water as used by others.

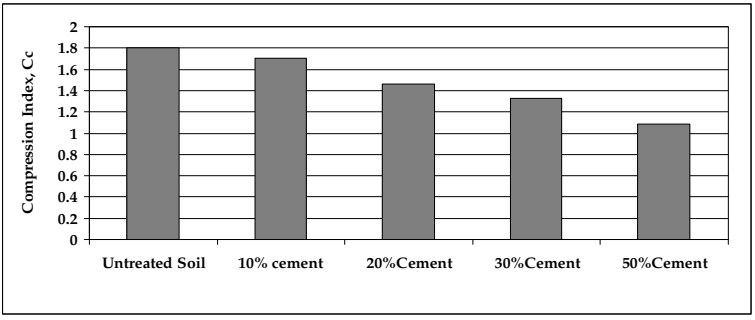

Figure 5. c_c versus cement ratio.

Coefficient of consolidation (c_v). There is a significant decrease in the c_v of the undisturbed samples with an increase in σ above the apparent pre-consolidation pressure (σ_c) (Huat, 2004). Farrell et al., (1994) reported that this decrease is more marked in the samples, which had higher organic contents.

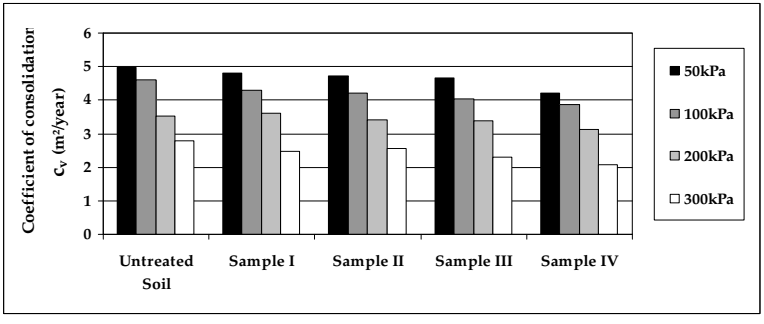

Figure 6. c_v versus σ with different cement ratio.

For fibrous peat, the results (Figure 6) indicate that the c_v decreases upon increasing the σ and cement ratio. The c_v decreased from 4.98 m^2/year (50 kPa, no cement) to about 4.2 m^2/year (50 kPa, 50% cement). Also, at 300 kPa, it decreased from 2.79 m^2/year (no cement) to 2.07 m^2/year (50% cement) and the reduction was about 60% by increasing σ from 50 to 300 kPa and cement ratio to 50%.

Coefficient of secondary compression (c_α). The secondary compression and associated settlement are often more significant for peat deposits than other geotechnical materials for the following three reasons: (i) Tropical peat soils deposits display the highest values of c_c, (ii) These soils deposits have the highest values of c_α/c_c and (iii) Primary consolidation of fibrous peat layers in the field is completed commonly within a few weeks or months (Mesri and Ajlouni, 2007). Primary consolidation and secondary compressions can take place simultaneously. However, it is assumed that the secondary compression is negligible during primary consolidation, and is identified after primary consolidation is completed (Hobbs, 1986; Kogure et al., 1986).

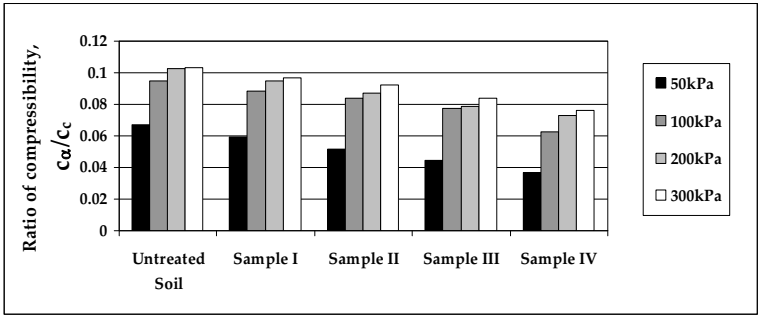

Figure 7. (c_α /c_c) versus σ with different cement ratio.

The c_α is determined from the slope of the e-log (t) curves during the period of 4 to 24 hours after load increment, assuming that the secondary compression would have started 4 hours after loading. The soil with c_α/c_c values of more than 0.064 is classified as soil with extremely high secondary compressibility (Mesri, 1973). The secondary compression behavior of soils is completely explained and predicted by the c_α/c_c law of compressibility (Mesri and Godlewski, 1979; Mesri et al., 1997).

Figure 7 shows the measured c_α/c_c of untreated fibrous peat and cement column reinforced fibrous peat. c_α/c_c of untreated peat increased with increasing the σ subsequently from 0.067 to 0.103 upon increase in σ from 50 to 300 kPa respectively. On the other hand, the c_α/c_c is influenced by the addition of cement and it declined from 0.067 to 0.037 for untreated and peat treated with 50% cement respectively at a consolidation pressure of 50 kPa. Further, it decreased from 0.103 to 0.076 for untreated and peat treated with 50% cement respectively at a consolidation pressure of 300 kPa (Figure 7).

Coefficient of volume compressibility (m_v). This parameter is very useful in estimating the primary consolidation settlement. The e-σ' curve is used to obtain coefficient of axial compressibility (a_v) and subsequently the m_v, while the e-log σ is used to obtain c_c and σ_c.

It is observed that from m_v versus σ plot (Figure 8) that m_v gradually decreases upon increase in the σ and cement ratio. Because of the hardened peat-cement matrix formed by cement particles bonding with adjacent soil particles in the presence of water in its pores, the compressibility characteristics of soils is improved. It was observed that m_v declined from 1.42×10^{-3} for untreated peat soil to 0.96×10^{-3} for peat soil added with 50% cement at a σ of 50 kPa.

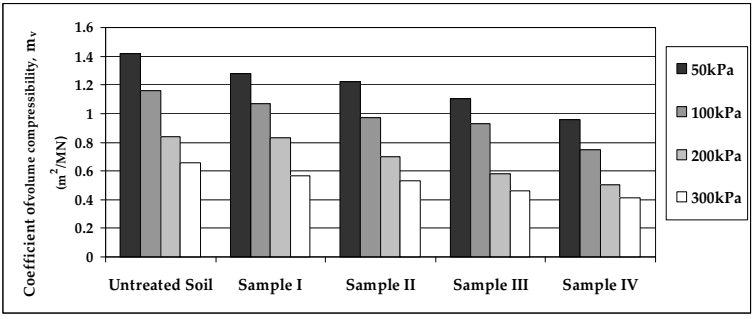

Figure 8. m_v versus σ with different cement ratio.

It is apparent from the m_v versus σ plot that the minimum consolidation pressure at 50 kPa was higher than the pre-consolidation pressure for the peat soil. Inversely, if consolidation pressure is lower than the pre-consolidation pressure, the soil sample would swell less and lower value would have been obtained for the m_v under consolidation pressure of 50 kPa.

As the sample consists predominantly of organic matter (table 2), it is obvious that cement reacted with only water in the soil during the process of stabilization. Mixing cement with water initiates a chemical process (hydration) which forms a hard cement paste. Janz and Johansson, (2002) stated when a cement particle undergoes hydration an extremely fine-pored cement gel forms around the particles**.** The reaction products constituting the cement gel include CSH gel, ettringite, and mono sulfate. Since the cement gel is porous and contains chemically combined water (water of crystallization), its volume will be greater than that of cement particle prior to reaction. Thus as the reaction between the cement and the water proceeds, the voids between the cement particles will gradually be filled with cement gel. At the same time the cement sets and gains strength and compressibility parameters of fibrous peat soil like c_v, c_c, c_α, and m_v improved resulting in less compressibility and settlement.

CONCLUSIONS

This study was carried out to investigate the influence of the various quantities of cement on compressibility parameters or settlement of tropical peat soil by installing a cement-peat column in undisturbed peat soil.

The following conclusions are drawn based on this study:

1. The c_c values from Rowe cell consolidation test for the natural fibric peat, sample I, II, III and IV is 1.79, 1.70, 1.46, 1.32 and 1.08 respectively, for σ of 50 kPa. It shows that by increasing the cement ratio, the c_c decreased by 5 to 60%.

2. The c_v of untreated peat soil is decreasing upon increase in σ and cement ratio up to 60%.

3. The c_α/c_c increased with increase in σ but decreased, along with m_v, with the increase in the cement content, showing that the settlement will decrease with an increase in cement content.

4. It is apparent that the cement gel formed due to the reaction of cement with water filled up the voids of the peat soil. At the same time, the hardened soil-cement matrix formed due to the bonding of cement with the adjacent soil particles improved the compressibility parameters (c_α/c_c, c_c, c_v, and m_v) resulting in a decreased settlement in fibrous peat.

REFERENCES

Ajlouni, M. A. (2000). “Geotechnical Properties of Peat and Related Engineering Problems." *PhD Thesis*, University of Illinois at Urbana-Champaign.

Alwi, A. (2007). “Ground Improvement on Malaysian Peat Soils Using Stabilized Peat-Column Techniques.” *PhD. Thesis*, University Malaya, Kuala Lumpur.

ASTM (1992). “*American Society for Testing and Materials Annual*.” Philadelphia, PA., U. S. A.

BS 1377 (1990). “Soils for Civil Engineering Purposes.” *British Standard Institution* (BSI.), London, U. K.

Colley, B. E. (1950). “Construction of highways over peat and muck areas.” *American highways*, Washington, D.C., 29(1): 3–6.

Deboucha, S., Hashim, R., and Alwi, A. (2008). “Engineering Properties of Stabilized Tropical Peat Soils,” *The Electronic Journal of Geotechnical Engineering* (EJGE). Vol. 13, Bund. E.

Duraisamy, Y., Huat, B.B.K., and Muniandy R. (2009). “Compressibility Behavior of Fibrous Peat Reinforced with Cement Columns” *Geotechnical and Geological Engineering Journal*, DOI: 10.1007/s10706-009-9262-3.

Edil, T. B. (2003). “Recent Advanced in Geotechnical Characterization and Construction over Peat and Organic Soils.” *In Proceeding of 2nd Int. Conf. on Advances in Soft Soil Eng. and Tech*., ed. Huat et al., Putra jaya, Malaysia, 3-25.

Edil, T. B. and Wang, X. (2000). "Shear Strength and K_0 of Peats and Organic Soils." *Geotechnics of high water content materials*, ASTM STP 1374, West Conshoho-cken, Pa., 209–225.

Hanrahan, E. T. and Rogers, M. G. (1981). "Road on peat: Observations and design." *J. Geotech. Eng. Div*., 107(10): 1403–1415.

Hobbs, N. B. (1986). "Mire Morphology and the Properties and Behavior of Some British and Foreign Peats." *Q. I Eng. Geol*., London, 19(1): 7-80.

Huat, B.B.K. (2004). "*Organic and Peat soil Engineering*." University Putra Malaysia, Serdang, Malaysia.

Janz, M. and Johansson S. (2002). *"*The Function of Different Binding Agents in Deep Stabilization," *Report 9, Swedish Deep Stabilization Research Center*, Linköping, Sweden.

Kalantari, B. and Huat, K. (2009). "Precast Stabilized Peat Columns to Reinforce Peat Soil Deposits." *The Electronic Journal of Geotechnical Engineering* (EJGE), Vol. 14, Bund. B.

Kazemian, S., Asadi, A. and Huat, B.B.K. (2009). "Laboratory Study on Geotechnical Characterization of Tropical Organic Soils and Peat." *International Journal of Geotechnics and Environment*. January, issue 1.

Kazemian, S., Huat B. B. K., Jit Ming Yeong, and Vahed, G. (2008). "Laboratory Investigations on Shear Strength of Organic Soils and Peat Reinforced with Cement Columns," *Proc. of Int. Graduate Con. on Eng. and Sci. (IGCES) UTM*, Johor Bahru, Malaysia.

Kogure, K., Yomuguchi, H., Ohira, Y. and Ishioroshi, H. (1986). "Physical and Engineering Properties of Peat Ground." *Proceeding Advances in Peat land Engineering*. Ottawa, Canada, 95-100.

Landva, A. O., and Pheeney, P. E. (1980). "Peat Fabric and Structure." *Canadian Geotechnical Journal*, 17(3), 416–435.

Larsson, S. (2003). "Mixing Processes for Ground Improvement by Deep Mixing", *Doctoral thesis published in Royal Institute of Technology, Stockholm*, Sweden.

Magnan, J. P. (1980). "Classification Geotechnique Des Sols: 1- A Propos De La Classification LPC." *Bulletin de Liaison des Laboratories des Ponts et Chaussees*, Paris, 19-24.

Mesri, G. & Ajlouni, M. (2007). "Engineering Properties of Fibrous Peats." *Journal of Geotechnical and Geoenvironmental Engineering*, ASCE, U.S.A., Vol. 133, No. 7.

Mesri, G. (1973). "Coefficient of Secondary Compression." *J. Soil Mech. and Found. Div*., 99(1), 123–137.

Mesri, G., and Godlewski, P. M. (1979). "Closure to Time and stress compressibility interrelationship." *Journal Geotechnical Engineering Div*., 105 (1): 106–113.

Mesri, G., Stark, T. D., Ajlouni, M. A., and Chen, C. S. (1997). "Secondary compression of peat with or without surcharging." *Journal Geotechnical Geoenvironmental Engineering*, 123 (5), 411–421.

Yulindasari (2006). "Compressibility Characteristics of Fibrous Peat Soil." *Master of Engineering Thesis*, Universiti Teknologi Malaysia.

Von Post, L. (1922). "Sveriges Geologiska Undersoknings Torvinventering Och Nagre av Dess Hittills Vunna Resultat, Sr. Mosskulturfor." *Tidskr* 1: 1-27.

Bearing Capacity of Rectangular Foundations near the Slopes with Nonassociated Flow Rules

N. Ganjian[1], F. Askari[2], and O. Farzaneh[3]

[1] PhD Candidate in Geotechnical Eng., Civil Engineering Department, College of Engineering, University of Tehran, P.O. Box: 11365-4563, Tehran, IRAN; FAX: +982144404928; Email: nganjian@ut.ac.ir, Corresponding author.
[2] Assistant professor, International Institute of Earthquake Engineering and Seismology, Tehran, IRAN; Email: Askari@iiees.ac.ir
[3] Assistant professor, Civil Engineering Department, College of Engineering, University of Tehran; Email: ofarzane@ut.ac.ir

ABSTRACT

A method of three-dimensional slope stability analysis is presented here based on the energy consideration to obtain the ultimate bearing capacity of rectangular foundations located near the slopes with coaxial nonassociated flow rule. Taking the eccentrically loaded foundation into account, a rotational failure mechanism consisted of several lateral surfaces is considered. The stress distribution along the rupture surface, needed to obtain the rate of dissipation of internal energy for the nonassociated flow rule, is established on the basis of extended Bishop's method and boussinesq theorem. The bearing capacity of rectangular foundations in different conditions is obtained using the proposed method and the effects of dilatancy angle are investigated. The results indicate that for the nonassociated flow rule materials, the bearing capacity of slopes reduces with decrease in the dilatancy angle. These influences increase in the case of mild slopes in frictional.

KEY WORDS

Rotational Failure Mechanism; 3D Bearing Capacity; Nonassociated flow rule.

INTRODUCTION

The assessment of the stability of slopes under surcharge loads or the determination of ultimate bearing capacity of foundations located near the slopes is a fundamental problem received wide attention across geotechnical communities because of its practical importance. Previous studies show that, in such a complex footing-on-slope

system, the ultimate bearing capacity of the footing may be governed by either the local foundation failure or the global slope failure. The non-eccentric loading, make this problem more difficult in superstructures located on top of the slopes under wind or earthquake conditions.

Numerous two-dimensional methods have been developed for the evaluation of stability of loaded slopes. However, all slope failures are three-dimensional (3D) in nature, especially for slopes under local loading. So, 3D stability analyses should be performed in the most cases of slope stability problems.

In general, proposed methods can be classified to the following types: a) Limit equilibrium approach. b) Characteristic line method. c) Limit analysis approach.

- The 3D limit equilibrium methods of columns, which are analogous to the two-dimensional methods of slices, have been most commonly used by engineers over the past several decades (Anagnosti, 1969; Hovland, 1977; Chen and Chameau, 1982; Ugai, 1985 and Hungr, 1987).
- The characteristic line method is based on integrating the equations of plastic equilibrium and is more rigorous, but still takes no account of the flow rule and can only deal with a restricted set of boundary conditions.
- In order to reduce the influence of the assumptions made in limit equilibrium methods, the methods of limit analysis (upper and lower bounds) based on the rigid plasticity theory were developed. In upper-bound theorem of limit analysis, it can be proved that the dissipation is a function only of the velocities. This property is used to compute the dissipation along the discontinuities, with the geometry being optimized to yield the minimum dissipated power and the lowest collapse load.

Some 3D upper-bound solutions have been presented assuming translational or rotational collapse mechanisms. Giger and Krizek (1976) used the upper-bound theorem of limit analysis to study the stability of a vertical corner cut subjected to a concentrated surcharge load. Michalowski (1989) presented a rigorous 3D solution for slope stability problems based on a translational collapse mechanism consisted of several rigid blocks which can also be used to estimate the bearing capacity of rectangular foundations. Farzaneh and Askari (2003) improved the results of Michalowski using combination of several lateral surfaces for each block and

extended his 3D analysis for nonhomogenous soils. Farzaneh et al. applied this 3D multi-rigid block mechanism for stability analysis of convex slopes in plan view under local loading. De Buhan and Garnier (1998) evaluated the upper bound bearing capacity of square foundations located near a slope examining both rotational and punching collapse mechanisms.

Taking the truly 3D geometry of the problem into account, here, a 3D rotational collapse mechanism consisted of a log-spiral bottom surface and combination of several lateral surfaces is considered to improve the solutions for bearing capacity of foundations under combined loading.

Since the most granular soils do not obey the associated flow rule, this assumption in the upper bound methods causes some overestimation of volumetric strain and consequently overestimation of limit loads. Davis (1968) pointed out that consideration of the angle of dilatancy could better predict the limit load and it always tends to the lower limit loads. Although considering the nonassociated flow rule violates the basic assumption of the upper bound theorem, applying the energy balance in an admissible velocity field, leads to the ability of studying the effect of dilatancy angle in slope stability analysis.

There are some researches about the influences of dilatancy angle on 2D stability of loaded slopes (Yin et al., 2001 and Yang et al., 2007). However, the studies about the influences of nonassociated flow rule on the 3D stability problems are very limited according to the literature. In the present article, by considering the energy balance at collapse, bearing capacity of rectangular foundations are computed using the proposed rotational collapse mechanism for soils with nonassociated flow rules. Since the rate of dissipation of internal energy for a nonassociated material depends on the value of normal stresses along the rotational rupture surface, the stress distribution is established using the extended Bishop's method and Boussinesq theorem.

THREE-DIMENSIONAL FAILURE MECHANISM

Proposed rotational collapse mechanism, as an extension of 2D rotational mechanism, consisted of a log-spiral cylindrical bottom surface and combination of several lateral

surfaces (shown in the Fig.1 as AEFD and BCFE). The known equation of bottom surface in polar coordinates is:

$$R = R_0 \exp[(\theta - \theta_0)\tan\phi] \tag{1}$$

where R_0 and θ_0 are the cylindrical coordinates of the start point of collapse on the surface and ϕ (=ψ) is the internal angle of friction.

Lateral surfaces can be adapted fulfilling the normality condition of upper-bound theorem through an equation of the following form:

$$z = f(r,\theta) \tag{2}$$

where (r, θ, z) are the cylindrical coordinates of a typical point P located on lateral surface. Compatibility of strains for associated materials means that at point P, the velocity vector across the surface makes an angle equal to the internal angle of friction (ϕ) with the tangent of slip surface or an angle equal to $\pi/2$-ϕ with the normal to the surface (**N**). Considering this assumption, the following differential equation can be driven:

$$\tan^2\phi\left(1+\left(\frac{\partial f}{\partial r}\right)^2\right) = \left(\frac{1}{r}\frac{\partial f}{\partial \theta}\right)^2 \tag{3}$$

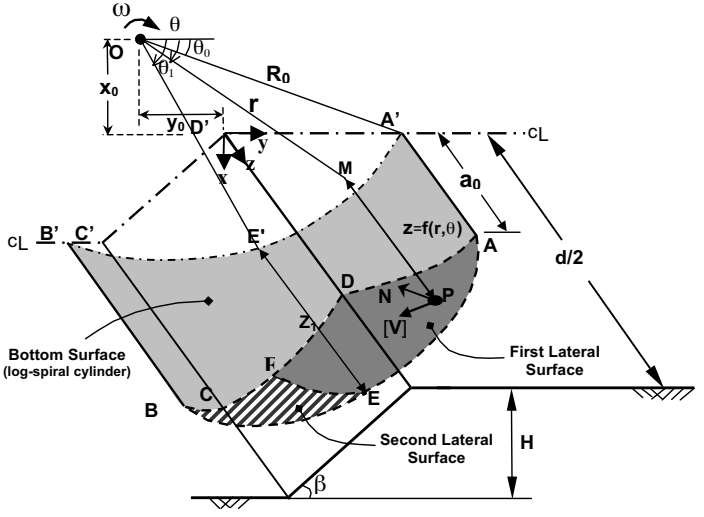

Figure 1. Proposed 3D collapse mechanism.

A possible class of solutions for above partial differential equation has been examined here as proposed by De Buhan and Garnier (1998):

$$z = f\ (r,\theta) = r\sinh\left(\theta\tan\phi + s\right) + b \tag{4}$$

where b and s are constants.

Considering a general point A(R_0, θ_0, a_0) on the lateral surface, the parameter b can be obtained as a function of parameters R_0 (which is itself a function of the coordinates of point O), θ_0, a_0 and s. Consequently, there are five independent geometrical variables (x_0, y_0, θ_0, a_0, and s) that should be optimized to obtain the critical failure mechanism.

De Buhan and Garnier (1998) used the rotational collapse mechanism with a lateral surface in each side to obtain bearing capacity of square foundations near the slopes. Performed analyses indicate that their proposed collapse mechanism extends laterally in frictional soils which results in overestimated limit loads.

To improve the results, combination of several lateral surfaces with the same rotational velocity and center of rotation, but different constant parameters (b_i and s_i), is proposed. For each additional lateral surface, two independent variables will be added to the five previous ones. Considering an arbitrary angle θ_1, coordinates of a point like E on the intersection of the bottom and first lateral surfaces, i.e. (R_1, θ_1, z_1), can be obtained. Crossing the second lateral surface from point E ($z_1 = R_1\sinh\left(\theta_1\tan\phi + s_2\right) + b_2$), b_2 is found as a function of θ_1 and s_2. In other words, the independent added variables are θ_1 and s_2. Based on the current study, a combination of three lateral surfaces in each side (with nine independent variables) is sufficient to obtain the appropriate results (Fig.2).

Many approaches have been developed to search for the critical failure mechanism in stability problems. Most procedures rely on traditional random generation techniques. The main limitation of these techniques is the uncertainty of the algorithm to find the global minimum limit load rather than the local minimum especially when the number of variable increases. Here, an alternative optimization method for determining the critical slip surface, called genetic algorithm (GAs), has been applied.

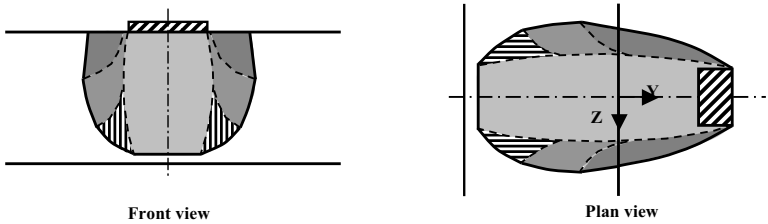

Figure 2. Schematic plans and front views of 3D rotational collapse mechanisms with combination of three lateral surfaces.

WORK AND ENERGY CALCULATIONS

Eq. 5 expresses the energy balance equation for a rigid collapse mechanism:

$$\int_A t_i [v]_i \, dA = \int_S T_i v_i dS + \int_V \gamma_i v_i dV \tag{5}$$

where the left term represents the rate of work dissipated by the traction t_i over the velocity jumps ($[v]_i$ is the relative velocity between two adjacent rigid blocks), and the last two terms represent the rate of external work of traction T_i over velocities v_i at boundary S, and of body forces γ_i over velocities v_i in volume V.

Assuming the associated flow rule (normality condition) for a Mohr-coulomb material means that the velocity jump becomes normal to the yield line and inclined to the velocity discontinuity at friction angle ϕ, as shown in Fig.3(a). Therefore, for the linear Mohr-Coulomb yield function, the internal energy dissipation is:

$$t_i [v]_i = c[v]\cos\phi \tag{6}$$

where, [v] is the resultant velocity jump and c is the cohesion of the material.

Thus, the internal energy dissipation will be independent of stresses along the rupture surfaces for associated materials.

In granular soils ($\psi \neq \phi$), assuming the normality condition, which is one of the main assumptions in the limit analysis theorem, generally causes the overestimation of volumetric strain. The effect of dilatancy angle on the stability of slopes can be investigated using a kinematically admissible velocity field comply with the kinematical boundary conditions and balancing the rate of internal energy dissipation with the rate of work of external forces.

As shown in Fig.3(b) for a nonassociated coaxial flow, the direction of [v] makes an angle ψ (dilatancy angle) with the plane of shear. The normal and shear stresses on the rupture plane representing E lie on a fictitious yield line, instead of the Mohr-Coulomb yield line. For this fictitious yield line we have:

$$\sigma_t = c^* + \sigma_n \tan\phi^* \tag{7}$$

where the values of the c^* and ϕ^* can be related by the following expressions (Davis, 1968):

$$\tan\phi^* = \eta \ \tan\phi \tag{8}$$

$$c^* = \eta \ c \tag{9}$$

$$\eta = \frac{\cos\psi \cos\phi}{1 - \sin\psi \sin\phi} \tag{10}$$

However, since the direction of [v] at the rupture plane is not normal to the supposed yield line, the internal energy dissipation will be obtained as:

$$t_i[v]_i = [v]\cos\psi \ [c^* + \sigma_n(\tan\phi^* - \tan\psi)] \tag{11}$$

Hence, in general, the energy expression depends on the distribution of normal stresses along the rupture surface for materials with nonassociated flow rule.

Drescher and Detournay (1993) proved that for translational collapse mechanisms, the limit load does not depend on the orientation of the velocity jump. So, a fictitious orientation and thus a fictitious flow rule (so as $\psi = \phi^*$) can be selected for which the specific energy dissipation is independent of σ_n:

$$t_i[v]_i = c^*[v]\cos\phi^* \tag{12}$$

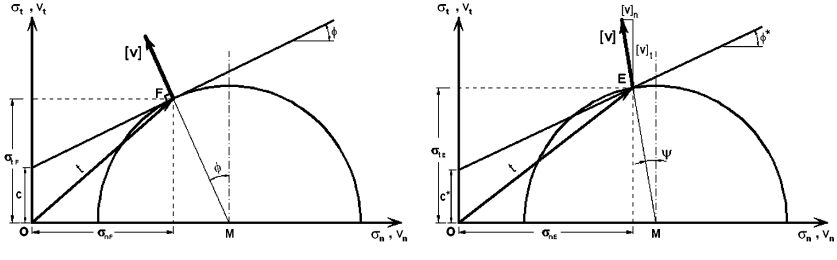

(a) **(b)**

Figure 3. Tractions and the direction of the velocity jump on the rupture plane for materials with (a) associated and (b) nonassociated flow rule.

However, in the case of rotational collapse mechanism, true orientation of the velocity jump should be considered. Thus, determination of the stress distribution along the rupture surface is necessary according to the Eq. 11.

Normal stress distribution along the rupture surfaces can be estimated using the limit equilibrium methods. Among the proposed methods of slices, Bishop's simplified method (Bishop, 1955) has been shown to produce somehow more accurate results when compared with other techniques. Hungr (1987) extended Bishop's method into three dimensions without any additional assumptions which expected to exhibit as a good performance as the original method. Here, the distribution of normal stresses along the proposed slip surfaces is generated by extension of Bishop's method considering fictitious yield line. More details and formulation of the extended Bishop's method into three dimensions is discussed by Hungr (1987). This limit equilibrium method of columns does not consider the shear resistance along the vertical sides of the sliding mass (Stark and Eid, 1998). In other words, the normal stresses generated by the earth pressure on the sides of the vertical columns along the vertical lateral surfaces are ignored. This will lead to an underestimation of the 3D factor of safety. Since the proposed lateral surfaces of used rotational collapse mechanism can be degenerated into vertical planes in the case of a nonassociated soil with ψ=0, removing mentioned limitation is imperative.

To include the normal stresses on vertical sides, at-rest earth pressure acting on the lateral vertical surface of the slide mass is considered as:

$$\sigma_n = k_0 \, \overline{\sigma}_v \tag{13}$$

where $\overline{\sigma}_v$ is the average vertical stress over the depth and k_0 is coefficient of earth pressure at rest (k_0=1-Sin ϕ_d). The excess stresses on lateral surfaces due to surcharge load are also considered using the Boussinesq theorem.

COMPARISONS AND NUMERICAL RESULTS

Wei et al. (2009) studied about the 3D stability and failure mode of locally loaded slopes based on the strength reduction method (SRM) using numerical finite difference code (Flac3D). Here, to compare the current results with those of

numerical methods, a locally loaded slope is considered. The slope geometry, dimensions of rectangular area of vertical loading and the soil properties are shown in Fig.4. Results of the analyses are compared in Table 1, for a loading q of 100 kPa and where the ratio of the loading length L to loading width B varies from 0 to 10.

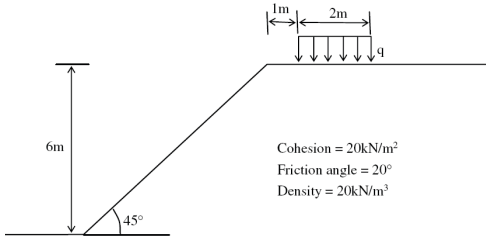

Figure 4. The geometry of the slope under local loading.

Table 1. Comparisons of safety factors for locally loaded slopes (q=100kPa)

L/B	0	1	2	4	6	8	10
WEI et al.	1.82	1.71	1.60	1.41	1.33	1.30	1.26
Farzaneh & Askari	1.94	1.82	1.63	1.43	1.35	1.29	1.26
Current	1.89	1.76	1.58	1.39	1.31	1.27	1.24

In the 3D analyses, when the loading ratio (L/B) is 1, 2, 4 and 6, the length of model chosen is 20m and when the L\B is 8 or 10, the length of model chosen is 30m. The results are nearly same as shown in this table, though the current results are somewhat less (better) for the slopes under rectangular foundations.

The described algorithm has been used to investigate the effects of nonassociativeness, or dilatancy angle, on the bearing capacity of rectangular foundations located near the slopes. Here, these effects are presented as some typical results.

Fig. 5 shows the influences of dilatancy angle (ψ) on the bearing capacity factor N'_c of a square foundation located in different distance from the slope (a/B) with the height of 6 meter and internal friction angle of ϕ=15° in the cases of centrically and eccentrically loading condition. Fig. 5(a) presents the bearing capacity factors versus

the ratio of dilatancy angle to friction angle of soil for a slope with angle of β=30°, while Fig. 5(b) corresponds to a slope with angle of β=60°.

Fig. 6 illustrates the bearing capacity factors, N'_c, of a square foundation near the slopes with the friction angle of ϕ=30° and different values of dilatancy angle assuming associated and nonassociated flow rules. As seen from these figures, reduction of ψ decreases the bearing capacity factors in both centrically and eccentrically loading conditions. This effect is more considerable where the friction angle and the distance of foundation from the slope increase.

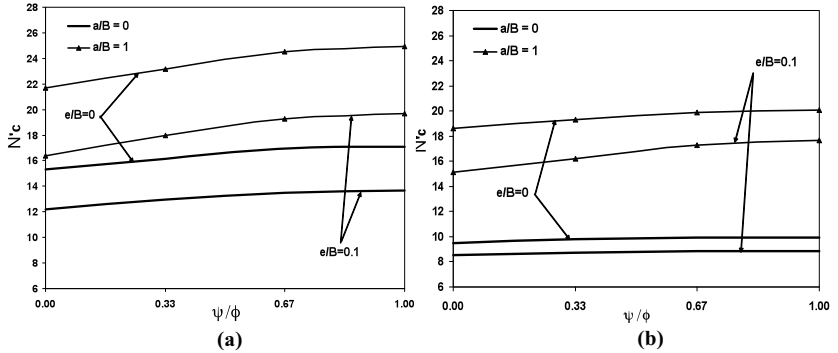

Figure 5. Bearing capacity factors N'c of square foundations near the slopes with H=6m and ϕ = 15°; (a) β = 30°, (b) β = 60°

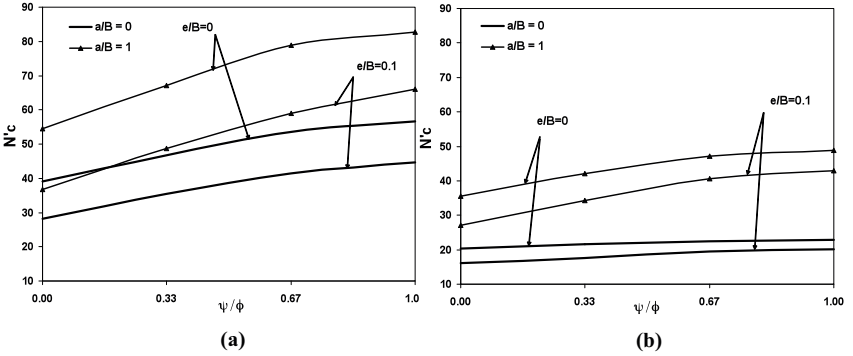

Figure 6. Bearing capacity factors N'c of square foundations near the slopes with H=6m and ϕ = 30°; (a) β = 30°, (b) β = 60°

Fig. 7 demonstrates the influences of dilatancy angle on the bearing capacity factor N'_{γ} of square foundations near the slopes with the friction angle of $\phi=30°$ in the cases of (a) $\beta=10°$ and (b) $\beta=30°$. As can be seen from Figs. 5 to 7, the effect of dilatancy angle is more significant for the mild slopes (smaller values of β).

To compare the influences of dilatancy angle on the bearing capacity factors N'_c and N'_{γ} in different conditions, the bearing capacity ratios are defined and presented in Fig. 8 for the slopes with the friction angle of $\phi=30°$ and $\beta=30°$. $(N'_c)_{\psi=\phi}$ and $(N'_{\gamma})_{\psi=\phi}$ are the bearing capacity factors, N'_c or N'_{γ}, corresponding to the associated slopes.

According to these numerical results, the reduction of bearing capacity is more in frictional soils. In other word, the decreasing of bearing capacity factors N'_{γ} is more considerable compared with that of N'_c.

It is also noticeable that nonassociativness leads to more decreasing of bearing capacity in the case of eccentrically loaded foundations.

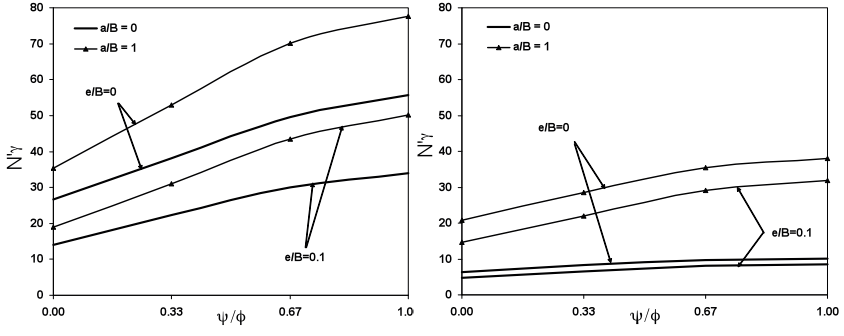

Figure 7. Bearing capacity factors N'_{γ} of square foundations near the slopes with H=6m and $\phi = 30^{\circ}$; (a) $\beta = 10^{\circ}$, (b) $\beta = 30^{\circ}$

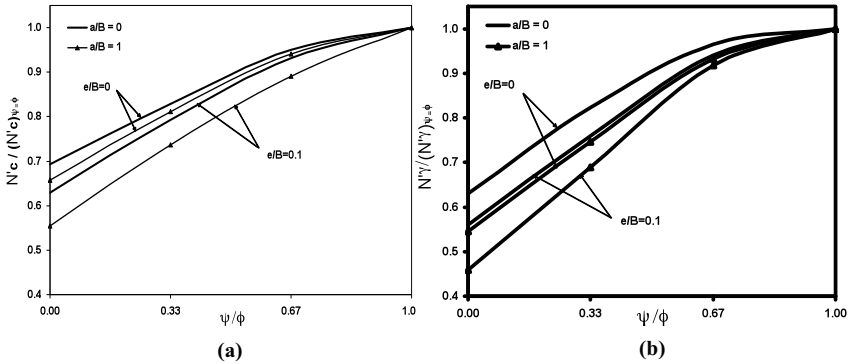

Figure 8. Bearing capacity ratios of square foundations near the slopes with $\phi = 30^{\circ}$ and $\beta = 30^{\circ}$; (a) $N'_c/(N'_c)_{\psi=\phi}$, (b) $N'_{,\gamma}/(N'_{,\gamma})_{\psi=\phi}$

CONCLUSIONS

A three-dimensional method based on the upper-bound theorem of limit analysis approach is provided to determine the bearing capacity of rectangular foundations under combined loading located near the slopes with associated flow material. Using the proposed 3D rotational collapse mechanism and applying energy dissipation method, bearing capacity factors for nonassociated slopes are determined and the effects of dilatancy angle on the bearing capacity of square foundations are investigated. The distribution of normal stresses along the rupture surfaces, needed in the case of stability analysis of nonassociated flow materials, is computed based on the extended Bishop's method and the assumption of Boussinesq theorem.

To evaluate the results of proposed mechanism, some comparisons with other solutions have been performed for associated flow materials.

According to the numerical results, the influences of dilatancy angle are very important in the case of determining the bearing capacity of foundations located near the slopes. The values of bearing capacity factors with nonassociated flow rule are smaller than those with the associated flow. The effects of dilatancy angle increase when the foundations are under eccentrically loading and located in more distance from the edge of mild slopes in frictional soils.

REFERENCES

Anagnosti, P. (1969). “Three-dimensional stability of fill dams”, Proceeding of the 7th International Conf. on Soil Mechanics and Foundation Engineering, Mexico, Vol. 2: 275-280.

Bishop, A. W. (1955). “The use of slip circle in the stability analysis of slopes”, Geotechnique, 5(1): 7–17.

Chen, R. H. and Chameau, J. L. (1982). “Three-dimensional limit equilibrium analysis of slopes”, Geotechnique, 33(1): 31 - 40.

Davis, E. H. (1968). “Theories of plasticity and the failure of soil masses”, In Soil mechanics: selected topics (ed. I.K. Lee), pp. 341-380.

De Buhan, P. and Garnier, D. (1998). “Three Dimensional Bearing Capacity Analysis of a Foundation near a Slope”, Soil and Foundations, 38(3): 153-163.

Drescher, A. and Detournay, C. (1993). “Limit load in translational failure mechanisms for associated and nonassociated materials”, Geotechnique, 43(3): 443–456.

Farzaneh, O. and Askari, F. (2003). “3D Analysis of Nonhomogeneous Slopes”, Journal of Geotechnical and Geoenviromental Engineering, 129(2): 137-145.

Farzaneh, O., Askari, F. and Ganjian, N. (2008). “Three Dimensional Stability Analysis of Convex Slopes in Plan View”, Journal of Geotechnical and Geoenviromental Engineering, 134(8): 1192-1200.

Giger, M. W. and Krizek, R. J. (1976). “Stability of vertical corner cut with concentrated surcharge load”, J. Geotech. Eng. ASCE, 102(1), 31 - 40.

Hovland, H. J. (1977). “Three-dimensional slope stability analysis”, Journal of Geotechnical and Geoenvironmental Engineering, 103(9): 971 - 986.

Hungr, O. (1987). “An extension of Bishop’s simplified method of slope stability analysis to three dimensions”, Geotechnique, 37(1):113-117.

Michalowski, R. L. (1989). “Three dimensional analysis of locally loaded slopes”, Geotechnique, 39(1): 27 - 38.

Stark, T. D. and Eid, H. T. (1998). “Performance of three-dimensional slope stability methods in practice”, Journal of Geotechnical and Geoenviromental Engineering, 124(11): 1049-1060.

Ugai, K. (1985). “Three dimensional slope stability analysis of vertical cohesive slopes”, Soils and Foundations, 25(3): 41-48.

Wei, W. B., Cheng, Y. M. and Li, L. (2009). “Three-dimensional slope failure analysis by the strength reduction and limit equilibrium methods”, Computers and Geotechnics, 36: 70-80.

Yang X., Gud N., Zhao L. and Zou J. (2007). “Influence of nonassociated flow rules on seismic bearing capacity factors of strip footing on soil slope by energy dissipation method”, Journal of Central South University of Technology, 14(6): 842-847.

Yin J., Wang Y. and Selvadurai, P. S. (2001). “Influence of non-association on bearing capacity of a strip footing”, Journal of Geotechnical and Geoenviromental Engineering, 127(11):985-989.

Assessment and Remediation of Geotechnical and Structural Deficiencies at a 5-Story Hotel Experiencing Large Differential Settlements

[1]Gregory L. Hebeler, Ph.D., P.E.; Rafael I. Ospina, P.E.
[2]Darren K. Howard, E.I.T.; Ralf Leistikow, P.E.

[1]Golder Associates Inc., 3730 Chamblee Tucker Rd., Atlanta, GA 30341, PH: (770) 496-1893, FAX: (770) 934-9476, Email: GHebeler@golder.com, ROspina@golder.com.
[2]Wiss, Janney, Elstner Associates, Inc., 2915 Premiere Parkway, Suite 100, Duluth, GA 30097; PH: (770) 923-9822, FAX: (770) 232-9044, Email: DHoward@wje.com, RLeistikow@wje.com

Abstract

This paper presents a case study of a forensic investigation and subsequent geotechnical and structural remediation of an operating 5-story hotel experiencing large differential settlements. The hotel construction consists of concrete masonry unit (CMU) load bearing walls and concrete hollow-core plank (HCP) floor framing founded on shallow strip and spread footings bearing on variably thick structural fill over sloping residual soils. Survey data 4 years following construction showed maximum settlements of 11 inches over the thickest fills, with trends indicating the potential for continued settlements. The building had experienced significant distress and concerns about its structural stability and life safety were raised. By working closely with the owner and each other, the geotechnical and structural consultants developed an effective and feasible approach to stabilize the foundation system and repair the structural elements while allowing the hotel to remain operational. This case study highlights the benefits of joint geotechnical and structural participation throughout the forensic and remediation process, and stresses the need to identify the full extent and root causes of building distress and to identify potential construction defects or omissions that may affect the available remediation options.

Background

The 5-story hotel was constructed from 2000 to 2001. Shortly following completion of the structure, settlement of the westernmost portion was reported in the range of 3 to 4-1/2 inches. The structural framing consists of a concrete slab-on-grade at the first floor and 8 inch thick HCP at the elevated floors, second through fifth. The HCPs are supported by reinforced CMU walls around the perimeter of the hotel and along the interior corridor; with the roof system consisting of plate connected wood trusses and plywood decking. The foundations consist of reinforced concrete continuous wall footings and isolated areas of spread column footings bearing on variably thick fill overlying sloping residual soils (Figure 1). A level survey from October 2005 indicated the maximum total settlement of the building was 11 inches at the southwest corner, as seen in the Figure 1 contours. Structural distress from the settlement was well hidden by the interior finishes and continued aesthetic repairs by

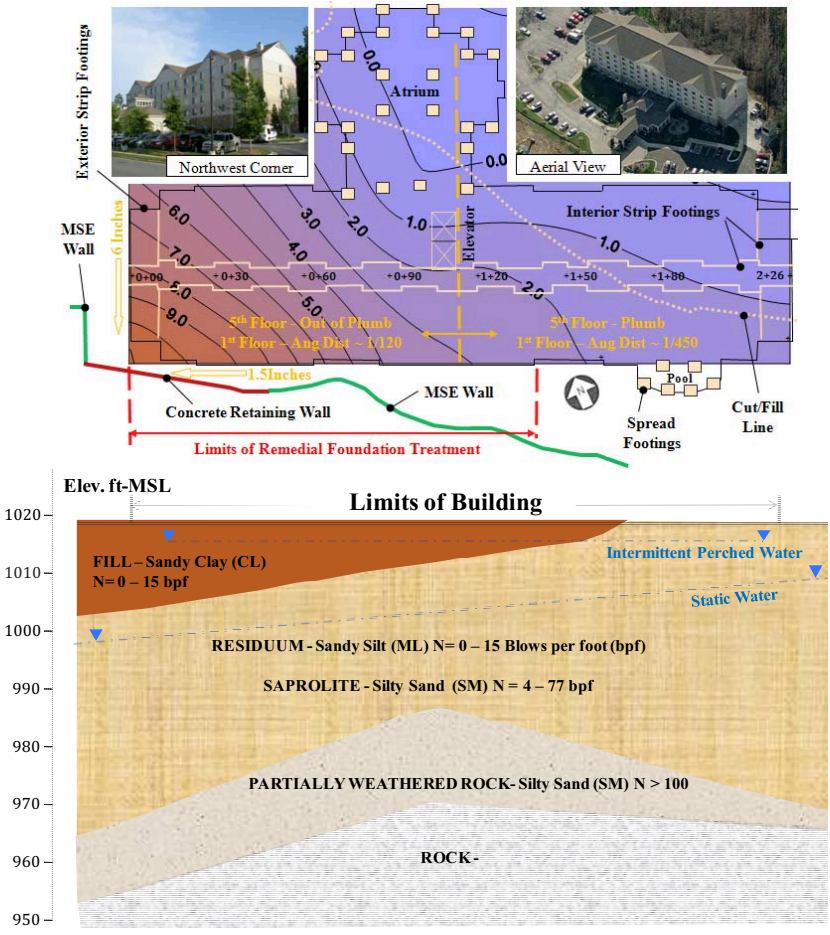

Figure 1. Upper: Layout with pre-remediation total settlement contours (in.), angular distortion, and 5th floor plumbness. Lower: Subsurface profile along main corridor.

the hotel maintenance staff. Prior to the authors' (Golder and WJE) involvement with the project, two other structural engineers had warned the hotel owner that additional building settlements would result in an unstable condition putting the building at risk of collapse. These assessments added urgency to the project and required Golder and WJE to quickly become familiar with the history of the building and assess the existing condition of the structural system. In addition to reviewing the available project documents and conducting an interior room by room survey, structural surveys were performed on the building exterior and roof framing. A subsurface

geotechnical investigation and corresponding laboratory testing were also conducted to assess the subsurface soil and groundwater conditions and to evaluate the depth to suitable bearing strata should deep foundation remediation be required.

Summary of Pre-Remediation Conditions

Only limited documentation and no survey data from the original construction of the building was provided to the team. Thus, an assumption that the floor slab was built to the design elevation was made to allow for evaluation of total and differential settlement magnitudes. In addition, only anecdotal estimates of the construction settlements and remedial actions were available, with no photographs or field reports found that clearly described the locations and magnitudes of the initial settlements, the resulting building damage, and whether remedial actions had been taken.

Geotechnical Pre-Remediation Conditions

The building is located in the Piedmont physiographic geologic province for which typical subsurface conditions consist of residual, saprolitic, and partially weathered rock materials generated from in place weathering of parent bedrocks that are most commonly granite or gneiss. As with many forensic geotechnical evaluations, access within the building for conventional machine-augered borings was limited, so a combination of investigation techniques was utilized, consisting of 12 exterior machine-augered borings (as per ASTM D 1586) to auger refusal (40 to 72 ft-bgs), two of which were completed as groundwater monitoring wells, and 9 hand auger borings through the 1st floor building slab advanced to hand refusal (2 to 14 ft-bgs) with incremental dynamic cone penetrometer testing (per ASTM STP 399).

Based on the historical review of project documents and the completed forensic investigation, the following pertinent observations were made regarding the pre-remediation geotechnical conditions:

- Continuous zones of very loose soils (SPT N values <4) were observed in both the fill and residual materials during pre- and post-construction investigations.
- Laboratory consolidation testing indicated the residual soils were 2.5 to 4 times more compressible than the moderately compressible fill soils, with both having high potential for secondary compression (long-term creep settlements).
- While the observed settlements were unusually high as compared to typical responses in this geology, they were in line with field and laboratory test results.
- Fill placement records indicated adequate compaction, and typical testing intervals; however, post construction investigations revealed very soft fill conditions, significant organic debris, and in-situ moisture contents well above optimum, leading to questions about the fill placement. Surface water control measures and the potential for leaking utilities were also investigated, to assess whether inundation from the observed perched water table could have factored in to the settlements via internal fabric collapse or other mechanisms.
- The building site was leveled using a variable fill thickness, and no state-of-practice engineering measures (e.g., preloading, post-fill delays, etc.) were implemented to control differential settlements prior to construction. The combination of variable fill conditions (from cut to 18 feet of fill), rapid

construction, and the highly compressible nature of the foundation and fill soils likely contributed significantly to the large differential settlements (see Figure 1).

Figure 2. Upper: Exterior wall to HCP connection detail and large void in keyway joint around reinforcing bar Lower: Separations and cracks in HCP at various areas.

Structural Pre-Remediation Conditions

The initial condition survey of the building interior and exterior was hindered by maintenance completed by hotel staff to correct aesthetic defects potentially caused by building settlements. Several rooms located just west of the central elevator core exhibited signs of extensive remedial work, racked door frames and separations between the HCPs, in addition to defects in the connections between the HCPs and the CMU walls and shear walls. Of these rooms, five were selected for a more detailed investigation involving the removal of select finishes to allow for exploratory openings. Subsequent follow-up investigations of six additional rooms were

completed to gain additional data and better gauge the extent of the conditions. The following conditions were typically noted, some of which are illustrated on Figure 2:

- Separated joints between HCPs
- Longitudinally cracked HCP with exposed prestressing strands
- Lack of reinforcing and grouted hollow cores at HCP to CMU wall connections
- Reduced bearing length at exterior and interior CMU walls
- Stepped and vertical cracks at re-entrant corners of exterior walls and interior corridor wall headers
- Areas of uninstalled No. 4 hooked bars at the HCP to CMU wall connections
- Voids in the grout around the No. 4 hooked bars at locations where installed
- Uninstalled No. 4 hairpin bars at the HCP to CMU shear wall connections

In March and August of 2006 two follow-up plumbness surveys were completed to verify previous data and to evaluate the exterior wall plumbness. Plumbness measurements of the corridor walls were also taken, which had not been measured in the previous surveys. The 2006 surveys were completed by removing a small area of the exterior insulation and finish system facade to allow direct measurement on the exterior CMU walls and slab edges. Prisms and a total station were used to shoot two points at each floor; one above, and one below the floor line. The plumbness survey showed that the maximum out-of-plumbness was 6 inches to the south and 4 inches to the west at the top of the 5th floor walls (see Figure 1), and that additional out-of-plumbness was occurring as settlement continued.

Remedial Repair Design

A remedial repair design was required to address multiple issues identified during the geotechnical and structural investigations, including: stabilization of the building foundations, repair of settlement induced building damage, and correction of construction defects.

Foundation Remedial Design

Several options for stabilization of the building foundations were evaluated with input and assistance from specialty geotechnical remediation contractors. The final evaluation of remedial options included: pressure grouting, compaction grouting, compaction grouted piles, underpinning with micropiles (pipe piles or push piers), and jet grouting. Comparative evaluation of alternatives considered cost (both remediation cost and impact on hotel revenue); long-term settlement control; uniformity of treatment; ease and accuracy of available verification monitoring; and applicability of the method given the site subsurface and building conditions. In the authors' experience, there are several issues unique to remedial design, as compared to conventional design, that should be considered during remedial option screening:

- Conducting thorough forensic evaluations to identify all mechanisms contributing to poor performance prior to the selection of a remedial option. The inherent redundancy of modern engineering codes and designs typically requires that multiple deficiencies exist at projects requiring remediation.

- When screening remedial options, consideration of stresses induced on existing structures from remedial work is important, and often results in the optimum remedial option differing from the optimum convention construction option.
- Accurate, cost effective, feasible, and accepted means of conducting construction quality control, assurance, and verification testing are paramount to success, as many remediation projects involve some level of litigation.
- Good communication between all involved parties, including properly educating the owner, is critical to ensure resolution of technical challenges, and to achieve owner satisfaction based on upfront discussions of risks and potential operational disruptions. In the current project, the owner's desire to keep the hotel in operation during remediation to maintain revenue flow and to retain key staff was a very high priority, which in the end outweighed stand alone remedial costs.

Based on the final evaluation of remedial options, pressure grouting was determined to be the least effective option, due to the possibility for uneven treatment, poor control, and inability to verify effectiveness. Compaction grouting was evaluated to provide good ground improvement but to not offer significant advantages for foundation underpinning. Conventional underpinning with micropiles or push piers required structural upgrades to the existing foundations, and would require installation from both sides of the strip footings to avoid inducing large eccentric loadings onto the footings and walls. Jet grouting was the most expensive option evaluated and had the potential to result in minor remediation induced settlements during load transfer. However, it was chosen because it allowed for underpinning from a single side of the strip footers since the large treatment diameter extended underneath the footing centerline, allowing work to predominantly occur from the exterior and within the main corridor, Figure 3. Ground improvement under the first floor slab was also considered, however, the owner opted to continue with monitoring and spot repairs as necessary due to the limited structural and safety hazards associated with additional slab settlements.

Structural Remedial Design

During the repair design, an analysis of the out-of-plumb perimeter and corridor walls was performed using calculated axial loads and the known out-of-plumbness to evaluate the additional moments induced on the walls. The axial loads and moments were then plotted on interaction diagrams to evaluate if the walls were still within acceptable values for combined axial loads and bending moments. The analysis showed that all walls were still within acceptable limits; however, repairs to damaged portions of the structure and of as-built construction deficiencies were still required.

Of primary importance was stabilizing the foundation from further movements, as the introduction of additional eccentricity would lead to unacceptable loading conditions. Also of concern were the large separations at the HCP joints, and the as-built deficiencies at the HCP and CMU wall and shear wall connections. Re-establishing continuity of the load path between the walls, diaphragm, and shear walls was vital to future stability and performance if the building was to remain in its eccentric state. To

accomplish this, retrofit repairs would be required at each of these three connections to repair settlement induced damage and as-built construction deficiencies.

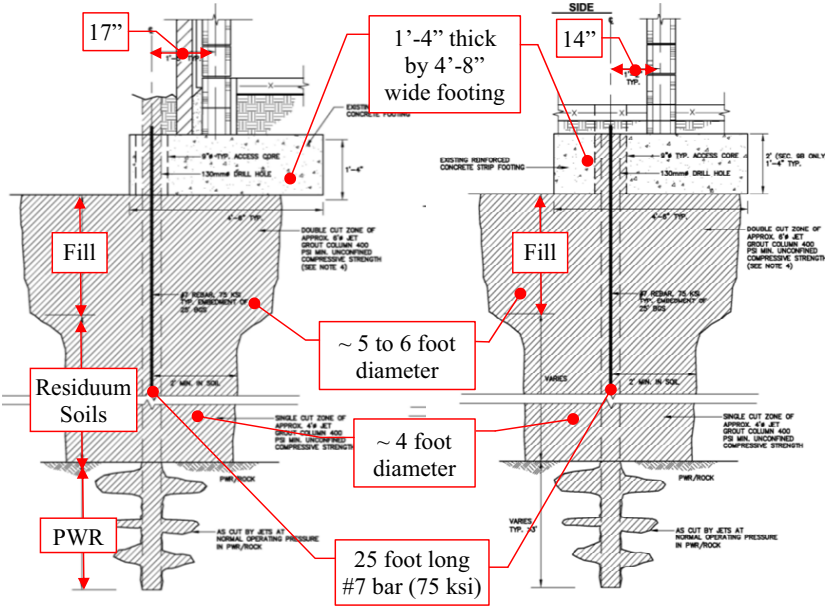

Figure 3. Jet grout column details and installation photos.

The options for retrofitting the connection between the HCP and the CMU walls were limited. Based on the forensic investigation, missing reinforcing bars and poorly grouted keyway joints were observed at the perimeter CMU wall connections, and no reinforcing bars were found at the corridor CMU wall connections. An option that was considered was identifying the locations of all missing bars using non-destructive testing equipment such as an electromagnetic rebar detector and intrusively inspecting the bar and grout at all other locations for voids. If voids were found around the bar, the joint could be remediated by further chipping and regrouting. However, this option did not address several issues, such as locations of short plank bearing on the walls and a different retrofit would still be required in areas with missing reinforcing bars. Based on these factors, the chosen remedial design used a steel angle bracket installed between the plank and the bond beam at the top of the wall at each keyway joint. This repair, while simple, addressed several issues: it supplemented the connection between the wall and the plank, it extended the bearing length of the plank, it was easy and quick to install, and it also supplemented the connection between the floor diaphragm and the shear walls.

Figure 4. Left and Bottom Right: Structural repairs between HCP plank joints
Upper Right: Steel angle bracket between CMU wall and HCP plank.

Areas where longitudinal cracks and separations had occurred within or along HCP joints were also discovered. The repairs were initially designed to be chipped out and regrouted if the separation was larger than 1/4 inch or to be epoxy injected if it was smaller than 1/4 inch. During remediation, the contractor had difficulty with the epoxy grouting and an alternative repair was developed. The alternative consisted of chipping out a small area of the open cell on each side of the keyway joint at 4 feet

on center and grouting a U-shaped reinforcing bar hairpin in place between the joints. The repair, while more disruptive and labor-intensive, was quick and easy to install.

Implementation of Remedial Design

The selected remedial designs were implemented in stages, with the foundation remediation conducted first so that structural repairs could be completed after the building was stabilized. At the request of the owner, the hotel was to remain operational during the repairs, with first floor rooms in the west wing taken out of service during the interior foundation repairs and additional rooms taken out of service on a rotating basis as necessary during structural repairs. The owner decided to proceed with plans for an interior remodel that was scheduled for the next few years. Against the recommendations of WJE, a remodeling contractor with minimal structural repair experience was selected to perform both the remodeling and structural repair work. As a consequence, more involvement and oversight by WJE was required, especially during the early work phases. Figure 4 illustrates some of the implemented structural repairs.

Jet grouting is a ground improvement process that uses high pressure fluid jets in combination with grout impregnation and mixing to create soilcrete columns. Jet grouting was completed using a triple phase jet grout process with a combination of two drill rig systems: (1) exterior locations enabled the use of a larger drill rig capable of faster production and (2) interior jet grout columns required the use of a specialized miniature electric powered, remote control operated drill rig capable of working in the space constraints of the hotel hallways. The jet grouting process was electronically controlled and monitored by a centralized control center consisting of the pumps, mixers, accessories, electronic controls, and recording devices.

Prior to production jet grouting, three geometric test columns were constructed utilizing different operating parameters to find the optimum rotation rate, lift rate, and treatment frequency for the site soil conditions. Each of the test columns were exhumed and examined for evaluation of the trial production parameters. Additionally, a non-production load test jet grout column was constructed and loaded to 1.5 times the design capacity of the columns as per the project specifications; with load test results showing deflections of 0.07 and 0.10 inches under the design and 1.5 times the design load, respectively. A total of 93 production jet grout columns were installed under the western portions of the building foundations to underpin and stabilize the structure. Some lessons learned or reinforced were:

- Based on the geometric test columns evaluation, it was found necessary to provide double jet-grout treatment in the upper more clayey fill soils to ensure more homogeneous soilcrete columns that achieved the 4 foot minimum design diameter. The double treatment limited the size and quantity of unmixed soil clods within the finish soilcrete columns which can act as weak zones, and is an effective procedure to improve jet grout effectiveness in fine grained soils.
- Handling of jet grouting cuttings efficiently and effectively is often the key to jet grouting production and success. The current site allowed for a slurry pit to be

dug in a portion of the hotel parking lot for waste management, and had a nearby lot for temporary cuttings storage which simplified operations and efficiency.
- Significant wood debris (up to 4 inches in diameter) were encountered during jet grouting (potentially indicating poor quality fill) resulting in many clogs to the vacuum lines used to manage the jet grout cuttings. This problem was overcome by conducting a "pre-cut" of the upper area directly under the footing to open up an area for the wood to accumulate without clogging the return feed that could then be cleaned during column completion, if necessary.

Conclusions and Lessons Learned

- The hotel was able to stay in operation and maintain high occupancy rates during the remedial activities, which resulted in significant overall cost savings to the owner and was a driving force behind the selected remedial option alternative. The success of the remedial work in and around an operating hotel highlights the importance of communication and teamwork between all parties during forensic investigations and subsequent remedial repairs.
- A qualified and experienced contractor, familiar with the specified materials and products is important to successful and timely completion of remedial repairs.
- Both the original and early post-construction geotechnical investigations at the site focused on the fill as the likely primary mechanism for settlement. Based on a more exhaustive subsurface and laboratory forensic evaluation it was estimated that approximately 60% of the site settlement occurred within the residual soil below the fill, and that data gaps existed in the earlier investigations due to their incomplete scope of investigation into all potential mechanisms. This example stresses the importance of not limiting forensic investigations by biased or otherwise pre-conceived notions, providing an example of economic and schedule efficiency by conducting thorough forensic investigation at the onset of observed poor performance so that all contributing factors can be discovered and addressed.
- The observed differential settlements, while atypical for the region, could have been predicted considering the applied loads and the site subsurface conditions. While economic and schedule constraints limit the type and extent of investigations and engineering analyses completed in support of designs, engineering consultants should use their experience, preferably in the earliest stages of projects, to identify potential conditions which, if encountered, will require additional, more thorough or robust investigation. Design professionals should maintain professional diligence when atypical conditions are encountered by educating their client about potential risks associated with forgoing these more robust assessments.
- This case study highlights the benefits of joint geotechnical and structural participation throughout the forensic and remediation process, and stresses the need to identify the full extent and root causes of building distress and to identify potential construction defects or omissions that may affect the available remediation options.

Optimization of Compaction Grouting in Collapsible Soils

Jason M. Cumbers, P.E., M.ASCE [1], Eileen M. Dornfest, P.G., CEG[2],
Daniel D. Overton, P.E., F.ASCE [3], Joe Harris[4]

[1] Project Engineer, Soil and Materials Engineers, Inc., 3301 Tech Circle Drive, Kalamazoo, Michigan, 49008 USA, 269-323-3555. cumbers@sme-usa.com

[2] Senior Engineering Geologist, Engineering Analytics, Inc., 1600 Specht Point Road, Suite 209, Fort Collins, Colorado 80525 USA, 970-488-3111. edornfest@enganalytics.com

[3] Principal Geotechnical Engineer, Engineering Analytics, Inc., 1600 Specht Point Road, Suite 209, Fort Collins, Colorado 80525 USA, 970-488-3111. doverton@enganalytics.com

[4] Vice President, Hayward-Baker, 11575 Wadsworth Blvd., Broomfield, CO 80020, 303-469-1136

ABSTRACT

Six multi-family residential buildings consisting of wood frame structures founded on post-tensioned slabs-on-grade were constructed in approximately 1995 in Basalt, Colorado. Collapsible soils had been identified at the site, in geohazard evaluations, as early as 1976 and a pre-construction geotechnical investigation indicated that the silty clay soils at shallow foundation depths could have high collapse potential when wetted. The buildings experienced between 4.8 and 13.0 cm (1.9 and 5.1 in.) of differential settlement between 1995 and December 2006. Compaction grouting test pads were constructed and pre- and post-grouting analyses of the soils were conducted to quantify changes in moisture content, density, compressive strength, and collapse potential of the soils. Introduction of water into the soils prior to grouting played a significant role in the improvement of soil conditions under the buildings. The grouting methodologies are summarized, and the resulting soil improvement at the test pads and stabilized buildings is discussed.

INTRODUCTION

Six multi-family residential townhomes consisting of wood frame structures founded on post-tensioned slabs-on-grade were constructed in approximately 1995 at the subject site in Basalt, Colorado, at the location shown in Figure 1. Collapsible soils were identified in the vicinity of the site as early as 1976 (Miller, 1976), and the pre-construction geotechnical investigation determined that collapsible soils existed at the site. Evidence of distress related to building settlement was first observed in approximately 1997.

A geotechnical investigation was conducted after excessive movement had occurred at the site in order to: 1) identify locations of collapsible soils at the site, 2) determine the future performance of the structures without foundation stabilization, and 3) evaluate compaction grouting as an alternative for foundation stabilization. The

investigation included drilling of exploratory borings across the site, collection of samples for laboratory testing, installation of moisture-access tubes, geological site reconnaissance, geotechnical laboratory testing, review of historic documents, and geotechnical analyses.

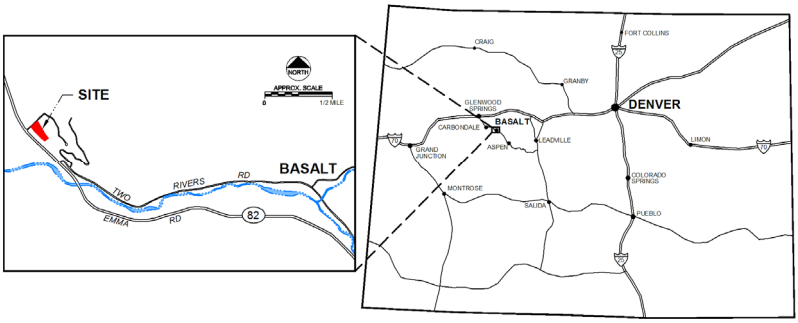

FIG 1. Location Map

GEOLOGIC SETTING

The site is located in the Roaring Fork river valley in central-western Colorado in the Southern Rocky Mountains physiographic province. The structures are constructed on Quaternary debris flow deposits and colluvial deposits derived from the Quaternary landslide deposits upslope and to the east of the site (Kirkham, et al., 1998 and Streufert et al., 1998). The subsurface materials at the site consist of moderately sorted sands, silts, and clays overlying fluvial gravels. The depth to the fluvial gravels ranges across the site from 5.5 to 11.9 meters (18 to 39 feet).

Collapsible soils are a common hazard in the area of the Roaring Fork River corridor. Collapsible soils are commonly found in arid to semi-arid environments where poorly indurated, clay- and silt-rich sedimentary rocks are present (White, 2003). The debris flow sediments at the site were generated from upslope landslide deposits. Debris flow deposits are typically deposited quickly and then quickly dry out before subsequent deposition takes place (White, 2003). This rapid desiccation leads to an open soil structure, with voids that can be seen with the naked eye as shown in Figure 2. Such voids were identified in the soils at the site. These soils have a relatively high apparent strength when dry, but the open structure collapses upon subsequent loading and/or addition of water.

BUILDING PERFORMANCE – PAST AND FUTURE

The buildings were constructed in 1995 on shallow post-tensioned slab-on-grade foundations on the native soils. Evidence of distress related to building settlement was first observed in 1997. Differential vertical settlement at each of the buildings at the site ranged from 4.83 to 12.95 cm (1.9 to 5.1 inches) from 1995 to December, 2006. Significant cosmetic distress was evident in several of the buildings, in the

form of cracked drywall, racked doorways and windows, separations between floors and walls, and perceivable sloping floors and ceilings.

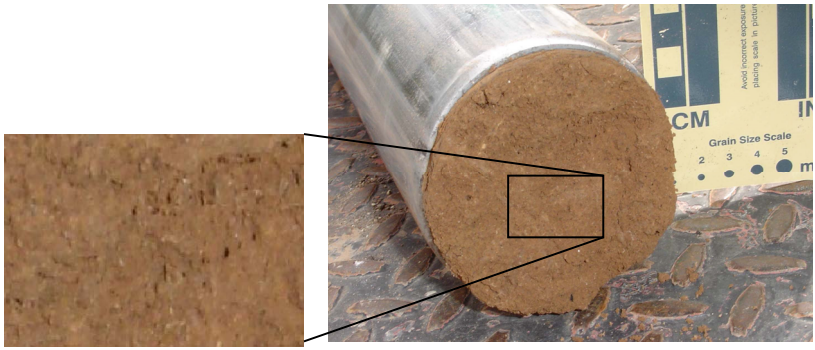

FIG 2. Photograph of a Typical Collapsible Soil Sample, with Visible Pore Spaces

Post-construction geotechnical investigations were conducted in 2004 and 2006 to evaluate the future performance of the structures. The collapse potential was calculated based on the soil profile encountered in each of the borings, and the results of the geotechnical laboratory investigation. Calculation of the collapse potential of a given layer in the soil profile was calculated by multiplying the percent collapse measured in the laboratory for each soil sample from a given layer by the thickness of that layer. The total collapse potential for each profile was then calculated by summing the collapse potential of the individual layers within the profile.

Results of the analyses indicated that collapse potential at the site ranged from 0.51 to 64 cm (0.2 to 25.2 inches). Results of the analyses of future collapse potential, in combination with relative elevation surveys at each building to determine current building out-of-levelness and future potential out-of-levelness were evaluated to determine which buildings would need to be repaired. It was determined that four of the six buildings would require foundation stabilization to perform adequately in the future, and compaction grouting was chosen as the preferred foundation stabilization alternative.

COMPACTION GROUTING TEST PADS

Compaction Grouting Theory

The goal of the compaction grouting mitigation was to reduce the total collapse potential such that if future potential collapse were to occur, it would not result in unacceptable performance of the structures and post-tensioned slabs. Degrees of saturation measured on samples obtained at the site in 2004 generally ranged from 30 to 80 percent. Data presented by Houston (1988) shows that a percentage of full collapse occurs as a result of partial wetting, and for a degree of saturation as low as 60%, the percent of collapse ranges from approximately 88% to 98% of the fully

wetted collapse potential. Thus, during remediation by compaction grouting, the goals are to increase the water content enough to cause a significant amount of the potential collapse to occur during the grouting process, and to densify the soil.

Compaction Grout Test Pads and Baseline Conditions

Four test pads were constructed at the site to determine the effectiveness of various methods of compaction grouting. Test Pads 1 and 2 were drilled with air rotary drilling methods and grouted with Hayward-Baker's standard method of compaction grouting. Test Pads 3 and 4 were drilled with rotary wash methods in order to increase the moisture content and compressibility of the soils and modifications were made to the compaction grout sequence, injection volumes and pressure criteria.

Borings were drilled to depths of 8.53, 7.92, 8.99 and 6.40 meters (28, 26, 29.5 and 21 feet) prior to grouting at Test Pads 1 through 4, respectively. Samples were obtained during drilling using Shelby Tubes and California Samplers. Laboratory testing was performed on the samples to determine pre-grouting moisture content, density, unconfined compression, and collapse potential. Moisture-access tubes consisting of vertical PVC casing were installed at each test pad to allow for insertion of a downhole nuclear moisture/density probe for the purpose of measuring the in-place water content and density of the soil surrounding the borehole before and after compaction grouting. A CPN model 501DR downhole nuclear density probe was lowered to the bottom of each tube and measurements of in-situ moisture content and density of the soil were determined at 0.61 meter (2-foot) intervals over the profile. Due to large variations in the soil density and moisture content, the readings displayed significant scatter and were difficult to quantify.

Compaction Grouting of Test Pads

Test Pads 1 and 2 were drilled with rotary air methods to the underlying river gravels and grouted by pumping low-slump, Portland cement grout through the drill casing that were left in place upon completion of grout hole drilling. In general, 0.14 cubic meters (5 cf) of grout was injected per 0.3 meters (1-foot) of hole depth, and the grout pipe was withdrawn in 0.3 meter (1-foot) increments once the desired injection volume or pressure had been achieved. The grouting was performed until one or more of the following cutoff criteria were obtained.

- Quantity: when 0.14 cubic meters (5.0 cf) of grout was injected per 0.3 meters (1 foot).
- Pressure: when 3,447 kPa (500 psi) was recorded at depths greater than 9.1 meters (30 feet), or when a pressure reading of 2,413 kPa (350 psi) was recorded at shallower depths.
- Movement: when undesirable movement of the slabs or ground surface was detected.

After reviewing the post-grouting collapse results from Test Pads 1 and 2, a second pair of test pads with a modified grouting procedure was proposed to improve the results. Test Pad 3 was located near Test Pad 2 in order to directly compare results of the two compaction grouting methods. Test Pad 4 was located near a third building in

order to optimize the compaction grouting procedure at that building. The modifications from the previous grouting procedure consisted of the following:

- Drilling was performed with rotary-wash drilling methods and the drill rods were left in place for 24 hours after drilling to allow the water to infiltrate into the soils.
- The grout hole grid was modified to result in less space between adjacent grout holes than at Test Pads 1 and 2.
- The sequence of grouting was modified from that performed at Test Pads 1 and 2. Grouting of the perimeter holes was performed first in order to provide confinement to the test pad, followed by grouting of the center holes.
- The minimum grout volume was increased to 0.65 m^3/m (7.0 cf/ft) for grout pressures less than 1,034 kPa (150 psi).

The average volume of grout injected at Test Pads 1 through 4 was 0.28 m^3/m (3.0 cf/ft), 0.35 m^3/m (3.8 cf/ft), 0.36m^3/m (3.9 cf/ft), and 0.33 m^3/m (3.6 cf/ft), respectively. These quantities were less than the volume cutoff criteria, because in many locations the pressure criterion was reached before the volume criterion. Post-Grouting test holes were drilled at each of the four Test Pads a minimum of 9 days after grouting was completed.

RESULTS OF TEST PAD STUDY

Monitoring of Moisture-access Tubes

Samples were collected during drilling for measurement of water content and dry density at each of the moisture-access tube locations. In addition, water content and total density was measured at each of the moisture-access tube locations both before and after compaction grouting. Table 1 shows the average increase in total unit weight at each of the test pads, as a result of compaction grouting. As shown in Table 1, an increase in unit weight of 1.1 and 1.7 % was obtained at Test Pads 1 and 2, respectively, and an increase in unit weight of 4.3 and 4.2 % was obtained at Test Pads 3 and 4, respectively.

Table 1. Increase in Unit Weight as a Result of Compaction Grouting

Test Pad No.	*Moisture-access Tube*	*Distance from Closest Compaction Grout Column m (ft)*	*Average Increase in Total Unit Weight (%)*
1	MA-1	1.72 (5.6)	+1.1
2	MA-2	1.62 (5.3)	+1.7
3	MA-3A	1.72 (5.6)	+4.3
4	MA-4A	1.72 (5.6)	+4.2
4	MA-4B	2.29 (7.5)	+3.4

Collapse Potential

The future collapse potential was calculated for pre-grouting and post-grouting test holes in Test Pads 1 through 4, in order to determine the effect of the compaction grouting on the collapse potential of the soil. The collapse potential was determined by saturation at overburden pressure. The gravimetric water content and collapse potential with depth for the soil profiles at Test Pads 1 through 4 are shown on Figures 3 through 6, respectively. Table 2 summarizes the results of the collapse potential for each boring location. The different drilling and grouting methods applied at Test Pads 3 and 4 resulted in a significant decrease in collapse potential from that resulting from compaction grouting at Test Pads 1 and 2. One plausible explanation for the poor results at Test Pads 1 and 2 is that the air rotary drilling methods may have disturbed the sensitive site soils and resulted in a greater collapse potential after drilling and grouting was performed.

Table 2. Summary of Predicted Collapse for Test Pads 1 through 4

Test Pad No.	*Boring ID*	*Collapse Potential Before Grouting* cm (inches)	*Collapse Potential After Grouting* cm (inches)
Test Pad 1	MFG-GP1A	21.8 (8.6)	-
	MFG-GP1B	-	49.8 (19.6)
Test Pad 2	MFG-GP2A	12.2 (4.8)	-
	MFG-GP2B	-	16.0 (6.3)
Test Pad 3	MFG-3	30.2 (11.9)	-
	MFG-3C	-	0.5 (0.2)
Test Pad 4	MFG-11	5.1 (2.0)	-
	MFG-4C	-	2.0 (0.8)

Conclusions of the Test Pad Study

Results of the test pad study indicated that compaction grouting performed in general accordance with the procedures followed at Test Pads 3 and 4 resulted in an increase in total unit weight of the soil profile, as well as a significant reduction in total potential collapse. Additionally, samples from Test Pads 3 and 4 tested for unconfined compressive strength showed increases in strength ranging from 60 to 181%, as a result of compaction grouting.

FOUNDATION MITIGATION USING COMPACTION GROUTING

Compaction Grouting Plan and Specifications

Geotechnical analyses of the test pad data indicated that a more robust compaction grouting procedure would be needed to obtain a more consistent level of soil improvement during foundation mitigation. The compaction grouting specifications for remediation stated that the grout holes were to be drilled with water and left for 24 hours prior to grouting to allow for the water used during drilling to infiltrate into the

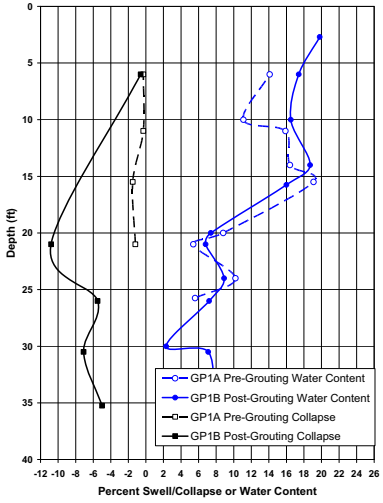

FIG 3. Collapse and Water Content Before & After Grouting at Test Pad 1

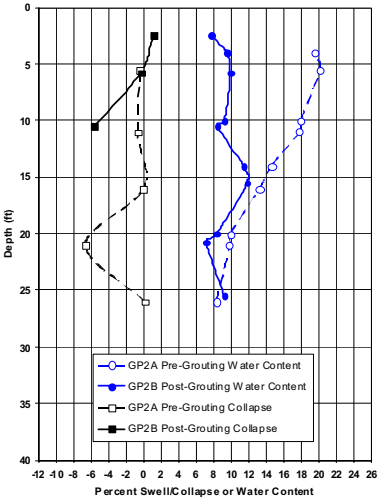

FIG 4. Collapse and Water Content Before & After Grouting at Test Pad 2

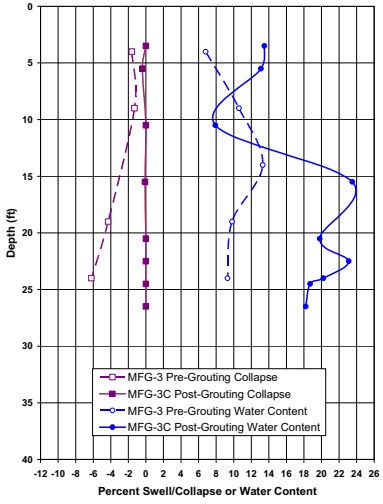

FIG 5. Collapse and Water Content Before & After Grouting at Test Pad 3

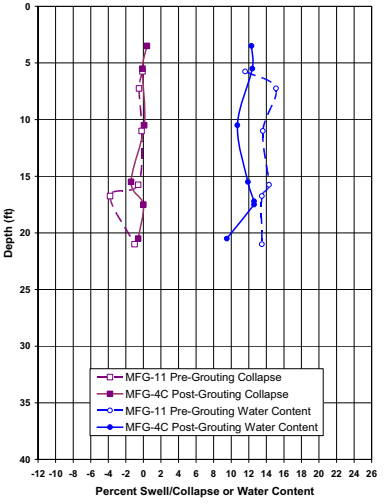

FIG 6. Collapse and Water Content Before & After Grouting at Test Pad 4

soils. The grout injection rate was specified as a maximum of 0.06 m^3 (2.0 cubic feet) per minute due to the clayey nature of the site soils. The grout pipes were installed to the underlying gravels and the holes were grouted in one-foot increments until one or more of the following cutoff criteria was obtained:

- Quantity: when 0.14 m^3 (5.0 cubic feet) of grout was injected per 0.3 m (1 foot).
- Pressure: when 3,447 kPa (500 psi) was recorded at depth greater than 9.14 m (30 feet), or when a pressure reading of 2,413 kPa (350 psi) was recorded at shallower depths. Grouting pressures below 1,034 kPa (150 psi) required that grouting continue until a minimum of 0.28 m^3 (10 cubic feet) of grout was placed.
- Movement: when undesirable movement of the structure was detected.

Post Grouting Verification Soil Borings

Two borings were drilled approximately four months after the completion of grouting at each building to collect samples for laboratory testing and analysis of post-grouting soil conditions. The boreholes were advanced to the underlying river gravels and Shelby tube samples were collected for laboratory testing at 0.61 meter (2-foot) intervals. A summary of some of the post-grouting laboratory test results are included in Figures 7 and 8.

Soil Improvement through Grouting

Figure 7 depicts a comparison between the collapse potential and the gravimetric water contents of the pre- and post-grouting boreholes at Building A. The pre- and post-grouting boreholes were located approximately 20 feet apart. Of particular interest is the significant increase in water content corresponding to a significant decreases in collapse of the post-grouting samples. The subsurface profile contains up to 78% fines, with the percentage generally increasing toward the bottom of the borehole. The average increase in total unit weight over the profile was 29%.

Figure 8 depicts a comparison between the percent collapse and the gravimetric water contents of the pre- and post- grouting boreholes at Building B. Based on the laboratory test results, improvement was observed to a depth of 4.3 m (14 ft) below the ground surface. However, below that depth the samples indicated lower water contents than the upper soils and post-grouting collapse of samples tested ranged from 3.5% to 6.3%, indicating the potential for collapse had not been reduced. While the percentage of fines did not appear to vary significantly between the top and bottom of the profile at Building B, the percentages of fines in the samples collected at Building B are significantly greater than the samples collected at Building A. The results appear to indicate that as the fines content of the samples exceeded 80%, the soil improvement achieved by grouting was significantly reduced.

The reduction in total potential collapse at Buildings A and B are summarized in Table 3. A significant reduction in collapse potential was observed at both buildings, although the remaining total future collapse potential is much less at Building A than Building B.

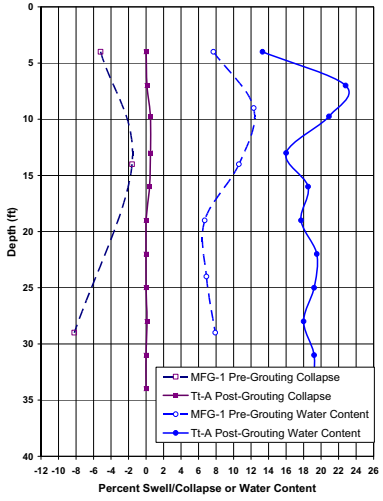

FIG 7. Pre- and Post-Grouting Collapse Potential and Gravimetric Water Content with Depth – Building A

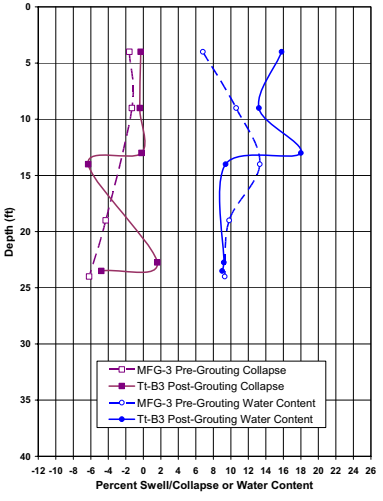

FIG 8. Pre- and Post-Grouting Collapse Potential and Gravimetric Water Content with Depth – Building B

Some confirmation of the stabilization was indicated for the lower soils at Building B by the unconfined compression results of one sample from 5.5 m (18 ft) and one sample from 7.2 m (23.5 ft) with unconfined compressive strengths of 406 kPa (8,480 psf) and 246 kPa (5,142 psf) respectively. These results are more than twice the unconfined compressive strength values determined for post-grouting samples at Test Pad 3, 102.1 kPa (2,132 psf).

Table 3. Summary of Predicted Collapse for Buildings A and B

Building	*Pre-Grouting Boring*	*Collapse Potential Before Grouting cm (inches)*	*Post-Grouting Boring*	*Collapse Potential After Grouting cm (inches)*
A	MFG-1	64 (25.2)	Tt-A	3.8 (1.5)
B	MFG-3	29.2 (11.5)	Tt-B	12.4 (4.9)
			Tt-B2	15.0 (5.9)
			Tt-B3	14.0 (5.5)

CONCLUSIONS

The conventional method of air rotary drilling of compaction grouting boreholes and subsequent grouting resulted in a negligible improvement in soil conditions at the site. The modified compaction grouting procedure, consisting of rotary wash drilling of the boreholes, allowing the drill rods to remain in place for 24 hours prior to compaction grouting, and modification to the volume and pressure injection criteria, resulted in a significant improvement of soil conditions during both the Test Pad Study and the foundation stabilization. Using the modified grouting procedure, collapse potential of the soil profiles was reduced by 3.0 to 62.5 cm (1.2 to 24.6 in) from pre-grouted conditions. Furthermore, increases in total density and unconfined compressive strength were also observed during both the Test Pad Study and the foundation stabilization.

Infiltration of water into the soils played a significant role in the improvement in soil conditions resulting from the modified compaction grouting procedure. Infiltration of water from the drilling procedure into the surrounding soils allowed for the softening and degradation of the internal soil strength and therefore an increase in the compressibility of the soils. This resulted in the soil accepting larger volumes of grout and an overall improvement in densification over that resulting from dry air rotary drilling and grouting methods. Review of the data indicated that as the fines content of the samples exceeded 80%, soil improvements were significantly reduced. This is theorized to be in response to the lower permeability and thus reduced water migration into the clay soils.

REFERENCES

Houston, S.L. (1988). *Pavement Problems Caused by Collapsible Subgrades. Journal of Transportation Engineering*. Vol. 114. No. 6. November. Paper No. 22902.

Kirkham, R.M., Widmann, B.L., and Streufert, R.K. (1998). *Geologic Map of the Leon Quadrangle, Eagle and Garfield Counties, Colorado.* Colorado Geological Survey Open-File Report 98-3. 1:24,000 scale.

Miller, A.E.. (1976). *Environmental and Engineering Geologic Map for Land Use.* Sheet No. 10E. 1:24,000-scale. In Charles S. Robinson & Associates, Inc., Snow Avalanche Hazard, Environmental and Engineering Geologic and Geologic Resource Maps, Eagle County, Colorado.

Streufert, R.K., Widmann, B.L., and Kirkham, R.M. (1998). *Geologic Map of the Basalt Quadrangle, Eagle, Garfield, and Pitkin Counties, Colorado.* Colorado Geological Survey Open File Report 98-1.

White, J.L., (2003), Collapsible Soils in Colorado, *In* Boyer, D.D., Santi, P.M., and Rogers, W.P., editors, Engineering geology in Colorado: contributions, trends, and case histories: Association of Engineering Geologists Special Publication 14 and Colorado Geological Survey Special Publication on CD-ROM.

Rethinking Waterproofing for Subsurface Structures

Clinton Deckard[1]
Peggy Hagerty Duffy[2], PE

[1]President, Construction Solutions, LLC, 229 Walnut Street, Jeffersonville, Indiana 47130
cdeckard@construct-solutions.com 812-725-7580 fax: 812-725-7584
[2]President, Hagerty Engineering, Inc., Vice President, Construction Solutions, LLC, 229 Walnut Street, Jeffersonville, Indiana 47130 pduffy@construct-solutions.com 812-725-7580 fax: 812-725-7584

ABSTRACT

Waterproofing for subsurface structures long has been accomplished using standard practices that typically are determined by cost and routine practice, regardless of the potential ramifications of poor functioning or failure. Repair measures for waterproofing often also follow faulty procedures that attempt to control water flow.

Experience with evaluating seepage problems has revealed inherent flaws in many of these standard procedures. Numerous projects involving seepage in areas with heavy groundwater flow have led to the conclusion that sump pumps and trench-type drain systems do not provide suitable control of water and often are relied upon with disastrous results.

A new approach to waterproofing proposes using crystalline concrete and various bentonite-based materials to prevent water from penetrating subsurface structures or to prevent water from seeping from subsurface structures. More advanced methods have been developed to arrest seepage where flow is heavy and cannot be stopped long enough to install waterproofing materials.

INTRODUCTION

Traditional Post-Construction Waterproofing Methods

Waterproofing subsurface concrete structures has been performed in a variety of ways for many years. Methods applied during construction range from spray-on petroleum-based products intended only to act as dampproofing to relatively expensive liners and surface treatments, such as bentonite sheets, that require very careful installation. The success of most methods applied during construction depends heavily on the diligence and experience of the personnel specifying and installing the chosen system. Even with careful planning and field supervision, conventional waterproofing methods often fail when the structure in question is subjected to significant water pressure.

Post-construction waterproofing involves even more difficulties than construction-phase activities. Many post-construction waterproofing projects take place because of seepage or flow that causes significant structural and/or cosmetic damage before the need for protection from water is identified. The subsurface orientation means that any work needed to be performed on the exterior of the structure will require excavation, possible

temporary retention, and potential underpinning of adjacent structures. In addition, most conventional waterproofing methods cannot be installed in flowing water.

Sump pumps long have been used to collect and discharge water flowing into subsurface structures. Older structures typically would include floor slabs sloped to drain toward the sump so that any water infiltrating the subsurface space would be directed toward the sump and be pumped out to a storm sewer or other exterior location. Basement wall cracks and other seepage points sometimes were allowed to seep, in unfinished spaces, and drain to a sump. In many instances, however, seepage points have been injected with epoxy or with urethane foam to arrest the inflow. Combined systems have become popular, particularly in the past 20 years, in which plastic sheeting is used to cover a seepage point so that the inflow is directed to a system of subsurface drains, usually located around the perimeter of the subsurface structure. The premise is that the seepage or infiltration is directed to the drains and then transported to a sump, where a pump discharges the water to some exterior location. The subsurface drains often are placed below the interior floor slab surface, and a thin layer of concrete is poured over the drains so that they are not visible.

Membranes and bentonite sheets usually are not considered for post-construction waterproofing projects due to the complications involved with excavating on the exterior of the structure and difficulties in replacing backfill in a constrained area without damaging an applied material.

Problems

The drawbacks to most commonly implemented waterproofing methods range from durability to capacity to tendency to increase health risks. The severity of the problems typically is proportional to the volume of seepage involved.

Epoxy injection can be successful in sealing concrete cracks and other seepage points subjected to moderate inflow. However, epoxy should be injected in a dry environment, and temporarily diverting or arresting inflow can be a significant problem. In addition, epoxy becomes brittle over time; experience with numerous cases of epoxy injection suggests a typical lifespan of about two to five years. Minor movement of the structure in question can cause the epoxy to shear and begin seeping again.

Urethane injection depends upon suitable displacement of compressible materials on the exterior of a subsurface structure without actually being able to see the area to be filled. Urethane foam is injected into a crack or other seepage point, and the theory is that the foam extends into any void spaces in the subsurface materials (soil, rock) and creates a barrier so that water cannot enter the same seepage point again. Unfortunately, injection often leads to reorientation of groundwater flow conditions outside the structure, and the new flow conditions can create erosion channels that allow new avenues for seepage to reach discontinuities in the exterior of the subsurface structure. Urethane foam also should be installed in dry conditions, so use of this method is difficult in situations of heavy inflow.

Any methods relying upon a sump pump for regular use are by nature dependent upon a power supply. Sump pump problems often occur during power outages caused by heavy rainfall events, at the very time when water removal is critical. Battery backup units can be purchased but are expensive. Furthermore, heavy inflow into a sump can wear out a pump quickly, necessitating frequent pump purchases and high costs.

Trench type systems rely on a pump and are, as such, susceptible to the aforementioned limitations and problems. These systems also include an inherent risk generated by unknowns associated with the seepage rate. Frequently a trench-type waterproofing system is installed after a heavy rainfall event when interior flooding occurs, or after persistent seepage has created a problem within a subsurface structure. Sizing of the trenches usually is accomplished based on observations of seepage or flow rates at the time. Some companies only use one size trench or trench pipe. Problems occur when future seepage or flow rates are greater than what can be handled by the trenches. At that point, water typically will back up at the floor-wall joint, usually at the base of some crack or other point of seepage that has been covered with plastic to direct seepage into the trench. Predicting future subsurface seepage rates can be very difficult, particularly in areas underlain by solutioned rock, such as limestone, where groundwater flows from a large subsurface watershed area. Hydraulic conditions in a karst terrain can lead to highly variable subsurface flow rates and volumes. As such, a seepage condition handled adequately by a trench type system for several years can change significantly during a period of heavy precipitation, overwhelming the waterproofing system and flooding the subsurface structure.

A secondary problem associated with trench-type systems is caused by the fact that water is directed into the interior of the subsurface structure, increasing the humidity and carrying with it mold and similar organisms that promote health problems. Inspection of many of the plastic “barrier” sheets removed from malfunctioning systems has encountered significant mold growth, as well as soils squeezing in from the exterior of the structure.

ALTERNATIVE METHODOLOGY

Crystalline Concrete

Repeated exposure to malfunctioning waterproofing systems led to an evaluation of possible alterative methods using existing and new technology. Crystalline concrete materials were tested and applied to determine if the technology could be used to provide a more durable waterproofing system that would prevent water from entering subsurface structures.

Crystalline concrete materials are produced by several manufacturers and are composed of proprietary blends of organic compounds and cementitious materials that react with unhydrated cement in concrete to grow long needlelike crystals within the void spaces in concrete. When crystalline materials are applied to the surface of concrete or are used to

fill a void space in a concrete structure, the crystals will grow out into the surrounding concrete, forming a barrier at the interface. Crystalline materials are hydrophilic, so they require exposure to water to be activated. Any minor recracking of concrete treated with crystalline materials will cause new crystals to form, effectively generating a perpetual resealing function. The original development of crystalline concrete took place in the 1940s and was designed for the concrete repair market. Product development has evolved over the years to include slurry coats, crack repair materials and methods, and admixtures for new construction.

Methodology

Most crystalline manufacturers publish standard crack repair methods, so these methods were followed to seal several conventional cracks in concrete basement walls over a 3- to 4-year period. None of the cracks involved ongoing foundation movement. The separations were chipped out with a concrete chipping hammer to produce a rectangular cut on the inside of each of the basement walls. (Cracks can be repaired from either the exterior or the interior of the wall, but interior access typically is easier and more cost-effective). A hydraulic cement-like material containing crystalline concrete first was placed in the crack to stop the flow of water. The rectangular cut then was filled with several layers of materials containing various concentrations of crystalline concrete, as per the manufacturer's recommendations. Finally, the crack surfaces were covered with a thin slurry coat of crystalline concrete.

All of the cracks treated in this manner were observed for at least two years after they were sealed. In several cases, minor seepage was observed along the edges of the treated area for a short time period (four to seven days) after the repairs were complete. Visible crystals soon formed, however, and the seepage stopped. Additional seepage was observed shortly after repairs were complete on one crack at the outside edge of the treated area, along the interface between the crystalline materials and the existing concrete. The seeping section was re-chipped out and retreated, and no further seepage was observed. No longterm seepage was observed from any of the cracks.

Permeability testing was conducted in the laboratory on concrete samples with a crystalline admixture. Longterm test results showed an effectively negligible permeability.

Given the success of treatment of the routine cracks, it was determined that crystalline materials would be used to treat more complex seepage problems. A number of cracks were treated on the outside of a process water holding tank at a steel mill in Illinois. The tank contained over 40 feet of water, so the head pressure on any repair materials would be substantial. Crystalline materials were used to seal the cracks, which have stayed dry for over two years.

Once it was confirmed that the basic function of crystalline materials was valid, cases with heavy inflow into subsurface structures were reconsidered. In many instances, seepage was not confined to one point, such as a single crack, but flowed from a number

of sources, including cracks, floor-wall joints, bad tie-holes, pipe penetrations, and other similar openings and discontinuities in the concrete. Each source was identified and treated, "chasing" the seepage until all avenues were sealed. Often closing off the flow of water in one location would cause seepage to occur at a location not observed previously. The chasing methodology evolved so that the worst point of seepage was identified first and treated, and subsequent locations were identified and treated in order of magnitude of flow. A slurry coat often was placed over an entire wall to provide a blanket barrier (in addition to the barriers installed at specific seepage points) where heavy moisture, poor concrete quality, or poor construction practices were encountered.

In each case, it was found to be critical that the apparent condition of the concrete as a whole be evaluated and that any evidence of original construction sequencing and procedures be noted. In many cases, an understanding of initial problems, such as cold joints, improper form ties, and honeycombing, guided the formulation of the waterproofing plan.

One installation issue presented itself repeatedly in situations where inflow was heavy. As with other types of waterproofing, placement of the crystalline materials was difficult under the force of moving water. Moderate flow could be arrested using the hydraulic cement-like crystalline material, but even that material eroded when subjected to heavy inflow. Extensive field testing was performed to identify a versatile material that could be used to stop the flow of water temporarily so that permanent crystalline concrete materials could be installed. Traditional water barriers, such as oak wedges, were not found to be easy to use in a wide range of opening sizes and flow rates. After substantial field testing was performed, a proprietary blend of expansive materials and a small dose of crystalline compounds was developed and was shown to be effective in stopping inflow of as much as 100 gallons per minute (gpm) without eroding. The material was easily shaped to fit a variety of opening sizes, and it did not exert sufficient pressure to damage the crystalline repair materials once they were in place.

Use of the temporary material has proven to be highly successful, particularly in two tunnel projects with heavy inflow. One of these projects was a hard rock tunnel, 180 feet below the ground surface and 160 feet below the top of the Ohio River. A large set of solution features was encountered in the shaley limestone along the tunnel alignment, and inflow from the features was estimated to be about 200 gallons per minute. The temporary material was inserted into the surface void spaces, where it expanded and sealed off the water flow. Material tested to seal a number of voids was in place, with no significant seepage, three weeks after it was installed. However, contracting issues changed the waterproofing approach, and the full plan involving crystalline concrete materials in a shotcrete barrier was not implemented. Similarly, the temporary materials were used to arrest the flow of water into a pedestrian tunnel at a steel mill in northern Indiana. Wells used to draw the water table down when the plant was built had been decommissioned, and groundwater was producing a heavy stream into a tunnel used by union workers 30 feet below the ground surface. Inflow was estimated to be about 60 gpm. The expansive materials were inserted into the primary seepage points, two holes adjacent to a staircase. The water flow was stopped in about ten minutes, but water

almost immediately began flowing into a below grade conference room and a stairwell landing. The sealing capability of the temporary material in the relatively small cross-sectional area of the two holes was such that it was difficult to reopen the holes when plant officials decided to resequence the waterproofing activities.

CASE STUDIES

A number of projects have been completed which have required a thorough evaluation of the seepage condition, original construction problems, and repair challenges to formulate the most effective waterproofing plan. Crystalline concrete has been used in each case, sometimes supplemented with the proprietary expansive material to temporarily stop heavy flow. Two cases in particular have been notable.

Residential Structure with Heavy Groundwater Flow

In 2008, Louisville, Kentucky, experienced a prolonged period of heavy rain during a time when the ground already was saturated. A residential structure in the east part of Louisville, constructed in the 1970s, had been subjected to seepage in the basement for many years. A steep slope on the northeast side of the site contained solutioned limestone layers that drained a large subsurface area through a network of interconnected voids. (See Figure 1). The depth and area of the network was such that flow from the rock layers at the elevation of the foundation of the house was constant. In fact, a subsurface flow channel was encountered when the foundation originally was constructed, and the builder notched the foundation wall to accommodate the flow and direct it to the gravel base layer under the basement floor slab, which discharged into a sump pump. (See Figure 2) Seepage and flooding occurred in the basement for many years, originating from numerous wall cracks as well as from the area of the notched foundation wall. Various waterproofing measures had been attempted at the house over the years, with little success. A trench-type system was installed in the basement in 2007 and included perimeter drains around most of the basement, a second sump pump, and battery backup units for both pumps. The perimeter drains were connected into the notch into the foundation wall in an attempt to control and direct the flow at that location. When the heavy precipitation occurred in 2008, the drain system backed up, flooding the basement.

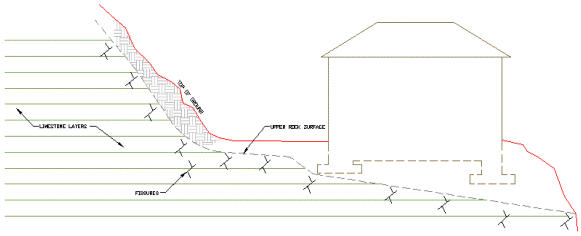

Figure 1

Elevation View of Residential Site

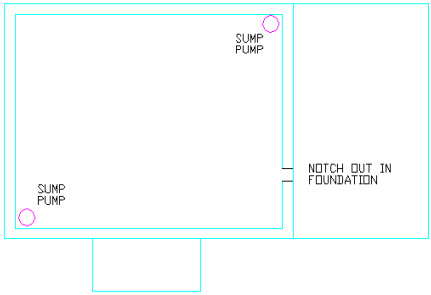

Figure 2
House Plan Showing Sumps and Foundation Wall Notch

The site was evaluated, and it was determined that the rock surface sloped to a nearby creek and overburden depths around the house were shallow, so water would not back up around the house if it was blocked from flowing through the notch in the foundation wall. The steep slope at the rear of the house did flow to a relatively level area immediately behind the house, so some regrading was designed to direct surface water runoff away from the house more quickly and to prevent most runoff from reaching the exposed portions of the basement walls. The decision then was made to remove the trench-type system in the basement, close the notch in the foundation wall, remove the two sump pumps, and use crystalline concrete materials to seal all avenues for seepage to enter the basement.

A combination of proprietary materials and hydraulic cement-type crystalline concrete materials was used to stop the flow of water through the notch in the foundation wall. The trenches then were removed and replaced with concrete containing a crystalline concrete admixture. Each basement wall crack was chipped out and repaired using crystalline materials. A significant volume of clay had squeezed through several of the cracks onto the plastic covering the separations, and mold was observed on the plastic, as well. The concrete surfaces exposed in the rectangular areas chipped out of each crack were required to be cleaned thoroughly to remove the clay from the concrete surface. Failure to remove the clay would have interfered with the ability of the crystalline material to grow into the surrounding concrete and stop water flow along the edges of the cracks.

After the cracks were sealed and the trenches were filled, a slurry coat of crystalline concrete was brushed over the treated surfaces. The treated areas then were allowed to seep for several days to activate the growth of the crystalline material. Several additional small seeps at the edges of the treated areas were identified and were chipped out and

treated. Once significant seepage was no longer observed, the sumps and pumps were removed and filled with concrete containing a crystalline admixture.

Two small seepage points appeared several months after repairs were complete. The areas in question were located in concrete in poor condition at the edges of the treated areas. These seeps were chipped out and sealed and no seepage has occurred since they were repaired.

Regrading of the rear of the property directed runoff away from the house, and standing water no longer occurs adjacent to the basement walls during heavy rainfall events. The small size of the yard and steepness of the adjacent slope will prevent rapid removal of all runoff during flood events, and existing window wells will be vulnerable to inflow during extreme weather events. However, in general, the subsurface portion of the house is dry and is not dependent upon pumps or power sources to remove seepage or inflow.

Elevator Pit

An elevator pit at the University of Louisville Ekstrom Library began experiencing seepage problems shortly after it was constructed. The pit extended 56 feet below the ground surface, and the localized groundwater surface was about 10 feet below the ground surface. Several contractors had attempted to stop seepage into the pit, but none of the methods were successful. In 2007, a trench-type system was installed to control the inflow; the system effectively acted as a straw, concentrating the inflow and increasing the seepage so that the constant rate of inflow was about 90 gpm. Multiple pumps were burnt up during a short time period, and the university was forced to purchase a number of standby units, based on the short life of the previous units subjected to the excessive inflow.

Seepage was occurring through a number of discontinuities in the concrete, and repair efforts began with installing the temporary proprietary materials to stop the flow of water at multiple locations so that the flow could be discharged from several select spots while the remainder was being sealed using crystalline concrete materials. The discharge points were under so much pressure that water spurted from them in what resembled fountains. Hoses were used to control the flow from the discharge points, and the surrounding areas were systematically sealed off using concrete containing a crystalline concrete admixture, and then crystalline concrete materials at specific seepage locations. The seepage was arrested slowly until only a few discharge points were left. At that point, the proprietary materials were used to stem the flow temporarily while crystalline concrete materials were applied. A slurry coat of crystalline concrete materials was placed over the entire bottom of the elevator pit to provide a blanket barrier against seepage.

Figure 2
Hoses Used to Direct Controlled Discharge

The pit was allowed to seep for several days to let the crystalline materials activate. Extensive crystalline growth was observed within a short period of time; in fact, significant crystal growth was observed within the first few days of treatment. Several small seeps were identified and re-treated after approximately one month, but no significant inflow has occurred since the repairs were made. The sump and pump are required to stay in place due to laws governing elevator pits, but the need for active seepage control has been eliminated.

LIMITATIONS

In general, the methodology developed for waterproofing subsurface concrete structures has been extremely effective. However, some limitations have been identified, as with most methods.

It is extremely important to address the structural capability of the structure in question at the start of the waterproofing program. Many post-construction waterproofing projects are required because there was no knowledge of subsurface water problems prior to construction. In those situations the subgrade walls often are not designed to resist hydrostatic pressure, and seepage through cracks and joints has served as a kind of pressure relief valve so that full hydrostatic pressure has not been applied to the walls and failure has not occurred. Successful waterproofing can change those conditions, and displacement or failure of subsurface walls can occur. Any waterproofing project should include an evaluation of the existing structural conditions and a plan for structural reinforcement, if necessary.

Subsurface structures involving concrete block can be treated using crystalline concrete materials, but the methodology is somewhat different and involves chasing seepage along

mortar joints and applying heavy slurry coats. In addition, the risk of structural inadequacy typically is much higher with concrete block walls.

Poor quality concrete can require either large scale removal and replacement or extended observations to identify areas where water has rerouted from the original seepage point to a less permeable yet available avenue. Similarly, structures located in stratigraphies with perched and/or trapped water can require longer periods of observation as the water is rerouted in the subsurface and finds new seepage points in the structure. The decision of how to approach the project often depends on the time available to observe the treated seepage points.

CONCLUSIONS

A methodology has been developed to perform post-construction waterproofing using crystalline concrete and proprietary materials designed to temporarily stop heavy inflow so the crystalline materials can be installed properly. Use of these methods allows interior trenches and sumps to be eliminated so that water is not drawn into the structure, creating unhealthy environmental conditions. Prevention of water from entering the structure also eliminates risks associated with trying to predict the maximum volume of flow that will be required to be handled by a collection or discharge system. The resealing characteristic of concrete treated with crystalline materials is a significant improvement over other sealants, such as epoxy, that have limited lives and are susceptible to breaches when subjected to minor movements. Assuming a structure has been evaluated to determine whether it can withstand the exterior hydrostatic pressure, and based on the idea that all information about seepage rates, patterns, and sources have been reviewed, waterproofing using the methods described appears to have the highest likely success rate.

Floor Level Surveys and Their Use in Geotechnical Investigations: Case Studies

K. Medji Sama, Ph.D., P.E.,[1] Debanik Chaudhuri, Ph.D., G.E.,[2] Michele F. Cyr, Ph.D., P.E.,[3] and Joanna L. Meldrum, P.E., P.G.[4]

[1] Senior Engineer, Exponent, Inc. 5401 McConnell Avenue, Los Angeles, CA 90066, e-mail: msama@exponent.com

[2] Senior Engineer, Exponent, Inc. 320 Goddard, Suite 200, Irvine, CA 92618, e-mail: dchaudhuri@exponent.com

[3] Senior Engineer, Exponent, Inc. 420 Lexington Avenue, Suite 1740, New York, NY 10170, e-mail: mcyr@exponent.com

[4] Senior Managing Engineer, Exponent, Inc. 149 Commonwealth Drive, Menlo Park, CA 94025, e-mail: jmeldrum@exponent.com

ABSTRACT

The measurement of building floor or foundation levelness using floor level surveys can be an important tool in construction quality control and engineering analysis and design. The processed results of floor level surveys are often used to evaluate conformity to construction guidelines, to form professional opinions regarding causation of distress and for selection of appropriate repair methodologies. In this latter case, the interpretation of results requires a great deal of judgment and experience.

This paper focuses on the application of floor level surveys in forensic geotechnical investigations. Following a brief discussion of required fieldwork, data acquisition, and data processing, three case studies are presented. These case studies serve to illustrate the importance of the adoption of an integrated approach in forensic geotechnical investigations by combining the floor survey results with other site observations and published and historical records.

INTRODUCTION

A floor level survey consists of the collection of relative elevations across a floor surface. The measurements are "relative" because they typically are taken with respect to a reference point that is, itself, located on the surveyed surface. The survey is simple to conduct and can be used for a variety of purposes. These include construction quality control (e.g. levelness of newly poured concrete slab), quality control and performance of foundation remediation activities, and structural and geotechnical forensic investigations. In geotechnical engineering, floor level survey data can be correlated with potential ground deformation mechanisms to determine whether such mechanisms are plausible scenarios.

The investigative process involves collection of raw field data, reduction of the field data, visual presentation of the data, and finally, interpretation of the results and correlation with other site observations. This last step is crucial as floor level surveys are most effective when integrated with other relevant data within the context of the problem at hand. In the remainder of this paper, the data collection and processing stage, and some of the issues typically involved in geotechnical investigations are discussed briefly. Three case studies are presented to illustrate the use and importance of floor level surveys in geotechnical investigations.

DATA COLLECTION, REDUCTION, PRESENTATION, AND INTERPRETATION

Water levels and manometers are the most commonly used devices to collect floor level survey data. As a result, floor level surveys are often referred to as manometer or water level surveys. Both water levels and manometers typically are accurate to approximately 2.5 mm (0.1 in). Occasionally, conventional surveying equipment, including laser levels, or proprietary devices (e.g. Dipstick®) are used to collect floor level survey data, particularly on larger slabs.

With the exception of data collected for F-number analysis (concrete floor flatness and levelness, ASTM E1155), there are no standard guidelines for the collection of floor level survey data points. In a typical floor level survey, elevation measurements are taken at regular intervals, when possible, on the floor surface. Typically, data points collected every 1.5 m (5 ft) for a residential slab are sufficient for analysis. Occasionally, collection of more closely spaced data may be necessary. The presence of furniture or other items, however, often prohibits access to certain areas of the floor surface and alters the regular spacing of the data points.

Different patterns of variations in floor elevation can be expected for different types of foundation systems. For example, localized depressions or sagging might be observed in floors supported by a pier-and-beam foundation. The type of foundation, expected deformation patterns and the purpose of the investigation should be taken into consideration when selecting the number and locations of field measurements to be collected for a floor level survey.

Following the collection of elevation readings, the data is typically reduced (and adjusted for changes in floor coverings, as necessary) to a format that is amenable to easy analysis and interpretation (e.g. graphical format). Generally, the data is reduced by normalizing the readings to a datum, usually chosen as either the highest or the lowest elevation point. This is achieved by assuming a zero elevation for the highest or lowest point, and adjusting the remaining data points relative to the zero datum. If the highest elevation point is assumed to be zero, then the rest of the data points will be transformed to negative numbers and vice versa. The difference between the largest and smallest relative elevation across a particular surface is termed the maximum (measured) elevation difference.

One of the most effective ways to interpret the data is by drawing contour lines (lines of equal relative elevations). This method allows one to readily visualize any trend in relative elevation or lack thereof. Typical contour plots are shown in the case studies section below. Contouring of the data is usually performed using commercially

available computer software packages, and the choice of contouring method may be influenced by several factors including the number of data points, data point spacing, trend in the data, etc. Such choice can, in turn, influence the resulting contour map. A detailed discussion on different contouring methods and their relative merits is beyond the scope of this paper.

Interpretation of floor level surveys during forensic investigations always involves some degree of judgment and can present considerable challenges. This is usually due to the lack of baseline or prior surveys to which to compare the data obtained during the investigation. Several authors have discussed the relative merits and pitfalls of the use of floor level surveys. Topics such as the correlation of relative floor elevations with superstructure distress (Skempton and McDonald,1956), the effect of the number of data points collected (Walsh and Miguel, 2003), the difficulty of interpreting floor level survey data when results of at least one prior survey are not available (Chen, 1975), and the potential pitfalls in using "pattern" recognition (Walsh 2007) have been addressed in the literature and are not explicitly covered here. Reference will be made, however, to some of these items within the case study section.

FLOOR LEVEL SURVEYS IN GEOTECHNICAL FORENSIC INVESTIGATIONS

Geotechnical engineers are called upon as forensic experts for various types of investigations. These include: assessment of foundation distress such as cracking of stemwalls, footings, or piers; investigation of the effects of leaks, poor drainage, and tree roots on foundation or slab-on-grade performance; evaluation of earth movement mechanisms related to expansive soils, slope creep, fill settlement; and wall finish or framing damage. During the course of such investigations, geotechnical engineers typically use a number of tools in addition to floor level surveys. These include site history review, visual observation of the damaged structure or foundations, indicators of potential ground movement (e.g. presence of ground cracks), proximity to slopes, condition of adjacent structures, nature of site soils and rocks, etc. Such tools are essential in interpreting the results of floor level surveys, and failure to take them into account can lead erroneous conclusions. This is particularly important in situations where the results of the floor level survey show no obvious pattern or when, for instance, the pattern of relative floor elevation is not consistent with the pattern of finish distress.

It is important to recall that relative floor elevations represent the state of the surveyed floor surface at the time the data was collected. Such condition can be frozen in time (i.e. no ongoing significant movement) or transient (e.g. in the case of ongoing ground movement). When viewed in that light, it becomes clear that a floor level survey, used as the sole basis for a professional opinion, may be of little use as current floor elevation patterns may be representative of a past phenomenon, not relevant to the present investigation. It is the task of the forensic engineer to synthesize and analyze all of the collected data and to reach conclusions as to the plausible cause(s) of the distress. Examples of the process are presented in the next section.

CASE STUDIES

To illustrate some of the practical uses of floor level surveys in forensic geotechnical investigations, three case studies are presented. These case studies demonstrate the use of an integrated approach, where floor level surveys are combined with additional observation and data, in a distress causation evaluation. The first case study also illustrates some of the variability inherent in the collection of floor elevation data.

Case Study I: Single-family residence

Site description and purpose of investigation: This case study involves a single-family residence consisting of a single-story wood-frame structure supported on a concrete slab-on-grade with continuous perimeter footing that was constructed circa 1965. The structure was constructed on a relatively flat building pad situated on a hillside lot. Grading of the building pad consisted of the placement of fill material to depths of 4 to 15 m with the thickest section of fill located near the top of the slope. The purpose of the investigation was to determine whether a water leak near the hallway bathroom had caused deformation of the concrete slab and finish damage.

Documents review: Review of property records revealed that a floor level survey had been performed as part of an evaluation in 1999, approximately two years prior to the water leak. Similar observations of finish distress were made at the time of the previous floor level survey as were made during the investigation of the current water leak.

Field observations: Three floor level surveys were performed in April, May, and August 2004, approximately three years following the reported water leak. Finish distress observed at the residence consisted of pervasive minor cracking at doors and window corners with several of the cracks occurring in previously patched areas; all consistent with distortion of the slab.

Discussion: The contours resulting from 1999 and April 2004 surveys are shown in Figures 1 (a) and 1 (b). The maximum elevation difference measured in 1999 was approximately 153 mm, while a maximum elevation difference of approximately 165 mm was measured in April 2004. The trend in the floor elevation surveys is similar and indicates that the slab is tilted generally downward from the northeast to the southwest. More details are captured in the April 2004 floor level survey as it contained approximately four times as many data points (182 versus 46). No noticeable local maximum or minimum was recorded near the location of the water leak (see Figure 1 (b)).

Given the location of the leak just outside the hallway bathroom, any resulting movement of the slab likely would have led to a relative high or low point in the vicinity of the leak. In addition, the pattern of finish cracking would have correlated better with the location of the leak than that observed during the site inspection (e.g. there could have been more significant cracking near the leak). A study of site topography and geotechnical data indicated that the southwest corner of the property - which is also located near a southwest facing descending fill slope- was underlain by as much as 15 m of fill, while the opposite corner of the building had less than 4 m of

fill. The leak was located on the shallower fill. Moreover, surficial soils at the residence were found to be expansive.

The observed pattern of relative floor elevations was in better agreement with the variable fill depth and the location of the slope than with the location of the leak as illustrated in Figure 2, which shows the results of the floor level survey superimposed on a topographic map. Based on this analysis, the observed distress at the residence was attributed to as-built conditions, long-term fill settlement, expansive soil movement, and slope creep, conditions that were exacerbated by poor drainage conditions at the property.

Comparison of various surveys: The contours for the four floor level surveys as well as the location of data points are shown in Figure 1. For the contours shown in Figure 1 (a) 46 data points were collected in 1999; for Figure 1 (b) 182 data points were collected in April 2004; for Figure 1 (c) 67 data points were collected in May 2004 and for Figure 1 (d) 52 data points collected in August 2004 (a subset of the data locations used in Figure 1(c)) were used. Although data were collected at roughly the same locations for Figures 1 (c) and (d), the operators were different, and the surveys were conducted approximately three months apart. For the April and August 2004 surveys, the operator and equipment were the same.

Examination of Figure 1 reveals that the overall trend shown by the contours (i.e. relative high and low points located at northeast and southwest corners of the slab) is essentially similar for all for surveys. The maximum measured differential elevation was approximately 153 mm in the 1999 survey, 165 mm in the April 2004 survey and 157 mm in the May and August 2004 surveys. The variability between the maximum elevation differences is within the aggregate accuracy of the devices used to collect the data. The April 2004 survey shows significantly more detail than all the other surveys due to the larger data set, but for purposes of evaluating the overall pattern of slab inclination fewer data points are sufficient. The contours shown in Figures 1(c) and (d) display some slight local differences. These are likely related to operator errors, differences in equipment, and the use of a slightly different number of data points.

Case Study II: Condominium complex I

Site description and purpose of investigation: This case study involves a condominium complex consisting of over 200 one-story, single-family units of conventional wood-frame structures with perimeter footings and reinforced slabs on grade. Grading at the site included the construction of fill slopes and the creation of level building pads, several of which were located at the top of the fill slopes. The purpose of the investigation was to determine whether alleged distress at the property was related to an earthquake or other phenomena. Although several mechanisms explaining the observed distress at the site were identified in the course of the investigation, only one such mechanism is discussed.

Field observations: The field investigation included collection of relative floor level data, visual observation of finish distress, subsurface investigation, etc. The contours

of the floor level surveys revealed that 75 percent of the surveyed units had a maximum floor elevation difference of 38 mm or less; 16 percent of those units had a maximum floor elevation difference between 38 mm and 57 mm, and 9 percent had a maximum floor elevation difference greater than 57 mm. The majority of the units had very little finish distress at the time of the investigation since the damage had been patched and painted in the years or months preceding the investigation. Some units, however, had significant finish distress and slab cracks.

Historical documents review: Review of historical documents revealed several interesting and noteworthy facts related to the site. The site was originally used for agricultural purposes and site grading and building construction occurred in the early to mid-1970s. Several mature heritage oak trees were present prior to construction. The local municipality required preservation of the trees as part of the grading plan. As such, a root protection system was designed that consisted of surrounding each tree with a masonry block tree well (at depths ranging from 0 to 1.5 m), placement of gravel within the dripline of the tree, and minimal compaction of fill placed within the dripline. Figure 3 shows a schematic of the grading detail near the oak trees. At the time of the investigation in the early-2000s, several of the oak trees or the tree wells (either empty or occupied by other tree species) were still present at the site. Several units had sections of their foundation and slab located within the dripline area, as illustrated in Figure 3.

Discussion: Figure 4 shows contours of relative elevations for several units within the site overlaid on a site plan showing the location of the heritage oak trees. This figure illustrates the correlation between units with relatively high floor deformation and the location of tree wells. Most of the units in the figure have maximum floor elevation differences less than 50 mm. Units with floor elevation differences of 50 mm to 100 mm were located in close proximity to the tree wells (although there are some exceptions) and showed a pattern consistent with settlement of loose fill below the tree's dripline (e.g. points of lowest relative elevation located in the section of the unit closest to the heritage oak trees). The investigation concluded that distress at the site was related primarily to long-term settlement of fill around tree wells and not to seismic effects on the structures or the soils.

Case Study III: Condominium complex II

Site description and purpose of investigation: This case study involves a condominium complex consisting of about 40 multi-unit, one- and two-story buildings with about 200 condominium units. The buildings' construction is conventional wood framing with slab on grade and perimeter concrete footing foundations on an essentially level parcel. After an earthquake, the owners and management of the complex were concerned about the serviceability and structural integrity of the buildings.

Field observations: Manometer surveys were performed in all ground floor units and tied between adjacent units so that the data could be reduced across each building. Elevation differentials across the building slabs ranged from less than 25 mm to 171 mm (accounting for floor finishes). As data was being collected and analyzed, it

became apparent that the units with the most structural distress (e.g. drywall cracks, etc.) also showed the greatest floor elevation differential. In addition, it was noted that units with relatively large floor elevation differentials were typically clustered along the central section of the site.

Historical aerial photograph review: During the review of historical aerial photographs, it was discovered that the site was an old orchard and that a natural drainage channel, relocated in a concrete open channel at the time of the investigation, cut roughly through its center. The results of the floor elevation survey were overlaid on an aerial photograph. A schematic showing the floor elevation survey data and the location of the drainage channel are shown in Figure 5.

Discussion: Examination of Figure 5 reveals that, with the exception of a few outliers, buildings with relatively large maximum floor elevation differences (i.e. greater than 66 mm) were generally located along the edge of the in-filled drainage channel, where fill soils had been placed during site grading. After additional testing and analysis of the static and dynamic behavior of the fill, the alleged earthquake damage at the site was instead attributed to long-term settlement of fill soils. Without review of the historical aerial photographs in conjunction with the floor level survey results, it would have been difficult to identify the potential cause of the observed distress.

CONCLUSION

This paper discusses the use of floor elevation surveys in geotechnical engineering investigations. Following a brief discussion of data collection, reduction, and interpretation, three case studies were presented that illustrate the use of floor elevations surveys in geotechnical forensic investigations. As seen through the case studies such surveys are most useful when integrated with other observations. There is no widely accepted methodology for the use of floor elevation surveys and, while they can be a valuable tool in the investigation of building distress, it is crucial that the investigator exhibit engineering judgment and be cognizant of the inherent limitations to their use.

REFERENCES

Chen, F. H. (1975) “Foundations on Expansive Soils”, Elsevier Scientific Publishing Company, Amsterdam.

Skempton, A. W., and McDonald, D. H. (1956) “The allowable settlement of buildings”, Proceedings of the Institute of Civil Engineers, Vol. 5 , No. 3, pp. 727-768.

Walsh, K. D. and Miguel, G. P. (2003) “Method for forensic analysis of residential floor-elevation data”, Journal of Performance of Constructed Facilities, ASCE, Vol. 17, No. 3, pp. 110-117.

Walsh, K. D. (2007), “Performance of methods of relative floor elevation measurements in residential structures”, Journal of Performance of Constructed Facilities, ASCE, Vol. 21, No. 5, pp. 329-336.

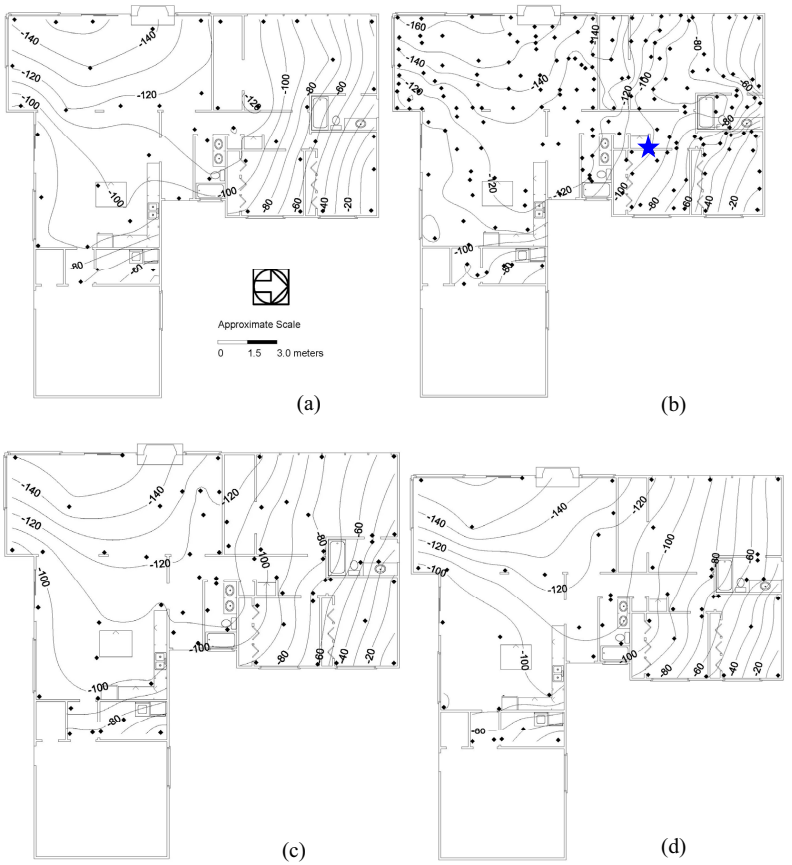

Figure 1. Case Study I: Relative floor elevation contours (in mm) and approximate data point locations with leak indicated by star. (a) 1999 survey by consultant A; (b) April 2004 survey by consultant B; (c) May 2004 by consultant C; (d) August 2004 survey by consultant B with readings taken at a subset of the May 2004 locations. The same equipment was utilized by consultant B for both surveys.

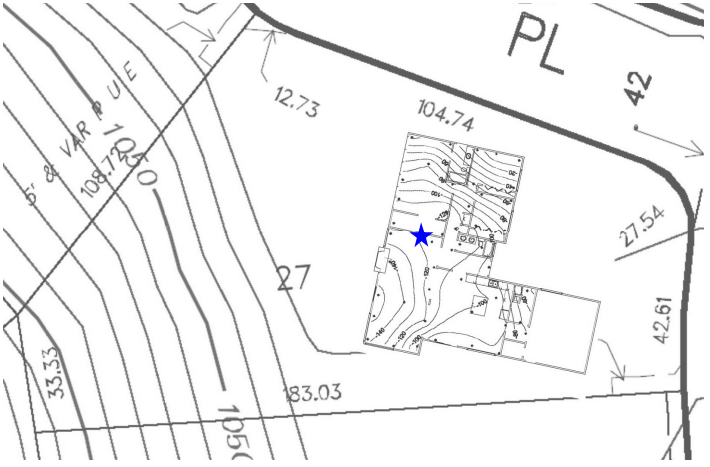

Figure 2. Case Study I: Schematic showing leak location and 1999 relative floor elevation contours of property overlaid on a topographic map (topographic map uses English units and shows 5 ft (1.5 m) contour lines).

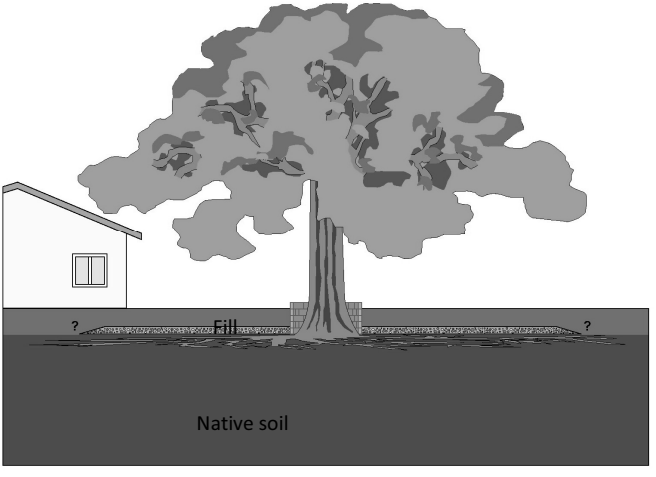

Figure 3. Case Study II: Schematic of typical layout around oak trees.

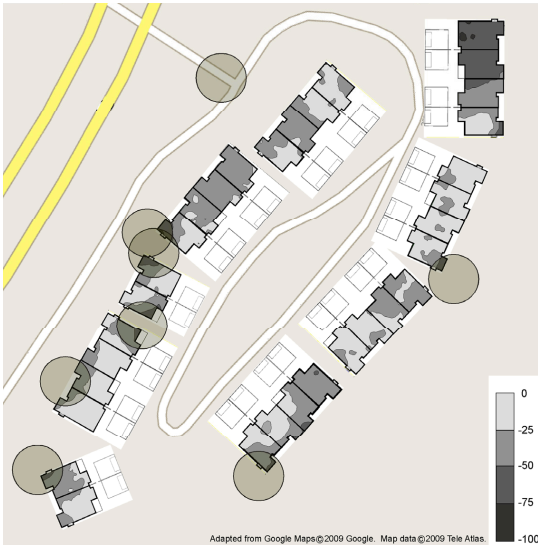

Figure 4. Case Study II: Relative floor elevation contours (in mm) for a section of the development. Note proximity of heritage oak trees (indicated by circles) to area of relatively high floor elevation difference.

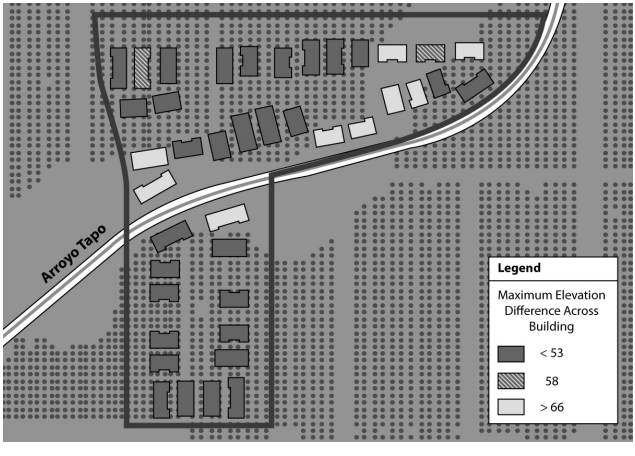

Figure 5. Case Study III: Schematic of project site showing location of buried drainage channel and condominium buildings shaded according to their maximum elevation difference (in mm).

Vibration Study of a Proposed Fitness Center Adjacent to a Server Room

Prasad Samarajiva, Ph.D., P.E.[1], and Dilip Choudhuri, P.E.[2]

[1]Associate, Walter P. Moore and Associates Inc., 1301 McKinney, Suite 1100, Houston, TX 77010, psamarajiva@walterpmoore.com

[2]Principal, Walter P. Moore and Associates Inc. 1301 McKinney, Suite 1100, Houston, TX 77010, dchoudhuri@walterpmoore.com

KEYWORDS: Floor Vibration, Fitness Center, Server Room, Sensitive Equipment, Human Perception, AISC, Natural Frequency, Monitoring

Abstract

Structural vibrations in a proposed fitness center area and the existing computer server room located on the third floor of multi story building was evaluated. Natural frequency of the concrete floor was evaluated in the proposed aerobics area. Aerobic activities were simulated by people spot jogging on the bare floor as well as the existing raised floor for 120, 150, 180 BPM metronomes. Vibration levels were monitored inside the computer server room, the proposed aerobics area and at a location close to the proposed treadmill area. Natural frequency of the concrete floor found to be not susceptible to structural resonance during aerobic activities. However, the vibration levels due to simulated aerobic activities in the computer server room were significantly above the published threshold for a computer equipment room. It was recommended that the floor system be modified to reduce floor vibrations in the server room.

Introduction

The building has 41 levels with approximately 25,000-ft2 floor area at each level. The foot print of the building shown in Figure 1 has a 200' base and 125' sides with a 45-degree internal angle. The perimeter encased columns on the base sides (200' sides) are spaced at about 15'. The perimeter composite columns on the other sides vary from 15'-20'. In the fitness center area (on Level 3), the steel beams (W21x44) which support the metal decks are spaced at about 10'-6" on center and the steel beam in-turn are supported by steel girders (W27x114) at 30' on center. According to the record drawings, the thickness of the composite metal deck is about 5 ¼". A rectangular area enclosed between two adjacent beams (10'-6") and two adjacent girders (30'-0") was considered to be an effective bay for vibration evaluation of the floor system. In the raised floor system, 24"x 24" floor panels are supported by steel posts and interconnecting beams.

The owner planned to convert a part of the third floor to a fitness center. The owner was concerned about potential vibrations in the fitness center due to aerobic activities, particularly with respect to transmission of vibrations to the adjacent

computer server room due to aerobic and exercise activities. In order to address the owners concerns, we conducted:

(1) Testing the floor to identify natural frequency

(2) Testing the floor with simulated exercise activities on the original raised floor.

Vital information of each of the above activities are described below.

Natural Frequency

The frequency at which an object tends to vibrate when disturbed from the at-rest state is known as the natural frequency of the object. If aerobic activities occur at or very close to the natural frequency for a sufficient period of time, undesirable amplifications of floor movements can occur. As a result the floor can be unusable or damaged cosmetically or in extreme cases damaged sustain structural damage. Therefore, it is critical to identify the natural frequencies of the floor system by conducting vibration testing.

Usually, the structural frequency response shows spikes at natural frequencies when structures are subjected to free vibration conditions such as the free weight drop case. Using the free weight drop case, we established the first natural frequency of the floor to be at 11 Hz (Figure 1). Usually, aerobic activities, walking and spot jogging result in vibrations in the range of 1-4 Hz which is substantially lower that the first natural frequency of 11 Hz. Therefore, structural resonance due to excitation from aerobic activities in the proposed fitness center is not likely to occur.

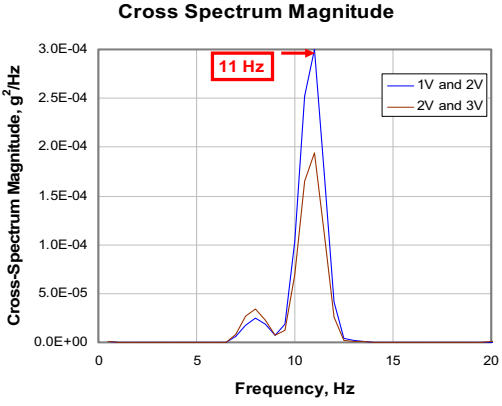

Figure 1. Frequency Response of the Floor. Red arrows indicate first natural frequency

Vibrations due to Aerobic Activities

Sensitive Equipment: Computer Room

Floors that support sensitive equipment need to provide vibration environments that are acceptable for the operation of the equipment. American Institute of Steel Construction (AISC) recommends a vibration threshold of 8000 micro inches/second peak particle velocity (PPV) for computer systems. Our testing indicated measured vibration levels well above the acceptable levels (8000 µin/s) for both Case 1 and Case 2 (Figure 2). Therefore, it will be necessary to take significant remedial actions to suppress vibration levels in the computer room below the sensitivity threshold of 8000 in/s PPV.

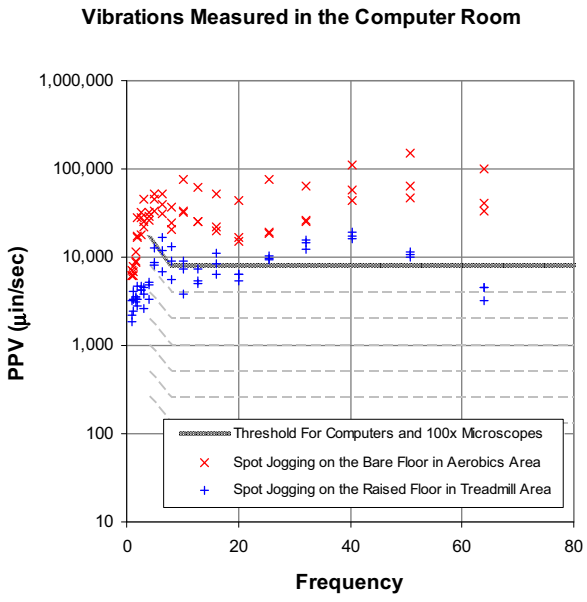

Figure 2. Vibration Response of the Floor in the Computer Room for Spot Jogging on the Bare Floor (Structural Slab) and existing Raised Floor

Human Perception

Vibrations were recorded for the following cases:

Case 1: Nine people spot jogging to 120, 150, and 180 beats per minute (BPM) metronomes on the structural floor slab (bare floor) after removal of the existing raised floorin the proposed aerobics area.

Case 2: Nine people spot jogging to 120, 150, and 180 BPM metronomes on the existing raised floor near by the proposed treadmill area.

Human response to floor motion is a very complex phenomenon. The threshold of perception of floor motion in a busy workplace can be higher than in a quiet apartment (AISC). The reaction of people who feel vibration depends very strongly on what they are doing. People in offices or residences do not like "distinctly perceptible" vibration (peak acceleration of about 0.5 percent of the acceleration of gravity, g), whereas people taking part in an activity will accept vibrations approximately 10 times greater (5 percent g or more). People dining beside a dance floor, lifting weights beside an aerobics gym, or standing in a shopping mall, will accept something in between (about 1.5 percent g).

In the Case 1 setup, our testing indicated that spot jogging on the bare floor causes vibration levels to exceed the perception threshold for people engaged in rhythmic activities in the treadmill area as recommended by AISC (Figure 3). Furthermore, the measured vibration levels significantly exceed the perception threshold for office use. It should be noted that the human perception threshold of vibrations are higher than that for a computer (sensitive equipment) room. Therefore, any remedial action to reduce the vibration below the computer threshold should automatically bring the vibrations well below the human perception threshold also. In addition, installation of a new floor system with equivalent or better vibration absorption characteristics can further reduce these vibration levels.

Spot jogging on the raised floor caused vibration levels below the perceptible limits for offices (Figure 4). However, the accelerometer aerobics area in this case was mounted on the bare floor. Therefore, installation of a new floor system with equivalent or better vibration absorption characteristics can further reduce these vibration levels.

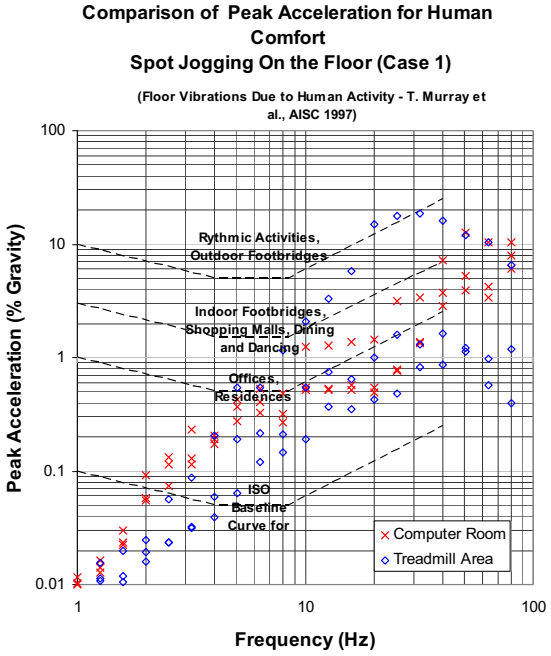

Figure 3. Vibration Response Measured at the Computer Room and the Proposed Treadmill Area to Spot Jogging on the Bare Floor in the Proposed Aerobics Area

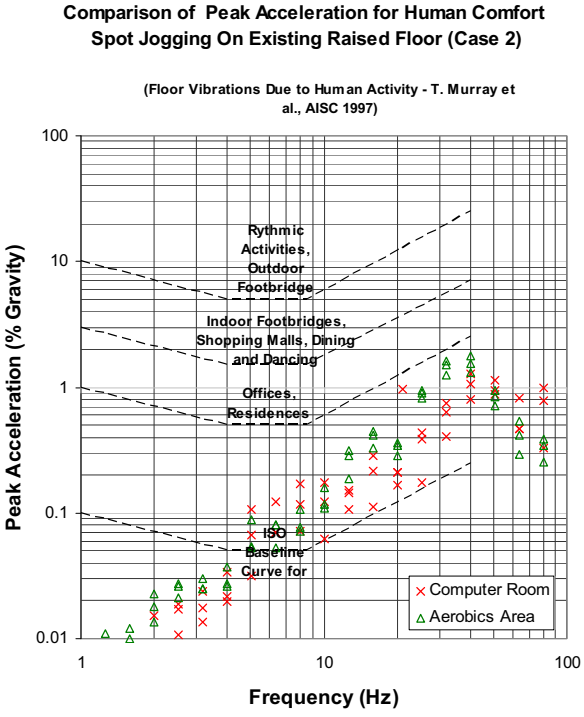

Figure 4. Vibration Response Measured at the Computer Room and the Proposed Aerobics to Spot Jogging on the Raised Floor in the Proposed Treadmill Area

Conclusions

Based on the vibration testing conducted in the proposed fitness center we offered the following conclusions and recommendations:

(1) Natural frequency (11 Hz) of the floor slab is sufficiently above vibration frequencies caused by aerobic activities. Therefore, it is very unlikely for the floor system encounter resonance related problems.

(2) Exercise activities on both Cases 1 and 2 causes' vibration levels in the computer room well above the acceptable level (8000 μin/s PPV). Therefore, it will be necessary to take significant remedial measure to reduce vibration levels in the computer room below the threshold of 8000 μin/s PPV.

(3) Spot jogging on the raised floor (Case 2) resulted in vibration levels below the threshold for offices. On the other hand, spot jogging on the bare floor (Case 1) caused vibration well above the threshold for offices and residences and exceeded the threshold for rhythmic activities. However, spot jogging on the bare floor is an unlikely scenario after the completion of fitness center construction with the proposed raised floor in place. It would be possible to further improve the conditions by using a floor system with better vibration damping characteristics than the existing raised floor system.

References

AISC (1997), Floor Vibrations Due to Human Activity, American Institute of Steel Construction, Inc, One East Wacker Drive, Suite 3100, Chicago, Illinois 60601-2001.

Shock and Blasting Effects on Power Transmission Structures

Kaoshan Dai[1], Eric Connor[2], Antoneta Koleva[3], Wenya Qi[1] and David Young[1]

[1]Department of Civil & Environmental Engineering, University of North Carolina at Charlotte, 9201 University City Blvd, Charlotte, NC 28223; PH (704) 687-2337; FX (704) 687-6953; email: kdai@uncc.edu
[2]Fluor Power Group, 6060 Piedmont Row Drive South, Suite 1000, Charlotte, NC 28287.
[3]Areva NP Inc., 7207 IBM Drive, Charlotte, NC 28262.

ABSTRACT

This paper presents outcomes of a blast effect on power transmission structure study, which mainly include discussions about considerations for blast plan establishment. The ultimate goal of this study is to provide scientific data and a systematic research procedure that would allow power companies to determine the best blast plan to secure power transmission assets during blasting. Through this study, the importance of peak-particle velocity, airblast, flyrock, fracture and mud-seams in blast planning has been identified. Factors such as blast distance and velocity, structure type and area geology should be included in the blast planning. A design example is included to demonstrate the procedures recommended herein.

KEYWORDS: Blast design; Power transmission structure; Ground vibration; Structural dynamics.

INTRODUCTION

Blasting is a most commonly used technique for groundbreaking for mining and construction purposes. Blast-induced ground vibrations, air vibrations, flyrock damages and subsidence are typical concerns during such operations. As a result, neighboring structures, which may include residential structures, power systems, pipelines, dams and water towers, can be affected by blasting operations.

Electric transmission poles are structures used to support conductors and shield wires of a transmission line. The integrity of these poles is critical to the reliability of power supply. In areas where blasting is used for mining or construction, these transmission structures can be endangered if the blasting is too close. There is a lack of industry-wide study on how transmission structures respond to blasting and no guidelines exist to regulate blasting near transmission structures. A common practice in the power industry is to limit ground motion by specifying maximum peak particle velocity. Some empirical criteria employed by power company engineers or blasting consultants are borrowed from the studies on residential structures and human annoyance (Siskin et al. 1980; Dowding 1985). For example, the peak particle velocity (PPV) of 50.8 *mm/s* ground vibration criterion was set forth and formed the basis for industrial standards for many years (Svinkin 2003). While these limits may yield prudent protection for low-rise houses, whether they are applicable to non-residential structures is questionable.

There is no nation-wide blast plan requirement currently in U.S. The information provided by the Vibrations Regulations Committee of the International Society of Explosive Engineers (ISEE 2009) summarizes regulations in some states or cities (Table 1). The allowable vibration levels vary from region to region due to geological variances. This conveys the significance of this research. Through blast monitoring at local surface mining and rock quarry locations at Southeastern U.S., this paper provides recommendations for blast design. An example is given to demonstrate the proposed procedure.

Table 1 Federal, state and local vibration regulations compiled by the ISEE Vibrations and Seismograph Section (Conner 2007).

Jurisdiction	Ground Vibration Limits (*mm/s*)	Jurisdiction	Ground Vibration Limits (*mm/s*)
Alabama	19.1 – 50.8	New Jersey	19.1 – 50.8
Arizona	none	New Mexico	19.1 – 31.8
Phoenix	25.4	New York	no regulations
Arkansas	25.4	Amherst	19.1 – 50.8
Florida	12.7	Clarence	19.1 – 50.8
Georgia	50.8	North Carolina	25.4
Idaho	no regulations	North Dakota	25.4
Lewiston	12.7	Ohio	50.8
Illinois	19.1 – 31.8	Oklahoma	25.4 – 50.8
Indiana	19.1 – 31.8	Oregon	N/A
Iowa	19.1 – 31.8	Gladstone	19.1 – 50.8
Kentucky	50.8	Pennsylvania	50.8
Louisiana	19.1 – 31.8	Rhode Island	12.7
Maine	50.8	South Carolina	25.4
Maryland	19.1 – 31.8	Tennessee	50.8
Massachusetts	19.1 – 50.8	Texas	19.1 – 31.8
Minnesota	25.4	Austin	43.2
Missouri	no regulations	Utah	19.1 – 31.8
Kansas City	19.1 – 31.8	Virginia	19.1 – 31.8
Montana	19.1 – 31.8	West Virginia	19.1 – 31.8
Nevada	no regulations	Charleston	50.8
Clark County	12.7	Wyoming	19.1 – 31.8
New Hampshire	50.8		

BLAST PLAN DESIGN CONSIDERATIONS

Blasting phenomena involve two critical aspects: rock fragmentation (near field effect) and explosive energy propagation. Explosions can generate high air pressure as well as strong ground vibrations. Blasting practices include drilling holes and filling them with explosive materials. For any given size of blast, an engineer will set up an 'explosive area.' Within this area, all the boreholes will be drilled and the detonators will then be tied together via detonation cords to a relay control. Although, conducting a blast within one hundred percent control is virtually impossible, a comprehensive consideration should include effects to reduce any possible

detrimental damages to nearby structures.

When a blast is detonated, some energy is vented into the atmosphere, causing a change in air pressure known as air blast. Explosive detonations create an incident blast wave, which reflects upon contact with a structure, and this wave-structure interaction imparts an impulse upon the structure. Ground movements caused by blasting may propagate to the structures and excite foundations (Figure 1). The majorities of annoyance complaints felt by people are facilitated by the air blast and ground vibration; it is these complaints, which dictate most blast limits for mining activities in existing documentation. In the case of transmission structures, air blast effects are the least detrimental. Ground vibrations generate excitations similar to the effects of natural earthquakes, although there are differences between these two vibrations in terms of excitation frequency and duration.

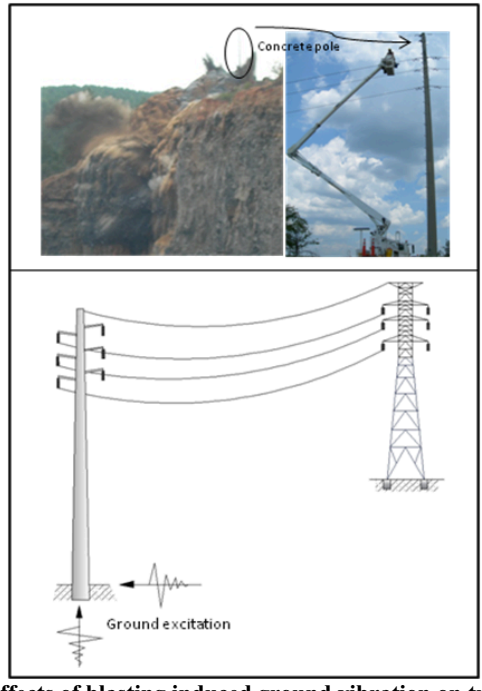

Figure 1. Effects of blasting induced ground vibration on transmission structures.

The amount of explosive materials used and the distance from the blast site determine the blasting levels. A reasonable ground motion limit at the location of structural foundations is a critical criterion in blast planning. Structural responses to strong ground excitations are crucial considerations for blast limit establishment. Since different types of transmission structures have different vibration characteristics, it is essential that a comprehensive blast plan takes into account of

structure types and site situations. Furthermore, the effect of a shock wave is a function of geological characteristics of a test site, although this is rarely addressed when setting safe limits.

Site conditions are important not only because of wave propagation but also because of the instabilities resulted from soft soils and ground fissures. Mudseam is a primary culprit in rock fracture (Figure 2). Upon detonation, pressure waves from explosions are inadequately confined, and the mudseam causes a premature release of gasses into the atmosphere. Therefore, it is crucial that mudseams and potential geological instabilities are recognized prior to developing a blast plan.

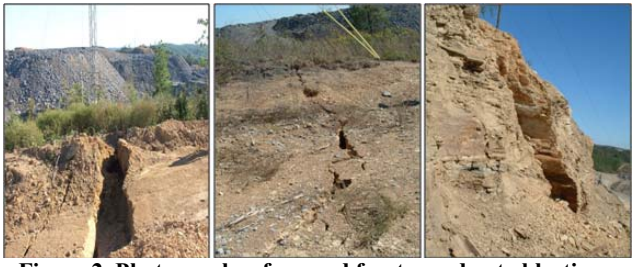

Figure 2. Photographs of ground fractures due to blasting.

Flyrock is defined as the rock propelled beyond the blast area by the explosion (IME 1997). In most flyrock cases, the penalties are much more severe than those in vibration cases. Flyrocks are hard to defend and the damage is most likely self-evident (Figure 3). Generally, flyrock is caused by a mismatch of the explosive energy with the strength of rock masses surrounding explosive charges (Kecojevic 2005), which promotes flyrock propulsion. Additional studies on flyrock phenomena can be found in works by Persson et al. (1984), Bajpayee et al. (2000), Fletcher and D'Andrea (1986), Rehak et al. (2001), Shea and Clark (1998), and Siskind and Kopp (1995).

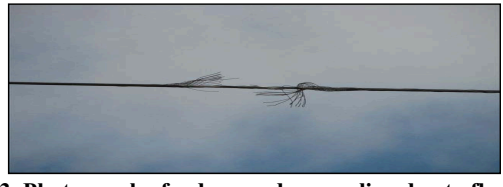

Figure 3. Photograph of a damaged power line due to flyrock.

BLAST PLAN ESTABLISHMENT AND RECOMMENDATIONS

Design of a reasonable blast plan typically starts with site geology investigation for potential rock fracture or problems that may lead to ground instabilities. Ground vibrations induced by detonation should not be beyond certain limitation in case they cause excessive excitations of the structures. The peak particle velocity of ground vibration, one representative value of ground vibration level, can be used to control ground movements at structure foundations. For establishment of such a blast limit,

structural dynamic characteristics should be identified. With available information of geological medium in which blasting wave propagates, empirical relations between the charge weight of blasting agents (ANFO, dynamite, etc), distance from blast to structure, and ground vibration limit at structure foundations can be developed through field study or by referring to available literatures. Combined the PPV blast limit and these empirical relations, the blast scale can be determined at the designated blast site. Figure 4 shows a flowchart that can guide one through the blasting design. Primarily, it is the blast design engineer's duty to ensure a safe blast. Thus, if a blast site has unusual conditions, additional procedures and precautions may be necessary.

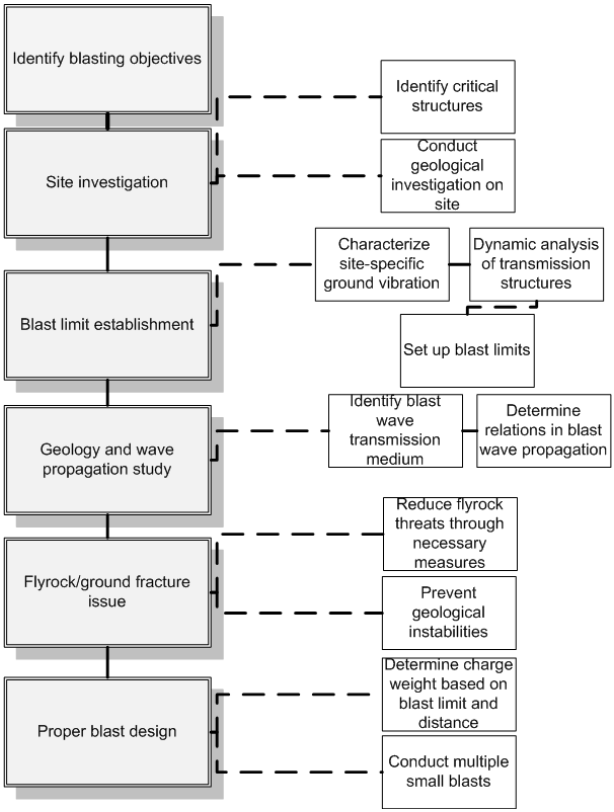

Figure 4. Blast plan consideration flowchart aide.

The following steps provide detailed elaboration to acquire necessary information for a reasonable blast design:

Site investigation

- Identify potentially endangered structures.
- Conduct geological reconnaissance and consult geological maps.

Blast limit establishment

- Characterize ground vibration as excitations at structure foundations.
- Perform dynamic analysis of transmission structures under ground motions.
- Set up blast limits based on structural performances.

Geology and wave propagation study

- Conduct geotechnical tests at the actual site to characterize blast wave propagation.
- Establish or refer to existing documentation to determine relations between charge weight, distance from blast to structure, and ground vibration limit.

Flyrock/ground fracture issue

- Set up a "safe zone" and use blasting mats if necessary to reduce flyrock threats.
- Indentify potential geotechnical instabilities and take measures to prevent them.

Blast plan establishment

- Back-calculate the blast scale based on ground motion limit, air pressure or other restrictions.
- Design blast monitoring to ensure safety of critical structures.
- Check to ensure that all local, state, federal blasting regulatory requirements are met (Table 1).
- Keep records for reference any problems develop within the blasting region.

AN EXAMPLE OF BLAST PLAN DESIGN

At this point, it may be beneficial to walk through an example of the process in developing a blast plan. The case considered is a concrete pole located within a surface coal mine located in south-eastern U.S. region:

Step 1: Determine the desired blast area perimeter/depth and rock fragmentation size.

- To help mining process of a layer of coal at a commercial surface coal mine, an estimation of 45.7 m × 27.4 *m* area need to be blasted with a depth of 45.7 *m*, and the rock should be fragmented into 25 cm square pieces.

Step 2: Survey the surrounding area for nearby structures and potential problems.

- An 18.3 *m* concrete pole is located 152.4 *m* from the blast origin and a 32 *m* guyed steel pole standing side by side with the concrete pole (Figure 5).
- Site characterization was established by site reconnaissance and consulting geological maps. The site can be described as shallow bedrocks with surface layer of stiff, silty sands. Such a site is characteristics of most Appalachian mountain regions with either carboniferous coal formations or mineral quarry.

Step 3: Blast limit establishment.

- Blast records were collected and analyzed at nearby sites and locations with similar geo-characteristics. Response spectra (Figure 6) were developed for dynamic analysis of the transmission poles under blasting induced ground vibration.
- Vibrational behaviors of the poles were studied (Figure 7). Dynamic characteristics such as natural frequencies were obtained, which were useful for the principal frequency consideration in blast design. They were also necessary information for structural response analysis.

- Through dynamic response analysis of the two poles under designed ground excitations, based on material level bearing capacity, a blast limit of 50.8 *mm/s* PPV was established, which meets the local blast regulatory requirements.

Step 4: Geology and wave propagation study.

- Site characterization was established by field testing with resultant average shear velocity of 451.1 *m/s*. Blast wave propagation medium was described as bedrocks with stiff sands on the top and average unit weight was estimated to be 2324.4 kg/m^3.
- According to the relation between charge weight W, distance from blast to structure R, soil density ρ, and ground vibration limit $\dot{u}$ (Equation 1) (Dowding 1985), when $\dot{u} = 50.8\,mm/\mathrm{s}$, $R = 152.4\,m$, $\rho = 2324.4\,kg/m^3$ in this case, charge weight per delay was calculated as $W = 4959.6\,kg$. In a proper blast design, charge weight per delay should be less than this value.

$$\dot{u} = 18.3\,mm/s\left(\frac{30.5\,m}{R}\right)^{1.46}\left(\frac{W}{4.5}\right)^{0.48}\left(\frac{2.4}{\rho}\right)^{0.48} \quad (1)$$

Step 5: Flyrock/ground fracture issues.

- The "safe zone" was set up 152.4 m around the perimeter of the blasting. Equation 2 (Lundborg 1975) was used to estimate the hole diameter for dynamite, in which L_{max} is the "safe zone" area radius and d is charge hole diameter. When $L_{max} = 152.4\,m$, the charge hole should be no more than $d = 67.8\,mm$. It was deemed necessary to use blasting mats to control flying debris.

$$L_{max} = 7.4 \times d^{2/3} \quad (2)$$

- No obvious ground fracture or instability issues were identified in site investigation. So there were no special geotechnical strengthening measures taken at pre-blast phrase.

Step 6: Proper blast design.

- All of the data obtained was given to a blasting consultant for the blast design. The blast plan consisted of 10 rows of six blastholes per row (Figure 8), and the diameter of each blasthole was 25.4 *mm* with charge weight per delay of 380.5 *kg*. 8 millsecond delay caps were used to stagger the explosions. The airblast level of 130 decibels was set (Dowding 1996).
- All landowners within 0.8 kilometer, who requested it, were notified of the date and approximate times of blasts. Prior to the blast, a warning whistle, audible within 0.8 kilometer of the excavation area, was sounded twice: first, 5 minutes before the detonation, and second, 1 minute before the detonation.
- Blast was monitored by vibration and air pressure monitoring equipment placed near and on the closest structures for which permission was granted; i.e. the transmission poles. Records were kept for reference.

Figure 5. Power transmission pole structures close to the blast site.

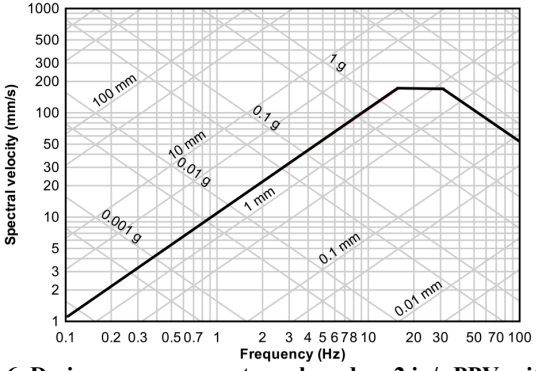

Figure 6. Design response spectrum based on 2 in/s PPV criterion.

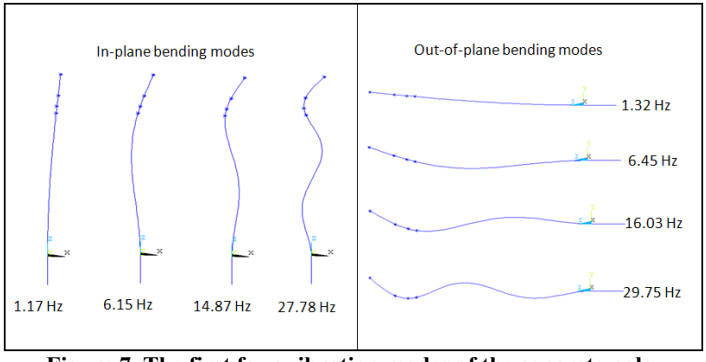

Figure 7. The first four vibration modes of the concrete pole.

Figure 8. typical blast site.

CONCLUSION

Contributing factors to unforeseen reactions during blasting include discontinuity in the geology and rock structure, improper blast hole layout and loading, insufficient burden, very high explosive concentration, and inadequate stemming (Kecojevic 2005). Blast design should be site specific and may include the following:

- Identify structures of concern.
- Determine safe vibration levels.
- Devise initial blast designs based on the desired level and site conditions.
- Refine the blast designs with other considerations such as flyrock and ground fracture issues.
- Select appropriate equipment(s) to accurately measure vibration levels.
- Implement vibration monitoring and keep blast records.

Since each blast site is different, understanding and learning from previous explosions is the best way to prepare for future blasts. The proposed blasting guidelines not only promote the safety of transmission structures, but they also encourage better safety practices at the blast site in general.

ACKNOWLEDGEMENT

The authors would like to acknowledge the support of Southern Company: Southern Company Transmission System Design Committee, Mr. Charles Munden and Mr. Dennis Mize. Special appreciation is extended to Mr. Colby Galloway, Mr. Luke Stafford, Mr. Eddie Sheffield of Southern Company, Mr. Bill Kitchens of the Alabama Department of Surface Mines, and Mr. Mac Sauls and Randall Franklin of the SAULS Seismograph group.

REFERENCES

Bajpayee, T.S., Rehak, T.R., Mowrey, G.L., Ingram, D.K. (2000). "A summary of fatal accidents due to flyrock and lack of blast area security in surface mining, 1989-1999." *Proc. of the 27th Annual Conference on Explosives and Blasting Technique,* International Society of Explosives Engineers, Cleveland, OH.

Conner, E.G. (2007). *Design of a blast plan for transmission structures*. Master Degree Thesis, University of North Carolina at Charlotte, Charlotte, NC.

Dowding, C. H. (1985). *Blasting vibration monitoring and control*. Prentice-Hall, Inc., Englewood Cliffs, N.J.

Dowding, C. H. (1996). Construction vibrations. Prentice–Hall, Saddle River, N.J.

Fletcher, L.R., and D'Andrea, D.V. (1986). "Control of flyrock in blasting." *Proc. of the 12th Annual Conference on Explosives and Blasting Technique*. International Society of Explosives Engineers, Cleveland, OH.

Institute of Makers of Explosives (IME). (1997). "Glossary of commercial explosives industry terms." *Institute of Makers of Explosives, Safety Publication*, 16(12), Washington, DC.

Kecojevic, V. and Radomsky, M. (2005). "Flyrock phenomena and area security in blasting-related accidents." *Safety Science*, 43(9), 739-750.

Lundborg, N., Persson, A., Ladegaard-Pedersen, A., Holmberg, R. (1975). "Keeping the lid on flyrock in open-pit blasting." *Engineering and Mining Journal,* 176(5), 95-100.

Persson, P., Holmberg, R., Lee, J. (1984). *Rock Blasting and Explosives Engineering*. CRC Press, New York, NY.

Rehak, T.R., Bajpayee, T.S., Mowrey, G.L., Ingram, D.K. (2001). "Flyrock issues in blasting." *Proc. of the 27th Annual Conference on Explosives and Blasting Technique*, 1, 165-175. International Society of Explosives Engineers, Cleveland, USA.

Shea, C.W. and Clark, D. (1998). "Avoiding tragedy: lessons to be learned from a flyrock fatality." *Coal Age*, 103, 51-54.

Siskind, D.E. and Kopp, J.W. (1995). "Blasting accidents in mines: a 16 year summary." *Proc. of the 21st Annual Conference on Explosives and Blasting Technique,* p. 224-239. International Society of Explosives Engineers, Cleveland, USA.

Siskind, D. E., Stagg, M. S., Kopp, J. W. and Dowding, C. H. (1980). "Structure response and damage produced by ground vibration from surface mine blasting." *Report of investigations 8507*. U.S. Bureau of Mines, Washington, D. C.

Svinkin, M. R. (2003). "Drawbacks of blast vibration regulations." *Vulcanhammer. net: geotechnical and marine engineering online library*. < http://www.vulcanhammer.net/svinkin/> (Dec.5, 2008).

Soil Contributions to Blasting Effects from Case Histories and Vibration Limits

Mark R. Svinkin, Member, ASCE[1]

[1]VIBRACONSULT, 13821 Cedar Road, #205, Cleveland, OH 44118-2376; PH (216) 397-9625; FAX (216) 397-9625; msvinkin@roadrunner.com

Abstract

The existing vibration limits were developed for 1-2 story houses surrounding coal surface mines, and these limits are applied for ground vibrations as the criteria for the possible crack formation in structures. However, other blast design, soil conditions and structures require different vibration limits. There are no regulations for multistory building vibrations from blasting and there are no limits to assess possible dynamic settlements of soil and structures triggered by ground vibrations from blasting. Nevertheless, numerous case histories are available in technical papers which describe tolerable and unacceptable soil and structural vibrations measured for different soil conditions and structures. These case histories are valuable sources of information to evaluate vibration effects on structures, analyze vibration levels that do not produce damage to structures, determine the areas of application of the existing regulations and assess tolerable vibration limits for various structures during blasting operations.

Introduction

Blasting operations conducted in urban areas are usually connected with potential problems of manifestation of vibration effects on adjacent and remote houses, buildings and other super and underground structures. Dynamic consequences of structural vibrations range from benign to harmful.

It is common that two significant questions come up at neighborhood areas around sites with blasting operations: what is the cause of damage to structures and what vibration limits have to be used at specified areas. It is necessary to underline that similar damage to structures can be produced by different group of static and dynamic loads such as environmental forces (temperature, humidity, wind, rain, snow, etc.), geotechnical hazards (heave, settlement, stability, sliding and failure), and dynamic effects from blasting. Determination of actual causes of damage to structures without the performance of a pre- and post-blast structure surveys is a complicated task, and

missing surveys are the basis for contradictory judgments of blasters and house owners.

Counteraction between both sides sometimes extends in large scales. On the one hand blasters stand up for their correct blasting operations without any damage to structures. On the other hand residents who believe that their houses were damaged by blasting joint efforts to push forward the legislature for diminishing the vibration limits, increase areas of pre-blasting survey and choose larger scaled-distances to decrease vibration effects on houses from blasting. Such restrictions can create substantial obstacles for production blasts without insurance of safe blasting.

Obviously, a number of resident complaints are related to public perception of blasting and public relations. However, there are case histories with real damage to structures from blasting. Vibration limits correctly determined can help to properly assess vibration problems during blasting. Case histories are large and valuable sources of information which can be used to determine vibration limits. In this paper, a number of case histories are analyzed with an emphasis on soil contributions to blasting effects on wave propagation and damage to structures.

The Existing Vibration Limits

Apparently, it is impossible to have universal regulations of blasting vibrations applied for different kinds of blasting, variety of soil conditions and types of structures. The available optional regulations, NFPA 495 (2006), include the vibration cosmetic cracking thresholds for assessment of surface coal mine blasting effects on 1-2 story residential houses, Figure 1. These criteria developed by the U.S. Bureau of Mines (USBM) have the following displacement and velocity values for the four ranges of the dominant frequencies: 0.76 mm (0.03 in) for 1-4 Hz, 19 mm/s (0.75 in/s) for 4-15 Hz, 0.2 mm (0.008 in) for 15-40 Hz, and 50.8 mm/s (2.0 in/s) for 40-100 Hz. The limit of 19 mm/s (0.75 in/s) for 4-15 Hz is used for drywall while the limit of 13 mm/s (0.5 in/s) for 2.5-10 Hz is applied for plaster, Siskind et al. (1980). The derivative version of the USBM safe limits shown in Figure 1 was included as the Chart Option into the surface coal mine regulations by the Office of Surface Mining Reclamation and Enforcement, OSM (1983).

The USBM vibration limits were built up on the basis of the two decades research studies of a correlation between ground vibrations and observations of blast damage to low-rise houses, and these limits are applied for ground vibrations as the criteria of possible crack formation in various structures. The USBM research study has been recognized as the great achievement which provides the safety of 1-2 story residential houses from vibrations generated by surface coal mining blasting. Obviously, these vibration limits can be successfully used for adequate blasting loads, similar structures and ground conditions they were developed for, but different limits should be used for other combination of dynamic loads, soil conditions and structures.

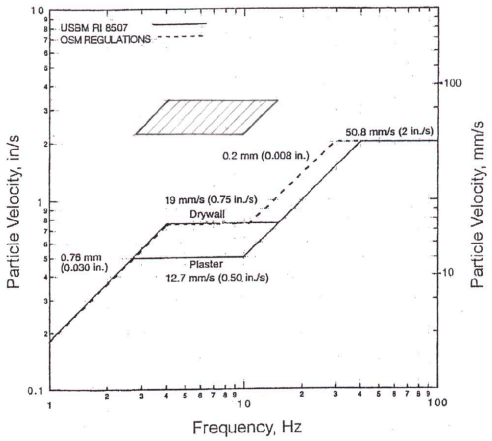

Figure 1. Safe level blasting criteria from USBM RI 8507 and the derivative version, the Chart Option from OSM surface coal mine regulations. Shaded area shows maximum velocities of resonant structural vibrations with amplification of 4.5. Data were modified from Siskind (2000). Plot was adapted from Svinkin (2008).

Siskind (2000) presented the accumulated results of research studies accomplished by the USBM and others on vibrations from blasting and their effects on low-rise houses, Figure 2. Ground vibrations were measured near 1-2 story residential structures from 718 blasts and 233 documented observations were obtained. Non-damaging blasts are not shown although some of them produced relatively high level of ground vibrations even exceeding 51 mm/s (2 in/s). These data indicate different vibration effects on structures depending on the dominant frequency and the peak particle velocity (PPV) of ground vibrations.

It is necessary to point out that the USBM criteria are conservative for assessment of direct blasting vibration effects on structures in the non-resonant frequency zones of structural vibrations when ground vibrations do not trigger plastic soil deformations under structures (Figure 2), but they cannot protect low-rise structures from appearance of cosmetic cracks by amplification of ground vibrations higher than 4.5x and beyond the 4-12 Hz frequency range, Svinkin (2003, 2004). Furthermore, the application of these limits to different super and underground structure is incorrect. AASHTO Designation: R 8-96 (2004) stated the application of the USBM limits to markedly different types of structures is common and inaccurate. Besides, the USBM limits do not actually take into account construction blasts with much higher frequency content. Dowding (1996) demonstrated examples where the dominant frequencies of ground vibrations from surface mining and construction blasting would lie between 12 and 18 Hz and 70 and 100 Hz, respectively. It means that the USBM limits cannot be used for construction blasts.

Some publications have stated that there are no problems with blasting vibration limits. For example, Aimone-Martin (2005) has asserted, that the safe blasting criteria defined by the U.S. Bureau of Mines in 1980 are widely used in the U.S. rock blasting industry. “This safe criteria is based on over 40 years of research and crack observations and has been scientifically supported since 1980 by experts in the field of structure response to rock blasting. There has been no scientific data to date that disputes this criteria.” On the one hand this statement is correct because the USBM criteria without doubt are good for the specific blast design, soil conditions and the types of structures they were developed for. On the other hand this statement is confusing because in a number of cases, these vibration limits are used for different blast, soil and structure conditions. Verification is necessary for the application of the USBM criteria for other blasts, soil and 1-2 story houses.

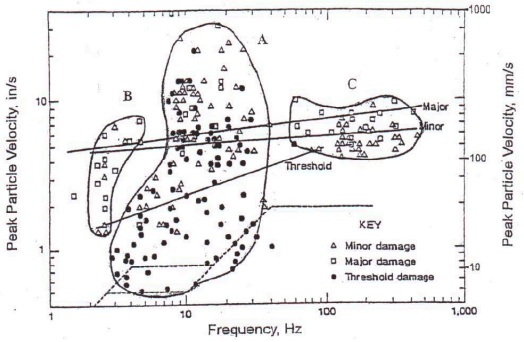

Figure 2. Ground vibrations from blasting and structural damage summary grouped in three zones. Dashed lines define USBM safe limits. Data were modified from Siskind (2000). Plot was adapted from Svinkin (2008).

Siskind (1991) wrote, “Vibration criteria for nonresidential cases are needed: concrete, power poles, pipelines, bridges, etc. Without reliable criteria for such cases, regulation is often based on relatively strict levels required to prevent cosmetic damage to residences”. Also, Siskind (2000) stated that most regulatory bodies, including OSM, recognize “that a more rigorous treatment may be needed in special cases, such as that outlined in RI 8507”.

Some states use single vibration limits between 6.4-51 mm/s (0.25-2.0 in/s) for PPV of ground vibrations that only aggravates problems with assessment of damage to houses because of lack of objectivity and ignorance of possible resonant structural vibrations.

The British Standard BS 7385 (1993) and the USBM criteria are depicted in Figure 3. It can be seen that the BS 7385 considers two lines of the safe limits depending on a type of buildings. Line 1 with the frequency-independent criterion of 51 mm/s (2 in/s) is applied to industrial and heavy commercial buildings. Line 2 with the frequency-based safe limits is similar to the USBM criteria and applied to residential or light commercial

type buildings. It seems the values presented in Figure 3 are small to represent structural vibrations. On the basis of similarity of two standards, it can be assumed that the BS 7385 requires measurement of ground vibrations as the criteria of possible structural damage. If so, the BS 7385 has similar restrictions of its application as the USBM criteria, Svinkin (2007).

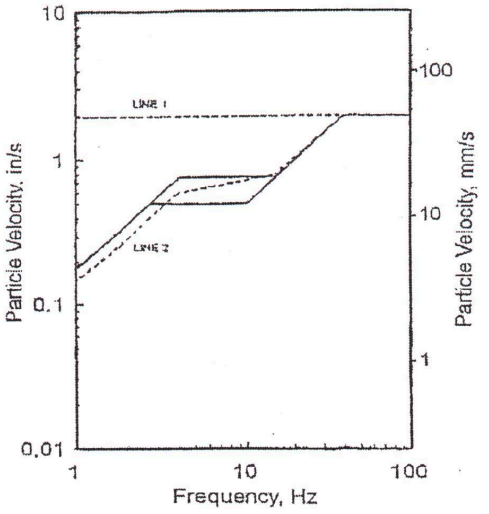

Figure 3. Vibration guidelines - USBM RI 8507 (solid line) compared to BS 7385 (dashed line). Line 1: reinforced or framed structures, industrial and heavy commercial buildings; line 2: unreinforced or light framed structures, residential or light commercial type buildings. From AASHTO Designation: R 8-96 (2004).

The German Standard DIN 4150 (1986) and the USBM criteria are depicted in Figure 4. DIN 4150 suggests three lines of time-dependent vibration limits for different types of structures. Lines 1-3 represent different kinds of structures described in the figure caption of Figure 4. Lines 2 and 3 are located below the USBM vibration limits. Line 1 is close to the upper boundary of the USBM vibration limits in the 4-100 Hz frequency range. Comments are needed regarding structures with particular sensitivity to vibrations. Such terminology is appropriate for devices and technology sensitive to vibration, but structure sensitivity is different. Resonant vibrations are dangerous for any kind of structures: from buildings under the preservation orders to industrial buildings. Dynamic settlements can also be devastated for any kind of buildings. However, industrial buildings have much higher resistance to direct vibration effects than 1-2 story residential houses. The basis for the guideline level of DIN 4150 is unknown, AASHTO Designation: R 8-96 (2004). Obviously, these criteria intended to minimize human perceptions and complaints. This approach would be sensible if construction operations

constantly affect houses and even at night. However, if blasts are performed 1-2 times per day, such an approach is unreasonable, Svinkin (2007).

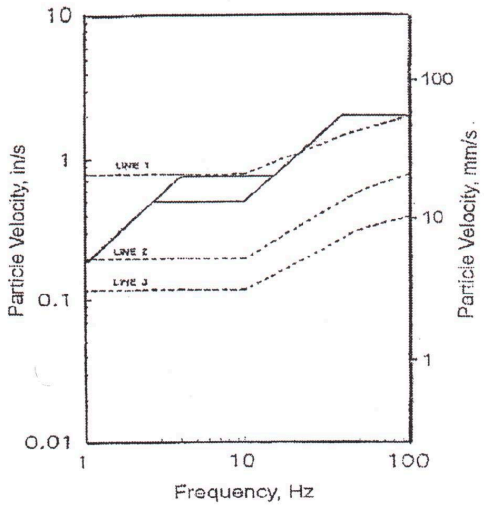

Figure 4. Vibration guidelines - USBM RI 8507 (solid line) compared to DIN 4150 (dashed line). Line 1: buildings used for commercial purposes, industrial buildings and buildings of similar design; line 2: dwellings and buildings of similar design and/or use; line 3: structures that because of their particular sensitivity to vibration, do not correspond to those listed in lines 1 and 2, and are of great intrinsic values (e.g. building that are under a preservation order). From AASHTO Designation: R 8-96 (2004).

The Russian limits of 30-50 mm/s (1.18-1.97 in/s) for vibrations of sound structures were found by the Moscow Institute of Physics of the Earth to assess the safety of structures from explosive effects of various blasts in the air, on the ground and under the ground at the time of the Second World War, Sadovskii (1946). So, for multi-story residential, commercial and industrial buildings, the frequency-independent safe limit of 51 mm/s (2 in/s) can be chosen for the PPV of structural, not ground, vibrations. This criterion automatically takes into account soil-structure interaction for the whole building frequency range. In the support of the proposed criterion, it is necessary to underline that according to Siskind (2000), the PPV of 51 mm/s (2 in/s) is the highest vibration level generated inside homes by walking, jumping, slamming doors, etc. Besides, this vibration limit is compatible with the European Standards, and it does not exclude higher allowable vibration levels. It is easy to demonstrate compatibility of the new simplified safe criterion and the USBM vibration limits, Figure 1. To evaluate tolerable structural vibrations, the smallest vibration limits of 13 mm/s (0.5 in/s) and 19 mm/s (0.75 in/s) have to be multiplied by 4.5, and their

products of 57 mm/s (2.25 in/s) and 85.5 mm/s (3.37 in/s) are higher than the simplified criterion of 51 mm/s (2 in/s), Svinkin (2007, 2008).

Soil and Structure Responses to Blasting

Blasting operations generate different body and surface waves which travel through the medium of soil deposits and rock. Elastic waves travel from dynamic sources and induce elastic soil deformations (ground vibrations) which levels depend on intensity of propagated waves. The structural responses to ground vibrations depend on soil-structure interaction. Ground vibrations can produce direct vibration effects on structures and trigger resonant structural vibrations of adjacent and remote structures. However, under certain circumstances such as a combination of non-cohesive soil deposits, water table levels and ground vibrations, elastic waves can be the cause of plastic soil deformations, e.g. liquefaction, densification and soil settlements triggered by small ground vibrations. Soil-structure interaction will be different for soil failure. The structural response to ground excitation depends on the soil response to waves propagated from the source and soil soil-structure interaction. Because elastic and plastic soil deformations cause dissimilar structural responses and damage, diverse thresholds have to be used for assessment of direct vibration effects, resonant structural vibrations, and plastic soil deformations (Svinkin, 2008).

The existing regulations were developed for assessment of elastic soil deformations and structural responses to ground vibrations from blasting. These criteria have nothing to do with plastic soil deformations. It is necessary to underline that there are no federal, state and local regulations of the critical vibration levels of ground vibrations which may trigger dynamic soil failure. Therefore, an experience from cases histories of soil failure contribution to structural damage from blasting is very important for assessment of vibration limits to cover plastic soil deformation effects triggered by blasting.

Low Attenuation of Propagated Waves in Saturated Soils

Case 1. Siskind and Stagg (2000) have made a comprehensive study of structural vibration damage to the ten typical houses from quarry blasting. The houses were selected at five areas in Miami-Dade County. Vibration measurements of ground and house structure vibrations were made from 42 quarry blasts during about a 2-month period from late February to late April 2000. The maximum distances between the active quarries and the test sites were in the 3.2-4.8 km (2-3 mi) range. Pre- and post-blasting condition surveys were made before and after vibration monitoring. Additional 756 vibration records from other reports were considered in the study.

The soil at the area consisted of 0.3-0.9 m (1-3 ft) of fine grained to fibrous peat followed by 0.6-1.2 m (2-4 ft) of sand followed 0.6 m (2 ft) of marl underlain by weakly to well cemented limestone. The groundwater table is virtually coincident with the surface of peat. The specific condition of wave propagation has been found

in the Miami-Dade County: attenuation with distances is less than found on similar sites in the north.

The report has revealed other interesting findings: (a) structure oscillations are superposition of vibrations with various frequencies including low frequencies of about 8 Hz, which are close to the natural frequencies of house horizontal vibrations, and very low frequencies of 2 to 4 Hz; (b) vibrations are of long duration at the houses with maximum duration about 17 second; (c) ground vibrations with the PPV of 19 mm/s (0.75 in./s) and with structure response of 6.1x would produce a global wall strain that is 1.5 times higher of the strain limit for crack formation. On the basis of vibration monitoring in the west and south-west Miami area, the authors concluded that the highest vibrations there would likely be under 3 mm/s (0.12 in/s).

Liquefaction in Sands

Case 2. Sanders (1982) has performed an assessment of liquefaction danger from explosively creating breaches in the Bird's Point – New Madrid fuze plug levee. Creation of two large crevasses would use tens tons of explosives that would cause liquefaction hazards to structures in the area. A rock layer was located at the depth greater than 30 m (100 ft). There were problems with the scarcity of borehole data below 4.5 m (15 ft) and the scarcity of data bearing on the investigation of blast-induced liquefaction. A data base from row charge experiments in soil was used in the assessment of the liquefaction hazards in the area.

This study had to determine a possible liquefaction PPV threshold, the maximum distance from a blast where the threshold could be expected, and availability of structures within the distance. The safety criterion of 10 cm/s (3.9 in/s) was found out as the conservative threshold for assessment of liquefaction hazards. The maximum distances at which liquefaction might occur from blasting were ascertained in the 300-383 m (1000-1275 ft) range. The report was reviewed by Dr. H.B. Seed, one of the founders of Earthquake Engineering, who used a totally different line of approach and concluded that the threshold of 10 cm/s (3.9 in/s) was reasonable.

Settlement in Sand and Clay Soils

Case 3. Charlie et al. (2001) have reported the potential responses of earth-fill and tailing dams, and other saturated earthen structures subjected to blast vibrations. Eight explosive tests were conducted on a 2.25 m (7.4 ft) high dam constructed of loose dilative sand, and they showed that significant increases in a residual pore pressure occurred when the PPV exceeded 1.5 cm/s (0.59 in/s) at shallow depths to 3.5 cm/s (1.38 in/s) at greater depths. Limited crest settlement occurred when the PPV exceeded 2.5 cm/s (1.0 in/s). Results of research studies and investigation of the field behavior of full-scale earth-fill and tailing dams indicate that the PPV below 2.5 cm/s (0.98 in/s) and 10 cm/s (3.94 in/s) are reasonable thresholds to limit pore pressure buildup in these dams sensitive and not sensitive to vibrations, respectively.

Case 4. Edwards and Northwood (1960) have presented the results of controlled blasting tests of six buildings on two different sites. Damage was correlated with explosive weight, distance, PPV of ground or structure vibrations, settlement and strain measurements in the buildings. The selected buildings were old but in good conditions except for quite localized areas in one or two of them. All had basements constructed with heavy stone masonry walls and frames with brick superstructures.

The soil at the first site consisted of 6.1 m (20 ft) loose wet sand underlain by soft marine clay. The water table was about 2.1 m (7 ft) below grade. Sand soil was frozen to a depth of about 0.3 m (1 ft) at the time of the test. The buildings at the first site: church, school and house with 305 mm (12 in) brick walls and plaster inside.

Large low-frequency (2-5 Hz) ground vibrations in the sand-clay soils were obtained within hundred feet of the source, and they did not occur at all at 457 m (1,500 ft) and beyond. Damage inspected in the buildings on sand-clay deposits: cracks were mainly vertical and some diagonal cracks developed in the basement and upper walls; cracks were from hairline to 13 mm (0.5 in) width; larger cracks were in walls closest to the blast. The authors concluded that the damage in the buildings on sand-clay deposits was caused by failure of the soil manifested in settlements under the building rather than by vibrations of building structures. The threshold level of 102-127 mm (4-5 in/s) was defined.

Damage to Foundation Walls

Case 5. Edwards and Northwood (1960) have conducted experiments of controlled blasting operations near buildings with the objective of producing damage. General information is the same as in Case 4.

The soil at the second site comprised well-consolidated glacial till which is a high shear strength material consisting of a highly compacted mixture of sand, clay, gravel and boulders. Till was frozen to a depth of about 1 ft at the time of the test. There were three houses at the second site: two with 305 mm (12 in) brick walls and plaster inside, and third with frame and vinyl sliding and wood fiber board inside.

Most of the high-frequency components of ground vibrations were obtained in the till soils. Damage inspected in the buildings on till: some horizontal cracks; most of the windows in the ground floor longitudinal walls were broken while those in the walls normal to the blast remained intact. Major damage was inflicted on one building on till soil. Considerable section of the rear basement wall fell away and the masonry walls above ground level were bulged out approximately 76 mm (3 in). The threshold level of 102-127 mm (4-5 in/s) was defined.

Vibration Limits and Surveys of Structures

Case histories presented above demonstrate various soil contributions to blasting effects on wave propagation and soil failure. Wave paths in saturated soils underlain

by rock had low attenuation and as a result ground vibrations had higher PPV. Consequently, the vibration limit of ground vibrations was decreased to 3 mm/s (0.12 in/s). This criterion is four times less than the smallest USBM vibration limit. However, the vibration thresholds of soil failure like liquefaction, settlement and soil movement damaged foundation walls were 1.5-5 times higher then the highest USBM limit in most cases.

The obtained results were determined for the specific cases, and the application of these criteria to other sites can be used only for preliminary assessment of blasting effects because each site is unique. It is necessary to keep in mind that changes of blast parameters, wave paths and structure types may yield different outcomes and require different safe criteria, Siskind et al. (1980), Siskind (1991), Siskind and Stagg (2000), Svinkin (2006, 2007). Such criteria are not always available. Therefore in addition to vibration measurements, it is imperative to use other approaches like the condition survey of houses and buildings that provides good opportunities for assessment of blasting damage to structures.

Pre- and post-blast surveys of structures have to be professionally performed because different kind of static and dynamic loading like environmental forces, geotechnical hazards, and dynamic effects of blasting can be the causes of similar structural damage, and such damage can exist before the beginning of blasting. It is common to consider only the effects of environmental forces such as temperature, humidity, wind, rain, snow, etc. on structural integrity. However, it is particularly important to analyze the geotechnical natural hazards at various distances from construction sites such as heave, settlement, stability, sliding and failure which may damage structures prior to construction, during and after construction. There are case histories which show the major effects of environmental forces and geotechnical causes on crack formation and structural damage in spite of blasting at various distances from houses and buildings. For example, the writer analyzed the results of pre- and post-blast structure surveys of the building and found that the geotechnical hazard, a soil failure started prior to the beginning of blasting, was the cause of damage to structures.

A pre-construction survey is the first step in the control of structural vibrations to ensure safety and serviceability of adjacent and remote houses, buildings and facilities. There are four goals of this survey: (1) document the existing cracks and other damage; (2) ascertain the cause(s) of the existing cracks and other damage; (3) assess susceptibility rating of structures; (4) determine mitigation measures of blasting effects on structures.

At some sites, the condition survey can provide more information about benign and harmful blasting effects on structures than vibration measurements performed during blast operations because the vibration criteria cannot embrace the whole spectrum of the blast effects on structures. The condition surveys must always accompany measurements of blasting vibrations. Surveys of structures and analysis of damage to structures should be performed by engineers who have an experience in Soil-Structural Dynamics and evaluation of blast effects on soil and structures. For

example, only Siskind and Stagg (2000) co-report presented the results of the great scope of study of the blasting effects on houses in Miami-Dade County in comparison with another three co-reports, Svinkin (2005).

Some blaster contractors try to decrease ground vibrations from blasting as much as possible. For example, Labriola (2006) has reported that on the basis of preliminary calculations the limit of 10 mm/s (0.39 in/s) was used as the threshold of ground vibrations near a pipeline in Tasmania in spite of that pipelines can withstand ground vibrations in the order of 120-250 mm/s (4.72-9.84 in/s) in accordance with Siskind et al. (1994).

Additional research is needed for improvement of the safety of structural integrity during blasting operations. Some research topics are outlined in Siskind (1991). In addition, it is necessary to point out the importance of studies of vibration responses of various structures to diverse blasts because structures are the final destinations of blast vibration effects.

Conclusions

Blasting can differently affect adjacent and remote structures, and the relation between blasting operations and building damage is often a subject of arguments when blasting is done not only in the vicinity of buildings but at distances of few miles.

The USBM criteria are a great work and these results can be applied for the blast, soil and structure condition they were developed for. The application of these vibration limits to different blast design, soil deposits, super and underground structures is incorrect and misleading, and such an approach can discredit the USBM vibration limits.

The existing regulations were developed for assessment of elastic soil deformations and structural responses to ground vibrations from blasting. These criteria have nothing to do with plastic soil deformations. It is necessary to underline that there are no federal, state and local regulations of the critical vibration levels of ground vibrations which may trigger dynamic soil failure. Therefore, an experience from cases histories of soil failure contribution to structural damage from blasting is very important for assessment of vibration limits to cover plastic soil deformation effects triggered by blasting.

Case histories presented demonstrate various soil contributions to blasting effects on wave propagation and soil failure. Soil influence increased ground vibrations, and consequently the vibration limit was decreased. In most cases, the vibration thresholds of soil failure like liquefaction, settlement and soil movement damaged foundation walls were found much higher than the biggest USBM limit.

A pre-construction survey is the first step in the control of structural vibrations to ensure safety and serviceability of adjacent and remote houses, buildings and facilities. Properly performed surveys provide the reliable arguments for protecting bluster contractors and house owners in possible litigations.

Additional research is needed for analysis of the structural responses to blast excitations and raising the safety and protection of structural integrity of various houses, building and facilities during blasting operations.

References

AASHTO Designation: R 8-96. (2004). *Standard Recommended Practice for Evaluation of Transportation-Related Earthborne Vibrations*, AASHTO Washington, D.C.

Aimone-Martin, C.T. (2005). *The Report. Structure Response Study, Cristal Ridge, MacDonald Ranch, and MacDonald Highlands*, Aimone-Martin Associates, Socorro, New Mexico.

British Standard Institution (1993). *Evaluation and measurement for Vibration in Building – Guide to Damage levels from Groundborne Vibrations. BS 7385*, Part 2, Milton Keynes, England.

Charlie, W.A., Lewis, W.A. and Doehring, D.O. (2001). "Explosive Induced Pore Pressure in a Sandfill Dam". *Geotechnical Testing Journal*, ASTM, V.24, No.4, 391-400.

DIN 4150 (1986). *Deutsche Normen: Erschütterungen im Bauwesen - Einwirkungen auf bauliche Anlagen*, Germany (in German).

Dowding, C.H. (1996). *Construction Vibrations*, Prentice Hall, Upper Saddle River.

Edwards, A.T. and Northwood, T.D. (1960). "Experimental Studies of the Effects of Blasting on Structures", *THE ENGINEER*, September 30, 538-546.

Labriola, A. (2006). *Blasting Risk Assessment for Gunns Limited Proposed Pulp Mill Development Site*, Tasmania, Orica Quarry & Construction Services.

NFPA 495. (2006). *Explosive Materials Code*. National Fire Protection Association, An International Codes and Standards Organization, Quincy, Massachusetts.

Office of Surface Mining Reclamation and Enforcement. (1983). *Surface Coal Mining and Reclamation Operations; Initial and Permanent Regulatory Programs; Use of Explosives. Federal Register*, Vol. 48, No. 46, March 8: 9788-9811.

Sadovskii, M.A. (1946). *The Simplest Methods of Determining Seismic Hazard Due to Massive Blasts*. Academy of Science, USSR, Moscow (in Russian).

Sanders, S.G. (1982). *Assessment of the Liquefaction Hazards Resulting from Explosive Removal of the Bird's Point – New Madrid Fuze Plug Levee*, TA7 W34M No. GL-82-5, U.S. Army Corps of Engineers.

Siskind, D.E., Stagg, M.S., Kopp, J.W., and Dowding, C.H. (1980). *Structure response and damage produced by ground vibrations from surface blasting, RI 8507*, U.S. Bureau of Mines, Washington, D.C.

Siskind, D.E. (1991). "Vibration Criteria for Surface Mine Blasting: Ten Years after Bureau of Mines RI 8507", *Proceedings of the 17th Annual Conference on Explosives and Blasting Technique*, Orlando, February 1991, V. 2, 1-12.

Siskind, D.E. (2000). *Vibrations from Blasting*. International Society of Explosives Engineers, Cleveland, Ohio.

Siskind, D. and Stagg, M., Wiegand, J.E, and Schulz, D.L. (1994). *Surface Mine Blasting Near Pressurized Transmission Pipelines, RI 9523*, U.S. Bureau of Mines, Washington, D.C.

Siskind, D. and Stagg, M. (2000). *The Co-Report. Blast Vibration Damage Assessment Study and Report,* Miami-Dade County, C3TS Project No.: 1322-01.

Svinkin, M.R. (2003). Drawbacks of blast vibration regulations. *Proceedings of the 29th Annual Conference on Explosives and Blasting Technique*, ISEE, Cleveland, Ohio, V. II: 157-168.

Svinkin, M. R. (2004). "Minimizing construction vibration effects", *Practice Periodical on Structural Design and Construction*, ASCE, V. 9, No. 2, 108-115.

Svinkin, M.R. (2005). Closure to "Minimizing construction vibration effects," by Mark R. Svinkin., *Practice Periodical on Structural Design and Construction*, ASCE, Vol. 10, No.3, 202-204.

Svinkin, M.R. (2006). "Regulations of Construction Vibrations". *Proceedings of 31st Annual Conference on Deep Foundations*, DFI, Hawthorne, New Jersey, 559-571.

Svinkin, M.R. (2007). "Assessment of safe ground and structure vibrations from blasting", *Vienna Conference Proceedings 2007,* (P. Moser, ed.), European Federation of Explosives Engineers, CD-ROM, 107-115.

Svinkin, M.R. (2008). "Soil and structure vibrations from construction and industrial sources", OSP 8, *Proceedings of 6th International Conference on Case Histories in Geotechnical Engineering*, Arlington, Virginia, August 11-16, CD-ROM.

Seismic Damage Control of Underground Structures associated with Reduced Stiffness of Soil Foundation

Mohammad Reza Okhovat[1] and Koichi Maekawa[2]

[1] PhD Candidate, Concrete Laboratory, Department of Civil Engineering, University of Tokyo, 7-3-1 Hongo, Bunkyo-ku, Tokyo, Japan, Postal Code: 113-8656; TEL (+81)03-5841-6100; FAX (+81)03-5841-6010; email: okhovat@concrete.t.u-tokyo.ac.jp
[2] Professor, Concrete Laboratory, Department of Civil Engineering, University of Tokyo; email: maekawa@concrete.t.u-tokyo.ac.jp

ABSTRACT

Liquefaction can significantly increase the deformation of soil around underground structures but at the same time, the stiffness and internal stress of soil are also dramatically reduced. Therefore, it is questionable that if it is really essential for the structure to accommodate all the free-field ground deformations as the conventional design approach currently requests. In the present study, a typical subway tunnel is subjected to earthquake excitations using dynamic Finite Element method coupled with soil and pore water considering the nonlinearity of both structure and soil foundation. The simulation is carried out in both drained and perfectly undrained conditions to clarify the effect of liquefaction on seismic response of the structures. The computational results imply that the required ductility of RC ducts can be moderated provided that the liquefaction risk is high. Furthermore, the effect of sheet piling on various types of tunnel damages such as uplift or shear deformation is also investigated. It is found that installation of sheet piles can cause the structure to suffer more damage due to the increase of relative stiffness between the structure and the soil.

INTRODUCTION

Liquefaction is a typical phenomenon in soft alluvial deposits in coastal areas on the occasion of strong earthquakes. It can cause severe damage to underground structures due to large deformation of soil, uplift or even floatation of structures. The relationship between the damage to structure and soil liquefaction was detected as early as in 1964 Niigata Earthquake and Alaska Earthquake (Hall and O'Rourke, 1991). Such damages to small pipelines or even large underground structures which were embedded in liquefiable soils were also found in many other earthquakes since then (Schmidt and Hashash, 1998). Therefore, various preventive countermeasures have been studied and developed so far to eliminate or alleviate damages to underground structures specially the uplift. Basically, they can be classified into three groups; soil improvement, drainage and suppression of shear deformations. Amid these strategies, installation of sheet pile walls is known to be effective and economical in reducing the uplift (Kimura *et al.,* 1995), however, its efficiency in

other kinds of damage mitigation of underground structures such as controlling the shear deformation response is rarely studied. Besides, more accurate analyses which can well cover the nonlinearity of soil, structure and their interaction are quite necessary now. In most of the previous researches regarding soil–underground structure interaction, however, either nonlinearities of structure were neglected or soil was modeled with very simplified assumptions.

On the other hand, seismic design actions for underground ducts are generally characterized in terms of forced displacement and/or mean strains imposed on the structure. The rational and practical approach is to implicitly consider the interaction of underground RC with surrounding grounds. First, free-field ground deformations due to a seismic event are estimated and second, the underground RC is designed to accommodate these deformations through fictitious soil spring. This approach is satisfactory especially when lower levels of shaking are anticipated or the underground facility is in a stiff medium such as rocks (Hashash *et al.* 2001).

In this paper, a subway tunnel having interaction with surrounding soil is analyzed using coupled dynamic Finite Element method. In order to determine the effect of liquefaction on seismic response of structures, both drained and perfectly undrained states of pore water are discussed. Liquefaction may greatly increase in the deformation of soil around structures, but at the same time, the stiffness and internal stress of soil are dramatically reduced, too. A question is raised, what is the resultant of the both kinematics in RC nonlinearity? Furthermore, the effect of sheet piling on various types of tunnel damages such as uplift, shear deformation or cracking pattern is also investigated. It is found that the installation of sheet piles can change the damage pattern of the structure which should be considered in the design procedure of sheet piles.

NONLINEAR CONSTITUTIVE MODELS

Constitutive Model for Reinforced Concrete. A reinforced concrete material model has been constructed by combining constitutive laws for cracked concrete and that for reinforcement. The fixed multi-directional smeared crack constitutive equations (Maekawa *et al*, 2003) are used as the relations of spatially averaged stresses and strains. Crack spacing or the density and diameter of reinforcing bars are implicitly taken into account in smeared and joint interface elements no matter how large they are.

The constitutive equations satisfy uniqueness for compression, tension and shear of cracked concrete. The bond performance between concrete and reinforcing bars is taken into account in terms of tension stiffening and the space-averaged stress-strain relation of reinforcement is assumed to represent the localized plasticity of steel. The hysteresis rule of reinforcement is formulated based upon Kato's model for a bare bar under reversed cyclic loads. This RC in-plane constitutive modeling has been verified by member-based and structural-oriented experiments. Herein, the authors skip the details of the RC modeling and refer to Maekawa *et al.*, 2003.

Constitutive Model for Soil. A nonlinear path-dependent constitutive model of soil which can predict the nonlinear response of layered soil under earthquake excitation

is essential to simulate the behavior of the entire RC–soil system properly. Here, the multi-yield surface plasticity concept (Maekawa *et al*, 2003) is applied to formulate the stress-strain relationship of the soil following Masing's rule for the shear hysteresis (Masing, 1926). The authors also use the framework of elasto-plastic and damaging concrete modeling to formulate the soil nonlinearity as follows.

The basic idea of this method is rather simple. First, the total stress applied on soil particle assembly, denoted by σ_{ij}, can be decomposed of deviatoric shear stresses (s_{ij}) and compressive mean pressure (p) as,

$$\sigma_{ij} = s_{ij} + p\delta_{ij}$$

where δ_{ij} is Kronecker's delta symbol.

Soil is idealized as an assembly of finite numbers of elasto-perfectly plastic components, which are conceptually connected in parallel. Each component is given different yield strength, so all components yield at different total shear strains, which results in a gradual internal yielding. Thus, the nonlinear behavior appears naturally as a combined response of all components. Hence, the authors propose the total shear stress carried by soil particles being expressed with regard to an integral of each component stress as,

$$s_{ij} = \sum_{m=1}^{n} s_{ij}^{m}(\varepsilon_{kl}, \varepsilon_{kl}^{m}, G^{m}, F^{m})$$

where G_o^m is the initial shear stiffness of the m-th component, and F^m is the yield strength of the m-th one. These component parameters can be uniquely decided from the shear stress-strain relation (Maki *et al.*, 2005).

In order to determine the volumetric nonlinearity of soil skeleton, the authors simply divide the dilatancy into two components according to the microscopic events of soil particles. One is the consolidation or negative dilation as unrecoverable plasticity denoted by ε_{vc}. The other is the positive dilatancy associated with alternate shear stress due to the overriding of soil particles, which is denoted by ε_{vd} as,

$$p = 3K_0(\varepsilon_0 - \varepsilon_v), \quad \varepsilon_v = \varepsilon_{vc} + \varepsilon_{vd}$$

where K_0 is the initial volumetric bulk stiffness of soil particles assembly. Herein, the authors skip the details of the soil modeling and refer to (Okhovat and Maekawa, 2009).

The multi-yield surface plasticity model has two main advantages. First, it can be easily applied to simulate the envelope of any shape and cyclic hysteretic curves. Second, the number of path-dependent parameters used to trace the cyclic loops is much less than that of nonlinear isotropic model (Maekawa *et al*. 2003).

Constitutive Model for Interface between RC and Soil. In this paper, the linear elastic model which assumes a bilinear relation for the opening/closure mode is employed to model the interfacial kinematics. The normal stress is zero in case of separation, which means no stress is transferred between the soil and the structure when the interface is open. On the other hand, the contact stiffness in closure mode is assigned a large value to ensure that no overlap is allowed, as shown in Figure 1(a). For shear sliding mode, shear stress–slip relation is assumed to be linear-plasticity as shown in Figure 1(b). The contact may slide if the applied shear stress exceeds the frictional shear strength, which is assumed to follow the Coulomb law.

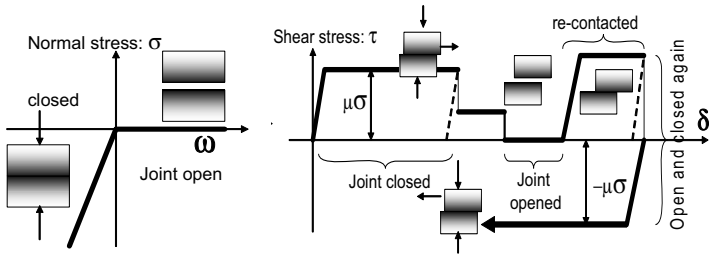

(a) Normal response (b) Shear response

Figure 1. Response of linear elastic interface model (Maekawa *et al*, 2008**)**

FINITE ELEMENT MODEL

Model Properties. To investigate the seismic behaviors of underground RC ducts, a typical subway tunnel section is modeled whose structural dimensions are shown in Figure 2. The center column to mainly support the dead weight of soil overlay has a rectangular cross section of 0.60 × 0.80 *m* and is idealized as firmly fixed to the slabs. The clear distance between two adjacent columns along the line is 3 *m*. The tunnel is stiffened with 45° haunches at the corners and has a longitudinal reinforcement ratio of 1.1% for side walls and slabs, 1.6% for the column, and web reinforcement ratio of 0.2% for all elements. Compressive strength of concrete and yield strength of steel are 24 MPa and 240 MPa, respectively.

The soil deposit is assumed to be loose sand with a friction angle of 30º and thickness of 15 *m* which is located on a 5-meter-thick layer of non-liquefiable soil which again lies on the bedrock as shown in Figure 2.

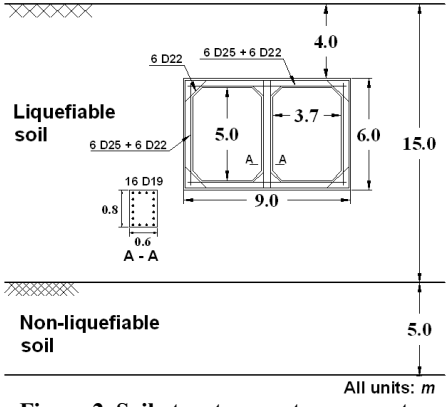

Figure 2. Soil-structure system geometry

By assuming the plane strain condition, the finite element mesh used in the analysis is composed of eight-node isoparametric two-dimensional elements for both

RC and soil. The RC-soil interfacial elements are placed at an interface in between the soil and the RC elements. Since the angle of internal friction of the model sand is 30°, the friction angle of the interface is obtained using the relation $\delta = \tan^{-1}[(2/3)\tan\phi]$, which is about 21°. The north-south component of the rock base acceleration measured at 1995 Kobe earthquake, which is scale-adjusted to 0.3g based on the measurement at Kobe meteorological observatory, is used as the input bed rock motion in the seismic analysis as shown in Figure 3.

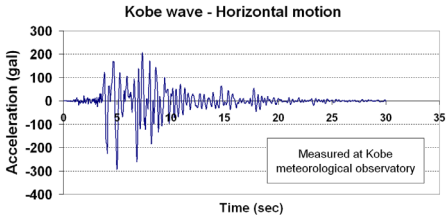

Figure 3. Input earthquake motion

Boundary Conditions. The boundary between the soil deposit and the bedrock is simply assumed to be fixed and would act as the bottom boundary of the analyzed domain at which the earthquake motion is imposed. The ground surface is assumed to be flat and free of loadings and the underground water level is assumed to locate up to the ground surface level when the soil is saturated.

The seismic behavior of the soil deposit in the far fields of the underground structure should assume the response of a free field. In the shaking table tests of soil-structures, a laminar shear box may be used to simulate the quasi-far-field boundary (Towhata, 2008). Here, quasi-far-field elements with a length of 10 *m* are placed at each extreme side of the analysis domain. The stiffness and unit weight of these elements are increased 100 times with respect to adjacent soil elements of the domain. As the far-field mode of seismic motion is simple shear, the length of the boundary condition (about the half of the domain height) is selected so that the bending deformation mode would not occur. This boundary allows the harmonized horizontal and vertical displacements similar to the case of laminar shear box.

Analytical Approach. The seismic analyses of the soil-structure system require that an initial stress field in equilibrium be obtained beforehand (Maekawa *et al*, 2003). Therefore, an initial static drained analysis was firstly performed to determine the initial stress field and static earth pressure on the duct. This static stress field is then used as the initial condition for the subsequent dynamic run with the input excitation.

Then, in order to investigate the effect of soil liquefaction on the damage of underground RC ducts, several models with and without the duct are analyzed in both drained and undrained states of pore water with various initial stiffness which is increased from 12 MPa to 230 MPa as shown in Table 1. The structure is assumed to be located inside the soil at a depth of 4 *m* without any change in the mesh property of the remaining soil elements.

Table 1. Material property for first soil layer

SPT *N*-value	G_0 (MPa)	D_r (%)
1	12	25
3	29	28
5	44	32
10	76	40
15	105	48
20	132	56
25	158	65
30	182	75
40	230	80

In order that the effect of the of sheet piling on the soil-structure response can be understood, an analysis is carried out with two sheet piles with a length of 18 *m* which are assumed to be installed at 0.5 *m* away from the both sides of the tunnel. The sheet pile is assumed to be made of steel with a Young modulus of 2.0 x 10^5 MPa and Poison's ratio of 0.3 using elastic elements. The thickness of the sheet pile is assumed to be 0.12 *m* so that its stiffness would be close to the sheet piles which are practically used. The sheet pile and the liquefiable soil (G_0 = 35 MPa) are assumed to be perfectly bonded. i.e., no interface element is used between them. The results are compared with those without considering sheet piles.

NUMERICAL RESULTS

Effect of liquefaction. Figure 4 shows the maximum shear deformation response spectrum of the RC duct and the soil volume which replaces it in the plain sandy grounds. It can be observed that the on-going practical design approach based on the free-field ground deformations can well predict the deformational demand on the underground RC structures in somehow stiffer soil mediums. In soft layers of soil which consists of loosely deposited sand, however, the design based on the free-field ground deformations would result in an overestimated deformational demand on the structural members as shown in Figure 4(a).

Besides, liquefaction may greatly bring about increased soil deformation which indicates that large soil strains with associated large degradation of the shear stiffness have developed within the ground. Hence, the underground RC duct which is located in the regions where the underground water level is high and designed without considering the interaction with the surrounding ground results in large amount of web reinforcement or large dimensions of structural elements for ductility demand. However, because of the deterioration of the surrounding soil stiffness which takes place in liquefied soil, the deformation demand on the RC duct would dramatically decrease resulting in less damage to the tunnel as shown in Figure 4(b). Therefore, that large amount of reinforcement or thick structural elements is not necessary. Finally, it should be pointed out that some countermeasures have to be considered to reduce the uplift of underground structure in liquefiable soils. Here, we investigate the effect of sheet piling as a widely used method in reducing the uplift.

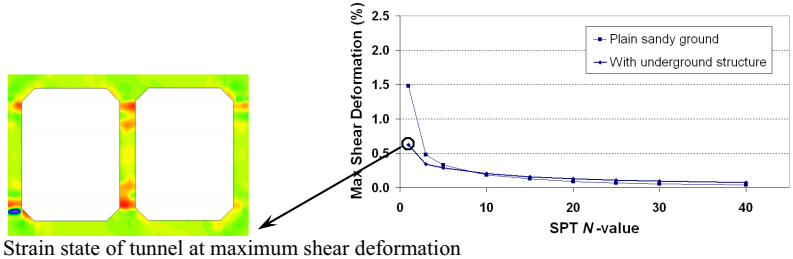

Strain state of tunnel at maximum shear deformation

(a) Drained condition

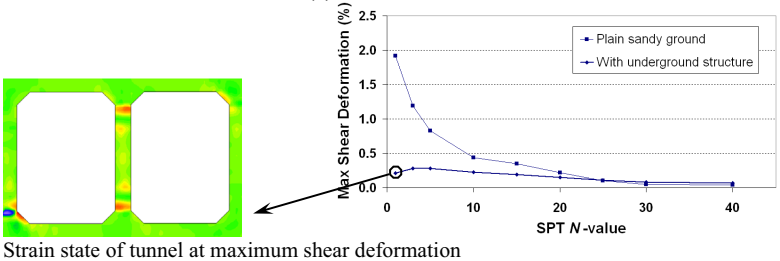

Strain state of tunnel at maximum shear deformation

(b) Undrained condition

Figure 4. Effect of soil stiffness on shear deformation

Effect of sheet piling. Many researchers have concluded that the effect of sheet piling in reducing the uplift of underground structures due to earthquake induced liquefaction is very obvious (Kimura *et al.,* 1995, Towhata, 2008). According to the finite element results in the present research, the uplift of the tunnel can significantly reduce when sheet piles with the length of are considered as shown in Figure 5. The deformed mesh after the earthquake motion for the cases with and without sheet piles is compared in Figure 6. It is clear that the floating of the subway tunnel is accompanied by the inward movement of liquefied soil under the structure which can push it upward. The sheet piles can reduce or even prevent such soil movement and therefore the uplift of the underground structure is much smaller.

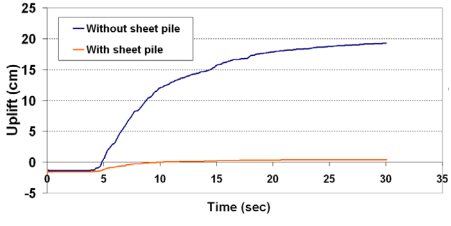

Figure 5. Effect of sheet pile in reducing uplift

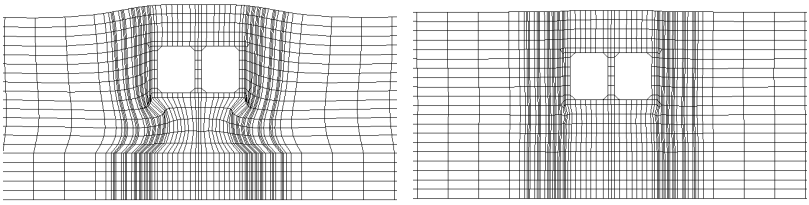

(a) Without sheet pile (b) With sheet pile

Figure 6. Part of the deformed mesh (enlarged 5 times)

Liu and Song (2006) propose that cutoff walls cannot always inhibit the development of excess pore water pressure. In comparison with the case without cutoff walls, the magnitude of excess pore pressure of the enclosed liquefiable soils depends on the soil properties and earthquake magnitude. The excess pore pressure responses for both of the above-mentioned cases at the location 2.5 *m* below of the centerline of the centerline of the tunnel are shown in Figure 7(a). The excess pore pressures are expressed in terms of the ratio of excess pore pressure to the initial effective overburden pressure. It can be understood that although the excess pore pressure in both cases develops almost similarly at the beginning of the seismic motion, it would decrease while the uplift of the tunnel takes place for the case without sheet pile. In fact, the flotation of the underground structure would cause larger shear deformation of soil which contributes to the lowering of excess pore pressure. The sheet piles alleviate the floatation so that the excess pore pressure remains nearly constant. Furthermore, the excess pore pressure 1.5 *m* above the structure in the case with sheet piles is smaller than that in the case without sheet piles as shown in Figure 7(b); however, it is clear that the soil could also liquefy with sheet piles installed.

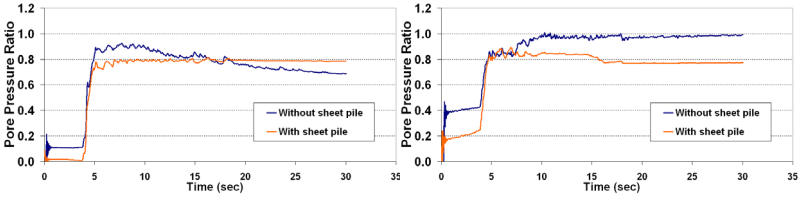

(a) 2.5 m below the tunnel (b) 1.5 m above the tunnel

Figure 7. The development of excess pore pressure

The shear deformation of the underground structure, on the other hand, has obviously increased when sheet piles are installed, as shown in Figure 8. The maximum shear deformation of the tunnel, for example, would rise from 0.28 % in the no sheet pile case to 0.37 % in the case with sheet piles. This is believed to be due to the increase of relative stiffness between the structure and the soil. In fact, the relative stiffness between the structure and the surrounding soil has the most significant influence on the distortion of the structure due to racking deformations

(Wang, 1993). When there is no sheet pile, the structure is rather stiff relative to the medium and does not deform so much. However, by restricting shear deformations in the enclosed soil, sheet piles can recover the soil stiffness degradation and thus more deformation demand would be applied to the underground structure. As a result, more damage would occur at the structural elements in the case with sheet piles as it can be observed in Figure 9.

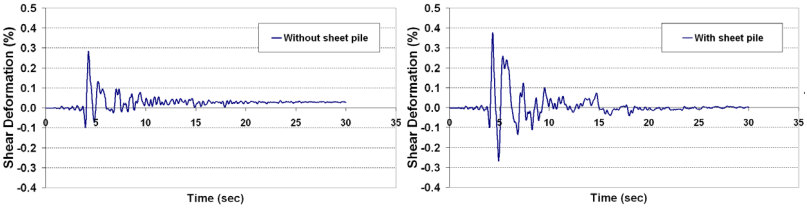

(a) Without sheet pile (b) With sheet pile

Figure 8. Shear strain response of the tunnel

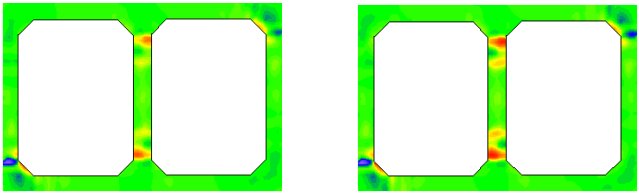

(a) Without sheet pile (b) With sheet pile

Figure 9. Shear strain state of the tunnel at the maximum shear deformation

CONCLUSION

In this paper, the nonlinear seismic response of an underground structure in dry and saturated liquefiable soils was investigated. From the numerical analyses, it can be concluded that in soft layers of soil which consists of loosely deposited sand, the design based on the large free-field ground deformations would result in high deformation demand on the structural elements which in turn requires large amount of reinforcement or large dimensions of structural elements. This situation would become even more severe in the regions where the underground water level is high because liquefaction may occur, which significantly increases the ground deformations. However, liquefaction would deteriorate the surrounding soil stiffness and thus the deformation demand on the tunnel would consequently decrease. Considering this issue could lead to a more optimum, economical and rational design of the RC underground structures.

Furthermore, it can be said that although installation of sheet piles can drastically alleviate the uplift of underground structures, it can cause the structure to suffer more damage due to the increase of relative stiffness between the structure and

the soil. Hence, a rational design of sheet piling should consider both of its positive and negative effects on the underground structure response.

REFERENCES

Hall, W. J., and O'Rourke, T. D. (1991) "Seismic behavior and vulnerability of pipelines." *Proc. Third Conf. Lifeline Earthquake Engineering*, 761-773.

Hashash, Y. M. A., Hook, J. J., Schmidt, B., and Yao, J. (2001). "Seismic design and analysis of underground structures." *J. Tunneling And Underground Space Technology*, 16(4), 247-93.

Japan Society of Civil Engineers (JSCE). (2002). *Recommended code and manual for seismic performance verification of out-door important structures of nuclear power plants*, Concrete Library.

Kimura, T., Takemura, J., Hiro-oka, A., and Okamura, M. (1995). "Countermeasures against liquefaction of sand deposits with structures." *Proc. First Int. Conf. on Earthquake Geotechnical Engineering*, Tokyo, 1203-1224.

Liu, H., and Song, E. (2006). "Working mechanism of cutoff walls in reducing uplift of large underground structures induced by soil liquefaction." *Computer Geotechnics*, 33(4), 209-221.

Maekawa, K., Irawan, P., and Okamura, H. (1997). "Path-dependent three-dimensional constitutive laws of reinforced concrete: formulation and experimental verifications." *Structural Engineering and Mechanics*, 5(6), 743-754.

Maekawa, K., Pimanmas, P., and Okamura, H. (2003). *Nonlinear mechanics of reinforced concrete*, Spon Press, London.

Maekawa, K., Fukura, N., and Soltani, M. (2008). "Path-dependent high cycle fatigue modeling of joint interfaces in structural concrete," *J. of Advanced Concrete Technology,* 6(1), 227-242.

Maki, T., Maekawa, K., and Mutsuyoshi, H. (2005). "RC pile-soil interaction analysis using a 3D-finite element method with fiber theory-based beam elements." *Earthquake Engineering Structural Dynamics*, 99, 1-26.

Masing, G. (1926). "Eigenspannungen and verfestigung beim messing," *Proc. of Second Int. Congress of Applied Mechanics*, Zurich, 332.

Okhovat, M. R., and Maekawa, K. (2009). "Seismic performance of large underground structures in unsaturated and liquefiable soils," *Proc. of Lifeline Earthquake Engineering in a Multihazard Environment,* ASCE, Oakland, 424-435.

Schmidt, B., and Hashash Y.M.A. (1998). "US immersed tube retrofit," *Tunnels Tunneling Int.*, 30(11), 22-40.

Towhata, I. (2008). *Geotechnical Earthquake Engineering*, Springer, Germany.

Wang, J.N. (1993). "Seismic design of tunnels: a state-of-the-art approach," Monograph, *Quade and Douglas Inc*, New York.

CANTILEVER ROOF STRUCTURAL FAILURE CAUSED BY EXCESSIVE CONSTRUCTON LOADS, FLAWED DESIGN, AND POOR MAINTENANCE

By Hal K. Cain,[1] Member, ASCE

ABSTRACT: A busy shopping center department store was suddenly brought to a standstill because of the collapse of the structural roof support system. This paper will explore the reasons leading up to the collapse. Those reasons include overloading the roof structural support system during re-roofing operations, design errors within the building structure, construction errors, and lack of maintenance of the building structure. Various roof loading conditions assumed during the re-roofing operations will be analyzed with the assistance of a computer structural analysis program. A torsional analysis will also be performed to determine if the structure collapsed by way of torsional overturning under load. Other modes of failure investigated were lateral buckling, web crippling and sidesway web buckling. The paper concludes that the structure failed due to under-designed cantilever beams, no weak axis bracing, excessive welding of joists to structural beams, poor maintenance of the building roof, and poor supervision of the Roofing Contractor.

INTRODUCTION

The Department Store in question is a two story structure, 420' 10" x 216'10", cantilever style construction. This one particular department store was only one store of many stores in a very large shopping mall. A building with this style of construction should have a service life of at least one hundred years if properly maintained. On a routine morning on May 4, 1999 a busy shopping Mall Department Store in Mobile, Alabama was brought to a standstill due to a roof collapse in a defined area approximately ten feet by fifteen feet. Roofers had been busy with preparation for re-roofing operations. The work crew had been scraping up rooftop gravel for disposal over the side of the building. However the work methods of the crew were such that they had piled up gravel over a fairly confined area approximately 4.27 m x 2.44 m x 21.59 cm high. Further a number of large workers were in the vicinity of the pile. Without warning a section of the roof structure, deck, and roofing collapsed downward into the storage section of the department store, rupturing a sprinkler pipe, and damaging the structure, HVAC ducting, and electrical cable and conduit. Fortunately the roof did not fall on any employees or shoppers at the store. The construction of the roof in the area of the collapse, as part of the cantilever construction, consisted of W8 x24 columns at 8.53 m on center, with a W 14 x 22 beam resting on top of the columns and bolted to the top plate of the column with four bolts. The corrugated roof deck was supported by steel roof joists 12 H 4 @ 1.22 m on center and 8 H 2 @ 1.22 m on center about the failure line of the beam that rotated and caused the collapse. The plans required a 1 ½" x 1 ½" x 3/16" angle

to be field welded from the bottom flange of the W 14 x 22 to the bottom chord of the roof joist within 1.68 m of the column support. The roof construction consisted of corrugated 9/16" form deck, zonolite (lightweight concrete) fill and a three-ply organic felt built-up roof, covered by river gravel ballast.

Similar failures of cantilever beam and post construction for Shopping Centers have occurred in the past as described in "Construction Failure," Second Edition, by Feld and Carper. This book describes the Station Square Shopping center Roof Failure, Burnaby B.C., Canada, in 1988, as well as the Magic Mart Store, Bolivar, Tennessee in 1983 that had catastrophic roof failures. The cause of these failures were related to an overloaded roof structure and lack of bracing of the compression flange at the column line. The failure of the Alabama roof structure is very similar, however the causation factors are quite different.

The purpose of this paper is to demonstrate and explain how a number of design and as-constructed conditions, not just an excess pile of materials and workers, worked together to cause a collapse that could have easily led to several fatalities, but did not.

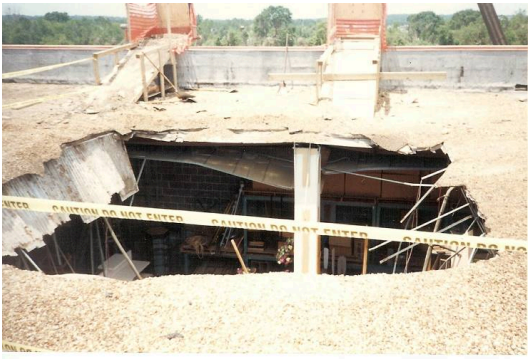

Figure 1. Collapsed area, the column straight ahead is on col. Line 7-K. Note corrosion on sheets.

Figure 2. Area of Failure

Figure 3. Beam rotation along K line, significant between column K and 6-8 as seen in photograph.

HISTORY & CONDITION ASSESSMENT OF BUILDING

The assessment of the roof immediately after the failure revealed that the zonolite fill lightweight concrete was wet and the roof decking material was corroded. An assessment by a Corrosion Engineer revealed that the roof form deck sheets had severe crevice corrosion at the lap splices of the sheets. A laboratory analysis of the zonolite concrete revealed moisture contents of 14 % to 16 %. It was discovered from the Store Manager that the roof had been leaking for the last six years. An inspection of the roof outside the area of failure revealed soft spots that were obviously wet, especially in the area of rooftop Cooling Towers for the main Chiller Plant.

An inspection in the Store room adjacent to the roof failure area revealed very severe corrosion of the metal deck in the operating area of the store room. Further, there were no flange braces anywhere between the W14 x 22 beams and the roof joists, as required by the contract drawings. Thus one has to conclude that the structure was not built according to the plans and the building was not being maintained properly.

STRUCTURAL COMPONENTS EVALUATION & QUALITY CONTROL

The collapsed roof joists and structural beam (W 14 x22) were taken to the Structural Steel Erector's lay down yard for temporary storage. The steel joists in the area of the collapse revealed poor quality welding although the welds provided more than adequate strength. The welding within the joist revealed lack of penetration and porosity in the weld. This is an issue with quality control in the fabrication shop of the bar joist manufacturer. The main structural support beam that failed (W 14 x 22) had a visible delamination mark and should have been rejected by the fabrication shop prior to shipment and maybe even prior to fabrication. This, however, was not the reason for the failure.

Close examination of the joist attachment area to the beam revealed that the joist support plate was welded solid to the top flange of the beam on three sides, creating a fixity or moment connection of the joist to the beam. This was seen in several areas along the top of the beam. It is worth noting that the 1972 Standard Specification for Open Web Steel Joists to steel supports should be two, 1/8" fillet welds 1" long or a ½" bolt. In other words, the connection should be a pinned connection, not a rigid connection. Joist manufacturers also have the same requirement shown on their standard details.

Figure 4. Note delamination in beam marked by welding inspectors at joist No. 1, above col. K-7. Note extensive welding and fixity of joists assisted in failure.

Figure 5. Bending of beam web plate about bottom fixed flange. Weak axis bending.

BUILDING CODE and BASIS of DESIGN

The Code used as the basis for design was the 1973 Standard Building Code. The basis of design for the steel joists was the Standard Specifications for Open Web Steel Joists, J & H Series, by the Steel Joist Institute, while the structural steel would have

been designed in accordance with the Manual of Steel Construction AISC, Sixth Edition. The roof live load required per the Standard Building Code is 20 pounds per square foot, and the dead load requirement is the weight of all permanent construction. The engineer of record designed the building for 25 psf dead load and 25 psf live load. The actual dead load was approximately 10 psf. Therefore the basis of design for loading was in fact conservative.

DESIGN CODE VIOLATION

The most obvious design violation was the specification to weld the steel joist on both sides of the support plate, 2" x 3/16". This is in violation of the Steel Joist Institute Specification 5.6 (b), Steel Supports. This specification states that "ends of joists resting on steel supports shall be connected thereto with the equivalent of two each - 1/8-inch fillet welds 1 inch long, or a ½-inch bolt." Further "In steel framing, where columns are not framed in at least two directions with structural steel members, joists at column lines shall be field bolted at the columns to add lateral stability." The joists were welded solidly to the W 14 x22 beam, creating a fixity condition that was an obvious quality control issue in the field.

CALCULATIONS

Certain load cases were modeled and calculations were made with the STAAD program. The main beam that failed in the analysis, the W 14 x 22 and supported along column line K, was loaded with the design basis load, and carrying roof joists that were supported by the beam as simple connections. Under this criteria the beam failed. The STAAD analysis re-designed the beam as a W 16 x 26 under the design load conditions.

Under the criteria of what we named Load Condition No. 2 with a pile of gravel 4.27 m x 2.44 m x 21.59 cm high, and one man standing in the area and under the actual dead weight of the roofing material, the beam does not reach a failure point based on the STAAD analysis. The bar joist, 12 H 4, exceeded its capacity along a 4.57 m length of its 7.31 m length.

Load condition No.3 was based on an area of gravel 4.27 m x 2.44 m x 21.59 cm high", four (4) people in the area and one loaded wheelbarrow. It is assumed that each person weighs 890 newtons. The bar joist under load, a 12H 4, has an ultimate capacity of 29.94 kn-m. The maximum moment produced was 28.24 kn-m. The joist did not fail, but was very close to its ultimate capacity. The W14 x 22 beam did not fail under the STAAD analysis, without torsion effects.

Loading Condition No. 4 was similar to Loading Condition No. 3 except six (6) people were used as a basis of line loading instead of four (4) people. No effects of torsion were considered, and the STAAD model was run. The W 14 x 22 main support beam passed the STAAD analysis, no failure. The allowable capacity of the 12 H 4 joists, (Joist No. 1 being directly over the column) 24' length, was exceeded,

but the ultimate capacity was not, however it was on the borderline of complete failure.
M (all) =20.11 kn-m, M (ult) = 29.94 kn-m, M (act) = 28.24 kn-m. Therefore M (act) < M (ult).

A torsional analysis was run since the overloaded roof joist sitting above Column K-7 (the column that failed) was solidly welded to the top of the column. The W 14 x 22 pulled completely over, almost a 90° turn. The torsional load was transferred to the W14 x 22 by the fixity across the top flange by the support plate of the roof joist. The loading on the structure was exerted by Load Condition No. 3 and No. 4, the pile of stones, wheelbarrow, and personnel working above.

A STAAD model was run and that analysis revealed torsional failure. Hand calculations were performed, and the results were close to results of the STAAD Analysis, but failure, nevertheless. The maximum torsionsal load transferred to the top of the W 14 x 22 was 107.37 kn-m. Most practicing structural engineers would consider a torsional moment of that magnitude on the beam to be excessive, without performing the first calculation. The summary of hand calculations are included herein.

Summary of Torsional Stresses

Location	Normal Stresses MPa		Shear Stresses MPa		
	Warping 6_w	Bending 6_b	Torsional τ_t	Torsional $\tau_{w(warping)}$	Bending τ
Centerline of Beam					
Flange (max)	-626.7	+26.2	-500.0		-3.4
Web (max)			-343.3	+17.5	-0.51
Beam Support					
Flange (max)	0	-74.7	-		
Web (max)	-		-	-247.6	

Max combined stresses

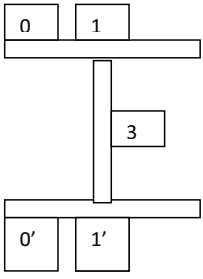

Pt. 0 The max normal stresses occur

at midspan or centerline.

Pt.0 $6_b + 6_w$ = -626.7 +26.2 = -600.5 Mpa (tension)

Pt. 0' 6 = 6b + 6w = + 600.50 (compression)

Maximum shear stress occurs at centerline or midspan of beam

At Pt. 1 - τ (sheer stress) = -500 + 26.2 = -473.8 MPa (acts toward left)

At Pt. 1'- τ = -473.8 MPa acts toward right

At Pt. 3 – τ = -343.3 MPa acts downward All failures > 240 MPa

Torsional failure

At Pt. 1 -473.8 MPa -473.8/ 240 = -1.97

At Pt. 3 -343.3 MPa -343.3/240 = -1.43
At Pt. 1' -473.8 MPa -473.8/240 = -1.97

Staad ProTorsion Analysis

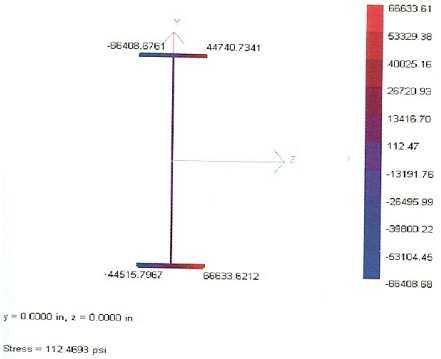

At Pt. 0 as above, stress due to torsional loads = 66.4 ksi = 442 MPa
At Pt.0' as above, stress due to torsional loads = 44.5 ksi = 297 MPa

Figure 7. Torsional stresses on Beam at Column Line

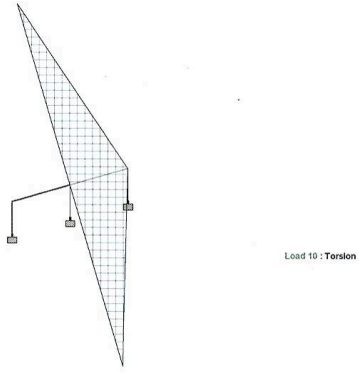

Figure 8. Torsional moment diagram of rotated beam

AISC (1967) Analyses of Failure Modes

Various analyses of failure modes were considered without the effects of torsion, or web plate bending. The loading produced by load case No. 3, the heaviest load, is considered a transfer by shear only. The calculations revealed that the beam should not have failed by lateral buckling, web crippling, or sidesway web buckling.

SHEAR CALCULATION: 1967 AISC Manual of Steel Construction (Section 2.4 Shear)

V_u = shear in kips
F_y = yield stress of steel (psi)
w= web thickness
d= depth of beam
$V_u = .00055F_ywd$
V_u = .00055 x 36 ksi x .23 in x 13.75 in
V_u = 62 kips (276 kn) V_{act} = 6.23 kips (27.8 kn)
$V_u > V_{act}$ therefore no failure

Section 1.10.10 Web Crippling

Web compressive stresses at the toe of fillets from compressive stress due to concentrated loads not supported by bearing stiffeners shall not exceed .75 F_y = .75 X 36 = 27 ksi (180 MPa)

Compressive stresses allowed on web: Section 1.10.10.2

$$[5.5 + \frac{4}{(386/13.75)^2}] \frac{10{,}000{,}000 \text{ lb/in}^2}{(h/t)^{-2}} \qquad \text{Formula 15}$$

h= clear distance between flanges
t= thickness of web
F_{cr} = compressive stress

$$F_{cr} = \frac{5.5 \times 10^7}{(13.75/.23)^2} \qquad \text{Formula 15}$$

F_{cr} = 1.54 X 10^4 = 15,400 psi or 15.4 ksi (102.7 MPa)
$V_{cr} = P_{cr}$ = 15.4 X 13.75 X .23 = 48.7 kips (216.6 kn)
Shear and web crippling are not a problem based on formula 15.
Stiffeners are not needed.

LATERAL BRACE

A lateral brace 1 ½" x 1 ½" x 3/16" was designed into the structure to run from the bottom chord of the joist to the lower flange of the W 14 x 22 Beam, 1.68 m from the end of each column (W 8 x 24). The braces were never installed. Maximum tension in the bottom chord of the truss was determined to be 82.7 kn at allowable capacity. The angle brace, however, could only transfer 5.43 kn before exceeding the ultimate bending stress in the angle. The angle brace, as designed, is not a brace at all. In a double curvature case such as this, lateral braces must be attached to both flanges to be considered a true brace. The brace in question does not meet this criteria. Even

though the brace would not have worked, it is a moot point since the brace was never installed. No Y axis bracing was installed along the beam line (K), and the result was tragic.

CONCLUSIONS AND RECOMMENDATION

The analysis of the failure of this building revealed multiple problems. Those problems consisted of design errors, steel fabrication quality issues, installation problems, and quality control during construction. The roof was not maintained well and the lack of proper supervision during the re-roofing operations allowed a substantial roof overload from personnel and gravel to exert a torsional load on the beam that ultimately failed. The roof joist over column K-7 was solidly welded to the top of the flange of the W 14 x 22 beam that allowed a torsional load to be exerted across the beam and twist the beam approximately at a 90 °angle. The Steel Joist Institute Specifications specify fillet welds on either side of the joist support plate to be 1/8" x 1" or a ½" bolt. The deteriorated condition of the metal roof decking also weakened the ability of the deck to transfer load across the structure. The angle braces between the bottom chord of the joist and bottom flange of the beam that should have been installed on each end of the beam within 1.68 m from the columns but were not, also weakened the structure.

The recommendation is that quality control should be exercised during the design phase of any project, during fabrication of structural steel and joist manufacturing components, and during construction to ensure that the building or structure has been built according to the plans. Further the building owner has a responsibility as well to ensure that the building is being properly maintained and that the Contractors performing repairs and especially re-roofing operations are properly supervised.

Appendix. References

Manual of Steel Construction, Sixth edition (1967), American Institute of Steel Construction
Manual of Steel Construction, Seventh edition (1970), American Institute of Steel Construction
Manual of Steel Construction, Eighth edition (1980), American Institute of Steel Construction
Standard Building Code, 1973, by the Southern Building Code Congress International, Inc.
Standard Specifications for Open Web Steel Joists, J and H series, November 1, 1972.
Torsional Analysis of Structural Steel Members, 1997 Steel Design Guide Series, American Institute of Steel Construction.
Construction Failure, Second Edition, 1997, by Jacob Feld and Kenneth L. Carper.

[1] Principal Engineer, Cain and Associates Engineers and Constructors, Inc, 3100 Cottage Hill Rd., Suite 201, Mobile, AL 36606

CONVENTION CENTER

STEEL TRUSS COLLAPSE

Presented By

Benjamin Lavon[1] & Andrew Goodrich[2]

Abstract

Bow truss 13 failed during construction of the David L. Lawrence Convention Center in February 2002. Bow truss 13 was designed to withstand the gravity loads and horizontal tension loads from the roof suspension system. The truss itself required stabilization during erection proceedings to prevent it from toppling over. During construction a change order was introduced directing that the bow truss be temporarily supported by a tension strut in lieu of the originally designed compression strut. In addition, no clear erection procedure was given in the shop drawings for the tension strut. During construction, the connection fastening the tension strut to the foundation block failed. Bow truss 13 rotated forward and then to the side, landing on the ground killing one steel erector/iron worker and injuring two others. To prevent this kind of failure of a non-self-supported structure in the future, proper and clear erection notes should always be provided during construction.

Introduction

An accident occurred at the project site of David L. Lawrence Convention Center on February 12, 2002. Bow truss "X13" collapsed during erection. As a result, one steel erector/iron worker was killed and two others injured. The truss was the thirteenth bow truss to be erected. The bow truss was erected in parts, as it was extremely heavy, approximately 150 tons (300 kips). The crane used for the truss erection was used to lift the steel pieces into place. However, the crane was not engaged to provide

[1]Benjamin Lavon, P.E., President, Feld Kaminetzky & Cohen, P.C. 237 West 35th Street, Suite 501, New York, NY 10001; PH (212) 687-8282 ; FAX (212) 661-8090; e-mail: blavon@FKCeng.com

[2]Andrew Goodrich, P.E., Associate, Feld Kaminetzky & Cohen, P.C.; e-mail: agoodrich@FKCeng.com

any stability measures via the hoist lines. Neither guy wires, nor crane hoist lines were provided for stability measures during the bow truss erection process. See Figure 1 for general description of the collapse.

At the time of the accident, erectors/iron workers were in the process of installing floor beams that connected bow truss "X12" to bow truss "X13". These floor beams provided some partial lateral restraint and stability to bow truss "X13". However, these measures proved to be inadequate.

Tension members were provided at the tension support, at point "A1.5", in order to resist tension loads during erection and to address stability measures.

Subsequent to the collapse, the firm of Feld, Kaminetzky & Cohen, P.C. (FKC) was retained on behalf of the insurance company, to investigate this failure and to provide our engineering opinion regarding the causes for the failure.

This presentation will discuss:

a. Review of existing project records, design and construction documents, engineering reports, building codes, OSHA files, laboratory reports, and correspondence.
b. Site visits to observe and record field conditions.
c. Office studies performed based on information obtained from field data and testing.
d. Discuss the causes for the collapse and lessons learned.

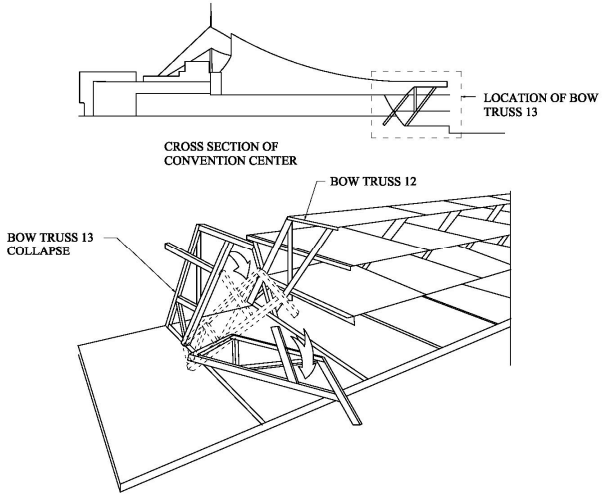

Figure 1. General Project Description.

Figure 2. General view of a Bow Truss. It weights 300 Kips.

For description of a bow truss refer to Figure 2.

Project Records

Sports and Exhibition Authority, the owner, contracted with an architect, to design the convention center facility and to provide construction administration services. The architect retained a structural engineer to provide structural design and prepare structural drawings, including erection procedures and to review shop drawings and erection procedures, stability measures, etc. The structural steel fabricator and erector for the project produced shop drawings, erection procedures, and structural calculations for the fabrication and erection of the structure including bow truss "X13". These documents were issued for review and comment to the structural engineer and the construction manager. A vendor provided the tension rods and nuts used for the tension support of bow truss "X13"at point "A1.5". The rods and nuts were sold to the erector and shipped to the site, to be installed by the erector.

Type of Construction

The structural system of the facility includes bow trusses on the north side and stern trusses on the south side. The bow trusses and the stern trusses are constructed of built-up structural steel members and provide support for the suspension roof cable system of the convention center structure. For general description of the structure see Figure 1.

There are fifteen rows of bow trusses and stern trusses altogether, Row "X1" to Row "X15". Each row has a different geometry and is increasingly longer and higher than the other. Row "X1" is the smallest and Row "X15" is the largest. The bow

trusses and stern trusses are supported by caisson foundations. In addition to the roof cables, the bow trusses support various floor beams of the facility, at three levels, Elevation 760'-2" (second floor), Elevation 786'-2" (third floor), and roof level.

Bow Truss "X13"

Bow Truss "X13" stood approximately 73 feet high and weighed approximately 150 ton (300 kips). A general description of the truss, including the tension strut, are shown in Figure 3.

A number of floor beams connected Bow Truss "X13" to Bow Truss "X12", at time of the accident. All the beams of the second level (760'-2" elevation) were installed, a total of twelve beams; seven beams of the third level (786'-2" elevation) were installed; there were no beams installed at the fourth level roof (806'-2" elevation). It is FKC's understanding that all the above beams were in the process of being installed and therefore only partially connected with bolts at the time of the accident.

Bow Truss "X13" was supported during erection at two supports: at support "A1", which was subjected to bearing (compression) loads and at support "A1.5", which was subjected to tension loads, that were generated due to the truss gravity loads and construction loads, via a tension member. See Figure 3 for locations of compression and tension connections and Figure 4 for erection procedure. The tension connection

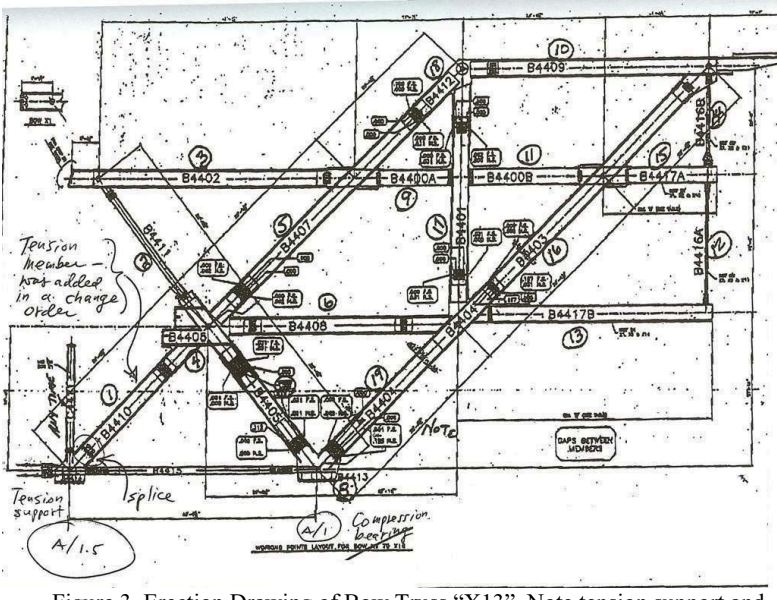

Figure 3. Erection Drawing of Bow Truss "X13". Note tension support and compression support.

failed during erection and is the subject of this investigation. See Figure 5 for the failed tension connection at the support.

The structure was not self supported and therefore required special and specific erection procedures in order to remain stable during construction.

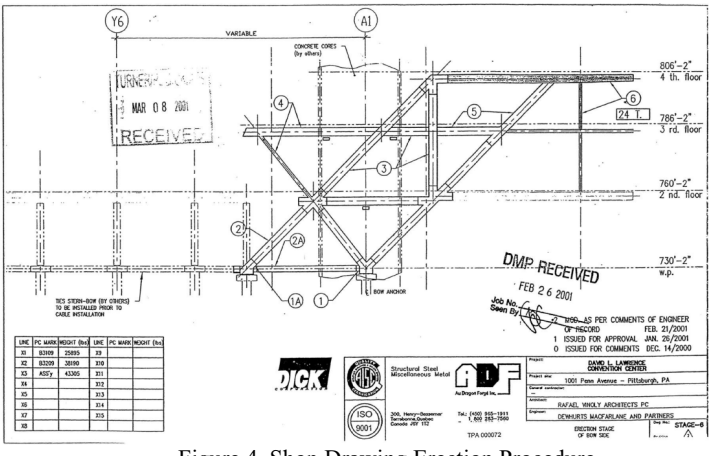

Figure 4. Shop Drawing Erection Procedure

Figure 5. Collapsed Truss During Erection – Note Tension Connection at support.

Tension Strut

The said tension member was a tension strut that was designed to transfer erection tension loads only, due to the bow truss self weight and construction loads at the time of erection/construction. This tension strut was introduced as a result of a change order. Originally, the structural drawings specified a vertical compression member (compression strut) to be provided in order to support the bow truss gravity loads and to prevent truss rotation during erection. The tension strut was specified as a diagonal member located at point "A1.5"; its purpose was to prevent rotation of the bow truss during erection. It should be noted that the connection between the tension strut and its support was originally designed as a rigid connection that could not be adjusted at any time. Refer to Figure 6. However, due to constructability issues, it was decided that an adjusted tension connection should be provided to allow for needed adjustment for the truss during the erection of the roof suspension cables. Refer to Figure 7.

Tension Connection

The tension connection, at point "A1.5", included eight threaded rods connecting the tension strut base plate to a tension support base plate assembly on the caisson foundation. See Figure 8. It was specified that an initial erection gap of approximately eight inches be introduced in between the base plates of the tension strut and the support. The erection gap would be bridged by an adjustable shim pack. The threaded rods would penetrate slotted holes in the tension strut base plate, would go through the shim pack, and penetrate slotted holes in the base plate of the support.

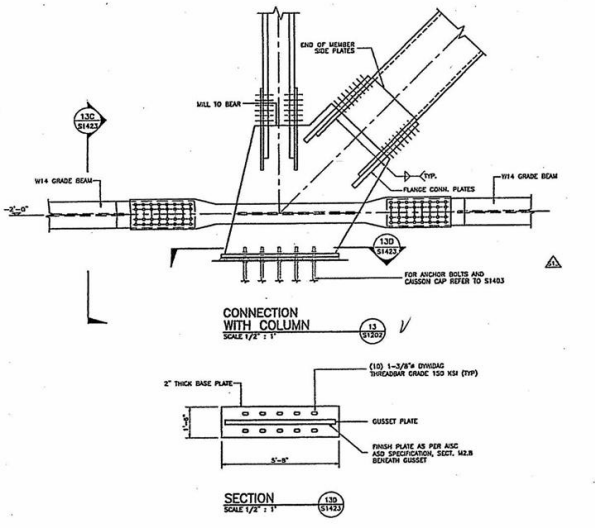

Figure 6. Tension connection, Design Detail – Fixed.

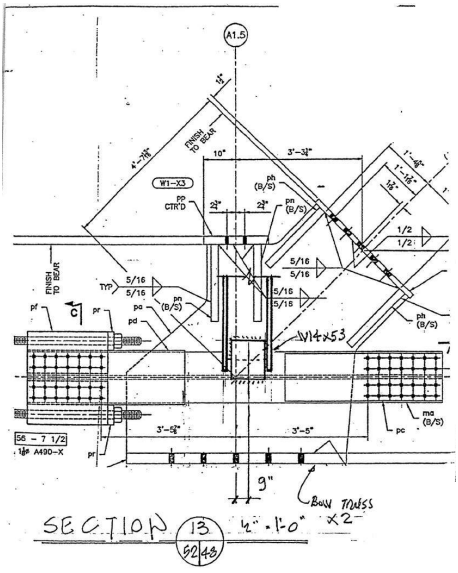

Figure 7. Tension connection, Shop Drawing Detail – Adjustable.

Figure 8. Tension Connection Detail – Adjustable

The eight threaded rods were a proprietary product, one-inch diameter, 1'-6", long grade 150 (150 ksi ultimate tension strength) steel alloy material. See Figure 9. The threaded rods required certain nuts to be utilized for strength and adjustment requirements. Therefore, hex nuts were to be used for strength and jam nuts were to

Figure 9. Failed Connection Rods at tension support – Note stripped threads

be used to lock the hex nut in position. However, the shop drawings were not clear and did not provide specifics regarding the nuts to be used, tightening procedures, sequences of the rods/nuts installation, nor did they include any specific information regarding hex nuts or jam nuts use.

The threaded rods and nut connections of the tension connection were the subject of FKC investigation, as they failed during erection. The construction field reports, accident reports, and FKC's own field inspection observations revealed that instead of the proper hex nuts and jam nuts needed for the rod connections, cut nuts were used. See Figure 10. Hex nuts, 2 inches long, are typically shown on the manufacturer's data sheets. The hex nuts are locked in position by jam nuts. However, cut nuts, approximately 3/4 inch long, were found on and around the failed threaded rods after the accident.

The vendor had shipped to the site cut nuts for erection, in lieu of jam nuts that are used for locking the hex nuts. However, the vendor failed to notify the construction manager and the erector that they had shipped cut nuts to the site.

FKC reviewed the probable applicable tension loads during erection. According to the fabricator's calculations, the originally estimated tension connection loads were 504 kips. The estimated tension loads were subsequently reduced to 435 kips.

However, according to the structural engineer's calculations, the tension loads were estimated at 366 kips. But, after the accident, the engineer's estimated tension loads

Figure 10. Failed Connection Rod Nuts at tension support – Note stripped threads

during erection were reduced to 109 kips. However, according to FKC estimates, the tension loads at the time of the accident, based on available data, were approximately 168 kips.

While all eight tension rods were installed in the failed tension connection, the erector did not install hex nuts and jam nuts, but rather cut nuts only. The sequence of the nut installation is unknown. It was found that the failed rods and nuts exhibited failure of the threads in the rods and nuts due to stripping (shearing off) of the threads, as examined in the field by FKC, and as reported by a testing agency that was retained subsequently. See Figure 10.

After the accident, a testing agency tested samples of hex nuts, jam nuts, and cut nuts in pull tests to determine the ultimate strengths of various combinations of rods and nuts. The test results were: jam nuts - 71.5 kips; cut nuts - 57.9 kips; hex nuts - 120 kips. Thus, using cut nuts was the weakest link of the tension connection by the threaded rods.

If the tension loads had been evenly applied to all eight tension rods during erection, the rods and nuts would have had sufficient structural capacity to resist the tension loads. However, due to connection eccentricity, dynamic shifting of the truss, and uncontrolled nut tightening by the erector, it was impossible to engage all the nuts to evenly distribute the tension loads among all the rods during erection. Further, due to erection adjustments, it is most likely that dynamic movements of the bow truss, as well as out-of-plumb of the truss, had subjected the tension connection and the threaded rods to unsymmetrical, unbalanced, and eccentric loads, thus causing single threaded rods to carry excessive tension loads, and cause overloading. The

overloading exceeded the rod/nut capacities, as evidenced by the failure mode of the stripped threads of the cut nuts and rods.

Conclusions and Recommendations

Erection of the bow trusses was not a straight forward procedure. Bow truss "X13" self weight was approximately 150 tons (300 kips). It had to remain plumb and stable during erection. The erection process was a complex one that needed proper coordination efforts and attention by all parties concerned - engineer, fabricator and erector.

Therefore, proper and clear erection notes and procedures should have been provided in order to direct the erector on all stages of erection. However, these were clearly missing from the shop drawings.

Optimizing the erection load distribution to the tension rods would have increased the tension connection strength and would have enhanced the truss stability.

Lessons Learned

1. Provide proper bracing and stability measures during erection, such as guy wires, crane hoist lines, and other methods to enhance stability during erection. Stability resistance loads are only 1% to 2% of the gravity loads.

2. When erecting a not self supported structure, special attention during erection is needed. Therefore, the structural engineer, the fabricator and erector, should devise proper procedures and stability measures for safe and successful erection.

3. Clear instructions and procedures should be provided by erectors supervisory personnel to their laborers. The erectors personnel should be provided with training, instructions, direction and supervision.

4. Erectors should be properly trained to avoid:
   a) Lack of, or confusing erection procedure.
   b) Unbalanced loads (created) during erection.
   c) Erection violations of OSHA provisions.
   d) Lack of proper training of its employees.
   e) Lack of proper supervision of its employees.
   f) Lack of proper inspections of its work.
   g) Use of improper hardware for critical connections.
   h) Lack of proper engineering review of the erection procedures and approval thereof – when dealing with complex erection.
   i) Design or fabrication changes that impact erection procedure.

Structural Robustness Evaluation

S. M. Marjanishvili, PhD, PE, SE[1], L. Leininger, PhD[2],
M. Miraglia[3] and I. Alsharkawi[4]

[1] Hinman Consulting Engineers, Inc., One Bush Street, Suite 510, San Francisco, CA 94104; PH (415) 621-4423; FAX (415) 621-4447; email: shalva@hce.com
[2] Hinman Consulting Engineers, Inc., One Bush Street, Suite 510, San Francisco, CA 94104; PH (415) 621-4423; FAX (415) 621-4447; email: lara@hce.com
[3] Hinman Consulting Engineers, Inc., 225 Reinekers Lane, Suite 250, Alexandria, VA 22314, PH (703) 416-6780; FAX (703) 836-4423; email: michael@hce.com
[4] Hinman Consulting Engineers, Inc., 225 Reinekers Lane, Suite 250, Alexandria, VA 22314, PH (703) 416-6780; FAX (703) 836-4423; email: iman@hce.com

ABSTRACT

This paper proposes a quantitative measure and mathematically reproducible definition of structural robustness as it pertains to a structure's ability to minimize the potential for structural progressive collapse. Structural robustness is defined by the structure's ability to withstand any unforeseen loading as well as initiating damage scenarios without a disproportionate response. Presented here is a study that finds that in the absence of the specific progressive collapse load scenarios and unknown location and extent of initiating damage, progressive collapse potential can be minimized by employing the concept of structural robustness as well as safety and reliability, which are all interdependent qualities of a structural system. This study also concludes that structural robustness represents a structure's ability to absorb small structural failures (perturbations) without affecting the overall structural integrity, and can be measured as a standard deviation of the progressive collapse dynamic resistance probability density function.

KEYWORDS

Progressive collapse, structural robustness, structural resilience, reliability

INTRODUCTION

The primary goal of the structural designer is to reduce the probability of failure of a structure to a level deemed acceptable to society. The current state of the practice is to achieve this goal by evaluating a structural system under defined (i.e. deterministic) loading scenarios and by providing the requisite structural resistance to the defined loads. The general consensus is that this approach results in a "robust" structure that is resistant to collapse. Exactly how this "robustness" is provided in the structure is unclear and the actual "robustness" of the structure is also left un-quantified, undefined and assumed to be enhanced through the design approach. This

assumption is certainly reasonable given the practical constraints of building design, but is perhaps unsatisfying because the actual robustness is left un-quantified. It is the goal of the research community to provide analytical approaches to quantify the reliability, overall "robustness" of the structure, and evaluate the performance of existing design guidance in reducing probability of failure. It is the aim of this paper to present a logical framework in order to quantify structural robustness and probability of failure as they pertain to the progressive collapse phenomenon.

ROBUSTNESS DEFINED

Remarkably, there is little common ground on the definition of robustness. A quick look at the dictionary reveals five variations of the adjective with three of those five including the word "strong" or "strength". The U.S. General Services Administration (GSA) Progressive Collapse Analysis and Design Guidelines describes robustness as the ability of the structure to resist failure "due to its vigorous strength and toughness". So, it is natural that structural engineers, when asked about the meaning of robustness, would reply with words like "strong", "resilient", "ductile", and "redundant". There is currently no direct guidance out of the United States building codes standards that link robustness with a quantifiable definition. Be that as it may, other engineering and scientific disciplines have various specific definitions of robustness, and it is helpful to examine them here. Insight from outside of the structural engineering community combined with specific definitions of structural engineering metrics will lead to an adaptation to the definition of robustness and a novel way to evaluate building systems.

In November of 2005, the Joint Committee on Structural Safety (JCSS) and the International Association for Bridge and Structural Engineering (IABSE) working Commission 1 convened a workshop on the robustness of structures. The European establishment has shown itself to lead the Americans in the integration of reliability metrics into their building code, and it should come as no surprise that they are leading the discussion of structural robustness as well. At the conclusion of the conference it was agreed the robustness is the "product of several indicators," many of which might be expected to be associated with robustness. The indicators identified include many of the aforementioned metrics: redundancy, ductility, variability of resistance, interdependency of failure modes, and joint performance, just to name a few. From the conclusions of the workshop, it was identified that the definition of robustness from Eurocode should be adopted and understood as the "ability of a structure to withstand events like fire, explosions, impact, or the consequences of human error, without being damaged to an extent disproportionate to the original cause" (prEN 1991-1-7:2004, 1.5.14).

Based on these conclusions it is evident that robustness is a complex metric not solely related to strength, but rather it is part of a system of indicators (one of which is strength), and that the quantification has to do with the structure's sensitivity to stimulus, regardless of the magnitude of the stimulus.

Furthermore, in a presentation by M. Faber at the Workshop COST C26 held in November 2006, definitions of robustness were explored as they are understood in other scientific disciplines. In his presentation, references are made to standards in structural engineering, software engineering, product development, control theory,

and others. In all cases, a pattern emerged wherein the robustness is quantified as the measure of deviation from the expected performance. It is not directly related to the measure of the performance.

Reliability techniques can be applied in structural engineering to compute the probability of failure based on a distribution of threats, or hazards, and a corresponding distribution of resistance to those hazards. The probability of failure is determined based on the relative positions of the load and resistance Probability Density Functions (PDFs) on a strength ordinate. Within the context of the definition of reliability, the probability of failure can be decreased by either: moving the relative positions of the PDFs to decrease overlap (decrease the load, increase the strength) or by decreasing the dispersion, or standard deviation of the PDFs (by increasing the certainty in the definition of either the load or the resistance).

In Protective Design, the load from the threat is unpredictable because the nature of the threat is always changing, evolving, and (usually) increasing in frequency and magnitude (TSWG, 2004). In this practice, it is difficult to predict any structure's reliability given the great dispersion that is expected in the load scenario induced by the threat, though it is possible to determine and influence the dispersion of the resistance function. Increasing the certainty in the structural resistance by decreasing the standard deviation of the resistance – regardless of the expected value of the resistance (or strength) – increases the reliability for a constant load PDF, and it also decreases the sensitivity of the structural response to loading stimuli. The physical outcome of a narrow PDF for resistance is that the reliability of the structure will likely be unaffected by small perturbations in loading. This outcome is consistent with the Eurocode definition of robustness as well as the expected behavior of robust systems in various scientific fields.

DEFINITIONS FOR PROGRESSIVE COLLASPE RESISTANCE

Before introducing an example of robustness quantification in the context of progressive collapse, important concepts and definitions will be briefly outlined that are typically used when discussing the potential for progressive collapse and improving the overall robustness of a structure.

Threat is defined as an intentional or accidental event that causes ***initiating damage***. Traditionally these threats include (but are not limited to) impact, explosion and fire.

Initiating damage for progressive collapse is a relatively small damage, that (under ***progressive collapse load***) triggers larger failures in structural systems (i.e., failures in ***progressive collapse resisting mechanisms***), which in its turn triggers more failures resulting in widespread collapse and eventually leads to a complete or partial collapse of a structure. It worth noting that, by definition, progressive collapse occurs when initiating damage is very small in comparison to final collapse of a structure. For example, in Protective Security, the initiating damage could be the removal of a single column as a result of a blast load.

Progressive Collapse Load is defined as a load, which causes progressive collapse. Although progressive collapse may be initiated by various *initiating damages*,

structural progressive collapse occurs under gravitational loads (i.e. dead and live loads), which are always present and are a main reason of structural progressive collapse occurrence.

To resist progressive collapse, a damaged structure develops ***progressive collapse resisting mechanisms***. Progressive collapse resisting mechanisms are defined as a structural system which forms in the damaged structure to resist progressive collapse load. A progressive collapse load path travels through structural connections at each structural element that may include slabs, beams, shear walls, columns, and foundations – all of which act as resisting mechanism along the load path. Subsequent element failures along progressive collapse resisting load path may trigger the formation of new progressive collapse resisting systems, until all resisting systems are exhausted and the structure collapses. It is worth noting that a damaged structure may develop multiple progressive collapse resisting mechanisms.

Strength is structural property comparing how strong the progressive collapse system is in comparison to the progressive collapse load (i.e. gravitational loads). Obviously, if structural system does not have sufficient strength it will collapse. In a probabilistic sense, strength is related to mean values of resistance probability density functions (PDF).

Continuity refers to element inter-connectivity that is required to form progressive collapse resisting mechanisms. Strength of the connections should be sufficiently large to allow progressive collapse load transfer from one component to another to form a resisting mechanism and thus preventing progressive collapse.

Ductility is a structural property describing a structure's ability to undergo inelastic deformation without failure (fracture or breakage). Since progressive collapse is a dynamic event, it is expected that progressive collapse load will be amplified dynamically by several times. Generally, it is uneconomical to design structural systems to respond elastically to dynamically amplified loads. Furthermore, in the case of the existing structure, it may not be possible to provide a retrofit solution to force the structure into elastic range. Therefore, it is expected that the progressive collapse resisting system will undergo inelastic deformations. We can conclude that progressive collapse resisting systems should have the ability to resist dynamically amplified gravitational load in inelastic range without collapse.

Structural Redundancy is an essential characteristic of a structural system related to existence and subsequent development of multiple progressive collapse resisting mechanisms. These mechanisms provide the load path for the building to arrest a potential progressive collapse.

Structural Reliability is structure's capacity to perform as designed under stated loading conditions. It is a measure of predictability of structural response to withstand initiating damage without progressive collapse, and is related to the probability of progressive collapse occurrence. Given an initiating load, the lower the probability of

progressive collapse occurrence, the more reliable the structure is under given gravity loading conditions. It is worth noting that to estimate structural reliability both loading as well as resistance PDFs must be defined.

Structural Robustness is defined by the structure's ability to withstand any unforeseen loading as well as initiating damage scenarios without a disproportionate response. There have been numerous studies performed to attempt to quantify and subsequently increase structural robustness. Structural robustness is very hard to quantify, however, it is relatively easy to identify once presented in the structure (see Agarwal & England, 2008). Intuitively it is obvious that structural robustness is related to structural safety and structural reliability. The main purpose of this paper is to propose a quantitative measure and mathematically reproducible definition of structural robustness.

Structural reliability, structural safety and structural robustness are interdependent qualities of a structural system that deserve further study in order to fully understand and realize the potential benefits of balancing these qualities with those of economics to meet future demands of the engineering community.

PROBABILISTIC APPROACH TO PROGRESSIVE COLLAPSE

The application of probabilistic concepts for the evaluation of progressive collapse potential is illustrated in this section. The premise of this approach is based on the assumption that the potential of progressive collapse is low if the probability of progressive collapse occurrence (following the initiating damage) under progressive collapse load is low, and vice versa: progressive collapse potential is high when probability of progressive collapse occurrence is high. This concept is best illustrated by performing a series of comparisons of two hypothetical structures which are referred to as Structure A and Structure B.

In the first series of examples, let us assume that both structures are equal in all terms aside from the mean value of the resistance (i.e., strength). Figure 1 plots the probability density functions (PDF) of load and the PDF of the two hypothetical structures. It can be deduced that Structure A has a smaller probability of progressive collapse occurrence than Structure B; therefore making Structure A more reliable than Structure B to resist progressive collapse occurrence under predefined load (usually dead and live), given that the initiating damage occurs.

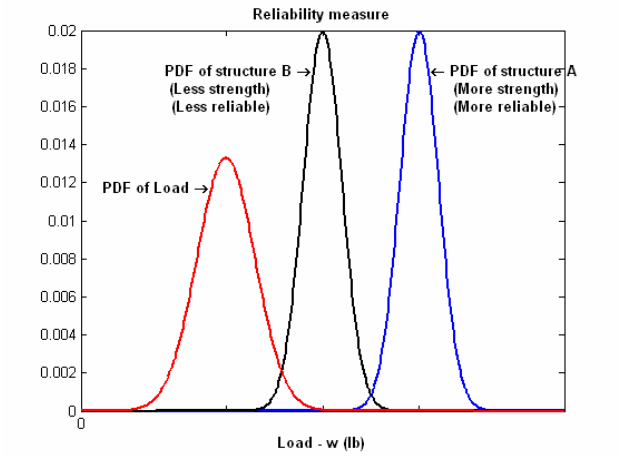

Figure 1. The measurement of reliability of a structure against progressive collapse occurrence based on mean value of the resistance for a given load distribution

A second hypothetical example deals with two structures, Structure A and Structure B, with different strengths and different standard deviations as presented in Figure 2. Let us assume that mean values and standard deviations of both structures differ in a specific way that yet results in equal probabilities of progressive collapse occurrence. Based on this example, we can conclude that both structures are equally reliable despite Structure A being stronger (by a mean value).

A third hypothetical example illustrates the effect of standard deviation of resistance PDF as shown in Figure 2. Let us assume that resistance PDFs of Structure A and Structure B differ in such a way that the probability of progressive collapse occurrence for Structure A is higher than structure B. In this example we may conclude that Structure A is more reliable than structure B despite of being weaker than Structure B.

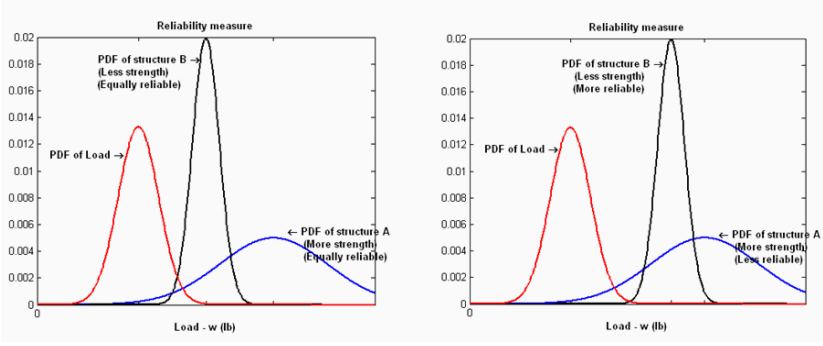

Figure 2. The measurement of reliability of a structure against progressive collapse occurrence based on mean value as well as standard deviation of resistance. The left graph depicts the PDF of Structure B having less strength and equal reliability. To the right, Structure B has less strength but more reliability.

Based on Figures 1 and 2 we can conclude that there is a unique relationship among structural reliability, structural strength (mean value of PDF) and standard deviations. This concept is well known in the theory of reliability (see Ang & Tang, 1975). In this paper, we take advantage of the concept that structural reliability can be improved by reducing standard deviation. The following section extends this concept in the measurement of structural robustness.

ROBUSTNESS FOR PROGRESSIVE COLLAPSE

To illustrate robustness concept, let us examine two hypothetical structures, Structure A and Structure B, where both structures have exactly the same strength (mean value of resistance PDF) but different standard deviations (see Figure 3). We can conclude that with everything being equal in Structure A and Structure B except standard deviations, Structure B is less reliable than Structure A since the probability of progressive collapse occurrence in Structure B is larger than it is in Structure A.

This means that in the absence of specific loading conditions (see the right graph in Figure 3), standard deviation by itself can improve structural reliability. However, in the absence of the specific loading condition, we cannot assert the level of reliability of the structure. Instead, we may be able to conclude that everything being equal, the structure with the smaller standard deviation is more reliable than one with a larger standard deviation. This is a basic premise of our proposed robustness measure.

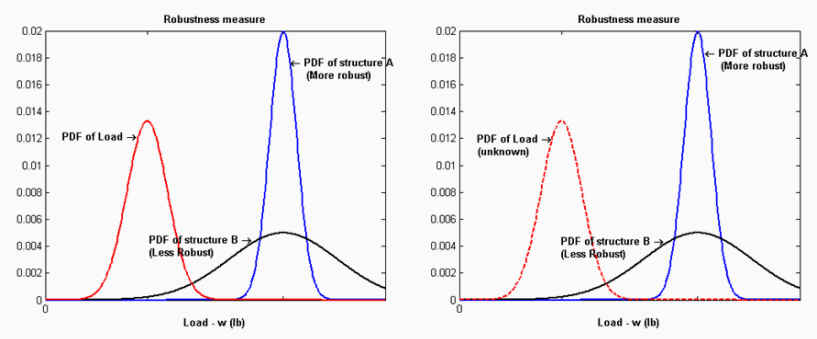

Figure 3. Robustness is an extension of structural reliability measured by a standard deviation of resistance function.

The traditional definition of structural robustness is a structure's ability to absorb initiating damage without propagating global effects (i.e., progressive collapse). The larger the initiating damage and the smaller the global structural effect, the more robust the structure is. Thus, structural robustness is a property of a structural system that measures its response to various (sometimes random) structural perturbations. In practice, this concept is applied to progressive collapse evaluation by instantaneously removing one or several major load-bearing elements and analyzing the remaining structure's capability to contain the damage.

Relating back to Figure 3, we can observe that Structure B is more sensitive to variation of progressive collapse load than Structure A (due to the larger standard deviation). This leads to the definition of structural robustness, which states that a *robust structural system is one which is insensitive to small variations in design assumptions.*

CONCLUSIONS AND RECOMMENDATIONS

Based on this study we draw the following conclusions:

- ✓ Provided that the specific progressive collapse load is known and the prescribed initiating damage has occurred, progressive collapse potential can be quantified in terms of the probability of progressive collapse occurrence and structural reliability concepts.
- ✓ In the absence of the specific progressive collapse load scenarios and unknown location and extent of initiating damage, progressive collapse potential can be minimized by employing the concept of structural robustness.
- ✓ Structural robustness represents a structure's ability to absorb small structural failures (perturbations) without affecting the overall structural integrity (i.e. without progressive collapse), and can be measured as a standard deviation of the progressive collapse dynamic resistance probability density function.
- ✓ Structural robustness is defined as structure which is insensitive to small variations in design assumptions
- ✓ Further studies need to be conducted to fully realize the potential of interdependency of structural reliability and standard deviation of resistance

PDF on overall structural risk, robustness, and ability to gracefully withstand future unforeseen loading conditions from unexpected initiating damages.

REFERENCES

Alimoradi, A., Pezeshk, S., Foley, C.M., June 2007, "Probabilistic Performance-Based Optimal Design of Steel Moment-Resisting Frames. II- Applications", Journal of Structural Engineering, ASCE, pp. 767

Ang, A.H.S., Tang W.H., 2007, "Probability Concepts in Engineering –Emphasis on Applications to Civil and Environmental Engineering", John Wiley & Sons, Inc.

Ang, A.H.S., Tang W.H., 1975, "Probability Concepts in Engineering Planning and Design-Vol.2, Decision, Risk and Reliability", John Wiley & Sons, Inc.

Agarwal, J., England, J., "Recent Development in Robustness and Relation with Risk", Structures and Buildings, Institution of Civil Engineering, Volume 161, issue SB4, August 2008

Benjamin, J.R, Cornell, C.A., 1970, "Probability, Statistics and Decision for Civil Engineers" McGraw-Hill, Inc., New York.

Department of Defense (DoD), 2005, Unified facilities criteria (UFC), design of buildings to resist progressive collapse UFC 4-023-03, DoD.

Downey E.K. a Ericksen,J., 2006, "Tolerances Illustrated", Modern Steel Construction Magazine, Steelwise, Steel Solutions Center

Ellingwood, B.R., 2006, "Load and Resistance Factor Criteria for Progressive Collapse Design", REC 06 Wksp.

General Services Administration (GSA), 2003, Progressive collapse analysis and design guidelines for new federal office buildings and major modernization projects. GSA.

Kang, Z., 2005, Robust Design Optimization of Structures under Uncertainties, Dr. –Ing. Thesis, Intitut fur Statik und Dynamic der Luft- und Raumfahrkonstruktionen, Universtat Stuttgart.

Marjanishvili, S., 2004, "Progressive Procedures for Progressive Collapse", Journal of Performance of Constructed Facilities, Vol. 18, No. 2

Marjanishvili, S., Buscemi, N., 2005, "SDOF Model for Progressive Collapse Analysis", Structures Congress 2005, ASCE, SEI

Marjanishvili, S., Agnew, E., 2006, "Comparison of Various Procedures for Progressive Collapse Analysis", Journal of Performance of Constructed Facilities, Vol. 20, No. 4

Marjanishvili, S., Tadepali, T., "Probabilistic failure model for structural components subjected to air-blast loads", 20th Conference on Military Aspects of Blast and Shock, MABS20, Oslo, Norway 2008.

Pretlove, A.J., Ramsen, M, Atkins, A.G., 1991, "Dynamic effects in progressive failure of structures" Int. J. Impact Eng., 11(4), 539-546

Rjanitsin, A.R., 1978. Theory of reliability of structural design. Stroiisdat, Moscow. (in Russian)

Schmidt, B.J., Bartlett, F.M., 2002, "Review of Resistance Factor for Steel: Data Collection", Canadian Journal of Civil Engineering, Vol. 29, pp 98-108

TSWG, 23 March 2004, "Vehicle Borne Improvised Explosive Devices in Worldwide Terrorism, A Contemporary Open Source Analysis".

Partial collapse of an historical masonry building

N. Augenti

Professor, Department of Structural Engineering, University of Naples Federico II, via Claudio 21, P.O. Box 80125, Naples (Italy); PH (+39) 081-7683102; FAX (+39) 081-7683491; e-mail: augenti@unina.it

ABSTRACT

On June 2007 the corner part of an ancient masonry building realized in the 20's of the last century at the centre of Salerno (Italy) fell down suddenly. The collapse occurred at the sunup, but no victims or injured people were caused only because that part of the building contained living rooms of apartments, rather than bedrooms.
The building, made up of tuff masonry and having six storeys, was one of the most beautiful palaces of the town for its location and the beauty of the façades.
During restoration works at the ground floor, retrofit interventions on masonry walls were been proposed and alarming cracks appeared along the masonry piers few days before the collapse. Despite these clear signs of alarm forecasting the disaster, no shoring structure was realized to avoid it.
In this paper all the investigation phases that allowed to define the mechanics of the collapse and to identify its causes are discussed.

INTRODUCTION

Collapse of buildings during restoration or strengthening works has become a recurrent phenomenon for several reasons. The main factors are usually: lack of preliminary inspections and assessment of the construction to be retrofitted; wrong or invasive interventions; lack of temporary shoring structures; no recognitions of alarming cracks; non-rapid safety interventions. This is why structural interventions aimed to upgrade the state of bearing elements may frequently cause their collapse.
The case described below shows that wrong design and construction procedures can induce damages and sometimes loss of human lives.

THE PARTIALLY COLLAPSED BUILDING

The present paper deals with one of the most beautiful buildings realized in the centre of Salerno (Italy) at the end of 20's. Such a building lies along the seafront between the City Hall and the Prefecture; it has six storeys in elevation, plus an underground one, and two staircases. The rooms placed at the ground floor are used by banks, restaurants, business activities, and a bar.
The building has a mixed structure consisting of tuff masonry walls, reinforced concrete (RC) structural elements (columns and beams), and floors slabs composed by RC joists and hollow bricks. Figure 1 shows the beautiful main façade of the building, having a great historical value.

Figure 1. Main façade of the building.

After 1929 (construction year), some modifications of the building were carried out, mainly consisting into the enlargement of rooms at the ground floor, where the entrances of trade activities are placed. Other substitutions of internal masonry walls with RC frames were made to enlarge net area of rooms of the trade activities. Such works induced stress concentrations in some façade masonry piers.

In mid-March 2007, restoration works of a bar started at the ground floor in the corner of the building with the seafront of Salerno. Moreover, such works consisted in repairing of some masonry walls through a partial substitution of old mortar joints with new cementitious-based ones.

After the removal of plaster from the walls and the substitution interventions were started, some cracks were observed on the masonry piers. The contractor decided to suspend the works and asked to the owners to take on the costs of strengthening interventions of the masonry piers. Pending the dispute resolution between the room owners, condominium, and contractor was solved, the cracks' width dramatically increased. Despite the rapid evolution of failures on some masonry piers placed in the corner of the building (according to the results of successive inspections), no shoring was realized to assure safety of the structure. Figures 2 and 3 show serious crushing cracks found on June 13, 2007, about 30 hours before the collapse into the thickness of the masonry piers placed in the corner zone of the building, inside the rooms under restoration.

Since the risk of collapse was not perceived, the technicians decided to design strengthening works and to submit them to the owners of the rooms placed at the ground floor, as wells as to the ones of the whole building.

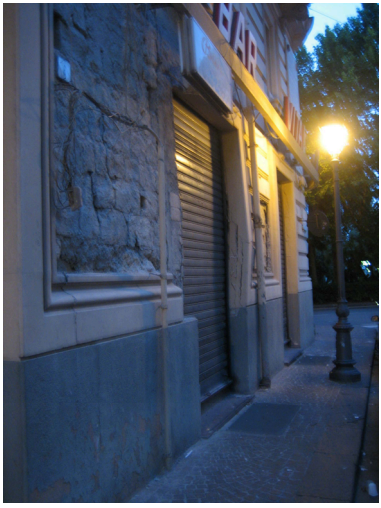

Figure 2. Crushing cracks.

Figure 3. Detail of crushing cracks.

THE COLLAPSE

On June 15, 2007, at about 3.30 a.m. a whole corner part of the building fell down suddenly. Figure 4 shows the ground floor plan of the building in which either the masonry piers, or the collapsed parts of floors, are drawn in red.

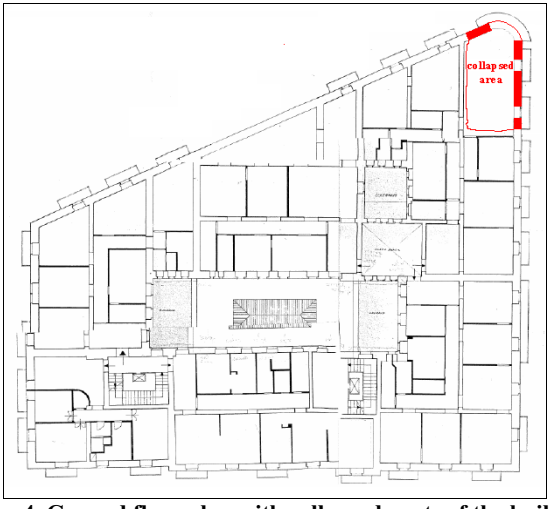

Figure 4. Ground floor plan with collapsed parts of the building.

The collapse did not cause victims only because the rooms placed at the ground and first floors were deserted at that early hour of the morning, and the corner part of the building contained living rooms, rather than bedrooms. No pedestrians or vehicles passed the adjacent streets in that moment, fortunately. Figure 5 shows the corner of the building before the collapse, while in Figure 6 one can see the same corner after the collapse and the removal of rubbles.

Figure 5. Corner before the collapse.

Figure 6. Corner after the collapse.

INVESTIGATIONS

In order to determine the causes of the collapse and the related responsibilities, the Judicial Authority opened a criminal procedure after the accident.
The author of this paper took part in the investigations as technical consultant of the aggrieved parties, which were the owners of the collapsed apartments.
The history of the building and of modifications made on the masonry structure was reconstructed first. A controlled demolition of rubbles was then carried out to bare the residual masonry walls in their conditions immediately before the collapse. Traces of the collapse mechanisms and of the structural interventions that were in progress immediately before the collapse were also observed on one of the masonry piers. In particular, it was possible to assess that the masonry walls were composed by two external leaves made up of squared tuff stones and lime mortar, and by an inner core made up of irregular stones and mortar.
Traces of interventions made a few days before the collapse were still evident along the internal leaf of the masonry walls. A part of the old mortar joints was been removed, so several stones were not connected themselves. The only residual masonry wall highlighted during the investigations is showed in Figures 7 and 8 outside and inside of the building, respectively. Traces leaved by the removal of

mortar joints are evident in the second figure. One can also see that the internal leaf was completely disconnected.

Figure 7. Residual masonry wall outside the building.

Figure 8. Residual masonry wall inside the building.

The splitting of the internal leaf induced by the removal of mortar joints was noted by observing carefully the cross-section of the masonry wall. Figures 9 and 10 show the fracture of masonry and the splitting cracks opened before the collapse.

After onsite inspections on the rubbles and the survey of the building's characteristics were complete, all loads acting on the structure at the moment of the collapse were estimated.

Therefore, a structural analysis of the building was carried out by means of different models, to estimate the most probable stress state at the moment of the collapse (Augenti 2004).

Crushing tests were conducted on the tuff stones constituting the masonry building. The technical consultants of the examining judge rejected onsite compression tests on masonry prisms proposed by the author of the present paper, based on similar investigations carried out by him on the school "F. Jovine" in San Giuliano di Puglia, which collapsed on October 31, 2002 (Augenti 2006).

CAUSES OF THE DISASTER

All the technical consultants agreed that the disaster was caused by the crushing of the masonry piers between the openings of the rooms placed at the ground floor in which restoration works were in progress (marked in red in Figure 4).

Figure 9. Fractured masonry pier.

Figure 10. Splitting cracks.

Instead, the conclusions about the responsibilities of the collapse were different. The technical consultants of the examining judge said that the disaster was been induced by the vulnerability of the building and by the law compression strength of tuff masonry. Thus, they stated that the building's owners were considered to be responsible of the collapse (Vitone and Palmisano 2008).

Either the author of the present paper, or the consultants of the Public Prosecutor, were in agreement to believe that the collapse were been caused by the weakening of the masonry piers after the removal of mortar joints from one of the wall leaves (Augenti 2008, Ascione and Ciarletta 2008). Such an operation disjointed the internal leaves of the masonry wall making it ineffective in terms of resistance. Since individual masonry units were disjointed, the thickness of the wall was drastically reduced so one of the external leaves was de facto eliminated. Moreover, these serious and delicate operations were been made without safety and shoring structures.

The author of this paper has already had experience of failures due to same causes because in 2003 he investigated on the partial collapse of a building situated in the centre of Naples. Also this disaster occurred during similar restoration works (Augenti 2007): the collapse of the roof and of a part of façades of the building occurred after the removal of mortar joints, without temporary shoring structures (see Figure 11).

The author showed also that a shoring structure, simply made a few hours before the disaster by closing the adjacent openings of the cracked masonry pier (see Figures 2 and 3), should have avoided the collapse. He had a similar experience in a building situated in the ancient centre of Naples. Also in that case some masonry walls of the ground floor underwent serious cracks, which were fully comparable with those occurred in the building of Salerno (see Figure 12), but the disaster was avoided by

closing quickly the adjacent openings of the masonry piers on the verge of collapse. At present, it is being prosecuted for the causes of the collapse and the related responsibilities.

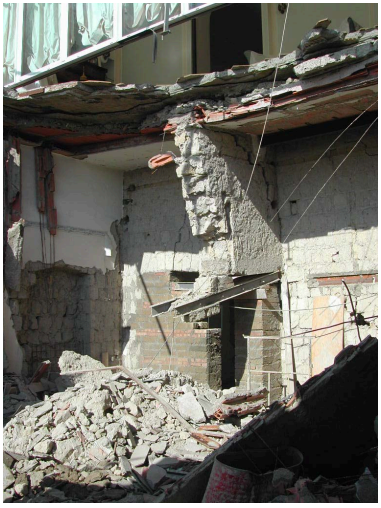

Figure 11. Collapse of a roof and of a façade in Naples.

Figure 12. Splitting cracks of another building in Naples.

CONCLUSIONS

This case study shows that restoration and strengthening interventions to be made on masonry structures must be necessarily preceded by an accurate structural analysis.
The modifications of the structure after its construction and the stress state due to actual loads must be studied. In addition, interventions must be non-invasive and structural safety must be assured during their execution.
Any work on bearing elements cannot start without shoring and safety structures able to avoid dangerous situations.
Finally, failures and crack patterns must be checked by skilled professionals able to propose quick safety interventions aimed to avoid collapses.

REFERENCES

Augenti, N. (2004). *Il calcolo sismico degli edifici in muratura*. UTET, Turin (in Italian).

Augenti, N. (2006). "The primary school collapse in San Giuliano di Puglia: Inquirie and Evaluations". *Proceedings of the 2nd International fib Congress, Naples, 5-8 June 2006*.

Augenti, N. (2007). Un crollo nel centro di Napoli durante lavori di consolidamento. *Proceedings of CRASC'06, Italian Conference on Collapses and Reliability*

of Structures, Messina, 20-22 April 2006, Flaccovio, Palermo (in Italian).
Augenti, N. (2008). *Relazione di consulenza relativa al crollo del Palazzo Edilizia.* Naples (in Italian).
Ascione, L. and Ciarletta, M. (2008). *Relazione tecnica dei consulenti della Procura*. Salerno (in Italian).
Vitone, A. and Palmisano, F. (2008). *Perizia tecnica per il GIP*. Bari (in Italian).

Lessons Learned from Marcy Bridge Collapse

D. J. Corr[1], D. M. McCann[2], and B. M. McDonald[3]

[1]Department of Civil & Environmental Engineering, Infrastructure Technology Institute, Northwestern University, 2145 Sheridan Road, Evanston, IL 60208
PH (847) 467-0890; FAX (847) 491-4011; email: d-corr@northwestern.edu

[2]Exponent, Inc., 185 Hansen Court, Suite 100, Wood Dale, IL 60191
PH (630) 274-3206; FAX (630) 274-3299; email: dmccann@exponent.com

[3]Exponent, Inc., 149 Commonwealth Drive, Menlo Park, CA 94025
PH (650) 688-6946; FAX (650) 328-3094; email: mcdonald@exponent.com

ABSTRACT

A pedestrian bridge near Marcy, New York collapsed during construction on October 12, 2002, injuring nine workers and killing one. The authors were retained to investigate the reasons for the bridge collapse, and whether the actions or omissions by the key players contributed. The pedestrian bridge was designed as a straight, single-span, composite box girder composed of a trapezoidal steel tub with stay-in-place forms and concrete deck. The collapse occurred while the concrete deck was being placed. Based on eyewitness accounts and the position and orientation of the debris, the mode of failure was consistent with lateral-torsional buckling of the entire girder cross-section. While conventional engineering training would preclude lateral torsional buckling of a beam bent about its weak axis as a potential failure mode, computer simulations using nonlinear analysis and eigenvalue buckling analysis confirm eyewitness accounts, that is, a point of bifurcation is reached during concrete placement on the torsionally flexible steel tub girder. Since this failure, which was slightly predated by a very similar failure in Sweden, the State of New York and AASHTO have appended bridge design specifications to explicitly require diagonal bracing between the top flanges in order to suppress this buckling mode. A discussion of the collapse and the failure mode follow, highlighting the lessons that the engineering community has learned from the collapse.

Keywords: Marcy Bridge, tub girder, composite bridge, lateral-torsional buckling, AASHTO.

INTRODUCTION

The composite tub girder is becoming a more popular bridge type in the United States. These bridges are composed of a steel tub girder with a trapezoidal shaped cross section topped with a concrete deck, which is typically formed atop steel stay-in-place forms that span between the girder flanges. The advantages include efficient use of materials (in areas of positive moment where the composite section is utilized), elimination of the need for falsework under the span, and torsional rigidity of the composite section, which is particularly beneficial for curved beams. When built without falsework, the design of composite bridges must include a check of constructability to ensure the ability to carry wet concrete and construction loads prior to achieving full composite strength. This check was required, for instance, by Section 10.61 of the AASHTO

Standard Specifications for Highway Bridges, 16th Edition, which (with interim revisions through 1998) was the basis for the New York State DOT specifications that governed the design of the subject bridge.

BRIDGE DESIGN

The subject pedestrian bridge (herein referred to as the Marcy Bridge) was designed to span approximately 170 feet across a new extension of the Utica-Rome expressway (NYS Route 49) in Marcy, New York. The bridge was intended to carry pedestrian traffic and small emergency vehicles only. The design consisted of a single trapezoidal steel tub girder with a composite reinforced concrete deck. The bridge was straight in plan, with no skew, and vertically curved in elevation. The tub girder was cambered approximately 2½ feet to achieve the intended final vertical profile. It was fabricated in two sections that were spliced (bolted) on site while supported by cranes; the erection was done without falsework or shoring. A schematic of the bridge cross-section showing the formwork in place during construction is provided in Figure 1.

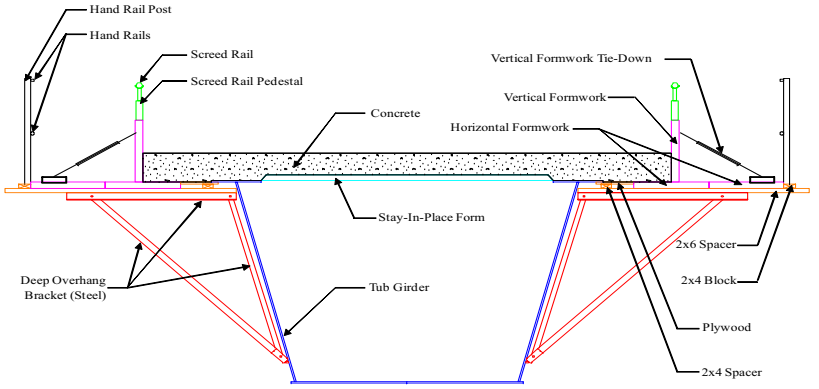

Figure 1. Cross-section showing formwork in place during construction.

Although the tub girder had internal diaphragms and struts to prevent distortion of the cross section during shipping and erection, it did not have top lateral bracing, that is, diagonal bracing in the plane of the top flanges. Prior to and during placement of the concrete deck, the tub girder cross section was closed only by stay-in-place forms, which were nominally connected to closure angles on each top flange and to each other using self-tapping screws. The arrangement of internal struts and diaphragms and stay-in-place forms is shown in the post-collapse photo provided in Figure 2. A close-up view of the stay-in-place form connections is shown in Figure 3. Despite the presence of the stay-in-place forms to close the section, the means of attachment was not sufficient to provide sufficient torsional strength or stiffness, and the section could be considered open and thus torsionally flexible. After curing, the concrete deck would have created a truly closed cross section, and the increased torsional stiffness would have

eliminated the potential for lateral-torsional buckling.

Torsional stiffness of a composite tub girder bridge can be increased prior to curing of the concrete slab by means of a top flange lateral bracing system to create a quasi-closed section. Such as system was neither prescribed in the design nor included as part of the fabrication, transportation and erection means and method. The technical literature (Heins and Blank, 1973, US Steel, 1978, and Chen et al., 2002) discusses the option of using adequately sized and connected stay-in-place forms to create an effectively closed cross section. While the Marcy Bridge utilized stay-in-place forms, the connections to the flanges and between the individual panels were not engineered for this purpose and did not provide sufficient strength and stiffness to constrain the lateral torsional mode.

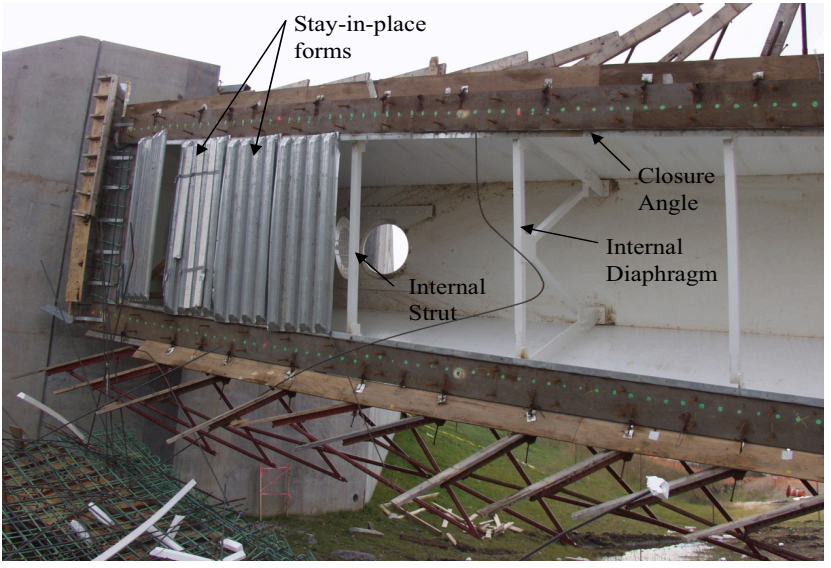

Figure 2. Post-collapse photo of the Marcy Bridge showing the internal diaphragms, struts, and stay-in-place forms.

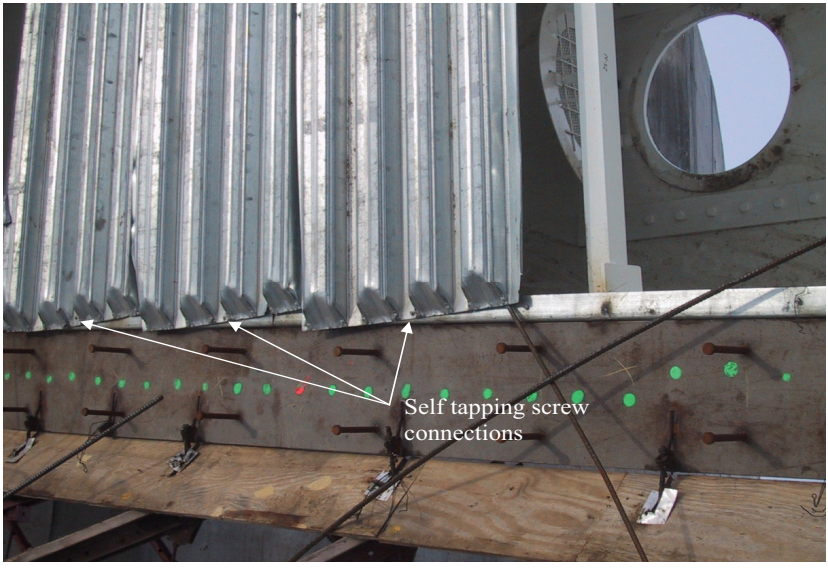

Figure 3. Close-up of stay-in-place form connections to closure angle at top flange of tub girder.

BRIDGE COLLAPSE

The flexibility of the open tub girder cross section without top flange lateral bracing described above, coupled with the vertical curve and long, slender geometry, made the Marcy Bridge susceptible to lateral-torsional buckling. The steel tub girder had been erected, including all stay-in-place forms, and the concrete was being placed starting at the east (fixed bearing) end on the day of the incident. The bridge collapsed during casting of the deck, shortly after placement of the wet concrete had passed midspan, injuring nine workers and killing one. Based upon eyewitness accounts and the position of the girder after the accident, it was evident that the failure mode was lateral-torsional buckling of the steel tub girder in which the entire girder cross-section participated; local buckling of a compression flange did not contribute. A photograph of the collapsed tub girder is shown in Figure 4.

Conventional treatment of global lateral-torsional buckling precludes the possibility of such buckling in members loaded in bending about their minor axis. In the case of the subject tub girder, the major axis is the vertical axis of symmetry, and the minor (horizontal) axis is located closer to the bottom flange than the top flanges, as depicted schematically in Figure 5. Transverse loads applied to the tub girder acting in the direction of gravity produce bending about its minor axis.

Figure 4. Collapsed steel tub girder.

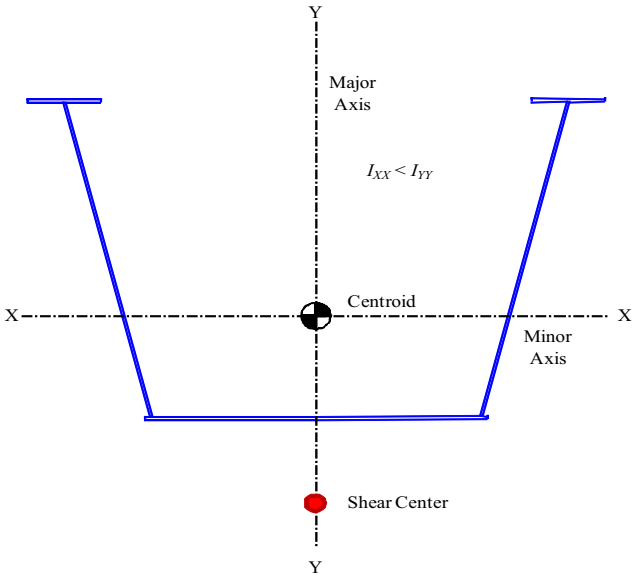

Figure 5. Schematic of the tub girder cross section depicting the major and minor centroidal axes and the shear center.

Given that engineers are often taught that lateral-torsional buckling is not a possible failure mechanism for beams loaded in bending around their minor axis, there were no explicit code requirements mandating top flange lateral bracing or other means to prevent lateral torsional buckling at the time of design. Top lateral bracing is, of course, required for curved girders wherein torsional resistance is required to carry the offset load. Design guides by US Steel (1979) and Bethlehem Steel (Heins and Hall, 1981) recommend the use of top flange lateral bracing, but it appears that those recommendations were not intended to prevent buckling during concrete placement but were based largely on concerns regarding the possibility of torsional overload and associated permanent deformations occurring during transportation and erection.

More rigorous mathematical treatment of the trapezoidal, open cross section reveals that it is indeed susceptible to lateral torsional buckling when loaded about its weak axis. References by Trahair (1993) and Attard (1990) provide the requisite theory, and Yura and Widianto (2005) provide an excellent summary of their work (and others) and the resulting buckling equations in their various forms. In summary, if one considers that the shear center of the tub girder is located below its bottom flange (see Figure 5), or if one considers camber/vertical curvature, then the resulting stability equations reveal that lateral torsional buckling of prismatic members loaded in bending about their weak axis is possible. Finite element models utilizing either eigenvalue buckling or geometric nonlinear analyses also reveal the lateral torsional failure mode, but such analyses have not been commonly used in the design of these bridges. The program UTrAp 2.0 has been developed with this capability (eigenvalue analysis) by Williamson et al. (2004) at the University of Texas at Austin. At the time of this writing, the online documentation for the program included the Marcy Bridge as an example.

While bracing requirements appear in bridge design standards in general terms, top flange lateral bracing was not an explicit requirement of the 16th Edition of the AASHTO Standard Specifications for Highway Bridges, adopted by New York State at the time of the design of the Marcy Bridge. Additionally, lack of clarity in the Specifications regarding lateral bracing during construction may have been confusing regarding requirements for stability versus requirements meant to control distortion of the steel tub cross section. As an outcome of the collapse, New York State Department of Transportation issued an Engineering Bulletin in July 2003 requiring full length lateral bracing systems for all tub girders that rely upon a composite concrete deck to form a closed cross section; similar provisions soon appeared in subsequent AASHTO specifications.

Interestingly, it appears that a similar bridge collapsed under similar circumstances in Sweden just a few months prior to the Marcy Bridge collapse in June 2002 (Ålenius, 2003). Though there appears to be little information publicly available regarding the collapse, a photograph indicates it was a trapezoidal tub girder with stay-in-place forms (no top flange lateral bracing visible) that collapsed in a lateral-torsional mode during concrete placement.

ANALYSIS

The authors' investigation of the Marcy Bridge collapse included post-

collapse inspection, review of witness statements, laboratory testing, and computer modeling of the tub girder using the finite element analysis software package ABAQUS. This analysis described herein was performed to calculate the capacity of the girder to resist buckling based on linear elastic eigenvalues; the buckling capacity calculated under these ideal conditions did not include the potential adverse effects of local yielding and initial imperfections. The finite element model was composed of plate elements for the girder flanges and webs, and combinations of plate and beam elements to model the internal diaphragms and struts. The analysis did not model the beneficial effect of the partially effective bracing provided by stay-in-place forms. Loads on the girder included self weight of the tub girder, the weight of the stay-in-place forms and reinforcing steel (full length), the weight of other formwork and work platforms, loads from the concrete screed machine, and the weight of approximately 90 feet of wet concrete from the east end of the bridge (consistent with witness descriptions and observations of the debris). An image of the finite element model of the tub girder in the undeformed state is shown in Figure 6.

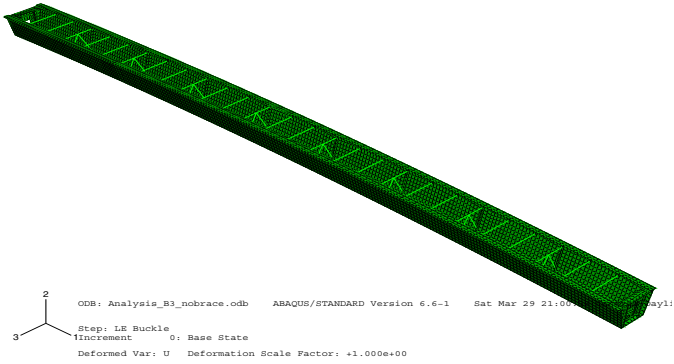

Figure 6. Finite element model of the steel tub girder in its undeformed state.

The first model represented the as-designed tub girder, including camber, with no top flange bracing. The first eigenvalue computed for this model was 0.67, meaning that buckling would occur when the quasi-statically incremented, monotonically increasing load reached 67% of the known load on the bridge at the time of collapse. Thus, the model without the stay-in-place forms underestimated the buckling strength of the bridge, likely due to the beneficial effect of the forms. The displaced shape for this mode is shown in Figure 7, exhibiting a clear global lateral-torsional mode.

A second model added a hypothetical top flange bracing system to the tub girder. This top flange bracing used spring (truss) elements in a K-brace pattern between the top flanges, at the locations of each internal diaphragm and strut. The axial stiffness for these hypothetical braces was taken to be equivalent to that of the practically feasible / nominal strut elements that might have been added at the

time of construction to span horizontally between the top flanges. The eigenvalue computed for this mode was 2.09, indicating that the buckling strength has increased by a factor of three. Thus, for this tub girder, the inclusion of even nominal top flange bracing effectively suppresses the first mode buckled shape, i.e., lateral torsional buckling. Addition of the top flange bracing shifted the first mode buckling to a mode associated local web and flange buckling as seen in Figure 8.

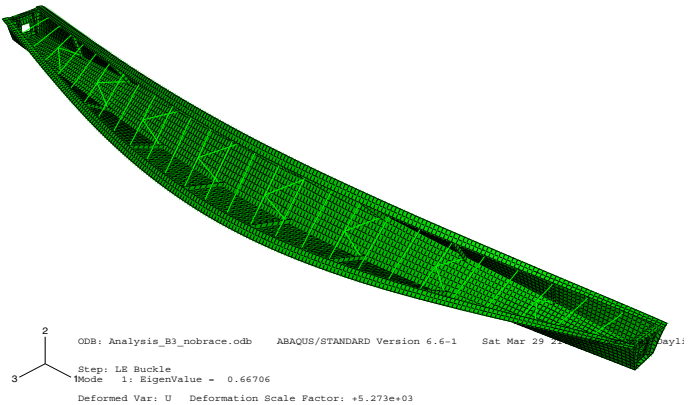

Figure 7. Buckled shape without top flange bracing exhibiting global lateral-torsional displaced shape.

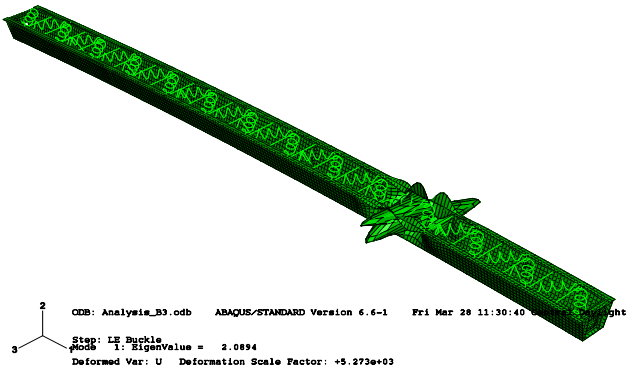

Figure 8. Buckled shape with top flange braces, with local flange and web buckling displaced shape.

DISCUSSION AND LESSONS LEARNED

The fundamental lesson to be taken from the tragic collapse of the Marcy Bridge is that designers and erectors must consider global lateral torsional buckling mode when evaluating the constructability of trapezoidal tub bridges without falsework or shoring. As engineers, we are often taught that such buckling cannot occur for prismatic members loaded in bending about their weak axis, and thus this failure mode was neither addressed in design specifications nor specifically referenced in industry design guides. However, the shape of the open trapezoidal cross section (which is torsionally flexible with a shear center below the member) coupled with the possibility of vertical curvature and/or camber, makes this type of bridge susceptible before the concrete has cured and the section is fully composite. Because of the tragedy, this lesson has already been incorporated into current design specifications, which now address this failure mode, typically by the use of top flange diagonal bracing (truss bracing in the plane of the top flanges). Tools to check the buckling capacity of these bridges without undue effort, such as UTrAp 2.0, are readily available to the designer, and calculation of this condition should become standard practice for checking constructability.

REFERENCES

AASHTO. (1996). *Standard Specification for Highway Bridges, 16th Edition,* American Association of State Highway and Transportation Officials, Washington, DC.

Ålenius, M. (2003). *Finite Element Modelling of Composite Bridge Stability*, MSc Thesis, Department of Mechanics, Royal Institute of Technology, Stockholm, Sweden.

Attard, M. (1990). "General Non-Dimensional Equation for Lateral Buckling," *Thin-Walled Structures 9*, 417-435.

Chen, B. S., Yura, J. A. and Frank, K. H. (2002). *Top Lateral Bracing of Steel U-Shaped Girders,* Texas Department of Transportation, FHWA/TX-02/1395-2F.

Heins, C. P. and Blank, D. (1973). "Box Beam Stiffening Using Cold Formed Decks," *Current Research and Design Trends*, ed. Yu, W.-W., Specialty Conference on Cold Formed Steel Structures, St. Louis, MO.

Heins, C. P. and Hall, D. H. (1981). *Designers Guide to Box Girder Bridges*, Bethlehem Steel Corporation, Bethlehem, PA.

Trahair, N. S. (1993). *Flexural-Torsional Buckling of Structures*, E&FN Spon, London.

US Steel. (1978). *Steel/Concrete Composite Box-Girder Bridges, A Construction Manual*, United States Steel Corporation, Pittsburgh, PA.

Williamson, E., Topkaya, C., Popp, D., and Yura, J. (2004). *UTrAp 2.0, Analysis of Steel Box Girders During Construction*, University of Texas at Austin.

Yura, J. A. and Widianto (2005) *Lateral Buckling and Bracing of Beam – A Re-evaluation after the Marcy Bridge Collapse.* Annual Technical Session Proceedings, April 6-9, 2005 in Montreal, Quebec Canada, Structural Stability Research Council. Rolla, MO.

From Concept to Collapse

Stewart M. Verhulst, M.S., P.E., M.ASCE[1]
Deepak Ahuja, M.S., P.E., M.ASCE[2]
Gregory G. Schober, M.S., P.E.[3]

[1]Nelson Architectural Engineers, Inc., 9701 Brodie Lane, Suite 201, Austin, Texas 78748; PH (512) 610-2800; email: sverhulst@architecturalengineers.com
[2]Nelson Architectural Engineers, Inc., 2470 Dallas Parkway, Suite 220, Plano, Texas 75093; PH (469) 429-9000; email: dahuja@architecturalengineers.com
[3]Nelson Architectural Engineers, Inc., 2470 Dallas Parkway, Suite 220, Plano, Texas 75093; PH (469) 429-9000; email: gschober@architecturalengineers.com

ABSTRACT

The development of new products is essential for the continued progress of the building industry. New products can improve the performance and efficiency of building systems; however, they must as a minimum maintain the same level of public safety provided by proven existing products.

This paper presents a case study of a new cold-formed steel joist roof framing system/product. The manufacturer designed and manufactured the product, taking it from the concept stage to implementation as a product sold for use in building structures.

One of the buildings with this new roof framing system experienced a roof collapse during a rainstorm. Investigation of the collapse led to the discovery of design errors of the joist product and defects in its fabrication, leading to questions regarding the safety of this product and its suitability for use in a roof system. This case study also highlights the role of the design professional with regards to the selection and verification of new building systems and products.

INTRODUCTION

In June 2004, a large section of a warehouse roof in the Dallas/Fort Worth, Texas area collapsed during a rainstorm. The collapse caused damage to multiple tenant spaces in this warehouse building. Fortunately, there was no injury or loss of life.

The roof framing for the warehouse building consisted of a cold-formed steel joist type system. The joists were similar in profile and geometry to open web steel joists; however, the chords and webs of the trusses were fabricated with cold-formed steel shapes. The subject structure was constructed approximately three (3) years after the

manufacturer developed this new roof framing product. Therefore, this cold-formed steel joist system was considered a new structural framing product.

The collapse of the roof was extensive, as indicated in Figure 1. The collapse affected the framing bays along one side of the building for a majority of the length of the building.

Evaluation of the failed joist members uncovered weld failures at the connections between cold-formed steel members of the joists. Several weld failures were observed at the interface between the weld metal and base metal. Additionally, the joists typically failed at the connection between the diagonal webs and the bottom chord, particularly at the end diagonal web. The failure pattern of the joists and other details regarding the failed joists are discussed further below.

PRODUCT CONCEPT AND DESIGN

The subject cold-formed steel joist product was developed in the late 1990's for long span applications. This product was developed at least in part to compete with conventional steel joists in the warehouse building market.

The steel shapes utilized in the joist product design consisted of rectangular channel sections with openings along one side to allow fit-up and assembly. The top and bottom chords had vertical extensions along the openings to facilitate the connections with the web members. Refer to Figures 2 and 3 for a representative view of the joists and the constituent members. It should be noted that, due to their open shapes, the joist members were susceptible to torsional instability in compression.

The web members were designed and fabricated to be connected to the chord members by welds. Due to the geometry of the connections and the chamfered corners of the web members, two predominant types of welds were utilized: flare bevel welds and fillet welds.

This joist product design was analyzed by the manufacturer using commercially available structural engineering software. This joist design analysis consisted of a traditional two-dimensional truss analysis of the individual members. Connection design was performed separately and welds were specified for each of the joist member-to-member connection points. The connection design apparently consisted only of the weld design and specification and did not include modeling for localized stress conditions at the member connections, such as Finite Element Modeling (FEM). In lieu of sophisticated FEM for the local stresses, the manufacturer performed product testing to evaluate the performance of the joists. It should be noted that the authors do not find fault with this approach, if the testing is performed in a thorough manner and in conformance with generally accepted standards (in this case the AISI Specifications). The testing procedures for the subject joist product will be discussed further in the "Manufacturing and Testing" section below.

Effective Length Factor in Design. During a review of the joist design performed by the manufacturer, the authors noted that an effective length factor of k=0.65 was used. As stated in the design manual from the manufacturer,

> *The values of "K" are generally taken as 0.65 in that all interior webs are either continuous or fully restrained by welding.*

Using k=0.65 as opposed to k=1.0 significantly increases the design capacity of the compression elements, in this case the vertical webs. In our opinion, the joist manufacturer's use of k=0.65 was (and is) not the industry standard for joist design and may be unconservative for the design of joists of this type. The industry standard for steel joists is to use k=1.0 for compression members, as is published by the Steel Joist Institute (SJI 1994) in its *Standard Specifications for Open Web Steel Joists*, *K-Series.*

In addition, the American Institute of Steel Construction (AISC 1989) states the following in its *Manual of Steel Construction: Allowable Stress Design*, 9th Edition:

> *Although translation of the joints in the plane of a truss is inhibited and, due to end restraint, the effective length of compression members might therefore be assumed to be less than the distance between panel points, it is usual practice to take K as equal to 1.0, since, if all members of the truss reached their ultimate load capacity simultaneously, the restraints at the ends of the compression members would disappear or, at least, be greatly reduced.*

Considering the subject joists, it was observed that joist chords were severely distorted in relation to the web members at several locations; indicative of a flexible connection rather than full restraint. While the use of k=0.65 in lieu of k=1.0 for compression members did not significantly contribute to the subject roof collapse discussed herein, it is the authors' opinion that the use of this k value did not conform with the industry standards and may result in unconservative roof framing designs using the new cold-formed joist product.

SJI has requirements for both the design and manufacture of joists conforming to its specification, including the submittal of detailed design data for the joists to SJI or an SJI-approved independent agency (SJI 1994). The subject joist product was not a certified or accepted SJI joist product and there was no evidence that such an independent design review was performed. Therefore this joist product was not subjected to the same scrutiny as would be an SJI-approved joist product.

It is the authors' opinion that this case study illustrates the need for new products to undergo a thorough and independent design review; and the need for Structural

Engineers to insist upon such measures before specifying a new product for use in construction.

MANUFACTURING AND TESTING

The subject joists were generally manufactured in an assembly line fashion. This included multiple welders welding the connections for each joist. After the joists were assembled and the connections were welded, the joists were dipped in paint.

The joist manufacturer performed tests on joists during the product development stage. Furthermore, during the production stage, the manufacturer implemented quality control testing for the joists. These test regimes are discussed below.

Product Development Testing. Testing of full-scale joists under load was conducted during the product development stage. Based on information available from the joist manufacturer, 18 joists were tested prior to production, and some additional tests were conducted during joist production, for a total of 41 full-scale joist tests. Of these 41 tests, 38 were performed with downward (gravity) loading and three (3) were performed with uplift loading.

The results of the product development testing indicated that the most common failure mode of the tested joists was buckling of the top chord. Buckling of the top chord would not be an expected failure mode for these joists in actual construction, where they would be connected to a roof or floor deck, and this calls into question whether manufacturer's testing sufficiently replicated the expected as-built conditions for these joists in service.

Another common failure mode during the product testing was failure at the bottom chord connections. Multiple tests indicated "tube tear out of B.C [bottom chord]" as the failure mode and some also included the note "welds critical". In a summary of the tests performed prior to production, the manufacturer stated the following:

> *Many conclusions were drawn from these initial tests* [Tests 1-18]. *It was concluded that the welds connecting the web members to the top/bottom chords were critical.*

The failure modes for the test joists were not the desired failure mode for this type of joist product. Specifically, the tear out failure at the bottom chords was a connection failure, indicating that the design capacity of the joist members was not developed. The documented bottom chord failures that were encountered during the product testing appear similar to the observed joist failures at the subject building. The evidence suggests that the manufacturer did not learn from its own testing, and proceeded to manufacture joists with deficient connections that were prone to improper modes of failure. There was no evidence of testing of isolated welded connections to test the connections separately from the full-scale joists.

The authors also discovered significant deficiency in the failure load results for the full-scale joist tests performed by the manufacturer. Section F2 ("Tests for Confirming Structural Performance") of the American Iron and Steel Institute Standard (AISI 1989 and UBC 1994) states the following:

> *...A successful confirmatory test shall demonstrate a safety factor not less than that implied in the Specification for the type of behavior involved.*

The applicable safety factors specified by the 1989 AISI Standard and the 1994 UBC were:

- 1.67 for tension members,
- 1.92 for compression members,
- 2.50 for welded connections.

Considering the actual loads for the subject structure (which was a common loading regime for a structure of this type), and using the lowest applicable factor of safety (1.67 for tension failure), only 12 of the 38 gravity load tests performed by the manufacturer failed at or above the minimum prescribed loading. Several of the recorded tests indicated failure loads of less than 75% of the equivalent expected failure load at the subject structure. Furthermore, the joist configuration used for the subject structure was not even included in the full-scale failure testing.

Due to the combination of insufficient testing and poor test performance for this joist product, the ability of the subject joists to resist the design loads was not adequately established prior to their use as roof framing members. The importance of independent verification testing for structural products and systems is highlighted by the requirements of SJI and similar organizations. Independent verification is necessary to remove bias from the test/approval program and to provide a reliable testing program on which customers and the public can rely.

Quality Control Testing. The manufacturer's quality control testing was limited to 1 out of every 50 joists, and the joists were to be tested to 110% of the design load. If the specimen passed the test, then it was to be put back into production for shipping. Therefore, there was no full-scale failure testing of the actual production joists.

In the authors' opinion, testing the joists to only 110% of the design load was insufficient for proper quality control and did not conform with the building code (1994 UBC), which required the test to meet or exceed the safety factor for confirmation of structural performance. Testing the joists only up to 110% of the design load would not be sufficient to detect manufacturing or design defects in the joists. Furthermore, based on the information available, the subject joists were not load tested, even to the 110% criteria, because this quality control testing was not implemented until after the subject joists were fabricated.

PRODUCT SELECTION AND APPROVAL

The Structural Engineer of Record (EOR) for the project was responsible for determining the suitability of this joist product for use as roof framing in the subject building structure. One common method for a manufacturer of a new product to provide product verification to architects, engineers and building officials was to have the product certified by an ICBO (now ICC Evaluation Services) report. This certification by an independent, accredited laboratory would certify that the product meets the appropriate code requirements. This joist product did not have any such certification.

For new structural framing products, the EOR should require verification of the product by independent, accredited agencies. For the subject structure, there is no evidence that the EOR received any such information regarding this joist product. Due to the deficiencies in the design, manufacture, and testing of the subject joist product, it is the authors' opinion that the EOR should not have selected and approved this product for use as roof framing.

COLLAPSE

The observations and the pattern of the roof failure at the site, in addition to the available weather data, were indicative of a gravity load failure, and roof uplift failure was ruled out as a possible or contributing cause. While the collapse occurred during a rain event, a storm drainage analysis of the subject roof indicated that the equivalent loads and stresses imposed on the individual joist members from the storm were less than those imposed by the full design loads (dead load + live load). Additionally, while the analysis of the joists under the storm loading indicated some overstressed members in *compression* (due to design errors, as discussed above), the overstresses obtained from the analysis did not exceed the factor of safety for the design. Therefore, the subject joists should not have failed under the loads imposed by the rain event.

Failure Mode. The shape of the collapsed joists did not exhibit evidence of plastic deformation (refer to Figure 4), nor was there evidence of compression failures at the joists. The primary failure mode for the collapsed joists was failure at the welded connections between the tension webs and the joist chords. The pattern of the joist framing failures and the condition of the joists after the collapse were indicative of sudden failures in the elastic range, not indicative of "ductile" failure. Furthermore, the roof collapse was extensive and was consistent with a progressive collapse, whereby an initial failure caused subsequent failures in adjacent joists and the collapse spread along the length of the building.

Welds. Weld failures were observed at the joists. The failure of many of the welds occurred at the junction between the weld and the base metal. This type of weld

failure was indicative of a lack of fusion and substandard welding, which was verified by metallurgical testing and evaluation.

At some welds, paint was observed at the weld surface, as indicated in Figure 5. As noted above, the joists were painted by dipping them after the welding was completed (during the manufacturing process). The presence of paint between the weld and the base metal was therefore indicative of a gap between the weld metal and the base metal from the time of fabrication. The gap indicates inadequate fusion.

Figure 6 below shows a failed joist at the subject building, where several web members detached from the bottom chord at the connections. The failure mode for each of these connections was separation of the base metal and the weld metal, indicative of a lack of fusion as discussed above. This type of weld failure at multiple connections of adjacent web members indicates that there were multiple poor welds for this individual joist, which was one of many that failed in this manner. Based on a review of the joists at the collapse area, poor welds were frequent. A metallurgical examination of welds from the subject joists indicated that the overall weld quality was unacceptable and that some welds were so poor that they had only 0-10% of the strength of a good weld. Refer to Figures 7 and 8 for typical poor welded connections which failed.

SUMMARY

The extensive and progressive nature of this collapse indicated that the new cold formed steel joist framing was deficient with regards to both load-carrying and load-sharing capabilities. The pattern of the joist failure was sudden and violent, and was consistent with failure of the welded connections. Inconsistent welding and poor weld quality were observed at joists throughout the collapse area. The poor weld quality had a significant impact on the strength of the welds and the overall load bearing capacity of the joists. The physical evidence from the failed joists indicated that they were not properly constructed to withstand the design loading and were susceptible to collapse.

Deficiencies in the design, testing, and manufacture of the joists were discovered during the evaluation of the collapse and by evaluating available information from the manufacturer. These deficiencies, especially the manufacturing deficiencies at the welded connections, contributed to the collapse event. Additionally the design deficiencies were indicative of improper design assumptions that could result in unsafe conditions at structures using this new product.

If the EOR had reviewed the product testing and standard practices of the manufacturer, he/she would have noted a lack of a proper testing program for the joists, many joist failures at equivalent loads less than the project design loads times the factor(s) of safety, and use of non-standard effective length factors. While this does not excuse the poor design and manufacture of the joist product, Structural

Engineers should not select and specify products without proven track records or proven independent testing and design verification.

REFERENCES

American Institute of Steel Construction (AISC). (1989). *Manual of Steel Construction: Allowable Stress Design, 9th Edition*. AISC, Chicago, IL, p. 5–138.

American Iron and Steel Institute (AISI). (1991). *Specification for the Design of Cold Formed Steel Structural Members, August 1986 Edition with December 11, 1989 Addendum.* AISI, Washington, DC.

International Conference of Building Officials (ICBO). (1994). *Uniform Building Code*. ICBO, Whittier, CA.

Steel Joist Institute (SJI). (1994). "Standard Specifications for Open Web Steel Joists, K-Series." SJI, Myrtle Beach, SC.

FIGURES

Figure 1. Overall view of roof collapse.

Figure 2. Web to top chord connection. Also note the weld failures.

Figure 3. Typical joist geometry. Note the failure at the end web connection at the bottom chord.

Figure 4. Collapsed joists. Note the lack of plastic deformation.

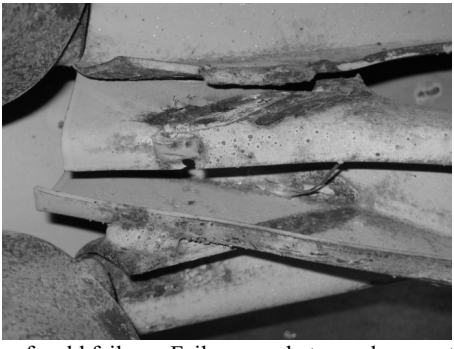

Figure 5. Close-up of weld failure. Failure was between base metal and weld metal. Note paint at surface of failed weld near middle of photo.

Figure 6. Failed joists. The webs failed at the bottom chord.

Figure 7. Failure at welded connection.

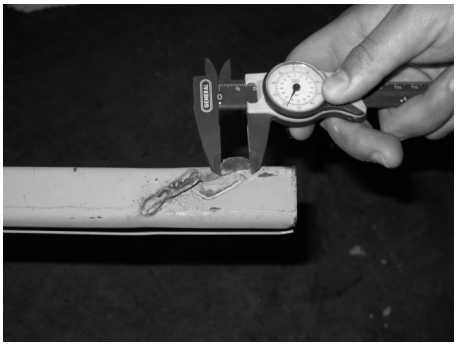

Figure 8. Failure at welded connection.

DESCRIPTION AND ANALYSIS OF CRIB WALL FAILURES

Gerald D. Lehmer, SE, PE, F ASCE[1],
Chukwuma G. Ekwueme, PhD, SE, PE, M ASCE[2]

[1]*Senior Consultant, Weidlinger Associates, Inc. 4551 Glencoe Avenue, Suite 350, Marina del Rey, CA 90292, Tel: 310-315-8430, Email: lehmer@wai.com*
[2]*Associate Principal, Weidlinger Associates, Inc., 4551 Glencoe Avenue, Suite 350 Marina del Rey, CA 90292 Tel: 310-315-8430, Email: ekwueme@wai.com*

ABSTRACT

Crib walls are a form of gravity retaining walls that are constructed of prefabricated interlocking concrete units. The space between the interlocking units or "crib" is filled with soil to provide weight and stability before the adjacent backfill is placed. In recent years, crib walls have been used in greater numbers and heights to solve varied retaining problems. This has resulted in an increasing number of failures. This paper discusses common problems with the design and construction of crib walls by summarizing five crib wall failures ranging in height from 20 to 40 feet that occurred recently in Southern California. The laboratory test procedures and test results performed during the forensic analyses of these failures is presented. Single and multiple assemblies of drycast crib elements were tested to destruction under laboratory conditions. Proper and improper construction procedures are also discussed and a crib wall design specification section is presented for inclusion in model building codes.

INTRODUCTION

In recent years, crib walls have been used in greater numbers and heights to solve more varied retaining problems. As a result, more failures have occurred. We have been involved in the investigation of approximately five recent failures. The findings derived during these investigations are discussed in the following paragraphs.

The most common type of crib wall in Southern California is the "New Zealand" type which is designed to be built by hand using individual members weighing about 130 lbs. maximum. The members are usually fabricated by the dry-process method similar to that used for concrete block. Members placed horizontally and parallel to the face of the wall are called stretchers; members perpendicular to the face are termed headers and these (headers) are alternated along a row with false headers which act as only spacers between stretchers. Stretchers and headers are made with one reinforcing bar in the center and the false headers are unreinforced. Figure 1 shows a typical crib wall.

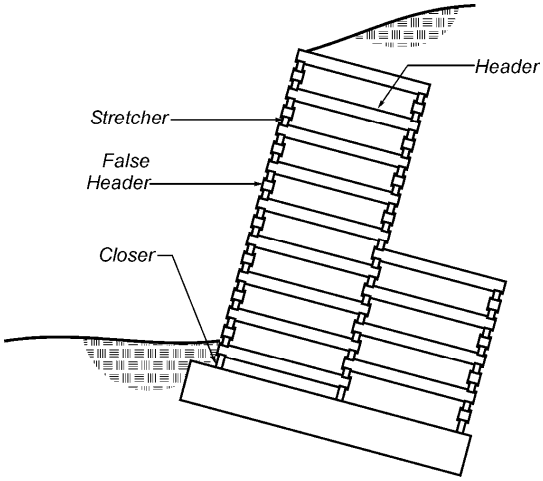

Figure 1 Cross-Section through a Typical Crib Wall

The reasons for failures of crib wall can be classified into three main categories – design issues, issues related to materials and quality control and issues related to construction.

DESIGN ISSUES

The following is a summary of some of the design issues that have not been adequately considered or have been ignored by some designers:

1. Adequate soil drainage behind the wall to ensure that the "drained soil" design load is not exceeded. Past investigation of failures reveals that crib walls are very sensitive to water intrusion into the cells or backfill. Adequate drainage is a required to prevent hydrostatic build-up, prevent wash-out of fines and ensure that the design assumptions regarding friction at the back of the wall are obtained. A majority of the crib wall failures in the past have been associated with heavy rains and/or with excessive moisture intrusion into the cells.

2. Adequate surface drainage at the top of the wall to prevent overtopping and erosion of soils in the front cell.

3. Sufficient compressive capacity in the crib members. Virtually all of the vertical overturning forces will have to be transferred through the bearing area between crib members. Review of crib wall failures reveals a common tendency for the members to split vertically at or near the compression areas, that is, at the intersections of headers or false headers and stretchers. In the past, designers have

failed to recognize that at many points in the wall, the crib skeleton will have to resist all the compression loads due to arching of the soils within the cells.

4. Stability of cell segments or stability of the entire wall if friction between the wall and soils is lost or even reversed causing uplift. Review of calculations for some walls which have failed revealed that the designer did not consider all possible loading conditions, that is, with or without vertical wall friction at the rear. The loss of wall friction for any reason could cause a lowering of the safety factors for sliding and overturning and an increase in the compression loading at the face of the wall.

5. Design compression stresses of individual members should be limited to that allowed for plain concrete.

6. Differential settlement between rows of stretchers causing bending and edge loading in members. Designers in the past have allowed significant differences in soil bearing across the section of the wall which in turn causes differential settlement between rows of stretchers. This may cause instability of the top single cell portion. Also, high compression stresses in the soil mass may cause settlements within the crib cells.

7. Insufficient compaction under and around stretchers and headers thereby reducing the cell area available to resist sliding.

ISSUES RELATED TO MATERIALS

The following is a summary of the issues related to the materials fabrication process:

1. The method of fabrication by the “Dry-Process” (similar to that for concrete block) provides excessive porosity in the members. In this method the water added is barely enough to hydrate the cement and the material is “pressed” into molds and immediately extracted and stacked to dry. As a result, the members appear very porous and a majority of them are already cracked when received at the jobsite. Also, there is great variability in the compression strengths within pallets of members or between pallets fabricated on the same day.

2. The effects of long-term corrosion are not clearly understood. Investigations have revealed that corrosion is predominant along lines of cracks and can be substantial after one or two years of building the crib wall and in particular appears to jeopardize the structural integrity of the front cell.

3. Variability in the location of the reinforcing bar in the section of the member causes wide variability in the member moment capacity.

4. Dimensional variability of the crib members is a direct cause of cracking in the members in particular when multiple headers / false headers are used. Tests

performed on assemblies of stacked crib members indicates that first cracking in stretchers can appear at values as low as 10% of ultimate if there is any appreciable difference in dimensions of headers below the stretchers.

ISSUES RELATED TO CONSTRUCTION

Past investigations indicate that poor workmanship is a direct cause of distress in crib walls. The following is a summary of the construction problems most frequently encountered.

1. Offsets in the vertical alignment of headers / false headers are a direct cause of the cracking of stretchers.

2. Stretchers (or closer at the rear of the wall) are butt-lapped in the compression area. This causes a reduction in the bearing area and a pinched-end condition at the ends of stretchers with usual cracking of headers and stretchers.

3. Asphalt roofing shingles (used as shims for alignment) do not cover the full bearing area or are not appropriately used to provide proper bearing.

4. Changes in the batter of wall members cause edge loading. As a result, the members become chipped or cracked.

5. Field-cut members not treated at the exposed end of rebar to prevent corrosion.

It is our opinion that with proper consideration of the above issues that crib walls can be constructed safely and economically in Southern California. Some limitations as to maximum height of walls and maximum equivalent fluid pressure should probably be specified until better field results can be documented.

EXAMPLES OF CRIB WALL FAILURES

The following provides examples of crib wall failures that were as a result of several of the reasons listed above

Wall Failure at Hebrew Union College

Cracking of the members was first observed in the crib wall at Hebrew Union College in 1990. When cracking was first observed, repairs were attempted by epoxy-injecting the cracked members and replacement of the broken members. However, while the epoxy repair was strong enough to prevent reopening of the crack in most cases, the cracks usually reappeared in the same member in close proximity to the repaired location. After continued cracking of the members, the height of the wall

was lowered by about 10 feet and a second shorter wall was built about 40 feet up slope from the first wall.

Additional cracking of the face members of the lower wall continued and was particularly sever after the heavy rains of February 1992. The cracking was most severe in the lower 8 to 10 feet of the wall and appeared to be uniform throughout the length of the wall. After a heavy storm, which lasted several days, a localized collapse occurred in the lower wall. Both crib walls were abandoned and replaced with a conventional cast in place reinforced concrete retaining wall.

An investigation revealed that crib wall failed due to a number of reasons. The prefabricated drainage sheets were incorrectly installed. The sheets were placed horizontally (instead of vertically) and ship-lapped in a manner that provided no positive connection between adjacent sheets for water to flow feely. In addition, misalignment of headers made the wall susceptible to differential movement. The failure of the wall was progressive. When a header or false header crushed, the vertical load was redistributed to adjacent highly stressed members, which then also failed. The cell backfill was unable to pick up any of the redistributed load because the soils under the members was not well compacted. If adequate compaction been performed, the soil mass would have taken some of the load from the failed member and this may have limited the progression of the failure.

Figures 2 and shows pictures of the crib wall failure, while figures 3 to 5 show photographs of the misaligned headers and false headers that were observed during an investigation of the wall.

In addition to the on-site observation oft he crib wall, a number of undamaged members was selected from the crib wall for testing in the laboratory. Compressive strength tests revealed that the compressive strength of the concrete in the members was less than required by the construction documents.

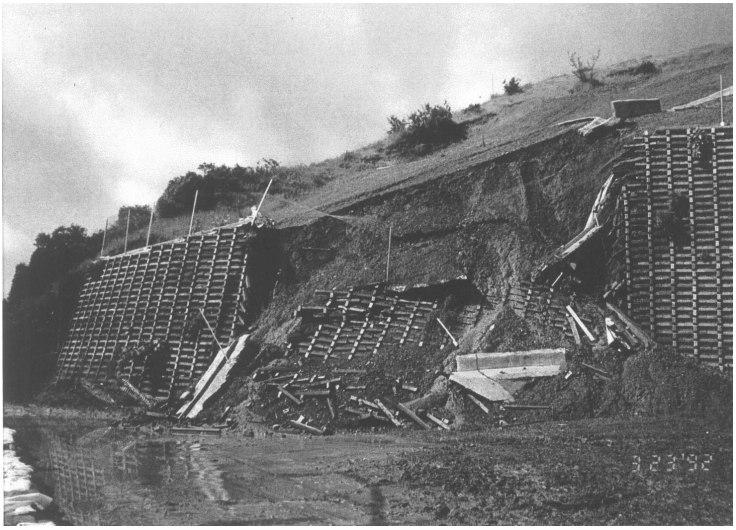

Figure 2 Overall view of crib wall failure.

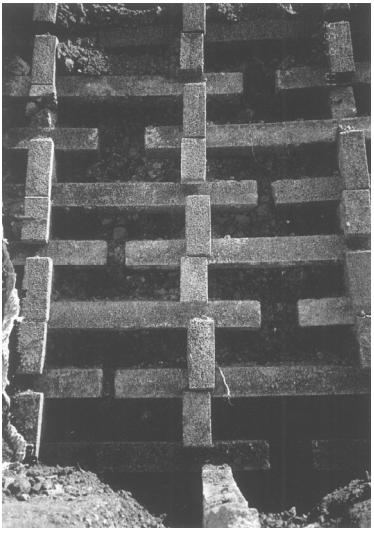

Figure 3 Back of a single cell showing bottom stretcher cracked at offset in line of headers.

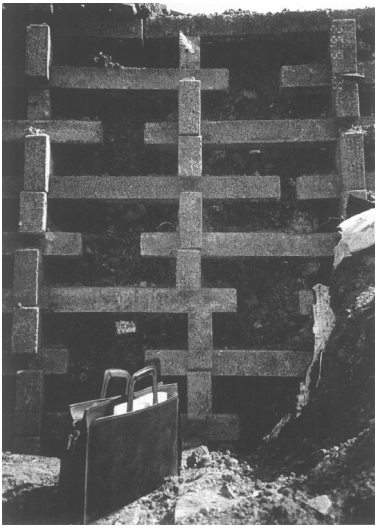

Figure 4 Back of a single cell showing offset in line of headers (third closer form bottom

Figure 5 Close up showing lower false header at right has punched into upper stretcher causing splitting and spalling of face lug.

Topanga Canyon Crib Walls G, H & D

The crib walls at Topanga Canyon consisted of six separate walls that wee investigated in 1993. Walls G, H and D exhibited the most damage. A major collapse occurred in wall G in which the cribs slid forward, one over the other. At to the locations and in other walls, distress was clearly evident in the bottom 8 to 10 feet of the wall. The damage typically consisted of bulging of the wall, crushed headers and false headers, broken stretchers, loss of fill from the front cell and differential vertical movements between rows of headers. Corrosion of the reinforcing steel was observed, particularly in members that had cracked and allowed moisture to penetrate. Figure 6 through 8 show typical damage to the walls.
Several test pits were dug during the investigation and they revealed severe cracking to numerous headers. The cracks typically consisted of a single vertical crack through the header located at the back of the compression area. While almost of the observed headers were cracked almost none of the false headers were damaged.

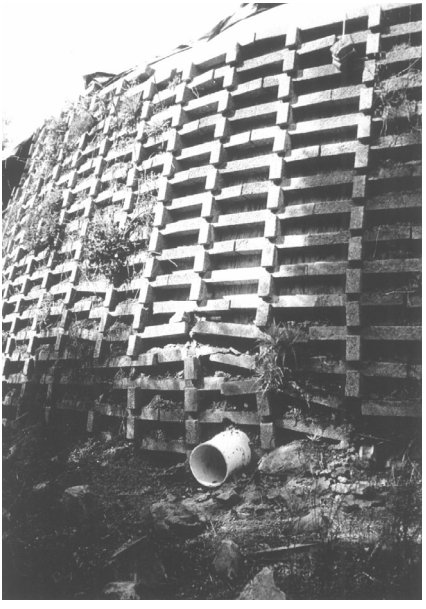

Figure 6 Damage at base of wall at a12-inch diameter pipe. Note plywood forms to retain slurry that was poured to replace washed out soil.

Figure 7 Damage at base of wall. Note plywood forms to retain slurry that was poured to replace washed out soil.

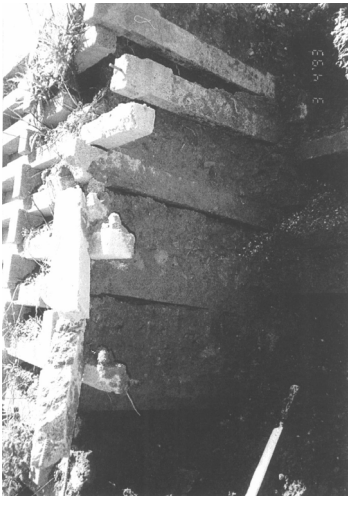

Figure 8 Side of crib wall south of failure area. Note voids under headers

The investigation if the crib walls identified several reasons for the failures. The actual plan layout of Wall G differed considerably from the approved plans in several locations. Two large curves were introduced during construction to avoid damaging

some oak trees. At numerous locations the stretchers were butt-lapped in the compression area, thereby decreasing the bearing area on the headers and increasing he applied compressive stresses. In addition, several drains were missing and compaction rests indicated that the compaction of the soil was significantly less than the 90% required by the construction documents. There were voids under several headers, which were about 2 to 3 inches deep. The ends of stretchers that were cut in the field were not treated to prevent corrosion of the reinforcing steel and this allowed corrosion to occur.

CONCLUSIONS

The numerous collapses of crib walls can be attributed to three main causes – design errors, issues related to materials and quality control, and issues related to construction. To prevent further collapses, it is imperative that each of these aspects is addressed during the design and construction of crib walls. It is particularly important to provide adequate drainage for the crib wall to prevent the increase in loads that occur during rainstorms when proper drainage is not provided.

The American Society of Civil Engineers (ASCE) Los Angeles Section Crib Wall Committee has developed proposed criteria for the design of crib walls in the Los Angeles area. The proposed criteria recommend that a continuous concrete footing should be provided under all crib wall elements and designed to distribute the vertical and overturning loads uniformly to the soil below the footing as prescribed for retaining walls in International Building Code (ICC, 2006) Section 1610 and for concrete footings in ACI 318. In addition, no soil-column effects are to be considered as reducing the bearing loads at the element intersections and the resultant upward reaction due to any load combination shall lie within the middle 1/3 of any cross-section of the wall or footing. Dry cast-crib wall elements should comply with the material standards as set forth in Section 2103 of the International Building Code (ICC, 2006) for concrete masonry units. The design of poured concrete crib wall elements should comply with IBC Section 1903 specifications for tests materials for concrete.

REFERENCES

International Code Council (ICC). (2006). *International Building Code*, International Code Council, Inc., Falls Church, Virginia.

American Concrete Institute (ACI). (2005). *Building Code Requirements for Structural Concrete and Commentary (ACI 318-05)*, American Concrete Institute, Farmington Hills, Michigan.

ROOF COLLAPSE CASE STUDY: DRAINAGE DESIGN ISSUES

James W. Jordan, SE, PE, M.ASCE[1]
Luke Sharara, PE, M.ASCE[1]

Abstract: A section of the roof for a warehouse structure collapsed after a rainstorm event during the summer of 2006. Given the location of the building, one may be surprised to find that such a roof would collapse after a rain event rather than a snow event.

Was it an unusually heavy rain event? Were there errors in the structural design of the building? Were there problems with the fabrication/installation of the roof joists, girders and columns? Were there errors in the design and installation of the roof drains and associated plumbing? Surprising, none of these issues proved to be the culprit.

This paper steps through our forensic evaluation of this case, and briefly reviews roof drainage design considerations. From the collection of weather data, through our consideration of various failure hypotheses, we will show the forensic methodology that led us to a very interesting conclusion.

[1]Rimkus Consulting Group, Inc., 8910 Purdue Road – Suite 170, Indianapolis, IN 46268; PH (317) 510-6484; FAX (317) 510-6488; email: lmsharara@rimkus.com, jwjordan@rimkus.com, rakimble@rimkus.com .

Introduction

Forensic evaluations of roof collapses in the Midwest portion of the United States present unique challenges for the investigating engineer. The structural design of building roofs in this region is typically governed by snow loads. As such, we would generally expect a roof collapse in the Midwest to result from snow overloading. The investigating engineer may be surprised to find that these collapses may occur during the summer months, when no snow loading is present.

When roof collapses for structures located in the Midwest occur during summer months, the investigating engineer will often find that a rain event was involved. In order to assess loading conditions from this scenario, the investigating engineer requires a good understanding of basic roof drainage design practices and

methodologies. Simply following design tables and charts from appropriate building codes may not account for a particular loading condition.

Case Study Background Information

The subject of this paper involves a large warehouse located in the upper Midwest, generally southeast of Lake Michigan. A portion of the roof collapsed during a thunderstorm event in July 2006. Figure 1 shows the damage as viewed the day after the collapse.

Figure 1: View of collapsed roof section in subject warehouse case study.

The roof collapse was isolated to a relatively small portion of the warehouse structure (see Figure 2). The construction of the roof system consisted of metal deck welded to steel joists, supported by steel columns and concrete wall panels. The debris contained failed roof joists, metal deck, and roofing materials. The concrete wall panels and structural steel framing (girders, columns) remained essentially intact. The affected portion of the lower roof was bounded by a wall on one side, parapets on two sides, and an upward sloped condition that led to a ridge on the remaining side. With this confinement, rainwater accumulation would have to exceed a depth of 36 inches (above the roof drain) before spilling over to adjacent roof areas.

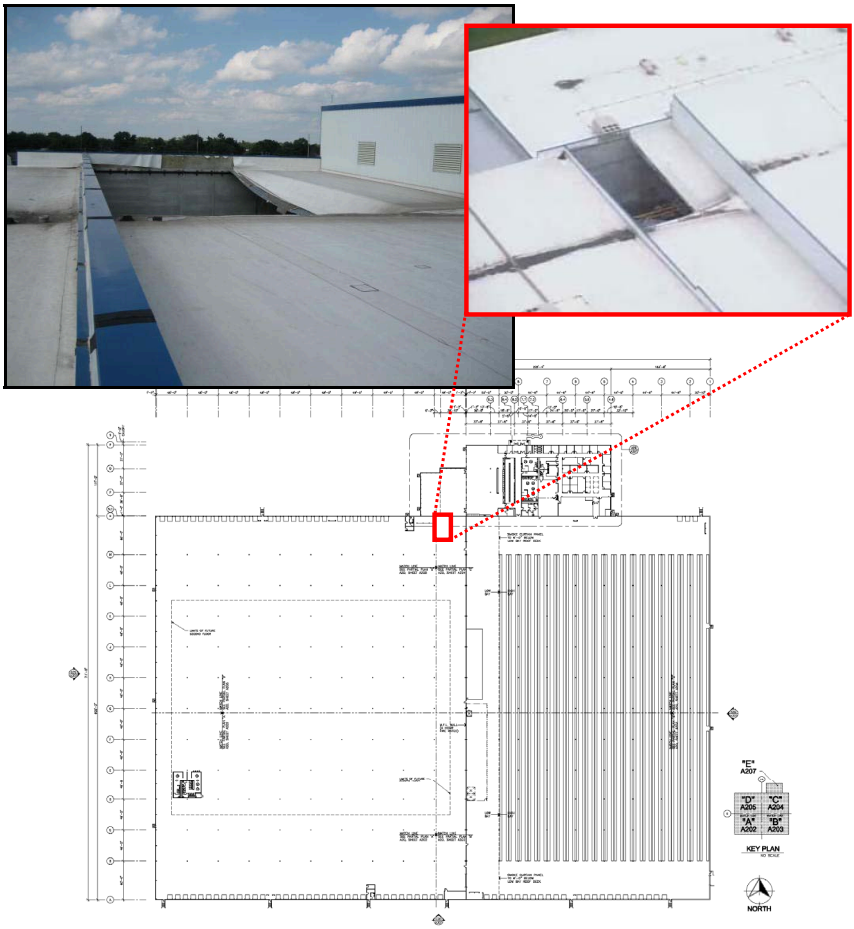

Figure 2: Views of the collapsed portion of roof.

Approach to Investigation

In this instance, we were retained to determine why the roof collapse occurred. Our general approach to performing this investigation consisted of:

1. Examining the evidence (debris, remaining structure)
2. Interviewing personnel at the site
3. Reviewing construction drawings and relevant building codes

4. Obtaining weather information
5. Performing analyses and formulating opinions
6. Preparing a written report of findings

Examining the Evidence

The failure of the steel roof joists was a primary factor in the collapse of the roof portion. During our investigation, the failed joists were recovered and examined (see Figure 3).

Figure 3: Roof joists collected from debris.

Multiple modes of failure were evident in the roof joists, including failed welds and detached web members, torn seat angles (at supports), and large deformations. No apparent defects were found, such as excessive porosity in weld metal, lack of weld metal fusion, improperly altered joists, lack of mechanical attachment to roof deck, etc. Based on the remaining evidence, the specific joist failure mechanism that initiated the collapse could not be determined.

We also examined the roof drains that served the portion of the roof that collapsed. There were two drains present, a primary drain and a secondary (emergency) drain (see Figure 4). Both drains were partially blocked with debris. We also noted that both drains were eight inch diameter, and connected to the same drainage pipe. The inlet elevation for the secondary drain was located two inches above that of the primary drain, so that rainwater accumulation would reach a depth of two inches before the secondary drain became effective.

Interviewing Personnel at the Site

Upon interviewing personnel at the site, we found out that a security camera recorded the failure from a remote location. The recording showed that the collapse occurred between 2 am and 3 am. The recording also revealed that the roof failure initiated at joists adjacent to the roof drain.

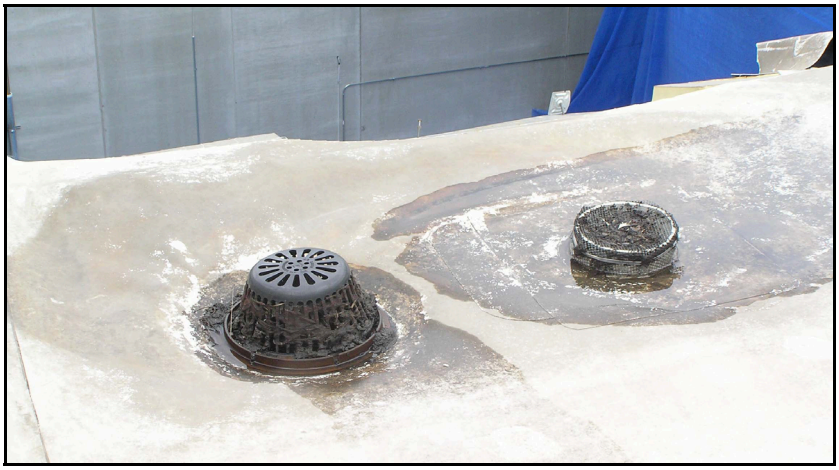

Figure 4: Remaining roof drains that served the portion of the roof that collapsed. Primary drain is on the left, and secondary drain is on the right.

Reviewing Construction Drawings and Relevant Codes

Upon reviewing the construction drawings, we noted the following:

1. The roof drainage system was essentially installed as specified in the drawings.
2. Due consideration had been given to snow drift loading for the design of the roof structure (a 20-foot tall wall was adjacent to the portion of the roof in question, which served a high bay portion of the building).
3. The adjacent high bay portion of the building had its own drainage system, distinctly separate from the low bay roof portion that collapsed.

Upon reviewing applicable building codes, we noted the following:

1. The 1997 Uniform Plumbing Code with State Amendments governed the design of the roof drainage system.
2. State Code Amendments permitted both the primary and secondary drains to be connected to a common drainage pipe, which was contrary to the 1997 Uniform Plumbing Code.
3. The strainer for the secondary drain was simply a flat screen stretched across the end of a pipe. This did not meet code requirements, which states that the

strainer openings should be 150 percent of the conductor area, such as that used for the primary drain in this case (see Figure 4).

4. The tributary area for the roof drains at the collapse area must include half of the adjacent wall height (for the wall between the high and low bay roofs).

Obtaining Weather Information

Information on the rain event was available from some internet sources, including that from the National Weather Service. Since we had a security video that documented the relatively precise time that the collapse occurred, we sought more detailed timing information on the rain event. We retained the services of a forensic meteorologist, who determined (within a reasonable degree of scientific certainty) the rainfall intensity and duration at various points during the storm. It was determined that approximately 1.6 inches of rain had fallen within an 18 minute period between the start of the rain event and the collapse at the site of concern. A total of 2.42 inches of rain fell over the 54 minute duration of the storm.

Performing Analyses and Formulating Opinions

We performed several analyses of the subject roof area considering varied severities of roof drainage obstruction. We found that 100 percent blockage (a very conservative estimate) of the drains would have loaded the roof joists to approximately 90 percent of their allowable design capacity. We also found that the rainfall event was reasonably within design requirements for the area (2.75 inches per hour, 60 minute duration). The results of these earlier analyses simply did not show an overload condition from this rain event on the affected area of the roof. Given that there were no apparent defects in the construction of the roof structure, and that the actual loading conditions for the tributary area of the affected roof were within allowable design values, we knew that we must look elsewhere for our answer to this perplexing problem.

So we began to review a typical design process for this type of structure. In particular, we reviewed the drainage design for adjacent building areas – including the high bay roof. The high bay roof was designed similarly as the low bay, with eight-inch diameter primary and secondary drains that served various tributary areas. We noted that the top of the wall between the high and low bay portions of the building did not have a parapet, but did have a flashing detail with a gravel stop as well as a sloped roof profile to direct rainwater away from the wall.

We took a closer look at the drainage design for the high bay roof area adjacent to the wall near the low bay roof collapse site. The drains appeared to be sized appropriately, per the 1997 International Plumbing Code. This code provided the permissible square foot area that may be attributed to a particular drain size. Based on the tributary area of the high bay roof, an eight-inch diameter drain was appropriate. The secondary drain also met code requirements, which state that the primary drain must be assumed to be completely blocked when sizing the secondary

drain, and that the inlet elevation of the secondary drain should be two inches above the inlet of the primary drain.

An iterative analysis was performed, where the volume of rainwater for each minute of the storm was compared to the flow rates of the high bay roof drains, and accumulated water depth (hydraulic head) at the drains were determined. This considers that the maximum flow rate of a particular drain is not achieved until a certain hydraulic head is obtained (see Figure 5). As a "rule of thumb", the designer should consider that a depth approximately equal to the drain radius may be required for the drain line to achieve its maximum design flow rate. We considered that the primary and secondary drains would have discharged water simultaneously during the rain event. In this case, we found that rainwater would accumulate to a depth of 3.8 inches on the upper roof portion during the subject rain event just prior to collapse of the lower roof portion. The ASCE paper "Roof Drainage Design and Analysis: Structural Collapses, Responsibility Matrix, and Recommendations" (prepared by James W. Jordan, presented at the 2005 Structures Congress) explains the iterative methodology for estimating rain water accumulation.

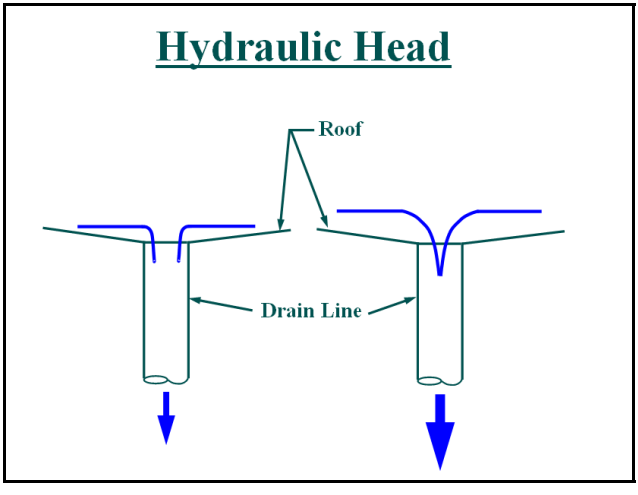

Figure 5: Conceptual cross-section of roof at drain, showing increased drainage flow rate with greater water depth.

Armed with this knowledge, we re-examined the construction drawings and took another look at the site. The detail at the roof edge for the high bay would retain water to a depth of three inches, which was less than that determined for the subject rain event. This meant that it was possible for unintended overflow of the high bay roof onto the low bay roof in the vicinity of the collapse. Considering the extra volume of water that would have overflowed from the upper roof during the subject rain event, it was possible for the affected roof joists to be loaded at approximately

250 percent of their allowable design capacity. See Figure 6 for an illustration of the overflow effect. We also found staining on the lower roof which supported our conclusion that overflow (spill-over) had occurred at the area of the collapse (see Figure 7).

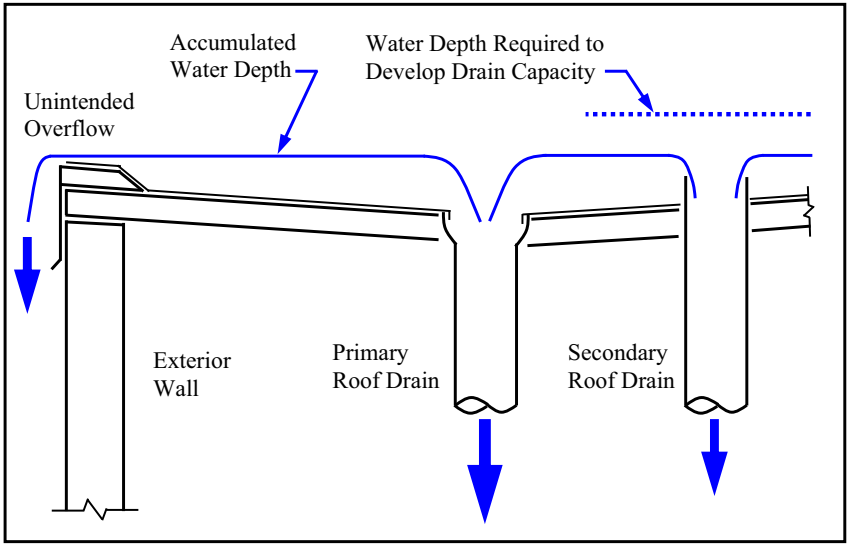

Figure 6: Schematic roof cross-section illustrating the unintended overflow (spill-over) condition. Please note that this sketch is not to scale.

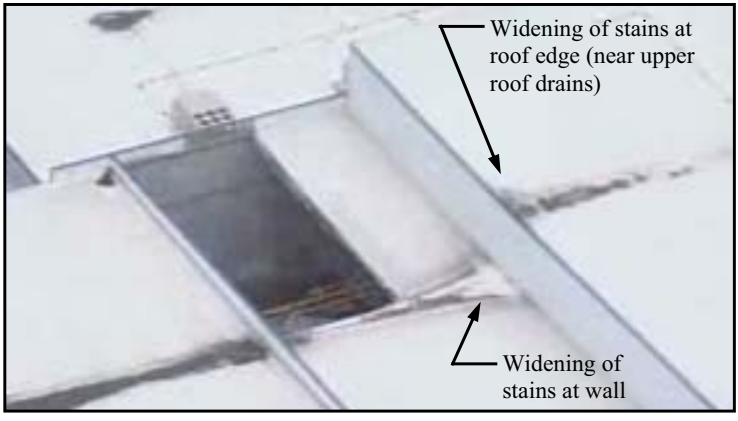

Figure 7: Enlarged view of aerial photograph with overflow evidence denoted.

Preparing a Written Report of Findings

Our findings were summarized and explained in a written report provided to our client. Generally, reports of this nature should include a listing of observations and other pertinent information, a succinct and easily understood summary of key conclusions, and a logical discussion of analyses that shows how the key conclusions were derived from the observations and gathered pertinent information. Appropriate references used in the evaluation should also be included in the report.

Summary

This case study provided an opportunity to discuss a general approach to performing a forensic engineering investigation. We reviewed several steps that were taken in our analysis. In this particular case, we found that the original hypothesis (construction defects) was not supported by the physical evidence. We also found that the rain event was not unusual and should not have produced loads that exceeded typical roof design loads for this building. Upon our initial evaluation of the roof drainage design, we found no obvious errors in the interpretation and use of the applicable building codes. After further analysis, we discovered that the roof drainage design had the unintended consequence of an overflow condition from an upper roof onto the lower roof in question. This condition was not readily apparent when using the various design tables allowed by the applicable code. As a result, roof drainage design defects were a key factor in the collapse of the affected lower roof system.

References

American Society of Civil Engineers (ASCE, 2005). "Minimum Design Loads for Buildings and Other Structures [ASCE/SEI 7-05]".

International Code Council, Inc. (ICC, 1997). "International Plumbing Code Commentary".

Janney, Jack R. (1986). "Guide to Investigation of Structural Failures". American Society of Civil Engineers (ASCE).

Jordan, James W. (2005). "Roof Drainage Design and Analysis: Structural Collapses, Responsibility Matrix, and Recommendations", Proceedings of the 2005 Structures Congress, American Society of Civil Engineers (ASCE).

Patterson, Stephen and Mehta, Madan (2001). "Roofing Design and Practice". Upper Saddle River, New Jersey. Prentice-Hall, Inc.

Failure of a Church Fresco: The Engineering of Art vs. The Art of Engineering

Michael P. Lester[1]

[1]Element Analytical, PLLC, PO Box 1091, Knightdale, NC 27545, PH (888) 875-5973; FAX (888) 875-5973; email: mlester@elementanalytical.com

ABSTRACT

St. Peter's Catholic Church in Charlotte, North Carolina, commissioned artist Ben Long to erect a fresco in the church sanctuary. The fresco was erected on the gabled south wall of the sanctuary. The work of art commenced in 1988 and it was completed in 1989, with assistance of apprentices and consultation of building professionals. In February 2002, the *buon fresco* partially collapsed from the wall of the sanctuary, which was constructed c. 1893. Coincidentally, the church was surrounded by ongoing construction activity for a large multi-use development, and the collapse reportedly occurred during removal of concrete pavement close to the structure. The church alleged, as did some investigators, that the collapse ensued because of adverse vibrations associated with the construction activity. This paper presents the evaluations of the author, including observations, analysis of vibration activity, and laboratory testing, which revealed the fresco failure commenced prior to surrounding construction because of inherent defects in the fresco installation.

DESCRIPTION

The church comprises wood and steel frame construction with solid masonry walls and a full basement. Portions of the structure date to the mid 1800's, when the church was reportedly reconstructed after a fire. The church entrance faces the street in a northwesterly direction. For reference, the church is taken to face north. The triptych fresco was applied by artist Ben Long to the south wall of the sanctuary in 1988 and 1989 (Figure 1). Prior to that application, an old layer of plaster was removed from the south brick wall and replaced with a layer of plaster

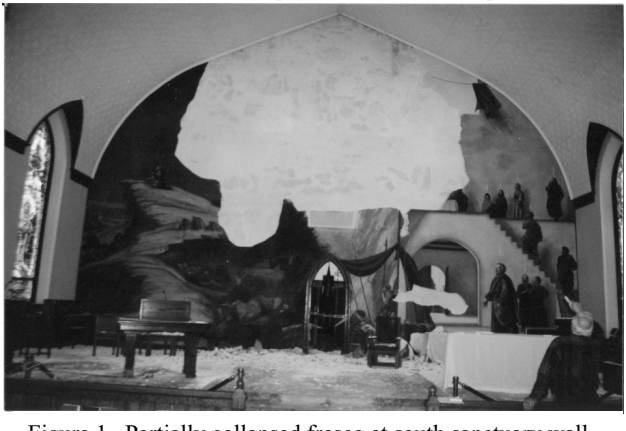

Figure 1. Partially collapsed fresco at south sanctuary wall.

consisting of Structo-Lite®, a proprietary gypsum-based bagged plaster mix manufactured by US Gypsum Company. The new plaster was specified by an architect consulting for the church during the renovation phase. The fresco covered a portion of the gabled south wall about 13.4 m (44 ft) wide and about 10.4 m (34 ft) high at the apex.

BACKGROUND

The church is adjacent to a mixed-use facility that was under construction and nearing completion when the incident occurred. The project included a multi-story underground parking garage, immediately adjacent to the church, and a multi-story mixed-use structure along the side of the project lot farthest from the church. Figure 2 depicts the church and its relationship to surrounding construction. The plaza between the church and multi-story building is atop a subsurface parking garage.

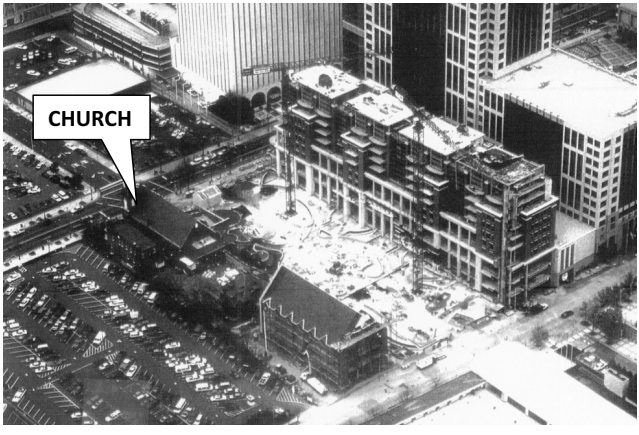

Figure 2. Aerial view of church and surrounding development.

Construction of the parking garage required blasting of rock to facilitate the subsurface structure, and included driving numerous piles, some very close to the church. To accommodate new facility construction, shoring was installed along the east wall of the church structure. On February 20, 2002, reportedly in the late morning, the fresco experienced catastrophic failure, when a large portion of the fresco fell to the sanctuary floor. The fresco collapse reportedly coincided with demolition activities by one of the subcontractors. That contractor was removing a section of sidewalk utilizing a pneumatic hammer mounted on a backhoe. The demolition activity had been under way several hours.

SCENE EXAMINATION

A limited scene examination was conducted in February 2002, in the company of a parish member. Much of the fresco remained on the floor at the time of that examination, with some of the larger pieces reportedly removed for safe keeping. Most of the fallen portion originated in the upper and middle area of the wall. The

plaster-like substrate, commonly referred to as the "scratch coat" in plaster work, had a smooth finish, and remained intact and affixed to the brick wall. That layer was the Structo-Lite material and was installed by a subcontractor in advance of the artist's activities. Closer examination of that gypsum plaster base revealed no visible cracking or other distress.

Examination of fallen pieces revealed double layers of plaster material. These layers were lime-based plaster. Both layers were somewhat friable under manual pressure. The under layer, or the "arriccio" in classic terminology, was the thicker of the two layers, measuring about 8.9 mm (0.35 in). Of the two layers, the arriccio contained larger, darker aggregate. The outer layer, called the "intonaco", measured about 5.3 mm (0.2 in). The intonaco contained smaller, tan-colored aggregate. It also contained the paint pigments of the fresco. The arriccio and intonaco (totaling about14 mm (0.55 in)) were well bonded. Figure 4 illustrates the fallen fresco cross section, magnified for clarity.

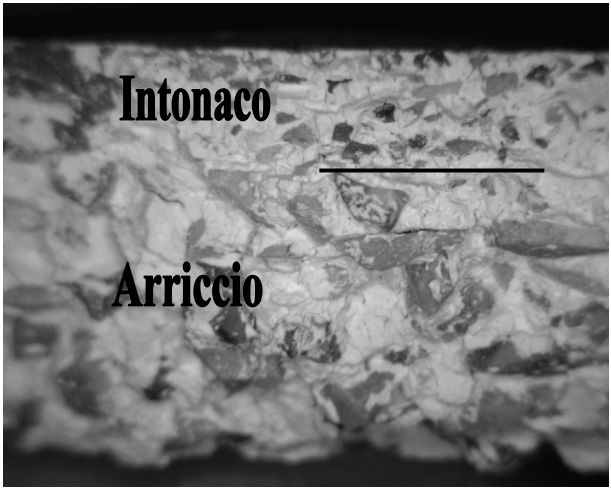

Figure 3. Enlarged cross-section of fresco remnant illustrating smaller aggregates of the intonaco. The line corresponds to the interface of the two layers, which are indicated.

Manual (fingertip) sounding of accessible fresco portions revealed detachment of the lower fresco portion along much of the wall length and lower height. While results were not recorded quantitatively, the exercise indicated widespread detachment of the fresco from the plaster substrate. Visual examination of newly exposed, fractured edges revealed gapping between the intonaco and base plaster. The gaps were present at most areas viewed and were discernible in the upper portions, even when viewed from the floor. Further examination revealed discoloration of the gypsum plaster substrate near roof level, an indication of probable water intrusion. With

permission, a few small pieces of the fresco were retained for further examination and potential laboratory testing.

INTERIM PERIOD

Shortly after the field investigation, a regimen of tests and evaluations were recommended; however, as is sometimes the case in forensic investigations, further work was halted. The case file was placed away until a couple years later when a client change took place under a mutual agreement. By that time, all fresco remnants, even those surviving pieces on the wall, had been removed, and the south wall of the sanctuary had been refinished. Fortunately, the change in clientele brought about a significant amount of case-related documents not previously available.

DOCUMENT REVIEW

Records associated with pile driving, if any were kept, were not available. Therefore, pending analysis would have to be based on speculative vibrations and building response. Conversely, the blasting subcontractor maintained field notes and blasting logs during construction. In addition, seismographs monitored and recorded ground vibrations associated with the blasts. The seismographs were placed at various locations around the site, very often including the church. The presented logs related 319 blasts on the site between January 4 and June 23, 2000. Invoicing records indicated some additional blasting took place after June 23. Each available blast and its associated data were entered in tabular form for evaluation. Information for some of the blasts was incomplete in that time of day, measured response, pounds of explosives, or specific blast location could not be derived. Nonetheless, review of the records yielded usable information regarding response of the church to blasting activity. The data suggested a seismograph was placed at the church for all significant blasting events. The highest recorded blast response was 1.17 inches per second (ips) peak particle velocity (PPV) at 25 Hertz on March 8, 2000. Interestingly, the fresco collapse occurred almost two years after pile driving and blasting activity on the site ceased. The following table, Table 1, is excerpted from the master spreadsheet.

Table 1. Measured Blast Response at Various Locations

				Parking Deck		Conv. Center		Duke Power		Monastery		Church		
Event	**Date**	**Time**	**Lbs/Del.**	PPV	Hz	PPV	Hz	PPV	Hz	PPV	Hz	PPV	Hz	**Dist.**
21	2/29	18:53	14.5	0.27	45	0.51	28	0.15	31	0.37	18	0.12	26	184
22	2/29	19:00	14.5	0.50	56	0.25	29	0.11	63	0.35	63	0.17	45	171
23	3/1	18:53	17	0.96	28	0.95	26	0.33	25	0.82	41	0.44	31	184
24	3/2	18:54	17	3.76	6	0.41	32	0.12	42	0.43	50	0.17	20	
25	3/3	18:52	14	0.38	42	0.74	29	0.28	26	0.25	21	0.12	42	
26	3/3	18:55	13	0.53	56	0.49	31	0.16	36	0.44	56	0.37	26	
27	3/7	19:01	11	1.15	24	0.27	33	0.08	36	0.24	63	0.21	35	
28	3/8	19:04	18	1.26	28	1.32	24	0.68	28	2.60	20	1.17	25	
29	3/10		8	0.26		0.14		0.09		0.22		0.11		224

Several reports were produced by other investigators in this case, and many of these reports, along with associated correspondence prepared subsequent to the fresco failure, were available for review. Most notable were reports from local engineering firms and one conservation condition report from an engineering/art specialist. Some of the investigators suggested pre-incident separation of the arriccio from the wall.

Of particular interest was a letter from one subcontractor that stated points on the eastern exterior portion of the church experienced between 0.18 and 0.30 inches of subsidence because of shoring movement. The letter speculated a potential cause of movement to be a blast that occurred on August 12, 2000. Given the absence of records to indicate blasting by the blasting subcontractor at or even around this date, the occurrence of such a blast on site was questionable. Moreover, records implied the occurrence of off-site blasting.

A favorable coincidence in this investigation was the commissioning of a local writer to document the story of the incident fresco and its artist. The author completed his story and, ultimately, a book was published. As part of the investigation, that text (Maschal 1993) was obtained and reviewed. The book provides information regarding the application of the plaster layers. The text also discusses the dislocation of a section of the arriccio just before the pigmenting (painting) process was to begin. Immediately after the incident, the architect was consulted and, eventually, the artist decided to continue with installation.

LABORATORY EXAMINATION

The retained pieces of fresco were examined visually and by optical microscope in the laboratory. No deleterious material was visible, and no remnants of the gypsum (Structo-Lite) base were observed. The contact surface of the arriccio contained numerous voids, a condition that would limit surface-to-surface contact for bonding. The arriccio also exhibited widespread fissuring, small randomly dispersed cracks, apparently the result of drying shrinkage immediately after installation. Figures 4 and 5 are magnified views of the contact side of the arriccio. Figure 5 is twice the magnification of Figure 4. The figures illustrate the widespread presence of voids and fissures in the arriccio surface.

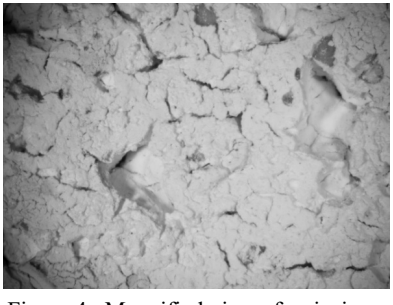

Figure 4. Magnified view of arriccio contact surface illustrating voids and fissures.

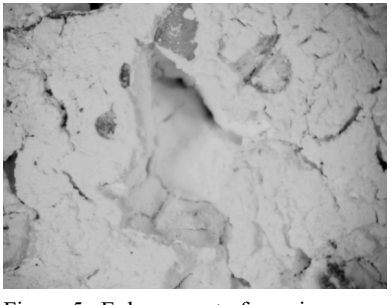

Figure 5. Enlargement of area in Figure 4.

LABORATORY TESTING

Review of product literature and texts on plaster gave no indication of adverse performance when gypsum-based and calcium-based plaster materials are joined. A search for testing standards failed to find any pertinent industry guidelines. Having interest in actual performance, a laboratory testing procedure was developed and implemented. Structo-Lite and calcium-based slaked lime putty were acquired and applied, in similar fashion as the fresco, to concrete pavers. The Structo-Lite (gypsum plaster) was applied and permitted to set for one week. It was applied in smooth and notched (1/8" V-notch trowel) finishes to twelve pavers (slabs), six of each surfacing. Figure 6 depicts six of the pavers coated with gypsum plaster. The lime putty was mixed with clean, moistened sand aggregate, similar in appearance to that of the incident arriccio, and applied to the gypsum substrate. The lime plaster

Figure 6. Partially prepared test slabs coated with gypsum plaster.

was applied to substrates that were either dry or moistened. Figure 7 depicts the pavers after application of the lime plaster. After 30 days, the slabs were cored by various means and with differing diameters to permit pull testing of the arriccio to gypsum substrate (Figure 8). A Shimpo FGV-500HX force gauge recorded load history and peak values while testing the samples to failure. The results of this testing are summarized in Table 2. The results were not statistically analyzed.

Figure 7. Test slabs with lime plaster coating over gypsum plaster base.

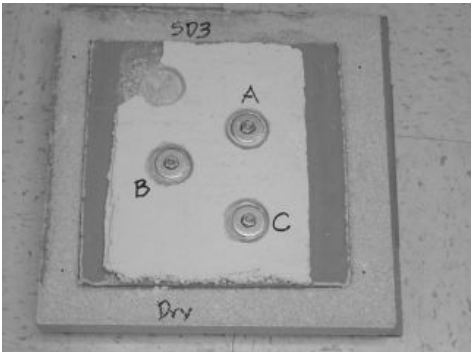

Figure 8. Test slab with three cores for testing.

Table 2. Sample data and test results.

Slab	Sample	Dia. (in)	Area (in^2)	Force (lbs)	t (psi)	Abs. Value (psi)	Comments
ND1	B	1.05	0.865901	-5.4	-6.23628	6.24	
ND2	B	1.75	2.405282	-62.9	-26.1508	26.15	Failed in matrix
	C	1.75	2.405282	-56.5	-23.49	23.49	
	D	1.75	2.405282	-12	-4.98902	4.99	
ND3	A	1.75	2.405282	-13.9	-5.77895	5.78	
	C	1.7	2.269801	-7.1	-3.12803	3.13	
SD1	A	2.25	3.976078	-33	-8.29964	8.30	
SD2	A	1.75	2.405282	-14.8	-6.15312	6.15	
SD3	A	1.75	2.405282	-35.9	-14.9255	14.93	Failed in matrix
	B	1.74	2.377871	-14	-5.88762	5.89	
	C	1.74	2.377871	-16	-6.72871	6.73	Failed in matrix
NM2	A	1.74	2.377871	-23.5	-9.88279	9.88	
	B	1.7	2.269801	-38.9	-17.1381	17.14	
	C	1.76	2.432849	-6.2	-2.54845	2.55	
	D	1.8	2.54469	-213.3	-83.8216	83.82	StrutoLite to StructoLite
NM3	A	2.25	3.976078	-55.6	-13.9836	13.98	
	B	2.25	3.976078	-25	-6.2876	6.29	
SM1	A	1.74	2.377871	-32.3	-13.5836	13.58	
	B	1.74	2.377871	-39.5	-16.6115	16.61	
	C	1.75	2.405282	-4	-1.66301	1.66	
SM2	A	1.7	2.269801	-50.1	-22.0724	22.07	
	B	1.72	2.323522	-46.8	-20.1418	20.14	
SM3	A	2.3	4.154756	-17.2	-4.13983	4.14	
Lime Cyl	A	1.03	0.833229	-20.9	-25.0831	25.08	
					Min.	**1.7**	NM2_D and Lime Cyl were not used in formulation of max/min/avg values
					Max.	**26.2**	
					Avg.	**10.9**	

One gypsum to gypsum application was placed and tested for comparison. That sample, NM2-D, failed at over seven times the average for the lime to gypsum samples and over three times the maximum value for the lime to gypsum samples. One lime plaster cylinder was cast and tested to failure. It failed at nearly twice the average bond strength of lime to gypsum plaster. Figure 9 contains graphical results of the testing. Table 3 lists interesting results regarding moistened versus dry and notched versus smooth substrates. Intuitively, the notched applications were expected to fail at higher values; however, the average was slightly less for the testing population. Similarly, the wetted substrate was expected to yield higher bond, and the moistened samples produced an average bond over 14% higher. One noteworthy observation was the difference in consistency between the incident samples and tested samples. Both sample types were friable; however, the laboratory samples had fewer voids, fewer fissures, and more stable aggregate retention under manual pressure.

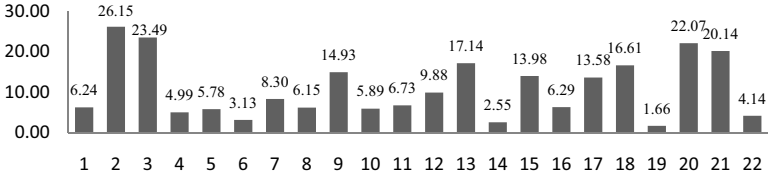

Figure 9. Lime plaster to gypsum plaster bond strength (psi) for 22 test specimens.

Table 3. Average of Test Results

Average Bond Strength (psi)		
Notched	vs.	Smooth
10.87396		10.92789
Wet	vs.	Dry
11.64116		10.16069

DISCUSSION

Lime has been used for centuries as a major constituent in cementitious materials, including mortars and plasters. Like many cementitious products, lime mortars/plasters are much stronger in compression than in shear or tension. Research failed to reveal an instance where lime was recommended for use over gypsum; however, no instances advising against such an application were discovered. While both materials are used in new construction as well as repair work, their intermingling is not common. Interestingly, research did show that slaked lime was used in the past to harden gypsum plaster (Eckel 1922), and sulfate contaminants (sulfate is a constituent of gypsum) are deleterious in the hydration of lime (Hassibi 1999 and

Potgieter 2003). Early observations indicated the fresco (lime plaster) to gypsum plaster bond was flawed. The pull tests strongly suggested an inability for the dissimilar materials to form a sturdy bond. The average bond strength of about 11 pounds per square inch (psi) is relatively low when compared to some other materials, but likely sufficient to support the fresco absent adverse exposure. Of interest was whether the bond quality prior to construction vibration exposure could be quantified. The friable arriccio coupled with copious voids and shrinkage cracking indicate the arriccio mixing and application were flawed at the time of installation.

Given the ineffective bond of the arriccio, the fresco lamina was sensitive to differential movement, especially differential in-plane movement. In this case, the most adverse response to blasting for the plaster-masonry assembly would be out-of plane deflections. It is recognized that an elevated mass, such as the masonry wall, would potentially experience amplified displacements as compared to ground movement. Nonetheless, significant blasting activity, yielding much higher PPV response than actually recorded would be required to induce structural damage in the masonry wall. By all accounts, the south wall of the church was absent distress, as was the interior gypsum plaster substrate. A well-bonded plaster will be unlikely to crack under nominal blasting influence when founded on a stiff wall. On the other hand, research by Dowding (2003) has shown that stresses associated with weather fluctuations and normal structure use can be more distressing on interior finishes. For instance, Dowding illustrates in one instance that measured (not estimated) crack displacement associated with a measured 0.75 ips PPV blast was much less than the measured displacement associated with a weather front. In fact, the weather front induced wall crack displacement 3.5 times that of the blast.

Lime plaster, gypsum plaster, and brick all have differing coefficients of thermal expansion. The brick wall is partially exposed to direct sunlight under a southerly exposure, and interior temperatures naturally fluctuate depending on environment and usage. These conditions set up considerable stresses associated with temperature swings. Consider the coefficient of thermal expansion, α, for different materials. One set of published values (Richardson 2001) lists clay brick at 5-8 x 10^{-6}/°C and gypsum plaster 10-12 x 10^{-6}/°C. All things equal, the plaster can expand two times the brick for each degree of temperature change. The difference between the brick and plaster could be as much as 7 x 10^{-6}/°C, or 0.000007 cm/cm·°C, indicating potential for significant differential strain. Now, consider a realistic 20°C change in temperature for the plaster over a section of wall 3 meters (9.8 feet) long. Using the lower limit, the change in length would be (Δ = 0.000010 cm/cm·°C x 20°C x 300 cm =) 0.06 cm (0.024 in). This movement exceeds the displacements, either measured or computed by reasonable analysis, by whole multiples. This crude exercise illustrates the improbability that speculative displacements were of any greater influence than normal environmental exposure. A similar exercise regarding changes in humidity can be undertaken. Oriard adapted data from research by Stagg, et al (1984) to illustrate how everyday activities can be compared to blasting. In that effort, it is indicated that jumping in a room can produce nearly 1.0 ips in a wall, slamming a

sliding door can generate about 1.3 ips, and driving a picture nail can generate about 2.0 ips (Oriard 2003). These comparisons illustrate how normal activities induce vibration in a structure. That research applied mainly to residential structures and, although extrapolation might not be appropriate, further illustrates that human activity can be significant. Accordingly, it could be said that the construction vibration induced no greater stress in the fresco assembly than did other nearby activities, city traffic, occupant usage, and environmental exposure.

In blasting cases, reference is often made to the Z-curve developed in earlier extensive blasting research by the US Bureau of Mines (Siskind 1980). This curve evolved out of studies into threshold damage and has been adopted by many federal, state, and local governments as a benchmark for acceptable blasting vibration. The curve limits the amount of vibration in ips for given frequencies (Hz). The 0.75 ips and 0.5 ips limits for drywall and plaster, respectively, at lower frequencies, are considered the point at which cosmetic damage could occur. The limits are based on a relatively high percentage confidence line. Generally, in newer construction, the limits need to be exceeded significantly before damage would be expected. Consequently, the limits do not truly apply in this case. First, the lower limit was based on residential lath and plaster construction, uniquely different from plaster on brick. Second, the threshold is for *older* plaster. The failure occurred when the fresco was a young age of thirteen years. Further, the fresco delamination is inconsistent with damage expected from the blasting activity experienced.

One last influence considered was moisture. The staining on the gypsum substrate near the wall apex was indicative of moisture intrusion. The presence of the discoloration on the gypsum surface indicates the fresco was detached from the substrate in that location. Moisture causes degradation in installations such as this and it would most likely disrupt the already insufficient bond between the arriccio and gypsum layers.

CONCLUSIONS

It was concluded through this investigation that:

1) Distress (bond failure) in the fresco predated the blasting activity.
2) Construction vibrations were beyond generally accepted limits in one or more instances, but they were insufficient to cause widespread delamination of typical plaster work.
3) Environmental conditions and normal exposure would likely induce stresses at or above those associated with the construction vibrations experienced.
4) The original mixing and application of the arriccio by the artist was defective.

The notion that the construction vibration greatly aggravated the weakened installation is likely accurate given the unstable condition present at the time surrounding construction took place. Ultimately, the cause of the fresco failure was defective installation, including the improper preparation and application of

materials, which resulted in imminent collapse. The collapse was simply the manifestation of an aged bond failure, a condition that predated construction activity.

REFERENCES

1. Wet Wall Tattoos, Ben Long and the Art of Fresco, Richard Maschal, John F. Blair, Publisher, 1993.
2. The Effects of Vibration and Environmental Forces, Lewis Oriard, ISEE, 1999.
3. Structure Response and Damage Produced by Ground Vibration from Surface Mine Blasting, Report of Investigation 8507 (RI8507), D.E. Siskind, M.S. Stagg, J.W. Kopp, C.H. Dowding, U.S. Bureau of Mines, 1980.
4. Micro-Meter Measurement of Cracks to Compare Blast and Environmental Effects. Charles H Dowding, Micheal Louis, 2003.
5. Defects and Deterioration in Buildings, 2nd Ed., Barry A. Richardson, Taylor & Francis, 2001.
6. An Empirical Study of Factors Influencing Lime Slaking, Part II: Lime Constituents & Water Composition, J.H. Potgieter, S.S. Potgieter and D. de Waal, 2003.
7. An Overview of Lime Slaking and Factors that Affect the Process, Mohamad Hassibi, 1999.
8. Cements, Limes and Plasters, 2nd Ed., Edwin C. Eckel, John Wiley & Sons, 1922.

Failures of Roofs under Snow Load: Causes and Reliability Analysis

M. Holicky[1] and Miroslav Sykora[2]

[1]Prof. Dr., Department of Structural Reliability, Klokner Institute, Czech Technical University in Prague, Solinova 7, 16608 Prague 6, Czech Republic; PH (+420) 224353842; FAX (+420) 224355232; e-mail: holicky@klok.cvut.cz
[2]Dr., Department of Structural Reliability, Klokner Institute, Czech Technical University in Prague, Solinova 7, 16608 Prague 6, Czech Republic; PH (+420) 224353850; FAX (+420) 224355232; e-mail: sykora@klok.cvut.cz

ABSTRACT

Collapses of a number of roofs in Europe during the winter 2005/2006 initiated discussions concerning reliability of the roofs exposed to snow loads. Presented overview of extensive investigations of structural failures is focused on causes and consequences of failures. Main observed causes may be subdivided into human errors and insufficient code provisions. Collapses developed from local failures particularly in cases of insufficiently robust structures. Probabilistic reliability analysis reveals that the model for snow loads in the Eurocodes should be modified. Obtained experiences provide valuable background information for future revision of current standards and for forensic assessments of failures of structures exposed to snow loads.

INTRODUCTION

Number of roofs collapsed during the winter period 2005/2006 in European countries such as Austria, Czech Republic, Germany and Poland. Forensic assessments of damaged structures were intended to answer the following questions:

- What were main causes of structural failures?
- Were observed snow loads exceptional?
- Is the reliability of structures designed according to standards sufficient?

Presented overview of extensive investigations of structural failures in the Czech Republic is focused on main causes and consequences of failures. Insufficient code provisions, identified as the cause common for most of damaged structures, are analysed in detail using probabilistic methods. Recommendations for design and assessment of structures exposed to snow loads are proposed.

CAUSES OF STRUCTURAL FAILURES

In total 249 structures mostly in highlands and lowlands in the Czech Republic were investigated, taking into account information provided by Police of the Czech Republic and the Fire Rescue Service of the Czech Republic. The structures were classified as follows:

1. Agricultural structures and other buildings where people usually do not enter (99 damaged structures),
2. Residential houses (68),
3. Industrial buildings (49),
4. Public buildings and other buildings where people gather (33).

Failures of timber roofs were observed in most cases while a lower number of the cases comprised steel roofs. In the latter cases, however, consequences of failures were more severe. In most cases buildings had pre-failure insufficiencies.

Main observed causes of structural damage were subdivided into human errors in design, during execution and use, and insufficient code provisions as indicated in Figure 1. These causes are briefly described in the following. More detailed description is provided in the report by Kucera (2006) and in the special issue of the journal Konstrukce (Structures), Cieslar (2006).

Errors in design

It was observed that gross errors in design such as inconsistencies with code provisions, incorrect loading widths, and numerical errors were less frequent. However, they may have had more severe consequences including the total collapse. Other design errors contributed to a lower extent. These included incorrect models for foundation conditions, local buckling of massive frames braced by insufficiently stiff roofs, torsional buckling, and low resistance of joints.

Errors during execution

Errors during execution (mostly use of low-quality materials for timber structures and inappropriate details) were observed in some cases. It was concluded that such errors had not been identified due to an inadequate quality control of design and execution.

Errors during use

The most frequent errors occurred during use. In particular incompetent interventions into structures (removal or reduction of sectional areas of structural members, new structural members) or installation of new facilities (suspended ceilings, air conditioning etc.) caused unexpected stresses in a structure and contributed to failures. Other errors during use included upgrades of structures without reliability assessment and lack of regards to experts' recommendations for strengthening. In some cases insufficient maintenance together with inappropriate details such as roof parapets with inside drainage yielded accumulation of water on a roof and caused an additional load unexpected in design. Snow load exceeding design assumptions was observed on roofs where snow was required to be removed.

Insufficient code provisions

Insufficient code provisions seem to be the most common cause of structural damage. Use of light-weight roof structures increases significance of snow load and an insufficient reliability level may be obtained by the partial safety factor design as indicated by the probabilistic reliability analysis described below.

In several cases a model for snow loads recommended in standards underestimated actual loads. Use of high-quality materials for heat insulation of roofs

protected snow from melting and caused its accumulation (often non-uniform). In several cases a significant load due to the combination of snow and ice on roofs, not considered in design codes, was observed. In few cases snow load was also present on roofs with a great angle of pitch.

In many cases multiple causes such as combination of the errors were observed. The causal network indicating the main identified causes and consequences is shown in Figure 1. Note that available information does not make possible to provide better statistics on the collapsed buildings, more discussion of the causes and their combinations.

CONSEQUENCES OF STRUCTURAL FAILURES

Four levels of damage were distinguished:

- Excessive deflection,
- Failure of a member or few members,
- Partial collapse (up to half of the roof or structure),
- Total collapse (more than half of the roof or structure) – see Figure 2.

In the causal network in Figure 1, the top two levels may represent local failure while the other two collapse. Remarkably, about 60 % of described failures were classified as total collapses and approximately 75 % as the partial or total collapse.

Collapsed structures had mostly insufficient robustness (no tying, low resistance of key members or inappropriate structural detailing). Apparently, robustness is a key property affecting development of collapse from a local failure. That is why the influence of robustness is included in Figure 1. Lack of robustness became important particularly in cases of multiple causes of failure.

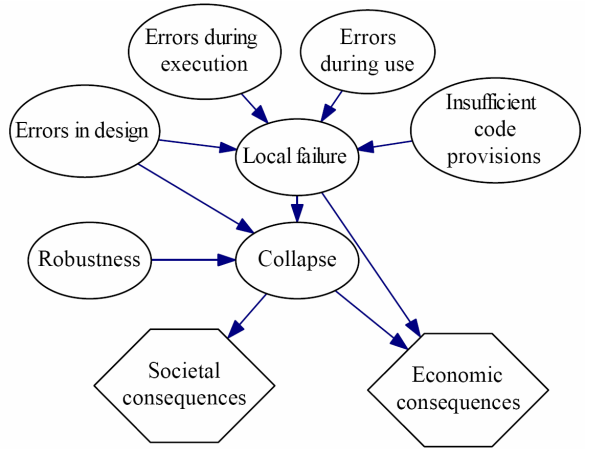

Figure 1. Causes and consequences of structural failures.

Figure 2. Collapse of a stadium.

Recent discussions have indicated that robustness is a complicated concept and is not understood uniformly within engineering society. In accordance with EN 1991-1-7 (2006), robustness is here understood as *the ability of a structure to withstand events like fire, explosions, impact or the consequences of human error, without being damaged to an extent disproportionate to the original cause*. At present robustness is investigated by researchers from more than 20 European countries within the COST Action TU0601, Faber et al. (2008).

Consequences were qualitatively classified by structural engineers as negligible, low, medium and severe. Two fatalities and one injury were reported. Frequency of the levels of damage for the different types of structures and consequences are indicated in Table 1.

The data in Table 1 may be used as the first estimate of the expected consequences related to a specific type of structure, given local failure/collapse. This may be utilized in risk assessments of structures exposed to snow loads. However, it is emphasized that the information in Table 1 is derived from a limited amount of data and should be considered as indicative only.

DETAILED ANALYSIS OF INSUFFICIENT CODE PROVISIONS

Since the insufficient code provisions were identified as the cause common to most of damaged structures, attempts were made to improve snow load models in design codes. In some European countries including the Czech Republic available measurements of snow loads have been newly evaluated and relevant standards such as National Annexes to EN 1991-1-3 (2003) promptly revised. The following probabilistic reliability analysis is aimed to verify whether the changes in standards guarantee a sufficient reliability of roofs exposed to snow loads.

Statistical evaluation of annual maxima of snow load on the ground

The Czech Republic as well as numerous other regions where roofs collapsed has continental climate. Snow load may increase until late winter or early spring. Drifts of snow may be important.

Table 1. Frequency of the levels of damage for the different types of structures and estimates of consequences.

Class of Structure	Excess. deflect.	Member failure	Partial collapse	Total collapse
1. Agricultural structures	10 %	5 %	20 %	65 %
2. Residential houses	0 %	15 %	20 %	65 %
3. Industrial buildings	10 %	20 %	15 %	55 %
4. Public buildings	5 %	50 %	15 %	30 %

□ negligible consequences, ▫ low consequences, ▪ medium consequences, ■ severe consequences.

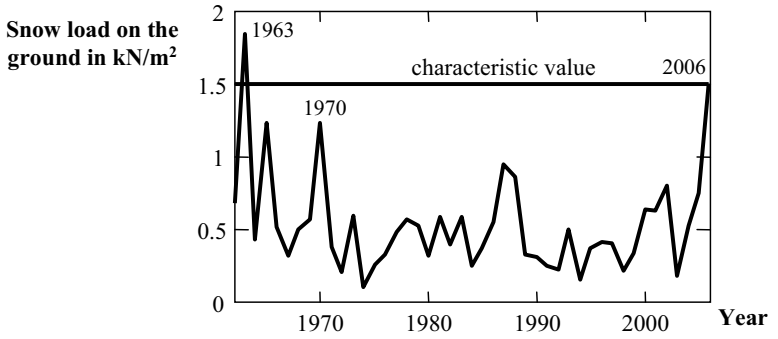

Figure 3. Annual maxima of snow load on the ground in Humpolec.

Annual maxima of snow load on the ground measured by the Czech Hydrometeorological Institute were analysed in detail. Four locations in the Czech Republic were selected. Three of them are in lowlands, close to large cities where a considerable number of new structures is constructed each year. The fourth one is in highlands (altitude 550 m) at the town of Humpolec where the ice-hockey stadium shown in Figure 2 collapsed under snow in 2006. Note that investigations of the stadium collapse were described in detail by Drdacky (2009). The time series of available measurements from Humpolec is indicated in Figure 3.

Point estimates of sample characteristics are estimated by the classical method of moments for which prior information on the type of an underlying distribution is not needed. It follows that means and standard deviations are different for various locations. The coefficient of variation varies within the narrow range from 0.65 to 0.7 while skewness varies between 1.0 and 2.0. However, the sizes of available samples (40-50) may be rather small to estimate credibly skewness.

The sample characteristics indicate that the annual maxima might be described by a two-parameter lognormal distribution having the lower bound at the origin (LN0) or by a more general three-parameter shifted lognormal distribution having the lower bound different from zero (LN). Other possible theoretical models are extreme value distributions: the type II called also the Fréchet distribution (Fre)

or type I, a popular Gumbel distribution (Gum). Gamma distribution (Gam) is also considered.

Probability density functions of the considered theoretical models and a sample histogram are shown in Figure 4 for the measurements from Humpolec. To compare goodness of fit of the considered distributions, Kolmogorov-Smirnov and chi-square tests are applied. It appears that the lognormal distribution LN0 is the most suitable model. However, favourable test results are obtained also for the other models.

Appropriate models should be selected on the basis of the statistical tests considering general experience with distributions of annual maxima. It is often assumed that the Gumbel distribution might be a suitable model, ISO 4355 (1994) and Soukhov (1998). Therefore, this distribution is considered hereafter although its constant skewness 1.14 is in most cases lower than the sample skewness.

Theoretical characteristic values of the snow load on the ground are further determined as the 0.98 fractile of the Gumbel distribution with the sample mean and standard deviation. The obtained values are in a good agreement with those provided in the National Annex to EN 1991-1-3 (2003). More specifically, the fractiles of the theoretical model are mostly by about 5 % lower than the characteristic values in the Eurocode.

In two of the considered locations, the snow loads recorded in 2006 slightly exceeded the characteristic values given in EN 1991-1-3 (2003). In view of this, the snow loads observed in 2006 may hardly be considered as “extreme” or “exceptional”.

It should be mentioned that the submitted analysis is based on annual maxima determined from weekly measurements. Several methods have been proposed to estimate daily snow loads from weekly measurements. The detailed analysis conducted by Sadovsky et al. (2008) indicates that the theoretical characteristic value may be increased by about 5 % when daily values are taken into account. Moreover, it appears that trends of snow loads may often be neglected.

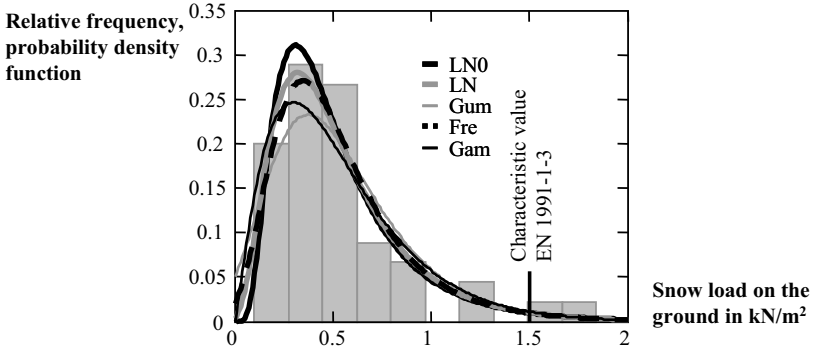

Figure 4. Histogram of the annual maxima and the selected theoretical models.

Reliability analysis

It is further assumed that a considered structure is designed in accordance with the principles of the present suite of the Eurocodes, EN 1990 (2002), EN 1991-1-1 (2003) and EN 1991-1-3 (2003). The characteristic load on the roof is determined as the product of the shape factor μ (for horizontal roofs equal to 0.8); exposure factor C_e; thermal factor C_t and characteristic value of the snow load on the ground s_k given in a snow map. The exposure and thermal factors are usually considered as unity, EN 1991-1-3 (2003), and hence are omitted hereafter.

Steel structural members are further considered only. Design of a member exposed to a permanent load G and snow load S can be based on the partial factor method described in EN 1990 (2002). Using the fundamental load combination (6.10), the design value of a generic resistance R of the member is determined from:

$$r_k / \gamma_{M0} = \gamma_G g_k + \gamma_Q s_{s,k} \quad (1)$$

where r_k is the characteristic value of resistance; γ_{M0} partial factor for resistance of a cross-section; γ_G partial factor for the permanent load; g_k characteristic value of the permanent load (equal to the mean value); γ_Q partial factor for the snow load; and $s_{s,k}$ snow load on the roof.

When structural members are not susceptible to stability phenomena, the partial factor for resistance is considered by the value 1.0 as recommended in EN 1993-1-1 (2005). Assuming unfavourable effects of the actions, the partial factor for the permanent load is 1.35 and for the snow load 1.5, EN 1990 (2002).

In the following effect of a load ratio on the reliability of structural members is analysed. The load ratio is defined as the characteristic value of the snow load on the roof over the total characteristic load:

$$\chi = s_{s,k} / (g_k + s_{s,k}) \quad (2)$$

For roofs, the realistic range of the load ratio may be from 0.4 up to 0.8. For a given load ratio and characteristic snow load on the roof, the characteristic permanent load follows from relationship (3):

$$g_k = s_{s,k} (1 - \chi) / \chi \quad (3)$$

Reliability of generic steel members is further analysed by probabilistic methods. The limit state function is written as follows:

$$g(\mathbf{X}) = K_R R - K_E (G + \mu S_{50}) \quad (4)$$

Table 2. Models for basic variables.

Variable	Symb.	Dist.	Partial fac.	X_k	μ_X	V_X
Resistance	R	LN0	1.0	Eq. (1)	$r_k e^{2V_R}$	0.08
Permanent load	G	Norm.	1.35	Eq. (3)	g_k	0.10
Shape coefficient	μ	Norm.	-	0.8	0.8	0.15
Snow on ground	S_{50}	Gum	1.5	s_k	$\approx s_k$	0.22
Resistance unc.	K_R	LN0	-	-	1.15	0.05
Load effect unc.	K_E	LN0	-	-	1.0	0.10

where K_R denotes model uncertainties in structural resistance; K_E model uncertainties in load effect and S_{50} are 50-year maxima of the snow load on the ground (corresponding to the design working life 50 years indicated in EN 1990 (2002) for building structures and other common structures). Models for the basic variables accepted from Holicky and Sykora (2008) are described in Table 2.

In the reliability analysis, the probability of failure and corresponding reliability index are determined:

$$P_f = P[g(\mathbf{X}) < 0]; \quad \beta = -\Phi^{-1}(P_f) \tag{5}$$

where $g(\mathbf{X}) < 0$ denotes failure; and Φ^{-1} is the inverse cumulative distribution function of the standardised normal distribution. The FORM method proposed by Hasofer and Lind (1974) is applied to estimate the indicators of a reliability level. Results of the reliability analysis are shown in Figure 5.

It follows from Figure 5 that the recommended values of the partial factors lead to a significant variation of the reliability index for all the considered locations. Moreover, for the considered range of the load ratio 0.4 – 0.8 the index decreases below the target value 3.8 recommended in EN 1990 (2002) and the reliability of a structural member seems to be insufficient. Recent study by Holicky and Sykora (2008) indicates that the partial factor for the snow load should be significantly increased.

It is, however, emphasized that generalization of these findings may be rather difficult. The resulting reliability is considerably dependent on the model uncertainties, which may differ for various types of members or structures under consideration. In addition variability of the snow load effect is significantly increased by uncertainties of the shape coefficient. The recent report by CEN/TC250 and JRC (2009) indicates that further research on the shape coefficient is desired.

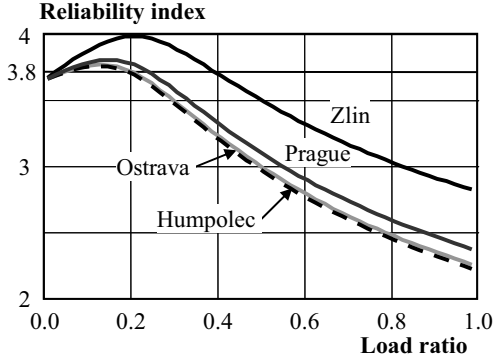

Figure 5. Variation of the reliability index with the load ratio.

CONCLUSIONS AND RECOMMENDATIONS FOR DESIGN

Presented experience gained within investigations of failures of roofs under snow load and analysis of their causes provides valuable background information for future forensic assessments. It is indicated that:

- The main observed causes of structural damage may be subdivided into errors in design, during execution and use, and insufficient code provisions.
- Collapses developed from local failures particularly in cases of insufficiently robust structures.
- In some locations snow loads recorded in 2006 slightly exceeded the characteristic values given in standards and thus may hardly be considered as "exceptional".
- Gumbel distribution is a suitable theoretical model for the annual maxima of snow loads on the ground.
- Reliability of roofs designed in accordance with the present suite of the Eurocodes is lower than the target level recommended in EN 1990 (2002).
- In the Czech Republic, characteristic values of the snow load on the ground well correspond to those derived from the theoretical model. However, the recommended values of the partial safety factor should be differentiated and in case of light-weight roofs increased.

It is emphasized that the presented results are significantly dependent on the assumed models for basic variables and should be considered as informative only.

Note that proper code provisions alone do not prevent collapses. Systematic quality control of design and execution needs to be applied.

In addition robustness aspects should be considered to reduce possible damage due to snow loads. Sufficient robustness may be achieved by an adequate system of ties, increased resistance of key members, secondary protection of key members and by appropriate structural detailing.

ACKNOWLEDGEMENTS

This study has been conducted at the Klokner Institute, Czech Technical University in Prague, Czech Republic, within the framework of the research project COST OC08059 Assessment of structural robustness supported by the Ministry of Education, Youth and Sports of the Czech Republic. Achievements of the COST Action TU0601 Robustness of structures have been utilized. Comments and suggestions of a reviewer that have considerably improved the paper are appreciated.

REFERENCES

CEN/TC 250 Structural Eurocodes & JRC (Joint Research Centre) (2009). *The Eurocodes and the construction industry (medium-term strategy 2008 – 2013),* Report, January 2009.

Cieslar, S. (2006). "Mimoradna priloha cisla 2/2006 Havarie strech – nazory odborniku (in Czech - special annex of No. 2/2006 Collapses of roofs – views of experts)", *Konstrukce (Structures),* 2006(2), 1-16.

Drdacky, M. (2009). "Lessons from the failure of a steel-structure ice-hockey hall under a snow load", Forensic Engineering: From failure to understanding, Proc. Fourth Int. Conf. on Forensic Engineering, Thomas Telford, London.

EN 1990 (2002). *EN 1990:2002 Eurocode - Basis of structural design,* CEN.

EN 1991-1-1 (2003). *Eurocode 1: Actions on structures - Part 1-1: General actions; Densities, self-weight, imposed loads for buildings,* CEN.

EN 1991-1-3 (2003). *Eurocode 1: Actions on structures - Part 1-3: General actions; Snow loads,* CEN.

EN 1991-1-7 (2006). *Eurocode 1: Actions on structures – Part 1-7: General actions – Accidental actions,* CEN.

EN 1993-1-1 (2005). *Eurocode 3: Design of steel structures - Part 1-1: General rules and rules for buildings,* CEN.

Faber, M. H. et al. (2008). *Proceedings of the 1st Workshop of the Action TU0601 Robustness of Structures,* Reprozentrale ETH Hönggerberg, Zurich.

Hasofer, A. M. and Lind, N. C. (1974). "An Exact and Invariant First Order Reliability Format", *J Engrg Mech Div (ASCE),* 100(EM1), 111-121.

Holicky, M. and Sykora, M. (2008). "Safety of lightweight steel roofs exposed to snow load", Proc. EUROSTEEL 2008, ECCS Southampton, Brussels.

ISO 4355 (1994). *Basis for design of structures - Determination of snow loads on roofs,* ISO.

Kucera, V. (2006). *Zprava c. 010-019840, Cast I. Analyza pricin havarii stresnich konstrukci v zimnim obdobi 2005 – 2006 (in Czech - Report No. 010-019840, Part I. Analysis of Causes of Roof Failures in the Winter 2005 – 2006),* Ministry of Industry and Trade of the Czech Republic.

Sadovsky, Z. et al. (2008). "Special features of the collection and analysis of snow loads", Proc. ESREL 2008, Taylor & Francis, London.

Soukhov, D. (1998). "The Probability Distribution Function for Snow Load in Germany", *LACER,* 1998(3), 263-274.

Analysis of an 1864 Long-Span Truss Roof

Donald Friedman, P.E., M. ASCE[1]

[1]Old Structures Engineering, PC, 260 West 35th Street, New York, NY 10001;
PH (212) 244-4546; FAX (917) 591-2189; email: df@OldStructures.com

Abstract
Philadelphia's Wagner Institute has a long-span roof completed in 1864, consisting of wood-and-iron arched trusses supporting wood purlins. The plaster ceiling below the roof is extensively cracked, and gaps in truss joints are present in some locations. The truss structure that supports the roof can be analyzed in several different ways, and this ambiguity makes interpretation of the signs of damage difficult. This paper includes a review of the possible mechanisms that could have been used at the time of construction incorporating the visible materials, including various forms of truss and tied arch. This review provided the key to analysis and interpretation of the damage.

Introduction

In any era, cutting-edge technology may be more difficult to understand than ordinary work. New technology of the past may have been a dead end that bears little relation to modern forms. This paper will use the long-span roof at the Wagner Free Institute in Philadelphia to illustrate the difficulty in analyzing structural technology that was advanced for its time and now obsolete.

Wagner's 1864 main building houses a natural-history museum. The three-story high exhibition hall at the second floor of the building is covered by a single-span roof that is a "balloon shed," or arched-truss roof. The roof form is a shallow segmental barrel vault supported by exposed trusses. These roofs were often used in the nineteenth century for railroad stations and armories; early examples in the United States include the 1866 Cleveland Union Depot, and the 1871 Grand Central Station and 1879 Seventh Regiment Armory in New York. Unlike these buildings, the Wagner roof arches begin four stories in the air, not at grade, and rest on relatively thin walls. This roof was built while structural analysis was still in its infancy. The first practical American treatise on analysis, Squire Whipple's *A Work on Bridge Building*, was published in 1847, and structural engineering was still rare in building design when Wagner was built 17 years later. (Whipple 1847; Condit 1960, 113-115, 208-210)

Minor but pervasive damage – cracks in the plaster ceiling below the purlins between the arched trusses, cracks in the fourth-floor wall plaster, and open splice joints in the

truss lower chords – were investigated as part of a structural analysis of the roof. Various possible mechanisms for carrying load were examined, including the trusses working as tied arches, the truss top chord working as tied arches with the lower chords and web braces acting only as local stiffening, the ceiling plaster and/or roof deck acting as tied vaults, and the trusses acting as beam-trusses, not dependent on arching action. The analysis showed that the method by which the trusses function depending on the amount of load: under dead load only, the top chord is a sufficient arch to carry the load, while under full snow load the bottom chord is also required.

The original designers worked with a new structural form, but neglected issues that affect load distribution such as wood creep, elongation of the tie rods, wall rotation, and looseness in the connections. These issues had to be accounted for to perform an analysis accurate to current standards. In short, the technology of the 1860s provided a lasting roof, but one that does not work in the way that the builders intended.

General Description of Structure

The main building of the Wagner Institute has a mixed structural system, including brick exterior bearing walls, interior cast-iron columns, and wood-joist floors. The building has four nominal floors: office and theater space at the ground floor, the main museum floor above, and two partial gallery floors at the top. The barrel-vaulted roof spans the full width of the building (18.3 m out to out) and consists of a waterproofing membrane over a wood deck, wood purlins (spanning perpendicular to the vault curve), and a plaster ceiling on wood lath. The obvious structural support for the roof is a set of eight arched trusses which are located below the roof so that the truss top chords are just barely embedded in the plaster. (See Figures 1, 2, and 3.)

Figure 1: Overall view of the main museum space, showing the 2nd floor, the 3rd and 4th floor galleries, and the arched trusses. (n.a. 2000)

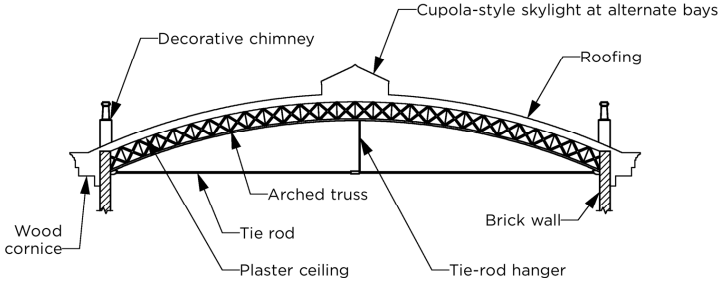

Figure 2: Roof Section, Visible Structure

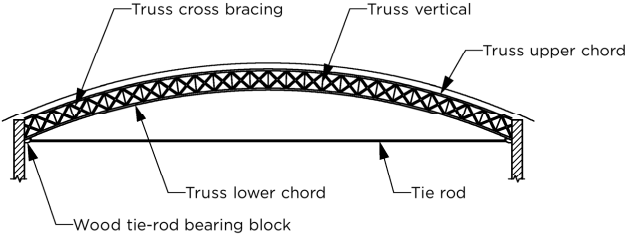

Figure 3: Roof Section, Major Structure

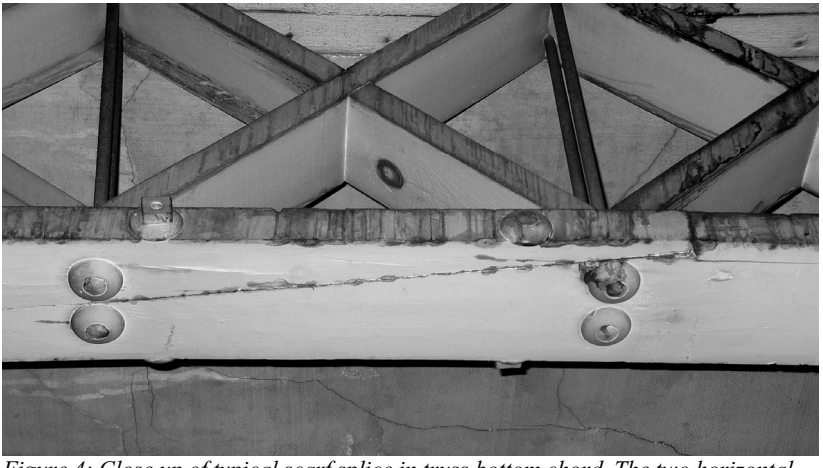

Figure 4: Close up of typical scarf splice in truss bottom chord. The two horizontal bolts tie the splice; two pairs of vertical rods and their bolted ends are visible.

Figure 5: Typical lower-chord connection.

Figure 6: Truss end connection, with lower chord bird's-mouthed to bearing block.

The trusses fairly represent ordinary building technology of the mid-1800s. The top and bottom chords each consist of a single wood member with one scarf-type splice. (See Figure 4.) At the splices, each half of the chord is tapered in width and

connected to the other half by three horizontal bolts. The wood cross-bracing within each truss panel is not positively connected to the chords but simply bears on prismatic wood blocks. The wrought-iron "verticals" that run perpendicular to the chords and define the truss panels are simply bolted through the bearing blocks and chords. (See Figure 5.) In other words, the verticals are capable of resisting tension but no compression, and the braces are capable of resisting compression but no tension. Finally, the wrought-iron tie rod at each truss passes through wood bearing blocks at each end to plate washers. The bottom chord is fastened into the end bearing block with a birds-mouth cut. (See Figure 6.) The wood deck and ceiling lath are through-nailed to purlins. The purlins rest on top of the trusses, so most of the purlin-to-truss connections are simple bearing with toe-nails; four connections per truss are reinforced with vertical bolts through the purlins and truss top chord.

Conditions Observed

Several patterns of damage were visible at the roof, but no gross deformation or deterioration of structural material. The most obvious damage was the presence of numerous cracks across the plaster ceiling, typically parallel or perpendicular to the vault and spaced at approximately 0.9 to 1.5 m on center. There was little separation or out-of-plane movement at the cracks in the ceiling; the only cracks observed with significant movement were similar vertical cracks in the side-wall plaster.

The side walls were out of plumb, with their tops tilted away from the interior. The tilt varied from zero to roughly 100 mm. There is no corresponding damage to the stucco on the exterior face of the walls; in most cases there was no difference between the interior plaster damage at the most-tilted and least-tilted areas.

Two forms of truss movement were observed: lateral sway and open joints. The first is sideways movement of the bottom chords accompanied by out-of-plane tilting of the cross-braces and verticals. The upper chords are restrained against lateral sway by their embedment in the plaster ceiling and the bolted purlins, while the remainder of the truss is free to move laterally. The lower-chord movements were in the form of a single or a double "S" curve along the chord length, up to roughly 75 mm sideways. Open joints were observed at the lower-chord splices, with up to 10 mm separations. No similar separation was observed in the upper-chord splices. Finally, as many as one-third of the cross-brace to bearing-block joints showed separation up to 6 mm.

Much of the information gained by probing was negatively useful, in that expected damage was not found. For example, even though the decorative wood cornice was in poor condition, with numerous repairs and rotted areas, truss ends exposed through probing were in good condition, apparently protected by the continuous main roof directly above. No splitting or crushing was seen at the truss end probes or the center top chord probe. Old weathering damage (deteriorated mortar) and repairs to the brick, including rebuilding and repointing, were observed at some locations. Given that the interior finish was observed to be wet-applied plaster over wood and expanded-metal lath, the repairs were probably made between the 1880s and 1930s.

Analysis

Because the roof was built before accurate truss and arch analysis methods were well known and because the vertical and bracing connections only allow force transfer in one direction, the trusses were likely were not designed in the current sense. Modern structural analysis of the roof encompassed both the expected structural mechanism (the trusses working as tied arches) and alternates. While the analysis showed that the alternates could not work, they help explain some of the damage noted.

The dead load of the roof, including the wood structure, plaster ceiling, and waterproofing, totals 1.2 kPa. Using the standard ASCE 7, *Minimum Design Loads for Buildings and Other Structures* (n.a. 2005), the maximum snow load is 1.1 kPa and the maximum wind pressure 0.48 kPa downward or 0.72 kPa upwards. Since the maximum downward wind pressure will not act simultaneously with the maximum snow load (the sloped roof and lack of parapets allow snow to drift entirely off of the building during high winds) and the wind uplift is less than the dead weight of the roof, the governing load combination is the sum of the dead and snow loads. The analyses below were performed for both this combination and for dead load only.

Mechanism 1: Tied Arch A (Figure 7)

The roof was analyzed with the purlins as simple-span truss-to-truss beams and the trusses as arches consisting of the top chords only.

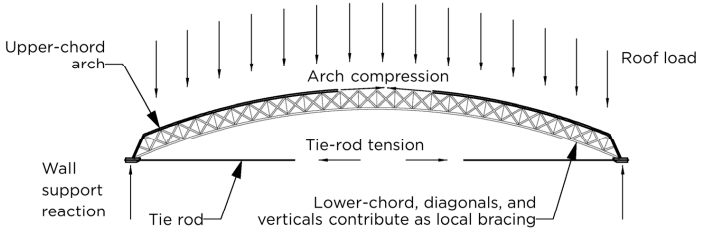

Figure 7: Tied Arch A Structural Model

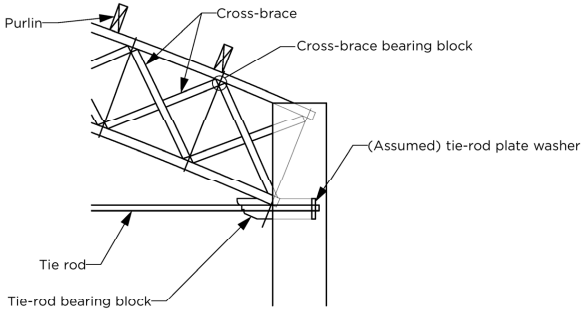

Figure 8: Truss End Detail

The tie rods were modeled as ending in plate washers that cover the rear of the end bearing blocks; later investigation confirmed the plate washers' existence. (See Figure 8) In this scenario, the truss verticals, cross-bracing, and lower chord serve only as local stiffeners to prevent small areas of unbalanced load from creating significant bending in the top chord arch. Under dead load only, this analysis provided acceptable results in terms of stress. The tie rods would lengthen approximately 10 mm under dead load and 19 mm under full load. Under full dead and snow load, the top chord would be overstressed in compression. Under a 16C temperature change, the truss center moves vertically roughly 6 mm. Under wind load from the side or unbalanced snow load caused by a combination of wind and snow, the arches could deflect asymmetrically as much as 40 mm. All of these movements would contribute to the ceiling cracks observed.

Because the loaded tie rods elongate and the masonry walls are too weak to resist the arch thrust, the walls would move outward as the roof was completed and the dead load increased from zero to its maximum. The truss ends, embedded in the masonry walls, are wood tie-rod bearing blocks. As the trusses were originally loaded, the tie rods would stretch, allowing the horizontal reaction caused by the arch form to push apart the bearing blocks. This reaction, transferred from the bearing blocks to the surrounding masonry, and applied more than 2 m above the upper gallery floor, would cause outward rotation of the walls. Any tie-rod slack or looseness in the end connections would cause similar outward rotation. When significant snowfall increased the truss loads, the tie rods would temporarily lengthen, likely causing additional permanent outward tilt. Forced outward rotation of the masonry would crack the mortar joints on the interior face and possibly crush them on the outside face and therefore would tend to be one-way motion. This type of ratchet mechanism, where walls move in only one direction after they have first moved, is common in old and unreinforced masonry. The amount of tilt observed was far less than would be required to create instability in the walls and is therefore not dangerous as long as the masonry condition is maintained.

Mechanism 2: Tied Arch B (Figure 9)

The roof was analyzed in a similar manner to Tied Arch A, but using both the top and bottom chords as compression members. The only different result is that the stresses were within acceptable limits for the combined dead and snow load.

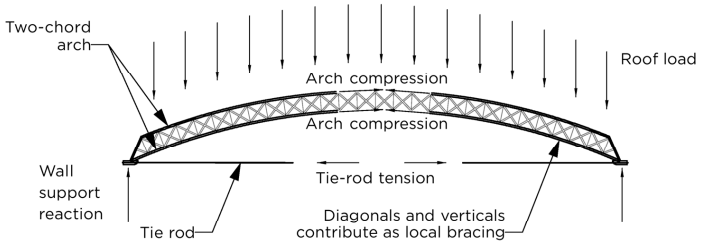

Figure 9: Tied Arch B Structural Model

Mechanism 3: Untied Arch (Figure 10)
This analysis is similar to Tied Arch 1, but neglecting the action of the tie rods to approximate conditions if the rods were installed with their end connections too loose to take up the outward arch thrust. The stresses in the truss itself are the same as in Mechanisms 1 and 2, but the bending stresses in the masonry wall from restraining the thrust are unacceptably high. Using the maximum allowable masonry bending tension, the roof can support less than 2 percent of the combined dead and snow load.

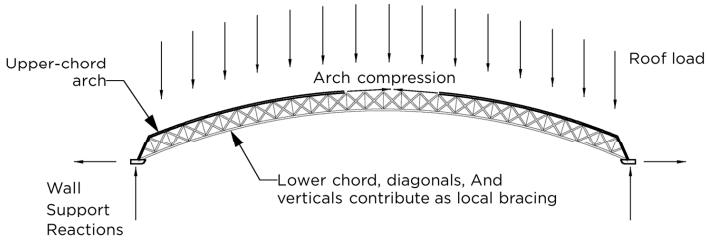

Figure 10: Untied Arch Structural Model

Mechanism 4: Vault A (Figure 11)
The wood plank that makes up the roof surface was analyzed as a vault. Skylights interrupt half of the between-truss vault panels, so this is a combined mechanism, where vault action takes place in the uninterrupted panels and the interrupted panels are carried by the trusses as tied arches. This type of load sharing is common when deflection from load in a primary structural member (in this case, the trusses) allows load to fall onto secondary members (the vaults). The stress in the wood was high, but not necessarily unacceptably so. However, the vaults create end thrust similar to the untied arch and therefore create unacceptably high bending stress in the walls.

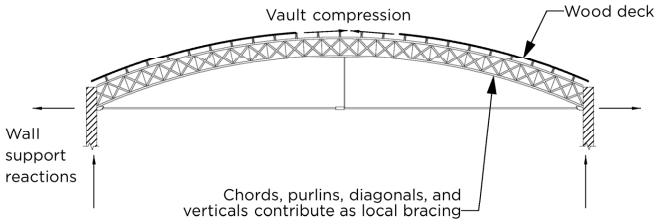

Figure 11: Vault A Structural Model

Mechanism 5: Vault B (Figure 12)
The combination of the wood plank and plaster ceiling was analyzed as a vault, similar to Vault A. The stress in the wood and plaster was acceptable, however the thrust problem is identical. It should also be noted that this mechanism contradicts empirical observation: if the plaster were in compression in half of the panels, there would be little or no cracking in those panels, which is not true.

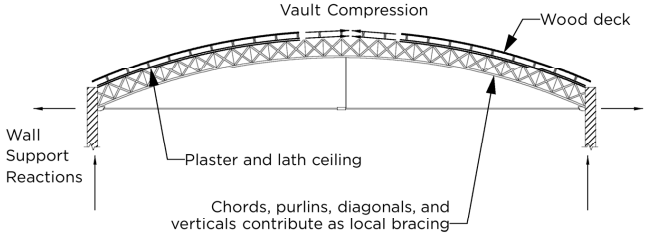

Figure 12: Vault B Structural Model

Mechanism 6: Trussed Beam (Figure 13)
The truss was analyzed working as a double-diagonal truss (ignoring the arch shape). The overall depth of 0.71m is shallow for the span of 18.3m, leading to calculated compressive and tensile stresses in the wood of roughly 34 MPa. This is so far from the allowable stresses in wood that this mechanism cannot be considered realistic.

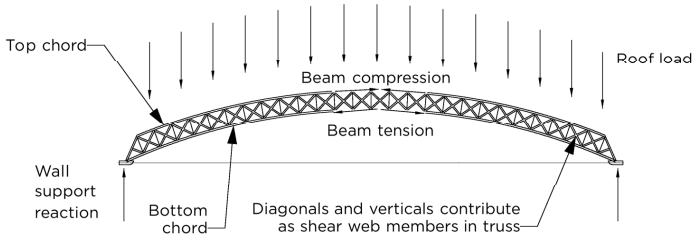

Figure 13: Trussed Beam Structural Model

Conclusions

The roof likely functions in the manner that it appears to, with tied-arch trusses carrying the purlins above. Given the lack of insulation and the open space allowing heat from three floors of radiators to collect at the roof, snow load has likely never reached the code maximum; maximum snow is rare even if the roof is a cold surface. In addition, the absence of parapets means that there are no valleys to collect snow. For most of the building's life, the roof has carried dead load plus small live loads from less-than-maximum wind and snow. It is likely that the ordinary and maximum load-carrying mechanisms are not identical: under ordinary load, the top chord is sufficient as an arch; as load increases during snowfall, the trusses deflect downward and shorten. When the lower chords shorten sufficiently to close the gaps at the splices, the lower chord will begin to carry load as an arch as well, effectively doubling the arch strength and stiffness.

The gaps at the lower-chord splices may represent nothing more threatening than wood shrinkage. Eighteen meters of timber can be expected to shorten 20 mm or more along the grain from drying in service. As the trusses shrank after their installation, the entire arch curve would have lowered, but not all pieces of lumber shrink equally. The difference between the gaps may represent different original rates of shrinkage between the various top and bottom chord pieces. Since the top chord is necessarily loaded in compression at all times, it cannot contain shrinkage gaps.

The upward motion of the roof from expansion on hot days, the downward movement from contraction on cold days and when snow or high winds load the roof, and the distortion caused by asymmetrical loads are sufficient to crack the plaster. Cracks in the wall plaster can be caused by similar thermal movement. The visible cracks by themselves were not dangerous but may be a sign that the portions of plaster keyed through the lath are cracked. The investigation showed no physical evidence or analytical result suggesting structural overstress. The damaged plaster was a life-safety hazard but one caused by natural movement of a long-span roof.

References

Condit, C. (1960). *American Building Art: The Nineteenth Century*, Oxford University Press, New York.

n.a. (2005) *Minimum Design Loads for Buildings and Other Structures, ASCE/SEI 7-05*, ASCE, Reston, VA.

n.a. (2000) Library of Congress, Prints & Photographs Division, HABS PA, 51-PHILA, 751-17

Whipple, S. (1847). *A Work on Bridge Building: Consisting of Two Essays, One Elementary and General, the Other Giving Original Plans and Practical Details for Iron and Wooden Bridges*., H. H. Curtis, Utica, NY.

LOAD DURATION EFFECT ON FAILURE OF AN OVERLOADED WOOD TRUSS STRUCTURE

Behnam Arya, PhD, PE, SECB, AM ASCE[1], Mohsen Kargahi, PhD, PE, SECB, M ASCE[2], and Gary C. Hart, PhD, PE, SECB, M ASCE [3]

[1]Associate, Weidlinger Associates, Inc., 4551 Glencoe Ave. Ste 350, Marina del Rey, CA 90292, PH: (310) 315-8430, FAX: (310) 315-8431, arya@wai.com
[2]Senior Engineer, Weidlinger Associates, Inc., 4551 Glencoe Ave. Ste 350, Marina del Rey, CA 90292, PH: (310) 315-8430, FAX: (310) 315-8431, kargahi@wai.com; and Lecturer, University of Southern California, Los Angeles, CA
[3]Professor Emeritus, Dept of Civil Engineering, University of California, Los Angeles, CA, and Managing Principal, Weidlinger Associates, Inc., 4551 Glencoe Ave. Ste 350, Marina del Rey, CA 90292, PH: (310) 315-8430, FAX: (310) 315-8431, hart@wai.com

ABSTRACT

This paper presents the analysis used to demonstrate how load duration affects the time required to cause failure of overloaded wood structures. A bowstring roof truss of a commercial building partially collapsed two months after remodeling. During remodeling, several industrial HVAC units and a new suspended ceiling were attached to the roof structure. However, failure of the truss did not occur immediately after the introduction of the new loads; it took approximately two months for the truss to collapse. A computer model of the roof trusses was created and a linear-staged analysis was performed. The load duration curve of wood developed by U.S. Forest Product Laboratory was used to determine the time-to-collapse after application of additional loads. The analysis showed it would take approximately two months for the truss to fail. The calculated time-to-failure closely matched the actual time of collapse of the bowstring trusses. Load duration curve shows that when the stress level in a member exceeds 60% of the ultimate strength of wood, failure is imminent.

Keywords: Failure Analysis, Forensic Engineering, Roof Collapse, Building Investigation, Bowstring Truss, Load Duration

INTRODUCTION

Understanding wood properties is essential for analysis and design of wood structures to recognize the limitations and to prevent misapplication of material. Performance of wood is affected by environmental and service conditions such as moisture, temperature, grade, construction, size, and load history. The magnitude of the load that results in failure depends on the duration of the load applied to the member. Structure can support larger load if the load is applied for a short duration of time or it can support smaller load if the load is applied over a long period of time. This paper presents the significance of load duration on the failure of a bowstring roof truss structure through a case study that was conducted in a failure investigation project.

Bowstring trusses are made of curved top chords and straight bottom chords. These trusses had been the dominant roof structural system from the 1940s to 1960s for commercial and industrial buildings. However, due to changes in design practice and some deficiencies of these trusses, the existing bowstring trusses have little or no additional reserve capacity to carry additional loads. Deficiencies of these trusses are discussed in several articles such as Gilham, and McKee (2007), Tigue and Kurt, and Kristie and Johnson (1996). Since the 1960s, load considerations for building roofs have changed to some extent. For instance, snow loads have been increased in some areas of the country. Furthermore, use of computers in recent decades has led to more accurate analysis methods. The methods originally used for analysis of these trusses were mainly graphical force diagrams calculating only axial loads. They did not take into account the continuity of the chords which results in large moments in truss members. Last but not least, allowable timber stresses in the code was changed in the 1960s. By 1968, tensile strength of the wood was significantly reduced by a factor of approximately 0.55. This was due to the inaccuracy of early testing procedures for obtaining wood strength properties that was improved in the 1960s. Therefore, the most common deficiency in early truss designs is inadequate tensile strength. As a consequence, the capacity of truss members in tension would have been 55% less than intended in the design.

The subject building of this paper was built in 1951 as a typical warehouse with dimensions of approximately 238 feet by 246 feet. The building's roof is flat with lightweight wood framing supported on 14 lines of bowstring trusses. There are three bowstring trusses in each truss line which span approximately 80 feet between steel box column supports. Bottom chords of the trusses were strengthened by tension rods. Top chords are partially supported from lateral movement by diagonal wood members (kickers) that connected the top chords to the roof joists. Cripple stud walls were provided on top chords to create the elevated support required for the building's flat roof. Figure 1 shows overall configuration of the roof framing and member sizes.

Over the past several decades, the building's function has changed with new business developments. Consequently, new equipment was installed over and under the roof structure to support new business demands. For instance, several heavy HVAC units had been recently placed on the building's roof to provide air circulation for newly installed sensitive equipment inside the building. Approximately two months after installation of the roof equipment, the bowstring trusses supporting these

units failed causing damage to the building structure. No warning signs were evident within the two-month period prior to the failure.

A failure analysis must consist of two major parts or phases. They are the Observation and Simulation Phases as discussed by Hart et al (2009). The following sections describe the tasks that were performed during these phases for this project.

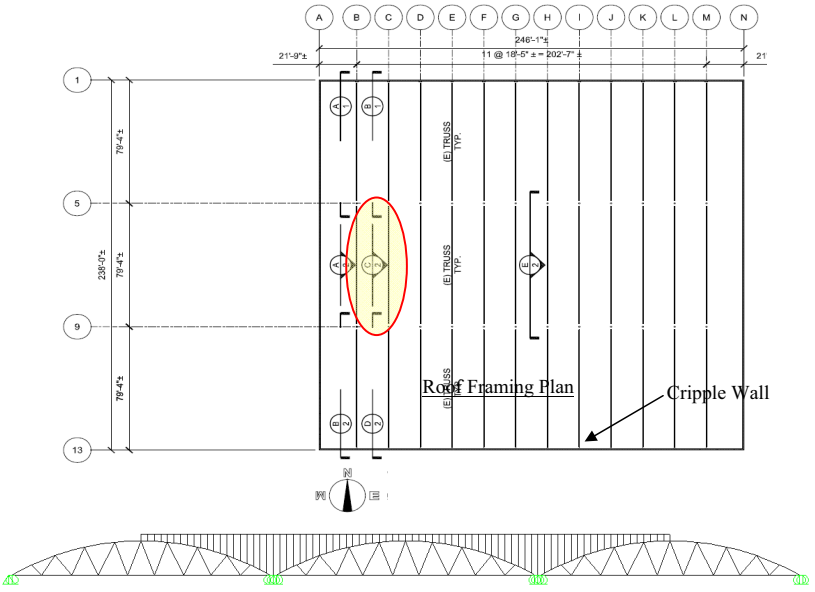

Typical Truss Elevation

Member Sizes:

Top and bottom chords are double 2x10; Web members are single 3x6 sandwiched between top and bottom chord members; Cripple walls are 2x6 @ 24" o.c.

Figure 1. Roof Framing Plan, HVAC units were placed over the hatched area

OBSERVATION PHASE: CONDITION ASSESSMENT

Post failure condition assessment of the structure was carried out through the following steps:

1. Conduct onsite investigation.
2. Review of the extensive post-failure photo and video documentation of the damage prepared by the engineer of record and building owner.
3. Review of pre-failure photographs and construction documents.
4. Identify damaged framing components and prepare a sketch of damaged trusses.

The investigation revealed extensive cracking and damage to the truss bottom and top chords in the area of collapse. Figures 2 through 5 shows damage observed in top and bottom chords after the collapse. The damage location numbers in these figures are used in the next section as analysis reference points. Our investigation in the attic directly below trusses revealed an excessive amount of utilities and conduits that were hung from the roof structure (see Figure 6).

Figure 7 shows a sketch of the location of the damaged truss members. During our investigation, we discovered that very limited survey of the structure and its condition was performed during the remodeling. In addition, no strengthening was provided for roof trusses to carry the additional loads. Very limited structural engineering calculations were performed which concluded that no strengtehning was required.

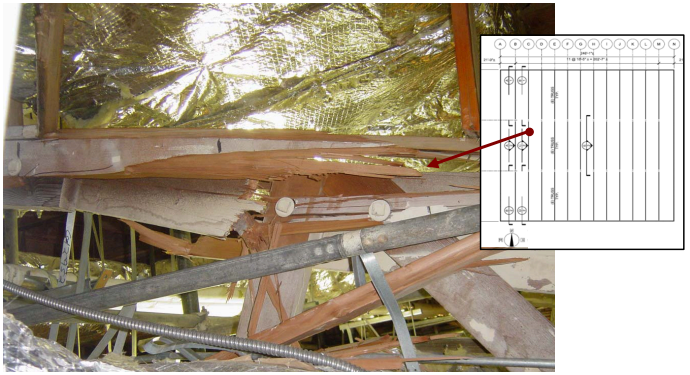

Figure 2. Top chord damage at damage location 1

Figure 3. Top chord damage at damage location 2

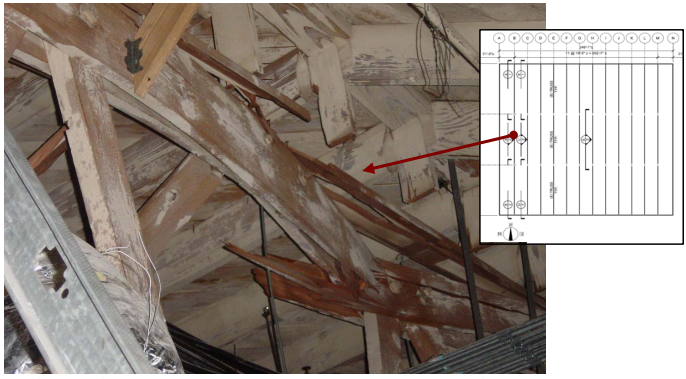

Figure 4. Top chord damage at damage location 3

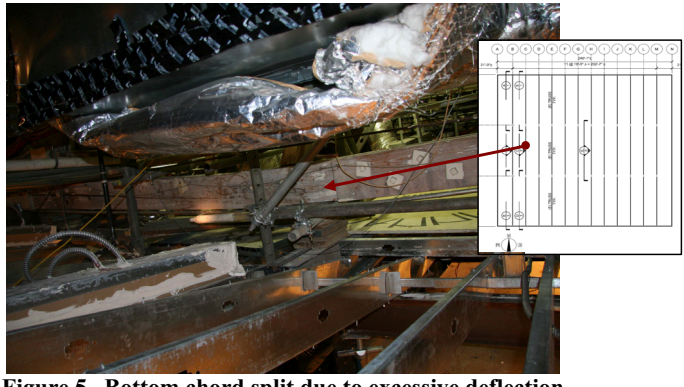

Figure 5. Bottom chord split due to excessive deflection

Figure 6. Excessive amount of conduit and utilities hung from roof structure

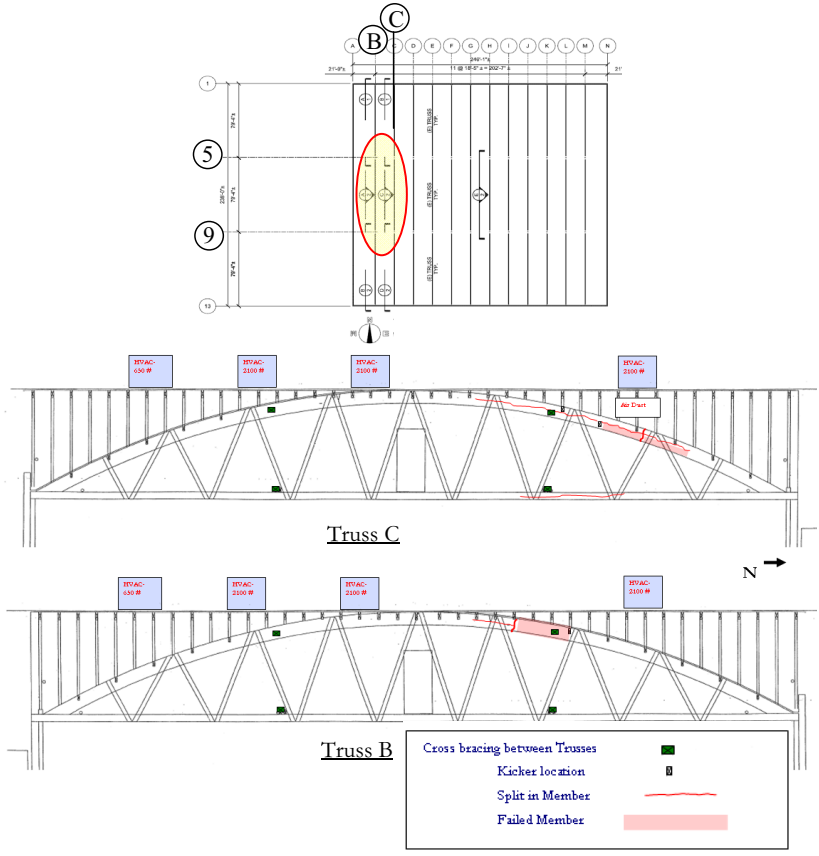

Figure 7. Failed trusses

SIMULATION PHASE: STRUCTURAL ANALYSIS

In addition to the visual investigation of the existing conditions, structural engineering calculations and analyses were conducted to determine the cause and mechanism of the failure. A two-dimensional computer model of the two failed roof trusses was created using SAP2000® structural analysis program. Properties of the structural elements including truss members, tension rods, cripple walls and kickers were obtained from available remodeling drawings and on-site investigations. The frame element option in SAP2000® was used to model the truss elements. It was assumed that no moment transfer could occur at the truss supports. As a result, a "pin" condition was used at the base of the trusses at the column locations. An overview of the computer model is shown in Figure 8. Damage locations observed on the trusses during the field investigation is also shown in this figure.

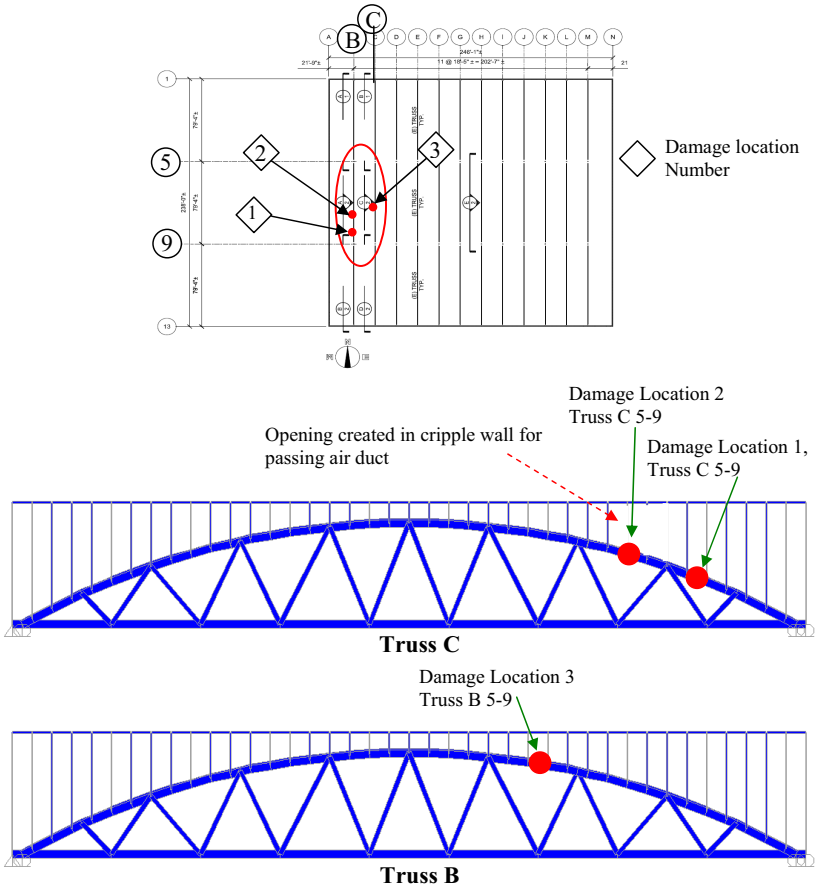

Figure 8. Overview of compute model and location of damage on failed trusses on plan and elevation

The weight of the truss and roof framing was determined based on the information obtained during the on-site investigation and measurement of the element dimensions. Equipment operational loads were determined from the manufacturer's specifications and utility and conduit loads were estimated based on the on-site measurements and engineering judgment. The weight of the architectural features, such as a suspended acoustic ceiling, was estimated using values published in common structural engineering design practice guidelines. Table 1 shows the gravity loads that were applied to the computer model.

Table 1. Various loads applied to roof trusses

ORIGINAL ROOF DESIGN LOADS			
Dead Load	12.0	PSF	According to available Information
Live Load	12.0	PSF	
Total	24.0	PSF	24 PSF
ROOF DEAD LOAD PRIOR TO INSTALLATION OF HVAC UNITS			
Roofing 5-ply felt	4.0	PSF	Consider roofing was repaired at least two times
1 x 8 sheathing	2.5	PSF	
Roof Joists (2 x 10 @ 24" O.C.)	2.0	PSF	
Sprinkler System	1.0	PSF	
Miscellaneous (Light fixtures, utility pipes, wires, conduits etc)	2.0	PSF	
Suspended Ceiling System	1.0	PSF	
Acoustic Tiles	1.5	PSF	
Truss	2.4	PSF	
Total	16.4	PSF	**17 PSF**
Live Load	12.0	PSF	
ROOF DEAD LOAD AFTER INSTALLATION OF HVAC UNITS			
Roofing 5-ply felt	4.0	PSF	Consider roofing was repaired at least two times
1 x 8 sheathing	2.5	PSF	
Roof Joists (2 x 10 @ 24" O.C.)	2.0	PSF	
Sprinkler System	1.0	PSF	
Mechanical Ducts	3.0	PSF	
Ceiling (2 layers of 5/8" GWB)	5.5	PSF	
Ceiling (Steel stud @ 16" OC)	1.0	PSF	
Ceiling (Steel stud @ 24" OC + hanger Stud)	0.5	PSF	
Miscellaneous (Light fixtures, utility pipes, wires, conduits etc)	3.0	PSF	
Roof Mechanical Pipes	2.7	PSF	
Truss	2.4	PSF	
HVAC Units (3x2100+1x650)x1.1=7645 lbs	3.00	LBS	
Total	30.6	PSF	**31 PSF**
Live Load	12.0	PSF	

To capture the mechanism of failure, the analysis was conducted in four stages:

Stage 1: Pre-construction dead loads applied to trusses.
Stage 2: Three vertical cripple wall studs were removed in truss C, 5-9 (this was done during the construction to let the air duct pass through); as a result loads are re-routed to the edges of cripple wall opening.
Stage 3: Post-construction dead loads were applied to trusses.
Stage 4: Failed elements were removed from truss C, 5-and truss B, 5-9; as a result loads are re-routed to adjacent trusses.

Table 1 shows that trusses were loaded approximately to 70% of their design loads prior to the installation of new equipment. After the installation of the new equipment and utilities over and under the roof structure, the amount of dead load surpassed the total design loads by approximately 30%. During the installation of the new equipment, some cripple wall studs over the top chords were removed to allow for the passage of air ducts. Creating an opening in the cripple wall introduced concentrated loads to the top chords at the edges of the cripple wall opening.

Using analysis results, the total compressive stress for each member of truss due to the combination of moment and axial forces was computed and compared with the ultimate stress of the wood members. Ultimate compressive and bending stresses of the wood were determined using National Design Specification (NDS) for Wood Construction, LRFD provisions (Edition 2005). Stress ratio in stages 1 (pre-construction dead loads) and 3 (post-construction dead loads) of the analysis for failed members are reported in Table 2.

Table 2. Ratio of applied stress to ultimate stress for locations where roof trusses failed

		Prior to Equipment Installation, Dead Load Only - Stage 1			After Equipment Installation, Dead Load Only - Stage 3		
Truss	**Damage Location**	**Axial Load (Kips)**	**Moment (K-in)**	**Combined Stress/ Ultimate Stress ratio**	**Axial Load (Kips)**	**Moment (K-in)**	**Demand/ Capacity ratio**
C 5-9	1	22.8	11	0.27	44.5	53.2	0.7
C 5-9	2	22.7	13.1	0.29	44.6	23.1	0.6
B 5-9	3	24.9	7.6	0.27	36.3	11.1	0.4

The analysis indicated that the maximum stress ratio prior to failure occurred in the top chord at damage location number 1 (approximately 0.7 of ultimate stress of wood in compression). This was expected since creating the opening in the cripple walls introduced new concentrated loads at this location, and therefore, the top chord at this location collected larger bending moments. It was concluded that the roof failure was initiated at this location.

Analysis results are consistent with the field investigation at this location where shattered top chord was observed (see Figure 2). It is worth mentioning that this location is not directly under the HVAC unit on the roof. It was also concluded that once the top chord of truss C at location 1 failed, it redistributed the applied loads which resulted in the failure of the top chord of truss C at location 2 (see Figure 3). Subsequently, this truss deflected vertically, approximately one foot causing damage to the bottom chord (see Figure 5) and ceiling finishes. In addition, redistribution of the load caused the failure of truss B. The top chord of truss B failed at location 3 where it was connected to truss C with transverse cross bracing. When the first truss went down, the cross bracing pulled the top chord of the adjacent truss (B) and caused it to buckle laterally (see Figure 4). Stage 4 of the analysis was done by removing the failed members of the trusses and reanalyzing the truss. Figure 9 shows the truss members with large stress ratios that were susceptible to damage. The locations of these members were consistent with the locations of damaged members observed during the investigation as seen in Figure 9.

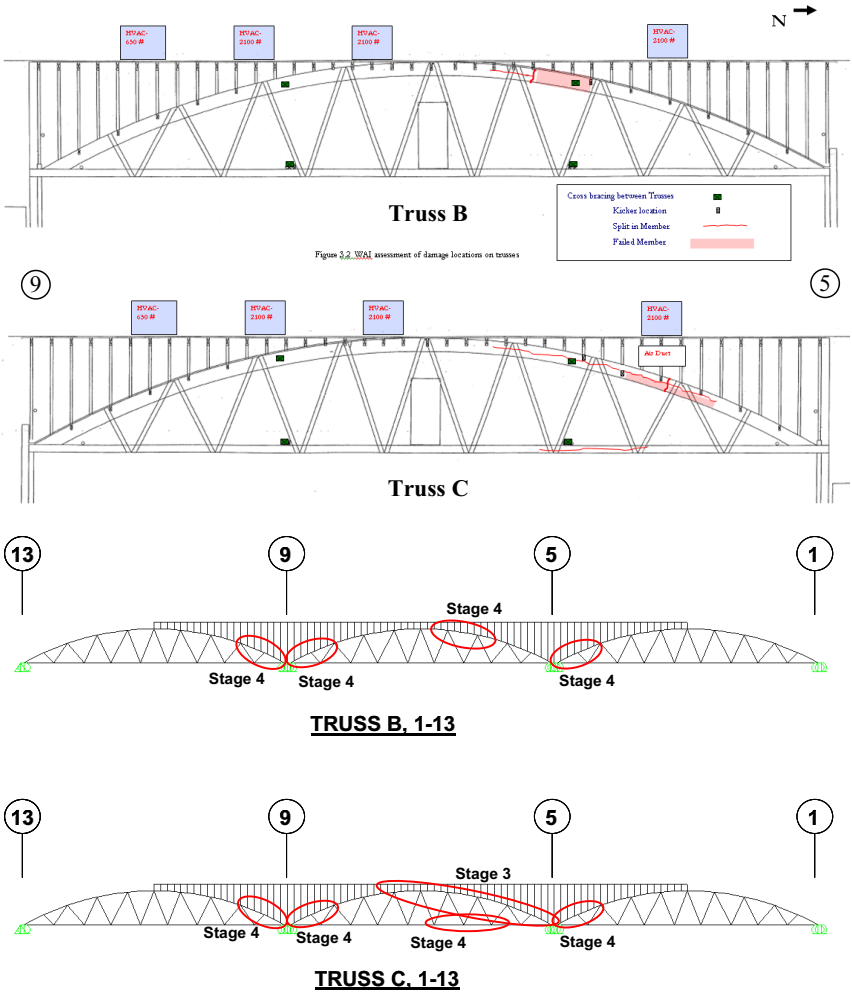

Figure 9. Comparison between location of truss members with large stress ratio and the location of damaged truss members observed during field investigation

The sequence of damage, however, does not explain why the bowstring truss that was overloaded did not fail immediately after application of the new loads. The answer lies in correlation between the level of stress in the truss members and the duration of the applied loads. Such a relationship has been developed by the U.S. Forest Product Laboratory, which was reproduced in Structural Engineering Handbook by Chen and Lui (1999), and adopted here as Figure 10. The curve in this

figure plots the ratio of applied stress to the ultimate stress of timber versus time-to failure. This curve was developed based on the results from several studies, taking into account compression, bending and shear behavior of wood specimens. No consideration is given in the reference for wood properties such as grade and density. Therefore, the authors' understanding was that this curve was developed considering the test results from specimens with various wood properties. Using this curve and the results from the computer model, for a maximum stress ratio of 0.7, it would take approximately two months for the critical truss member to fail. The calculated time-to-failure closely matched the reported time of collapse of the bowstring trusses.

It is also noted that according to the load duration curve when the stress level in a member exceeds 60% of the ultimate strength of the timber, failure is imminent. Therefore, the load duration curve can be used as a tool for the investigation of failure of wood structures. This analysis also confirmed that the bowstring trusses did not have much reserved capacity for additional loads as described earlier in this paper.

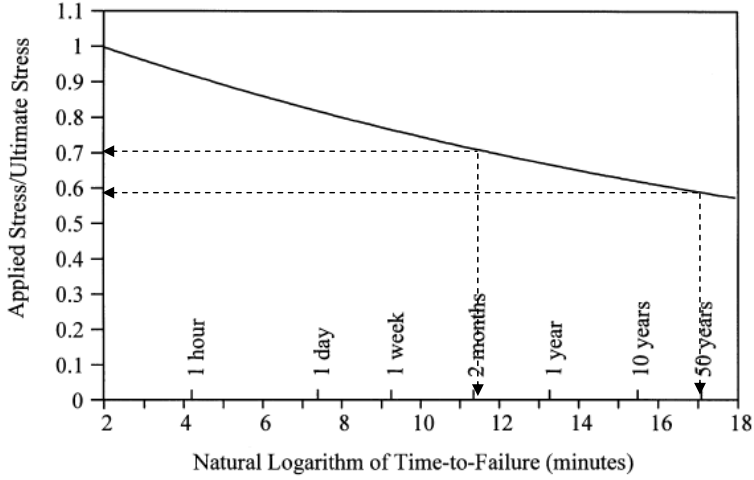

Figure 10. Load duration behavior of wood, the stress ratio of 0.7 in critical member of truss resulted in a two-month delayed failure, Also note that for to prevent failure in an average building with about 50 years of service life stress ratio should not exceed 60%

CONCLUSIONS

This paper presented the effect of load duration on the failure of two in-service bowstring trusses supporting weight of newly installed heavy industrial equipment. No strengthening was provided for these trusses. Our failure analysis consisting of Observation and Simulation Phases showed that roof trusses had no additional reserve capacity and would ultimately fail under the added sustained loads. It was determined

that the delay in roof collapse was due to the level of the stress in truss members and load duration effect. The lessons learned from this study are:

1. Load duration has significant effect on the load resisting behavior of wood structures that should be considered in a failure investigation.
2. Failures might not occur immediately after the addition of loads.
3. Failure curve is an excellent tool for forensic investigation of wood structures.
4. During the design or strengthening of wood structures, service compressive stress ratio shall not exceed 60% of ultimate stress of structural elements.
5. Prior to introducing new loads to existing structures, a detailed condition assessment of the structure must be performed including field investigation and reviewing load history of the structure.
6. Calculations must be performed to determine the load capacity of the existing structure and the required strengthening for additional loads.
7. Bowstring trusses have no reserve capacity and therefore, strengthening is absolutely necessary prior to introducing any new load to them, unless observations and simulations show otherwise.

ACKNOWLEDGMENTS

The authors would like to acknowledge Mr. Mike Cochran, Associate Principal of Weidlinger Associates, Inc for his constructive input during the project.

REFERENCES

American Forest & Paper Association (2005), National Design Specification (NDS) for Wood Construction, American Wood Council, Washington DC.

Chen, W.F. and LUI, E.M. (1999), "Structural Engineering Handbook", CRC Press, Boca Raton, FL.

Hart, G. C., Jain, A. and Arya, B. (2009), "Damage Investigation: Infill Concrete Frames", Accepted for publication in the 11th Canadian Masonry Symposium, Toronto, Ontario, May 31- June 3, 2009.

Kristie, Richard J. and Johnson, Arne P. (1996), "Investigating and Repairing Wood Bowstring Trusses", Practical Periodical on Structural Design and Construction, Volume 1, Issue 1, pp. 25-30 (February)

SAP2000 Version 11 (2008), Integrated Software for Structural Analysis & Design, Computer and Structures Inc, Berkeley, CA, USA.

Tigue, David B. and Hoigard, Kurt R., "Vintage Timber Truss Roofs: Claims Waiting to Happen", article posted on Wooden Roof Structures Inc website, http://woodenroofinc.com/services.htm

United States Department of Agriculture (USDA) (1987), *Wood Handbook: Wood as an Engineering Material,* Agriculture Handbook 72, Forest Products Laboratory, USDA, Madison, WI.

Structural Engineering Responsibilities and Structural Components: A Premanufactured Wood Truss Case Study

Stewart M. Verhulst, M.S., P.E., M.ASCE[1]
Deepak Ahuja, M.S., P.E., M.ASCE[2]

[1]Nelson Architectural Engineers, Inc., 9701 Brodie Lane, Suite 201, Austin, Texas 78748; PH (512) 610-2800; email: sverhulst@architecturalengineers.com
[2]Nelson Architectural Engineers, Inc., 2470 Dallas Parkway, Suite 220, Plano, Texas 75093; PH (469) 429-9000; email: dahuja@architecturalengineers.com

ABSTRACT

Structural Engineers have a duty to their clients and the public to provide safe designs. Typically, the Structural Engineer of Record is responsible for the structural design of the overall project, including specification of the design loads, issuance of design documents, and review of submittals.

When structural components are used, the engineer for the Component Designer/Manufacturer is responsible for the design of individual structural components. This can constitute a significant portion of the structural design on ae project. Structural Engineers must understand their duties and must also be aware of the extent to which structural component design is (or is not) being performed by a Professional Engineer.

In the subject case study, the Component Designer/Manufacturer's licensed engineer was not familiar with the project layout and only reviewed the design output for the individual components, without regard for the framing layout and the resulting loading conditions. As a result, the project was built with structural inadequacies, which necessitated extensive repairs.

INTRODUCTION

General. In the building industry, Structural Engineers have a duty to their clients to provide proper and safe designs and a duty to ensure public safety in their designs. The Structural Engineer typically fulfills these duties by directly supervising the design work, as designated by issuance of sealed documents and by reviewing submittals and shop drawings for the structural members and materials used for construction. For premanufactured wood trusses discussed in this case study, the Component Designer/Manufacturer is also typically required to provide sealed documents. The Component Designer/Manufacturer in this case study created the layout scheme for many of the primary framing components. The study outlined herein shows the effect of significant structural design being performed by a Truss Designer/Manufacturer without the oversight of a licensed Structural Engineer.

Structural Engineers must understand their duties and be aware of the extent to which framing component design is (or is not) being performed by a licensed engineer.

Structural components. Structural components are commonly used in buildings with highly repetitive structural loading conditions. For instance, warehouse buildings typically have structural components such as steel joists for roof framing. For this type of component design in simple structures, component manufacturers often provide tables and charts as design aides to the engineer.

Component design for more complex structures is somewhat different. If the loading conditions for the components vary and are not repetitive, it is necessary to determine the loading for each component and then design the component to meet the loading requirements. Engineering work is required to determine the correct load magnitudes and loading conditions for each component.

The manufacture of many types of structural components, including metal plate connected wood trusses, is a volume business. With many different manufacturers making basically the same type of product, there are competitive market pressures, dictating tighter profit margins. There are economies of scale involved. There are project schedules to meet. This is not to say that *quality* is not a concern of the component manufacturers; it is just a fact that *quantity* and *speed* are deciding factors to success in the marketplace.

CASE STUDY

Overview. This case study considers a condominium project located in Dallas, Texas. The project included three (3) buildings of similar construction. There were a total of 17 condominium units, but there were only four (4) distinct unit floor plan layouts. Therefore, the unit layouts were repeated in the three (3) buildings. The condominium buildings were three-story buildings (plus an attic) and were built in 2000-2001.

The condominium buildings were wood-framed structures. The 1st floor was supported by a reinforced concrete slab-on-grade foundation with piers. The framing at the 2nd and 3rd floors consisted of metal plate connected wood trusses and engineered wood beams - both glued laminated (glulam) beams and parallel strand lumber (PSL) beams. The vertical support consisted of wood stud walls, with groups of studs serving as columns for concentrated loads. The interior finishes were typical for residential construction in the area, including wood floors, carpet, and gypsum board walls and ceilings. In addition to the floor loads, there was some brick veneer supported by the framing (i.e., not continuously supported to the foundation), and there were balconies off the attic areas, at the highest level of the units.

The authors were retained to investigate the complaints of the unit owners, which included deflections and uneven floors and ceilings. Specifically, the structural design was evaluated to determine if structural deficiencies were contributing to the deflections and to the floor levelness issues.

The authors' investigation began less than three (3) years after the construction of the condominiums was completed. The unit owners had several complaints, including but not limited to: uneven floors, sloping countertops, cracks in

finishes, separations in wood flooring, cracks in brick veneer, and sticking and swinging doors. Although the investigation encompassed several issues and causes of distress, this discussion is limited to the issues related to the design of the floor framing.

A floor elevation survey was performed for each unit type to determine the extent and pattern of floor unlevelness for each framing layout. Based on these elevation surveys and the visible distress, a pattern of deflection was observed at some of the interior walls and framing support locations. The surveys also ruled out foundation movement as a cause of unlevelness at the 2nd and 3rd floors. Refer to Figure 1 for the relative elevations at the 2nd and 3rd floors of one of the units.

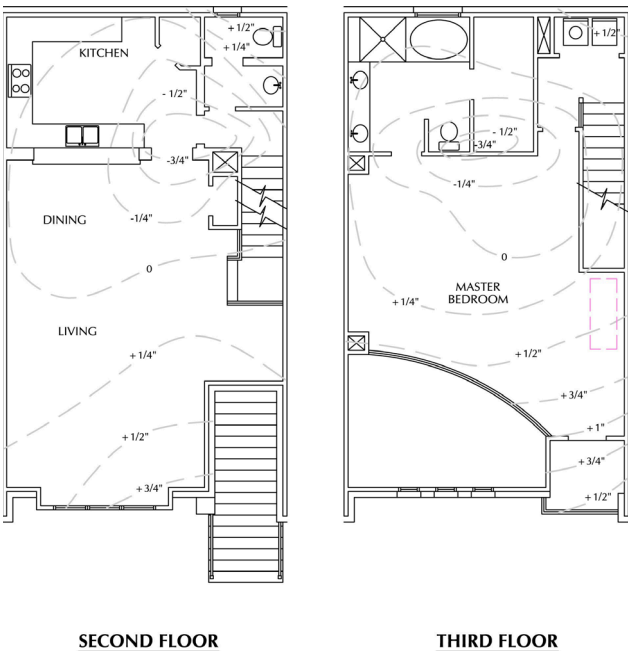

Figure 1. Elevation surveys at 2nd and 3rd floors of one condominium unit. The lowest elevations occur below a non load-bearing wall at each floor.

The overall patterns of floor unlevelness indicated that there were load transfer deficiencies at the floor framing. For the unit depicted in Figure 1, the exterior walls were load-bearing and all of the interior walls, except for the stairway wall, were not intended to be load-bearing. Also, as indicated in Figure 1, the lowest points at the 2nd floor and 3rd floor occurred where the truss framing was supported on walls that were not intended to be load-bearing. These non load-bearing walls were not continuously supported to the foundation.

Structural design. The structural design for the project was performed by a combination of the Structural Engineer of Record and the Truss Designer/Manufacturer. The Structural Engineer of Record was responsible for the overall structural design, including the foundation and lateral load resisting systems. The Truss Designer/Manufacturer was responsible for the design of the metal plate connected wood trusses.

The Structural Engineer of Record prepared the original structural framing layout schematic. However, the Truss Designer/Manufacturer prepared a different layout scheme for the truss and beam framing at the floors. This revised layout scheme was customized for the design of the trusses and beams and was adopted for construction.

The Truss Designer/Manufacturer designed the trusses and produced floor framing layout drawings (the "Truss Placement Plans") along with individual drawings for each of the trusses. The individual truss "cut sheet" drawings (the combination of the layout drawing and individual truss drawings is referred to as the "shop drawings" herein) were signed and sealed by a licensed Professional Engineer, an employee of the Truss Designer/Manufacturer.

Loads and load transfer issues. The Structural Engineer of Record provided the loads to be used for the truss design. These loads included a typical dead load of 20 psf (0.96kPa) and a floor live load of 40 psf (1.92 kPa) at the living spaces (increased to 60 psf (2.88 kPa) at the balconies). The Truss Designer/Manufacturer had to calculate the loads throughout the structure, taking into account special loads and all load transfer conditions. These calculations constituted a significant portion of the design of the truss framing and would have been required regardless of the framing layout.

Furthermore, some of the non load-bearing walls were included on the Truss Placement Plans and it was not clearly indicated which walls were load-bearing and which walls were not. Refer to Figure 2 below, which indicates the Truss Placement Plans for the 2nd floor of one of the unit types. At the very least, the truss shop drawing layout plan was confusing regarding the locations of the load-bearing walls. The result was that the Truss Placement Plans were confusing to the framer who erected the framing, and was even confusing to the Professional Engineer working for the Truss Designer/Manufacturer.

Based on the authors' review of the design documents and the measured floor elevations, the primary deflections and relative low points in the floors occurred at walls that were *not* designated as load-bearing, indicating load transfer from non load-bearing walls into the framing below (refer to Figure 1).

Some destructive testing was performed at the framing to observe the connections and the possibility of load transfer at the non load-bearing walls. Nearly all of the truss and beam framing was in contact with, and therefore was bearing on, the walls below (refer to Figure 3). This condition essentially made every wall a load-bearing wall.

Consequently, the load from these walls was transferred into the framing below. This framing was designed to support the weight of the wall only and was not designed to support loads transferred from above.

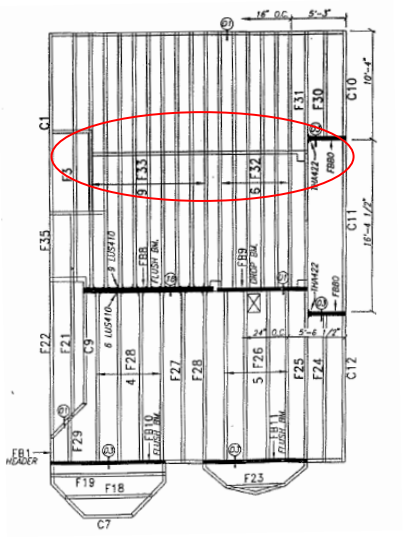

Figure 2. Example of the Truss Placement Plans. The wall below the mid-span of the trusses marked "F32" and "F33" was not intended as load-bearing, but was included in the Placement Plans.

Figure 3. Truss bearing on a wall not designed as load-bearing. Note the nail connecting the truss to the wall (follow arrow).

In addition to the interior load transfer issues, it was also determined that some of the truss and beam framing was underdesigned. The magnitude and location of some of the loads used for the component design (by the Truss

Designer/Manufacturer) were incorrect, primarily due to incorrect calculations considering tributary areas and load transfers.

One area where unconservative loads were commonly used in the design was at the upper level concrete balconies. The design for the premanufactured trusses did not consider the proper dead load or live load for these balconies. Another area where the loading was incorrectly calculated occurred where wood framing was supporting brick veneer. Although brick veneer support is a safety issue unto itself, some of the brick load was supported by the truss framing. This brick load was not accounted for in the truss design.

The load transfer issues and the use of unconservative loads for component design resulted in undersized structural members and unsafe conditions. These conditions existed to some degree in each of the four (4) unit types, and all three (3) of the buildings were similarly affected.

The subject condominium structures were certainly not uniquely complex structures. However, because of the varying loading conditions and load transfer issues, they were not simple structures either. With 3-story framing plus an attic and roof, there were a variety of load transfer and support conditions requiring consideration (and calculation). Because the walls were not all "stacked" (they did not all line up from floor to floor), some of the floor framing trusses at the attic and 3rd floor were not bearing on walls that were continuous to the foundation. Also, because the structures had three (3) stories plus an attic and roof, the magnitudes of the structural loads caused increased demand on the structural framing compared to the typical one or two-story structures for which this type of wood framing is commonly utilized.

DISCUSSION

Standards of practice for engineering. The Component Designer/Manufacturer is required to perform structural engineering to determine the loading for each of the components, based on the design loads provided by the Structural Engineer of Record.

Each state has jurisdiction over the practice of engineering in that state. Therefore, each state has laws and rules for the practice of engineering, although these are generally similar from state to state. Generally, a Professional Engineer is required to directly perform or directly supervise all engineering work sealed by the engineer. As a point of reference, the State of Texas (Texas Board of Professional Engineers 2007) provides a definition of the practice of engineering, which includes: "design, conceptual design, or conceptual design coordination for engineering works, products or systems", and "development or optimization of plans and specifications for engineering works, products, or systems". Furthermore, the "direct supervision" required of an engineer for engineering work product is defined as follows:

> *The control over and detailed professional knowledge of the work prepared under the engineer's supervision. The degree of control should be such that the engineer personally makes engineering decisions or personally reviews and approves proposed decisions*

prior to their implementation. The engineer must have control over the decisions either through physical presence or the use of communications devices.

An independent licensed Professional Engineer (not directly employed or contracted by the manufacturer) cannot directly supervise the engineering work performed by a Component Designer/Manufacturer. Therefore, the Component Designer/Manufacturer is required to employ a licensed Professional Engineer to perform or directly supervise the engineering work for the component design. This ensures that all of the calculations for the structural design of a building are performed under the direct supervision of a licensed Professional Engineer.

If the above states the theory of what should be done, what is the reality? Are all calculations for component design performed under the direct supervision of a licensed Professional Engineer? While Structural Engineers of Record do have a duty to ensure public safety, they are not required to perform work outside their scope of service. Structural Engineers of Record are typically required to review shop drawings, such as those prepared by a Component Designer/Manufacturer, but they are not required to retrace all of the design calculations performed by the Component Designer/Manufacturer to determine if the components were designed correctly. The Structural Engineer of Record is required to review the shop drawings for conformance with his/her design, but this does not constitute a line-by-line verification of the engineering work performed by the Component Designer/Manufacturer.

The Truss Plate Institute (TPI) is an organization that creates standards for the wood truss industry in the USA. In the commentary for the National Design Standard for Wood Truss Construction (Truss Plate Institute 2003), TPI describes the duties of a Truss Designer as follows:

7.0 TRUSS DESIGNER RESPONSIBILITIES

7.1 The Truss Designer shall prepare the Truss Design Drawings based on the truss design criteria and requirements set forth in writing by the Owner, Building Designer or Contractor, by the Building Structural System Design Documents, and in conformance with the requirements set forth in the Truss Design Standard.

While TPI does not discuss specific engineering responsibilities or protocol, the Truss Designer is performing engineering work, and is therefore required to conform to the standard of practice for engineering. As noted above, this includes direct supervision by a licensed Professional Engineer over all engineering work.

Engineering roles. For the case study project, the Truss Designer/Manufacturer created the Truss Placement Plans, which indicated the floor framing layout for each of the units, and performed the design of the floor trusses. There was an engineering seal on the shop drawing for each truss on the project. The Truss Placement Plans, however, were not sealed.

Representatives of the Truss Designer/Manufacturer gave deposition testimony regarding the project, providing some insight into the design process and methods used. Based on this deposition testimony, the Professional Engineer who sealed the truss drawings, by his own admission, did not have any involvement in the calculation of the loads for the trusses. This work was performed by a "designer", an employee of the Truss Designer/Manufacturer who was not a Professional Engineer. The employee who designed the project was therefore not directly supervised by the Professional Engineer who sealed the truss drawings. This conduct is a violation of the standards of practice for engineering.

Deposition testimony further revealed that the Professional Engineer who sealed the truss drawings was not familiar with the architectural floor plans or structural drawings for the project, and was not even familiar with the Truss Placement Plans that accompanied the signed and sealed truss drawings. Furthermore, this Professional Engineer testified that it was *not* common practice for the engineer sealing the truss drawings to review the structural and architectural drawings.

In fact, while looking at the Truss Placement Plans for the project (prepared by his employer) during the deposition, this engineer incorrectly identified non load-bearing walls as load-bearing. The engineer stated that he was not familiar with the Truss Placement Plans and the framing layout. This admission indicated that the engineer was also not familiar with the loading conditions and the load path through the framing.

The question then becomes: If the Professional Engineer employed by the Truss Designer/Manufacturer is not responsible for this engineering work, who is responsible? The Structural Engineer of Record had the understanding that the Truss Designer/Manufacturer's Professional Engineer was responsible for the totality of the truss design, including the determination of individual truss loading and load paths. The Structural Engineer of Record must review the shop drawings and must also perform load calculations for other structural members and systems. However, the Structural Engineer of Record cannot have direct supervision over engineering decisions that are made and implemented by representatives of the Truss Designer/Manufacturer. In this scenario, the Truss Designer/Manufacturer had the responsibility to provide supervision by a licensed and qualified Professional Engineer over their engineering work. For this case study, this was not done in accordance with the requirements of the standard of practice for engineering.

While there were shortcomings in the shop drawing review by the Structural Engineer of Record, some of the design errors made by the Truss Designer/Manufacturer may have not been caught even with a thorough review of the shop drawings. Shop drawing review is one "line of defense" to detect design errors, but it cannot be used as a crutch by those preparing the shop drawings.

It was further discovered that the "designer" and the Professional Engineer for the Truss Designer/Manufacturer had as many as fifty (50) projects ongoing at the time and that this was a typical workload. This indicates a significant volume of engineering work for one Professional Engineer. The case study project included 118 different trusses plus some channel frames. The Truss Designer/Manufacturer's Professional Engineer estimated that it would take 1 1/2 hours to review the drawings

and calculations for a project of this size. This time estimate equates to less than 1 minute per truss and is not nearly enough time to perform an adequate review of the engineering work. Also, this review does not comply with the previously noted requirements for direct supervision, as the Professional Engineer did not have control over the project and did not make or approve many of the engineering decisions.

Because the engineering design of structural components was not performed under the direct supervision of a Professional Engineer, the Component Designer/Manufacturer did not comply with the duties of the engineering profession and there is an increased likelihood of structural deficiencies. This is an important issue, as unsupervised engineering work can result in an increased danger to the public.

SUMMARY

The case study discussed herein illustrates a situation where a Component Designer/Manufacturer performed significant engineering work on a building design. A substantial portion of this engineering work was not performed under the direct supervision of a licensed Professional Engineer.

While the Structural Engineer of Record is responsible for the overall structural design on a project, it is not in his/her scope of work to perform an exhaustive review of the calculations and design work performed by a Component Designer/Manufacturer. Structural Engineers must be aware of their scope of work as it pertains to structural components. Structural Engineers should delineate what work they are responsible for and what work is the responsibility of others. The Structural Engineer of Record for the project highlighted in this case study did approve the shop drawings, but he did not perform an exhaustive calculation review, nor was he required to do so.

An unlicensed individual performed critical engineering work, without direct supervision by a licensed Professional Engineer. Due to this lack of proper supervision over the design, structural deficiencies in the design were not identified prior to the completion of construction. As a result, extensive repairs were required to the structural framing after the construction was completed and the individual homeowners had occupied the buildings, creating inconvenience and significantly increasing the cost of the repairs.

Considering the engineering design of structural components, the ultimate responsibility resides with the Component Designer/Manufacturer. It is not acceptable for these components to be designed by unlicensed individuals without direct supervision by a licensed Professional Engineer. The authors acknowledge that component design and manufacture is often a volume business, requiring repetitive designs with quick turnaround times. However, for more complex projects, such as multi-story structures with load transfers, structural engineering work cannot be adequately performed under these conditions. The Component Designer/Manufacturer must provide proper supervision by licensed Professional Engineers over their engineering work.

Even though it is the duty of the Component Designer/Manufacturer to perform the design work for these components, the Structural Engineer of Record

should perform a thorough review (not an exhaustive review or re-doing of the work) of the shop drawings, with special consideration for unique structural complexities such as load transfers. This review may uncover mistakes that indicate a lack of supervision by the Component Designer/Manufacturer.

While the authors realize that it is already accepted practice for Structural Engineers of Record to review shop drawings, our goal is to highlight that Structural Engineers should be aware of what work is (and what work is not) being performed under the direct supervision of a licensed Professional Engineer working for the Component Designer/Manufacturer.

We recommend that Component Designers/Manufacturers ensure that their design processes comply with the standard of practice for engineering, including direct supervision over all engineering design by a licensed Professional Engineer. We further recommend that, as a part of their shop drawing review for structural components, Structural Engineers of Record attempt to better understand whether or not all of the engineering work has been performed with the proper amount and quality of supervision.

The authors' concern is that it is generally accepted by Structural Engineers that component design, including the distribution of loads to individual members, is being performed under the direct supervision of licensed Professional Engineers. Based on this case study, this is not necessarily true in every case. Component Designers/Manufacturers must provide direct engineering supervision over their engineering designs, and Structural Engineers are advised to understand and verify the extent to which a Component Designer/Manufacturer has provided this direct engineering supervision. When Component Designers/Manufacturers are performing engineering design, they must comply with the standard of care for licensed Professional Engineers.

REFERENCES

Structural Engineers Association of Texas (SEAoT). (1998). *Guideline for Practice*, Second Printing.

Texas Board of Professional Engineers. (2008). *Texas Engineering Practice Act and Rules Concerning the Practice of Engineering and Professional Engineering*, Texas Board of Professional Engineers, Austin, TX, p.36.

Truss Plate Institute (TPI). (2003). *National Design Standard for Metal Plate Connected Wood Truss Construction*, TPI, Madison, WI, p.77.

Wood Truss Council of America (WTCA). (2002). *Metal Plate Connected Wood Truss Handbook, Third Edition*, WTCA, Madison, WI, p.H-1 – H-10.

INVESTIGATION OF COLLAPSE OF WOOD-FRAMED WAREHOUSE DURING CONSTRUCTION

R. Scott Silvester P.E.[1] and Charles J. Russo, P.E.[2]

[1]Senior Project Manager, Simpson Gumpertz & Heger Inc., 2101 Gaither Road, Suite 250, Rockville, MD 20850; PH (301) 417-0999; email: rssilvester@sgh.com
[2]Senior Principal, Simpson Gumpertz & Heger Inc., 2101 Gaither Road, Suite 250, Rockville, MD 20850; PH (301) 417-0999; email: cjrusso@sgh.com

ABSTRACT

Temporary stability bracing is required to hold wood trusses true to line and dimensions, plumb, and in a stable condition until permanent truss bracing and other permanent components necessary for the overall stability of the structure are completed. Industry guidelines provide prescriptive recommendations for temporary bracing of metal plate connected wood trusses to inform truss installers, contractors, and builders of record about handling and stability considerations for wood trusses. This paper presents a case study involving the collapse of an 11,000 sf wood-framed warehouse during construction and includes the procedures used to investigate the technical and procedural causes of the collapse along with an overview of industry guidelines for temporary bracing of wood trusses during construction.

BACKGROUND

During the summer of 2002, a Pennsylvania-based licensed general contractor began construction of an 11,000 sf wood-framed structure to replace an existing commercial building destroyed by fire. At the time the project started, the Commonwealth of Pennsylvania had not yet adopted a statewide building code. The owner of the property simply needed to apply for a zoning application to obtain the building permit for the project. The planned project did not have an architect of record or an engineer of record. As such, construction drawings and technical specifications did not exist. A simple hand sketch on an 8-1/2 in. by 11 in. sheet defined the overall building layout (Figure 1). Reportedly, the general contractor prepared the sketch during a meeting with the owner where they discussed the general requirements for the new building.

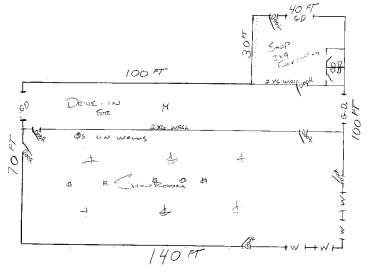

Figure 1. Contractor's Sketch of Building Layout

THE STRUCTURE

When completed, the warehouse would be a single-story structure constructed of metal plate connected wood trusses and wood-framed walls. The main section of the warehouse has approximate dimensions of 140 ft (east to west) by 70 ft (north to south) with a smaller, 30 ft (north to south) by 40 ft (east to west), section at the southwest corner. The roof structure consists of wood trusses spaced at 2 ft o.c. that span the north-south direction in the main section and the east-west direction in the smaller section at the southwest corner. By intent, the trusses would span across the 70 ft width of the main section. An interior wood-framed partition wall, oriented east-west, divided the main section. The exterior walls and central wall of the main section consist of 16 ft tall 2x6 studs at 16 in. o.c. The exterior cladding for the walls and the roof consists of metal panels.

THE COLLAPSE

In early September 2002, the general contractor erected the prefabricated, metal plate connected wood trusses on load-bearing, wood-framed stud walls that they previously constructed. Following the erection of the trusses and up to the morning of the collapse, a duration of one-week, employees of the general contractor reportedly worked to install wood purlins on top of the trusses in preparation to install the metal roof panels. During this period, an electrical subcontractor worked on the framed structure to install electrical wiring. On the morning of the collapse, the general contracting crew reportedly stopped working after a few hours because of the wind conditions, and subsequently left the project site. The electrical subcontractor remained behind and continued to work. Shortly thereafter, the entire structure collapsed to the ground (Figure 2). The collapsing roof trusses and stud walls impacted the electrical workers causing injuries.

Figure 2. Collapsed Structure

Local fire and rescue companies responded to the incident. During their efforts, some of the collapsed components were cut and removed from their resting position to facilitate extraction of the electrical workers. The removed components were retained on site.

INVESTIGATIVE PLAN

We received the assignment as the principal investigator to determine the cause(s) of the collapse about 1-1/2 months subsequent to the collapse. As principal investigator, we developed an investigative plan that consisted of the following general tasks:

- Collect background information on the structural system, the construction procedures, and the activities prior to the collapse.
- Conduct an initial site visit to gain familiarity with the site and to establish the extents to which collapsed debris has been modified by others.
- Conduct a field investigation to document the overall configuration of the debris (which includes identification of how the building collapsed, damaged and undamaged components, the configuration of the framing components and their connections, movements from original positions and the relative positions of the collapse components), and the configuration of the framing components and their connections.
- Obtain weather records from local measurement stations.
- Determine loads imposed on the structure such as dead loads, live loads, and wind loads.
- Estimate the likely capacities of the structural framing and temporary bracing.
- Advance failure hypothesis using the collected evidence and results of the structural analysis.

The following sections summarize pertinent information obtained from these respective tasks.

COLLECTION OF BACKGROUND INFORMATION

Other than the simple hand sketch discussed earlier and a few wood truss design sheets, there was no project documentation – no architectural or structural drawings, no details for the construction, no superintendent logs, no third party inspection reports, etc. Fortunately, the general contractor was extremely cooperative and granted us the opportunity to meet with them and collect information on the procedures and details used to construct the load-bearing, wood-framed walls and the roof trusses prior to collapse, to discuss their recollection of the events during the morning of the collapse, and to obtain copies of their construction progress photographs and their photographs immediately after the collapse.

Figures 3 and 4, given to us by the contractor, provided valuable information on the state of construction of the building in the days prior to the collapse. Significant features visible in the photographs included the following:

- Two in-plane diagonal braces are visible on the interior side of the studs of the north wall. The diagonals do not extend the full height of the wall.
- Out-of-plane, top-of-wall braces are installed on the visible portions of the three walls in the photographs (north, east, and south). The wall braces are

single-piece wood components attached to the top of a wall stud and to a temporary wood nailer on the top of the concrete slab.

- Five diagonal ground braces and five vertical ground braces are installed on the east gable end truss. The diagonal ground braces are single-piece wood components. The center-to-center spacing and angles relative to the ground of the diagonal ground braces vary. The vertical ground braces, or stiffbacks, do not extend the full height of the building and are not always aligned with diagonal ground braces.

Figure 3. Construction – Stud Walls

Figure 4. Construction – Ground Braces

The photographs taken by the general contractor immediately after the collapse showed the following relevant features:

- The superstructure of the main portion of the building, wood-framed stud walls and roof trusses, collapsed in its entirety (Figure 5). The collapsed trusses lay on each other in a domino fashion, as do the studs of the walls. The superstructure collapsed toward the east and slightly to the south.
- The heels of the trusses detached from the top plates of the walls. A combination of toe nails and Simpson Strong-Tie hardware connectors attached the heels of the truss to the top plates.
- Roof purlins existed on the top chord of the northern portion of the roof trusses from the eave to the ridge. The purlins butted end to end; they were not lapped. A few purlins existed on the top chord of the southern portion of the roof trusses.
- Two rows of Simpson Strong-Tie Spacer Bracers existed on both the northern and southern portions of the roof trusses.
- Two of the diagonal ground braces for the trusses on the east end of the structure were visible. One is fractured at an unknown portion of its length. Only the lower portion of the second brace is visible and shows the distorted nailed connection to a metal stake in the ground (Figure 6).
- Built-up T-shaped stiffbacks were visible along the east end of the structure.

Figure 5. Collapse – Trusses

Figure 6. Collapse – Trusses and Walls

EXAMINATION OF COLLAPSE DEBRIS

When we arrived on site for our initial visit, we discovered that certain components had been removed from their original resting position as part of the rescue and site cleanup operations. Luckily, the majority of the debris remained in its original position, and components that were previously removed were still on site in organized piles, with the exception of the east end gable truss and the associated ground braces. From the information collected during this initial visit, we planned examination procedures.

With the assistance of a contractor and in the presence of the other investigating consultants retained by involved parties, we implemented the disassembly of the debris for the purpose of observing and documenting the remaining components and their relative interaction. Prior to starting the disassembly, we marked each component with a unique identification mark, documented its condition with photographs and video, and recorded its relative position with measurements to adjacent components and a project benchmark. We then proceeded to systematically remove components from the debris pile one at a time, examining and documenting each one. We learned the following pertinent information from the disassembly process:

- The three rows of horizontal strapping on the north and east walls consisted of 1x3 lumber fastened into the narrow face of the each wall stud with two nails. Segments of horizontal strapping were also evident on the south wall.
- We did not discover remnants of the diagonal wall bracing on the interior of the north stud walls, as shown in the pre-collapse photograph, during the disassembly process.
- We did not discover remnants of diagonal wall bracing on the interior of the south stud wall during the disassembly process.
- Diagonal corner braces were present on the interior of the studs on the east wall, which was consistent with the pre-collapse photograph.
- Top chord lateral bracing of the trusses consisted of four rows of Simpson Strong-Tie Spacer Bracers, and to some extent, the installed 2x4 roof purlins. The roof purlins were fastened to the top chords with two nails per truss. The roof purlins were butted end to end, not lapped. We did not find diagonal top chord bracing of the trusses during disassembly.

- Bottom chord lateral bracing consisted of two rows of 2x4s nailed into the top edge of the bottom chord and two rows of 2x4s nailed into the lower portion of a vertical web member just above the bottom chord. For both bracing configurations, one nail fastened the brace to each truss. We did not find diagonal bottom chord bracing of the trusses during disassembly.
- Diagonal web bracing of the trusses, consisting of single 2x4s, existed in two locations. Nail penetrations in the vertical webs of adjacent trusses indicated the first location to be near the east wall and the second location about 70 ft toward the west. The diagonal web bracing attached into the side of the web members with one nail into each truss.

WIND RECORDS

We obtained recorded weather data from four National Oceanic and Atmospheric Association National Climatic Data Centers near the project site. Table 1 summarizes the recorded wind speeds (5-second gusts) and general direction of the wind at the reported time of the collapse.

Table 1. Recorded Wind Speeds

Recording Station	Wind Speed (MPH)	General Wind Direction	Relative Location to Project Site
Station 1	23 – 27	South, southeast	30 miles southwest
Station 2	25 – 29	Southeast	40 miles northwest
Station 3	30 – 35	Southeast	70 miles southeast
Station 4	23 – 30	South, southeast	90 miles southwest

We also reviewed the recorded weather data at the above-referenced stations for the period of time from the day following the completion of truss installation up to the day of the collapse. The recorded data during this time showed maximum daily wind speeds (5-second gusts) in the range of 8 to 16 mph, which are significantly lower than the recorded wind speeds at the time of the collapse.

STRUCTURAL ANALYSIS

Loads Acting at Time of Collapse. We calculated lateral wind pressures on the erected components using drag coefficients for the member shapes and shielding effects. Based on the recorded weather data, we performed our calculations considering a 25 MPH lower bound and a 35 MPH upper bound. We converted the recorded wind speeds to 3-second gusts and made adjustments for wind direction with respect to the trusses. The resulting cumulative horizontal force on the array of trusses was 1,650 lbs (lower bound wind) and 3,200 lbs (upper bound wind).

The top chord, web, and bottom chord braces within the array of trusses distribute most of the horizontal load to the east gable end. We estimated that the cumulative horizontal force resisted by the group of five ground braces to be 1,350 lbs to 2,600 lbs.

Strength of Temporary Bracing. We calculated the strength limit state for the temporary ground braces (Spruce-Pine-Fur, Stud Grade). The nominal compressive strengths of the ground braces ranged from 115 lbs to 135 lbs, with a 620 lbs cumulative strength of the group. There was not sufficient information to evaluate the connections of the ground braces to the structure or the metal stake in the ground.

INDUSTRY REFERENCES

In 1989, Truss Plate Institute (TPI) published "DSB-89: Recommended Design Specification for Temporary Bracing of Metal Plate Connected Wood Trusses". The publication provides technical guidance for the design of temporary stability bracing for metal plate connected wood trusses for use by licensed engineers, architects, and truss design engineers.

A second industry reference available at the time of the subject construction, and for about a decade prior to the construction, is "HIB-91: Commentary and Recommendations for Handling, Installing and Bracing Metal Plate Connected Wood Trusses" published by the Truss Plate Institute (TPI). TPI developed the temporary bracing recommendations contained in HIB-91 in accordance with the procedures of DSB-89. The publication includes a 100+ page booklet, which is the commentary and recommendations, and a six-page foldout summary sheet intended for use by truss installers, contractors, and builders of record. In fact, the Summary Sheet explicitly references the contractor to obtain and read the booklet.

Prescriptive temporary bracing recommendations are shown on the summary sheet for various intervals of truss spans up to 60 ft. Temporary bracing consists of top chord lateral and diagonal bracing, bottom chord lateral and diagonal bracing, cross bracing of the web members, and ground bracing. For truss spans larger than 60 ft, HIB-91 recommends that a registered professional engineer be consulted. The DSB-89 and HIB-91 publications only address stability bracing to hold the trusses true to line and dimensions, plumb and in a stable condition until permanent truss bracing and other permanent components necessary for the overall stability of the structure are completed.

DISCUSSION

General. Temporary bracing is often required during construction because many elements of the completed structure, which are necessary for strength, stiffness, stability, and continuity, may not exist at certain times during the construction process. Maintaining the structural integrity of a partially completed structure can be achieved by sequencing the construction in order to avoid creating vulnerable incomplete portions of a structure, by completing the primary gravity-load-resisting system and lateral-load-resisting system as the structure is erected, or by providing suitable temporary bracing and/or supports with adequate strength and stiffness. The HIB-91 Summary Sheet is the document which industry organizations, such as TPI and Wood Truss Council of America (WTCA), recommend that truss manufacturers include in the delivery of trusses to the project site to inform the contractor of such temporary bracing considerations for wood trusses.

For example, the top and bottom chord lateral braces shown in HIB-91 reduce the unbraced lengths of the chords to temporarily minimize the potential for buckling and to collect lateral stability loads until a permanent plywood or metal-panel roof is installed to provide this lateral bracing. The top and bottom chord diagonal braces and web cross braces provide temporary load paths to resolve lateral stability loads through the assembled truss system and into the supporting structure until a permanent roof diaphragm is installed to provide this load path. The lateral load system of the supporting structure, whether temporary, permanent, or a combination of the two, should be properly designed, constructed, and braced before the trusses are installed.

Truss Bracing. Since the 70 ft design span of the main trusses exceeds the 60-ft limitations of the HIB-91 guidelines, a registered professional engineer should have been consulted to evaluate the necessary stability bracing for the main trusses. The general contractor did not consult with a professional engineer, and a comparison of the installed temporary bracing with the illustrations in HIB-91 shows the general contractor did not even comply with the prescriptive recommendations for the largest applicable truss span of 60 ft.

HIB-91 recommends the truss bracing system consist of lateral and diagonal top chord braces, cross braces in webs, and lateral and diagonal bottom chord braces. The frequency and spacing of these bracing components varies by the interval of the truss span. The general contractor did not install a bracing system that included all of the recommended components. Figures 7 and 8 show HIB-91 recommendations for top chord bracing and the as-built top chord bracing, for comparison.

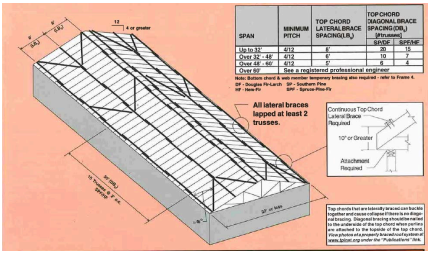

Figure 7. HIB-91 Top Chord Bracing

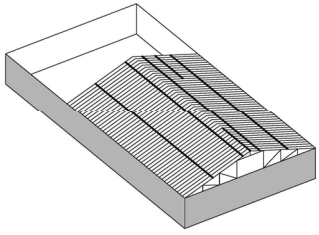

Figure 8. As-Built Top Chord Bracing

HIB-91 prescribes diagonal bracing in conjunction with lateral bracing to form triangulation for stability, otherwise a lateral force, if large enough, can cause the entire group of trusses to collapse sideways with lateral braces acting only as truss spacers as they fall. The installed bracing system essentially consisted of top and bottom chord lateral bracing, but no diagonal top and bottom chord braces were installed and the web bracing was minimal. The lack of dedicated load paths to resolve lateral loads through the assembled truss system and into the wall system results in an accumulation of lateral load passed through the truss assembly to the ground braces alone, and not into the supporting shear walls.

Regarding ground braces, HIB-91 directs the contractor to align ground braces with top chord lateral braces and, when possible, to locate ground braces and lateral braces at truss panel points. The general contractor did neither. In addition, HIB-91 cautions that "ground braces are seldom sufficient in strength unless braced themselves with lateral braces in the weak direction and/or support struts in the strong direction." The general contractor installed 2x diagonal ground braces with estimated lengths of 28 ft to 30 ft and partial height stiffbacks on the end walls. The installed system does not comply with the prescriptive recommendations of HIB-91. In addition, these long and slender diagonal ground braces do not meet slenderness requirements for temporary construction and have minimal axial capacity to resist the applied lateral loads. Figures 9 and 10 show HIB-91 recommendations for ground bracing and as-built ground bracing, for comparison.

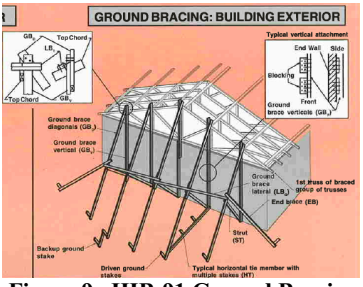

Figure 9. HIB-91 Ground Bracing

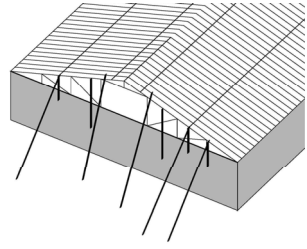

Figure 10. As-Built Ground Bracing

Wind. The HIB-91 bracing recommendations do not explicitly address resistance of the truss assembly to wind exposure. Inherently, the prescriptive bracing system has a defined load path and nominal resistance to lateral wind loads, but the prescriptive recommendations such as frequency of diagonals, cross bracing, and fastening methods, are based on lateral stability loads.

The recorded wind speeds from surrounding weather stations at the time of the collapse are in the mid-20 mph to mid-30 mph range. These recorded wind speeds are not an extraordinary weather event, and are well within the wind conditions that any contractor with a building under construction needs to anticipate. The predominant recorded wind direction at the time of the collapse is southeast, which is consistent with the general direction of the collapse of the partially completed structure. The estimated cumulative horizontal force on the group of five ground braces is 1,350 lbs to 2,600 lbs. The estimated nominal strength of the group of five ground braces is 620 lbs, which does not consider the strength of the connections to the structure and the metal stakes in the ground.

For reference, in the days prior to the collapse, the recorded maximum daily wind gusts from the weather stations are about half the velocity of gusts recorded on the day of collapse. Since wind pressure is proportional to the velocity squared, the cumulative wind force on the trusses around the time of collapse was on the order of 5 times greater than the previous days.

Wall System. The lateral-load-resisting system of the structure includes the stud-framed walls behaving as shear walls to transfer the lateral loads from the roof system down to the foundation. At the time of the collapse, the partially completed wall system consisting of 16 ft tall 2x6 studs spaced at 16 in. o.c., with a few horizontal rows of 1x3 strapping attached to the exterior side of the wall studs. During disassembly, we observed diagonal corner braces on the east wall. We did not observe diagonal braces on the remaining portions of the north and south walls. The estimated horizontal forces transferred to the north and south walls were relatively small, and the installed components likely provided some measure of lateral-load resistance. However, as evidenced by the totality and the nature of the failure of the wall system, the constructed stud walls lacked adequate lateral-load resistance under the impact of the collapsed trusses.

CONCLUSIONS

From our investigation described above we concluded the following:

- The wind initiated the collapse of the partially completed structure.
- The recorded wind speeds from surrounding weather stations at the time of the collapse do not constitute an extraordinary weather event.
- The wind speeds are well within the wind conditions that the general contractor needed to anticipate with a building under construction. The erected truss system lacked adequate bracing to provide stability of the partially completed roof structure to resolve lateral loads through the assembled trusses and into a suitable lateral-load-resisting system.

REFERENCES

Truss Plate Institute (TPI). (1989). *DSB-89: Recommended Design Specification for Temporary Bracing of Metal Plate Connected Wood Trusses*. Madison, WI.

Truss Plate Institute (TPI). (1991). *HIB-91: Commentary and Recommendations for Handling, Installing and Bracing Metal Plate Connected Wood Trusses – Booklet and Summary Sheet.* Truss Plate Institute (TPI), Madison, WI.

Engineering Ethics and Structural Calculations

Joshua B. Kardon, PhD, SE, M. ASCE[1]

[1] Joshua B. Kardon + Company Structural Engineers, 1930 Shattuck Avenue, Suite C, Berkeley, California 94704; PH (510) 548-1892; FAX (510) 548-1895, email: jbkse@jbkse.com.

ABSTRACT

Various organizations publish and promulgate Codes of Ethics which are intended to guide practitioners in their relationships with their clients, with their colleagues, and with the general public.

Structural computations are intended to substantiate the judgment of the engineer and present the engineer's design intent. They also depict, for the purpose of explaining to others, the modeling and analysis of the intended structure, and its anticipated response to the demands which it must withstand to provide intended performance over its intended useful life.

This paper examines the correlation between the ethical responsibility of the engineer and the modeling and mathematical computations used by the engineer. Examples will be presented where there has been a disconnect between the structural computations and the ethical responsibility of the engineer.

ENGINEERING ETHICS

Canon 1 of ASCE's Guidelines to Practice Under the Fundamental Canons of Ethics includes, "Engineers shall recognize that the lives, safety, health and welfare of the general public are dependent upon engineering judgments, decisions and practices incorporated into structures, machines, products, processes and devices." This paper examines the correlation between that ethical responsibility of the engineer and the modeling and mathematical computations used by the engineer.

"Ethics" are the formal or professional rules that specify conduct or behavior (and the study of those rules). Codes of Ethics of organizations present the rules their members are expected or required to follow (Griggs, 2009). Engineering students learn of ethics from courses devoted entirely to engineering ethics, or from case studies integrated into their other undergraduate and graduate level courses (Pritchard, 1992). Practicing engineers often are made aware of ethics in the context of professional societies' proscriptions against conflicts of interest or unfair competition (e.g.: NSPE, 2007; ICC, 2009), in continuing education courses required by licensing agencies, and in columns, articles and opinion pieces that appear in professional publications. Engineering ethics is not an abstract concept that only is of academic concern, but is a necessary consideration in the every-day application of engineering art, science and service.

THE PURPOSE OF COMPUTATIONS

Structural engineers use drawings and specifications to convey their engineering design intent, and produce computations to substantiate their engineering choices. What an engineer chooses to include in the drawings and computations is a product of that engineer's education and experience, and a response to the particular project conditions and constraints.

Building codes describe the minimum requirements of engineering design and construction, and as such define a lower bound for the engineer's intent, judgment, decisions and practices. For the most part, building codes do not specify the contents of the engineer's computations.

Drawings and calculations are the manifestations and presentations of the engineering judgments, decisions and practices to which Canon 1 refers, therefore, one place to see that the engineer has met the ethical obligation defined in Canon 1 is the document presenting the engineer's written computations.

EXAMPLES

Two recent examinations of engineering computations are instructive regarding the roll of engineering ethics in structural calculations.

Example 1, Residential Parking Platform. The author recently participated in the investigation of allegedly defective design and construction of a single family residence (Kardon, 2007). The property was on a steep down-slope lot, and included a detached parking platform of heavy timber post and beam construction with a concrete topping slab. The structural engineer of record (SER) produced computations for the parking platform, including a written statement on the first page of those computations describing his intent that the platform resist lateral (seismic) loads through torsion, transferring the entire lateral load to the grade beam/retaining wall at the street. The space beneath the parking level was not enclosed by walls other than the retaining wall at the street.

Engineering mechanics tells us that to resolve the lateral loads on the parking platform, torsion has to be resisted by a couple (with two opposing forces normal to the plane of the retaining wall) and a shear force (along the ledger connected to and parallel to the retaining wall). Nowhere in the computations was there a derivation of the couple resisting the torsion generated by the lateral load on the platform, and no details were depicted on the drawings for transfer of the couple forces to the retaining wall. Other than in the written statement on the first page, the calculations were mute concerning the resolution of the design forces on the platform. No mechanical connectors were designed, constructed or installed to adequately transfer the couple induced by the torsional response of the parking platform.

The SER stated his intent that the platform transfer lateral loads through torsion, but did not incorporate torsional behavior in his computations. The resolving couple was not computed, the forces perpendicular to the retaining wall were not defined, and engineering details for the transfer of those loads were never produced. Because they were not detailed, those connections were not constructed.

The mere statement of intent did not fulfill the engineer's responsibility to incorporate that intent into the structure. The judgment, decision and practice of the

engineer, that is, to have a structure built that transfers lateral load on the parking platform through torsion, was not incorporated into the structure.

Resolution. The SER was not asked to visit the site during construction of the parking platform, and was informed that the platform was not going to be constructed in accordance with his design documents. The fact that the engineer's computations did not conform to his own stated intent was irrelevant because the SER's design was never executed in construction. Even if the platform were to fail in an earthquake, because the construction differed from the SER's design, and was completed without the SER's participation, there would likely be no liability on the part of the engineer of record.

Example 2, Engineering Evaluation of the I-35W Bridge. In a draft report titled, "Fatigue Evaluation and Redundancy Analysis, Bridge No. 9340, I-35W Over Mississippi River,"(2006) produced by a large engineering firm for the State of Minnesota, 52 fracture critical main truss members were identified, the failure of any of which would have resulted in the collapse of the bridge. Figure 1 is a view of the bridge included in that report. The report included input and output of several computer-based analyses of the bridge, each with one of the critical members removed to model the failure. The analysis included impact loads generated by the assumed sudden tension failure of the member examined, as well as calculated dead loads and assumed traffic loads.

The computer output presented in the report included graphic images of the "deformed" shape of the computer model after each of the assumed failures. A reproduction of one such graphic output is shown in Figure 2.

On August 1, 2007, the bridge collapsed, killing 13 people and injuring 145. Figure 3 is a view of a portion of the collapsed bridge.

The 299 page report did not include any mention of the possible effects of the collapse of the bridge. The writers of the report did not warn the State of Minnesota of the real world consequences of the computed collapse. The report that included the graphic representation of the computations predicting the collapse of the bridge did not also include the recognition that the lives, safety, health and welfare of the general public are dependent on the judgment which produced those computations. Nowhere in the report is there a warning that the computational output depicted in Figure 2 is equivalent to the real world catastrophe depicted in Figure 3.

Resolution. Official reports (NTSB, 2008) of the cause of the collapse of the I-35W released after significant forensic investigations were completed have stated that the cause of the collapse was the original inadequate design of gusset plates at the panel points of the bridge trusses in combination with increased loading from previous modifications, and from traffic and concentrated construction loads on the bridge on the day of the failure. The "Fatigue Evaluation and Redundancy Analysis" produced a year prior to the collapse did not include any evaluation of the gusset plates. The draft report states, "Local effects of gusset plated truss joints are not addressed in the model" (page 3-4), and, "No deductions (of truss member capacities) are made for the rivet holes because holes are only present at the gusset plate connections at the panel

points. The strength of the connections will be checked separately" (page 4-4). That separate check was included in Section 6.6.2 of the Fatigue Evaluation and Redundancy Analysis report. The entire Section 6.6.2 is reproduced in Appendix 1 at the end of this paper.

Section 6.6.2 of the Fatigue Evaluation and Redundancy Analysis justifies the existing gusset plates by referring to the AASHTO Standards requirement assumed to have been used in the original design, which requires the connection "be designed for a capacity based on the average of the calculated design stress in the member and the allowable stress of the member at the point of connection, but in any event, not less than 75% of the capacity of the member." The section goes on to state, "An examination of the plans indicated the likelihood of the use of the 75% member capacity rule in the truss connection design, since relatively less *(sic)* connection bolts were used for lightly loaded truss members compared with more heavily loaded members of comparable section dimensions."

It is apparent from this writing that the actual capacities of the gusset plate connections at the truss panel points was not the subject of engineering computations that substantiated the engineering judgments and recommendations of the draft report. The draft report states that the actual connection capacities "were not calculated . . . because of the complexities and uncertainties in possible failure sections of the gusset plates and in ultimate capacities of rivets and bolts." The capacities of the truss members were adjusted based on assumed connection capacities.

It is not clear to this author that the draft Fatigue Evaluation and Redundancy Analysis should have included a specific computation of the gusset plates, or if it had, whether such a computation would have disclosed a critical design defect which might have averted the tragedy of August 1, 2007. What is clear, however, is that the draft report relied on the unverified assumption that the original connections were in compliance with design standards of the time, and did not include specific calculation of the connector capacities because of "complexities and uncertainties." It seems to this author that in situations involving life-safety performance of a significant structure, reliance on assumptions should be verified, and calculations performed, even, or especially, when complexities and uncertainties exist.

CONCLUSION

Engineering computations are not just a formality of paperwork for which engineers can charge a fee, but are part of the ethical obligation of the engineer to recognize that the lives, safety, health and welfare of the general public depend on the judgment, decisions and practices of the engineer.

FIGURES

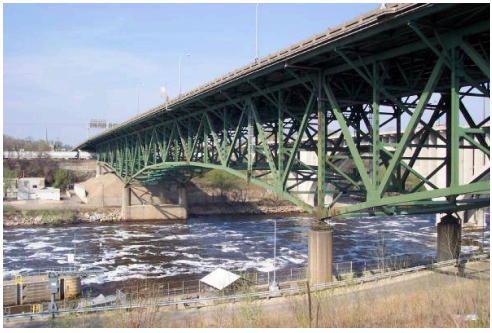

Figure 1: I35-W Bridge Prior to Collapse

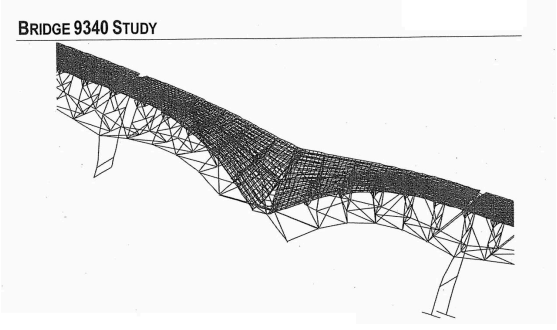

Figure 2: Analysis Model of Failed Bridge

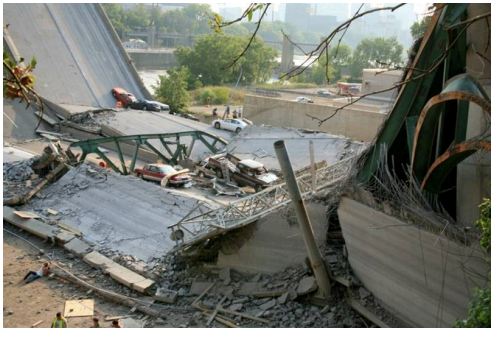

Figure 3: Collapsed Bridge

APPENDIX 1

"Fatigue Evaluation and Redundancy Analysis, Bridge No. 9340, I-35W Over Mississippi River,", Section 6.6.2:

6.6.2 Connection Capacity Check

Another consideration in the capacity check is the connections, such as the gusset joints of truss members. For connection design using the Allowable Stress Design method, the basic AASHTO criterion is: "Connections for main members shall be designed for a capacity based on the average of the calculated design stress in the member and the allowable stress of the member at the point of connection, but in any event, not less than 75% of the capacity of the member." This is a general requirement that applies to tension, compression, bending, or shear. In the original design of Bridge 9340 that followed the 1961 AASHTO *Standard Specifications for Highway Bridges,* the general requirement for connection design was the same. An examination of the plans indicated the likelihood of the use of the 75% member capacity rule in the truss connection design, since relatively less connection bolts were used for lightly loaded truss members compared with more heavily loaded members of comparable section dimensions.

The connection capacities were not calculated based on the actual dimensions of the gusset plates and the rivets/bolts because of the complexities and uncertainties in possible failure sections of the gusset plates and in ultimate capacities of rivets and bolts. Instead, the calculated member capacities as discussed in Section 4.3 were adjusted to consider the truss connection capacities per the following:

•A member design force (P) was determined in accordance with the stress table in the original design sheet for each member at the service load level
•A member ultimate axial capacity (C) was determined based on its actual plate dimensions
•For truss members with a design force less than 75% of its capacity, i.e., $P/C < 0.75$, the connection capacity is assumed to be 75% of member capacity
•For truss members with a design force greater than 75% of its capacity, i.e., $P/C \geq 0.75$, the connection capacity is assumed to be $(r_{conn})C$, where $r_{conn} = [(P+C)/2]/(C)$, which should vary between 0.75 and 0.99.
•In member capacity check using Eq. (6-4), the calculated member force interaction ratio (R) is divided by r_{conn} to consider a reduction of the member capacity due to the relatively weaker connection.

For example, a truss member has: P = 100 kips, C = 120 kips, and thus $r_{conn} = [(P+C)/2]/(C) = 0.92$. If the force interaction ratio using Eq. (6-4) is calculated as R = 0.90 considering the axial and in-plane and out-of-plane bending effects, the adjusted interaction ratio considering the relatively weaker connection capacity is $R/r_{conn} = 0.90/0.92 = 0.98$.

ACKNOWLEGEMENTS

Figure 1: Photograph by John A. Weeks III, 2008, reproduced with permission of photographer.

Figure 2: Provided by the Minnesota Department of Transportation

Figure 3: Photograph by Tim Davis, EIT, 2007, reproduced with permission of photographer.

REFERENCES

URS Corporation (2006). "Fatigue Evaluation and Redundancy Analysis, Bridge No. 9340, I-35W Over Mississippi River," Minneapolis, MN.

Griggs, Francis E., Jr., F. ASCE, (2009). "New Look at the Code of Ethic." *Journal of Professional Issues in Engineering Education and Practice,* ASCE, 135(1), 40-46.

International Code Council (ICC) (2009). "Expectation of Ethical Conduct," CP37-09.

Kardon, Joshua B., (2007). Joshua B. Kardon + Company Structural Engineers, Berkeley, California, Project Number 1663.

National Society of Professional Engineers (NSPE), (2007). "Code of Ethics for Engineers," Alexandria, Virginia.

National Transportation Safety Board (NTSB) Press Release, November 14, 2008. http://www.ntsb.gov/Pressrel/2008/081114.html>(Mar. 23, 2009)

Pritchard, Michael S., Editor, (1992). "Teaching Engineering Ethics, a Case Study Approach," Center for the Study of Ethics in Society, Western Michigan University, National Science Foundation, Grant No. DIR-8820837.

Testifying Regarding the "Standard of Care"

Joshua B. Kardon, PhD, SE, M. ASCE[1]

[1] Joshua B. Kardon + Company Structural Engineers, 1930 Shattuck Avenue, Suite C, Berkeley, California 94704; PH (510) 548-1892; FAX (510) 548-1895, email: **jbkse@jbkse.com**.

ABSTRACT

Forensic experts are asked to provide testimony concerning technical issues in disputes involving failures and defects. Among the most critical of the areas of testimony, certainly from the perspective of an engineer defendant, is the presentation of opinion concerning the "standard of care" and whether a defendant met that level of performance. The evaluation of an engineer's performance, the definition of the duty the defendant owed the plaintiff, and the comparison of the defendant's performance with that "standard" are all questions of fact addressable by an expert witness.

This paper discusses necessary components of a valid and reliable method an expert can use to support testimony concerning the standard of care.

THE STANDARD OF CARE

Engineers have a duty to provide their services in a manner consistent with the "standard of care" of their professions. A good working definition of the standard of care of a professional, derived from case law (*City of Mounds View*, 1978; *Gagne*, 1934, and others), is presented in a standardized jury instruction, Book of Approved Jury Instructions, 6.37, "The Duty of a Professional," (BAJI, 1986), which reads:

> In performing professional services for a client, a professional has the duty to have that degree of learning and skill ordinarily possessed by reputable professionals, practicing in the same or similar locality and under similar circumstances. It is his or her further duty to use the care and skill ordinarily used in like cases by reputable members of his or her profession practicing in the same or similar locality under similar circumstances, and to use reasonable diligence and his or her best judgment in the exercise of professional skill and in the application of learning, in an effort to accomplish the purpose for which he or she was employed. A failure to fulfill any such duty is negligence.

The standard of care is the boundary between a non-negligent error and a negligent error. Although this boundary is a sharp line, that is, one is either on the negligent side or the non-negligent side, the placement of the line is not fixed. The boundary is determined in every instance when a jury answers the question, "Was this engineer negligent?"

EXPERT TESTIMONY

According to U. S. Federal Rule of Evidence 702—informed by case law such as *Daubert* (1993) and *Kumho* (1999)—the purpose of expert witness testimony is to "assist the trier of fact to understand the evidence or to determine a fact in issue." Expert testimony is admissible in Federal Court if (1) the testimony is based upon sufficient facts or data, (2) the testimony is the product of reliable principles and methods, and (3) the witness has applied the principles and methods reliably to the facts of the case (Federal, 2001).

To assist the trier of fact (the jury or the judge) to determine the standard of care and the decision regarding the defendant's conformance to the standard of care, it is appropriate and necessary for an expert to testify concerning the engineer's duties. The jury should be aided in determining the facts by answering the following questions:

1. Does the defendant have the degree of learning and skill ordinarily possessed by reputable professionals, practicing in the same or similar locality and under similar circumstances?
2. Did the defendant use the care and skill ordinarily used in like cases by reputable members of his or her profession practicing in the same or similar locality under similar circumstances?
3. Did the defendant use reasonable diligence?
4. Did the defendant use his or her best judgment?
5. Did the defendant do all that in an effort to accomplish the purpose for which he or she was employed?

To answer those questions, the following also have to be determined:

6. Who are "reputable professionals?"
7. What are "same or similar" localities and circumstances?
8. What is "skill?"
9. What is "care?"
10. What are "like cases?"
11. What learning and skill are "ordinarily possessed?"
12. What care and skill is "ordinarily used?"
13. What is "reasonable diligence?"
14. What is "judgment?"
15. What is the defendant's "best judgment?"
16. What was the purpose for which the defendant was employed?

Any valid and reliable method an expert uses to support an opinion regarding the standard of care as defined above should answer those questions. An early task for the expert is to describe or acknowledge as pertinent the following terms (Webster's, 1993, 2004):

Learning: Knowledge or skill acquired by instruction or study; formal education.

Skill: Knowledge of the means or methods of accomplishing a task; the ability to use one's knowledge effectively and readily in execution or performance; technical expertness; proficiency; a learned power of doing a thing competently; a developed or acquired aptitude or ability.

Ordinarily: In the ordinary course of events; to the usual extent; moderately; without distinction.

Reputable: Enjoying good repute; of excellent reputation; held in esteem; estimable (worthy of esteem or respect, deserving good opinion); respectable (conventionally correct in conduct).

To "have that degree of learning and skill ordinarily possessed by reputable professionals" means to have received instruction, study, or formal education, and to have knowledge of means or methods, or to have developed or acquired an aptitude or ability to accomplish the engineering task to the usual extent that engineers conventionally correct in conduct and deserving of good opinion obtain or have in the ordinary course of events. This means the engineer does not have a duty to attain the highest level of academic achievement, nor to pursue the highest academic degree, nor to have extraordinary knowledge, aptitude, or ability. One indicator of adherence to this duty is possession of an engineering license. States that licence or register engineers typically demand a minimum level of learning in the form of several years of work under the direct supervision of a licensed engineer, and/or the possession of a relevant degree from an appropriate accredited institute of higher learning. States establish the existence of minimum levels of aptitude and ability by requiring that licensees or registrants pass a written examination (Kardon, 2003).

To "use . . . skill ordinarily used in like cases by reputable professionals" means to bring to bear the knowledge of engineering means or methods, or to exercise the aptitude or ability to accomplish the engineering task, to the usual extent that engineers conventionally correct in conduct and deserving of good opinion exercise in the ordinary course of events. This means the engineer is not bound to carry out every engineering task perfectly, or with an extraordinary level of skill, but has a duty to do so as is usually done, including an acceptable degree of mistake or error (Kardon, 2003).

Similar: Marked by correspondence or resemblance.

Locality: Particular spot, situation, or location.

Circumstances: Surrounding conditions.

The learning, care, and skill that are required are those possessed and used by reputable engineers "practicing in the same or similar locality and under similar circumstances." To evaluate whether an engineer met that duty, one must know relevant aspects of the locality of the engineer's practice, and relevant circumstances

under which the engineer's services were provided. Aspects of the locality and circumstances which may be relevant to the question of an engineer's actions include, but are not limited to, the local conventional materials and practices, the predominance of a particular soil type in the area, the state of the real estate market, the form of contract used, the architectural complexity of the structure, and the intended occupancy and use of the structure.

Care: Joan Tronto (1993) identifies five elements of the ethic of care, all of which are pertinent in engineering (Kardon, 2005). Tronto's five elements of care are:

- Attentiveness: Caring about; noticing the need to care, or recognizing the need of others.
- Responsibility: Taking care; having more than an obligation, but a responsibility arising in part from one's position or knowledge.
- Competency: Care Giving; having the ability to carry out the caring act effectively and correctly.
- Responsiveness: Care Receiving; being receptive to care, being aware of the care receiver's perceptions.
- Integrity: Knowledge on the part of the care giver of the situations, needs, and competencies of all the parties to the care interaction, including an assessment of needs in a social and political, as well as personal, context.

Reasonable: Being or remaining within the bounds of reason, not extreme, not excessive, well balanced; sensible (having or containing sense or reason, characterized by or resulting from sober, serious examination and study).

Diligence: Persevering application; devoted and painstaking application to accomplish an undertaking; assiduity (constant, unremitting attention or close, persistent, energetic application).

A professional has the duty to use "reasonable diligence" in the exercise of skill and learning. This means the engineer must apply a well balanced, sensible level of effort to the engineering tasks; the effort must involve or result from serious examination, but the effort need not be extreme, excessive, or beyond the bounds of reason. In evaluating the reasonableness of an engineer's diligence, one can examine the depth of the engineer's examination of loads, components, systems, and materials; the breadth of alternate design choices examined; the type and rigor of the investigation or of the structural design analysis methods used, and the suitability of the analysis method in consideration of the requirements of the structural system. It is difficult to define a reasonable level of diligence. Every time an engineer selects a design approach, chooses an analysis method, or selects a particular element or member of a structure or system to investigate or analyze, the engineer strikes a balance between doing too much and doing too little (Kardon, 2003). Evaluation of diligence must take into account the concept that "rigor is not a substitute for imagination (Klein, 1999)."

Judgment: The mental or intellectual process of forming an opinion or evaluation by

discerning and comparing; the power or ability to decide on the basis of evidence; the wise or just exercise of the capacity to judge; discernment; discretion.

Gary Klein describes the problem-solving abilities people bring to bear in making decisions as "sources of power (Klein, 1999)." These abilities can be considered aspects of judgment. They include:

- Intuition (pattern recognition, having the big picture, achieving situation awareness)
- Mental simulation
- Using leverage points to solve ill-defined problems
- Seeing the invisible (perceptual discriminations and expectancies)
- Storytelling
- Analogical and metaphorical reasoning
- Reading peoples' minds (communicating intent)
- Rational analysis
- Team mind (drawing on the experience base of the team)

Klein also found other judgments and abilities that apply to decision making:

- Judging the typicality of a situation
- Judging typical goals
- Recognizing typical courses of action
- Judging the solvability of a problem
- Detecting anomalies
- Judging the urgency of a problem
- Detecting opportunities
- Making fine discriminations
- Detecting gaps in a plan of action
- Detecting barriers that are responsible for gaps in a plan of action

Best judgment: A professional has a duty to "use his or her best judgment" in the exercise of skill and learning. This is the only obligation the professional has that is described in the superlative. In evaluating the judgment of an engineer, one must refer to that particular individual's "best," not the best judgment of all engineers. To determine whether the individual's best judgment was used, one must examine the judgment actually brought to bear.

Judgment is informed by knowledge gained from experience, and the best judgment of a particular engineer arises from that individual's own experience. To determine an engineer's best judgment, one must consider the knowledge and experience of that engineer, including knowledge gained from formal education, and examine how that engineer's judgment was applied in the situation in question.

Purpose: An investigation of the purpose for which the defendant engineer was employed must take into account the specifics of the contract under which the defendant engineer provided services, and the scope of those services, including the modifications of that contract arising from the specific performance of the parties as

well as from written or oral contract changes.

The investigation must also take into account the fact that engineers are licensed or registered by the states in which they practice, for the purpose of protecting the public, and are bound by that license to act in a manner to fulfill that purpose. Additionally, the actions of engineers who are members of professional societies are defined or guided by those societies' codes of ethics, and members are asked to perform in accordance with those codes for the purposes stated in them (Davis, 1998).

METHODS

Testimony concerning the standard of care should address each of the issues itemized above. In any one particular case, one or several of the issues might be moot or irrelevant, or might not be evidence for which the court requires expert testimony. For instance, an expert witness may not be required to testify as to the level of learning a defendant possesses.

On the other hand, many of the above issues do reasonably require expert testimony. One such area of testimony is the comparison of the defendant's actions or performance with those of reputable professionals. Often, such testimony is based on surveys of other practitioners. The validity and reliability of a survey upon which testimony is based can be challenged if the survey population is incorrectly defined, if the survey sample is not appropriately selected, if the sample size is not statistically significant, or if the survey results are not statistically evaluated.

A method has been proposed (Kardon, 2003) that does not rely on statistically questionable surveys, but is based on the deductive logic of case-based reasoning, which is an analogical reasoning technique that utilizes past problem solutions to solve current problems (Maher, Balachandran, & Zhang, 1995). This reasoning technique has been used for two general tasks: diagnosing or interpreting a new situation in order to classify it as being included or excluded from a group of known previous situations, and solving a problem by applying a previously discovered solution to a new situation (Leake, 1996). The proposed method lends itself well to the first type, interpretive case-based reasoning. The basics of interpretive case-based reasoning involve the following steps (Leake, 1996):

1. Assessment: Characterizing the new problem situation;
2. Retrieval: Identifying relevant past situations similar to the new one;
3. Comparison: Using those past situations to suggest a classification of the new one;
4. Learning: Updating the knowledge base with the learning from the new situation.

In many instances, case-based reasoning will be sufficient for an individual expert witness to use in independently arriving at opinions regarding the performance of a defendant engineer. In some situations, however, such as those in which hypothetical situations are relied upon, where the problem situation is complex or unique, or where the question of a defendant's negligence hinges on arcane or highly

technical facts, validity and reliability of the case-based reasoning approach may require more than the knowledge and experience of the individual expert witness. In those instances, the proposed method utilizes the Delphi process to support case-based reasoning.

The Delphi process, developed in the early 1950's by the RAND Corporation (Dalkey & Helmer, 1962), was devised as a means to obtain a consensus of expert opinion concerning predictions of complex, uncertain future events. It is "a means for aggregating the judgments of a number of individuals in order to improve the quality of decision making" (Delbecq, Van de Ven, & Gustafson, 1975). In the proposed method, it will be used to obtain a consensus of opinion concerning the characterization of the problem situation, the identification of relevant past situations, and (or) the suitability of the comparison between the problem situation and the relevant past situations.

CONCLUSIONS

As a basis for expert opinion, the proposed method has its strengths and weaknesses. Among the method's weaknesses is its possible sensitivity to threats to internal validity. The expert applying the method might be able to influence its results at each step of the case-based reasoning process. It might be possible to build bias into the Delphi process in the selection of the panelists and in the creation of the questionnaires.

Among the method's strengths is the transparency of the reasoning used. The choices an expert makes in characterizing the problem situation, in retrieving relevant reasoning cases, in comparing the problem situation with the retrieved cases, are all accessible to examination by all sides in a dispute. The qualification of the panelists, the questions asked of them, their reasoning, and their consensus, are also accessible. The reasoning for the expert's opinion can be understood and evaluated by the trier of fact, and can help the trier of fact assess the opinion evidence presented by the expert. A judge or jury does not typically possess the special knowledge the expert does, but does possess the normal ability to understand logical reasoning. The method allows the jury to answer the ultimate question of the defendant's negligence.

REFERENCES

Book of Approved Jury Instruction (BAJI) (1986), California Jury Instructions, Civil, West Publishing Company.

City of Mounds View v. Walijarvi, 263 N. W. 2d 420, 424 Minn. 1978.

Dalkey, Norman; Helmer, Olaf, (1962). "An Experimental Application of the Delphi Method to the Use of Experts," Memorandum RM-727-PR (Abridged), The RAND Corporation, Santa Monica, California.

Daubert v. Merrill Dow Pharmaceuticals, Inc., 509 U. S. 579, 113 S. Ct. 2786, 125 L. Ed. 2d 469 1993.

Davis, Michael, (1998). Thinking Like an Engineer: Studies in the Ethics of a Profession, Oxford University Press, Oxford.

Delbecq, Andre L.; Van de Ven, Andrew H.; Gustafson, David H., (1975). Group

Techniques for Program Planning: A Guide to Nominal Group and Delphi Processes, Scott, Foresman and Company, Glenview, Illinois.

Federal Rules of Evidence, (2001). U. S. Government Printing Office, Washington, DC.

Gagne v. Bertran, 43 C. 2d 481, 275 P. 2d 15 1934.

Kardon, Joshua B., (2003). "The Standard of Care of Structural Engineers," Doctoral Dissertation, University of California, Berkeley.

Kardon, Joshua B., (2005). "The Concept of 'Care' in Engineering."American Society of Civil Engineers, Journal of Performance of Constructed Facilities, 19(3), 256-260.

Klein, Gary, (1999). Sources of Power: How People Make Decisions, MIT Press, Cambridge, Massachusetts.

Kumho Tire Co., Ltd. v. Carmichael, 97-1709 131 F.3d 1433 1999.

Leake, David B., (1996). "CBR in Context: The Present and Future," Case-Based Reasoning, Experiences Lessons & Future Directions, David B. Leake, Ed., MIT Press, Cambridge, Massachusetts.

Maher, Mary Lou; Balachandran, M. Bala; Zhang, Dong Mei, (1995). Case-Based Reasoning in Design, Lawrence Erlbaum Associates, New Jersey.

Merriam-Webster Dictionary, Collegiate Dictionary, (2004). 11th Edition, Merriam-Webster, Springfield, Massachusetts.

Tronto, Joan C., (1993). Moral Boundaries: A Political Argument for an Ethic of Care, Routeledge, New York.

Webster's Third New International Dictionary of the English Language, (1993). Unabridged, Merriam-Webster, Springfield, Massachusetts.

The First University Master on Forensic Engineering

N. Augenti

Professor, Department of Structural Engineering, University of Naples Federico II, via Claudio 21, P.O. Box 80125, Naples (Italy); PH (+39) 081-7683102; FAX (+39) 081-7683491; e-mail: augenti@unina.it

ABSTRACT

A 2nd level university Master degree on Forensic Engineering coordinated by the author has been instituted at University of Naples Federico II in the present academic year 2008-2009. It is the first Master of Science degree regarding this field of engineering in Italy and in the rest of Europe, with exception of United Kingdom.
Professors of the Faculties of Engineering and Law are involved in the Master degree and teach eighteen courses of engineering and five of law, respectively. The programme is aimed to create two different professional figures: the Civil Forensic Engineer and the Industrial Forensic Engineer.
Only graduates in engineering are admitted to the Master courses and its duration is one year.
This paper describes the subjects, the contents of the courses, the main objectives and the great interest showed about the Master degree. On 25 available positions, as many as 53 civil and industrial engineers made application in time.

INTRODUCTION

Forensic Engineering applies scientific principles and methods of engineering in solving legal technical problems. Based on its nature, engineering and jurisprudence are jointed together, as well as technique and law. While legal medicine is widely acknowledged by both scientific and professional community, Forensic Engineering has been recognized only about twenty years ago in the United States of America and is taking the first steps in Europe.
Forensic Engineer is thus a professional that, in a broad sense, investigates the causes and responsibilities of an accident whereas, in a strict sense, works as technical consultant on behalf of judicial authority or parties in a judicial process. Therefore, the engineer studies the most probable reasons for which an unexpected performance has occurred. The problem under investigation may be a failure, a defect, or a damage, for any type of construction or product. This discipline includes all the fields of Engineering: along with the most famous civil area (addressed to structural failures and collapses, forensic estimate, building trade, etc.), a very interesting industrial area exists and it is full of forensic activities such as those regarding mechanical, chemical, and electric fields. All these subjects are included in a new **2nd level Master degree on Forensic Engineering** born on August 6, 2008 at University of Naples Federico II, which is described in detail in this paper.

DISSEMINATION OF FORENSIC ENGINEERING

Forensic Engineering is very spread in Anglo-Saxon Countries where public organizations and associations were born and now promote its evolution and dissemination, based on the initiative of insurance societies and some industries. Since in Italy and in the rest of Europe this field of engineering is not included in traditional university courses and is transversal with respect to different types of disciplines, it is currently not very known. Nevertheless, it can offer large job perspectives in the future.

While this subject was entrusted only to personal initiatives and seen as an art in the past, it has been recently under a tentative of codification, aimed to become a science. At the same time such a profession, treated by few practitioners earlier which handed down the rules of work, has become a topic of university courses to train new skilled figures having academic credentials.

In Europe and manly in Italy, this discipline is officially born on August 6, 2008 at University of Naples Federico II where a 2nd level Master degree on Forensic Engineering has been instituted. This MSc programme is the first initiative in Italy and in the rest of Europe aimed to create a new professional class of civil and industrial engineers, highly specialised in the activity of technical consultant on behalf of judicial authority or parties.

Figure 1 shows a poster containing the main information for anyone who might be interested to enrol in. On 25 available positions, as many as 53 civil and industrial engineers made application in time.

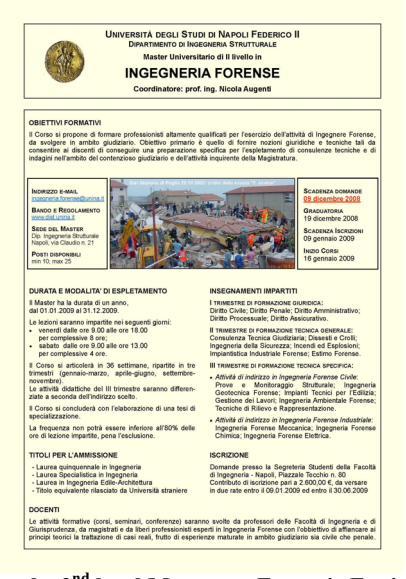

UNIVERSITÀ DEGLI STUDI DI NAPOLI FEDERICO II
DIPARTIMENTO DI INGEGNERIA STRUTTURALE
Master Universitario di II livello in
INGEGNERIA FORENSE
Coordinatore: prof. ing. Nicola Augenti

OBIETTIVI FORMATIVI
Il Corso si propone di formare professionisti altamente qualificati per l'esercizio dell'attività di Ingegnere Forense, da svolgersi in ambito giudiziario. Obiettivo primario è quello di fornire nozioni giuridiche e tecniche tali da consentire ai discenti di conseguire una preparazione specifica per l'espletamento di consulenze tecniche e di indagini nell'ambito del contenzioso giudiziario e dell'attività inquirente della Magistratura.

INDIRIZZO E-MAIL
ingegneria.forense@unina.it
BANDO E REGOLAMENTO
www.ssd.unina.it
SEDE DEL MASTER
Dip. Ingegneria Strutturale
Napoli, via Claudio n. 21
POSTI DISPONIBILI
min 10, max 25

SCADENZA DOMANDE
05 dicembre 2008
GRADUATORIA
19 dicembre 2008
SCADENZA ISCRIZIONI
09 gennaio 2009
INIZIO CORSI
16 gennaio 2009

DURATA E MODALITA' DI ESPLETAMENTO
Il Master ha la durata di un anno, dal 01.01.2009 al 31.12.2009.
Le lezioni saranno impartite nei seguenti giorni:
- venerdì dalle ore 9.00 alle ore 18.00 per complessive 8 ore;
- sabato dalle ore 9.00 alle ore 13.00 per complessive 4 ore.

Il Corso si articolerà in 36 settimane, ripartite in tre trimestri (gennaio-marzo, aprile-giugno, settembre-novembre).
Le attività didattiche del III trimestre saranno differenziate a seconda dell'indirizzo scelto.
Il Corso si concluderà con l'elaborazione di una tesi di specializzazione.
La frequenza non potrà essere inferiore all'80% delle ore di lezione impartite, pena l'esclusione.

INSEGNAMENTI IMPARTITI
I TRIMESTRE DI FORMAZIONE GIURIDICA:
Diritto Civile; Diritto Penale; Diritto Amministrativo; Diritto Processuale; Diritto Assicurativo.
II TRIMESTRE DI FORMAZIONE TECNICA GENERALE:
Consulenza Tecnica Giudiziaria; Dissesti e Crolli; Ingegneria della Sicurezza; Incendi ed Esplosioni; Impiantistica Industriale Forense; Estimo Forense.
III TRIMESTRE DI FORMAZIONE TECNICA SPECIFICA:
- *Attività di indirizzo in Ingegneria Forense Civile:* Prove e Monitoraggio Strutturale; Ingegneria Geotecnica Forense; Impianti Tecnici per l'Edilizia; Gestione dei Lavori; Ingegneria Ambientale Forense; Tecniche di Rilievo e Rappresentazione.
- *Attività di indirizzo in Ingegneria Forense Industriale:* Ingegneria Forense Meccanica; Ingegneria Forense Chimica; Ingegneria Forense Elettrica.

TITOLI PER L'AMMISSIONE
- Laurea quinquennale in Ingegneria
- Laurea Specialistica in Ingegneria
- Laurea in Ingegneria Edile-Architettura
- Titolo equivalente rilasciato da Università straniere

ISCRIZIONE
Domande presso la Segreteria Studenti della Facoltà di Ingegneria - Napoli, Piazzale Tecchio n. 80
Contributo di iscrizione pari a 2.600,00 €, da versare in due rate entro il 09.01.2009 ed entro il 30.06.2009

DOCENTI
Le attività formative (corsi, seminari, conferenze) saranno svolte da professori delle Facoltà di Ingegneria e di Giurisprudenza, da magistrati e da liberi professionisti esperti in Ingegneria Forense con l'obbiettivo di affiancare ai principi teorici la trattazione di casi reali, frutto di esperienze maturate in ambito giudiziario sia civile che penale.

Figure 1. Poster on the 2nd level Master on Forensic Engineering at Naples.

MASTER PROGRAMME AT UNIVERSITY OF NAPLES FEDERICO II

The 2nd level Master on Forensic Engineering take place at the Department of Structural Engineering, University of Naples Federico II (see the webpage www.ingegneriaforense.unina.it). The courses are divided into three quarters which deal with fundamentals of law, engineering subjects common to civil and industrial areas, and advanced engineering topics which are specifically addressed to civil or industrial areas.
In particular, the first quarter includes the following subjects: civil law; criminal law; administrative law; process law; and insurance law.
The second quarter comprises: forensic technical consulting; failures and collapses; safety engineering; fires and explosions; forensic industrial plants engineering; and forensic estimate.
Finally, the third quarter is divided into the following areas: civil forensic engineering and industrial forensic engineering. the former includes: testing and structural monitoring; geotechnical forensic engineering; building plants; works management; techniques of survey and graphics; and environmental forensic engineering. the latter includes: mechanical forensic engineering I; mechanical forensic engineering II; chemical forensic engineering I; chemical forensic engineering II; electric forensic engineering I; and electric forensic engineering II.
A MSc thesis will be discussed at the end of the Master courses by each post-graduate student.
The Master school is directed by the author of the present paper and members of Scientific Board are: prof. E. Cosenza (dean of the Faculty of Engineering); prof. L. de Giovanni (dean of the Faculty of Law); prof. E. de Rosa (coordinator of the industrial area); prof. G. Manfredi (director of Department of Structural Engineering); prof. V. Patalano (coordinator of the judicial area and vice-chancellor of University of Naples Federico II). The logo of the Master school is showed in Figure 2.

Figure 2. Logo of the Master on Forensic Engineering at Naples.

FURTHER ACTIVITIES IN ITALY

Since the beginning of the new millennium three Conferences on Collapses, Reliability and Retrofit of Structures were already held in Italy on 2001 (Venice), 2003 (Naples), and 2006 (Messina). The topics of these conferences are de facto a part of the wider field of Forensic Engineering. This is why the University of Naples

Federico II has organised the **IF CRASC'09** Congress, that is the fourth Congress on Collapses, Reliability and Retrofit of Structures (**CRASC**, in Italian) joined to the first Congress on Forensic Engineering (**IF**, in Italian). **IF CRASC** is thus a natural evolution of the traditional field of interest of Structural Civil Engineering to the industrial area and engineering legal aspects. Such a Conference will be held on December 2-4 of the present year at Naples.
The logo, specifically created for this Congress, is intended to express the indissoluble contiguity of the themes of Forensic Engineering with Collapses, Reliability and Retrofit of Structures, born in 2008 and 2000, respectively, close to the Mt. Vesuvius under initiative of University of Naples Federico II (see Figure 3).

Figure 3. The logo of IF CRASC Conferences.

Aim of IF CRASC'09 is to promote the exchange of knowledge and experiences between academics, professionals, public servants, operators of private companies, jurists and magistrates, in their own respective fields of work in Civil and Industrial Forensic Engineering.
This initiative is aimed, however, also to encourage a new synergy among engineers, lawyers and judges in order to contribute to a better administration of justice and to a spreader legality.
Third objective is to create a new professional figure of Forensic Engineer by defining its own skills and regulating its job activity. In this way, the Congress is also aimed to gather all the engineers engaged in the activity of technical consultant for judicial authority or parties, in the frame of dispute resolution, whose professional figure is not officially recognized.
Main topics of IF CRASC'09 are: engineering legal aspects; civil forensic engineering; industrial forensic engineering; education and ethics; collapses and failures; structural reliability; and retrofit of structures.
Delegates should present the paper at the conference during oral or poster sessions. Italian and English will be the official languages of the Conference for both oral and poster presentations. For more information about this initiative one can refer to the webpage www.ingegneriaforense.unina.it and/or send an email to the address ingegneria.forense@unina.it.
American Society of Civil Engineers (ASCE), and specifically its Technical Council on Forensic Engineering (TCFE), is also promoting IF CRASC'09 Conference and abstract proposals are encouraged from USA.

CONCLUSIONS

The 2nd level Master course on Forensic Engineering instituted on August 6, 2008 by the Faculty of Engineering at University of Naples Federico II is the first one in Italy and Europe (with exception of United Kingdom). Aim of the Master programme is to create two skilled professional figures able to fulfil the role of technical consultant for the judicial authority: the Civil Forensic Engineer and the Industrial Forensic Engineer. Professors of the Faculties of Engineering and Law are involved in the Master school and teach eighteen courses of engineering and five of law, respectively. Therefore, post-graduate students learn not only advanced engineering tools, but also fundamentals of law, so a complete professional ability is reached.
The Master degree organised by University of Naples Federico II is the first step towards the dissemination of Forensic Engineering in Italy. IF CRASC'09 Congress that will be held in Naples on December 2-4, 2009 is another initiative aimed to promote exchange of knowledge about Forensic Engineering, as well as collapses, reliability and retrofit of structures.

Education: The Challenge and How Forensic Engineering Can Help

D. T. P. Phillips PhD PE CEng[1]

[1] *Senior Lecturer, Faculty of Science and Engineering, University of Limerick, Limerick, Ireland, P: +353 (0)61 202683, E: declan.phillips@ul.ie*

ABSTRACT

Education of construction professionals for a dynamic and challenging industry requires a sea change in how we educate. The traditional didactic methods no longer engage the student who operates in a world of instant information, instant messaging and instant coffee! The student body are no longer prepared to be drip fed information in discrete modules on diverse civil engineering topics. Furthermore, at the end of a bachelors degree, these modules will not necessarily coalesce to produce a competent well rounded graduate ready for training in the practice of engineering.

The traditional lecture based method is, at best, challenged to produce graduates with the skills needed in a 21st century economy. Therefore, engineering education needs a unifying student led approach to direct their learning. Many professional bodies have recognised the need for change and accordingly commissioned vision reports to chart the skills demanded by the environment in which we now operate. To this end, the following paper summarises how forensic engineering can be used as a means of promoting problem solving skills in undergraduate students. I argue that forensic engineering case histories provide the means of developing these skills and others without impacting on the technical rigour demanded of an accredited engineering programme.

INTRODUCTION

We operate in an environment where information is instantly available. Certainly the undergraduate student exploits this to a maximum. However, what is often lost in this transaction is the rigour required of the student to understand and synthesise the information. This takes much greater effort than merely reviewing the information. Michael Jordan (the legendary Chicago Bull) remarking on his success stated "I have missed more than 9000 shots in my career; I have lost almost 300 games. Twenty six times, I've been entrusted to take the game winning shot ……. and missed. I have failed over and over again in my life and that is why I succeed." Like Jordan, crafting the skill of perseverance when solving problems must be cultivated in the student if they are to succeed in the 21st century. A successful learning experience can be a solitary journey and the pace of learning does not always ensure a speedy outcome or

triumph at the first hurdle. Nevertheless, the sense of accomplishment when understanding is reached makes the endeavour worthwhile.

The paper summarises how I draw upon forensic engineering and the literature on teaching and learning to develop the desired learning outcomes in undergraduate students. Issues presenting obstacles to learning, at least in an Irish context, are also presented although; anecdotal evidence suggests the same issues transcend all international boundaries and waters. A case history involving a fatal foundation failure is used to orientate an investigative programme involving model foundation tests.

WHAT ISSUES ARE CAUSING PROBLEMS

Our educational methods have substantially remained as they were a century ago; the lecture, tutorial and laboratory are virtually unchanged. Using an analogy with the newspaper industry, we know the sale of newspapers throughout the world is diminishing and many newspaper companies face receivership. This is because the 'news' is now instantly available through the internet and mobile phones. So the paper media must innovate or become extinct. We continue to transmit our information in large theatres to an audience who now operate with a different currency – digital media. Perhaps this explains why student retention in mathematics, science and engineering remains a problem. Attracting and retaining bright students into the profession may be better served if we as educators also move with the times. We need to modify our teaching and assessment methods so that they facilitate the lifestyle of today's learner, for example, could a well rehearsed lecture be transmitted on-line and the lecturers' time more effectively utilised by designing and facilitating small group based challenges or exercises?

A second factor, free university fees are available (at the time of writing) to all Irish students provided they reach the required academic standard in their second level examinations. This may have invoked subliminal messages on the perceived value of education. The construction boom over the past 12 year has resulted in the current generation of graduates obtaining their choice of employment opportunities with attractive salaries. Never before has this small island nation experienced the construction of so many new buildings, roads, bridges, tunnels and ports. However, this period in our history has come to an abrupt end, prompted in part by the uncertainty in world markets. This unfortunate situation serves as an opportunity for students to re-focus on the value of their education and the role it plays in obtaining employment in a very competitive world.

Finally, personal and social problems are far more prevalent in today's undergraduate. These issues add an extra dimension to the challenge of teaching, and need to be addressed with sensitivity and care. Most educational institutions have pastoral and counselling centres for students, but as educators we need to be cognisant of the fact that we are often in a position to first recognise when a student is having difficulties and requires assistance.

HOW TO TEACH

It is easy to recognise excellent teaching, a skilled teacher can engage a class and inspire a student to explore and experience the pleasure of becoming a problem solver. Inevitably such teachers have a good rapport with their students. If one has been privileged to experience (at least) one wonderful teacher, the encounter creates a lasting impression. Albom (1997) rhetorically extols the virtues of such a teacher:

> "Have you ever really had a teacher? One who saw you as a raw but precious thing, a jewel that, with wisdom, could be polished to a proud shine?"

Many engineers become teachers upon receipt of a PhD. Without formal training in the skills of the craft, they tend to teach the same way that they were taught. So, if poor teaching has been their dominant experience, such experiences are likely to be replicated in their approach and so the cycle of poor teaching prevails.

Dennis and Larson (2005), quoting a study by Seymour and Hewitt, present the damning result that, the overwhelming majority of math, science and engineering (MSE) students in the United States cite poor teaching as the number one reason students leave MSE programmes. Clearly a change in our approach to teaching engineers has become a priority.

The American Society of Civil Engineers (ASCE) is to be commended in this regard. Over the past decade they have championed and financially supported the ExCEEd (Excellence in Civil Engineering Education) programme. Over 500 practicing university teachers have graduated from the one-week intensive programme with skills enabling them to become more effective teachers. These ambassadors of excellence in teaching have no doubt, initiated a redress of the Seymour and Hewitt findings.

ESSENTIAL CHARACTERISTICS FOR EFFECTIVE TEACHING

One must be fundamentally interested in teaching, be passionate about their subject and like being around young people. In my experience, the following can be considered the minimum essentials for effective teaching

Knowledge of Learning Styles

As Plato (c380 BC) noted, one must know something about the learner to teach them. Often when we teach we use one mode of delivery for 'all' students, yet different students learn in different ways. Our educational system today continues to "teach" in large lecture halls filled with students in the notion that real and deep learning is taking place. This 'one size fits all' approach to learning is not supported by the research. Felder and Spurlin (2005) use the 'Index of Learning Styles' (ILS) model to illustrate the non-homogeneity of learning styles that exist within a student

cohort. Personal experience indicates that even within groups as small as eight, the learning styles can be quite diverse (Phillips, 2009). Therefore opportunities for students to learn through the various learning style dimensions must be presented with every teaching opportunity. This enables students to develop the skills to act in variable and unfamiliar learning contexts and to manage learning tasks independently and professionally.

Blooms Taxonomy

Bloom (1956) outlines the hierarchical nature of learning and the importance of giving students the opportunity to operate at each level of learning (Figure 1). Bloom's taxonomy facilitates the structuring of learning outcomes so that student performance in the cognitive domain can be evaluated.

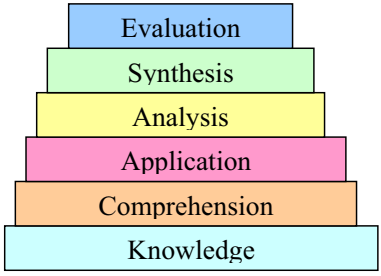

Figure 1: Bloom's Taxonomy for the Cognitive Domain

The Power of Oration

Thankfully the art of story telling is a skill that will transcend and surpass the communication 'gimmicks' advanced by the techno-age. Prior to the invention of print, and the advent of the internet, people used stories to pass cultures and traditions from generation to generation. This is just as prevalent today; I watched in admiration as President Obama wooed a nation and captivated the world with his oratory abilities. In his victory speech in Chicago's Grant Park, President Obama captured the attention of the audience right from his opening line "Is there anyone out there who still doubts that America is a place where all things are possible, who still wonders if the dreams of our founders is alive in our time, who still questions the power of our democracy, tonight is your answer" (Obama, 2008). The president went on to tell of the life experiences of Ann Nixon-Cooper, a 106 year old Afro-American lady from Atlanta The images painted in our minds were vivid, as if we personally met Ms. Nixon-Cooper and listened to her story spanning over a century of life in America.

Imagine the power of such an approach in education not to mention the increase in attendance at lectures! Replacing the in-flexible and much loved crutch of PowerPoint as a teaching tool with wonderful stories and lessons form civil engineering's rich legacy is a winning formula. I understand that the late Professor Ralph Peck successfully adopted this approach exclusively in his teachings on soil mechanics and foundation engineering (DiBiagio and Flaate, 2000). In creating the context for learning using personal experience and anecdotes, Professor Peck became internationally known as a passionate and outstanding educator. For example, in "Art and Science in Subsurface Engineering," Peck (1962) craftily draws upon the observational and diagnostic skills of the medical practitioner to illustrate how these same skills can be developed in the geotechnical engineer when assessing challenging problems in ground engineering. Unfortunately, the academic profession today lacks people with Professor Peck's portfolio of professional practice. Instead recruitment of faculty in 2009 favours research orientated individuals over practitioners.

TURBULENCE BETWEEN RESEARCH AND TEACHING

In a thought provoking paper, Felder (1994) highlights the different goals of teaching and research and makes the case for striking a balance between researchers and practitioners on university faculty. Dennis and Larson (2005) also allude to the different goals of teaching and research and propose a broadening of the term 'scholarship' to incorporate the exemplar teacher in addition to the researcher so the educational interests of tomorrow's engineers are better served. The following extracts from Felder (1994) highlights the differences between teaching and research:

> "It is no secret that **research** is a major time sink. It takes time - preferably in large uninterrupted blocks - to define problems, generate support, collect, read, and understand all relevant published work on the topic, plan a method of attack, make false starts and wander down blind alleys, wait out the inevitable unproductive periods, clean out logical flaws or weak points, replicate experiments, explore possible consequences and applications of results, write papers, and give seminars. Doing all that is under any circumstances a full-time job; doing it well enough to gain national recognition - now the principal criterion for promotion and tenure almost everywhere - requires an intensity of effort that tolerates few distractions.
>
> That excellent **teaching** takes just as much time and intensity of effort is not as well appreciated. …. Most course notes and texts are written from the point of view of someone who already understands the concepts …. To make it comprehensible to most students, the instructor must first provide examples to establish relevance and motivate interest …. and finally provide more examples and participatory exercises to solidify understanding. Finding a way to do all that for just one relatively straightforward concept can take hours or even days - and a course contains lots of concepts.

> Making up good problems is another time-intensive chore. Students almost never learn anything nontrivial in formal lectures…. For true learning to take place, however, the problems must vary in scope and difficulty …... Relatively few textbooks offer problems that provide the necessary variety and scope; the burden on the instructor is to collect problems from several sources and to make up and work out solutions to others. Doing so takes *immense* amounts of time."

Felder (1994) in acknowledging these differences offers advice and guidance on how we might accomplish a balance between the important role of research and the need for excellence in teaching to inspire creativity and thinking that lead to independent learners.

THE UNIVERSITY OF LIMERICK RESPONSE

In President Kennedy's 1961 address to the US congress he outlines a vision to put a man on the moon. Kennedy states "For while we cannot guarantee that we shall one day be first, we can guarantee that any failure to make this effort will make us last." It is in this spirit that we must reform how we educate the engineer of tomorrow. To this end, the University of Limerick's new programme in civil engineering present a number of deviations from the 'traditional' programme (http://ulcivilengineering.blogspot.com/) the main differences being:

- The programme is delivered through a blend of problem based learning (PBL), workshops and seminars.
- All core staff lecturing on the programme has, at a minimum, five years experience in professional practice and are chartered members of the professional body.
- The programme team is led by a professor with over twenty-eight years in professional practice designing some of the most challenging structures built in Ireland.
- All core staff receive professional training in 'teaching engineering' during their first year of employment.
- The civil engineering students are educated alongside architects; the other primary stakeholders in the building profession.

HOW FORENSIC ENGINEERING CAN HELP

A first year engineering module introduces the fundamentals of structural and geotechnical engineering. This is done in the absence of any formal instruction in the disciplines. The goal is to focus on an interesting engineering case that illustrates an important lesson or concept while encouraging learning and inspiring further self directed research in the area. Strategies for incorporating forensic engineering case histories in geotechnical engineering are outlined in Phillips and McCabe (2007) and Phillips (2008). This paper summarises a foundation failure that caused the collapse of a five storey building on Manhattan's Lower East Side (Figure 2). The collapse is

investigated using model foundation tests designed to replicate the conditions observed during the actual forensic engineering investigation (Figure 3). The case history and model foundation tests are an interesting preface to a discussion on the effects of eccentric loading on foundations.

Figure 2: Collapse of the five storey masonry structure during renovation works (Source Kaminetzky (1991)).

Figure 4 illustrates the building anatomy and renovation work underway on a five storey building over basement. The investigation uncovered errors in both design and supervision of the works but Kaminetzky (1991) concludes the failure was triggered during placement of a 90mm thick concrete slab on the third floor (Figure 4a).

Several of the foundations were found to be cast at less than half the size on the design drawings. Of the three interior foundations, two had been cast eccentrically to the centre line location (Figure 4b). The report describes these foundations as being visibly tilted and pitched from one end to the other by up to 127mm. A follow up analysis of the loads acting at the time of the collapse revealed that even under the optimum possible bearing capacity, the soil beneath these foundations experienced a 25% over stress on its ultimate capacity and therefore 'had to fail.' This case emphasises the need for a detailed method statement outlining the work schedule and sequences for foundation renovations in old structures. The discrepancy between the as-designed and as-constructed foundations is shown in Figure 5. Model pad foundations similar to those employed in the case study are tested in the laboratory under concentric loading and the results compared to the findings when the footings are loaded eccentrically. Soil information associated with the tests is limited to grading characteristics and relative density (D_r). Figure 6 confirms the compromised condition of the Delancey Street footings

(a) Embedded 50 mm Square Pad

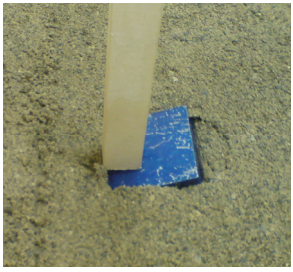

(b) Eccentrically loaded 50 mm Square Surface Pad

Figure 3: Model Tests on Pad Foundations.

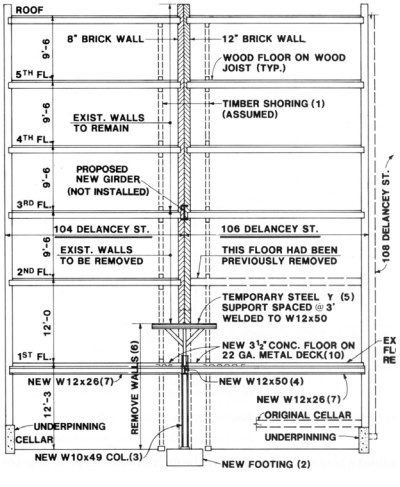

a) Cross Section

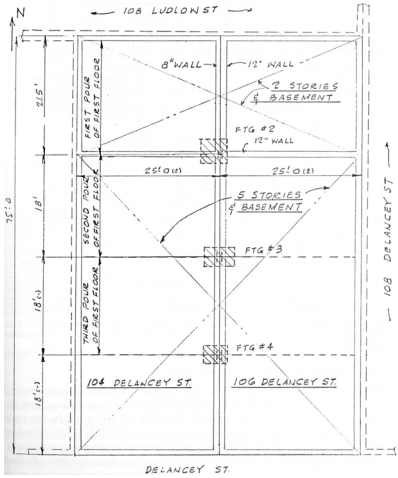

b) Foundation Plan

Figure 4: (a) Cross section showing temporary works (b) Foundation Plan (Source Kaminetzky (1991)).

FOOTING SIZE AND AREA			
FOOTING NO.	AS DESIGNED	AS CONSTRUCTED	REMARKS
FOOTING #2	5'-6"X 8'-6"=46.75sf	4'-8"X4'-7"= 21.4 sf	FOOTING CAST ECCENTRIC TO SUPPORTED COLUMN
FOOTING #3 (TOP AREA)	5'-6"X7'-0" = 38.5sf	5'-9"X3'-6" = 20.1 sf	FOOTING CONCENTRIC WITH SUPPORTED COLUMN BUT SIDE SLOPES, RESULTING IN AN ECCENTRIC BEARING SURFACE
FOOTING #3 (BOTTOM AREA)	5'-6"X7'-0" = 38.5sf	3'-9"X 3'-6" = 13.1sf	
FOOTING #4	5'-6"X7'-0" = 38.5sf	4'-2"X 3'-4"=13.9sf	FOOTING CAST ECCENTRIC TO SUPPORTED COLUMN

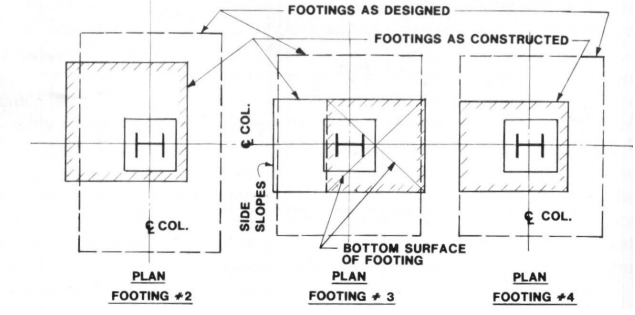

Figure 5: Details of the as designed and as constructed footings at Delancey Street (Source Kaminetzky (1991)).

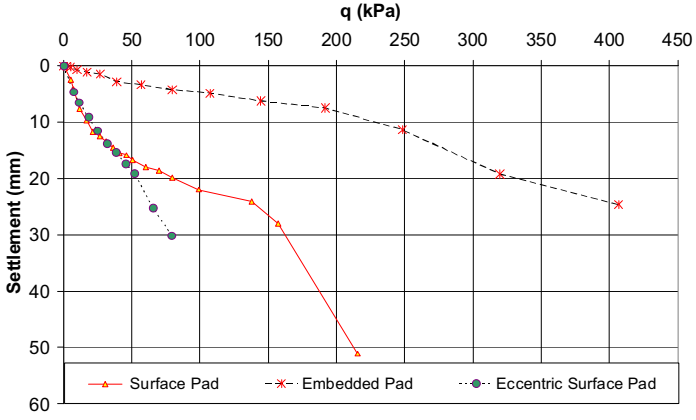

Figure 6: Influence of eccentric loading and embedment on 76mm square pads (Sand D_r = 60%).

CONCLUDING REFLECTION

In my opinion, a successful teacher must embrace change and be innovative in their pursuit to capture the imagination and creativity locked in the minds of every young student. Forensic engineering case studies play an important part in facilitating these outcomes particularly when merged with laboratory and/or field experimentation. They provide for effective learning and training of engineers. The simplistic approach of 'learning by doing' engages the student and focuses their attention, in this case, on the critical modes of shallow foundation failure. This is accomplished with basic engineering concepts of density and stress. To be successful, this approach must be informed and underpinned with a sound understanding of the fundamentals of teaching and learning.

REFERENCES

Albom, M. (1997). *Tuesdays with Morrie,* Time Warner Paperback, ISBN 0 7515 2737 8.

Bloom, B. S. (1956). Taxonomy of Educational Objectives: Cognitive Domain, Longman, N.Y.

Dennis, N. and Larson, D. (2005), *Defining Who Should Teach the Body of Knowledge*, Proceedings, 2005 ASEE Annual Conference, Portland, OR, June 12-15, No. 1789.

DiBiagio, E. and Flaate, K. (2000). *Ralph B. Peck: Engineer, Educator, Man of Judgment,* Pub.No. *207,* NGI Publication Series.

Felder, R (1994). *The Myth of the Superhuman Professor.* J. Engng. Education, 82(2), pp. 105-110.

Felder R. and Spurlin, J. (2005). *Application, Reliability and Validation of the Index of Learning Styles*, Int. J. Engng. Ed., Vol. 21, No1, pp. 103-112.

Kaminetzky, D. (1991). *Design and Construction Failures: Lessons from Building Failures*, McGraw Hill, ISBN 0070335656.

Obama, B. (2008). *Change we can believe in,* Canongate Books, ISBN 978 1 84767 432 6.

Peck, R.B. (1962). *Art and Science in Subsurface Engineering*, International J. of Soil Mechanics & Foundations, Geotechnique, pp. 60-66.

Phillips D.T. (2008). *Benefits of case based instruction in undergraduate geotechnical education*, Paper 11.14a, Sixth International Conference on Case Histories in Geotechnical Engineering, Arlington, Va.USA. August 11-16, 2008.

Phillips, D. T. and McCabe, B.A (2008). *Launching Geotechnical Education into the 21st Century,* 1st Int. Conf. on Education and Training in Geo-Engineering Sciences: Soil Mechanics and Geotechnical Engineering, Engineering Geology, Rock Mechanics, pp.439-442, CRC Press, ISBN 9780415475938.

Phillips, D. T. (2009). *Learning styles of first year construction management and engineering students from 2006 to 2009,* unpublished data.

Wind Related Failures of Temporary Construction Installations

Dan Eschenasy, PE, M.ASCE, New York City Buildings Department
Deschenasy@buildings.nyc.gov

Introduction

The intent of the paper is to instigate a discussion on the adequacy of wind design and construction practices for temporary installations such as scaffolds, formwork or sidewalk sheds. The paper presents data collected on incidents ranging over a period from January 2006 to July 2009. It describes patterns of collapse for various types of installations following gusts in the range of 40 to 60 mph, significantly lower than the code specified wind speeds. Some of the collapses led to worker and pedestrian injuries. Two cases involved a fatality each.

In all the cases, the forensic investigators determined without difficulty that accidents were due to improper contractor practice and/or lack of engineering design. The author suggests that the accidents could have been avoided by some basic rule of thumb instructions. The relative low wind pressures that led to the collapses might also require clarifications and reevaluation of some wind design requirements for temporary installations.

History of Wind Regulation in New York City

Up to 1968, the New York City building codes paid limited attention to wind loads and design. The code allowed the wind loads to be neglected for most structures under 100ft. For the other structures the designer had to provide for a wind load to of 20 psf independent of the height of the structure. The 1968 Building Code introduced requirements that all buildings be designed for wind and introduced wind pressures dependent on height. The 2008 Building Code aligned itself for the most part to the ASCE 7, *Minimum Design Loads for Building and Other Structures*, but also for buildings less than 200 ft (300 ft in Manhattan), it gives the designers the latitude to use simplified provisions that are similar to the 1968 Code. No major tall building accidents were recorded in the city on buildings built before 1968. The new code does not introduce any major change in the provisions for the wind design of temporary construction installations described in the Chapter 33 –Safeguards During Construction or Demolition. Nor are there any new significant wind related measures for site safety.

ASCE 37 Design Loads on Structures during Construction is not specifically referenced by the new building code, but calculations based on its load combinations and reductions are accepted by the New York City Buildings Department (the department).

Data on Wind Related Incidents

The data analyzed in this study covers the period from January 2006 untill July 2009 and was extracted from the department's incident database. For the purpose of this study, an incident is defined as a call to the department's emergency operation center that resulted in sending an inspector to investigate within a very short period of time, usually one hour. Almost each incident could potentially result in a person being injured or in serious property damage. The calls to the center are usually made by city agencies such as police, fire or the Office of Emergency Management and are based on credible reports from the field.

The period studied was characterized by unprecedented construction activity in the city. Over this period, every year, the number of incidents of all types has increased. This does not necessarily reflect an actual increase in the number of incidents or construction activity, but more accurate reporting. It is a result of the department's efforts to improve accountability, enforcement and response time. There is thus a slight bias in the data. More and more, high rise construction incidents are called in the emergency center by department's own inspectors based on information received from site safety managers employed by the contractors. There were no such wind related calls in 2006 against 15 in the first half of 2009. The slight bias is thus towards events involving construction activities on high rise buildings, especially in 2009.

We excluded from the statistics incidents produced by falling trees. Over the period, there were 13 such incidents. Some of them resulted in buildings being vacated as the felled trees had blocked exits or destroyed fire escapes. Typically these events did not involve injuries. They are excluded from further discussion as tree protection, inspection and care are not covered by the Building Code.

Wind Conditions. There were seven days when we registered more than five wind related incidents. In each gusts were reported over 40 mph. The wind event in each of these seven days appears to have lasted several hours, although reliable data on the duration was not found. See Table 1. Particular wind conditions at individual locations are not known.

An experiment compared wind speed readings at JFK, LaGuardia and Newark airports as well as Central Park meteorological stations to those recorded continuously at a downtown construction site where anemometers had been installed at several levels. As expected, the correlation was poor.

From October 2007 the department has issued 48 wind advisories that require specific precautionary inspection and site housekeeping actions. To keep the data normalized, the events during a local tornado that occurred in Brooklyn were not included in the statistics.

DATE	Max. Gusts (various sources)	Max. Wind LGA	Max. Wind JFK
Saturday, October 28, 2006		34 mph	37 mph
Wednesday, August 08, 2007	55 mph	21 mph	22 mph
Monday, December 03, 2007		32 mph	33 mph
Wednesday, January 30, 2008	51 mph	33 mph	37 mph
Saturday, March 08, 2008	51 mph	34 mph	39 mph
Tuesday, June 10, 2008	55 mph	39 mph	22 mph
Thursday, February 12, 2009	55 mph	43mph	37 mph

TABLE 1 High Wind Days

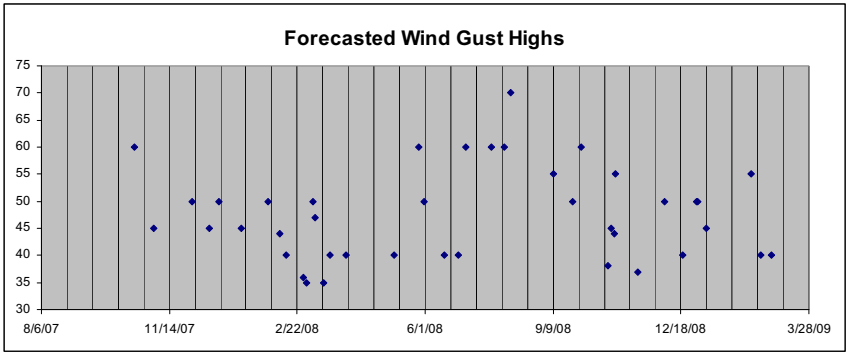

PHOTO 1 Advisories issued since Oct. 2007 – based on forecasted gusts.

Tornado in Brooklyn. In the early morning hours of July 8th 2007 an EF-2 tornado hit the Bay Ridge and Sunset Park residential areas of Brooklyn. There was no significant warning before the event. The tornado was of short duration and winds reached speeds between 110 and 135 mph. It was only the fifth tornado to hit the city since 1950.

The building stock in the affected areas consisted of attached two and four story bearing masonry structures supporting wood joists Some facades had brick veneer on wood studs. The damage was located on several blocks some noncontiguous with some additional individual buildings located hundred of yards away. The typical damage was located at cornices and roofs. Several chimneys fell puncturing the neighboring roofs. Building Department inspectors used ATC forms to inspect the blocks affected. DOB has vacated 20 properties and partially vacated 17 properties in the Bay Ridge and Sunset Park area. 2 buildings had to be demolished. The building damaged and incidents related to the tornado and enumerated in this section, were not included in the statistics discussed further in this paper. See Photo 2

The discussion in this paper, however, incorporates the incidents that occurred the same day in other city neighborhoods where gusts reached about 50 mph.

Injuries and Fatalities. There were 13 incidents involving fatalities and injuries. Multiple injuries occurred in two fence collapses during which four and respectively two people suffered minor injuries. In one scaffold accident, one person died and another was injured. Only one injury occurred in an event in an existing building and in the absence of construction activity.

Photo 2 Bearing wall collapse during tornado

Photo 3 CMU wall collapse lead to fatality

Construction Related Incidents.

The data is classified in two major categories depending on whether or not it is the result of construction operations. The *Construction* category includes also events that do not involve construction activity per se, but that entail temporary installations required to support construction operations. A cursory review of the data in Photo 4 reveals that the largest percentage of incidents belongs to the *Construction* category. Both fatalities and 16 of the 17 injuries were in *Construction*. Within this category the largest number of incidents involves temporary construction installations. In most cases, these installations should be engineered or should be installed based on standardized drawings or procedures.

The *Non-Construction* category denotes events that involved existing buildings (that were not undergoing repair). The vast majority of these incidents involve some failure of the envelope, usually localized at roofing, parapet or cornice. There was one case of a wood frame vacant building that collapsed. These *Non-Construction* incidents were not analyzed in detail for this study. Ratios of *Construction* to *Non-Construction* seems to vary for different high wind days. Surprisingly, no significant difference was noted when the ratios were calculated with incidents for the seven high wind days removed from consideration. The assumption was that in these days, with higher gusts and winds sustained for longer time periods, there would have been more façade damage.

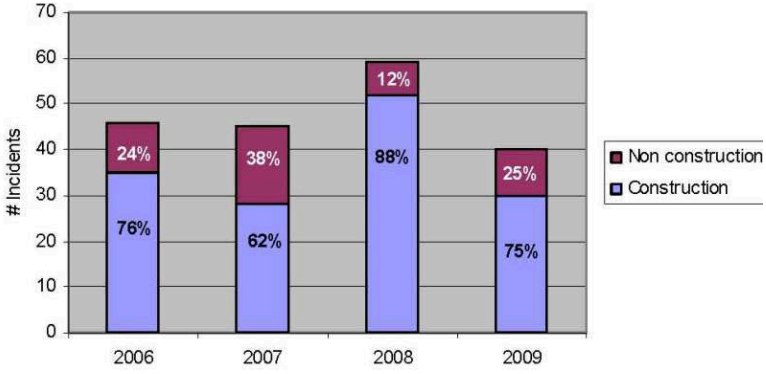

PHOTO 4 *Construction* vs. *Non-Construction* wind incidents.

Fatalities during Construction Activities. During a wind event that reached 45 mph gusts an 18 ft tall scaffold collapsed. The scaffold had been installed on the roof of a 13 story about to be completed building. It was used by workers placing stucco on the bulkhead. The scaffold was wrapped with 2lbs mesh. As a result of the collapse, one worker died and one was injured. In an unpublished draft report, Deodat Ramsarran of the Forensic Engineering Unit found the scaffold to have been assembled with frames of different makes, from disparate manufacturers. The scaffold had been attached to the wall with 20 gage wires that were not sufficient to prevent overturn.

A 30 ft high unsupported wall fell over a construction worker on a day that registered 45 to 55 gusts. The initial forensic findings indicate that the wall was not supported, the reinforcement was improper and there was poor adherence of the mortar to the bloc. The un-shored wall collapsed during a sudden gust. See Photo 3.

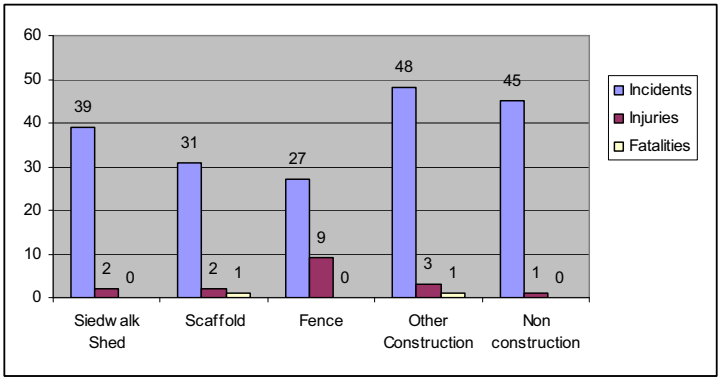

Photo 5 Injuries and Fatalities

Although neither report was final at the time of the writing of this paper, it seems obvious that poor construction practice was the cause. The sudden wind load only exploited the deficiencies.

Temporary Construction Installations

The list Construction incidents includes one building collapse and two serious glass curtain wall events. These do not seem to be typical. Temporary installations (scaffolds, sheds, fences and formwork) account for over three quarters of the total. See Photo 6. Construction wind related incidents are discussed in the rest of the paper.

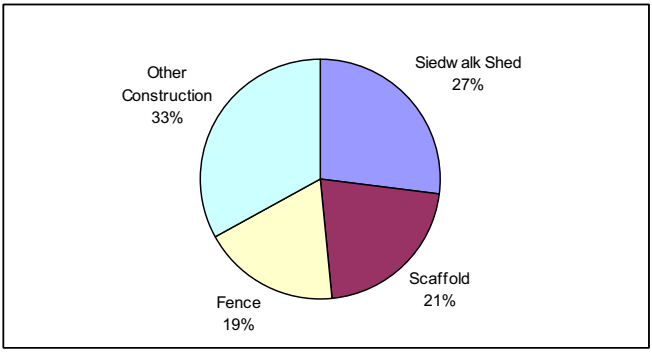

Photo 6 Distribution of temporary installation incidents in *Construction* category

Construction Fences. There were 29 fence failures related to wind. Many involved separation of the plywood from the post; others were described as partial collapse (overturn) exceeding 8 feet in fence perimeter length. This is the category with the most injuries, albeit minor. There were 4 events that resulted in 9 injuries. The building code requires the fences to be built solid and be eight feet tall. It does not provide specific details on how to install or design such fences. Some additional simple instructions such as minimum number and type of nails could reduce the accidents.

Sidewalk Sheds. The sidewalk sheds are structures intended to protect pedestrian from falling objects resulting from defective facades or from construction activities. They are most often installed following the discovery of a façade defect, and are kept in place until the repair is concluded. Because many times the installation follows a professional's determination that a potential dangerous façade condition might be present, the speed of erection and the immediate availability of components are of essence. The code requires the installations to be designed to sustain a 300 psf or a 150 psf vertical load, to account for the potential impact of falling debris, but the posts are set on the existing sidewalk surface without any foundation or penetration.

Typically, the legs are not anchored to the sidewalk, nor are the frames to the building. The common designs use one of the two department approved prototypes. These prototypes were approved in the 1950s, a period when wind design was not required by code.

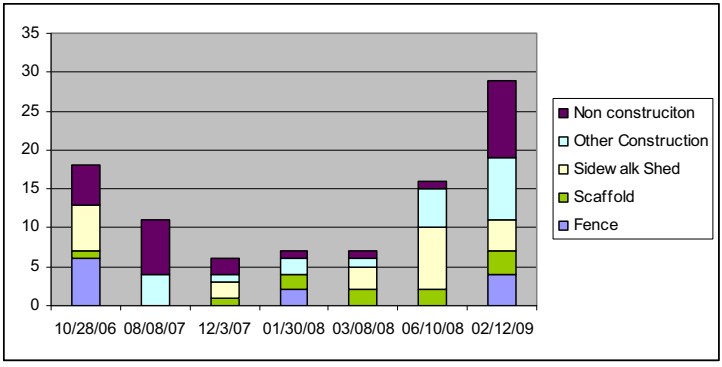

Photo 7 Distribution of incidents - High Wind Days

There have been 39 wind related sidewalk shed incidents. They ranged from one sheet of parapet flying in the wind to entire installation overturning. The overturning occurs when the shed is not loaded. The failures did not produce any pedestrian injuries, but destroyed the vehicles parked in front. See Photo 9.

Photo 8 Form collapse at 15th Floor

Photo 9 Sidewalk shed overturn

Simplified stability calculations of some of the overturned sheds, proved that these configurations were liable to overturning, but at wind pressures somewhat higher than the gusts registered citywide the day of the collapse. Calculations using ASCE -7 open building formulas yield larger pressures and uplift and seem to predict more closely the overturning. At the time of this writing, a competition for new sidewalk shed designs is taking place. It is intended to improve both the safety and the aspect of these installations

Scaffolds. There were 31 scaffold wind related incidents. Aside the accident described above that involved one fatality and one injury; there was another resulting in an injury. This category covers both hanging scaffolds (6 incidents) and supported scaffolds (25 incidents). In 7 incidents, the supported scaffold was described as leaning due to improper attachments to the building. In 13 incidents, entire scaffolds or significant sections actually collapsed. In most of these cases it was due to insufficient or defective ties to the building. During two of the suspended scaffold accidents workers were stuck in the air during high winds.

The building code requires plans and/or specifications to be submitted for all scaffolds taller than 40 feet. The designs, including the anchorage to buildings, need to provide a minimum factor of safety of four. In the vast majority of cases scaffolds are assembled using steel or aluminum stock pipe frames. They are enclosed with wire or plastic meshes. Typically, the wind calculations apply the wind pressure only on the area of the weave, totally discounting the aperture area. This is most likely insufficient, but there are no code provisions or other engineering guidance as to what percentage of the covered area should be considered.

Formwork for Concrete Operations. There were five formwork shoring incidents. Another five incidents involved plywood used as formwork. One of the incidents involved the collapse of the entire formwork and shoring at the 15th floor of a construction site. Site stabilization and debris removal required two days of traffic stoppage on the major artery in front of the construction site. The investigation concluded that the shoring had been installed without sufficient bracing. See Photo 8 During an incident at a different site, the formwork flew off the 17th floor unto the avenue below. The shoring had been sufficiently braced and did not suffer. Under the wind uplift pressure the formwork had dislodged and bent the rebars already installed. The traffic had to be stopped for 12 hours.

The code requires formwork shoring design only for formwork shoring installed over a 14 ft. height. In most cases, contractors reuse the same typical drawings. These drawings or the manufacturer instructions, in the case of prefabricated support frames, indicate the need to brace the system, but do not provide specific details. The drawings also do not take in account the increase in wind pressures as the construction reaches higher elevations. Investigations proved that when installed, the bracing and anchoring can maintain the stability of the supporting frames.

Calculations of formwork uplift are not being performed and there is no special technical consideration given to the possibility of such event. Simplified calculation performed by this engineer, using a base 45-50 mph wind speed, assumed present during the specific accident, did not show uplift of the plywood likely to occur. The failure could be explained when using values from ASCE-7 formulas for open buildings with monoslope roofs. In fact the uplift could be prevented by the attachment of the formwork plywood to the joists using a tighter nailing schedule. One should note that once the concrete is poured, uplift will not occur. The period from formwork installation to concrete pour varies from one day to one week. In lieu

of specific uplift calculations, one can improve safety by enforcing prescriptive nailing schedules based on the elevation of the formwork installation.

Discussion

For most of the incidents inspected, the code provisions were found sufficient to prevent the accidents, especially at the moderate gust levels observed in this paper. When wind pressures start to manifest and as they increase in strength, they just put in evidence pre-existing weaknesses in the design or installation of the temporary structures. It is not the wind, but negligent practices that are the cause of the accidents. Sometimes the negligence is gross. The highest number of injuries were due to construction fences, the installations least covered by the code. In all cases, designs using the code specified hurricane wind speed would have ensured safety. Additional studies are suggested to balance safety against onerous requirements (e.g. unreduced hurricane wind speed). The wind reductions need to be incorporated in the formulas that most appropriately describe the physical condition. It was observed that not all calculations submitted to the department take in account the added wind pressure due to height or exposure.

When used for the analysis of specific cases of shed overturn and of uplift of formwork, the ASCE-7 *open buildings* formulas seemed to predict better the event. The full adequacy of the use of these formulas for such temporary installations needs to be assessed.

The relatively low ratio of number of injuries to number of incidents is probably due to the fact that in most cases, the collapse is not instantaneous. Probably it takes several successive gusts to bring total failure and this time interval might have allowed some sheltering. It is likely that the two fatalities were also associated with almost instantaneous rise in wind speed.

The high number of scaffold failures relative to those of sheds point to a serious problem as one would expect a larger number of shed incidents. Since they offer a larger surface exposed to wind, the scaffolds sustain larger wind pressures. The Building Code requires that the scaffold anchorage be designed for the specific conditions of each project. The higher level of safety expected from such designs does not seem to be always present. Scaffold design can be improved by clarifications regarding what percentage of netting area should be considered in calculations.

The construction installations discussed above are intended to be kept in place for periods ranging from less than one week (formwork shoring) to two years (construction fences). They cannot be dismantled or significantly reinforced in a short period of time. Special inspections on the eve of a predicted wind event can only result in repairs of the most obvious defects. Periodic inspections, not just emergency inspections induced by wind advisories, can reduce accidents as they allow more time for the repair. Where proper design is lacking, advisories and subsequent inspections will yield only limited safety improvements.

A CASE STUDY OF FAILURE DUE TO INAPPROPRIATE USAGE OF FORMING SCAFFOLD SYSTEM

Y. Pashang Pisheh[1], H. R. Shafiei[2] and M. Hatambeigi[3]

[1]S.M. ASCE, Ph.D. Candidate of Geotechnical Eng., Department of Civil and Environmental Engineering, Amirkabir University of Technology, Tehran, IRAN; PH (+98912) 3595494; Email: yadolah_p@yahoo.com
[2]M.S. Student of MBA-Project Management, Industrial Management Institute, Tehran, IRAN; PH (+98912) 3331765; Email: hrshafiei@yahoo.com
[3]B.S. Civil Engineering Graduate, Department of Civil Engineering, Imam Khomeini International University, Qazvin, IRAN; PH (+98912) 5882400; Email: mahya2464@yahoo.com

ABSTRACT

One of the major reasons for disasters during construction of massive concrete structures is the failure of weak and defective scaffolding systems. During the construction of Bojnourd cement factory, the failure of forming system related to the concrete slab of the bypass clinker silo led to collapse and crush of the fresh concrete slab and death and injury of some labors in the site. In this paper, using in-situ and numerical investigations, the main causes of the accident are studied. So, by making use of Finite Element Method, the forming system including scaffold grids has been modeled and analyzed respected to common and extra loading applied on the elements. Various analyses were carried out in existence and absence of the proper lateral bracing system considering P-Delta effects in scaffolding elements. Based on the current study, application of improper connections in vertical elements of scaffolding piers, weak lateral bracings in two orthogonal directions, and discontinuity in scaffolding performance were distinguished as the main reasons for occurrence of this destructive event.
KEYWORDS: Concrete Structures; Failure; Forming Systems; Scaffolding

INTRODUCTION

Formwork failures are the causes of many accidents during construction of cast in place concrete structures. This kind of failure usually occurs during or soon after fresh concrete placement and is related to collapse of temporary supporting structures

or premature removal of formworks. Generally, some unexpected events cause one member to fail, then others become overloaded or misaligned and as a result, the entire formwork structure collapses. Such failures often involve serious injuries, loss of lives, property damages, and construction delays. The dramatic 1970 failure of the 17-story Commonwealth Avenue building in Boston, Massachusetts, killed four workers. Fifty six lost their lives in the Willow Island, West Virginia, due to the cooling tower collapse in 1978. In 1982, thirteen construction workers were killed in collapse of the temporary structure supporting Riley Road Interchange Freeway Ramp in East Chicago, Indiana (Feld and Carper, 1997). On December 24, 2006, a formwork collapse occurred during the construction of concrete slab of bypass clinker silo which was being built in Bojnourd cement factory in northeast of Iran (Pashang Pisheh et al., 2007). The structure has a thick reinforced concrete slab with 1.2 m thickness retained on a reinforced concrete wall. During concrete pouring for the slab in elevation of +11.5 m, after placing about sixty centimeters of the fresh concrete, the supporting structure of the formwork collapsed resulting in death of three and injury of seven construction workers and a one-month delay in project. Figures 1 and 2 represent the former and latter status of collapsed concrete slab respectively.

Figure 1. Bojnourd cement silo during construction of concrete slab.

Figure 2. Collapsed slab of Bojnourd cement silo.

CAUSES OF THE FORMWORK FAILURE

In many cases of formwork failures, the collapse is a principal result of inadequate accuracy in evaluation of various acting loads and material strength in formwork design. Except these basic factors illustrated in codes and standards (OSHSCI 1993; ACI Committee 318; ACI Committee 347), other main reasons can be classified as below (Peurifoy and Oberlander, 1995):

- inadequate shoring or supporting elements
- Improper stripping and shore removal
- Inadequate bracing of members
- Lack of control of rate of concrete placement
- Improper or inadequate connections
- Improper or inadequate bearing details

In construction of Bojnourd cement silo, the steel forms of the 15-meter-diameter slab was supported by scaffolding piers system consisted of vertical, horizontal, and diagonal steel tubes. So, strips of these scaffolding structures with width of 1 to 1.5 m and 0.2 to 0.3 m of free distance were situated along each other. To integrate and brace these separate strips several horizontal steel elements were used in various heights. Figures 3 and 4 show partial plan and sectional views of scaffolding piers arrangement used as the supporting structure of the slab formwork.

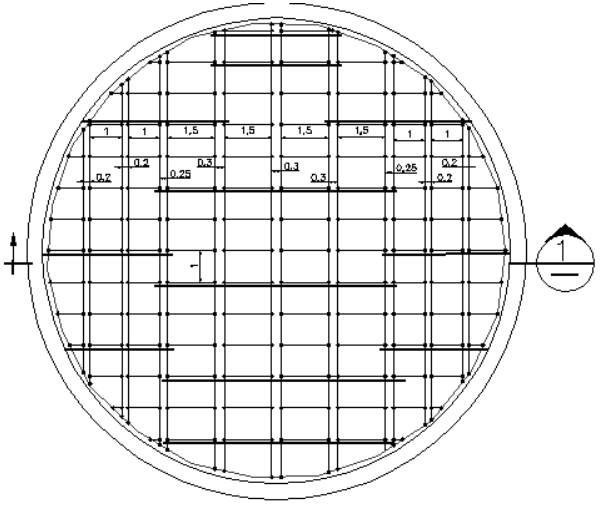

Figure 3. Plan view of the slab formwork supporting piers.

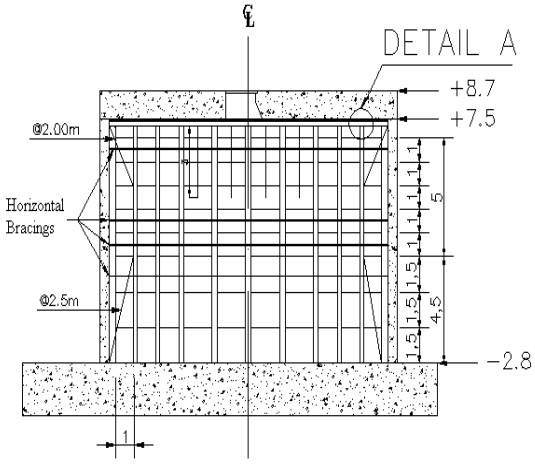

Figure 4. Sectional view of the slab formwork supporting piers.

As shown in Figure 3, the lateral bracing system in the structure is mainly restricted to horizontal elements between supporting strips, whereas diagonal elements were not used properly to brace the structure against the lateral loads produced by different factors such as concrete pouring and fresh concrete vibration. Furthermore, to erect the scaffolding piers to reach the formwork elevation, instead of application of proper standard hinge connections, the adjacent vertical upper and lower piers are connected to each other just by means of a 32-mm-diameter steel bar bounded by a steel o-ring. Thus, the joints behavior under intense lateral loads which may result in generating tensile internal load in the vertical elements could be changed from pinned joint to a roller bearing. More in-situ investigations performed on the causes of slab formwork failure confirmed these connections as a weak point in the used scaffolding system during concrete pouring in the day of the accident.

In addition, application of scaffold tubes with internal diameter of 44 mm (12 mm greater than connecting bars diameter) led to formation of a little void in the joints; therefore, an eccentricity shaped in locations between upper and lower elements corresponding to the separate adjacent vertical piers. This can cause P-Delta effects generation and consequently increase of produced stresses and decrease of elements strength against buckling in case of the compressive loads in the vertical fairly slender supporting elements. The connection detail of the vertical scaffolding piers and corresponding eccentricity of these elements is illustrated in Figure 5. It is worth noting that due to relatively small thickness of tubes used in the formwork supporting structure, in addition to the weaknesses mentioned above, the local effect of the piers connector bars was appeared as scaffold tubes tearing in several joints after the formwork collapsed (see Figure 6).

Figure 5. Eccentricity formed because of improper connections in the supporting piers.

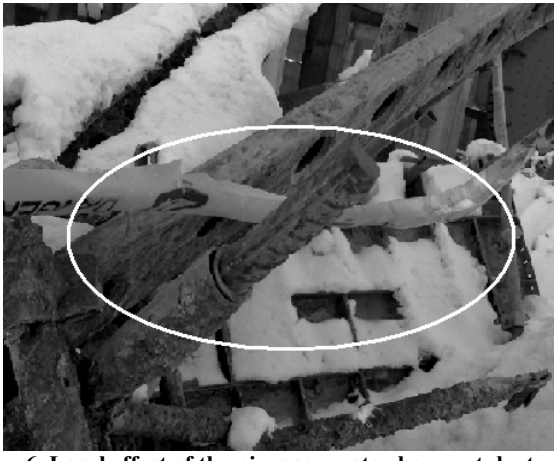

Figure 6. Local effect of the piers connector bars as tube tearing.

NUMERICAL INVESTIGATIONS

Modeling the structure. In order to assess the formwork supporting structure of Bojnourd cement silo slab and corresponding probable defects, the scaffolding piers under various kinds of loads have been modeled by Finite Element Method through which the structure behavior in conditions of existence and absence of proper bracing system has been studied (see Figure 7). In the mentioned Finite Element model, the formwork supporting structure has been modeled as separate piers system contained

vertical, horizontal, and diagonal straight frames of steel tubes with internal diameter of 44 mm and thickness of 3 mm. Each separate pier was connected to adjacent pier by several similar horizontal steel tube elements in various heights of the structure as it is already illustrated in Figures 3 and 4. The forces applied on the forming supports include dead and live loads plus impact. Dead loads include the weight of the formworks and any supporting sections, the fresh concrete plus the weight of construction materials stored on the forms and slab while the supports are still in place. Live loads, however, include the weight of the workers and construction equipments that move over the decking or the concrete as it is being placed, or soon thereafter. The impact factor related to the fresh concrete impact during placement and other moving equipments can be considered according to the construction method or available standards and codes. According to the above, the loads used in the numerical analyses have been introduced as below:

- The weight of the formworks = 150 kg/square meter
- The weight of the fresh concrete = 2500 kg/cubic meter
- Live loads = 350 kg/square meter
- Lateral extra loads = 500 kg/meter
- The impact factor = 1.25

It must be noted that in the current study analyses, the joints connecting every two 3-meter-high vertical piers have been considered as hinged joints and the roller node formation because of the improper connections usage was ignored to produce initial stability for the numerical model.

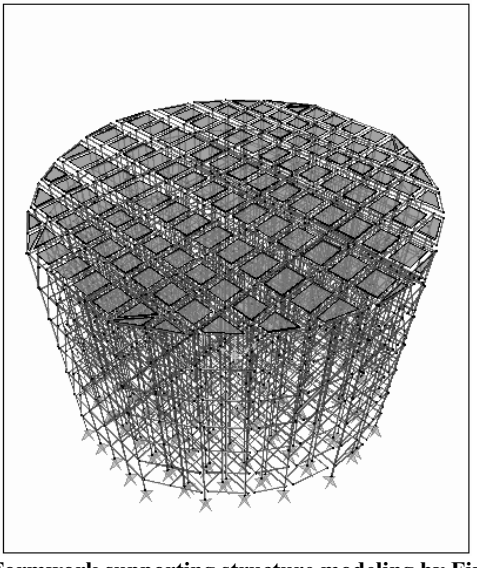

Figure 7. Formwork supporting structure modeling by Finite Element Method.

Existence of proper lateral bracing system in the structure. In this case of analyses, the supporting structure has been analyzed with assumption of adequate bracing elements existence in two directions in the first, middle, and last spans of the scaffolding piers strips. As it is illustrated in Figure 8 for one of the separate strips, in this situation, the structure is completely stable under all kinds of loads, and the maximum horizontal displacement of the structure in the critical loading combination is just restricted to 10 mm in the highest elevation of the structure beneath the formwork.

Inadequate lateral bracing of the structure. According to the material weakness and aging been occurred in some of the elements as well as improper installation of bracings in some of the spans, in these series of analyses, the diagonal bracings in the sixth altitudinal span were eliminated. So, the analysis of the supporting structure was performed with assumption of bracing absence in this span. As shown in Figure 9, absence of diagonal bracings or usage of aged and improper elements in one or more spans of the supporting structure under lateral loads results in excessive horizontal displacements and consequently instability occurrence in the supporting piers. Hence, the structure becomes unstable with increasing resulted displacement between upper and lower elements of the unbraced span.

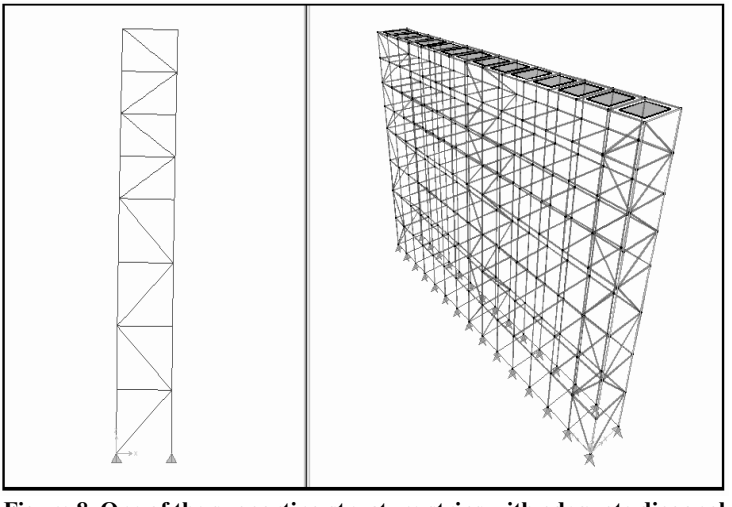

Figure 8. One of the supporting structure strips with adequate diagonal bracings.

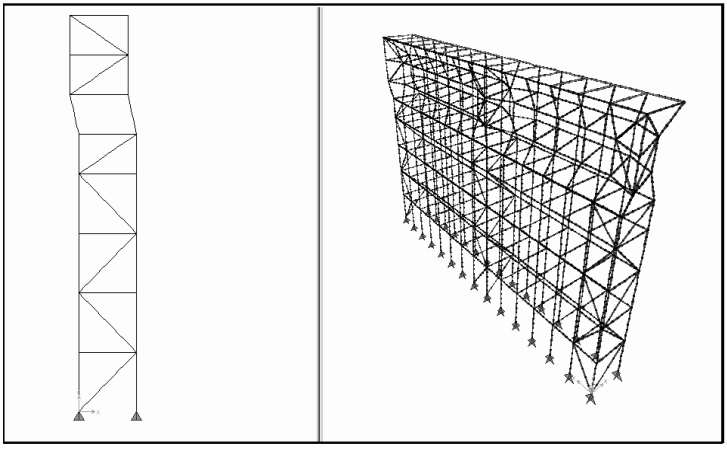

Figure 9. The supporting structure strip with inadequate lateral bracings.

Assessment of P-Delta effects in the scaffolding piers. P-Delta is a non-linear effect that occurs in every structure where elements are subjected to axial loads. As structures consist of more slender and less resistant to deformation elements, the necessity of considering the P-Delta effects increases. Since the magnitude of P-Delta effects is related to axial loads as well as slenderness of individual elements, it seems that investigation of this effect in the accident of Bojnourd cement project would be valuable. As mentioned, the use of steel bars as connectors with diameter smaller than the internal diameter of scaffold tubes can be considered as a weak point during the formwork collapse. As it can be seen in Figure10, the relative rotation and resulted out of plumb about 7 degrees between upper and lower elements in the joint spots due to existence of the void space can lead to a 360-milimeter horizontal displacement from vertical axe for every 3-meter-high vertical pier; this can cause increase of internal stresses in elements or P-Delta effects due to vertical and horizontal loads. Therefore, corresponding P-Delta effects in the braced structure elements even in absence of lateral loads can result in decrease of elements strength in compression and formation of buckling in several elements situated in the lower elevations of the supporting structure. Thus, in order to investigate the P-Delta effects, one of the scaffolding strips has been modeled under applying only the vertical loads and relating effect of the 360-mm displacement occurred between two adjacent 3-meter-high piers. It was illustrated that the lower elements of the piers which support a 3.2-tone axial load in the common state, experience an axial load about 4.5 tones in case of this eccentricity existence (see Figure 11). Since the comparison of the results of two analyses, with and without P-Delta, illustrates the magnitude of the P-Delta effects (Rutenberg, 1982), for the mentioned structure with these improper connections, the contributions from the P-Delta effects are highly amplified and can change the internal forces by 40 percent or more. Consequently, this increase in displacements and internal forces could be one of the main causes of the formwork collapse.

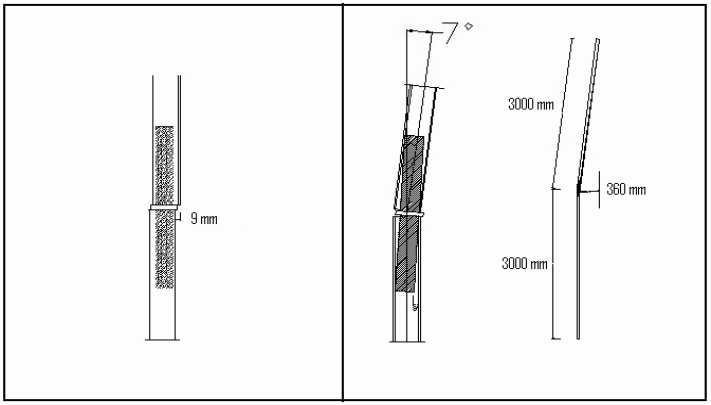

Figure10. Relative rotation and resulted out of plumb between upper and lower elements in the joining location of piers.

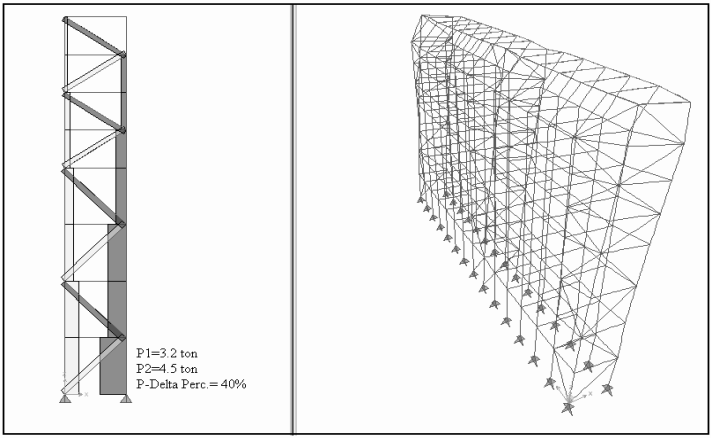

Figure11. P-Delta effect on the internal compressive forces of a supporting pier.

SUMMARY AND CONCLUSIONS

The failure of forming system related to the concrete slab of the bypass clinker silo of Bojnourd cement factory was assessed. Based on the in-situ investigations mentioned in this study and numerical analyses performed on the formwork supporting structure, the main causes of the formwork collapse can be listed as below:

- The lateral bracing for vertical scaffolding piers particularly in the 3-meter-high lower piers was performed inadequately and also diagonal elements were not used properly.

- The connecting horizontal elements used between the separate piers did not have enough capacity to create an integrated lateral supporting system.
- The use of a 32-milimeter-diameter steel bar to join the scaffold tubes with 44 mm internal diameter led to a 360-milimeter horizontal displacement for every 3-meter vertical pier and creation of P-Delta effects in these elements.

REFERENCES

Building Code Requirements for Reinforced Concrete. (1989). ACI Committee 318, American Concrete Institute, Detroit, MI.

Feld, J., and Carper, K. L. (1997). "Construction failure." Wiley, New York.

Guide to Formwork for Concrete. (1994). ACI Committee 347, American Concrete Institute, Detroit, MI.

Occupational Safety and Health Standards for the Construction Industry. (1993). Part 1926, Subpart Q: Concrete and Masonry Construction, U.S. Department of Labor, Washington, DC.

Pashang Pisheh, Y., Shafiei, H. R., and Soleimani, A. H. (2007). "Accident report of Bojnourd cement factory project." Boland Payeh Co., Central technical office, Tehran, Iran.

Peurifoy, R. L., and Oberlender, G. D. (1995). "Formwork for concrete structure." Third edition, McGraw-Hill, New York.

Rutenberg, A. (1982). "Simplified P-Delta analysis for asymmetric structures." ASCE, Journal of the structural division, 108(9).

Defects, Damage, and Repairs Subject to High-cycle Fatigue: Examples from Wind Farm Tower Design

by

Nestor A. Agbayani, P.E., S.E., SECB, M.ASCE

Minner, Stinnett, Koo & Agbayani (MSKA)
Structural and Civil Engineers
1716 Oak Street, Suite 21
Bakersfield, CA 93301-3040
Tel: (661) 324-9724
E-mail: nagbayani@mskaengineering.com

Abstract

Wind farm towers are the steel lattice or tube towers serving as the support structures for large power-generating wind turbines. This paper presents a variety of wind farm tower problems encountered over two decades of practice in the wind energy industry. Wind towers are subject to turbine operational loads that cause very high-cycle fatigue loading and can give rise to unusual tower problems requiring special repairs. Problems unique to wind towers include: structural damage or collapse from turbine overspeed ("runaway" condition); tower resonance with turbine operational frequencies; turbine fires; and excessive localized member vibrations. Further, wind towers can suffer from construction-related problems: fabrication and weld defects; design deviations; accidental dents and gouges during transport; construction errors during tower erection; and wind-induced vortex shedding oscillations. Each tower problem is discussed in terms of its cause, evaluation method, mitigation strategies, and repair options with special consideration for high-cycle fatigue.

Introduction

Wind Tower Structural Systems. Figure 1 shows typical lattice and tubular tower structures. The lattice tower legs and diagonal web members are steel angle (i.e., L-shape) members that are connected with high-strength bolts at their joints. The tubular tower is a fabricated tube consisting of "can" segments formed from flat steel plate. Figure 2 shows how cans are welded together to form longer tubular sections. The lattice towers were used predominantly in the early days (early 1980's) of the US wind industry. Lattice towers ranged from heights of 20 m to 60 m. However, in the last decade, the utility-scale wind industry has transitioned to almost exclusive use of tubular towers that routinely reach heights of 80 m.

Codes, Standards, and Certification. The commercial wind turbine industry evolved in Europe, and European wind turbine manufacturers continue to dominate the global market. Since the US has no specific wind turbine tower design standards, European wind industry standards are the basis for most wind tower design. Wind turbines and towers are certified by a handful of established European certification

agencies, such as Germanischer Lloyd (GL) and Det Norsk Veritas (DNV). Certification is achieved by demonstrating design compliance with IEC standards, e.g., IEC (1999), or agency-specific standards, e.g., GL (2003). Achieving certification is the industry standard for establishing the commercial legitimacy of a turbine-tower system in a way that is analogous to a UL listing for an electronic device or to an ICC test report for a structural product.

Figure 1. Typical lattice towers (left) and tubular towers (right). (Photographs courtesy of MSKA.)

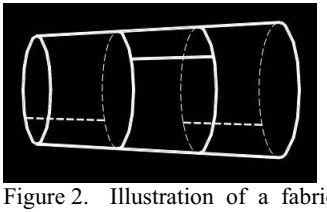

Figure 2. Illustration of a fabricated tube comprised of "can" segments welded together at circumferential weld seams. (Detail courtesy of MSKA.)

High-cycle Fatigue. A typical modern utility-scale wind tower with a 20- or 30-year design life is subject to "megacycle" fatigue, which is low-stress, high-cycle fatigue on the order of several hundred million cycles. It is not unusual for fatigue loading to govern over the usual Code wind or seismic forces. For these reasons, consideration of fatigue is imperative in the assessment of defects, damage, and repairs. Based on provisions of Eurocode 3, Section 9, (ENV, 2002) detailed examples of wind tower fatigue calculations using *S-N* curve methods can be found in Agbayani and Kyatham (2008 and 2009). Fatigue damage is calculated using Miner's Rule linear damage summation method (Miner, 1945).

Overview of Damage and Defects in Wind Towers

In the discussions that follow, tower problems are grouped by structure type (lattice or tube). However, a few problems common to both tower structure types are discussed here.

Turbine "Runaway." Near or total tower collapse can be caused by turbine "runaway," which is a condition of uncontrolled turbine rotor overspeed. The typical

scenario starts with a mechanical or electrical failure in the turbine's rotor braking systems. For example, the failure of a turbine's lightning protection system might leave other electrical systems susceptible to failure after lighting strike. Excessive blade rotation speed breaks off a turbine blade, resulting in both a blade projectile and a large magnitude eccentric rotor loading condition. By chance should the projectile miss the tower, the remaining blades can strike the tower due to the unexpected rotor deflections from the eccentric loading. Figure 3 shows a tower with local buckling damage due to a runaway turbine scenario.

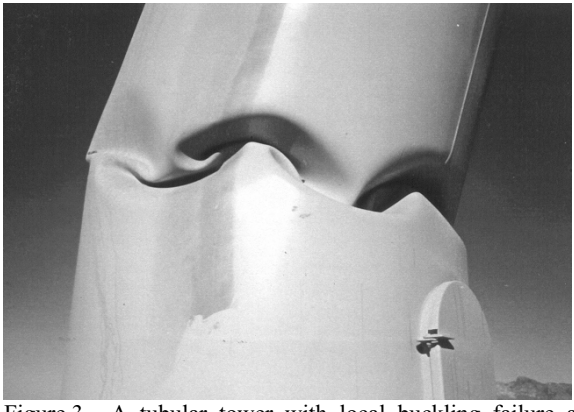

Figure 3. A tubular tower with local buckling failure after a turbine overspeed condition due to lightning strike. (Photograph courtesy of MSKA.)

Tower Resonance. Most modern wind turbines have one or more fixed operational frequencies. The system itself (consisting of the turbine, tower, and foundation) has natural frequencies corresponding to the system's natural modes of vibration. The fundamental mode is the simple back and forth lateral displacement of the tower as an inverted pendulum. Resonance characterized by the build-up of large displacements may occur if there is inadequate separation between a turbine operational frequency and a system natural frequency. Lack of frequency separation could stem from gross error in tower design or from more subtle problems such as the turbine being significantly out of specification for mass or operational speed. A resonance scenario usually involves large tower displacements shortly after start of turbine operation. When the turbine sensors detect excessive displacement, they trigger a fault condition known as an "emergency shutdown" to protect the tower from damaging oscillations. The result is lack of power generation. Possible retrofit measures to provide frequency separation include: shifting the system frequency by stiffening the tower or increasing the tower top mass; or changing the turbine operational frequency usually by reprogramming its controller to operate slower (unfortunately resulting in less power generation).

Turbine Fires. A turbine may catch fire due to an electrical or mechanical problem. An assessment is made to separate cosmetic damage from more serious damage that

has affected the chemistry and mechanical properties of the steel. Affected portions of the tower are usually scrapped and totally replaced with new components.

Damage and Defects in Lattice Towers

The bygone era of small lattice towers (early 1980's) has now transitioned into the era of large tubular towers. For this reason, the defects and damage in lattice towers are only briefly mentioned here for the sake of historical interest. Fleets of lattice towers have now fulfilled most of their 20- to 30-year design life, and many towers have outlived their original turbine. However, no structural system is perfect, and along the way various problems have been encountered with lattice towers.

Lack of Field Fit-up. With lattice towers comprised of hundreds of members, connection plates and bolts, the occasional lack of field fit-up is usually due to a fabrication error. Erection of a single initial prototype tower essentially ensures that any blunders in geometry contained in either the engineering plans or the fabricator shop/assembly drawings can be corrected before the mass production phase.

Excessive Local Vibrations. Lattice towers can be susceptible to local vibrations. In contrast to overall tower vibration, specific pairs of web members or specific groups of web members may undergo excessive out-of-plane vibrations. Continual vibration during turbine operation would point to local resonance with an operational frequency, a rotor imbalance, or gearbox problem. Sporadic local vibration may indicate resonance of a transient nature such as with a pass-through frequency during turbine start-up. Inevitably, loose bolts accompany excessive vibration. An effective remedy for a loose bolt is usually a new replacement bolt properly pre-tensioned and included with a nut-locking device (for redundancy).

Fatigue Cracks in Welded Connections. While lattice towers are comprised mostly of field-bolted connections, a few welded connections exist in lattice towers such as at the leg-to-top mounting ring connection. Fatigue cracks have been observed in tower top ring plates, usually at locations of stress concentrations or with high residual stresses.

Other Damage. Other problems are known to have befallen lattice towers: flood damage undermining or scouring the foundations; intentional vandalism, such as bolt removal, with intent to cause full or partial tower collapse; accidental vehicle impact; total tower collapse due to overwhelming extreme wind event, etc.

Damage and Defects in Tubular Towers

Tower Wall Dents. Towers occasionally are dented by mishandling or accidents during fabrication, transport, or erection. See Figure 4. Excluding fatigue failure and connection failures, the most likely design limit state (or failure mode) for a tubular tower structure is local buckling of the tower shell. See Figure 3. For this reason, a dent in a tubular tower shell is considered a serious problem, because a dent is like

the onset of a local buckle. With a dent, the very condition that the structural design attempts to avoid has already occurred. According to Troitsky (1990):

> About the worst thing that can happen to a tubular structure either during construction or operation is for it to develop a buckle. The buckle may be defined as a localized failure in the form of a wrinkle or indentation caused by over-stress or instability of the wall of tubular structure on the compression side of the structure subjected to bending. . . . Theoretical analyses . . . of the effect of imperfections on the buckling behavior of cylinders have clearly demonstrated that relatively small imperfection amplitudes can drastically reduce the critical load of the shell. . . . The results of the . . . analysis indicate that an initial imperfection amplitude equal to the shell thickness is sufficient to reduce the buckling load to only 20 percent of the corresponding value for the perfect cylinder.

For these reasons, dents in the tower wall should be limited in size to that allowed by defined fabrication tolerances. Dent tolerances are found in various European standards such as DIN 18800. Should a dent's size exceed tolerances, then a repair is necessary. Repair involves the careful pushing out of the dent until it is either removed or at least until the dent's size is reduced below maximum tolerances. Where a dent affects a main tower weld, the weld is subject to NDT inspection after the dent repair.

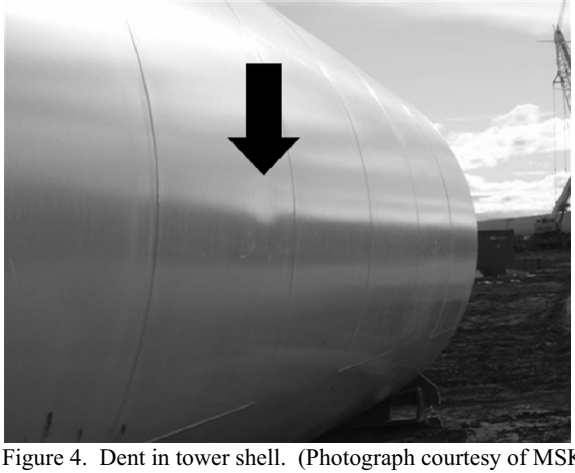

Figure 4. Dent in tower shell. (Photograph courtesy of MSKA.)

Tower Wall Surface Defects. Wall surface scratches, indentations, and gouges may result from accidents or mishandling. See Figure 5. Other examples of surface defects include: identification marks by physical indentation; miscellaneous streak indentations from unknown contact or rubbing; intentional fabrication marks; rolling marks, etc. While they may seem insignificant from the standpoint of tower ultimate

strength, surface defects have the potential to be locations of fatigue crack initiation, so these otherwise minor defects are considered to be a serious problem when subject to high-cycle fatigue. At the very least, the small surface defects should be ground smooth to prevent stress-rising notch effects. Plate defect tolerances are usually based on engineering judgment informed by plate defect limits such as found in ASTM A6 or weld notch/undercut defect tolerances as found in AWS (2004). For deeper defects, base metal repair by welding is an option. However, in light of the high-cycle fatigue environment, repair by field welding should be considered a last resort and undertaken with great caution. The possibility exists that a low-quality repair by field welding may result in the weld material itself cracking or acting as an even larger notch. To prevent the "fix" from being worse than the problem, a repair procedure and welding specification should be developed in consultation with an expert welding engineer who can address weldability issues.

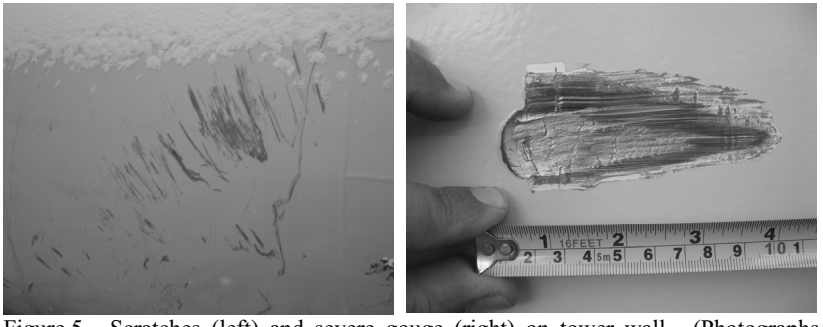

Figure 5. Scratches (left) and severe gouge (right) on tower wall. (Photographs courtesy of MSKA.)

Tower Paint/Coating System Problems. The tower paint/coating system protects the tower from corrosion. When the tower paint is damaged or found to be locally flawed (e.g., peeling, blistering, etc.) it is imperative to perform robust paint repairs compatible with the original 20- or 30-year-life coating system. Specialized paint specification is best left to knowledgeable coating specialists. Interestingly, while foul weather exposure is easy to imagine for a tower's exterior, less obvious is routine moisture exposure on the interior surfaces of a tubular tower due to condensation in the slightly warmer conditions within the tower caused by heat from electrical systems. Similarly, corrosion too has a subtle aspect. Obviously, extensive corrosion can reduce the strength of a structural component, but a less obvious consideration is the aggravating effect of corrosion on fatigue. Corrosion-fatigue is a complex phenomenon, but stated in simple terms: corrosion in the presence of fatigue increases susceptibility to cracking, hastens the onset of cracking, and reduces fatigue life. The surface roughness, pitting, cracking, notching effects, and the resulting chemical and material property changes in steel that result from corrosion are contributing factors to this behavior. In a high-cycle fatigue environment, maintaining the integrity of the paint is especially critical to prevent corrosion and to prevent premature fatigue damage.

Tower Wall Can Joint Offsets. The tower is a fabricated tube consisting of "can" segments welded together with circumferential weld seams (i.e., "girth" welds). See Figure 2. Where the plate edges at the can-to-can joints do not abut within the permissible tolerances for misalignment, repair or mitigation is necessary. The misalignments cause additional stresses due to joint eccentricity resulting in reduced fatigue life. The circumferential can joints must comply with constructional details that have a fatigue Detail Category (DC) classification. The DC usually has a misalignment tolerance built into its definition. The flawed detail can be assessed accounting for the misalignment. A satisfactory fatigue life may indicate that repair is not required. However, if the risk or engineering judgment requires a repair, a mitigation strategy is to provide fatigue life increase by applying post-weld improvement techniques such as weld profile improvement. The stress-riser effect of the joint offset can be removed by grinding the weld surface smooth with a flush slope transition across the joint weld surface. Fatigue life enhancements are described in Section 8.4 of AWS (2004) or Section 3.5.3 of IIW (2003).

Tower Splice Flange "Toe-to-Toe" Contact. Splice flanges are the bolted ring plates that join tower sections. A cross section through the tower flange is L-shaped somewhat like a person's foot with the flange having a "heel" and "toe." Figure 6 depicts the required "heel-to-heel" initial contact condition for splice flanges coming into contact. When two tower sections are joined together during the erection process, the high-strength splice bolts are pre-tensioned by application of an installation torque. Ideally, the splice flanges should close with perfect flat contact, but in reality, contact is not perfect. Of the imperfect contact conditions, initial heel contact is permissible, but initial toe contact is prohibited. The reason is fatigue. Clamping the flange closed starting from initial *toe* contact represents a pre-pried condition that leaves the splice bolts susceptible to fatigue. In contrast, clamping the flange closed starting from initial *heel* contact provides a load path through the heel contact pressure that protects the splice bolt from prying forces. The repair is flange contact surface grinding to provide either perfect flat contact or initial heel-to-heel contact.

Tower Splice Flange Gaps. When flanges make initial heel contact, a toe gap (lack of contact at the flange toes) naturally exists. See Figure 6. The toe gap disappears as the flanges are clamped together during bolt installation. Flange toe gaps result when the full effort of the bolt pre-tension installation fails to close the initial gaps. See Figure 7. This condition is a problem because the splice bolts at gaps are more susceptible to fatigue damage. Gaps prevent the desired load paths and contact stress distributions assumed in the flange analytical models used for design. Residual flange gaps are typically discovered after tower erection but just after the bolt installation process, so disconnecting the tower sections for flange grinding is not a practical option. Careful flange gap shimming using precision stainless steel shims is the typical repair. The width and extent of flange gaps are measured and mapped around the entire flange circle. The *GL Rules* (GL, 2003) requires that the shimming material match the elastic modulus of the steel flanges, so this prevents the use of

construction grade metal-to-metal filler putties or bonding agents. Moreover, the long-term properties of these filler materials under fatigue loading are unknown.

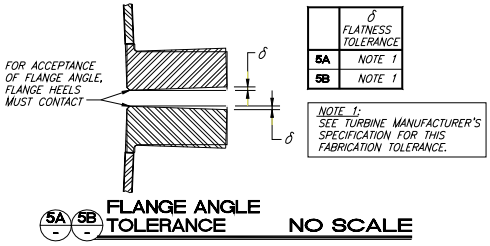

Figure 6. Typical detail showing required initial heel-to-heel contact at tower splice flanges. (Detail courtesy of MSKA.)

Vortex Shedding Oscillations. During the stages of tower section erection prior to topping out with the wind turbine, the tower sections resemble steel stacks or chimneys. These cylindrical structures are known to be sensitive to vortex shedding oscillations, which are across-wind vibrations resulting from the periodic shedding of vortices from upper portions of the tower. Excessive and sometimes violent displacements from prolonged resonant vortex shedding can damage the tower and its connections. After the critical wind speed for vortex shedding is calculated, the project manager should make every effort to avoid leaving the partially-completed tower in the susceptible condition. Total avoidance of a vortex shedding situation is best. However, when work stoppages are unavoidable, some mitigation strategies exist to diminish wind-induced vibrations such as: aerodynamic methods, damping methods, and stiffening methods (ASME, 2006). Only two are generally used in the wind industry. The use of large diameter ropes to form temporary helical strakes (i.e., "candy striping") is an aerodynamic method that has been used in the wind industry. If only a single tower is left in a susceptible configuration, the tower erection contractor will sometimes leave the large crane boom attached to the tower top as a temporary support.

When vortex shedding has occurred, a visual inspection for damage should be performed, and fatigue calculations should be performed to estimate the fatigue damage that has resulted. Methods to quantify vortex shedding into fatigue loading are contained in steel stack standards such as ASME STS-1 (ASME, 2006) or German standards such as DIN 4133. Project site anemometer data can be used to accurately determine the amount of time that wind speeds were within an interval where vortex shedding oscillation was likely. This wind speed interval around the critical wind speed is known as the "lock-on" range. In most cases, the partially constructed tower can be left in place, and no repairs are required. However, if excessive damage is indicated, then disassembly of the tower for repairs or further inspection may be necessary.

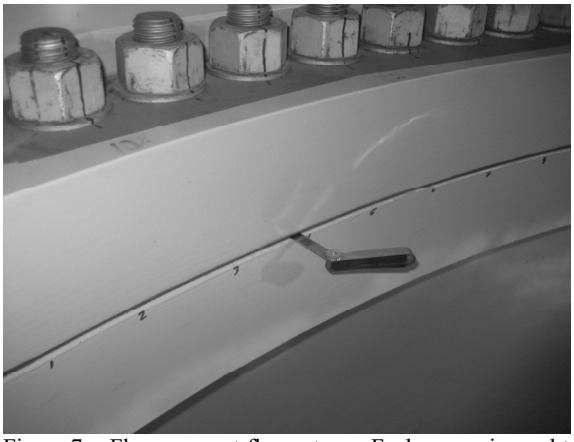

Figure 7. Flange gap at flange toes. Feeler gage is used to determine thickness and extent of the gap. (Photograph courtesy of MSKA.)

Accidental Deviation from Fatigue Details. Sometimes what appears to be an innocuous deviation from approved details could prove to be a serious problem. One such case occurred at the welded connection of miscellaneous support brackets at the interior wall surface of the tower. A small 8 mm bracket plate that was 50 mm in depth was to be fillet welded to the tower wall. A fabricator provided deeper 65 mm bracket plates (due to availability) and reasoned that the greater depth would result in more bracket plate strength and more weld strength. While the fabricator's reasoning was basically correct, the deviation unintentionally created a significant reduction in the tower shell's fatigue life. The original 50 mm dimension came from a limit in a fatigue construction detail defined as Detail Category (DC) 80 (ENV, 2002). The DC value is a nominal fatigue strength in units of stress in Megapascals, so the higher the DC, the better (higher) the fatigue resistance. The lengthening of the weld from 50 mm to 65 mm resulted in a change from DC 80 to DC 71, which shortened the fatigue life by approximately 38%. Where many brackets are affected, total removal and replacement is not a practical solution. One mitigation strategy would be to provide fatigue life increase by applying post-weld improvement techniques such as weld toe grinding of the fillet weld toes.

Other Damage. A myriad of other problems has occurred with tubular towers. These include: tornado damage; weld quality problems; field problems with high-strength bolt installation at tower splice flanges; permanent tower tilt after foundation settlement; tower mis-siting (i.e., towers sent to the wrong location), etc. Complete tower collapse from foundation overturning instability has been known to happen. Also, other foundation-related problems have been encountered: anchor bolt fracture after installation; grout cracking (beneath tower base plate) due to an over loading event, drying shrinkage, or freeze-thaw exposure; and punching shear failure of embedded steel foundation components.

Conclusion

Examples of damage, defects, and repairs of wind farm towers illustrate special considerations for high-cycle fatigue loading. Other examples illustrate problems due to dynamic loads such as resonance, vortex shedding, and other vibration problems.

References

Agbayani, N., and Kyatham, V., (2008), "Megacycle Fatigue Analysis Demystified: Examples from Wind Farm Tower Design," *Proceedings of the 2008 Structural Engineers Association of California (SEAOC) Convention*, SEAOC, Sacramento, California, 303-320.

Agbayani, N., and Kyatham, V., (2009), "Fatigue-driven Wind Farm Towers: A Practical Introduction to Fatigue Calculations," *Proceedings of the 2009 Structures Congress*, ASCE/SEI, Reston, Virginia, 2119-2132.

ASME (2006), ASME STS-1-2006 *Steel Stacks*, American Society of Mechanical Engineers (ASME), Three Park Avenue, New York, New York.

AWS (2004), AWS D1.1/D1.1M:2004, *Structural Welding Code–Steel*, American Welding Society (AWS), Miami, Florida.

ENV (2002), Prestandard prEN 1993-1-9:2002, *Eurocode 3: Design of Steel Structures – Part 1.9: Fatigue Strength of Steel Structures*, 2002, European Committee for Standardization (CEN), Brussels, Belgium.

IEC (1999), International Standard IEC 61400-1, *Wind Turbine Generator Systems–Part 1: Safety Requirements*, Second Edition, 1999-02, International Electrotechnical Commission, Geneva, Switzerland.

IIW (2003), Document XIII-1965-03/XV-1127-03, *Recommendations for Fatigue Design of Welded Joints and Components*, 2003 (Updated 2004), International Institute of Welding (German Delegation), Paris, France.

GL (2003), *Germanischer Lloyd Rules and Guidelines, IV–Industrial Services, Part 1–Wind Energy, Guidelines for the Certification of Wind Turbines*, 2003, Germanischer Lloyd WindEnergie GmbH, Hamburg, Germany.

Miner, Milton A. (1945), "Cumulative Damage in Fatigue," *Journal of Applied Mechanics*, vol. 12, Transactions American Society of Mechanical Engineers, vol. 67, pp. A159-A164.

Troitsky, M. S. (1990), *Tubular Steel Structures—Theory and Design*, Second Edition, James F. Lincoln Arc Welding Foundation, Cleveland, Ohio, 2-3.

Crane Safety—an Industry in Flux

David B. Peraza, PE, Member ASCE [1]
Jeffrey A. Travis, PE, SE, Member ASCE [2]

[1] Exponent, 420 Lexington Avenue, Suite 1740, New York, NY; Ph 212-895-8100; email: dperaza@exponent.com
[2] Exponent, 1011 Warrenville Rd., Suite 215, Lisle, IL; Ph 630-743-7705; Email: jtravis@exponent.com

Abstract

The recent rash of crane accidents across the United States, and even internationally, has raised the public's awareness of the potential hazards posed by crane use in the construction industry. This paper will provide a broad overview of the rapidly changing regulations relating to crane operations, as well as review crane accident statistics, the causes of milestone crane accidents, and summarize new regulations at local and national levels.

Statistics

As reported by The Center for Construction Research and Training (CCRT), from 1992 to 2006, data from the Bureau of Labor Statistics indicates that there were 632 construction worker deaths resulting from crane accidents, or an average of 42 worker deaths per year. The leading cause of death from these accidents, roughly 25%, was electrocution from contact with power lines. Crane collapses accounted for about 14% of the reported deaths. Surprisingly, for over half of the crane collapses, the cause is listed as unknown. The other crane collapses were attributed mostly to ground conditions, overloading, or shifting of the load. Of the reported crane collapses, approximately 40% involved mobile cranes.

In 2008, a review of trade and news media by CCRT indicated that there were 54 construction worker fatalities associated with crane accidents, an approximately 30 % increase over the annual average from 1992 to 2006. In addition to the construction workers, there were four bystander fatalities. Several of the crane accidents were high-profile, occurring in dense urban areas with resulting high-consequence, and they occurred within a short span of time. These crane accidents resulted in heightened public awareness and a general outcry to tighten safety standards.

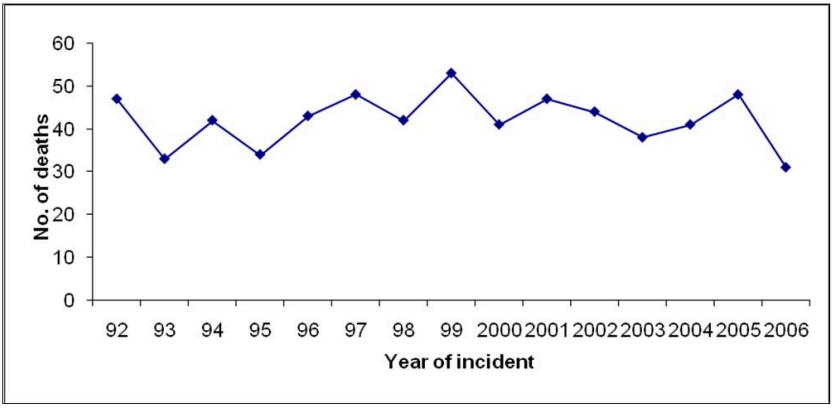

Figure 1: Crane-Related Deaths of Workers, 1992-2006. Based on US Bureau of Labor Statistics, Census of Fatal Occupation Injuries Research File. Graphic from The Center for Construction Research and Training.

Milestone Crane Accidents

Miller Park, WI (July 14, 1999)

The collapse of "Big Blue" at the new Miller Park baseball stadium resulted in 3 fatalities to ironworkers, caused extensive damage to the remainder of the roof structure and bleachers, and delayed opening day for one year. The collapse occurred in 26 mph sustained winds, during the lowering of a 180 foot by 100 foot lattice roof panel into position. "Big Blue" was one of the largest mobile cranes in the country, with a height of 540 feet and a rated lifting capacity of over 500 tons. The collapse was possibly the most extensively photographed crane accident in history, even being captured on videotape by OSHA employees who happened to be on site.

OSHA citations and a jury trial concluded that the failure was due to the "sail effect" of the lattice roof panel, which caused the crane to tip over to the side. A jury found the firm responsible for the roof erection as 97% negligent and awarded the widows $100 million, which was reduced on appeal. The negligence was due to the decision to proceed with the lift, even though the wind speed that day was well above the value given in the crane's load chart. Ross (2007) provides detailed information about the accident and engineering analysis. An unpublished engineering investigation by the author, prior to joining Exponent, also concluded that the crane had been overloaded by wind forces.

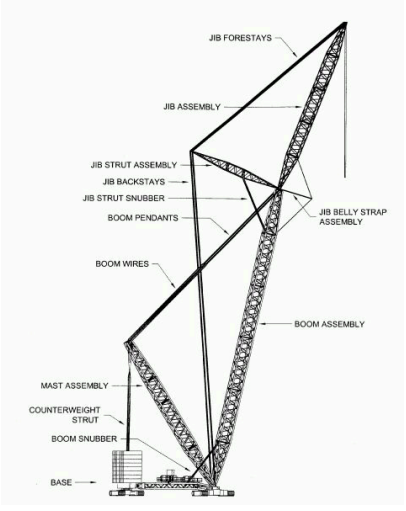

Figure 2: "Big Blue" crane

Anecdotally, wind does not appear to be a common cause of crane collapses. The US Bureau of Labor does not even have a category for crane collapses due to wind. Possibly the low incidence of this type of failure is due to the rarity of lifting loads that have unusually large "sail" characteristics. Despite its notoriety, this crane accident did not result in any changes to existing crane regulations or standards, or any identifiable new regulations. It did result in much more rigorous engineering evaluation of each subsequent crane pick at Miller Park and adherence to lifting protocols once construction resumed.

San Francisco, CA (November 28, 1989)

The collapse of a luffing boom tower crane resulted in the death of three ironworkers, the crane operator, and one bystander, and injured 22 persons. The collapse occurred during a climbing operation with the upper portion of the crane falling 16 stories, or approximately 290 feet, to the street below.

The tower crane was erected by the steel erection subcontractor and certified by the crane manufacturer on August 22, 1989. The climbing of the crane was to be done by the steel erection subcontractor. On October 17, 1989, the San Francisco area experienced an earthquake. Subsequently, the steel erection subcontractor and crane manufacturer examined the crane and found it to be free of any structural damage.

The initial tower erection included the first nine tower sections. On November 9, 1989, the crane was climbed to a greater height, including tower sections 10, 11, and 12. Also added at that time was the tie-in collar at the tenth floor. On November 27, tower sections 13, 14, and 15 were added. The next tie-in collar was added at the 16th floor. On November 28, during the climbing operation to add tower section 16, the crane collapsed.

As a result of this accident, the state of California passed legislation regulating certain tower crane operations, initially requiring that cranes be inspected regularly by licensed crane inspectors. California was the first state to adopt such regulations. The city of San Francisco approved an ordinance based on the state regulations. The

San Francisco code requires a contractor to identify the location of proposed crane operations on a Crane Site Safety Plan; comply with tower crane safety regulations; the presence of a safety representative during tower crane erection, jumping, and dismantling; and employment of a flag person to redirect traffic when loads are lifted over streets or walkways.

According to statistics from the California Division of Occupational Safety and Health, this measure appears to have been effective. In the three years prior to California adopting the stricter regulations, there were 10 fatal accidents and 30 injuries involving cranes where the new regulations would have required operator certification. In the three years following the introduction of the stricter regulations, only three fatal accidents and 13 injuries were recorded.

New York City, NY (March 15, 2008)

The collapse of a tower crane on East 51st street in Manhattan claimed seven lives; six of whom were construction workers and the other who was a bystander inside a nearby building that was impacted.

At the time of the collapse, workers were in the process of climbing or "jumping" the crane. They had increased the height of the crane by inserting tower sections, and were adding another brace level. The brace consisted of a collar, and three steel members connecting the collar to the building slabs. At the time, the collar was suspended from the tower using four synthetic slings. During the tie-in operations, the slings failed, allowing the collar to slide down the tower. The sliding collar impacted the collar at the 9th floor, with the two collars subsequently sliding down and impacting the collar at 3rd floor, which resisted the impact. The tower then rotated away from the building, impacting a building across the street and causing the tower sections to fail. The upper tower sections fell onto a neighboring low rise building.

Figure 2: The base of the tower crane that collapsed on March 15, 2008 in New York City. The collars slid down the tower. Source: New York County District Attorney's Office.

Six months after the collapse, OSHA issued citations against the crane's erector, the general contractor, and the concrete subcontractor. The citations against the erector were for willful misuse of synthetic rigging slings that were used to support a collar through which the tower was braced to the building.

The master rigger for the crane erection was indicted with multiple charges of manslaughter, criminally negligent homicide, assault and reckless endangerment.

The Department of Buildings of the City of New York also conducted an investigation, and it issued a report one year after the accident. The main findings were:

- The collar was suspended from the tower at only four points, contrary to the manufacturer's recommendations, which require the use of eight points.
- The points on the collar from which it was suspended from the tower were not intended for that purpose by the manufacturer.
- The synthetic slings used to suspend the collar were choked around the tower in a manner that is not in accordance with industry practice, and which reduces the strength of the slings. Specifically, the slings were not protected from the sharp edges of the vertical tower members, and the slings were bunched and edge loaded in a V-shaped area.
- One of the four slings was in a deteriorated condition and should not have been used.

The report also found other deficiencies, which did not play a significant role in the collapse, such as improper welding of the tieback beams.

This was the second incident related to the use of nylon slings. On December 14, 2007, a crane was lifting a 7 ton bundle of metal studs using nylon slings at 200 Murray Street, when the slings failed and the load fell onto a construction trailer, severely injuring an architect

As a direct result of the subject tower crane collapse, the City of New York adopted a law that prohibits the use of nylon slings, except for those situations where they are specifically recommended by a manufacturer.

New York, NY (May 30, 2008)

The collapse of a tower crane on East 91st Street on Manhattan's Upper East Side resulted in the deaths of the crane operator and a construction worker, and serious injuries to another construction worker. The cab, counterweights, machine table, and boom separated from the uppermost tower section and fell against an adjacent apartment building, shearing off balconies before landing in the street.

The failure occurred at a weld along the circumference of the turntable. Initial investigations are focusing on the quality of that weld, which was made as a repair.

Figure 3: The quality of the weld around the circumference of the turntable is the focus of investigations for the May 30, 2008 tower crane accident in New York City

The failure has prompted questions about procedures for quality control and quality assurance regarding repairs made to cranes. One possibility that is being explored by the City of New York is the possibility of registering and tracking key crane components throughout their life on a national basis.

Miami, FL (March 25, 2008)

The collapse of a tower crane resulted in the deaths of two construction workers and injuries to five others. During a climbing operation, a 20 foot tower section fell 30 stories and through the roof of the construction office.

The tower section that was to be inserted had been lifted from ground level by the crane, and had been transferred to the overhead trolley attached to the climbing frame. Once hung from the trolley, the tower section was to be winched in through the climbing frame and attached to the main tower. The subject tower section had been transferred to the trolley prior to it falling. Winds were on the order of 18 to 24 mph at ground level.

Initial investigations are focusing on the mechanism that is used to hang the tower section from the trolley, and on whether the winds played a role in causing that mechanism to fail.

Three days after this accident, Miami-Dade County passed regulations requiring that crane operators be certified. A federal judge later ruled that the county crane laws

were not enforceable, because they were superseded by federal OSHA regulations, and that enacting them would subject firms to duplicative laws.

Bellevue, WA (November 16, 2006)

The collapse of a 210 foot tall tower crane at the corner of Northeast Fourth Street and 108th Avenue Northeast resulted in the death of one bystander, injury to one construction worker, and damage to three neighboring buildings. The crane was located at the site of Tower 333, a 20-story office building which was under construction. The crane operator was trapped in the cab and rode the crane down. Firefighters eventually were able to extricate the operator from the cab.

The base of the tower crane was located on a steel frame, located several levels above the lowest basement levels. At the time of the accident, the crane was rotating, but it did not have a load on its hook. It had been in use for about two months.

In May of 2007, the State of Washington Department of Labor & Industries (L&I), fined the structural engineer who designed the dunnage beam crane base and also fined the general contractor. According to the L&I report, the tower crane foundation was under-designed. It states that the overturning moment and the slewing moments were not included in the design of the dunnage, and that the design was not approved by the crane manufacturer.

Houston, TX (July 18, 2008)

The collapse of one of the largest mobile cranes in the United States at a refinery in Houston resulted in the deaths of 4 construction workers and injury to 7 others. The crane stood 300 feet tall with a 400-foot boom. The crane had recently arrived at the site, and had performed a test lift that day. It was scheduled to begin work the following week.

In January of 2009, OSHA cited the crane supplier for unsafe practices, consisting of elevating the boom to an unsafe angle which allowed the crane to tip over backward. The operator, though he had operated other large cranes, had never operated nor been trained to operate this particular crane, which was a custom-built unit.

Changes in Regulations

Current OSHA crane regulations were enacted approximately 40 years ago, and have long needed updating. In 2003, OSHA formed the Crane and Derrick Negotiated Rulemaking Advisory Committee (CDAC) which consisted of representatives from industry, labor and government and was tasked with developing a new safety standard for the construction industry to aid in reducing the number of crane related fatalities. In October 2008, OSHA published its proposed crane rules and invited public comment. In March 2009, public hearings were held to discuss the new crane

standard. One of the key, and controversial, changes is the requirement that crane operators be certified. The new rules are expected to be adopted sometime during 2009.

In the wake of the 2008 crane accidents in Manhattan, the Department of Buildings and the City of New York swiftly enacted new regulations and measures, which include:

- The requirement that written plans and specifications be prepared by an engineer for the erection, jumping, and dismantling of a tower crane.
- The use of nylon slings was generally prohibited. Nylon slings shall only be used if the manufacturer's manual specifically recommends that nylon slings be used. Nylon slings should never be used unless softening mechanisms have been applied to all sharp edges.
- Minimum training requirements for the crew performing the erection, jumping or dismantling.
- Requiring that safety coordination meetings be held prior to erection or jumping a crane.
- A building inspector must be present whenever a tower crane is raised or lowered.

Other changes being considered by the NYC Department of Buildings include:

- Mandatory Labeling Requirements for Critical Crane Components. This would be a universal system of labeling each key structural component of the crane in order to track it throughout its lifetime. The labeling will include the climbing frame, machine deck, engine, cab, A-frame, turntable, all mast and boom sections and other critical parts.
- Impose Additional Requirements for Testing. This would require suitable testing of critical crane components including, but not limited to, the climbing frame, machine deck, engine, cab, A-frame, and turntable as well as connections, joints, pins, bolts, tiebacks, and collars.

On March 18, 2008, Miami - Dade County passed a new ordinance requiring the following:

- Site inspections of cranes.
- Crane operator certification.

The State of California and City of San Francisco have adopted the following crane regulations:

- Crane safety is under the jurisdiction of the state Occupational Safety and Health Administration.
- Requires inspection certification prior to and following erection of tower cranes using procedures developed for San Francisco Building Code requirements.
- Periodic inspections to ensure appropriate anchorages are in place.

The State of Washington passed legislation to extensively improve crane safety, and the Division of Occupational Safety and Health developed corresponding rules. Most of the new requirements go into effect on January 1, 2010. The laws require certification of crane operators, certification of crane inspectors, and certification of cranes. The laws also require that all non-standard tower crane bases be approved by an independent professional structural engineer.

The State of Utah passed legislation requiring that crane operators must be licensed. However, they do not require tower crane erection certification.

The City of Chicago requires all crane operators to be certified. For tower cranes, the foundation design must be designed by a licensed structural engineer and submitted to the city for review. The Department of Buildings employs seven crane inspectors.

The State of Idaho conducts inspections according to federal OSHA policy. The state does random construction inspections.

Conclusion

The recent changes in regulations are being spurred by a spate of crane accidents that have occurred across the county. The rapid changes in regulations are resulting in widely differing practices across the country. The enactment of new OSHA regulations will be an important factor in "leveling the playing field" in many respects.

The primary changes in the coming years from federal, state, and local regulations, will address these issues:

- Licensing of crane operators
- Training for riggers
- Training for signal persons
- Tracking key crane parts
- Requiring cranes to be certified
- Requirements regarding inspection during erection, climbing, and disassembly

- Design of crane foundations and tiebacks by a structural engineer
- Inspection of foundations and tiebacks
- Licensing for crane inspectors
- Requiring that repairs be approved by the crane manufacturer

References

"Crane-Related Deaths in Construction and Recommendations for Their Prevention," The Center for Construction Research and Training, Silver Spring, MD, Revised January 2009

Ross B, McDonald B, and Vijay Saraf, "Big blue goes down. The Miller Park crane accident," Engineering Failure Analysis, 2007; 14(6): 942-961.

"51st Street Crane Investigation Report," Ove Arup & Partners Consulting Engineers, PC, March 2009

CAL/OSHA Crane Accident Investigation Summary, Tower Crane Collapse November 28, 1989, Department of Industrial Relations, Division of Occupational Safety and Health, May 1990.

ANATOMY OF A TOWER CRANE COLLAPSE – AN OPPORTUNITY TO LEARN

Charles J. Russo, P.E.[1] and Elizabeth A. Puchek[2]

[1]Senior Principal, Simpson Gumpertz & Heger Inc., 2101 Gaither Road, Suite 250, Rockville, MD 20850; PH (301) 417-0999; email: cjrusso@sgh.com
[2]Staff II – Structures, Simpson Gumpertz & Heger Inc., 2101 Gaither Road, Suite 250, Rockville, MD 20850; PH (301) 417-0999; email: eapuchek@sgh.com

ABSTRACT

This paper describes an investigation of the collapse of a 250+ ft tall, hammerhead, freestanding tower crane during a Category 2 hurricane at a construction site in southeast Florida. The investigation showed that the technical cause of the collapse was a tensile failure of the anchor bolts connecting the lowest tower section to the expandable legs cast into the concrete foundation. A subsequent independent study revealed that the out-of-service design-base wind speed for the tower, originally designed and manufactured in the mid-1980s under the *Rules for the Design of Hoisting Appliances* by the European Handling Federation (FEM 1.001), to be inappropriate for the expected wind conditions in southeast Florida during hurricane season. Our work showed that the collapse during this specific hurricane event would not have occurred if the tower crane in this configuration were more appropriately rated to resist wind conditions consistent with SEI/ASCE 37: *Design Loads on Structures During Construction*.

BACKGROUND

We received an assignment in fall 2005 to investigate the cause(s) of a collapse of a 250+ ft tall, hammerhead, freestanding tower crane during a Category 2 hurricane at a construction site in southeast Florida. The maximum recorded wind speeds (3-second gusts) at nearby recording stations at the time of collapse were around 100 MPH with a northwest direction. Our investigation included the following tasks:

- Collect background information on the as-built tower crane, including manufacturer, configuration, and installation records, and the activities prior to the collapse.
- Collect eyewitness accounts of the collapse.
- Conduct a field investigation to document the overall configuration of the debris, which includes identification of how the tower crane collapsed, damaged and undamaged components, movements from original positions and the relative positions of the collapse components, and the configuration of the framing components and their connections.
- Obtain weather records from local measurement stations.

- Develop initial hypotheses regarding the cause(s) of the failure and then test them in the context of the collected background information and findings from our field investigation.

Our assignment stopped after development of initial failure hypotheses due to the limited involvement of our client with this aspect of the project, Had we continued with our assignment, our investigation would have included the following additional effort:

- Establish actions imposed on the structure from dead loads and wind load.
- Estimate the likely capacities of the structural components of the tower crane and anchor bolts.
- Obtain material information on the components of the tower crane and the anchor bolts. Possibly conduct material testing of the anchor bolts and a metallurgical analysis of the fractured surfaces of the anchor bolts.
- Advance our failure hypotheses in consideration of the additional information.

Following several nationally reported incidents involving tower crane collapses and subsequent to litigation proceedings associated with our previous assignment with the collapse in southeast Florida, the authors of this paper conducted independent research as a learning exercise to further investigate the out-of-service stability of frequently used 1980s generation freestanding tower cranes. Our independent research included (1) a review of the design procedures of *Rules for the Design of Hoisting Appliances* by the European Handling Federation (FEM 1.001), a commonly referenced design standard for this vintage of tower cranes, (2) a comparison of design wind pressures using procedures of FEM 1.001 and provisions of ASCE 7: *Minimum Design Loads for Building and Other Structures* and SEI/ASCE 37: *Design Loads on Structures During Construction*, (3) a series of structural analyses as part of a parametric study of different wind pressures to determine the overturning moment and base reactions, and (4) discussions with general contractors, building departments, and engineering consultants regarding the design/use of freestanding tower cranes. For our own interest, we also revisited our previous assignment to advance our initial failure hypotheses.

This paper describes aspects of our investigative assignment and independent research. The paper does not contain the information collected from our discussions with general contractors, building departments, and engineering consultants regarding the design/use of freestanding tower cranes.

THE TOWER CRANE

The freestanding, hammerhead tower crane involved in the collapse in fall 2005 is part of a common fleet of European manufactured cranes originally designed and fabricated in the 1980s. The tower crane had the following characteristics:

- The individual tower sections were 19+ ft in height and 7 ft square in plan dimensions, and consisted of wide-flange corner columns (roughly 9 in. deep and 9 in. wide) and pipe diagonals (3.5 in. dia.). Individual tower sections are bolted together with four bolts per corner column.

- The freestanding configuration had a 250+ ft hook height, a 300 ft overall height (tower top), and a 246 ft hook reach. Figure 1 shows a graphic representation of the tower crane at the project site.
- The base of the tower attached to expendable legs (structural steel assemblies fabricated and provided by the tower crane supplier) cast into the concrete foundation. Each corner column attached to an expendable leg with four anchor bolts. Figure 2 is a graphic representation of the base connection.

Figure 1. Tower Crane

Figure 2. Base Connection

INVESTIGATIVE ASSIGNMENT

Field Investigation. We visited the project site 4 days after the collapse to conduct our field investigation. With the exception of the counterweights and the anchor bolts, the collapsed debris remained in its original resting position. The general contractor marked each of the anchor bolts with unique identifications, and collected and safely stored them at the project site. We learned the following pertinent information from our field investigation:

- The tower mast fell in a northwesterly direction, rotated clockwise 90°, and collapsed onto a nearby two-story structure causing significant property damage (Figure 3).

Figure 3. Collapsed Tower Crane

- The jib fell in a westerly direction across the adjacent building (Figure 3). The counterjib and counterweights were oriented more northerly than the tower mast.

- Primary structural components of the first and second tower sections buckled and/or experienced failed connections. Damage at the northwest and southwest corners was more severe than damage at the other two corners.

- The southeast corner column of the first tower section was essentially straight with only minor deformation (Top left column in Figure 4).
- The northeast corner column of the first tower section had flexural deformation toward the northwest (Top right column in Figure 4).
- The southwest corner column of the first tower section had flexural deformation toward the northwest (Bottom left column in Figure 4).
- The northwest corner column of the first tower section severely buckled and twisted (Figure 5). The lower portion pushed back to the south, the buckled shape occurred just above the first panel point, and the column rotated clockwise over the next panel section.

Figure 4. Tower Base

Figure 5. Tower Base

- Primary structural components in the remaining 11 tower sections showed little to no structural damage.
- The anchor bolts at the southeast corner failed in tension, as evidenced by the cup-and-cone fractures on three of the bolts (Figure 6) and the stripping of threads on fourth bolt. The bolts are essentially straight.

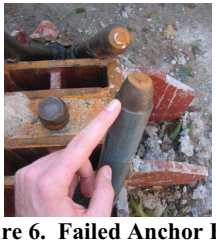

Figure 6. Failed Anchor Bolts

- The anchor bolts at the northeast corner failed in tension, as evidenced by the cup-and-cone fractures on three of the bolts and the stripping of threads on the fourth bolt. The bolts were slightly bent and the steel plate assembly of the expendable leg had moderate deformations. The bends in the bolts and the associated local bearing deformations in the plate assembly were oriented toward the northwest.
- Three of the four anchor bolts at the southwest corner failed in tension, as evidenced by the cup-and-cone fractures. The fourth bolt, the northwestern bolt, failed in shear (Figure 7). The southeastern bolt is straight; the remaining

bolts are bent toward the northwest (Figure 8). The steel plate assembly of the expendable leg had significant deformation from bearing of the bolts, which indicated an overall clockwise twisting behavior, and significant deformation from bearing of the column along the northwest corner (Figure 7).

Figure 7. Bolt Shear and Plate Deformation

Figure 8. Anchor Bolt Orientation

- At the northwest corner, the northern two anchor bolts failed in tension. The southern two anchor bolts remained in place but bent.
- The anchor bolts measured 1.65 in. (42 mm) in diameter at the threads and the body of the shaft, but the section of bolt immediate below the threads had a manufactured reduced diameter of 1.42 (36 mm) over a length of 1.65 in. (42 mm) (Figure 8).
- Other than the local deformations in plate assemblies, the expendable legs did not show signs of visible distress.
- The concrete pile cap did not show visible signs of distress.

Information from Others. We obtained the following information from others:

- The general contractor maintained staff at the project site during the hurricane to monitor the construction site. An eyewitness account bracketed the time of the collapse to a half hour window, and reported that the jib weathervaned and the tower mast rocked in an oscillating manner in a southeast to northwest direction prior to the collapse.
- Experts in the field of crane operations examined the operable components of the collapsed crane and reported that the slewing unit rotated and permitted weathervaning of the jib.
- More than a half dozen cranes collapsed in southeast Florida during this hurricane.

Initial Failure Hypotheses. The conditions of the anchor bolts, components of the tower sections, and the general layout of the fallen tower suggested failure initiated within the first tower section and/or the anchor bolts. We evaluated several hypotheses with different components initiating failure and tested them against the collected physical evidence.

The most probable of our initial hypotheses placed the origin of failure at the anchor bolts in the southeast connection to the expendable leg. The southeast corner would be the outermost corner resisting a northwest wind and, therefore, would

experience the most tensile force. All of the anchor bolts failed in tension and the anchor bolts and corner column were essentially straight. The hypothesis had the remaining failure sequence as the northeast corner (all anchor bolts failed in tension), and then the southeast corner (3 bolts in tension and 1 in shear) and northwest column (buckling and twisting), resulting in the global rotation of the tower mast. The shear failure of the last anchor bolt and the plate deformation in the southwest corner likely coincided with local yielding of the northwest column and then buckling and twisting of the northwest column.

WIND PRESSURE

FEM 1.001. FEM 1.001 prescribes out-of-service wind pressures as a function of the height of the tower crane. These wind pressures (converted from SI units) are 16.8 psf from 0 to 66 ft, 23.0 psf from 66 to 328 ft, and 27.2 psf above 328 ft. These wind pressures correspond to wind speeds of 80 MPH, 94 MPH, and 103 MPH using the static-pressure relationship. Procedurally, the design wind load may be taken as constant over these vertical height intervals or the pressure at the top of the crane may be used as a constant pressure over the entire height. Stability against out-of-service wind load is evaluated using a load factor of 1.0 on the dead weight and 1.2 on the wind load.

FEM 1.001 contains a note to the crane designer that the prescribed wind pressures may be modified in consideration of local weather data when the cranes are to be used for extended periods in locations where wind conditions are exceptionally severe.

ASCE 7 and SEI/ASCE 37. The wind provisions, and specifically the wind velocity profiles, contained in ASCE 7 represent the most current understanding of wind characteristics based on recorded information, research, and statistical evaluation. The wind velocity profile uses a power-law relationship with gradient heights of the boundary layer and power-law exponents defined by exposure categories.

Given that tower cranes consist of standard components (tower sections, jib sections, counterjib sections, etc.) that are generally used throughout the United States, we selected three target design wind speeds for our parametric study. We selected the following 3-second gust wind speeds: 90 MPH, which represents Washington, DC, Baltimore, MD, and a large portion of the continental United States; 110 MPH, which represents Boston, MA, Jacksonville, FL, and other cities in the southeastern United States; and 150 MPH, which represents Miami, FL.

Using the gradient height and power-law exponent for Exposure Category B, we calculated the profile of wind pressures for the different wind speeds from grade to an elevation of 300 ft. Figure 9 shows the profiles of wind pressure with height for FEM 1.001, FEM 1.001 with the load factor of 1.2, and the three target wind speeds.

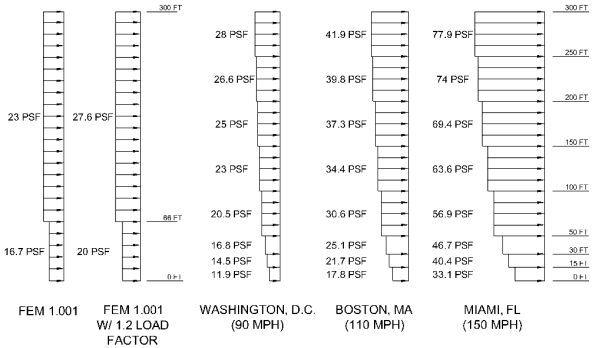

Figure 9. Vertical Profile of Wind Pressures

The intention of SEI/ASCE 37-02 is to provide minimum design load requirements during construction. This standard addresses partially completed structures and temporary structures used during construction. The wind provision includes a reduction factor on the design wind speed obtained from ASCE 7 (specifically ASCE 7-95), which is based upon the premise of maintaining the same statistical probability of exceeding the design mean recurrence interval. For a reasonable construction period of 1 to 2 years, the reduction factor would be 0.85.

STRUCTURAL ANALYSIS

We performed a series of structural analyses on a specific tower crane configuration as part of a parametric study to evaluate the stability of the freestanding tower crane under different wind profiles. The focus of our study was to determine overturning moment and base reactions for comparison to the nominal strengths of the wide flange corner columns of the tower mast and the anchor bolts.

Structural Model. We chose to use the freestanding tower crane from our southeast Florida investigation (7 ft square base dimensions, 250 ft hook height, 246 ft hook reach). We obtained a part list and erection manual for the tower crane to determine geometries and weights. The tower section consists of the following components: the corner columns are IPBV 220, Grade ST 53-2 steel; the pipe diagonals are 88.9 mm dia., 7.1 mm wall thickness, Grade ST 53-2 steel; the anchor bolts are M42, Grade A490M steel. We modeled the tower crane using the finite-element based computer software FEMAP and performed a linear analysis incorporating second-order effects using ABAQUS.

We obtained manufacturer's engineering information on the base reactions (overturning moment, vertical base reaction, and lateral base reaction) for FEM 1.001 wind loads for this specific tower crane configuration. For comparison, the results of our finite-element analysis using FEM 1.001 wind loads produces base reactions that are within 5% of the reported manufacturer's engineering information.

Wind Loads. We calculated the wind forces on the various components of the tower crane accounting for wind-pressure shape coefficients for the components, shielding effects from aligned and shadowed component, and wind direction at an angle to the component. We considered two wind directions for our analysis: a face-on wind direction (perpendicular to a side of the tower mast) and a diagonal wind direction (aligned with the diagonal of the square tower mast). We calculated an increase in wind force on the tower mast of slightly more than 10% when the wind direction is applied along the diagonal as compared to a face-on wind application. In both cases, the jib is free to weathervane.

For the FEM 1.001 wind pressures, we applied the maximum pressure over the entire height of the tower crane. For the target cities, we applied the interval pressures calculated from ASCE 7 and shown in Figure 9. We did not apply a gust factor to our wind load calculations, as would typically be done for the flexible tower cranes when considering wind speeds developed on a fastest mile basis. The wind speed contours in ASCE 7-02 are based on a new and more complete analysis of hurricane wind speeds and account for peak gust speeds in the given return period.

Tower Capacities. We calculated nominal strengths for the components of the tower section and the anchor bolts using the strength limit state provisions of 2005 AISC Specification for Structural Steel Buildings. We calculated the following nominal strengths:

- Corner Column – Nominal compressive strength of 1,130 kips; nominal tensile strength of 1,115 kips. The column is considered to be laterally braced at panel points.
- Anchor Bolts - Nominal tensile strength (yielding) 215 kips per bolt, which is controlled by the reduced diameter.

In the context of base reactions, the maximum compressive base reaction under each column cannot exceed the nominal compressive strength of the column (1,130 kips) and the maximum tensile base reaction cannot exceed the cumulative strength of the group of four anchor bolts (860 kips).

Results of Analyses. Table 1 reports the overturning moment at the base of the tower, the maximum compressive reaction, the maximum tensile reaction, and the total lateral reaction associated with face-on directional wind loading.

Table 1. Analysis Results for Face-on Wind Loading

	FEM	1.2 * FEM	90 MPH	110 MPH	150 MPH
Overturning Moment (ft-kips)*	6,155	7,700	7,200	11,545	22,790
Compressive Reaction (kips)*	510	630	585	890	1,675
Tensile Reaction (kips)*	345	465	420	720	1,505
Lateral Reaction (kips)*	45	55	50	70	130

***** - Reported value rounded to the nearest unit of 5

The more severe condition for the base reactions of the square tower is when the wind is oriented along its diagonal. Table 2 reports the overturning moment at the

base of the tower, the maximum compressive reaction, the maximum tensile reaction, and the total lateral reaction associated with wind loading directed along the diagonal of the tower.

Table 2. Analysis Results for Wind Loading Directed Along Diagonal

	FEM	1.2 * FEM	90 MPH	110 MPH	150 MPH
Overturning Moment (ft-kips)*	6,550	8,175	7,620	12,180	23,950
Compressive Reaction (kips)*	740	900	850	1,305	2,485
Tensile Reaction (kips)*	575	740	680	1,140	2,320
Lateral Reaction (kips)*	50	60	50	75	140

* - Reported value rounded to the nearest unit of 5

Using the results of the parametric study for wind directed along the diagonal, we used interpolation to approximate wind speeds associated with the limiting tensile and compressive strengths of the components. Using interpolation, which will slightly overestimate the wind speeds, we estimated 98 MPH wind speed will produce a tensile base reaction equal to the nominal tensile strength of the group of anchor bolts and 103 MPH wind speed will produce a compressive base reaction equal to the nominal compressive strength of the corner column. For both estimated wind speeds, we also checked the axial demands on the pipe diagonals and the bolted connections between tower sections to evaluate whether a local strength limit state is initiated. For both cases, strength limit states were not reached.

We applied the 0.85 wind reduction factor of SEI/ASCE 37-02 to the 110 MPH wind speed (diagonal direction) and calculated an overturning moment of 10,120 ft-kips, a compressive reaction of 1,100 kips, a tensile reaction of 930 kips, and a lateral reaction of 65 kips.

DISCUSSION

Our structural analyses show that the overturning moment and base reactions on the out-of-service, 250-ft hook height, freestanding tower crane resulting from wind provisions and stability requirements of FEM 1.001 are comparable to the overturning moment and base reactions that one would anticipate in a region of the United States with a 90 MPH ASCE 7-02 design wind speed (3-second gust). The tower crane reaches strength limit states at about 100 MPH wind speed (98 MPH for nominal tensile strength of anchor bolts and 103 MPH for nominal compressive strength of corner column).

As discussed earlier, SEI/ASCE 37 includes a provision to reduce the design wind speed from ASCE 7 for temporary structures in consideration of the expected construction period. Given a 1 to 2 year construction period, the reduction factor is 0.85. We interpolated the results of our parametric study and estimate that the strength limit state for the anchor bolts occurs at a design wind speed of 104 MPH in consideration of the permitted 0.85 reduction factor in SEI/ASCE 37. Therefore, the tower crane, with its standard tower section and anchor bolts, would not be suitable in a region where the out-of-service wind speed, as mapped by ASCE 7, is anticipated to

exceed about 100 MPH without the benefit of SEI/ASCE 37 provisions, or exceed about 104 MPH with the benefit of the 0.85 reduction factor. While not part of our independent study, one could perform a more rigorous analysis based on the probability of failure to estimate these limiting wind speeds.

Along the east coast of the United States, the mapped design wind speeds of ASCE 7 of 100 MPH and higher are associated with Atlantic hurricanes. Outside of hurricane season, SEI/ASCE 37 indicates that a 90 MPH design wind speed may be considered. Therefore, the subject tower crane would be suitable for periods outside of an anticipated hurricane. Upon notice of an impending hurricane, the subject tower crane would need to be lowered to a freestanding height such that the anticipated wind speeds will not produce forces that reach strength limit states of the components.

Evaluation of Collapsed Tower Crane. The 250+ ft tall, hammerhead, freestanding tower crane that was the focus of our investigation is the same tower crane that we used in our parametric study. The maximum recorded wind speeds (3-second gusts) at nearby recording stations at the time of collapse were around 100 MPH, and the wind had a northwest direction. Our study showed that at wind profiles associated with this magnitude wind speed and direction, forces anticipated in the tower section reach the strength limit state for the anchor bolts. When these anchor bolts have a demand-to-strength ratio of 1.0, the northwestern column under compression has a demand-to-strength ratio of 0.9. The analysis results support our initial failure hypothesis that collapse initiated at the southeast anchor bolts.

CONCLUSIONS

Our study demonstrated that the out-of-service, FEM 1.001 design wind speed/pressures for the erected tower crane configuration were not appropriate for the expected wind conditions in southeast Florida during hurricane season, which is 140 MPH based on the mapped wind speeds in ASCE 7-02. In addition, our study also showed that the collapse during this specific hurricane event in fall 2005 would not have occurred if the tower crane in this configuration were more appropriately rated to resist wind conditions consistent with SEI/ASCE 37.

REFERENCES

American Society of Civil Engineers (ASCE/SEI 7-02). (2002). *Minimum Design Loads for Buildings and Other Structures.* Reston, VA.

American Society of Civil Engineers (SEI/ASCE 37-02). (2002). *Design Loads on Structures During Construction.* Reston, VA.

European Handling Federation (FEM 1.001, Third Edition). (1987). *Rules for the Design of Hoisting Appliances*. Paris, France.

European Handling Federation (FEM 1.001, Third Edition - Revised). (1998). *Rules for the Design of Hoisting Appliances*. Paris, France.

Damage Assessment of Houses and Buildings from an Engineering Point of View

Charles R. Norman P.E.[1]

[1]Consulting Engineer, Private Practice, and Former Professor at McNeese State University, Lake Charles, LA, charles_norman@bellsouth.net

ABSTRACT

This paper addresses methods of assessing damage to buildings and houses based on an engineering approach that utilizes forensics along with codes and standards to determine the extent of the damage. The various causations of the damage include wind, fire, floods, earthquakes and blasts. A general approach to the examination of the risks is outlined, and the elements that a report should contain are addressed. Emphasis is placed on the decisive role that corroborating information plays in determining the extent and the proximate cause of damage.

INTRODUCTION

Engineers are often asked to inspect buildings and houses (risks) to evaluate the damage caused by an event such as a hurricane, tornado, fire, flood, earthquake, etc. These risks may include non engineered, marginally engineered, or pre engineered structures. Professional engineers have a point of view that deals with loads, structural resistance, degree of damage, mechanical and structural integrity, material strength, etc. The evaluation may be used to assess the amount of damage, methods of repairing the risks, and safety of the risk, and to determine if the risk is a constructive total loss or total loss. Typically engineers refer to builders and contractors to assess the cost of repairing the damage.

The different approaches that engineers use depend upon the risk, the amount of damage to the risk, and the engineer. A home that is completely destroyed will be approached differently from a home with minor damage. However, the end result is to determine the amount of damage that was caused from the event.

This paper presents engineering methods to inspect houses and buildings. These methods should be useful to inspectors, adjusters, engineers, architects, and owners to identify damage that must be repaired to restore proper mechanical and structural integrity as well as cosmetic appearance. It also addresses causation methodology and describes the concept of constructive total loss.

The methods include acquiring the necessary information to document the design of the risk, determining the loads and energy imparted to the risk, documenting the visual physical damage, evaluating the extent of the physical damage from the loads, and the preparation of a written report.

EXAMINING THE OUTSIDE

An engineering inspection should begin with documentation of the location and physical appearance of the structure from the external. In other words, photograph the front and rear view, and the two side views of the structure. (Figure 1)

If available, aerial photos are useful. Also, document the physical address and exposure of the risk. Exposure is identified in ASCE-07. This is an important issue for hurricane and tornado wind loads. Occasionally, a GPS reading is also used to locate the risks in reference to winds on radar.

The exterior shape of the structure, type of roof, outside finish, location and type of windows, and attached structures such as carports should be identified. Attention should be paid to details of the roof such as age, gauge, number of nails per shingle, type of shingle, etc. Type and wind rating of windows is also important.

If the home is on a slab, the pinning of the bottom wall plates, the thickness of the slab, footings, grade beams, post tension slab, etc. must be documented. If the home is on piers or piling, the size, height, location of piers, etc. must be photographed. For elevated structures, the bracing must be documented. In the case of wind and flood related damage assessments, the elevation of the grade, bottom floor or lowest horizontal member must be determined. This is important to determining the height of water entering a structure.

All roof planes must be evaluated to identify sagging or bulging rafters. It is best to photograph these planes as well. A wavy roof plane is important to document since is may be related to vibration from wind or fire damage.

If the structure has been destroyed, the documentation of the structure prior to the event must be obtained from the owner, local government official, etc. In the case of a tree(s) falling onto a structure, several photographs from different angles must be taken to document the damage zone. If the tree was removed, a measurement of the weight of the tree or an estimate is required. Differential measurements of the floor should also be taken to evaluate the affects of the tree impact on the foundation. This includes documenting movement of piers.

Photographing structures around the subject risk is also helpful, particularly for wind related damage. Nearby structures that are engineered should be included.

Figure 1. Documenting the views.

EXAMINING THE INSIDE

Once the outside has been documented, the inside must be inspected and documented. This includes photographing the inside ceilings, walls, doors, cabinets, floors, attic sections, insulation, and wiring. Photographs of damaged and non damaged areas should be included. Some examples of damage to the inside include cracked sheetrock, separated molding and trim, cracked ceramic floor coverings, distorted walls and door frames, cracks in chimney, moisture and mildew behind walls, cracked glass, uneven cabinets, floors that vibrate, walls separated, etc. In the attic, the rafter to top ridge plate must be inspected. Also, most of the rafters and rafter to top wall plate should be inspected. Documenting the bracing in the attic frame and damage to rafters should be considered. (Figure 2)

The engineer should discuss with the owner any plumbing or electrical problems. If there were inspections done by a licensed inspector or another engineer prior to the visit, these documents should be reviewed by the engineer. A floor plan is required. Most of the time an insurance inspector will draw a floor plan. Sometimes the owner will have an engineering drawing of the floor plan. Other times, a professional foundation repair company will have drawn the floor plan. The overall size of the building envelope is critical to evaluating wind, flood, fire and earthquake related damage.

In the framing, the type of connections should be documented. This includes identifying hurricane clips and straps, bolting, and toe nail connections. The spacing and size of the rafters, ridge plate, decking, strong backs, cross bracing, type of insulation, etc. must be documented.

All of the above information is useful in determining the resistance of the risk to applied loads from tornadoes, hurricanes, earthquakes, floods, etc. Engineers should also consider the weaker and stronger aspects of the structure in evaluating the extent of the damage.

Figure 2. Separated rafter to ridge beam and broken rafters.

FOUNDATIONS

Foundations require special attention since they support the structure and also provide anchoring of the structure. Types of foundations include concrete slabs, piers (various types), structural frame and pilings. Structures may be on grade or elevated. Elevated structures require bracing and this must be evaluated and documented. For houses gravity set onto piers, termite plates must be considered in the design and resistance of the structure.

During the inspection of a home, unlevelness of the foundation, cracked slab and/or flooring coverings, out of plumb walls, etc. must be noted. If the structure is unlevel, then the engineer or a professional foundation repair expert familiar with laser level or water level technology must be called to evaluate the structure. This data can be used by professional engineers to further evaluate the need for repair and repair plans for the structure.

RATING RESISTANCE OF STRUCTURES

Structures may be rated for hurricane and tornado winds. The scale is F0 to F5 based on the Fujita scale. The Enhanced Fujita (EF) scale is a very useful method of rating the resistance of structures and also determining the degree of damage. (Figure 3) The Beaufort and Mach scales are also useful in determining damage. The Saffir-Simpson scale does not have adequate detail to perform damage assessment, but can be useful if categorizing wind associated with Categories of hurricanes. Individual components such as roofs, siding, windows, and manufactured houses may be rated according to the Fujita scale. Individual components are often wind tunnel or wind speed rated according to the manufacturer. Pre-engineered structures are often wind rated and this may be used to determine the resistance of a structure. Examples are metal buildings, flag poles, tall towers, and signs.

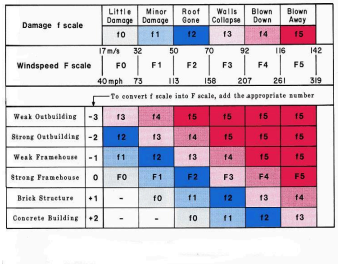

Damage f scale		Little Damage	Minor Damage	Roof Gone	Walls Collapse	Blown Down	Blown Away
		f0	f1	f2	f3	f4	f5
Windspeed F scale	17 m/s	F0	F1	F2	F3	F4	F5
	40 mph	73	113	158	207	261	319
To convert f scale into F scale, add the appropriate number							
Weak Outbuilding	-3	f3	f4	f5	f5	f5	f5
Strong Outbuilding	-2	f2	f3	f4	f5	f5	f5
Weak Framehouse	-1	f1	f2	f3	f4	f5	f5
Strong Framehouse	0	F0	F1	F2	F3	F4	F5
Brick Structure	+1	-	f0	f1	f2	f3	f4
Concrete Building	+2	-	-	f0	f1	f2	f3

Table 4.

One- and Two-Family Residences (FR12)

Typical Construction

- Asphalt shingles, tile, slate or metal roof covering
- Flat, gable, hip, mansard or mono-sloped roof or combinations thereof
- Plywood/OSB or wood plank roof deck
- Prefabricated wood trusses or wood joist and rafter construction
- Brick veneer, wood panels, stucco, EIFS, vinyl or metal siding
- Wood or metal stud walls, concrete blocks or insulating-concrete panels
- Attached single or double garage

DOD*	Damage description	EXP	LB	UB
1	Threshold of visible damage	65	53	80
2	Loss of roof covering material (~20%); gutters and/or awning; loss of vinyl or metal siding	79	63	97
3	Broken glass in doors and windows	96	79	114
4	Uplift of roof deck and loss of significant roof covering material (>20%); collapse of chimney; garage doors collapse inward or outward; failure of porch or carport	97	81	116
5	Entire house shifts off foundation	121	103	141
6	Large sections of roof structure removed; most walls remain standing	122	104	142
7	Top floor exterior walls collapsed	132	113	153
8	Most interior walls of top story collapsed	148	128	173
9	Most walls collapsed in bottom floor, except small interior rooms	152	127	178
10	Total destruction of entire building	170	142	198

* DOD is degree of damage

Figure 3. The Fujita Scale pegged to damage-causing wind speeds. Example of Enhanced Fujita (EF) Scale implemented in U.S. on February 1, 2007.

IDENTIFYING THE DAMAGE

The engineer must be careful to identify all damage. Mistakes are created when damage is overlooked or omitted. A good example of this is a foundation. If the foundation is unlevel, repairs to a structure may not take or last very long. In some cases, it may not be possible to effectuate repairs unless the foundation is leveled. Another example is missing damage to a roof frame that has been racked or distorted. An attic frame that had little bracing and was damaged by severe winds may require mitigation to restore the mechanical and structural integrity. The damage must include distortion of the upper framing.

In general, damage can be grouped as follows. This is not an all inclusive list.
Structural: Structural includes damage to members such as overstressing, breaking, loss of joint strength, deck separation, and separation of members, distortion of frame members, and movement or failure of foundation. Structural damage may also include a weakening of the structure due to fatigue.
Mechanical: Mechanical damage includes reduction in mechanical properties, failure in plumbing and HVAC, corrosion of materials, abrasion of materials and finish, water damage to insulation and sheetrock, separation of dissimilar materials, failure of roof materials and attachments, failure of windows, loss of seals, etc.
Cosmetic: Cosmetic damage includes separation of trim and molding, cracking of paneling and sheetrock, failure of outside bricking or siding, loss of shutters, gutters, fascia, soffit, separation in wood floor coverings, water damage to inside contents from wind and infiltration, etc.
Safety and Health issues: Mold and mildew issues. Handrail damage around porches, walkways and stairways, electrical wiring and plumbing issues, leaks in gas pipes, electrical riser damage, etc.
Environmental issues: Asbestos materials damaged, leaks in pipes, containment of environmental sensitive MSDS materials, etc.
Economic issues: Cost to comply with new codes, regulations, elevations for FEMA.

DOCUMENTING THE DAMAGE

Physical damage can be photographed. Some of the more difficult damage to photograph is small cracks in light materials, but these can be identified on the photographs. Most of the time more than one picture is needed to identify the damage. For example, pictures of several rafters to ridge plate connections or lifted decking are important. Outside pictures of damage are also important in using damage scales. (Figure 4) There are instances where photographs do not show all damage.

Occasionally, a sketch of the damage is helpful. For example, a tree fallen onto a structure is usually sketched to show where the tree hit the floor plan of the risk and this is used to assess the damage zone. A section of a structure that has twisted relative to another section can easily be sketched. A contour map of the differential measurements of elevations of a slab or floor should be sketched.

Computer analyses of the damage can be useful. For example, when the wind or earthquake loads are imposed on a beam or a frame a computer generated analysis with graphics may be useful. Floor and ceiling beams that are damaged from excessive loads due to wind can be analyzed by hand or using computer analysis to show the moments, loads, deflection, and stresses.

A complete structural analysis of the entire structure can be performed for damage assessment, primarily to support the physical evidence. These analyses are expensive and are not usually done unless requested. They are useful to determine how a structure fails and what the proximate cause of failure when two or more events load a structure. In many cases, component failure occurs prior to complete structural failure.

Water damage to wood materials is important to document. For example, the long term exposure of wood to outside elements such as rain and sun can reduce the mechanical strength of the timber members by 50%. This may result in sagging of roof lines and ceilings. Mold and mildew growth can also be documented. Experts in determining, measuring, and treating mold are called in to evaluate health risks to owners. Exposure of metal structures to saltwater can cause excessive corrosion of the materials and weaken the structure.

Figure 4. Documenting damage from a fallen tree and exterior wind and water.

DATA FROM EVENT

A very important part of the engineering evaluation is to document the data from the event that caused the damage. For example, the magnitude and direction of hurricane winds along with the duration and timeline of the winds is important. The building envelope and angle of attack are crucial to understanding the performance of the risks to wind. The radius of maximum winds, the eye wall and the sustained and gust winds are critical to describing the wind field. Usually there is very limited amount of wind recordings made in a large hurricane. Therefore it is critical to describe the wind field and location of the building or structure in the wind field. Figure 5. In the case of the combination of two or more events, the time line for each event and the combination of events is important. For example, a hurricane that has hurricane force winds prior to the combination of wind and water forces must be documented. Tornadoes are rated using the Enhanced Fujita scale for wind speed and damage. Earthquakes are documented using the Richter scale and epicenter. Fires are rated according to BTU and type of fire. The National Weather Service, NOAA, FEMA, USGS, the US Army Corps of Engineers and local authorities provide information on major events in the area of concern. In each of these events, considerable engineering data and science is available to provide the engineer with loads on structures. These sciences are provided in codes and standards such as the NFPA Life Safety Code, NFPA Fire Protection Handbook, and the ASCE “Minimum Design Loads for Buildings and other Structures” ASCE 7-05. The engineer must utilize this information to assess the loads and timing of loads that caused damage to a structure.

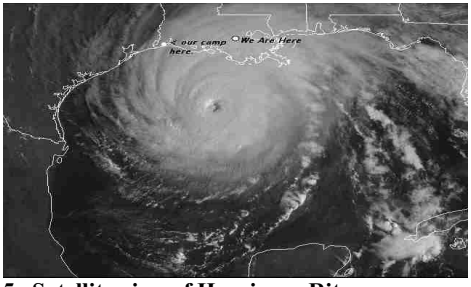

Figure 5. Satellite view of Hurricane Rita.

ROLE OF THE ENGINEER

The role of the engineer is to evaluate damage to the risk in terms of its design resistance, the magnitude of the loads and energy that reached the structure, the forensics available that show the damage and to use the loads and energy imparted to the structure to determine the extent of the damage. In the case of more than one event, each event and the combination of events should be included in the analysis. Also, all available information, data, forensics, and engineering methods must be corroborated to fully understand and evaluate the damage. In some cases this may be difficult to do. However, in all cases engineering methods must be employed to assess the damage.

Some of the questions that an engineer can consider in corroborating information for different events are

- What were the magnitudes and directions of the winds and how long did they last?
- How much water entered the risk and how fast was the water traveling?
- What was the timing of the wind vs. water?
- What type of fire occurred and how large was it?
- What are the fire resistant ratings of the various materials?
- What is the size and duration of the earthquake?
- What is the rating of the blast?
- What are the debris tracks and fields?
- What are the characteristics of the damage?

TOTAL LOSS

A complete loss of a risk can be a total loss or a constructive total loss. If the risk is destroyed by an event and only debris remains, it is a total loss. A constructive loss is a partial loss but the damage is so extensive that repairs would cost as much or more than the property is worth or the limit of insurance policy. Another constructive loss is a partial loss and the cost to repair and bring the risk to new required standards would exceed the value of the property. Also, the cost of repairs may exceed the cost to rebuild a new structure and the loss may be declared a constructive total loss.

In the case of a total loss, the engineer must consider the proximate cause of the loss. If only one event happened to the risk, the proximate cause is somewhat easier to determine. In the case of two or more events such as wind and water, the engineer must consider the timeline and magnitudes of the forces and energy for each event. If the timeline is not developed and considered, errors may occur in attributing the damage to each event. The risk shown in Figure 6 was a home located near the Gulf Coast and a major hurricane reached the site and destroyed the risk. Figure 6 also shows part of the risk after the storm. In this case, the proximate cause of the constructive total loss was hurricane wind forces even though flood waters reached the home during the storm.

Opinions that are based solely on the magnitudes of the forces and energy from a narrow timeline may be subject to error. A better approach is to consider the damage to the risk as they occur. In other words, winds that attacked a structure for 8 to 10 hours prior to water reaching the structure must be considered separately for their damage. Although the structure may have been destroyed, the knowledge of the design resistance to wind may indicate that the structure failed due to wind loads prior to water reaching the structure. Thus an evaluation of the resistance of the risk to the winds will help the engineer evaluate the degree of damage to the risk for wind prior to a subsequent event. The same is true if water and wind reach a structure concurrently. A damage assessment for each type load can be used to determine the degree of damage from each providing an engineering approach is used to superimpose the loads.

The risk in Figure 7 illustrates a total loss where wind alone loaded the structure for 10 hours, wind and water combined to load the structure for 5 hours, and the risk was declared a constructive total loss due to wind damage. Storm surge did not reach the bottom floor of the risk.

A risk can also be declared uninhabitable due to an event prior to a second event. In the case of a hurricane, a risk along the coast could become uninhabitable due to hurricane force winds prior to storm surge or flood waters arriving at the site.

Forensic data is also useful in determining the severity of an event. The fractured piece of metal roofing in the tree as shown in Figure 7 helped to identify severe winds that destroyed a risk close by.

Figure 6. Risk after storm illustrating a complete loss.

Figure 7. A constructive total loss and forensic evidence showing winds.

OTHER CONSIDERATIONS

In general, the engineer is trying to inspect and document damage to a risk before the risk has been disturbed. Therefore the engineer should inspect soon after the incident. That is not always possible. However, photographs that others took can be used as well. In all cases, the engineer should visit the risk site and document the forensic evidence even though the site may have been disturbed. When a site visit is scheduled it is important for the owner to be notified and asked to attend the inspection. Examples of errors include a visit to the wrong site, evaluating a structure that was destroyed without knowing how the structure was designed and constructed, and failing to recognize outside or additional structures. Following are additional considerations.

- Engineers should be called early.
- Engineers should be free to investigate.
- Adequate time must be allowed for a thorough inspection.
- Engineers should be free to talk to the owner, adjuster, etc.
- All available information on the event should be provided.
- Engineers must keep in mind the safety of the risk, the protection of the economic assets of the owner, and the separation of damage from more than one event.
- Engineers must be prepared to render opinions on the efficient or proximate cause of a total loss or a constructive total loss.

REPORT ON DAMAGE ASSESSMENT

The report on the damage assessment is the focal point of the investigation. It should address the scope of work and the findings and in some cases recommendations. The purpose of the report should be clearly stated. If the engineer is limited in the scope of work, this must be clearly stated. However, in most cases the engineer must be free to evaluate the damage and the causation of this damage for the entire risk. Limiting the scope of the investigation can influence the outcome. For example, limiting an investigation to a single event when more than one event occurred may result in errors in determining the proximate cause of the damage. Items to include are

- Name, address, general location and date of examination.
- Persons attending the site investigation and reviewing the findings.
- Identification and timing of event(s) causing the damage.
- Role of the engineer or assignment given to engineer.
- Characterization of loads and or energy causing the damage.
- Characterization of the resistance of the risk to the event(s).
- Forensic data that is available.
- Analysis of damage and extent of damage based on engineering methods.
- Findings along with summary & conclusions.
- Photographs.

SUMMARY

Damage assessments of risks by engineers are important to owners, insurance companies, mortgage holders, local, state, and federal governments, and persons interested in purchasing or repairing a damaged risk. Engineering damage assessments are on the increase because engineers apply good engineering principles and practice in evaluating a risk and in developing repair plans.

Engineers typically do not exclude any part of a damage assessment since they need to examine the entire structure to determine the extent of the damage and in some cases the proximate cause of damage. There are recognized engineering methods based on studies, building codes, engineering codes & standards that are available to engineers and these should be utilized.

Repair plans are often the second part of an engineer's damage assessment and they require detail analysis, detail drawings, and prioritizing items to be repaired.

The proximate cause of damage is best determined using engineering methods that utilize the magnitudes of loads and energy. Also, the timeline for the loads and energy imparted, particularly when more than one event reaches a structure, is a very important consideration. All available data and information must be corroborated to determine the relative damage caused by more than one event.

REFERENCES

ASCE, "Minimum Design Loads for Buildings and Other Structures", *ASCE* 7-05, Reston, Va., 2005.

International Code Council (ICC). (2006). *International Building Code,* ICC, Falls Church, Va., 2002.

International Code Council (ICC). (2006). *International Residential Code,* ICC, Falls Church, Va. NFPA, 2002).

NFPA, *SFPE Handbook of Fire Protection Engineering.* 3rd Edition, Quincy, Ma., 2002.

National Weather Service. *Enhanced Fujita Scale*. Texas Tech University, Lubbock, TX, June, 2004.

Norman, C. R. (2007) "Damage Assessment of Homes and Buildings-Distinguishing between Storm Surge and Wind", ASCE-SEI, Longbeach, CA.

INVESTIGATION OF LOAD CAPACITY AND SERVICEABILITY OF ASSEMBLED CONCRETE BLOCKS (DOX PLANK)

Anthony M. Dolhon[1], P.E., M.ASCE; Dennis D. Rolander[2], P.E., M.ASCE; Mark R. Chauvin[3], P.E., M.ASCE; and David S. Finley[4], E.I.T., AM.ASCE

[1] Senior Associate, Wiss, Janney, Elstner Associates, Inc., 14 Washington Road, Suite 501, Princeton Junction, New Jersey 08550; Telephone: (609) 799-7799; Facsimile: (609) 799-7088; E-mail: adolhon@wje.com
[2] Senior Associate, Wiss, Janney, Elstner Associates, Inc., 2751 Prosperity Avenue, Suite 450, Fairfax, Virginia 22031; Telephone: (703) 641-4601; Facsimile: (703) 641-8822; E-mail: drolander@wje.com
[3] Senior Associate, Wiss, Janney, Elstner Associates, Inc., 600 Highway 169 South, Minneapolis, Minnesota 55426; Telephone: (952) 545-0295; Facsimile: (952) 544-6954; E-mail: mchauvin@wje.com
[4] Associate II, Wiss, Janney, Elstner Associates, Inc., 9655 Sweet Valley Drive, Suite 3, Cleveland, Ohio 44125; Telephone: (216) 642-2300; Facsimile: (216) 642-6288; E-mail: dfinley@wje.com

Abstract

This paper presents a literature survey of roof and floor slab systems constructed of assembled concrete blocks as manufactured in the 1940s, 1950s, and 1960s with a retrospective on load capacity considerations and serviceability. Assembled concrete blocks were formed by assembling a row of lightweight hollow core concrete blocks into a prestressed plank. The most common system, which came to represent the industry, was Dox Plank named for its inventor Bernard A. "Doc" Vander Heyden. Mr. Vander Heyden patented improvements in the planks and the methods of constructing them in 1954 and 1965. This survey of United States patents, manufacturers' design data, and design theory will aid the forensic engineer in an investigation of the load capacity and serviceability of existing systems. This survey identifies the original design parameters, such as the allowable unit stresses, area of embedded steel, material properties, etc.

Introduction

Past performance of buildings in service can be an indicator of future performance. However, when past performance alone is insufficient to evaluate serviceability, or when changing the building use, or adding dead loads, further investigation and analysis may be warranted. This analysis can be challenging, if not incomplete, without a basic understanding of original design theory, material properties,

manufacturing, and installation methods in use at the time of construction. This paper presents a literature survey of assembled concrete blocks as manufactured in the 1940s, 1950s, and 1960s used in roof and floor slabs to aid the forensic engineer in an investigation of the load capacity and serviceability of existing systems that remain in service today.

Description

Assembled concrete blocks (Fig. 1) were made of lightweight hollow core concrete. They were formed by placing blocks end to end in a row to form a plank and placed upside down on a work table. The blocks within the plank were compressed by an external means using approximately 20,000 pounds of clamping force applied to the ends of the planks. Once the blocks were compressed together reinforcing steel bars were then laid into the aligned channels and grouted into place. Once the grout cured the externally applied compression was removed, thereby forming a minimally prestressed plank.

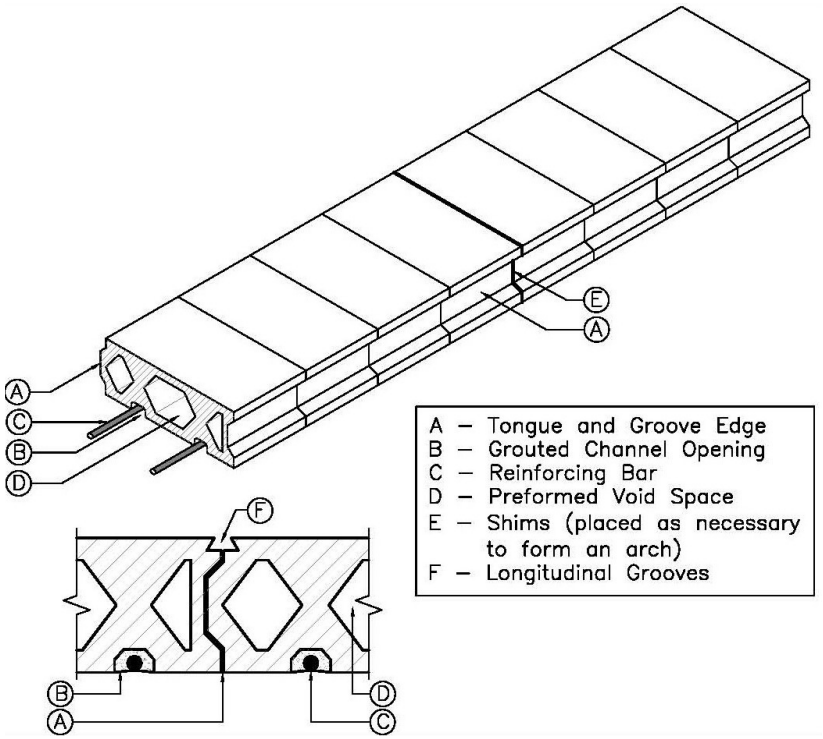

Fig. 1. Typical Dox Plank

Once the planks were delivered to the jobsite, they were hoisted into position and laid side by side to form a roof or floor slab. Each plank had tongue and groove edges for shear transfer to aid in forming a more cohesive slab. Longitudinal grooves were cast into the upper corners of the blocks to increase composite action and to increase the overall strength of the slab assembly once a thin concrete topping (usually up to 2 inches) was cast on top of the planks. Some of the earliest plank systems lacked the longitudinal grooves.

The planks had the advantage of being manufactured in the factory, thereby providing greater supervision, control, and uniformity than would otherwise be available on the jobsite. The planks were able to be erected quickly. Once in place the slab served as a working platform and as a ceiling. The lightweight aggregate and hollow cores reduced the overall weight of the slab. The cores could be used as conduits for utilities or as air ducts. The undersides of the planks formed a flat ceiling which may, or may not, have been plastered.

Historical Significance

During the 1920s, the American Concrete Institute (ACI) formed Committee 711 and tasked it to undertake a critical examination of the state-of-the-art in practice and construction methods used with precast concrete joists and superimposed concrete floor systems, and also to make recommendations for minimum standard requirements.

On July 25, 1929, Committee 711 submitted its initial report to ACI. It was titled, "Precast Joist Concrete Floor Systems." The report was first published in January 1940 (ACI, 1940), but it was not until November 1952 that Committee 711 first recognized the popularity of assembled concrete blocks by introducing standards specific to those systems.

Assembled concrete block systems gained popularity as an economical alternative to wood and light steel joists for relatively light loads. They were not recommended for roofs or floors with heavy loads or moving machinery due to the potential for impact forces and vibrations.

Assembled concrete block systems emerged as an attempt to eliminate or to minimize the cost of carpentry that was otherwise necessary for formwork used in cast-in-place concrete. Assembled concrete block systems were particularly well suited for residential and light commercial construction, such as schools, office buildings, and motels.

Variations in proprietary assembled concrete blocks generally consisted of differences in the external clamping action, grouting process, external tensioning, camber, block shapes, and the manufacturing apparatus. Most of these variations are structurally insignificant and cataloging the variations between proprietary systems is outside of the scope of this paper.

Among the proprietary systems that attracted the most attention was Dox Plank, initially known as "Doc's Blocks." It was named for its inventor Bernard A. "Doc" Vander Heyden, who patented improvements in the planks and in the methods of construction in 1954 and 1965. He founded the Dox Plank Manufacturers Association, which licensed approximately 25 manufacturers across the eastern United States in the 1950s and 1960s. Although Dox Plank is just one variation of an assembled concrete block system, it came to represent the industry.

The production of high strength steel reinforcement (especially wire strands) and the increased compressive strength of concrete lead to the advent of presetressed concrete in the 1950s, which improved upon many of the disadvantages of conventionally reinforced concrete. The introduction of hollow core, prestressed planks captured the market formerly dominated by Dox Plank, which naturally led to the decline and discontinuation of the Dox Plank system in construction.

Dox Plank Patents

On June 19, 1944, Mr. Vander Heyden filed an application with the United States Patent Office, which was a continuation of an earlier application that was filed on May 17, 1943, for improvements to a system of prestressed planks using concrete blocks and the method of manufacture. Patent No. 2,696,729 was granted on December 14, 1954 (Vander Heyden, 1954).

The stated objective given in Patent No. 2,696,729 was, "To provide a strong but light and porous cementitious plank combining great strength with a high thermal and acoustical insulation factor, which together with its light weight, adapts it for making of roofs and floors, and the like." The patent identified 13 claims distinguishing it from other patents using concrete and clay tile block.

The patent provisions stated that the planks are to be supported at their ends and that the planks are manufactured by grouting reinforcing bars throughout the length of the planks, so as to distribute the compressive stress to individual blocks rather than concentrating it within the end blocks. The reinforcing bars are not threaded nor do they extend beyond the end blocks.

The patent provisions also stated that the manufacturing process provided a means for grinding the face of individual blocks, aligning the channels and hollow cores within a row of blocks, placing reinforcing bars at predetermined positions in the plank, compressing the assembly of blocks, grouting the reinforcing bars while the assembly of blocks remains in compression, and transferring compressive stress in the blocks through the bond with the reinforcing bars, thereby forming a minimally prestressed plank. The provisions also included a process to create an arch in the plank.

On December 29, 1960, Mr. Vander Heyden filed an application for additional improvements in the method of manufacturing a concrete plank. Patent No. 3,172,932 was granted on March 9, 1965. It identified ten claims

pertaining to prefabricated or drilled access ports for pressure grouting in special blocks provided at predetermined intervals along the length of the plank and to provide a step-by-step process for grouting (Vander Heyden, 1965).

Manufacturers' Design Data

The Dox Plank Manufacturers Association licensed those manufacturers that complied with Patent No. 2,696,729. Each manufacturer produced its own technical manual which included standard specifications, design assumptions, design tables, and installation details (Dox Plank Manufacturers Association, 1960 est.).

The standard specifications in effect in the 1940s, 1950s and 1960s indicated that the design was performed in accordance with the prevailing building regulations given in ACI 318-41, ACI 318-51, or ACI 318-56 and the corresponding ACI 711-46, ACI 711-53, or ACI 711-58. Table 1 provides the allowable unit stresses in concrete, taken from ACI 711-58.

Table 1. Allowable Unit Stresses in Concrete

Description		Allowable Unit Stresses, (psi)				
		For Any Strength of Concrete as Fixed by Test in Accordance with ACI 711 Section 302	When Strength of Concrete is Fixed by the Water-Content in Accordance with ACI 711 Section 302			
			Compressive Strength, $f_c'(psi)$			
			2,000	2,500	3,000	3,750
		$n = \frac{30{,}000}{f_c'}$	$n = 15$	$n = 12$	$n = 10$	$n = 8$
Flexure, f_c Extreme fiber stress in compression	f_c	0.45 f_c'	900	1,125	1,350	1,688
Shear, v Flat slabs at distance, d, from the edge of column capital or drop panel	v_c	0.03 f_c', but not to exceed 75 psi	60	75	75	75

Note: Allowable unit stresses shown were based upon ACI 711-58.

The specifications also indicate that the compressive strength of all concrete was generally 2,500 pounds per square inch, or greater. The maximum tensile stress of reinforcing steel was to be 20,000 pounds per square inch. The ratio of net area to the gross area of a typical plank was approximately 0.55. The concrete topping, if provided, was to be reinforced with welded wire fabric. On roof slabs and other areas where no concrete topping was provided, a grout coat with a 1 to 3 cement to sand mix ratio was to be thoroughly swept into the top surface of the plank after it was placed. The bearings were specified as a minimum of 3 inches on masonry and concrete beams and 2-1/2 inches on structural steel.

Design Theory

The design of simple span planks under a uniformly distributed load using the prevailing Working Stress Design method derived from a T-beam section in accordance with the ACI Reinforced Concrete Design Handbook (ACI, 1955) yielded the following standard formula used in the original design of Dox Planks:

$$M_s = A_s f_s j d \tag{1}$$

$$M_c = f_c \left(1 - \frac{t}{2 k d}\right) b t j d \tag{2}$$

$$V_c = v_c b' j d \tag{3}$$

$$V_u = u \sum o j d \tag{4}$$

$$V_h = \frac{U_h I}{2 (kd - 1)} \tag{5}$$

where the values of j and k are illustrated in Fig. 2,

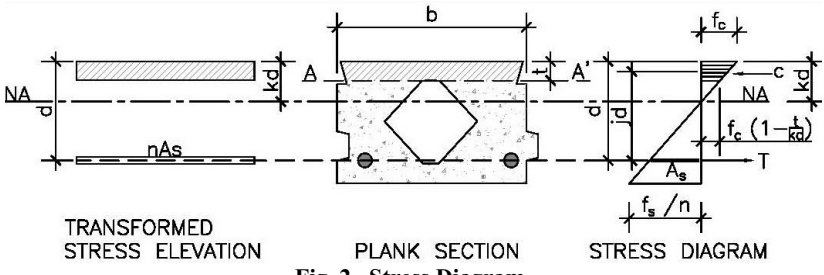

Fig. 2. Stress Diagram

$$j = 1.0 - \left[\frac{\left(k - \frac{2\,t}{3\,d}\right)}{\left(2\,k - \frac{t}{d}\right)} \text{ x } \frac{t}{d} \right] \tag{6}$$

$$k = \frac{\frac{n\,A_s}{b\,t} + \frac{t}{2\,d}}{\frac{n\,A_s}{b\,t} + 1.0} \tag{7}$$

Additional Load Capacity Considerations

Dox Plank systems essentially behave as a collection of simply supported beams. The cross section of a typical Dox Plank is comparable to a box beam with top and bottom flanges and side web elements.

In a Dox Plank, the primary flexural compression element (i.e., the bonded concrete topping, if present) and the primary flexural tension element (i.e., the reinforcing bars grouted in the bottom channel openings) are continuous over the entire span length. Thus, the demands sustained by these elements are similar to the demands sustained in a conventional cast-in-place or precast concrete beam, and the flexural capacity of Dox Plank can be established using typical flexural design principles. However, Dox Plank must be treated differently in shear. This is due to the regular, closely spaced, web discontinuities at the unbonded butt joints between the ends of adjacent Dox units along the span length. These discontinuities alter the distribution of shear stresses as compared to that which would be sustained in a continuous beam web. Fig. 3 illustrates a free body diagram of a single Dox unit.

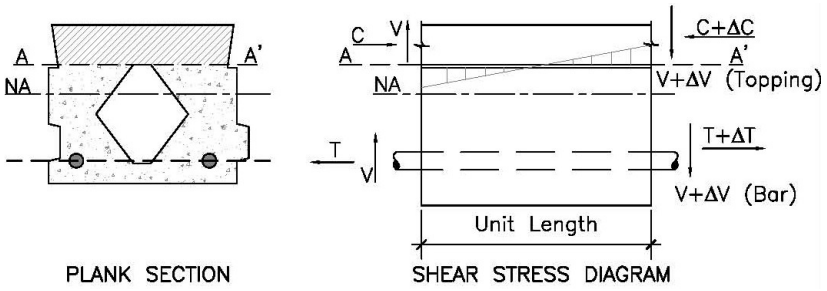

Fig. 3. Free Body Diagram

On the section of the Dox unit below Plane A-A' in Fig. 3, the only external forces are the net horizontal force in the reinforcing bar (ΔT) and the small fraction of the total shear taken by the bar at each end ($\Delta V\ bar$). Unless the reinforcing bar carries most of the interface shear, which is not realistic, summing the moments about the center of the block will result in significant moment associated vertical flexural stresses in the web of the Dox unit. If the tensile stress levels are high enough, web failure can compromise plank capacity. In a member with a continuous web, this does not occur.

The presence of significant web tensile stresses of the type shown in Fig. 3 is a characteristic of flexural members with closely spaced web discontinuities. In this manner, the Dox Plank system is comparable to Sheffield Tile Deck System (Hill, 2003). The magnitude of these tensile stresses relative to the tensile strength of the concrete used to fabricate the Dox unit must be evaluated to establish the true flexural strength of the Dox Plank system. In some instances, these stress levels will

control the ultimate capacity. Although manufacturer load tables given in the Technical Manuals of the Dox Plank catalogs provide guidance regarding the capacity of a Dox Plank system, their development did not include consideration of the local stress mechanism described above. Therefore, the effect must be evaluated to ensure that the appropriate limiting strength is established.

Serviceability

Some of the performance issues associated with a Dox Plank system include conventional versus prestesssed concrete, simple span design, minimal reserve capacity, creep, and corrosion of embedded steel reinforcement.

Reinforcement used in the Dox Plank system is mild steel. The precompression forces are of the magnitude of 20,000 pounds with incidental prestress force transferred to the reinforcement. Therefore, Dox Planks are considered to be conventionally reinforced despite early claims as being prestressed.

Dox Planks were generally intended for simple span construction with a pair of reinforcing bars at the bottom of the section, or wire mesh in the topping slab. Subsequent engagement of non-structural partition walls positioned below the planks could produce unintended stress reversals for which the planks are unreinforced.

Dox Plank manufacturers typically prepared designs resulting in the lightest possible planks with minimal reserve load capacity. Subsequent alterations to buildings with Dox Plank need to be performed to ensure that the planks have the capacity for the additional loads.

The concrete blocks used in a Dox Plank are made with lightweight aggregate giving the blocks an extremely low modulus of elasticity. Period manufacturers technical design data indicates that the modulus of elasticity of the block is 1,666,667 pounds per square inch. As with other low modulus concretes, deflection (particularly creep) can become problematic. Other deflection issues can result in differential deflection between planks.

The concrete block used to make the Dox Plank was touted as being porous in part to improve the acoustical properties of the plank soffit. High porosity is correlated with low resistance to carbonation and low resistance to water penetration. Therefore, the exposure of the planks to water intrusion, such as leaks in roof structures, overhangs, and balconies, corrosion of the embedded reinforcement can become problematic.

Concluding Remarks

This paper provides a literature survey of the manufacture, load capacity, and serviceability of assembled concrete block systems, in particular Dox Plank, used in the construction of roof and floor slabs in the 1940s, 1950s, and 1960s with a retrospective focusing on load capacity considerations and serviceability.

References

American Concrete Institute, Reported by ACI Committee 711 (1940). "Precast Joist Concrete Floor Systems." *Proceedings of the American Concrete Institute*, Volume 36, Title 36-15, *Journal of the American Concrete Institute*, January 1940, 297-312.

American Concrete Institute, Reported by ACI Committee 318 (1945). ACI Standard, "Building Regulations for Reinforced Concrete (ACI 318-41)." *Proceedings of the American Concrete Institute*, Volume 41, Title 41-23, *Journal of the American Concrete Institute*, Volume 16, No. 6, June 1945, 559-619.

American Concrete Institute, Reported by ACI Committee 711 (1946). ACI Standard, "Minimum Standard Requirements for Precast Concrete Floor Units (ACI 711-46)." *Proceedings, American Concrete Institute*, Volume 43, Title 43-6, *Journal of the American Concrete Institute*, Volume 18, No. 2, October 1946, 133-146.

American Concrete Institute, Reported by ACI Committee 318 (1951). ACI Standard, "Building Code Requirements for Reinforced Concrete (ACI 318-51)." *Proceedings, American Concrete Institute*, Volume 47, Title 47-43, *Journal of the American Concrete Institute*, Volume 22, No. 8, April 1951, 589-652.

American Concrete Institute, Reported by ACI Committee 711 (1953). ACI Standard, "Minimum Standard Requirements for Precast Concrete Floor Units (ACI 711-53)." *Proceedings, American Concrete Institute*, Volume 50, Title 50-1, *Journal of the American Concrete Institute*, Volume 25, No. 1, September 1953, 1-15.

American Concrete Institute, Reported by ACI Committee 317 (1955). Reinforced Concrete Design Handbook, Second Edition 1955.

American Concrete Institute, Reported by ACI Committee 318 (1956). ACI Standard, "Building Code Requirements for Reinforced Concrete (ACI 318-56)." *Proceedings, American Concrete Institute*, Volume 52, Title 52-57, *Journal of the American Concrete Institute*, Volume 27, No. 9, May 1956, 913-986.

American Concrete Institute, Reported by ACI Committee 711 (1958). ACI Standard, "Minimum Standard Requirements for Precast Concrete Floor and Roof Units (ACI 711-58)." *Proceedings, American Concrete Institute*, Volume 55, Title 55-4, *Journal of the American Concrete Institute*, Volume 30, No. 1, July 1958, 83-94.

Dox Plank Manufacturers Association, Dox Plank Technical Manual published for Dox Plank of Minnesota, Nabco Plank Company, Baltimore Concrete Plank Corporation, Dox Planks of Northeastern PA, and Dox Block System, 1960 (est.).

Heyden, Bernard A. Vander (1954). "Cementitious Plank and Method of Constructing It." *United States Patent Office*, Patent No. 2,696,729, Patented December 14, 1954.

Heyden, Bernard A. Vander (1965). "Method of Manufacturing a Concrete Plank." *United States Patent Office*, Patent No. 3,172,932, Patented March 9, 1965.

Hill, Howard J. (2003). "Investigation of a Sheffield Structural Tile Floor Failure Indicates a Dangerous Design/Development Oversight." *ASCE Practice Periodical on Structural Design and Construction*, Volume 8, Issue 4, November 2003, 190-194.

UNCERTAINTY INFORMATION PROCESSING IN REPAIR AND REHABILITATION

Ratna Divya Y.[1], Natarajan C.[2], Rajaraman A.[3]

[1, 2] *Department of Civil Engineering, National Institute of Technology, Tiruchirappalli, India. E-mail: lc_nataraj@yahoo.com*
[3] *Department of Civil Engineering, Indian Institute of Technology M, Chennai, India.*

ABSTRACT

In India, natural disasters can cause considerable amount of damage in terms of lives and financial investments. The after effects of disasters in mitigating the effects to repair and rehabilitation can take considerable amount of time as experts visit the site to get a personal assessment. The information flow is language independent and it is possible to communicate with persons on site either in visual or oral manners. In this paper, the role of uncertainties in visual and oral communications provided by the various groups of visitors is addressed. A methodology is proposed in which the statistical nature of the input information relating to damage parameters like location, spread and intensity are translated into engineering inputs that enable the modeling of the problem, which is followed by assessment ,diagnostics and possible rehabilitation measures.

KEYWORDS*: uncertainty, fuzzy randomness, repair and rehabilitation.*

INTRODUCTION

Realistic analysis of structures requires reliable (input) data as well as well-matched computational models. Unfortunately, actual data and numerical models will always contain uncertainties. Contrast to deterministic structural analysis, fuzzy probabilistic structural analysis takes account of the uncertainties in data and model. For damage analysis, damage parameters such as damage intensity, location of damage and spread of damage, are also characterized by uncertainties. If an event such as a random test result from a load test is observed as random values on several different occasions under constant boundary conditions, this constitutes a stochastic uncertainty. The uncertainty characteristic randomness is then assigned to this stochastic random event. *If the number of observations are only available to a limited extend, or the sample elements are of doubtful accuracy (non-precise), an information deficit exists*. If stochastic methods were used to solve the problem, gaps between the data quality requirements and actual non-precise data may result. The impreciseness results from the informal uncertainty in terms of either non-precise recognition of data or statistical inference (determining stochastic input parameters, such as expected values, variances and probability distribution functions). This informal uncertainty can be described by using uncertainty characteristic fuzziness and can be mathematically quantified. The uncertainty consisting of randomness and fuzziness,

is summarized in the characteristic fuzzy randomness. The fuzzy random data are then managed with the aid of the uncertain *fuzzy probability.*

In this paper, the fuzzy characterization methodology has been tested on a damaged beam element with uncertainty consideration as functions of damage intensity only. Other damage parameters such as spread of damage and location of damage are not considered. The analysis also considered four support conditions namely cantilever, simply supported, fixed and propped cantilever cases.

METHODOLOGY

Beam element considered in the analysis is shown in Fig 1.

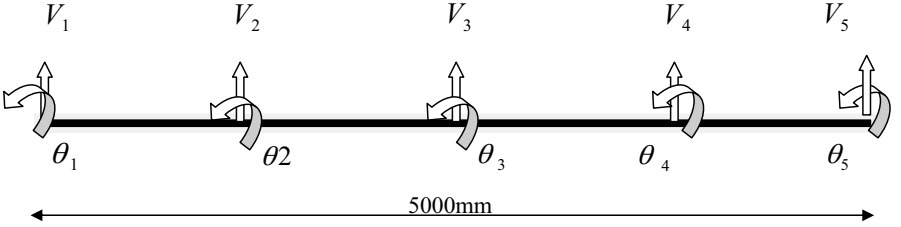

Figure. 1. Beam element

Table 1 Details of beam element

Length of the beam	5000mm
Cross section of beam	230mm * 300mm
Young's modulus of concrete	27386N/mm^2
Load applied	100kN

Application of damage parameters in the beam element is shown in Fig 2.

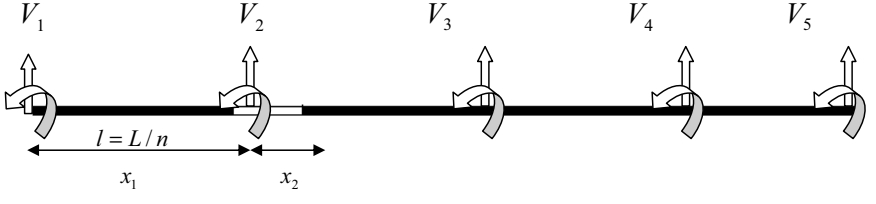

Figure 2. Damaged beam element

Location of each damaged portion of the element and its spread are expressed as a ratio to the length of the undamaged element, and are represented as $\beta$and γ , respectively. The percentage reduction in EI value can be taken into account using one more parameter which is represented as α in the present study.

$$\alpha \text{ is known as intensity parameter} = 1 - \frac{\%reduction}{100}$$

β is known as location parameter for a damaged element = $\frac{x_1}{l}$

γ is known as spread parameter for a damaged element = $\frac{x_2}{l}$

The parameters defined above are considered in the formulation of the stiffness matrices of the beam element.

Stiffness matrix of the damaged element

$$[Ke_1]=\begin{bmatrix} \frac{12EI\alpha}{(\gamma l)^3} & \frac{6EI\alpha}{(\gamma l)^2} & \frac{-12EI\alpha}{(\gamma l)^3} & \frac{6EI\alpha}{(\gamma l)^2} \\ \frac{6EI\alpha}{(\gamma l)^2} & \frac{4EI\alpha}{(\gamma l)} & \frac{-6EI\alpha}{(\gamma l)^2} & \frac{2EI\alpha}{(\gamma l)} \\ \frac{-12EI\alpha}{(\gamma l)^3} & \frac{-6EI\alpha}{(\gamma l)^2} & \frac{12EI\alpha}{(\gamma l)^3} & \frac{6EI\alpha}{(\gamma l)^2} \\ \frac{6EI\alpha}{(\gamma l)^2} & \frac{2EI\alpha}{(\gamma l)} & \frac{-6EI\alpha}{(\gamma l)^2} & \frac{4EI\alpha}{(\gamma l)} \end{bmatrix}$$

The stiffness matrix of undamaged element is

$$[Ke_1]=\begin{bmatrix} \frac{12EI}{(l)^3} & \frac{6EI}{(l)^2} & \frac{-12EI}{(l)^3} & \frac{6EI}{(l)^2} \\ \frac{6EI}{(l)^2} & \frac{4EI}{(l)} & \frac{-6EI}{(l)^2} & \frac{2EI}{(l)} \\ \frac{-12EI}{(l)^3} & \frac{-6EI}{(l)^2} & \frac{12EI}{(l)^3} & \frac{6EI}{(l)^2} \\ \frac{6EI}{(l)^2} & \frac{2EI}{(l)} & \frac{-6EI}{(l)^2} & \frac{4EI}{(l)} \end{bmatrix}$$

where l=L/n; n= number of elements in the beam. Static condensation procedure is then applied to the stiffness matrix into 10 X 10 matrix. All slave degrees of freedom (degrees of freedom at intermediate node points) are expressed in terms of master degrees of freedom (degrees of freedom at the ends of the beam).

Augmentation of the damaged beam element

The stiffness matrix formulated for the damaged beam element can be applied to any finite element model. The augmentation has shown in the flowchart, which explains how the damaged beam element and normal beam finite element be augmented and solution is carried out.

The combination of the uncertainty model with a deterministic algorithm based on the Finite Element Method (FEM) gives the desired output (reduced stiffness). For this purpose Monte Carlo simulation is used.

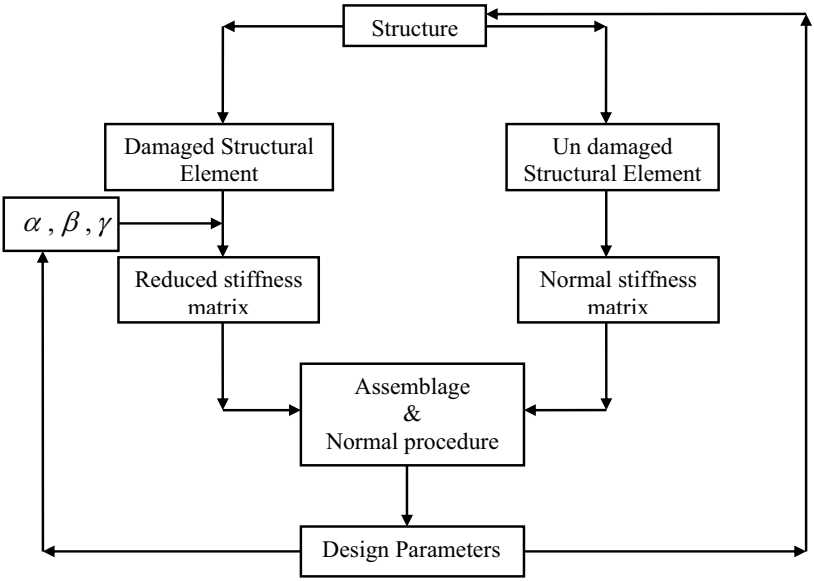

Figure 3. Augmentation of damaged beam element

RESULTS AND DISCUSSIONS

After converting oral descriptions of damages, such as slightly damaged, severely damaged, into numerical value, damage intensity is expressed as 50% stiffness reduction. Uncertainty is expressed as ± 10% deviation to the 50% intensity of damage. Three sets of data with sample sizes 100, 50, 10 with range of 50% ± 10% are used as input. The four boundary conditions are applied to all samples and the corresponding reduction in stiffness are calculated for two non-central damage locations, namely: 1) Damage near the left support; and 2) Damage at 1/3 of the span. The input parameters are shown in Table 2. Table 3 shows the reduced stiffness from both deterministic and stochastic (simulation) analyses are compared. The results from the two analyses are shown to be reasonably close to each other.

Table 2 Stiffness values for the damaged and undamaged conditions

Support Condition / **Condition of the beam**	**Cantilever**	**Simply supported**	**Fixed**	**Propped Cantilever**
Undamaged	340.13 N/mm	5442.1N/mm	21769N/mm	12439N/mm
50% damage at 1/3 of the span	65.37N/mm	1232.2N/mm	7132.1N/mm	2638.9N/mm
50% damage at the left end	97.61N/mm	2496.4N/mm	10930N/mm	4839.9N/mm

Table 3 Comparison of deterministic and simulation result for one set

Support Condition / Condition of the beam		Cantilever	Simply supported	Fixed	Propped Cantilever
50% damage at 1/3 of span	From Deterministic	65.37N/mm	1232.2N/mm	7132.1N/mm	2638.9N/mm
	From Simulation	56.28N/mm	1042.0N/mm	6597.1N/mm	2348.3N/mm
50% damage at the left support	From Deterministic	97.61N/mm	2496.4N/mm	10930N/mm	4839.9N/mm
	From Simulation	81.20N/mm	2266.8N/mm	10432N/mm	4539.7N/mm

The reduction in stiffness values in each sample is on the high side from simulation than from deterministic analysis (more than 50%). This reduction in stiffness for ± 10% deviation is 13% to 17% more in the case of cantilevered beam, 8.48% to 15.7% in case of simply supported beam, 4.2% to 7.6% in case of fixed beam, and 5.72% to 11.13% in case of propped cantilever, respectively. Parametric study has been carried out on these samples to observe how the sample sizes, support condition of the beam, location of damage are influencing the stiffness degradation.

Parametric study

Parameters considered are as follows:

1. Number of samples for analysis - P1 (100 for all support conditions).
2. Uncertainty randomness in evidence of deterministic input - P2.
3. Uncertainty randomness in stiffness degradation 50 ± 10% - P3.
4. Uncertainty randomness in stiffness degradation (P3) with respect to sample sizes 50 and 10 are P4 and P5, respectively.
5. Uncertainty randomness in stiffness degradation with respect to location of damage and support conditions also can be observed.

The results of one set of input are presented here to demonstrate the role of uncertainty presence in these parameters.

Type of beam	P1	P2	P3	P4	P5
Cantilever damage at support	100	46	84	39(78%)	7(70%)
Cantilever damage at 1/3from support	100	46	93	44(88%)	7(70%)
Simply supported damage at left support	100	46	100	50(100%)	10(70%)
Simply supported damage at 1/3 from left support	100	46	90	40(80%)	7(70%)
Fixed damage at left support	100	46	100	50(100%)	10(100%)
Fixed damage at 1/3 from left support	100	46	100	50(100%)	10(100%)
Propped cantilever damage at support	100	46	100	50(100%)	10(100%)
Propped cantilever damage at 1/3 from left support	100	46	100	46(92%)	7(70%)

where P1 is the sample size of 100 with 50% as mean value of damage intensity with ± 10% deviation. Various factors that may influence this reduced stiffness including:

1. In the case of *cantilever beam with damage at support:* 84% of samples are falling within 50% reduced stiffness and the remaining 16% of samples are showing the possibility of reduced stiffness greater than 50%. Again, this value is varying with sample size: in case of sample size of 50, 22% and in case of sample size of 10, 30% are showing the possibility of reduced stiffness to be more than expected.

2. In case of *cantilever beam with damage location at 1/3rd from the support:* 7% of the samples are showing the possibility of stiffness degradation to be more than

expected: in case of sample size of 50, 12%, and sample size of 10, 30% are showing the possibility of reduced stiffness to be more than expected, respectively.

3. In the case of *simply supported beam with damage at the support:* all samples are showing the reduction in stiffness to be within the expected range.

4. In *simply supported beam with damage location at 1/3rd from left end:* all samples are showing the reduced stiffness to be within the expected range. But for sample size of 50, 20%, and for sample size 10, 30% of values are showing the possibility of reduced stiffness to be more than expected, respectively.

5. In case of *fixed beam with two damage locations and the case of propped cantilever with damage at the support:* All sample sizes are showing the reduction in stiffness to be within the expected range that is 50% ± 10%. But in case of propped cantilever when damage is at 1/3rd from left support for sample sizes 50 and 10 8% and 30% of values are showing the possibility of reduction in stiffness to be more than the expected.

The sample sets are checked for distribution fit assuming normal distribution. Distribution fit has been performed on all support conditions and sample sizes.

UNCERTAINTY MODELING

Monte Carlo simulation with quasi random number is used in uncertainty modeling. This quasi random number sequence is also called the low discrepancy sequence; this sequence discrepancy is a measure of its uniformity. Quasi-random number generators (QRNGs) produce highly uniform samples of the unit hypercube and are designed to minimize the *discrepancy* between the distribution of generated points and a distribution of equal proportions of points in each sub-cube of a uniform partition of the hypercube. As a result, QRNGs systematically fill the "holes" in any initial segment of the generated sequence.

To find uncertainties for any input number, exponential fit is used with 100, 50 and 10 value sets. Uncertainty in input for any number and uncertainty in output in terms of structural damage is then determined, so that the repair measures can be adjusted. General expression for the power fit is:

$$f(x) = a * x^{b} \quad \text{.....(1)}$$

The values of a and b in equation (1) obtained from this modeling are 45.92 and -1.273 and the fit is shown in Figure 4.

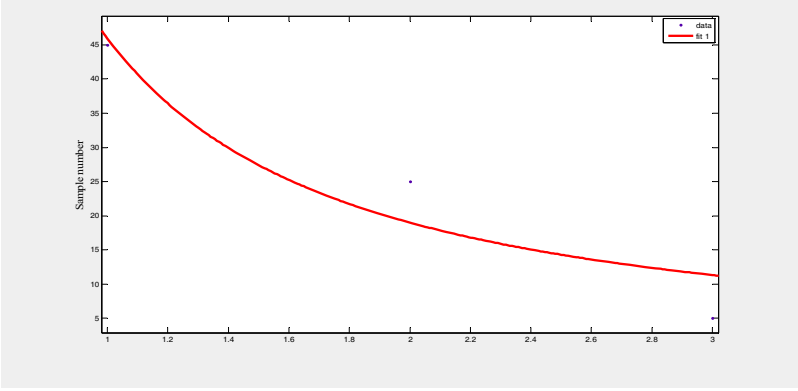

Figure 4 Power fit for input uncertainty

Uncertainty percentages for different sample sizes are calculated and tabulated in table 5. This uncertainty can be calculated for any number of samples.

Table. 5 Uncertainty variations with respect to sample size

Sample size	100	75	50	35	27	24	10	7
Uncertainty in %	13.6	14.13	15.78	17.39	18.67	19.28	24.49	27.0

As the sample size is increasing uncertainty is decreasing which shows the importance of sample size to suggest appropriate rehabilitation meaures.

Similar uncertainty modeling is also performed for output (stiffness) data. For the considered deviation, all samples are showing stiffness less than 50% of original stiffness, except in fixed beam case where damage is at left support. The power fit curve for all conditions except for fixed beam with damage is at left support is shown in Figure 5. The fit curve for fixed beam with damage is at left support is shown in Figure 6. Examples of using sample sizes of 7 and 23 to compare the uncertainty effects are shown in Table 6.

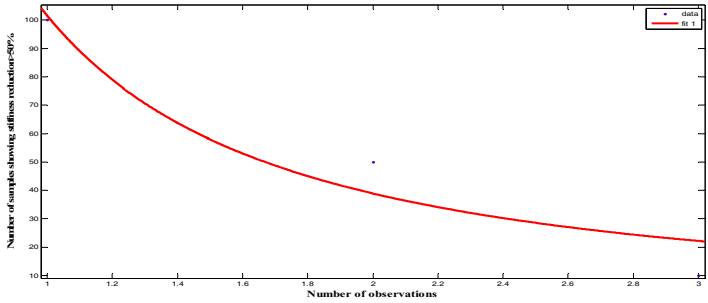

Figure 5. Power fit for output uncertainty modelling for all support conditions except for fixed beam when damage is at left support

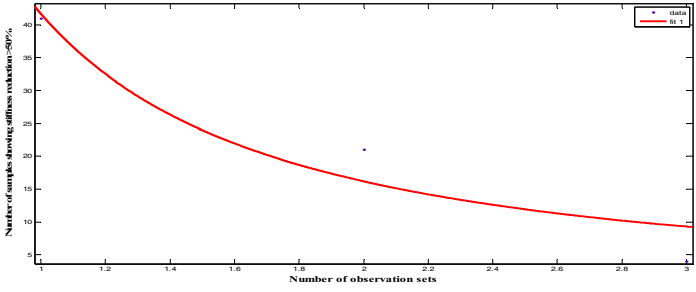

Figure 6. Power fit for output uncertainty modelling for fixed beam when damage is at left support

Table 6 Comparison of input and output uncertainties for all support condition

Beam type	Input uncertainty (in %)		Output uncertainty (in %)	
	Sample size 7	Sample size 23	Sample size 7	Sample size 23
Cantilever	27	19.5	48.22	30.57
Simply supported	27	19.5	48.22	30.57
Fixed	27	19.5	20.45	13.23
Propped cantilever	27	19.5	48.22	30.57

CONCLUSIONS

Random (Fuzzy) probabilistic structural analysis permits the simultaneous consideration of different uncertainties including: randomness, fuzzy randomness, etc. The parametric study showed that if damage location is at or near the support,

the fixed beam shows the best performance in terms of damage prediction. This trend changes when the damage location is shifted to the center of the beam, in which case, simply supported beam shows the best prediction.

Uncertainty in intensity will be reflected interms of reduction in stiffness, uncertainty in observations (Considering the effect of sample size and latitude) on intensity will give reduction in siffnessmore than expected (the one from determinist approach) and hence uncertainty consideration will lead to better rehabilitation methods.

REFERENCES

Abdel Wahab M. M, De Roeck G and Peeters B(1999),“ Parameterization of Damage in Reinforced Concrete Structures Using Model Updating”, Journal of Sound and Vibration,**228**: 717-730.

Bernd Möller, Wolfgang Graf, Michael Beer.(2003),“Safety assessment of structures in view of fuzzy randomness”, *Journal of Computers and Structures*,**81**:1567-1582,.

J.-U. Sickert, M. Beer, W. Graf & B. Möller.(2002), Fuzzy Probabilistic Structural Analysis Considering Fuzzy Random Functions, *Fifth World Congress on Computational Mechanics*, Vienna, Austria.

J. Maeck, M. Abdel Wahab, B. Peeters, G. De Roeck, J. De Visscher, W. P. De Wilde, J. -M. Ndambi and J. Vantomme.(1998), Damage identification in reinforced concrete structures by dynamic stiffness determination, *Journal of Engineering Structures*,**22**,1339-1349.

Lars Peter Hansen and Thomas J. Sargent.(2004), “Certainty Equivalence” and “Model Uncertainty”, *An international conference at the Federal Reserve Board* on March,.

M. Chandrasekhar, Ranjan Ganguli.(2007), Uncertainty handling in structural damage detection using fuzzy logic and probabilistic simulation, *Journal of Mechanical systems and signal processing,***23**:384-404,.

S.Shifana Fatima.(2009),“*Dynamic nonlinear fracture mechanics for composite materials*”, PhD thesis from National Institute of Technology Trichy,.

Failure and repair in cultural heritage conservation

Miloš Drdácký[1] & Zuzana Slížková[2]

[1]Institue of Theoretical and Applied Mechanics of the Academy of Sciences of the Czech Republic (ITAM AS CR), Prosecká 76, Praha 9, 190 00, Czech Republic; fax 00420286884634; e-mail: drdacky@itam.cas.cz
[2] ITAM AS CR, Department of Particulate Media, Prosecká 76, Praha 9, 190 00, Czech Republic; fax 00420286884634; e-mail: slizkova@itam.cas.cz

ABSTRACT

Architectural heritage objects exhibit a vast variety of damage and failures which is difficult to categorize for the sake of designing general preventive or repair and conservation measures. The authors studied sensitivity of historic structures and elements to weather and disasters within several international research projects using their personal experience and research as well as records of damage and failures gathered in literature and special databases. It should be emphasized that any historic structure or element cannot be dealt with unless its material characteristics and a general environmental situation, (e.g. hydro-geological conditions), have been taken into account, which must be reflected in evaluating results and designing mitigation strategies. This paper presents selected examples from a developed information system containing data on typical damage and failures related to weathering effects and disasters action, namely wind, floods and landslides. In specific cases, not the historic structure but its surroundings and supporting structure are prone to failure, which can adversely affect their behaviour and response and cause damage to cultural heritage objects. The approach is documented by preventive strategies and measures and accompanied with life expectancy and repair cost estimates.

INTRODUCTION

The lifespan and serviceability of materials, elements, buildings and ensembles of architectural heritage are influenced by various factors, including to which type of action they are subjected. A great deal of attention is devoted to those which affect the physical existence of the object or building. Nevertheless, almost all intangible heritage features and values, especially historic cities, can be severely damaged, which is definitely a defect and can even attain the dimension of a failure. We can divide the aforementioned factors causing the deterioration of the physical state of monuments into three categories according to the period of their action: i) before the production of the object or building, ii) during the production/construction phase and iii) during the service life of the object or building, (Drdácký 2001). Even though historic buildings exhibit numerous defects and failures caused by factors originating before their construction, which is an important issue for conservation

theories and approach definitions, the third aforementioned category is the most important one for architectural heritage, and it can be divided into the following groups: weathering effects, biological factors, incompatibility, loads, operation, concept, design, materialization and alterations to the building or object, unexpected events & "injuries". Climate change influences or acts in synergy with weathering effects namely action of radiation, heat, water, air, wind and air pollutants, and biological factors. Weathering as well as biodegradation occurs in both the exterior and the interior spaces.

Most technical materials, namely building materials, elements and structures are created as non-homogeneous composite systems, which combine materials of different physical, chemical and biological characteristics. They respond to the acting loads and influences differently, and when a common threshold of tolerance is surpassed a defect or failure occurs. In the case of architectural heritage, the intangible values are to be taken into account, too. In practice we distinguish between at least the following types of such an incompatibility: physical, chemical, biological, architectural (including aesthetic) and social.

Historic buildings are subjected to various loads that we usually describe as static, periodic (repeated or dynamic) and movement of supports. The resulting stresses are caused by exterior forces, (e.g. gravitation, pressure, uplift forces, inertia forces), which can have different directions, intensity and duration, and by deformations, (e.g. induced: temperature or moisture difference dilatation, subsoil movement, vibrations or from internal material characteristics: creep, shrinkage, crystallization). They cause local material damage and failure by shear, tension, compression or fatigue (mechanical as well as environmental).

Use of monuments brings about numerous degradation factors, first of all, wear, which gradually exhausts the lifespan of the object or building. Wear and threat of failure increase with inappropriate use of cultural heritage buildings, which can act mechanically (overloading) or in the area of building physics (unsuitable change of interior climate, creation of diffusion barriers). On the other hand, the operational danger is reduced by means of regular and timely maintenance, which is one of the most important safeguarding factors.

The initial concept, design and construction of the object or building influence its lifespan most significantly. An inappropriate choice of construction site, water retention, snow or pollutants, wrong details, insufficient insulation, insufficient ventilation and non-suitable materials or technologies can decrease substantially the life of a historic building. We consider such a work defective or even a failure. However, such a flawed concept, design or materialization of a monument in the field of conservation is barely rectified, because such attributes are sometimes understood as a part of cultural heritage which should be conserved. The authors do not agree with such an approach and support conservation approaches which in an acceptable way and after proper documentation improve the building to prolong its life and safeguard its original parts. In any case, the conceptual errors are frequently associated with restoration works and similar changes made to historic objects and buildings.

Unexpected events do not represent the most frequent cause of damage and failures, nevertheless, their consequences are mostly catastrophic and disastrous,

therefore this contribution is more focused on them. They involve floods, earthquake, landslides, avalanches, strong winds, windstorms, hurricanes, and fires, but also man made disasters, e.g. wars, vandalism, explosions, impacts of all kinds of vehicles or floating objects etc. However, the extent of the contribution does not allow dealing with all problems and a reasonable choice had to be adopted.

RANKING OF HISTORIC STRUCTURES, ELEMENTS AND SITUATIONS ACCORDING TO THEIR SENSITIVITY TO THE WEATHER AND DISASTER EFFECTS

Damage and failure analysis of historic objects aims at gathering of knowledge which enables to design and suggest measures mitigating the adverse effects of various situations, loads and conditions. A wide variety of historic structures and materials as well as the scope of possible damage makes designing of widely applicable measures and methods difficult and, therefore, the authors adopted an approach of generalization based on ranking of historic structures, elements and situations according to their sensitivity to the weather and natural disaster effects into five categories depending on the acting loads or environments.

Serious damage to buildings caused by climatic reasons – windstorms, hurricanes or floods – definitely belonged among the most remarkable events to be noted in chronicles and other written sources. Together with large fires, often started by thunderstorms, they make the numerous groups of records in chronicles. The windstorm damages of roofs were recorded relatively often in the past and still represent one of the major threats to historical objects including parks and gardens. Churches with their high roofs and in particular steep spires represent the largest group of buildings mentioned in written sources. Outlook towers with timber structures on the tops of the hills and standing for the most part separately from the traditional settlements were maybe the most endangered building type, especially around the 1900. Quite unusual is one report from 1842, which speaks about the menhir in Klobuky (Central Bohemia) falling to the ground due to a hurricane. Most of the damage caused by strong winds touched the roof covering. Wooden shingles were in this sense much more resistant than for example ceramic or slate tiles. Copper sheets when used in pitched roofs of a larger extent caused serious problems too. The total collapse of an all-timber structure of a roof spire was usually not the result of structural faults in timber construction but was connected with longer established existing problems, as for example rotten wall plates or roof leakage. That means that the periodic monitoring of wood condition within the constructions is essential to prevent future damages. A combination with other structural failures – cracking in masonry or vaulting – could be very dangerous leading to a collapse of the building as a whole. The following ranking of cultural heritage objects has been suggested:

W0 Wind resistant structures and elements * W1 Vibration prone elements and structures • *windows and window glazing,* • *architectural elements (e.g. pinnacles)* * W2 Wind releasable elements • *roof covering* * W3 Structure susceptible to partial damage by wind • *roofs,* • *windmills,* • *tall sculptural works* * W4 Structures and elements vulnerable to overall collapse due to wind action • *free*

standing walls and elements (attic gables, ruin walls, fencing walls, chimneys, menhirs, poles, etc.), • *light and tall buildings (towers, timber houses, etc.),* • *trees*.

During flood situations historic materials, structures and territories (landscape, gardens etc.) are subjected to unusual loads and actions. First of all, we have to have in mind that the law of Archimedes is valid and therefore all flooded objects are uplifted and some can even flow away from their original position, even inside interiors, where streams can occur, too. Naturally, static and dynamic pressures can destroy structures as well as trees and this phenomenon may be multiplied with the impact of floating objects or the creation of barriers from the floating objects or erosion of subsoil under foundations. Wet materials and structures are mostly losing their strength and stiffness characteristics and they exhibit substantial volumetric changes. Besides the mechanical action, during and especially after floods substantial chemical attacks are present also, mostly due to water pollution and salt efflorescence during drying processes. Therefore, the general ranking of structures and elements according to their sensitivity to flood is much more difficult than in any other situation. Generally, many effects occur after the flood as, e.g. compacting of infill, which can cause failure of partition walls, buckles of floors as a consequence of the uplift forces, cracks in vaults due to uneven settlement after the flood and many others.

F0 Flood resistant structures * F1 Structures from materials with a high moisture volumetric change • *timber structures and elements,* • *combined structures from different moisture expansion materials,* • *some soils* * F2 Structures from materials of strength highly degrading due to moisture • *dried brick masonry,* • *masonry with clay (low lime or cement contents) mortars,* • *decayed timber structures and elements,* • *infill subsoil and fine particle subsoil* * F3 Structures susceptible to partial damage due to flood • *timber parts prone to uplifting and floating away,* • *large bridges,* • *pavements* * F4 Structures and elements vulnerable to overall collapse or displacement due to flood • *small bridges and walkways,* • *free standing walls,* • *light improperly anchored objects (summer-houses, etc.)*.

Taking into account the sensitivity of structures and elements to weather effects regardless materials from which they are created, we logically sort the structures according to their exposure conditions and morphological characteristics which influence water retention or the eddies and flows around the monuments. The last item is reflected in the robustness categories in which material types are also mentioned.

Sculpture and building surfaces ***exposed to rain*** are divided into five categories: R0 Sheltered from rain * R1 Partly exposed to rain or/and moderate rain water runoff • *vertical surfaces moderately exposed to winds* * R2 Exposed to rain or/and heavy rain water runoff • *roofs,* • *inclined surfaces of sculptures,* • *vertical surfaces exposed to prevailing and strong winds* * R3 Complex shapes with horizontal surfaces • *cornices,* • *balconies,* • *decorative architectural elements* * R4 Complex shapes with water traps • *roof and façade details*.

Structures and elements exposed to threat of ***rising dampness*** are classified as: D0 Natural moisture contents * D1 Occasional moisture occurrence • *walls which are damp due to splattered water (bridge parapet walls, ..),* • *structures occasionally*

affected by an elevated water table * D2 Permanent moisture contents • *masonry highly contaminated with hygroscopic salts or materials,* • *masonry covered with damp proof layers* * D3 Permanent high moisture contents • *buildings in lagoons,* • *cellars or caves* * D4 Cyclical alterations under water/open air • *bridge piers,* • *watermills,* • *marine structures*.

Structures and elements ***exposed to sunshine*** (heat and light effects): S0 Sheltered against light * S1 Sheltered against direct sunshine * S2 Partly exposed to sunshine • *buildings in shadow of trees* * S3 Fully exposed to sunshine • *south-east oriented façade* * S4 Fully exposed to sunshine with elevated heat exchange • *south + SW +W oriented facades or roofs,* • *flat roofs and pavement*.

Robustness (***volume of mass, detailing and material***) of the element or structure: M0 Robustly resistant to weather effects * M1 Robust in form, sensitive material • *porous materials,* • *materials with low freeze/thaw resistance,* • *water soluble materials,* • *corrosion prone materials (alterations, crust creation)* * M2 Resistant material, sensitive details • *details with notches (stress concentration, manufacturing defects, ..)* * M3 Form prone to uneven strains and gradients • *edges, corners, protuberances,* • *subtle elements fixed to massive parts* * M4 Sensitive material & sensitive details.

STRATEGIES AND MEASURES PREVENTING OR MITIGATING DAMAGE TO CULTURAL HERITAGE OBJECTS

Strategies and measures mitigating damage to cultural heritage are suggested in relation to the above mentioned groups of vulnerable materials or elements. Preventive strategies and measures against wind effects involve: i) Regular inspection of structural health (all categories); ii) Long term monitoring of structural health (W3, W4); iii) Installation of warning systems (special cases of W3, W4); iv) Regular maintenance (all categories); v) Change of tuning of a structure or element (W1); vi) Improved building envelope (roofing, façade) anchoring (W2); vii) Improved sensitive structural parts anchoring into supporting structures (W3); viii) Change of wind effect on the element or building (change of wind flow conditions) (W1, W2, W3); ix) Structural strengthening and/or additional supports of the whole structure (W4). Typical examples are given in the next paragraph.

Preventive measures in flood prone areas are based on: i) Regular inspection of structural health (all categories); ii) Emergency plans and guidelines (all categories); iii) Early warning and information systems (all categories); iv) Prepared technical means against flood – stable or temporary with easy installation (all categories); v) Temporary strengthening and additional supports (F2, F3, F4); vi) Decreasing load measures (dismantling bridge parapet walls, openings allowing balancing of water pressure) (F3, F4); vii) Improved anchoring of sensitive structural parts into supporting structures (F3, F4); viii) Removal of floating objects or “dams” from the stream (F3, F4); ix) Guidelines for “after the flood” activities, e.g. preventing damage from fast settlement, material disintegration, fast salt crystal growth, pollution and climatic effects etc. (all categories)

TYPICAL PREVENTIVE MEASURES FOR WIND AND WEATHERING

Regular inspection of structural health. Regular inspection of structural health concerns all categories of vulnerability to the wind effects and represents a basic condition for properly and in-time maintenance of historical objects and prevention of damages and failures. The scope and procedure of the regular inspection is generally oriented to checking of historical materials and structures irrespectively to a probable deteriorating or damaging action mainly for economy reasons. There are several guidelines available for such an inspection, e.g. The ISE guidelines (Clancy) 1991, Hollis 2000. From the wind action point of view the following characteristics are of importance: anchoring of slender or light parts (glass window tables, window frames or shutters, façade cladding, architectural elements as e.g. pinnacles, crosses on towers or roofs, free standing sculptures, roof structures, roof covering – namely on ridges, attic gables, chimneys, menhirs, poles etc.); stiffness ensuring elements (reinforcing struts or ties); measures ensuring overall stability (ballast loads or anchoring ropes). The anchoring must be checked as a system including the structures which provides supports. There should be also checked the health of trees which can damage buildings in their vicinity. From the weathering point of view the surface layers and elevated moisture are of the great importance. Therefore, the tightness of the envelope against penetrating water or snow, (at reasonable diffusion characteristics), and the damp rise structures and voids must be carefully checked.

Long term monitoring of structural health. In special cases of highly vulnerable structures, long term monitoring of structural health is recommended, which concerns mainly structures from the group W3 and W4. In this case, the number of stress cycles is recorded and a risk of fatigue is assessed. Selected objects of higher cultural historical value or objects made form weathering sensitive materials (namely some stones) or fragile structures are subjects for long term monitoring of structural health. Optical devices and special sensors are mostly used.

Early warning systems. Installation of warning systems is usually connected with the above mentioned monitoring of structural health or with simple moisture measurements detecting leaking of roof covering layers. In such a case it helps to prevent biological decay and corrosion of roof structures. However, it might be also used for monitoring special cases in structural groups W3 and W4.

Regular maintenance. Regular maintenance concerns all categories and it represents one of the most important strategies against damages and failures. Unfortunately, the regular maintenance is almost neglected and it is guilty for the majority of failures of built heritage. Lack of regular maintenance causes material decay and loss of mechanical characteristics decisive for structural resistance to acting winds. It also influences substantially the subsequent measures listed below. The maintenance action is usually initiated as a result of the regular inspection or it can be carried out really regularly on a basis of maintenance plans, which is a better approach. The maintenance action in most cases does not need design work or even an engineering supervision. It can rely only on skills of properly trained craftsmen, which substantially shortens the time to action and prevents development of a defect into a more serious damage or even a failure. A maintenance guide is a useful tool and should combine tips for inspection with recommendations how to fix an

identified problem. In the case of wind action, the work should be focus on the state of fixtures and anchors, the completeness of the roof covering and on a possible decrease of wind loading or danger from falling objects. Regular maintenance significantly improves life cycles of historical materials and objects. It prevents development of serious damages from weathering action and prolongs time between restoration works. Here cleaning and renewal of protective paints or penetration represents one of the most desirable measures. "Soft" techniques must be applied and only the deposits which prevent "breathing" of object skin are to be removed.

Change of tuning of a structure or an element. Problems of vibration of some architectural details or slender structures can be solved using change of tuning of a structure or a structural or architectural element. There are different techniques available for such a purpose – from passive mass damping or stiffness change to active dampers, necessary mostly in cases of combined wind and other dynamic loading. This measure applicable for structures of the vulnerability category W1.

Improved anchoring of building envelope. Improved anchoring of building envelope i.e. namely roofing and façade elements is important for wind releasable structures (W2). Roof tiles require proper filling of joints with mortar and on steep roofs and ceramic tiles covering an increased number of fixing screws or strips is suggested, Fig. 1. Mortars with natural fibres exhibit the best life performance.

Figure 1. Proper mortar filling and anchoring by means of screws.

Improved anchoring of sensitive structural parts. Improved anchoring of sensitive structural parts into supporting structures is relevant to structures susceptible to partial damage by wind (W3), especially roofs, windmills or tall sculptural works. Roof frames are typically anchored by ties into masonry walls of a building or a tower, Fig. 2. Very sensitive to wind action are decorative elements placed on the roofs or gables, as e.g. crosses which are mostly anchored into timber poles vulnerable to biological decay. Additional supports here improve also mechanical behaviour and loading of anchoring cantilever pins which are bent and may fail due to repeated cyclic loading. Careful inspection and enhanced anchoring is very important at free standing sculptures.

Change of wind effect on the element or building. Change of wind effect on the element or building, especially a change of wind flow conditions can be effectively applied in structural categories W1, W2 and W3. A typical measure consists in change of surface characteristics, change of near surroundings (wind flow breakers) or larger surroundings, (e.g. planting of trees), in order to decrease the wind load.

Figure 2. Strengthening of masonry with timber beams and anchoring of tower roof frames.

Structural strengthening and/or additional supports. Structural strengthening and/or additional supports of the whole structure are utilized in the following situations: i) free standing walls and elements (attic gables, ruin walls, fencing walls, chimneys, menhirs, poles, etc.), ii) light and tall buildings (towers, timber houses, etc.) and iii) trees. Light buildings, mainly timber towers require additional supports (cables) or increased ballast preventing overturning. In some cases only structural strengthening may be sufficient to ensure the desired stability and strength, Fig. 2 (right).

Water disposition. Water in all forms is considered the most harmful agent for historic materials and structures and the water carry away must be fast and effective. All parts where water can accumulate must be provided with adequate water outlets. The expected increase of precipitation amount calls for appropriate changes in dimension of gutters. Water must be carried away from the vicinity of a building, not only from the roof and then left to moisture the subsoil around foundations. All facilities for water drainage must be regularly cleaned and kept in function.

Surface protection against water penetration. Prevention of water penetration or soaking into material is one of measures which are considered indispensable in some cases, as e.g. for ceramic roof tiles. On the other hand, an opinion of professionals on their use for façades is not so uniform. There exists a wide scope of materials for surface protection – from invisible agents to paints, namely the so called sacrificed paints or layers. Even though in the majority of European countries the hydrophobization of stone façades is not accepted, for stone sculptures it seems to be quite common. The effectiveness of hydrophobization can be seen from Fig. 3.

Protection against excessive heat & light variations. Historic materials and structures can be effectively protected against excessive heat and light action by means of different shelters, filters and coats. In rooms, curtains and window shutters can be installed.

Architectural improvements. A specific problem arises in the restoration of monuments with historical (authentic) faults. During restoration works the faulty cornice details are usually restored with original errors. This approach should be

changed, and the durability should be superior to formal copying of original details or repairs of appearance in justified cases. This applies primarily to the remediation of natural expansion cracks made without an adequate technical solution. Typical problems involve: missing expansion joints (unaccommodated volumetric temperature and moisture changes), faulty details (mostly cornices), unsuitable materials, insufficient protection against climatic factors, rising damp. The faulty details should be improved in order to prevent consequences presented on Fig. 4.

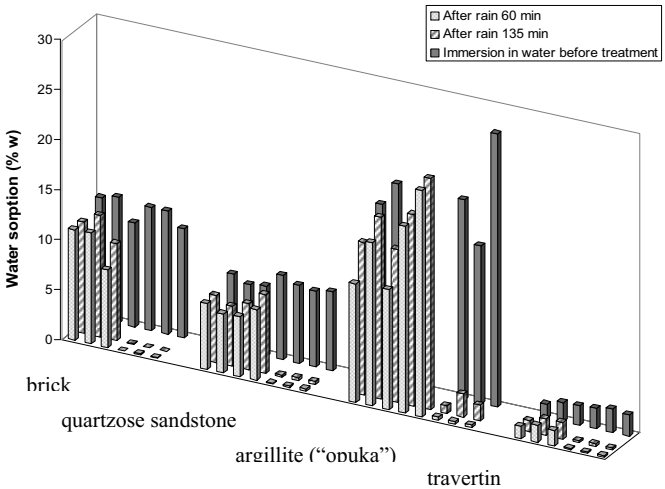

Figure 3. Windy rain impact on brick and stone samples protected by water repellent (right group of columns for each material) and unprotected (left group of columns for each material)

Figure 4. Examples of faulty details which are to be improved (from the left to the right: water trap on a Gothic façade, short eaves and non suitable material (copper), missing eaves on horizontal surfaces – one year after façade renovation)

Replacement of originals by replicas. Severely deteriorated or very precious heritage objects subjected to harmful effects can be saved by replacement of the original with a replica. Such a method is quite expensive but relatively safe if the original is placed into environment ensuring physical and chemical conditions necessary for its long term sustainability.

RELATION OF REPAIR CYCLES TO DAMAGE OR FAILURE IDENTIFICATION

According to general definition used by Technical Council on Forensic Engineering of the American Society of Civil Engineers a failure is an unacceptable difference between expected and observed performance. This definition is well applicable to assessment of historic buildings and monuments where their overall physical lifetime is not decisive for a necessity to repair their outer skin.

Lifetime is defined according to the BRE as a *mean time to failure (MTTF)* or a *return period (RP)*, which is dependent on the data available. The MTTF is estimated from the known lifetimes of several similar objects, the RP is calculated from data known for one object on which an identical element has failed several times during the life of the object. The MTTF is known and published for civil engineering materials and systems, the RP is rather a subject of individual studies associated with restoration works. The practical (or real) lifetime values change in dependence to the environmental factors, conservation technologies, materials and approaches, state policy as well as to changes in critical damage or serviceability definitions. The interventions are further influenced by costs of repair or restoration works which are different in different countries. Typical relative costs of repair of historic façades and masonry in European countries are summarized in the Table 1.

Repaired part	Czech Republic	United Kingdom	Italy	Norway
Masonry	1	12,1924	18,3986	5,8958
Façade	1	10,0593	11,4403	10,7287

ACKNOWLEDGEMENT

The authors gratefully acknowledge support from Institutional research plan grant AV0Z 20710524, the Czech Grant Agency GA ČR grant No.103/09/2067 and the "NOAH'S ARK" Project of the 6th Framework Programme of the European Commission.

REFERENCES

Drdácký, M.F. (2001): Learning from failures - experience, achievements and prospects, in "Forensic Engineering – the investigation of failures" (ed. B.S.Neale), Thomas Telford Pub., pp.165-174, ISBN 0 7277 3094 0, London.

Guide to surveys and inspections of buildings and associated structures (2008), B.Clancy (ed.), IStructE, London.

Hollis, M., Gibson, Ch. (2000): Surveying buildings, 4th Edition, RICS Books, Coventry.

Forensic Evaluation Techniques for Masonry and Concrete Construction

Gerald A. Dalrymple, P.E.[1]

[1]Whitlock Dalrymple Poston & Associates, P.C., 10621 Gateway Boulevard, Suite 200, Manassas, VA 20110; PH (703) 257-9280; FAX (703) 257-7589; email: adalrymple@wdpa.com

ABSTRACT

The paper discusses methods of nondestructive testing used in masonry and concrete evaluations. Many of the methods discussed were first used to evaluate concrete structures and have been adapted for use with masonry. Test methods discussed include: Infrared Thermography (IRT), Surface Penetrating Radar (SPR), and Impact Echo (IE) testing methods. These test methods can be used as evaluation tools for existing construction and as quality assurance tools for new construction offering advantages over visual inspection alone. The paper addresses the basic technical aspects of the test methods so that the audience has a general working knowledge of the test methods and understands the limitations of each.

INTRODUCTION

Have you ever had to convince an inspector that a masonry wall was grouted? Have you ever cut an opening in a wall that was supposed to have been grouted only to find that it was not? Have you ever wondered if the reinforcing specified for a masonry wall or concrete slab was actually installed? If so, how did you answer all of these questions in the past? Banging on masonry face shells with a hammer? Making Swiss cheese out of walls and slab sections with hammer drills and core rigs? There are better ways to address these issues with better accuracy and less destruction of completed work.

Surface Penetrating Radar (SPR), Infrared Thermography (IRT), and Impact Echo (IE) are powerful nondestructive test methods that aid in the assessment of masonry and concrete structures. The testing techniques permit rapid "on-the-spot" evaluation of existing construction conditions and document existing conditions in a portable electronic format.

MASONRY EVALUATION

SPR and IRT can be used to verify reinforcing steel placement and filling of the grout spaces in reinforced masonry construction. These methods are only useful after grouting operations are completed and grout curing has progressed to a point where

there is not free water within or on the grouted section. Nondestructive testing can usually be started approximately one to two weeks after grout placement.

SPR and IRT are two methods that have demonstrated advantages in assessing grout placement. SPR has the added advantage of identifying reinforcement embedded in grouted cells. Each of these methods permits survey of a section with access to only one face and, as such, have an advantage over pulse velocity methods and x-ray methods which require access to both faces of the component being surveyed.

Surface Penetrating Radar

SPR utilizes the principles of electromagnetic wave propagation and reflection to distinguish between different material interfaces. The SPR unit emits a series of discrete electromagnetic wave pulses which travel through the material being surveyed. When the wave passes through different materials, the propagation of the wave is altered; and some or all of the wave energy is reflected from the interface of the two materials.

Air, steel, masonry units, and grout within a masonry wall reflect the radar signal at interfaces between them. Steel is a perfect reflector of electromagnetic waves while masonry, grout, and mortar reflect only a portion of the electromagnetic energy. Air causes rapid attenuation of the electromagnetic wave and is readily distinguishable in the reflected wave signal.

The output from the SPR system can be used to identify conditions in the masonry. Radar signals are processed by a mobile computer and displayed in real time on the screen as a series of bands. The shade of the band is a function of the phase and amplitude of the reflected signal. Based on the shades and shapes of the reflected signals, three basic conditions within a grout space can be detected:

- Void in Grout Space: Air inside of a grout space reflects the signal as the wave passes through the masonry at the air interface. The resulting reflection (as shown in this publication) from masonry to air is displayed as a black-white-black band.
- Reinforcing Bar Embedded in Grout Space: Since steel objects are perfect reflectors, the reflection from a reinforcing bar is always inverted and displayed as a white-black-white band. The shape of the band is that of a hyperbola due to the discrete diameter of the bar and reflection of the signal as the antenna passes over the bar.
- Grout Filled Grout Space, No Reinforcement: The dielectric constant of grout and masonry are very similar. Therefore, the reflection of the wave at the grout/masonry interface will have a low amplitude and appear as a gray shade.

The characteristics of the wave reflection also permit calculation of the depth of embedded steel reinforcement relative to the surface of the antenna. The SPR method, however, cannot be used to directly determine reinforcing bar diameters from the reflected wave. Figure 1 shows representative SPR output from a reinforced concrete masonry unit column.

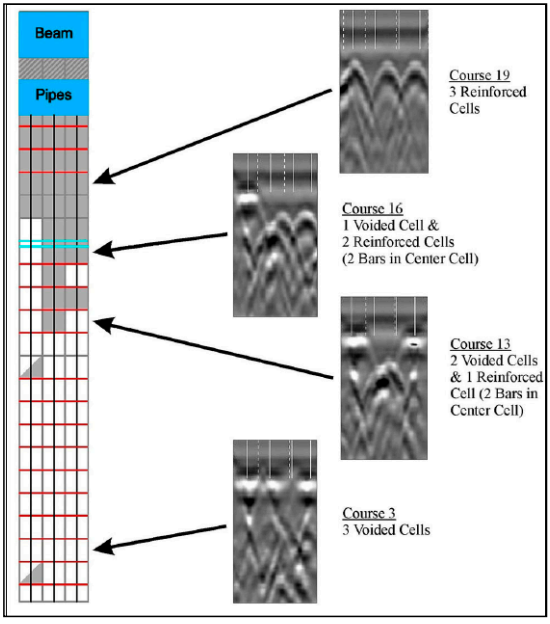

Figure 1. SPR survey results of a reinforced masonry column

Under favorable conditions, the SPR signals can be used to determine approximate splice lengths of bars when the bars are placed side by side relative to the line of the antenna scanning direction. The perfect reflection of the wave and the characteristic hyperbola shape of the steel reflection hides materials directly behind the steel object so that they are not detectable by the method.

In older masonry construction, brick header courses were often used to structurally bond the exterior brick wythe to structural clay tile or concrete masonry back-up wythes. Identifying true brick header courses can be difficult for brick bond patterns such as Flemish bond shown in Figure 2. In the case of the wall shown, true masonry headers were located every sixth brick course, and the remaining headers in the bond pattern were false or clipped headers making visual determine of true header courses impossible. SPR can be used to identify true header courses quickly due to the different depth of reflection of the SPR signal between full and clipped headers, Figure 3. We have not been able to use SPR to reliably identify cracked masonry headers due to the often extremely small void at the crack which is beyond the resolution of the method.

Figure 2. Flemish bond pattern with clipped masonry headers

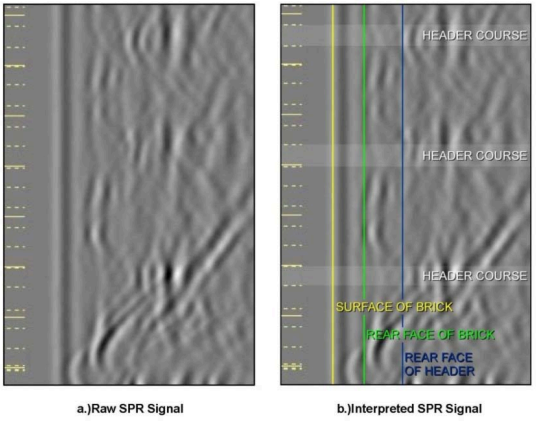

Figure 3 – SPR output used to identify full masonry header courses

Infrared Thermography

IRT uses the principles of thermal energy absorption, transmission, and emission to distinguish between hollow and grout filled cells in masonry. Since this method can only differentiate between hollow and solid masonry cells (steel cannot be detected), it is often coupled with a pachometer survey or SPR survey to locate and evaluate reinforcement installation. Detailed information, such as positioning of reinforcement and splice lengths, cannot be determined with IRT alone.

An infrared camera is used to detect relative differences in thermal radiation from a masonry surface. Hollow or insulated masonry cells act as a thermal barrier in masonry construction. Solidly grouted cells act as a heat sink and transmit the majority of the thermal energy through the masonry section.

Because the majority of the heat is transmitted through a grouted cell, very little thermal energy is emitted back in the direction of the heat source. In short, hollow or

insulated cells emit more energy than solid grouted cells. An infrared camera detects these minute differences in emitted thermal energy. As a result, when viewed with an infrared camera, hollow cells are displayed in a sharp and distinct contrast to grouted cells. In examples in this paper, cells that are not grout filled appear as lighter gray shades.

Thermal sources can be the sun (solar energy) or an artificial heat source, such as a heater or heat lamp. Optimum conditions for IRT testing occur when there is a combination of both, such as testing an air-conditioned building in the summer on a hot sunny day. In this example, the exterior masonry surfaces are exposed to solar energy and develop high exterior temperatures while the interior masonry surfaces are exposed to lower conditioned interior air temperatures. The thermographic image would thus display hollow cells as hot (as they emit the thermal energy) and the solid grouted cells displayed as cool (as the energy is transferred through the wall).

A sample photograph from infrared thermography is shown in Figure 4. Note the hollow cells appear white (hot) where the solid cells appear black (cold). In this example, the thermographer can rapidly and easily assess the grout placement, particularly the grout voids and misalignment of grouted cells. With the use of a camcorder linked to an infrared camera, survey data can be recorded, taped, and printed with ease for use in evaluating conditions.

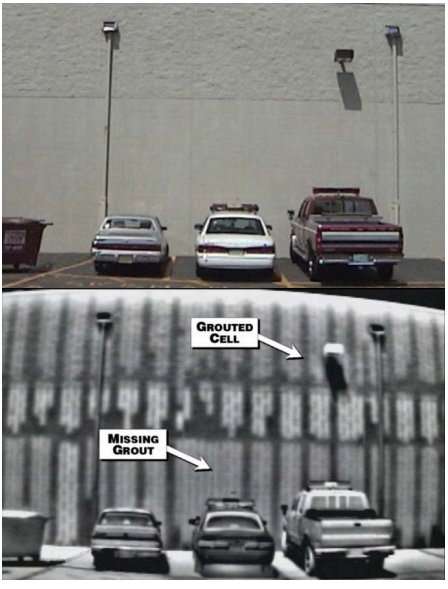

Figure 4. IRT survey results of reinforced masonry wall

CONCRETE EVALUATION

Concrete evaluation is best performed using SPR and Impact Echo. The fundamentals of SPR are the same as those discussed for masonry evaluations. Typically in concrete evaluations it is desired to determine the location, cover depth, and spacing of reinforcing steel, stirrups, post-tensioning tendons, grouted post-tensioning ducts, and conduits. All of this data can be gathered using SPR, typically with access required to only one surface.

The location of voids, cracks, and defects within concrete components is often better handled by IE. For some situations it is advantageous to use SPR in conjunction with IE. For example, it is relatively simple to locate post-tensioning ducts in beams and girders using SPR. SPR cannot be used to assess the presence of grout with the steel ducts due to the full reflection of the radar wave by the steel casing. Voids in the grout within the ducts can be located by IE after the location of the duct is defined by SPR.

Figure 5 shows a typical SPR signal from evaluation of a reinforced concrete slab-on-grade. As in masonry construction, the reinforcing steel is identified by the hyperbola in the shape of the reflection.

The depth of the reinforcing bar and overall concrete thickness is calculated and displayed by the equipment based on the input dielectric constant of the base material. A dielectric constant can be assumed for initial scans and calibrated by probe openings to verify the actual depth of embedded steel or by verifying the depth or thickness of the concrete section at the location along the scan. Calibrating the SPR equipment to the specific concrete in the structure can result in determination of concrete cover depth within approximately 1/4 inch.

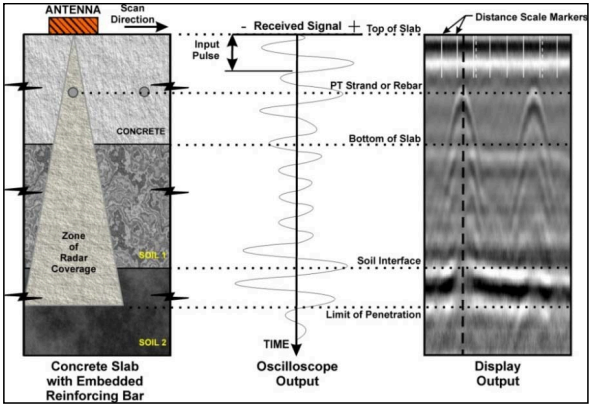

Figure 5. Typical SPR signal in concrete

The SPR data can also be used to estimate concrete thickness, where the thickness of the concrete section does not exceed the limits of the SPR signal penetration.

SPR survey is often most useful for verifying as-built construction where no original design drawings are available or where construction was not monitored or inspected and some post concealment verification is desired. Figure 6 shows a signal taken during the survey of a 30 year old parking structure where verification of reinforcing bar installation patterns was desired at column strips and middle strips in the structural slab. The survey produced as-built bar spacing patterns, cover depths, and bar cut-off locations so that a strength evaluation of the structural slab could be performed.

The location and depth of reinforcing bars are easily verified by SPR; however, SPR cannot be used to verify reinforcing bar diameters. Exploratory probe openings are required to verify reinforcing bar sizes. As with conventional reinforcing, SPR can be used to verify the location, grouping patterns, and trajectory of un-bonded post-tensioning tendons and ducts for bonded post-tensioning tendons.

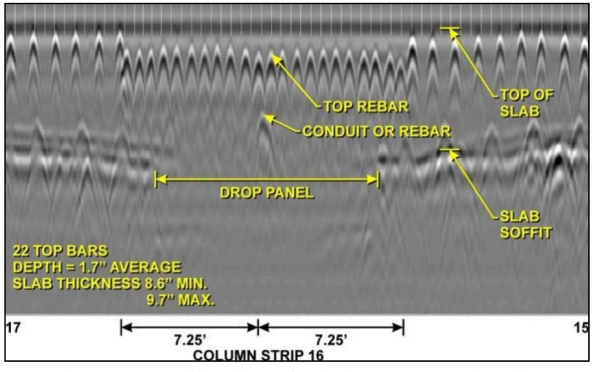

Figure 6. Verification of reinforcement using SPR

SPR can also be used to locate areas clear of reinforcement, post-tensioning tendons, and electrical conduits where it is necessary to core or cut concrete to permit installation of ducts, piping, access hatches, or other equipment that requires penetrations in slabs or walls.

SPR is quite versatile and can be used to solve a number of problems when evaluating structures. We have used SPR for the following evaluations in addition to the basic uses described above.

- Locate chimney flues in multi-wythe masonry bearing wall systems;
- Locate voids below concrete slab-on-grade construction caused by soil settlement and undermining of slab sections by water travel.

Impact Echo Testing

Impact echo (IE) is a nondestructive test method developed for flaw detection in concrete structures. The method is based on analysis of stress waves generated by an elastic impact on a concrete surface. Development of the method began in early 1980 at the National Institute of Standards and produced basic testing equipment and an understanding of stress wave propagation in concrete plates. Further research and development has expanded the capabilities of impact echo to include analysis of columns, beams, hollow pipes as well as slabs.

During testing a transient stress wave is introduced into the test specimen by means of a mechanical impact on the surface using calibrated impacting balls. The stress pulse propagates through the depth of the specimen as compression and shear waves and as a surface wave along the exposed surface. The waves are reflected by internal flaws and the extreme boundaries of the specimen. Reflected waves are monitored by a displacement transducer placed at the point of impact. Due to the reflection of waves by internal flaws such as voids and cracks, the method is only successful in locating the first reflecting flaw in the component. Thus, underlying flaws may go undetected unless the opposite surface of the component is available for testing. Figure 7 shows impact echo testing in progress.

Figure 7. Impact echo testing to locate post-tensioning ducts

Impact echo is often mislabeled as pulse-velocity or pulse-echo techniques which rely on the use of high frequency transducers. Impact echo uses both low and high frequency domains as required based on the geometry and type of flaw investigated.

Impact echo testing is effective on concrete components up to approximately 24 inches in thickness. The age of the concrete at the time of testing is generally not a factor.

Therefore, impact echo has surpassed the pulse-velocity and pulse-echo techniques in versatility for practical testing requirements. Typical applications of impact-echo include:

- Slab and pipe thickness measurements, a hundred or more data points can be collected per day

- Void detection in grouted post-tensioned tendon ducts in beams and girders, Figure 8
- Detection of corrosion induced delaminations at inaccessible surfaces of retaining walls, tanks, pipes, and tunnel linings
- Detection of cracks within the body of concrete components
- Quality assurance to assess bonding characteristics of repair materials and overlays

Figure 8. Location of voids in grouted post-tensioning ducts

IE has limited uses in the evaluation of masonry because the geometry of masonry units, unit core patterns, cavities, and intermixing of mortar and grout complicate the signal forms and make interpretation difficult. When dealing with 100 percent solid masonry units or solid grouted masonry units it is possible to use IE to identify masonry header courses and solid grouted masonry cells and to distinguish grouted masonry cells from ungrouted cells. Figure 9 presents IE signals from a header bonded masonry wall system. The clipped header is distinguished from the full header by the shift in the signal peak to a higher frequency.
If the wavespeed in the substrate, C, is known, the depth to the reflecting interface can be calculated with the following equation:

$$T = \frac{C}{2f}$$

In the equation, T is the depth to the interface and f is the frequency of the P-wave reflections from the interface. The wavespeed can be measured from a surface wave or from an element of known thickness.

Using the above equation with a field measured wavespeed of 2,192 m/s, the observed length of the full header is 8.0 inches and the clipped header is 4.6 inches.

SELECTING THE BEST TEST METHOD

No single test method is applicable for all conditions and all construction types. Often several methods combined with selective destructive testing is required to evaluate a problem.

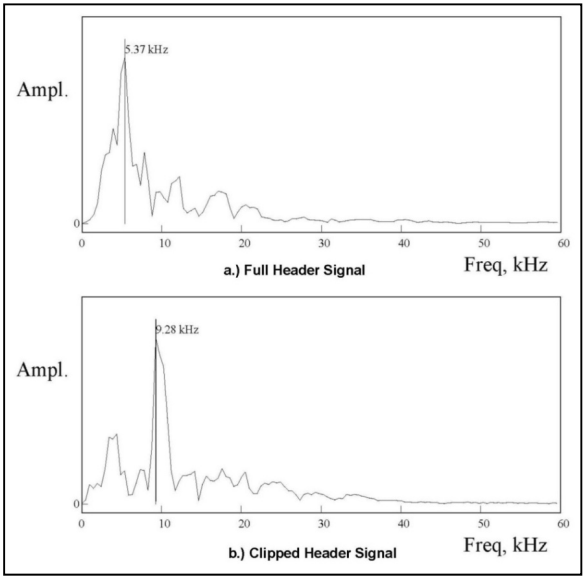

Figure 9. IE signals from brick masonry headers

SPR and IE testing are often limited by voids and/or air spaces within construction. The signal will not penetrate air spaces in typical masonry cavity wall construction; therefore, the method is often limited if access to the back-up wythe is not available.

Likewise, IRT is very dependent on the thermal conditions of the element being tested. If a sufficient thermal gradient cannot be developed across the component, IRT will be ineffective.

It is advisable to plan for some destructive testing to verify the results obtained from the nondestructive testing method selected. Probe openings will be required to calibrate equipment to accurately assess cover depth and to verify reinforcement bar sizes and post-tensioning tendon sizes which cannot be determined nondestructively through the methods discussed.

SUMMARY

Nondestructive test methods can be extremely valuable in the assessment of masonry and concrete structures and permit the collection of more comprehensive data than could be collected through destructive testing alone. The test methods discussed can also be used for quality assurance testing and inspection of work in progress as well as verifying as-built conditions of existing structures.

GROUND PENETRATING RADAR – DECIPHERING THE SIGNALS

Amy S. Graver, P.E.[1], Charles J. Russo, P.E.[2], and Matthew R. Sherman, P.E.[3]

[1]Senior Staff I – Structures, Simpson Gumpertz & Heger Inc., 2101 Gaither Road, Suite 250, Rockville, MD 20850; PH (301) 417-0999; email: asgraver@sgh.com
[2]Senior Principal, Simpson Gumpertz & Heger Inc., 2101 Gaither Road, Suite 250, Rockville, MD 20850; PH (301) 417-0999; email: cjrusso@sgh.com
[3]Associate Principal, Simpson Gumpertz & Heger Inc., 41 Seyon Street, Building 1, Suite 500, Waltham, MA 02453; PH (781) 907-9000; email: mrsherman@sgh.com

ABSTRACT

Ground penetrating radar (GPR) continues to gain use as a non-destructive investigative tool for existing reinforced concrete structures. Structural engineers conducting a flexural strength evaluation as part of a condition appraisal can use GPR to identify the relative positioning of reinforcement within the concrete element for use in their calculations. Different techniques can be used to convert the recorded time signals from the GPR into depth measurements. These techniques could include implementing an equipment-based default for the dielectric constant for the surveyed concrete, selecting a user-defined dielectric constant for the surveyed concrete, or creating a site-specific calibration using depth measurements recorded at destructive exploratory openings. Ultimately the usefulness of the GPR information to the structural engineer is a function of the accuracy of the technique used to convert the recorded time signal to an estimated depth. This paper presents a case study on the implementation of several conversion techniques, and compares how these techniques affect the estimated depths to reinforcement to be used in the strength calculations.

INTRODUCTION

Structural engineers conducting a flexural strength evaluation as part of a condition appraisal of an existing reinforced concrete structure can use ground penetrating radar (GPR) to collect a substantial amount of information, such as the relative positioning of reinforcement within the concrete framing elements or the thickness of the element, in a relatively short amount of time. As such, GPR continues to gain use as a non-destructive investigative tool. GPR equipment is relatively simple to use (Figure 1) and manufacturers generally provide quality training sessions on how to operate the equipment. Unfortunately, technicians and/or investigators often mistake the simple operation of the equipment for a false sense of simplicity regarding the overall process of using GPR as an investigative technique. A consistent question asked by structural engineers receiving estimated depths of reinforcement and overall thicknesses of slabs is “how accurate are these results?” The answer highly depends on the effort spent post-processing the collected data.

This paper presents a case study that shows the overall process of using GPR as an investigative technique. The case study includes the implementation of several conversion techniques and compares how these techniques affect the estimated depths to reinforcement needed to make strength calculations.

Figure 1. GPR Equipment in use

BACKGROUND ON GPR

Simply put, GPR uses an antenna to transmit and receive radar energy (Figure 2) and measures the time it takes to get a reflection. A reflection occurs when the radar energy encounters a change in the dielectric constant. The dielectric constant is a measure of how electromagnetic signals (radar) move through a material. The dielectric constant is associated with a velocity expressed in inches per nanosecond (in./ns) through a mathematical relationship with the speed of light in a vacuum.

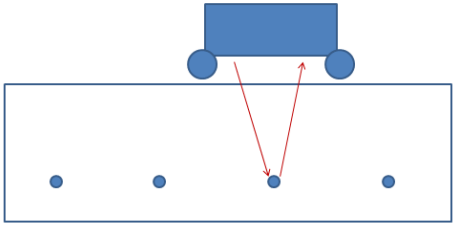

Figure 2. Reflected radar

In a reinforced concrete structure, reflections occur at the interfaces between concrete, steel, and air. For reference, air has a lower dielectric constant than concrete, and concrete has a lower dielectric than steel. The reflection is positive when the radar energy travels from a material of lower dielectric constant to a material of higher dielectric constant. Conversely, the reflection is negative when traveling from a higher to a lower dielectric constant. The recorded GPR survey image contains a series of positive and negative reflections (Figure 3) associated with the different materials encountered and each of these reflections is recorded as the cumulative time in nanoseconds (ns) that it takes the signal to leave the radar unit and

return from the reflection. The recorded survey images and stored GPR time records depict the concealed components of the reinforced concrete as a series of time intervals. However, the structural engineer needs distances, not times. And therefore, the GPR time records must be converted from time to distances.

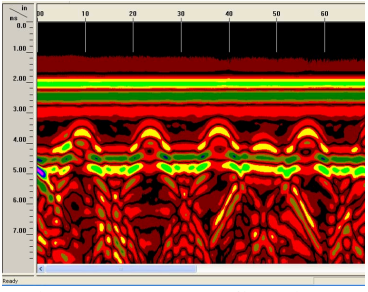

Figure 3. Recorded GPR signal

CALIBRATION TECHNIQUES

The conversion of GPR recorded time (ns) to a distance (in.) involves the multiplication of the recorded time and a conversion velocity (in./ns) associated with the dielectric constant of the material. Several common conversion techniques include an equipment-based default for the dielectric constant for the surveyed concrete, selecting a user-defined dielectric constant for the surveyed concrete, or creating a site-specific calibration using physical measurements obtained during the investigation (Figures 4 and 5), most often through exploratory openings and core sampling.

Figure 4. Exploratory opening to record depth of cover and Size of reinforcement

Figure 5. Recorded slab thickness from extracted core sample

Through the use of case study, we will further discuss the following conversion techniques:

- Method 1: Dielectric Constant – The simplest conversion is to multiply the recorded time (ns) by the velocity (in./ns) that corresponds to a dielectric constant selected to be representative of the concrete. The dielectric constant may be an equipment-based default or can be input directly into the GPR equipment by the operator.
- Method 2: Site-specific Calibration – A site-specific calibration can be created by correlating a number of recorded times to physical measurements obtained during the investigation. The calibration essentially determines the site-specific dielectric constant. The case study examines various site-specific calibration techniques, including the following:
  - Use two recorded times and associated physical measurements to create a calibration, and convert the time records.
  - Make a series of exploratory openings, record the depth of cover to the reinforcing bars, create a calibration, and convert the time records.
  - Make a series of exploratory openings and record the depth of cover to reinforcing bars, make a series of drilled or cored holes and record the overall thickness, create a calibration, and convert the time records.

CASE STUDY FOR CONVERSION OF GPR TIME RECORDS TO DISTANCES

Background. The case study involves a structural condition assessment of a reinforced concrete flat plate in an apartment building that is several years old for the purpose of performing a flexural strength evaluation. Allegedly the No. 5 top reinforcing bars were not properly positioned within the depth of the slab and the investigating engineer intends to use GPR to survey the existing construction so they can report the relative position of the negative flexural top reinforcement within the existing slab. The GPR survey is limited to the topside of the slab and not all locations can be accessed. The case study will demonstrate different conversion techniques of the recorded time from the GPR survey.

A limitation of the case study is that the GPR survey is restricted to the topside of the slab. When converted, the GPR time records will represent distances referenced from the topside of the slab. Flexural strength calculations by the structural engineer require depths to reinforcement from the compressive side of the element. Negative flexural strength needs the depth to the top reinforcement as measured from the bottom of the slab up to the reinforcement. This depth must be obtained by first converting the GPR time record associated with the top and bottom of the slab (transition from air to concrete and concrete to air; overall thickness of the slab) to a distance, subtracting the converted GPR time record associated with the top reinforcement (transition from air to concrete and concrete to steel; clear cover), and subtracting half of the diameter of the reinforcing bar.

Data for Case Study Simulations. We used collected GPR time signals and physical measurements from a previous survey of a flat plate concrete slab to populate the data for the study. The data consist of 32 GPR time records and associated physical measurements for the distance from the top of the slab to a top reinforcing bar and 32 GPR time records and associated physical measurements for the overall thickness of the slab. Physical measurements were recorded to the nearest 1/16 in. We will use only the GPR time records associated with known physical measurements for the simulations of the case study in order to evaluate the results.

Method 1: Dielectric Constant. Hardened concrete is a composite material consisting of a specific combination of fine aggregate, coarse aggregate, cement, water, and air. The moisture content of hardened concrete is influenced by the environment in which it exists. It should come as no surprise to the reader that all concrete is not the same. Similarly, it should come as no surprise that there is not a unique dielectric constant for "concrete". The dielectric constant of hardened concrete typically falls somewhere between 4.5 and 12, where most moderately dry concrete would fall between 6 and 6.5, and 12 would be indicative of a moist concrete.

We can select a dielectric constant for the concrete, but ultimately we are looking to use that constant to calculate a velocity that we can use to convert GPR time records to distance. Table 1 summarizes the relationship between the dielectric constant and the related conversion velocity. The reported velocity accounts for the total time duration of the two-way travel as depicted in Figure 2.

Table 1. Dielectric Constant and Conversion Velocity

Dielectric Constant	Conversion Velocity (in./ns)
4.5 (More Dry)	2.78
6.0	2.41
6.25	2.36
6.5	2.31
9.0 (More Moist)	1.97

As mentioned earlier, the investigator could choose to use the equipment-based default value for the dielectric constant or enter one manually. We will explore the latter. When selecting a dielectric constant, the investigator will enter a value based on experience and knowledge of the surveyed concrete, or take a single physical measurement and estimate a dielectric constant (using more than one physical measurement is considered a site-specific calibration and will be discussed in Method 2). If we decided to use the first technique and select a dielectric constant based on experience, what dielectric constant would you select based on the initial background statement? Select one and see how your choice compares in the results of the following simulation.

Using the second option, we need to obtain a single physical measurement during the field investigation. From the recorded data intended for calibration, we randomly selected one set of companion data (recorded GPR time record and physical measurement) related to the distance to the reinforcing bar (Data 1), and one set of companion data for the overall slab thickness (Data 2). Table 2 summarizes two data points.

Table 2. Reference Recorded Time and Measurement for Method 1

Reference Data for Trial	GPR Time Record (ns)	Measured Distance (in.)
Data 1 – Distance to Top Reinforcing Bar	0.969	2 -1/16
Data 2 – Overall Thickness	2.438	5 -5/8

We multiplied the recorded GPR time record for each of the reference datum in Table 2 by the velocities associated with the dielectric constants shown in Table 1 and compared the resulting estimates for the distance to the actual physical measurements. The subject slab for the case study is several years old and is an interior slab, and therefore, we would expect the range for the dielectric constant to be between 6 and 6.5. Table 3 shows the results if the physical measurement from Data 1 were used to estimate a dielectric constant and Table 4 shows the results if Data 2 were selected.

Table 3. Conversion for Data 1

Dielectric Constant	4.5	6.0	6.25	6.5	9.0
Conversion Velocity (in./ns)	2.78	2.41	2.36	2.31	1.97
Conversion to Distance (in.)	2.70	2.33	2.29	2.24	1.91
Physical Measurement (in.)	*2.06*	*2.06*	*2.06*	*2.06*	*2.06*
Deviation from Measurement (in.)	0.64	0.27	0.23	0.18	-0.15

Table 4. Conversion for Data 2

Dielectric Constant	4.5	6.0	6.25	6.5	9.0
Conversion Velocity (in./ns)	2.78	2.41	2.36	2.31	1.97
Conversion to Distance (in.)	6.78	5.87	5.75	5.64	4.80
Physical Measurement (in.)	*5.62*	*5.62*	*5.62*	*5.62*	*5.62*
Deviation from Measurement (in.)	1.16	0.25	0.13	0.02	-0.83

Considering either Data 1 or Data 2, the investigator could select a dielectric constant of 6.5 and use the corresponding conversion velocity to convert all the time records into distances. Following the conversion of the 64 GPR time records of this simulation using a dielectric constant of 6.5 with an associated conversion velocity of 2.31 in/ns, the average of the converted distances to the top reinforcement is 2.10 in. and the average of the converted measurements for overall thickness is 5.90 in.

The investigator should closely review the statistics of the GPR results and evaluate the most appropriate manner in which to use them. To demonstrate the influence of the GPR results on the overall objective of the case study, which is a flexural strength evaluation by the structural engineer, we will assume the investigator decided on a simple procedure to calculate an effective depth of the top reinforcement using the reported GPR averages. The structural engineer would calculate an effective depth to the top reinforcing bars by subtracting the average of the converted distances from the top of the slab to the top reinforcing bars and half of the diameter of the reinforcing bar from the average of the converted measurements for the overall slab thickness yielding an effective depth of 3.49 in.

The 64 physical measurements have the following characteristics: an average measured distance from the top of the slab to the top reinforcing bar of 1.73 in. and an average measured overall slab thickness of 5.77 in. The effective depth, using the simple procedure described above, is 3.73 in. Since flexural strength is almost directly related to the effective depth, the GPR estimate would underestimate the strength by about 6%.

Method 2: Site-specific Calibration. Method 2 involves creating a calibration for the GPR time records using site-specific physical measurements obtained during the investigation. A common question is "how many measurements are enough?" To answer that question, the investigator needs to weigh the objective of the assignment, the sensitivity of the analysis to the GPR results, and the cost to obtain the physical measurements for calibration. We prepared the case study for Method 2 to illustrate the influence how the number and type of physical measurement affects the conversion of GPR time records to distances. Since we are using only the time records associated with known physical measurements, we can directly evaluate the GPR results.

The site-specific calibration is determined by plotting the GPR time record (X Axis) against the physical measurement (Y Axis) and applying linear regression to get the best-fit straight line. Statistically, we can measure how well the line approximates the collected data using the R-squared value. The calibration has the

form of a linear equation, $D = mT + b$, with m and b determined from the linear regression, T is the GPR time record, and D is the estimated distance associated with the time record. For comparison, the conversion for Method 1 would have the form $D = mT$, with m being the corresponding velocity (Table 1).

A common mistake witnessed by the authors when reviewing GPR results from investigations conducted by others is the reliance on only shallow physical measurements often made at the closest reinforcing bars to the exposed surface. For a calibration plot, the domain of the GPR time records is bounded at the low end by the time records associated with shallow measurements and the upper end by the time records associated with the deeper measurements and overall thickness measurements. When only shallow measurements are used, the linear regression is anchored only at the low end of the time domain and the upper end is not represented. If this calibration is applied to all time records, including those with times at the upper end, the estimated distances can be significantly inaccurate.

We randomly selected sets of companion data (GPR time records and associated physical measurements) from our field investigation to incrementally construct site-specific calibrations as follows: two near-surface measurements; continue to add a single near-surface measurement up to a total of 10 points, use all 32 near-surface points, use 10 near-surface points and 10 overall thickness points, and finally, use all 64 companion data points (near-surface and overall thickness). Each simulation is recalibrated to get the best fit line. Figures 6 and Figure 7 contain calibrations for Simulations 2 and 12, respectively.

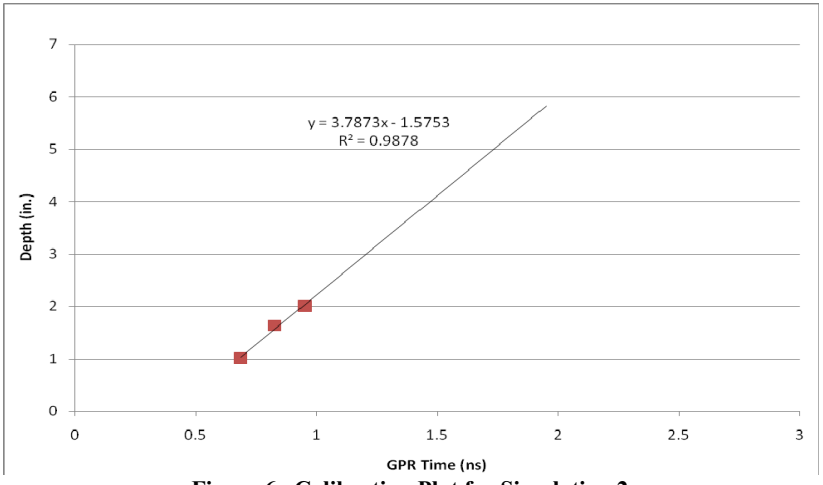

Figure 6. Calibration Plot for Simulation 2

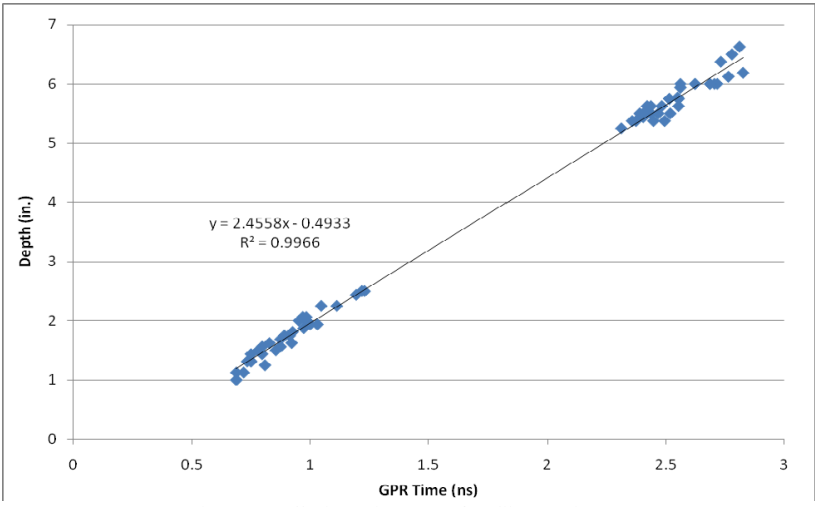

Figure 7. Calibration Plot for Simulation 12

At each interval, we used the incremental site-specific calibration to convert GPR time records to distances and then to calculate the average distance to the top reinforcement, the average overall thickness, and the effective depth using these averages. Table 5 summarizes the results of the simulations.

Table 5. Conversion Using Site-Specific Calibration

Incremental Calibration	Avg. Distance to Top Reinf. (in.)	Avg. Overall Thickness (in.)	Effective Depth (in.)
(1) 2 near-surface points	1.98	9.32	7.03
(2) 3 near-surface points	1.86	8.09	5.91
(3) 4 near-surface points	1.84	7.96	5.81
(4) 5 near-surface points	1.81	7.48	5.36
(5) 6 near-surface points	1.76	6.58	4.51
(6) 7 near-surface points	1.77	6.58	4.50
(7) 8 near-surface points	1.77	6.59	4.51
(8) 9 near-surface points	1.74	6.79	4.73
(9) 10 near-surface points	1.75	6.92	4.86
(10) 32 near-surface points	1.73	6.07	4.03
(11) 10 near-surface and 10 overall thickness points	1.74	5.83	3.78
(12) 32 near-surface and 32 overall thickness points	1.73	5.77	3.73
Actual Values from Physical Measurement	***1.73***	***5.77***	***3.73***

Simulations 1 through 9 have inaccurate estimates of the overall thickness as a result of applying a calibration that is only anchored at the low end of the time domain. While not as inaccurate, Simulation 10 suffers from a similar bias with its low-end calibration, despite the use of 32 calibration points. It is not until the calibration points for full-depth cores are used that the accuracies increase.

CLOSING REMARKS

GPR is a valuable tool available to investigating engineers. We can collect a substantial amount of information in a relatively short amount of time, but conversion of the collected GPR time records and the use of the results are as important as the objective of the primary assignment.

The case study demonstrates different conversion techniques, from the simple selection of a dielectric constant either from experience or a single-point physical measurement, to a series of site-specific calibrations using increasingly more physical measurements from different sources. The simulations of the case study demonstrate why the answer to the question “How accurate are the GPR results?” is not as simple as some may believe or desire.

INTEGRATION OF NDT RESULTS INTO THE EVALUATION OF DISTRESSED STRUCTURES

Keith Kesner, M. ASCE, Ph.D., P.E.[1] and Michael D. Brown, Ph.D., E.I.T.[2]

[1]Associate, WDP & Associates, P.C., 50 Washington St., Suite 751, So. Norwalk, CT 06854; PH (203) 354-4503; FAX (203) 354-4528; email: kkesner@wdpa.com
[2]Staff Engineer, WDP & Associates, P.C., 402 W. 7th Street, Austin, TX 78701; PH (512) 473-0018; FAX (512) 542-9033; email: mbrown@wdpa.com

ABSTRACT

Nondestructive test methods (NDT) are available for the assessment of many types of defects in existing structures including: the evaluation of reinforcing steel corrosion, determination of defect location, accurate assessment of the member sizes, and reinforcement locations. The use of these methods has increased as engineers and owners become aware of their capabilities. However, recent experiences have suggested that the integration of the NDT results into the evaluation process is lagging, and often the results of the NDT program end up as little more than report filler. Worse, the lack of NDT verification can result in incomplete or erroneous conclusions about the structure. Integration of NDT results into the evaluation process requires an understanding of both the output of the test methods and how the results impact structural performance. The successful integration of NDT results into the evaluation process is described.

KEYWORDS

Nondestructive testing, evaluation, impact-echo, corrosion, vibration, monitoring, structure

INTRODUCTION

The use of nondestructive test methods in the evaluation of structures has the potential to provide significant improvements in the ability of engineers to evaluate existing structures with defects. The use of NDT methods for flaw detection in concrete structures is described in ACI 228.2 as well as other references (ACI 228.2, 1998). These references provide guidelines on the use of the methods, spacing of testing points, and provide methods for verification of test results. The use of these methods has grown as engineers become more comfortable and familiar with them. The successful use of NDT requires field verification of test results, the lack of verification can result in an incomplete or erroneous conclusion regarding the nature and significance of defects in a structure (Cuoco, 2009).

The output data from the NDT methods varies significantly depending upon the methods selected and the nature of the evaluated structure. The output data can also

be described as quantitative – a physical value is measured during the testing or qualitative – a relative measure is assessed or a property inferred from the test results. Both types of results can be used in the evaluation of structures. The following sections describe the integration of results from various test methods and demonstrate how the use of NDT improves the evaluation process and allows improved engineering solutions to be developed.

QUANTITATIVE VERSUS QUALITATIVE NDT METHODS

NDT methods can be sorted into methods that provide either qualitative or quantitative information. Table 1 shows a summary of commonly used NDT methods [ACI 228.2R, 1998, ACI 222.1R 2002, Rodriguez, et al, 1993], with a classification of the results from the methods into qualitative or quantitative information. Depending upon the type of structure and the nature of the problem being evaluated either type of data can be used in the evaluation process. Some methods also can provide either quantitative or qualitative results depending upon how the testing is conducted.

Table 1. Commonly Used NDT Methods for Concrete Structures

Method	Output	Classification
Impact-Echo	Thickness, Flaw location	Generally quantitative
Surface Penetrating Radar	Thickness, reinforcement location, anomaly location	Generally quantitative
Instrumentation of structures	Varies (strain, displacement, etc)	Quantitative
Hammer sounding	Delamination indication	Qualitative
Impulse-response	Relative stiffness	Qualitative / Comparative
Half-Cell Corrosion Potential [ASTM C876]	Half-cell potential	Quantitative
Corrosion Rate Measurement	Corrosion rate	Quantitative

The results obtained from qualitative NDT results, such as a thickness measurement obtained from an impact-echo test, or the location of reinforcing steel obtained from surface penetrating radar can typically be directly integrated into analyses models. Similarly the results from instrumentation, such as accelerations or strains can be directly integrated into structural analysis models or directly compared to the results of such models. A distinct advantage of quantitative NDT is that they can be verified by physical measurement or through the use of multiple test methods.

Quantitative results such as those obtained from corrosion tests such as a corrosion potential test result or corrosion rate measurements also can be used both in both analysis models, such as models used to predict the life cycle of a structure or in the modeling of the effects of corrosion damage on the capacity of a structure. Verification of corrosion test results can be more complicated than measurement of physical properties. Methods to verify corrosion test results include use of multiple

test methods, physical probes to examine steel conditions and repetition of test results to verify repeatability.

Results obtained from qualitative test methods such as the impulse-response method are more difficult to evaluate, verify and incorporate. The impulse response method results in the measurement of the dynamic stiffness and mobility of the structure at the test location. Both of these parameters are significantly affected by the boundary conditions at the test location. Only in ideal situations, can a comparison be made between results obtained from damaged areas and results from undamaged sections or other structures with a similar geometry and material properties. Depending upon the test geometry, other NDT methods can also be used to verify test results.

INTEGRATION OF NDT RESULTS

The following sections provide a brief summary of case studies where the results from NDT methods were used in the evaluation process. The case studies are intended to highlight examples where NDT results were either directly used in analysis models, or were used to guide the selection of repair strategies. In all of the case studies described below, a verification program to confirm the test results and equipment performance was included in the evaluation process. Complete details of the verification programs are not included for brevity.

Evaluation of Corrosion Induced Spalling Using Impact-Echo Method

The impact-echo method was used in the evaluation of a reinforced concrete cantilever retaining wall [Kesner, 1999]. The 60 ft long wall sections were used to create a recreational marina. Long-term exposure to seawater resulted in corrosion of the reinforcing steel at the base of the 10 ft tall wall sections. Due to the non-redundant nature of the cantilever wall section, when the corrosion damage exceeded a critical value, the wall section failed with little or no warning. To address the corrosion damage, and to improve the seismic performance of the sections, a caisson system with ties was developed (Figure 1). An impressed current cathodic protection system was used to mitigate future corrosion.

The evaluation involved using the impact-echo method to locate areas where corrosion damage resulted in spalling of the concrete on the back-face of the wall which was below grade and could not be inspected visually. The transition from nondestructive testing to structural assessment was made by assuming that the reinforcing steel at locations with concrete spalling was completely corroded. In analysis terms, at locations with corrosion damage, the fixed cantilever condition was assumed to be a hinged joint. This assumption was a conservative one as verification core tests (Figure 2) indicated that some amount of reinforcing steel was present at the delaminated concrete sections. Incorporation of the impact-echo test results into the analysis models allowed for the tailoring of the number of caissons added to the actual extent of damage in a given wall panel. The analysis models,

which incorporated the results of the impact-echo testing, resulted in a significant reduction of the cost of the project.

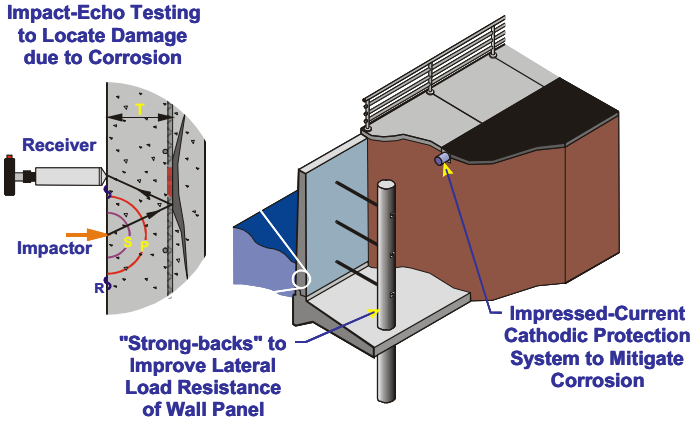

Figure 1. Schematic of cantilever retaining wall with caissons installed, impact-echo test location shown at the base of the wall.

Figure 2. Concrete core samples removed for verification of test results. Note significant remaining reinforcing steel cross-section.

Evaluation of Possible Vibration Damage in Industrial Structure

The frame consisted of a cast-in-place structure that was approximately 60 ft tall, and the upper most beams in the frame were precast and attached to the cast-in-place

portion by long anchor bolts extending up from the CIP columns and passing through the precast beams (Figure 3). The upper layer of beams supported a bank of 8 large industrial fans that ranged from 6 to 10 ft in diameter. After a number of years in service, significant cracking was observed in the precast beams at the joint to the cast-in-place portion of the frame. A large vertical crack can be seen in the right-hand portion of Figure 3. Prior to repairing the structure, the effects of fan vibrations on the forces in the connections were investigated to mitigate similar damage to the repaired structure.

To perform the investigation, a series of field measurements were made to measure the dynamic accelerations experienced by various portions of the structure. Measurements were taken in all three directions at most of the beam column joints as well as the fan housings. During the field measurements, various combinations of the 8 fans were starting-up, running-down, or in a steady state condition. An effort was made to measure the fans individually to determine if a single unit was responsible for a disproportionate amount of the vibrations. Approximately 240 test runs were performed, monitored, and recorded for later analysis.

After data collection, a series of Fast Fourier Transforms (FFTs) were performed on the acceleration records to examine the relative intensities of the various frequency components of the recorded data. A portion of the recorded acceleration recorded is shown in Figure 4, and the FFT corresponding to that data is shown in Figure 5. Overall, the maximum recorded accelerations were on the order of 2% of gravity. The data were analyzed by combining the many acceleration records into a small number of acceleration vs. frequency envelopes. Envelopes were constructed by grouping similar measurements (such as: measurement in the N-S direction with accelerometers mounted on fan housings). The FFT envelope for this case is shown in Figure 6. The data indicated a relatively large peak at approximately 19 Hz (Figures 5 and 6). However, the magnitude of the acceleration for this frequency was still relatively small (~0.75% of g). For each group, the maximum acceleration at each frequency was determined to determine a curve, similar to Figure 6, that the resembled a design spectrum. The experimentally determined design spectrum was finally used in combination with a modal analysis of the structure to estimate the maximum expected lateral forces due to fan vibrations.

Based on these results, it was determined that the dynamic forces on the beam-column joints were quite small and likely not the cause of the observed damage. Further investigation revealed that the damage was likely due to poor detailing within the structure. These details produced very large amounts of cover (4 to 5 in.), and that cover was spalling while the underlying concrete was still intact.

The use of instrumentation was a crucial part of the evaluation as it allowed for a reasonable means to determine the forces on the damaged sections. By examining the magnitude of these forces in a rational manner, a possible cause of damage was eliminated. This allowed the assessment to identify the actual mechanism responsible for the damage, and to develop appropriate repairs.

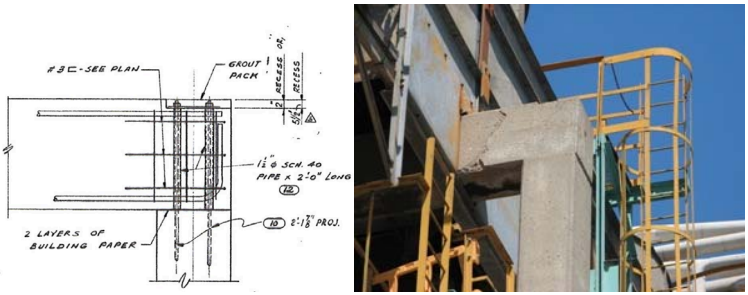

Figure 3. Detail (left) and Photograph (right) of precast beam/cast-in-place column connection.

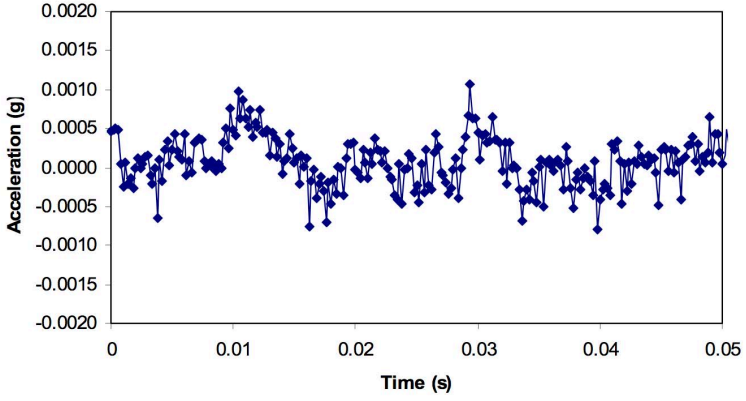

Figure 4. Sample of recorded acceleration data.

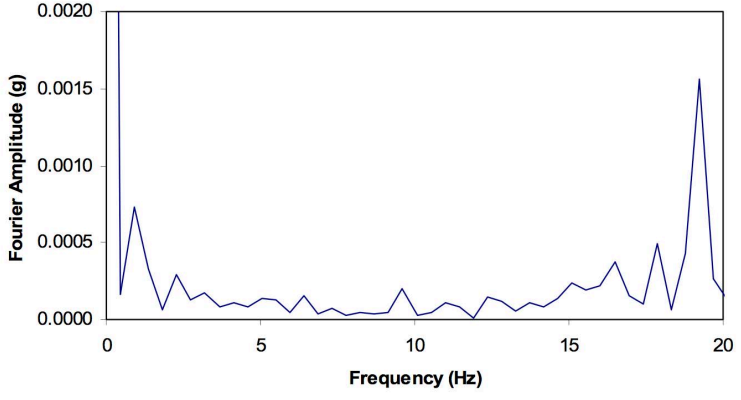

Figure 5. FFT plot resulting from data in Figure B.

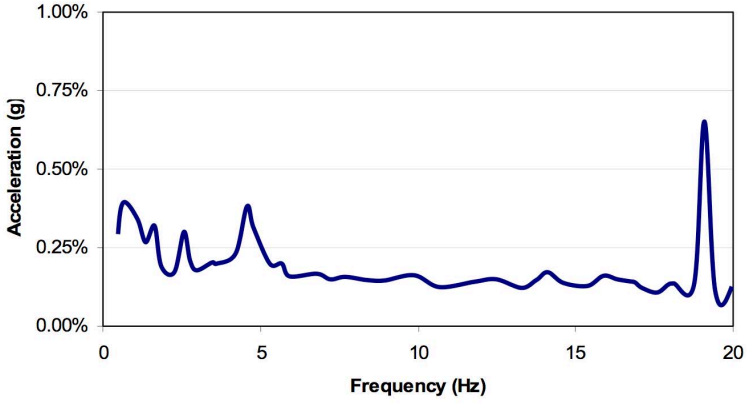

Figure 6. Envelope of FFT data.

Corrosion Evaluation – Concrete Shell Structures

The structural capacity of a concrete shell structure was recently evaluated due to concerns that the integrity of the reinforced concrete shell structures had been compromised by long-term leakage through the roof of the structure resulting in corrosion damage to the concrete members. The concrete shell structure was constructed in the late 1970's, and currently serves as both an indoor athletic field house and an exterior playing field [Tully, 1979]. The structure is a comprised of a series of rectangular concrete shells, supported by concrete columns (Figure 7). The evaluation was developed to assess the current condition of the structure, with an emphasis the current condition of steel reinforcement.

To assess the condition of the structure, a series of nondestructive tests and probes were performed on five of the concrete shells. Three of the tested shells were identified as "bad" shells, and the other shells were identified as "good" locations. The "bad" shells were characterized by visible stains on concrete surfaces and active leakage. Figures 8 and 9 show the typical conditions that motivated the evaluation. After completion of the field testing, a series of structural analyses were performed. Results from the testing were combined with results from structural analyses to develop an informed opinion with respect to the long-term integrity of the structure.

Electrochemical test methods were used to evaluate the potential for reinforcing steel corrosion. In each shell, a series of half-cell corrosion potential tests (ASTM C876) were taken at an approximate spacing of 7 ft on center. Corrosion rate measurements (Rodriguez, 1993) were made at the locations with the highest (most negative) corrosion potentials. None of the corrosion potential tests indicated active corrosion at the time of testing. However, the corrosion rates indicated corrosion damage was likely to occur in the future. These results indicate that some level of corrosion

current (flow of electrons associated with a corrosion process) is occurring; however, the amount of corrosion current is not sufficient to generate conclusive (more negative) half-cell corrosion potential values.

Figure 7. Shell structures at field house

Figure 8. Water leakage and efflorescence on interior shell space.

Figure 9. Staining on interior surfaces at "bad" shells.

The highest amounts of corrosion activity were identified in "wet" areas which occurred along the paths followed by leaking water as it flowed towards the drains in the shells. Tests performed in dry areas of the shells resulted in near zero half-cell corrosion potentials indicated that corrosion was not likely occurring. The testing was performed in winter, during moderate interior temperatures, and moderate amounts of humidity. Greater amounts of corrosion activity may have been recorded had the testing been performed during the warmer summer months.

Testing was performed on two "good" shells that had only a limited amount of visible leakage and were generally drier than the "bad" shells. Corrosion rate measurements were taken at the locations with the most negative corrosion potential. All of the electrochemical tests indicated that no active corrosion was occurring in shells 8 and 13. The measured values were consistent with the dry appearance of the concrete on the shell interior and probes that indicated no corrosion was occurring.

The corrosion testing indicated that, at worst isolated corrosion activity was occurring in the shells. Based upon these results, and the results from impact-echo and other physical tests, a decrease in structural capacity was not expected. Accordingly, the recommendations for the structure were primarily intended to mitigate the flow of water through the shell roof. If significant corrosion damage had been observed, the analysis models would have been adjusted to account for the variation from the design capacity. Specifically, using the corrosion rate measurements, an estimate of the loss in reinforcement cross-section over time would be been developed. This would allow for estimations of the decrease in capacity over time as corrosion degraded both the reinforcing steel development (bond) and cross-sectional area.

SUMMARY

The case studies described in the preceding sections highlight the integration of the results from various NDT methods into structural analysis models and in the development of appropriate repair strategies. The successful use of NDT arises from the selection of test methods where test output can be integrated into analysis models or provide an indication of ongoing deterioration. Based upon the author's experience, test methods that provide quantitative data can be integrated into evaluation models. Prior to the use of NDT results, verification of the results through direct measurement, destructive testing or other methods is required.

The integration of NDT into analysis models can be accomplished in a variety of manners. The simplest integration is through the use of actual thickness measurements obtained via NDT or the actual reinforcing steel locations to create more realistic analysis models. Results from corrosion testing can be used to guide the selection of repair strategies or be integrated into service life prediction models. Corrosion rate measurements can also be estimate the impact of the loss of cross-section on capacity.

REFERENCES

ACI 228.2R-98, (1998). "In-place Methods for Determination of Strength of Concrete." American Concrete Institute, 1998, Farmington Hills, MI.

ACI 222R-01, (2001). "Protection of Metals in Concrete Against Corrosion," Report prepared by ACI Committee 222 – Corrosion, 2001, 41 pp.

ASTM C876, (2004). "Standard Test Method for Measurement of Half-Cell Corrosion Potential", ASTM, West Conshohocken, PA.

Cuoco, D.A., (2009), "The Right Decision," Letters to the Editor, Civil Engineering, July 2009, Vol. 79, Issue No. 7, p. 9.

Kesner, K.E., Poston, R.W., Salmassian, K., and Fulton, G.F., (1999). "A Case Study in Sustainable Restoration: The Marina del Rey Seawall Repair Project," Concrete International, December 1999, Vol. 21, No. 12.

Rodriguez, J., Ortega, L.M., Garcia, A.M., (1993). "Corrosion Rate Measurements in Concrete Bridges by means of the Linear Polarization Technique Implemented in a Field Device," *ACI Fall Convention*, November 1993.

Tully, D., (1979) "Hypar Recreation Complex Built Under Football Field," Concrete International, August 1979, Vol. 1, No. 8, pp. 50-57.

The Application and Advantages of Surface Penetrating Radar in Subgrade Void Detection Beneath Slabs-On-Grade

Justin Norvell, E.I.T.[1] and John Grill, P.E.[2]

[1]Staff Engineer, WDP & Associates, P.C., 402 W. 7th Street, Austin, TX 78701; PH (512) 473-0018; FAX (512) 542-9033; email: jnorvell@wdpa.com
[2]Senior Engineer, WDP & Associates, P.C., 10621 Gateway Boulevard, Suite 200, Manassas, VA 20110; PH (703) 257-9280; FAX (703) 257-7589; email: jgrill@wdpa.com

ABSTRACT

Settlement of subgrade resulting in poor performance of slabs-on-grade is a common problem in structures. On a recent project, significant amounts of soil slurry infiltrated the basement of a large manufacturing warehouse. The washout of the underlying soil and resulting settlement was sufficient to cause visible dynamic deflections when subjected to routine forklift traffic. These observed conditions indicated the void space beneath the slabs would be moderately deep and widespread.

This paper discusses the application of surface penetrating radar (SPR) to identify the locations of subgrade voids and provides a comparison to other nondestructive test (NDT) methods. Impulse response and impact-echo can be used to locate these voids; however, these methods have inherent limitations and often require more destructive testing for confirmation of results. Due to its accuracy and ease of use, SPR is an ideal NDT method for this application.

INTRODUCTION

Poor performance of slabs-on-grade is commonly evidenced by cracking or settling of the concrete slab. A common cause of these flaws is the settlement and/or erosion of the subgrade materials. Poor preparation of the underlying soils can result in consolidation settlement over time, creating a void directly beneath the slab. In addition, water can erode significant amounts of soil, resulting in similar subgrade voids. Once voids are present, the slab no longer performs as intended, resulting in cracking, deflection, and shifting of the slab.

Typical repairs for voided subgrades include removal and replacement of the subgrade or injection of a filler material, such as grout, into the voids. A critical aspect of either repair is the identification of the extent of subgrade voids. Voids may extend far beyond the areas visibly damaged. If not addressed, these remaining voids may compromise the effectiveness of repairs and potentially allow damage to occur after the repairs have been completed, ultimately increasing costs. Therefore, methods that accurately identify the limits of the subgrade voids enhance the effectiveness of repairs and the ability to formulate more accurate repair cost estimates.

Nondestructive methods are typically desirable when identifying the extent of voids beneath a slab-on-grade since they minimize cosmetic damages to the slab and can essentially map the areas which need repairs, rather than relying on blind “hunt and

peck" techniques. Every nondestructive test method has its own strengths and weaknesses, and therefore, no one method is the "best" for every job.

When selecting the ideal NDT method for a project, several factors must be taken into consideration. The test method's level of accuracy over the desired range (plan area as well as depth of penetration) must be considered. Work hours and work space may be restricted and environmental conditions may be harsh, requiring the method be highly portable and durable. The amount of destructive verification must also be considered. An extremely wide array of conditions and requirements will play a part in the selection of the proper test method for each individual project.

The following sections will describe the application of surface penetrating radar (SPR) to the detection of subgrade voids, and show the advantages of SPR compared to other test methods.

SLAB SUBGRADE VOID DETECTION METHODS

Several NDT methods are available to identify voids below a slab-on-grade. Each method has its own strengths and weaknesses; therefore, proper selection is critical to the success of the investigation. Regardless of the NDT method used, comparative study of areas indicative of both solid contact and voids, along with destructive verification, is often required to validate the obtained results. The following section discusses some common NDT methods for detecting air voids below slabs-on-grade and criteria used to select the appropriate method for field application.

IMPACT-ECHO

The impact-echo method (IE) is a NDT method that utilizes stress wave propagation for detection of slab thicknesses, voids, honeycombing and other flaws in concrete and masonry structures (Sansalone and Streett, 1997). An IE test system is comprised of three components: an impact source, a receiving displacement transducer, and a portable computer with a data acquisition card. The impact source is a hardened steel sphere on a spring steel rod. The receiving transducer is a broadband piezoelectric displacement transducer; a thin lead strip is used to provide acoustic coupling between the transducer and the concrete surface. A portable computer, complete with data-acquisition card and software, is used for signal acquisition and analysis.

Testing Procedure

When conducting impact-echo testing, a transient stress pulse is introduced into the member by striking the impactor on the surface as illustrated in Figure 1. The stress pulse propagates into the object along spherical wavefronts. The waves are reflected by internal cracks or interfaces, such as voids, cracks, and delaminations, as well as by the external boundaries of the member. The arrival of these reflected waves at the surface where the impact was generated produces surface displacements that are monitored by the transducer. If the transducer is placed close to the impact point, the waveform is dominated by displacements caused by P-wave arrivals.

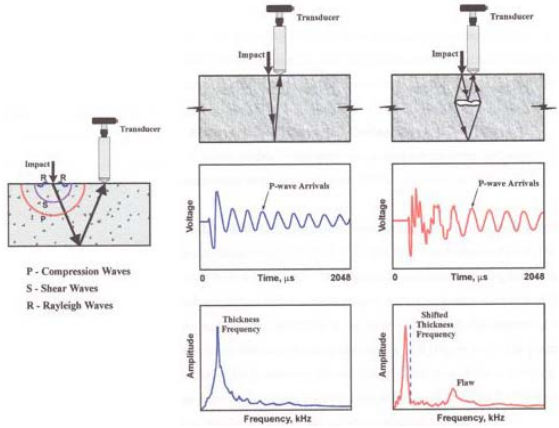

Figure 1. Schematic of the impact-echo test method.

Application to Subgrade Void Detection

The IE test method has been used as a reliable NDT technique for locating defects in many types of concrete structures as well as estimating slab thickness. In addition, IE can be adapted for application in void detection, which is achieved through comparative testing of the resultant waveforms of both voided and non-voided areas (Wouters et al 1999). Although the acoustic impedance (the resultant of density and wavespeed), which defines whether wave energy is reflected or refracted, of concrete is much different than water or air, the acoustic impedance of soil is only slightly lower than that of concrete. Since the acoustic impedance of air is low as compared to concrete, most of the wave energy generated in the concrete is reflected back to the transducer. However, when the concrete has good contact with the subgrade, some of the energy is refracted through the concrete/soil interface and therefore causes more wave energy dissipation as compared with the voided subgrade. (Sansalone and Streett 1997)

Since IE is a single point test, data is gathered only at discrete locations. When using this method to gather data over a large area, the balance must be found between spacing of the test grid and the level of accuracy required. A tight test grid, while providing more detailed results, requires more time to acquire data. On the other hand, a large test grid will leave gaps in the data leading to less refined results. In addition, IE requires intimate contact with the concrete surface to be tested. Therefore, floor coverings, such as carpet, tile, and some types of waterproof membranes, must be removed prior to testing.

IMPULSE RESPONSE

Impulse response (IR) is also a NDT method that uses stress wave propagation for detection of flaws in concrete structures. An IR test system comprises three components: an impact source, a receiving transducer, and a portable computer with the ability to perform data acquisition. The impact source is an instrumented hammer

capable of measuring the striking force. The receiving transducer is a low frequency velocity transducer. A portable computer, complete with data-acquisition capability, is used for signal acquisition and analysis.

Testing Procedure

When conducting IR testing, a forced vibration is introduced into the member by striking the hammer on the surface. The resulting waveform is then measured as the transducer, near the impact, monitors the movement of the member being tested. Both the impact and the impact response are measured over time. This impulse response is dependent on characteristics of the element being tested, such as material properties, support conditions, etc. IR is generally a comparative NDT method; in that, multiple tests are required to infer meaning for the data obtained.

Application to Void Detection

Although IR is primarily used to test the integrity of concrete piles (Malhotra and Carino, 2004), it has also been used for detection of subgrade voids (Amick et al 2009). Since the response is dependent on the stiffness of the material being tested and its support, voids are typically identifiable when compared to responses obtained in non-voided areas. Areas without subgrade contact are more flexible and exhibit higher mobility. However, as slab thickness increases, stiffness also increases. Therefore, the thicker the slab, the less likely you are to have distinctions in the data due to the self-supporting nature of thick slabs. Like impact-echo, IR is also a single point test method and requires removal of some concrete coverings. Therefore, economy limits accuracy when large areas are being tested. Due to variability within test results, impulse response requires more verification than other techniques.

SURFACE PENETRATING RADAR

Surface (or Ground) Penetrating Radar (SPR) is a nondestructive evaluation technique which uses electromagnetic energy to locate objects, subsurface flaws, or interfaces within a material. A typical SPR system consists of a portable computer specifically intended for radar data collection and interchangeable antennas of different frequencies. A SPR antenna housing contains both the transmitting and receiving antennas. Antennae are available in many wave frequencies. As the frequency of the antenna increases, penetration depth increases, but resolution decreases. For typical concrete and masonry applications, a high frequency antennae (1500 or 1600 MHz) is used, which typically gathers data up to a depth of approximately 18 to 24 in. The use of a survey wheel aids in data interpretation by providing a distance scale over the scan.

Testing Procedure

When collecting SPR data, the operator moves the antennae along the survey line at a slow walking speed. A real time visual display of the material cross section is presented on the computer for interpretation. The transmitting antenna emits a train of discrete amplitude modulation (AM) radio wave pulses while the receiving antenna collects the scattered pulses as they return to the antenna housing. The time it takes for a radar wave to travel through an object is dependent on the dielectric constant of

the material. If this constant is known, the depth of an embedded object or interface may be determined by measuring the time it takes to receive the reflected signal. The output is fed to sampling circuitry before being digitally processed by a computer.

Data Interpretation

The color and intensity of the patterns in the output are related to the amplitude of the reflected signals. Figure 2 illustrates a typical SPR scan and sample signal output. The first low amplitude gray band corresponds to the concrete surface. The bands of alternating light and dark areas that appear in the remainder of the output correspond to the positive and negative reflections of the input wave from subsurface objects. Reflections from a lower dielectric media to a higher one, such as from concrete to steel, will undergo a phase inversion, or reversal, and the boundary will show up as a bright signal (assuming the input wave is dark). Conversely, the boundary from concrete to air (higher dielectric to lower) will show up as a dark signal. SPR antennae are specifically tuned to detect cylindrical objects, such as rebar, conduit, pipes, etc. These types of features show up as hyperbolas, or arch shapes, on the data record, as seen in Figure 2. Steel shows up more distinctly than other media due to the high reflective property of electrically conductive materials, and as a result, SPR is particularly well suited for locating post-tensioning tendons and mild reinforcing steel in concrete slabs.

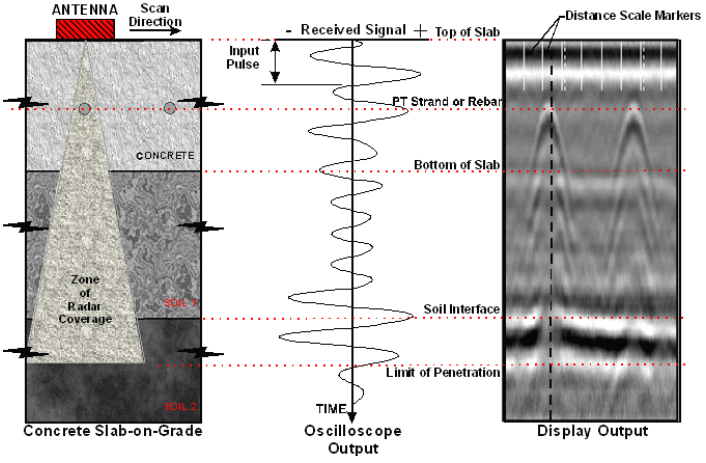

Figure 2. Typical SPR scan.

Application to Void Detection

As described in the preceding section, reflections of the electromagnetic waves can be interpreted to identify the presence of embedded objects, subsurface flaws and boundaries between dissimilar materials. In this manner, SPR can be used to identify air-filled voids beneath a concrete slab-on-grade. The boundary between a higher dielectric media to a lower dielectric media, as in the case of the transition from

concrete to air, will appear as a black band. Thus, the presence of air voids can be identified in the SPR data record by the high amplitude negative reflection, or black band, generated at the interface between the concrete and air. When no void is present, the bottom of the slab usually cannot be clearly seen because the dielectric constant of concrete is similar to that of the underlying soil.

As opposed to stress wave methods, SPR is continuously recording data. Therefore, large amounts of data can be collected in a relatively short period of time. SPR can collect data over a variety of materials typically covering concrete, such as carpet, tile, and various membranes. However, foam insulation commonly exhibits similar reflections as airspace in radar scans, limiting its effectiveness in some situations. In addition, SPR may have difficulty detecting very small voids (less than ½ in. deep).

COMPARISON OF TEST METHODS

The three NDT methods discussed each have the capability to identify subgrade voids. However, each of the methods also has inherent limitations. When determining the appropriate test method, several factors must be considered – the expanse of the tested element; the level of accuracy required; the allotted time for testing; and the condition of the tested element, including the addition of membranes or facades.

Since SPR continuously records data, it often provides more complete data and eliminates errors in data interpretation when compared to single-point methods. SPR provides a graphic of the scanned element and leaves less chance to misinterpret the data provided; therefore, SPR often requires less destructive verification to identify location of voids. Essentially, single point methods can only identify localized conditions and do not provide information adjacent to the test point. Therefore, a small flaw with limited dimensions may be interpreted as a more wide spread flaw. SPR can be performed quickly and it is most effective when testing large areas. SPR is robust and can be used in a variety of environments. In addition, SPR can be used when coatings are present, unlike stress wave methods. The drawback of using SPR is that it is typically only capable of identifying large voids, usually greater than ½ in. deep, while stress wave methods may be able to identify smaller flaws. It should be noted that none of the methods presented have the ability to estimate void depth.

CASE STUDY

During the summer of 2008, a normally-reinforced, concrete slab, less than five years old, at an industrial warehouse had and was experiencing potentially significant damage and dynamic deflection. Damage was primarily evidenced by slab-on-grade cracking and settling near drain inlets. Deflections were noted in areas where heavy machinery (forklifts) was used. In addition, soil-water slurry was infiltrating the basement through electric conduit. An estimated 900 cu ft of washed out soil was removed from the facility. A limited investigation by plant personnel indicated that some of the water drain conduits had been damaged during construction and others were not present at all. The facility is cleaned nightly with significant volumes of water to wash away byproducts of the processing operations. The damaged or missing drain conduits allowed these large volumes of water to flow beneath the slab. Based on these observations, it was apparent to plant personnel that subgrade voids were

present and were likely extensive. The observations also indicated the voids were large, or deep.

The main level of the facility is primarily supported by a 7-inch concrete slab-on-grade. Other portions are elevated above a subgrade basement level. The main level of the warehouse has approximately 160,000 sq ft of total space. Only about 65,000 sq ft of the main level supported by the slab-on-grade was of importance to the client for this investigation. No evidence of washout or damages to the slab-on-grade were observed in the basement areas.

The warehouse had multiple partitions, including pre- and post-processing areas with varying temperatures and environmental conditions. Mechanical processes ran continuously between 5:00 am and 3:00 pm, immediately followed by daily cleaning and inspections that kept the facility occupied and essentially on a continuous 24-hour schedule. This constant activity made it improbable to shut down operations without a incurring a significant loss in revenue. Large amounts of cleaning water ponded throughout the facility. Some areas of the slab were also covered with a urethane overlay.

The test method selected for this project had to be able to endure harsh environments (high and low temperatures and wet floors), account for urethane coatings, be easily and quickly relocated, and gather data over large areas in short amounts of time. Based on these limitations and the assumption that the voids were deep, SPR was determined to be the best option, primarily due to its ruggedness and ease of use as compared to other NDT techniques. Although significant amounts of water can affect SPR scans, any standing water in the test areas was pushed aside immediately prior to testing.

PRELIMINARY VISIT

In order to gain an understanding of the facility and test the applicability of SPR for this case, a preliminary site visit was performed. During this visit, the optimal equipment setups were determined to enhance the signal results and reduce the need for post processing. Trial scans were performed in a small area where both subgrade voids and solid contact was assumed to exist. A 1,500 MHz antenna was used, which is typical for structural applications. The following system parameters were determined through preliminary testing: five signal gain points were adjusted as necessary throughout the facility to increase the visibility at the bottom of the slab; since tests needed to be completed quickly, scans were recorded at 60 scans per ft as opposed to a more detailed scanning rate; the color table was set to indicate voids as a black-white-black band; and the dielectric constant of 6.25 was determined to be adequate for comparison of signals.

Three locations were scanned using the pre-determined setup parameters. Signal interpretations were performed on-site and three locations were chosen for destructive verification. At two of these locations, SPR indicated the presence of a void directly below the slab. The third location indicated solid contact between the slab and subgrade. The cores verified the SPR results. Figure 3 shows an SPR scan with a black-white-band indicative of a voided location. Immediately adjacent to the void,

the bottom of the slab is not clearly evident. Figure 4 shows the core verification. The right figure is identifying the depth the concrete dropped after coring.

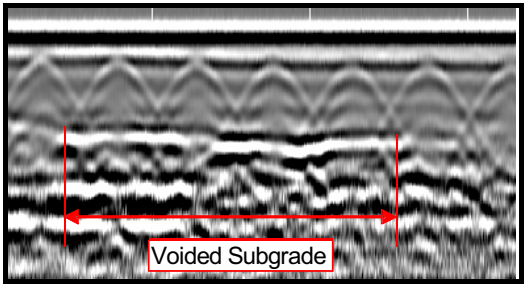

Figure 3. SPR scan indicating voided subgrade (Note the black-white-black band indicating the bottom of the slab).

Figure 4. Core verification of voided subgrade (left: apparent subgrade void after core removal; right: depth of void under core)

PRIMARY VISIT

After completion of the preliminary visit and confirmation of the results, an additional visit was planned to develop a map of the voided areas. In order to minimize the number of SPR scans and, subsequently, time in the field, a grid was created by scanning in two orthogonal directions. The spacing of the scans ranged from 2 ft to 15 ft, without exceeding 4 ft in both directions simultaneously. However, about 10% of the area scanned exceeded these spacing guidelines due to active facility operations limiting access to these areas. Standing water was mostly displaced from the scanning area prior to testing. Due to the large area that required scanning, signal interpretation was not performed on-site. Scan locations were documented on site plans so that the limits of subgrade voids could be easily mapped. SPR analysis software was used to review the scans and document the locations of solid contact and probable subgrade voids.

Additional destructive verification (concrete cores) was performed at two locations during the primary visit, making a total of five verification cores in all – three locations in areas in which SPR had indicated voids, one location in which solid contact was indicated, and one location where indications were not readily clear. The core at the unclear site revealed the subgrade to have good contact with the concrete slab. The remaining cores verified SPR results confirming voids were readily identified by clearly distinguishable reflections (distinct black and white contrasts).

A contour map of identified conditions, as illustrated in Figure 5, was developed for the Client. Approximately 14%, or 8,900 sq ft, of the 65,000 sq ft scanned indicated the presence of subgrade voids. These areas typically were adjacent to basement walls, indicating that the subgrade loss and settlement was likely due, in part, to lack of compaction of fill material. Failure to obtain proper compaction of fill soils against basement walls would lead to increased soil settlement in these areas. Voided areas were also prevalent near drain conduit. The settlement/erosion of the subgrade was exacerbated by the large supply of water coming from damaged or missing drain conduits.

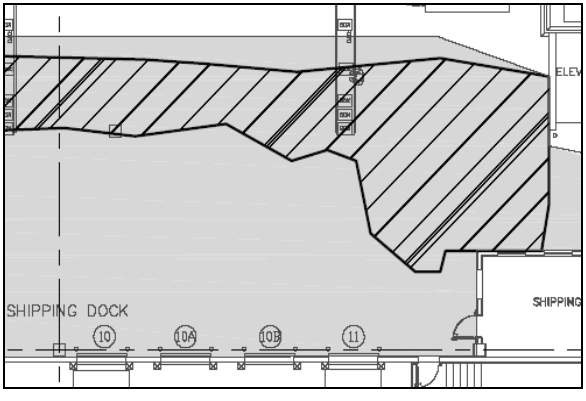

Figure 5. Typical contour map identifying voided subgrade (diagonal hatching) within area scanned with SPR (gray hatching).

Two repair options were made available to the client. The first was to remove the slab in areas containing subgrade voids. The fill would then be replaced and compacted and a new slab would be cast and connected to the existing slab with dowels. The second repair option was to inject cementitious grout under low pressure into the voided areas. The second option was recommended, as it would likely be less costly and less disruptive to plant operations.

SUMMARY

The identification of subgrade voids in the processing facility proved to be challenging in many ways. The extreme environmental conditions were difficult for the engineers and the equipment used. Working quickly around areas where water pools and around byproducts of the manufacturing processes was difficult and had to

be executed without delay. In order for plant operations to continue uninterrupted, the investigation had to be performed in a limited amount of available work hours, which required the NDT method to be flexible, quick, and easy to use.

Over a total of six days, SPR was used to gather data representative of 65,000 sq ft of the slab-on-grade with essentially no disruption in the plant's daily production. Approximately 8,900 sq ft (14%) of slab area was identified to have subgrade voids. Although the depth of the voids cannot be identified, the core verifications indicated an approximate void depth of 3 in., resulting in an approximate volume of 2,100 cu ft of voids to be repaired. Equipped with plans identifying the scanned areas, the extents of the subgrade voids, and the approximate volume of voids, the Owner was able to seek accurate repair cost estimates and perform repairs with less risk of cost overruns due to unforeseen conditions.

SPR is certainly not a failsafe method for detecting voids. However, SPR's durability and flexibility, its ability to collect large amounts of continuous data in a short period of time, and its ease of use in the field confirmed it as the appropriate NDT method for this particular case study. As a result of using SPR, destructive verification was limited and data was gathered in a very short amount of time without disruption in plant operations. Comparable sampling by IE or IR testing methods would likely have required significantly more time in the field, destructive verifications, and potential disruption to the facility's operations.

For other applications, a different NDT method may be more beneficial than SPR. Perhaps a combination of NDT methods may be the most cost-effective and beneficial solution for a particular project. Ultimately, every survey and assessment is unique. Careful analysis of the site conditions and limitations should always be performed to ensure selection of the proper test method and verification procedures. A relatively small amount of pre-planning and reasoning can significantly reduce the overall project costs to the Client and ultimately provide a better finished-product accurately tailored to the Client's needs.

REFERENCES

1. Wouters, J. P., Peterson, J. E., Kesner, K. E., Poston, R. W., 1999, "Impact-Echo Locates Subgrade Voids," *Concrete International*, Vol. 21, No. 5, pp. 23-27.

2. Sansalone, M. J. and Streett, W. B., 1997, *IMPACT-ECHO Nondestructive Evaluation of Concrete and Masonry*, Ithaca, NY.

3. Malhotra, V. M. and Carino, N. J., 2004, *Handbook on Nondestructive Testing of Concrete*, 2nd Edition, CRC Press, West Conshohocken, PA.

4. Amick, H., Xiong, B., Tang, N., Gendreau, M., 2009, "Voids Beneath Slabs-on-Ground," *Concrete International*, Vol. 31, No. 7, pp. 29-33.

In-Situ Evaluation of Structures Using Load Testing

Nestore Galati, PhD[1] and Tarek Alkhrdaji, PhD, PE[2]

ABSTRACT

In-situ load testing is commonly used to assess the safety or the serviceability of an existing or new structural system or part of its elements for a particular external load condition. The most frequently used load testing procedure includes the in-situ load test method described in Chapter 20 of the ACI 318 - Building Code Requirements for Structural Concrete and the Cyclic Load Test method in ACI 437 and ACI 437.1R. This paper describes the load testing programs used for two field projects to evaluate the load capacity of existing and upgraded structural components. The main objective of this paper is to describe the process for determining the test load level, loading procedure, instrumentation, evaluation criteria and load test outcomes. The first case study is for the evaluation of the sidewalks for a historical steel bridge in which the supporting beams lost up to 70% of the original cross-section due to extensive corrosion. The load test was performed in order to assess whether the sidewalks were able to safely support the pedestrian load. The second case study is for the evaluation of a typical bay in an old reinforced concrete (RC) pan-joist floor system. The floor was being considered to support new telecommunication equipment that required an increase in the capacity of the floor system. Load tests were performed for typical existing members and members upgraded using externally bonded FRP reinforcement as well as bonded RC overlay.

[1] Design Engineer, Structural Group, Inc., Strengthening Division, 7455 New Ridge Rd., Suite T, Hanover, MD, 21113, ngalati@structural.net

[2] Engineering Manager, Structural Group, Inc., Strengthening Division, 7455 New Ridge Rd., Suite T, Hanover, MD, 21113, talkhrdaji@structural.net

INTRODUCTION

Load testing of concrete structures in the United States is a century old tradition with some applications carried out as early as in the 1890s [Birkmire, 1894]. In the early days, in-situ load testing was the most direct proof of performance of, at the time, proprietary and novel construction materials and methods. The American Concrete Institute (ACI) began formalizing load test procedures for concrete structures in 1920 [ACI, 1920]. Subsequent codes [ACI, 1936] defined the deflection evaluation criterion as a function of the span and the total depth of the member. This formed the deflection criterion that is still in effect to date [ACI, 2005]. Notable investigations into load testing of concrete structures documenting the practice of the last few decades can be found in a variety of literature [FitzSimons and Longinow, 1975; RILEM, 1984; and Bungey, 1989].

Today, in-situ load testing is commonly used to assess the load carrying capacity of structural members as affected by design or construction errors, verify new methods of repairs or strengthening, verify if the existing members can carry loads different that those used for the original design, and demonstrate the safety of a structure that has experienced damage due to corrosion and degradation. There are currently two methods used for in-situ load testing of concrete structures: The 24-hour load test procedure, as prescribed in Chapter 20 of the ACI 318 Building Code [ACI 318, 2005], and the Cyclic Load Test (CLT) method, as prescribed in ACI 437 Strength Evaluation of Existing Buildings and ACI 437.1R Load Tests of Concrete Structures (ACI 437R, 2003; ACI 437.1R, 2007). Each of these documents is published by the American Concrete Institute (ACI).

The ACI 318 load test method and its evaluation criteria are widely referred to as the 24-hour load test because the test load is held in place on the structure for a period of 24 hours. Because residual displacements must be measured 24 hours after the test load has been removed, the actual test duration (not including setup) takes at least 48-hours to complete.

The CLT method includes testing the structure with repeated loading/unloading cycles with a load magnitude that increases as the test progresses, rather than a constant load applied for a predetermined length of time. This provides improved information regarding the behavior of the structural system.

Both the 24-hour and the CLT methods allow the use of dead weight (water bladders, sand bags, steel plates, etc.) or hydraulic jacks to apply load to the structure. However, the use of dead weights may not be safe since the load cannot be removed quickly, and the use of hydraulic jacks is typically considered to be safer since the applied load can be quickly removed at the first signs of overstress or failure.

Analytical models are typically used to design the load test and to evaluate the effects of structural characteristics such as load sharing with adjoining or adjacent members, effects of the magnitude and location concentrated loads, effect of using concentrated loads versus original distributed loads, and the effects of support fixity on load distribution. In some instances, the analytical models are refined after the test is completed by adjusting the boundary conditions and stiffness of the adjacent

elements to match the actual measured deformations of the structure. Once the model has been calibrated, the analytical model may also be used to accurately determine the internal forces caused by external loads.

Determination of the test load level and loading procedure are not entirely straightforward and are discussed next using two field case studies. A general description of the loading levels, cycles, and the number of steps are given in each case study.

CASE STUDY 1: LOAD TESTING OF HISTORICAL STEEL BRIDGE

The bridge under investigation was constructed at the beginning of the century and has experienced extensive corrosion of the steel members, as showed in Figure 1. Due to the age of the bridge, no engineering drawings and construction records were available. The original sidewalks on both sides of the bridge were 10 ft wide. Concrete-filled steel buckle plates, which were riveted to supporting steel stringers and floor beams, supported the sidewalk decks and the full area of the roadway decks (see Figure 2).

The buckle plates are supported by three longitudinal lines of stringers under the sidewalks consisting of riveted, built-up, steel members. The stringer lines 1 to 3 are referred as “fascia stringers,” “sidewalk struts,”and “curb stringers,” respectively.

The transverse floor beams under the sidewalks (brackets) cantilevers approximately 4 ft (1219 mm) out from each vertical post, which are spaced every 7 ft - 3 in (2210 mm) on center along the length of each span.

In the 1960s, the eastbound roadway was widened by decreasing the width of the upstream sidewalk. This was accomplished by reducing the length of the anchor spans of the sidewalk brackets by 4 ft (1219 mm) and moving the curb stringers closer to the sidewalk struts. The roadway buckle plates adjacent to both sidewalks were removed and the roadway decks were reconstructed as reinforced concrete slabs. The buckle plates, concrete sidewalk slabs, and all the other original structural members outboard of the sidewalk struts were retained at both sidewalks.

Due to the extensive corrosion and complexity of the structure, the development of numerical models would not be reliable unless calibrated with field measurements. For this reason, the consulting engineer on this project requested a cyclic load test to be performed on the structure in order to asses the existing capacity and to collect experimental data that can be used to calibrate a 3-D FEM model of the structure.

A total of six (6) tests were performed on the two sidewalks, three tests on each side of the bridge. The first test area was located at the downstream side of the bridge (downstream load tests). This area included two sidewalk bays with a total area of about 14 ft - 6 in (4420 mm) by 9 ft (2743 mm). The second test area was located at the upstream side of the bridge (upstream load tests). This area also included two sidewalk bays with a total area of about 14 ft - 6 in (4420 mm) by 4 ft (1219 mm). The evaluation comprised of three load tests for each test area.

The first load test involved testing the sidewalk slabs for negative bending moment by simultaneously loading two adjacent spans. The second test involved testing the sidewalk slabs for positive bending moment by loading only one span. The third test involved testing of the steel brackets by applying the load to the sidewalk directly over the bracket.

The test loads, which were to be applied as concentrated forces, needed to create internal forces in the structure that should be at least equal to those produced by the applicable load combination per ACI 318-05. The design live load is 100 psf (4.8 kPa) uniform live, which is uniformly distributed over the entire sidewalk area, as prescribed by the State Building Code where the bridge is located. The load test magnitude for the bracket at the upstream side was performed with a load intensity of 1.3D + 1.6L, corresponding to the full design-load prescribed by the state where the bridge is located.

Equivalent Point Loads

The test loads were determined by considering the sidewalk as a continuous beam spanning above the steel brackets for the upstream load-test area, and between brackets and their anchor-span extension for the downstream load-test area. After determining the flexural and shear demands, the analysis was repeated with the introduction of concentrated loads that produced similar flexural and shear demands. The analysis considered loading configurations with pairs of point loads, spaced at 3 ft longitudinally. The load configurations for the downstream load tests are illustrated in Figure 3.

Load Test Setup

The loads were generated by 30-ton-capacity hydraulic jacks, connected in parallel, which reacted against a system of steel counterweights placed at the ground level. The load was transferred through ½" (12mm) post-tensioning cable, passing through 1 in. (25mm) diameter holes drilled in the slab, and locked against the counterweight systems and to the hydraulic jacks (See Figure 4)

During the load tests, loads, displacements and strains were continuously monitored in real-time by load cells, direct-current-variable-transformer (DCVT) transducers, and strain gauges (SG) connected to a data-acquisition system. The data-acquisition system recorded data at a rate of 5 Hz from all devices, and displayed in real time the load vs. deflection curves of critical locations on a computer screen. The DCVT transducers measured vertical displacements at 14 locations. Strain gauges measured strains at 6 critical locations on the steel buckle plates and steel bracket. The use of hydraulic jacks, and continuous monitoring of the structure during the load tests, ensured that the loads could be rapidly removed in case signs of distress developed, preventing permanent damage to the structure.

Load Test Procedure and Results

The structure was tested following the cyclic load testing protocol of ACI 437 (ACI 437.1R-07). For each load test, repeatability, permanency and deviation from linearity were evaluated, even though they were not developed for steel structures. The most important criterion for a steel structure would be the deviation from

linearity because failing of this parameter would be a clear indication that steel yielding has occurred.

No evident signs of distress were detected in the structure during the load tests. The load-deflection envelopes indicated that the test sidewalks and brackets had a linear behavior, passing all the ACI-437 acceptance criteria.

Discussion of Results

The load tests indicated that there was a substantial longitudinal stiffness in the sidewalks, which was attributed to the interaction among adjacent deck slabs (buckle plates and concrete fill), brackets, and railing. Load-sharing mechanisms were evident based the following observations:

1. At the downstream side, the recorded deflections in the center bracket are similar to the two adjacent brackets for both the Negative-Moment and Positive-Moment tests, as shown by the deflected shapes of the sidewalks along Load Lines 1 (See Figure 5).
2. The mid-span deflections generated by the Negative-Moment tests are larger than the deflections caused by the Positive-Moment tests. This is an indication of load sharing between adjacent spans.
3. The recorded deflections at the free-end of the brackets are only slightly greater than the deflections measured at the mid-region of the bracket (see figure 6).
4. A more pronounced slope between the end and middle points, and consequent larger deflection, would be expected if the bracket end would be entirely disengaged from the sidewalk deck.

The load sharing mechanism previously described allowed the structure to sustain the entire design load and to meet the acceptance criteria of ACI 437 even though the structure was substantially corroded.

CASE STUDY 2: LOAD TEST EVALUATION OF UPGRADE FLOOR SYSTEM

The following case study discuses the strengthening and cyclic load test that was performed on the second-level structural floor of a building located in downtown Cleveland, Ohio. The nine-story building was constructed in 1917. Originally, the second floor of the building was occupied by a department store. With the high percentage of internet traffic between New York and Chicago running through fiber optic lines, downtown Cleveland is becoming a prime location for the telecom industry. To meet the demand of this industry, the owner of the building decided to upgrade the floor on the second level to house telecommunications equipment. Telecom hotels are essentially warehouse spaces for internet related telecommunications and other high-tech equipment that usually requires structural floor capacity in the range of 125 psf (6.0 kPa) to 175 psf (8.4 kPa).

Building Description

The building was constructed with masonry over a concrete incased steel frame and a reinforced concrete floor system. The ceiling height is approximately 14 ft (4270 mm), and the column spacing varies from 19 to 23 ft (5800 to 7000 mm). Due to the age of the building, very limited construction and maintenance records were available. The existing engineering drawings provided only floor plans and geometry of the members. No information regarding material properties and reinforcement details were available. All dimensions and section geometries were field-verified.

The floor system consists of reinforced concrete joists supporting a concrete slab monolithically cast with the joists. The concrete slab is 3 ½ in. (89 mm) thick and reinforced with #3 (#10) steel bars spaced at 18 in. (457 mm) on centers. The joists are 27.6 ft (8410 mm) long, 6 in. (153 mm) wide, and 15.5 in. (394 mm) deep. Field investigation of the joists revealed that they are typically reinforced with two 1-in (25 mm) square bars at mid-span, one of which is bent up at approximately 5.5 ft (1676 mm) from each end and extend above the support. There was no information on reinforcement details at the supports. The field investigation also revealed that an additional straight bar is provided over the support at the location of the bent up bars. No information of material characteristics was available for the joists. Due to time constrains, a nominal concrete strength of 3,500 psi (24 MPa) and steel yield strength of 33,000 psi (227 MPa) were assumed for the preliminary analysis of the joists. These values were based on the typical material strength recoded for structures with similar age. The assumed values were later verified through testing.

Localized destructive investigation of the joists revealed that the joists do not have any steel shear reinforcement. Preliminary analysis of the existing floor system indicated that the existing beams and slab are capable of carrying the proposed loads. The joists, on the other hand, were deficient and their capacity was limited to approximately 96 psf (4.6 kPa), governed by the shear strength of the joists. To house telecommunication equipment, the floor needed to be upgraded to carry its own weight, a super imposed dead load of approximately 25 psf (1.2 kPa), and a service live load of 150 psf (7.2 kPa) acting over the entire surface of the floor. The super-imposed dead load is a result of the concrete overlay required to level the existing concrete slab.

Strengthening and Load Testing

The cyclic load tests were designed to locally verify the performance of some typical joists that appeared to be the "weakest link." To this end, the joists were loaded near their ultimate strength and their response was measured in terms of deformation and crack width. The cyclic load testing procedure involved applying concentrated loads to the test joists at predetermined locations to simulate the effect of maximum flexural forces at mid span and maximum flexural and shear forces at the supports of the test joists.

Analytical modeling of the joists indicated that the maximum moments and shear forces could be produced using two-point loads spaced 6 ft (1830 mm) apart. The load was applied using hydraulic jacks that pulled against a reinforced concrete

micro-pile that was installed on the ground floor below. A high strength steel bar was used to connect the jacks to transfer the load to the micro-pile. Linear variable differential transformers (LVDTs) were used to measure joists deflections at five locations along their lengths (see Figure 7). A load cell was used to measure the applied load. Measurements were collected using a data acquisition system that allowed for real-time monitoring of the applied load and the behavior of the test joists. During the test, deflections and crack width were monitored for stability.

Two load tests were performed on the joists. Test 1 was performed on two joists that were isolated by saw-cutting the concrete slab along a line between the joists. Prior to testing, the joists were strengthened for shear using carbon FRP strengthening systems applied in the form of U-strips 12 in. (305 mm) wide and spaced at 18 in. (457 mm) on center. The load test was terminated when the mid-span deflection became unstable and inelastic behavior was observed. Large residual deflections were measured when the load was removed.

Results of the first test indicated that failure of the joist was governed by yielding of reinforcement at the support. No failure signs were observed at joists mid-span. Based on the test results, the joist was rated for a super-imposed dead load of 25 psf (1.2 kPa) plus a live load of 135 psf (6.5 kPa). The shear performance was adequate with no shear cracks or failure signs observed.

Bonded reinforced concrete overlay was used to address the observed joist deficiency. The overlay consisted of 3 in. (76 mm) thick concrete reinforced with steel wire mesh. To ensure adequate bond between existing and new concrete, the slab surface was prepared by aggressive abrasion blasting to remove all weak concrete and provide an open-pore structure. Pull-off tests were performed on the overlay to verify that failure will not occur at the interface.

After the overlay was applied, Test 2 was performed on the same two joists to verify the overall behavior of the strengthened system. The test was performed following the same procedure outlined earlier. However, the joists were only loaded to 85% of the ultimate as recommended by ACI 318 to prevent excessive damage to the upgraded joists. During testing, a number of flexural cracks developed on top of the slab (through the overlay) at both ends of the joists (at the negative moment region) (see Figure 8). The number and distribution of the cracks indicated that sufficient bond existed between the existing and new concrete. This behavior confirmed that a composite behavior was achieved. The load test results demonstrated the improvement stiffness and deflection behavior of the joists after strengthening (see Figure 9). Based on the test results, the strengthened joists were rated for the self-weight plus 36 psf (1.7 kPa) super-imposed dead load (RC overlay) and 150 psf (7.2 kPa) live load.

CONCLUSIONS

This paper presented the process of load testing using the cyclic load testing (CLT) method that were used to perform in-situ evaluation for two projects: a historical bridge sidewalk and a reinforced concrete pan-joist floor system in a

building. For both structures, the load test was conducted without disrupting the normal operation of the structures.

Load testing is a method of strength evaluation that is more representative of the performance of the strengthened structural member than analytical approaches and can provide valuable information regarding the health and performance of a strengthened structural element.

REFERENCES

American Concrete Institute (1920), "Standard Specification No. 23 – Standard Building Regulations for the Use of Reinforced Concrete".

American Concrete Institute (1936), "Building Code Regulations for Reinforced Concrete," ACI 501-36T.

ACI Committee 437 (2003), “Strength Evaluation of Existing Concrete Buildings (ACI 437R-03)”, American Concrete Institute, Farmington Hills, Michigan, 28 pp.

ACI Committee 437 (2007), “Test Load Magnitude, Protocol and Acceptance Criteria”, (ACI 437.1R-07), American Concrete Institute, Farmington Hills, MI, 2006, 83 pp.

American Concrete Institute (2005), “Building Code Requirements for Structural Concrete”, ACI 318-05, American Concrete Institute, Farmington Hills, Michigan, pp. 443.

Birkmire, W. (1894) “Skeleton Construction in Buildings,” John Wiley & Sons, New York, 80pp.

Bungey, J., (1989), The Testing of Concrete in Structures, Second Edition, Chapman and Hall, New York, New York, 228 pp.

FitzSimons, N., and Longinow, A., (1975), “Guidance for Load Tests of Buildings,” Journal of the Structural Division, American Society of Civil Engineers; pp. 1367-1380.

RILEM Technical Committee 20-TBS, (1984), “General Recommendation for Statical Loading Test of Load-Bearing Concrete Structures In Situ (TBS2)”, RILEM Technical Recommendations for the Testing and Use of Construction Materials, E & FN Spon, London, England, pp. 379-385.

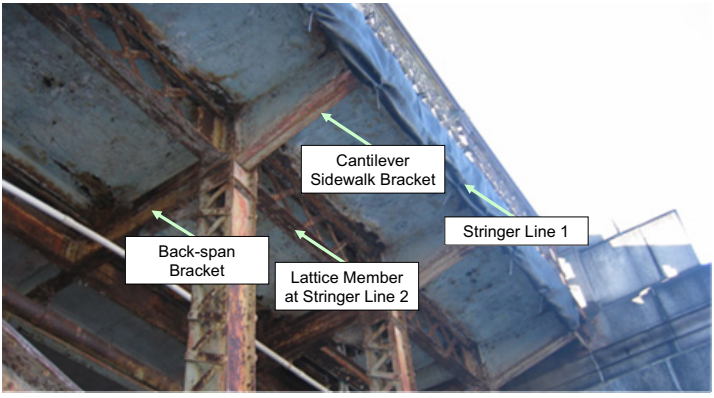

Figure 1 – Extensive corrosion at the downstream side of the bridge

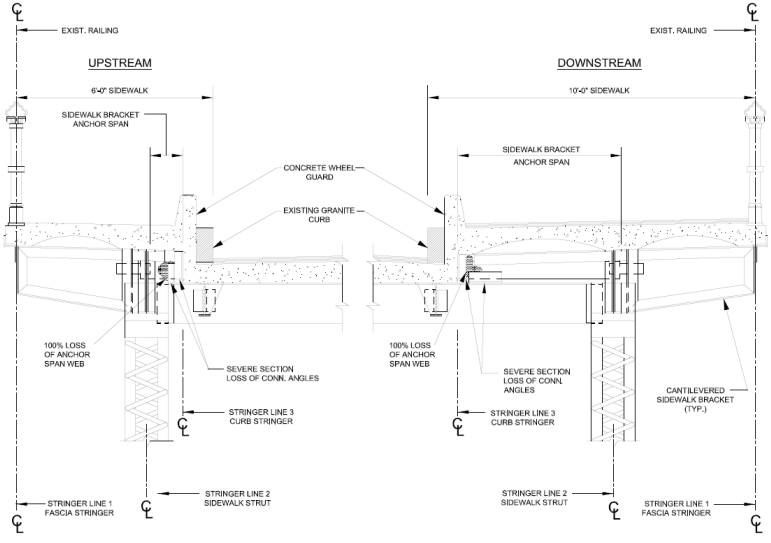

Figure 2 - Bridge cross-section

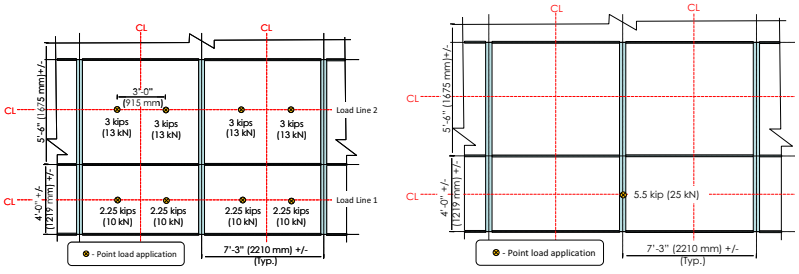

Figure 3 - Load Configuration for Downstream Load Tests

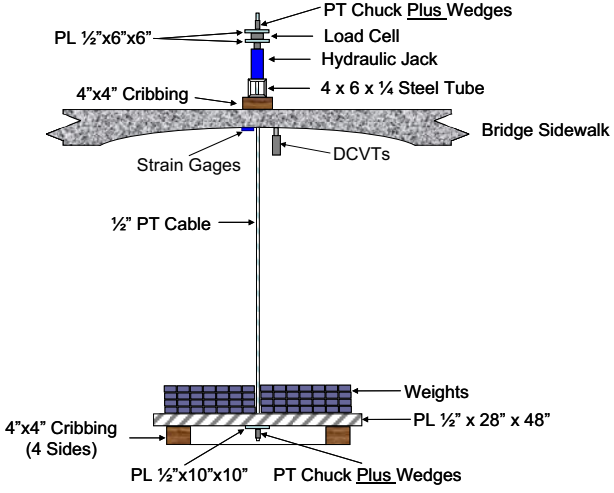

Figure 4 - Schematic of the Load Test

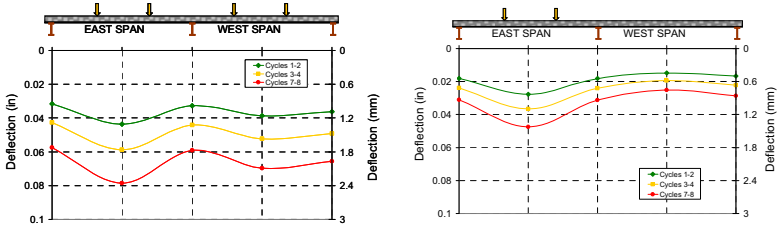

a) Negative Moment b) Positive Moment

Figure 5 - Downstream Test: Deflection along Line 1

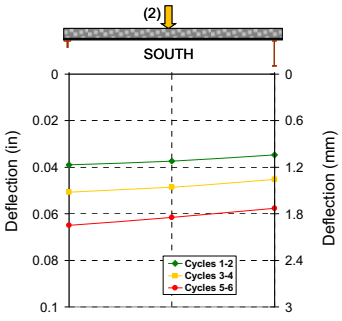

a) Negative Moment

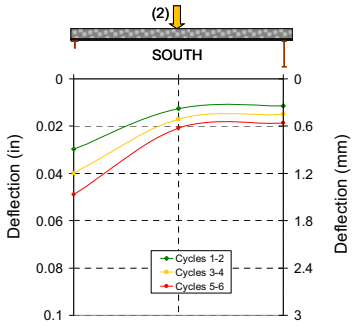

b) Positive Moment

Figure 6 - Downstream Test: Deflection along Line A

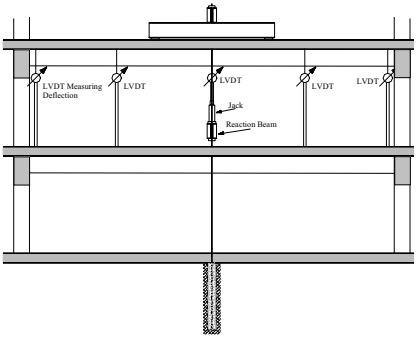

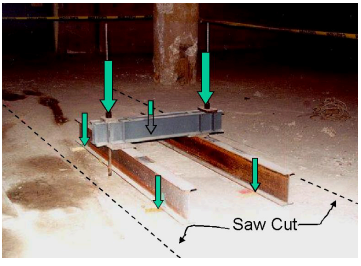

Figure 7 - Diagnostic Load Test Setup

Figure 8 - Cracks in the negative moment region

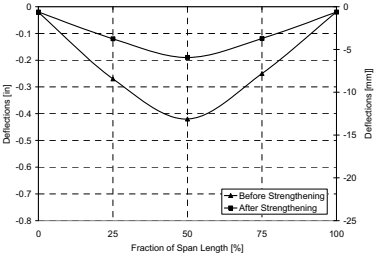

Note: P = 19.6 kip (87 kN) before strengthening, P = 14.7 kip (65 kN) after strengthening

Figure 9 - Effect of strengthening on joist profile (Test 1 & 2)

A Method to Assess Peak Storm Wind Speeds Using Detailed Damage Surveys

Gregory A. Kopp (M. ASCE)[1], Murray J. Morrison, Bahareh Kordi, and Craig Miller

Boundary Layer Wind Tunnel Laboratory, University of Western Ontario,
London, ON, N6A 5B9, Canada.
[1]Email. gakopp@uwo.ca

ABSTRACT

A detailed damage survey of a single, wood-framed, structure, which had a complete roof failure during the passage of a gust front in southern Ontario, was performed. Radar data was used to estimate upper level wind speeds associated with the gust front. Details pertaining to the structural failure, including the debris field, were obtained. Wind tunnel pressure time histories, in a simulated atmospheric boundary layer, were used to establish the roof height, gust wind speed at failure. This speed was smaller than the upper level speed found from the analysis of the radar. The flight of the roof was also examined, and confirmed the wind speeds obtained from the analysis of the failure. The study illustrates that detailed damage surveys, which incorporate the use of wind tunnel test data and debris flight in the analysis, can shed considerable light on the details of the wind speeds at failure, reducing the uncertainty caused by the many assumptions in such analyses.

INTRODUCTION

The paper focuses on the results from a detailed damage survey from the passage of a gust front in southern Ontario in June 2008. It is now common to conduct damage surveys following large storms (such as hurricanes and large tornadic events) to capture overall damage and repetitive patterns of failure. The results of such studies are important to solving problems caused by severe wind storms. It is also important to have knowledge of the wind speeds which caused such damage in order to assess design practice, construction methods and building codes. These speeds are rarely available at the surface, where the structures are and where the damage occurs. The current study is focussed around the question of determining wind speed from damage, and takes the approach of finding detailed case studies which can illuminate the issues around this, such as, for example, the bounds of the peak gust speeds and the duration of such peaks. In particular, the current study focuses on using both (structural) failure observations and subsequent flight of the debris to infer both upper and lower bounds on the wind speeds, rather than just the lower bounds associated with the failure observation. In order to accomplish this, other tools are required, and in the current study, both scale model wind tunnel experiments and numerical analysis of debris flight are utilized.

One issue, where there is currently little information, is the role of unsteadiness and gust duration during downbursts, microbursts and gust fronts. Wind-induced pressures in boundary layer (or hurricane) winds typically have short duration peaks, but little is known about these for thunderstorm (downburst) winds. For boundary layers, peak pressures are of shorter duration for higher wind speeds and are typically less than a few seconds (and often less than a second) for damaging winds in

hurricanes. However, downbursts appear to have steadily increasing speeds over a longer time frame, on the order of tens of seconds to minutes, so it is not clear whether different aerodynamic phenomena and gust structures are involved with the peak pressures and failures.

One method to infer wind speed from damage has been to use pressure coefficients in the wind provisions of the ASCE 7. To do this is a significant assumption, particularly if the damage is to smaller wood-frame structures such as houses. The reason for this is that the MWFRS coefficients were developed to envelope wind tunnel data and were obtained for buildings generally of much larger size than typical houses, for example. Surrounding structures also alter the loads in less than straightforward ways. To address this, we have analyzed detailed wind tunnel pressure data for the failed building, considering local terrain and surrounding details. Obviously, this cannot be done for each structure in a large storm, but for particular case studies, we believe it is beneficial. One of the objectives of the current work is to describe such a methodology. In conjunction with detailed aerodynamic data, the structural response is also crucial. It is well known that the fluctuating pressures on a structure have substantial gradients over the surfaces and this has a profound effect of the performance of the structure and the failure mode, particularly for massively statically-indeterminant structures like wood-frame houses with relatively small spacings between trusses (compared to the metal frame buildings used in the development of the ASCE 7). Recent, laboratory-based, full-scale tests to failure at the '3 Little Pigs' Project at UWO illustrate the importance of these mechanisms, mechanisms which cannot be inferred via analyses based on static, code coefficients.

An additional source of information about gust speeds at failure is in the debris field. Fujita and Wakimoto (1981) used this method effectively, as have other researchers. Flight trajectories of debris depend on when the element failed during the gust, the magnitudes of the pressures during the particular gust, and local aerodynamics after the element has failed. Given the non-stationary and gust duration effects of the wind in downbursts, one might expect different behaviour for debris flight in downbursts, when compared with hurricanes. This point is also addressed in the current study, through the use of wind tunnel pressure data to define the initial speeds and accelerations of the failed roof and the numerical models, assuming quasi-steady theory (amongst other factors), to determine the average gust speed during the flight. Recent work on the role of initial conditions on debris flight by the authors illustrates that these effects are crucial for relatively small debris elements like shingles and tiles. In the current work, the effects on a large debris element, i.e., an entire roof, are examined.

Thus, the goal of the current work is to develop a methodology to examine failure wind speeds for structures using as much information as possible, including wind tunnel studies and analysis of debris flight. Results obtained by applying this approach, for the single case study of a gust front at Tupperville, Ontario, are presented.

STORM DETAILS AND RADAR DATA

Doppler weather radar data was obtained from the National Climatic Data Centre (NCDC) for the National Weather Service (NWS) WSR-88D radar station KDTX

located just to the north-west of Detroit, Michigan. This station is located approximately 100 km to the immediate west of Tupperville, Ontario, and provides coverage of much of south-western Ontario on the Canadian side of the border, in addition to the area covered on the US side. Both base Level II radar data and processed Level III data products for the period 8-9 June, 2008 were obtained from the NCDC for this station. At this stage we have not considered the base Level II data in detail, and instead focus on the use of the Level III base velocity measured at the lowest elevation angle of the radar to corroborate the inferred surface wind speeds from other sources. An examination of the radar data suggests that in the vicinity of Tupperville, the front of the storm was moving eastwards with a forward speed of around 27-32 m/s. Although the radar only measures the wind speed component directed along the radar beam, given the location of Tupperville, relative to the radar station (due east, and the motion of the storm at this point (due east also), it would seem reasonable to infer that the true wind speeds are likely to be fairly close to the measured base velocities in this sector.

In a conventional boundary layer these wind speeds would then place an upper limit on the corresponding likely surface gust wind speeds. In this case, however, we are dealing with a gust front in which the maximum wind speeds nearer the surface are likely to be higher than the upper level wind speeds, which, given the elevation angle of the radar beam and the distance between the radar station and Tupperville, corresponds to a height of around 550 m above ground. Unfortunately at this point in time it has not proven possible to quantify exactly what the likely increase in surface wind speeds should be. The damage on the ground is assessed in the remainder of the paper to estimate these speeds at heights of less than 10m.

DAMAGE SURVEY

Following the storm, a damage investigation was under taken by the authors, in partnership with Environment Canada (EC). The majority of the observed damage was due to trees being uprooted and broken branches, with these sometimes causing secondary damage to adjacent structures. The single exception was a commercial storage building which had its roof completely removed during the storm. The North and East walls had collapsed outwards, while the South and West walls remained partially standing. The plan dimensions of the building were 24.35 m by 15.24 m, with an eaves height of 4.88 m and a roof slope of 4 on 12 ($\varphi = 18°$). Two large 4.57 m roller doors were located on the North side of the building, these doors were found closed and in their tracks. The roof was found to the North East of the structure and appeared to have landed upside down, the furthest piece of debris was found 84 m from the East side of the building. Figure 1(a) shows the debris field looking back towards the structure (facing West), and also shows the upstream fetch for the estimated wind direction at the time of the investigation, which is a typical open country terrain. A layout of the building debris field along the cardinal directions at the building site is shown in Figure 1(b), the south gable end wall was found closest to the building (location A), while the North gable was found further away (location B) which is consistent with the observation that the roof landed upside down. The narrow debris swath from the building indicates that the damage is due to straight line

and not tornadic winds. This is supported by meteorological data which confirms that there was no sign of tornadic activity in the region during this storm event.

Examination of the roof debris revealed that the roof truss spacing was 1.22 m on center, with batons at 0.61m centers. Trusses were held down with 2-3 toe-nail connections using 10d twisted shank nails.

Thus, from the observations of the debris field, the roof, and the walls, it appears that the failure was of the complete roof (in more-or-less one piece) by overturning about the east wall. From the observations of the walls, in appears highly unlikely that internal pressures played any part in the global roof failure. Following this damage investigation and based on the structural failure discussed above Environment Canada rated this storm to have been a gust front with F1 damage (Note that Canada still uses the F-scale, not the revised EF-scale.)

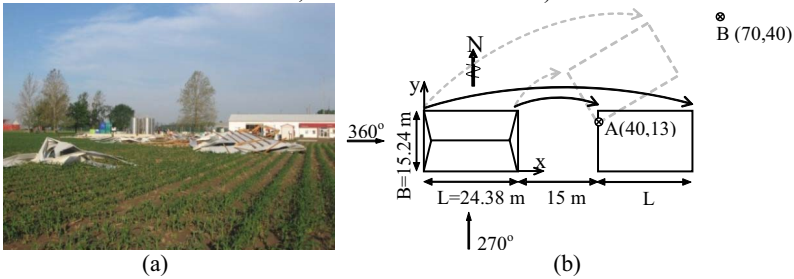

(a) (b)

Figure 1. (a) Picture of the debris field looking west towards the building. (b) Building plan dimensions and debris field location

INTEGRATED PRESSURE ANALYSIS

The current analysis concentrates on the failure of the roof and estimates the wind speed required to produce the observed damage. In addition, effort was placed on putting bounds on the gust wind speed at the time of failure. In order to estimate the wind speed from a wind tunnel pressure test, several assumptions and simplifications are required. The influence area for each structural connection (i.e., toe-nail) is assumed to be equal to its geometric tributary area. The ultimate capacity of toe-nail connections can vary substantially, depending on the type of wood and moisture content, the angle and location of the nail, in addition to other factors such as age and deterioration. The capacity of the toe-nails are assumed to be equal to be 1850 N/connection from Visscher et al. (2007) with a variation of 20%. This value seems reasonable when compared with measured capacities found by other researchers (Robinett 2002, Cheng 2004). The assumed value for the weight of the roof is 88N/m^2, within about ± 15%.

The fact that the roof landed upside down indicates that the roof likely failed by overturning of the entire roof about the leeward (East) wall, as discussed above. Perhaps the most significant assumption of this analysis is that pressure coefficients obtained for traditional boundary layer winds are similar to those generated under thunderstorm winds. There is some indication in the literature that this may not be the case (Chay and Letchford 2002), although such a conclusion also involves significant assumptions. The current work cannot address this question, and, in any

case, detailed data are not really possible to obtain for buildings of this size with currently available downburst wind tunnels.

In order to estimate the failure wind speeds, pressure data were selected from the NIST aerodynamic database (Ho et al. 2005) for a building which closely matched the dimensions of the damaged building. The model building selected has full scale plan dimensions of 24.38 m x 38.1 m an eaves height of 4.88 m at the tested length scale of 1:100 and a roof slope of 3 on 12 (θ = 14°). The aspect ratio of the model building to the damaged building is nearly identical. In order to match the full scale dimensions, the length scale of the wind tunnel model was reinterpreted using a value of 1:64. However, it is worth noting that the gable slope did not match perfectly. Additional details on the NIST aerodynamic database can be found in Ho et al. (2005), while discussion of scale mismatches can be found in St. Pierre et al. (2005). Since the wind direction at failure is not known precisely, the analysis was conducted for wind angles ranging from 315° to 360° which are believed to be the bounding wind angles from the field investigation. (Note that these wind angles are defined in Figure 1(b), and that 360° is due east.)

The individual reaction forces at the connections (R^n), the overall roof uplift force (Fv), and the overturning moment about the leeward wall (East Wall) (M_x) can be calculated from;

$$R(t)^n = qCr^n(t); \quad Fv(t) = qCf(t); \quad M_x(t) = qCm_x(t) \tag{1}$$

where q is the dynamic pressure and $Cr^n(t)Cr$, $Cf(t)$, and $(Cm_x(t))$ are force and moment coefficients for the individual connection(s), overall roof uplift and overturning moment, respectively. These coefficient time series are calculated from the wind tunnel pressure coefficient (Cp) time series and have an overall length of approximately 1 hour at full scale (assuming normal boundary layer scaling). If the connections are assumed to be brittle and fail instantaneously once the force has exceeded the hold down (HD) resistance ($R^n_{HD}, Fv_{HD}, M_{xHD}$), the hourly mean failure velocities at roof height can be obtained from;

$$V^{R^n}_{H,3600s,O.C.} = \sqrt{\frac{2}{\rho}\frac{R^n_{HD}}{\check{C}r^n}}; \quad V^{Fv}_{H,3600s,O.C.} = \sqrt{\frac{2}{\rho}\frac{Fv_{HD}}{\check{C}f}}; \quad V^{M_x}_{H,3600s,O.C.} = \sqrt{\frac{2}{\rho}\frac{M_{xHD}}{\check{C}m_x}}; \tag{2}$$

By assuming quasi-steady theory, the gust wind speed $V^{M_x}_{H,gust,O.C.}$ can be determined from,

$$V^{M_x}_{H,gust,O.C.} = \sqrt{\frac{\check{C}m_x}{\bar{C}m_x}}V^{M_x}_{H,3600s,O.C.} \tag{3}$$

where $\bar{C}m_x$ is the mean moment coefficient. Similarly $V^{R^n}_{H,gust,O.C.}$ and $V^{Fv}_{H,gust,O.C.}$ can be determined through the same procedure.

In addition, to facilitate comparison to the ASCE7-05, the hourly roof height wind speeds are also converted into ASCE7-05 3s gust wind speeds following the procedure outlined in St. Pierre et al. (2005) where, again a typical boundary layer wind profile is assumed. From the profile data presented by Holmes et al. (2008) it appears likely that such an approach may overestimate the wind speed at 10m.

Following this analysis, the gust wind speed ($V^{M_x}_{H,gust,O.C.}$) required to fail the roof in overturning about the leeward wall was 39.5 m/s for a wind angle of 360°. This would assume that the roof is completely rigid and there was "perfect" load sharing between the structural connections (i.e. toe-nails). In contrast, if it is assumed that

there is no load sharing between structural elements, the first individual toe-nail connection would fail at a wind speed of 22.3 m/s for the same wind direction. In reality the true structural stiffness will lie somewhere between these two cases, but ultimately the current results indicate that individual connections would fail before the roof would fail in overturning about the eastern wall. However, the debris field indicates that the entire roof was removed from the structure as a single piece. This suggests that there may have been a sequential failure of the connections prior to the flight of the roof.

To evaluate this hypothesis further, a sequential connection failure analysis was conducted. The results for a wind angle of 360° are shown in Figure 3. The horizontal axis represents the sequence of failed connections i.e., 0 meaning no connections have failed, 1 meaning a single connection has failed, and so on. Once a connection has failed its load is redistributed to adjacent connections but because of the high spatial variation of the wind these connections may require a higher wind speed to fail. For example in Figure 3 once the wind speed has passed 22.3 m/s the connections corresponding to steps 0-8 would have failed; however, to continue the failure (step 9) a higher wind speed would be required. In contrast, the overturning moment remains constant while the hold down force has diminished, reducing the wind speed required to overturn the entire roof at each failure step. Ultimately the wind speed required to overturn the entire roof becomes less than the wind speed required to fail the next connection, and the estimate for the failure wind speed for this wind angle is found. Based on the estimated values for the weight and hold down forces, the calculated failure gust wind speeds ranged from 23.3 (335°) to 25.1 (350°) m/s at roof height depending on wind angle. This is equivalent to a 3 second gust speed at 10m (i.e., equivalent to the wind speed provided in the ASCE7-05) of 27.3 to 30.4 m/s. Increasing and decreasing the building weight and toe-nail strength, as described above, causes these estimates to vary by approximately ±2 m/s.

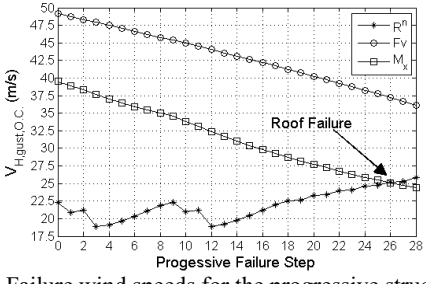

Figure 2. Failure wind speeds for the progressive structural failure

The ultimate failure velocities found using this method provide an estimate of the lower bound of the peak velocity for this storm. The actual peak velocity for this storm could have been much higher, but in order to place an upper bound on the wind speed, other indicators would have to be used such as analysis of nearby structures that have not failed or debris flight analysis, which will be discussed in more detail below. We do note, however, that there were no other failures in Tupperville.

DEBRIS FLIGHT ANALYSIS

As discussed above, since we know the origin of the debris and its landing location, we may be able to estimate the failure wind speed based on the flight trajectory.

There are several challenges with estimating gust wind speeds from debris field observations. First of all, the wind speeds are modified substantially by the presence of the structure. For small elements, like roof shingles, the failure and subsequent flight depends intimately on the local flow field above the roof and in the wake downstream of the structure, as well as the gust duration and the details of the debris element. For large elements, like a complete roof, this is also true, although the modification of the flow field is less likely to be important, while the gust duration is more important due to the relatively slow accelerations of larger, heavier objects. The second challenge is that the wind velocity changes continuously during gust fronts and downbursts, typically starting from lower velocities, increasing to a maximum, and then decreasing (as shown by Holmes and Hangan, 2008). On top of this, there is superimposed turbulence. Based on when the actual failure happens, how long the failed element takes to accelerate, and the speed the element can travel at, the wind velocity at failure may be substantially different from the wind speed while the element flies. Finally, the failure may not lead to a clean breakaway from the structure so that parts of the failed element hang on a little longer, perhaps lowering the initial accelerations or causing the shape of the element to change, altering the aerodynamic coefficients.

Assuming a clean break from the walls, the flight of a complete roof might be amenable to a relatively simple method, like that of Tachikawa (1983). In the present work, our intention is to compare the range of possible flight speeds with the wind speeds obtained from the failure analysis using the pressure data.

In the current work, two methods were used to predict the wind speed during failure and the subsequent flight, both based around the work of Tachikawa. In the first case, very simple initial conditions were used under the assumption that the plate aerodynamics hold from the moment of failure; the other links to the pressure integration to provide more accurate initial conditions and to transition from the building aerodynamics to the plate flight aerodynamics. Details are given below.

Flight analysis assuming uniform, smooth flow

The same numerical approach as first presented by Tachikawa (1983), and recently extended by Kordi and Kopp (2009a), is applied first. A flat plate with an initial angle of attack is released into the uniform horizontal wind flow and Newton's 2nd law is applied to predict the motion. As proposed by Tachikawa, the forces applied on the element are divided into static and rotational components; thus, by applying the quasi-steady theory, the two-dimensional equations are solved and the flight trajectory is obtained. For the numerical calculations of the roof flight, some additional assumptions are required:

(i) Since the force and moment coefficients for any kind of roof with different angles of attack are not available, the roof is considered as a thin flat plate with the aspect ratio, $AR=L/B$, of 0.5. (ii) The plate travelled towards the east in a two-dimensional domain. The assumed landing location is shown in Figure 1(b) by the solid rectangle.

(iii) The rotational force and moment coefficients are assumed to be negligibly small since the roof landed relatively close to the house. (iv) The overturning moment is calculated about the eastern wall unless the roof has elevated enough so that it will be able to rotate freely about its center of mass. (v) When the axis of rotation changes from the eastern edge to the center of mass, the rotational velocity over the eastern edge is assumed to be translated to the center of mass, with an additional translational velocity normal to the plate. The horizontal, u, and vertical, v, velocity components of the additional translational velocity can be calculated as follows;

$$\mathrm{v} = \frac{\omega L}{2}\cos(\theta) \qquad u = \frac{\omega L}{2}\sin(\theta) \tag{5}$$

Based on these assumptions, the equations of motion are written as

$$m\frac{d^2x}{dt^2} = (\frac{A\cdot\rho_{air}}{2}).(C_{DS}\cos\beta - C_{LS}\sin\beta)\,V_{rel}^2 \tag{6}$$

$$m\frac{d^2z}{dt^2} = (\frac{A\cdot\rho_{air}}{2}).(C_{DS}\sin\beta + C_{LS}\cos\beta)\,V_{rel}^2 - mg \tag{7}$$

Rotation about the east wall: $$I_o\frac{d^2\theta}{dt^2} = \left(\frac{A\cdot L\cdot\rho_{air}}{2}\right)\left(C_{NS}.\frac{c+0.5L}{L}\right)V_{rel}^2 - mg\frac{L}{2}\cos\theta \tag{8a}$$

Rotation about the center of mass: $$I\frac{d^2\theta}{dt^2} = \left(\frac{A\cdot L\cdot\rho_{air}}{2}\right)\left(C_{NS}.\frac{c}{L}\right)V_{rel}^2 \tag{8b}$$

where A is the area of plate, I and I_o are the moment of inertia of the plate about the centerline and the edge, respectively, g is the gravitational acceleration, ρ_{air} is the air density, V_{rel} is the relative wind velocity, β is the angle of attack of the relative wind velocity with respect to the horizontal, and x, z, and θ are the horizontal, vertical, and rotational displacement of the plate, respectively. C_{DS}, C_{LS}, and C_{NS} are the static drag, lift, and normal force coefficients acting on the plate and c is the distance of the centre of pressure to the centre of the plate.

Using published static force and moment coefficients, Eqs. (6) - (8) can be solved for any wind velocity. Based on the field observations, it seems more probable that the eastern edge of the roof had first landed on the ground. Having this condition in mind, horizontal wind gust velocities for a flat plate with m=3365Kg, L=24.4m, B=15.2m, and different initial angles of rotation varying from 2^o to 40^o was found to be in the range of 19-22 m/s. The duration of flight was about 3 to 5.5 seconds. Figure 3(a) shows the flight trajectory for the plate with θ_0=10^o. It should be noted that the first point of impact for these cases is about 34m, and not 40m as observed in the field. This seems physically reasonable since the roof may have slide on the ground for several meters after impact.

Flight analysis using the pressure data for the initial condition

Based on the failure analysis, the type of failure is recognised to be an overturning moment about the east wall. Using the time series of M_x and F_v for five distinct peaks, and integrating the aerodynamic moment and uplift over time, the angular and vertical velocities and displacements at the time of release were estimated. Since it is unknown for how long the aerodynamics of the building governs the flight before asymptoting into the aerodynamic coefficients for the free, thin plate, three different points of transition were considered, specifically, θ equal to 2^o, 10^o, and 20^o. The

calculated failure wind speed from the integrated pressure analysis, $V_{H,gust,O.C}^{M_x}$, is about 24 m/s. Assuming that the failure wind velocity remains constant during the course of failure and flight, the angular and vertical velocities and displacements of the three transition points can be used as the initial values to calculate the flight trajectory for each case by solving Eqs. (6) - (8) and making the same assumptions as before, namely the smooth uniform flow and using the flat plate coefficients. Figure 3(b) shows the results for the second transition point at θ=10°.

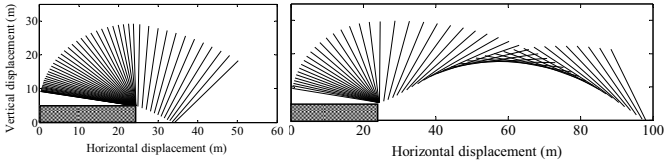

(a) (b)

Figure 3. Numerical calculation of the flight trajectory of the plate with m=3365Kg, L=24.4m, B=15.2m, and θ_0=10° in a wind gust speed of (a) 20.4 m/s and (b) 24 m/s, where the initial condition from the pressure data was applied.

From the above calculations several observations can be made:

(i) The impact location of the farthest tip point of the plate for the three transition points are 85m, 98m, and 125m, respectively. Thus, the actual flight most likely occurred in a lower wind velocity than this failure velocity, otherwise, the roof would have flown much farther than actually observed. Since the flight duration is about 3-5 seconds it is possible that the flight occurred in a wind velocity lower than the failure wind speed if the failure occurred near the peak storm wind speed.

(ii) Based on these calculations, it appears that the average wind speed during flight of the roof was in the range of 19-23 m/s. For it to have been higher, would require that the failure did not occur 'cleanly' and/or that the roof was significantly deformed so that either the net lifting area of the roof or aerodynamic coefficients differed substantially from the assumed values. For example, if the force coefficients decrease by 20% or the area decreases by 1/3, the required wind velocity increases by about 2 m/s. Thus, we conclude that the flight of the roof occurred in an average wind speed within the range of 19-25 m/s.

CONCLUSIONS

Wind speeds associated a gust front which passed through Tupperville, Ontario on the evening of June 8, 2008 were examined in detail from radar data and analyses of the global roof failure of a medium sized wood-framed, metal clad building. The radar data indicated an upper level wind speed of 27-32 m/s. Integration of wind tunnel pressure data indicated a range of failure wind speeds of 22-25m/s for a flexible roof and 39m/s if the roof were assumed to be rigid. Analysis of the debris field of the roof indicated that roof height (gust) speeds were likely less than 25 m/s (55 mph).

It is not clear from this data how to relate the roof height wind speeds to the standard 10m height. If one makes standard boundary layer approximations, which are not likely to be completely valid for a gust front, it is evident that this structure

failed at below the design wind speeds. Roof flexibility means that individual roof-to-wall connections see higher loads and failure occurs at much lower wind speeds as a consequence. For the structure under examination, the truss spacing of 1.2m coupled with very flexible metal cladding allowed the toe-nails to see higher loads than if the roof had been made much stiffer in the lateral direction.

The paper has illustrated that it may be possible to obtain reasonable estimates of failure wind speeds using detailed damage surveys of both structural failures and the debris field, coupling this with analysis of wind tunnel aerodynamic data and numerical analysis of debris flight. Given that thunderstorm winds cause the bulk of the wind damage across North America, outside of the hurricane regions, and that there is little information about the wind speeds, wind profiles and time scales of these events, we propose that detailed damage surveys be more commonly used as a tool to build a database of information regarding such storms. In addition, it is clear that the assumptions that have been developed in wind engineering for dealing with more stationary winds, such as hurricanes or large synoptic storms, are inadequate and that a great deal more information about the profiles and gust structure are required so that a framework for unsteady processes can be developed.

REFERENCES

Chay, M. T., and Letchford, C. W. (2002). "Pressure distributions on a cube in a simulated thunderstorm downburst—Part A: stationary downburst observations." *Journal of Wind Engineering and Industrial Aerodynamics,* 90(7), 711-732.

Cheng J. (2004). “Testing and analysis of the toe-nailed connection in the residential roof-to-wall system.” *Forest Products Journal*, 54(4), 58-65.

Fujita, T.T. and Wakimoto, R.M. (1981). “Five scales of airflow associated with a series of downbursts on 16 July 1980.” *Monthly Weather Review*, 109, 1438-1456.

Ho, T. C. E., Surry, D., Morrish, D., and Kopp, G. A. (2005). “The UWO contribution to the NIST aerodynamic database for wind loads on low buildings: Part 1.” *J. Wind Eng. Ind. Aerodyn.,* 93(1), 1-30.

Holmes, J.D., Hangan, H., Schroeder, J.L., Letchford, C.W., and Orwig, K.D. (2008) “A forensic study of the Lubock-Reese downdraft.” *Wind Struct.*, 11(2), 137-152.

Kordi, B., and Kopp, G.A. (2009a). “Evaluation of the quasi-steady theory applied to windborne flat plates in uniform flow.” *ASCE J. Eng. Mech.*, 135(7), 657-668.

NRCC (National Research Council Canada). (2005). “National Building Code of Canada (2005)” National Research Council Canada, Ottawa, Canada.

Robinett, D. S. (2002). "Assessment of retrofits for high wind resistance." Clemson University, Thesis Dissertation.

St. Pierre, L. M., Kopp, G. A., Surry, D., and Ho, T. C. E. (2005). "The UWO contribution to the NIST aerodynamic database for wind loads on low buildings: Part 2." *J. Wind Eng. Ind. Aerodyn.,* 93(1), 31-59.

Structural Engineering Institute. (2006). *Minimum design loads for buildings and other structures.* American Society of Civil Engineers, Reston, Va.

Tachikawa, M. (1983). “Trajectories of flat plates in uniform flow with application to wind-generated missiles.” *J. Wind Eng. Ind. Aerodyn.* 14, 443–453.

Visscher, B. T., and Kopp, G. A. (2007). "Trajectories of roof sheathing panels under high winds." *J. Wind Eng. Ind. Aerodyn.,* 95(8), 697-713.

WIND GUST PHENOMENA ON AN INDUSTRIAL FACILITY DURING HURRICANE GUSTAV

Rolando E. Vega[1], Ph.D., P.E., Member ASCE, Ph.D. Wind Engineering;
Ben F. Harrison[2], P.E., Member ASCE, M.S. Civil Engineering

[1]ABS Consulting Inc., 14607 San Pedro, Suite 215, (210) 495-5195,
rovega@absconsulting.com
[2]ABS Consulting Inc., 14607 San Pedro, Suite 215, (210) 495-5195,
bharrison@absconsulting.com

ABSTRACT

An industrial facility near Baton Rouge, LA experienced significant damage from Hurricane Gustav. Observed damage patterns indicated that a localized gust resulted in damage to sections of the facility that were disproportionately higher than to the remainder of the facility. One of the wind speed data sources available was a local meteorological tower which measured an equivalent 3-second wind gust of 70 miles per hour (mph at 10 meters). The National Oceanic Atmospheric Administration (NOAA) – Hurricane Research Division experimental product H*WIND estimated a 3-second gust of 62 mph for the site. However, after a careful examination of all the data sources and structural analysis, it was estimated that the probable peak wind speed experienced in a section of the facility was at least 80 miles per hour. The latter implies that the damage observed at the facility was produced by a gust factor that was on the order of 15% larger than the average gust estimated for non-hurricane regions.

KEYWORDS: forensic, gust, meteorological, turbulence, wind

INTRODUCTION

This paper presents the findings of the wind damage forensic investigation conducted by ABS Consulting at an industrial facility following Hurricane Gustav. The content of this paper has been reviewed by and is disclosed with authorization by the facility owner. First, structural damage indicators are presented and evaluated to aide in the determination of the probable wind speed experienced by the facility. This is followed by a presentation of the hurricane wind data near the facility and a brief discussion of the methodology utilized to correct the wind speed data to a reference height, exposure and averaging time.

DAMAGE INDICATORS

The ABS Consulting team surveyed the damage to an industrial facility after Hurricane Gustav. The field investigation identified eight wind speed damage indicators for evaluation. Wind speed damage indicators are objects damaged by extreme wind speeds that may either be analyzed to estimate the wind speed which occurred or used to assess the relative wind speed for similar objects at different locations. Wind speed indicators were utilized by the team to assess whether a localized gust wind speed was experienced at the facility which exceeded expected values during Hurricane Gustav and to confirm wind speed estimates obtained from structural analysis. The wind speed damage indicators identified in Figure 1 and shown in Figure 2 are:

(1) Stripped trees and dislocation of foliage farther upwind
(2) Siding damage near flow separation points along periphery of a structure
(3) Siding panel detachment on a major building
(4) Considerable roof damage to wooden canopy
(5) Tilting of signage posts along gust wind direction
(6) Dislocation of garage door from railing system along gust wind direction
(7) More stripped trees downwind
(8) No other damage indicators in the rest of the facility, including in the vicinity of the local meteorological tower

Having inspected areas inside and outside the path of damage including the vicinity of the local meteorological tower, identified in Figure 1, it is evident that the facility experienced a gust phenomenon during Hurricane Gustav. The wind speed damage indicators in Figure 2 show that a portion of the site was most probably subjected to higher gust wind speeds than measured by the local meteorological tower. All damage indicators indicated a consistent wind direction for the gust thus discarding the possibility of a tornado.

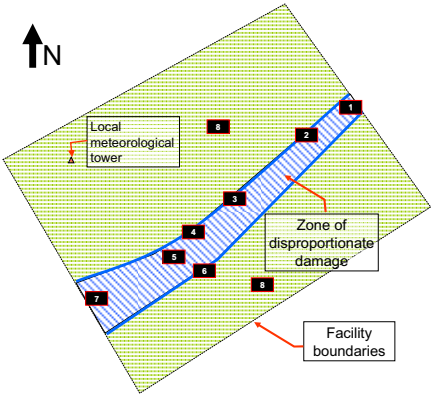

Figure 1: Path of wind damage indicators

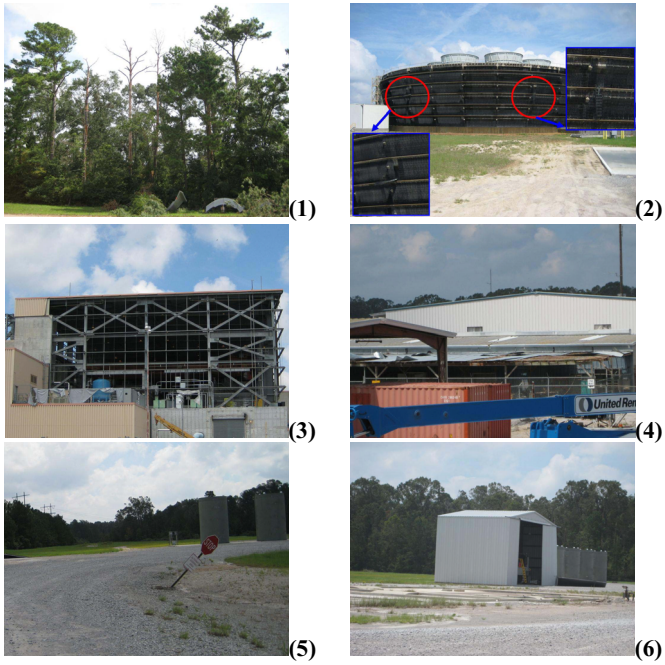

Figure 2: Some wind damage indicators observed at the facility

MEAN WIND SPEED PROFILE

Strictly speaking, the models available to date to extrapolate mean wind speed and turbulence intensities to different heights were developed for straight line winds. Nevertheless the widely available velocity profiles are used for all type of winds including: straight line, hurricanes and thunderstorm winds assuming a near-neutral atmospheric stability under extreme wind conditions.

The atmospheric boundary layer of interest to the investigation was the surface boundary layer (SBL) which extends to approximately 10% of the full atmospheric boundary layer (Panofsky and Dutton, 1983). The mean velocity profile in the SBL may be modeled in a number of ways but can be principally determined by the surface roughness. Ground friction is responsible for the change in wind velocity with height. This is believed to be particularly true for strong neutrally stable winds (i.e. wind speeds > 8m/s); while for low and moderate wind speeds, the velocity profile is a product of mechanical and thermal mixing. There are three widely accepted models to describe the average velocity profile in the SBL; power law, logarithmic law and an empirical quasi-logarithmic function (Deaves and Harris, 1978).

The logarithmic law was used to adjust mean wind speeds as a function of height above ground level, z, as shown by Equation 1. The surface roughness, z_0, is

characterized by the upwind terrain exposure on which Wieringa (Wieringa, 1993) gives a comprehensive evaluation for different terrain classifications. Since the necessary meteorological measurements for a direct quantification of the roughness length were not available to the investigation team, the latter literature and experience was used to make the necessary corrections based upon site inspection of terrain exposure. The von Karman constant (k) is approximately equal to 0.40. When the average surface roughness, height above ground level and wind speed are quantified or measured, the friction velocity (u_*) in that exposure can be estimated. Prior to using the logarithmic law to estimate mean wind speed at other heights, the friction velocity is adjusted for the appropriate exposure, as described in the following section. However, a simple height correction factor for mean wind speeds in a constant exposure was utilized irrespective of the friction velocity and von Karman value, as given by the ratio of wind speeds at the two heights using Equation 1.

$$U(z) = \frac{u_*}{k} \cdot \ln\left(\frac{z}{z_0}\right) \tag{1}$$

Upwind Exposure Considerations

Values of surface roughness were determined from visual inspection and referencing values readily available in literature (Wieringa, 1993). Once the surface roughness was determined for the site an exposure correction factor was estimated. Three basic methods to correct wind speeds for exposure were considered during the investigation. These basic methods include:

1. Wieringa's 60 meter blending height concept (Wieringa, 1976), see Equation 2
2. Bietry's friction velocity correction (Simiu and Miyata, 2006), see Equation 3
3. Simplified Deaves and Harris friction velocity correction (Tieleman, 2008), see Equation 4

Figure 3 and Figure 4 show a simple comparison of the methods for a constant 10 meter height when the correction is applied from a reference open terrain with z_0=0.02m to other common exposures (Figure 3) and from various common exposures to the same reference open terrain (Figure 4). Notice that no correction is needed (F=1.0) when the reference and station roughness are the same. Assuming a constant instrument height, comparison of the three methodologies becomes an evaluation of the "blending height" concept as a means to describe a correction of the friction velocity for exposure (i.e. $u_*(z_{0r})/u_*(z_{0s}) = f(z_{0r},z_{0s})$). Since it is recognized in literature (Simiu and Scanlan, 1996) that the Bietry model must be subjected to empirical adjustments for large roughness lengths ($\approx z_0$>0.3m) the pragmatic assumption in this investigation was to accept the simplified Deaves and Harris model as most appropriate.

$$F_{Wieringa} = \frac{U_r}{U_s} = \frac{\ln(60/z_{0s})}{\ln(60/z_{0r})} \cdot \frac{\ln(z_r/z_{0r})}{\ln(z_s/z_{0s})} \tag{2}$$

$$F_{Bietry} = \frac{U_r}{U_s} = \left(\frac{z_{0s}}{z_{0r}}\right)^{0.0706} \cdot \frac{\ln(z_r/z_{0r})}{\ln(z_s/z_{0s})} \quad (3)$$

$$F_{Simplified(D-H)} = \frac{U_r}{U_s} = \frac{\ln(10^5/z_{0s})}{\ln(10^5/z_{0r})} \cdot \frac{\ln(z_r/z_{0r})}{\ln(z_s/z_{0s})} \quad (4)$$

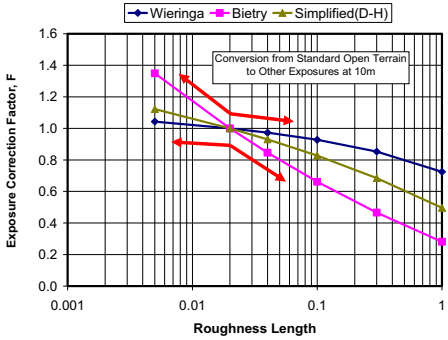

Figure 3: Exposure correction factors to adjust mean wind speeds from a standard open terrain with z_0=0.02m to various common exposures.

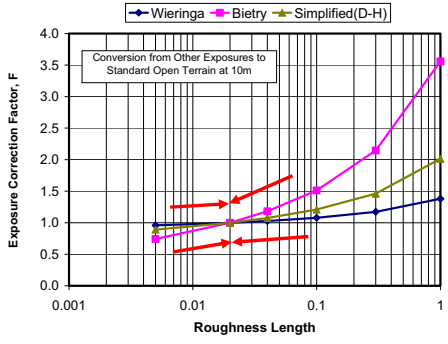

Figure 4: Exposure correction factors to adjust mean wind speeds from various common exposures to a standard open terrain with z_0=0.02m.

Wind Speed Averaging Times

An averaging time is a discrete time used to characterize the wind. Short averaging times, such as 3-second or 5-seconds, are measures that better describe turbulence due to their smaller averaging time. Longer averaging times, such as 10-minutes or 1-hour, correspond to sustained wind speeds and do not give information about the wind turbulence. The different data sources for wind speed and design standards used to design structures of interest at the facility utilized averaging times

that differ from one another and from modern code definitions of wind speed. Therefore, in order to adequately explain the observed damage and determine local wind speeds at the facility, corrections for wind speed averaging times were necessary.

For decades, Durst's (Durst, 1960) studies have been adopted as the standard to correct short averaging time (peak) wind speeds to equivalent hourly sustained winds over flat open terrain for non-hurricane conditions. The Durst curve, as shown in Figure C6-4 of ASCE 7-05 (ASCE 7, 2005), is widely used to convert wind speeds with different averaging times in flat open terrain for all wind types. Krayer and Marshall (Krayer, 1992), however, found that gust factors, resembled in the Durst curve for extratropical storms, are about 10% higher for hurricane conditions. A supplementary curve to the Durst curve is sometimes used for hurricane applications, as illustrated in (ASCE 7, 1995). However, the validity of Krayer and Marshall's finding was later refuted (Vickery, 2000) as not truly representative of hurricanes. Given the insufficiently dense spatial data collection during hurricanes in the past, whether there is a unique averaging time wind speed correction for hurricanes or not remains an open question within the wind engineering community. Therefore, based upon the current standard of practice, the investigation used the original Durst curve.

WIND DATA SOURCES

Several sources of wind data were used for meteorological evaluation during the investigation. Three of the sources were local meteorological towers while a fourth source was based on a composite model developed by NOAA's Hurricane Research Division. In summary, the wind data sources used in the investigation were:

(1) Local meteorological tower near the facility.
(2) National Weather Service – Meteorological Station at Baton Rouge Airport
(3) Texas Tech University – StickNet platform near Baton Rouge, LA
(4) NOAA – Hurricane Research Division (HRD) H*WIND wind field composite

In order to compare measurements of wind speeds coming from different data sources, it has to be assured that values are based upon a common exposure, height and averaging time. The available methodologies for adjusting wind speeds are discussed in the following sections.

Local Meteorological Tower

A 45.7 meter (150 feet) meteorological tower is located near the facility at approximately 1km to the northwest, as shown previously in Figure 1. The meteorological tower collects wind speed and direction measurements at two heights: 10 and 45.7 meters using a 3-cup anemometer and vane. Sparsely populated trees with an approximate mean height of 15 meters near the meteorological tower influence the wind speed measurements at the 10 meter elevation. An upwind roughness length of z_0=0.8 meter was deemed appropriate for the wooded area (i.e. pine forest) under consideration. With such upwind roughness the absolute lowest

acceptable observation height should be at $z \approx 20 \cdot z_0 \approx 16$ meters (Wieringa, 1993) if not more.

The local meteorological tower was assumed to have a flat uniform upwind exposure and the wind data from the 45.7 meter height was used for analysis purposes of this investigation and adjusted for height where necessary. Figure 5 shows the 10 minute average and 10 second instantaneous wind speeds at 45.7 meter level. The 10 minute average and 10 second peak gust at this height were 50.5 mph (22.6 m/s) and 77 mph (34.4 m/s), respectively.

After correcting the tower data for upwind exposure considerations, elevation and averaging time, the equivalent 3 second peak wind speed at 10 meters of 70 mph (31 m/s) was measured at the facility.

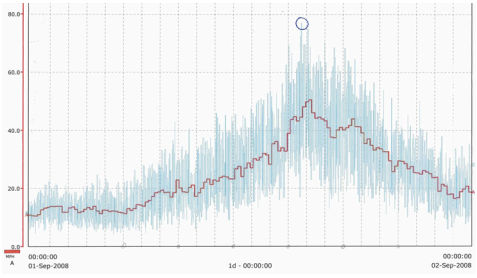

Figure 5: Wind Speed Measured at the Local Meteorological Tower

National Weather Service – Baton Rouge Airport

A network called ASOS (Automated Surface Observing System) is maintained by the National Weather Service. Most of the meteorological stations are located at airports in uniform flat open terrain. The closest ASOS station during Hurricane Gustav is located at the Baton Rouge Airport and the wind speed statistics obtained during the event are shown in Figure 6. The ASOS stations records 2-minute (sustained) and 5-second (peak) averages in knots. After correcting the ASOS data for upwind exposure considerations and averaging time, the equivalent 3-second gust at 10 at the airport was approximately 101 mph (45.2 m/s). Given the location of the building site with respect to the hurricane path this wind speed value should serve as an upper bound to the expected wind speed at the building site.

A. LOWEST SEA LEVEL PRESSURE/MAXIMUM SUSTAINED WINDS AND PEAK GUSTS

METAR OBSERVATIONS...
NOTE: ANEMOMETER HEIGHT IS 10 METERS AND WIND AVERAGING IS 2 MINUTES

LOCATION ID LAT LON DEG DECIMAL	MIN PRES (MB)	DATE/ TIME (UTC)	MAX SUST (KT)	DATE/ TIME (UTC)	PEAK GUST (KT)	DATE/ TIME (UTC)
KBTR-BATON ROUGE AIRPORT 30.54 -91.15	982.1	01/1953	080/053	01/1940	060/079	01/1912

Figure 6: National Weather Service Post-Storm Report for Hurricane Gustav at the Baton Rouge Airport

Texas Tech University – StickNet Meteorological Station

In 2008 Texas Tech University (TTU) deployed a new measurement platform called StickNet. StickNet is a rapidly deployable research quality 2.25 meter height meteorological station that measures the wind environment of hurricanes, thunderstorms and tornadoes. On September 1, 2008 TTU deployed 20 of their 24 StickNet platforms for Hurricane Gustav. One of the stations, Station 0101A, was located approximately 20 miles west southwest relative to the Baton Rouge Airport and towards the path of the storm and measured 10 minute and 3 second averages of 33.7 mph (15.1 m/s) and 62 mph (27.7 m/s), respectively. Towards the east northeast (i.e. direction of strongest winds) the terrain is flat and open with a fetch distance that exceeds half a mile to a line of trees. The influence of these trees was considered minimal, and having a similar exposure to the facility, a roughness length of $z_0 \approx 0.1$ meters was assumed. Consequently, using Equation 4 and an averaging time conversion factor of 1.42 to convert from 10 minute to 3 seconds, gives an approximate 3 second wind speed at 10 of 70.8 mph (31.7 m/s).

NOAA-HRD (H*WIND) Wind Data Compilation

Since 1996 the Hurricane Research Division (HRD) of the National Oceanic and Atmospheric Administration (NOAA) has released results of an experimental product, called H*WIND, that assimilates and syntheses disparate observations into a consistent framework for height, exposure, and averaging time. The wind surface analysis system creates a wind field based on the integration of several data sources (e.g. 10 meter meteorological stations, ships, buoys, coastal platforms, surface aviation reports, reconnaissance aircraft data adjusted to the surface, etc.). Although NOAA HRD wind field composites are sophisticated they are a research tool in experimental phase that need verification and validation by a Meteorologist or Wind Engineer. H*WIND provides the maximum 1-minute sustained winds from which the maximum 3-second gust is obtained through averaging time corrections. The maximum 3 second gust wind speed for the facility based upon this dataset was approximately 62 mph.

STRUCTURAL ANALYSIS

Of special interest to the forensic investigation team was the Damage Indicator (3) shown in Figure 2. Damage indicator 3 was a large steel building that had lost a significant percentage of its cladding during the hurricane. As part of the investigation, structural engineers identified the failure mode of the cladding, which was engineered to release from the building during extreme wind events to protect the frame of the structure. The cladding was fastened to the building girts with an angle and a rivet (BSPQ-6) designed to release the panel from shear failure at a specified pressure, as shown in Figure 7. The engineered release mechanism provided a reliable indicator of the minimum wind pressures the building was subjected to. A large number of failed cladding fasteners were collected for a metallurgic study to

determine strength of the installed materials and compare the results to the design specifications. A structural analysis was carried out to determine the minimum wind pressure required to produce the damage to the cladding. This analysis provided a reliable estimate of the pressures required to result in the observed damage.

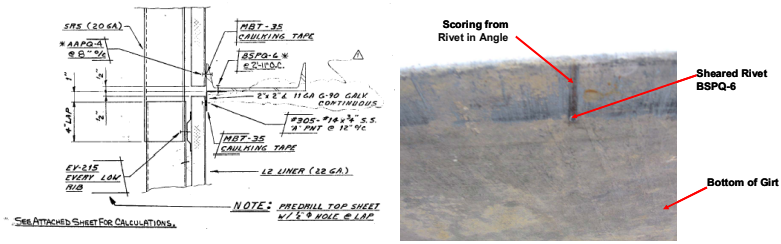

Figure 7. Wall Panel Fastener Detail & Photo of Failed Rivet

Having determined the pressure required to fail the fasteners and release the panels, ASCE 7-05 (ASCE, 2005) was used to determine the required wind speed to produce the observed damage. Results from this analysis indicate that the required 3 second gust to produce such damage was approximately 80 mph (35.8 m/s). The wind speed assessment based upon the observed structural damage was independent of the meteorological estimate of the wind speed at the facility. These results support the hypothesis stated before that gust wind speeds at the building exceeded the values suggested by the meteorological tower located at approximately 1 kilometer to the northwest of the area with disproportionate damage.

CONCLUSIONS

A summary of the adjusted wind speeds discussed previously is shown below in Table 1. These values, when evaluated in perspective with the wind damage indicators, suggest that an estimated 3 second gust of 80 miles per hour occurred at the facility resulting in the observed damage. Both TTU and NWS stations are located several miles away from the building site and were utilized with due regard for this fact. The local meteorological tower and the NOAA – HRD (H*WIND) experimental product are unique in that they are location specific and are therefore better descriptors of the hurricane strength decay over land for the site under consideration. Nonetheless, the H*WIND experimental product seem to slightly underestimate the average 3 second gust when compared to the local meteorological tower. The average 3-second gust from the local meteorological tower was estimated to be 10-15% lower (i.e. ≈ 70mph/80mph) than the actual gust experienced in a portion of the facility. If the assumed roughness length was inappropriate by, say, z_0=0.8 ± 0.4 meters, estimation of the gust wind speed from the local meteorological tower still gives between 8% and 21% (i.e. 74mph/80mph and 63mph/80mph) lower values than estimated by structural analysis of damage indicators. It is therefore concluded that the Durst curve for correction of averaging times in hurricane conditions might need a reassessment.

Table 1: Summary of adjusted wind speeds to the building exposure (z0=0.1m) and at a height of 10 meters.

Source	Wind Speed (3 second in mph) Height = 10m; z_0=0.1m
Local Meteorological Tower	70
NOAA – HRD (H*WIND)	62
TTU – StickNet (0101A probe)	71
NWS Baton Rouge Airport (ASOS Station)	101

ACKNOWLEDGEMENT

The authors are very grateful for the collaboration of the facility owner who was very kind to approve this article and generous helping the ABS Consulting team during the investigation. The authors also recognize the members of the ABS Consulting team: Nelson Durán, Robert C. Konz and Johnny Waclawczyk.

REFERENCES

ASCE 7 (1995), *Minimum Design Loads on Buildings and Other Structures*, American Society of Civil Engineers, Reston, Virginia.

ASCE 7-05 (2005), *Minimum Design Loads on Buildings and Other Structures*, American Society of Civil Engineers. Reston, Virginia.

Deaves, D.M., Harris, R.I., (1978). *A mathematical model of the structure of strong winds*, CIRIA Report 76, Construction Industry Research and Information Association, London.

Durst, C.S. (1960), *Wind speeds over short periods of time*, The Meteorological Magazine Volume 89: 181-187.

Holmes, J. D., (2001) *Wind Loading of Structures*. London, Spon Press, 356.

Krayer, W. R., and Marshall, R. D. (1992), *Gust factors applied to hurricane winds*. Bull. American Meteorological Soc., 73 : 613–617.

Panofsky, H.A. and Dutton, J.A., (1983). *Atmospheric Turbulence*. Wiley-Interscience, New York.

Simiu, E. and Scanlan R.H., (1996), *Wind effects on structures: fundamentals and applications to design*, New York, John Wiley & Sons, 1996, 688.

Tieleman, H.W., (2008) *Strong wind observations in the atmospheric surface layer*, Journal of Wind Engineering and Industrial Aerodynamics, Volume 96: 41-77.

Vickery, P. J., Skerlj, P. S., Steckley, A. C., and Twisdale, L. A. (2000), *Hurricane wind field and gust factor models for use in hurricane wind speed simulations*: J. Structural Eng., Volume 126 : 1203–1221.

Wieringa, J. (1976), *An objective exposure correction method for average wind speeds measured at a sheltered location*: Quart. J. R. Met. Soc., Volume 102: 241-253.

Wieringa, J. (1993), *Representative roughness parameters for homogeneous terrain*, Boundary Layer Meteorology, Volume 63: 323-363.

Wind-Induced Curtain Wall Damage and Moment Resisting Frame Performance: The Emergency Response, Stabilization, Analysis, Testing and Retrofit of a 36-Story Urban High-rise

William D. Bast, P.E., S.E., M.ASCE[1]
Ken R. Maschke, P.E., S.E., M.ASCE[2]
Scott G. Nacheman, M.Sc.Eng. AIA, M.ASCE[3]
Adam Abbes Yala, Ph.D., P.E.[4]

[1] Principal, Thornton Tomasetti, Inc. 330 North Wabash Ave., Suite 1500, Chicago, Illinois 60611. Phone 312.596.2014. WBast@ThorntonTomasetti.com
[2] Project Engineer, Thornton Tomasetti, Inc. 330 North Wabash Ave., Suite 1500, Chicago, IL 60611 KMaschke@ThorntonTomasetti.com
[3] Vice President, Thornton Tomasetti, Inc. 330 North Wabash Ave., Suite 1500, Chicago, Illinois 60611. Phone 312.596.2408. SNacheman@ThorntonTomasetti.com
[4] Senior Associate, Thornton Tomasetti, Inc. 330 North Wabash Ave., Suite 1500, Chicago, Illinois 60611. Phone 312.596.2164. AYala@ThorntonTomasetti.com

ABSTRACT:

On the evening of April 2, 2006 a severe wind storm passed through the downtown of a major Midwest urban municipality. This event resulted in distress to a 36 story high rise structure with approximately 10% of its curtain wall visibly missing and unknown damage to the balance of the building's cladding and structural systems.

This paper will present the authors' involvement with the initial emergency response to the property where they immediately worked with contractors to stabilize the remaining curtain wall, designed and erected temporary enclosures and shoring systems, and began an assessment of damage.

Moreover, the paper will discuss the 3-dimensional analytical model of the building's cladding and structural frame that was developed for the purpose of determining the extent of damage, in addition to the wind tunnel analysis, field instrumentation, tuned damper study and other analysis that provided critical data for the design of the curtain wall over clad to be installed at the building.

INTRODUCTION

On Sunday April 2, 2006 a severe thunderstorm with elevated wind speeds passed through a Midwestern city in the early evening. National Weather Service reports indicated that straight line winds reached speeds of nearly 80 miles per hour. The storm's wind and rain resulted in minor damage to a number of the city's structures; however, one building was affected in a particularly severe manner.

During the storm, portions of the building's exterior wall separated from the main building structure.

The initial hazard zone was primarily confined to the end 30 foot bays at the affected corners of the building. In addition, there were isolated and random breaches in the glazing throughout the building. The disengagement of some of the cladding elements (mullions and glazing) resulted in falling debris deposited about the adjacent parking lot. In addition to the loss of cladding components, several of the remaining elements (glass, mullions and convector covers from the perimeter heating units) were unsafely supported by the damaged framing matrix. These elements created a large potential hazard below the building due to the height of the damaged area of the building and the potential for these loose components to become airborne projectiles in moderate to high wind situations.

Figure 1: Area of curtain wall disengagement

Late on April 3, 2006 Thornton Tomasetti was contacted by the Building Management and asked to respond to the scene to evaluate and stabilize the visibly damaged areas of the structure. It was determined by the City and Management that the area surrounding the site would remain closed for another day, and that all contractors and consultants would mobilize the following day. On Wednesday April 5, 2006, Messrs. William Bast, Dudley McFarquhar and Scott Nacheman (all of Thornton Tomasetti) performed a site visit to view the condition of the building and perform an initial assessment of the extent and nature of distress. This assessment focused on the building structure as well as the building exterior envelope. During this time Michael Lewis of Façade Forensics and Tom Rowe of Wiss Janney Elstner Associates also collaborated in the evaluation process.

Thornton Tomasetti personnel maintained a sire presence through Saturday April 8 to assist in the design and oversight of installation of temporary stabilization systems for the missing curtain wall components.

The curtain wall had detached from floors 15 to 33 at the end west bay of the north elevation of the building. Curtain wall framing separation from its anchorage had also occurred from floors 24 to 34 at the end south bay of the west elevation, and floors 30 to 34 at the end west bay of the building south elevation. Due to the geometry and connectivity of the framing elements, some of the detached elements remained suspended from the building in large sections. In addition to the detached framing, there were many occurrences where the building envelope was breached (i.e. broken glass panes) during the storm.

On April 6, 2006 implementation of temporary and long-term stabilization systems commenced. Thornton Tomasetti personnel assisted staff from Jungclaus-Campbell and their subcontractors with on-site engineering and decision making with regard to the securing of the loose sections of curtain wall components and interior equipment.

Wire rope tiebacks were attached to the curtain wall mullions and connected to the building's steel framing as well as anchor plates that were installed into the concrete floor.

Raker shoring was implemented at the partition walls that enclosed offices that no longer contained exterior curtain walls. Due to the lack of enclosure, these partition walls were now subjected to exterior wind loading conditions. Provisions were made utilizing walers and strongbacks so that the rakers could be relocated to the 'exterior' of the partition walls, thereby bracing the walls for both pressure and suction conditions. Moreover, the partitions needed to be extended to the underside of the steel deck, so that they could act as 'demising' walls until such time as an exterior enclosure was implemented.

On April 12, 2006, a second site visit was performed by Scott Nacheman and Adam Yala. During this visit, additional observations were made at various floors and designs for temporary enclosures and interior wall bracing systems were developed.

It was determined that new 'mullions' comprised of W-shape members would span between the floor slabs, and that galvanized steel deck would act as the new temporary exterior 'skin' of the building. Drainage and weep details were considered so that the new enclosure would adequately serve as a building skin until such time as repairs were implemented.

On-site evaluations and consulting regarding temporary stabilization and enclosure continued on a regular basis as required based on contractor progress through the end of April.

INITIAL WIND TUNNEL ANALYSIS RESULTS - STRUCTURAL LOADS

A structural review and wind tunnel study were conducted to determine the local wind environment and its impact on the main structural system and cladding of the building. All subsequent analyses were based on the addition of an overclad curtain wall system instituted to remediate the damaged façade.

Review and analysis of the building was based largely on the existing structural drawings dated February 6, 1968. The building is comprised of a 32-story tower which sits above of a low-rise podium. It has a foundation system comprised

of isolated spread footing on soil with a high bearing capacity. The building is laterally supported by steel moment frames in both principal directions. This type of lateral force resisting system is no longer typically used for structures of such height.

To analyze the existing structure and determine its behavior under gravity and wind loading, a structural analytical model was built using ETABS© software (Figure 2). During several site visits, modifications to the original design drawings were observed. The analytical model was updated to reflect these conditions and thus represent the most accurate current state of the structure.

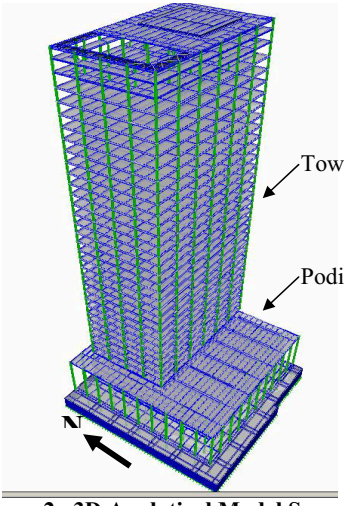

Figure 2. 3D Analytical Model Screen Shot

The gravity loads applied to the model were based on those given on the original design drawings. The structure's self weight was determined directly from the modeled steel and concrete elements. Design live loads were typically taken as 2.4 kN/m^2 (50 psf) for office space, plus 1 kN/m^2 (20 psf) for partitions. The exterior curtain wall load included 0.6 kN/m^2 (12 psf) for the existing system, plus another 0.7 kN/m^2 (15 psf) for the new overclad curtain wall system.

Factors were applied to these gravity loads to determine an appropriate total building mass for use in the wind tunnel study. The natural period of vibration of a building is based on its mass and stiffness. The flexible nature of this building, combined with the added mass of the new curtain wall system, resulted in natural periods of vibration of 8.58 sec., 7.14 sec., and 6.93 sec. for the first three modes, respectively. This information was used by the wind tunnel laboratory to determine the equivalent static wind loads applied to the structure.

The main structural wind loading shown on the design drawings was compared with the current building code and the equivalent static loads provided by the wind tunnel laboratory [1]. Main structural wind loads are computed differently than cladding suctions and pressures, where very high local forces are often considered. The original drawings considered 1 kN/m^2 (20 psf) at the base of the

building, up to 2.3 kN/m^2 (48 psf) at the top. The current building code calls for 0.5 kN/m^2 (10 psf) at the base of the building, up to about 1.1 kN/m^2 (24 psf) at the top. The equivalent static wind loads provided by the wind tunnel laboratory varied greatly from both the original design and code required loads.

In the following graphs, the design wind load from three different sources is given for each story. Wind from the north/south direction blows on the broad face of the tower. Figure 2 shows that the wind tunnel equivalent static forces closely follow the code required loads up to the 15th floor. At that point, they go through a transition period, before closely matching the original design loads. Wind from the east/west direction blows on the more narrow face of the tower. The wind tunnel equivalent static forces, shown in Figure 3, start near 0 kN and increase linearly throughout the building height to a maximum force almost twice the original design load. The wind tunnel laboratory attributed this difference to dynamic effects. A large portion of this dynamic effect comes from the inertial load due to mass at the top of the building wanting to continue moving, essentially "pulling" the tower beyond the wind effect alone.

The loads described above were given for a 50-year return period event [2]. The derivation of the wind loads also assumed a damping ratio of 2.0% of critical. Damping slows the free vibration of a building and causes an excited structure to eventually return to the steady state. The amount of damping is usually empirically derived from the type and use of the structure. However, with the development of sensitive instrumentation, some consultants now advertise the ability to estimate the amount of damping in a building from field measurements.

Different damping values may be assumed when determining the equivalent static wind loads versus the performance design for occupant comfort. Under maximum design loads, the building can undergo large sway movements which warrant the use of higher damping values. Whereas, at the lower load magnitudes used to estimate occupant comfort, lower damping values are usually used.

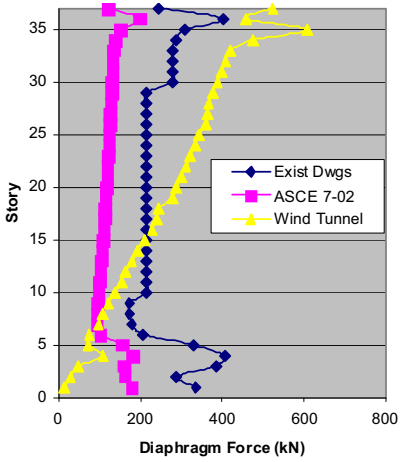

Figure 2. Applied Lateral Wind Forces (N-S)

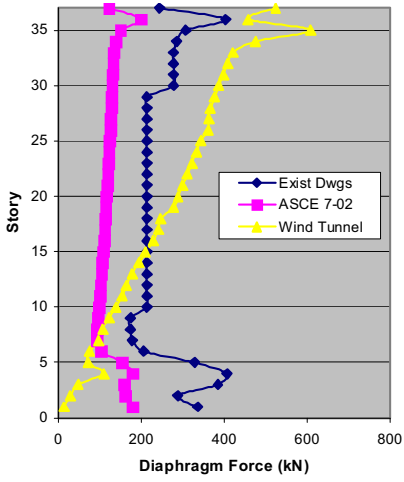

Figure 3. Applied Lateral Wind Forces (E-W)

INITIAL WIND TUNNEL ANALYSIS RESULTS - OCCUPANT COMFORT

For tall buildings responding to wind loads, occupant comfort is based on the perceptibility of motion. Table 1 summarizes the responses in each principal direction for 1.5% damping and an event with a 10-year return period at the 36th floor of the building. Accelerations at the building corners are usually taken as the governing condition, since less acceleration is felt near the center of the building. These accelerations are felt by occupants, much like the movement of a vehicle is felt when it accelerates. Torsional velocity provides a measure for the discomfort that is felt when an occupant observes objects moving with respect to their position. References provided by the wind tunnel laboratory indicate that occupants are highly sensitive to seeing stationary objects like the horizon or adjacent buildings appear to move [3].

Table 1: Wind Load Response (Damping = 1.5%, 10-yr. Return)

Variable	Response	Acceptable Criteria
X Acceleration (milli-g)	21.1	20-25
Y Acceleration (milli-g)	15.9	20-25
Corner Acceleration (milli-g)	25.3	20-25
Torsional Velocity (milli-rad/sec)	7.7	3.0

The criteria for acceptable accelerations were very nearly met. However, the predicted torsional velocity far exceeded the criteria. The large torsional velocity can

be related to the long natural period of the torsional mode of vibration (3rd mode). This behavior is a fundamental characteristic of the building structure.

INITIAL WIND TUNNEL ANALYSIS RESULTS - STRUCTURAL RESPONSE

In addition to occupant comfort, the structural response to the equivalent static wind forces was also a concern. As previously noted, the equivalent static wind loads recommended by the wind tunnel study were much greater than those prescribed by the governing code. Additionally, the wind tunnel laboratory recommended combining the components of the equivalent static loads (North/South, East/West, and torsional) according to a set of 24 different load combinations. These combinations helped to account for blowing on the building from any azimuth. The structural engineer specifically analyzed three components of the structural response: inter-story drift, footing capacity, and steel moment frame strength.

The ratio of the inter-story height (L) to the inter-story drift (Δ) is a measure of the flexibility of a structure. Most buildings are typically designed for a drift ratio around 400 to 500. Under code loading in the North/South direction, the building displayed a drift ratio (L/Δ) around 350. This suggests a relatively flexible structure. However, under the wind tunnel loads, the drift increased such that the ratio dropped to around 300.

The effect on the footings was then considered. According to the code required wind loadings, about five footings were overstressed and would require reinforcing. However, the addition of the wind tunnel load cases increased the total number of overstressed footings to 20. The footings were efficiently designed, so that the bearing capacity of the soil closely matched the concrete strength of the footing.

Therefore, even if an increased bearing capacity could be determined by in-situ investigation, the footings themselves would still require reinforcing.

Finally, the effect of the wind tunnel loads on the main lateral wind resisting moment frames was reviewed. Nearly all steel columns and beams were overstressed under the wind tunnel load combinations. Whereas, under the code prescribed loads, few members were overstressed. The wind tunnel loads essentially decreased the factor of safety for the structural elements to a factor of 1.

TUNED SLOSHING LIQUID DAMPER (TSD)

The wind tunnel laboratory's report also provided equivalent static wind loads for increased damping in the first mode –translation in the east/west direction. Such an increase in damping could be accomplished by employing a tuned sloshing liquid damper (TSD). The increase in damping effectively reduced the equivalent static loads to more closely match the loads given on the original design drawings.

To get a better perspective for what this meant to the building structure, the structural engineer compared the base shear and overturning moments for the various load conditions (as noted in Table 2). For 3.8% of critical damping, the base shear in the east/west direction was reduced by 25% in comparison to the original wind tunnel loads (2% critical damping). The base shear for 3.8% critical damping was also less than the base shear computed from the original design drawings. However, since the equivalent static loads for 3.8% damping were greater than the original design

drawings above the 20th floor, the overturning moment was still approximately 5% greater.

Table 2: East/West Base Shear & Overturning Moment

	ASCE 7	Design Drawings	Wind Tunnel 2% Damping	Wind Tunnel 3.8% Damping
Base Shear	4,760 kN (1,070 k)	9,300 kN (2,090 k)	9,880 kN (2,220 k)	7,380 kN (1,660 k)
Overturning Moment	381,00 kN-m (281,000 k-ft)	740,000 kN-m (546,000 k-ft)	1,026,000 kN-m (757,000 k-ft)	760,000 kN-m (575,000 k-ft)

BUILDING PROPERTY MEASUREMENTS

In order to 'fine tune' and value engineer the TSD, it was recommended that the building's actual dynamic properties should be measured in the field.

A specialty consultant was engaged to perform measurements of the building's dynamic response characteristics. During the period from November 9th through 11th, 2007, data was acquired from the building under mild ambient wind conditions, 20-23 km/hr (13-14 mph) maximum [4].

The specialty consultant used several data analysis techniques to obtain the dynamic characteristics of the building. For example, the half-power bandwidth technique enabled evaluation of damping from forced vibration tests without knowing the applied force.

Their own computational model, based on the design drawings, was used to decipher the building's dynamic response from the data. The model provided insight into the coupling between various modes of vibration and the contribution of building geometry to dynamic response and was used to correlate measured modes with specific mode shapes. Classical descriptions of mode shapes (torsional, translational, etc.) were difficult to apply to the buildings' actual mode shapes because of the large amount of coupling among the modes - especially for modes higher than the fifth mode.

The first measured mode demonstrated a period of 5.0 seconds for translation in the north-south direction. The first 'torsional' mode had a period of 1.7 seconds.

Measured damping ratios ranged from approximately 1% to 8% of critical. The specialty consultant opined that the 4% of critical damping would exist when the building was subjected to large excitation - such as design wind forces.

This relatively high amount of damping (4% versus 2% assumed by the wind tunnel laboratory for a typical high-rise steel structure) appeared to be the result of many damping mechanisms activated at low amplitude. These mechanisms include such phenomena as soil-structure interaction, stiffness due to architectural features (such as partitions and curtain walls, floor slab to frame connections, structural joints, concrete floor slabs, the concrete podium to tower interface), and connection to the adjacent concrete parking structure.

CALIBRATION OF ANALYTICAL MODEL

The first mode of vibration, measured at a period of 5.0 seconds, was considerably less than that calculated using the structural engineer's 3-dimensional ETABS© model, which yielded a corresponding period of 8.5 seconds. The measurements revealed a stiffer and/or lighter building than that of the model (the building period is a function of mass and stiffness).

The structural engineer proceeded to 'calibrate' the analytical model in an effort to arrive at results similar to those measured. The first four revisions instituted rigid zone factors at the beam/column connections and modified the dead load and cladding weight contributions to mass. Models 5 and 6 considered the superstructure beams to be partially composite (these beams were not designed as composite beams, but likely behaved compositely under low amplitude motion). Model 7 considered the podium as fixed at level 5 to provide an upper-bound estimate of the effect of the garage structure which was separated from the podium by an expansion joint. Finally, Models 8 through 11 considered the effects of modeling the glass and metal curtain wall system as a 'skin' membrane acting over the outer surface of the superstructure. These last models had a particularly significant effect in lowering the torsional period of the building to values close to those measured in the field.

The structural engineer concluded that Model 5 was a realistic, valid model of the structure; it had a translational first mode period of 6.4 seconds. It was decided that the other models (6 through 11) served to partially confirm that the specialty consultant's results at low wind speeds and low amplitudes measured the stiffening effects of non-structural components. These could not reliably be counted upon during a design wind event.

Therefore, the Model 5 dynamic properties were sent to the wind tunnel laboratory for re-computation of equivalent static wind forces. The dynamic properties of the building can have a significant impact on the effective wind forces borne by the building, so the new, stiffer building properties were logically expected to reduce the effect of the equivalent static wind forces.

REVISED EQUIVALENT STATIC WIND FORCES

Using the Model 5 properties for mass distribution, fundamental periods, and mode shapes, the wind tunnel laboratory performed a desk-top study to recalculate the equivalent static wind forces under a range of critical damping percentages varying from 2% to 4%.

As can be seen in Table 3, there was a dramatic reduction in the overturning moment values due to the revised dynamic properties and 3% critical damping. An even greater reduction in wind forces occurs with 4% critical damping – the damping value recommended for use by the specialty consultant.

Table 3: Base Shear and Overturning Moments

Building Type	Base Shear E/W	Base Shear N/S	Overturning Moment E/W	Overturning Moment N/S
Existing Structure (Loads Tabulated on Existing Drawings)	9,300 kN (2,090 k)	14,500 kN (3,260 k)	740,000 kN-m (546,000 k-ft)	1,239,000 kN-m (914,000 k-ft)
Structure w/ Overclad	4,760 kN	7,430 kN	381,000 kN-m	639,000 kN-m

(Loads Computed from ASCE-7 '99)	(1,070 k)	(1,670 k)	(281,000 k-ft)	(471,000 k-ft)
Initial wind tunnel – 2% critical damping	9,880 kN (2,220 k)	10,450 kN (2,350 k)	1,026,000 kN-m (757,000 k-ft)	1,037,000 kN-m (765,000 k-ft)
Revised wind tunnel- 3% critical damping	7,120 kN (1,600 k)	9,790 kN (2,200 k)	717,000 kN-m (529,000 k-ft)	915,000 kN-m (675,000 k-ft)

CONNECTION INVESTIGATION

Some degree of structural damage or degradation was suggested as a potential cause of this higher-than-expected amount of critical damping. In an attempt to rule out this possibility, a limited investigation of selected beam-to-column moment resisting connections was conducted.

Nine moment connections, at floors 5, 7 and 8, were opened for visual examination and magnetic particle testing for cracking or other defects. Each of these connections was part of the main wind force resisting system. Some beam-to-column connections were calculated to be overstressed by as much as 39% when subjected to the equivalent static wind loads originally presented by the wind tunnel laboratory. The highest amounts of calculated overstress in these connections were located near the base of the tower.

The general contractor was asked to expose the bare metal of these connections so that potential cracking of the base metal and welds could be visually and non-destructively examined. In order to expose the steel, the general contractor removed column cladding and parts of the ceiling construction and then removed the fireproofing around the joint.

None of the exposed connections had any visible signs of distress. Magnetic particle testing was performed on certain welds within these connections; the testing did not reveal any weld cracking. Ultrasonic or shear wave testing was performed on one of the weld groups; this testing did not reveal any weld cracking either.

SUMMARY AND CONCLUSIONS

Under the initial wind tunnel study the building was found to be quite lively. Given relatively flexible dynamic properties and 2% critical damping, the equivalent static wind loads represented a large magnification of the code-calculated main building lateral loads. With these results, it was estimated that a TSD of significant size would be necessary to increase the effective critical damping to the 3.8-4.1% range. Later, when building measurements revealed a stiffer structure, the revised studies concluded that critical damping of only 3% would be required to achieve base shears and overturning moment equivalent to the original design assumptions.

The building under study in this investigation contains a steel moment frame main wind force resisting system in both principal directions. This type of lateral system is not as stiff or as efficient as other systems that were under development when this building was designed in the late 1960's - including braced frame and tube structures. Recent studies of the more efficient framing systems have measured critical damping in these buildings ranging from roughly 1.0 to 2.0% [5]. Other studies for buildings of this height have suggested damping values as high as roughly 3.1%. The critical damping values measured by the specialty consultant are significantly higher than these references would estimate.

The measurements also revealed a stiffer building than would be determined by typical analytical models. The structural engineer is of the opinion that the specialty consultant's measurements, taken at low amplitudes with highly sensitive equipment, are likely upper bound estimates of both damping and stiffness for the structure. For this reason, the revised wind tunnel study used the dynamic properties of a calibrated analytical model that differed from the values measured by the specialty consultant at low amplitude. Further, the revised wind tunnel study used a lower range of critical damping percentages, rather than just the 4% value recommended by the specialty consultant.

Based upon the measured dynamic properties, the revised analytical model properties, the revised equivalent static wind forces, and the limited connection investigation, the structural engineer concluded that a TSD would not be required to reduce the equivalent static wind forces applied to the building. No overstress in the building superstructure was observed under these conditions.

REFERENCES

[1] XU Z., HO T.C.E., *A Study of Wind Effects* [Internal Report], The Boundary Layer Wind Tunnel Laboratory, The University of Western Ontario, London, Ontario, December 2006

[2] *Minimum Design Loads for Buildings and Other Structures (SEI/ASCE 7-02),* American Society of Civil Engineers, Reston, Virginia, 2003, pp. 274-276.

[3] ISYUMOV N., "Motion Perception, Tolerance and Mitigation", 5th World Congress of the Council on Tall Buildings and Urban Habitat, Amsterdam, Netherlands, May 1995, pp. 1-4.

[4] CHIU G.L.F., [Internal Report], STRAAM LLC, Hong Kong, China. December, 2007, pp. 1-2.

[5] GAMBLE S., "Supplementary Damping of Buildings," *Structural Engineer,* December, 2007, pp. 24-27.

The Enhanced Fujita Scale: For Use Beyond Tornadoes?

J. Arn Womble[1], Douglas A. Smith[2], Kishor C. Mehta[3] and James R. McDonald[4]

[1]Wind Engineering Consultant, WindForce Assoc./LNSS Assoc.; Instructor, Wind Science and Engineering Research Center, Texas Tech Univ., Lubbock, TX 79409. arnwomble@aol.com
[2]Professor of Civil Engineering, Wind Science and Engineering Research Center, Box 41023, Texas Tech University, Lubbock, TX 79409. doug.smith@ttu.edu
[3]Horn Professor of Civil Engineering, Wind Science and Engineering Research Center, Box 41023, Texas Tech University, Lubbock, TX 79409. kishor.mehta@ttu.edu
[4]Professor and Chair of Civil Engineering, Wind Science and Engineering Research Center, Retired, Box 41023, Texas Tech University, Lubbock, TX 79409. mcdonald3182@sbcglobal.net

ABSTRACT

The Enhanced Fujita (EF) Scale was developed specifically for the estimation of wind speeds based on damage caused by tornado winds. Recently, the question has arisen as to whether or not the EF Scale can be reliably used in reverse to predict the amount of wind damage based on measured or estimated hurricane wind speeds, particularly when wind action is co-mingled with severe storm-surge action and evidence of the exact level of wind damage is obliterated. In considering such use of the EF Scale, we examine separately its two major components: (1) Degrees of Damage and (2) ranges of tornado wind speeds associated with these damage levels. Our experience suggests that, in general, the EF Scale properly describes the overall progression of damage with increasing wind speeds in both tornadoes and hurricanes; however, the wind speeds associated with various degrees of damage are generally expected to be different for structures exposed to hurricanes and tornadoes. Use of the EF Scale to predict hurricane damage based on peak wind speeds is therefore discouraged.

DEVELOPMENT AND USE OF THE EF SCALE

The original Fujita Scale (Fujita, 1971) was designed as a wind speed scale to provide relative ratings of tornado intensity (McDonald et al., 2009). The scale divided intensity into multiple wind speed ranges and attempted to describe the type of damage one might expect for each wind speed range. This original Fujita Scale did not account for differences in the resistance of various structures. Prior to the 1970s, there was little understanding of the true magnitudes of maximum wind speeds in tornadoes due to a scarcity of tornado wind speed measurements. Engineering-oriented investigations of tornado damage subsequently highlighted the importance of

the wind resistance of structures (Minor, McDonald, and Mehta, 1972).

The Enhanced Fujita Scale (WISE, 2006) was developed to address variations in construction quality, to add additional damage indicators, to improve consistency of intensity ratings, and to provide more realistic estimates of tornado wind speeds (McDonald et al., 2009). The EF Scale was implemented by the National Weather Service in 2007. The EF Scale defines Degrees of Damage (DOD) for 28 different Damage Indicators (DI), e.g., residential structures, commercial buildings, and trees. The DODs follow the general progression of damages with increasing wind speeds, based on engineering-oriented studies of tornado damage over the previous three decades. As actual measurements of tornado wind speeds still remained scarce, the developers of the EF Scale used an elicitation process, comprised of experts in the study of tornado damage, to develop estimates of wind speed ranges (including expected, lower-bound, and upper-bound speeds) associated with each DOD for each DI. Examples of DODs and wind speed ranges are shown in Table 1. McDonald et al. (2009) provide additional details on the development of the EF Scale.

Table 1. EF Scale Damage Descriptions for One- and Two-Family Residences.

DOD	Damage Description	Wind Speed* (mph)		
		Expected Value	Lower Bound	Upper Bound
1	Threshold of visible damage	65	53	80
2	Loss of roof covering material (<20%), gutters and/or awing; loss of vinyl or metal siding	79	63	97
3	Broken glass in door and windows	96	79	114
4	Uplift of roof deck and loss of significant roof covering, material (>20%); collapse of chimney; garage doors collapse inward; failure of porch or carport	97	81	116
5	Entire house shifts off foundation	121	103	141
6	Large sections of roof structure removed; most walls remain standing	122	104	142
7	Exterior walls collapsed	132	113	153
8	Most walls collapsed, except small interior rooms	152	127	178
9	All walls collapsed	170	142	198
10	Destruction of engineered and/or well constructed residence; slab swept clean	200	165	220

*3-sec gust, open-country terrain, 10 m height

The EF Scale is intended specifically to establish tornado intensity from the resulting levels of damage to various DIs; it is deployed by estimating the wind speed for a specific level of damage. By reviewing several damaged buildings or other DIs, a range of storm wind speeds is ascertained, which in turn establishes the tornado intensity ranging from EF0 to EF5. McDonald et al. (2009) and WISE (2006) give further details on the EF-Scale rating protocol.

The EF Scale is *not* designed to establish the damage level of a specific building from a specific wind speed, and if used in this manner, it is likely to give results with a gross error. For example, Figure 1 graphically shows the ranges of wind speeds associated with various DODs for a single-family residence. From multiple DOD observations acquired in a tornado damage investigation, it is possible

to obtain a range of associated wind speeds and to therefore assign an EF rating to the tornado event. However, entering the plot with a specific wind speed, say 110 mph, results in associated DODs ranging approximately from DOD 3 to DOD 7 – far too great a range to accurately predict wind damage to a single structure.

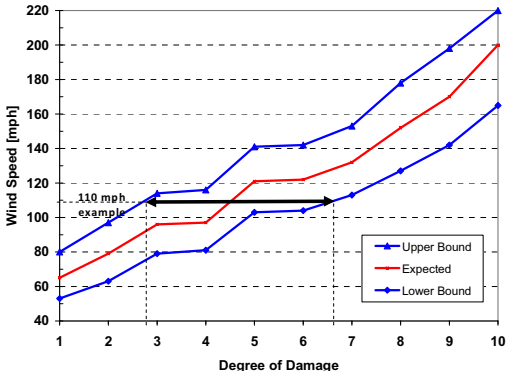

Figure 1. Example EF-Scale windspeed ranges vs. DODs.

WIND SPEEDS IN TORNADOES AND HURRICANES

The wind speed ranges of the EF Scale represent the best estimates of the engineering and meteorological communities at the time of its development. We stress that the tornado wind speed ranges represent well-founded *estimates* rather than widespread measurements. It is significant that the EF Scale ultimately serves to rate tornadoes based on damage, rather than on known wind speeds. An intensity scale based on wind speeds rather than damage would be independent of construction quality in various locations and could therefore be used universally in all parts of the U.S. and beyond (Doswell, 2007). A wind speed-based tornado scale, however, is not useful in practice due to the lack of known wind speeds in tornadoes; damage thus remains the best indicator available on a routine basis in tornadoes (Doswell, 2007).

While wind speeds in tornadoes are necessarily estimated based on damage, the knowledge of actual wind speeds in hurricanes has increased significantly over the past decade. Developments in mobile radar equipment and ruggedized portable anemometers have made direct measurements of hurricane wind speeds feasible (Giammanco, Schroeder, and Edwards, 2006; Gurley et al., 2005; Schroeder and Smith, 2003). In-situ measurement of hurricane wind speeds has greatly increased our understanding of the hurricane parameters important for engineering design (Vickery, 2009). Such direct measurement of wind speeds has been accomplished at a greater pace for hurricanes than for tornadoes, due primarily to longer lead times and larger spatial extents of hurricanes that better enable the strategic placement of measurement equipment in the path of the storm.

Whereas *direct measurement* of wind speeds in severe hurricanes has become more-or-less standard, the *estimation* of wind speeds for tornadoes using damage as a proxy indicator remains a practical necessity (Doswell, 2007) – at least for the near future. Efforts are currently underway to extend such in-situ measurements to

thunderstorms and tornadoes (e.g., Weiss and Schroeder, 2008; Orwig and Schroeder, 2007). Further analysis of tornado wind speed measurements and associated damages may well lead to future refinements of wind speeds in the EF Scale.

DAMAGE MECHANISMS IN TORNADOES & HURRICANES: SIMILARITIES AND DISSIMILARITIES

Whether caused by tornado, hurricane, downburst, or straight-line winds, the general appearance of wind damage to a particular structure, without reference to specific wind speeds, is very similar (Marshall, 1993). For a given wind speed, however, the anticipated damage can vary significantly between types of storms, due to temporal and spatial characteristics of the winds as well as resistances of the structures themselves. Apart from specific magnitudes of wind speeds, the progression of damage to structures with increasing wind speeds is generally expected to be similar for tornadoes and hurricanes, as observed by engineering investigations of tornado and hurricane damage over the past 40 years (e.g., Teasdale, 2008; Marshall, 1993; Minor and Mehta, 1979; Minor et al., 1977).

This progression of wind damage to structures is also crucial in establishing damage causation, such as distinguishing wind-induced damage from damage caused by foundation settlement or storm-surge action. Much anecdotal evidence exists for the improper use of EF Scale to determine the extent of wind damage occurring before the subsequent destruction by storm surge (Womble and Smith, 2009). For instance, the pier-and-beam residence shown in Figure 2 was removed from its foundation by storm surge during Hurricane Katrina. Forensic reports citing wind action as the cause of destruction reasoned that the damage was consistent with EF Scale DOD 5 from Table 1: "*Entire house shifts off foundation*." (As originators of the EF Scale, co-authors Mehta and McDonald interject that DOD 5 does not likewise include "transport of intact residence off-site.") It is unlikely for such structures to be moved by wind action without first experiencing lesser DODs.

Even in attempting to establish wind action as the damage causation using the DODs and wind speeds of the EF Scale, other nearby DIs should also be investigated, e.g., hardwood and softwood trees (Table 2). By *strict application* of wind speeds presented throughout the EF Scale, shifting of a residence (DOD 5, Table 1) should be associated with damage to trees as described by DOD 5 ("trees debarked with only stubs of largest branches remaining") or DOD 4 ("trunks snapped") for hardwood and softwood trees, as well as certainly DOD 3 ("trees uprooted"). As shown in Figure 2, such damage to trees did not occur. Storm-surge action, however, can be expected to move inadequately founded pier-and-beam residences without major damage to roof coverings or to nearby trees. Obviously, selective application of DODs is to be avoided in establishing damage causation.

In addition to the DODs, the EF Scale gives *estimated* ranges of wind speeds expected to cause these levels of damage. We note that wind speeds required to cause similar levels of damage to structures in tornadoes and in hurricanes can be quite different.

Despite many similarities in their loading of structures, tornadoes and hurricanes have differences that can be of significance in the resulting wind loads. Sudden atmospheric pressure changes are more closely associated with tornadoes but are found to be of little consequence in the failures of most structures, such as single-family residences (Marshall, 1993; Mehta, 1976; Minor, 1976). Order-of-magnitude

differences in the radius of rotation for hurricanes and tornadoes is significant for the spatial distribution of damage across an entire region but are of little difference in the wind loading of individual structures that are small relative to the radius of rotation (Marshall, 1993). (For tornadoes as well as hurricanes, individual structures experience essentially a turbulent straight-line wind that shifts direction with time.)

Figure 2. Pier-and-beam residence moved off its foundation by storm surge during Hurricane Katrina. Note the condition of roof coverings and surrounding trees. EF Scale DOD-5 (Table 1) is not applicable to this situation.

Table 2. EF Scale Damage Descriptions for Trees.

DOD	Damage Description	Wind Speed* (mph)		
		Expected Value	Lower Bound	Upper Bound
	Softwood: Pine, Spruce, Fir, Hemlock, Cedar, Redwood, Cypress			
1	Small limbs broken (up to 1" diameter)	60	48	72
2	Large branches broken (1" - 3" diameter)	75	62	88
3	Trees uprooted	87	73	113
4	Trunks snapped	104	88	128
5	Trees debarked with only stubs of largest branches remaining	131	112	153
	Hardwood: Oak, Maple, Birch, Ash			
1	Small limbs broken (up to 1" diameter)	60	48	72
2	Large branches broken (1" - 3" diameter)	74	61	88
3	Trees uprooted	94	76	118
4	Trunks snapped	107	93	134
5	Trees debarked with only stubs of largest branches remaining	143	123	167

*3-sec gust, open-country terrain, 10 m height

Rapid changes in temperature and air density in thunderstorms as well as differing vertical velocity components may also be responsible for differences in the pressure distributions on building surfaces resulting from hurricanes and tornadoes; such effects are currently under investigation by others (e.g., Mason, James, and Letchford, 2009; Lombardo and Smith, 2008).

Large differences in the time of exposure to elevated wind speeds in tornadoes and hurricanes *can* also be significant in the damage ultimately resulting to a structure, due to the possibility of fatigue failures induced by cyclic loading. Unusually slow-moving tornadoes can also produce DODs beyond that typically expected in other tornadoes (Phan and Simiu, 1998). The possibility of cyclic-loading failures in hurricanes has gained moderate attention within the engineering community. Some engineers have suggested that the EF scale, without modifications, is applicable to hurricane damage prediction because cyclic loading may counteract the increased resistance of many structures in hurricane-prone regions. In our experience, however, the likelihood of fatigue failure is frequently overstated. Fatigue failures in hurricanes appear to be the exception rather than the norm, as they generally require both an unusually slow-moving and intense storm to apply enough cycles of pressure of sufficient magnitude. When these conditions are met, however, the effect can be dramatic, as evidenced by Cyclone Tracy in 1974 (Marshall, 1976).

Womble and Smith (2009) discuss that widespread fatigue failures are *not* generally expected for tropical cyclones such as Hurricane Katrina having relatively low wind speeds and typical storm-translation speed. We examine this issue further with the aid of typical time histories of wind speed and wind direction (Figure 3) measured during the passage of Hurricane Katrina at Stennis International Airport, MS (Giammanco et al., 2007). Whereas the elevated winds of a tornado will typically act on a building for seconds to minutes, the time history shows that hurricane winds are active for many hours. Note, however, that the highest wind speeds (Region B in Figure 3) are short-lived, and that during this time associated with the nearby passing of the eye, the wind direction changes rapidly. Changes in wind direction cause the highest wind pressures to be experienced by different sections of a building, thus minimizing the chance for a particular component to receive maximum loading throughout the storm.

BUILDING RESISTANCES IN U.S. MIDWEST & HURRICANE REGIONS

Damage occurs when loads exceed resistance, and therefore the resistance of buildings is obviously of extreme importance in the consideration of damage from tornadoes and hurricanes. The overall building stock in hurricane-prone regions of the U.S. (Atlantic and Gulf coasts) is generally expected to exhibit higher resistance than the overall building stock in the Midwestern (interior) U.S. Although tornadoes can likewise occur along the hurricane coasts, we observe that Midwestern U.S. tornadoes have comprised the bulk of engineering-oriented investigations of tornado damage from which the estimated wind speed ranges of the EF Scale have been compiled. The historical map of windstorm damage surveys conducted by the Institute for Disaster Research (now Wind Science and Engineering Research Center) of TTU (Figure 4) demonstrates the relative number of Midwestern and coastal-area tornadoes in the TTU damage database.

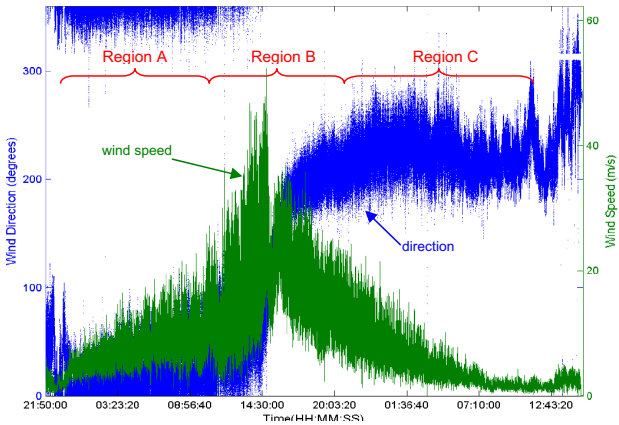

Figure 3. Time histories of Hurricane Katrina wind speed and direction measured in-situ at Stennis International Airport by TTU-HRT tower.

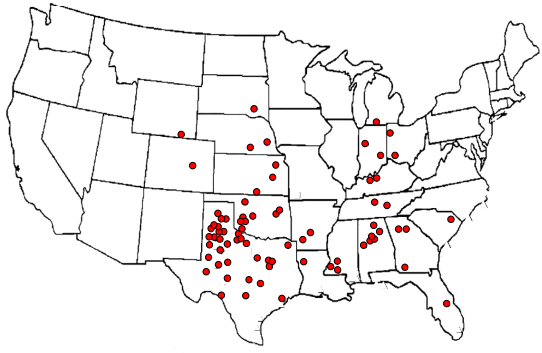

Figure 4. Locations of TTU tornado damage investigations 1970-2002, up to the time of EF Scale creation. Midwestern/interior U.S. tornadoes are far more prevalent than Atlantic- and Gulf-coast tornadoes in this database.

Consequently, the wind speeds associated with various DODs in the EF Scale are expected to vary between tornado- and hurricane-prone areas. We expect the overall hurricane-coast building stock to have superior wind resistance relative to the overall building stock in the Midwestern U.S., where strong tornadoes are most prevalent and with which the EF Scale was developed. This is not to say that inferior construction is not found along the coast; however, the overall coastal building stock

is expected to have superior wind resistance due to heightened (and ever-increasing) awareness of vulnerability to strong winds as well as increasingly strict enforcement of building codes in many coastal areas.

The acknowledged need for greater wind resistance in U.S. hurricane areas can be found in design maps dating back to the earliest-known wind load specifications of the 1940s and 1950s (ASA, 1945, 1955) through present day (ASCE, 2005), all of which acknowledge increased design velocity pressures or wind speeds in hurricane-prone regions. ASCE 7-05 specifies design-level 3-sec gust wind speeds of 100–150 mph in hurricane-prone areas, as opposed to 90 mph in the Midwestern U.S. (Note that such an increase in wind *speeds* near the coast equates to an increase in wind *loads* of up to 2.78 times [= $(150 \text{ mph}/90 \text{ mph})^2$] compared to design wind speeds in the Midwestern U.S.) We further note that prevalent wind load standards (including ASCE 7-05) intentionally include hurricane wind speeds in the specification of minimum design wind speeds for hurricane-prone areas of the U.S., whereas these load standards do not incorporate tornado wind speeds in the specification of minimum design wind speeds for the Midwestern U.S.

EF SCALE – NOT A HURRICANE DAMAGE PREDICTOR

Forensic engineers are seeking a tool for estimation of hurricane damage from a known (or estimated) wind speed when direct physical evidence of wind damage has been removed. As we have discussed above, the EF Scale was not designed to serve in this capacity. Rather than predicting wind damage occurring at a given wind speed, the EF Scale is intended to rate an overall tornado event using wind damage to a number of different Damage Indicators. Tornado wind speed ranges for the EF Scale are necessarily based on estimates of experts, rather than on measurements of tornado wind speeds. Furthermore, application of the EF Scale for building stocks for which it was not "calibrated" can potentially lead to inaccuracies in wind speed estimates for tornadoes (Doswell, 2007) as well as hurricanes. The EF Scale can be used to assign consistent damage ratings (i.e., DODs) to buildings and other DIs, apart from wind speeds. We note that this usage of the EF Scale is different, however, than predicting certain damage from a known or estimated wind speed.

CONCLUSIONS & RECOMMENDATIONS

Our investigations of tornado and hurricane damage suggests that DODs in the EF Scale properly describe the general progression of damage to structures with increasing wind speeds in both tornadoes and hurricanes and that, apart from associated wind speeds, this progression itself is helpful in establishing wind damage causation. However, the actual wind speeds associated with these DODs are expected to be different in tornadoes and hurricanes. This disparity in wind speeds for tornadoes and hurricanes stems from inherent differences in both the loading and resistance of building stocks in tornado- and hurricane-prone areas of the U.S. In most cases, the wind speeds of the EF Scale are expected to overestimate hurricane damages for the overall building stock in hurricane-coast areas. Relatively rare cases of very intense and slow-moving storms may increase the chances for fatigue failures, and in such cases the wind speeds of the EF Scale could underestimate damages for hurricanes. Without careful adjustment for the above factors, use of the EF Scale to predict hurricane damage is discouraged.

With emerging technologies for measuring wind speeds in hurricanes and correlating these wind speeds with observed damage, storm-specific and region-specific damage functions can be generated to serve as better estimators of likely hurricane damage than the EF Scale extended beyond its intended purpose. The feasibility of obtaining in-situ measurements of wind speeds (as in Figure 3) has been greater for hurricanes than for tornadoes. Many such data have been collected in the past decade, and more are being collected with each hurricane season. In addition, damages to nearby structures have been captured by remote-sensing images and/or ground surveys (Womble, Smith, and Adams, 2008). Such damages can be correlated with known wind speeds to produce more accurate relationships of damage and wind speeds than were available to our team in developing the EF Scale.

As technological innovations enable us to better measure wind speeds within tornadoes, such techniques can likewise help to refine the wind speeds of the EF Scale and can also indicate whether or not simple wind speed adjustment factors can be applied to the tornado EF Scale to extend its application to hurricanes.

REFERENCES

ASA (1945, 1955). *American Standard Building Code Requirements for Minimum Design Loads in Buildings and Other Structures,* A58.1, Am. Stds. Assoc. Inc.

ASCE (2005). *ASCE 7-05 Minimum Design Loads for Buildings and Other Structures.*

Doswell, C.A. III, Brooks, H.E., and Dotzek, N. (2007). "On the implementation of the Enhanced Fujita Scale in the USA," 4th European Conf. on Severe Storms, Sept. 10-14, 2007, held in Trieste, Italy.

FEMA (2000). *Hazus-MH MR2*. Technical Manual Developed by the Department of Homeland Security, FEMA Mitigation Division, Washington, D.C.

Fujita, T.T. (1971). *Proposed characterizations of tornadoes and hurricanes by area and intensity*, SMRP 91, Dept. of Geophysical Sciences, Univ. Chicago, 42 pp.

Giammanco, I.M., Schroeder, J. L., and Hirth, B.D. (2007). *Hurricane Katrina Deployment Summary*, Hurricane Research Team, Wind Science and Engineering Research Center, Texas Tech University, Lubbock, Texas.

Giammanco, I.M., Schroeder, J.L., and Edwards, B. (2006). *A Summary of Texas Tech University's 2005 Hurricanes at Landfall Project,* Preprint, AMS 27th Conference on Hurricanes and Tropical Meteorology, held in Monterrey, California. 24-28 April 2006.

Gurley, K., Masters, F., Prevatt, D., and Reinhold, T. (2005). *Hurricane data collection, FCMP deployments during the 2004 Atlantic Hurricane Season*, 10th Americas Conference on Wind Engineering, Baton Rouge, LA, May 31–June 4, 2005.

Lombardo, F.T. and Smith, D.A. (2008). "Investigation of Thunderstorm Winds on an Instrumented Building," *Proc. ASCE/SEI Structures Congress,* held in Vancouver, B.C. 24-26 April 2008.

Marshall, R.D. (1976). *Engineering aspects of Cyclone Tracy, Darwin, Australia, 1974,* Building Science Series 86, U.S. National Bureau of Standards.

Marshall, T.P. (1993). "Lessons learned from analyzing tornado damage." *The Tornado: Its Structure, Dynamics, Prediction, and Hazards*. Geophysical Monograph 79, American Geophysical Union.

Mason, M.S., James, D.L., and Letchford, C.W. (2009). "Wind pressure measurements on a cube subjected to pulsed impinging jet flow," *Wind & Structures*, 12, 77-88.

McDonald, J.R., Mehta, K.C., Smith, D.A., and Womble, J.A. (2009). *The Enhanced Fujita Scale: Development and Implementation*, forthcoming, 5th Forensic Engineering Congress, ASCE, Washington, DC. 10-15 November 2009.

Mehta, K. C. (1976). "Windspeed estimates: Engineering analyses," in *Proceedings of the Symposium on Tornadoes*, pp. 89-103, Texas Tech University, held in Lubbock, Texas. 22-24 June 1970.

Minor, J. E. and Mehta, K.C. (1979). "Wind damage observations and implications," *Journal of the Structural Division*, ASCE, 105(ST11), 2279-2291.

Minor, J.E., McDonald, J.R., and Mehta, K.C. (1977). *The tornado: An engineering oriented perspective*. NOAA Technical Memorandum, ERL NSSL-82, National Severe Storms Laboratory, Norman, OK, p. 103.

Minor, J. E. (1976). Applications of tornado technology in professional practice, in *Proceedings of the Symposium on Tornadoes*, 375-392, Texas Tech University. Held in Lubbock, Texas. 22-24 June 1970.

Minor, J. E., Mehta, K.C., and McDonald, J.R. (1972). "Failures of structures due to extreme winds." *Journal of Structural Division*, ASCE, 98(ST11), 2455-2471.

Orwig, K. D., and Schroeder, J.L. (2007). "Near-Surface Wind Characteristics of Extreme Thunderstorm Outflows," *Journal of Wind Engineering and Industrial Aerodynamics*, 95 565-584.

Phan, L.T. and Simiu, E. (1998). *The Fujita tornado intensity scale: a critique based on observations of the Jarrell tornado of May 27, 1997*, NIST Tech Note 1426, U.S. Dept. Commerce, Gaithersburg, MD 20 pp.

Schroeder, J. L. and Smith, D.A. (2003). "Hurricane Bonnie Wind Flow Characteristics," *Jnl. of Wind Eng. & Industrial Aerodynamics*, 91 767-789.

Teasdale, D. (2008). "Field Evaluation of Damage from Wind and Flooding," *ASCE/SEI Structures Congress,* held in Vancouver, BC. 24-26 April 2008.

Vickery, P.J., Wadhera, D., Twisdale, L.A., and Lavelle, F.M. (2009). "U.S. hurricane wind speed risk and uncertainty," *Journal of Structural Engineering*, 135(3), 301-320.

Weiss, C.C. and Schroeder, J.L. (2008). "StickNet- A new portable rapidly deployable surface observing system", *88th Annual Meeting of the American Meteorological Society*, held in New Orleans, Louisiana. 20-24 January 2008.

WISE (2006). *A recommendation for an Enhanced Fujita Scale*, Rev.2, Wind Science and Engineering Research Center, Oct. 2006; available from http://www.wind.ttu.edu/EFScale.pdf, Internet. Accessed 22 March 2009.

Womble, J.A. and Smith, D.A. (2009). "Common Misconceptions in Determining Wind/Water Damage Causation." *ASCE/SEI Structures Congress,* held in Austin, Texas. 30 April – 02 May 2009

Womble, J.A., Smith, D.A., and Adams, B.J. (2008). "Use of Emerging Remote-Sensing Technologies to Determine Neighborhood Wind/Water Damage Patterns," *Proc. ASCE/SEI Structures Congress,* Vancouver 24-26 Apr. 2008.

Ground Damage Assessment from Tornado-Borne Projectiles

Charles E. Pierce[1], Jonathan Jenkins[2], Lesley Joseph[3]

[1]Associate Professor, Department of Civil & Environmental Engineering, University of South Carolina, 300 Main Street, Columbia, SC, 29208; PH 803-777-3855; FAX 803-777-0670; email: piercec@cec.sc.edu
[2]Undergraduate Research Assistant, Department of Civil & Environmental Engineering, University of South Carolina, 300 Main Street, Columbia, SC, 29208; PH 803-777-3855; FAX 803-777-0670; email: jon.jenkins02@gmail.com
[3]Undergraduate Research Assistant, Department of Civil & Environmental Engineering, University of South Carolina, 300 Main Street, Columbia, SC, 29208; PH 803-777-3855; FAX 803-777-0670; email: lesleysjoseph@gmail.com

ABSTRACT

Tornados often create and transport large amounts of debris that can be ejected at high velocities. There have been empirical and theoretical studies conducted on missile transport and impact, but ground damage from tornado-borne projectiles has not been well documented in the field. This paper summarizes the evidence and extent of ground damage from tornados and proposes a method for field data acquisition and assessment. Impact velocities of projectiles can be estimated using field measurements of ground deformations coupled with projectile and soil properties. Ground damage has the potential to adversely affect subsurface infrastructure if the penetration is deep enough to strike a buried pipeline or if the ground impact transfers sufficient energy to induce local settlement around a buried pipeline. With reliable data, ground damage assessment can be considered for inclusion as part of the Enhanced Fujita Scale for tornado classification.

INTRODUCTION

In 1973, a method to classify tornados by estimating their wind speeds was developed by Ted Fujita, which he named the Fujita Tornado Damage (F) Scale. This scale estimated wind speeds by assessing tornado damage. Classifications ranged from F0 to F5; at higher wind speeds, it was noted that tornado missiles can be produced. For example, an F2 tornado might generate “light-object missiles” and “cars lifted off ground,” while a more intense F4 tornado might result in “cars thrown and small missiles generated.”

In 2007, the Enhanced Fujita (EF) Scale was developed to relate more specific tornado damage observations to wind speeds. The recommended EF Scale is compared to the original F Scale in Table 1. It should be noted that wind speeds in the EF ratings have been reduced from the original F ratings. This revision was necessary because the higher wind speeds were unverified based on damage assessments.

Table 1. Fujita Tornado Damage (F) Scale versus Enhanced Fujita (EF) Scale

Fujita Tornado Damage (F) Scale		Enhanced Fujita (EF) Scale	
Rating	**Wind Speed (mph)**	**Rating**	**Wind Speed (mph)**
F0	<73	EF0	65-85
F1	73-112	EF1	86-110
F2	113-157	EF2	111-135
F3	158-206	EF3	136-165
F4	207-260	EF4	166-200
F5	261-318	EF5	>200

To evaluate tornado intensity, observations of damage to structures are identified and correlated to those on a list of 28 damage indicators (DIs). The list is comprised of specific structures with differing construction methods and materials, such as a 1- or 2-family residence (DI No. 2), strip mall (DI No. 10), and elementary school (DI No. 15). Slender structures represent DI Nos. 25 to 28 and include free-standing towers, poles and trees. For each DI, several degrees of damage (DOD) are identified that range from minor visible damage to complete destruction. DODs are arranged so that each one corresponds to a higher expected wind speed. After all observed DIs/DODs have been determined, upper and lower bounds for wind speeds are estimated to assign one of the six EF ratings.

Although the original F Scale addressed missile transport, it was decided not to include missile transport as part of the EF Scale because reliable data are still rare. Correlations of missile transport and wind speeds have not been well established. The omission of missile transport in the EF Scale indicates that more research in this area is much needed. When sufficient field data are acquired, ground damages from tornado-borne projectiles can be considered as additional damage indicators in the EF Scale.

PRIOR RESEARCH

There is significant published literature that investigates the formation of a tornado vortex and how it lifts, transports, and ejects projectiles. For example, Rotunno (1979) combined lab-scale experimentation with theoretical modeling to create a tornado vortex and examine its characteristics. Researchers have analyzed the known velocities of various projectiles as well as the potential velocities that can be achieved for missiles specifically produced by tornados (e.g. Iotti 1975; Costello et al. 1977; Kar 1979a). Others have studied the impact loading of tornado-borne projectiles (e.g. Kar 1978; Kar 1979b; Dunn and Twisdale 1979). Perhaps the most comprehensive work on the creation and impact loading of tornado-borne projectiles is summarized by Corbett et al. (1996). Corbett et al. (1996) reviewed published literature to explore the impacts of different projectiles over a range of velocities on multiple target media, including aluminum, steel, concrete, and soils. More recently, Chen and Lia (2002)

performed a series of penetration tests using concrete, steel, and soil media and generated a general non-dimensional formula to predict penetration depth due to normal impact of a non-deformable projectile.

Some studies on ground impacts have concentrated on a specific soil or rock type, such as sand (e.g. Boguslavskii et al. 1996a, 1996b), gravel (e.g. Pichler et al. 2005, 2006), and limestone (e.g. Ben-Dor et al. 2003; Warren et al. 2004). Other studies take a more generalized approach to analyzing the effects of a projectile on soils. Byers et al. (1978) discuss the various methods used to launch projectiles and to monitor projectile impact and penetration into earth media. Yew and Stirbis (1978) present a penetration model that uses physical projectile characteristics to mathematically predict penetration depth into earth media.

PROJECTILE CHARACTERISTICS

Most tornado-borne projectiles consist of smaller debris, such as wood boards like the one shown in Figure 1. Larger projectiles can also be generated during tornados, and in the strongest events, such objects can be transported great distances and cause significant damage. According to eyewitness reports and documented damage assessments, some of the largest objects that have been lifted and transported by tornados include refrigerators and pianos; fertilizer tanks (see Figure 1) and propane tanks; and cars (see Figure 1), vans, farm wagons, school buses, and tractor-trailers. For instance, an empty fertilizer tank weighing 26,000 pounds was moved about 3,900 feet during a tornado that passed through Lubbock, Texas in May 1970. In August 1990, a tornado in Illinois displaced a tractor-trailer, which ended up in a field about 1,100 feet from the road after bouncing five times. While there is sufficient visual evidence of ground impacts, the extent of ground damage from both small and large projectiles has not been adequately quantified in the field.

Figure 1. Examples of tornado projectiles.

Depending on their characteristics, projectiles can cause direct or indirect damage to the ground. Direct, or visible, damage is defined herein as damage created when a projectile indents and/or penetrates the ground surface. Small, slender objects are the most common penetrating projectiles. As shown in Figure 1, a fractured wood board, which is lightweight and has a small impact surface area, has been observed to partially penetrate the ground. Although there is photographic evidence of partial

penetration, there are no quantifiable measurements of projectile characteristics or penetration depths. It is also possible for shorter projectiles to fully penetrate the ground, resulting in complete burial, although there is no published documentation of such occurrences in the field. Penetration depth is important when pipelines, utilities, and other subsurface infrastructure are buried at shallow depths. If a projectile penetrates the ground and contacts a buried pipe, then there is some risk of damage. Direct impact can cause punctures and immediate leaks or, in other cases, it can initiate damage such as cracking that induces gradual development of a slow but long-term leak. Protection of sensitive pipelines, such as regional gas line networks and water lines at nuclear facilities, is a priority for these industries.

Indirect damage is more common with larger objects that have considerable weight and large impact surface areas, like the tank and cars shown in Figure 1. Indirect damage occurs when a significant amount of energy is transferred from the projectile to and through the ground at impact. Direct damage such as crater formation may or may not occur. While larger projectiles are not expected to make direct contact with buried infrastructure, as might be the case with smaller projectiles, the energy that is transferred through the ground can cause soil deformations leading to immediate or long-term structural damage to pipelines or utilities.

PROPOSED FIELD MEASUREMENT OF GROUND DAMAGE

While there has been significant experimental and theoretical research published to date, there remains a lack of field data about tornado-borne projectiles and ground impacts. Observations of damage from tornados have not routinely included measurements of projectile characteristics, ground conditions, or ground deformations. There are three main reasons for the lack of field measurements. First, in the EF Scale, there are no damage indicators (DIs) for surface infrastructure, such as pavements, parking lots, culverts, ditches, embankments, or other ground surfaces. Second, observations of projectile impacts on DIs are not required for primary assessment of degrees of damage (DODs), although such impacts might be noted as secondary evidence. Grounded projectiles, however, might be overlooked entirely. Third, the field meteorologist(s) responsible for damage assessment often must cover a large area in a relatively short period of time, so quantifiable measurements are not a required part of EF classification. In other words, the purpose of having a descriptive checklist of DIs/DODs is so that an accurate qualitative assessment can be completed without the need for measurements.

Field data is needed to quantify actual ground damage and compare it to prediction models. To this end, a ground damage assessment form has been created to collect field evidence of ground damage from projectiles, although the form has not yet been implemented. First, the depth of indentation and/or penetration is measured along with crater dimensions. Second, the projectile orientation is measured, which is especially important if the projectile has partially penetrated the ground. Third, the physical condition and properties of each object (e.g. mass, dimensions, impact surface area) are needed to estimate the impact stresses. Due to the irregular shape of

most projectiles and the irregular projectile movements that can be generated, there are multiple strike surface areas that can be produced when an object impacts the ground. For example, an object like a car can land right side up or upside down, on its side, or on its front (head lights) or rear (tail lights) face. Impact positions can also occur at an angle other than perpendicular. Each position produces a different surface stress and dictates how an object indents or penetrates the ground. Fourth, the soil conditions and properties must also be measured using appropriate field tools and techniques.

PREDICTION OF GROUND DEFORMATION

Depth of Indentation. Labiouse et al. (1996) developed the following empirical formula that describes the impact force of an object based on tests performed to determine the required soil thickness over artificial rockfall protection sheds:

$$F_{MAX} = 1.765 M_E^{2/5} R^{1/5} (WH)^{3/5} \quad \textbf{(1)}$$

where M_E is the elastic modulus of the soil, R is the curvature radius of the impacting mass, W is the weight of the impacting mass, and H is the height of fall. Mayne and Jones (1983) proposed an equation to determine the impact force of a large object that was derived from the Law of Conservation of Linear Momentum and the authors' experience with dynamic compaction:

$$F_{MAX} = \sqrt{\frac{32WHGr_0}{\pi^2(1-\nu)}} \quad \textbf{(2)}$$

where W is the weight of the impacting mass, H is the height of drop, r_0 is the radius of the impacting mass, G is the dynamic shear modulus of the soil, and ν is the Poisson's ratio of the soil. To determine the maximum indentation depth in the soil, an empirical formula developed by Peila et al. (2007) can be used. This formula was produced using data from experimental rockfall testing and utilized the preceding equations to obtain impact force of an object:

$$\delta = \frac{mv^2}{F_{MAX}} \quad \textbf{(3)}$$

where m is the mass of the impacting object, v is the impact velocity, F_{MAX} is the computed maximum force, and δ is the resulting depth of indentation.

Depth of Penetration. An empirically derived penetration equation, based on the modified Petry formula, can be used to predict penetration depths of multiple objects into various soil conditions. The modified Petry formula is:

$$Z = \frac{W}{A} K \log_{10}\left[1 + \frac{V^2}{215{,}000}\right] \quad \textbf{(4)}$$

where Z is the total distance of penetration, W is the projectile weight, A is the projectile cross-sectional area, K is a constant for different soil types, and V is the impact velocity. The empirical penetration prediction equation proposed by Young (1969) was derived to bridge the gap between the widely used Petry formula and other empirical equations, taking into account a more complete understanding of penetration. The empirical penetration prediction equation is as follows:

$$Z = 0.53SN\left(\frac{W}{A}\right)^{1/2} \ln(1 + 2V^2 10^{-5}), \text{ V} < 200 \text{ fps} \quad \textbf{(5)}$$

$$Z = 0.0031SN\left(\frac{W}{A}\right)^{1/2} (V - 100), \text{ V} \geq 200 \text{ fps} \quad \textbf{(6)}$$

where S is a soil constant and N is the nose performance coefficient, which accounts for different nose shapes compared to a flat nose. These two empirical equations were based on numerous tests of penetration of multiple objects into various earth media. It is recognized that Equations 4 through 6 do not explicitly incorporate soil properties in the same manner as Equations 1 and 2.

SAMPLE DEPTH CHARTS

Depth of Indentation. A sample set of indentation charts is illustrated in Figure 2 based on the theoretical impact from a 1.89 m^3 (500 gallon) propane tank in three conditions: empty, half-filled, and filled. Two strike surfaces are assumed: a direct vertical impact (smaller surface area), which occurs when the tank is dropped on its top or bottom, and a direct horizontal impact (larger surface area), which occurs when the tank is dropped on its side. In the field, it is possible that the impact occurs at some angle in between the vertical and horizontal positions. The impact position might be discernible from observations and measurements of a surface crater. A constant drop height of 10 m was selected for the sample charts. Video evidence has shown large objects, such as cars, reaching heights of at least 10 m inside a tornado. In this example, the tank is treated as a rigid, incompressible body.

Depths of indentation are plotted as a function of increasing velocities using Equations 2 and 3 for soft clay and dense sand. Poisson's ratio, ν, is assumed to be 0.3 for both soil conditions. However, the shear modulus for soft clay is assumed to be much lower than for dense sand. Table 2 shows the values used in the calculations.

Under the most extreme conditions assumed in this example, the indentation depth exceeds 3.0 m, which would translate to full burial of the tank into the ground. While such an impact is not probable, the charts illustrate that there is a considerable range

of indentation depths for large projectiles like a propane tank, especially if the ground conditions are soft.

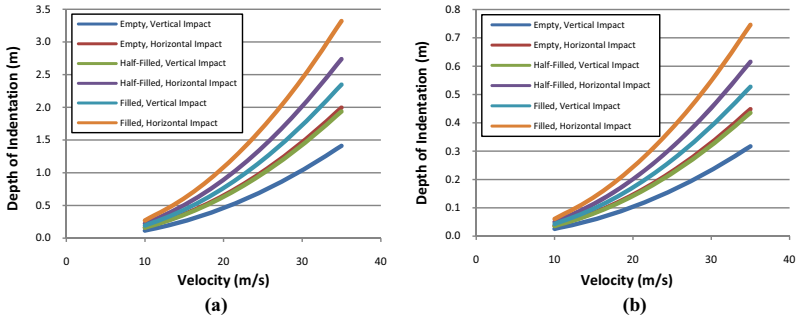

Figure 2. Predicted indentation depths for propane tank in (a) soft clay and (b) dense sand.

Table 2. Assumed Values for Calculating Depth of Indentation of Propane Tank

Radius, r_0 (m)	Drop Height (m)	Mass (kg)	Shear Modulus (MPa)
0.235 [horizontal] 0.470 [vertical]	10	500 [empty] 1,000 [half-filled] 1,500 [filled]	2.0 [soft clay] 37.5 [dense sand]

Depth of Penetration. A sample set of penetration charts is illustrated in Figure 3 for two slender objects, a wooden plank and a hollow aluminum pole. These are common objects that can be found in and around homes or on construction sites. These two objects have different mass, dimensions, shape, and material properties. For the hollow pole, the outside diameter was used to calculate the cross-sectional area since the object, after penetrating the ground, is assumed to be filled with soil creating a soil plug. The shape of the end penetrating the ground was projected to be either flat or an ogive shape. The ogive shape was assumed to represent a splintered wooden plank and the compressed or fractured end of an aluminum pole. The same two soil conditions were assumed: soft clay and dense sand. Each soil has a corresponding soil factor as presented in Young (1969). Table 3 shows the values used in the calculations.

Depths of penetration are plotted as a function of increasing velocities using Equations 5 and 6. Impact velocities were modeled up to 97.5 m/s (320 ft/s) to account for projectile velocities that might be generated from an EF4 or EF5 tornado. A nuclear site safety analysis to assess potential projectile penetration through pipelines might consider such high velocities for worst case scenarios.

It is apparent that projectile shape and soil media have a significant influence on the depth of penetration. The wooden plank with an assumed ogive shape had the greatest penetration depth; it was almost twice as deep as the others. Penetration in dense sand is predicted to be less than 1 m even in the worst case scenario. Penetration in soft clay, however, is predicted to be on the order of meters and as deep as 14 m. However, one must keep in mind that these predictions do not account for increased side frictional resistance that will develop as depth of penetration increases.

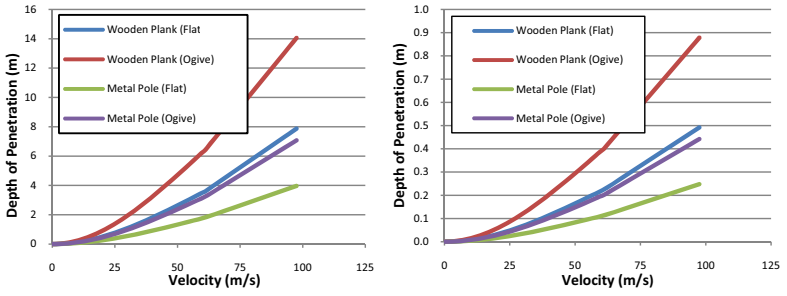

Figure 3. Predicted penetration depths in (a) soft clay and (b) dense sand.

Table 3. Assumed Values for Calculating Depths of Penetration

Object	Weight, lb (kg)	Area, in^2 (10^{-3} m^2)	Nose Coefficient	Soil Constant
Wooden Plank	15 (6.80)	5.25 (3.39)	0.56 [splintered] 1 [intact]	40 [soft clay] 2.5 [dense sand]
Metal Pole	2 (0.90)	2.76 (1.78)		

CONCLUSIONS

The Enhanced Fujita Scale provides a more detailed observational method for tornado classification based on structural damage. However, it does not include missile transport and impact in its determination of degrees of damage. It also does not include surface infrastructure, such as pavements, parking lots, culverts, ditches, embankments or other ground surfaces in its list of damage indicators. There is evidence of ground damage from tornado-borne projectiles, ranging from small debris like wood boards to large objects like cars and trucks. Evidence is qualitative and limited to eyewitness accounts, brief commentaries, photographs and video images. Empirical and theoretical studies provide a better understanding of the mechanics of missile transport and impact, but there remains a need to collect quantitative field measurements for comparison to prediction models. Damages incurred from projectiles can be direct, such as visual evidence of ground surface penetration or indentation, or indirect, where visual evidence at the ground surface is difficult to obtain. In all cases, the extent of ground deformations is a function of

projectile characteristics, projectile velocities, and ground conditions. With this information, correlations between ground damage and wind speeds can be formulated such that ground damage assessment can be considered for inclusion in the Enhanced Fujita Scale.

ACKNOWLEDGEMENTS

This research was supported through the Louis Stokes South Carolina Alliance for Minority Participation (LS-SCAMP) program. The authors wish to acknowledge Mr. Mark Malsick, Severe Weather Liaison, State Climate Office, South Carolina Department of Natural Resources and Mr. Steve Naglic, Warning Coordination Meteorologist, National Weather Forecast Office in Columbia, South Carolina for their assistance.

REFERENCES

Ben-Dor, G., Dubinsky, A., and Elperin, T. (2003) "Shape Optimization of Impactor Penetrating into Concrete or Limestone Targets." *International Journal of Solids and Structures.* 40 (17): 4487 – 4500.

Boguslavskii, Y., Drabkin, S., Jurin, I., and Salman, A. (1996a) "Theory and Practice of Projectile's Penetration in Soils." *ASCE Journal of Geotechnical Engineering*. 122 (10): 806 – 812.

Boguslavskii, Y., Drabkin, S., and Salman, A. (1996b) "Analysis of Vertical Projectile Penetration in Granular Soils." *Journal of Physics D – Applied Physics*. 29 (3): 905 – 916.

Byers, R.K., Yarrington, P., and Chabai, A.J. (1978) "Dynamic Penetration of Soil Media by Slender Projectiles." *International Journal of Engineering Science*. 16 (11): 835 – 844.

Chen, X.W. and Lia, Q.M. (2002) "Deep Penetration of a Non-Deformable Projectile with Different Geometrical Characteristics." *International Journal of Impact Engineering*. 27 (6): 619 – 637.

Corbett, G.G., Reid, S.R., and Johnson, W. (1996) "Impact Loading of Plates and Shells by Free-Flying Projectiles: A Review." *International Journal of Impact Engineering.* 18 (2): 141 – 230.

Costello, J.F., Simiu, E., and Cordes, M. (1977) "Tornado-Borne Missile Speeds." *ASCE Journal of the Structural Division*. 103 (6): 1275 – 1288.

Dunn, W.L. and Twisdale, L.A. (1979) "A Synthesized Windfield Model for Tornado Missile Transport." *Nuclear Engineering and Design.* 52: 135 – 144.

Iotti, R.C. (1975) “Design Basis Velocities of Tornado-Generated Missiles.” *Transactions of the American Nuclear Society*. 21: 351 – 353.

Kar, A.K. (1978) “Impact Load for Tornado-Generated Missiles.” *Nuclear Engineering and Design*. 47 (1): 107 – 144.

Kar, A.K. (1979a) “Residual Velocity for Projectiles.” *Nuclear Engineering and Design*. 53 (1): 87 – 95.

Kar, A.K. (1979b) “Loading Time History for Tornado-Generated Missiles.” *Nuclear Engineering and Design*. 51 (3): 487 – 493.

Labiouse, V., Descoeudres, F., and Montani, S. (1996) “Experimental Study of Rock Sheds Impacted by Rock Blocks.” *Structural Engineering International*. 3 (1): 171–175.

Mayne, P. and Jones, J.S. (1983) “Impact Stresses During Dynamic Compaction.” *ASCE Journal of Geotechnical Engineering*. 109 (10): 1342 – 1346.

Peila, D.C., Oggeri, C., and Castiglia, C. (2007) “Ground Reinforced Embankments for Rockfall Protection: Design and Evaluation of Full–Scale Tests.” *Landslides*. 4 (3): 255 – 265.

Pichler, B., Hellmich, C., and Mang, H.A. (2005) “Impact of Rocks onto Gravel Design and Evaluation of Experiments.” *International Journal of Impact Engineering*. 31 (5): 559 – 578.

Pichler, B., Hellmich, C., Mang, H.A., and Eberhardsteiner, J. (2006) “Loading of a Gravel-Buried Steel Pipe Subjected to Rockfall.” *ASCE Journal of Geotechnical and Geoenvironmental Engineering.* 132 (11): 1465 – 1473.

Rotunno, R. (1979) “Study in Tornado-Like Vortex Dynamics.” *Journal of the Atmospheric Sciences*. 36 (1): 140 – 155.

Warren, T.L., Hanchak, S.J., and Poormon, K.L. (2004) “Penetration of Limestone Targets by Ogive-Nosed VAR 4340 Steel Projectiles at Oblique Angles: Experiments and Simulations.” *International Journal of Impact Engineering*. 30 (10): 1307 – 1331.

Yew, C. and Stirbis, P. (1978) “Penetration of Projectile into Terrestrial Target.” *ASCE Journal of the Engineering Mechanics Division*. 104 (6): 1466 – 1469.

Young, C.W. (1969) “Depth Prediction for Earth-Penetrating Projectiles.” *ASCE Journal of the Soil Mechanics and Foundations Division*. 803 – 817.

The Enhanced Fujita Scale: Development and Implementation

James R. McDonald[1], Kishor C. Mehta[2], Douglas A. Smith[3] and J. Arn Womble[4]

[1]Professor and Chairman of Civil Engineering, Texas Tech University Wind Science and Engineering Research Center, Retired. email: mcdonald3182@sbcglobal.net
[2]Horn Professor of Civil Engineering, Texas Tech University Wind Science and Engineering Research Center, TTU, Lubbock, Texas 79409. email: kishor.mehta@ttu.edu
[3]Professor of Civil Engineering, Texas Tech University Wind Science and Engineering Research Center, TTU, Lubbock, Texas 79409. email: doug.smith@ttu.edu
[4]Wind Engineering Consultant, WindForce Associates, Inc./LNSS Assoc.; Instructor, Texas Tech University Wind Science and Engineering Research Center, TTU, Lubbock, Texas 79409. email: arnwomble@aol.com

ABSTRACT

The original Fujita Scale (F Scale) was introduced as a means of estimating the intensity of tornadoes and hurricanes by relating appearance of damage to wind speeds. The relationships were based on the extensive experience of Dr. Fujita but were never independently verified. Furthermore, the importance of construction quality was not recognized, and the number of damage indicators was limited. The Wind Science and Engineering group at Texas Tech University agreed to lead an effort to improve the original scale. The improved scale, known as the Enhanced Fujita Scale (EF Scale), defines 28 damage indicators and a number of degrees of damage for each one. A process of expert elicitation was used to relate estimates of expected, upper and lower bound wind speeds for each degree of damage. The Enhanced Fujita Scale was then correlated with the Fujita Scale by means of a regression equation. The National Weather Service implemented the Enhanced scale in February 2007. In its present form, the EF Scale is applicable only to tornado intensity.

INTRODUCTION

The Enhanced Fujita Scale (EF Scale) was implemented by the National Weather Service in February 2007 as the official measure of tornado intensity in the U.S. The EF Scale replaces the Fujita Scale (F Scale), which had been used since 1971. This paper identifies the need and traces the development and implementation of the EF Scale.

THE FUJITA SCALE

Dr. T. T. Fujita devised the Fujita Scale (Fujita, 1971) as a means of distinguishing weak tornadoes from intense tornadoes. Because of Fujita's

renowned reputation as a tornado expert, the new scale was almost immediately accepted as a standard for rating the strength of tornadoes. At the time, there was a keen interest in and need of defining the significant characteristics of tornadoes.

Using the analogy of the Beaufort Scale for describing ranges of wind speed, Fujita defined categories F0 to F12, which ranged from 40 mph to Mach 1. The practical range of wind speed expected in tornadoes is from F0 to F5. The common frame of wind speed reference at the time was the fastest-mile wind speed. Recognizing the importance of wind duration, Fujita reasoned that only a fraction of a mile of wind is required to destroy structures and trees. The F-Scale wind speed was thus defined as a fastest quarter-mile wind speed *at the height of the damage* above ground (Fujita, 1971). Note that standardized height and terrain were not utilized in the original F Scale.

Fujita then attempted to describe the type of damage one might expect for each wind speed range from F0 to F5. Table 1 summarizes the wind speed ranges and damage descriptions. A set of photos, which showed typical damage in each category, accompanied Fujita's damage descriptions. The damage associated with a category is assumed to be caused by winds in the range of the category. In assigning an F-Scale rating to a tornado, the most severe damage observed in the path was used as the basis for the rating.

NEED FOR IMPROVEMENT

While the Fujita Scale served a useful purpose over the years, various limitations and discrepancies have been documented. The correlation of appearance of damage and wind speed was never independently verified. The relationships were based on Fujita's considerable experience and judgment. The descriptions did not recognize variations in construction quality. The movement of large objects and pieces of debris had no analytical basis. Another limitation is the relatively small number of damage indicators mentioned in the descriptions, thus making it difficult to assign a rating when there is nothing in the path on which to base the assessment. A further concern was the general inconsistency in assigning F-scale ratings. In many cases, ratings by different individuals varied by one or more categories. One person might assign an F0 while another would call it F2 based on similar damage. Analytical calculations of wind speeds to cause certain damages indicate that the F-scale categories F3, F4 and F5 overestimate the wind speeds to cause the described damage (Minor, et al. 1977; Phan and Simiu 1998).

APPROACH

With the above-listed limitations and deficiencies, there was a general consensus that something needed to be done. Researchers at the Wind Science and Engineering (WISE) Center at Texas Tech University volunteered to address the problem. WISE personnel, including authors Mehta and McDonald, organized and coordinated an effort to improve the Fujita Scale or to develop an entirely new one. It was agreed that whatever was to be done must be done openly with all persons and organizations who had an interest and need for the Fujita Scale.

A steering committee co-chaired by authors McDonald and Mehta was organized with the purpose of setting goals, objectives and an initial plan of action. The steering committee confirmed the need for action on the F Scale and proceeded to organize a forum to define the problems and establish a strategy for improvement. Attendance at the forum was by invitation. Twenty-six persons who had some connection to the use and application of tornado technology were invited, and 23 attended the 1½-day meeting. The forum participants agreed with the steering committee's recommendation that the Fujita Scale should be modified (enhanced) rather than a new concept developed.

Table 1: Damage Descriptions of the Original Fujita Scale (Fujita, 1971).

F0	**40 – 72 mph**	**Light Damage**
	Some damage to chimneys and TV antennas; breaks twigs off trees; pushes over shallow-rooted trees	
F1	**73 – 112 mph**	**Moderate Damage**
	Peels surface off roofs; windows broken; light trailer houses pushed or overturned; some trees uprooted or snapped; moving automobiles pushed off the road	
F2	**113 – 157 mph**	**Considerable Damage**
	Roof torn off frame houses leaving strong upright walls; weak buildings in rural areas demolished; trailer houses destroyed; large trees snapped or uprooted; railroad boxcars pushed over; light object missiles generated; cars blown off highway	
F3	**158 – 206 mph**	**Severe Damage**
	Roofs and some walls torn off frame houses; some rural buildings completely demolished; trains overturned; steel-framed hangar-warehouse-type structures torn; cars lifted off the ground; most trees in a forest uprooted, snapped or leveled	
F4	**207 – 260 mph**	**Devastating Damage**
	Whole frame houses leveled, leaving piles of debris; steel structures badly damaged; trees debarked by small flying debris; cars and trains thrown some distances or rolled considerable distances; large missiles generated	
F5	**261 – 318 mph**	**Incredible Damage**
	Whole frame houses tossed off foundations; steel-reinforced concrete structures badly damaged; automobile- sized missiles generated; incredible phenomena can occur	
F6 – F12	**319 mph to sonic speed**	**Inconceivable Damage**
	Should a tornado with the maximum wind speed in excess of F5 occur, the extent and types of damage may not be conceivable.	

The forum agreed to the following strategies, which were followed throughout the study:

- Identify additional damage indicators
- Correlate appearance of damage and wind speed
- Preserve the use of the historical data base
- Seek input and consensus from users

The Wind Science and Engineering Center at Texas Tech University agreed to expedite the action plan formulated by the forum.

THE ENHANCED FUJITA (EF) SCALE CONCEPT

The EF Scale has the same format as the F Scale. The categories are EF0 to EF5, but the wind speed ranges are different. Damage indicators are still used but take on a different form. Twenty-eight damage indicators (DIs) consisting of buildings, structures and trees were defined. The buildings considered range from weak structures such as barns, manufactured homes and residences to very strong engineered structures. Canopies, poles and towers are included along with two types of trees. Each DI is carefully defined so it can be easily recognized in a damage path even if the structure is heavily damaged or destroyed. Table A1 in the Appendix lists all 28 DIs.

A new feature was introduced that significantly improves the EF Scale. For each DI, several Degrees of Damage (DODs) are defined. The DODs represent progressive steps of damage to a structure requiring increasing wind speeds. The damage ranges from initiation of visible damage to near or total destruction. This feature changes the paradigm in assigning intensity of a tornado: the EF Scale assesses wind speed based on damage; whereas the F Scale fit damage to predetermined wind speed ranges.

An expected value of wind speed is associated with each DOD under a set of "normal" conditions. For buildings, "normal" includes no glaring weak links in the load path, traditional construction quality, appropriate building materials, compliance with local building code and proper maintenance. Deviations from these normal conditions are taken into account by establishing a lower and upper bound wind speed in addition to the expected value for each DI. Conditions worse than the norm suggest an actual wind speed less than the stated expected value. Conditions better than the norm indicate the actual wind speed is greater than the stated expected value.

CORRELATION OF DAMAGE AND WIND SPEED

Correlation of damage and wind speed presented a challenge that had not been previously undertaken in the form presented here. Conventional measurements of wind speeds in tornadoes are nearly impossible. Structural calculations working backwards from damage to wind speed have been accomplished on a very limited basis. The amount of supporting data relating to the strength of components and structural systems would have been overwhelming for this project. Doppler radar

is capable of measuring wind speeds in tornadoes, but there has to date been little correlation with observed damage in the field. None of these conventional approaches provided a practical method for this effort.

EXPERT ELICITATION APPROACH

A method of expert elicitation was developed to estimate certain earthquake parameters that could not be measured either directly or indirectly. The Senior Seismic Hazard Analysis Committee (SSHAC, 1997) established a protocol for conducting the elicitation process. The group of experts making the elicitation is a sample of the population of all experts. Properly done, their results are considered the same as if all the experts made the assessments. The experts make their best estimates of the expected, lower and upper bound wind speeds to cause the damage described in the DODs of each DI. The individual estimates of the panel members are then averaged. Several rounds of estimates are made with discussions and guidance from a Technical Facilitator/Investigator (TFI), who conducts the elicitations and group interactions. A final step in the process is a peer review of the process and results.

ELICITATION RESULTS

The DODs are arranged in ascending values of expected wind speeds to form a scenario of progressive damage to the DI. As an example, Table 2 shows the information furnished for a one or two family residence: a description of typical construction, a table of DODs with their associated wind speeds and a plot of wind speed versus DOD. (The wind speed frame of reference is 3-second gust speed at 33 ft above ground in open terrain.) Similar tabulations can be found in WISE (2006) for the 28 DIs that make up the current set.

CORRELATION WITH FUJITA SCALE

Both the steering committee and forum made very clear that usefulness of the historical database of F-Scale tornado ratings (dating to the 1950s) was to be preserved. (Tornadoes prior to the 1970s were rated based on historical accounts of damage.) This meant that a correlation was needed between the Fujita Scale and the Enhanced Fujita Scale. A means of transforming the F-Scale rating of a tornado to the equivalent EF Scale was needed. To accomplish the correlation, a second panel of experts was assembled. National Weather Service (NWS) personnel were selected, who had extensive tornado damage investigation experience. Their objective was to assign a Fujita Scale rating to each DOD. The ratings were averaged and then converted to an expected wind speed by Fujita's F Scale versus wind speed equation (Fujita, 1971). The F Scale wind speeds were converted to equivalent 3-second gusts to be compatible with the EF Scale wind speeds.

Table 2. Damage Indicator Description: One- and Two-Family Residence.

Typical Construction Features

- Asphalt shingles, tile, slate or metal roof covering
- Flat, gable, hip, mansard or mono-sloped roof or combination thereof
- Plywood/OSB or wood plank roof deck
- Prefabricated wood trusses or wood joist and rafter construction
- Brick veneer, wood panels, stucco, EIFS, vinyl or metal siding
- Wood or metal stud walls, concrete blocks or insulating-concrete panels
- Attached single or double garage

Degrees of Damage

DOD	Damage Description	Wind Speed* (mph)		
		Expected Value	Lower Bound	Upper Bound
1	Threshold of visible damage	65	53	80
2	Loss of roof covering material (<20%), gutters and/or awing; loss of vinyl or metal siding	79	63	97
3	Broken glass in door and windows	96	79	114
4	Uplift of roof deck and loss of significant roof covering, material (>20%); collapse of chimney; garage doors collapse inward; failure of porch or carport	97	81	116
5	Entire house shifts off foundation	121	103	141
6	Large sections of roof structure removed; most walls remain standing	122	104	142
7	Exterior walls collapsed	132	113	153
8	Most walls collapsed, except small interior rooms	152	127	178
9	All walls collapsed	170	142	198
10	Destruction of engineered and/or well constructed residence; slab swept clean	200	165	220

*3-sec gust, open-country terrain, 10 m height

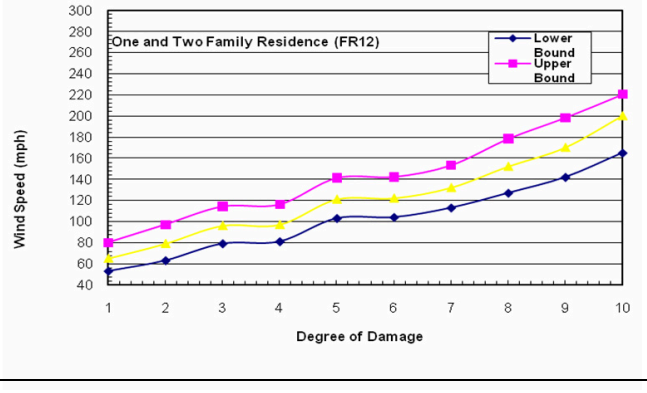

A plot of EF Scale wind speed versus F Scale wind speed for every DOD is shown in Figure 1 (WISE, 2006). Linear regression analysis of the data gives a correlation equation with a correlation coefficient of 0.91.

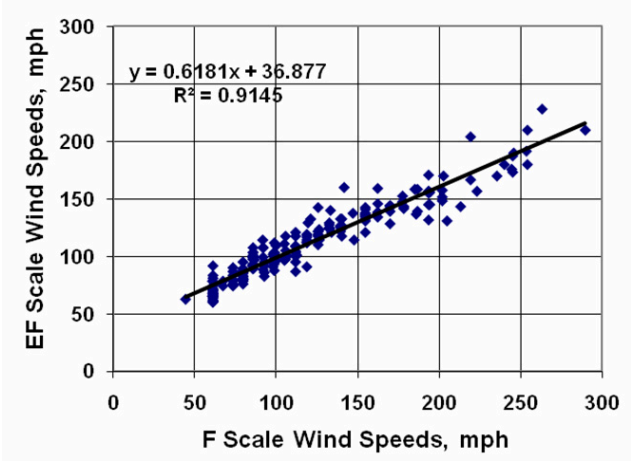

Figure 1. Correlation of Enhanced and Original Fujita Scales.

EF SCALE DEFINED

Using the regression equation, the wind speeds that define the F Scale ranges were converted to equivalent EF Scale wind speeds. These wind speeds define the EF Scale wind speeds in each category. The F Scale and the EF Scale wind speeds are compared in Table 3. In order not to imply more accuracy than justified, the final EF Scale wind speeds have been rounded to the nearest 5 mph as shown in Table 4. With this approach, a Fujita Scale "F3" translates to an "EF3", but the wind speed ranges are different.

Table 3. Correlation of F Scale and EF Scale Wind Speed Ranges.

Original Fujita Scale		Enhanced Fujita Scale	
Category	**Wind Speed* Range, mph**	**Category**	**Wind Speed* Range, mph**
F0	45 – 78	EF0	65 – 85
F1	79 – 117	EF1	86 – 109
F2	118 – 161	EF2	110 – 137
F3	162 – 209	EF3	138 – 167
F4	210 – 261	EF4	168 – 199
F5	262 – 317	EF5	200 – 234

*3-sec gust, open-country terrain, 10 m height

Table 4: Final EF Scale Wind Speed Ranges.

EF Scale Categories	Wind Speed* Range, mph
EF0	65 – 85
EF1	86 – 110
EF2	111 – 135
EF3	136 – 165
EF4	166 – 200
EF5	>200

*3-sec gust, open-country terrain, 10 m height

APPLICATIONS

The EF Scale is used to rate damage to individual buildings, structures and trees. The scale is also used by NWS personnel to rate the intensities of tornado events. The rating of an individual building in a damage path is accomplished by first identifying the DI that matches the building type and construction. The observed damage is then matched to the DODs. The highest DOD is used to estimate the maximum winds. The final step is to determine if conditions suggest the wind speed is lower or higher than the expected value for the controlling DOD. The observer makes a judgment based on the deviation of conditions from the norm and establishes the wind speed estimate for the observed damage. The assigned EF Scale rating of the damaged building is the one whose range of wind speeds contains the estimated value.

Rating a tornado event follows the same approach except several different buildings or structures are considered in estimating wind speed to cause the most intense damage in the tornado path. The NWS investigators generally conduct an aerial survey to identify potential DIs and to define the extent of the damage path. They identify two or more DIs that seemingly indicate the highest wind speed in the path. Their location is pinpointed within the damage path. The steps described for rating individual buildings or structures are followed to estimate the wind speeds. These results are considered in making an estimate of the maximum wind speed in the damage path. The EF Scale rating of the storm is assigned to the category that contains the estimated maximum wind speed. Pertinent data related to the tornado event are recorded, and an oversight committee reviews the results for an intense tornado before the EF Scale rating becomes official.

IMPLEMENTATION OF EF SCALE

After a thorough review of the proposal, the National Weather Service completed implementation of the EF Scale in February 2007. Training materials were developed to assist NWS field personnel in applying the EF Scale for rating the intensities of tornadoes. Several online training modules were developed. NWS personnel obtain certification by successfully completing the courses. More details of the research and methodology used to develop the EF Scale can be

found on the web site of the TTU Wind Science and Engineering Research Center (WISE, 2006).

IMPLICATIONS

The major improvements of the EF Scale are the more accurate wind speed ranges in each category because of the increased amount of detail that goes into determining the rating. As shown in Table 3, the wind speeds in EF3, EF4 and EF5 are less than the corresponding categories of the F Scale. This reduction has an impact on the results of tornado hazard assessments. For example, the U.S. Nuclear Regulatory Commission recently reduced the design wind speeds for nuclear power plants based on hazard assessments using the EF Scale wind speeds (USNRC, 2007).

The additional damage indicators and the introduction of degrees of damage will lead to more consistent ratings of tornado intensity. There will still be instances where no damage indicators are found that match the ones available today. Research is needed to explore other damage indicators that are commonly found in these open areas. Crops, other kinds of trees and vegetation as well as farm equipment and crop storage facilities need to be studied. These can be added to the DI list when sufficient evidence is available.

CONCLUSIONS

Continued use of the EF Scale by the NWS will lead to more consistent and more accurate estimates of tornado intensities. It corrects some of the deficiencies of the Fujita Scale, particularly the overestimation of wind speeds in the F3-F5 categories. More indicators are available for making the wind speed estimates, and there is provision for adding additional ones as the research data become available. The correlation between the F Scale and the EF Scale preserves the historical tornado records and makes it possible to use them consistent with future tornado occurrences.

ACKNOWLEDGEMENT

Funding for this effort was provided through the Windstorm Mitigation Initiative, a cooperative agreement between the National Institute of Standards and Technology and the Texas Tech University Wind Science and Engineering Center.

REFERENCES

Fujita, T.T. (1971). “Proposed characterizations of tornadoes and hurricanes by area and intensity”. SMRP 91, Department of Geophysical Sciences, University of Chicago, 42 pp.

McDonald, J.R. and Mehta, K.C. (2001). "Summary Report". Fujita Scale Forum, Wind Science and Engineering, Texas Tech University, Lubbock, TX, 36 pp.

McDonald, J.R. (2002). "Development of an enhanced Fujita Scale for estimating tornado intensity". Preprints, 21st Conference on Severe Local Storms, AMS, San Antonio, TX, August 2002, pp 174-177.

Minor, J.E., McDonald, J.R. and Mehta, K.C. (1977). "The tornado: An engineering oriented perspective". NOAA Technical Memorandum, ERL NSSL-82, National Severe Storms Laboratory, Norman, OK, p 103.

Phan, L.T. and Simiu, E. (1998). "The Fujita tornado intensity scale: a critique based on observations of the Jarrell tornado of May 27, 1997". NIST Tech Note 1426, U.S. Department of Commerce, Gaithersburg, MD 20 pp.

SSHAC. (1997). "Recommendations for probabilistic seismic hazard analysis: guidelines on uncertainty and use of experts". NUREG/CR-6372, UCRL-ID-122160, Vol. 1, Lawrence Livermore National Laboratory, Livermore, CA 133 pp.

USNRC. (2007). "Design-basis tornado and tornado missiles for nuclear power plants". Reg. Guide 1.76, Rev. 1, US Nuclear Regulatory Commission, Washington DC.

WISE. (2006). "A recommendation for an Enhanced Fujita Scale, Rev. 2.". Wind Science and Engineering Research Center, October 2006; www.wind.ttu.edu/EFScale.pdf.

APPENDIX

Table A1: Damage Indicators for the Enhanced Fujita Scale.

No.	Damage Indicator	No.	Damage Indicator
1	Small Barns or Farm Outbuildings	15	Elementary School
2	One- or Two-Family Residences	16	Junior or Senior High School
3	Manufactured Homes - Single Wide	17	Low-Rise Building (1-4 Stories)
4	Manufactured Homes - Double Wide	18	Mid-Rise Building (5-20 Stories)
5	Apartments, Condos, Townhouses	19	High-Rise Building (More than 20 Stories)
6	Motels	20	Institutional Building
7	Masonry Apartment or Motel	21	Metal Building System
8	Small Retail Building	22	Service Station Canopy
9	Small Professional Building	23	Warehouse Building
10	Strip Mall	24	Electrical Transmission Lines
11	Large Shopping Mall	25	Free Standing Towers
12	Large, Isolated Retail Building	26	Free-Standing Light, Luminary & Flag Poles
13	Automobile Showroom	27	Hardwood Trees
14	Automobile Service Building	28	Softwood Trees

Distinguishing Between Storm Surge and Wind Damages to Buildings and Structures

Charles R. Norman P.E.[1]

[1] Consulting Engineer, Private Practice, and Adjunct Professor at McNeese State University
P.O. Box 5715
Lake Charles, LA 70606 Email: charles_norman@bellsouth.net

ABSTRACT

This paper addresses methods and guidelines for assessing damages and distinguishing between damages caused by wind, flood and storm surge to homes and buildings from a hurricane event. These methods are based on an engineering approach that utilizes forensics, engineering science along with codes and standards to determine the extent of the damages and various causations. A general approach to the examination of the risks is outlined, and the elements that a report should contain are addressed. Emphasis is placed on the decisive role that corroborating information plays in determining the extent and proximate cause of damages.

INTRODUCTION

Engineers are often asked to inspect buildings and homes (risks) to evaluate the damages caused by a hurricane. These risks may include non engineered, marginally engineered, or pre engineered structures. Professional engineers have a point of view that deals with loads, structural resistance, degree of damage, mechanical and structural integrity, material strength, etc. The evaluation may be used to assess the amount of damages, methods of repairing the risks, safety of the risk, to determine if the risk is a constructive total loss or total loss, and to segregate or distinguish damages attributable to "wind" or to "flooding and storm surge". Typically engineers refer to adjusters or contractors to provide cost to repair.

The different approaches that engineers take depend upon the risk, the amount of damages to the risk, and the engineer. A home that is completely destroyed will be approached differently from a home with minor damages. However, the end result is to determine the amount of damages that were caused from the event and distinguish between damages caused by flood, storm surge and wind.

This paper presents an engineering approach to inspect homes and buildings, and methods of distinguishing between flooding, storm surge and wind related damages. These methods should be useful to inspectors, adjusters, engineers, architects, and owners to identify damages that must be repaired. In addition, the efficient or proximate cause of a total loss or constructive total loss may be determined.

EXAMINING THE BUILDING ENVELOPE

An engineering inspection should begin with documentation of the location and physical appearance of the structure (Figure 1). If the structure was destroyed by

a hurricane, a photograph(s), drawing, or detail description of the structure before the storm is critical. Research has shown that the building envelope plays a vital role in the performance of the structure to winds (Minor, J. E. 1997, 2005).

If available, aerial photos are useful. Also, document the physical address and exposure of the risk. Exposure is identified in ASCE-07. The tracking of the hurricane relative to the risk is required.

The exterior shape of the structure, type of roof, outside finish, location and type of windows, and attached structures such as carports should be identified. Attention should be paid to details of the roof such as age, gauge, number of nails per shingle, type of shingle, etc. This includes wind rating of roof, windows, etc.

If the home is on a slab, the pinning of the bottom wall plates, the thickness of the slab, footings, grade beams, post tension slab, etc. must be documented. If the home is on piers or piling, the size, height, location of piers, etc. must be photographed. For elevated structures, the bracing must be documented. In the case of wind and flood related damage assessments, the elevations of the grade, bottom floor or sill must be determined to evaluate the height of water entering the home.

Photographing structures around the subject risk is also helpful.

Figure 1. Documenting the envelope.

EXAMINING THE INSIDE

Once the outside has been documented, the inside must be inspected and documented. This includes photographing the inside ceilings, walls, doors, cabinets, floors, attic sections, insulation, and wiring for damaged and non damaged areas.

Some examples of damages to the inside include cracked sheetrock, wet insulation, separated molding and trim, cracked ceramic floor coverings, distorted walls and door frames, cracks in chimney, moisture and mildew behind walls, cracked glass, uneven cabinets, floors that vibrate, walls separated, etc. Also, all available rafters and rafter to top wall plate should be inspected. Documenting the bracing in the attic frame should be considered. (Figure 2)

A floor plan is required. Most of the time an insurance inspector will draw a floor plan. Sometimes the owner will have an engineering drawing of the floor plan. Other times, a professional foundation repair company will have drawn the floor plan. The overall size of the building envelope is critical to evaluating wind, flood, and storm surge related damages.

In the framing, the type of connections should be documented. This includes identifying hurricane clips and straps, bolting, and toe nail connections. The spacing and size of the rafters, ridge plate, decking, strong backs, cross bracing, type of insulation, etc. must be documented.

All of the above information is useful in determining the resistance of the risk to applied loads from tornadoes, hurricanes, floods, etc. It is also helpful for engineers to consider the weaker and stronger aspects of the structure in evaluating the extent and causation of the damages.

All water marks inside and outside a structure from flooding and storm surge should be identified and documented. It is important that water marks due to run up be distinguished from marks due to slow rising water.

Figure 2. Broken rafters and damage zone.

FOUNDATIONS

Foundations require special attention since they support the structure and also provide anchoring of the structure. Types of foundations include concrete slabs, piers (various types), structural frame with integrated pilings, etc. Structures may be on grade or elevated. Elevated structures require bracing and this must be evaluated and documented. For homes gravity set onto piers, termite plates must be considered in the design and resistance of the structure.

During the inspection of a home, unlevelness of the foundation, cracked slab and/or flooring coverings, out of plumb walls, etc. must be noted. If the structure is unlevel, then a professional foundation repair expert familiar with laser level or water level technology must be called to evaluate the structure. This data can be used by professional engineers to further evaluate the need for repair and repair plans.

Identifying the soil type and properties such as strength, composition, etc. must include in the evaluation an analysis of the resistance to movement from loads and flooding.

RESISTANCE RATING OF STRUCTURE

Structures may be rated for hurricane and tornado winds. The scale is F0 to F5 based on the Fujita scale now called the Enhanced Fujita (EF) Scale (Figure 3). The enhanced EF scale is a very useful method of rating the resistance of structures and also determining the degree of damage (DOD). (Figure3). Individual components such as roofs, siding, windows, and manufactured homes may be rated according to the EF scale. Individual components are often wind tunnel or wind speed rated according to the manufacturer. Pre-engineered structures are often wind

rated and this may be used to determine the resistance of a structure. Examples are metal buildings, flag poles, tall towers, and signs.

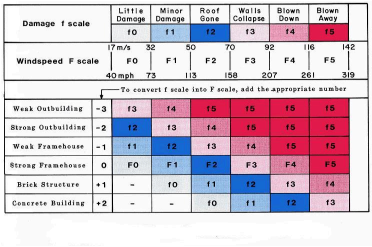

Damage f scale		Little Damage	Minor Damage	Roof Gone	Walls Collapse	Blown Down	Blown Away
		f0	f1	f2	f3	f4	f5
Windspeed F scale	17 m/s	32	50	70	92	116	142
	40 mph	73	113	158	207	261	319
To convert f scale into F scale, add the appropriate number							
Weak Outbuilding	-3	f3	f4	f5	f5	f5	f5
Strong Outbuilding	-2	f2	f3	f4	f5	f5	f5
Weak Framehouse	-1	f1	f2	f3	f4	f5	f5
Strong Framehouse	0	F0	F1	F2	F3	F4	F5
Brick Structure	+1	-	f0	f1	f2	f3	f4
Concrete Building	+2	-	-	f0	f1	f2	f3

Table 4.

One- and Two-Family Residences (FR12)

Typical Construction

- Asphalt shingles, tile, slate or metal roof covering
- Flat, gable, hip, mansard or mono-sloped roof or combinations thereof
- Plywood/OSB or wood plank roof deck
- Prefabricated wood trusses or wood joist and rafter construction
- Brick veneer, wood panels, stucco, EIFS, vinyl or metal siding
- Wood or metal stud walls, concrete blocks or insulating-concrete panels
- Attached single or double garage

DOD*	Damage description	EXP	LB	UB
1	Threshold of visible damage	65	53	80
2	Loss of roof covering material (~20%), gutters and/or awning; loss of vinyl or metal siding	79	63	97
3	Broken glass in doors and windows	96	79	114
4	Uplift of roof deck and loss of significant roof covering material (>20%); collapse of chimney; garage doors collapse inward or outward; failure of porch or carport	97	81	116
5	Entire house shifts off foundation	121	103	141
6	Complete removal of roof structure removed; most walls remain standing	122	104	142
7	Top floor exterior walls collapsed	132	113	153
8	Most interior walls of top story collapsed	148	128	173
9	Most walls collapsed in bottom floor, except small interior rooms	152	127	178
10	Total destruction of entire building	170	142	198

* DOD is degree of damage

Figure 3. See EF Scale at www.spc.noaa.gov/efscale/
Also see National Weather Service *Enhanced Fujita Scale* for examples.

Water forces may be calculated using principles from fluid mechanics. Water forces may be compared to wind forces in units of pounds per square foot. A major difference between wind and water are the physical properties such as viscosity, density, and speed. Using the weather data, a comparison between the two forces can be made. Also, the height of the forces reaching the structure must be included. For example, storm surge may not cover the entire envelope of the structure whereas wind may cover the entire envelope. It is important to identify the levels and areas of materials over which the different forces act. In other scenarios, a combination of both wind and water may reach the structure. Debris tracks and debris fields may be helpful in separating out damages from wind vs. water. Hurricane winds and storm surge may cause debris tracks in an entirely different directions.

IDENTIFYING THE DAMAGES

The engineer must be careful to identify all damages. Mistakes are created when damage is overlooked or omitted. A good example of this is a foundation. If the foundation is unlevel, repairs to a structure may not take or last very long. In some cases, it may not be possible to effectuate repairs unless the foundation is leveled. Another example is missing damages to a roof frame that has been racked or distorted. An attic frame that had little bracing and was damaged by severe winds may require mitigation to restore the mechanical and structural integrity. The damages must include distortion of the upper framing.

In general, damages can be grouped as follows (not all inclusive).

Structural: Structural includes damages to members such as overstressing, breaking, loss of joint strength, deck separation, separation of members, distortion of frame members, and movement or failure of foundation. Structural damages may also include a weakening of the structure due to fatigue or a complete collapse of a structure or structural member. Damages may not always be visible.

Mechanical: Mechanical damages include reduction in mechanical properties, failure in plumbing and HVAC, corrosion of materials, abrasion of materials and finish, water damage to insulation and sheetrock, separation of dissimilar materials, failure of roof materials and attachments, failure of windows, loss of seals, etc.

Cosmetic: Cosmetic damages include separation of trim and molding, cracking of paneling and sheetrock, failure of outside bricking or siding, loss of shutters, gutters, fascia, soffit, separation in wood floor coverings, water damages to inside contents from wind and infiltration, partially damaged roof.

Safety and Health issues: Mold and mildew issues. Handrail damage around porches, walkways and stairways, electrical wiring and plumbing issues, leaks in gas pipes, electrical riser damage, etc. Habitability (is the risk inhabitable?).

Environmental issues: Asbestos materials damaged, leaks in pipes, containment of environmental sensitive MSDS materials, etc.

Economic issues: Cost to comply with new codes, regulations, etc.

DOCUMENTING THE DAMAGES

Physical damages can be photographed. Some of the more difficult damages to photograph are small cracks in light materials, but these can be identified on the photographs. Most of the time more than one picture is needed to identify the damage. For example, pictures of several rafters to ridge plate connections or lifted decking are important. Outside pictures of damages are also important in using damage scales. (Figure 4)

Occasionally, a sketch of the damage is helpful. For example, a tree fallen onto a structure is usually sketched to show where the tree hit the floor plan of the risk and this is used to assess the damage zone. A section of a structure that has twisted relative to another section can easily be sketched. A contour map of the differential measurements of elevations of a slab or floor should be sketched.

Computer analyses of the damages can be useful. For example, when the wind or storm surge forces are imposed on a beam or a frame, a computer generated analysis with graphics may be useful. Floor and ceiling beams that are damaged from excessive loads due to wind can be analyzed by hand or using computer analysis to show the moments, loads, deflection, and stresses.

A complete structural analysis of the entire structure can be performed for damage assessment, primarily to support the physical evidence. These analyses are expensive and are not usually done unless requested. They are useful to determine how a structure fails and what the proximate cause of failure when two or more events load a structure. In many cases, component failure occurs prior to complete structural failure.

Satellite pictures can be useful to document damages to roofs and the amount of water infiltration and damage that was done to the inside of a structure. By locating the structure on satellite, the roof can be examined to assist in determining the extent of the degree of damage.

Water damage to wood materials is important to document. For example, the long term exposure of wood to outside elements such as rain and sun can reduce the mechanical strength of the timber members by 50%. This may result in sagging of

roof lines and ceilings. In addition, nailed wood connections are weakened and must be mitigated. Mold and mildew growth can also be documented. Experts in determining, measuring, and treating mold are called in to evaluate health risks to owners. Exposure of metal structures to saltwater can cause excessive corrosion of the materials and weaken the structure.

Figure 4. Documenting exterior damages from a fallen tree.

DATA FROM EVENT

A very important part of the engineering evaluation is to document the data from the event that caused the damage. For example, the magnitude and direction of hurricane winds along with the duration and timeline of the winds is important. The building envelope and angle of attack are crucial to understanding the performance of the risks to wind. In the case of the combination of two or more events, the time line for each event and the combination of events is important. For example, a hurricane that has hurricane force winds prior to the combination of wind and water forces must be documented. Tornadoes are rated using the EF scale for wind speed and damages. The National Weather Service, National Hurricane Center, NOAA, FEMA, the US Army Corps of Engineers and local authorities provide information on major events in the area of concern. In each of these events, considerable engineering data and science is available to provide the engineer with loads on structures. These sciences are provided in codes and standards such as the ASCE "Minimum Design Loads for Buildings and other Structures" ASCE 7-05. The engineer must utilize this information to assess the loads and timing of loads that caused damages to a structure. (Figure 6).

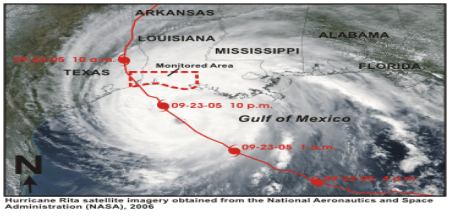

Figure 6. Satellite image of Hurricane Rita.

ROLE OF THE ENGINEER

The role of the engineer is to evaluate damages to the risk in terms of its design resistance, the magnitude of the loads and energy that reached the structure, the forensics available that show the damages and to use the loads and energy imparted to the structure to determine the extent of the damages. In the case of more than one event, each event and the combination of events should be included in the analysis. Also, all available information, data, forensics, and engineering methods must be corroborated to fully understand and evaluate the damages. In some cases this may be difficult to do. However, in all cases engineering methods must be employed to assess the damages.

Some of the questions that an engineer can consider in corroborating information for different events are

- What were the magnitudes and directions of the winds and moving water?
- How much water entered the risk and how fast was the water traveling?
- What was the timing of the wind vs. water?
- What is the sequence of damages?
- What were the barometric pressure readings near or at the site?
- Were hydrographs near the structure and what were the recordings?
- Were two or more water movements present at the site?
- What are the debris tracks and fields?
- Did the Army, etc. drop floating buoys ahead of the hurricane to measure winds, pressure, direction, etc?
- What are the characteristics of the damage in terms of material failures (broken, torn, twisted, fatigued, etc.)?

TOTAL LOSS

A complete loss of a risk can be a total loss or a constructive total loss. If the risk is destroyed by an event and only debris remains, it is a total loss. A constructive loss is a partial loss but the damage is so extensive that repairs would cost as much or more than the property is worth or the limit of insurance policy. Another constructive loss is a partial loss and the cost to repair and bring the risk to new required standards would exceed the value of the property. Also, the cost of repairs may exceed the cost to rebuild a completely new structure and the loss may be declared a constructive total loss.

In the case of a total loss, the engineer must consider the proximate cause of the loss. In the case of two or more events such as wind and water, the engineer must consider the timeline and magnitudes of the forces and energy for each event. If the timeline is not developed and considered, errors may occur in attributing the damages to each event. The risk shown in Figure 7 was a home located near the Gulf Coast and a major hurricane reached the site and destroyed the risk. In this case, the proximate cause of the constructive total loss was hurricane wind forces even though flood waters reached the home during the storm.

Opinions that are based solely on the magnitudes of the forces and energy from a narrow timeline may be subject to error. A better approach is to consider the damages to the risk as they occur. In other words, winds that attacked a structure for many hours prior to water reaching the structure must be considered separately for their damages. Although the structure may have been destroyed, the knowledge of the design resistance to wind may indicate that the structure failed due to wind loads prior to water reaching the structure. The same is true if water and wind reach a structure concurrently.

The risk in Figure 8 illustrates a total loss where wind alone loaded the structure for 10 hours, wind and water combined to load the structure for 5 additional hours, and the risk was declared a constructive total loss due to wind damages. Storm surge did not reach the bottom section of the risk.

A risk can also be declared uninhabitable due to an event prior to a second event. In a hurricane, a risk could become uninhabitable from wind prior to flooding.

Figure 7. House before and after Hurricane Rita.

Figure 8. Constructive total loss and forensic evidence showing winds.

Hinkley (2006) presented several guidelines for determining wind vs. water causation during hurricanes. Following is an outline containing several considerations that are consistent with the Hinkley guidelines.

- Determine engineering elevations of structure and surrounding areas. Old or new elevation certificates may be useful.
- Determine high water marks inside and outside. Distinguish between water marks that are flood, water run up, splash, and wind driven water.
- Determine the distance of risk to coastline, tributaries, lakes, rivers, etc.
- Nature of soils supporting the structure.
- Rate the permeability of structure to water and wind.
- Evaluate the method and materials of construction. Determine the resistance rating in terms of equivalent pressure. Perform a component analysis of roofs, windows, doors, exterior walls, etc.

- Always observe nearby structures. Distinguish between structures that are pre engineered, marginally engineered, and non engineered.
- Identify precursors, i.e. damages that pre existed.
- Look for forensic evidence all around the site.

OTHER CONSIDERATIONS

In general, the engineer is trying to inspect and document damages to a risk before the risk has been disturbed. That is not always possible. However, photographs that others took can be used as well. In all cases, the engineer should visit the risk site and document the forensic evidence even though the site may have been disturbed. When a site visit is scheduled it is important for the owner to be notified and asked to attend the inspection. Without the owner's presence, errors may occur that effect the outcome of the investigation. Following are additional considerations.

- Engineers should be called early and free to investigate.
- Adequate time must be allowed for a thorough inspection.
- Engineers should be free to talk to the owner, adjuster, etc.
- All available information on the event should be provided.
- Engineers must keep in mind the safety of the risk, the protection of the economic assets of the owner, and the separation of damages from more than one event.

REPORT ON DAMAGE ASSESSMENT

The report on the damage assessment is the focal point of the investigation. It should address the scope of work and the findings and in some cases recommendations. The purpose of the report should be clearly stated. If the engineer is limited in the scope of work, this must be clearly stated. However, in most cases the engineer must be free to evaluate the damages and the causation of these damages for the entire risk. Limiting the scope of the investigation can influence the outcome. For example, limiting an investigation to a single event when more than one event occurred may result in errors in determining the proximate cause of the damages. Items to include in the report are

- Name, address, general location and date of examination.
- Persons attending the site investigation and reviewing the findings.
- Identification and timing of event(s) causing the damage.
- Role of the engineer or assignment given to engineer.
- Characterization of loads and or energy causing the damages.
- Characterization of the resistance of the risk to the event(s).
- Forensic data that is available. Document with photographs.
- Analysis of damages and extent of damages based on engineering methods.
- Findings along with summary & conclusions.

SUMMARY

Methods of assessing and separating wind and water related damages to risks by engineers are important to owners, insurance companies, mortgage holders, local, state, and federal governments, and persons interested in purchasing or repairing a damaged risk. Engineers should not exclude any part of a damage assessment since they need to examine the entire structure to determine the extent of the damages and the proximate cause of damages.

The proximate cause of damages is best determined using engineering methods based on the magnitudes of loads and energy, forensics, and the resistance of the structure and its components. Also, the timeline for the loads and energy imparted, particularly when more than one event reaches a structure, is a very important consideration.

The methodology in this paper has been applied to approximately 1200 different structures that were damaged by Hurricanes Rita and Katrina. These investigations helped determine damages attributable to both wind and water. More than 95 % of the cases have been resolved by separating wind and water damages. These methods are also being used in Hurricanes Humberto, Gustav, and Ike.

REFERENCES

ASCE. (2005). *Minimum Design Loads for Buildings and Other Structures*. ASCE 7-05, Reston, Va.

Hinkley, J. M. (2006). *Guidelines for Determination of Wind versus Water Causation of Hurricane Damage*. Forensic Engineering Conference, ASCE. Cleveland, Ohio

International Code Council (ICC). (2006). *International Building Code, and International Residential Code,* ICC, Falls Church, Va.

Minor, J. E. (1997). *New Philosophy Guides Design of the Building Envelope*. Proc., ASCE Structures Congress, ASCE, Reston, VA., 1-5.

Minor, J. E. (2005). *Lessons Learned from Failures of the Building Envelope in Windstorms*. J. Architectural Engineering.

National Weather Service. *Enhanced Fujita Scale*. Texas Tech University, June 2004. Lubbock, TX.

Norman, C.R. (2006). *Damage Assessments to Homes and Buildings from an Engineering Point of View*. ICC Conference, Orlando, Florida.

Cladding Performance of High-Rise Buildings in the Houston CBD during Hurricane Ike

Rolando E. Vega[1] and Robert C. Konz[2]

[1]ABS Consulting, 14607 San Pedro Ave., San Antonio, TX 78232; PH (210) 495-5195; email: rovega@absconsulting.com
[2]ABS Consulting, 16855 Northchase Dr., Houston, TX 77060, PH (281) 673-2735; email: rkonz@absconsulting.com

ABSTRACT

In 1983, Hurricane Alicia caused extensive glazing damage to high-rise buildings in the Central Business District (CBD) of Houston with fastest-mile winds reaching 80 mph (~94 mph 3-second gust). Twenty five years later, Hurricane Ike also passed near the Houston CBD causing significant glazing damage despite 15-20% lower wind speeds. Straightforward kinetic energy calculations of hurricane Alicia and Ike show that Ike can cause comparable or even more damage than Alicia if cladding components start failing at 60 mph (1-min) winds. While both hurricanes followed virtually identical headings, Alicia passed west of the CBD and Ike to the east, providing a unique opportunity to understand extreme wind environments in an urban area for different angles of attack. This paper discusses post-Ike glazing and rooftop appurtenance damage observed in sixteen high-rise buildings within the Houston CBD, including those affected during Alicia.

INTRODUCTION

Hurricane Ike made landfall at Galveston Island, Texas on September 13, 2008 with sustained winds of 110 mph. Hurricane Alicia in 1983 made landfall at the southwest tip of the Galveston Island. While both hurricanes followed virtually identical headings, Alicia passed west of the CBD and Ike to the east, as shown in Figure 1. Sixteen buildings were surveyed by ABS Consulting using ground and aerial observations. Damage to cladding and rooftop appurtenance damage are discussed.

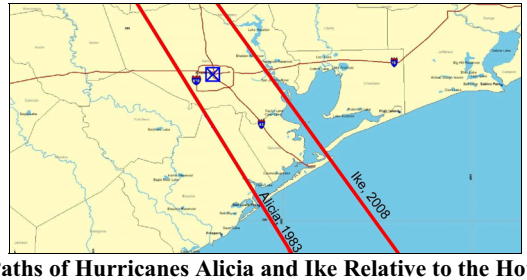

Figure 1: Paths of Hurricanes Alicia and Ike Relative to the Houston CBD.

Previous investigations of the Houston CBD after Hurricane Alicia [Beason et al. 1984; Kareem, 1986; Williams and Kareem, 2003] concluded that wind-borne

debris was the principal source of glass breakage and degradation. Further, several mitigation measures were recommended in hurricane-prone areas including prohibition of loose gravel roofing ballast, control of debris at construction sites, and better design for penthouse structures.

Post-event damage observations by ABS Consulting suggest that the extent of damage from Ike was similar to Alicia, wind-borne debris continues to be a principal cause of damage in urban environments, and localized atmospheric turbulence and interference effects need further study. For some time it has been recognized [Minor and Beason, 1976] that both local wind pressures and windborne missiles are principally responsible for the performance of window glass in windstorms. It should be noted that these potential causes of damage are not acting independently but rather in combination (e.g. local wind pressures may accelerate debris or produce glass failure thus transporting these missiles by the wind field or other localized wind phenomena to impact other building surfaces).

Current practice for wind design of new construction in the US is guided by ASCE 7 to avoid or reduce wind-borne debris risks in hurricane-prone regions. In such wind-borne debris regions impact-resistant glazing or protective coverings are required for certain portions of the building. A strict definition of "wind-borne debris regions" as currently defined by ASCE 7, exclude the Houston CBD. Since overall winds in the CBD reached only tropical storm speeds, a revised definition may warrant consideration.

WIND VECTOR AND KINETIC ENERGY COMPARISONS – IKE VS. ALICIA

Powell and Georgiou [1987] made a detailed assessment of the meteorology and structural response of the Allied Bank Plaza Tower during Hurricane Alicia. Wind speeds as a function of time could be approximated from the time-history presented in Powell and Georgiou with the exception that wind speeds were corrected to a standard height of 10 meters. Time-histories for Hurricane Ike can be approximated from the composite wind field created by H*WIND [Powell et al., 1998]. The H*WIND product assembles available measured data into a common averaging time, exposure and height and is made available online as a gridded file (and other formats). Using these corrected data for open terrain, approximated wind speeds and directions were estimated for a given latitude and longitude. Wind speeds and directions for Ike and Alicia were then plotted into a common time frame such that the magnitude and duration of the events could be compared in Figures 2 and 3. Note that while hurricane Alicia had a higher maximum wind speed, Ike had a longer duration.

A measure to compare damage potential between hurricanes is the Integrated Kinetic Energy (IKE) approach proposed by Powell and Reinhold [2007]. The IKE methodology is believed to better characterize damage potential due to wind and storm surge when compared to any other method because it uses more precise evaluation of the wind field in the entire storm domain and not just the maximum winds. Note in Figure 4 that despite the higher maximum wind speed during Alicia, Ike had a longer duration that produced comparable damage by winds associated with a tropical storm, i.e. 1-minute sustained wind speeds between 37 and 73 mph.

The kinetic energy approach does not take into account wind directionality. In Figure 3, the wind directions in the CBD for Ike and Alicia have counter-rotating direction shifts. For wind tunnel studies of asymmetrical floor plans, this becomes important. The wind directionality issue on hurricane-prone regions is in part considered by the random walk process of the Monte Carlo simulation approach used to produce the wind speed maps of ASCE 7. However, studies to assess the wind directionality issue probabilistically in hurricane-prone regions have not been exhaustive.

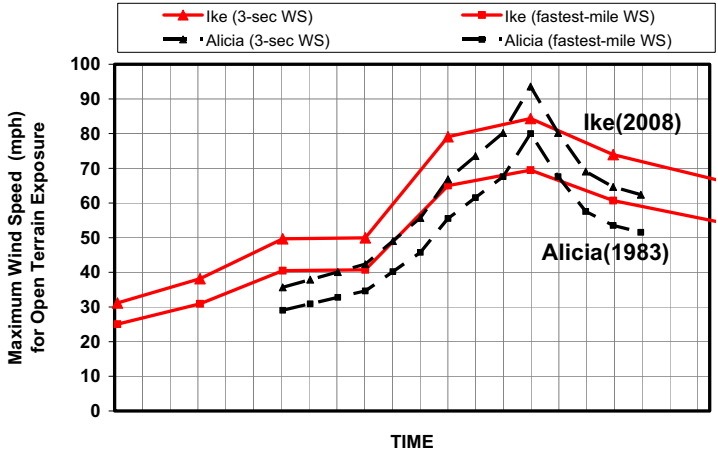

Figure 2: Wind Speed Time Histories for Hurricanes Alicia and Ike

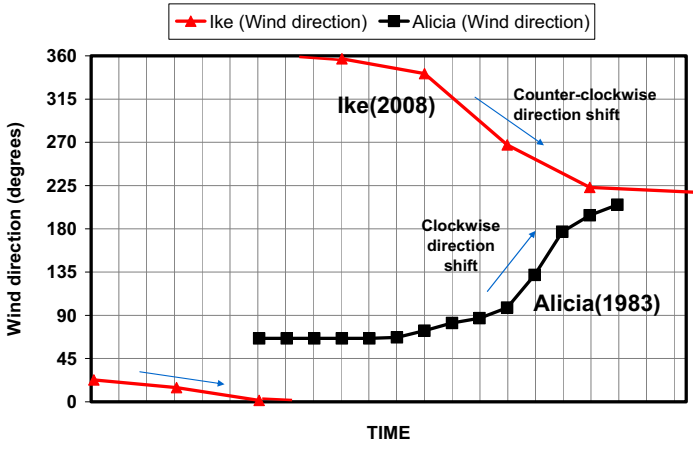

Figure 3: Wind Direction Time Histories for Hurricanes Alicia and Ike

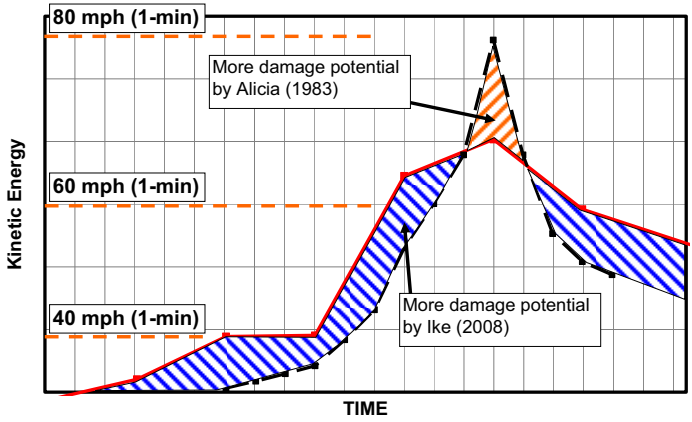

Figure 4: Kinetic Energy Potential Time Histories for Hurricanes Alicia and Ike.

OVERVIEW OF SURVEYED BUILDINGS

Damage assessment of the Houston CBD after Alicia focused on an area with significant damage along Louisiana Street. Major damage investigations involving Houston CBD included Beason, Meyers and James [1984], Kareem [1985], Kareem [1986], Powell and Georgiou [1987] and the Williams and Kareem [2003]. In general, their conclusions agree that windborne debris was the principal cause of damage. Furthermore, Beason et al. [1984] alludes to roof gravel of El Paso Energy (Tenneco) Building and other rooftop objects on the Total Plaza (Entex) Building becoming wind-borne debris. The shape of broken glass still in place after the storm suggested small-missile impacts and the predominant wind directions during the storm and the damage height correlation provided further justification. Table 1 and Figure 5 show the surveyed buildings during the assessment for hurricane Alicia in the Houston CBD.

During the damage survey of the Houston CBD after hurricane Ike ABS Consulting engineers performed aerial and ground surveys of several high-rise buildings. Several buildings exhibited “minor” (a few window pane failures), “moderate” (more than a few but probably unacceptable for the wind speeds), and “extensive” damage that goes beyond simple explanations from wind engineering concepts. Table 2 and Figure 6 show the surveyed buildings, damage level and related figures.

Table 1. Damage by Building from Hurricane Alicia

Bldg. No.	Bldg. Name in 1983 (2008)	Wind Damage From Alicia
1	One Shell Plaza	Some glazing damage breakage on the southwest face
2	Allied Bank (Wells Fargo)	Serious glazing damage on southeast and southwest faces below 40th floor
3	InterFirst (Enterprise Plaza)	Significant glazing damage on northeast and southeast faces
4	Hyatt Regency	Lost 80-100 windows including a few large panels at the northeast and southwest plaza level. Revolving rooftop restaurant lost a few large window panes.
5	Sheraton (Omni)	Significant glazing damage on northeast face
6	Entex (Total Plaza)	Glazing damage primarily along east corner of northeast face, particularly spandrel glazing
7	Milam (Centerpoint Energy)	Glazing damage primarily on northeast face at roof level of Tenneco Building
8	Tenneco (El Paso Energy)	No documented damage but mentioned as a considerable debris source

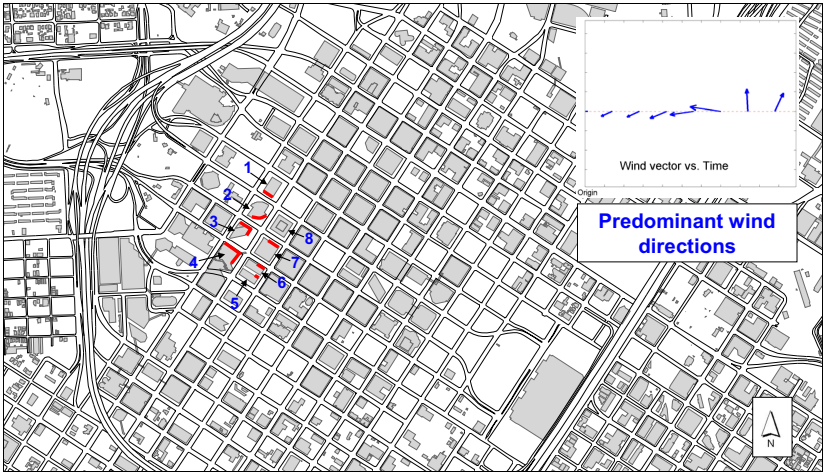

Figure 5: Damaged Buildings in the Houston CBD Surveyed by Kareem [1986] and Beason et al. [1984] in the Aftermath of Hurricane Alicia

Table 2. Damaged Buildings Surveyed by ABS Consulting After Hurricane Ike.

Bldg. No.	Bldg. Name in 2008	Bldg. Height	No. of Floors	Year Built	Damage Level
1	Chase Tower	305	75	1982	Extensive
2	Chase Center	73	20	1982	Extensive
3	Niels Esperson	125	32	1927	Minor
4	One Shell Plaza	218	50	1971	Minor
5	2 Houston Center	176	40	1974	Minor
6	Wells Fargo Plaza	302	71	1983	Extensive
7	El Paso Energy	153	33	1963	Moderate
8	Texaco Heritage Plaza	232	53	1987	Minor
9	Centerpoint Energy	226	47	1974	Extensive
10	Hyatt Regency	122	30	1972	Minor
11	Total Plaza	158	35	1971	Extensive
12	Three Allen Center	209	50	1982	Minor
13	One Allen Center	138	34	1972	Minor
14	1400 Smith Street	211	50	1983	Moderate
15	1500 Louisiana Street	183	40	2002	Extensive
16	Wedge International	168	43	1983	Heavy

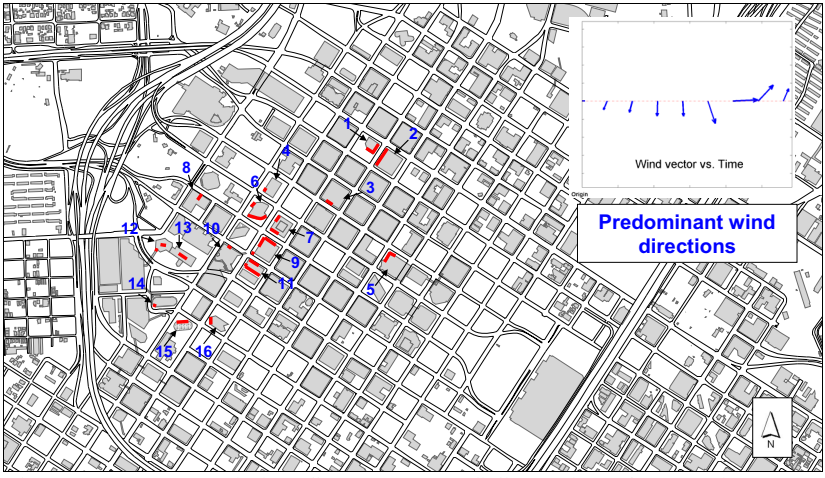

Figure 6: Damaged Buildings Surveyed by ABS Consulting After Hurricane Ike.

The 75-story JP Morgan Chase Tower suffered extensive glazing damage on the lower portion of the southeast face during reports of vortices by local news media. The following observations by the damage reconnaissance team from ABS Consulting support the formation of these reported vortices.

Figure 7 shows the relative locations of Chase Tower, Chase Center and the Calpine Center. An aerial view of the hypothesized wind flows in shown in Figure 8, and Figure 9 depicts the relative heights of Chase Tower and Calpine Center.

The wind tunnel study for the design of Chase Tower, completed in 1982, likely did not consider the upwind Calpine Center, built in 2003. The curved shape of the Calpine Center, capable of producing downwind vortices, may have been sensitive to the Reynolds number and perhaps, even in a wind tunnel study, may not be fully represented. As states, "Strict scaling of the mean wind and the turbulence Reynolds number for the approach flow is generally not possible for wind-tunnel model studies of buildings and structures." [Isyumov 1999]

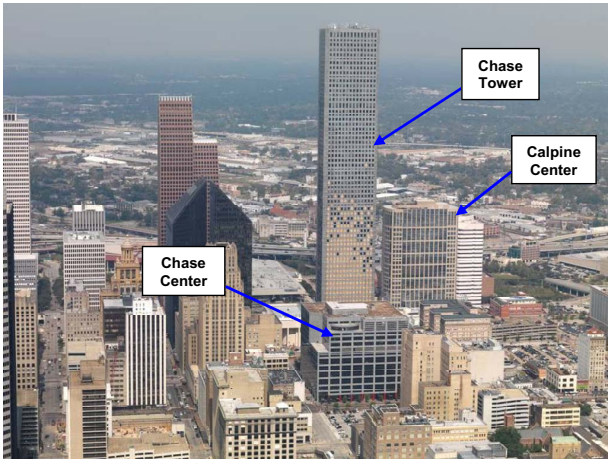

Figure 7: Southeast Face of Chase Tower with Chase Center in Foreground. ***(Photo by EQECAT/ABS Consulting)***

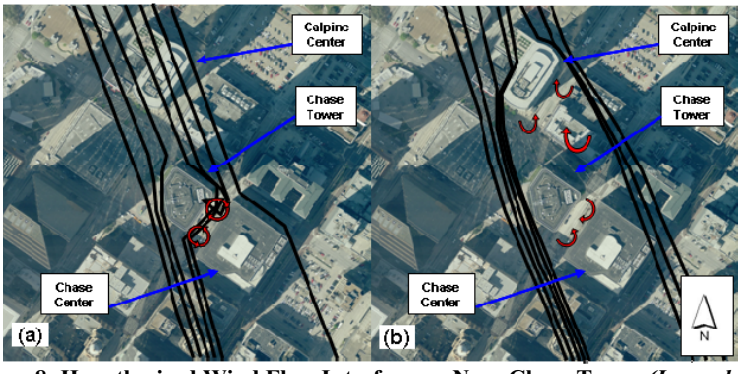

Figure 8: Hypothesized Wind Flow Interference Near Chase Tower ***(Image by ABS Consulting)***

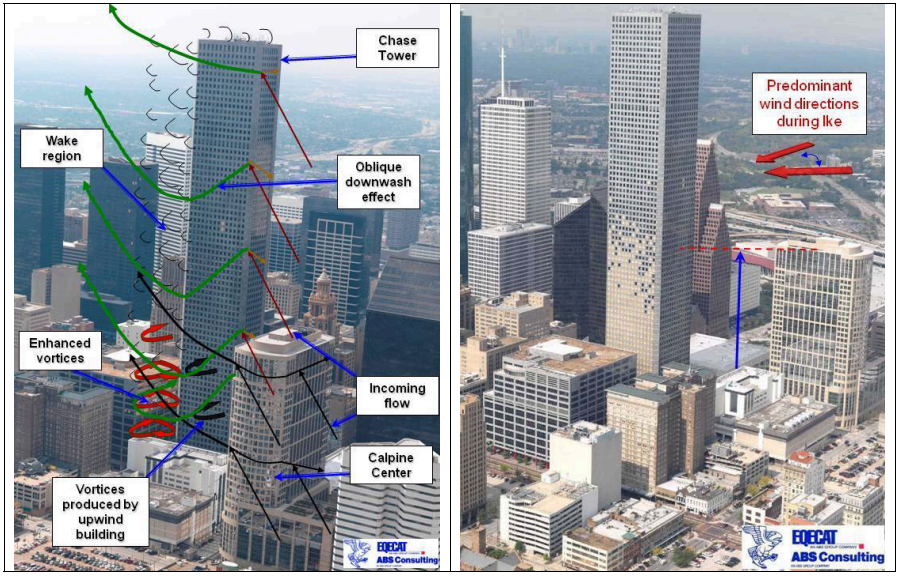

Figure 9. Hypothesized Wind Environment and Relative Heights of Chase Tower and Calpine Center.

Chase Center, located southeast of Chase Tower, sustained extensive cladding damage. Observed damage was concentrated on the northwest facade of the building; this damage could have been cuased by extreme wind flow recirculation, (between Chase Tower and Chase Center, carrying glass fragments of Chase Tower failed glazing.

Wedge International Towers, at 1400 Smith Street and 1500 Louisiana Street sustained extensive glazing damage (Figure 10 and Figure 12). Interference effects from adjacent buildings and wind-borne debris may have contributed significantly to the damage. The oblong tower at 1400 Smith experienced concentrated cladding damage along the curved southwest surface, perhaps an indication of relatively high negative pressures due to flow separation around the curved surface. The tower at 1500 Louisiana, also oblong, experienced cladding damage along the north facade.

Figure 10: Glazing Damage of Wedge International Towers ***(Photos by EQECAT-ABS Consulting)***

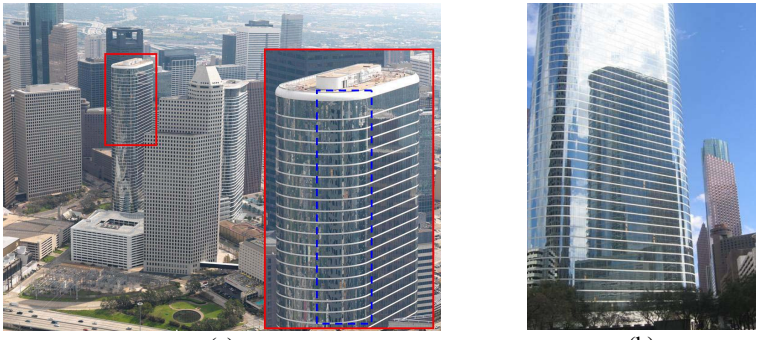

(a) (b)

Figure 11: Possible Flow Separation Line at 1400 Smith Street. ***(Photos by EQECAT-ABS Consulting)***

CONCLUSIONS AND RECOMMENDATIONS

- Wind speeds in the Houston CBD resulting from Hurricane Ike were equivalent to tropical storm intensities.
- Direction and duration of extreme winds, not just velocity, should be considered for the design of large buildings in urban environments.
- The Integrated Kinetic Energy (IKE) index proposed by Powell and Reinhold [2007] should be considered as a descriptor of damage.
- Current practice for wind design still results in significant cladding damage.
- Previous recommendations regarding avoidance of wind-borne debris sources are critical for acceptable building performance for urban areas in hurricane-prone regions.
- New policies or requirements are needed to investigate the effects of new construction to its surrounding urban environment or neighboring buildings.

REFERENCES

ASCE 7-05, Minimum Design Loads on Buildings and Other Structures, American Society of Civil Engineers. Reston, Virginia. 2006.

Durst, C.S., Wind speeds over short periods of time, The Meteorological Magazine, 89 (1960): 181-187.

Simiu, E. and T. Miyata, (2006), Design of Buildings and Bridges for Wind, New Jersey, John Wiley & Sons, 308.

Kareem, A., Performance of cladding in Hurricane Alicia, Journal of Structural Engineering, 112 (1986): 2679-2693.

Powell, M. D., S. H. Houston, L. R. Amat, and N Morisseau-Leroy, The HRD real-time hurricane wind analysis system. J. Wind Engineer. and Indust. Aerodyn. 77&78 (1998): 53-64.

Powell, M. D. and T. A. Reinhold, Tropical cyclone destructive potential by integrated kinetic energy. Bull. Amer. Meteor. Soc., 87 (2007): 513-526.

Powell, M. D. and P. N. Georgiou, Response of the Allied Bank Plaza Tower During Hurricane Alicia, Journal of Wind Engineering and Industrial Aerodynamics, 26 (1987): 231-254.

Isyumov, N., Wind Tunnel Studies of Buildings and Structures, ASCE Manuals and Reports on Engineering Practice No. 67. 1999.

Beason, W., G.E. Meyers, and R.W. James, Hurricane Related Window Glass Damage in Houston, Journal of Structural Engineering, ASCE. 110 (1984): 2843-2857.

Savage, R.P, Hurricane Alicia, Galveston and Houston, Texas, August 17-18, 1983, National Research Council (U.S.), Committee on Natural Disasters – Commission on Engineering and Technical Systems, National Research Council (1984).

Williams, T. and A. Kareem, Performance of building cladding in urban environments under extreme winds, 11th International Conference on Wind Engineering, Lubbock, Texas, June 2-5, 2003.

Minor, J.E., W.L. Beason, Window Glass Failures in Windstorms, Journal of the Structural Division, 102 (1976): 147-160.

Structural Evaluation Procedures and Case Studies of Damage Related to Wind Storms, Tornadoes, and Hurricanes

Kerry S. Lee, MBA, P.E., MASCE[1]
Jessica M. Caffey, M.S.[2]
Daniel M. Killian, B.S., P.E.[3]

[1] Director of Engineering, Nelson Architectural Engineers, Inc., 2740 Dallas Parkway, Suite 220, Plano, Texas 75093; email: klee@architecturalengineers.com; phone: 469-429-9000
[2] Senior Associate, Nelson Architectural Engineers, Inc., 2740 Dallas Parkway, Suite 220, Plano, Texas 75093; email: jcaffey@architecturalengineers.com; phone: 469-429-9000
[3] Project Director, Nelson Architectural Engineers, Inc., 2740 Dallas Parkway, Suite 220, Plano, Texas 75093; email: dkillian@architecturalengineers.com; phone: 469-429-9000

Abstract

This paper will discuss structural forensic investigative procedures used to assess wind storm damage, tornado damage, and methods to differentiate between hurricane wind and storm surge damage. Several structures or facilities are considered on a case study basis to determine commonalities and differences in the types and extent of wind-related damages. In several cases, comparisons to storm surge-related damages were conducted as part of the investigation.

This paper will address the factors impacting the types and degree of wind-related damages exhibited by each structure. Wind forces related to hurricanes, tornadoes, and wind storm events vary in strength, duration, and directionality; however, common wind-related damages were observed as a result of the differing wind events. Though commonalities in the types of damage were observed, the extent of damage varied depending on the type of construction, quality of construction, age of the structure, and orientation of the structure to the wind forces.

Investigation Procedure

In determining the cause and extent of distress to a structure damaged by a wind storm, tornado, or hurricane, a protocol of data collection is utilized. Once on site, it is standard to photographically document all observed distress and take plumbness data. Other valuable information in determining the cause and extent of damage include aerial photographs and relevant wind data.

There is no substitute for a site visit shortly after the storm event to accurately document the damage at the site. Being able to observe and document distress prior to repairs being made allows for more accurate data to be collected. Photographs should be taken in a systematic pattern.

Plumbness measurements are taken to check for structural racking. Aerial imagery can be an important factor if the subject site is not observed immediately following a storm event and prior to repairs. Weather data relevant to a specific storm and subject site is important in determining the effects of the wind on the subject structure. The directionality and wind speeds are important factors in determining if the distress observed is consistent with the storm event.

ANALYSIS

Photographs and Graphical Distress Mapping

Reviewing photographs of the observed distress and graphical mapping of distress on illustrations of the structure are important steps in assessing patterns of distress for comparison to storm data. In the event that the subject structure is not evaluated immediately following a storm event, aerial imagery, photographs taken by others, and any repair documents can play an important role in determining the pre and post-storm condition of the structure, and the cause and extent of damage. The comparison of the pre and post-storm aerial imagery can provide useful information on the pattern of distress at the roofing system.

Plumbness

The plumbness measurements are evaluated to determine if an overall pattern of out-of-plumbness exists at a structure which could indicate structural damage to the lateral load resisting system. When analyzing the plumbness readings it is important to look at the overall patterns or trends, such as movement in one direction or twist, which could indicate damage to the structural system.

Weather Data

Weather data relevant to a specific storm and subject site is important in determining the effects of the wind on the subject structure. The directionality and wind speed experienced at a subject structure assist in determining what types of distress would be expected at a specific structure; however, it should be noted that construction defects, design defects, and material defects often result in distress at lower than expected wind speeds.. The directionality and wind speeds are important factors in determining if the distress observed is consistent with the storm event.

Internal Pressure

Velocity pressure used in the design of a structure is outlined in section 6.5.10 of ASCE 7-05. The equation for design velocity pressure (q_z) is given in equation 6-15 of ASCE 7-05 as: $q_z=0.00256\ K_z\ K_{zt}\ K_d\ V^2\ I\ (lb/ft^2)$. K_z, K_{zt}, and K_d are all factors used to modify wind pressures due to structure height, wind directionality, and the surrounding topography. A basic 3-second wind gust speed (V) is also utilized.

The engineer must take the internal pressure coefficient into account per Equation 6-18 in the ASCE 7-05. Figure 6-5 in ASCE 7 provides the internal pressure coefficients for open, partially enclosed, and enclosed structures. The internal pressure coefficient for an enclosed structure is +- 0.18, where the internal pressure

coefficient for a partially enclosed structure is given as +- 0.55. This increased coefficient effectively triples the internal pressure in a partially enclosed structure compared to one that is considered enclosed. In addition, ASCE 7 commentary indicates that the internal pressure coefficient could be increased further. "Taken in isolation, the internal pressure coefficients can reach values of +- 0.8 (or possibly even higher on the negative side)." (ASCE 7-05)

During the exposure transition, design wind pressures on the windward wall and roof effectively transition from a positive pressure in the direction of wind flow to a negative pressure, acting in the opposite direction from the prevailing wind. In addition to the pressure reversal on the windward side, the pressures acting on the leeward side and ends of the structure increase by 60% and 63%, respectively. If an internal pressure coefficient of 0.8 is used, this increase in leeward pressure increases by an average of 200% from the values obtained for an enclosed structure. "An opening on the windward face of the building can also lead to a failure by allowing positive pressures to occur that, in conjunction with negative pressures, can 'blow the building apart.'" (FEMA, 2000)

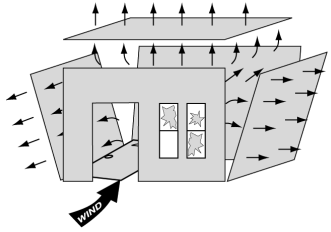

Figure 1. Building Failure Due To Internal Pressurization (FEMA, 2000)

Structures can transition from an enclosed to partially enclosed condition as openings in the building envelope are created. Such openings can be created by flying debris damaging windows and doors. "When glazing is breached by missiles, development of high internal pressure results, which can overload the cladding or structure if the higher pressure was not accounted for in the design." (ASCE 7-05) This immediate pressure increase can have a "popping" effect on the building's connections, significantly weakening and possibly failing them if the connections were not designed to withstand the additional force. "Building failures occur when winds produce forces on buildings that the buildings were not designed or constructed to withstand. Failures also occur when the breaching of a window or door create a large opening in the building envelope. These openings allow wind to enter the buildings, where it again produces forces that the buildings were not designed to withstand." (FEMA, 2000)

Lateral Loads

During a windstorm event residential structures are subjected to lateral loading in the form of wind, storm surge, or a combination of both. If the loads are not successfully transferred, failure of the structure may occur.

The magnitude of lateral loading associated with wind is dependent on the height of the structure above grade and the velocity of the wind. Wind velocity increases at higher elevations above grade. In addition, when the wind velocity is increased, the air pressure exerted on the structure during a given time period increases, thus increasing the magnitude of the lateral force applied on the structure.

Lateral forces related to storm surge are resisted by a structure in a similar manner. As the depth of the storm surge rises, the water on the exterior of the structure creates an increasing lateral force on the structural framing.

Due to the differences in the density of air and water, the lateral loading related to storm surge is typically far greater than that related to wind on a given area. The density of dry air at sea level is approximately 1/800 the density of water. Therefore, if wind and water moving at the same velocity impact a surface, water will impose a force several magnitudes greater than wind.

Case Study 1

Eight school campuses in southern Louisiana were impacted by Hurricane Rita in September 2005. Observations at the campuses were not performed until August 2006. At the time of the investigations, repairs had been performed or complete facilities had been demolished. This made the aerial imagery and photographs taken by others immediately following the storm key in determining the condition of the structures after the storm event.

During the site investigation, photographs were systematically taken to document the condition of the remaining structures. Also, a plumbness survey was taken at the interior and exterior walls at the remaining structures. Post-storm photographs by others and aerial imagery were heavily relied upon in determining findings. Several of the campuses located at various locations along the gulf coast are discussed below.

School A

At School A, approximately three to six feet of storm surge was incurred at the structure. The post-storm photographs taken by others indicated that the south non-structural stack bond concrete masonry unit walls had collapsed in a manner consistent with being pushed inward at the bottom, which is indicative of storm surge damage as shown in Figure 2. Additionally, the post-storm photographs showed that the papers and posters in the classrooms were still attached to the walls, as shown in Figure 3, indicating that the winds were not strong enough to damage the papers taped or tacked, to the walls, much less a CMU wall.

Figure 2. Collapsed CMU walls

Figure 3. Papers still intact at interior

The aerial photos taken shortly after Hurricane Rita indicated that the high gymnasium flat roof was significantly damaged by wind. However, the aerial imagery did not indicate significant damage to the lower flat or metal sloped roofs. The plumbness survey performed did not indicate any evidence that the structure had been "racked" or displaced due to lateral wind pressures.

School B

School B was located further inland and incurred minimal water from storm surge. The post-storm photographs taken by others indicated a large amount of lost shingles at the sloped roofs. The post-storm photographs did not indicate any displaced flat roof membrane at the flat roof areas.

The plumbness survey performed did not indicate any evidence that the structure had been "racked" or displaced due to lateral wind pressures. However, separations and fractures were typical throughout the plaster, CMU, and brick walls. Mortar joint separations were typical at the corner intersections and above doors and windows. The majority of the separations and fractures had previously been repaired indicating evidence of long-term foundation movement. The CMU at the interior CMU walls were laid in a stack bond pattern with no interlocking of the walls. According to the construction drawings, the vertical cells of the CMU walls were unreinforced except for dowels into the foundation at the bottom of the wall at select locations. The construction drawings only indicated the placement of a single bond beam at the top of the walls. No intermediate bond beams or corner reinforcement were indicated. This lack of reinforcement and bond pattern provided minimal resistance to distress within the wall as a result of normal foundation movement and thermal effects.

School C
School C was located approximately two miles north of the Gulf of Mexico and incurred approximately eight to ten feet of water from storm surge. At the time of the investigation, the structures had been completely demolished; therefore, findings were all based on aerial photographs and post-storm photographs by others. The pre-storm aerial imagery indicated that several temporary classroom structures were located on the campus, adjacent to the main structure. The post-storm photographs by others indicated a large amount of debris in the roof joists. Additionally, the post-storm aerial imagery indicated that the south edge of the roofing was peeled back, consistent with storm surge damage. Based on the pre-storm and post-storm aerial imagery, it was apparent that any temporary classroom structures were completely destroyed by storm surge. Further, the post-storm photographs indicated that the wind-related distress was minor and limited to the higher roof areas of the structure.

School D
School D was located approximately four miles north of the Gulf of Mexico and 12 miles east of School C. School D incurred approximately ten to twelve feet of water from storm surge. At the time of the investigation, the structures had been completely demolished; therefore, findings were all based on aerial imagery and post-storm photographs by others. The post-storm photographs and post-storm aerial imagery indicated limited and minor wind-related damage to the flat roof system. Therefore, it was evident that the majority of the damage was related to the approximately ten to twelve feet of storm surge.

Case Study 1 - Conclusions
The type and quality of construction also impacts the extent of damage experienced at a structure. For example, at School A, the sloped metal panel roofs and lower flat roofs incurred far less damage than did the higher flat roof.

It is critical to document the distress and study the locations and the patterns; including evidence of previous repairs. For example, at School B, a large amount of mortar joint separations were observed throughout the facility; however, the plumbness survey did not indicate a pattern of lateral movement. A study of the locations of the CMU wall distress showed a highly consistent pattern to the distress and also many areas of previous repairs. The type of construction of the walls (stack bond CMU walls) was the primary cause of the distress; wide spread distress was observed within the walls as a result of normal foundation movement and thermal effects.

Finally, all of the schools' wind-related damages varied significantly from campus to campus, even the structures that were located relatively close to each other. Therefore, assumptions cannot be made of the post-storm condition of a structure based only on the condition of surrounding structures. The quality and type of construction; the age; the presence or lack of a good maintenance program; design,

construction and material defects; and the orientation of the building all play a central role in how much damage a building sustains from a wind storm.

Case Study 2

Several structures in Plaquemines Parish Louisiana were investigated for wind-related versus storm surge related damages as a result of Hurricane Katrina. Plaquemines Parish was located directly in the path of Hurricane Katrina. The area of Plaquemines Parish investigated is protected by a levee along the west side adjacent to the Gulf of Mexico and by a levee along the Mississippi river to the east. Breaches in the levee system were reported, but the exact location(s) of the breaches were not known.

Adjacent structures in the area were observed to be either heavily damaged with extensive wind distress to the roof, cladding systems, and framing systems, or to be completely destroyed. Many structures were observed to have floated due to buoyancy.

The cladding of the structures as well as the framing, was generally completely destroyed by Hurricane Katrina, as shown in Figure 4. Typically, the brick was observed to have fallen away from each face of the structure while the wood wall framing and windows ranged from partially intact to completely collapsed, as shown in Figures 4 and 5.

Figure 4. Typical condition of remaining structure

Figure 5. Brick veneer distress

Figure 6. Typical roof distress

The roofs of the structures investigated were observed to be completely dislocated

from the structure and some of the roofs were observed to have been deposited on the ground, while others were completely gone. Additionally, extensive wind damage was observed to the roof shingles at the displaced roof systems, as shown in Figure 6.

Overall, measured wind speed information was not available for Plaquemines Parish. It was evident that the wind gust speeds at the sites were in excess of 100 mph; the closest measured wind gust was 114 mph recorded at the Grand Isle Buoy (approximately 25 miles southwest from the structures). Further, the NOAA National Climactic Data Center (NCDC) indicated sustained winds of 127 mph at landfall. Based on observations at the site, the forces from the wind were structurally significant.

The subject structures indicated common evidence of structures that had burst, or effectively exploded consistent with internal pressure build-up. The brick veneer on the structures was typically observed to have fallen outward from each face of the structure, which is consistent with a bursting or explosion of the structure due to high wind forces.

The entire roof system at the subject structures observed in Plaquemines Parish, including the attic framing and decking, were typically dislocated from the structures. Based upon site observations, it was evident that the structural destruction to the structures observed was the result of high wind forces with a subsequent contribution from storm surge.

Case Study 3

A residential structure in North Texas was impacted by high winds and tornadic activity. The damage observed at the subject structure was isolated and the surrounding structures and trees were effectively undamaged, showing the power and selectivity of a tornado.

The north pitch of the structure was severely damaged with large portions of the roof decking and rafters displaced from the northwest and northeast planes of the roof and deposited into the yard at the east elevation (Figure 7). Missing and fractured rafters, ridge beam, and hip and valley members were observed at the north side of the structure as shown in Figure 8. Minimal damage was observed at the south pitch of the roof framing system.

Figure 7. Condition of structure

Figure 8. Roof framing distress

Case Study 4

Over 30 residential structures located on Port Bolivar, Texas were evaluated after Hurricane Ike. The structures evaluated were typically elevated one and two-story structures supported by wood pilings. Elevation heights taken from available FEMA flood elevation certificates were compared with actual in-field measurements of elevated structural components above grade. Based on the comparison of in-field measurements and available survey data, the height of the storm surge was approximated to be in excess of 20 feet above sea level.

Typical observations at the ground level of the structures included undermined concrete seal-slabs, displaced and missing breakaway wall framing, and in some cases, a significant amount of soil scouring and erosion (Figure 9). The exterior siding and any impacted wood framing was typically displaced by storm surge and wave action. In addition, many of the wood pilings were displaced as the deck support framing was removed (Figure 10). Roof distress was typically limited to isolated areas of loose and missing shingles.

Figure 9. Erosion of soil

Figure 10. Missing/displaced framing

A plumbness survey was performed at each structure at the structural wood pilings and at the interior walls of the structure. Only a few of the structures observed indicated lateral movement consistent with structural damages related to lateral pressures associated with either wind or storm surge beneath the structure. In addition, perceptible lateral movement was experienced in two of the structures where an extensive amount of soil scouring was observed below the structure.

The wind speeds at the sites reached approximately 90 – 100 mph (3-second gust). Based on observations and measurements at the sites, the forces from the wind did not cause significant lateral movement of the structures. Additionally, lateral pressures exerted on the structures related to storm surge did not cause significant lateral movement of the structures. Although an extreme amount of destruction was observed on the Bolivar Peninsula, relatively little damage was observed on well built structures that were elevated higher than the storm surge.

CONCLUSION

A protocol of data collection is required when evaluating the cause and extent of distress to a structure damaged by a wind storm, tornado, or hurricane. Photographing and graphically mapping the observed distress at a site creates permanent evidence of the condition of the subject structure and the pattern of distress immediately following a storm event. However, reviewing documentation taken by others is commonly used to re-create the scene.

Wind forces related to hurricanes, tornadoes, and wind storm events vary in strength, duration, and directionality; however, common wind-related damages were observed as a result of the differing wind events. Though commonalities in the types of damage were observed, the extent of damage varied depending on the type of construction, quality of construction, age of the structure, and orientation of the structure to the wind forces.

The case studies presented herein show the different factors that affect the type and extent of distress a structure can experience during a wind event. Significant factors contributing to the extent of damage a structure incurs include the quality and type of construction; the age; the presence or lack of a good maintenance program; design, construction and material defects; and the orientation of the building all play a central role in how much damage a building sustains from a wind storm.

It is critical that proper structural forensic investigative procedures be used to assess damage and collect accurate and significant data. Further, the assessment of damage patterns established from site-specific data, observations, and documentation combined with weather data and other information sources allow for an accurate determination of the cause and extent of damage at a structure.

References

American Society of Civil Engineers (ASCE). 2005. *ASCE 7-05 Minimum Design Loads for Buildings and Other Structures,* U.S.A.: ASCE.

Federal Emergency Management Agency (FEMA). July 2000. *Design and Construction Guidance for Community Shelters*.

NOAA/National Climactic Data Center (NCDC). October 2005. "Hurricane Katrina: A Climatological Perspective Preliminary Report" (Technical Report 2005-01).

An Investigation of Building Damage Caused by Thunderstorm Winds

Scott M. Adan, Ph.D., P.E., S.E.[1] and Rene Luft, Sc.D., P.E., SECB[2]
and Nicholas G. Wetzel, P.E.[3]

[1]Senior Project Manager, Simpson Gumpertz & Heger Inc., The Landmark @ One Market, Suite 600, San Francisco, CA.; (415) 495-3700; email: smadan@sgh.com
[2]Senior Principal, Simpson Gumpertz & Heger Inc., The Landmark @ One Market, Suite 600, San Francisco, CA.; (415) 495-3700; email: rluft@sgh.com
[3]Staff II Structures, Simpson Gumpertz & Heger Inc., The Landmark @ One Market, Suite 600, San Francisco, CA.; (415) 495-3700; email: ngwetzel@sgh.com

ABSTRACT

In June 2004, thunderstorm winds caused significant structural damage to a downtown Tulsa, Oklahoma 15-story building. Damage was concentrated on the east facade of the building's multi-story glass atrium. The atrium is constructed with a framework of vertical steel trusses and horizontal struts. Eyewitness accounts from inside the atrium described a shaking or pulsing of the exterior glass curtain wall while wind gusts of up to 56 mph were recorded at a nearby weather station. On the building's sixth floor, the alternating wind pressures caused the failure of several horizontal strut connections. Without the horizontal support, the vertical structure deformed outward dislodging approximately thirty glass panels and damaging much of the surrounding structural support. In the ensuing investigation, a number of structural deficiencies and construction defects were uncovered in the curtain wall framework. This paper describes the sequence of events that led to the damage and summarizes the investigation's findings.

INTRODUCTION

By definition, a thunderstorm is considered severe when wind gusts exceed 58 mph (NOAA, 2004). In June 2004, winds from a severe thunderstorm caused significant structural damage to a downtown Tulsa, Oklahoma 15-story building. The damage was concentrated on the east facade of the building's multi-story glass atrium. As shown in Figure 1, the atrium is constructed with a framework of vertical steel trusses and laterally supporting horizontal struts. A system of horizontal steel girts connect and support the trusses in-plane.

The building core provides lateral support to the curtain wall structure with pinned horizontal struts, connecting the vertical steel trusses to adjacent concrete floor slabs. The horizontal struts are round structural steel tubes attached to both the building and the vertical steel trusses with stainless steel connection pins, retained by snap rings. At the building, the pins are connected to dual steel gusset plates (Figure 2a). The dual gusset plates are welded to a steel plate embedded at the edge of the floor slab. At the vertical steel trusses, the pins are connected to a steel clevis (Figure 2b). The building provides in plane lateral support to the curtain wall structure with two pairs of stainless steel cable cross braces, located at the end bays of the curtain wall (Figure 1b).

The vertical steel trusses are stacked one over the other and are supported vertically at the building's fourth floor. The vertical trusses typically span 32 feet between even numbered floors, except between the tenth and twelve floors where they span 36 feet. The vertical trusses are spaced 16 feet on center in the longitudinal direction. The horizontal tubular girts are spaced 8 feet on center vertically and connect to the truss chords with a seated steel angle connection.

A steel connector at each end of the truss attaches the upper and lower trusses, the horizontal struts, the horizontal girts, and any cable cross bracing (Figure 2b). This truss end connection (Figure 3) consists of four basic machined parts: an adjusting clevis; a truss jack base; a jack screw or toggle stud; and an adjustment or toggle bar. The toggle stud and the adjusting clevis permit vertical and horizontal field adjustment of the connection.

(a) (b)

Figure 1. Atrium curtain wall structure (a) vertical trusses and horizontal struts (b) horizontal cross braces

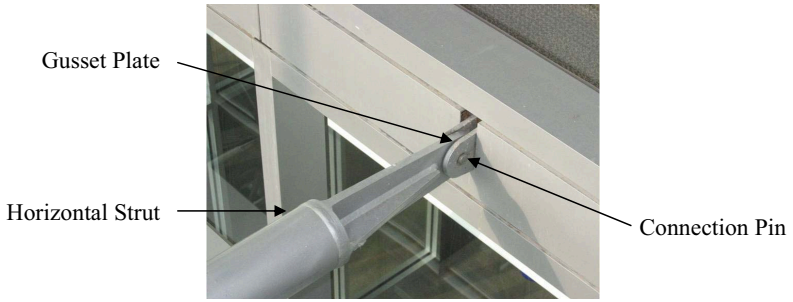

(a)

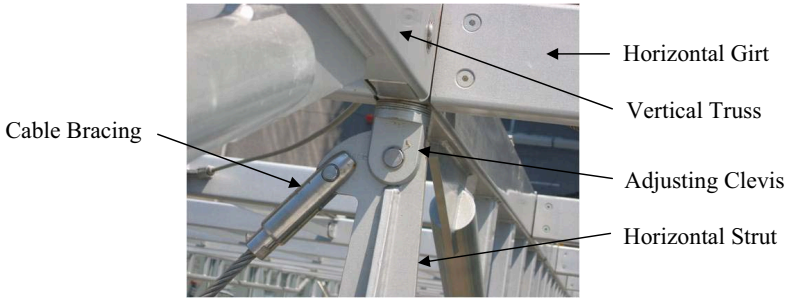

(b)

Figure 2. Curtain wall strut connections (a) interior to building slab (b) exterior to curtain wall

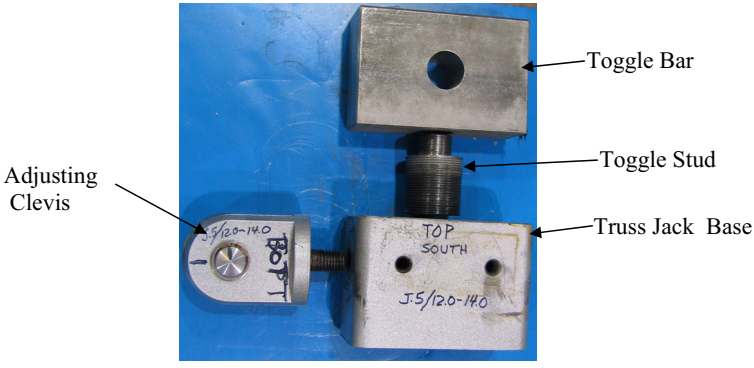

Figure 3. Truss end connection showing the adjusting clevis, the truss jack base, toggle stud and toggle or adjustment bar.

DESCRIPTION OF THE THUNDERSTORM

In June, 2004, a series of strong thunderstorms passed through the Tulsa, Oklahoma, metropolitan area. The thunderstorms generated severe winds within the downtown business district and caused widespread structural damage. As it passed through the Tulsa area, the storm's general direction was from northwest to southeast. However, wind direction within the storm varied widely and by significant amounts. Sustained wind speeds of 44 mph and gusts of up to 56 mph were recorded at the nearby Tulsa International Airport.

Based on records available from the surrounding weather stations as well as meteorological theory, a wind analysis of the event (by others) determined that peak wind velocities as high as 75 mph occurred in the downtown area. Due to storm microbursts, the wind direction oscillated between 340 and 25 degrees, and the oscillations occurred in a matter of seconds. Figure 4 shows a plan of the building with respect to the wind directions.

During the storm, eyewitness accounts from inside the building described a shaking or pulsing of the exterior glass wall. On the building's sixth floor, the alternating wind pressures caused the failure of several horizontal strut connections supporting the vertical steel trusses. Without support, the vertical structure deformed outward dislodging approximately thirty exterior glass panels and damaging much of the surrounding structural support as shown in Figure 5. The panels then crashed onto the street and sidewalk below.

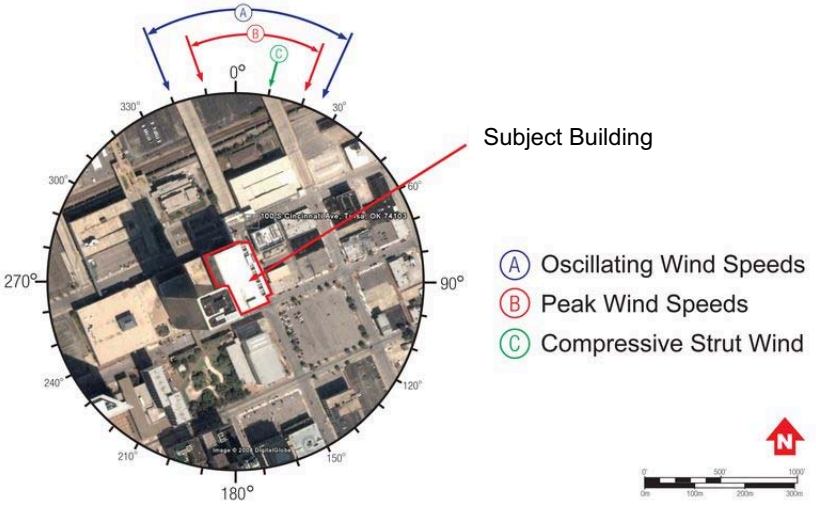

Figure 4. Wind directions relative to the building

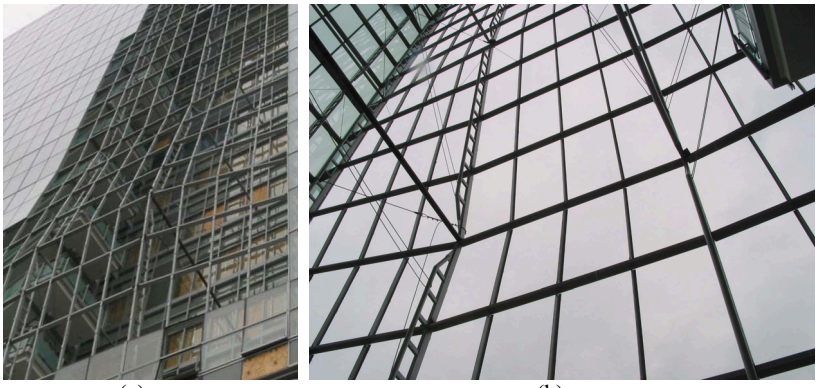

(a) (b)

Figure 5. Curtain wall damage (a) exterior and (b) interior view

WIND TUNNEL STUDY

A wind tunnel analysis (performed by others) following the event determined that areas of the curtain wall were subjected to strong turbulence from adjacent buildings. Figure 6 shows a partial sixth floor plan of the building structure where the damage occurred. The wind tunnel analysis concluded that the horizontal strut along Column Line "J" experienced strong positive (tension) forces for wind directions from about 300 to 20 degrees with a peak at about 340 degrees; and the same strut experienced strong negative (compression) forces for wind directions from about 0 (360) to 80 degrees with a fairly constant "peak" at about 30 to 50 degrees. In the cross over directions between 0 (360) to 20 degrees the struts could experience tension or compression.

The study concluded that the 340-degree wind direction and the 0-degree wind direction could alternate repeatedly within seconds, creating the oscillating effect reported by witnesses within the building. The wind study, therefore, showed that horizontal struts would rapidly alternate between tension and compression, and that the curtain wall would vibrate from only a 20 degree change in wind direction.

SITE INVESTIGATION FINDINGS

The primary damage to the curtain wall structure occurred nearest to the north corner of the building between Column Lines "J" and "K" (Figure 6). The steel trusses experienced severe lateral distortion between the fourth and eighth floors. The distorted shape simulated a three-dimensional bulge as shown in Figure 5, with the peak lateral displacement occurring at the sixth floor along Column Line "J.5."

Our investigation determined that two local structural failures triggered the damage to the curtain wall. Both failures occurred at horizontal struts which support the curtain wall structure in the lateral or east-west direction. The first failure

occurred when a connection pin at Column Line "J" at the sixth floor became disengaged from the gusset plates at the end of a horizontal strut (Figure 2a). The alternating tension and compression forces in the horizontal strut and consequential vibration, allowed the pin to "walk" out of its partially engaged position. Following the event, the pin was found inside one of the two connecting gusset plates. The connection pin was missing one of the two retainer clips. Figure 7 shows touch-up paint on both the pin and within the plate hole opposite the pin, indicating the pin was not fully engaged through both plates at the time of painting. Without the pin, the horizontal strut dropped down and away from the gusset plates. The opposite end of the strut remained attached to the exterior vertical truss, but the truss was no longer supported laterally.

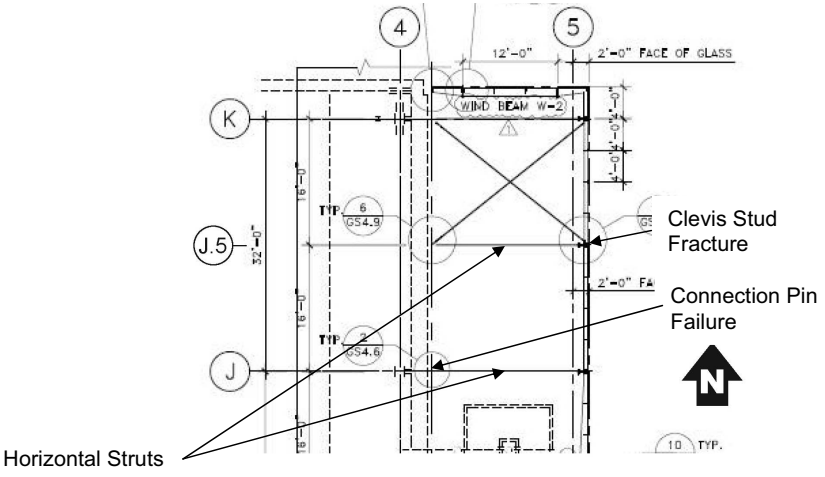

Figure 6. Sixth level partial framing plan.

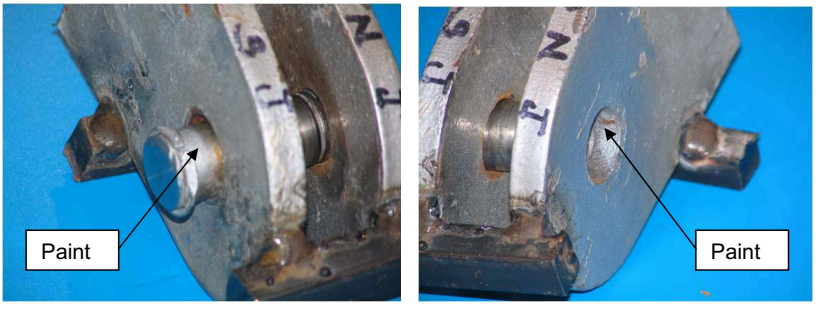

(a) (b)

Figure 7. Interior gusset and pin (a) left side (b) right side

A positive wind gust during and after the loss of lateral support of the vertical trusses distorted the horizontal tubular girt inwards and caused a rapid and dynamic rotation in the adjacent vertical truss framework (Figure 8). The distortion was measured at approximately 8 to 10 degrees. The rotation of the vertical truss along Column Line "J.5" was restrained by the horizontal strut. This rotation, due to eccentricity in the connection of the strut and the trusses, placed the strut in compression and the clevis stud in bending. The bending moment caused by the imposed rotation of the horizontal girt, places tension on the north side of the stud. This rotation and consequential bending caused the threaded clevis stud to fracture (Figure 9).

Following the stud fracture, the horizontal strut fell down and away from its attachment to the truss jack base, leaving the vertical truss at Column Line "J.5" without lateral support. The opposite end of the strut remained attached to the building.

As mentioned previously, the triggering wind gust, positive (inward) along Column Line "J" dislodged some of the glass panels around the vertical truss, and it caused the clevis stud at Column Line "J.5" to fracture. With the two adjacent vertical trusses now laterally unsupported, a subsequent negative wind gust pulled the curtain wall outward. In the failed framework, the outward movement at Column Line "J.5" is greater than the outward movement at Line "J." In addition, the damage close to Column Line "J.5" is more significant than at "J." This deformed shape is consistent with the initial disengagement of the pin along Column Line "J."

LABORATORY FINDINGS

The failed clevis stud fracture surface and orientation are crucial in the determination of the failure sequence. The clevis stud initially fractured under tensile stresses applied on its north side as Figure 9 indicates. The orientation or direction of the stud fracture is determined from the matching piece that remained in the truss end connection.

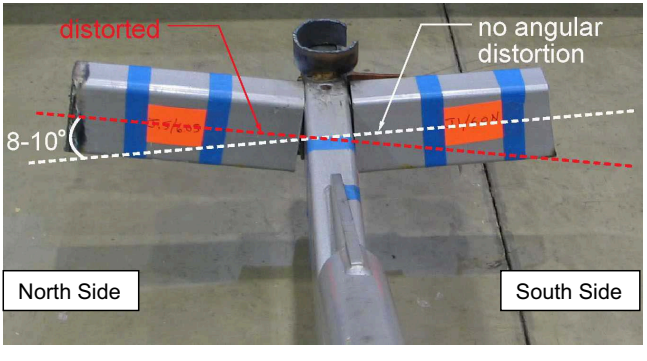

Figure 8. Column Line "J.5" truss and distorted horizontal girt

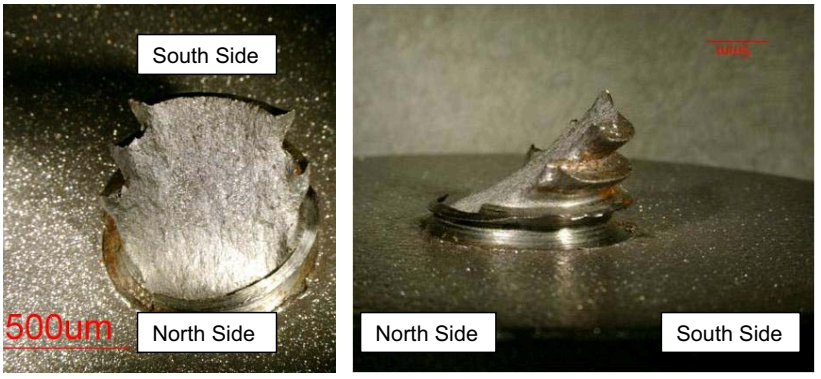

(a) (b)

Figure 9. Adjusting clevis stud fracture (a) front and (b) side microscopy view.

The fracture surface (Figure 9b) consists of two parts: a primarily tensile and a primarily shear component. Based on the orientation of these surfaces, we concluded the stud initially fractured under tensile stresses on its north side close to the 3-inch diameter disk of the clevis. The fracture surface indicates that the origin of the fracture is approximately 2-mm away from the clevis disk surface. The fracture then propagates at approximately a 45 degrees angle relative to the stud centerline; this propagation is evidenced by the chevron marks on the fracture surface. The fracture surface transitions from that caused primarily by tension to that caused primarily by shear (tension and shear are always forces on the clevis stud). When examining the threaded surface of the stud, the threads appear deformed or bent southward. This bending of the threads is also consistent with a bending moment that applies tension on the north side of the stud (Figure 9b).

If all the horizontal struts remain connected, no wind force applied to any of the exterior atrium walls imposes a bending force that applies tensile stresses on the north side of the clevis stud. This is the side closest to the attached cable brace (Figure 6). The effect of wind, from any direction and of any speed, is to place the attached cable brace in tension. This tension force imposes a bending moment on the clevis stud. The moment places the south side of the stud in tension. Given that no wind force is capable of failing the stud in the fractured orientation, the clevis stud fracture could not have been the trigger of the failure.

FAILURE THEORIES

Failure theory is the science of predicting the conditions under which solid materials lose their strength under the action of external loads. Any failure theory must be consistent with the physical evidence remaining after a failure occurs, and to the extent possible, with other available evidence. This fundamental investigative

point is often overlooked.

The physical evidence we obtained in our investigation included: the deformed shape of the steel framework remaining on the building; the origin of the fracture obtained from microscopy; the orientation of the fracture obtained from matching the clevis to the broken stud inside the truss jack base; the chevron marks on the fracture surface; and the deformed shape of the fractured stud. Other evidence obtained included: eye witnesses accounts describing a vibration of the curtain wall prior to the failure; the wind analysis indicating the wind characteristics and directions; and the wind tunnel study showing that forces in the horizontal struts could vary between tension and compression, and that the alternating positive and negative pressures on the curtain wall could make it vibrate. All the evidence is consistent with our failure theory.

Multiple approaches can be used in determining the cause and sequence of failure. One approach is to apply code provisions to the structure that failed, and determine whether code forces amplified by safety factors overload the failed elements. In this instance, amplified code forces would overload the stud that failed; however, code forces would also cause tension in the cable brace. Tension in the cable brace is inconsistent with the fractured stud. (A deviation from code requirements may have important legal implications, but it does not necessarily explain a failure).

Another approach is to question code requirements and show that they are insufficient for the subject failure. In this instance, wind speeds from microbursts may have exceeded wind speeds assumed by the developers of the code; however, the magnitude of code forces does not explain the failure since no wind force imposes bending moments consistent with the failure.

When performing an analysis as part of a failure investigation, the question arises as to the appropriate method of structural analysis. The most common, and initial analysis, should be one based on linear elastic static analysis. Such an analysis, in most investigations, is sufficient. In this instance, nonlinear structural analysis was a requirement because of the imposed displacements. A dynamic analysis was also required because of the rapidly changing forces and the curtain wall movements before and during the failure.

INVESTIGATION FINDINGS

Wind analysis and wind tunnel tests show that wind directions changed during the storm and pressures on building walls fluctuated between inward and outward. Consequently, the forces in horizontal struts alternated between tension and compression. The alternating wind pressures, and vibrations associated with a change in direction of strut forces, disengaged a connecting pin at the end of a horizontal strut.

Structural analyses and microscopy show that, to explain the failure, both inward and outward wind pressures at the same location of the building are required and that large displacement theory is needed to explain the direction of the stud fracture. After the connection pin disengaged, wind pressures on the surrounding

structural elements increased dramatically and caused rapid and dynamic rotation in the adjacent vertical truss. The geometry of the connection between the truss and the horizontal struts restrained the rotation of the connection, and forces occurred that are in a direction opposite to those applied by cable braces. The adjacent clevis stud fractured from restraint to imposed rotation.

With the loss of two supports, the vertical structure deformed outward dislodging glass panels and damaging much of the surrounding structure

CONCLUSIONS

Failure investigations are an iterative process in which a theory is developed, carried through by analyses, and the results compared with the known facts and other evidence. Inconsistencies between analysis results and known facts of the failure lead to modified theories, and hence to modified results. The modified results are once again compared with the known facts and other evidence. Once a good match is achieved between the results of the analysis, the observed facts, and the ancillary evidence, a higher degree of confidence is established in the failure theory.

Failure theories must be consistent with the facts. Facts that were significant in our investigation are the characteristics of the wind, the impact of the wind on the building, the deformed shape of the remaining structure, and the nature and orientation of the fracture surface. Analysis of the fracture surfaces in the clevis stud was critical. It defined the origin of the fracture, the direction of propagation of the fracture, and the nature and direction of forces that caused the fracture.

Code analysis, while useful to establish adequacy of design, does not necessarily lead to the correct theory of failure. Similarly, analyses of the adequacy of the code provisions do not always lead to a correct explanation of a failure. Building codes are written to assist engineers design buildings; using code provisions often is the incorrect approach to explain a failure.

REFERENCES

National Oceanic and Atmospheric Administration (NOAA). (2004). *National Weather Service Glossary*, http://www.weather.gov/glossary/.

Repair and Rehabilitation of a 28 Year-Old Overhead Water Tank

C. Natarajan[1], S.E. Chen[2] and S.S. Fatima[3]

[1]Chair and Professor, Dept. Civil Eng., National Institute of Technology, Tiruchirappalli.
[2]Associate Professor, Dept. Civil and Env. Eng., University of North Carolina at Charlotte, 9201 University City Blvd., Charlotte, NC 28223-0001, USA, email: schen12@uncc.edu.
[3]Research Scholar, Dept. Civil Eng., National Institute of Technology, Tiruchirappalli.

ABSTRACT

Reinforced Concrete (RC) overhead reservoirs are important water-supply systems that may fail due to aging and other durability problems. To maintain the integrity of these structures, proper inspection and repairs are necessary. A case study on a near thirty-year old overhead water reservoir, located in Tiruchirppalli, India, is presented. An important lesson learned in the case study is the need for frequent inspection and proper repair and rehabilitation schemes to prevent further deterioration. This paper discusses the issues associated with the maintenance of the water tank and describes in detail the repair process.

KEYWORDS: Repair, Rehabilitation, Water Storage Structure

INTRODUCTION

There are several reasons why structures may become structurally inadequate, including: errors in engineering design or detailing, construction-induced defects, inappropriate material selections or use of sub-quality materials, overstressing, misuse of structure, lack of maintenance, change in environmental conditions beyond anticipation, or aging, etc. While some of the causes can be predicted and avoided, other causes may be beyond human control, such as the occurrence of floods, earthquakes or fire. Structural distresses resulted from above causes may exist in the form of cracks or spalls, unsightly stains, settlements, sagging of load bearing/ transmitting members, and total collapses. In general, structural distress degrades the utility of the structure and/or mars the aesthetics of the structure. Repair, retrofitting and rehabilitation are required to remedy such situations.

In India, the codes of practice lay down the general design loads, design practices and acceptable norms for construction and in some cases, the maintenance procedures (Central Public Works Department 2002; Indian Institute of Technology Madras 2007; Walker 1999). Most of them treat cracks with special interests and explain the importance of cracks to concrete structures (Suresh 2003). It is very important to perform early diagnosis of cracks or other damages in the inspection stages - based on the inspection results to establish prompt repair (Kanakaraj 2005) and rehabilitation schemes to lengthen the life expectancy of structures (Kim et al. 2006 & Raghavan 2005).

It is important to distinguish between retrofit, repair and rehabilitation of a structure. All three terms refer to the modifications carried out on a structure, but in different contexts. Repair refers to the minor interventions that are typically dealing with non-structural components in nature (Allen et al. 1993; Mailvagnan 1992; Emmons 2001). Both 'retrofit' and 'rehabilitation' refer to structural interventions with the purpose of strengthening the structure**.** The difference between the two terms is subtle. Rehabilitation aims to regain the original strength of the structure, while retrofit aims to strengthen the structure to satisfy the design requirements (Indian Institute of Technology Madras 2007; Kay 1992).

This paper provides a glimpse of the repair practices in India through the presentation of the repair of a 20 year-old elevated water tank. Elevated water tanks are commonly used to store, treat and distribute water through an efficient distribution network in Tiruchirappalli, India. These units are important in terms of design, safety, and maintenance to enable a continuous and hygienic flow of water to the residents. Negligence to these structures often leads to heavy water loss.

To avoid unexpected deterioration of a water tower, approaches towards waterproofing of the structure have been recommended to prevent leakages and seepages (Manjrekar 2004). Many of the techniques call for specialized knowledge and technology for designing efficient waterproofing treatments including the selection of site-specific materials and methodologies for execution (Perkins 1996, Reddy & Rao 2006).

PHYSICAL DETAILS

Constructed in 1980, the water tank discussed in this paper has a capacity of 2.0 million liters (Table 1). The plan and sectional elevation of the particular water tank is shown in Figure 1. During recent inspection, the following problems have been identified:

1. Cracks were found on several reinforced concrete (RC) columns (Figure 2) and beams at lower level.
2. Water leakage was identified at sidewalls and base slabs.
3. Spall of concrete in RC columns and exposure of braces reinforcement were identified.
4. The spiral stair column, steps and the handrails were severely damaged due to corrosion.
5. The handrails at the roof slab of the water tank were completely damaged and in some places, completely unavailable.
6. Parts of the water tank floor were undulated and some concrete fell from the roof.

DIAGNOSIS

Based on physical observations, it was inferred that the distress in the water tank columns, braces, sidewalls and staircases are due to a combination of reasons:

1. Presence of poor quality concrete in distressed region.
2. Honey combing in concrete.

3. Improper handling of concrete during construction, resulted in cracking of concrete at base wall joints.
4. Improper packing of concrete at joints between concrete and steel pipes.
5. Continuous leakage, which have led to further spall of concrete and corrosion of steel.
6. Contaminations such as chlorides and sulfates may be present in the water used for construction.

Table 1: Details for the water tank

Client	Tiruchirappalli City Corporation K. Abisekapuram Zone
Year of Construction	1980
Capacity of the tank	2.0 million liters
Cost of the water tank	10 million rupees
No. of Columns	40
Centre Circular Column	1
Height of Column	1.60 m (Below Ground level) 2.46 m (1st level) 4.96 (2nd level) 7.38 (3rd level) 9.84 (4th level)
Bracing Beam	64 #/level × 3 levels = 192 total
Diameter of the Tank	17.85 m (Inner compartment) 25.71 m (Outer compartment)
Tank Height	4.45 m at slab bottom 7.57 m at dome slab bottom 3.00 m at Water filling height

REHABILITATION CONSIDERATIONS

The deterioration in concrete usually manifests in the form of carbonation, corrosion of reinforcing steel, cracking, spalling and excessive deflection, etc. Factors affecting deterioration of reinforced concrete structures as well as the mechanism of deterioration are well-understood (ACI Committee 364, 1993). Remedial measures for water retaining/storage structures should consider water sealing. Vulnerability of construction joints and plugging continuity can be enhanced by using hydrophilic polymers, which when meets water will form insoluble polymer gel. The corroded portions of steel should be removed completely and a corrosion-resistant barrier film should be applied on the reinforcement steel (such film should inhibit further corrosion). Strong, passive, moisture insensitive layer can replace the lost cover of the concrete.

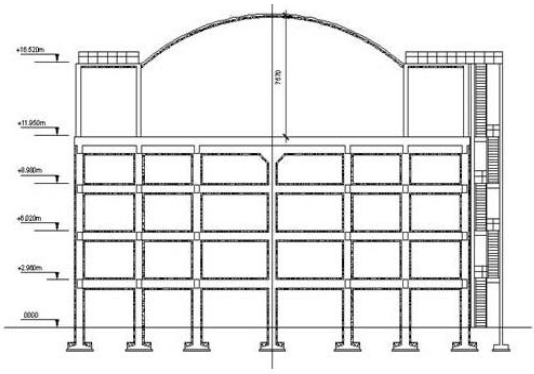

Sectional Elevation

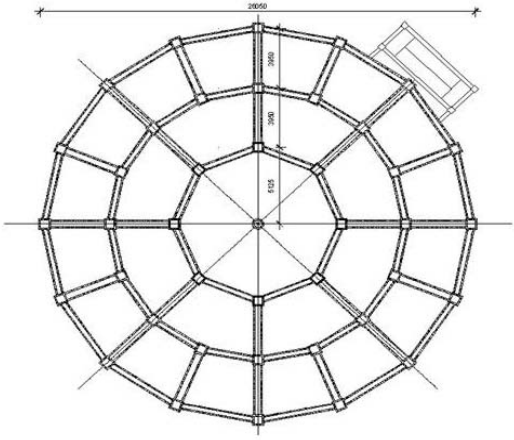

Plan View

Figure 1: Schematic view of the plan and elevation of the water retaining structures

Figure 2: Columns of the water retaining structure before rehabilitation

THE REPAIR WORK

Based on the nature and extent of damages from the visual inspection and non-destructive test reports, it has been decided to strengthen the overhead tank by the following: The internal finish of 25mm thick cement mortar plaster was removed; and the surface was cleaned and washed. A bond coat slurry was applied over the wet surface. Two layers of hot dip galvanized 22 gauge orthogonal woven wire mesh with 12mm size mesh opening, were provided and fixed to suitable width. Overlapping of the mesh was provided in both directions at a clear spacing of 4mm, and a clear cover of 40mm. Glazed tiles using CM 1.3 was provided on both side walls and floor slab.

During rehabilitation, reinforced concrete members were supported by props. Loose concrete are removed by means of chisel and hammer from the reinforcement plaster. Rusts from reinforcement were removed by means of wire brush. Rust removing solution was also applied by brush or cotton swabs. Figure 3 shows the sequence of repair process: poor concrete around the column was carefully chipped away (Figure 3(a)); soil around the foundation of the columns was then removed (Figure 3(b)); a new layer of steel (woven wire mesh, Figure 3(c)) and concrete was laid above the existing foundation (Figure 3(d)). To strengthen the foundation, concrete jacketing was applied (Figure 3(e)). Anti-corrosive chemical paint was then applied over the rusted steel. Figure 3(g) shows a nicely finished concrete column foundation.

A new RC column is constructed beside the existing damaged column and bracing beam (Figure 4(a)). Additional reinforcements are also added to the damaged beams (Figure 4(b)). Figure 4(c) shows the concrete repair process on the bracing beams. The flooring of the tank was repaired with chemical bonds and M20 grade concrete. Figure 5 shows the dismantling and repair of the staircase support. Figure 6 shows the staircase before and after repair.

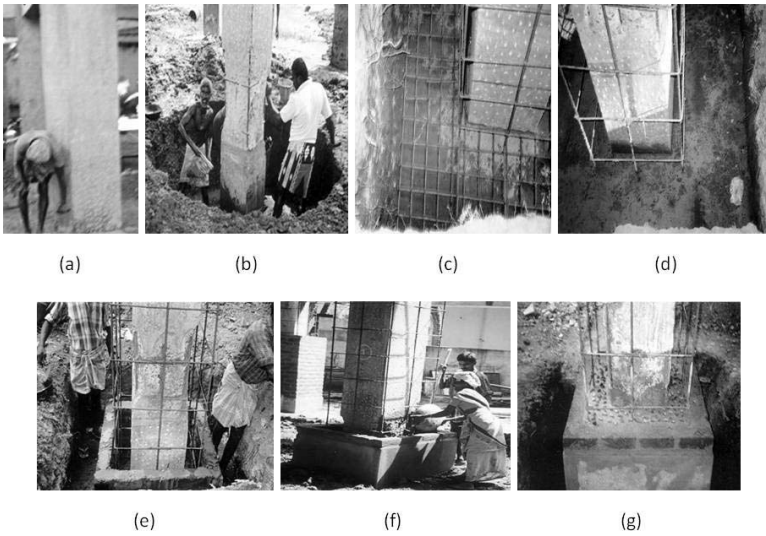

Figure 3: Rehabilitation of damaged columns of water retaining structure: (a) Chipping of the column; (b) Earthwork excavation; (c) Additional reinforcement provided for footing and column; (d) After concrete laid for column footing; (e) Jacketing of the existing column; (f) Concreting; (g) After concrete laid for the column.

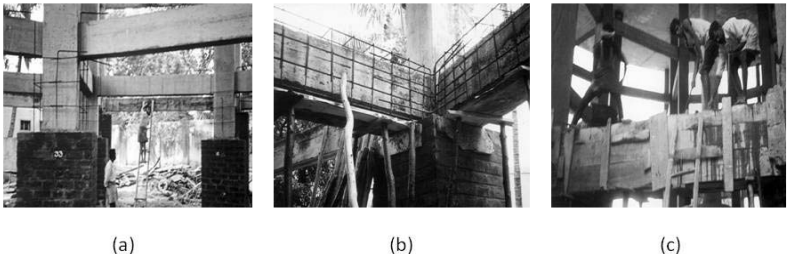

Figure 4: Rehabilitation of damaged beams at the first level of bracing of the water retaining structure: (a) Chipping of beam; (b) Additional reinforcement for the damaged beam; (c) Concreting.

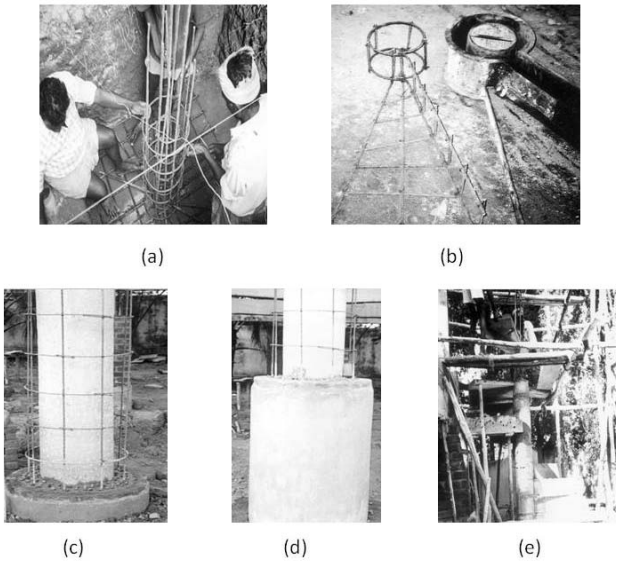

Figure 5: Depicting the rehabilitation steps/measures involved in stair case: (a) Providing reinforcement for the footing and column of the staircase; (b) Reinforcement of the spiral stair case; (c) After Ist stage of concreting; (d) After 2nd stage of concreting; (d) Erection of stair case.

DISCUSSION AND SUMMARY

A well-protected water tank is critical to the well being of the population it serves. The water tank presented in this paper represents structures constructed in India during the early seventies and eighties that have encountered unique engineering problems and now are in desperate need of repairs. Some of these engineering-related problems include:

- Use of concrete with high water-cement ratio and strengths around 15Mpa - 20Mpa.
- Lack of advanced technology to place concrete at elevated heights.
- No control of water contaminants: continuous contact of chlorine resulting in the corrosion of steel (Page et al 1996; Schiessl 1988) particularly in the free board area and the soffits of top slab.
- Lack of details concerning concrete construction joints resulting in heavy leakage through the joints.
- Pouring of concrete in non-watertight shutter.
- Unskilled workmanship for these specialized constructions.

Figure 6: Staircase of the water retaining structure before and after rehabilitation

Figure 7: Overall view of the tank after rehabilitation

Today however precautions are being taken during the construction of these structures which include the use of high quality construction materials/chemicals, proper corrosion and surface protection, use of high range water reducing admixtures, use of self compacting admixtures, so that concrete itself can be made watertight. Another consideration in repairing such structures is that emptying the reservoir usually poses a problem. This is due to the imperative need to minimize the close-down time so that the water supply can be restored as soon as possible. This involves proper planning and involves alternative arrangements for water supply. For more than two decades, the most popular method of repairs in India involves shotcreting, concrete jacketing and replastering (Ropke 1982).

The cost of the rehabilitation of the water tank is about 1.4 million rupees: which represents a cost effective solution as contrast to the costs that would be needed to demolish and reconstruct the entire water retaining structure. Figure 7 shows the water tank after rehabilitation.

REFERENCES

ACI Committee 364. (1993). *Guide for Evaluation of Concrete Structures Prior to Rehabilitation.*

Allen, R.T.L., Edwards, S.C., and Shaw J.D.N. (1993). *The repair of concrete structures*, Blackie Academic and Professionals, London.

Central Public Works Department (2002). *Handbook on repair and rehabilitation of RCC buildings*, Director General (Works), Central Public Works Department, New Delhi.

Indian Institute of Technology, Madras (2007). *Handbook for repair, rehabilitation and restoration*, Narosa Publishers, New Delhi.

Kanakaraj, A., (2005). "Using Correct Repair materials." *New Building Materials and Construction World*, 10 (8), 26-28.

Kay, T. (1992). *Assesment and renovation of concrete structures.* Longman Scientific & Technical, New York.

Kim YM, Kim CK, Hong SG. (2006). "Fuzzy based state assessment for reinforced concrete building structures." *Journal of Structural Engineering* 28 (9), 1286-97.

Mailvagnan, N.P. (1992). *Repair and protection of concrete structures.* CRC Press Inc. Boca Ranton. Florida. USA.

Manjrekar, S.K. (2004). "Water proofing of concrete structures." *New Building Materials and Construction World*, 9 (10), 10-20.

Page, C. L., Bamforth, P. B., and Figg, J. W., (1996). *Corrosion of reinforcement in concrete construction*. The Royal Society of Chemistry.

Perkins, P.H., (1996). *Repair, protection and waterproofing of concrete structures.* E & FN Spon, London.

Emmons, P.H. (2001). *Concrete Repair and Maintenance-Problem Analysis, Repair Strategy, Techniques.* Galgotia Publications, New Delhi, India.

Raghavan, N. (2005). "Some aspects connected with repair and rehabilitation of structures." *New Building Materials and Construction World*, 10 (8), 20-25.

Ropke, J.C. (1982). *Concrete Problems – Causes and Cures*. McGraw-Hill, New York, NY.

Schiessl, P. (1988). *Corrosion of Steel in Concrete,* RILEM Report. Chapman and Hall, London.

Reddy, P.S. and Rao, E.J., (2006). "Knowledge and technology Management for waterproofing using construction chemicals". *New Building Materials and Construction World*, 11 (10), 130-138.

Suresh, N., (2003). "Detection of cracks in concrete." *New Building Materials and Construction World*, 8 (9), 29-37.

Walker, M., (1999). "An overview of rehabilitation methods and selection of an appropriate system controlling concrete degradation." *Proceedings*, 1999 International Congress - Creating with Concrete, Dundee, Scotland.

EVALUATION OF DAMAGE TO CONCRETE BUILDINGS FOR INSURANCE CLAIMS: NEW GENERATION APPROACHES

Gary C. Hart, PhD, CE, SECB[1],
Anurag Jain, PhD, PE, SECB[2]

[1] *Professor Emeritus, Dept of Civil Engineering, University of California, Los Angeles, CA, and Managing Principal, Weidlinger Associates Inc., 4551 Glencoe Avenue, Suite 350, Marina del Rey, CA 90292, Tel: 310-315-8430, Email: hart@wai.com*
[2]*Principal, Weidlinger Associates, Inc., 4551 Glencoe Avenue, Suite 350 Marina del Rey, CA 90292, Tel: 310-315-8430, Email: jain@wai.com*

ABSTRACT

Imagine that a hurricane or an earthquake has occurred. Your assignment, either for an owner or for an insurance company, is to recommend what rehabilitation, if any, is needed to bring the building back to it pre-event condition. There are two parts to this rehabilitation: Building Lateral Force Resisting System and the Building Envelope. This paper will only address the former and will focus on concrete buildings even though the concepts apply to all buildings. This paper shows that the concepts presented in recent publications by FEMA and ATC (especially ATC-63) and the experiences of the authors that it is scientifically possible and practical within reasonable budget constraints to complete the above defined assignment.

INTRODUCTION

It is possible to scientifically quantify the prior condition of the building's lateral force resisting system using laboratory and analytical tools that were developed over the last decade by FEMA, ATC and PEER, and then to scientifically quantify the damaged building using the same methods. This approach enables the performance of the damaged building to be compared with the performance of the pre-event building in future events and for all limit states (not just the collapse limit state). If rehabilitation is needed, then different repairs can be proposed and evaluated until the rehabilitation returns the building to its pre-event condition. The proposed method in ATC-63 [1] is especially noteworthy because the method of directly incorporating uncertainty into the evaluation process. This is very important because it allows further use of limited information that comes from having a limited project budget. It also directly provides for the uncertainty reduction with expanded scopes of work that could include (1) more field evaluation, (2) more advanced and structural analysis models, and (3) more accurate estimation of site specific future loading, etc. This scientific approach has the benefit of encouraging constructive communication between experts employed by different parties by requiring the documentation of the assumptions, analysis performed, etc. and then the identification of common ground and differences, and then perhaps proposing to remove the differences.

ATC-63 and other methods that incorporate uncertainty have evolved over the past several decades and the field of Bayesian Decision Making has become accepted within probability and statistics, spanning many different disciplines. For example, the Wall Street Journal described the retired chairman of the Federal Reserve, Alan Greenspan, as a Bayesian Decision Maker. In simple terms, Bayesian Decision Making entails the updating of uncertainty and resulting decision by the incorporation of new data or information. When we are making decisions, or more specifically, offering an expert opinion, it is a fact of life that we have uncertainty in our opinion and that we can use more information to reduce our uncertainty and increase our confidence.

In the structural engineering field, we are often asked to offer opinions with very limited information and typically in a very short time frame. For example, consider the green, yellow or red tagging of buildings immediately after an earthquake. It is in the culture of structural engineering to make decisions with limited information and with little time or budget for information gathering, and we do it often in the area of post-earthquake and post-hurricane damage estimation.

It is possible that a structural engineering expert is asked to state his or her opinion under not the best of conditions and thus will not state an opinion unless they have a minimum level of confidence in that opinion. Table 1 shows different levels of confidence in both qualitative and numerical terms that are used to describe the confidence in an opinion [2].

Table 1. Qualitative to Numerical Transformation of Confidence, adapted from [2]

Expression	Single-numbered (median) Probability Equivalent (%)	Range (%)
Almost Certain	90	90-99.5
Very Likely	85	75-90
Likely	70	65-85
Even Chance	50	45-55
Possible	40	40-70
Unlikely	15	10-25
Very Unlikely	10	2-15
Almost Impossible	2	0-5

What is very clear to all doing investigation work is that it must always now have two basic parts which are Observation and Simulation. A prior paper [2] presented the method for quantifying confidence consistent with Table 1.

THE OBSERVATION PART

Observation could involve reading the published literature and learning from laboratory tests conducted on concrete structural members and full scale buildings. For example, Figure 1 shows basic information about concrete buildings with masonry infill and the different failure modes that must be considered in the observation phase. Also, it illustrates the different cracking patterns that can be expected during field observation. The observation phase has a goal of obtaining field information to better understand basic behaviour characteristic of the performance of the frame and the building.

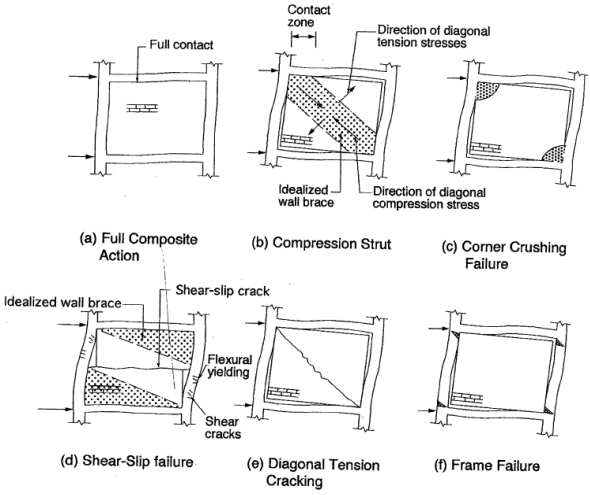

Figure 1. Infill Concrete Frame Failure Modes (Drysdale and Hamid, 2008) [3]

The observation of concrete buildings and structural members in the load path after they have either been tested in a laboratory or subjected to hurricane or earthquake loading always provides very valuable information to a structural engineer. A good laboratory test plan combines the professional experience of the test planners and structural engineering analyses of the expected performance of the test specimen. In the controlled environment of a laboratory, the loading that the load path member is subjected to is usually well known. Therefore, learning from the test either in the laboratory or full scale is very important because it tells us how this load carrying member-infill is expected to perform and also provides a way on how we can perform reality checks on our structural engineering modeling.

It is also important to utilize appropriate investigation tools during the observation phase. For instance, one important question to answer in the investigation of concrete masonry infill walls in a concrete building is whether the masonry cells are grouted or not. The spacing of grouted cells is also of interest to verify agreement

of as-built condition with the construction documents. This is also valuable information for the simulation phase of the investigation to accurately model the structure. Infrared cameras are excellent tools to detect grouting of masonry walls. These cameras are heat sensitive devices that let you see and measure thermal energy emitted from an object. The products of investigation with an infrared camera are thermographic pictures that can accurately identify areas of solid grouting within a masonry wall, see Figure 2. Another question to answer is whether the masonry wall is reinforced. The authors have successfully used a Micro Covermeter, a metal detector type device designed to locate and determine the size of reinforcing bars, as well as concrete cover.

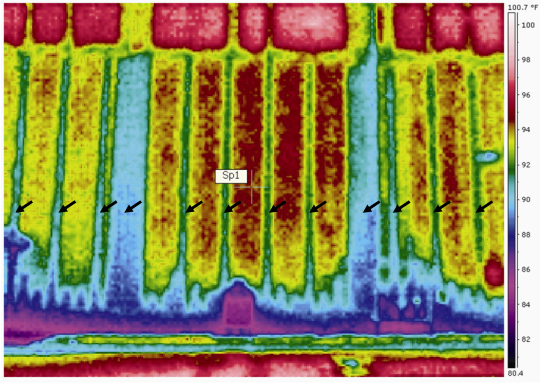

Figure 2. A Thermographic Photograph Taken by an Infrared Camera Shows Areas of Solid Grouting within a Masonry Wall, Note that Arrows Show Cells with Solid Grouting

We could go on and on with respect to destructive and non-destructive testing but the bottom line is that it is an important part of an insurance claim role by the structural engineer.

THE SIMULATION PART

It is essential that a structural analysis must be performed on a concrete building involved in an insurance claim if the ATC-63 method is to be used to measure performances. The word simulation is just a decision making term for what we structural engineers call a structural analysis model of the concrete building. Also, the structural engineer working on an insurance claim must select from a spectrum of structural engineering models to estimate structural response and performance to fit the clients' budget and required degree of confidence. This selection process directly impacts the confidence in analysis results.

To illustrate one of the many limit states that the simulation part can focus on, consider Figure 3. A structural element loses its energy capacity after it experiences a

first cycle of response. Therefore, a limit state may be the energy absorbing capacity of the infill wall as a component.

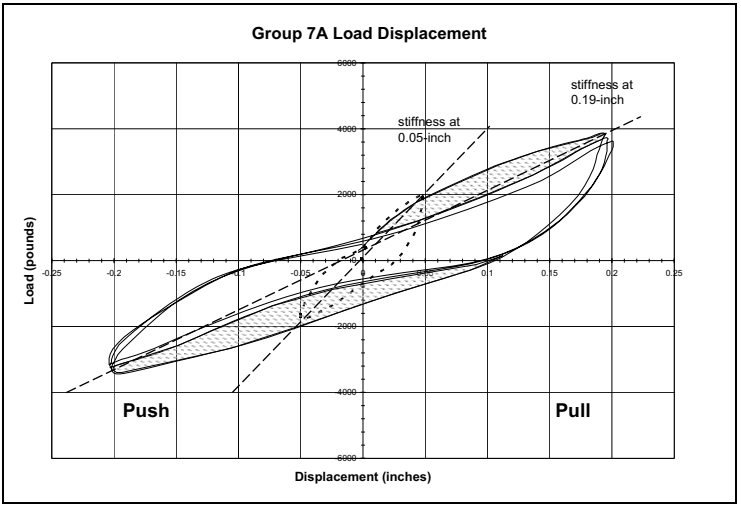

Figure 3. Loss of wall strength and energy capacity up to a defined level of displacement (1 in = 25.4 mm)

Or we can focus on what is commonly called a Fragility Curve, see Figure 4. It shows how the simulation part can focus on the determination of the damage from the earthquake and how we can determine the changes in the fragility curve.

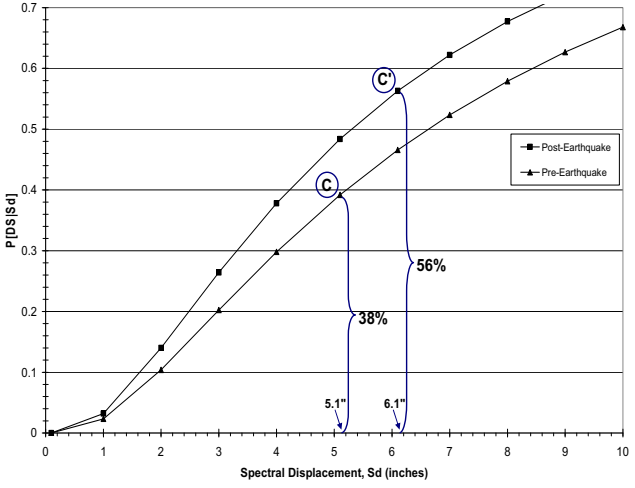

Figure 4. Consider Pre and Post Earthquake Fragility Curve (1 in = 25.4 mm)

Another example in the simulation part is work we can perform to determine the relative importance of the elements in the load path of the concrete building. First, the concrete frame can be modeled without masonry infill. Then the masonry infills can be added to the structural analysis model. The difference between response curves of the concrete frame and the combination of frame and masonry yields the force-displacement response of masonry units as shown in Figure 5. This simulation information can be used to tell us that the stiffness property of the masonry infills in the global computer model has a significant impact on the load path of the concrete building.

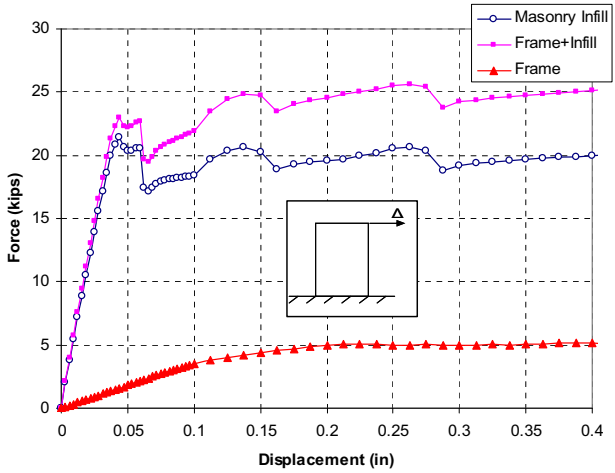

Figure 5. Force-displacement response of the wall panel due to Monotonic Horizontal Displacement at the top of Wall Panel (1 in = 25.4 mm) [4]

RATIONAL APPROACHES

Experts may not agree that the implementation of ATC-63 is the right approach for a scientific quantification of performance. As previously mentioned, there are other choices. For example, one way to incorporate the concepts of Structural Reliability and calibrate the pre-earthquake or severe wind condition of the building is to use the procedures described in FEMA 356 [5] and ASCE/SEI 41-06 [6]. The building analysis procedures as defined in FEMA 356 or ASCE/SEI 41-06 can be used to calculate the building response for each of the building components in the earthquake or hurricane load path. This response is described in terms of the components deformation ratio. For example, for a concrete building each of the structural members in the load path load in their pre-event condition can have their deformation ratio calculated and for illustration the ratios could be 2.0 and 3.0 for the 10% (BSE-1) and 2% (BSE-2) in 50-year earthquakes, respectively. Therefore, the pre-

earthquake building is calibrated to be at these deformation levels and does not meet either the Life Safety or the Collapse Prevention Performance Level. If the desire is to restore the post-earthquake building to its pre-earthquake condition, then first the post-earthquake building is analyzed to determine its response and component deformation ratios. Then the building is rehabilitated by the structural engineer to bring the component deformation levels back to, as a minimum, their pre-earthquake values. For example, using the previously illustrated concrete structural member the post-earthquake deformation ratios might be reduced to 1.5 and 2.0 for the 10% and 2% in 50 year earthquake. The rehabilitation would then increase these components deformation ratios back to 2.0 (from 1.5) and 3.0 (from 2.0) for the 10% and 2% in 50 year earthquake. Then the structural engineer can inform the participants in the insurance claim that concrete structural members can also at an additional cost be brought up to acceptable levels for a Basic Safety objective.

The FEMA 356 and ASCE/SEI 41-06 approach was developed for earthquakes. However, its application for hurricanes or severe winds is equally valid and is straightforward. An advantage of the above approach is that it provides a well documented approach for analysis and response description that is professionally accepted. It also provides a rational basis for discussion among structural engineers on the opposite sides of an insurance claim to discuss their assumptions and agree on some and disagree on others. Then the impact of this disagreement on the claim cost aspect under the responsibility of the structural engineer can be documented for our clients.

Another example of a rational way to perform work on an insurance claim is to incorporate the concepts of structural reliability and calibrate the pre-earthquake, hurricane or severe wind condition of the building is to use the methodology in the FEMA HAZUS [7] documentation. As with the previously discussed approach this methodology applies equally well for hurricane or severe wind damage. This fragility analysis based method is an improvement from a scientific structural engineering perspective over the previously discussed method. For a defined level of earthquake ground motion, e.g. a 10% in 50 year earthquake, or a 2% in 50 year earthquake, or both, the structural engineer can first define the earthquake ground motion at the building site. Similarly in hurricane or severe wind insurance claims the site specific wind speeds and loads can be determined. Then the capacity of the building can be determined and this is done by developing a load versus deflection – or capacity (pushover) curve – using nonlinear structural analysis methods. Then a fragility curve can be developed using this pushover curve and the uncertainty in the ground motion, uncertainty in the capacity of the structural, and uncertainty in the expected damage gives the expected displacement of the structure. It is very important to note that the quantification of these uncertainties requires the use of probabilistic structural analysis methods. Because uncertainty usually reduces with the application of more advanced analysis methods it also directly rewards technology transfer. The result for the pre-earthquake analysis of the building is a probability that the building will respond to the selected earthquake (e.g. the 10% in 50 year earthquake) in each of five FEMA HAZUS defined damage state. The five damage states in order from least damage are None, Slight, Moderate, Extensive and Complete. For example, the analysis of the pre-earthquake building could result in the following 5%, 20%, 40%,

25% and 10% probability of being in the None, Slight, Moderate, Extensive and Complete Damage States for a 10% in 50 year earthquake.

This analysis provides a calibration of the pre-earthquake condition of the building. The building in its post-earthquake condition can then be analyzed using the same FEMA HAZUS procedure and the probability of being in each of the five damage states can be calculated (e.g. it could be 2%, 10%, 50%, 30%, and 8% probability of being in the None, Slight, Moderate, Extensive and Complete Damage States for a 10% in 50 year earthquake). To bring the building back to its pre-earthquake condition these probabilities must be brought back to their pre-earthquake lines.

It is very important to note that if the owner desires to provide the fees to develop a more confident estimate of the ground motion, the capacity curve, and the threshold of damage for this specific building, then even if the same target displacement results there will be a reduction in uncertainty in the estimate. If this is the case then the total variability in the damage state estimate will decrease. Tables 2 and 3 illustrate the benefit of uncertainty reduction in insurance claims.

Table 2. Probability of Experiencing Different Damage States

Damage State	Pre-Earthquake Building	Post-Earthquake Building
None	3	2
Slight	15	7
Moderate	44	35
Extensive	28	34
Complete	10	22

Table 3. Probability of Experiencing Different Damage States after Advanced Analysis and Uncertainty Reduction

Damage State	Pre-Earthquake Building	Post-Earthquake Building
None	0	0
Slight	3	0
Moderate	68	38
Extensive	28	56
Complete	1	6

THE ATC-63 APPROACH: NEWER AND BETTER

The management at ATC since its founding has always selected excellent project teams that leave their individual bias at the door and work for the goodness of the profession. This was done in the case of ATC-63 and the project team credentials are great. Also, ATC assembled other outstanding structural engineers at full day

meetings, such as the one we joined with approximately 100 in attendance. In short, the ATC-63 document can certainly be viewed as an excellent addition to the scientific base of structural engineering and also that this base is accepted by the profession.

The ATC-63 approach directly incorporates uncertainty into the evaluation process and therefore allows the direct use of limited information that comes from a limited budget for such assignments. It is now possible using today's available spectrum of structural engineering analysis (Simulation) options to define the prior condition of the building's infill concrete lateral force resisting system using Observation (laboratory) and Simulation (analytical) tools that have been developed in the last decade. It is also possible to evaluate the damaged building using the same methods. The performance of the damaged building can then be compared with the performance of the pre-event building to the same future events. If rehabilitation is needed then it can be proposed and evaluated until the building is returned at a minimum to its pre-event performance condition.

The structural engineer not only has to carry out the steps discussed in ATC-63 but he or she must be able to support their position. Structural engineering is to a great extent about making informed decisions. We are all better if we are put on the "hot seat" about the work we did and also our basis for making a decision. For example, in developing a good computer model of a building, and especially a non-linear computer model, we must select the type of structural model we are going to use for the structural members and joints. Then for that member or joint model we must select the numerical values of the parameters in that model. First, the structural engineer learns because he or she must study the latest laboratory test data and published literature. Next, the expert always learns by asking questions and listening to the other expert structural engineers' decisions.

Appendix F of the ATC-63 document presents an excellent roadmap on how the ATC-63 Methodology can be adapted to the collapse evaluation of individual buildings. This evaluation can be used as part of a seismic rehabilitation or a post earthquake study of a building.

The structural engineer can now address reality and use good structural models of buildings with real estimates of strength, stiffness and as a result answer this very important question.

It is often necessary for the structural engineer to evaluate a building for something other than collapse limit state. For example, one possible limit state could be yielding of any member in a building. Or the limit state could be the roof deflection experienced by a building before and after an earthquake. Reading ATC-63 enables the learning of tools. Then the structural engineer can identify limit states that are of interest to the client. Then he or she can perform an analysis using the tools of ATC-63 to answer questions for the selected limit state.

ATC-63 Recognizes and Rewards Experimental Testing. The value of the uncertainty for any limit state will decrease with testing. Today many universities have excellent laboratories that can do testing focused on a specific building's components and we will by reducing uncertainty in all future projects.

CONCLUSIONS

It is the beauty of the HAZUS and ATC-63 approaches that the tools of modern risk and reliability analysis are used to define the uncertainties associated with the different steps in the damage estimation process. This enables a direct rewarding for the transfer of technology into insurance claim work that impacts so many people.

ACKNOWLEDGMENTS

Thank you to Dr. Charles A. Kircher, ATC and FEMA for developing tools for reporting on post-earthquake or wind building performance other than pretty slides and often insulting comments and hot air.

REFERENCES

1. ATC-63 Project Report - 90% Draft (2008) “Quantification of Building Seismic Performance Factors” Redwood City, California
2. Hart, G.C., King, S.A and Hortacsu, A. (2009) “Converging Confidence of Expert Opinions”, *The Structural Design of Tall and Special Buildings Journal*, 18(2), 171-179
3. Drysdale, R.G. and Hamid, A.A. (2008) “Masonry Structures Behaviour and Design” The Masonry Society, Boulder, CO
4. Ewing, R.D., El-Mustapha, A.M. and Kariotis, J.C. (2000) “FEM/I, A Finite Element Computer Program for the Nonlinear Static Analysis of Reinforced Masonry Building Components” Rancho Palos Verdes, CA
5. FEMA 356 (2000) “Prestandard and Commentary for the Seismic Rehabilitation of Buildings”, ASCE, Reston, VA
6. ASCE/SEI 41-06 (2007) “Seismic Rehabilitation of Existing Buildings”, ASCE, Reston, VA
7. HAZUS$^{®MH}$ (2003) “Multi-hazard Loss Estimation Methodology”, FEMA Mitigation Division, Washington, D.C.

Structural Complexities and Durable Solutions for the Rehabilitation of a Reinforced Concrete High Rise Residential Building within a Marine Environment

Andrew Wilson, P.E.[1], Tracy Marcotte, PhD, P.E.[2], Mark Yerges[3], Robert Schaeffer, P.E.[4], and Eric Godfrey[5]

Abstract: The rehabilitation of a 17-story, concrete framed residential building presented an interesting and under-documented technical challenge in the design and execution of structurally complex, effective, and durable repairs. The case study is located on the southern New Jersey shore in which numerous columns within the exposed parking levels were structurally debilitated from on-going marine exposure, poor original construction, and previous improper repair attempts. Initial investigations of the deteriorated elements indicated that conventional localized concrete repairs would require significant concrete removals that could undermine the structural stability of the building as a whole, and an alternate remedy was implemented.

Introduction

Marine environments are notoriously aggressive to reinforced concrete structures with moist, chloride-laden winds depositing chlorides directly onto concrete surfaces. Reinforced concrete is an inherently adaptable, cost-effective, and sustainable building material provided that it is designed to resist the marine exposure, and this is typically handled in the design process by specifying suitable concrete cover depths atop the reinforcing steel. ACI 318R (e.g., 1963, 1971, 2008) governs this design area and typically, concrete cover depths from 1.5 to 3 in. are mandated depending upon the environmental conditions (exposure to moisture) and whether the concrete is cast on ground or left exposed (slabs-on-ground versus columns or beams).

Inherent in this protection strategy is the underlying assumption that minimum concrete quality requirements are met to provide long-term corrosion resistance for plain carbon reinforcing steel: low water/cementitious ratios, well-consolidated concrete, any cracks are repaired, and minimum cover depths are achieved.

Even with good quality concrete that is well-constructed, the ingress of deleterious substances over decades, primarily chlorides and carbon dioxide, initiates corrosion of the reinforcing steel. Per ACI 222.3R (2003), the localized attack of chlorides is particularly challenging to repair because localized repairs often shift the corrosion attack to a new area of the repaired structure, beginning the process anew. Service life prediction models can be developed for new concrete structures and those in service (ACI 365.1R, 2001) to predict the ingress of these deleterious species and validate options to achieve more durable concrete structures. Worldwide, a tremendous investment in durable concrete and its repair has been underway in earnest since the 1970s.

---

[1] Project Manager, CVM Facilities Renewal, Oaks, PA e-mail: awilson@cvmfr.com
[2] Associate, *ibid.*
[3] Staff Engineer, *ibid.*
[4] Associate, *ibid.*
[5] Principal, *ibid.*

It is, therefore, unsurprising that reinforced concrete structures after a few decades of service merit repair and intervention measures. For the case study presented in this paper, numerous repair cycles have been implemented in the parking garage level after 20 years of service. Overall, structural concerns, the inconvenience of the repair programs on the operations of the building, and the inability of the ownership to develop confidence in a maintenance program prompted a request for a comprehensive engineering evaluation and design to achieve long-term, durable reinforced concrete repairs.

General Building Description

The case study building is a seventeen story condominium complex constructed circa 1974 on the Atlantic Ocean coastline in Margate, New Jersey, with eleven residential floors built upon three open parking levels, and an enclosed ground floor serving as the lobby and common areas. Structurally, the building is composed of cast-in-place reinforced concrete columns, two-way floor slabs, and shear walls. The exterior envelope is a drained cavity wall system constructed of back-up CMU block walls with a concrete masonry brick veneer. This paper focuses upon the repair challenges presented by the deteriorated, reinforced concrete columns located within the open parking garage areas of the 2nd, 3rd, and 4th floors.

FIGURE 1 – South (open lower levels) and east (enclosed lower levels) elevations of the condominium building as viewed from the Atlantic Ocean shoreline.

Evaluations

Preliminary Investigations and Document Review

The investigative program was developed using ASCE's Guideline for Structural Condition Assessment of Existing buildings (SEI/ASCE 11, 1999) and ACI 364.1R, Guide for Evaluation of Concrete Structures Prior to Rehabilitation (ACI 364.1R, 2007), as guidance. Limited original architectural design drawings were available for review to establish design intent along with a few assessment reports prepared by other investigators. Of particular interest was a corrosion diagnostic report prepared in 1993, that documented the following results in localized areas: continuity, electrochemical potential (half cell) measurements, and chloride contamination profiles. These electrochemical and corrosion data were significant as they offered a

snapshot of corrosion activity at that time, and provided a reference point for our investigation.

Figure 2 presents the documented chloride profile data for two of the concrete columns within the garage. These were designated as "interior" columns, in that they were not a part of the façade. It is clear from the measured chloride levels, however, that the marine environment does reach the interior of the garage and poses an environmental risk to the building elements if unprotected. Even in 1993, chloride levels are in excess of that generally thought to initiate and sustain corrosion (ACI 222R, 2001). ACI 222R reports that there is not a single minimum value above which corrosion is guaranteed to initiate, and corrosion thresholds should be thought of as a range of values dependent upon cement type, water/cementitious materials ratio (w/cm), the presence of supplementary cementitious materials, and the corrosion resistance of the reinforcement. Below 0.20% mass of cement, corrosion is rarely reported to initiate and cause distress for plain carbon steel within any cementitious cover.

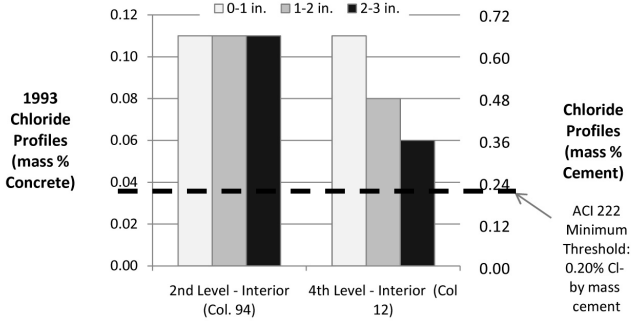

FIGURE 2 – Chloride profiles for two reinforced concrete columns measured in 1993 by a corrosion specialist.

With chloride levels as high as shown in Figure 2, it is evident why numerous rounds of repairs have been necessary. Earlier repairs appear to have been largely cosmetic as field observations of the previously implemented repairs indicated that significant deterioration of the reinforced concrete cover continued unabated. Concrete was easily removed due to delamination at the steel interfaces and corrosion of the primary vertical column reinforcement and stirrups was evident. A representative area is shown in Figure 3. Thus, comprehensive structural, materials, and corrosion risk evaluations were merited if long-term repairs were to be designed and implemented.

Detailed Investigation

An in-depth and detailed investigation was designed to facilitate a thorough evaulation of the building conditions, including analyses of loading conditions, testing of the concrete materials properties, intensive forensic studies, and service life modeling to tailor and validate options for rehabilitation.

FIGURE 3 – Typical concrete failure and corroded reinforcement at column.

FIGURE 4 – A representative probe area for a damaged concrete column at splice.

Prior to performing the destructive investigations, a preliminary structural analysis was performed to validate the structural capacity of the building to undergo additional concrete removals. The analysis indicated that under full dead and live loads, the existing columns had some reserve capacity, but not enough to allow the removal of concrete around the entire perimeter of the vertical rebar without risking potential column overload and instability. Investigative techniques were subsequently developed and executed so as to remain below the capacity limits of the existing columns.

Forensic Investigations – Reinforcement & Concrete Probes

Concrete probes were conducted at representative locations to observe the condition of the concrete and embedded reinforcement: "good", "bad" and previously repaired areas were studied to capture the range of conditions. The following specific observations were collected during this process:

1. Concrete deterioration and reinforcing steel corrosion was underway at many of the columns. Most severely at the exterior building columns at the garage levels, designated as "Perimeter" columns.
2. Where concrete deterioration was most severe no mechanical tools were needed to remove the concrete cover atop the corroding steel.
3. The condition of the underlying steel appeared to be in relatively good condition with little, if any, loss of cross-section.
4. Numerous failed localized patch repairs were encountered that were reportedly. 5 to 10 years old

The observed premature failures appeared to be typical of cosmetic concrete repairs where corrosive activity was not directly addressed. Other specific observations of the reinforcing steel included:

1. The steel reinforcement installed during initial construction was mild carbon steel without any inherent corrosion resistance.

2. The reinforcement placement, spacing, splicing, and concrete cover were typically inconsistent. The variations in the reinforcement placement and a lack of adequate cover were generally in excess of tolerances acceptable under building code requirements and general building practices, although not unusual for buildings of this vintage.

Most significant of the probe findings was that the corrosive deterioration appeared to be widespread enough to create potential serviceability deficiencies in the structural building components. These probe findings reinforced the need for an in-depth materials testing program and structural analyses of the building components was necessary to mitigate structural stability concerns during repairs and beyond.

Forensic Investigations: Sampling and Material Testing

A project specific field and laboratory testing program intended to ascertain essential information regarding the material properties of the existing concrete (compressive strength, density, chloride contamination, etc.) and the configuration, size and spacing of internal reinforcements was implemented using industry standard techniques described in ACI 364.1R and SEI/ASCE 11.

The concrete testing program indicated the following:

1. *Petrographic analysis*: The original concrete appeared to be of relatively good quality with a water/cement ratio of approx. 0.45, well-consolidated, non-air-entrained, no supplementary cementitious materials, and likely did not contain high levels of chloride concentrations when placed.
2. *Compressive strength tests*: The concrete compressive strength varied from approximately 4,500 psi to approximately 7,600 psi.
3. *Chloride profiles*: Significant contamination exists at the majority of the locations tested, as shown in Figure 5. Chlorides of sufficient concentration to support active corrosion are generally present at the depth of the primary reinforcing steel.
4. *Carbonation depth measurements*: The measured carbonation depths ranged from 0.04 to 0.4 in., and, therefore, had generally not progressed to primary reinforcement steel depths.

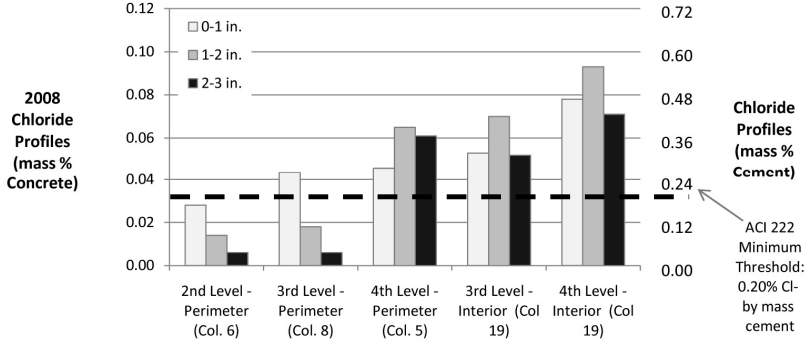

FIGURE 5 – Chloride profiles for five reinforced concrete columns measured during the current investigation.

Structural Load Capacity Analysis

Visual examinations, physical measurements, materials property measurements, and non-destructive and concrete removal examinations were used to analyze the structural load capacity of the building. A steel strength value of 60 ksi and concrete compressive strength of 5,000 psi were assumed in the analysis.

With this information, the effects of deterioration and section loss on the capacity of structural elements were simulated, and modified building loading scenarios were developed to best simulate the actual building loading that the columns would most probably be subjected to during the construction/repair process. The following conditions and assumptions were used:

1. The building depended on shear walls for the lateral support system, and the columns were not intended nor required to assist in lateral support.
2. Load run-downs for columns were performed to determine factored column loads at various column locations and floor levels (Load factors of 1.4DL + 1.7LL and 1.2DL + 1.6LL were used for the analysis).

The above conditions and assumptions permitted the evaluation of the consequences of potential loss of concrete cross-section for two areas of the column: at the lower portion of the column within the splice zone of the vertical reinforcement, and the upper portion of the column where no splicing occurred (Figure 4).

Maximum permissible concrete removal extents were estimated based upon the in-place dead load. The analysis concluded that removal of concrete to fully expose the corroding reinforcement steel could result in overloading of the remaining concrete core and potential buckling of the vertical reinforcement rebar. However, removal of concrete to the center of the vertical bars at the full column perimeters would not result in overloading of the columns (reduction of nearly 50% of the concrete section).

Demand/Capacity ratios were determined based upon potential concrete section reduction scenarios when subjected to dead loading conditions only. The section was then analyzed again, as a fully repaired section, using only the factored Live Load. This Live Load demand/capacity ratio on the fully repaired section was then added to the demand/capacity ratio for the factored Dead Load on the reduced column section to ensure that when the column was subject to Live Load in its repaired state, that the “combined” demand /capacity would not exceed 1.0.

Service Life Modeling

LIFE 365, Version 2.0, is a shareware computer modeling program that estimates the time-to-corrosion initiation and life-cycle costs for reinforced concrete exposed to chlorides. The following basic assumptions were inputted that reflected the reinforced concrete design criteria:

1. Original concrete w/c: 0.45
2. Original design intent for concrete cover depth per ACI 318-71: 2 in.
3. No supplementary cementitious materials

4. Either a sealer or a membrane was assumed in the model to represent the paint system applied to the columns.
5. Weather conditions similar to Atlantic City, NJ.
6. Marine spray exposure, given that the open garage levels are within 100 ft of the ocean.
7. A general assumption that the cement type and composition is approximately similar to that used to calculate the diffusion constants.

Under these assumptions, the service life model predicted that 0.05% chlorides by mass of concrete will reach the surface of the embedded steel within 7-10 years, with a standard corrosion propagation period after initiation assumed to be 6 years. According to this prediction, corrosion-related damage might not have become evident in the covering concrete until the late 1980s or early 1990s. This result is consistent with the chloride data collected in 1993 (Figure 2), as a certain level of corrosion-related damage to the concrete cover would remain undiscovered and tolerable until the building owners initiated an investigation.

With regard to options for rehabilitation, it is generally accepted that durable localized concrete patch repairs should replicate the surrounding concrete to remain as closely as possible to avoid the formation of galvanic cells (i.e., steel that is partly embedded in the new repair and the original concrete will suffer enhanced corrosion at the interface of the two materials). The presence of chlorides complicates this since the original concrete is not sufficiently resistant to the ingress of chlorides. Simple installations of new concrete patch repairs, however well the substrate is prepared, are destined to fail, even if coated with a sealer or membrane. Additional corrosion mitigation measures were, therefore, considered to achieve a longer service life for the repairs as described in the subsequent section.

Rehabilitation Design and Execution

Design Goals

The evaluations and structural modeling indicated that repair techniques requiring full removal of deteriorated concrete to fully expose the corroded reinforcement steel could result in overloading of the remaining column section. Furthermore, shoring of the structure was deemed to be prohibitive due to the building configuration and structural support system. Rehabilitation repair designs were needed to address the structural loading limitations without requiring shoring or unloading of the columns. Additionally, original construction deficiencies and marine exposure added complexity to the rehabilitation design process: long-term durability of the new rehabilitation repairs was prioritized by the building owners as continued, regular construction activity within the building was undesirable.

Structural Design

The limitations for concrete reduction as determined during the structural load capacity analysis were used as the limits of concrete removals. A minimum Load/Capacity ratio of 0.9 was used for design.

The loading conditions used in the load capacity analysis considered only dead loads (construction phase), and neglected all live loading. However, the rehabilitation repair designs needed to accommodate service live loading of the repaired column. While the design of reinforcement of the columns to accommodate

the additional live loading was relatively straight-forward, considerations of the redistributions of loading of the axial column into the reinforced patch sections were not. The following considerations were taken into account to determine the viability of redistribution of loading into the reinforced patch:

1. Concrete patch areas of axially loaded reinforced concrete columns are ineffective in carrying axial loading unless loads are relieved prior to installation of the patch.
2. Shrinkage of the concrete patch leads to further stress relaxation in the concrete portion of the patch.
3. Shrinkage compensating or non-shrink concrete mixes limit but do not eliminate shrinkage and/or creep.
4. The stresses induced in reinforcement steel within the patch areas of axially loaded reinforcement concrete columns will generally increase as the concrete patching undergoes shrinkage and creep.

After consideration of these criteria, a reinforced concrete patch was designed to jacket the existing reinforcement steel and the concrete core. The jacketed reinforcement was designed to incorporate the following, shown in Figure 6:

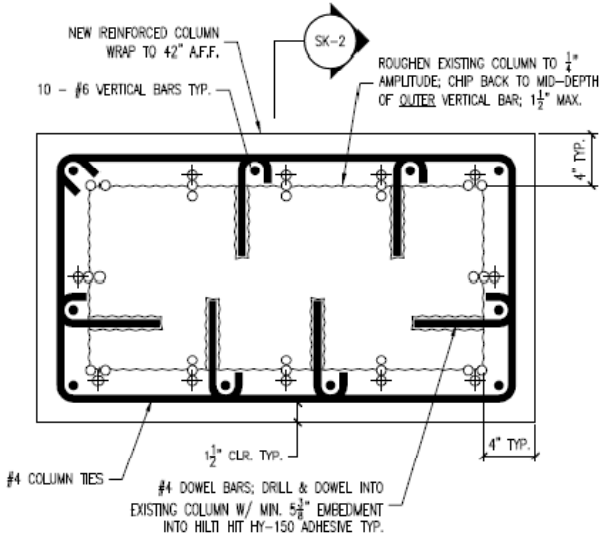

FIGURE 6 – Concrete Jacketing Plan Design Sketch

1. The reinforcement steel in the patched jacket area was to be anchored to the existing concrete core with epoxy-set mechanical dowels to induce transfer of loading from the concrete core to the new reinforcement steel.
2. The reinforcement steel in the patched jacket area was placed directly adjacent to the existing partially exposed reinforcement steel to induce splice load transfer.
3. Stirrup reinforcement was placed within the patched jacketed area to confine the concrete core.

4. Embedded galvanic anodes were installed at the perimeters of the new patches to protect the steel embedded within the new and original concrete areas.
5. The new and exposed steel was coated with a polymer coating to enhance the bond of the steel to the concrete, and theoretically stifle the cathodic reaction of the steel within the patch material, thereby minimizing the anticipated anodic reactions at the perimeter of the new patches.
6. An air-entrained concrete patch material with a 28-day compressive strength of 6000 psi was selected for ease of installation in localized areas, and approximate similarity to the original concrete to remain.

Although re-distribution of existing dead loading from the concrete core and existing reinforcement steel into the reinforced jacketed column was not anticipated, the jacketed area was designed to accommodate significant loads based on the following:

1. The jacketed portion was designed to accommodate an additional applied live loading. Although the existing loads were not relieved from the columns prior to repairs, the building was essentially unoccupied and live loading was considered to be "relieved". Future live loading would result in the addition of load that would be re-distributed into the patched section.
2. By limiting the extent of the concrete removals, chloride concentrations sufficient to support active corrosion would remain at the depth of the primary reinforcing steel. As described above, chloride contamination was considered to be the primary factor contributing to the observed corrosion damage to the reinforced concrete structural elements, and some continued deterioration of the primary reinforcement and concrete core was anticipated. Therefore, the new reinforced concrete jacket was designed to accommodate any load transfer from the concrete core in the event of further deterioration. A representative area of column jacketing in progress is shown in Figure 7 with a completed column line of rehabilitated perimeter columns shown in Figure 8.

FIGURE 7 – View of reinforced formed column jacketing rehabilitation.

FIGURE 8 – View of completed column rehabilitations

Concluding Remarks

Numerous concrete repair programs had previously been implemented with limited success. Significant deterioration and failures of the original and repaired building components resulted in significant reinforced concrete section loss to building columns. Evaluations of the building conditions indicated that traditional concrete repairs could undermine the stability of the existing structure causing potential serviceability deficiencies and potential structural failure. Further exacerbating the situation was the impracticality of installing shoring to support the flat plate slab construction of the building during repairs.

The design of appropriate and constructible concrete repairs required intensive forensic evaluations of the existing conditions as well as a full engineering evaluation and modeling of the existing building structure. The resulting repair program included significant additions of structural reinforcement, concrete repairs and incorporation of a galvanic protection system to slow future corrosion activity while limiting the impact on the buildings structural stability. A more extensive galvanic protection program is now under consideration to prolong the overall building service life expectancy within the marine environment, as further deterioration of additional areas is anticipated within the next 10 years.

Column jacket repairs were executed at multiple locations incorporating structural reinforcement and durable concrete patch repairs. The executed repairs were implemented without requiring additions of shoring or relief of loading from the existing columns.

References

ACI 222R (2001) "*Protection of Metals in Concrete against Corrosion*", American Concrete Institute, Farmington Hills, MI.

ACI 222.3R (2003) "*Design and Construction Practices to Mitigate Corrosion of Reinforcement of Concrete Structures*", American Concrete Institute, Farmington Hills, MI.

ACI 318R (1963, 1971, 1977) "*Building Code Requirements for Reinforced Concrete"*, American Concrete Institute, Detroit, MI.

ACI 364.1R (2007) "*Guide for the Evaluation of Concrete Structures Prior to Rehabilitation*", American Concrete Institute, Farmington Hills, MI.

ACI 365.1R (2001) "*Service Life Prediction"*, American Concrete Institute, Farmington Hills, MI.

LIFE 365, Version 2.0 (Released 2008) Available from the National Ready Mixed Association of America http://www.nrmca.org/research/Life365_Instructions.asp

SEI/ASCE 11 (1999) "*Guideline for Structural Condition Assessment of Existing Buildings*", American Society for Civil Engineers, Reston, VA.

FORENSIC ASSESSMENT OF PERFORMANCE DEFICIENCIES OF A NEW DEPARTMENT STORE

M. Holický

Czech Technical University in Prague, Klokner Institute, Solinova 7, 166 08 Praha 6, Czech Republic; PH (420) 602 347 609; FAX (420) 224 355 232; e-mail: holicky@klok.cvut.cz

ABSTRACT

Load bearing structure of a new department store consists of flat (double ribbed) reinforced concrete slabs supported directly on columns within span distances 12 x 12 m. Slabs above the first and second storey cantilever out beyond the edge columns by 3 m. After few years in service, serious performance deficiencies concerning cladding as well as interior partitions and other secondary elements were observed. Analysis of load effects showed that although the structure was safe (with respect to the ultimate limit states), the large span cantilevered slabs had insufficient stiffness. Serviceability deficiencies of the department store were primarily caused in design by lack of consideration of deflection due to permanent load and shrinkage. Several construction faults and overloading of the structure enhanced unfavorable deformation defects. It appears that causal (Bayesian) network may provide valuable insights into causal links between observed deficiencies, overall performance and utility of the building.

INTRODUCTION

The recently built department store in a new suburban town is one of the most important social facilities of a large urban locality in Prague. Overall performance of this type of buildings is being closely observed by public and local authorities. Unfortunately, shortly after its completion, several performance defects (cracks, deflections) were observed.

Incidentally, at the same time another department store of the same user collapsed. This was perhaps the reason why all the performance deficiencies were sensitively recorded and publicly reported. Engineering climate seems to play a significant role in the subsequent assessment of structural damage. Observed defects were often exaggerated and interpreted as a structural condition indicating insufficient safety against collapse, not just serviceability deficiencies.

Load bearing structure of the department store consists of flat (double ribbed) reinforced concrete slabs supported directly on columns within span distances 12 x 12 m. Slabs above the first and second storey cantilever out beyond the edge columns by 3 m. After few years in service, serious performance insufficiencies concerning cladding as well as interior partitions and other secondary elements were observed. Due to the public perception of the apparent faults the second storey was closed and the whole building was reconstructed.

DESCRIPTION OF THE STRUCTURE

The plan view dimensions of the building are 78 × 53 m. The load-bearing structure consists of reinforced concrete double ribbed slabs of the total thickness 0.45 m supported directly by columns of the cross section 0.5 × 0.5 m or 0.7 × 0.7 m located within span distances 12 × 12 m (see Figure 1).

Figure 1. Internal view of the structure.

The slabs are provided with in-depth heads, 1.65 × 1.65 m (at the edge columns) and 3.35 × 3.35 m (at the interior columns), where the coffer ceiling is replaced a by solid slab. In the remaining part of the slab, the ribs of the cross section 0.18 × 0.38 m support a thin plate (of the thickness 0.07 m and interior spans 0.8 × 0.8 m). Equivalent thickness of a solid slab having the same rigidity would be 0.34 m only, which indicates that the stiffness of the slab is very low. Moreover, slabs above the first and second storey cantilever out beyond edge columns by 3 m.

Design loads of the slab above the ground floor considered in the original analysis consist of a permanent part 7.0 kN/m^2 and a variable part 4.0 kN/m^2, corresponding values for the slab above the first floor are 7.2 kN/m^2 and 1.5 kN/m^2. However, the actual permanent load of this slab is, due to the actual roof and ceiling, greater and could be as high as 10 kN/m^2. Nevertheless, the ultimate strength of the slab is sufficient, and no strengthening of the load bearing structure was needed.

Non-bearing elements of the second storey consist of façade cladding, interior partition walls and interior built-in components like glass walls and shelf stands. Cladding of the building consists of large glass windows, brick walls and window pillars, located within regular distances of 2.4 m. The window pillars, reinforced by steel ties anchored into the floor and ceiling, were built in the bearing slabs without any movement joints. Similarly all interior masonry partition walls, reinforced by rolled steel elements of I- and U-section were constructed without any separation from the roof slab. Expansion joints were not used in any interior built-in components. All of these non-bearing structures were evidently designed without a appropriate consideration of differential deflection of floor and ceiling slabs due to their different stiffness and loading.

PERFORMANCE DEFECTS

After few years in service serious performance problems concerning cladding as well as interior non-bearing structures were observed and analyzed by Holický (2001). The most alarming were perhaps the defects appearing in the non-bearing structural components: visible deformations, cracks in the partition walls (see Figures 2 and 3) and façade (see Figures 4 and 5).

Tensile cracks of the window pillars and cladding elements were particularly noticeable near the exterior corners of the building (see Figures 4 and 5). Also, deformed doorframes and a buckled shelf stand were visible and impressive. There were also sporadic shear cracks in the slab ribs close to the hidden column heads; however, they were mostly near construction joints. These cracks, which were of smaller importance for the overall damage assessment of the building, were the only detected defects of the load bearing structure.

ASSESSMENT

All of the defects of non-bearing structures in the first floor are caused by differential deflections of the floor slab (above the ground floor) and of the roof slab, primarily due to permanent load and shrinkage. As mentioned above, the permanent load of the roof is greater by 3 kN/m^2 than that of the slightly less flexible floor slab. This could lead to considerable differences in deflections of the slab midpoints (shortening of the clearance by to 30 mm) and cantilevered slab points deflection (extension of the clearance up to 5 mm, at the corners up to 10 mm). Also shrinkage may lead to similar differences in slab deflections; midpoints shortening and cantilevered points extension of the clearance may reach 5 mm (at corners 10 mm).

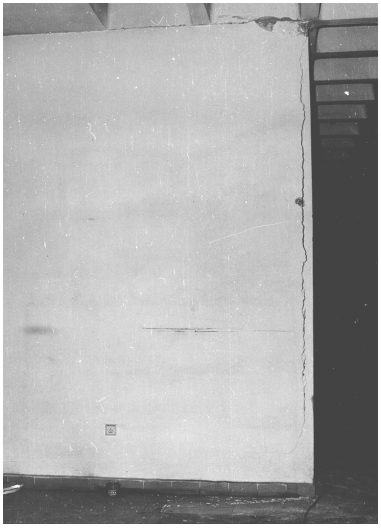

Figure 2. Crack in the partition wall.

Figure 3. Crack in the partition wall.

Figure 4. Crack in the façade corner.

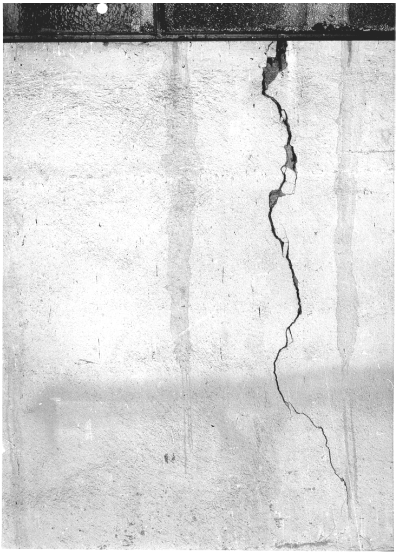

Figure 5. Crack in the façade wall.

Deformations due to a temporary load and temperature are of smaller importance and may cause a maximum clearance 6 mm and shortening 1 mm, cantilever clearance extension or shortening less than 1 mm. The observed deformation effects correlate well with theoretical results. Unfortunately, no verification of structural deformations were made in the original design. This was partly due to inadequate provisions of the contemporary standards.

Another construction fault mentioned above concerns the permanent load of the roof slab. Due to the actual self-weight of the ceiling and roof (sloped concrete layers) the permanent load of the slabs is approximately by 30 % greater than that assumed in the design calculation. However, this discrepancy arises from the neglect of some load components in the design calculation. Also the actual permanent load of the slab above the ground floor may be slightly greater than that considered in design. Even though the deformation effects would be considerably lower if the actual load equaled the assumed load, many of the serviceability defects would have appeared anyway. This concerns, above all, the cracks in the cladding elements, particularly at the exterior corners of two-way cantilevered slabs. Most of the observed defects were primarily due to general lack of considering deflection in the design and due to inaccurate determination of the design load. Construction errors, however, considerably enhanced deformation effects.

REPAIR

Although there were almost no defects apparent on the load bearing structure (except sporadic shear cracks in the ribs), it was decided to close the first floor and to reconstruct damaged interior partitions and other non-bearing structural components as well as the cladding components. Interior partitions including steel elements were separated from the ceiling and new movement joints were covered by panel strips. The cantilevered slabs were mutually tied up by ties placed near the window pillars. These measures were proposed by the designer, even though an additional analysis showed that the expected deformations due to temporary load and temperature were limited, and in some cases could be admitted without any modification of the non-load-bearing structures.

PUBLIC PERCEPTION

Public perception (recently discussed by Lewis (1995)) played an important role in the assessment and final decision concerning the building. The new department store soon became a building closely watched by a large number of users and local authorities. Moreover, at the same time another department store suffered from construction faults and this was partly the reason why all the performance deficiencies were carefully recorded (similar experience was described by Lewis (1995)). This unfavorable engineering climate seems to enhance the intensity of public perception. The observed defects were often exaggerated and regarded as indicators of insufficient structural safety. Widespread public perception of the defects and discrepancies appearing in expert assessments were reported in

newspapers and finally resulted in a strong public demand for strengthening the building.

THEORETICAL MODEL OF PUBLIC PERCEPTION

Public perception and expert assessments indicated that there is no distinct point in any commonly used performance indicator x (e.g. deflection, crack width) separating acceptable and unacceptable magnitude of the indicator. On the contrary, there seems to be a transition region $\langle a, b \rangle$ in which the structure gradually becomes unserviceable and the degree of caused damage $\nu(x)$ increases. This characteristic aspect of serviceability limit states was discussed in detail by Holický (1988 and 1999). A conceivable model for $\nu(x)$ is indicated in Figure 6 as a tri-linear function. The values of $\nu(x)$ are within the conventional interval from 0 to 1. There is no damage below a certain lower limit value a, and full damage above the upper limit b.

Figure 6. Theoretical model of public perception.

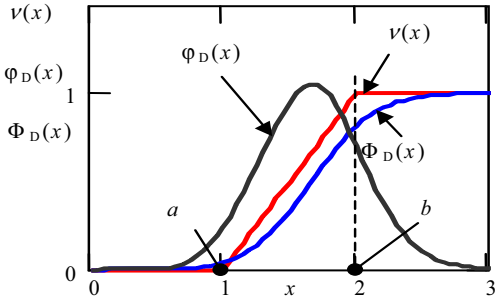

Obviously, at any damage level $\nu(x)$ there may be a perception scatter expressed by the distribution function $\Phi_P(x,\mu_P,\sigma_P)$, for which lognormal distribution having the mean $\mu_P = x$ and standard deviation $\sigma_P = s \times a$, where s is a relative measure of scatter related to the lower bound a, is accepted here. Taking into account all levels $\nu(x)$, the cumulative damage $\Phi_D(x)$ is defined by Holický (1999)

$$\Phi_D(x) = K \int_a^b \nu(\xi)\, \Phi_P(x,\xi,\sigma_P)\mathrm{d}\xi$$

where K is the normalizing factor to normalize $\Phi_D(x)$ into the interval from 0 to 1, and ξ is the integration variable. The cumulative damage $\Phi_D(x)$ and a corresponding density function $\varphi_D(x)$, shown in Figure 6 for $a = 1$, $b = 2$ and $s = 0.3$, can be considered as generalized probabilistic models (involving economic aspects). The cumulative damage $\Phi_D(x)$ can be used to specify in a rational way the required serviceability constrains as discussed by Holický (1999).

Further, considering an appropriate load effect E (e.g. deflection, crack width) having the mean μ_E and an assumed coefficient of variation w_E (=0.2), the expected perception level $\pi(\mu_E)$ can be defined similarly as the failure probability in the theory of structural reliability (e.g. Stewart and Melchers (1997)) as

$$\pi(\Delta,\sigma_P,\mu_E) = \int_{-\infty}^{+\infty} \varphi_E(x)\, \Phi_D(x)\, dx$$

Here $\varphi_E(x)$ is the probability density function of E. Gamma distribution having the mean μ_E is assumed. The mean μ_E equal to the lower limit of the transition region a, $\mu_E = a$, and the standard deviation $\sigma_E = 0.2\mu_E$ (the coefficient of variation 0.2) is assumed in the example shown in Figure 7, where the expected perception level $\pi(\Delta,\sigma_P,\mu_E)$ is indicated as a function of the ratio $\Delta = (b\text{-}a)/a$ for selected σ_P. Figure 8 shows $\pi(\Delta,\sigma_P,\mu_E)$ versus μ_E.

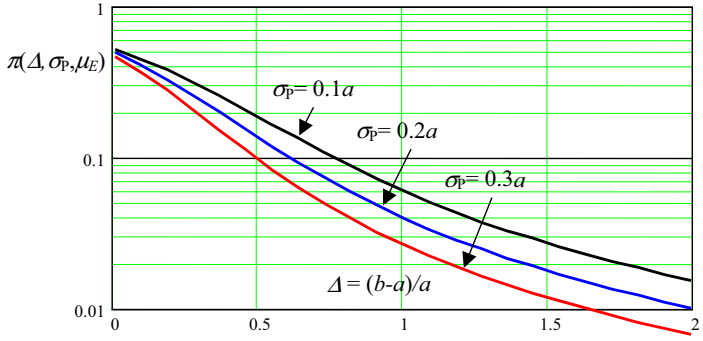

Figure 7. Perception level $\pi(\Delta,\sigma_P,\mu_E)$ for $\mu_E = a$.

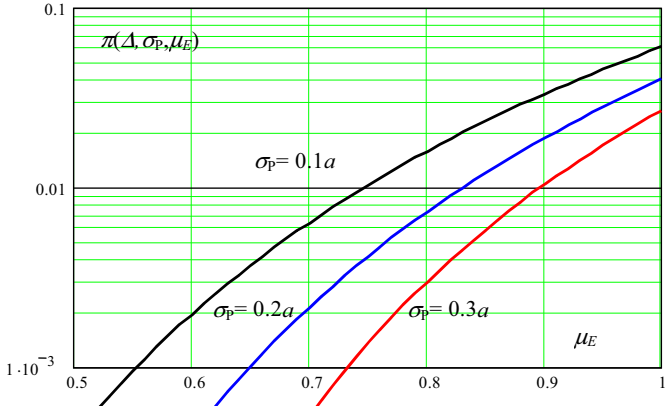

Figure 8. Perception level $\pi(\Delta,\sigma_P,\mu_E)$ for $\Delta = 1$.

It follows from Figure 7 and 8 that the expected damage (perception) level $\pi(\Delta,\sigma_P,\mu_E)$ is strongly dependent on both the ratio $\Delta = (b\text{-}a)/a$ and the mean μ_E, which may further depend on the sensitivity or experience of the observer. This finding explains the observed differences in public perception and the discrepancies in expert assessments.

EFFECTS OF EXPECTED CONSEQUENCES

In addition to psychological aspects, assessment of a structure may be affected also by the expected economic (and other) consequences. Both these factors may be considered explicitly or implicitly only. On the one hand consideration of expected consequences may lead to a rational specification of structural constraints; on the other hand it may significantly affect the assessment of the structure. Moreover, the expert assessor may use uncertain data and information. The following analysis investigates the possible effects of expected consequences.

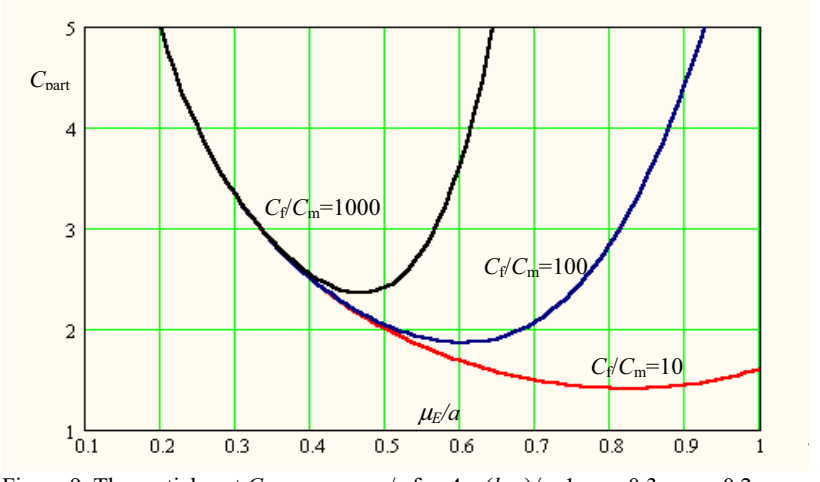

Figure 9. The partial cost C_{part} versus μ_E /a for $\Delta = (b\text{-}a)/a$=1, σ_P=0.3a, σ_E=0.2μ_E.

Assume that the optimum mean μ_E of the load effect E would correspond to the minimum of the total cost C_{tot}. Assuming a given coefficient of variation w_E, the optimum mean μ_E of the load effect E (the most suitable value assessed by an expert) may be obtained from the minimum of the total expected cost of a structure. Consider the total cost C_{tot} as a sum

$$C_{tot} = C_0 + C_m/\mu_E + \pi(\Delta,\sigma_P,\mu_E)\, C_f$$

where C_0 denotes the initial cost independent of μ_E, and C_m/μ_E is an additional cost affected by the modification of the mean μ_E, where C_m is a relevant marginal cost.

Finally the multiple $\pi(\Delta,\sigma_P,\mu_E)$ C_f describes the expected cost due to structural failure. Obviously the minimum C_{tot} will occur when the partial cost

$$C_{part} = 1/\mu_E + \pi(\Delta,\sigma_P,\mu_E)\, C_f/C_m$$

is the minimum, where $C_{part} = (C_{tot} - C_0)/ C_f$. Figure 9 shows the partial cost C_{part} for the following parameters: $(b\text{-}a)/a$=1, σ_P=0.3a, σ_E=0.2μ_E.

It follows from Figure 9 that the optimum mean μ_E may be expected from 0.5a to 0.8a. However, for an extremely high cost of failure C_f (greater than 1000 C_m) the optimum mean will be lower than 0.5a. Obviously, depending on the assumed cost ratio C_f/C_m the optimum (the most suitable) mean μ_E of the load effect E may considerably vary.

CAUSAL NETWORK

A simple causal (Bayesian) network describing causal links between observed deficiencies, particular requirements and overall performance of the building is shown in Figure 10. Software GeNIe (2007) was used to evaluate the network.

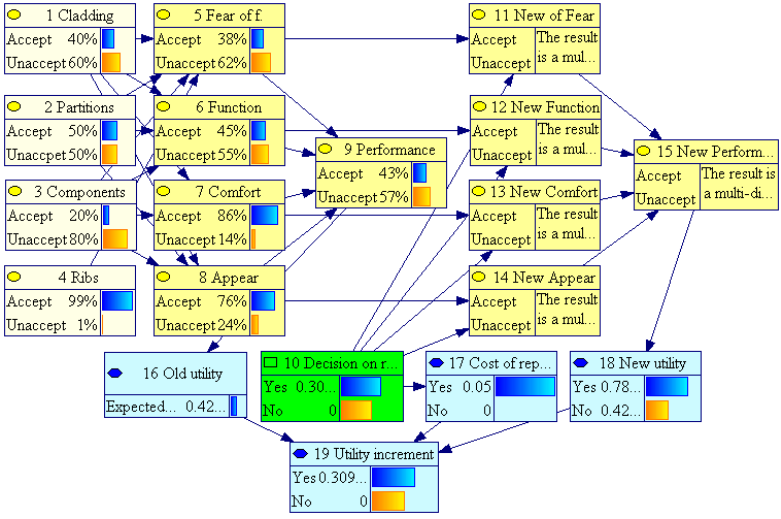

Figure 10. The causal (Bayesian) network describing causal links between observed deficiencies, particular requirements, overall performance and utility.

The network includes four initial nodes (1 to 4) representing observed performance deficiencies. Four structural requirements are described by nodes 5 to 9. The node 9 introduces the level of overall performance (within the scale from 0 to 1).

Decision node 10 indicates a choice of the extent of a possible repair. In general, several degree of the repair is conceivable.

The following nodes 11 to 15 correspond to the previous nodes 1 to 5. The nodes 11 to 14 represent potentially observed performance deficiencies after repair (not all the insufficiencies could be completely removed), the node 15 a newly reached performance level. The remaining nodes 16 to 19 are devoted to an assessment of utility of the structure before and after the repair and possible increase of the total utility due to repair (node 19). The values indicated in Figure 10 are just indicative results of an expert judgment.

CONCLUDING REMARKS

1. The performance deficiencies of the department store were primarily caused in design by lack of considering the deflection due to permanent load and shrinkage.
2. The construction faults (the additional permanent load and imperfect anchoring of ties) enhanced the unfavorable load effects of the structure.
3. The current engineering climate seemed to play an important role in the public perception, structural assessment and in the decisions concerning an intervention.
4. There is no distinct value that would uniquely separate acceptable and unacceptable structural conditions at the serviceability limit states.
5. The disturbing variance in public perception and in the expert assessment of the observed defects may be well explained by the proposed model for public perception.
6. There seems to be an optimum value of the performance indicator that would lead to the minimum total cost and that may be considered as the most suitable criterion.
7. Causal (Bayesian) network may provide valuable insights into causal links between observed deficiencies, criteria and overall performance of the building.

REFERENCES

GeNIe (2007), *Home page: http://genie.sis.pitt.edu*, *e-mail: genie@mail.sis.pitt.edu.*

Holický, M. (1988), "Fuzzy concept of serviceability limit states." *Symposium on serviceability of buildings*, NRC Canada, 1988, pp. 19-25.

Holický, M. (1999), "Fuzzy probabilistic optimization of building performance." *Automation in Construction*, 8/1999, pp 437-443.

Holický, M. "Performance Deficiency of a Department store - Case Study." *IABSE International Conference on Safety, Risk and Reliability - Trends in Engineering*, Malta, March 2001, pp 321-326.

Lewis, R. (1995) "The public perception of risk." *RSA Journal*, November 1995, pp. 52-63.

Steward, M.G. and Melchers, R.E. (1997) "Probabilistic risk assessment of engineering systems." Chapman & Hall, London.

ACKNOWLEDGEMENT

This research is a part of the research project GAČR: 103/09/0693 "Assessment of Safety and Risks of Technical Systems".

Restoration of Life Star Rooftop Heliport at Hartford Hospital

Howard Epstein[*] and George Torello, Jr.[+]

[*]Professor, Department of Civil and Environmental Engineering
University of Connecticut, Storrs, CT 06269-2037, U.S.A.

[+]Principal, George Torello Engineers, P.C.
215 Essex Plaza, Essex, CT 06426, U.S.A.

Abstract

This 20 year-old, 75' x 120' concrete structure, originally built for landing four medical helicopters, was presented to Torello Engineers with serious structural deficiencies, a deteriorated landing slab and structurally insufficient safety outriggers. Torello Engineers was charged with investigating the extent of repair needed and redesigning the structure. Among the challenges of this project was the need to keep Life Star Helicopters operational during rehabilitation of the landing surface and no disruption of other hospital services. Because the height of the heliport being more than 150 feet in the air, it was difficult to provide access for future repairs. Construction materials that will provide a long life but require little maintenance were used including stainless steels, polypropylene fibers and epoxy coating systems. The new design eliminated deficiencies and provided upgrades to the facility to accommodate landing of larger helicopters including Marine One, in the event of a Presidential emergency.

Description of the Project

This 20 year-old,75' x 120' concrete structure, originally built for landing four medical helicopters was presented to Torello Engineers with serious structural deficiencies a deteriorated landing slab and structurally insufficient safety outriggers. Torello Engineers was charged with investigating the extent of repair needed and redesigning the structure.

Initial investigation determined the condition of the 1986 concrete monolithic beam and slab system was not sufficient to meet the requirements of Life Star operations on the roof of the hospital. Specifically, years of exposure to the elements

and de-icing chemicals had contributed to the corrosion of the steel outriggers that support safety netting at the perimeter of the flight deck. Extreme deterioration of the concrete landing surface was producing loose debris which posed a risk to the safe operation of the aircraft. The existing waterproofing was badly disintegrated, and could no longer retain the water. A Ground Penetrating Radar survey (Figure 1) was performed to determine the extent of concrete deterioration. Structural rehabilitation was imperative to ensure continued safe operation of the air rescue service.

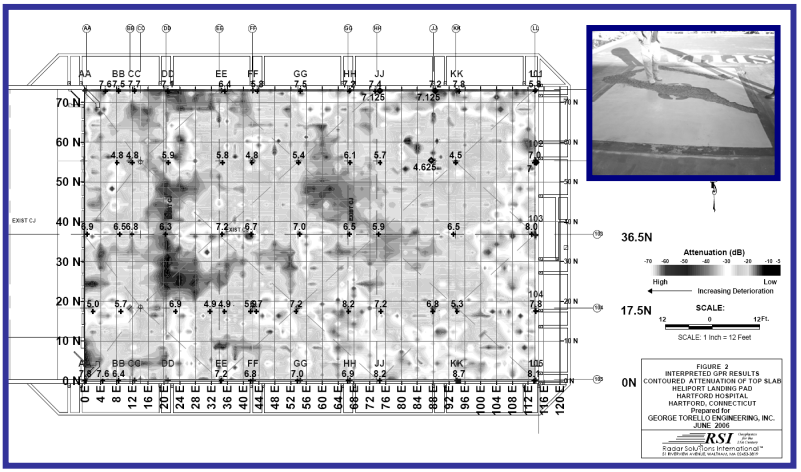

Figure 1. Ground Penetrating Radar deterioration mapping of the landing pad

The outrigger corrosion (Figure 2) was serious and would have required extensive demolition to repair or replace the structural steel tubes. Custom designed marine grade 316L stainless steel paddle plates were used that bypassed outrigger connections. Drainage systems were designed and constructed on the surface and beneath the concrete slab, improving flow and drainage. The new drainage details were designed to accommodate storm water and possible fuel spillage.

Figure 2. Severely corroded outriggers

Helicopters Continue to Fly

The challenge to the Hospital staff, Torello Engineers, and Petra Construction, was the need to keep helicopters operational during rehabilitation. Several design scenarios were considered and final construction methods were developed that would ensure continued operations during construction. During repairs, helicopters were in operation with little change to the daily routine. Only during a brief construction phase were the helicopters relocated to a ground landing site. Odor free construction materials and methods were selected and used to eliminate any disruption to the care and comfort of the 800 patients in the Hospital below. All work was performed in accordance with the latest International Building Code and FAA regulations.

420 tons of deteriorated concrete were broken into disposable sized pieces and were removed without damage to the structure below. A temporary containment enclosure (Figure 3) was constructed around the perimeter to protect the workers and control the air-born products from sand blasting and painting. This protected the Hospital patients on the floors below from odors, and allowed repairs to continue uninterrupted during aircraft take-offs and landings.

Figure 3. Protection of construction and scaffolding to the 13th floor allowed for continued operations.

Durability

Given the extreme height of the rooftop heliport and its inaccessibility for future repairs, durability of the heliport rehabilitation was paramount. Construction materials were carefully selected to assure a long life. The use of stainless steels, polypropylene fibers and epoxy coating systems require little maintenance. A detailed operations and maintenance manual was prepared for the client. Figure 4 shows the placing of stainless steel bars on the portion of the landing pad that was upgraded.

Figure 4. Stainless steel rebars used throughout

Innovative Design Features

'Paddle' Plates - The extent of the outrigger corrosion was more than just surface deep. The existing connections anchoring the outriggers to the building were so corroded that they could not be repaired. Stainless steel paddle plates were designed to bypass all seriously corroded connections. The strength of the new connections was designed to surpass the yield strength of the outriggers. Twenty six new 316L stainless steel paddle plates were custom fabricated and welded to the existing carbon steel outriggers. The paddles were then connected to the existing concrete structure with stainless steel anchor bolts. Figure 5 shows two of these plates during their installation. Each plate was bent up slightly to conform to the geometry of the existing outriggers. The plates were wrapped around the concrete curb and bolted to the concrete slab (stainless bolts).

Figure 5. Paddle plates provide unique bypass for existing deteriorated connections.

The plates and welds were sized so that they would be stronger than the capacity of the existing cantilevered steel outriggers. This design was deliberate so that if the outrigger tubes were ever overloaded the failure would not be due to any fracture but would be yielding of the steel. Welding stainless steel is a difficult operation. Weld designs, procedure qualifications, and welder testing were done first. Ongoing inspections of all stainless steel welding were meticulously performed. Figure 6 shows plan, side view and a section through a paddle plate.

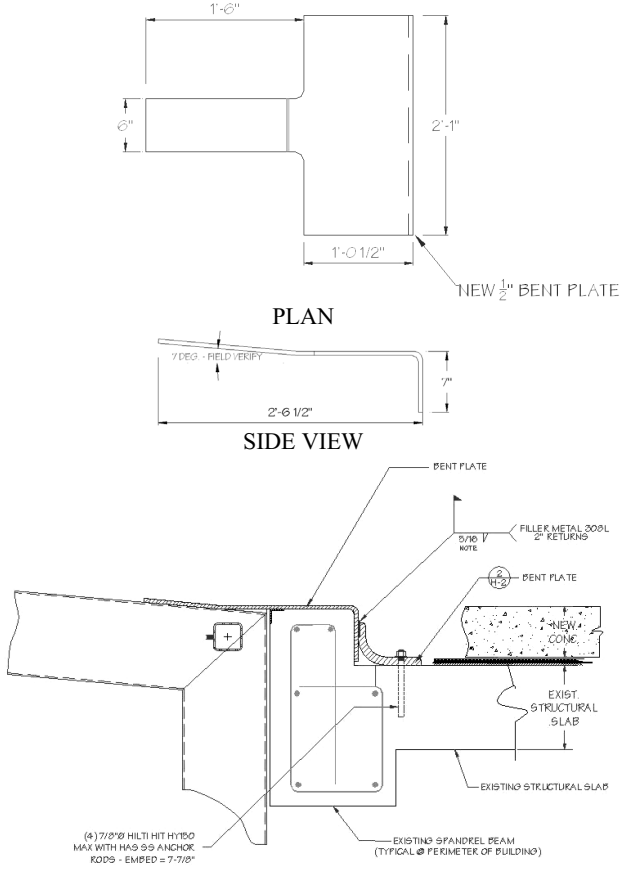

Figure 6. Geometry of the paddle plates.

Drainage - Unique design details provide secondary drainage for water or fuel infiltration. Two drainage systems were constructed; surface and beneath the concrete slab. Great care was taken providing drainage details to accommodate storm water and possible fuel spillage. Figure 7 shows a cross section through a drain.

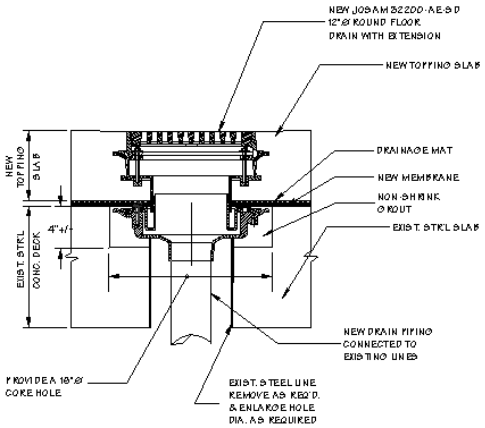

Figure 7. Dual drainage paths provide backup for fuel spills and water infiltration.

Composite Slab - Stainless steel anchor pins were used to tie the underlying concrete wearing slab and structural slab together increasing the structural capacity to accommodate a Presidential helicopter (Figure 8a). This resulted in an 18" thick composite slab. A fluid applied membrane encapsulates composite stainless steel pins insuring water tightness of roof deck below the presidential landing pad (Figure 8b).

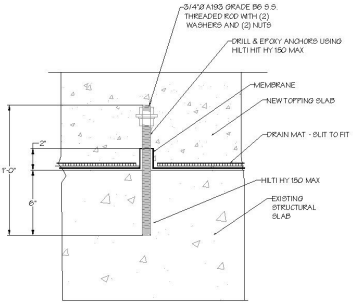

(a) (b)

Figure 8. The composite slab for the Presidential helicopter landing pad.

Other Features of the Project

As rehabilitative work progressed, the hospital engineering staff and Torello Engineers integrated additional design enhancements including a new electrically operated 46' x 18' bi-fold door that is fully operable during all weather conditions. Also upgraded were new beacons, landing field lights and paint striping of five individual landing pads. Torello Engineers worked with the bi-fold door manufacturer to upgrade the wind load capacity of the door structure so it could resist

hurricane force winds at the 13th floor elevation. Also, the existing safety netting needed replacing. New stainless steel support rings were added to the outriggers.

To accommodate the vital services of Life Star during reconstruction of the landing area, a critical path schedule was developed to meet the needs of the heliport's operations. Petra Construction Corporation, working closely with Torello Engineers, was able to complete construction of the strengthened heliport on August 29, 2008, 3 days ahead of the scheduled completion date.

OWNERS COMMENTS: Many times during the planning, it seemed almost impossible that budget constraints and other obstacles would allow this project to go ahead. Details were developed and cost estimates made about one year ahead of when construction was to begin. Working with the "team" which included Torello, Petra, Tilcon Connecticut Inc., Marion Testing & Inspection, Hospital staff and the pilots, a plan was worked out and a critical path schedule was developed with hard and fast start and finish dates. The owner commented that not only was this an amazing feat, but the completed project is probably the best elevated hospital heliport in the U.S.A.

Figure 9. Pilots and Life Star team members along with the engineering and construction teams meet at the flight line as the hospital president dedicates the revitalized facility.

Figure 10. Life Star helicopters help to save lives at a moment's notice.

This page intentionally left blank

Subject Index

Page number refers to the first page of paper

Accidents, 577
Aircraft, 809
Airport and airfield runways, 809
Asphalts, 194
Assessment, 115, 244, 278, 577, 709, 799

Blasting, 115, 325, 335, 487
Bridge failures, 105, 133, 395
Bridges, girder, 395
Bridges, pedestrian, 395
Bridges, railroad, 105
Bridges, wood, 133
Buckling, 395
Building envelope, 23, 55
Buildings, high-rise, 688, 739, 789
Buildings, low-rise, 143, 278, 335, 759
Buildings, multistory, 318
Buildings, nonresidential, 729
Buildings, residential, 55, 184, 288, 729, 789

California, 43, 115, 414
Canada, 668
Case studies, 13, 85, 234, 308, 335, 424, 477, 536, 749
Cement, 255
Chimneys, 175
Cladding, 13, 739, 799
Coal mining, 214
Coastal environment, 789
Collapsible soils, 288
Colorado, 55, 234, 288
Columns, 143, 255
Composite materials, 66
Compression, 255
Computation, 497
Concrete blocks, 587
Concrete construction, 617
Concrete slabs, 647
Concrete structures, 298, 536, 627, 779, 789, 799
Connecticut, 809
Conservation, 607
Construction, 163, 487, 527
Construction methods, 1
Corrosion, 637
Cracking, 647
Cranes, 556, 567, 577
Curtain walls, 688
Czech Republic, 799

Damage, 125, 194, 348, 546, 577, 668, 699, 709, 729, 739, 749, 759, 779
Defects, 546
Deformation, 348
Deterioration, 204
Diagnosis, 74
Differential settlement, 278
Drainage, 204, 424
Ducts, 153

Earthquakes, 33, 43, 779
Electric transmission structures, 325
Engineering education, 512, 517
Estimation, 699, 719
Ethics, 497
Europe, 444
Evaluation, 184, 433, 627
Expert witness, 504

Failures, 33
Fatigue, 546
Flexural strength, 627

Floods, 163, 729, 308
Forensic engineering, 153, 224, 244, 424, 465, 504, 512, 517, 617, 678, 799
Foundations, 265, 348
Frames, 487, 688
Frost heave, 234
Fuzzy sets, 597

Graduate study, 512
Ground motion, 325
Grouting, 288

Health care facilities, 809
Historic sites, 387, 607
History, 335
Humidity, 153
Hurricanes, 678, 719, 739, 749, 779

Identification, 74
In situ tests, 657
Industrial plants, 678
Infiltration, 23
Infrastructure, 115
Inspection, 55
Installation, 527
Insurance, 779
Internal pressure, 13
Internet, 214
Italy, 387

Land use, 214, 244
Leakage, 96
Leveling, 308
Load bearing capacity, 265, 587, 799
Load duration, 465
Load tests, 657

Mapping, 214
Masonry, 66, 96, 387, 617
Massachusetts, 105
Mathematics, 378
Microbes, 153
Moisture, 23, 43, 298
Monitoring, 637

Natural disasters, 597
New Jersey, 789
New York, 96, 368, 395
New York City, 368, 395
Nondestructive tests, 627, 637
North Carolina, 433

Oklahoma, 759
Optimization, 288
Oregon, 133

Pennsylvania, 454
Professional practice, 497
Progressive collapse, 378
Public safety, 404

Radar, 627, 647
Ratings, 55
Recreational facilities, 318
Rehabilitation, 55, 85, 546, 597, 769, 789
Remediation, 278
Reservoirs, 769
Restoration, 809
Retaining walls, 414
Roofs, 13, 184, 194, 204, 358, 424, 444, 454, 465, 587

Safety, 477, 556
Scaffolds, 536
Sealing, 96
Security, 115
Seismic effects, 348
Serviceability, 587, 607, 657
Settlement, 255, 647
Shear strength, 255
Sinkholes, 214, 224
Slabs, 587
Slope stability, 265
Snow loads, 444
Soft soils, 255
Soil compaction, 288

Soil liquefaction, 348
Soil pollution, 244
Stability, 143
Steel, 368
Stiffness, 348
Storage facilities, 487
Storm surges, 729
Storms, 759
Stress waves, 214
Structural analysis, 125, 378, 454, 497, 637, 657, 668, 749
Structural design, 163, 477
Structural dynamics, 325
Structural failures, 1, 13, 43, 55, 74, 115, 175, 358, 368, 387, 404, 414, 424, 433, 444, 465, 487, 504, 527, 536, 567, 607
Structural members, 477
Structural reliability, 378, 444
Subgrades, 647
Subsurface environment, 298
Sulfates, 234
Surveys, 308, 668
Sustainable development, 23

Temperature effects, 153
Texas, 175, 404, 739
Thermal factors, 43
Timber construction, 143
Tornadoes, 699, 709, 719, 749
Towers, 546, 567
Trusses, 368, 454, 477
Tunnels, 125

Uncertainty principles, 597
Underground structures, 298, 348
United Kingdom, 244

Veneers, 33, 85
Vibration, 318, 325, 335, 433, 637
Virginia, 85

Walls, 33, 43, 66, 74, 96, 234
Water, 23
Water flow, 298
Water tanks, 769
Wind forces, 749, 759
Wind gusts, 678
Wind loads, 163, 194, 527, 668, 688, 729
Wind speed, 699, 709, 719
Wood structures, 465, 477, 487

This page intentionally left blank

Author Index

Page number refers to the first page of paper

Adan, Scott M., 759
Agbayani, Nestor A., 546
Ahuja, Deepak, 143, 404, 477
Alkhrdaji, Tarek, 657
Alsharkawi, I., 378
Arya, Behnam, 465
Asadi, Afshin, 255
Askari, F., 265
Augenti, N., 387, 512

Bagley, Aaron D., 234
Bast, William D., 688
Beasley, Kimball J., 74
Brown, Michael D., 637

Caffey, Jessica M., 749
Cain, Hal K., 358
Cesare, Joseph A., 234
Chancey, Ryan, 143
Chaudhuri, Debanik, 308
Chauvin, Mark R., 587
Chen, Shen-En, 214, 769
Choudhuri, Dilip, 318
Connor, Eric, 325
Corr, D. J., 395
Cumbers, Jason M., 288
Cyr, Michele F., 308

Dai, Kaoshan, 325
Dalrymple, Gerald A., 617
Deckard, Clinton, 298
DeLeon, Marco A., 194, 204
Dethlefs, Richard, 133
Díaz de León, Alicia , 96
Dolhon, Anthony M., 587
Dornfest, Eileen M., 288
Drdácký, Miloš, 607
Drerup, Michael J., 96

Duffy, Peggy Hagerty, 298
Dunlap, Gary S., 175

East, Bradley L., 204
Ekwueme, Chukwuma G., 414
Epstein, Howard, 809
Eschenasy, Dan, 527

Farzaneh, O., 265
Fatima, S. S., 769
Finley, David S., 587
Fowler, David W., 143
French, Warren R., 13
Friedman, Donald, 454

Galati, Nestore, 657
Ganjian, N., 265
Glascoe, Lee G., 115, 125
Glenn, Lewis A., 125
Godfrey, Eric, 789
Goodrich, Andrew, 368
Graver, Amy S., 627
Grill, John, 647

Harris, Joe, 288
Harrison, Ben F., 678
Hart, Gary C., 779, 465
Hatambeigi, M., 536
Hebeler, Gregory L., 278
Holický, M., 444, 799
Howard, Darren K., 278
Huat, B. K. Bujang, 255

Ingargiola, John, 163

Jain, Anurag, 779
James, C. L., 244
Janardhanam, R., 214

Jenkins, Jonathan, 709
Jordan, James W., 424, 184
Joseph, Lesley, 709

Kardon, Joshua B., 497, 504
Kargahi, Mohsen, 465
Kazemian, Sina, 255
Kesner, Keith, 637
Killian, Daniel M., 175, 749
Kimble, Ross A., 184
Koleva, Antoneta, 325
Konz, Robert C., 739
Kopp, Gregory A., 668
Kordi, Behareh, 668
Krnjajic, Milovan, 125

Lattanzio, Stephen M., 23, 153
Lavon, Benjamin, 368
Lee, Kerry S., 175, 749
Lehmer, Gerald D., 414
Leininger, L., 378
Leistikow, Ralf, 278
Lester, Michael P., 433
Luft, Rene, 759

Maekawa, Koichi, 348
Marcotte, Tracy, 789
Margraf, Jonathan, 115
Marjanishvili, S. M., 378
Martin, Zeno, 133
Maschke, Ken R., 688
McCann, D. M., 395
McDonald, B. M., 395
McDonald, James R., 719, 699
McMichael, Larry, 115
Mehta, Kishor C., 699, 719
Meldrum, Joanna L., 308
Miller, Craig, 668
Miraglia, M., 378
Morris, Joseph P., 125
Morrison, Murray J., 668
Morse, Roger G., 153, 23

Nacheman, Scott G., 688
Natarajan, C., 769, 597
Noble, Charles, 115
Norman, Charles R., 577, 729
Norvell, Justin, 647

Okhovat, Mohammad Reza, 348
Ospina, Rafael I., 278
Overton, Daniel D., 288

Pazera, M., 43
Pennington, Steven M., 105
Peraza, David B., 66, 556
Peterson, J. E., 85
Phillips, D. T. P., 517
Pierce, Charles E. , 709
Pietrasik, Pamela C., 194
Pisheh, Y. Pashang, 536
Prasad, Arun, 255
Puchek, Elizabeth A., 567

Qi, Wenya, 325

Rahim, Irman B. A., 255
Rajaraman, A., 597
Ratna Divya, Y., 597
Rens, Kevin L., 55
Rolander, Dennis D., 587
Royston, H. James, 55
Russo, Charles J., 487, 567, 627

Sama, K. Medji, 308
Samarajiva, Prasad, 318
Schaeffer, Robert, 789
Schober, Gregory G., 404
Searls, C. L., 33
Shafiei, H. R., 536
Shah, L. A., 244
Sharara, Luke M., 184, 424
Shelton, T., 85
Sherman, Matthew R., 627
Silvester, R. Scott, 487
Simons, Kenneth B., 1
Slížková, Zuzana, 607
Smith, Douglas A., 699, 719

Stubblefield, T. N., 33
Svinkin, Mark R., 335
Syed, Mohiuddin, 214
Sykora, Miroslav, 444

Tezak, Scott, 163
Thomas, B. R., 244
Torello, George Jr., 809
Totten, P. E., 43
Travis, Jeffrey A., 556

Vega, Rolando E., 678, 739
Verhulst, Stewart M., 143, 204, 404, 477

Wetzel, Nicholas G., 759
Wilson, Andrew, 789
Womble, J. Arn, 699, 719

Yala, Adam Abbes, 688
Yerges, Mark, 789
Young, David, 325

Zisman, E. D., 224